SHOUT
SHARE
IT

MBL

Volume 199

Number 1

THE BIOLOGICAL BULLETIN

AUGUST 2000

Published by the Marine Biological Laboratory

Thanks Galileo, Hooke and Leeuwenhoek for the incentive.

We walk in the footsteps of visionaries.
And see with the eyes of disciples.

Galileo up close: astronomer, physicist, mathematician, dethroner of Aristotle, defender of Copernicus and, yes, credited with making double convex lenses and the first biological bservations with a microscope. A compound microscope. n 1624.

Hooke: 43 years later, the compound microscope eveals living things are composed of cells.

Leeuwenhoek: invents the first practical microscope nd discovers bacteria.

Armed with the knowledge and inspiration of these nd other Olympians, secure in the history of our own ccomplishments and aware that the mind's eye should lways focus on challenging the enigmatic as well as he undeniable, Olympus has created the BX2 series of linical and research microscopes, noteworthy for their nhancements in optics, imaging and ergonomics.

And each so individual, it deserves the nomenclature My Microscope.

From possibility to actuality, it is wonderful to behold.
A posse ad esse est mirabile visu.

Welcome to the next golden age of microsopy.

BX2
Microscope Series

The BX41
The new standard in laboratory microscopy vis-a-vis performance, versatility, operation.

Uncanny digitized imaging: enhanced with the **DP11 digital camera**, delivering high-resolution image recording beyond the norm.

Unusually insightful optics: observe magnifications from **1.25x to 100x without changing the condenser.** Choice of condensers includes Abbe, swing-out, phase-contrast and darkfield.

Unerringly precise-motion stage: selectable for right/left hand. Discover speed, ease, touch, comfort, and clinical accuracy.

Uncommonly easy-to-operate controls: extended fine-focus knob; forwarded-positioned illumination intensity dial; tactile X-Y control.

The BX45

The new standard in ergonomic microscopy. A dramatic metamorphosis: innovative, intelligent, insightful design improvements specifically addressing the needs of those spending hours looking through a microscope.

The **lowest low-position stage: three inches lower** than standard microscopes, offering the promise of minimum effort and hand movement when changing specimens.

The **tilting, telescoping observation tube:** a marvel of adjustability, it can be changed to accommodate any observation position. 80mm higher and 70mm closer to the operator than a conventional tilting tube. And the eyepoint can be moved forward by 45mm and inclined from 0–25 degrees.

The BX51

The new standard in research microscopy. The words "new" and "standard" really don't do it justice. How about "ingenious" or "original," "paragon" or "prototypical." Prepare yourself for a higher power.

The **6-position filter cube turret:** Not 4, not 5, but 6, so single and multi-band imaging of new fluorochromes and fluorescent proteins is faster, simpler and exclusively tailored.

5
6
2
4
5
6
WU
IG
WIY

The **rectangular field stop: ours alone.** By cleverly matching the camera's field of view, only the area requiring fluorescence excitation is exposed. Which means that the surrounding areas are protected from photo bleaching.

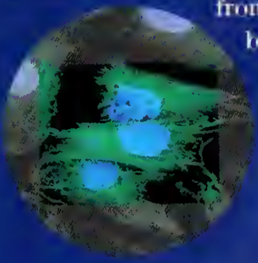

The **fluorescence excitation balancers:** another **Olympus exclusive.** A continuously variable excitation bandwidth. Visualization is enhanced, differentiation of multi-labels is immeasurably improved, capturing of images is at an unheard-of level.

Triple Labeled Specimen (l to r):

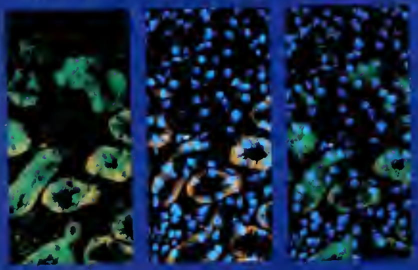

- with prevalent FITC and Cy3
- with prevalent DAPI and Cy3
- with balanced fluorescence emission

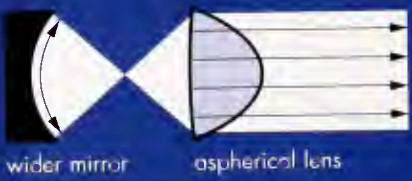

The **aspherical collector lens:** *sui generis*, in a class by itself. Specimens appear **brighter** and **more evenly illuminated**; and achromatic performance now incorporates wavelengths from UV to IR.

The **universal condenser: with 8 positions**, it can accept optical inserts for DIC, phase, brightfield and darkfield illumination. And the advanced Nomarski DIC system has been expanded and optimized to encompass prisms for enhanced contrast and image resolution.

OLYMPUS®
FOCUS ON LIFE

Visit us at www.olympusamerica.com
or call 1-800-455-8236

© Olympus America Inc.

THE
BIOLOGICAL BULLETIN
AUGUST 2000

Marine Biological Laboratory
Woods Hole Oceanographic Institution
Library

AUG 21 2000

Woods Hole, MA 02543

Editor	Michael J. Greenberg	The Whitney Laboratory, University of Florida
Associate Editors	Louis E. Burnett	Grice Marine Biological Laboratory, College of Charleston
	R. Andrew Cameron	California Institute of Technology
	Charles D. Derby	Georgia State University
	Michael LaBarbera	University of Chicago
Section Editor	Shinya Inoué, *Imaging and Microscopy*	Marine Biological Laboratory
Online Editors	James A. Blake, *Keys to Marine Invertebrates of the Woods Hole Region*	ENSR Marine & Coastal Center, Woods Hole
	William D. Cohen, *Marine Models Electronic Record and Compendia*	Hunter College, City University of New York
Editorial Board	Peter B. Armstrong	University of California, Davis
	Ernest S. Chang	Bodega Marine Lab., University of California, Davis
	Thomas H. Dietz	Louisiana State University
	Richard B. Emlet	Oregon Institute of Marine Biology, Univ. of Oregon
	David Epel	Hopkins Marine Station, Stanford University
	Gregory Hinkle	Cereon Genomics, Cambridge, Massachusetts
	Makoto Kobayashi	Hiroshima University of Economics, Japan
	Esther M. Leise	University of North Carolina Greensboro
	Donal T. Manahan	University of Southern California
	Margaret McFall-Ngai	Kewalo Marine Laboratory, University of Hawaii
	Mark W. Miller	Institute of Neurobiology, University of Puerto Rico
	Tatsuo Motokawa	Tokyo Institute of Technology, Japan
	Yoshitaka Nagahama	National Institute for Basic Biology, Japan
	Sherry D. Painter	Marine Biomed. Inst., Univ. of Texas Medical Branch
	J. Herbert Waite	University of California, Santa Barbara
	Richard K. Zimmer	University of California, Los Angeles
Editorial Office	Pamela Clapp Hinkle	Managing Editor
	Victoria R. Gibson	Staff Editor
	Carol Schachinger	Editorial Associate
	Carol Marrama	Subscription & Advertising Secretary

Published by
MARINE BIOLOGICAL LABORATORY
WOODS HOLE, MASSACHUSETTS

Cover

Among the "primitive" chitons of the suborder Lepidopleurina, the eggs have a smooth jelly coat, and the sperm—equipped with a typical, prominent acrosome—probably can enter an egg at any point on its surface. All other chitons have eggs with more elaborate spinous or cupulous hulls that focus sperm to specific regions on the surface. Moreover, these sperm have evolved a long nuclear filament tipped by a minute acrosome which interacts with the egg in specific ways. Differences in the form of the egg hull and in the mechanism of fertilization among chitons are providing insights into the evolution of this ancient molluscan taxon.

In this issue (pp. 59-67), John Buckland-Nicks and Alan Hodgson describe fertilization in *Callochiton castaneus* from South Africa. This chiton retains a mixture of primitive and derived characters that together produce a novel mechanism of fertilization, which is represented on the cover.

In the background of the cover is an unfertilized egg of *C. castaneus*, from which the jelly coat and part of the vitelline layer have been stripped to reveal a honeycomb of egg membrane cups. In the intact egg, these cups coincide with the bases of regularly spaced pores in the jelly coat. Fertile sperm seeking the egg locate one of these external pores and swim down it to the vitelline layer. The minute acrosome digests a pore, and the needle-like nuclear filament bridges the distance to the egg membrane cup.

The micrograph superimposed on the background shows a fertilizing sperm in the process of injecting chromatin into the egg cortex. The unusual aspect of fertilization in these chitons is that the sperm organelles are apparently abandoned in a membrane bag on the egg surface. If this is indeed the case, then inheritance, not only of mitochondria, but also of centrioles and other cytoplasmic components, would be maternal.

CONTENTS

Volume 199, No. 1: August 2000

RESEARCH NOTE

Bolton, Toby F., Florence I. M. Thomas, and Celere N. Leonard
Maternal energy investment in eggs and jelly coats surrounding eggs of the echinoid *Arbacia punctulata* 1

PHYSIOLOGY

Johnson, M. L., P. M. J. Shelton, E. Gaten, and P. J. Herring
Relationship of dorsoventral eyeshine distributions to habitat depth and animal size in mesopelagic decapods 6

Dietz, T. H., A. S. Udoetok, J. S. Cherry, H. Silverman, and R. A. Byrne
Kidney function and sulfate uptake and loss in the freshwater bivalve *Toxolasma texasensis* 14

Vollmer, Steven V., and Peter J. Edmunds
Allometric scaling in small colonies of the scleractinian coral *Siderastrea siderea* (Ellis and Solander) 21

DEVELOPMENT AND REPRODUCTION

Torrado, Mario, and Alexander T. Mikhailov
Frog Lim-1-like protein is expressed predominantly in the nervous tissue, gonads, and early embryos of the bivalve mollusc *Mytilus galloprovincialis* 29

Gibson, Glenys D., and Jennifer M. L. Harvey
Morphogenesis during asexual reproduction in *Pygospio elegans* Claparede (Annelida, Polychaeta) 41

Watson, G. J., F. M. Langford, S. M. Gaudron, and M. G. Bentley
Factors influencing spawning and pairing in the scale worm *Harmothoe imbricata* (Annelida: Polychaeta) . . . 50

Buckland-Nicks, John, and Alan N. Hodgson
Fertilization in *Callochiton castaneus* (Mollusca) 59

Hirose, M., R. A. Kinzie III, and M. Hidaka
Early development of zooxanthella-containing eggs of the corals *Pocillopora verrucosa* and *P. eydouxi* with special reference to the distribution of zooxanthellae 68

CELL BIOLOGY

Wakefield, Timothy S., Mark A. Farmer, and Stephen C. Kempf
Revised description of the fine structure of *in situ* "Zooxanthellae" genus *Symbiodinium* 76

ECOLOGY AND EVOLUTION

Barnes, David K. A., and Mathew H. Dick
Overgrowth competition between clades: implications for interpretation of the fossil record and overgrowth indices 85

* * *

Annual Report of the Marine Biological Laboratory R1

THE BIOLOGICAL BULLETIN

THE BIOLOGICAL BULLETIN is published six times a year by the Marine Biological Laboratory, 7 MBL Street, Woods Hole, Massachusetts 02543.

Subscriptions and similar matter should be addressed to Subscription Manager, THE BIOLOGICAL BULLETIN, Marine Biological Laboratory, 7 MBL Street, Woods Hole, Massachusetts 02543. Subscription per year (six issues, two volumes): $225 for libraries; $95 for individuals. Subscription per volume (three issues): $112.50 for libraries; $47.50 for individuals. Back and single issues (subject to availability): $40 for libraries; $20 for individuals.

Communications relative to manuscripts should be sent to Michael J. Greenberg, Editor-in-Chief, or Pamela Clapp Hinkle, Managing Editor, at the Marine Biological Laboratory, 7 MBL Street, Woods Hole, Massachusetts 02543. Telephone: (508) 289-7428. FAX: 508-289-7922. E-mail: pclapp@mbl.edu.

http://www.mbl.edu/BiologicalBulletin/

The home page for the electronic companion to THE BIOLOGICAL BULLETIN—*the Marine Models Electronic Record*—and other BIOLOGICAL BULLETIN publications is available on the World Wide Web at the address shown above.

THE BIOLOGICAL BULLETIN is indexed in bibliographic services including *Index Medicus* and MEDLINE, *Chemical Abstracts, Current Contents, Elsevier BIOBASE/Current Awareness in Biological Sciences*, and *Geo Abstracts*.

Printed on acid free paper,
effective with Volume 180, Issue 1, 1991.

POSTMASTER: Send address changes to THE BIOLOGICAL BULLETIN, Marine Biological Laboratory,
7 MBL Street, Woods Hole, MA 02543.

Copyright © 2000, by the Marine Biological Laboratory

Periodicals postage paid at Woods Hole, MA, and additional mailing offices.
ISSN 0006-3185

INSTRUCTIONS TO AUTHORS

The Biological Bulletin accepts outstanding original research reports of general interest to biologists throughout the world. Papers are usually of intermediate length (10–40 manuscript pages). A limited number of solicited review papers may be accepted after formal review. A paper will usually appear within four months after its acceptance.

Very short, especially topical papers (less than 9 manuscript pages including tables, figures, and bibliography) will be published in a separate section entitled "Research Notes." A Research Note in *The Biological Bulletin* follows the format of similar notes in *Nature*. It should open with a summary paragraph of 150 to 200 words comprising the introduction and the conclusions. The rest of the text should continue on without subheadings, and there should be no more than 30 references. References should be referred to in the text by number, and listed in the Literature Cited section in the order that they appear in the text. Unlike references in *Nature*, references in the Research Notes section should conform in punctuation and arrangement to the style of recent issues of *The Biological Bulletin*. Materials and Methods should be incorporated into appropriate figure legends. See the article by Lohmann *et al.* (October 1990, Vol. **179:** 214–218) for sample style. A Research Note will usually appear within two months after its acceptance.

The Editorial Board requests that regular manuscripts conform to the requirements set below; those manuscripts that do not conform will be returned to authors for correction before review.

1. ***Manuscripts.*** Manuscripts, including figures, should be submitted in quadruplicate, with the originals clearly marked. (Xerox copies of photographs are not acceptable for review purposes.) The submission letter accompanying the manuscript should include a telephone number, a FAX number, and (if possible) an E-mail address for the corresponding author. The original manuscript must be typed in no smaller than 12 pitch or 10 point, using double spacing (*including* figure legends, footnotes, bibliography, etc.) on one side of 16- or 20-lb. bond paper, 8 by 11 inches. Please, no right justification. Manuscripts should be proofread carefully and errors corrected legibly in black ink. Pages should be numbered consecutively. Margins on all sides should be at least 1 inch (2.5 cm). Manuscripts should conform to the *Council of Biology Editors Style Manual*, 5th Edition (Council of Biology Editors, 1983) and to American spelling. Unusual abbreviations should be kept to a minimum and should be spelled out on first reference as well as defined in a footnote on the title page. Manuscripts should be divided into the following components: Title page, Abstract (of no more than 200 words), Introduction, Materials and Methods, Results, Discussion, Acknowledgments, Literature Cited, Tables, and Figure Legends. In addition, authors should supply a list of words and phrases under which the article should be indexed.

2. *Title page.* The title page consists of a condensed title or running head of no more than 35 letters and spaces, the manuscript title, authors' names and appropriate addresses, and footnotes listing present addresses, acknowledgments or contribution numbers, and explanation of unusual abbreviations.

3. ***Figures.*** The dimensions of the printed page, 7 by 9 inches, should be kept in mind in preparing figures for publication. We recommend that figures be about 1 times the linear dimensions of the final printing desired, and that the ratio of the largest to the smallest letter or number and of the thickest to the thinnest line not exceed 1:1.5. Explanatory matter generally should be included in legends, although axes should always be identified on the illustration itself. Figures should be prepared for reproduction as either line cuts or halftones. Figures to be reproduced as line cuts should be unmounted glossy photographic reproductions or drawn in black ink on white paper, good-quality tracing cloth or plastic, or blue-lined coordinate paper. Those to be reproduced as halftones should be mounted on board, with both designating numbers or letters and scale bars affixed directly to the figures. All figures should be numbered in consecutive order, with no distinction between text and plate figures and cited, in order, in the text. The author's name and an arrow indicating orientation should appear on the reverse side of all figures.

Digital art: The Biological Bulletin will accept figures submitted in electronic form; however, digital art must conform to the following guidelines. Authors who create digital images are wholly responsible for the quality of their material, including color and halftone accuracy.

Format. Acceptable graphic formats are TIFF and EPS. Color submissions must be in EPS format, saved in CMKY mode.

Software. Preferred software is Adobe Illustrator or Adobe Photoshop for the Mac and Adobe Photoshop for Windows. Specific instructions for artwork created with various software programs are available on the Web at the Digital Art Information Site maintained by Cadmus Professional Communications at http://cjs.cadmus.com/da/home.html

Resolution. The minimum requirements for resolution are 1200 DPI for line art and 300 for halftones.

Size. All digital artwork must be submitted at its actual printed size so that no scaling is necessary.

Multipanel figures. Figures consisting of individual parts (*e.g.*, panels A, B, C) must be assembled into final format and submitted as one file.

Hard copy. Files must be accompanied by hard copy for use in case the electronic version is unusable.

Disk identification. Disks must be clearly labeled with the following information: author name and manuscript number; format (PC or Macintosh); name and version of software used.

Color: The Biological Bulletin will publish color figures and plates, but must bill authors for the actual additional cost of printing in color. The process is expensive, so authors with more than one color image should—consistent with editorial concerns, especially citation of figures in order—combine them into a single plate to reduce the expense. On request, when supplied with a copy of a color illustration, the editorial staff will provide a pre-publication estimate of the printing cost.

4. *Tables, footnotes, figure legends, etc.* Authors should follow the style in a recent issue of *The Biological Bulletin* in preparing table headings, figure legends, and the like. Because of the high cost of setting tabular material in type, authors are asked to limit such material as much as possible. Tables, with their headings and footnotes, should be typed on separate sheets, numbered with consecutive Roman numerals, and placed after the Literature Cited. Figure legends should contain enough information to make the figure intelligible separate from the text. Legends should be typed double spaced, with consecutive Arabic numbers, on a separate sheet at the end of the paper. Footnotes should be limited to authors' current addresses, acknowledgments or contribution numbers, and explanation of unusual abbreviations. All such footnotes should appear on the title page. Footnotes are not normally permitted in the body of the text.

5. ***Literature cited.*** In the text, literature should be cited by the Harvard system, with papers by more than two authors cited as Jones *et al.*, 1980. Personal communications and material in preparation or in press should be cited in the text only, with author's initials and institutions, unless the material has been formally accepted and a volume number can be supplied. The list of references following the text should be headed Literature Cited, and must be typed double spaced on separate pages, conforming in punctuation and arrangement to the style of recent issues of *The Biological Bulletin*. Citations should include complete titles and inclusive pagination. Journal abbreviations should normally follow those of the U. S. A. Standards Institute (USASI), as adopted by BIOLOGICAL ABSTRACTS and CHEMICAL ABSTRACTS, with the minor differences set out below. The most generally useful list of biological journal titles is that published each year by BIOLOGICAL ABSTRACTS (BIOSIS List of Serials; the most recent issue). Foreign authors, and others who are accustomed to using THE WORLD LIST OF SCIENTIFIC PERIODICALS, may find a booklet published by the Biological Council of the U.K. (obtainable from the Institute of Biology, 41 Queen's Gate, London, S.W.7, England, U.K.) useful, since it sets out the WORLD LIST abbreviations for most biological journals with notes of the USASI abbreviations where these differ. CHEMICAL ABSTRACTS publishes quarterly supplements of additional abbreviations. The following points of reference style for THE BIOLOGICAL BULLETIN differ from USASI (or modified WORLD LIST) usage:

A. Journal abbreviations, and book titles, all underlined (for *italics*)

B. All components of abbreviations with initial capitals (not as European usage in WORLD LIST *e.g.*, *J. Cell. Comp. Physiol.* NOT *J. cell. comp. Physiol.*)

C. *All* abbreviated components must be followed by a period, whole word components *must not* (*i.e.*, *J. Cancer Res.*)

D. Space between all components (*e.g.*, *J. Cell. Comp. Physiol.*, not *J.Cell.Comp.Physiol.*)

E. Unusual words in journal titles should be spelled out in full, rather than employing new abbreviations invented by the author. For example, use *Rit Vísindafjélags Islendinga* without abbreviation.

F. All single word journal titles in full (*e.g.*, *Veliger*, *Ecology*, *Brain*).

G. The order of abbreviated components should be the same as the word order of the complete title (*i.e., Proc.* and *Trans.* placed where they appear, not transposed as in some BIOLOGICAL ABSTRACTS listings).

H. A few well-known international journals in their preferred forms rather than WORLD LIST or USASI usage (*e.g., Nature, Science, Evolution* NOT *Nature, Lond., Science, N.Y.; Evolution, Lancaster, Pa.*)

6. ***Reprints, page proofs, and charges.*** Authors may purchase reprints in lots of 100. Forms for placing reprint orders are sent with page proofs. Reprints normally will be delivered about 2 to 3 months after the issue date. Authors (or delegates for foreign authors) will receive page proofs of articles shortly before publication. They will be charged the current cost of printers' time for corrections to these (other than corrections of printers' or editors' errors). Other than these charges for authors' alterations, *The Biological Bulletin* does not have page charges.

Reference: *Biol. Bull.* **199:** 1–5. (August 2000)

Maternal Energy Investment in Eggs and Jelly Coats Surrounding Eggs of the Echinoid *Arbacia punctulata*

TOBY F. BOLTON[1,*], FLORENCE I. M. THOMAS[1], AND CELERE N. LEONARD[2]

[1] *Department of Biology, University of South Florida, Tampa, 4202 East Fowler Avenue, Tampa, Florida 33620-5150; and* [2] *Department of Biology, Tuskeegee University, Tuskeegee, Alabama 36088*

In free-spawning marine invertebrates, the amount of maternal energy that is invested in each egg has profound implications for all life-history stages of the offspring. The eggs of echinoids are freely spawned into the water and are surrounded by several structurally complex extracellular layers. These extracellular layers, or jelly coats, do not contribute energy to embryonic development but must impose an energy cost on the production of each egg. The investment of maternal energy reserves in the jelly coats of echinoid eggs may have important implications for the number of eggs that can be produced (i.e., *fecundity) and the amount of energy that can be invested in each egg. We estimated the degree to which maternal energy is invested in the jelly coats surrounding eggs of the echinoid* Arbacia punctulata. *Estimates were derived from measurements of the amount of energy contained in the combined eggs and jelly coats, and in the eggs alone. The amount of energy contained in* A. punctulata *eggs ranged from 2.70 to 5.53 ×* 10^{-4} *J* egg^{-1}*. The amount of energy contained in the jelly coats ranged from 0.13 to 0.48 ×* 10^{-4} *J jelly* $coat^{-1}$*. The mean concentration of energy in the eggs was 2.15* mm^{-3} *and 0.29 J* mm^{-3} *in the jelly coats. These results indicate that between 3% and 11% (mean = 7%) of the total energy invested in each* A. punctulata *egg is partitioned to the jelly coat alone. A significant positive relationship was found between the volumes of the jelly coats and the amount of energy they contained. Based on this relationship and an analysis of differences in the size of jelly coats between echinoid species, we suggest that the degree to which energy is invested in jelly coats may vary among echinoid species and is therefore likely to be an important life-history characteristic of these organisms.*

In free-spawning marine invertebrates, the egg contains all the maternal energy provisioned for the development of each offspring. The amount of maternal energy invested in individual eggs is central to many theories on the evolution of life-history patterns in marine invertebrates and is widely considered to have profound implications for all stages of marine invertebrate life cycles (1–5). The eggs of echinoids are freely spawned into the water column where fertilization and development take place. Several extracellular layers surround the eggs of echinoids. These extracellular layers (commonly, and from here on, referred to as "jelly coats") are structurally complex, consisting of several concentric layers of polysaccharide fiber networks embedded in a glycoprotein matrix (6, 7). The jelly coats surrounding the eggs of echinoids are thought to play important roles in fertilization processes (8–10) and may also protect eggs from physical forces that they are exposed to during and after spawning (11, 12). The jelly coats of some echinoid species disintegrate soon after contact with seawater (13) or following fertilization, and do not contribute energy to embryonic development.

Although the jelly coats surrounding the eggs of echinoids do not contribute energy to embryonic development, they must impose an energy cost on the production of each egg. Assuming that the amount of maternal energy available for reproduction is finite, the investment of energy in jelly coats may have important life-history implications. These potential implications include a reduction in the number of eggs that can be produced (*i.e.*, fecundity), a reduction in the amount of energy that can be invested in each egg, or both. Although previous studies have shown that there is substantial extra-embryonic investment in the gelatinous matrices of egg masses that are deposited on the benthos by some marine invertebrates (14, 15), the energy invested in jelly

Received 2 February 1999; accepted 18 April 2000.

[*] To whom correspondence should be addressed.

coats surrounding the eggs of a free-spawning species has not been considered specifically.

We estimated the amount of maternal energy that is invested in the jelly coats surrounding eggs of the echinoid *Arbacia punctulata*. These estimates were derived from wet oxidation (16, 17) measurements of the amount of energy contained in the combined eggs and jelly coats, and in the eggs alone. The wet oxidation method yields an estimate of the amount of organic carbon contained in a sample, which can be directly interpreted as a measure of the amount of energy that it contains. This method has been used in previous studies of maternal energy investment in marine invertebrate eggs (18–21), so our data can be directly compared with earlier results.

The amount of energy contained in the combined egg and jelly coat (mean ± SD = $3.97 \pm 0.79 \times 10^{-4}$ J egg^{-1}) was significantly higher (paired sample t test: $t = 8.33$, df = 9, $P < 0.0001$) than the amount of energy contained in the egg alone (mean ± SD = $3.69 \pm 0.57 \times 10^{-4}$ J egg^{-1}; Table 1). The average (±SD) amount of energy contained in the jelly coat was $0.28 \pm 0.10 \times 10^{-4}$ J jelly coat^{-1}, and constituted 7.4% of the total amount of energy contained in the combined egg and jelly coat (Table 1).

The concentrations of energy (mean joules per cubic millimeter) in the eggs and jelly coats were calculated from the amount of energy each contained (Table 1) and their respective volumes (Table 2). The concentration of energy in eggs was 2.15 J mm^{-3} (*i.e.*, $3.69 \times 10^{-4} \times 5847 = 2.15$ J mm^{-3}, where the combined volumes of 5847 eggs are equivalent to 1 mm^3). The concentration of energy in the jelly coats was 0.29 J mm^{-3} (*i.e.*, $0.28 \times 10^{-4} \times 10{,}416 = 0.29$ J mm^{-3}, where the combined volumes of 10,416 jelly coats are equivalent to 1 mm^3). The concentration of energy in the egg was 7.4 times greater than the concentration of energy in the jelly coats (*i.e.*, concentration of energy in the eggs [2.15 J mm^{-3}] divided by the concentration of energy in the jelly coat [0.29 J mm^{-3}] = 7.4).

Before exposure to seawater, the volume (mean ± SD) of the combined egg and jelly coat was $2.67 \pm 0.30 \times 10^{-4}$ mm^3, and the volume of the egg alone was $1.71 \pm 0.19 \times 10^{-4}$ mm^3 (Table 2). The volume of the jelly coat alone was $0.96 \pm 0.48 \times 10^{-4}$ mm^3 (Table 2); thus, the jelly coat constituted 36% of the volume of the combined egg and jelly coat prior to exposure to seawater (*i.e.*, $0.96/2.67 \times 100 = 35.9\%$). After exposure to seawater, the volume of the jelly coats increased substantially to $9.27 \pm 2.42 \times 10^{-4}$ mm^3 (Table 2) and constituted 84% of the combined volume of the egg and jelly coat.

Linear regression analyses on data contained in Tables 1 and 2 showed no significant relationship between the volumes of the jelly coats and the volumes of the eggs. Similarly, no significant relationship was found between the amount of energy contained in the jelly coats and the amount of energy contained in the eggs. A significant pos-

Table 1

The amount of energy contained (mean ± SD × 10^{-4} J, n = 10) in the combined egg and jelly coat, and in the egg and jelly coat alone for each female Arbacia punctulata; *the proportion of total energy in the combined egg and jelly coat that is partitioned to jelly coat is also given*

Female	Combined egg and jelly coat	Egg	Jelly coat	Energy partitioned to jelly coat (%)
1	4.06 (0.20)	3.93 (0.18)	0.13	3.3
2	3.50 (0.22)	3.15 (0.13)	0.35	10.0
3	5.53 (0.17)	5.32 (0.31)	0.21	3.8
4	4.45 (0.15)	4.12 (0.34)	0.32	7.2
5	4.77 (0.69)	4.29 (0.43)	0.48	10.1
6	3.86 (0.30)	3.59 (0.25)	0.26	6.7
7	3.42 (0.41)	3.05 (0.44)	0.37	10.8
8	2.70 (0.02)	2.47 (0.46)	0.23	8.5
9	3.46 (0.30)	3.11 (0.07)	0.34	9.8
10	4.04 (0.57)	3.89 (0.85)	0.14	3.5
Overall	3.97 (0.79)	3.69 (0.57)	0.28 (0.10)	7.4 (2.8)

Specimens of *Arbacia punctulata* were collected subtidally between July and August 1998 from marina walls at Panama City, Florida. Eggs were obtained from 10 of these specimens by intra-coelomic injection of 0.5–1 ml 0.5 *M* KCl. The amount of energy contained in the combined egg and jelly coat and in the egg alone was determined using a modification of the wet oxidation method given by Parsons *et al.* (16). Energy determinations were made from large samples of eggs that were estimated to yield at least 7.8 joules (J).

The jelly coats were removed from half of the eggs obtained from each female by pouring them through a 100-μm Nytex screen. Thus, samples of eggs with and without jelly coats were obtained from each female for analysis. The concentration of eggs in each sample was determined by replicate counts ($n = 7$–20) of 10-μl aliquots of well-suspended eggs from each sample. To ensure that the eggs were not damaged by the removal of the jelly coats, eggs were examined microscopically (400× magnification) for any signs of injury to the egg membrane or leakage of yolk from the egg. The viability of eggs from five females was assessed from fertilization assays in which samples of eggs with and without jelly coats were incubated in dilute sperm suspensions (dry sperm diluted by 10^{-4} in seawater). Embryos were allowed to divide to the four-cell stage before being recorded as viable. The proportion of eggs with jelly coats that were fertilized was compared to the proportion of eggs without jelly coats that were fertilized from each female (paired sample t test, $\alpha = 5\%$, on arcsine transformed proportions).

Three subsamples of eggs with jelly coats and without jelly coats were taken from samples of eggs from each female and placed in separate containers. The jelly coat material was eliminated from subsamples by removing the supernatant above the eggs and refilling the container with seawater that had been filtered through a 0.22-μm membrane. This process was repeated several times with all subsamples of eggs. To ensure that all of the jelly coat material had been removed from the subsamples, a vital stain (Janus green) was added to the final supernatant solutions, which were then examined microscopically.

The amount of energy contained in each egg (mean ± SD joules egg^{-1}) was calculated from the total amount of energy in each subsample and the number of eggs that each subsample contained. The concentrations of energy (joules per cubic millimeter) in the eggs and jelly coats were calculated from the amount of energy each contained (Table 1) and their respective volumes (Table 2). A paired sample t test ($\alpha = 5\%$) was used to determine whether there were differences in the amount of energy contained in the combined eggs with jelly coats compared to the amount of energy contained in the egg alone. Relationships between the volumes and the amounts of energy contained in eggs and jelly coats were examined using linear regression analyses. The significance of these relationships were tested by one-way ANOVA ($\alpha = 5\%$).

Table 2

Volumes (mean ± SD × 10^{-4} mm^3, n = 10) of the combined egg and jelly coat, and of the egg and jelly coat alone before and after contact with seawater, for Arbacia punctulata

	Before contact with seawater			After contact with seawater	
Female	Egg	Egg and jelly coat	Jelly coat	Egg and jelly coat	Jelly coat
1	1.43 (0.22)	3.32 (0.77)	1.89	10.61 (3.08)	9.18
2	2.14 (0.44)	3.49 (0.74)	1.35	11.78 (1.63)	9.64
3	1.73 (0.79)	2.61 (0.35)	0.84	7.45 (1.76)	5.75
4	1.16 (0.31)	2.78 (0.73)	1.62	9.69 (4.04)	8.53
5	1.67 (0.23)	2.56 (0.56)	0.89	15.23 (2.84)	13.56
6	1.73 (0.79)	2.42 (0.31)	0.69	12.77 (1.92)	11.04
7	1.73 (0.79)	2.40 (0.17)	0.67	11.65 (1.60)	9.92
8	1.74 (0.18)	2.29 (0.32)	0.55	12.22 (1.98)	10.42
9	1.70 (0.14)	2.22 (0.25)	0.52	11.15 (1.81)	9.45
10	1.99 (0.52)	2.56 (0.61)	0.57	7.20 (1.19)	5.21
Overall	1.71 (0.19)	2.67 (0.30)	0.96 (0.48)	11.02 (2.51)	9.27 (2.42)

The volumes of the combined eggs and jelly coats and of the eggs alone were calculated from their respective diameters (D) and the equation for the volume of a sphere ($4/3\pi[D/2]^3$). The volumes of the jelly coats were calculated by subtracting the volumes of the eggs alone from the volumes of the combined eggs and jelly coats. Before the eggs of *Arbacia punctulata* contact seawater (*i.e.*, prior to spawning), the jelly coats lie in close proximity to the eggs. After contact with seawater, the jelly coats hydrate and increase substantially in volume. The volumes of jelly coats before hydration were used in calculations of the amount of energy they contain. To determine the pre-hydration volume, the thickness of the coat was measured, using an ocular micrometer in a compound microscope (200× magnification), from the distance between adjacent eggs and added to the mean diameter of the eggs. The edges of jelly coats after exposure to seawater were visualized by adding india ink to the egg suspension, and diameters were measured in the manner described above.

itive relationship was apparent between the amount of energy contained in the jelly coats and their volumes ($r^2 = 0.482$, $F = 7.44$, $P = 0.025$). However, no significant relationship was found between the amount of energy contained in the eggs and the volumes of the eggs.

Microscopic examination of eggs from which the jelly coats had been removed did not reveal any damage to the integrity of the membrane surrounding the eggs. Eggs from which jelly coats had been removed were fertilized at the same rate as eggs with jelly coats at a standard sperm concentration. Thus we assume that the removal of the jelly coats did not result in any leakage of yolk from the eggs or any reduction in their viability.

Our results indicate that approximately 7% (range = 3%–11%) of the maternal energy invested in the combined eggs and egg jelly coats of *A. punctulata* is partitioned to the jelly coats alone (Table 1). The amount of energy contained in the eggs of the *A. punctulata* tested in this study was about half of that reported for this species in a previous study (18). Similarly, the concentration of energy in the eggs of the *A. punctulata* measured here is about half of the average concentration of energy contained in eggs of free-spawning marine invertebrates with planktotrophic larval development (22). Large differences in the amount of energy contained in eggs from different populations of marine invertebrate species have been reported previously (19, 20). Differences in the quality of the yolk content of eggs between populations of the echinoid *Arbacia lixula* have also been reported (23, 24). These population differences in the energy content of the egg and of the quality of the yolk may be the result of variation in the quality and quantity of food available to the adult (22) or of differences in the productivity of the waters in which larvae develop (25).

The degree to which maternal energy is partitioned to the jelly coats of *A. punctulata* eggs (mean = 7.4%) is small relative to the amount of extra-embryonic energy partitioned to the gelatinous matrices of benthic egg masses of some other marine invertebrates. Although these gelatinous matrices contain less energy per unit weight than the eggs they encompass, they constitute a large proportion of the total maternal energy investment in the mass. For example, in species of the prosobranch gastropod genus *Conus*, up to 50% of the maternal energy invested in egg masses is partitioned to the gelatinous matrix (14). Similarly, in species of opisthobranch gastropods, up to 58% of the total energy investment in egg masses is partitioned to the gelatinous matrix (15).

While the amount of energy invested in the jelly coats of *A. punctulata* eggs is small relative to that of the gelatinous matrices of benthic egg masses, it may nonetheless have important life-history implications. Although the jelly coats of echinoid eggs do not contribute energy to embryonic or larval development, they do impose energy costs on the production of each egg. Within the context of current life-history theory (1–5), the investment of energy in the production of jelly coats may influence the number of eggs

Table 3

Size indices of the jelly coats surrounding the eggs of six echinoid species

Echinoids	Source of data*	*n*	Diameter of egg (μm)	Diameter of combined egg and jelly coat (μm)	Relative size index (±SD)
Strongylocentrotus purpuratus	1	NA	80	120	1.50
Strongylocentrotus franciscanus	1	NA	130	196	1.51
Strongylocentrotus droebachiensis	2	50	160	260	1.61 (0.16)
Arbacia punctulata	3	100	69	126	1.83 (0.15)
Lytechinus variegatus	2	125	143	298	2.09 (0.27)
Dendraster excentricus	4	NA	125	205	1.64

The size indices are the ratio of the diameter of the combined egg and jelly coat (after contact with seawater) to the diameter of the egg alone. A larger index indicates larger jelly coat relative to the size of the egg. SD = standard deviation; NA = not available.

* 1—Lessios, 1990 (25); 2—Bolton and Thomas, unpubl. data; 3—this study; 4—Timko, 1979 (26).

produced, the degree to which energy is invested in individual eggs, or both. Assuming that the maternal energy available for reproduction is finite, and that the amount of energy in each egg is constant, the investment of energy in jelly coats may compromise the number of eggs that could be produced (*i.e.*, may reduce fecundity). This study indicates that approximately 7% of total energy investment in the combined egg and jelly coats is partitioned to the jelly coats alone. Accepting the assumptions given above, the investment of energy in jelly coats may reduce the potential fecundity of *A. punctulata* by about 7%. Alternatively, assuming that the amount of energy available for reproduction is constant, and that the number of eggs produced is also constant, the partitioning of energy to jelly coats may reduce the amount of energy that could be invested in each egg. If this is the case, the investment of energy in jelly coats may compromise offspring growth, survivorship, and reproductive output.

No significant relationships were apparent between the volumes of jelly coats and eggs or the amount of energy contained in jelly coats and eggs. This indicates that the amount of maternal energy invested in jelly coats is independent of the amount of energy invested in eggs. Similarly, no relationship was found between the amount of energy invested in eggs and the volume of the eggs. A significant relationship was apparent, however, between the amount of energy invested in jelly coats and the volume of jelly coats. This suggests that it may be possible to infer the relative degree to which maternal energy is invested in the egg jelly coats of different species from the volumes of these coats.

The proportion of maternal energy invested in jelly coats relative to that invested in eggs is likely to vary among echinoid species. For example, an index of relative size of the jelly coats surrounding eggs of a particular species can be obtained by taking the ratio of the diameter of the egg plus jelly coat to the diameter of the egg alone. Thus, the relative size of the jelly coats to the size of the egg can be compared among species independently of actual differences in egg size. When this index is calculated for the few echinoid species for which data are available (26, 27), differences are apparent (Table 3). Since the amount of energy contained in the jelly coats of *A. punctulata* is positively related to the volume of the jelly coats, it is possible that the proportion of energy invested in the jelly coat relative to that invested in the egg could be inferred from this index. If this is the case, ecologically important differences in the degree to which energy is invested in jelly coats may exist among echinoid species.

The jelly coats surrounding the eggs of echinoids are not unique: the eggs of many free-spawning marine invertebrates are surrounded by extracellular structures and exhibit enormous diversity in size, structure, and form (28–30). Therefore, the investment of energy in the extracellular structures surrounding their eggs may impose substantial reproductive costs on many of these species and should be considered in theories of their life-history evolution. Further measurements of the degree to which maternal energy is invested in the extracellular structures surrounding the eggs of free-spawning marine invertebrates are clearly needed.

Acknowledgments

This research was supported by NSF grants IBN-9723779 and OCE-9701434 awarded to Dr. Florence I. M. Thomas. We thank Julien Lartigue, Chris Cornelisen, Gregory DeLozier, Kristen Edwards, and two anonymous reviewers for helpful comments on this manuscript.

Literature Cited

1. **Vance, R. R. 1973a.** On reproductive strategies of marine invertebrates. *Am. Nat.* **107:** 339–352.
2. **Christiansen, F. B., and T. M. Fenchel. 1979.** Evolution of marine invertebrate reproductive patterns. *Theor. Popul. Biol.* **16:** 267–282.
3. **Strathmann, R. R. 1985.** Feeding and non-feeding larval development and life-history evolution in marine invertebrates. *Annu. Rev. Ecol. Syst.* **16:** 339–361.
4. **Havenhand, J. N. 1993.** Egg to juvenile period, generation time, and

the evolution of larval type in marine invertebrates. *Mar. Ecol. Prog. Ser.* **97:** 247–260.

5. **McEdward, L. R. 1997.** Reproductive strategies of marine benthic invertebrates revisited: facultative feeding by planktotrophic larvae. *Am. Nat.* **150:** 48–72.
6. **Bonnell, B. S., C. Larabell, and D. E. Chandler. 1993.** The sea urchin egg jelly coat is a three-dimensional fibrous network as seen by intermediate voltage electron microscopy and deep etching analysis. *Mol. Reprod. Dev.* **35:** 181–188.
7. **Bonnell, B. S., S. H. Keller, V. D. Vacquier, and D. E. Chandler. 1994.** The sea urchin jelly coat consists of globular glycoproteins bound to a fibrous fucan superstructure. *Dev. Biol.* **162:** 313–324.
8. **Vaquier, M., and G. W. Moy. 1977.** Isolation of binding: the protein responsible for the adhesion of sperm to sea urchin eggs. *Proc. Natl. Acad. Sci. USA* **74:** 2456–2460.
9. **Nomura, K., and S. Isaka. 1985.** Synthetic study of the structure-activity relationship of sperm activating peptides from the jelly coat of sea urchin eggs. *Biochem. Biophys. Res. Commun.* **126:** 974–982.
10. **Levitan, D. R. 1996.** Effects of gamete traits on fertilization in the sea and the evolution of sexual dimorphism. *Nature* **382:** 153–155.
11. **Thomas, F. I. M., K. A. Edwards, T. F. Bolton, M. A. Sewell, and J. A. Zande. 1999.** Mechanical resistance to shear stress: the role of echinoderm egg extracellular layers. *Biol. Bull.* **197:** 7–10.
12. **Thomas, F. I. M., and T. F. Bolton. 1999.** Shear stress experienced by echinoderm eggs in the oviduct during spawning: potential role in the evolution of egg properties. *J. Exp. Biol.* **202:** 3111–3119.
13. **Kidd, P. 1978.** The jelly and vitelline coats of the sea urchin egg: new ultrastructural features. *J. Ultrastruct. Res.* **64:** 204–215.
14. **Perron, F. E. 1981.** The partitioning of reproductive energy between ova and protective capsules in marine gastropods of the genus *Conus*. *Am. Nat.* **118:** 110–118.
15. **Lee, C. E., and R. R. Strathmann. 1998.** Scaling of gelatinous clutches: effects of siblings' competition for oxygen on clutch size and parental investment per offspring. *Am. Nat.* **151:** 293–310.
16. **Johnson, M. J. 1949.** A rapid micromethod for estimation of non-volatile organic matter. *J. Biol. Chem.* **181:** 707–711.
17. **Parsons, T. R., Y. Maita, and C. M. Lalli. 1984.** *A Manual of Chemical and Biological Methods for Sea Water Analysis.* Pergamon Press, New York. 173 pp.
18. **Strathmann, R. R., and K. Vedder. 1978.** Size and organic content of eggs of echinoderms and other invertebrates as related to developmental strategies and egg eating. *Mar. Biol.* **39:** 305–309.
19. **McEdward, L. R., and L. K. Coulter. 1987.** Egg volume and energetic content are not correlated among sibling offspring of starfish: implications for life-history theory. *Evolution* **41:** 914–917.
20. **McEdward, L. R., and F. Chia. 1991.** Size and energy content of eggs from echinoderms with pelagic lecithotrophic development. *J. Exp. Mar. Biol. Ecol.* **147:** 95–102.
21. **McEdward, L. R., and S. F. Carson. 1987.** Variation in egg organic content and its relationship with egg size in the starfish *Solaster stimpsoni*. *Mar. Ecol. Prog. Ser.* **37:** 159–169.
22. **Jaeckle, W. B. 1995.** Variation in the size, energy content, and biochemical composition of invertebrate eggs: correlates to the mode of larval development. Pp. 49–77 in *Ecology of Marine Invertebrate Larvae*, L. R. McEdward, ed. CRC Press, Boca Raton, FL.
23. **George, S. B. 1990.** Population and seasonal differences in egg quality of *Arbacia lixula* (Echinodermata: Echinoidea). *Invertebr. Reprod. Dev.* **17:** 111–121.
24. **George, S. B., C. Cellario, and L. Fenaux. 1990.** Population differences in egg quality of *Arbacia lixula* (Echinodermata: Echinoidea): proximate composition of eggs and larval development. *J. Exp. Mar. Biol. Ecol.* **141:** 107–118.
25. **Lessios, H. A. 1990.** Adaptation and phylogeny as determinants of egg size in echinoderms from two sides of the Isthmus of Panama. *Am. Nat.* **135:** 1–13.
26. **Timko, P. 1979.** Larviphagy and oophagy in benthic invertebrates: a demonstration for *Dendraster excentricus*. Pp. 91–98 in *Reproductive Ecology of Marine Invertebrates*, S. E. Stancyk, ed. University of South Carolina Press, Columbia, SC.
27. **Strathmann, M. F. 1987.** *Reproduction and Development of Marine Invertebrates of the Northern Pacific Coast.* University of Washington Press, Seattle.
28. **Berrill, N. J. 1975.** Chordata: Tunicata. Pp. 252–255 in *Reproduction of Marine Invertebrates.* Vol. II. A. L. Giese and J. S. Pearse, eds. Academic Press, New York.
29. **Pearse, J. S. 1975.** Polyplacophora. Pp. 39–43 in *Reproduction of Marine Invertebrates.* Vol. V. A. L. Giese and J. S. Pearse, eds. Academic Press, New York.
30. **Mozingo, N. M., V. D. Vaquier, and D. E. Chandler. 1995.** Structural features of the abalone egg extracellular matrix and its role in gamete interaction during fertilization. *Mol. Reprod. Dev.* **41:** 493–502.

Reference: *Biol. Bull.* **199**: 6–13. (August 2000)

Relationship of Dorsoventral Eyeshine Distributions to Habitat Depth and Animal Size in Mesopelagic Decapods

M. L. JOHNSON[1,*], P. M. J. SHELTON[1], E. GATEN[1,†], AND P. J. HERRING[2]

[1] *Department of Biology, University of Leicester, University Road, Leicester LE1 7RH, UK; and*
[2] *Southampton Oceanography Centre, Empress Dock, Southampton SO14 3ZH, UK*

Abstract. Eyeshine distribution patterns recorded from the eyes of 19 mesopelagic decapod species were examined and related to the depths at which the species are found. For most species examined, eyeshine was found to be brighter ventrally than dorsally. Deep-water decapod species that do not undergo diel vertical migrations had brighter dorsal eyeshine than migratory species. Eyeshine intensity increased with body size in five of the species examined and decreased in two. These changes in eyeshine intensity may be an adaptation to variations in depth distributions that occur with increasing body size. It is suggested that the depth and size-related changes reflect the importance of remaining camouflaged in the mesopelagic realm and are an example of ecologically functional development.

Introduction

Many species active at low light levels possess a well-developed reflective tapetum behind the retina that effectively doubles the path length of light through the photoreceptor cells (Lythgoe, 1979). This doubling increases the photon-capturing efficiency of the eye without requiring an increase in eye size (Land, 1981). In most arthropod species that have superposition compound eyes, light reflected by the tapetum and not absorbed by the rhabdoms is visible as eyeshine (Kunze, 1979). Eyeshine consists of a circular patch of light that fills about half of the eye and represents the effective aperture (Land, 1981). Since approximately 80%–90% of the blue-green light entering the eye is absorbed by the rhabdoms (Johnson, 1998), eyeshine is orange-red when the eye is illuminated with white light.

The ecology of the mesopelagic realm is dominated by the vertical distribution of its inhabitants (Herring and Roe, 1988). Few expeditions have comprehensively studied the way in which species are distributed in the water column in a particular area over any significant length of time. As a result, we have little knowledge of how ecological factors affect vertical distributions and daily vertical migrations. In addition, the picture is complicated by community variation and differences in migratory behavior that may be associated with factors such as the intensity and angular distribution of light, hydrography, season, reproduction, ontogeny, feeding, interspecific interactions, and capture methods (Foxton, 1970; Jerlov, 1974; Longhurst, 1976; Marshall, 1979; Roe, 1984; Domanski, 1985; Herring and Roe, 1988; Gonzalez *et al.*, 1997). Our knowledge of mesopelagic ecology is derived for the most part from spot samples taken at various unrelated locations, seasons, and times of day. These samples have demonstrated that, although there are clear underlying patterns of diurnal behavior (Foxton, 1970), the preferred depths for all species are highly variable.

For many deep-sea species, shielding and reflecting pigments in the eye probably do not move in response to changes in light intensity (Nilsson, 1982; Shelton *et al.*, 1986). In addition, previous studies have suggested that, as with some nocturnal insects (Laughlin and Weckström, 1993), deep-water decapods may lack the physiological gain-control mechanisms necessary for light adaptation (Nilsson and Lindström, 1983; Johnson *et al.*, 2000). Mesopelagic species are thus limited by the range of light intensities in which their eyes can function, and they must migrate to avoid downwelling light intensities that exceed

Received 18 February 2000; accepted 12 June 2000.

* Present address: Biology Department, University of Hull, (Scarborough Campus), Filey Road, Scarborough, YO11 3ZZ, UK

† To whom correspondence should be addressed. E-mail: gat@le.ac.uk

their physiological limits. Therefore, given the structured way in which light varies with depth (Kirk, 1983) and the fact that the dynamic range of the eyes dictates to some degree the depths inhabited, the eyes of mesopelagic decapods should show physiological and anatomical associations with their preferred depth.

Here we suggest that, with respect to sensitivity, the ideal eye would have a complete tapetum equally reflective in all regions. Such an eye would have uniform sensitivity in all regions. However, in an earlier study of selected mesopelagic shrimps, it was found that tapeta are often incomplete or have regional variations in their reflectivity (Shelton *et al.*, 1992). This is in spite of the fact that such animals live in a dim environment where bioluminescence plays a major role in inter- and intra-specific communication (Burkenroad, 1943; Herring, 1990; Morin and Cohen, 1991) and where maximizing sensitivity must be of considerable importance. It was concluded that any reduction in reflectivity must be an adaptation to reduce visibility to predators. It was shown that in many species there is a decreasing gradient of eyeshine intensity along the anteroposterior axis of the eye. In other cases there is a large hole in the tapetum. The anteroposterior gradient seems to be associated with reducing the visibility of the shrimp to predators during the escape response. At such times, the eye swings forward so that the least reflective part of the eye is exposed to the predator (Shelton *et al.*, 2000).

We set out to investigate the features of eyeshine in mesopelagic decapods and to suggest how the variations found may be related to their life history and depth distribution. The current paper investigates differences in reflectivity along the dorsoventral axis of a range of mesopelagic shrimps. It was found that, as with the anteroposterior axis, there are considerable differences in reflectivity between dorsal and ventral regions. We conclude that the design of the eye in mesopelagic species is constrained by competing factors—the need to see and the need to avoid being seen.

Materials and Methods

Shrimps were taken from depths of between 0 and 2250 m during RRS *Discovery* cruise 204 (1995) in the eastern Atlantic north of the Cape Verde Islands (25° W, 20° N). The use of an RMT 1 + 8 net system allowed sampling at discrete depths, and a closing cod-end maintained animals in good condition while they were brought to the surface (Roe and Shale, 1979; Wild *et al.*, 1985). Light-induced damage of the eye was prevented, and the general condition of the animals was maintained by sorting and storing them in dim red light and placing them in refrigerated aquaria until required. All were utilized within 2 h of capture.

Mesopelagic species can be split broadly into two groups: those that undergo diel vertical migrations and those that live in deep water and do not migrate (Fig. 1). Species such as *Sergestes corniculum, Oplophorus spinosus, Parapandalus richardi,* and *Systellaspis debilis* are generally found above 1000 m and migrate close to the surface at night (Hiller-Adams and Case, 1988; Cartes *et al.*, 1994; Institute of Oceanographic Sciences (IOS) Database). Other species such as *Acanthephyra pelagica, Gennadas valens,* and *Sergia robustus* undergo diel vertical migrations of less magnitude and are rarely caught above 300 m (Domanski, 1985; Hiller-Adams and Case, 1988; IOS Database). *Systellaspis cristata, Acanthephyra gracilipes,* and *Bentheogennema intermedia* are examples of virtually nonmigratory species that are generally found between 700 and 1000 m (Domanski, 1985; IOS Database).

Eyeshine distribution and intensity was examined using a variation of the protocol developed by Shelton *et al.* (1992). Shrimps were mounted on a rotatable rod projecting into a polythene chamber filled with chilled seawater. The chamber was sealed with a glass coverslip to prevent distortion of the image by water surface movement. Measurements were carried out only on animals that had eyestalks in the laterally extended position, as they are during normal forward swimming. The preparation was examined through a Zeiss binocular microscope with a video camera attachment, and illumination was provided by a Schott KL 1500 halogen light source. The microscope was focused and the specimen was manipulated under dim red light. To record eyeshine intensity, preparations were axially illuminated with green (520 nm broadband filter; Wratten No. 59) light *via* a small mirror oriented at about 45° to the light beam just outside the field of view. Eyeshine was recorded using a JVC TK-1085E color video camera (with the automatic gain control switched off) and a Panasonic VHS video recorder. The preparation was rotated around the longitudinal axis by 20° increments from the dorsal to ventral points. For comparison, and to more easily assess any physical damage, the eye was then observed using white light (no filter). Video images were analyzed on a Kontron image analysis system. Average brightness across the eyeshine patch was measured in gray-scale units (1-255 GSU) and the patch diameter measured. Depth distributions were taken from the most appropriate literature or the IOS database. Where the information was available, the mean depth and the 95% confidence interval for range were used. If only range was available, then the midpoint was taken.

Results

Eyeshine distribution patterns were observed and recorded from 136 eyes from 19 species (Table 1).

Eyeshine patch diameter

There were noticeable differences in the diameter of the eyeshine patches under the two different colors of light

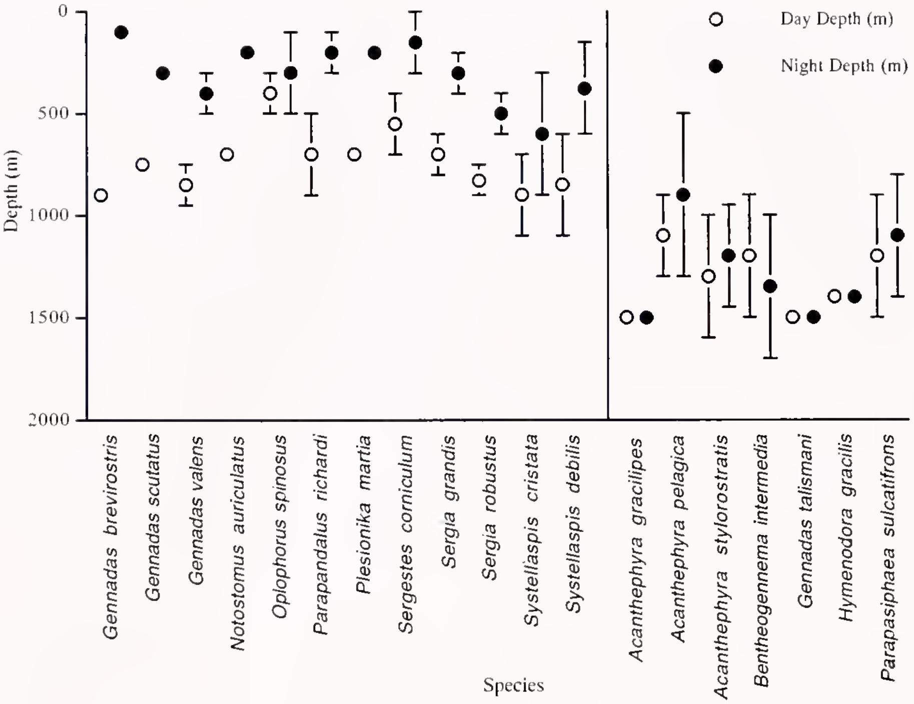

Figure 1. Estimated depth distributions for the 19 species of mesopelagic decapods examined. Data points indicate the mean or midpoint of the range which, when data are available, is indicated by the error bars. The species are separated into two depth classifications depending on their depth distribution and migratory behavior. Those that are commonly found to occur above 1000 m are classed as migratory. Depth data are from the following sources: Hiller-Adams and Case (1988)—*Gennadas valens, Oplophorus spinosus, Parapasiphaea sulcatifrons, Sergia grandis, S. robustus, Systellaspis cristata, S. debilis;* Cartes *et al.* (1994)—*Plesionika martia;* Crosnier and Forest (1973)—*Notostomus auriculatus, Sergestes corniculum;* Heffernan and Hopkins (1981)—*Gennadas brevirostris, G. scutatus, G. talismani;* Domanski (1985)—*Acanthephyra pelagica, A. stylorostratis, Bentheogennema intermedia, Parapandalus richardi;* Institute of Oceanographic Science database—*Acanthephyra gracilipes, Hymenodora gracilis.*

used. Generally the eyeshine patch diameter appeared smaller under green light and larger under white light. Often when illuminated with white light, the exact edge of the eyeshine patch was not clear since a band of eyeshine of a different character (color and intensity) would surround the main patch. To allow eyeshine patch diameters resulting from green and white light to be compared, the relative eyeshine patch diameter (eyeshine patch diameter/eye diameter) was calculated. This allowed a better comparison of animals of different sizes. The results of a two-tailed t test of the data from all the species examined suggested that there was a significant difference resulting from illumination by green or white light ($t = 10.85$, $P > 0.001$, $n = 128$). The relative eyeshine patch diameter resulting from green incident light (0.33 ± 0.09 mm) was 27.5% smaller than that resulting from white light (0.46 ± 0.10 mm).

Because there was a significant difference in the diameter of the eyeshine patch under white and green light, this study used only the measurements of diameter and intensity made under green illumination, which more closely resembles the light that mesopelagic species would experience normally (Kirk, 1983).

Eyeshine distribution along the dorsoventral axis

For the 19 species examined, the general trend is for eyeshine to be brightest ventrally (Table 1). The degree to which eyeshine intensity varies around the eye differs between species. In nonmigratory and deeper-living species, such as *Acanthephyra pelagica* and *Acanthephyra stylorostratis*, eyeshine is usually of similar intensity dorsally and ventrally (Fig. 2a). Migratory species that come close to the surface during the night, such as *Parapandalus richardi, Plesionika martia* (Fig. 2b), *Oplophorus spinosus*, and *Systellaspis debilis* (Fig. 2 c, d), have eyeshine that is brighter ventrally than dorsally. In *Sergestes corniculum*, because it hangs vertically during normal swimming, the eyeshine pattern is offset by 90° so that the more reflective posterior region of the eye is directed downwards (Shelton *et al.*, 1992).

Table 1

*Dorsal (in **bold** text) and ventral eyeshine intensities with standard errors*

Species	C	*n*	Eyeshine intensity by size class (carapace length, mm)			
			0–5	5–10	11–15	16+
Acanthephyra gracilipes	N	2		**84.0 ± 5.5** 85.8 ± 7.3		
Acanthephyra pelagica	M	8	**50.4** 78.5		**68.7 ± 17.5** 88.7 ± 9.8	**104.5 ± 7.8** 98.3 ± 6.5
Acanthephyra stylorostratis	N	2				**78.1 ± 4.6** 70.53 ± 2.3
Bentheogennema intermedia	N	2			**56.0 ± 3.3** 78.4 ± 14.6	
Gennadas brevirostris	M	5		**42.8 ± 11.3** 110.7 ± 18.4		
Gennadas scutatus	M	3		**32.9 ± 4.1** 54.2 ± 22.3		
Gennadas talismani	N	3		**79.6 ± 9.7** 95.5 ± 36.6		
Gennadas valens	M	3		**45.1 ± 11.4** 96.1 ± 15.3		
Hymenodora gracilis	N	2			**63.7 ± 4.4** 72.8 ± 11.4	
Notostomus auriculatus	M	4		**34.2 ± 1.6** 37.2 ± 6.8	**25.2 ± 3.2** 42.1 ± 6.9	
Oplophorus spinosus	M	16	**30.7 ± 0.2** 48.1 ± 10.1	**31.2 ± 0.7** 56.1 ± 3.3	**35.8 ± 1.4** 48.5 ± 5.7	**48.9 ± 9.6** 48.7 ± 24.0
Parapandalus richardi	M	2		**27.9 ± 0.9** 45.3 ± 15.7		
Parapasiphaea sulcatifrons	N	2		**75.8 ± 3.5** 42.1 ± 0.4		
Plesionika martia	M	4			**31.9** 46.7	**31.1 ± 1.1** 82.4 ± 22.1
*Sergestes corniculum**	M	7		**33.8 ± 0.8** 45.7 ± 8.4	**39.6 ± 18.0** 48.6 ± 5.7	**30.8 ± 2.5** 69.9 ± 19.1
Sergia grandis	M	7		**32.2 ± 0.8** 33.5 ± 0.8	**33.1** 48.7	**51.3 ± 3.2** 94.8 ± 9.1
Sergia robustus	M	4		**31.4 ± 0.2** 35.5 ± 0.5		**40.8** 46.8
Systellaspis cristata	M	3		**43.6** 82.3	**64.3** 81.2	**67.3** 74.8
Systellaspis debilis	M	12	**33.6 ± 2.2** 46.0 ± 4.6	**30.8 ± 2.7** 41.2 ± 6.0	**28.7 ± 1.6** 34.8 ± 1.3	

Species have been classified (C) as nonmigratory (N) and migratory (M) according to the depth and distance of their daily vertical migration cycle (Fig. 1). Eyeshine intensity is measured in gray-scale units (GSU).

* For *Sergestes corniculum*, anterior and posterior eyeshine intensities were used in place of dorsal and ventral (see text).

Animal size, eyeshine intensity, and distribution

Good size ranges (>5 mm range) were obtained for nine species. For five species (*Acanthephyra pelagica, Oplophorus spinosus, Sergia grandis, Sergia robustus,* and *Systellaspis cristata*) both dorsal and ventral eyeshine increased with carapace length (Table 1). For two species (*Plesionika martia* and *Sergestes corniculum*) there was no clear trend with regard to dorsal eyeshine, but ventral eyeshine was greater in larger specimens. In *Notostomus auriculatus* and *Systellaspis debilis,* both dorsal and ventral eyeshine intensity decreased with increasing carapace length. A typical example of eyeshine distribution in large and small specimens is shown by *O. spinosus* (Fig. 2c). *S. debilis* is unusual in that eyeshine intensity is markedly greater in small specimens than large (Fig. 2d). For four species where size ranges and numbers captured permitted, dorsal eyeshine was plotted against carapace length (Fig. 2 e, f). The two

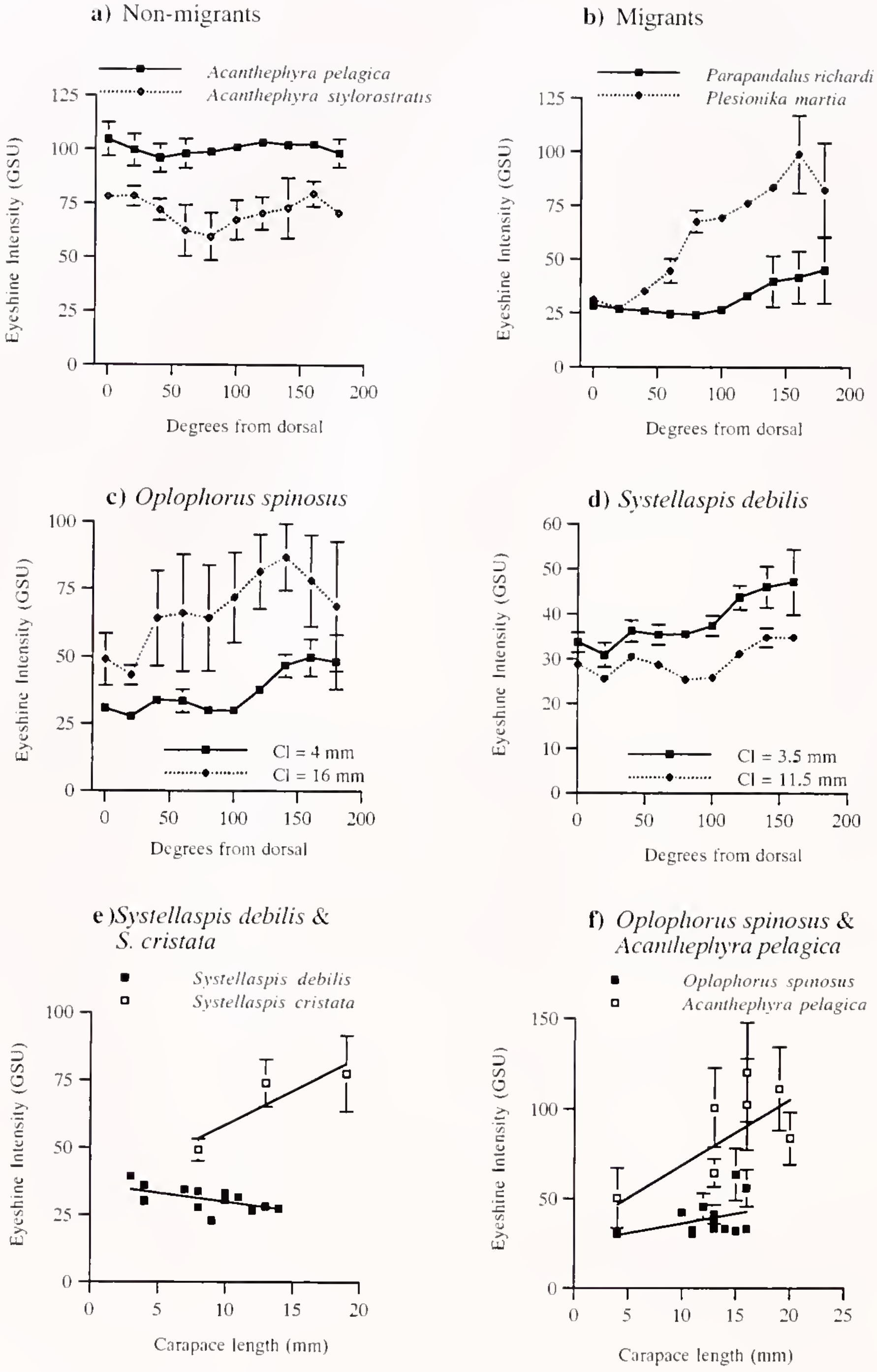

Figure 2. Size- and depth-related variations in eyeshine distributions. (a, b) Dorsoventral eyeshine intensity distributions for four species of decapod. In the two migratory species *Parapandalus richardi* and *Plesionika martia*, eyeshine intensity is markedly brighter ventrally than dorsally. In the deep migratory (*Acanthephyra pelagica*) and nonmigratory (*A. stylorostratis*) species, eyeshine does not vary significantly from dorsal to ventral (c, d) Dorsoventral eyeshine distributions for two species of migratory decapod showing how eyeshine intensity differs between large and small specimens. In *Oplophorus spinosus*, eyeshine is brightest in large specimens. In *Systellaspis debilis*, eyeshine is brightest in smaller specimens. (e, f) Changes in dorsal eyeshine intensity with increasing carapace length for four species of mesopelagic decapod. For two species (*Systellaspis cristata* and *Oplophorus spinosus*), positive and significant correlations were found ($n = 3$, $r = 0.896$, $P < 0.05$ and $n = 16$, $r = 0.459$, $P < 0.10$ respectively). Although a positive trend is also found for *Acanthephyra pelagica* ($n = 8$, $r = 0.614$), it is not significant. In the case of *Systellaspis debilis*, dorsal eyeshine intensity decreases with increasing carapace length ($n = 15$, $r = 0.560$, $P < 0.05$).

deep-water species (*Acanthephyra pelagica* and *Systellaspis cristata*) showed a significant increase in dorsal eyeshine intensity with increasing carapace length. In *Oplophorus spinosus*, the increase in dorsal eyeshine intensity was less pronounced, and in *Systellaspis debilis*, as is also demonstrated by Figure 2b, eyeshine actually decreased with increasing carapace length.

Depth distribution and eyeshine intensity

In the present study it was found that for the largest size classes of each of the 19 species examined (Table 1), there were significant correlations between $\log_{10}$ depth and $\log_{10}$ dorsal eyeshine intensity (Fig. 3 a, b). In the case of the relationship between eyeshine intensity and daytime depth, the correlation was markedly improved when *Oplophorus spinosus* was excluded from the analysis. This species has much higher dorsal eyeshine intensity for its daytime depth distribution than would normally be expected. It is possible that this anomaly is related to the unusually small amplitude of its vertical migration pattern (Foxton, 1970), which suggests that this species may be able to light adapt (thereby reducing eyeshine) to some degree. Ventral eyeshine appears to vary independently of depth (Fig. 3 c, d). Analysis of variance showed that migratory species have significantly lower ($F = 3.12$, $P = 0.095$) $\log_{10}$ dorsal eyeshine intensity (1.69 ± 0.21, $n = 13$) than nonmigrants (1.85 ± 0.15, $n = 6$). A comparison of ventral eyeshine between the two groups showed that there was no significant difference ($F = 2.29$, $P = 0.15$) between migratory (1.81 ± 0.14) and nonmigratory species (1.92 ± 0.15).

Discussion

Eyeshine intensity varies as a result of the efficiency and quantity of reflecting and absorbing pigments within the eye (Gaten *et al.*, unpubl.). Our examination of mesopelagic decapods has demonstrated that the distribution patterns of their dorsoventral eyeshine intensity vary with the species' estimated habitat depths. With increasing habitat depth,

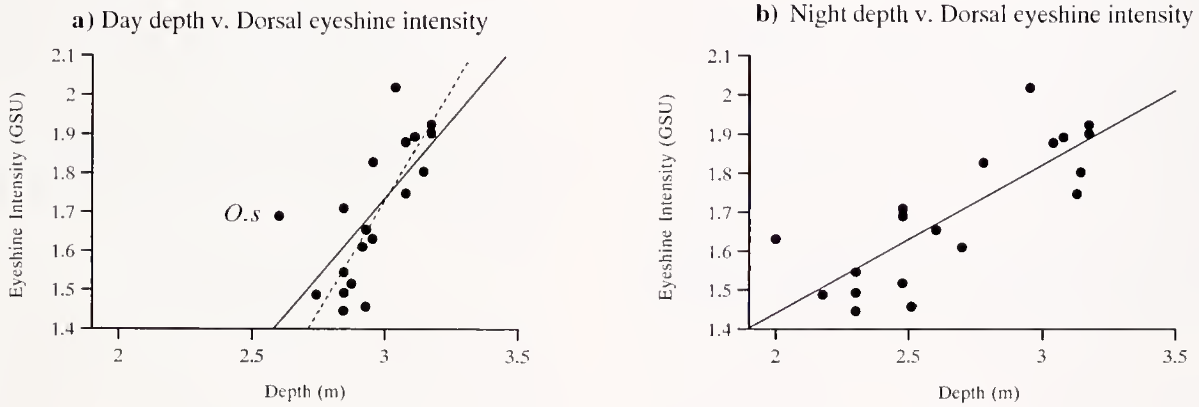
a) Day depth v. Dorsal eyeshine intensity

b) Night depth v. Dorsal eyeshine intensity

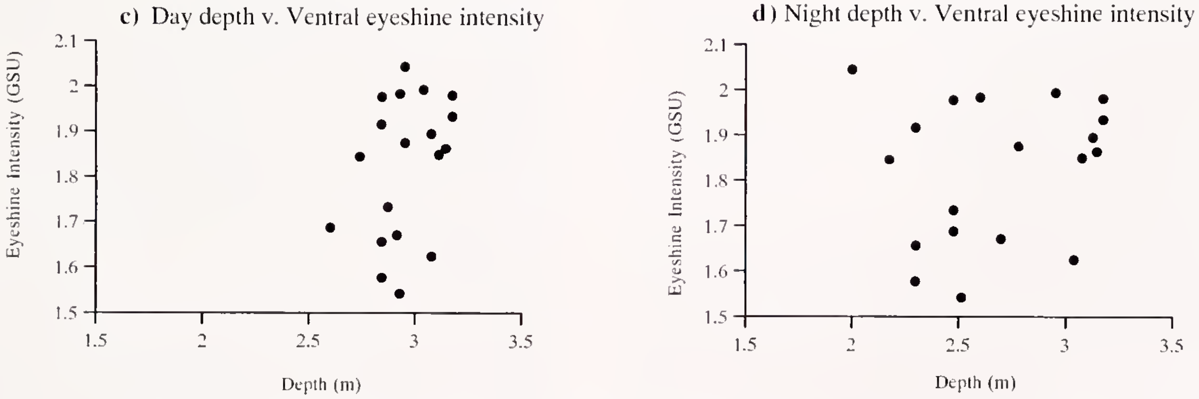
c) Day depth v. Ventral eyeshine intensity

d) Night depth v. Ventral eyeshine intensity

Figure 3. Eyeshine intensity in relation to depth distributions for adult mesopelagic species ($n = 19$) with least-squares lines fitted. Significant positive correlations were found for dorsal eyeshine intensity and day depth [(a) $r = 0.68$, $P < 0.001$] and night depth [(b) $r = 0.81$, $P < 0.001$]. When *Oplophorus spinosus* (*O.s* in Fig. 3a)—which exhibits higher dorsal eyeshine intensity than expected for its estimated daytime depth distribution—is excluded, $r = 0.82$. Ventral eyeshine intensity was poorly correlated with both day [(c) $r = 0.34$, n.s.] and night [(d) $r = 0.17$, n.s.] depths.

dorsal eyeshine was brighter, and the difference in intensity between dorsal and ventral regions of the eye decreased. In all species examined except *Systellaspis debilis* and *Notostomus auriculatus*, eyeshine intensity in at least one region of the eye increased with carapace length. Ventral eyeshine showed no significant depth-related trend. The variation in eyeshine distribution suggests that dorsal eyeshine intensity is related to the degree to which each shrimp species is exposed to downwelling light. This is supported by theoretical evidence which suggests that for any given eye, there are ideal distributions of reflecting and shielding pigments that optimize both sensitivity and resolution (Warrant and McIntyre, 1991). For most superposition compound eyes, the tapetum should, ideally, be formed of reflecting pigment enclosing the proximal third of each rhabdom. This has the effect of doubling the path length of light (by reflecting unabsorbed photons back through the target rhabdom) and restricting the bleed of light between adjacent rhabdoms. Despite the prevailing low levels of ambient light normally experienced by mesopelagic species, the distributions of these pigments generally deviate from the theoretical ideal (for maximum sensitivity) in the dorsal part of the eye (Gaten *et al.*, 1992; Johnson, 1998). This suggests that there is a requirement to remain camouflaged that outweighs the need for highly sensitive vision dorsally.

Generally we have found that with increasing carapace length, eyeshine intensity increases, and that the increase is more pronounced dorsally than ventrally. If the supposition that dorsal eyeshine intensity is determined by habitat depth is true, then it follows that where eyeshine increases with carapace length, juvenile mesopelagic decapods should be found closer to the surface than adults. Size-related differences in vertical distribution have been observed for some mesopelagic decapods, euphausiids, and copepods (Foxton, 1970; Baker, 1970; Hays, 1996). The study of the ontogeny of eye anatomy of mesopelagic decapods has shown that juveniles often have apposition eyes, that superposition optics develop with age, and that the ventral portion develops first (Gaten and Herring, 1995). Our description of the way in which eyeshine distribution patterns develop with size agrees with this finding.

The current results are consistent with the view that gradients of reflectivity along the dorsoventral axis and dorsal holes in the tapetum reduce the visibility of the eye to predators (Shelton *et al.*, 1992, 2000). The gradients are necessary because of the characteristic distribution of irradiance in the ocean. Here the brightness of upwelling light is two orders of magnitude lower than that of the downwelling light, and the light field is symmetrical about the vertical axis (Kirk, 1983). Low reflectivity in upwardly looking parts of the eye reduces the contrast between the light reflected from the tapetum and that arising from the dim background. In downwardly looking parts of the eye, a highly reflective ventral tapetum is unlikely to increase visibility, because the levels of upwelling light are low.

The variations in eyeshine distribution shown here are an example of how the development of sense organs can be linked, in a functional manner, to variations in depth distribution. Small decapods can only have small eyes and are limited in the degree to which they can vertically migrate by the inverse relationship between body size and energy requirements for swimming (Longhurst, 1976). A small apposition eye is sufficient in the relatively well-lit upper regions of the pelagic realm, where juvenile and adolescent pelagic decapods and euphausiids are to be found (Baker, 1970; Foxton, 1970; Marshall, 1979), but as shrimps increase in size and daily movement to the ecological refuge provided by depth (King and Butler, 1985) becomes a viable strategy, their eyes develop to suit a more oligophotic environment.

Acknowledgments

We gratefully acknowledge the assistance given by the officers and crew of RRS *Discovery* and Tony Rice of Southampton Oceanography Centre for allowing MLJ to participate in cruise 204. Many thanks also to Jeremy Brooks for technical assistance with eyeshine measurements and to Matt Sheehy for his comments on the manuscript. MLJ was supported by NERC grant GT4/92/5/A. PMJS and PJH acknowledge support of NERC grants GR9/0019A and GR3/11212.

Literature Cited

Baker, A. de C. 1970. The vertical distribution of euphausiids near Fuerteventura, Canary Islands ('Discovery' SOND Cruise, 1965). *J. Mar. Biol. Assoc. UK* **50:** 301–342.

Burkenroad, M. D. 1943. A possible function of bioluminescence. *J. Mar. Res.* **5:** 161–164.

Cartes, J. E., J. C. Sorbe, and F. Sardà. 1994. Spatial distribution of deep-sea decapods and euphausiids near the bottom in the northwestern Mediterranean. *J. Exp. Mar. Biol. Ecol.* **179:** 131–144.

Crosnier, A., and J. Forest. 1973. *Les Crevettes Profondes de L'Atlantique Oriental Tropical*, Volume XIX. ORSTOM, Paris.

Domanski, P. A. 1985. The Azores front: a zoogeographic boundary? *UNESCO Tech. Pap. Mar. Sci. No.* **49:** 73–83.

Foxton, P. 1970. The vertical distribution of pelagic decapods (Crustacea: Natantia) collected on the Sond Cruise 1965. *J. Mar. Biol. Assoc. UK* **50:** 939–960.

Gaten, E., and P. J. Herring. 1995. Morphology of the reflecting superposition eyes of larval oplophorid shrimps. *J. Morphol.* **225:** 19–29.

Gaten, E., P. M. J. Shelton, and P. J. Herring. 1992. Regional morphological variations in the compound eyes of certain mesopelagic shrimps in relation to their habitat. *J. Mar. Biol. Assoc. UK* **72:** 61–75.

González, J. A., M. V. Tuset, I. J. Lozano, and J. I. Santana. 1997. Biology of *Plesionika narval* (Crustacea, Decapoda, Pandalidae) around the Canary Islands (Eastern Central Atlantic). *Est. Coast Shelf Sci.* **44:** 339–350.

Hays, G. C. 1996. Large-scale patterns of diel vertical migration in the North Atlantic. *Deep-Sea Res.* **43:** 1601–1615.

Heffernan, J. J., and T. L. Hopkins. 1981. Vertical distribution and feeding of the shrimp genera *Gennadas* and *Bentheogennema* (Decapoda: Penaeidea) in the eastern Gulf of Mexico. *J. Crustac. Biol.* **1:** 461–473.

Herring, P. J. 1990. Bioluminescent communication in the sea. Pp. 245–278 in *Light and Life in the Sea*, P. J. Herring, A. K. Campbell, M. Whitfield, and L. Maddock, eds. Cambridge University Press, Cambridge.

Herring, P. J., and H. S. J. Roe. 1988. The photoecology of pelagic oceanic decapods. *Symp. Zool. Soc. Lond.* **59:** 263–290.

Hiller-Adams, P., and J. F. Case. 1988. Eye size of pelagic crustaceans as a function of habitat depth and possession of photophores. *Vision. Res.* **28:** 667–680.

Jerlov, N. G. 1974. Significant relationships between optical properties of the sea. Pp. 77–94 in *Optical Aspects of Oceanography*, N. G. Jerlov, ed. Academic Press, London.

Johnson, M. L. 1998. Aspects of visual function and adaptation of deep-sea decapods. Ph.D. Thesis, University of Leicester, Leicester, England. 262 pp.

Johnson, M. L., P. M. J. Shelton, and E. Gaten. 2000. Temporal responses in the eyes of marine decapods from coastal and deep sea habitats. *Mar. Biol.* **136:** 243–248.

King, M. G., and A. J. Butler. 1985. Relationship of life history patterns to depth in deep-water caridean shrimps (Crustacea: Natantia). *Mar. Biol.* **86:** 129–138.

Kirk, J. T. O. 1983. *Light and Photosynthesis in Aquatic Ecosystems.* Cambridge University Press, Cambridge.

Kunze, P. 1979. Apposition and superposition eyes. Pp. 441–502 in *Handbook of Sensory Physiology*, H. Autrum, ed. Springer-Verlag, Berlin.

Land, M. F. 1981. Optics and vision in invertebrates. Pp. 471–492 in *Handbook of Sensory Physiology*, H. Autrum, ed. Springer-Verlag, Berlin.

Laughlin, S. B., and M. Weckström. 1993. Fast and slow photoreceptors—a comparative study of the functional diversity of coding and conductances in the Diptera. *J. Comp. Physiol. A* **172:** 593–609.

Longhurst, A. R. 1976. Vertical migration. Pp. 116–137 in *The Ecology of the Seas*, D. H. Cushing and J. J. Walsh, eds. Blackwell Scientific, Oxford.

Lythgoe, J. N. 1979. *The Ecology of Vision.* Oxford University Press, Oxford.

Marshall, N. B. 1979. *Developments in Deep-Sea Biology* (Blandford Press, Poole, England.

Morin, J. G., and A. C. Cohen. 1991. Bioluminescent displays, courtship and reproduction in ostracodes. Pp. 1–16 in *Crustacean Sexual Biology*, T. B. J. Martin, ed. Columbia University Press, New York.

Nilsson, H. L. 1982. Rhabdom breakdown in the eye of *Cirolana borealis* (Crustacea) caused by exposure to daylight. *Cell Tissue Res.* **227:** 633–639.

Nilsson, H. L., and M. Lindström. 1983. Retinal damage and sensitivity loss of a light-sensitive crustacean compound eye (*Cirolana borealis*). *J. Exp. Biol.* **107:** 277–292.

Roe, H. S. J. 1984. The diel migrations and distributions within a mesopelagic community in the north east Atlantic. 2. Vertical migrations and feeding of mysids and decapod crustacea. *Prog. Oceanogr.* **13:** 269–318.

Roe, H. S. J., and D. M. Shale. 1979. A new multiple rectangular mid-water trawl (RMT 1 + 8 M) and some modifications to the Institute of Oceanographic Sciences' RMT 1 + 8. *Mar. Biol.* **50:** 283–288.

Shelton, P. M. J., E. Gaten, and C. J. Chapman. 1986. Accessory pigment distribution and migration in the compound eye of *Nephrops norvegicus* (L.) (Crustacea: Decapoda). *J. Exp. Mar. Biol. Ecol.* **98:** 185–198.

Shelton, P. M. J., E. Gaten, and P. J. Herring. 1992. Adaptations of tapeta in the eyes of mesopelagic shrimps to match the oceanic irradiance distribution. *J. Mar. Biol. Assoc. UK* **72:** 77–88.

Shelton, P. M. J., E. Gaten, M. L. Johnson, and P. J. Herring. 2000. The 'eye-blink' response of mesopelagic Natantia; eyeshine patterns and the escape reaction. *Crustacean Issues* **12:** 253–260.

Warrant, E. J., and P. D. McIntyre. 1991. Strategies for retinal design in arthropod eyes of low F-number. *J. Comp. Physiol. A* **168:** 499–512.

Wild, R. A., E. Darlington, and P. J. Herring. 1985. An acoustically controlled cod-end system for the recovery of deep-sea animals at *in situ* temperatures. *Deep-Sea Res.* **32:** 1583–1589.

Reference: *Biol. Bull.* **199:** 14–20. (August 2000)

Kidney Function and Sulfate Uptake and Loss in the Freshwater Bivalve *Toxolasma texasensis*

T. H. DIETZ[1,*], A. S. UDOETOK[1], J. S. CHERRY[1], H. SILVERMAN[1], AND R. A. BYRNE[2]

[1]*Department of Biological Sciences, Louisiana State University, Baton Rouge, Louisiana 70803; and*
[2]*Department of Biology, State University of New York College at Fredonia, Fredonia, New York 14063*

Abstract. *Toxolasma texasensis* acclimated to an artificial pondwater (PW) maintained a concentration of SO_4 in the blood of about 1–2 mmol l^{-1}. The anion transport inhibitor DIDS (5, 5′-diisothiocyanatostilbene 2, 2′-disulfonic acid) reduced the uptake of $^{35}SO_4$ from the bathing medium by 54%. The clearance of polyethylene glycol (PEG) injected into the blood of *T. texasensis* ranged between 0.8 and 1.3 ml g^{-1} dry tissue h^{-1}, and provided an estimate of renal filtration in PW-acclimated animals. The clearance of radioactive $^{35}SO_4$ simultaneously injected into the same animal was about 16% of the PEG clearance, suggesting that sulfate was being reabsorbed by the kidney. Para-aminohippuric acid was cleared about 4.6 times faster than PEG, indicating that this organic acid was subjected to secretion in addition to filtration. When the normal osmotic gradient was abolished by acclimating *T. texasensis* to 10% seawater (SW), the PEG clearance decreased to 0.17 ml g^{-1} dry tissue h^{-1}. Sulfate clearance in animals acclimated to PW or 10% SW was the same. However, in mussels acclimated to 10% SW, the calculated amount of SO_4 reabsorbed was significantly reduced relative to mussels acclimated to PW. *T. texasensis* conserved SO_4 when acclimated to PW, and reduced reabsorption when acclimated to the sulfate-rich 10% SW. When mussels acclimated to 10% SW were returned to PW, there was a transient increase in sulfate clearance during the first 8 h because filtration exceeded reabsorption.

Introduction

The characteristics of solute (K, La, Na, sucrose, mannitol) penetration through the epithelia of the unionid *Toxolasma texasensis* are intermediate to those of other freshwater bivalves (Dietz and Byrne, 1990; Dietz *et al.*, 1995; Wilcox and Dietz, 1995; Byrne and Dietz, 1997; Zheng and Dietz, 1998b; Dietz and Byrne, 1999). Previous studies indicated that the passive movements of solutes and water across the epithelia of *T. texasensis* were relatively slower that those of the dreissenid *Dreissena polymorpha* (Scheide and Dietz, 1986; Dietz and Byrne, 1997, 1999). To maintain ionic homeostasis, an animal must be able to accumulate and retain solutes; then to preserve water balance, it must excrete a volume of water equivalent to that taken up osmotically. Kidney filtration can be estimated by measuring the clearance of marker solutes from the blood, and it is a useful index from which kidney function and osmotic water movement can be monitored (Potts, 1954b; Murphy and Dietz, 1976; Hevert, 1984; Kirschner, 1991; Dietz and Byrne, 1997, 1999).

Unionid bivalves accumulate sulfate at the rather slow rate of 0.04 μmol g^{-1} dry tissue h^{-1} (Dietz, 1978). Thus, sulfate is a relatively nonpenetrating anion, and therefore it has been used for short-term studies of independent ion transport (Krogh, 1939; Scheide and Dietz, 1982; Byrne and Dietz, 1997; Zheng and Dietz, 1998a; Dietz and Byrne, 1999). However, sulfate is present in millimolar concentrations in the blood of freshwater mussels (Potts, 1954a; Dietz and Byrne, 1999) and is a component of various organic molecules (*e.g.*, amino acids, mucopolysaccharides) found in molluscs (Eriksson *et al.*, 1984; Kornprobst *et al.*, 1998).

Sulfate balance was studied recently in *D. polymorpha*, which has the highest epithelial solute permeability of any freshwater bivalve tested (Dietz and Byrne, 1999). In the present study, kidney function was examined in a unionid

---

Received 2 February 2000; accepted 16 May 2000.

* To whom correspondence should be addressed. E-mail: zothom@lsu.edu.

Abbreviations: DIDS, 5, 5′-diisothiocyanatostilbene 2, 2′-disulfonic acid; PAH, para-aminohippuric acid; PEG, polyethylene glycol; PW, artificial pondwater; SW, artificial seawater.

bivalve, *Toxolasma texasensis*. The unionids have a longer freshwater ancestry (Triassic) than the dreissenids, which invaded freshwater in the Pleistocene (Haas, 1969). Sulfate uptake and the characteristics of the renal clearance and conservation of $^{35}SO_4$ that was injected into the body fluids were studied.

Materials and Methods

Animal acclimation

Toxolasma (=*Carunculina*) *texasensis* was collected from ponds near Baton Rouge, Louisiana. The animals were stored, unfed for at least 1 week before use, in aerated artificial pondwater (PW) at 22° ± 2°C. The pondwater composition (in millimoles per liter) was 0.5 NaCl, 0.4 $CaCl_2$, 0.2 $NaHCO_3$, 0.2 $MgSO_4$, 0.05 KCl (Dietz *et al.*, 1994). Some mussels were acclimated to an artificial seawater (SW) that was diluted with PW to be about 10% SW (~106 mosm kg^{-1}) for more than 13 d before use. In 10% SW the mussels become isosmotic, and the osmotic gradient is minimal. The stock SW composition (in millimoles per liter) was 449.1 NaCl, 27.5 $MgSO_4$, 24.4 $MgCl_2$, 9.9 $CaCl_2$, 6.6 KCl, 2.4 $KHCO_3$, 0.8 KBr, 0.4 H_3BO_3, 1076 mosm (salinity = 35‰) (Chambers and De Armendi, 1979).

Solute analyses

Samples of blood (200–300 μl) were obtained from mussels by pericardial puncture and centrifuged for 3 min at 8000 × *g* before analysis (Fyhn and Costlow, 1975). The osmolality of blood or bathing medium was determined on undiluted samples by freezing point depression. Sodium and potassium concentrations were determined by emission flame photometry. Calcium and magnesium concentrations were determined by atomic absorption spectroscopy from samples diluted with La_2O_3/HCl. Chloride concentration was determined by electrometric titration.

Sulfate was determined by a turbidimetric method that formed a precipitate with barium in a total volume of 0.8 ml (Dietz and Byrne, 1999). A 50-μl sample of blood or bathing medium was added to 450 μl deionized water. To each sample, 100 μl of 4.1 mol l^{-1} NaCl in 0.2 mol l^{-1} HCl was added and vortexed. A 100-μl aliquot of glycerol, ethanol, dibutyl phosphate (2:1:0.15 by volume) was added and vortexed. The SO_4 was precipitated as $BaSO_4$ crystals by the addition of 100 μl of 1 mol l^{-1} $BaCl_2$ and immediately sonicated for 10 s to form crystals of a reproducible size (Dietz and Byrne, 1999). Turbidity was measured spectrophotometrically at 400 nm and was compared to a standard curve that was linear up to 1 mmol l^{-1} Na_2SO_4.

Sulfate uptake

Sulfate uptake was measured by the appearance of the radiolabeled SO_4 in the blood (Dietz and Byrne, 1999). Each animal was placed in a separate container and used once. The bathing medium was PW (0.2 mmol l^{-1} SO_4), and trace amounts of $^{35}SO_4$ were added to give a specific activity of 100,000 dpm μmol^{-1}. After 3 h, bath samples were collected, and the radioactivity was measured using a xylene/Triton X-114 liquid scintillation cocktail (Wiegman *et al.*, 1975) and a Beckman LS6000 counter. After the samples were collected, each mussel was removed, blotted dry, and weighed; a blood sample was then taken and processed as described above. The tissue was removed from the shell, and the soft tissue was dried overnight (90°C) to determine dry mass. The amount of $^{35}SO_4$ that accumulated in the mussel blood during the exposure to the isotope was used to calculate the uptake of sulfate (nanomoles per milliliter) in the blood by dividing the amount of radioactivity in a known volume of blood (dpm per milliliter) by the specific activity of the bathing medium (dpm per nanomole). In some studies, SO_4 uptake was measured for 3 h from PW containing 0.5 mmol l^{-1} of the anion transport inhibitor 5, 5′-diisothiocyanatostilbene 2, 2′-disulfonic acid (DIDS) adjusted to pH 7.3 with Tris. The uptake studies were performed under indirect illumination to minimize photodegradation of DIDS.

Solute clearance

Radioactive tracers [^{3}H-polyethylene glycol (PEG, 4 kDa), and Na_2 $^{35}SO_4$] dissolved in deionized water were injected [10 μl, 1 μCi of each isotope (1 Ci = 37 GBq)] into the foot muscle of each specimen, and the animal was returned to the appropriate acclimation medium for 3 h to allow isotope equilibration. The clearance of the radioisotope from the body fluids of *T. texasensis* was determined using the procedures of Dietz and Byrne (1997, 1999). In brief, after the 3-h equilibration, the animals were rinsed three times to remove adsorbed isotope and transferred to separate containers with 30 ml of the appropriate experimental bathing medium. The mussels resumed siphoning within 10–20 min, bath samples were collected at times 0 and 1 h, and the radioactivity was determined by double-label counting procedures, as needed, using a programmable Beckman LS6000 scintillation counter. After the final sample of bathing medium was taken, each mussel was removed, blotted dry, and weighed; a blood sample was then collected. The tissue was removed from the shell, and the soft tissue was dried overnight at 90°C and reweighed.

The clearance of the isotope was calculated from the total amount of radioactivity that accumulated in the bathing medium during the 1-h interval (dpm per hour) divided by the isotope radioactivity in the blood (dpm per milliliter) at the end of the clearance study (Murphy and Dietz, 1976). The clearance of solute from the blood was expressed as milliliters of blood per gram of dry tissue per hour. Because of the potential damage due to pericardial sampling, blood was collected only at the end of the experiment. Calculated data assumed that the specific activity of the blood remained constant during the 1-h clearance measurement. The specific activity of the blood probably decreased exponentially during the experiment, and clearance may be underestimated by 20%–24% (Murphy and Dietz, 1976; Dietz and Byrne, 1997).

Urine samples were not collected from the bivalves; thus the urine volume and urine:blood ratio of radioactive tracer were not determined directly. The method used for calculating clearance would determine the equivalent volume of blood that would have to be cleared of the tracer by all routes (kidney, epithelial, digestive tract), but our previous studies indicated that most of the loss is renal (Dietz and Byrne, 1997) and that contamination of the blood with bathing medium was rare and minimal (Dietz *et al.*, 1997).

The PEG marker was considered to represent the amount of material filtered by the kidney in bivalves (Dietz and Byrne, 1997, 1999). Thus, clearance values of other solutes(x) were compared with PEG clearance for each specimen to distinguish filtration (equal clearance values), reabsorption [clearance(x) < PEG], or secretion [clearance(x) > PEG]. Sulfate clearance was calculated by the method described above for PEG. The sulfate concentration in the blood of each specimen was measured and converted into the amount of sulfate filtered (micromoles of sulfate per gram of dry tissue per hour) into the kidney by multiplying the PEG clearance (milliliters of blood cleared of PEG per gram of dry tissue per hour) by the blood sulfate concentration (micromoles of sulfate per milliliter of blood). Knowing the specific activity (dpm μmol^{-1}) of $^{35}SO_4$ in the blood, the quantity of $^{35}SO_4$ excreted (dpm per gram of dry tissue per hour) was converted into the total quantity of sulfate eliminated (micromoles of sulfate per gram of dry tissue per hour) for each specimen, and this value represented sulfate excretion. The sulfate reabsorption was calculated as the difference between the filtered and excreted sulfate values for each animal.

Clearance studies were performed on mussels acclimated either to PW or to 10% SW: animals in PW were hyperosmotic to the bathing medium; those in 10% SW were isosmotic. Animals acclimated to 10% SW were transferred to PW for 1, 4, 8, 24, 48, or 72 h to observe the changes in renal clearance when they experienced an increased osmotic gradient. Clearance was measured for 1 h, ending at each time interval specified, and the amounts of sulfate filtered, excreted, and reabsorbed were calculated.

Para-aminohippuric acid (PAH, 194 Da) was injected into mussels together with PEG (15 μl, 1 μCi) to compare clearance values. The method used was similar to that described above for the double-label ^{3}H-PEG and $^{35}SO_4$ studies. Both ^{3}H- and ^{14}C-label for both PEG and PAH, and identical results were obtained. The clearance of PAH was rapid, thus the equilibration time was shortened from 3 h to 1 h.

Table 1

Blood solute concentration in pondwater-acclimated Toxolasma texasensis *with or without exposure to 0.5 mmol l^{-1} DIDS for 3 h*

Solute	Control	Treated
Total solute, mosm kg^{-1}	40 ± 2	39 ± 2
Na, mmol l^{-1}	19.4 ± 1.3	19.9 ± 1.2
K, mmol l^{-1}	0.4 ± 0.0	0.5 ± 0.1
Ca, mmol l^{-1}	3.5 ± 0.2	3.4 ± 0.2
Mg, mmol l^{-1}	0.3 ± 0.0	0.4 ± 0.0
Cl, mmol l^{-1}	12.3 ± 0.6	12.5 ± 0.8
SO_4, mmol l^{-1}	1.8 ± 0.2	1.7 ± 0.1
$^{35}SO_4$, nmol ml^{-1}	13 ± 1	6 ± 2*

Data are mean ±1 standard error, $n = 5$, * $P < 0.05$.

Statistical analyses

All data are expressed as the mean ± 1 standard error (SE). An animal was used once, and *n* indicates the number of animals in each treatment group. Data were analyzed for differences between treatment groups by performing a one-way analysis of variance (ANOVA). When the ANOVA was significant, the Fisher's protected least significant difference method was used to determine differences between specific means ($P < 0.05$).

Results

Solute balance and SO_4 uptake

Toxolasma texasensis is a hyper-regulator in freshwater, and the solute concentrations measured in the blood were maintained at higher levels than those in the PW bathing medium (Table 1). Sulfate had the lowest concentration of any anion in the blood (1.7–1.8 mmol l^{-1}), but this concentration was about 8 times higher than in the medium (0.2 mmol l^{-1}). Thus, SO_4 is concentrated to the same level as Cl (Table 1).

The SO_4 influx is slow in unionids (Dietz, 1978); thus we did not measure the unidirectional influx of SO_4 by the disappearance of isotope from the bathing medium. Less than 1000 dpm ml^{-1} of $^{35}SO_4$ would disappear from the bath after several hours, and compared to the 20,000 dpm ml^{-1} (30 ml bath volume) present in the bathing medium, this difference could not be distinguished with liquid scintillation counting techniques. The amount of $^{35}SO_4$ that accumulated in the blood over the incubation interval was small, but significantly greater than zero. The uptake of $^{35}SO_4$ was reduced 54% (significant at $P < 0.05$) by exposure to 0.5 mmol l^{-1} DIDS, but none of the other solutes measured in the blood were affected (Table 1).

Table 2

Volume of blood cleared of polyethylene glycol (PEG) and $^{35}SO_4$, and calculated sulfate processing by the kidney of Toxolasma texasensis *acclimated to pondwater (PW), 10% seawater (SW), or when returned to PW for various periods*

		Clearance, ml g^{-1} dry tissue h^{-1}		Sulfate, μmol g^{-1} dry tissue h^{-1}		
Treatment	*n*	PEG	Sulfate	Filtered	Reabsorbed	Excreted
10% SW	10	0.17 ± 0.05a	0.09 ± 0.02a	0.48 ± 0.14a	0.23 ± 0.08a	0.25 ± 0.07ab
1 h PW	5	0.57 ± 0.17b	0.21 ± 0.05a	1.34 ± 0.54b	0.84 ± 0.38ab	0.51 ± 0.18b
4 h PW	7	1.24 ± 0.12c	0.76 ± 0.13b	2.97 ± 0.37c	1.17 ± 0.32b	1.80 ± 0.31d
8 h PW	5	1.32 ± 0.18c	0.77 ± 0.15b	1.77 ± 0.25b	0.81 ± 0.25ab	0.97 ± 0.08c
24 h PW	5	1.25 ± 0.15c	0.09 ± 0.02a	1.66 ± 0.11b	1.54 ± 0.10bc	0.12 ± 0.02ab
48 h PW	5	1.32 ± 0.19c	0.10 ± 0.04a	1.74 ± 0.20b	1.62 ± 0.21bc	0.11 ± 0.03ab
72 h PW	5	0.93 ± 0.15bc	0.03 ± 0.00a	2.03 ± 0.39b	1.97 ± 0.38c	0.06 ± 0.01a
PW	11	0.76 ± 0.11b	0.12 ± 0.02a	1.33 ± 0.24b	1.17 ± 0.24b	0.17 ± 0.02ab

Data are expressed as mean ±1 standard error. Values within a column that have different letters are significantly different using Fisher's protected least significant difference method ($P < 0.05$).

Solute clearance

We previously reported values for clearance of radioactive inulin from the blood of *Ligumia subrostrata* and *T. texasensis* (Murphy and Dietz, 1976; Scheide and Dietz, 1986); in this study similar results were obtained using PEG: 0.77 ± 0.04 ml g^{-1} dry tissue h^{-1} ($n = 6$). However, the clearance of $^{35}SO_4$ administered simultaneously (0.09 ± 0.03 ml g^{-1} dry tissue h^{-1}) was 12% of the clearance of ^{3}H-PEG, suggesting that filtered SO_4 was being reabsorbed by the renal tissue.

The osmotic uptake of water should be high in PW-acclimated *T. texasensis,* but low in 10% SW-acclimated animals. Thus, filtration measured by the clearance of PEG should be at a relatively high rate in the former and lower in the latter acclimation medium. The clearances from animals that were doubly labeled with $^{35}SO_4$ and ^{3}H-PEG were measured from animals acclimated to either PW or 10% SW (Table 2). The animals in 10% SW were isosmotic with the medium (Table 3) and would have experienced a lower osmotic uptake of water and therefore reduced filtration, as reflected in the clearance of PEG. The sulfate clearance was about 16% of the PEG clearance in the PW-acclimated animals. However, the mussels acclimated to 10% SW had similar clearances ($P > 0.1$) for both $^{35}SO_4$ and ^{3}H-PEG. The SO_4 clearance in 10% SW-acclimated animals appeared to be unchanged relative to the PW-acclimated mussels. However, because the clearances of SO_4 and PEG were similar, these data suggest that 10% SW-acclimated animals had reduced their reabsorption of SO_4 (Table 2). The SO_4 concentration in the blood of *T. texasensis* acclimated to 10% SW was significantly higher ($P < 0.05$) than in PW-acclimated controls (Table 3), but was the same as in the 10% SW bathing medium (~2.7 mmol l^{-1} SO_4).

When *T. texasensis* was transferred from 10% SW into

Table 3

Concentration of solutes in the blood of Toxolasma texasensis *acclimated to pondwater (PW), 10% seawater (SW), or returned to PW for various periods*

	mosm kg^{-1}	Ion concentration, mmol l^{-1}					
Treatment	Total solute	Na	K	Ca	Mg	Cl	SO_4
10% SW	110 ± 1f	45.1 ± 0.7e	1.6 ± 0.1e	2.1 ± 0.2a	3.3 ± 0.3e	41.1 ± 1.7e	2.8 ± 0.2c
1 h PW	102 ± 2e	41.0 ± 0.7d	1.1 ± 0.0d	2.8 ± 0.2b	3.6 ± 0.2e	36.2 ± 1.1d	2.1 ± 0.4ab
4 h PW	79 ± 1d	29.6 ± 0.7c	0.9 ± 0.0cd	2.1 ± 0.1a	2.7 ± 0.2d	24.9 ± 0.8c	2.4 ± 0.1bc
8 h PW	67 ± 1c	27.7 ± 0.5c	0.7 ± 0.1bc	2.6 ± 0.1b	1.8 ± 0.2c	21.0 ± 0.3b	1.4 ± 0.2a
24 h PW	55 ± 1b	20.1 ± 0.7b	0.6 ± 0.0ab	3.0 ± 0.2bc	1.3 ± 0.1bc	15.5 ± 0.6a	1.4 ± 0.2a
48 h PW	45 ± 3a	16.4 ± 1.1a	0.4 ± 0.0a	2.6 ± 0.1b	1.0 ± 0.1b	12.0 ± 0.8a	1.4 ± 0.2a
72 h PW	46 ± 1a	16.6 ± 0.2a	0.6 ± 0.1ab	2.9 ± 0.2b	0.8 ± 0.1ab	12.3 ± 0.5a	2.1 ± 0.1abc
PW	44 ± 2a	19.1 ± 0.9b	0.5 ± 0.0a	3.5 ± 0.2c	0.4 ± 0.0a	12.7 ± 0.7a	1.7 ± 0.2a

Data are expressed as mean ±1 standard error, with 5–11 animals for each treatment. Values within a column that have different letters are significantly different using Fisher's protected least significant difference method ($P < 0.05$).

PW, PEG and $^{35}SO_4$ clearance increased (Table 2). Although there was an immediate rise in osmotic uptake of water, only PEG clearance increased significantly during the first hour relative to 10% SW animals, but clearance of both solutes was elevated by 4 h. The clearance of PEG was restored to the same level as that found in PW mussels by 72 h. In contrast, the $^{35}SO_4$ clearance remained elevated for 8 h and then returned to PW control levels by 24 h. The elevation in SO_4 excretion was due to a significant increase in filtration. During the first hour after transfer to PW, the SO_4 clearance remained statistically the same as the PEG clearance. By 4 h, the SO_4 clearance was significantly less ($P < 0.05$) than the corresponding PEG clearance. The reduction in SO_4 clearance was due to the rapid restoration of sulfate reabsorption (Table 2). During the first hour of re-acclimation to PW, the sulfate concentration in the blood returned to the same level as in the PW-acclimated controls; recovery was due to dilution caused by the osmotic uptake of water combined with increased levels of filtration (Table 3). However, 48 h were required for the total solute and most of the other measured ions to return to PW levels (Table 3).

To determine whether the renal tissue of *T. texasensis* could secrete organic acids, radioactive PEG and PAH were both injected into PW-acclimated animals. The clearance was 1.26 ± 0.08 ml g^{-1} dry tissue h^{-1} for PEG, and 5.75 ± 0.65 ml g^{-1} dry tissue h^{-1} for PAH ($n = 10$). PAH is a smaller molecule than PEG, but the volume of blood cleared of PAH by filtration was likely to be the same as for PEG. The additional PAH clearance was due to secretory mechanisms and amounted to 4.49 ml g^{-1} dry tissue h^{-1}; this value was 3.5 times the amount of PAH cleared by filtration.

Discussion

Toxolasma texasensis has a tubular kidney with functional characteristics similar to those found in other invertebrates and vertebrates. The kidney forms urine by ultrafiltration, for which PEG serves as a useful marker (Hevert, 1984). Some solutes can be added to the urine by the process of secretion, as well as filtration, and PAH is an organic acid that is subject to secretory activity. Most of the PAH eliminated by the kidney of *T. texasensis* was through secretory mechanisms. The importance of secretion in the elimination of PAH has also been documented in the snail *Achatina fulica* (Martin *et al.*, 1965). At low concentrations of PAH in the blood, most of this solute is secreted by the snail kidney rather than filtered. The third major process responsible for urine formation is solute reabsorption. In this study, we have focused on the characteristics of sulfate reabsorption by the kidney of *T. texasensis.*

Toxolasma texasensis was able to maintain a sulfate concentration in the blood of about 1–2 mmol l^{-1} while acclimated to an artificial PW containing 0.2 mmol l^{-1} SO_4. Sulfate balance was maintained by transport systems in the epithelia, including the kidney. Sulfate concentrations in the blood and pericardial fluid are the same, which suggests that the anion is freely filtered in molluscs (Potts and Todd, 1965) as it is in vertebrates (Mudge *et al.*, 1973). Thus, filtration in bivalves was assumed to be the same for sulfate as for PEG, but the renal reabsorption of SO_4 reduced its clearance from the blood by more than 80% relative to PEG clearance. Renal reabsorption of sulfate was reduced in animals that were acclimated to 10% SW for almost 2 weeks. During acclimation to 10% SW, the concentration of SO_4 in the blood increased to about 2.8 mmol l^{-1} (equal to the bathing medium). These data contrast with the somewhat more rapid SO_4 transport rates observed in *Dreissena polymorpha,* and with the apparent cessation of SO_4 reabsorption in that species when acclimated to 10% SW (Dietz and Byrne, 1999). The low blood SO_4 concentration of 0.7 mmol l^{-1} reported for the unionid *Anodonta cygnea* (Potts, 1954a) is similar to concentrations we observed in *T. texasensis,* but is less than half the concentration found in *D. polymorpha* (Dietz and Byrne, 1999).

In previous studies, the clearance values for PEG, inulin, and high-molecular weight dextran from the blood of *D. polymorpha* were similar, and we concluded that these three solutes were probably measuring the renal filtration rate (Dietz and Byrne, 1997, 1999). PEG clearance values in PW-acclimated *T. texasensis* were about 1 ml g^{-1} dry tissue h^{-1}, and were similar to inulin clearances reported for the freshwater snail *Lymnaea stagnalis* (de With and van der Schors, 1984). When *T. texasensis* was acclimated to 10% SW, the PEG clearance decreased to about 0.2 ml g^{-1} dry tissue h^{-1}. Although pondwater-acclimated *D. polymorpha* clear the blood of PEG at about double the rate observed for *T. texasensis,* the response by the kidney was the same in both species when the osmotic gradient was abolished by acclimation to 10% SW (Dietz and Byrne, 1997, 1999; this study).

In the sulfate-rich 10% SW environment, *T. texasensis* became isosmotic and isoionic for SO_4 and reduced its renal reabsorption. All freshwater bivalves studied become isosmotic when exposed to dilute seawater (Wilcox and Dietz, 1998; Jordan and Deaton, 1999). They have limited tolerance, but may survive in an environment in which total solutes approach 400 mosm kg^{-1}. Freshwater bivalves can maintain cellular volume regulation under moderate osmotic challenges; their ability to mobilize free amino acids is restricted, however, and this restriction may be responsible for the limit to their survival (Dietz *et al.*, 1998; Jordan and Deaton, 1999).

Transferring mussels from 10% SW to PW would increase the osmotic uptake of water and the subsequent excretion of water by the kidney. After the transfer, PEG clearance was rapidly elevated to values exceeding those observed for PW-acclimated *T. texasensis.* Because of elevated filtration, it was 24 h before SO_4 clearance returned to PW control levels, even though SO_4 reabsorption was immediately reestablished. *D. polymorpha* also required about 24 h to reestablish SO_4 reabsorption to PW control levels (Dietz and Byrne, 1999). However, *D. polymorpha* did not elevate PEG clearance above that found in PW-acclimated animals. Unlike the unionids, *D. polymorpha* has maximum renal filtration (PEG clearance) when acclimated to PW, and filtration cannot be increased even when the mussel is subjected to higher osmotic uptake of water (Dietz and Byrne, 1999).

Recent studies have examined mechanisms of sulfate transport in a variety of preparations (Larsen and Simonsen, 1988; Cole and Rastogi, 1991; Tenenhouse and Martel, 1993; Grassl, 1996; Dietz and Byrne, 1999). Toad skin is capable of active sulfate influx from a Ringer's solution containing 1 mmol l^{-1} SO_4, using an anion exchange mechanism (Larsen and Simonsen, 1988). The anion transport inhibitor, DIDS, significantly decreased the amount of $^{35}SO_4$ label that accumulated in the blood of freshwater bivalves, suggesting that sulfate uptake was linked to an anion exchange mechanism (Dietz and Byrne, 1999; this study).

Sulfate reabsorption is subject to regulatory mechanisms in freshwater bivalves. When mussels were acclimated to 10% SW, the concentration of SO_4 in the blood rose, and renal reabsorption was reduced in both unionids and dreissenids; thus, conservation of this anion was minimal (Dietz and Byrne, 1999; this study). Freshwater bivalves that are acclimated to PW are in a low SO_4 environment, but transport systems and conservation mechanisms both allow them to maintain a SO_4 concentration almost 10 times higher than that in the medium.

Acknowledgments

We thank Paul Bruce and Chris Thibodaux for technical assistance. The Louisiana Alliance for Minority Participation provided support for A.S.U. This study was partially supported by the Louisiana Sea Grant College grant NOAA 46RG0096 Project R/ZMM-1 and 46RG0096 R/ZMM-5.

Literature Cited

Byrne, R. A., and T. H. Dietz. 1997. Ion transport and acid-base balance in freshwater bivalves. *J. Exp. Biol.* **200:** 457–465.

Chambers, E. L., and J. de Armendi. 1979. Membrane potential, action potential and activation potential of eggs of the sea urchin, *Lytechinus variegatus*. *Exp. Cell Res.* **122:** 203–218.

Cole, D. E. C., and N. Rastogi. 1991. Sulfate transport in human placenta: further evidence for a sodium-independent mechanism. *Biochim. Biophys. Acta* **1064:** 287–292.

de With, N. D., and R. C. van der Schors. 1984. Urine composition and kidney function in the pulmonate freshwater snail, *Lymnaea stagnalis*. *Comp. Biochem. Physiol.* **79A:** 99–103.

Dietz, T. H. 1978. Sodium transport in the freshwater mussel, *Carunculina texasensis* (Lea). *Am. J. Physiol.* **235:** R35–R40.

Dietz, T. H., and R. A. Byrne. 1990. Potassium and rubidium uptake in freshwater bivalves. *J. Exp. Biol.* **150:** 395–405.

Dietz, T. H., and R. A. Byrne. 1997. Effects of salinity on solute clearance from the freshwater bivalve, *Dreissena polymorpha* Pallas. *Exp. Biol. Online* **2:** 11 (http://link.springer.de/).

Dietz, T. H., and R. A. Byrne. 1999. Measurement of sulfate uptake and loss in the freshwater bivalve *Dreissena polymorpha* using a semimicroassay. *Can. J. Zool.* **77:** 331–336.

Dietz, T. H., D. Lessard, H. Silverman, and J. W. Lynn. 1994. Osmoregulation in *Dreissena polymorpha:* the importance of Na, Cl, K, and particularly Mg. *Biol. Bull.* **187:** 76–83.

Dietz, T. H., R. A. Byrne, J. W. Lynn, and H. Silverman. 1995. Paracellular solute uptake by the freshwater zebra mussel *Dreissena polymorpha*. *Am. J. Physiol.* **269:** R300–R307.

Dietz, T. H., S. J. Wilcox, R. A. Byrne, and H. Silverman. 1997. Effects of hyperosmotic challenge on the freshwater bivalve *Dreissena polymorpha:* importance of K^+. *Can. J. Zool.* **75:** 697–705.

Dietz, T. H., D. S. Neufeld, H. Silverman, and S. H. Wright. 1998. Cellular volume regulation in freshwater bivalves. *J. Comp. Physiol. B* **168:** 87–95.

Eriksson, G., B. Särnstrand, and A. Malmström. 1984. Equilibration of [^{3}H]glucosamine and [^{35}S]sulfate with intracellular pools of UDP-N-acetylhexosamine and 3′-phosphoadenosine-5′-phosphosulfate (PAPS) in cultured fibroblasts. *Arch. Biochem. Biophys.* **235:** 692–698.

Fyhn, H. J., and J. D. Costlow. 1975. Anaerobic sampling of body fluids in bivalve molluscs. *Comp. Biochem. Physiol. A* **52:** 265–268.

Grassl, S. M. 1996. Sulfate transport in human placental brush-border membrane vesicles. *Biochim. Biophys. Acta* **1282:** 115–123.

Haas, F. 1969. Family Unionidae. Pp. 411–467 in *Treatise on Invertebrate Paleontology*, R. C. Moore, ed. Geological Society of America, Boulder, CO.

Hevert, F. 1984. Urine formation in the lamellibranchs: evidence for ultrafiltration and quantitative description. *J. Exp. Biol.* **111:** 1–12.

Jordan, P. J., and L. E. Deaton. 1999. Osmotic regulation and salinity tolerance in the freshwater snail *Pomacea bridgesi* and the freshwater clam *Lampsilis teres*. *Comp. Biochem. Physiol. A* **122:** 199–205.

Kirschner, L. B. 1991. Water and ions. Pp. 13–107 in *Environmental and Metabolic Animal Physiology*, C. L. Prosser, ed. 4th ed. Wiley-Liss, New York.

Kornprobst, J.-M., C. Sallenave, and G. Barnathan. 1998. Sulfated compounds from marine organisms. *Comp. Biochem. Physiol. B* **119:** 1–51.

Krogh, A. 1939. Osmotic regulation in aquatic animals. Cambridge University Press, Cambridge.

Larsen, E. H., and K. Simonsen. 1988. Sulfate transport in toad skin: evidence for mitochondria-rich cell pathways in common with halide ions. *Comp. Biochem. Physiol. A* **90:** 709–714.

Martin, A. W., D. M. Stewart, and F. M. Harrison. 1965. Urine formation in a pulmonate land snail, *Achatina fulica*. *J. Exp. Biol.* **42:** 99–123.

Mudge, G. H., W. O. Berndt, and H. Valtin. 1973. Tubular transport of urea, glucose, phosphate, uric acid, sulfate, and thiosulfate. Pp. 587–652 in *Handbook of Physiology, Renal Physiology*, J. Orloff and R. W. Berliner, eds. American Physiological Society, Washington, DC.

Murphy, W. A., and T. H. Dietz. 1976. The effects of salt depletion on blood and tissue ion concentrations in the freshwater mussel, *Ligumia subrostrata* (Say). *J. Comp. Physiol.* **108:** 233–242.

Potts, W. T. W. 1954a. The inorganic composition of the blood of *Mytilus edulis* and *Anodonta cygnea*. *J. Exp. Biol.* **31:** 376–385.

Potts, W. T. W. 1954b. The rate of urine production of *Anodonta cygnea*. *J. Exp. Biol.* **31:** 614–617.

Potts, W. T. W., and M. Todd. 1965. Kidney function in the octopus. *Comp. Biochem. Physiol.* **16:** 479–489.

Scheide, J. I., and T. H. Dietz. 1982. The effects of independent sodium and chloride depletion on ion balance in freshwater mussels. *Can. J. Zool.* **60:** 1676–1682.

Scheide, J. I., and T. H. Dietz. 1986. Serotonin regulation of gill cAMP production, Na, and water uptake in freshwater mussels. *J. Exp. Zool.* **240:** 309–314.

Tenenhouse, H. S., and J. Martel. 1993. Na^+-dependent sulfate transport in opossum kidney cells is DIDS sensitive. *Am. J. Physiol.* **265:** C54–C61.

Wiegman, T., M. G. Woldring, and J. J. Pratt. 1975. A new cocktail for liquid scintillation counting of aqueous radioimmunoassay samples. *Clin. Chim. Acta* **59:** 347–356.

Wilcox, S. J., and T. H. Dietz. 1995. Potassium transport in the freshwater bivalve *Dreissena polymorpha*. *J. Exp. Biol.* **198:** 861–868.

Wilcox, S. J., and T. H. Dietz. 1998. Salinity tolerance of the freshwater bivalve *Dreissena polymorpha* (Pallas, 1771) (Bivalvia, Dreissenidae). *Nautilus* **111:** 143–148.

Zheng, H., and T. H. Dietz. 1998a. Ion transport in the freshwater bivalve *Corbicula fluminea*. *Biol. Bull.* **194:** 161–169.

Zheng, H., and T. H. Dietz. 1998b. Paracellular solute uptake in the freshwater bivalves *Corbicula fluminea* and *Toxolasma texasensis*. *Biol. Bull.* **194:** 170–177.

Reference: *Biol. Bull.* **199:** 21–28. (August 2000)

Allometric Scaling in Small Colonies of the Scleractinian Coral *Siderastrea siderea* (Ellis and Solander)

STEVEN V. VOLLMER* AND PETER J. EDMUNDS

Department of Biology, California State University, 18111 Nordhoff Street,
Northridge, California 91330

Abstract. Although most physiological traits scale allometrically in unitary organisms, it has been hypothesized that modularity allows for isometric scaling in colonial modular taxa. Isometry would allow increases in size without functional constraints, and is thought to be of central importance to the success of a modular design. Yet, despite its potential importance, scaling in these organisms has received little attention. To determine whether scleractinian corals are free of allometric constraints, we quantified metabolic scaling, measured as aerobic respiration, in small colonies (≤40 mm in diam.) of the scleractinian *Siderastrea siderea*. We also quantified the scaling of colony surface area with biomass, since the proposed isometry is contingent upon maintaining a constant ratio of surface area to biomass (or volume) with size. Contrary to the predicted isometry, aerobic respiration scaled allometrically on biomass with a slope (b) of 0.176, and colony surface area scaled allometrically on biomass with a slope of 0.730. These findings indicate that small colonies of *S. siderea* have disproportionately high metabolic rates and SA:B ratios compared to their larger counterparts. The most probable explanations for the allometric scaling of aerobic respiration are (1) a decline in the SA:B ratio with size such that more surface area is available per unit of biomass for mass transfer in the smallest colonies, and (2) the small size, young age, and disproportionately high growth rates of the corals examined. This allometric scaling also demonstrates that modularity, alone, does not allow small colonies of *S. siderea* to overcome allometric constraints. Further studies are required to determine whether allometric scaling is characteristic of the full size range of colonies of *S. siderea*.

Introduction

Body size affects diverse biological variables ranging from physiological to life-history traits (Schmidt-Nielson, 1984). In unitary organisms, most processes scale allometrically (Schmidt-Nielson, 1974)—that is, they change disproportionately with size—as a result of physical and geometric constraints on body size, structure, and function (Gould, 1966; Schmidt-Nielson, 1974). Classic examples of these constraints include the limits that the skeleton places on the size of terrestrial mammals (Schmidt-Nielson, 1974; Economos, 1981) and the limits that flight muscles place on the size of flying birds (Pennycuick, 1972). Constraints often are inherent to the design of organisms, yet they can be minimized, in theory, by minor changes in geometry or shape (Brody, 1945; Gould, 1966). Profound changes in size, however, require design modifications, including elaborate structural changes and the development of complex internal systems (Gould, 1966; Schmidt-Nielson, 1984). Such changes probably evolve over relatively long time scales (Gould, 1966, 1977).

The relationship between surface area and volume is fundamentally important to scaling arguments, especially for surface-area-related phenomena such as metabolism and thermal regulation (Gould, 1966; Schmidt-Nielson, 1984), because most processes scale allometrically as a result of decreasing ratios of surface area to volume (SA:V) that are associated with volumetric increases in body size (Gould, 1966). In cases where geometric similarity is maintained with increasing size (that is, where there is geometric isom-

---

Received 23 September 1999; accepted 30 May 2000.

* To whom correspondence should be addressed. Current address: Department of Organismic and Evolutionary Biology, 16 Divinity Ave., Box 90, Harvard University, Cambridge, MA 02138. E-mail: svollmer@oeb.harvard.edu

etry, or constancy of shape), surface area (y) scales to the two-third power of volume (x) according to the allometric equation: $y = ax^b$. This equation describes a case of functional allometry arising from geometric isometry, where a is a constant and b is the scaling exponent with a predicted value of .067 (Schmidt-Nielson, 1984; Peters, 1983). Thus, all things being equal and with geometric isometry, all surface-area-related processes (heat loss, gas exchange, etc.) also should scale to the two-thirds power of mass, *i.e.*, the surface rule (Rubner, 1883). However, most organisms do not maintain geometric similarity as they grow (McMahon, 1973), and therefore the scaling exponents of many surface-area-related processes deviate from the predicted value of 0.67 (Kleiber, 1932, 1961). Metabolism, for example, often scales to the three-quarter power in interspecific analyses ($b = 0.75$) (Zeuthen, 1953; Hemmingsen, 1960), whereas intraspecific exponents vary widely depending on the organism (Altman and Dittmer, 1968; Peters, 1983). Such deviations can be explained, in part, by geometric allometry involving changes in the shape of exchange surfaces; these changes maintain high SA:V ratios and minimize surface-area-related constraints (Gould, 1966). In an extreme case, organisms might overcome geometric constraints entirely by maintaining a constant SA:V ratio with increasing body size (Gould, 1966). However, the maintenance of a constant SA:V ratio is likely only in organisms with relatively unusual body plans—for example, the dorsoventral flattening in flatworms (Gould, 1966), and the incorporation of non-respiring biomass in corals, bryozoans, hydroids, and other colonial modular organisms (Gould, 1966; Sebens, 1987a).

It has been hypothesized that colonial modular organisms overcome the allometric constraints typically associated with volumetric increases in body size by maintaining a constant SA:V ratio as colony size increases (Jackson, 1979; Hughes and Hughes, 1986). Purportedly, this is achieved by subdividing the biomass of the colony into individual units (*i.e.*, modules) of similar size (Hughes and Hughes, 1986) and growing through modular iteration (Jackson, 1979; Hughes and Cancino, 1985). As a result, physiological processes should not be functionally constrained by declining SA:V ratios, but instead should scale proportionally (*i.e.*, isometrically, $b = 1$) to both the number of modules and the total colony biomass (Jackson, 1979; Sebens, 1979, 1987a), thereby allowing indeterminate colony growth (Sebens, 1987a). In turn, this proposed isometry is thought to be critical to the success of colonial modular organisms (Hughes and Hughes, 1986), because it should provide access to the beneficial fitness consequences of increased size (Jackson, 1977; Sebens, 1982; Hughes and Jackson, 1985; Karlson, 1988) without the constraints of allometry.

However, despite the theoretical importance of isometry in colonial modular organisms, few studies have tested this prediction, and the available data are contradictory. Aerobic respiration, for example, scales isometrically with mass in the bryozoan *Electra pilosa* ($b = 0.97$; Hughes and Hughes, 1986) but allometrically in the soft coral *Alcyonium siderium* ($b = 0.88$; Sebens, 1987b). Moreover, chemical engineering and mass transfer theory predict that many colonial modular organisms with simple geometries should display allometric scaling (Patterson, 1992a). In this study, we revisit scaling in colonial modular organisms to determine whether their body plans do, indeed, provide a comprehensive escape from allometric constraints. More specifically, we test the null hypotheses that aerobic respiration (hereafter referred to as respiration) and the surface-area-to-biomass (SA:B) ratio scale isometrically (*i.e.*, proportionately) in the scleractinian *Siderastrea siderea*. Respiration was selected to examine the scaling of physiological traits because of its importance in generating ATP for synthetic and muscular work. The SA:B ratio was selected as a proxy for the SA:V ratio because biomass (B) can be determined easily with a gravimetric approach, and it is proportional to volume with a constant tissue density.

Siderastrea siderea was used as a model system for a colonial modular taxon because, as a scleractinian, it provides a consummate example of this structural clade. Additionally, *S. siderea* is ecologically important on Caribbean reefs (Goreau, 1959) and can be identified readily to species (Foster, 1979, 1980). The study was restricted to small (≤40 mm diam.), juvenile colonies (Soong, 1993) because they are tractable to investigation within the constraints of laboratory chambers designed to measure metabolism. Juvenile corals also have a strong effect on the population biology of reef corals (Bak and Meesters, 1999), and thus studies of their biology are likely to result in a better understanding of the processes driving coral demography. The full size range of *S. siderea* (to ≈1 m diam. and >100 y old, Foster, 1979) was not included because large colonies were rare at the study site (the north coast of Jamaica) and cannot be accommodated easily in laboratory apparatus. Thus, although the results of this study provide a valid test of scaling in an important life-history stage of a colonial modular taxon, the findings cannot be extrapolated beyond the size range of the colonies investigated.

Materials and Methods

Respiration

Small colonies of *Siderastrea siderea* were collected from 8.5 m depth on the forereef at Dairy Bull, about 2 km east of Discovery Bay, Jamaica, in January 1997. They were transported to the Discovery Bay Marine Laboratory (DBML) where they were epoxied (Z-Spar A-788) to tiles made of acrylic plastic. The epoxy was applied to the exposed skeleton so that only living coral tissue was left uncovered. Within 24 h, the tiles were secured to racks and returned to the collection site to recover. After more than 1 week of recovery, corals were selected haphazardly from the racks, returned to the laboratory, and placed in a darkened container supplied with flowing seawater. The corals were kept in darkness overnight, prior to respiration measurements, to avoid the confounding effect of light history on the respiration of symbiotic corals (Edmunds and Davies, 1988).

Respiration rates were measured as oxygen flux using polarographic oxygen electrodes that were connected to an oxygen meter (Cameron OM400) and inserted into the top of clear acrylic chambers. The chambers were designed to expose the corals to unidirectional flow while retaining the minimal volumes necessary for respirometry with small organisms (Fig. 1). A small chamber was used for corals roughly 20 mm in diameter, and a large chamber for corals 21 to 40 mm in diameter. Both chambers consisted of a circular working area with volumes of 332 and 680 ml, respectively, and were regulated at ambient seawater temperature (26°C) using a water jacket and bath (Haake D1). Water flow inside the chambers was created by a stirbar rotating at a constant rate. Flow rates at the periphery of the chambers, where the corals were located, were quantified using brine shrimp cysts (Johnson and Sebens, 1993), and were not significantly different between chambers (Mann Whitney *U* test, $U_s = 683.5$, $n_{1,2} = 40$, $P = 0.26$). The pooled flow rate for both chambers was 5.8 ± 0.1 cm s^{-1} (mean ± SE, $n = 80$).

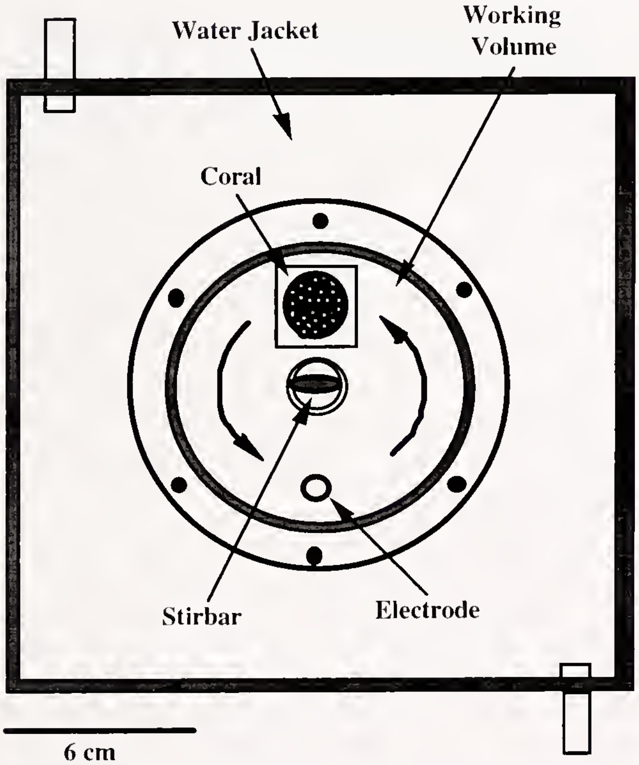

Figure 1. Plan view of the respiration chamber (drawn to scale). The chamber consisted of a cylindrical working volume (5 cm high × 14 cm in diam., 680 ml in volume) surrounded by a water jacket. A centrally located stirbar created a unidirectional flow (5.8 ± 0.1 cm s^{-1}) over the coral colony located on the periphery of the chamber; arrows indicate direction of flow.

Two oxygen electrodes were used (Strathkelvin E5046 and YSI Model 5739), and both were calibrated using a zero solution (0.01 *M* sodium tetraborate and sodium sulfite) and air-saturated seawater. Salinities were determined using a refractometer, barometric pressure was recorded, and oxygen solubilities were determined from Weiss (1970). Corals were placed into the chambers filled with filtered seawater (0.45 μm, FSW), and respiration rates were measured in darkness following 15-min acclimation to the chamber. All measurements were completed at an oxygen saturation above 80% (Edmunds and Davies, 1986), and data were recorded using a data acquisition system (Datacan, Sable Systems). Controls were run daily in the same manner using FSW alone. The rates of change in pO_2 in the experimental and control trials were calculated using simple linear regression ($r^2 > 0.94$). After accounting for controls, the respiration rate per coral (micromoles of oxygen per coral per hour) was calculated to examine metabolic scaling.

Surface area and biomass

After respiration measurements were completed, surface areas were estimated using the aluminum foil method (Marsh, 1970). In this technique, aluminum foil was molded over the surface of the coral; the foil was then removed, dried, and weighed; and the surface area was estimated using a previously derived relationship between area and weight. Dry tissue biomass was quantified by preserving the corals in 5% formalin in seawater, decalcifying in 5% HNO_3, and drying the resulting tissue tunic at 60°C for 7 days (Edmunds and Davies, 1986). Preliminary experiments using tissue from the anemone *Anthopleura xanthogrammica* demonstrated that the formalin and acid treatment resulted in a loss of 2.7% ± 0.7% (mean ± SE, $n = 10$) of the dry tissue. Therefore, the values of dry tissue biomass in the present study are likely to be slightly conservative.

Statistical analyses

Logarithmic linear regression was used to examine the scaling relationships. The slope of the regression provides the scaling exponent (*b*), and all analyses were completed using natural logarithms (ln). The scaling of metabolism was estimated by a regression analysis with the log of respiration (per coral) as the dependent variable and the log of dry tissue biomass as the independent variable. Changes in the ratio of surface area to volume were estimated by regression analysis with the log of surface area as the dependent variable and the log of dry tissue biomass as the independent variable, assuming that biomass and volume are related linearly. Model II (reduced major axis) regression analyses were used because the independent variables

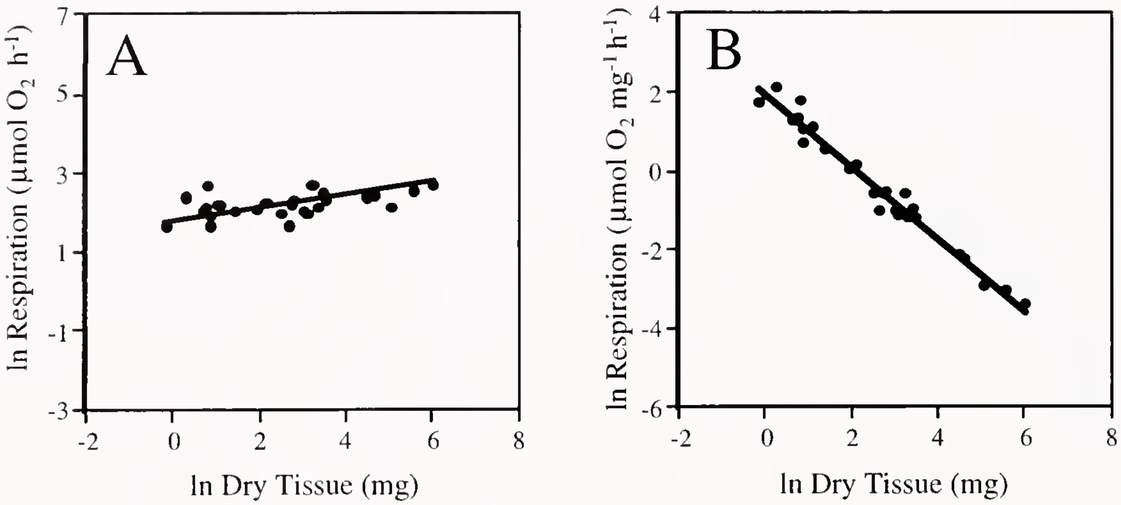

Figure 2. Respiration plotted against biomass in small colonies of *Siderastrea siderea.* (A) Regression of the log of the respiration rate per coral on the log of dry tissue biomass; regression equation: $y = 0.176x + 1.717$, $r = 0.499$. The slope of 0.176 ± 0.031 (±SE, $n = 26$ corals) deviates significantly from 1 ($t = 26.59$, df = 24, $P < 0.0001$), indicating allometric scaling. (B) Regression of the log of the mass-specific respiration rate on the log of dry tissue biomass (recalculated from the data in Fig. 2A); regression equation: $y = -0.924x - 1.9752$, $r = 0.986$.

were subject to measurement error (Ricker, 1973; Sokal and Rohlf, 1995). In this technique, the slope (or scaling exponent) is obtained by dividing the standard error of the dependent variable by the standard error of the independent variable, which results in a slope greater than that generated by least-squares linear regression (Sokal and Rohlf, 1995). The null hypothesis of isometry was tested using a t test (H_o: $b = 1$), where a significant deviation ($P \leq 0.05$) indicates an allometric relationship.

Results

Respiration

Respiration rates were estimated in 26 corals ranging in diameter between 3 and 37 mm. The regression of the log of respiration rate (micromoles of oxygen per coral per hour) on the log of colony dry tissue biomass (Fig. 2a) was significant ($F_{(1,24)} = 7.952$, $P < 0.01$), and produced a slope of 0.176 ± 0.031 (±SE, $n = 26$ corals), which deviated significantly from 1 ($t = 26.59$, df = 24, $P < 0.0001$). This significant departure from a slope of 1 indicates that respiration scaled allometrically on biomass such that respiration increased disproportionately more slowly than colony size (biomass). As a result, a doubling of biomass corresponds to only a 13% increase in the respiration rate per colony (Fig. 2a), and a 47% decline in mass-specific respiration (micromoles of oxygen per milligram of tissue per hour) (Fig. 2b).

Surface area on biomass

The scaling of colony surface area with biomass was quantified in 25 of the 26 corals; 1 coral was excluded as an outlier due to high leverage (Sokal and Rohlf, 1995). The regression of the log of surface area on the log of the dry tissue biomass of the colonies (Fig. 3) also was significant ($F_{(1,23)} = 294.973$, $P < 0.0001$), and the slope of 0.730 ± 0.041 (±SE, $n = 25$ corals) deviated significantly from 1 ($t = 6.60$, df = 23, $P < 0.0001$). This indicates that colony surface area scaled allometrically with biomass such that surface area increases disproportionately more slowly than

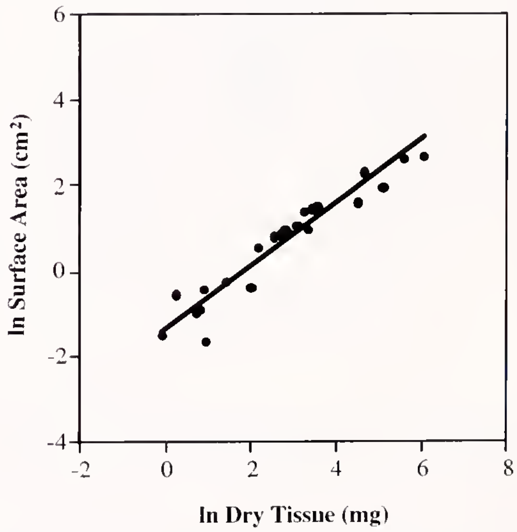

Figure 3. Colony surface area plotted against biomass in small colonies of *Siderastrea siderea.* Regression of the log of colony surface area on the log of dry tissue biomass; regression equation: $y = 0.730x - 1.356$, $r = 0.963$. The slope of 0.730 ± 0.041 (±SE, $n = 25$ corals) deviates significantly from 1 ($t = 6.60$, df = 23, $P < 0.0001$), indicating allometric scaling.

biomass, and the ratio of surface area to biomass declines with increasing colony size. As a result, a doubling of biomass corresponds to only a 66% increase in surface area. Moreover, the slope of 0.730 for surface area on biomass does not deviate significantly (t = 1.453, df = 23, P = 0.1597) from the expectation of geometric isometry (b = 0.67). Thus, the modular design of these small corals does not confer significantly higher ratios of surface area to biomass than would be expected if geometric similarity was maintained.

Discussion

Contrary to the isometric scaling predicted for colonial modular organisms (*sensu* Hughes and Hughes, 1986), respiration and surface area scaled allometrically with biomass in small colonies of *Siderastrea siderea*. As a result, both mass-specific respiration and the surface-area-to-biomass (SA:B) ratio declined with colony size. Thus, although respiration scales isometrically in at least one colonial modular organism—the encrusting bryozoan *Electra pilosa* (Hughes and Hughes, 1986)—the present results show that isometric scaling is not axiomatic with a colonial modular design. Instead, allometry describes the size-dependency of two traits in *S. siderea*, and has been demonstrated previously for respiration in the octocoral *Alcyonium siderium* (Sebens, 1987b) and predicted on the basis of chemical and mass-transfer theory (Patterson, 1992a). Although comparisons across taxa are difficult due to the wide variation in intraspecific metabolic scaling exponents, the exponent of 0.176 calculated for small colonies of *S. siderea* falls within the observed range (b = 0.15 − 1.28) of intraspecific exponents for metazoans (see Peters, 1983; Patterson, 1992a). Metabolic scaling exponents in unitary anthozoans range from 0.54 to 0.94 (Patterson, 1992a) and include the solitary scleractinian *Fungia scutaria* (b = 0.79; Krupp, 1982; exponent calculated in Patterson, 1992a). As for metabolic scaling in small colonies of *S. siderea*, we posit that the unusually small scaling exponent (b = 0.176) is a result of the changes in the SA:B ratio and the developmental stage of the small colonies investigated.

Maintaining a constant surface-area-to-volume (SA:V) ratio (and, with invariate biomass density, a constant SA:B ratio) is the theoretical basis for isometry in colonial modular organisms (Jackson, 1979). However, isometry can occur only where colony biomass is restricted to a single layer of modules with conserved dimensions; this design is typical of hydroids, scleractinians, and cheilostome bryozoans (Jackson, 1979). However, where there is metabolically active biomass outside the modules, the SA:B ratio decreases as extra-modular biomass increases volumetrically. Thus, the extra-modular biomass in octocorals (*i.e.*, the coenenchyme) and compound ascidians (*i.e.*, the gelatinous matrix) should favor allometric scaling (Jackson, 1979; Sebens, 1987a). These predictions are supported by experimental data from the encrusting bryozoan *Electra pilosa* and the fleshy octocoral *Alcyonium siderium* (cited above). However, although the single layer of uniformly sized polyps in scleractinians also should allow for a constant SA:B ratio, this is not the case for *S. siderea*, where colony surface area scales allometrically on biomass (b = 0.730). Thus, in small colonies of *S. siderea*, the SA:B ratio declines with increasing colony size, such that larger colonies have disproportionately more biomass than their smaller counterparts (Fig. 3).

The functional basis for the allometric scaling of the SA:B ratio is unknown, but it is probably related to calcification (Barnes, 1973) and the selective pressure for rapid growth in small corals (Jackson, 1977). Thus, the smallest corals may sustain high rates of linear growth (*i.e.*, calcification) at the expense of tissue growth, so that the existing tissues are "stretched" thinly over the increasing surface area. Then, as the colonies become larger, they may concentrate resources on tissue growth, thereby increasing biomass and tissue thickness. Support for this hypothesis comes from two studies. First, reanalysis of the data of Jokiel and Morrisey (1986) for the coral *Pocillopora damicornis* demonstrates allometric scaling of surface area with biomass (b = 0.700 ± 0.057, mean ± SE, n = 6) as well as respiration (b = 0.840 ± 0.041, mean ± SE, n = 6) (Jokiel and Morrisey, 1986). Thus, biomass is added more rapidly than surface area and, as in *S. siderea*, the resulting allometric scaling of the SA:B ratio provides a possible explanation for the allometric scaling of respiration in *P. damicornis*. Second, trade-offs in growth between skeleton and tissue, similar to those proposed for *S. siderea* (described above), have been reported for *Porites* from the Great Barrier Reef (Barnes and Lough, 1993), as have systematic differences in tissue thickness for the same species (Barnes and Lough, 1992). Indeed, the positive relationship between tissue thickness and colony height in *Porites* (Barnes and Lough, 1992), together with the large amount of extra-modular biomass (≈90% by thickness, Barnes and Lough, 1992), might be prominent in this genus. Thus, variation in tissue biomass, thickness, or both with colony size may be a general feature of scleractinian corals. However, in addition to putative changes in tissue thickness driving the observed changes in the SA:B ratio, it is possible that the SA:B ratio was biased by the use of the aluminum foil method (Marsh, 1970) to measure the surface area. This technique is widely used for determining the surface area of corals with relatively smooth and unconvoluted surfaces like those in *S. siderea* (see Hoegh-Guldberg, 1988, for an alternative approach), but it is unable to quantify the area of the expanded polyps. Quantifying the area of expanded polyps is made difficult by their highly variable morphology and degree of expansion and, as a result, previous studies have relied on geometric approximations to obtain polyp or tentacle area (Sebens, 1981). Regardless of the methodological difficulties, currently there is no evidence of systematic variation in polyp dimensions with colony size (*i.e.*, allometry); moreover, polyp dimensions may be highly conserved for mass-transfer purposes (Patterson, 1992a). Thus, given that the thickness of coral tissues is known to vary (*e.g.*, Barnes and Lough, 1992), we believe that changes in the SA:B ratio are more likely to be driven by tissue thickness than by the area of expanded polyps. Still, a definitive test of the hypothesized mechanism of variation in the SA:B ratio is required, and this will necessitate an analysis of tissue thickness and skeletal extension as a function of colony size.

The allometric scaling of the SA:B ratio in *S. siderea* could drive the scaling of respiration through indirect effects on mass transfer of metabolites to the coral tissue. Mass transfer with the surrounding seawater is determined, in part, by surface area, which decreases relative to biomass as *S. siderea* increases from 3 to 37 mm in diameter. Thus, all things being equal (*i.e.*, excluding the boundary layer arguments described below) and within the size range studied here, small corals should maintain relatively higher fluxes of metabolites than large corals, which could support the higher respiration rates observed in the small corals (Fig. 2). Additionally, increases in biomass will be accompanied by increases in biovolume that probably lengthen diffusion pathways (*i.e.*, the tissue thickness) and reduce the rates of solute transport (Patterson, 1992b). For the colony size range studied, the respiration of large *S. siderea* therefore may be depressed by limitations on the delivery of oxygen to metabolically active tissue. This hypothesis could be tested by measuring the magnitude of the flow dependency of respiration (*sensu* Patterson and Sebens, 1989), with the expectation of a greater effect in larger colonies than in smaller ones.

Although the scaling of the SA:B ratio provides a testable hypothesis to explain the scaling of respiration in *S. siderea*, it does not exclude the possibility that other factors might also be important. Of these, variation in energy expenditure among developmental phases (*i.e.*, colony sizes) has the greatest potential to explain, in part (or entirely), the allometric scaling of respiration. In benthic marine invertebrates, scaling exponents typically are affected by the size range and developmental phase of the organisms investigated (Zeuthen, 1953). Lower exponents are characteristic of early and late developmental phases and of the extremes of the natural size range. For example, metabolic scaling exponents (b) for the mussel *Mytilus edulis* change from 0.80 in recruits (<0.1 mg) to 0.95 in sub-adults (0.1 to 1 mg) and to 0.65 in adults (>1 mg) (Zeuthen, 1953). The low scaling exponents in the smallest (*i.e.*, youngest) size classes demonstrate that their metabolic rates are relatively high compared to those of the larger sub-adults, and are thought to be a consequence of the elevated energy expenditure necessary to sustain accelerated growth (Zeuthen, 1953). Size and age are poorly related in scleractinians (Hughes and Jackson, 1980), but the colonies of *S. siderea* used in the present study (≤37 mm diam.) are young relative to the largest colonies of this species (≈1 m diameter and >100 y old; Foster, 1979), and the smallest corals (3 mm diam.) may be only a few months old (Van Moorsel, 1988). Regardless of age, small corals are probably exposed to selective pressure for rapid growth (Jackson, 1977), as occurs in other colonial modular organisms (Jackson, 1977; Sebens, 1982; Karlson, 1988), because of the mortality risks of being small (Jackson, 1977). Thus, in addition to the SA:B explanation for allometric scaling in small colonies of *S. siderea* (described above), it is possible that the respiration rate (per coral) in the smallest colonies is elevated by the high metabolic rate of young tissues or by the costs of responding to the selective pressure for rapid growth.

Two other hypotheses could account for allometric scaling of respiration in small colonies of *S. siderea*—namely, mass transfer effects (*sensu* Patterson, 1992a) and the populations of endosymbiotic zooxanthellae—but these are not supported by the available data. The "mass transfer hypothesis" focuses on the importance of mass transfer in moving metabolites between the coral tissue and seawater and driving coral respiration (Patterson and Sebens, 1989; Patterson *et al.*, 1991). The boundary layers next to the coral have a critical role in determining rates of mass transfer (Denny, 1988; Patterson, 1992b) and are a function of the interaction of the flow regime with the size and shape of the coral colony. Based on these relationships, Patterson (1992a) predicted that metabolic scaling in aquatic organisms could be explained with a mass transfer argument. In short, changes in organism size and shape can be sufficient to alter mass transfer and support the allometric scaling of metabolism, with exponents similar to published values (Patterson, 1992a). For hemispherical objects like the small colonies of *S. siderea* used in the present study, the mass transfer explanation for metabolic scaling (*sensu* Patterson, 1992a) would predict an exponent (b) of ≈0.47 (Helmuth *et al.*, 1997). This is 2.7-fold higher than the allometric scaling exponent we calculated for respiration in small colonies of *S. siderea* that have hemispherical colonies ($b = 0.176$). One reason for this discrepancy is that the colonies used (3–37 mm diam.) were probably too small to establish their own equilibrium boundary layers (Denny, 1988) and were, instead, affected by upstream roughness elements in the respiration chamber (Gardella and Edmunds, unpubl. data). In other words, small colonies of *S. siderea* may be an exception to the mass transfer argument for allometric scaling (*sensu* Patterson, 1992a), because they all are too small (*i.e.*, ≤37 mm diam.) to affect their own boundary layers directly.

The "zooxanthellae hypotheses" focus on the role of the zooxanthellae in contributing to the respiration of the colony (*i.e.*, the cnidarian host plus algal symbionts) (Muscatine *et al.*, 1981; Edmunds and Davies, 1986) to account for allometric scaling of coral respiration. Thus, changes in the density or metabolic activity of zooxanthellae should affect the respiration of the colony and, if these changes are correlated with size, could affect metabolic scaling. In *S. siderea*, zooxanthellae densities cannot account for allometric scaling of respiration, because zooxanthellae densities scaled isometrically with biomass (Vollmer, 1999). It is possible, however, that the respiration rate per zooxanthella varied with colony size, but this possibility cannot be examined experimentally at the current time because zooxanthellar respiration can only be measured *in vitro*, and these rates may be different from those attained *in hospite* (Gates *et al.*, 1999). In the absence of *in hospite* determinations of zooxanthellar respiration, and given that zooxanthellae densities scale isometrically, we conclude tentatively that the zooxanthellae are unlikely to be a proximal cause of the allometric scaling of respiration in small *S. siderea*.

This study demonstrates allometric scaling in small colonies of *Siderastrea siderea* and underscores two mechanisms that probably drive this scaling—*i.e.*, disproportionate changes in the SA:B ratio and the developmental stage of the colonies examined. Because both mechanisms may be associated with the rapid growth necessary to escape the risky life-history stage of being small, allometric scaling probably has strong fitness consequences. While it remains to be seen whether the present findings are applicable to other species, or to a larger size range of colonies, further studies of allometric scaling in scleractinians will be valuable.

Acknowledgments

This research was submitted in partial fulfillment of the Master of Science degree to S. V. Vollmer at California State University, Northridge (CSUN). We thank R. C. Carpenter, D. Carlon, and three anonymous reviewers for their comments on earlier drafts of this paper. Field work was made possible through the generosity of M. Haley and the staff of the Discovery Bay Marine Laboratory (DBML), and numerous dive buddies who assisted in the field, including G. F. River and S. Tallack. This research was funded with a grant from the CSUN Office of Graduate Studies and International Programs (SVV) and a CSUN Research and Grants Award (PJE). This is DBML contribution number 623.

Literature Cited

Altman, P. L., and D. S. Dittmer. 1968. *Metabolism*. Federation of the American Society of Experimental Biologists, Bethesda, MD.

Bak, R. P. M., and E. H. Meesters. 1999. Population structure as a response of coral communities to global change. *Am. Zool.* **39:** 56–65.

Barnes, D. J. 1973. Growth in colonial scleractinians. *Bull. Mar. Sci.* **23:** 280–298.

Barnes, D. J., and J. M. Lough. 1992. Systematic variations in the depth of skeleton occupied by coral tissue in massive colonies of *Porites* from the Great Barrier Reef. *J. Exp. Mar. Biol. Ecol.* **159:** 113–128.

Barnes, D. J., and J. M. Lough. 1993. On the nature and causes of density banding in massive coral skeletons. *J. Exp. Mar. Biol. Ecol.* **167:** 91–108.

Brody, S. 1945. *Bioenergetics and Growth*. Reinhold, New York.

Denny, M. W. 1988. *Biology and Mechanics of the Wave-swept Environment*. Princeton University Press, Princeton, NJ.

Economos, A. C. 1981. The largest land mammal. *J. Theor. Biol.* **89:** 211–215.

Edmunds, P. J., and P. S. Davies. 1986. An energy budget for *Porites porites* (Scleractinia). *Mar. Biol.* **92:** 339–347.

Edmunds, P. J., and P. S. Davies. 1988. Post-illumination stimulation of respiration rate in the coral *Porites porites*. *Coral Reefs* **8:** 7–9.

Foster, A. B. 1979. Phenotypic plasticity in the reef corals *Montastraea annularis* (Ellis & Solander) and *Siderastrea siderea* (Ellis & Solander). *J. Exp. Mar. Biol. Ecol.* **39:** 25–54.

Foster, A. B. 1980. Environmental variation in skeletal morphology within the Caribbean reef corals *Montastraea annularis* and *Siderastrea siderea*. *Bull. Mar. Sci.* **30:** 678–709.

Gates, R. D., K. Y. Bil, and L. Muscatine. 1999. The influence of an anthozoan "host factor" on the physiology of a symbiotic dinoflagellate. *J. Exp. Mar. Biol. Ecol.* **232:** 241–259.

Goreau, T. F. 1959. The ecology of Jamaican coral reefs. I. Species composition and zonation. *Ecology* **40:** 67–90.

Gould, S. J. 1966. Allometry and size in ontogeny and phylogeny. *Biol. Rev. Camb. Philos. Soc.* **41:** 587–640.

Gould, S. J. 1977. *Ontogeny and Phylogeny*. Belknap Press of Harvard University Press, Cambridge, MA.

Helmuth, B. S. T., E. F. Stockwell, and D. R. Brunbaugh. 1997. Morphological and environmental determinants of mass flux of corals. *Proc. 8th Int. Coral Reef Symp.* **2:** 1103–1108.

Hemmingsen, A. M. 1960. Energy metabolism as related to body size and respiratory surfaces, and its evolution. *Rep. Steno Mem. Hosp. Nord. Insulin Lab.* **9:** 6–110.

Hoegh-Guldberg, O. 1988. A method for determining the surface area of corals. *Coral Reefs* **7:** 113–116.

Hughes, R. N., and J. M. Cancino. 1985. An ecological overview of cloning in Metazoa. Pp. 153–186 in *Population Biology and Evolution of Clonal Organisms*, J. B. C. Jackson, L. W. Buss, and R. E. Cook, eds. Yale University Press, New Haven.

Hughes, D. J., and R. N. Hughes. 1986. Metabolic implications of modularity: studies on the respiration and growth of *Electra pilosa*. *Philos. Trans. R. Soc. Lond.* **313:** 23–29.

Hughes, T. P., and J. B. C. Jackson. 1980. Do corals lie about their age? Some demographic consequences of partial mortality, fission and fusion. *Science* **209:** 713–715.

Hughes, T. P., and J. B. C. Jackson. 1985. Population dynamics and life histories of foliaceous corals. *Ecol. Monogr.* **55:** 141–166.

Jackson, J. B. C. 1977. Competition on marine hard substrata: the adaptive significance of solitary and colonial strategies. *Am. Nat.* **111:** 743–767.

Jackson, J. B. C. 1979. Morphological strategies of sessile animals. Pp. 499–555 in *Biology and Systematics of Colonial Organisms*, G. Larwood and B. R. Rosen, eds. Academic Press, London.

Johnson, A. S., and K. P. Sebens. 1993. Consequences of a flattened morphology: effects of flow on feeding rates of the scleractinian coral *Meandrina meandrites*. *Mar. Ecol. Prog. Ser.* **99:** 99–114.

Jokiel, P. L., and J. I. Morrissey. 1986. Influence of size on primary production in the reef coral *Pocillopora damicornis* and the macroalga *Acanthophora spicifera*. *Mar. Biol.* **91:** 15–26.

Karlson, R. H. 1988. Size-dependent growth in two zoanthid species: a contrast in clonal strategies. *Ecology* **69:** 1219–1232.

Kleiber, M. 1932. Body size and metabolism. *Hilgardia* **6:** 315–353.

Kleiber, M. 1961. *The Fire of Life.* Wiley, New York.

Krupp, D. A. 1982. The composition of the mucus from the mushroom coral, *Fungia scutaria. Proc. 4th Int. Coral Reef Symp., Manila* **2:** 69–73.

Marsh, J. A. 1970. Primary productivity of reef-building calcareous red algae. *Ecology* **51:** 255–265.

McMahon, T. A. 1973. Size and shape in biology. *Science* **179:** 1201–1204.

Muscatine, L., L. R. McCloskey, and R. E. Marian. 1981. Estimating the daily contribution of carbon from zooxanthellae to coral animal respiration. *Limnol. Oceanogr.* **26:** 601–611.

Patterson, M. R. 1992a. A chemical engineering view of cnidarian symbioses. *Am. Zool.* **32:** 566–582.

Patterson, M. R. 1992b. A mass transfer explanation of metabolic scaling relations in some aquatic invertebrates and algae. *Science* **255:** 1421–1423.

Patterson, M. R., and K. P. Sebens. 1989. Forced convection modulates gas exchange in cnidarians. *Proc. Natl. Acad. Sci. USA* **86:** 8833–8836.

Patterson, M. R., K. P. Sebens, and R. R. Olson. 1991. *In situ* measurements of flow effects on primary production and dark respiration in reef corals. *Limnol. Oceanogr.* **36:** 936–948.

Pennycuick, C. J. 1972. *Animal Flight.* Edward Arnold, London.

Peters, R. H. 1983. *The Ecological Implications of Body Size.* Cambridge University Press, Cambridge.

Ricker, W. E. 1973. Linear regression in fishery research. *J. Fish. Res. Board Can.* **11:** 559–623.

Rubner, M. 1883. Ueber den Einfluss der korpergrosse auf Stoffund Kraftwechsel. *Z. Biol.* **19:** 535–562.

Schmidt-Nielsen, K. 1974. Scaling in biology: the consequences of size. *J. Exp. Zool.* **194:** 287–308.

Schmidt-Nielsen, K. 1984. *Scaling: Why Is Animal Size So Important?* Cambridge University Press, Cambridge.

Sebens, K. P. 1979. The energetics of asexual reproduction and colony formation in benthic marine invertebrates. *Am. Zool.* **19:** 683–697.

Sebens, K. P. 1981. The allometry of feeding, energetics, and body size in three sea anemone species. *Biol. Bull.* **161:** 152–171.

Sebens, K. P. 1982. Competition for space: growth rate, reproductive output, and escape in size. *Am. Nat.* **120:** 189–197.

Sebens, K. P. 1987a. The ecology of indeterminate growth in animals. *Annu. Rev. Ecol. Syst.* **18:** 371–407.

Sebens, K. P. 1987b. Coelenterata. Pp. 55–120 in *Animal Energetics,* T. P. Pandian and F. J. Vernberg, eds. Academic Press, New York.

Sokal, R. R., and F. J. Rohlf. 1995. *Biometry.* Freeman, New York.

Soong, K. 1993. Colony size as a species character in massive reef corals. *Coral Reefs* **12:** 77–83.

Van Moorsel, G. 1988. Early maximum growth of stony corals (Scleractinian) after settlement of artificial substrata on a Caribbean reef. *Mar. Ecol. Prog. Ser.* **50:** 127–135.

Vollmer, S. V. 1999. Physiological scaling in small scleractinians. Master's thesis. California State University, Northridge, California.

Weiss, R. F. 1970. The solubility of nitrogen, oxygen, and argon in water and seawater. *Deep-Sea Res.* **17:** 721–735.

Zeuthen, E. 1953. Oxygen uptake as related to body size in organisms. *Q. Rev. Biol.* **28:** 1–12.

Reference: *Biol. Bull.* **199:** 29–40. (August 2000)

Frog Lim-1-like Protein Is Expressed Predominantly in the Nervous Tissue, Gonads, and Early Embryos of the Bivalve Mollusc *Mytilus galloprovincialis*

MARIO TORRADO AND ALEXANDER T. MIKHAILOV*

Developmental Biology Unit, Institute of Health Sciences, University of La Coruña, As Xubias,
La Coruña 15006, Spain

Abstract. In a few well-known cases, the biological consequences of the disruption of *lim-1* homeodomain (HD) genes have demonstrated the important roles of these genes in vertebrate development, especially in the nervous tissue, kidney, and gonads. Functional assay approaches require information not only about *lim-1* gene organization, but also about properties and tissue localization of Lim-1 proteins. Although *lim-1* genes have been identified in certain phyla of invertebrates, no information is available on Lim-1 proteins and genes in bivalve molluscs. Our study represents the beginning stage of identification of the Lim-1-related proteins in marine bivalves. Using antibodies against the C-terminal region of the *Xenopus laevis* Lim-1 protein, we describe cross-reactive antigen patterns in adults and early embryos of the mussel *Mytilus galloprovincialis*, as well as in sea urchin and chick embryos. In adult mussels, nervous ganglia and gonads display the most prominent Lim-1 immunoreactivity. Further, the antibodies verified the prediction that mussel Lim-1 antigens, like Lim-1 HD proteins in general, can be localized in the nucleus. Moreover, antibody detection allowed us to identify the Lim-1-like antigens in unfertilized mature eggs, as well as in very early embryos of bivalve molluscs and sea urchins (*Strongylocentrotus purpuratus*). In mussel eggs and embryos, Lim-1 antigens are expressed in multiple forms (40, 45, and 65 kDa), as detected by SDS-PAGE followed by Western blot. Taken together, the observations emphasize the conservation of the Lim-1 protein expression pattern in the nervous tissue and gonads of different animal groups, and demonstrate that Lim-1-like polypeptides can be maternally accumulated in eggs and, therefore, are present in very early embryos before zygotic expression of the genes begins.

Introduction

A cysteine-rich zinc finger domain, named LIM, was first identified in the *Caenorhabditis elegans* homeobox genes *lin-11* and *mec-3*, and in the rat DNA binding factor *Isl-1*. Then the LIM domain was found in a variety of proteins including transcription factors, cytoskeletal proteins, and LIM kinases (Dawid *et al.*, 1998; Bach, 2000). LIM domains appear to play a primary role in protein-protein interactions, through the formation of dimers with identical or different LIM domains or by binding distinct proteins (Breen *et al.*, 1997; Dawid *et al.*, 1998; Curtis and Heiling, 1998; Hobert and Ruvkun, 1998; Hobert and Westphal, 2000).

Phenotypic analysis of patterns of *lim* gene expression reveals that the genes can participate in a number of important events in early embryonic development, as well as in cell fate determination and cell differentiation at advanced stages of organogenesis. Moreover, some *lim* genes are constitutively expressed in adult tissues, where they may contribute to certain tissue-specific functions (Dawid *et al.*, 1998; Hobert and Westphal, 2000). The early and late ontogenetic expression phases of *lim* genes suggest that they have multiple and distinct functions at different stages of the animal life cycle. In the latter context, the LIM containing homeodomain (HD) *lim-1* genes have been most extensively studied in a range of animals.

Lim-1 encodes a protein with a pair of LIM domains located N-terminal to the HD. In vertebrates, *lim 1* was originally identified in the frog, *Xenopus laevis*, as *Xlim 1* (Taira *et al.*, 1992). In *X. laevis*, the *Xlim-1* is expressed in

Received 13 December 1999; accepted 8 May 2000.

* To whom correspondence should be addressed: E-mail: margot@udc.es

Abbreviations: LIM, an abbreviation derived from the names of three homeodomain transcription factors, containing a cysteine-rich zinc-finger domain (*i.e.*, LIM-domain): Lin-11 of *Caenorhabditis elegans*, Isl-1 of the rat, and Mec-3 of *C. elegans*; MW, molecular weight; SDS-PAGE, sodium dodecylsulfate polyacrylamide gel electrophoresis; HD, homeodomain.

the Spemann's organizer during gastrula stages, and in late embryos primarily in the nervous system and kidney (Taira *et al.*, 1992, 1994, 1997; Wallingford *et al.*, 1998; Carroll *et al.*, 1999a; Carroll and Vize, 1999). Similar patterns of *lim-1* expression have been observed in fishes (Toyama *et al.*, 1995; Carroll *et al.*, 1999b), chickens (Tsuchida *et al.*, 1994), mice (Fujii *et al.*, 1994; Shawlot and Behringer, 1995; Li *et al.*, 1999), rats (Furuyama *et al.*, 1994; Karavanov *et al.*, 1998), and humans (Dong *et al.*, 1997). The biological consequence of the disruption of *lim-1* HD genes or modifications of their expression patterns have demonstrated the crucial role of these genes in development, especially in the nervous tissue, kidney, and gonads (Shawlot and Behringer, 1995; Shawlot *et al.*, 1999; Taira *et al.*, 1997; Carroll and Vize, 1999).

In invertebrates, *lim-1* related genes have been identified in nematodes, fruit flies, and sea urchins. The *lin-11* gene of *C. elegans* (the closest homolog of amphibian and mammalian *lim-1*) is expressed in different subsets of neurons and in the vulva, and it is essential for uterine morphogenesis (Hobert *et al.*, 1998; Hobert and Westphal, 2000; Newman *et al.*, 1999). In *Drosophila*, the gene termed *dlim 1* is expressed in the head, the brain lobes, and in neurons of the ventral nerve cord (Lilly *et al.*, 1999). The *lim-1*-related HD gene of the sea urchin (*Hemicentrotus pulcherrimus*), *HpLim1*, is detected in early embryos and involved in the differentiation of endoderm, mesenchyme, and aboral ectoderm (Kawasaki *et al.*, 1999).

Thus, although expression in neural tissues seems to be a common feature of Lim-1-related HD factors in both vertebrates and invertebrates, most of these factors are also characterized by their expression in excretory and reproductive organ systems. These expression phenotypes have been described mainly at the molecular level by analysis of *lim-1* gene transcription patterns. An alternative approach is the analysis of post-translational Lim-1 expression by immunochemical methods. This approach makes it possible to measure this factor at the protein level in different cell types and to detect other tissues that express the polypeptide at different stages of development and in the adult state (Karavanov *et al.*, 1996; Brown *et al.*, 1999; Lilly *et al.*, 1999; Shimono and Behringer, 1999; Mauch *et al.*, 2000).

To our knowledge, no information is available on Lim-1 proteins (genes) in marine bivalve molluscs, although such data would be useful for further comparative analysis of Lim-1 expression patterns and functions in invertebrates and vertebrates (Hobert and Westphal, 2000). Our study represents the beginning stage of the identification of Lim-1-related proteins in bivalve molluscs. We describe the distribution patterns of immunoreactive Lim-1-like proteins in adults and early embryos of the mussel *Mytilus galloprovincialis*. We also report the first examination of Lim-1 antigen signals in sea urchin (*Strongylocentrotus purpuratus*) embryos, as well as in different compartments of the chick embryo brain.

Materials and Methods

Animals and embryos

Adult mussels (*Mytilus galloprovincialis*) and sea urchins (*Strongylocentrotus purpuratus*) were purchased during the spawning season (April–May of 1999) from commercial suppliers in La Coruña (Galicia, NW Spain). Published procedures (Sprung and Bayne, 1984; Holland and Holland, 1993; Mikhailov *et al.*, 1996) were followed for stripping of animals to obtain oocytes and sperm and for the subsequent *in vitro* fertilization and culture of embryos. At each chronological stage, the bulk of the embryos were re-collected, placed on ice, and typed morphologically under a dissecting microscope (Nikon). The embryos, selected according to morphology, were put into centrifuge tubes containing sterile seawater and permitted to settle to the bottom of tubes or pelleted by low-speed centrifugation; then the upper solution was discarded. Fertilized chicken (*Gallus gallus*) eggs were obtained from the cooperative chick network hatchery (Ferrol, Province of La Coruña, Galicia) and incubated at 37°C. Different brain regions (forebrain, optic lobes, and cerebellum) were microsurgically isolated in cold minimum essential medium (MEM; Gibco) and pelleted by low-speed centrifugation.

Tissue dissection and processing

Before use, adult mussels (*M. galloprovincialis*) were kept in a dry state for 1 h at 4°C. Mussels were opened with the aid of scalpel and placed on ice; a small portion of gonad material was microscopically examined to determine the sex of the individual. Different tissues and organs (gonad, foot, labial palps, hepatopancreas, gill, and fragments of posterior adductor muscle) were excised, rinsed in sterile seawater, and blotted on sterile filter paper. To obtain cell suspensions of sperm or oocyte, gonad follicle biopsy was performed as described in Torrado and Mikhailov (1998). Then, follicle luminal masses were aspirated and resuspended in ice-cold sterile seawater; the released cell suspension was microscopically tested for the presence of spermatozoa or oocytes. The sperm suspension was then centrifuged (100 × *g*, 5 min, 2°C), the oocytes were permitted to settle to the bottom of the tubes, and the rinse solution was discarded. For some experiments, gonad collecting tubules (with adjacent connective tissue) were dissected manually from the ripe male or female gonad and the excised tissue was microscopically examined to definitively determine the absence of gametes (spermatozoa or oocytes) in the tubule lumen. Isolated tissues were additionally shaken in ice-cold sterile seawater for 20 min; after settling, rinse solutions were discarded. Pedal ganglia (see Fig. 4A) were microsurgically dissected under a stereomicroscope (Nikon), pooled in ice-cold sterile seawater, and pelleted by low-speed centrifugation. When the samples were not homogenized immediately, they were stored at −85°C for several days.

Spent male gonads were sampled in 1998, and the corresponding frozen and Bouin-fixed tissue fragments were stored in liquid nitrogen and ethanol (70%), respectively.

Sample preparation

Mussel and sea urchin eggs and embryos were resuspended in cooled deionized water containing 2 m*M* EDTA (Merck), 6 *M* urea (Merck), and the protease inhibitor cocktail P2714 (Sigma). The supernatants obtained after centrifugation (30,000 × *g*, 8°C, 30 min) were mixed with SDS sample buffer containing the protease inhibitor cocktail, kept for 1 h at room temperature, and stored at −30°C until use. All other tissue samples were first homogenized in 1:5 (v/v) ratio in 100 m*M* Tris (Sigma), 2 m*M* EDTA (Merck) solution, containing the protease inhibitor cocktail. After centrifugation (10,000 × *g*, 2°C, 30 min), the supernatants were discarded, and the pellets were then re-extracted and assayed as described for embryos.

Antibodies

Anti-XLim-1 antibodies were a generous gift from Dr. A. A. Karavanov and Prof., Dr. I. Dawid. These polyclonal rabbit antibodies produced against the C-terminal region of the XLim-1 downstream of the HD (amino acids 265-403) (Taira *et al.*, 1992) have been characterized and shown to cross-react with Lim-1 proteins of fishes, mice, rats, and humans (Karavanov *et al.*, 1996, 1998). Gamma-globulin fraction was obtained from anti-XLim-1 serum with the aid of the Mab Trap G II Kit for antibody purification (Pharmacia), according to the manufacturer's protocol. The fraction was concentrated using concentrator units (Millipore), supplemented by glycerol (Merck) at a final concentration of 50%, and stored at −20°C in aliquots. Chemicon has recently commercialized these anti-XLim-1 antibodies.

Protein determination

Protein concentration was measured (Ultrospec 1000E spectrophotometer, Pharmacia) according to the Bradford method using rabbit immunoglobulin G (Sigma) or bovine serum albumin (Sigma) as standards.

SDS-PAGE assays

For all separations, the Mini-Protean II electrophoretic cell (Bio-Rad) was used. Samples were electrophoresed using 5% stacking and 10% resolving Tris-glycine SDS-polyacrylamide gels (Bio-Rad). The gels were stained with Coomassie blue R250 (Sigma) or electrophoretically transferred to membranes. The apparent molecular weights of the bands were determined by comparing low and high molecular weight calibration kits (Pharmacia) in the same gel. A micro-preparative variant of SDS-PAGE was performed as previously described (Mikhailov *et al.*, 1997) using a Mini-Protean II comb with one reference well. After electrophoresis, the reference gel strip was stained and used for isolating the Lim-1-containing fraction in the remaining gel slab. Alternatively, whole gel slabs were stained with Coomassie solution (0.0004% in 20% methanol and 3% acetic acid), and fractions of interest were cut out (Mikhailov *et al.*, 1996). The protein was eluted from gel fractions so obtained using a model 442 electro-eluter (Bio-Rad) in accordance with the manufacturer's recommendation; eluted solutions were concentrated using microconcentration units (Amicon, the 30-kDa cut-off membrane).

Blotting assays

Proteins resolved in 10% SDS-PAGE were transferred to nylon (Nytran, Schleicher and Schuell) or nitrocellulose (Optitran, Schleicher and Schuell) membranes by routine methods (Mikhailov *et al.*, 1997) using the mini Trans-Blot cell (Bio-Rad). Protein loading and localization of molecular weight standards was verified by membrane staining with amido black (Merck) or Ponceau S (Sigma). For immunodetection, the blots were incubated in blocking solution containing 20% of normal horse serum (Sigma) at room temperature for 1 h and further assayed as described in Mikhailov and Simirsky (1991). As primary antibodies, rabbit anti-XLim-1 or rabbit pre-immune (negative control) gamma-globulin fractions were used at appropriate dilutions. Peroxidase-labeled anti-rabbit immunoglobulins (Sigma) were used as the second-stage reagent, and diaminobenzidine (Sigma) was used to develop the blots. The relative amounts of antibody-labeled proteins were quantified by densitometry (GS-700 densitometer, Bio-Rad) and image software (Molecular Analysis, Bio-Rad). For total carbohydrate detection, blots were treated with an Immun-Blot kit (Bio-Rad) for glycoprotein detection as described (protocol 1A) by the manufacturer; chicken egg ovalbumin (Sigma) and rabbit liver carboxylesterase (Sigma) were used as positive controls. For a precise comparison of the position of the glycoprotein signal with that of Lim-1 immunoreactivity, the blot membrane was cut (along the direction of electrophoretic separation) at the middle of the run pocket width; one half was treated with Immun-Blot kit and the other with anti-XLim-1 antibodies (see Fig. 3C,D).

Deglycosylation assay

Extracts and Lim-1-containing fractions of mussel pedal ganglia and forebrains of 16-day-old chick embryos were desalted (using Microcon units), re-dissolved in 250 m*M* sodium phosphate (Merck), pH 6.0, and treated with an enzymatic deglycosylation kit (Bio-Rad) according to the manufacturer's denaturing protocol. Briefly, both neurominidase (EC 3.2.1.18) and *O*-glycosidase (EC 3.2.1.97) were first added to the reaction vials; after the incubation and denaturation step, *N*-glycosidase F (EC 3.5.1.52) was added to the mixture. To determine deglycosylation efficiently, samples (before and after deglycosylation) were subjected to SDS-PAGE followed by Coomassie staining (to detect the shift in band mobility) or blotting. Blots were treated with an Immun-Blot kit (Bio-Rad) for glycoprotein detection to additionally check the efficiency of the deglycosylation reaction. Bovine fetuin (Bio-Rad) and rabbit liver carboxylesterase (Sigma) were used as positive controls.

Ultrafiltration procedures

Lim-1-containing fractions isolated from mussel pedal ganglia and forebrains of 16-day-old chick embryos were subjected to subsequent ultrafiltration using Microcon micro-units with 100-kDa and 50-kDa cut-off YM membranes (Amicon) according to the manufacturer's recommendation. Bovine serum albumin (Sigma) and chicken ovalbumin (Sigma) solutions (1 mg/ml) were used as reference proteins. To prevent aggregation, urea (Merck) and SDS (Bio-Rad) were added to starting protein solutions at final concentrations of 6 *M* and 1%, respectively. Each sample was first applied on the Microcon-100 unit and centrifuged at 2500 × *g* for 30 min at 10°C. The resulting filtrate was then introduced into a sample reservoir of the Microcon-50 unit and centrifuged at 12,000 × *g* for 20 min at 10°C. The volume of each retained and filtered fraction so obtained was adjusted to that of the starting sample, and the solutions were subjected to SDS-PAGE followed by Western blot with anti-XLim-1 antibodies.

Immunocytochemistry

Mussel pedal ganglia were fixed in 100 m*M* 3-(*N*-morpholino) propane sulfonic acid (MOPS; Sigma), 2 m*M* $MgSO_4$ (Panreac), 2 m*M* EGTA (Merck), 3.8% formaldehyde (Panreac) for 1 h at room temperature. Standard histological techniques were used for sample dehydration, embedding in paraffin, sectioning at 6 μm, deparaffinization, and rehydration (Mikhailov and Simirsky, 1991). The slides were precoated with 3-aminopropyltriethoxysilane (Sigma). Prior to immunostaining, sections were blocked with 20% normal horse serum in 50 m*M* Tris-HCl, pH 8.0. Sections were then incubated with different dilutions of the anti-XLim-1 immunoglobulin fraction (3 h at room temperature or overnight at 4°C) and secondary antibodies conjugated to alkaline phosphatase (Boehringer-Mannheim). Antibody dilutions were prepared in blocking solution. All incubations were followed by six washes (10 min in each) in 50 m*M* Tris-HCl, pH 8.0. Staining was developed using 5-bromo-4-chloro-2-indolyl-phosphate (Sigma) and 4-nitro blue tetrazolium chloride as substrates (Sigma) as described in Karavanov *et al.* (1996). The sections were mounted in Permount (Fisher) and examined under the Nikon Microphot microscope. Control experiments were included (1) omitting anti-XLim-1 antibodies, (2) replacing the latter by normal rabbit immunoglobulins (Sigma), and (3) using anti-XLim-1 antibodies preadsorbed by fixed pedal ganglia or by foot tissue of *M. galloprovincialis*. Fixation was done in 3.8% formaldehyde as above, followed by a methanol wash. Using micro-forceps, fixed tissues were ground, rehydrated in 50 m*M* Tris-HCl, pH 8.0, blocked in blocking solution for 2 h, pelleted by a low-speed centrifugation, resuspended in anti-XLim-1 antibody solution (at 1/50 or 1/200 dilution), and incubated overnight at 4°C. For some experiments, anti-XLim-1 antibodies were depleted prior to staining by incubation at 1/50 dilution with hyperfixed *Xenopus laevis* embryos (this was performed by Dr. A. A. Karavanov and Dr. A. T. Mikhailov in the laboratory of Prof. I. Dawid).

Histological analysis

A portion of male ripe and spent gonads of *M. galloprovincialis* was fixed in Bouin's solution, embedded in paraffin, cut into 6-μm sections, and stained with hematoxylin-eosin; the gonadosomatic index was estimated from the sections and expressed as the percentage of the gonad occupied by follicle structures (Mikhailov *et al.*, 1996; Torrado and Mikhailov, 1998).

Results and Discussion

In this study we used rabbit polyclonal antibodies against a C-terminal region (as an immunogen) of the *Xenopus laevis* Lim-1 protein (*i.e.*, anti-XLim-1 antibodies). It has been shown that these antibodies detect the Lim-1 protein in *X. laevis* and also cross-react with Lim-1 polypeptides of the mouse (Karavanov *et al.*, 1996; Shimono and Behringer, 1999) and rat (Karavanov *et al.*, 1998). These studies have also demonstrated the high specificity of the antibodies to Lim-1 proteins and the absence of any discrepancy between the expression patterns of protein and mRNA. Note that the transcriptional activation domain of *Xlim-1* resides in its carboxyl terminus (Breen *et al.*, 1997).

Although it is generally accepted that the C-terminal peptide is a good choice for the production of antibodies specific to a protein of interest (Hancock and Evan, 1992), we decided to test, additionally, the degree of "specificity" of the *Xlim-1* C-terminal region (used as an immunogen) for Lim-1 proteins. Using the BLAST program (Altschul *et al.*, 1997), we performed alignments of the C-terminal sequence of *Xlim-1* with all the protein sequences listed in the SWISSPROT database (Bairoch and Apweiler, 2000). The most similar (similarity 80%–90%; Fig. 1) sequences, which were aligned first, are those of the fish, chick, mouse, and human Lim-1. Frog and fish Lim 5 factors are characterized by significantly lower primary structural similarity (47% and 46%, respectively) to the *Xlim-1* C-terminus sequence. It is significant that the regions of homology reside only in the C-terminus of the sequences mentioned above. Other sequences returned by the BLAST program displayed values of similarity with the C-terminus of *Xlim-1* (used as a query) that are not distinguishable from those

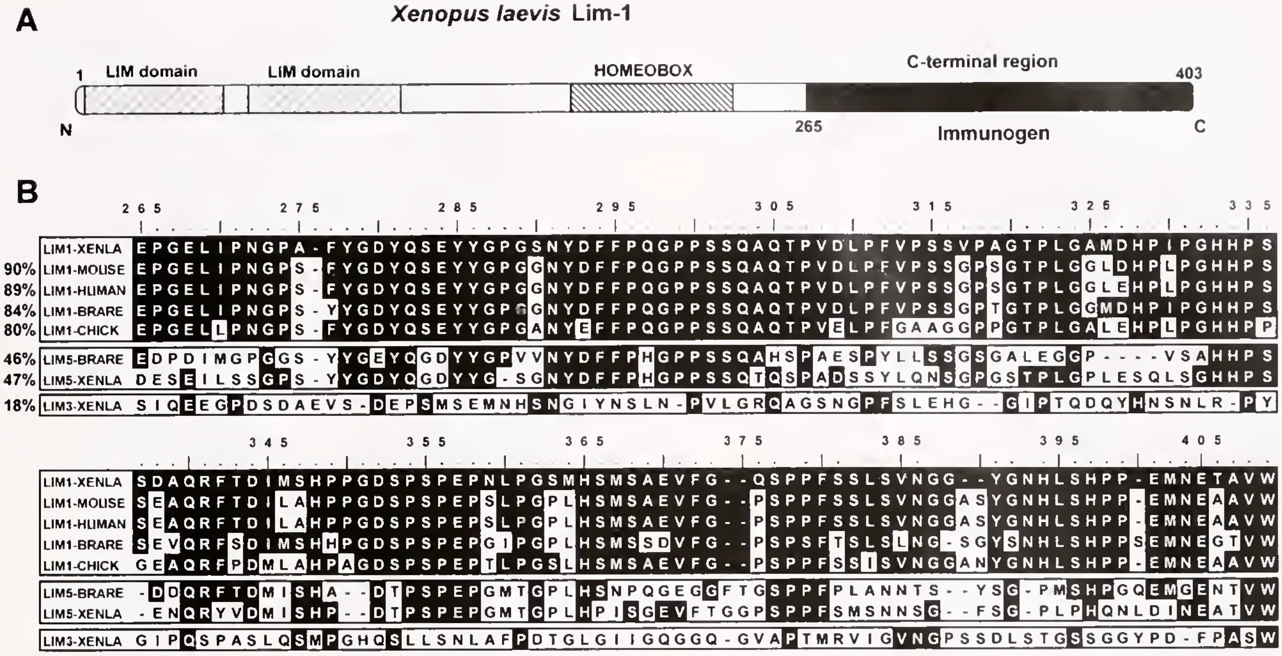
A
Xenopus laevis Lim-1
1
LIM domain
LIM domain
HOMEOBOX
C-terminal region
403
N
265
Immunogen
C
B
265 275 285 295 305 315 325 335
LIM1-XENLA EPGELIPNGPA-FYGDYQSEYYGPGSNYDFFPQGPPSSQAQTPVDLPFVPSSVPAGTPLGAMDHPIPGHHPS
90% LIM1-MOUSE EPGELIPNGPS-FYGDYQSEYYGPGGNYDFFPQGPPSSQAQTPVDLPFVPSSGPSGTPLGGLDHPLPGHHPS
89% LIM1-HUMAN EPGELIPNGPS-FYGDYQSEYYGPGGNYDFFPQGPPSSQAQTPVDLPFVPSSGPSGTPLGGLEHPLPGHHPS
84% LIM1-BRARE EPGELIPNGPS-YYGDYQSEYYGPGGNYDFFPQGPPSSQAQTPVDLPFVPSSGPTGTPLGGMDHPIPGHHPS
80% LIM1-CHICK EPGELLPNGPS-FYGDYQSEYYGPGANYEFFPQGPPSSQAQTPVELPFGAAGGPPGTPLGALEHPLPGHHPP
46% LIM5-BRARE EDPDIMGPGGS-YYGEYQGDYYGPVVNYDFFPHGPPSSQAHSPAESPYLLSSGSGALEGGP----VSAHHPS
47% LIM5-XENLA DESEILSSGPS-YYGDYQGDYYG-SGNYDFFPHGPPSSQTQSPADSSYLQNSGPGSTPLGPLESQLSGHHPS
18% LIM3-XENLA SIQEEGPDSDAEVS-DEPSMSEMNHSNGIYNSLN-PVLGRQAGSNGPFSLEHG--GIPTQDQYHNSNLR-PY
345 355 365 375 385 395 405
LIM1-XENLA SDAQRFTDIMSHPPGDSPSPEPNLPGSMHSMSAEVFG--QSPPFSSLSVNGG--YGNHLSHPP-EMNETAVW
LIM1-MOUSE SEAQRFTDILAHPPGDSPSPEPSLPGPLHSMSAEVFG--PSPPFSSLSVNGGASYGNHLSHPP-EMNEAAVW
LIM1-HUMAN SEAQRFTDILAHPPGDSPSPEPSLPGPLHSMSAEVFG--PSPPFSSLSVNGGASYGNHLSHPP-EMNEAAVW
LIM1-BRARE SEVQRFSDIMSHHPGDSPSPEPGIPGPLHSMSSDVFG--PSPSFTSLSLNG-SGYSNHLSHPPSEMNEGTVW
LIM1-CHICK GEAQRFPDMLAHPAGDSPSPEPTLPGSLHSMSAEVFG--PSPPFSSISVNGGANYGNHLSHPP-EMNEAAVW
LIM5-BRARE -DDQRFTDMISHA--DTPSPEPGMTGPLHSNPQGEGGFTGSPPFPLANNTS--YSG-PMSHPGQEMGENTVW
LIM5-XENLA -ENQRYVDMISHP--DTPSPEPGMTGPLHPISGEVFTGGPSPPFSMSNNSG--FSG-PLPHQNLDINEATVW
LIM3-XENLA GIPQSPASLQSMPGHQSLLSNLAFPDTGLGIIGQGGQ-GVAPTMRVIGVNGPSSDLSTGSSGGYPD-FPASW

Figure 1. Multiple alignment of the deduced amino C-terminal sequence of *Xlim-1* with those identified from BLAST search comparisons. (A) Schematic structure of the frog Lim-1 deduced from the previously published *Xlim-1* sequence (Taira *et al.*, 1992). The C-terminal region, which was used to generate anti-XLim-1 antibodies (Karavanov *et al.*, 1996), is shown in black. (B) The complete sequence of the *Xenopus* (XENLA) C-terminus is shown aligned with those of mouse, human, zebrafish (BRARE), and chick Lim-1s as well as with *Xenopus* Lim-5 and Lim-3 and zebrafish Lim-5. All the protein sequences were obtained from the SWISSPROT database (Bairoch and Apweiler, 2000). Black—identical amino acid residues. Dash—gaps. Comparison shows that both the size and the sequence of the XLim-1 C-terminus are highly similar (80%–90% of similarity; extent internal homology above seven amino acid residues) to that of Lim-1 proteins from other species. At the same time, the XLim-1 C-terminal sequence reveals no more than 50% of similarity (extent internal homology below seven amino acid residues) with that of Lim-5 proteins. No significant similarity was observed in the case of the *Xenopus* Lim-3.

expected by chance (Fig. 1, see *Xenopus* Lim-3 as an example).

It is generally accepted that short peptides (below about seven amino acid residues) are of insufficient size to function as immunogenic and antigenic epitopes (Hancock and Evan, 1992). Using the CLUSTAL W program (Thompson *et al.*, 1994), we performed a multiple sequence alignment of the XLim-1 C-terminal region with that of the Lim-1 and Lim-5 proteins identified from BLAST searches (see above). As shown (Fig. 1), the XLim-1 C-terminus shares a high sequence homology with a number of Lim-1 proteins but not with Lim-5 factors. Given the above criteria, it is probable that the XLim-1 C-terminus (used as immunogen) could generate successful antibodies characterized by a high cross-reactivity with Lim-1 proteins in other species. At the same time, it may be predicted that antibodies against the XLim-1 C-terminus possess a much lower cross-reactivity with Lim-5 proteins. Note that anti-XLim-1 antibodies used in this study cross-react with Lim-1 factors from various species but do not cross-react with the closely similar XLim-5 protein on tissue sections (Karavanov *et al.*, 1996).

Collectively, the data indicated that the *Xlim* C-terminal sequence (used as an immunogen to generate anti-XLim-1 antibodies) is highly conserved among most of other known *lim-1* genes and seems to be diagnostic for their protein products. This would in turn account for the use of the corresponding antibodies in selective (discriminative) immunochemical screening of Lim-1-related proteins in different species. This suggestion is supported by the results of application of anti-XLim-1 antibodies for immunocytochemical Lim-1 protein detection in frog, mouse, and rat tissues (Karavanov *et al.*, 1996, 1998; Shimono and Behringer, 1999).

Anti-Xlim-1 antibodies cross-react with mussel, sea urchin, and chick tissue antigens

SDS-PAGE followed by immunoblot analysis of a protein extracted from isolated pedal ganglia of *Mytilus galloprovincialis*, mature oocytes of *Strongylocentrotus purpuratus*, and brain tissues of chick embryos revealed a single band with an apparent molecular weight (MW) of approximately 65, 70, and 65 kDa, respectively (Fig. 2). Note that the open reading frame of the chicken (Tsuchida *et al.*,

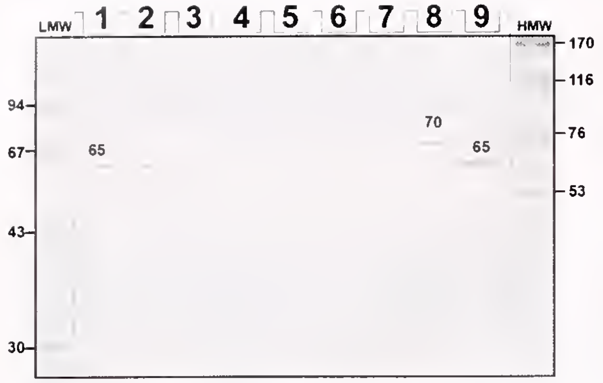

Figure 2. Cross-reactivity of anti-XLim-1 antibodies with mussel, sea urchin, and chick tissue antigens. Equal amounts (about 100 μg/pocket) of total protein extracted from different tissues were resolved in a 10% SDS-PAGE, blotted on membranes, and probed with anti-XLim-1 antibodies at 1/500 dilution. Membrane strips containing electrophoretically separated molecular weight markers were stained with Ponceau S. *Mytilus galloprovincialis* organs and tissues: Lane 1—male pedal ganglia; Lane 2—female pedal ganglia; Lane 3—male muscle adductor posterior; Lane 4—male gills; Lane 5—male foot; Lane 6—male hepatopancreas; Lane 7—male labial palps. Lane 8—*Strongylocentrotus purpuratus* eggs. Lane 9—forebrain tissues of 16-day-old chick embryos. LMW and HMW—low and high molecular weight calibration kit proteins (30–170 kDa), respectively. 65 and 70—molecular weights of antibody-labeled proteins, kDa.

1994) and sea urchin (Kawasaki *et al.*, 1999) *lim-1* gene encodes a protein with a predicted MW about of 45 kDa. The high MW value of the Lim-1 antigens is apparently not due to aggregation with other molecules, because it did not change when the antigens were extracted and electrophoretically analyzed in the presence of 6 *M* urea. In addition, observed low migration of mussel and chick Lim-1 antigens in SDS-PAGE is not due to their interactions with non-polymerized products of polyacrylamide gel (data not shown).

The discrepancy between the theoretical (45 kDa) and apparent (65 kDa) MWs of the Lim-1 antigens could be due to post-translation modifications in the protein molecules. In *X. laevis*, three Lim-1 bands were detected (by SDS-PAGE followed by Western blot with anti-XLim-1 antibodies) in embryos injected with the full-length synthetic *Xlim-1* mRNA. The fastest band of the "triplet" co-migrated with the protein product obtained from the same mRNA in a cell-free translation system, whereas other fractions were characterized by a lower electrophoretic migration. The latter suggested that a portion of the protein could be subject to post-translational modifications in the embryo (Karavanov *et al.*, 1996).

Using the ScanProsite tool (Hofmann *et al.*, 1999), we found that the *Xlim-1* sequence contains three potential sites for glycosylation, one of which resides in the C-terminus of the protein. By analogy with the XLim-1 protein, we proposed that mussel and chicken Lim-1 antigens run more slowly than predicted in SDS-PAGE, probably due to a glycosylation of the corresponding proteins. To investigate this option, we performed two experiments. First, Lim-1-containing fractions isolated from mussel pedal ganglia and chick embryo brain tissues (Fig. 3A, B) were electrophoresed on SDS-PAGE, blotted onto nylon membrane, and treated with the Immun-Blot kit for glycoprotein detection. Although a portion of each fraction displayed positive staining, the zones corresponding to Lim-1 antigens were absolutely negative (see Fig. 3C, D). Next, the same fractions were treated with the Bio-Rad deglycosylation kit, which enzymatically cleaves all *N*-linked and most *O*-linked oligosaccharides from glycoproteins. Treated and untreated Lim-1-containing fractions were subjected to SDS-PAGE followed by Western blot. All comparisons failed to identify any change in electrophoretic mobility of treated Lim-1 antigens (Fig. 3E, F). Thus, the difference between the predicted (45 kDa) and the apparent (65 kDa) MW of the Lim-1 antigens studied is apparently not due to the post-translational glycosylation of protein products.

To begin characterizing effective size values, Lim-1-containing fractions of mussel pedal ganglia and chick embryo brains were subjected to a subsequent ultrafiltration using 100- and 50-kDa cut-off membranes (Fig. 3G). Since mussel proteins tend to aggregate during ultrafiltration (Mikhailov *et al.*, 1997), the SDS and urea were added to starting Lim-1 and reference protein (*i.e.*, bovine albumin and chicken ovalbumin) solutions. Using SDS-PAGE followed by Western blot, we found that about 50% of the Lim-1 immunoreactivity, characteristic of Lim-1-containing fractions, is retained by the 100-kDa cut-off membrane, whereas no more than 40% of the immunoreactivity is detected in the filtrate. The latter is completely retained by the 50-kDa cut-off membrane. Such retention and recovery patterns are more similar to those of bovine serum albumin (MW 67 kDa) than to those of chicken ovalbumin (MW 43 kDa). In particular, about 60% of the bovine albumin was retained by the 100-kDa cut-off membrane, whereas more than 70% of the chicken ovalbumin passed through the membrane (data not shown). This raises the possibility that the effective MW (size) of the Lim-1 antigens studied could be larger than the theoretical one (45 kDa).

Taken together, the results indicate that the apparent MWs of the Lim-1 polypeptides, immunochemically detected in *M. galloprovincialis* pedal ganglia, *S. purpuratus* embryos, and chick embryo brain tissues, seem to be 40% higher than those calculated from deduced amino acid sequences derived from sea urchin (Kawasaki *et al.*, 1999), chick (Tsuchida *et al.*, 1994), and frog (Taira *et al.*, 1992) cDNA *lim-1* clones. We could not find any reference to apparent MWs of the Lim-1 proteins detected in frog, sea urchin, and chick tissues. For the other family of the zinc-finger transcriptional factors, aberrantly high MW values (in SDS-PAGE) have been found to be due to the particular amino acid composition of the C- and N-terminal domains (Klenova *et al.*, 1997). Examination of amino acid composition of the chicken, sea urchin, and frog Lim-1 C-terminal regions revealed that they are enriched with proline (18%, 20%, and 17%, respectively). Since polypeptides with a high proline content can give abnormally high MW values by SDS-PAGE (Hames, 1990), we suggest that the proline-rich C-terminus of the Lim-1 proteins may be responsible, at least in part, for their behavior when analyzed by SDS-PAGE (as could be the case of Lim-1 antigens studied). It is unlikely that Lim-1-like tissue antigens detected in this work are multimeric forms or aggregates that include other components, because reducing agents were present at all stages of the separation. Further studies should elucidate the significance of our findings and explain the discrepancy between the apparent MW of Lim-1 proteins immunochemically detected in chicken and sea urchin tissues and that deduced from the coding region of the corresponding cloned cDNAs.

Mussel pedal ganglia and gonads display the most prominent Lim-1-like immunoreactivity

In adult *M. galloprovincialis*, the most prominent Lim-1 immunoreactivity examined by Western blot analysis was detected in the pedal ganglia and gonads, in both males and females (Figs. 2, 5, 6). A very weak immunostaining was observed in gills and muscle tissues but not in hepatopancreas, foot, or labial palps (Fig. 2). Pronounced Lim-1 antigen accumulation in mussel nervous tissues and gonads raises a question about its possible functional importance. In this respect, it is interesting to note that mice carrying a disruption of the *lim-1* gene (Shawlot and Behringer, 1995) fail to develop the head and also lack kidneys and gonads.

Immunohistochemical staining was used to further characterize the Lim-1 expression pattern in the mussel nervous tissue. Figure 4 illustrates the nuclear localization of the antigen in neurons of pedal ganglia. To avoid the possibility of nonspecific cross-reactivity, we used anti-XLim-1 antibodies depleted prior to immunostaining by incubation with hyperfixed *X. laevis* embryos. This procedure results in the decrease of background and the enhancement of the signal-to-noise ratio (Karavanov *et al.*, 1996). The positive immuno-signal of mussel nuclei was blocked by adsorption of anti-XLim-1 antibodies with fixed pedal ganglia but not with fixed *M. galloprovincialis* foot or hyperfixed *X. laevis* embryo, providing additional support for tissue-specificity of immunodetection of the antigen. We reason that observation of a Lim-1-like positive signal in nuclei of mussel pedal ganglia is consistent with the generally accepted

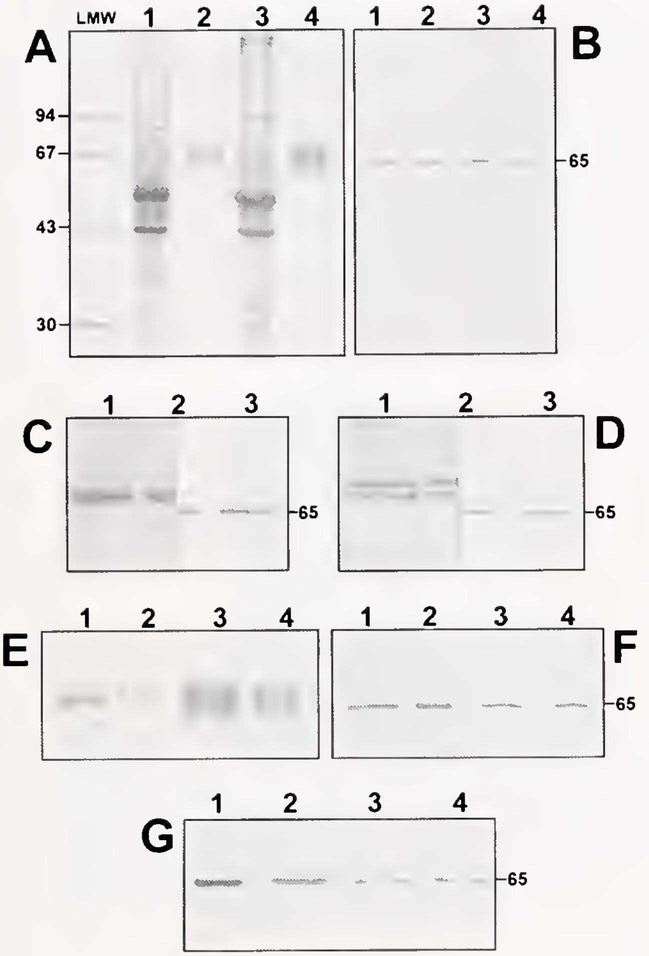

Figure 3. Characterization of mussel and chick Lim-1-like antigens. Lim-1-containing fractions isolated from mussel and chick tissues were subjected to SDS-PAGE followed by Western blot with anti-XLim-1 antibodies. Coomassie (A) and antibody (B) staining: Lane 1 and Lane 2—total extract and Lim-1-containing fraction of 16-day-old chick embryo forebrains, respectively; Lane 3 and Lane 4—total extract and Lim-1-containing fraction of *Mytilus galloprovincialis* pedal ganglia, respectively; LMW—low molecular calibration kit proteins (30–94 kDa). Note that fractions display the Lim-1 immunoreactivity similar to that of tissue extracts. In further experiments, chick (C) and mussel (D) Lim-1-containing fractions (Lanes 1, 2, and 3, respectively) were resolved in 10% SDS-PAGE and blotted on membranes. Each membrane was cut into two parts (see "Materials and Methods"): one part was treated with an Immun-Blot kit for glycoprotein detection (Lane 1 and a half of the Lane 2); the other (a half of the Lane 2 and Lane 3) was treated with anti-XLim-1 antibodies. Note that immunolabeled Lim-1 antigen bands do not reveal any glycoprotein-specific reaction. Next, chick and mussel fractions were treated with a deglycosylation kit and subjected to SDS-PAGE followed by Coomassie staining of the gel (E), or blotted on membranes followed by antibody staining of the membrane (F): Lane 1 and Lane 2—untreated and treated chick Lim-containing fraction, respectively; Lane 3 and Lane 4—untreated and treated mussel Lim-1-containing fraction, respectively. Note that the electrophoretic position of antibody-labeled bands in treated Lim-containing fractions corresponds to the 65-kDa value, as is the case for untreated fractions (see F; Lane 1 *versus* Lane 2, and Lane 3 *versus* Lane 4). Finally, chick Lim-containing fraction was subjected to subsequent ultrafiltration. Retained and filtered proteins were subjected to SDS-PAGE followed by Western blot with anti-XLim-1 antibodies (G). Immunostaining (signal quantitation, %): Lane 1—isolated Lim-1 fraction (100%), Lane 2—Lim-1 fraction retained by the 100-kDa cut-off membrane (~50%); Lane 3—Lim-1 fraction partially passed through the 100-kDa cut-off membrane (~40%); Lane 4—the latter retained by the 50-kDa cut-off membrane (~30%). 65—molecular weight of Lim-1-like antigens, kDa. Positions of bovine serum albumin (67 kDa) and chicken egg ovalbumin (43 kDa) are shown on (A).

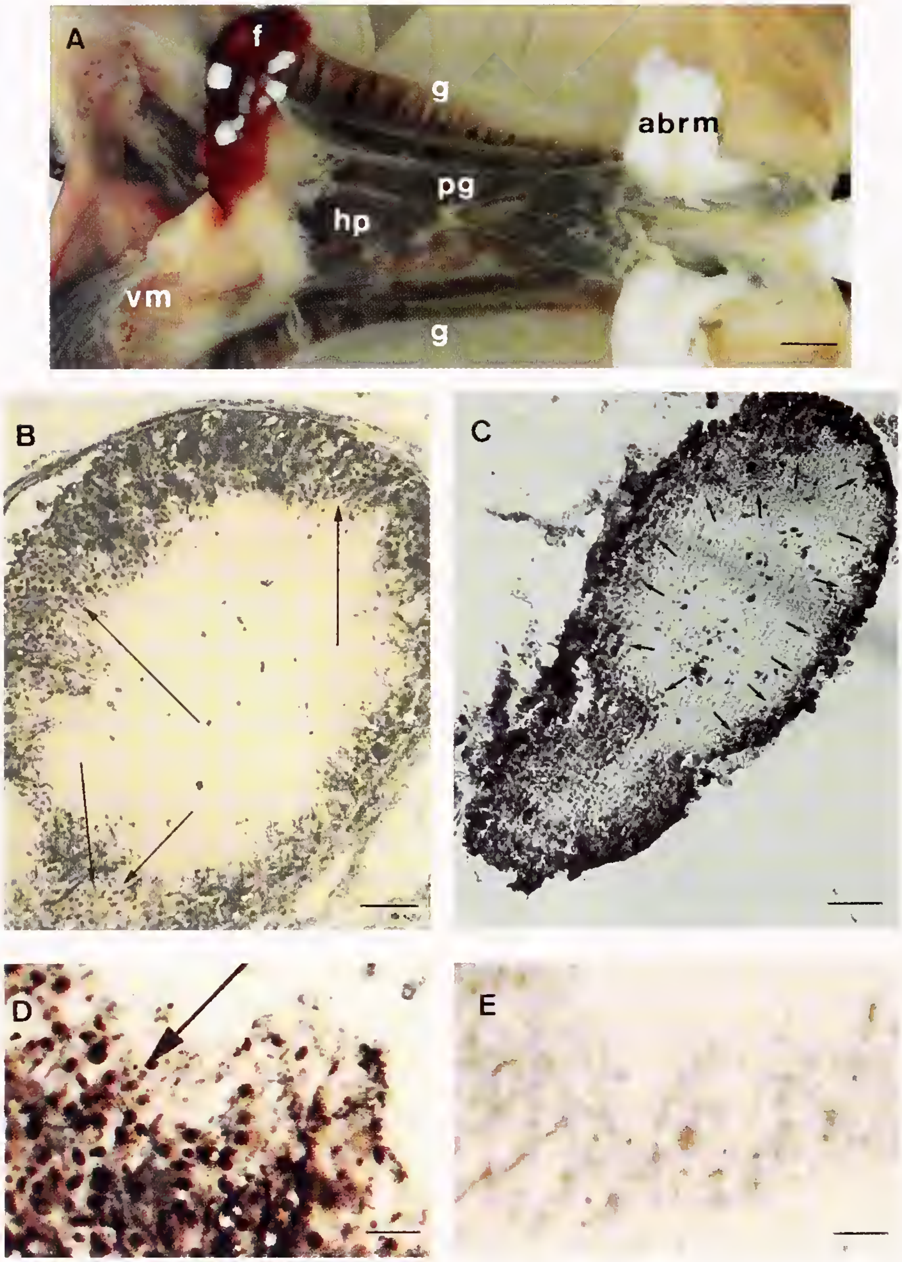

Figure 4. Tissue section visualization of Lim-1 immunoreactivity signal in *Mytilus galloprovincialis* pedal ganglia. (A) Localization of the pedal ganglion in the mussel. The anterior end of the animal is to the right; pg—pedal ganglion; g—gills; hp—hepatopancreas, f—foot; vm—visceral mass; abrm—anterior byssal retractor muscle. Ganglia were dissected, fixed, paraffin-embedded, and processed for immunohistochemistry using primary anti-XLim-1 antibodies and secondary antibodies conjugated to alkaline phosphatase. (B) Section treated with anti-XLim-1 antibodies depleted by hyperfixed *Xenopus laevis* embryos. Note the positive staining of nuclei (long arrows). (C) Section treated with anti-XLim-1 antibodies preadsorbed by fixed foot tissues of *M. galloprovincialis*. Short arrows point to a nuclear region (arranged on entire circumference of the ganglion) that is positive for anti-XLim-1 antibody staining. (D) Higher magnification of the section in (B), showing intensive immunostaining in isolated nuclei. (E) Section treated with anti-XLim-1 antibodies preadsorbed by fixed pedal ganglia of *M. galloprovincialis*: no immunoreactivity is observed in the nuclei (scale bar: A—5 mm; B—50 μm; C—100 μm; D and E—20 μm).

putative function of Lim-1 HD proteins as transcription factors.

In the *M. galloprovincialis* ripe male gonad, Lim-1 positive signals (*i.e.*, a major 60-kDa and a minor 65-kDa band) were detected in somatic gonad tissues, but not in sperm cells (Fig. 5A, C). In spent male gonads (*i.e.*, gonads that do not contain sperm cells and consist of gonad tubules and mantle connective tissue) a very weak 60-kDa immunoreactivity was found. At the histological level, not only sperm but also mature Sertoli cells were undetectable in seminiferous tubules of the spent gonad (Fig. 5B). The results suggest that in mussel male gonad, the 60-kDa antigen is mainly associated with Sertoli cells. This finding is consistent with data on Lim-1 protein cell localization in the fetus testis of the rat (Karavanov *et al.*, 1996). The minor 65-kDa band seems to be also characteristic for gonad somatic tissue, although its precise cell association remains to be elucidated.

Next we questioned whether the Lim-1 distribution in the *M. galloprovincialis* female gonad was similar to that in the male gonad. In the female ripe gonad, antibody staining revealed two Lim-1-like antigens with MWs of approximately 65 and 40 kDa (Fig. 6). In the oocyte-free gonad portion, containing mainly collecting tubules and mantle mesenchyme cells, only the 65-kDa fraction was detected. In mature spawned oocytes, both the 65- and the 40-kDa Lim-1 antigens were found. The 40-kDa band does not appear to be an artifact of degradation caused by sample processing. Detection of the 40-kDa Lim-1 antigenic polypeptide in the mussel female gonad is perhaps not surprising, because the *X. laevis* ovary contains the 2.7-kb maternal *Xlim-1* mRNA that is smaller than the larger zygotic 3.4-kb transcript found in the adult brain (Taira *et al.*, 1992). It should be noted that in immature oocytes (obtained by biopsy of female gonad follicles), neither 65-kDa nor 40-kDa antigens were found (see Fig. 6, Lane 3).

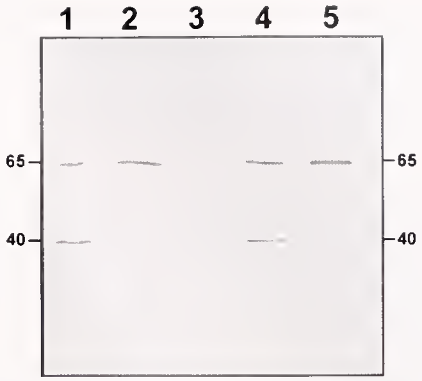

Figure 6. Analysis of Lim-1 antigen distribution in female gonads of *Mytilus galloprovincialis* using SDS-PAGE followed by Western blot with anti-XLim-1 antibodies. Lane 1—gonad biopsy containing somatic tissues, gonad ducts, fluids, and oocytes; Lane 2—gonad collecting ducts; Lane 3—immature oocytes obtained by biopsy of gonad follicles; Lane 4—spawned mature eggs; Lane 5—cerebellum of 16-day-old chick embryos (reference). 40 and 65—apparent molecular weight values of Lim-1 antigens, kDa.

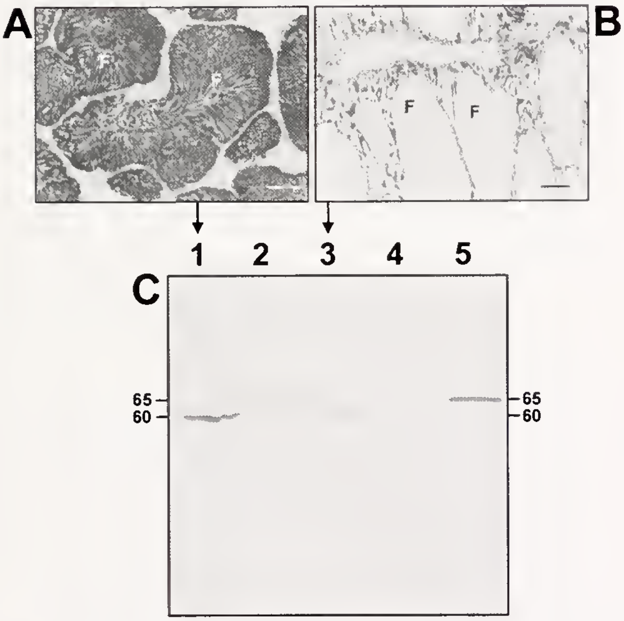

Figure 5. Analysis of Lim-1 antigen distribution in male gonads of *Mytilus galloprovincialis*. Histological sections of ripe male gonad before (A) and after (B) complete spawning (spent gonad). Note that the gonad samples are characterized by the same patterns of follicle (F) morphogenesis and gonadosomatic index values (in both samples, about of 90% of gonad volume was occupied by follicles) (scale bar—100 μm). (C) Extracts prepared from complementary gonad (Lane 1 and Lane 3; arrows) of the same animals, as well as from somatic tissues (Lane 2) and sperm cells (Lane 4) of the other ripe gonad before spawning, were subjected to SDS-PAGE followed by Western blot with anti-XLim-1 antibodies. Lane 1—gonad biopsy containing somatic tissue, gonad ducts, fluids, and sperm; Lane 2—gonad tube-free sample containing the mantle connective tissues only; Lane 3—spent gonad; Lane 4—mature sperm cells; Lane 5—optic lobe of 16-day-old chick embryos (reference). 60 and 65—apparent molecular weight values of Lim-1 antigens, kDa.

It is clear from these results that the 65-kDa Lim-1 form in the female is associated with somatic tissues of the gonad just like the Lim-1 variants detected in the male gonad. At the same time, in the female gonad the 65-kDa antigen is also characteristic of mature eggs. The 40-kDa antigen, despite our uncertainty regarding its precise nature, is specific to the female germ line. It is likely that neither of the two antigens are expressed at early phases of oocyte differentiation, but are expressed and accumulated in eggs at terminal stages of their maturation. Therefore, the *M. galloprovincialis* female gonad pattern obtained by Western immunoblot analysis for Lim-1 antigens may be interpreted as a compound profile of the 65-kDa variant, which originates from both somatic tissues and eggs, and of the 40-kDa form, which seems to be specific to mature oocytes only.

Dynamics of Lim-1-like immunoreactivity during early development

Observations on female gonads have led us to examine the patterns and timing of maternal expression of the 65-kDa and 40-kDa Lim-1 variants during early development of *M. galloprovincialis*. Both antigen signals, already seen in unfertilized and fertilized eggs, persist in embryos during cleavage. At the beginning of the blastula stage, the intensity of immunostaining of both the 65-kDa and the 40-kDa antigens decreases. In stereoblastulae, instead of these two Lim-1 antigenic variants, only 45-kDa immunoreactivity was observed. The latter was first detected in 8-cell embryos, and its intensity reached a maximum in blastulae (Fig. 7A).

Data from a variety of sources are consistent with the fact that zygotic transcription of *lim-1* genes begins before gastrulation at or very shortly after the midblastula transition (Taira *et al.*, 1992; Rebbert and Dawid, 1997; Curtiss and Heiling, 1998; Kawasaki *et al.*, 1999). It may be speculated that in mussels, the 65- and 40-kDa signals are due to Lim-1-related maternal molecules stored in the full-grown oocytes, whereas the 45-kDa protein reflects zygotic activity of the gene. Such an interpretation may explain why multiple Lim-1 antigen variants have been detected in embryos of *M. galloprovincialis* at early blastula stages, but there is no definitive proof. It remains to be established how the compound profile of Lim-1 protein variants relates to maternal and zygotic gene expressions as well as to possible post-translation modifications of the primary gene product (Karavanov *et al.*, 1996) or to the so-called premature termination of translation processes involving both untranslated and coding regions of the zinc-finger transcriptional factors (Klenova *et al.*, 1997).

In sea urchin embryos, expression of the *lim-1*-related gene (*Hplim-1*) has been studied at the transcriptional level (Kawasaki *et al.*, 1999), so we decided to examine the Lim-1 antigen dynamics in the course of sea urchin early embryogenesis. Levels of Lim-1 immunoreactivity during *S. purpuratus* development are shown in Figure 7B. A relatively high-abundance signal of the Lim-1 antigen, already seen in eggs, persists in embryos to the blastula stage, decreases dramatically in unhatched blastulae, and increases again in late (post-hatched) blastulae. In more advanced embryos (*i.e.*, at prism and pluteus stages), trace amounts of the Lim-1 antigen were detected. Although the developmental kinetics of the Lim-1 protein in *S. purpuratus* is quite similar to that of the *Hplim-1* mRNA in *H. pulcherrimus* (Kawasaki *et al.*, 1999), the most interesting finding revealed by Western blot is that the Lim-1 antigen is present at relatively high levels very early during development. Note that *H. pulcherrimus* fertilized eggs and cleavage embryos contain a trace amount of the *Hplim-1* mRNA that becomes abundant only at the blastula stage just after hatching (Kawasaki *et al.*, 1999).

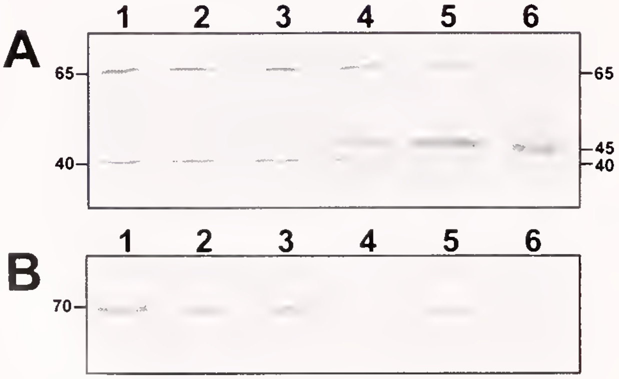

Figure 7. Patterns and timing of Lim-1 antigen expression in the course of early development of *Mytilus galloprovincialis* and *Strongylocentrotus purpuratus*. The extracts from eggs and embryos were subjected to SDS-PAGE followed by Western blot with anti-XLim-1 antibodies. (A) *M. galloprovincialis:* Lane 1—unfertilized eggs; Lane 2—fertilized eggs; Lane 3—4- and 8-cell embryos; Lane 4—16- and 32-cell embryos; Lane 5—early blastulae; Lane 6—stereoblastulae. (B) *S. purpuratus:* Lane 1—unfertilized eggs; Lane 2—fertilized eggs; Lane 3—8- and 16-cell embryos; Lane 4—unhatched blastulae; Lane 5—hatched blastulae; Lane 6—prism larvae. 40, 45, 65, and 70—apparent molecular weight values of Lim-1 antigens, kDa.

Thus, Lim-1-like polypeptides, which share common epitopes with the C-terminus of the frog XLim-1 protein, have been detected in both *M. galloprovincialis* and *S. purpuratus*. In these species, characterized by very different modes of early embryogenesis, the similar developmental kinetics of the Lim-1 antigens has been demonstrated. Whether this likeness leads to similar developmental consequences remains to be elucidated. In sea urchin embryos, ectopic expression of the *Hplim-1* inhibits endoderm and mesoderm differentiation, directing all embryonic cells to form oral ectoderm (Kawasaki *et al.*, 1999). It is widely accepted that maternally expressed gene products, stored in the egg, establish initial differences within the early embryo that, in turn, could contribute to further regionalization of the embryo body (Raff, 1996). The work described here particularly highlights the fact that in the marine invertebrates studied the Lim-1-like proteins maternally accumulated in the egg could persist after fertilization and be present in the early embryo long before zygotic expression of the genes is activated.

As mentioned above, the present study represents the first step in the identification and characterization of Lim-1-like proteins in marine bivalves. If it were accepted that the antibodies used recognize epitopes of the XLim-1 C-terminal sequence, then their cross-reactivity would appear to be specific for Lim-1-related proteins in many species (see Fig. 1). The corresponding immunochemical data obtained on rats (Karavanov *et al.*, 1996, 1998) and mice (Shimono and Behringer, 1999) confirm this assumption. Moreover, there is similarity between Lim-1 antigenic patterns observed in bivalves and those detected with the aid of the same antibodies in other species. This involves (1) the immunodetection of the Lim-1 protein in both ganglia and somatic gonads (bivalves—this work; rats—Karavanov *et al.*, 1996), and (2) the nuclear localization of Lim-1 immunoreactivity in tissue sections (bivalves—this work; frog and rats—Karavanov *et al.*, 1996; mice—Shimono and Behringer, 1999). In addition, the developmental dynamics of the Lim-1 antigen (this work) and *Hplim-1* mRNA (Kawasaki *et al.*, 1999) in sea urchin embryos appears to be very similar.

On the basis of the HD sequence similarity, vertebrate Lim-1 proteins, as well as Lim-5 and Lim-6 factors, have been included in the so-called LIN-11 class of LIM-HD proteins (Hobert and Westphal, 2000). Two *lim-1*-related genes have been recently identified in sea urchins (Kawasaki *et al.*, 1999) and fruit flies (Lilly *et al.*, 1999), and we suggest that they may be added to the same LIN-11 group. To the best of our knowledge, this study is the first report that describes Lim-1-like protein patterns in bivalve mollusc, sea urchin, and chick embryo tissues. Clearly, much remains to be learned about the corresponding factors involved, especially in bivalves. Nevertheless, it seems likely that the results obtained provide precedents for further identification of *lim-1*-related genes and characterization of their protein products in bivalve molluscs.

Acknowledgments

The authors thank Dr. A. A. Karavanov and Prof., Dr. I. B. Dawid for the gift of anti-XLim-1 antibodies as well as for comments and contributions at a time during which many aspects of this study were discussed and developed. We also extend our gratitude to two extremely helpful anonymous referees. The work was supported by the XUGA grant 16101A 98 from the Galicia Government to ATM and by a postdoctoral fellowship from the Institute of Health Sciences (University of La Coruña, Spain) to MT.

Literature Cited

Altschul, S. F., T. L. Madden, A. A. Schäffer, J. Zhang, Z. Zhang, W. Miller, and D. J. Lipman. 1997. Gapped BLAST and PSI-BLAST: a new generation of protein database search programs. *Nucleic Acids Res.* **25:** 3389–3402.

Bach, I. 2000. The LIM domain: regulation by association. *Mech. Dev.* **91:** 5–17.

Bairoch, A., and R. Apweiler. 2000. The SWISS-PROT proteins sequence database and its supplement TrEMBL in 2000. *Nucleic Acids Res.* **28:** 45–48.

Breen, J. J., A. D. Agulnick, H. Westphal, and I. B. Dawid. 1997. Interactions between LIM domains and the LIM domain-binding protein Ldb1. *J. Biol. Chem.* **273:** 4712–4717.

Brown, S., C. Biben, L. M. Ooms, M. Maimone, M. J. McGrath, R. Gurung, R. P. Harvey, and C. A. Mitchell. 1999. The cardiac expression of striated muscle Lim protein 1 (SLIM1) is restricted to the outflow tract of the developing heart. *J. Mol. Cell Cardiol.* **31:** 837–843.

Carroll, T. J., and P. D. Vize. 1999. Synergism between *Pax-8* and *lim-1* in embryonic kidney development. *Dev. Biol.* **214:** 46–59.

Carroll, T. J., J. B. Wallingford, and P. D. Vize. 1999a. Dynamic patterns of gene expression in the developing pronephros of *Xenopus laevis*. *Dev. Genet.* **24:** 199–207.

Carroll, T. J., J. B. Wallingford, D. Seufert, and P. D. Vize. 1999b. Molecular regulation of pronephric kidney. *Curr. Top. Dev. Biol.* **44:** 67–100.

Curtiss, J., and J. S. Heiling. 1998. DeLIMiting development. *Bioessays* **20:** 58–69.

Dawid, I. B., J. J. Breen, and R. Toyama. 1998. LIM domains: multiple roles as adapter and functional modifiers in protein interactions. *Trends Genet.* **14:** 156–162.

Dong, W. F., H. H. Heng, R. Lowsky, Y. Xu, J. F. DeCoteau, and M. D. Minden. 1997. Cloning, expression, and chromosomal localization of the human LIM/HOMEOBOX gene. *hLim-1. DNA Cell Biol.* **16:** 671–678.

Fujii, T., J. G. Pichel, M. Taira, R. Toyama, I. B. Dawid, and H. Westphal. 1994. Expression patterns of the murine LIM class homeobox gene *lim 1* in the developing brain and excretory system. *Dev. Dyn.* **199:** 73–83.

Furuyama, T., S. Inagaki, Y. Iwahashi, and H. Takagi. 1994. Distribution of *Rlim*, an LIM homeodomain gene, in the rat brain. *Neurosci. Lett.* **170:** 266–268.

Hames, B. D. 1990. One-dimensional polyacrylamide gel electrophoresis. Pp. 1–148 in *Gel Electrophoresis of Proteins*, B. D. Hames and D. Rickwood, eds. IRL Press, Oxford.

Hancock, D. C., and G. I. Evan. 1992. Synthesis of peptides for use as immunogens. Pp. 23–32 in *Immunological Protocols*, M. Manson, ed. The Humana Press, Totowa, NJ.

Hobert, O., and G. Ruvkun. 1998. A common theme for LIM homeobox gene function across phylogeny? *Biol. Bull.* **195:** 377–380.

Hobert, O., and H. Westphal. 2000. Functions of LIM-homeobox genes. *Trends Genet.* **16:** 75–83.

Hobert, O., T. d'Albert, Y. Liu, and G. Ruvkun. 1998. Control of neural development and function in a thermoregulatory network by the LIM homeobox gene *lin-11*. *J. Neurosci.* **18:** 2084–2096.

Hofmann, K., P. Bucher, L. Falquet, and A. Bairoch. 1999. The PROSITE database, its status in 1999. *Nucleic Acids Res.* **27:** 215–219.

Holland, N. D., and L. Z. Holland. 1993. Embryos and larvae of invertebrate deuterostomes. Pp. 21–32 in *Essential Developmental Biology. A Practical Approach*, C. D. Stern and P. W. H. Holland, eds. IRL Press, New York.

Karavanov, A. A., J.-P. Saint-Jeannet, I. Karavanova, M. Taira, and I. Dawid. 1996. The LIM homeodomein protein Lim-1 is widely expressed in neural, neural crest and mesoderm derivatives in vertebrate development. *Int. J. Dev. Biol.* **40:** 453–461.

Karavanov, A. A., I. Karavanova, A. Perantony, and I. Dawid. 1998. Expression pattern of the rat *lim-1* homeobox gene suggests a dual role during kidney development. *Int. J. Dev. Biol.* **42:** 61–66.

Kawasaki, T., K. Mitsunaga-Nakatsubo, K. Takeda, K. Asaka, and H. Shimada. 1999. *Lim 1* related homeobox gene (*HpLim1*) expressed in sea urchin embryos. *Dev. Growth Differ.* **41:** 273–282.

Klenova, E. M., R. H. Nicolas, A. F. Carne, R. E. Lee, V. V. Lobanenkov, and G. H. Goodwin. 1997. Molecular weight abnormalities of the CTCF transcription factor: CTCF migrate aberrantly in SDS-PAGE and the size of the expressed protein is affected by the UTRs and sequences within the coding region of the CTCF gene. *Nucleic Acids Res.* **25:** 466–474.

Li, Y. H., S. S. Cheah, J. M. Deng, W. Shawlot, and R. R. Behringer. 1999. Sequence and genomic organization of the mouse *lim1* gene. *Mamm. Genome* **10:** 444–446.

Lilly, B., D. D. O'Keefe, J. B. Tomas, and J. Botas. 1999. The LIM homeodomain protein *dlim1* defines a subclass of neurons within the embryonic ventral nerve cord of *Drosophila*. *Mech. Dev.* **88:** 195–205.

Lim, H. N., and J. R. Hawkins. 1998. Genetic control of gonadal differentiation. *Bailliere's Clin. Endocrinol. Metab.* **12:** 1–16.

Mauch, T. J., G. Yang, M. Wright, D. Smith, and G. C. Schoenwolf. 2000. Signals from trunk paraxial mesoderm induce pronephros formation in chick intermediate mesoderm. *Dev. Biol.* **220:** 62–75.

Mikhailov, A. T., and V. N. Simirsky. 1991. *Immunochemical Methods in Developmental Biology (A Manual)*. Nauka, Moscow. p. 176.

Mikhailov, A. T., M. Torrado, J. Méndez, and M. J. López. 1996. Annual cycle of expression of connective tissue polypeptide markers in the mantle of the mussel *Mytilus galloprovincialis*. *Mar. Biol.* **126:** 77–89.

Mikhailov, A. T., M. Torrado, L. I. Korochkin, M. A. Kopantzeva, and J. Méndez. 1997. Male-predominant carboxylesterase expression in the reproductive system of mollusks and insects: immunochemical and biochemical similarity between *Mytilus* male associated polypeptide (MAP) and *Drosophila* sex-specific Esterase S. *Comp. Biochem. Physiol.* **118B:** 197–208.

Newman, A. P., G. Z. Acton, E. Hartwieg, H. R. Horvitz, and P. W. Sternberg. 1999. The *lin-11* LIM domain transcription factor is necessary for morphogenesis of *C. elegans* uterine cells. *Development* **126:** 5319–5326.

Raff, R. A. 1996. *The Shape of Life: Genes, Development and the Evolution of Animal Form.* University of Chicago Press, Chicago.

Rebbert, M. L., and I. B. Dawid. 1997. Transcriptional regulation of the *Xlim-1* gene by activin is mediated by an element in intron I. *Proc. Natl. Acad. Sci. USA* **94:** 9717–9722.

Shawlot, W., and R. R. Behringer. 1995. Requirement for *Lim1* in head-organizer function. *Nature* **374:** 425–430.

Shawlot, W., M. Wakamiya, K. M. Kwan, A. Kania, T. M. Jessell, and R. R. Behringer. 1999. *Lim 1* is required in both primitive streak-derived tissues and visceral endoderm for head formation in the mouse. *Development* **126:** 4925–4932.

Shimono, A., and R. R. Behringer. 1999. Isolation of novel cDNAs by subtractions between the anterior mesoendoderm of single mouse gastrula embryos. *Dev. Biol.* **209:** 369–380.

Sprung, M., and B. L. Bayne. 1984. Some practical aspects of fertilizing of the eggs of the mussel *Mytilus edulis* L. *J. Cons. Int. Explor. Mer* **41:** 125–128.

Taira, M., M. Jamrich, P. J. Good, and I. B. Dawid. 1992. The LIM domain-containing homeobox gene *Xlim-1* is expressed specifically in the organizer region of *Xenopus* gastrula embryos. *Genes Dev.* **6:** 356–366.

Taira, M., H. Otani, M. Jamrich, and I. B. Dawid. 1994. Expression of the LIM class homeobox gene *Xlim-1* in pronephros and CNS cell lineages of *Xenopus* embryos is affected by retinoic acid and exogastrulation. *Development* **120:** 1525–1536.

Taira, M., J.-P. Saint-Jeannet, and I. B. Dawid. 1997. Role of the *Xlim-1* and *Xbra* genes in anteroposterior patterning of neural tissue by the head and trunk organizer. *Proc. Natl. Acad. Sci. USA* **94:** 895–900.

Thompson, J. D., D. G. Higgins, and T. J. Gibson. 1994. CLUSTAL W: improving the sensitivity of progressive multiple sequence alignment through sequence weighting, position-specific gap penalties and weight matrix choice. *Nucleic Acids Res.* **22:** 4673–4680.

Torrado, M., and A. T. Mikhailov. 1998. Male-associated polypeptide (MAP) expression in different compartments of the reproductive system of the mussel *Mytilus galloprovincialis:* immunocytochemical and Western blot study. *Cell Tissue Res.* **294:** 537–547.

Toyama, R., M. L. O'Connell, C. V. E. Wright, M. R. Kuehn, and I. B. Dawid. 1995. Nodal induces ectopic *goosecoid* and *lim 1* expression and axis duplication in zebrafish. *Development* **121:** 383–391.

Tsuchida, T., M. Ensini, S. B. Morton, M. Baldassare, T. Edlung, T. M. Jessell, and S. L. Pfaff. 1994. Topographic organization of embryonic motor neurons defined by expression of LIM homeobox genes. *Cell* **79:** 957–970.

Wallingford, J. B., T. J. Carroll, and P. D. Vize. 1998. Precocious expression of the Wilms' tumor gene *xWT1* inhibits embryonic kidney development in *Xenopus laevis. Dev. Biol.* **202:** 103–112.

Reference: *Biol. Bull.* **199:** 41–49. (August 2000)

Morphogenesis During Asexual Reproduction in *Pygospio elegans* Claparede (Annelida, Polychaeta)

GLENYS D. GIBSON* AND JENNIFER M. L. HARVEY

Department of Biology, Acadia University, Wolfville, Nova Scotia, Canada B0P 1X0

Abstract. The spionid *Pygospio elegans* reproduces both asexually and sexually. Using scanning electron and bright field microscopy, we examined morphogenesis following asexual reproduction to determine how "lost" body regions were regenerated after a worm spontaneously divided. Asexual reproduction occurred through transverse fission and divided the parent worm into 2 to 6 fragments (architomy). All fragments retained their original anterior-posterior polarity. Regeneration in all fragments followed a specific series of events: wound healing (day 1); extension of the blastema to generate lost body regions—specifically, the head and thorax for posterior fragments and the tail and pygidium for anterior fragments (days 2–3); segmentation (days 3–6); and differentiation of segment- or region-specific structures (days 4–8). This pattern occurred regardless of where the original division took place. Subsequent growth occurred through addition of terminal setigers anterior to the pygidium followed by differentiation of tail setigers into abdominal setigers, leaving the tail region about 6 to 10 setigers in size. Division rates were compared in worms from three populations in Nova Scotia, Canada. Worms from two populations (Conrad's Beach, Starr's Point) divided more frequently (about 1.2 and 1.3 weeks between divisions, respectively) than worms from Bon Portage Island (3.5 weeks between divisions). Fragments containing the original head (original mouth intact, generally much larger fragment) had a higher survivorship than fragments containing the original tail.

Introduction

Asexual reproduction is the process of forming two or more offspring from one parent body without involving gametes, or cells with a meiotically reduced chromosome number (Balinsky, 1975; Solomon *et al.*, 1993). Although polychaetes reproduce sexually, asexual reproduction, through fission or budding, also occurs in many families including spionids, cirratulids, syllids, and sabellids (Barnes, 1980). In the spionid *Pygospio elegans,* asexual reproduction occurs through transverse fission of the parent body into fragments, each of which will regenerate "lost" body regions (Rasmussen, 1953). Asexual reproduction has been widely reported in *P. elegans,* with most authors reporting its occurrence or testing environmental factors that may influence rates of division (Anger, 1984; Wilson, 1985). Despite the prevalence of asexual reproduction in this species, morphogenesis during post-fission regeneration has not been described.

Pygospio elegans is a tubiculous polychaete that is common on mud and sand flats and has a cosmopolitan, temperate distribution (Anger, 1984; Wilson, 1985). Adults grow to be 12 mm long, and feed on detritus (Wilson, 1985) and phytoplankton (Anger *et al.*, 1986). Rasmussen (1953) first described asexual reproduction in this species. He reported that both females and males could divide anywhere in the body and generally formed three to four fragments. Each fragment stayed in the original tube until regeneration was complete, about 8 d after division (20°C). Subsequently, several authors reported asexual reproduction in *P. elegans* from populations from the eastern seaboard of the United States (Hobson and Green, 1968), Washington State (Wilson, 1985), and the Baltic Sea (Anger, 1984; Gudmundsson, 1985). *P. elegans* also reproduces sexually, and it exhibits considerable flexibility in reproduction, as both planktotrophic and adelphophagic (a form of lecithotrophy) larval development have been reported in worms from different populations (*e.g.*, Thorson, 1946; Hannerz, 1956; Hobson and Green, 1968; Anger, 1984; Anger *et al.*, 1986; Schlötzer-Schrehardt, 1991; Morgan *et al.*, 1999).

Received 23 July 1999; accepted 4 May 2000.

* To whom correspondence should be addressed. E-mail: glenys.gibson@acadiau.ca

Our objective is to describe morphogenesis during post-fission regeneration in *P. elegans*. We use bright field and scanning electron microscopy (SEM) to describe morphogenesis after spontaneous divisions to determine (1) if anterior and posterior body regions show similar patterns of regeneration; and (2) how subsequent growth occurs. We use the term *regeneration* to refer to the replacement of lost body regions (*e.g.*, the head, thorax, tail) and *growth* as the addition of setigers to increase size, once the major body regions have formed. Also, we examine the rates of fission and fragment mortality in laboratory-maintained worms originating from three populations. No sexual reproduction was observed during the present study.

Materials and Methods

Adult specimens of *Pygospio elegans* were collected between May and September from three sites: Bon Portage Island, Starr's Point, and Conrad's Beach, Nova Scotia. At each site, sediments containing worms were sieved (500-μm mesh), and tubes were brought into the laboratory. *P. elegans* was identified following Bromley and Bleakney (1984). Worms were placed in either 250-ml Pyrex crystallizing dishes or 150-ml custard dishes, with seawater and defaunated sand. Dishes containing stock cultures were submerged in larger trays of seawater and aerated. Cultures were maintained at 20°C on a photoperiod of 16 h light. Worms were fed a mixture of dehydrated, ground *Enteromorpha* and Tetramin fish food suspended in seawater twice weekly. Seawater was changed once a week.

Stock cultures were sieved daily, and worms were isolated if they could be identified as having divided on that day (presence of a clean, smooth blastema) or showed signs that fission was about to occur (constriction of the body wall). Isolated worms were cultured separately to prevent movement of worms among culture dishes. Regeneration was observed with bright field and scanning electron microscopy. Fragments, anesthetised in 7% $MgCl_2$, were examined and photographed daily from fission to the completion of regeneration (8 d post-fission) using bright field techniques (n = 25 worms). Fragments at each stage of regeneration (2 to 3 fragments per stage for both anterior and posterior fragments) were prepared for SEM by fixation in 2.5% glutaraldehyde followed by post-fixation in 1% osmium tetraoxide, both in 0.1 *M* cacodylate buffer and seawater (Gibson *et al.*, 1999). After fixation, regenerates were dehydrated in an ascending series of ethanol, critical point dried with a Bio-Rad E3000 critical point drier, coated with gold-palladium with a Hummer II sputter coater, and observed with a JEOL JSM-25S or JEOL T330A scanning electron microscope. Growth was followed in additional worms that had completed the regeneration process (n = 12 worms). After the head and thorax or tail and pygidium had been regenerated, growth was examined by counting the number of setigers in each body region for a 17-d period.

Intact worms that showed no signs of a recent asexual event were cultured in isolation to determine rates of regeneration. Worms were observed from Bon Portage Island (n = 15), Starr's Point (n = 15), and Conrad's Beach (n = 10). Dishes were sieved weekly over a 6-week period. Original worm size was determined as the number of setigers at the beginning of the experimental period. Each week, the number of fragments per dish was noted, as well as the size of the fragments (number of setigers) and the degree of regeneration. Data were compared among the three study populations using one-way ANOVA in Statworks 1.2 (Cricket Software). Where significant differences were noted, a post-hoc Scheffé comparison was also performed using SPSS 8.0 (SPSS Inc.).

Results

Adult morphology

The overall body plan of *Pygospio elegans* is divided into four regions: the head, thorax, abdomen, and tail. The *head* is characterized by two ciliated palps, a prostomium with two or three pairs of eyes and paired nuchal organs (Fig. 1a). The *thorax* contains 10 to 12 abranchiate setigers, each with a single dorsal ciliary band, capillary notochaetae, and a lateral tuft of cilia. Neurochaetae are simple capillary on setigers 1 to 8 and hooded hooks on setigers 9 to 12 (Fig. 1b). The *abdomen* is 25 to 35 setigers in length. Each abdominal segment has paired branchiae and either a single (first few abdominal setigers) or double ciliary band, with two closely apposed bands of tufted cilia. Abdominal setigers also have capillary notochaetae, a lateral tuft of cilia, and neurochaetae that are hooded hooks (Fig. 1c). The *tail* contains 6 to 12 abranchiate setigers. Tail setigers have capillary notochaetae, neurochaetae that are hooded hooks, and a lateral tuft of cilia. There is a reduced ciliary band on the first few tail setigers only. The pygidium consists of four cirri, each with tufts of cilia on the inner surface (Fig. 1d). Male *P. elegans* have a pair of branchiae on the second setiger (Fauchald, 1977) and dorsal organs on each setiger (Schlötzer-Schrehardt, 1991). Only four males (n = 200 worms) were observed during the present study. No morphological differences were noted (SEM) between worms from the three study populations.

Morphogenesis following fission

In all cases, fragments retained their original anterior-posterior polarity. Posterior fragments regenerated only the head and thorax, and anterior fragments regenerated only a new tail and pygidium. Subsequent growth involved elongation of the tail by the addition of terminal setigers. We based our description on division into two fragments, as that

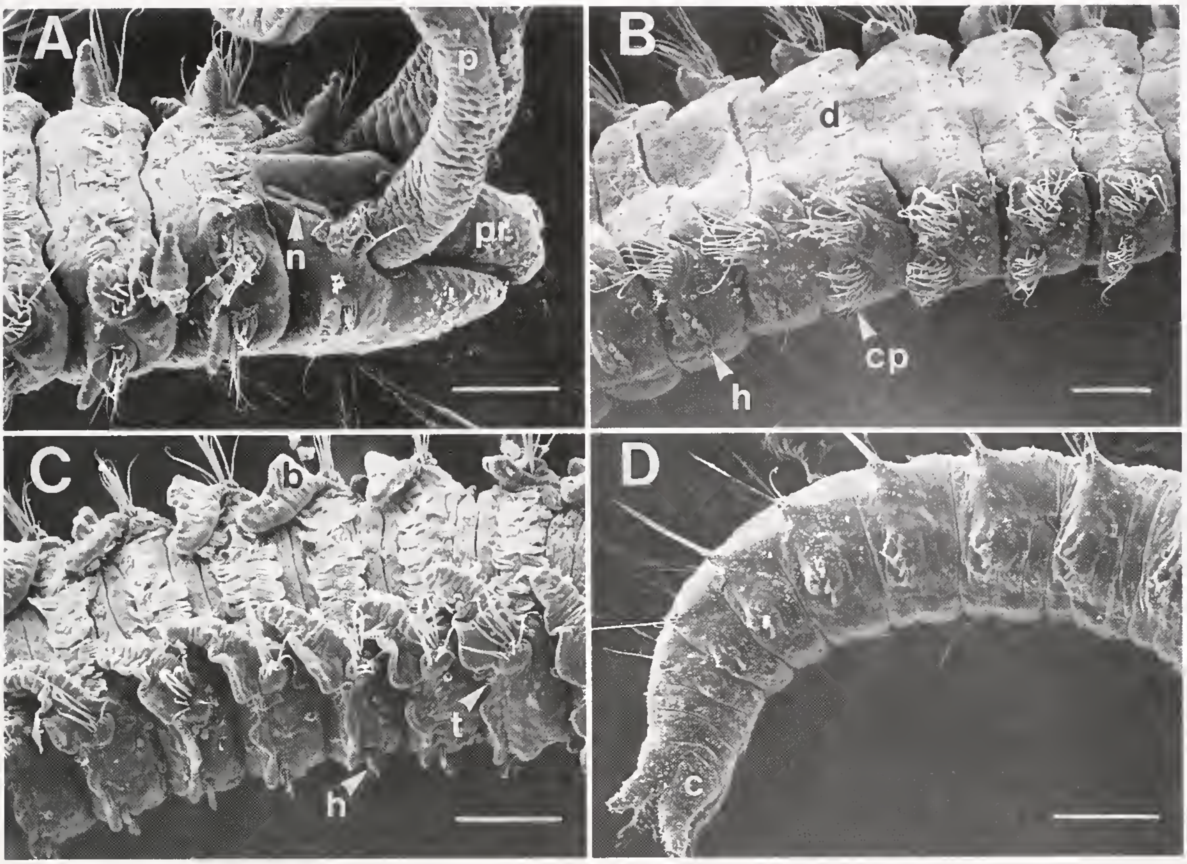

Figure 1. Scanning electron micrographs of adult *Pygospio elegans.* (A) Head and anterior thorax including the reduced first setiger. (B) Thorax, showing both anterior setigers with capillary neurochaetae and posterior setigers with neurochaetae that are hooded hooks. (C) Abdomen, characterized by branchiate setigers and a double dorsal ciliary band. (D) Tail and pygidium. b = branchus, c = cirrus, d = dorsal ciliary band, h = hooded hook, n = nuchal organ, cp = capillary chaetae, p = palp, pr = prostomium, t = tuft of cilia. Scale bar = 100 μm.

was the most common form of fission observed in the present study. The maximum number of fragments observed per division was six, and regeneration in all fragments followed the same basic pattern. Table 1 provides a list of the structures that were observed during regeneration and the time at which the regenerated structures were first observed.

On day 1, transverse fission began as a muscular constriction in the body wall, usually in the abdominal region located at a point about two-thirds along the length of the worm. Constriction of the body wall continued until the gut separated and the two fragments, each anchored to the substrate *via* mucous, pulled apart. The anterior fragment consisted of the head, thorax, and most of the abdomen (about 25 or more pairs of branchiae), while the posterior fragment consisted of the tail, pygidium, and usually about five or fewer branchiate abdominal setigers. The epidermis healed quickly and formed a smooth surface the same day as division occurred (Fig. 2a). On day 2, the blastema of both the anterior and posterior fragments showed a small amount of new tissue with tiny, scattered tufts of cilia on an otherwise smooth epidermis (Fig. 2b).

Regeneration on day 3 is characterized by rapid development of the blastema and formation of lost body regions (Table 1). As the anterior blastema increases in size, the regenerated head and thorax are readily distinguished (Fig. 2c). The head has palp buds, small dorsal depressions indicating formation of the nuchal organs, and a slightly rounded prostomium. The thorax shows the initial formation of 3 to 6 setigers, visible with both SEM and bright field microscopy. The gut, visible with bright field microscopy, has extended into the thorax near the parental abdomen. The tail blastema is smaller than the anterior blastema and shows 2–3 slight wrinkles, suggesting early segmentation. Bright field microscopy also revealed the formation of segments and as well as the extension of the gut into the tail region. Cirri buds are also visible (Fig. 2d).

On day 4, regeneration is characterized by further segmentation and early differentiation of region-specific structures. The anterior blastema has 8 to 12 well-defined seti-

Table 1

Summary of morphogenesis during regeneration in Pygospio elegans

Structure	Day 1	Day 2	Day 3	Day 4	Day 5	Day 6	Day 7	Day 8
Anterior blastema		+						
Head			+					
Eyes (no. pairs)						1–2	2–3	2–3
Mouth				*	**	**	**	**
Nuchal organ			*	**	**	**	**	**
Palps			*	**	**	**	**	**
Prostomium			*	**	**	**	**	**
Thorax			+					
Setigers (no.)			3–6	8–12	10–12	10–12	10–12	10–12
Notopodial lobe					*	**	**	**
Notochaetae					*	**	**	**
Ciliary tuft					*	**	**	**
Neuropodial lobe					*	**	**	**
Neuropodial capillary chaetae						*	**	**
Neuropodial hooded hooks						*	**	**
Posterior blastema		+						
Tail			+					
Setigers (no.)			2–3	3–6	3–6	5–7	5–7	5–7
Notopodial lobe					*	**	**	**
Notochaetae					*	**	**	**
Ciliary tuft					*	**	**	**
Neuropodial lobe					*	**	**	**
Neuropodial hooded hooks						*	**	**
Pygidium			+					
Cirri			*	**	**	**	**	**
Ciliary tufts				*	**	**	**	**

+ = body region recognizable, * = structure visible as a bud or rudiment, ** structure well developed but smaller than in parent.

gers in the thorax (Fig. 2e, f), each with two dorsal tufts of cilia. The mouth and prostomium are visible on the regenerating head, and the nuchal organs have small cilia. The gut has extended from the original abdomen to the head (Fig. 2f). Segments are further developed in the posterior blastema as well, with 3 to 6 well-defined setigers, each with paired lateral pits in the region of the presumptive noto- and neurochaetae. Differentiation of the pygidium involves extension of the cirri and the appearance of small tufts of cilia on the inner surface (Fig. 2g).

On the fifth day post-fission, the anterior blastema has regenerated the entire thoracic region and shows early differentiation of segment-specific structures. The number of thoracic setigers (10 to 12) that regenerated in the anterior blastema is similar in all specimens regardless of where fission occurred in the parent worm. The head has an elongate prostomium. The thoracic setigers develop neuropodial and notopodial buds, with a few small capillary notochaetae and a small tuft of cilia between the neuropodium and the notopodium (Fig. 3a). The gut extends through the thorax, and the mouth is complete (Fig. 3b). On the same day, the 3 to 6 setigers of the posterior blastema also develop parapodial buds, a few notopodial capillary chaetae on setigers nearest the abdomen, and small lateral tufts of cilia. The pygidium has larger cirri with tufts of cilia (Fig. 3c).

Regeneration on day 6 involves greater differentiation of segment-specific structures and addition of posterior setigers to restore the parental organization of the tail. The regenerated head has elongate, ciliated palps, a blunt prostomium (Fig. 3d), and 1 to 2 pairs of subdermal eyes (Fig. 3e). The thorax has dorsal bands of cilia on each setiger and well-developed notopodial chaetae throughout. Also in the thorax, the neuropodia exhibit short capillary chaetae on setigers 1–8 and a single hooded hook per setiger from setiger 8 posteriorly. The tail blastema has the 5 to 7 setigers characteristic of this region, with capillary notochaetae and notopodial hooded hooks that decrease in number from three on the proximal, earliest-forming setiger, to one on the later-developing terminal setiger (Fig. 3f). Lateral tufts of cilia are present on all setigers. The pygidium has cirri that are mature in size and have well-developed tufts of cilia.

By day 7, the anterior blastema has regenerated a head and thorax that are identical to those of the parent worm except in setiger size and number of chaetae (Fig. 3g). Subsequent development in this region involves an increase in setiger size but not number. In the tail, setiger size and chaetae number also increases (Fig. 3h). By day 8, the

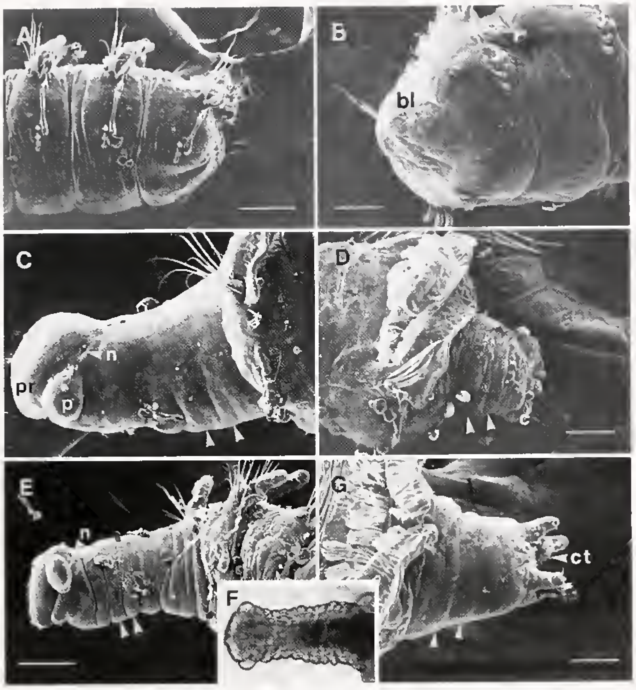

Figure 2. Early regeneration in *Pygospio elegans* following spontaneous transverse fission. (A) Day 1 post-fission, anterior fragment. (B) Day 2, posterior fragment with blastema. (C) Day 3, anterior blastema, showing regenerated head, thorax, and evidence of early segmentation. (D) Day 3, posterior blastema, showing regenerated tail and buds of cirri. (E) Day 4, regenerated head and thorax with segments. The head has a regenerated mouth, palp buds, and a rounded prostomium. (F) Day 4, regenerated head and thorax showing extension of the gut into regenerated tissue. (G) Day 4, regenerated tail and pygidium. A–E, G are scanning electron micrographs, F is a bright field micrograph. bl = blastema, c = cirri bud, n = nuchal organ, p = palp bud, pr = prostomium, t = tuft of cilia. Arrows indicate setigers. Scale bar = 100 μm for A and E, 50 μm for B–D and G.

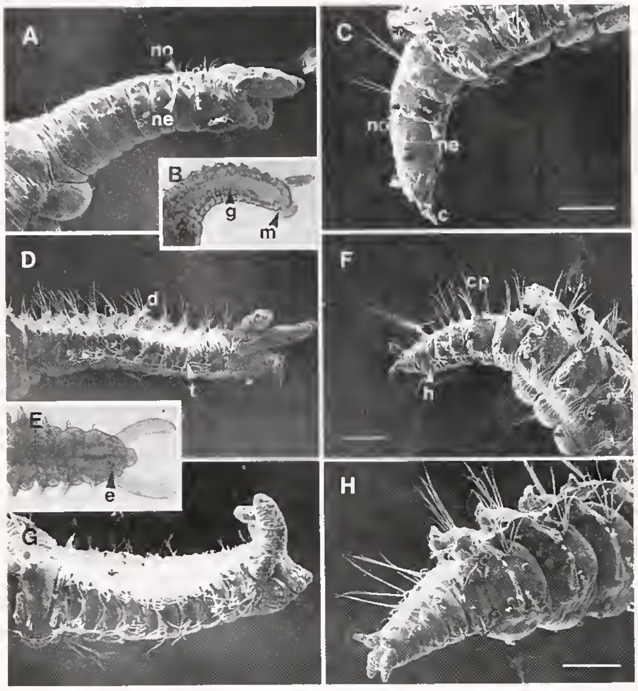

Figure 3. Completion of regeneration in *Pygospio elegans*. (A) Day 5 post-fission, anterior regenerate. (B) Day 5, anterior regenerate showing development of the gut, mouth, and setigers. (C) Day 5, posterior blastema. (D) Day 6, anterior regenerate. (E) Day 6, regenerated head with two pairs of eyes. (F) Day 6, regenerated tail and pygidium. (G) Day 7, anterior regenerate. (H) Day 7, posterior regenerate. A, C, D, F–H are scanning electron micrographs, B and E are bright field micrographs. c = cirrus, cp = capillary chaetae, d = dorsal ciliary band, e = eyes, g = gut, h = hooded hooks, m = mouth, ne = neuropodium, no = notopodium, t = tuft of cilia. Scale bar = 100 μm, anterior and posterior fragments for each day are shown at the same magnification.

regenerated thorax and tail have an increased number of chaetae, and are similar to the pre-fission organization except for setiger size. Also on day 8, the gut extends through the new tail to the pygidium.

In all fragments, regeneration produces only specific body regions, regardless of where fission occurred in the parent. Anterior fragments regenerate only the pygidium and the 6 to 12 abranchiate setigers of the tail. Posterior fragments regenerate only the thorax (10 to 12 setigers) and head. Mid-worm fragments concurrently regenerate both anterior and posterior regions as described above, with the result that these fragments regenerate the head and thorax and tail and pygidium but not the abdomen, regardless of the size of the original fragment (Fig. 4). After regeneration, worms grow to their pre-fission size by increasing setiger size and setiger number. During the growth phase, new setigers will only form immediately anterior to the pygidium; new setigers do not form in the thorax or abdomen once regeneration is complete. Newly formed terminal setigers develop chaetae and parapodial lobes typical of the

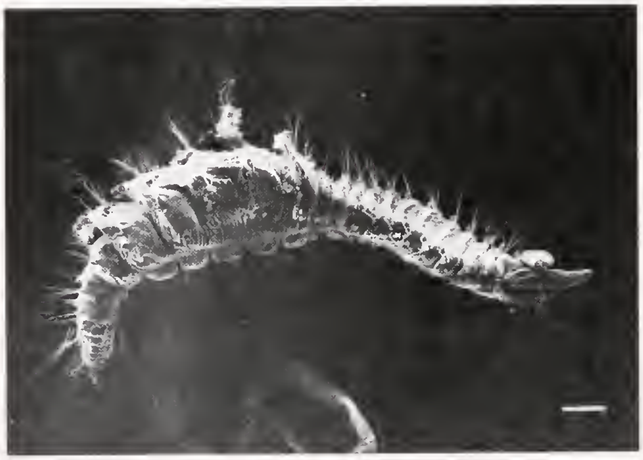

Figure 4. Scanning electron micrograph of a specimen of *Pygospio elegans* regenerating from a mid-worm fragment, about 6 days after fission. The larger, parental setigers originated from the abdominal region and have branchiae. Both the anterior (head, thorax) and posterior (tail, pygidium) regions have regenerated. Scale bar = 100 μm.

tail region (Fig. 5). As the tail region increases in setiger number, anterior tail setigers differentiate into abdominal setigers by forming dorsal ciliary bands and branchiae buds. About one-half of a setiger is added each day during the growth phase (n = 11 worms, mean ± SD 0.52 ± 0.23).

Occasional anomalies were noted in this general pattern. For example, Figure 6 shows a *P. elegans* that regenerated two thoracic regions and heads, both containing extensions of the gut. Such anomalies, although rare, reinforced the general pattern of regeneration described above. For both heads, the blastema gave rise to a specific number of setigers, and segmentation was followed by differentiation.

Population comparison

Frequency of spontaneous division and mortality were compared in *P. elegans* originating from the three populations. Specimens from all three populations were roughly the same size at the start of the experiment and ranged from 25 to 62 setigers overall (Table 2). Worms from Starr's Point and Conrad's Beach divided about once per week (1.3 and 1.2 weeks between divisions, respectively), while worms from Bon Portage Island divided less frequently (3.6 weeks between divisions; Table 2), although sample sizes were low for the Starr's Point and Bon Portage Island worms. Most worms divided into two fragments, but up to six fragments per division were observed. Conrad's Beach worms divided at the smallest size (average of 34 setigers), whereas those from Starr's Point and Bon Portage were, on average, larger before undergoing fission (42 and 45 setigers, respectively; Table 2).

Mortality was also compared among regenerating fragments. Fragments were classified according to the remaining original body region into anterior (containing the original head, thorax, and anterior abdomen), mid-worm (abdominal setigers only), and posterior fragments (original pygidium, tail, and a few abdominal setigers). Anterior and mid-worm fragments had a relatively low mortality, approximately 14% for all three populations combined (Table 2), although few mid-fragments were observed because most worms spontaneously divided into two fragments (anterior, posterior) only. Posterior fragments had the highest mortality overall, about 80% among all three populations (Table 2).

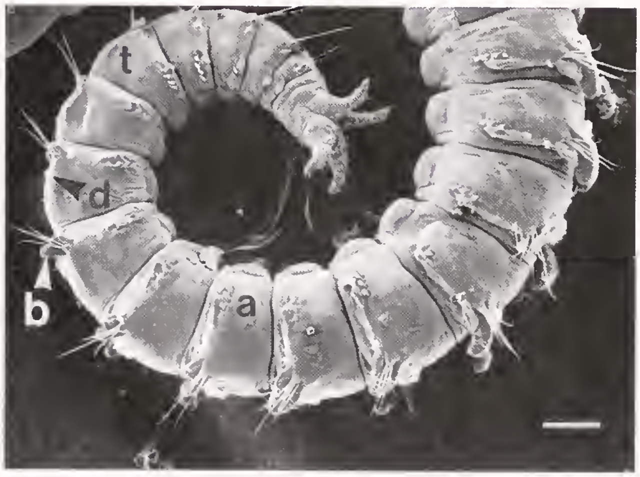

Figure 5. Growth in *Pygospio elegans*. Growth occurs through the addition of terminal setigers, immediately anterior to the pygidium. New setigers develop the parapodial lobes and chaetae characteristic of the tail (t). Transitional setigers show branchiae buds (b) and tufts of dorsal cilia (d) as they gradually differentiate into abdominal setigers (a). Scale bar = 100 μm.

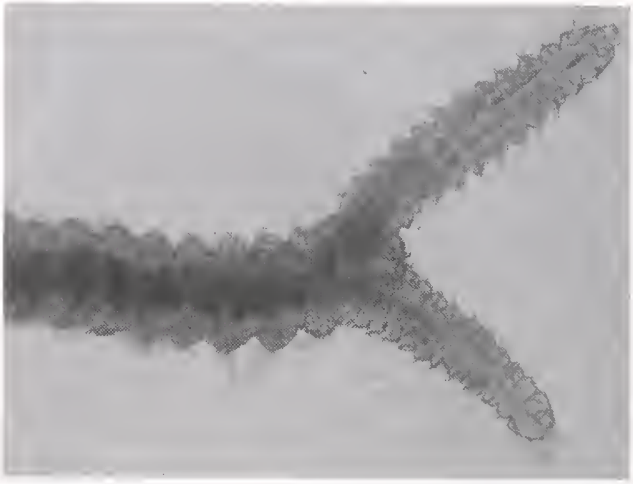

Figure 6. Bright field micrograph of a two-headed individual of *Pygospio elegans*, formed after a spontaneous asexual event.

Discussion

Morphogenesis after asexual reproduction in *Pygospio elegans* involved two phases: regeneration of lost body regions (*e.g.*, head, thorax, tail) followed by appositional growth as terminal setigers were added. During regeneration of the anterior region, the blastema extended to form the head and thorax, segmented to divide the thorax into 10–12 setigers, and subsequently developed segment-specific structures (*i.e.*, chaetae). Regeneration of the posterior blastema was similar and also involved formation of a finite, though variable, number of setigers (6 to 12). The origin of blastemal tissues was not examined in the present study, but probably involves the growth of existing tissues (*e.g.*, epidermis) in combination with the migration of mesodermal—and possibly endodermal—neoblasts, as occurs in other annelids (Hill, 1970; Christensen, 1994).

Once the thorax or tail had become reestablished, growth occurred but was restricted to a growth zone immediately anterior to the pygidium; new setigers did not appear elsewhere in the body. Growth by the formation of terminal setigers is common in spionid adults and larvae. The abdo-

Table 2

Asexual reproduction in Pygospio elegans

Trait	Population			ANOVA
	Bon Portage	Starr's Point	Conrad's Beach	
Original size (no. setigers)	42.1 ± 3.2	35.4 ± 1.2	41.6 ± 3.0	$F_{(2,39)} = 2.2, P = 0.12$
	$n = 15$	$n = 15$	$n = 10$	
Fission				
No. Weeks between divisions	3.6 ± 0.5	1.3 ± 0.3	1.2 ± 0.1	$F_{(2,28)} = 26, P = 0.000$
	$n = 5$	$n = 3$	$n = 21$	CB = SP < BP
Size at division (no. setigers)	44.6 ± 3.3	41.5 ± 2.1	34.0 ± 1.9	$F_{(2,53)} = 5.5, P = 0.007$
	$n = 17$	$n = 11$	$n = 26$	CB < BP, SP ns
No. Fragments per division	2.2 ± 0.1	2.2 ± 0.1	2.7 ± 0.2	$F_{(2,52)} = 2.4, P = 0.10$
	$n = 17$	$n = 11$	$n = 26$	
Mortality (no. dead/no. fragments per type)				% Mortality
Anterior fragment	6/26	0/11	3/29	13%
Middle fragment	1/2	1/2	2/24	14%
Posterior fragment	14/14	7/8	11/18	80%

Data are means, standard errors, and sample sizes (n) for traits indicated, in a comparison between laboratory-maintained worms from three populations. The final column gives results of a one-way ANOVA among populations and results of a post-hoc Scheffé comparison among populations, where significant differences were found.

men increased in size only during the growth phase as tail setigers differentiated into abdominal setigers by developing branchiae and dorsal cilia. In all fragments, regeneration produced only specific body regions, regardless of where fission occurred in the parent. For example, one worm divided in the original thoracic region and, after fission, had only a head and nine thoracic setigers. This individual regenerated only a tail and pygidium; abdominal setigers redifferentiated from tail setigers as growth proceeded. Many worms were observed to undergo a second asexual event before growth was complete (often 8 to 10 days after fission), and several individuals divided almost immediately after fission (days 1–3) as evidenced by the presence of fragments at different stages of regeneration in a single culture.

Spionids, in general, are not as well known for their ability to regenerate as are some other polychaetes, such as sabellids. Asexual reproduction by regeneration is common, however, in the spionids *Polydora tetrabranchia* (Campbell, 1955) and throughout the genus *Polydorella* (Radashevsky, 1996). In *Polydorella,* unlike *P. elegans,* new individuals are formed by paratomy, resulting in a chain of clones. Otherwise, morphogenesis during an asexual event in *Polydorella dawydoffi* is similar to architomy in *P. elegans:* the new individual forms through development of a growth zone (similar to the blastema reported here), elongation to form specific anterior body regions (*i.e.*, head and thorax), segmentation resulting in a specific number of thoracic setigers, and differentiation to form region-specific structures such as the chaetae, eyes, and branchiae. Once the new head has formed in *Polydorella,* transverse fission occurs and the two daughter worms separate (Radashevsky, 1996). Although asexual reproduction does not appear to be widespread in spionids, regeneration as a response to tissue loss (*e.g.*, palps or the tail) occurs frequently in *Polydora cornuta* (Zajac, 1985, 1995), *Boccardia proboscidea* (Gibson, pers. obs.), and *Streblospio benedicti* (Harvey, pers. obs.). Further work may reveal whether the restricted potential for asexual reproduction within the spionids could have arisen by decoupling regeneration and reproduction, as has been suggested in the oligochaete *Paranais litoralis* (Bely, 1999).

Although the mechanisms leading to the restoration and differentiation of body regions are not known, it seems likely that the regulatory genes important in embryogenesis may play a role. For example, *distal-less* is known to be important in the development of parapodia in polychaete embryos (Panganiban *et al.*, 1997) and possibly is reactivated during regeneration, although this remains to be demonstrated. In an asexual race of *Dugesia tigrina* (platyhelminth), lost body regions are defined during regeneration by Hox genes that have sequences very similar to those found in annelids (Bayascas *et al.*, 1998). Interestingly, in this race of *D. tigrina,* Hox genes were found to be permanently expressed in adults, perhaps contributing to the impressive regenerative capabilities of this species (Bayascas *et al.*, 1998).

There were no differences among populations in original size and number of fragments per asexual event in *Pygospio elegans,* although time between divisions and size at division did vary. Rasmussen found that rates of division increased at low temperatures, and Wilson (1985) found that division rates increased at low worm densities. Anger (1984) observed that the number of individuals (in an asexual population) increased at low salinity and temperature. In the present study, fission was observed in isolated worms that were maintained under constant conditions (34 ppt, 20°C and with an abundance of food); therefore, these conditions were unlikely to contribute to the differences in division we observed among laboratory cultures.

Posterior fragments (original tail) had a higher mortality than did anterior fragments (original head). Posterior fragments were much smaller than anterior fragments; had few branchiate, abdominal setigers (5–6 on average, *vs.* 25 for anterior fragments); and lacked a mouth until day 5 post-fission and therefore were unable to feed immediately after division. Differences in mortality could be due to fragment size (*e.g.*, energy reserves or number of neoblasts available) or lack of a mouth. However, the few mid-worm fragments observed during the present study had a high survivorship, despite their small size. Despite the high mortality of posterior fragments, extensive laboratory culturing by others indicates a net population growth through asexual reproduction (Anger, 1984; Wilson, 1985).

Although *P. elegans* is known to reproduce sexually (Thorson, 1946; Hannerz, 1956; Anger, 1984; Anger *et al.*, 1986; Morgan *et al.*, 1999), only asexual reproduction was noted in the worms observed in the present study (more than 200 in total). This suggests that asexual reproduction is the dominant reproductive mode in these populations during the study period (May–September). Anger (1984) reported a population in the Kiel Bight, Baltic Sea, that reproduces exclusively through asexual reproduction; two additional populations were predominantly sexual, although occasional fragmentation was noted. Anger (1984) attempted to induce specimens of *P. elegans* from these three populations to switch between sexual and asexual reproduction by varying culture conditions (temperature and salinity) but found that worms retained the reproductive mode of their original population, leading her to suggest the potential for cryptic species. Other investigators have reported seasonal differences in reproductive mode within a single population, with asexual reproduction being dominant in the spring or summer, and sexual reproduction prevalent in the fall or winter (Rasmussen, 1973; Hobson and Green, 1968; Wilson, 1985). Rasmussen (1953) also noted that fission could be induced in *P. elegans* by temperatures of 4°–5°C.

In addition to asexual reproduction, *P. elegans* exhibits considerable flexibility in sexual reproduction, including both planktotrophic and adelphophagic larval development (*e.g.*, Thorson, 1946; Hannerz, 1956; Hobson and Green, 1968; Anger, 1984; Anger *et al.*, 1986). This suggests the potential for reports of *P. elegans* to include cryptic species, but Morgan *et al.* (1999) clearly demonstrated that poecilogony does exist in this species, based on a molecular (allozyme) comparison of populations with planktotrophic or adelphophagic development. Poecilogony in *P. elegans* is, in several regards, similar to that of the spionids *Boccardia proboscidea* (Blake and Kudenov, 1981; Gibson, 1997) and *Polydora cornuta* (MacKay and Gibson, 1999), which also reproduce by means of planktotrophic and adelphophagic larval development. Such flexibility makes *P. elegans* a valuable model for tests of the ecological consequences of life-history variability, as well as for understanding the developmental mechanisms underlying a change in development mode.

Acknowledgments

We thank H. Smith for general and field assistance, and H. Taylor for assistance with the SEM. P. Allen-Wojtas and S. Carbyn of the Electron Microscopy and Imaging Laboratory, Agriculture and Agri-Food Canada, Kentville, Nova Scotia, provided facilities and assistance with SEM. The manuscript has benefited from comments from M. Gibson and I. Paterson. This research was funded by an NSERC grant to G. Gibson and Nova Scotia Summer Career Placement to J. Harvey.

Literature Cited

Anger, V. 1984. Reproduction in *Pygospio elegans* (Spionidae) in relation to its geographical origin and to environmental conditions: a preliminary report. *Fortschr. Zool.* **29:** 45–51.

Anger, K., V. Anger, and E. Hagmeier. 1986. Laboratory studies on larval growth of *Polydora ligni*, *Polydora ciliata*, and *Pygospio elegans* (Polychaeta, Spionidae). *Helgol. Meeresunters* **40:** 377–395.

Balinsky, B. I. 1975. *An Introduction to Embryology*, 4th ed. W. B. Saunders, Philadelphia. Pp. 592–595.

Barnes, R. D. 1980. *Invertebrate Zoology*, 4th ed. Saunders College, Philadelphia. Pp. 467–528.

Bayascas, J. R., E. Castillo, and E. Saló. 1998. Platyhelminthes have a Hox code differentially activated during regeneration, with genes closely related to those of spiralian protostomes. *Dev. Genes Evol.* **208:** 467–473.

Bely, A. 1999. Decoupling of fission and regenerative capabilities in an asexual oligochaete. *Hydrobiologia* **406:** 243–251.

Blake, J., and J. Kudenov. 1981. Larval development, larval nutrition and growth for two *Boccardia* species (Polychaeta: Spionidae) from Victoria, Australia. *Mar. Ecol. Prog. Ser.* **6:** 175–182.

Bromley, J. E., and J. S. Bleakney. 1984. *Keys to the Fauna and Flora of Minas Basin.* National Research Council of Canada, Atlantic Research Laboratory. NRCC Pub. No. 24119. 141 pp.

Campbell, M. 1955. Asexual reproduction and larval development in *Polydora tetrabranchiata* Hartman. Ph.D. thesis, Duke University, Durham, NC. 95 pp.

Christensen, B. 1994. Annelida–Clitellata. Pp. 1–23 in *Reproductive Biology of Invertebrates: Vol. VI Asexual Propagation and Reproductive Strategies*, K. Adiyodi and R. Adiyodi, eds. John Wiley, Chichester, UK.

Fauchald, K. 1977. *The Polychaete Worms: Definitions and Keys to the Orders, Families, and Genera.* Natural History Museum of Los Angeles County, Science Series 28: 1–190. Los Angeles. Pp. 25, 156–160.

Gibson, G. 1997. Variable development in the spionid *Boccardia proboscidea* (Polychaeta) is linked to nurse egg production and larval trophic mode. *Invertebr. Biol.* **116:** 213–226.

Gibson, G. D., I. Paterson, H. Taylor, and B. Woolridge. 1999. Molecular and morphological evidence of a single species, *Boccardia proboscidea* (Polychaeta: Spionidae) with multiple development modes. *Mar. Biol.* **134:** 743–751.

Gudmundsson, H. 1985. Life history patterns of polychaete species of the family Spionidae. *J. Mar. Biol. Assoc. UK* **65:** 93–111.

Hannerz, L. 1956. Larval development of the polychaete families Spionidae Sars, Disomidae Mesnil, and Poecilochaetidae N. Fam. in the Gullmar Fjord (Sweden). *Zool. Bidr. Uppsala* **31:** 1–204.

Hill, S. 1970. Origin of the regeneration blastema in polychaete annelids. *Am. Zool.* **10:** 101–112.

Hobson, K. D., and R. H. Green. 1968. Asexual and sexual reproduction of *Pygospio elegans* (Polychaeta) in Barnstable Harbor, Massachusetts. *Biol. Bull.* **135:** 410 (abstract).

MacKay, J., and G. Gibson. 1999. The influence of nurse eggs on variable larval development in *Polydora cornuta* (Polychaeta, Spionidae). *Invertebr. Reprod. Dev.* **35:** 167–176.

Morgan, T. S., A. D. Rogers, G. L. J. Paterson, L. E. Hawkins, and M. Sheader. 1999. Evidence for poecilogony in *Pygospio elegans* (Polychaeta: Spionidae). *Mar. Ecol. Prog. Ser.* **178:** 121–132.

Panganiban, G., S. Irvine, C. Lowe, H. Roehl, L. Corley, B. Sherbon, J. Grenier, J. Fallon, J. Kimble, M. Walker, G. Wray, B. Swalla, M. Martindale, and S. Carroll. 1997. The origin and evolution of animal appendages. *Proc. Natl. Acad. Sci. USA* **94:** 5162–5166.

Radashevsky, V. I. 1996. Morphology, ecology and asexual reproduction of a new *Polydorella* species (Polychaeta: Spionidae) from the South China Sea. *Bull. Mar. Sci.* **58:** 684–693.

Rasmussen, E. 1953. Asexual reproduction in *Pygospio elegans* Claparede (Polychaeta sedentaria). *Nature* **171:** 1161–1162.

Rasmussen, E. 1973. Systematics and ecology of the Isefjord marine fauna (Denmark). *Ophelia* **11:** 1–507.

Schlötzer-Schrehardt, U. 1991. Ultrastructural differentiation of nuchal and dorsal organs during postembryonic and sexual development of *Pygospio elegans* Claparede (Polychaeta: Spionidae). *Ophelia Suppl.* **5:** 633–640.

Solomon, E. P., L. R. Berg, D. W. Martin, and C. A. Villee. 1993. *Biology*, 3rd ed. Saunders College Publishing, Philadelphia. Pp. 219, 1028–1029.

Thorson, G. 1946. Reproduction and larval development of Danish marine bottom invertebrates. *Meddr. Kommn. Havunders.* (Plankton). **4:** 1–523.

Wilson, W. H., Jr. 1985. Food limitation of asexual reproduction in a spionid polychaete. *Int. J. Invertebr. Reprod. Dev.* **8:** 61–65.

Zajac, R. N. 1985. The effects of sublethal predation on reproduction in the spionid polychaete *Polydora ligni* Webster. *J. Exp. Mar. Biol. Ecol.* **88:** 1–19.

Zajac, R. N. 1995. Sublethal predation on *Polydora cornuta* (Polychaeta: Spionidae): patterns of tissue loss in a field population, predator functional response and potential demographic impacts. *Mar. Biol.* **123:** 531–541.

Reference: *Biol. Bull.* **199:** 50–58. (August 2000)

Factors Influencing Spawning and Pairing in the Scale Worm *Harmothoe imbricata* (Annelida: Polychaeta)

G. J. WATSON[1,*], F. M. LANGFORD[2], S. M. GAUDRON[2], AND M. G. BENTLEY[2]

[1] *Institute of Marine Sciences, Ferry Road, Eastney, University of Portsmouth, Portsmouth, P04 9LY, UK; and* [2] *Department of Marine Sciences and Coastal Management, Faculty of Agriculture and Biological Sciences, Ridley Building, University of Newcastle, Newcastle-upon-Tyne, NE1 7RU, UK*

Abstract. Endocrine and environmental factors control reproduction of the polynoid scale worm *Harmothoe imbricata*. We confirmed that the rate of vitellogenesis was greater in winter specimens transferred from ambient regimes of photoperiod and temperature to a light:dark (LD) photoperiod of 16:8 at 10°C and showed that the number of females spawning was significantly greater than for those transferred to LD8:16 at 10°C. The endocrine mediation of this response was investigated using prostomium implantations. Significantly more LD8:16 females implanted with prostomia from LD16:8 conditioned females spawned than LD8:16 females implanted with LD8:16 prostomia. Females without prostomia failed to spawn. LD16:8 exposure may increase levels of a possible "spawning hormone" in the prostomium. Spawning proceeded in these LD16:8 females and allowed spawning to occur in LD8:16 females implanted with LD16:8 prostomia. In LD8:16 prostomia, titers of the spawning hormone reached the threshold in significantly fewer individuals, so that significantly fewer females implanted with LD8:16 prostomia spawned.

Using Y-maze choice chambers, pair formation was shown to be under pheromonal control, with males being attracted to mature females but not to females carrying fertilized oocytes or to LD8:16 conditioned females. Production of this attraction pheromone can, therefore, be manipulated through photoperiodic control, suggesting a link between oogenesis, spawning, and pheromone production.

Introduction

The polynoid scale worm *Harmothoe imbricata* is a common inhabitant of temperate intertidal rocky shores, where it lives under rocks and small stones. It is an active carnivore that preys upon other small invertebrates. The reproductive biology of this species is relatively well understood. It is a dioecious, iteroparous species with an annual cycle of reproduction (Daly, 1972, 1974; Garwood, 1980). Females develop two cohorts of oocytes: the first is grown slowly during the winter months to be spawned in March; the second is produced rapidly and spawned about 30 days after the first. During the breeding season individuals pair, a behavior in which a male lies closely along the dorsal surface of the female (Daly, 1972). Cohorts of oocytes, once spawned, are fertilized and carried under the female's dorsal elytra (scales) during embryogenesis. Embryos are released as trochophores after about 16 days.

Oogenesis is initiated in late September without any specific environmental input. During the autumn, the first cohort grows under conditions of decreasing environmental temperature, and growth is accelerated by exposure to low temperatures (Garwood, 1980). The stabilization of oocyte development also requires exposure to a light-dark (LD) cycle with a photophase less than 13 h for between 42 and 55 days during the late autumn period. If these photoperiods are not experienced, oocyte development is aborted (Clark, 1988). Once the winter solstice has passed, natural populations respond to a second photoperiodic input. An exposure to LD cycles with a photophase above 10 or 11 h increases oocyte growth rate and may synchronize oogenesis and spawning among individuals (Garwood and Olive, 1982; Clark, 1988).

Although environmental manipulation affects both oogenesis and spawning, the endocrine role in mediating these

Received 23 November 1999; accepted 31 May 2000.

* To whom correspondence should be addressed. E-mail: gordon.watson@port.ac.uk

influences has received comparatively little attention. Bentley *et al.* (1994) and Lawrence (1996) confirmed the presence of a gonadotrophic hormone from the prostomium that probably mediates oogenesis, and it seems likely that the hormone is secreted only under the appropriate regimes of photoperiod and temperature. Nevertheless, the role of the endocrine system in spawning is unknown in this species. In a number of other polychaete species, the implantation or injection of prostomia into individuals has been used to investigate their endocrine control of reproduction and spawning (Golding, 1983; Bentley *et al.*, 1984; Pacey and Bentley, 1992; Bentley *et al.*, 1994; Watson *et al.*, 2000). In the work reported here, transplantation experiments establish the role of the endocrine system in mediating photoperiodic influences, and environmental manipulation is used to investigate the effect of photoperiod on spawning and oogenesis of the first cohort of oocytes.

Pheromones coordinate and control reproduction in a number of marine invertebrates, including species of the opisthobranch mollusc *Aplysia* (Zeeck *et al.*, 1990, 1996; Painter *et al.*, 1998), by inducing spawning and by attracting other individuals towards spawning animals. In this paper we provide evidence of an attraction pheromone produced by female *Harmothoe imbricata* to attract males for mating, and we examine the influence of environmental manipulation on its production.

The results presented here provide the first link between environmental conditioning, endocrine activity, and pheromonal control of attraction for pairing and spawning in a polychaete species. *Harmothoe imbricata* is thus likely to become a model species for the investigation of environmental-endocrine-pheromone interactions.

Materials, Methods, and Results

Photoperiodic control of oocyte growth and spawning mediated by the endocrine system

Collection and maintenance of animals. Specimens of *Harmothoe imbricata* were collected from the intertidal zone of three rocky shores in E. Scotland, UK: St Andrews (56°20′N, 2°47′W), Kingsbarns (56°18′N, 2°38′W) and Fife Ness (56°16′N, 2°35′W). Individuals were maintained in glass crystallizing dishes containing 100 ml of TFSW (twice-filtered seawater, pore size 0.34 μm) and provided with a cleaned *Patella vulgata* shell for shelter. All worms were hand-fed pieces of *Mytilus edulis* muscle once per week, after which the water was changed. All individuals were collected in December and January and kept at 10°C and ambient photoperiods until the experiments commenced on 9 February 1999.

To assess their state of maturity, individuals were narcotized in 5% ethanol in seawater and a small incision was then made in the lower edge of the 16th setiger. For microscopic analysis, a small sample of coelomic fluid and blood vessel was removed using a 20-μl glass micropipette. The diameters of about 30 oocytes from five randomly chosen females from each treatment group were measured using a compound microscope. Sperm activity was assessed after dilution.

Experimental protocol. On 9 February 1999, half of the females were transferred to conditions of 16 h light and 8 h dark (LD16:8) at 10°C. The individuals that remained in LD8:16 conditions were termed LD8:16 controls while those transferred to the LD16:8 were termed LD16:8 controls. Oocyte diameters were measured from five randomly selected individuals from the two groups on this day and subsequently once per week for 3 weeks.

Prostomium (PM) transplants were performed on 26 February 1999, 2 weeks after photoperiod manipulation had commenced. Individuals from the LD16:8 control and the LD8:16 control were narcotized as described above to provide prostomia. They were termed LD16:8 donors and LD8:16 donors, respectively. The PM was accessed by removing the first two scales and then excised with iridectomy scissors. Once removed, the PM was trimmed of excess flesh and tentacles and then placed in seawater on ice until implanted. Both sets of PM donors were then returned to seawater to recover from the narcotization.

Individuals designated to received the implanted PM were also narcotized, and a PM was inserted through an incision in the 20th setiger. This was far enough from the head to prevent any interference with movement. Twenty-five LD16:8 control females were used as PM donors and their PMs were implanted into females from the LD8:16 control group. They were termed LD8:$16^{\mathrm{PM(LD16:8)}}$ females (the superscript notation refers to the conditions that the female, from which the prostomium used for implantation was removed, was exposed to). As a control, eight LD8:16 control females were also implanted with LD8:16 control PMs, and these were termed LD8:$16^{\mathrm{PM(LD8:16)}}$. After implantation, all PM recipients and PM donors were returned to their respective photoperiod treatments. All individuals were examined daily for evidence of spawning (the presence of oocytes under the elytra). The diameters of about 30 oocytes were measured from individuals that had spawned.

Statistical analyses. The nature of the oocyte diameter data (unbalanced nesting and sample sizes) precluded analysis using a multiple ANOVA for all data. Instead, mean oocyte diameters for each female were obtained, and these data were then assessed using one-way and two-way ANOVAS. Subsequent pairwise comparisons were performed using Tukey tests. The numbers of spawning individuals were analyzed for independence by using an R × C contingency table and the chi-square statistic (χ^2); pairwise comparisons were performed subsequently using a modified Tukey test.

Results: photoperiodic control of oocyte growth. Mean oocyte diameters of LD8:16 and LD16:8 controls and PM recipients (LD8:16$^{\text{PM(LD8:16)}}$ and LD8:16$^{\text{PM(LD16:8)}}$ are shown in Figure 1. Analysis, using a two-way ANOVA, of the mean oocyte diameters of the LD8:16 and LD16:8 controls for weeks 1 to 3 shows that significant differences were present between weeks ($F = 28.64$, $P < 0.001$), but not between treatments. There were also significant interaction effects ($F = 7.407$, $0.05 > P > 0.001$). Pairwise comparisons using a Tukey test confirm that the mean diameters of LD16:8 and LD8:16 controls were not significantly different from each other in week 1. By week 2, LD16:8 control diameters increased significantly when compared to week 1, whereas LD8:16 control diameters did not increase. By week 3, LD8:16 control diameters increased significantly when compared to week 2. At the same time, all mean oocyte diameters of all treatments were not significantly different from each other when analyzed with a one-way ANOVA. ($F = 0.11$, $P > 0.05$). Analysis of all treatments in week 4 shows that there were significant differences between the treatments ($F = 9.56$, $0.05 > P > 0.001$). However, pairwise comparisons reveal that only the LD16:8 control mean diameter was significantly greater than the LD8:16 control and LD8:16$^{\text{PM(LD8:16)}}$. No other pairwise comparisons were significantly different.

Results: photoperiodic control of female spawning mediated by the endocrine system. During the experimental period, all individuals in all treatments were monitored daily for spawning; the cumulative percentage of individual spawning females is shown in Figure 2. Over the duration of the total experimental period (9 February-14 March), 96% (24 individuals) of the LD16:8 controls spawned, with the majority (16 individuals) spawning on 23 February and another 8 spawning between 24 and 28 February. In comparison, only 33% of the LD8:16 control females spawned during the experimental period, one on 19 February, two on 23 February, and another on 25 February.

During the experimental period for prostomial manipulation (26 February–14 March), 80% of the LD8:16$^{\text{PM(LD16:8)}}$ treatment group spawned, with 10 individuals spawning on

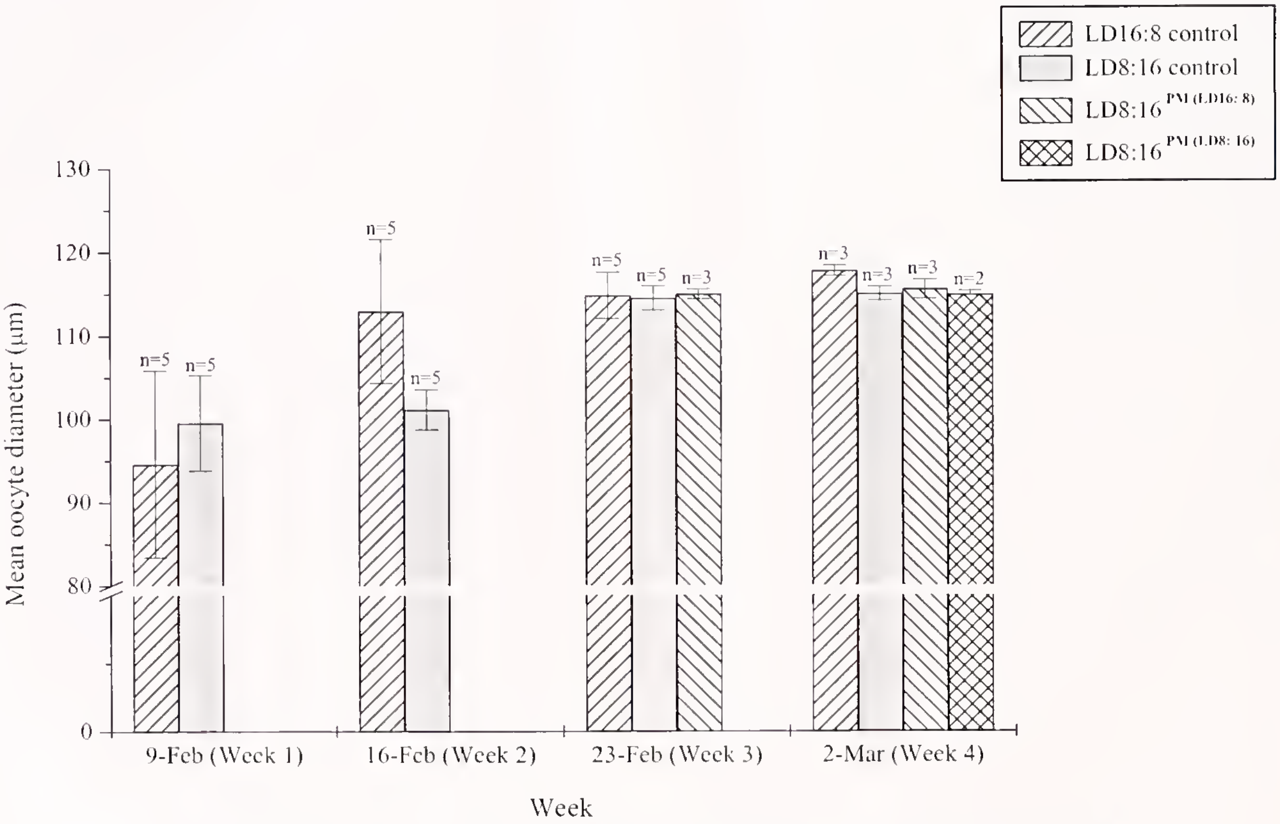

Figure 1. Mean weekly oocyte diameter (±95% confidence limits) of female *Harmothoe imbricata* exposed to various treatments at 10°C: LD16:8 control, females maintained in long-day photoperiod (LD16:8); LD8:16 control, females maintained in short-day photoperiod (LD8:16); LD8:16$^{\text{PM(LD16:8)}}$, females maintained in LD8:16, each implanted with one prostomium from an LD16:8 control female; LD8:16$^{\text{PM(LD8:16)}}$, females maintained in LD8:16, each implanted with one prostomium from an LD8:16 control female. All individuals were collected in December and maintained in ambient photoperiod at 10°C prior to the start of the experiment on 9 February 1999 (week 1). All transplantations were performed on 26 February 1999 (week 3); n = number of females sampled, 30 oocytes were counted per female.

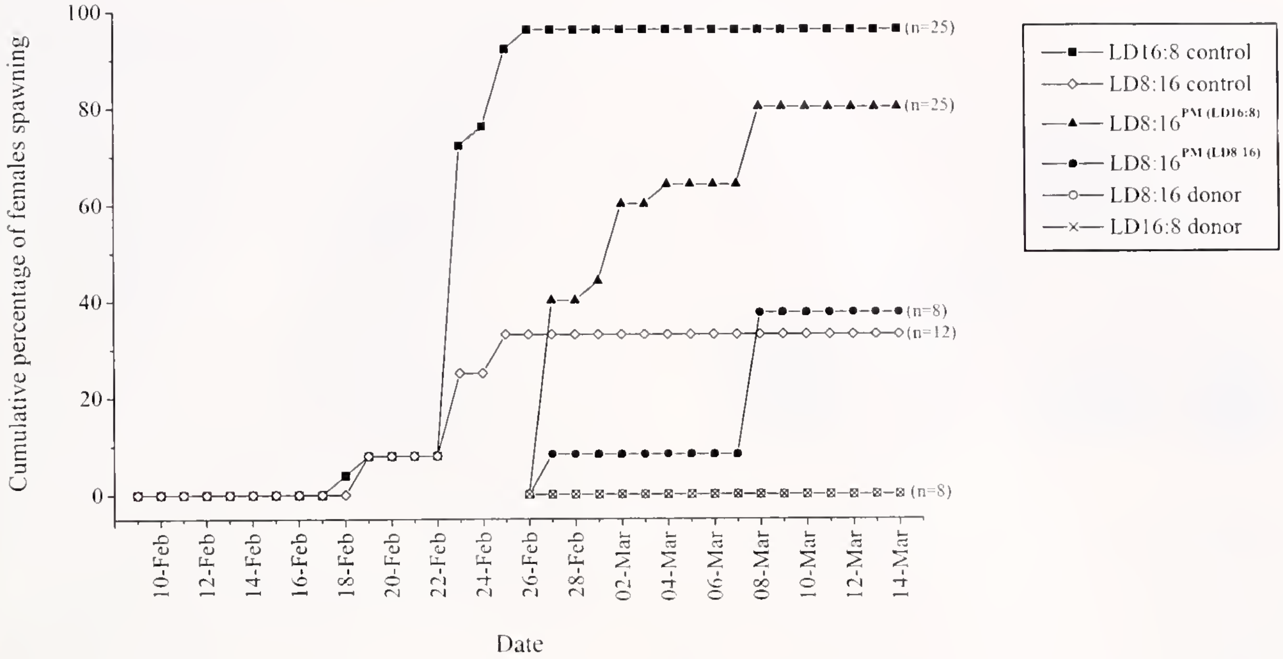

Figure 2. Cumulative percentage of spawning female *Harmothoe imbricata* after exposure to various treatments at 10°C. LD16:8 control, females maintained in long-day photoperiod (LD16:8); LD8:16 control, females maintained in short-day photoperiod (LD8:16); LD8:$16^{PM(LD16:8)}$, females maintained in LD8:16 and each implanted with one prostomium from an LD16:8 control female; LD8:$16^{PM(LD8:16)}$, females maintained in LD8:16 and each implanted with one prostomium from an LD8:16 control female; LD8:16 donor, LD8:16 control females used as prostomial donors; LD16:8 donor, LD16:8 control females used as prostomial donors. All individuals were collected in December and maintained in ambient photoperiod prior to the start of the experiment on 9 February 1999, start of photoperiodic conditioning. All transplantations were performed on 26 February 1999. *n* is the number of females in each treatment group.

27 February and a further 10 spawning between 1–8 March. In contrast, only 37.5% (3 individuals) of the LD8:$16^{PM(LD8:16)}$ treatment group spawned, and none of the LD8:16 or LD16:8 donors spawned.

Statistical analysis using an R × C test of independence and the χ^2 statistic reveals highly significant differences between the total proportion of spawning to nonspawning females between all treatments ($\chi^2 = 68.409$, $P < 0.001$). Statistical analysis of pairwise comparisons, using a modified Tukey test, shows that all pairwise comparisons were significantly different from each other, except the following treatments: LD8:16 control compared with LD8:$16^{PM(LD8:16)}$, and LD8:16 donor compared with LD16:8 donor.

Pheromone influence on pairing behavior

Y-maze behavioral bioassays. Six Y-mazes, the dimensions of which are shown in Figure 3A, were constructed from 5-mm-thick clear acrylic plastic. Each was sealed with silicon sealant and allowed to cure by soaking in seawater for several days prior to use. Each arm had a removable acrylic partition with 0.4-mm-diameter holes drilled through to allow pheromonal diffusion. All experiments were performed at 10°C in ambient illumination.

Animals. Animals were collected from the Fife Ness site during March and April and maintained as described above. Individuals collected in March and April (classed as "old" and "new," respectively) were sexed, and their state of maturity assessed as described above. Of the old individuals collected, 10 females were carrying fertilized oocytes and 7 females still had fully grown oocytes in the coelomic cavity. Of the males collected, 18 had active sperm in their coelomic cavity. Of the new individuals collected, 10 females had not spawned and 10 males had sperm in their coelomic fluid.

Experimental protocol. The basic experimental protocol is summarized in Figure 3B. Before each set of experiments, each maze was washed in fresh water before air-drying. During a run of experiments each maze was washed in TFSW between tests. After each maze was filled, a potential stimulus animal was placed in one arm of the maze behind the partition. After 1 min, a test male was placed in the base of the maze. To minimize handling, a glass tube was used in positioning the test animals. Each test was run for 30 min (except the first directional bias test with old males, see below), after which the position of the test male was noted. At the end of the 30 min, a response was considered positive if the test male was in the arm with the stimulus animal,

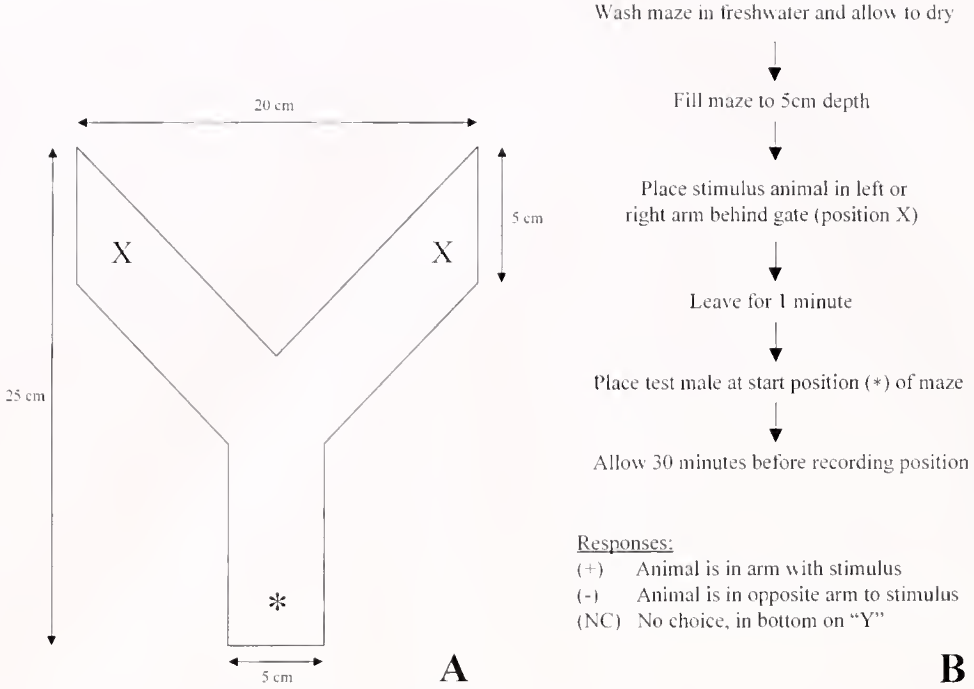
20 cm
5 cm
25 cm
X
X
*
5 cm
A
Wash maze in freshwater and allow to dry
Fill maze to 5cm depth
Place stimulus animal in left or right arm behind gate (position X)
Leave for 1 minute
Place test male at start position (*) of maze
Allow 30 minutes before recording position
Responses:
(+) Animal is in arm with stimulus
(-) Animal is in opposite arm to stimulus
(NC) No choice, in bottom on "Y"
B

Figure 3. (A) Schematic diagram of Y-maze for the investigation of pheromonal attraction of male *Harmothoe imbricata* to various stimuli. Dashed lines represent removable partitions. Depth of seawater in Y-maze: 5 cm. (B) Summary flow diagram of the experimental protocol.

negative if it was in the opposite arm, and a no choice if it was in the base of the Y. During an experimental run, all potential stimulus individuals were alternated between each arm in consecutive experiments and cross-tested with all test males.

Tests performed. All tests were performed within 2 weeks of collection. To assess for any directional bias ("handedness") and for chance levels of attraction in the maze, two sets of experiments were performed in which males were placed in the Y-maze with no stimulus animal. In the first experiment, nine old males were each run three times in the Y-maze and the position of the animal was recorded after 10 min. From observations of the males, it was suspected that this time period was not sufficient for the test animals to complete exploratory behavior before settling. A further six old males were tested without a stimulus six times each, and their position was recorded after 30 min. All subsequent tests were run for 30 min. Old males were tested against each of the following: old mature females (two sets) and old females carrying fertilized oocytes. New males were tested against each of the following: new mature females, new females maintained in short days, and old males. All statistical significance was assessed using χ^2 analyses.

Results. The first set of experiments was performed with old (collected in March) males and females (Fig. 4). To assess for any directional bias and for chance levels of attraction, the positions of the males were recorded 10 min after being introduced into the maze. Fifty-three percent of

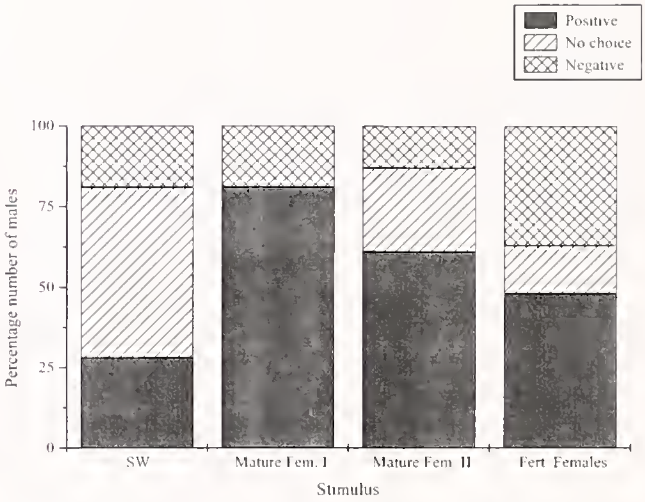

Figure 4. Percentage response of old (collected March 1999) male *Harmothoe imbricata* to various stimuli in a Y-maze run at 10°C. SW, no stimuli added (number of runs = 36 [6 males × 6 tests]); Mature Fem. I, mature old females (number of runs = 27 [9 males × 3 females]); Mature Fem. II, second group of mature old females (number of runs = 63 [7 males × 9 females]); Fert. Females, females carrying fertilized oocytes under their elytra (number of runs = 27 [9 males × 3 females]). The position of each male was recorded 30 min after introduction to the maze. Responses were classed as positive if the male was in the arm containing the stimulus (or designated as stimulus if seawater only), negative if in the arm with no stimulus, or no choice if it moved to neither arm.

these males moved to the arbitrarily labeled positive arm and 47% moved to the negative arm. However, this experiment was omitted from the graph and from statistical analysis because the males had not completed their exploratory behavior within the 10-min time frame. The experiment was, therefore, repeated with a further six old males whose positions were recorded 30 min after introduction. In the 36 tests performed, 28% of the males moved to the arbitrarily positive arm and 19% to the negative arm, while 53% made no choice. This result was not significantly different form an expected value of 33.3% moving to each arm or making no choice ($\chi^2(2) = 2.60$, $P > 0.05$).

These nine old males were then tested against three old mature females, and a significantly higher level of attraction ($\chi^2(2) = 23.07$, $P < 0.001$) was observed: 81% of the males moved to the positive arm and the other 19% moved to the negative arm (without the females). To confirm this attraction response, a further test was performed with 11 males and 7 old mature females. Sixty-one percent of the males moved to the positive arm, 13% moved to the negative arm, and 26% made no choice. This level of attraction was also significantly higher than shown for the seawater 30-min control ($\chi^2(2) = 10.58$, $0.05 > P > 0.001$).

An additional experimental run was performed using the nine old males and three old females that had spawned in the field and were carrying fertilized oocytes under their elytra. In the 27 tests performed, 48% of the males moved to the positive stimulus arm, 37% moved to the negative arm, and 15% made no choice. Statistical analysis of this data shows that this was a significantly higher level of attraction than shown for the seawater control ($\chi^2(2) = 9.69$, $0.05 > P > 0.001$). However, if the no choice and negative results are combined and compared statistically with the positive stimulus, there was no significant difference between the treatments ($\chi^2(1) = 2.74$, $P > 0.05$), confirming that the differences were due to the decrease in no choices and not to an increase in positive results. Statistical analysis also shows that there was a significantly lower level of attraction for fertilized females than for both mature female I ($\chi^2(2) = 6.87$, $0.05 > P > 0.001$) and mature female II experiments ($\chi^2(2) = 7.97$, $0.05 > P > 0.001$).

The second set of experiments was performed with new animals collected in April (Fig. 5). To assess again for directional bias, six new males were tested with no stimulus, and their position was recorded after 30 min. Thirty-three percent and 36% of the males moved to the arbitrary positive and negative arms respectively, with 31% making no choice. This was not significantly different from an expected value of 33.3% moving to each arm or making no choice ($\chi^2(2) = 0.593$, $P > 0.05$).

These new males were then tested against six new mature females. A significantly higher level of attraction was observed when compared to the seawater test, with 61% of the males moving to the positive arm, 22% to the negative arm, and 17% making no choice ($\chi^2(2) = 12.95$, $0.05 > P > 0.001$).

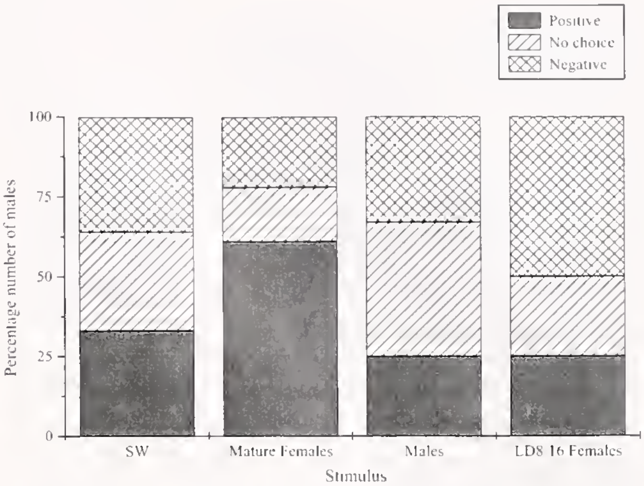

Figure 5. Percentage response of new (collected April 1999) male *Harmothoe imbricata* to various stimuli in a Y-maze run at 10°C. SW, no stimuli added (number of runs = 36 [6 males × 6 tests]); Mature Females, mature new females (number of runs = 36 [6 males × 6 females]); Males: new males tested against themselves (number of runs = 36 [6 males × 6 males]); LD8:16 Females, females maintained in short days (LD8:16) for 3 months (number of runs = 36 [6 males × 6 females]). The position of each male was recorded 30 min after introduction into the maze. Responses were classed as positive if the male was in the arm containing the stimulus (or designated as stimulus if seawater only), negative if in the arm with no stimulus, or no choice if it moved to neither arm.

These six new males were also tested against themselves. Twenty-five percent moved to the positive arm, 33% moved to the negative arm, and 42% made no choice. Statistical analysis of these data shows that this was not a significantly different level of attraction when compared to the seawater control ($\chi^2(2) = 0.506$, $P > 0.05$), and males were significantly less attractive than mature females ($\chi^2(2) = 12.61$, $0.05 > P > 0.01$).

These males were also tested against six mature females that had been maintained in LD8:16 cycles for 3 months. Twenty-five percent moved to the positive arm, 50% moved to the negative arm, and 25% made no choice. Levels of attraction for this test also did not differ significantly from seawater ($\chi^2(2) = 0.7$, $P > 0.05$), and LD8:16 females were significantly less attractive than mature females ($\chi^2(2) = 10.5$, $0.05 > P > 0.001$).

Discussion

Photoperiodic control of oocyte growth

The rate of oogenesis of the first oocyte cohort in *Harmothoe imbricata* can be altered by manipulation of temperature and photoperiod (Garwood, 1980; Garwood and Olive, 1982; Clark, 1988). A period of exposure of 42–55 days of less than 13 h (winter conditions) photophase is required to prevent the first cohort of oocytes from being aborted. In experiments in this study, females had been maintained in ambient photoperiods prior to the experiments commencing in February. They were, therefore, not exposed to either LD16:8 or LD8:16 conditions until after the critical minimum number of days had been reached, thus preventing resorbtion.

In the field, once females have been exposed to this critical period of LD8:16 cycles, an increasing ambient photophase (after the winter solstice) allows oogenesis to proceed normally. Above a critical photoperiod of 10–11 h photophase, oogenesis is accelerated; however, an increased number of winter condition cycles (between 55 and 73) is required for this response to be exhibited (Garwood, 1980; Garwood and Olive, 1982; Clark, 1988). The results presented in Figure 1 confirm that an increase in photoperiod (LD16:8 conditions) accelerates oogenesis. The results also show that the response to LD16:8 conditions was rapid, with effects occurring within 1 week from exposure. However, oocyte growth continued under LD8:16 conditions, as by 23 February both LD16:8 and LD8:16 conditions had oocytes that were not significantly different from each other.

Incubating prostomium homogenate with oocytes *in vitro* significantly increases their uptake of radiolabeled amino acid and their subsequent protein synthesis (Bentley *et al.*, 1994; Lawrence, 1996). These authors suggested the presence in the prostomium of a gonadotrophic hormone that promotes and controls oogenesis. The manipulation of photoperiod and temperature may, therefore, be acting directly on the levels of this hormone and it is this hormone level that subsequently mediates oogenesis. Ambient conditions (increasing photophases) in January and February may sustain oogenesis by increasing the circulating titers of this substance. The exposure of females to LD16:8 conditions may have triggered a burst of secretion of the hormone (above the levels normally experienced in February), inducing an increase in mean oocyte diameter that occurred in week 2. Females exposed to continued LD8:16 conditions had no burst of secretion; instead, oogenesis continued at a constant rate, resulting in the delayed increase (week 3) in mean oocyte diameter.

By week 3, oocytes were fully grown—approximately 120 μm (Daly, 1972); data from Figure 1 show that, in these experiments, oogenesis was complete by 23 February. Data also show that implantation of prostomia had no effect on oocyte diameter and did not induce oocyte degeneration. The diameters of spawned oocytes from females implanted with LD8:16 or LD16:8 prostomia were not significantly different from each other, from the LD8:16 controls in weeks 3 and 4, or from the LD16:8 control in week 3. In week 4, the mean oocyte diameters of LD16:8 controls were significantly higher than those in any other treatment, although this is more likely to be due to the low numbers of females sampled than to any effect of the treatment.

Photoperiodic control of spawning mediated by the endocrine system

Early transition through the critical photoperiod can advance the time of spawning; long days or photoperiods with greater than 11 h photophase can cause the first cohort of oocytes to be spawned about 1 month earlier than the natural date (Garwood and Olive, 1982). In this study, females carrying fertilized oocytes were collected from the field on 3 March 1999. We calculated that their natural spawning data was late February to early March. From the results presented in Figure 2, exposure to a LD16:8 photoperiod did not induce notably earlier spawning dates when compared to a LD8:16 photoperiod, and neither was different from the natural date. Instead, when compared to LD16:8 exposure, LD8:16 exposure actually prevented spawning in the majority of females. Ninety-six percent of the LD16:8 females spawned, as opposed to only 33% of the LD8:16 females.

We conclude that the presence of the prostomium is required for spawning to occur in *H. imbricata*, as none of the females that were used as LD16:8 or LD8:16 donors spawned. Examination of the oocytes form these donors also showed that they had not increased in diameter after prostomium removal and had begun to degenerate (data not shown). The prostomium is, therefore, required for the maintenance of oogenesis and for spawning to occur. Nevertheless, a failure to spawn after prostomium removal cannot, at present, be attributed solely to a loss of endocrine function because it may also be due to the severance of nervous connections controlling spawning.

To investigate whether the inhibition of spawning through exposure to LD8:16 photoperiods is endocrine mediated, we implanted LD8:16 control females with prostomia from females maintained in LD16:8 or LD8:16 photoperiods for 2 weeks. Although the implantation of prostomia is an established technique for investigating the role of endocrine substances in polychaetes (see Golding, 1987), this is the first time that it has been used successfully for *H. imbricata*. Previous attempts with this species resulted in the degeneration of the implanted prostomium (P. J. W. Olive, University of Newcastle upon Tyne, pers. comm.). Prostomia implanted during our experiments showed no obvious degeneration with light microscope analysis up to one month after implantation (data not shown). It should be noted that implantation of prostomia is not an ideal technique for identifying the putative spawning hormone in this species. Future investigations will focus on the development of *in vitro* bioassays to reduce the numbers of prostomia used and to meet the levels of sensitivity and reliability that are essential for purification studies.

The results presented in Figure 2 show that 80% of the LD8:16$^{\mathrm{PM(LD16:8)}}$ females spawned, as opposed to 37.5% of the LD8:16$^{\mathrm{PM(LD8:16)}}$ females. These results confirm that the implanted prostomia were still functioning as endocrine organs. We suggest the following hypothesis for the endocrine control of spawning. A spawning substance present in the prostomium is required for spawning to occur. The titers of this substance, as with the gonadotrophic hormone, are mediated by photoperiod. The exposure of females to lengthening photophases (ambient conditions in February) increases the titers of this spawning substance to a level above which spawning can occur. Exposure of females to LD16:8 conditions also allows titers of the spawning substance to reach the threshold level, so that nearly all the females spawn. In contrast, only a small proportion of the females exposed to LD8:16 conditions have titers of the spawning substance that reach the threshold, so significantly fewer spawn. Implanting the prostomia of an LD16:8 exposed female into an LD8:16 female also provides a source of higher levels of spawning hormone and thus increases the total circulating titers, enabling the LD8:16 females to reach the threshold required for spawning to occur. Implanting the prostomia of an LD8:16 exposed female into an LD8:16 female provides a second source of the hormone, but at lower concentrations. In most females, the combined level of hormone is lower than the threshold, so most fail to spawn.

The nature and action of a spawning substance in *H. imbricata* may take two forms. It could be a "true" spawning substance like that found in *Nephtys hombergii*. In that species, a hormone released from the supraesophageal ganglion induces spawning by acting on the musculature to allow the release of gametes through the anus (Bentley *et al.*, 1984). The maturation of the gametes is independent of the spawning hormone; they mature once released into seawater (Olive, 1976; Olive and Bentley, 1980).

The other form of spawning substance induces gamete maturation and subsequent spawning either directly or indirectly. This form occurs in *Arenicola marina*. Oocytes mature through a two-step system involving a substance from the prostomium and then a second substance in the coelomic fluid. The latter, termed the coelomic maturation factor (CMF), induces the oocytes to mature; these oocytes are subsequently spawned (Watson and Bentley, 1997). It is unclear whether CMF also acts on the musculature to facilitate spawning. However, in male *A. marina*, the sperm maturation factor (8, 11, 14 eicosatrienoic acid) not only induces maturation of the sperm but also produces specific behavioral changes associated with spawning (Pacey and Bentley, 1992).

In *H. imbricata*, oocytes are released from the ovaries at prophase of the first meiosis a few days before spawning. They mature to metaphase of meiosis I in the coelomic fluid, are collected by the nephridia, and spawned (Daly, 1972). Further experiments are required to elucidate whether the putative spawning substance from the prostomium can induce spawning of immature oocytes or actually induces the maturation of the oocytes that are subsequently spawned.

Pheromone influence on pairing behavior

Initial observations of the test males in the Y-maze indicated that 10 min was not sufficient time for them to complete their exploratory behavior. After 10 minutes most of the males were still actively searching. In all subsequent experiments we allowed 30 min for the males to settle before their position was recorded. This time period was sufficient for the males to settle and complete their exploratory behavior.

Results presented in Figures 4 and 5 provide the first evidence that pheromones are involved in the reproductive behavior of *H. imbricata*. Specifically, these data indicate that a mature female with fully grown oocytes in its coelomic cavity releases a waterborne substance or substances that attracts significantly more mature males than are attracted by seawater, males, or females that are carrying fertilized oocytes.

Harmothoe imbricata is a solitary species outside the breeding season, but it reproduces by forming single copulating pairs (Daly, 1972). This method of reproduction requires mature individuals to locate each other, but at low population densities, chance encounters may be infrequent. An attraction pheromone released by a mature female increases the chances that a male will find her and, therefore, increases the number of successful fertilizations. The pheromone may also maintain the pair bond and could suppress the cannibalistic tendencies of both individuals, allowing pairing to proceed. Once the female has fertilized oocytes, she stops releasing the pheromone and becomes unattractive to the male; this is confirmed by the data shown in Figure 5.

One of the best-studied attraction pheromones in marine invertebrates is attractin, a peptide found in the egg cordon of the opisthobranch mollusc *Aplysia* spp. The function of this 58-residue peptide is to attract other individuals to the mating aggregation and to induce mating (Painter *et al.*, 1991, 1998). Pheromones are also a component of a number of polychaete reproductive strategies, particularly in some nereid species (for review, see Zeeck *et al.*, 1996). However, these pheromones have been isolated only from species such as *Platynereis dumerlii* and *Nereis succinea* that swarm *en masse* in the water column (Zeeck *et al.*, 1988, 1996; Hardege *et al.*, 1998). The results presented here are, therefore, the first report of a waterborne cue being used as an attraction pheromone from a polychaete that reproduces following pair formation.

Although the evidence for pheromones in marine invertebrates is steadily growing, the environmental control of pheromone production has not been investigated. The effect of environmental manipulation (particularly photoperiod) on oogenesis is confirmed and the influence of photoperiod on spawning in *Harmothoe imbricata* has been described for the first time (Garwood and Olive, 1982; Clark, 1988). Establishing a link between the photoperiodic input and the production of a pheromone that regulates spawning behavior is an important step. Results presented in Figure 5 show that females maintained in LD8:16 photoperiods were only as attractive to mature males as seawater or other males. Just as LD8:16 exposure may prevent the production (or the attainment of threshold levels) of the putative spawning hormone and thus prevent spawning, it may also prevent the production of the attraction pheromone. The relationship between the spawning hormone and pheromone production requires further investigation, but the production of the two may be intricately linked, and they may be the same or similar substances.

Acknowledgments

The authors acknowledge the support of NERC grant GR3/10521 to MGB. The authors declare that the experiments comply with the current laws of the country in which the experiments were performed.

Literature Cited

Bentley, M. G., P. J. W. Olive, P. R. Garwood, and N. H. Wright. 1984. The spawning and spawning mechanisms of *Nephtys caeca* (Fabricius, 1780) and *Nephtys hombergi* (Savigny, 1818) (Annelida: Polychaeta). *Sarsia* **69:** 63–68.

Bentley, M. G., J. Boyle, and A. A. Pacey. 1994. Environmental influences on endocrine systems controlling reproduction in polychaetes. *Mem. Mus. Natl. Hist. Nat.* **162:** 37–44.

Clark, S. 1988. A two phase photoperiodic response controlling the annual gametogenic cycle in *Harmothoe imbricata* (L.) (Polychaeta: Polynoidae). *Invertebr. Reprod. Dev.* **14:** 245–266.

Daly, J. M. 1972. The maturation and breeding of *Harmothoe imbricata* (Polychaeta: Polynoidae). *Mar. Biol.* **12:** 53–66.

Daly, J. M. 1974. Gametogenesis in *Harmothoe imbricata* (Polychaeta: Polynoidae). *Mar. Biol.* **25:** 35–40.

Garwood, P. R. 1980. The role of temperature and day length in the control of the reproductive cycle of *Harmothoe imbricata* (L.) (Polychaeta: Polynoidae). *J. Exp. Mar. Biol. Ecol.* **47:** 35–53.

Garwood, P. R., and P. J. W. Olive. 1982. The influence of photoperiod on oocyte growth and its role in the control of the reproductive cycle in the polychaete *Harmothoe imbricata* (L.). *Int. J. Invertebr. Reprod.* **5:** 161–165.

Golding, D. W. 1983. Endocrine programmed development and reproduction in *Nereis*. *Gen. Comp. Endocrinol.* **52:** 456–466.

Golding, D. W. 1987. Brain-body interactions in *Nereis*. Deactivation of the cerebral neuroendocrine system by ganglion transplantation. *Int. J. Invertebr. Reprod.* **12:** 281–294.

Hardege J. D., C. T. Müller, and M. Beckmann. 1998. A waterborne female sex pheromone in the ragworm, *Nereis succinea* (Annelida: Polychaeta). *Polychaete Res.* **17:** 18–21. [ISSN 0961-320X. Available from C. Mettam, Univ. of Wales Cardiff, PO Box 915, Cardiff CF1 3TL, UK]

Lawrence, A. J. 1996. Environmental and endocrine control of reproduction in two species of polychaete: potential bio-indicators for global climate change. *J. Mar. Biol. Assoc. UK* **76:** 247–250.

Olive, P. J. W. 1976. Evidence for a previously undescribed spawning hormone in *Nephtys hombergii* (Annelida: Polychaeta). *Gen. Comp. Endocrinol.* **28:** 454–460.

Olive, P. J. W., and M. G. Bentley. 1980. Hormonal control of oogenesis, ovulation and spawning in the annual reproductive cycle of the polychaete *Nephtys hombergii* Sav. (Nephtyidae). *Int. J. Invertebr. Reprod.* **2:** 205–221.

Pacey, A. A., and M. G. Bentley. 1992. The fatty acid 8, 11, 14 eicosatrienoic acid induces spawning in the male lugworm *Arenicola marina*. *J. Exp. Biol.* **173:** 165–179.

Painter, S. D., M. G. Chong, M. A. Wong, A. Gray, J. G. Cormier, and G. T. Nagle. 1991. Relative contributions of the egg layer and egg cordon to pheromonal attraction and the induction of mating and egg-laying behavior in *Aplysia*. *Biol. Bull.* **181:** 81–94.

Painter, S. D., B. Clough, R. W. Garden, J. V. Sweedler, and G. T. Nagle. 1998. Characterization of *Aplysia* attractin, the first water-borne peptide pheromone in invertebrates. *Biol. Bull.* **194:** 120–131.

Watson, G. J., and M. G. Bentley. 1997. Evidence for a coelomic maturation factor (CMF) controlling oocyte maturation in the polychaete *Arenicola marina* (L.). *Invertebr. Reprod. Dev.* **31:** 297–306.

Watson, G. J., M. E. Williams, and M. G. Bentley. 2000. Can synchronous spawning be predicted from environmental parameters? A case study of the lugworm *Arenicola marina*. *Mar. Biol.* (in press).

Zeeck, E., J. D. Hardege, H. Bartels-Hardege, and G. Wesselmann. 1988. Sex pheromone in a marine polychaete: determination of chemical structure. *J. Exp. Zool.* **246:** 285–292.

Zeeck, E., J. D. Hardege, and H. Bartels-Hardege. 1990. Sex pheromones and reproductive isolation in two nereid species, *Nereis succinea* and *Platynereis dumerilii*. *Mar. Ecol. Prog. Ser.* **67:** 183–188.

Zeeck, E., T. Harder, M. Beckmann, and C. T. Müller. 1996. Marine gamete release pheromones. *Nature* **382:** 214.

Reference: *Biol. Bull.* **199:** 59–67. (August 2000)

Fertilization in *Callochiton castaneus* (Mollusca)

JOHN BUCKLAND-NICKS[1,*] AND ALAN N. HODGSON[2]

[1]*St. Francis Xavier University, Department of Biology, Antigonish, Nova Scotia, Canada B2G 2W5; and*
[2]*Rhodes University, Department of Zoology and Entomology, Grahamstown 6140, South Africa*

Abstract. A fine-structural study of fertilization in *Callochiton castaneus* has revealed that the mechanism of sperm penetration into the egg is intermediate between the primitive condition found in members of the order Lepidopleurida and the more derived condition found in the Chitonida. *C. castaneus* sperm have the long needlelike nuclear filament and reduced acrosome that characterizes all Chitonida, but they have retained several plesiomorphic features such as an unspecialized mid-piece and a lack of flagellar reinforcement. As in some Lepidopleurida but unlike any Chitonida, the egg hull in this species comprises a thick, smooth jelly coat permeated by pores that permit sperm rapid access to the vitelline layer. The jelly coat is delicate and quickly dissolves when a sperm concentrate is used, suggesting that excess acrosomal enzymes may be responsible. Once the sperm have penetrated the vitelline layer, the long nuclear filament bridges the gap to cups in the egg membrane. However, once the fertilization membrane is raised, the perivitelline space exceeds the length of the nuclear filament, preventing other sperm from penetrating the egg. A fertilization cone forms around the nuclear filament of the penetrating sperm, but it does not appear to engulf the body of the sperm. Rather, the nuclear chromatin is injected into the egg as a long thread. The remaining sperm organelles are apparently abandoned on the egg surface. If this is the case, it would be a significant departure from fertilization in other molluscs and many other metazoans, in which sperm organelles, such as centrioles and mitochondria, enter the egg.

New sperm and egg characters, as well as significant differences in fertilization, indicate that Callochitonidae are basal to all other members of the order Chitonida and may warrant separation as the sister taxon to the suborders Chitonina and Acanthochitonina.

Introduction

Sirenko (1997) recently classified extant chitons into two orders, Lepidopleurida (suborders: Lepidopleurina and Choriplacina) and Chitonida (suborders; Chitonina and Acanthochitonina). Lepidopleurida are considered basal to chitons in general, because they possess many primitive traits. For example, shell valve structure and articulation is simpler and ties in well with the fossil record (Sirenko, 1997); also they are the only chitons known to have typical aquasperm with prominent acrosomes, and eggs with smooth hulls (Hodgson *et al.*, 1988; 1989; Eernisse and Reynolds, 1994; Buckland-Nicks, 1995; Pashchenko and Drozdov, 1998). Presumably, in the ancestor of all members of Chitonida, the sperm acrosome became reduced to a minute vesicle atop a long needlelike extension of the nucleus, since this arrangement is found in all extant Chitonida (Buckland-Nicks *et al.*, 1990) but not in any Lepidopleurida examined to date (Hodgson *et al.*, 1988; Pashchenko and Drozdov, 1998). The intermediate condition of a prominent acrosome and short nuclear filament was recently discovered in the lepidopleurid *Deshayesiella curvata* (Pashchenko and Drozdov, 1998).

The term egg "hull" is used here instead of "chorion" as in previous publications (Buckland-Nicks *et al.*, 1988a, b; Buckland-Nicks, 1993, 1995), to describe the noncellular envelope enclosing the egg and its vitelline layer, because Richter (1986) showed that both the vitelline layer and the hull of chitons are formed by the egg and not by the follicle cells as in other Metazoa (for review of terminology, see Eernisse and Reynolds, 1994).

Chiton eggs evolved from having smooth unspecialized hulls, with fertilization presumably occurring anywhere on the surface, to having elaborate spinous or cupulous hulls that focus sperm to specific regions of the egg surface

Received 7 December 1999; accepted 25 May 2000.

* To whom all correspondence should be addressed. E-mail: jbucklan@stfx.ca

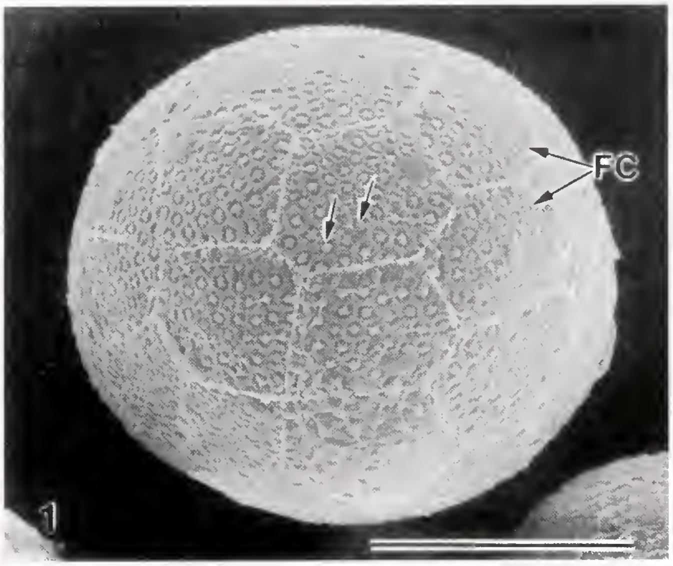
FC
1

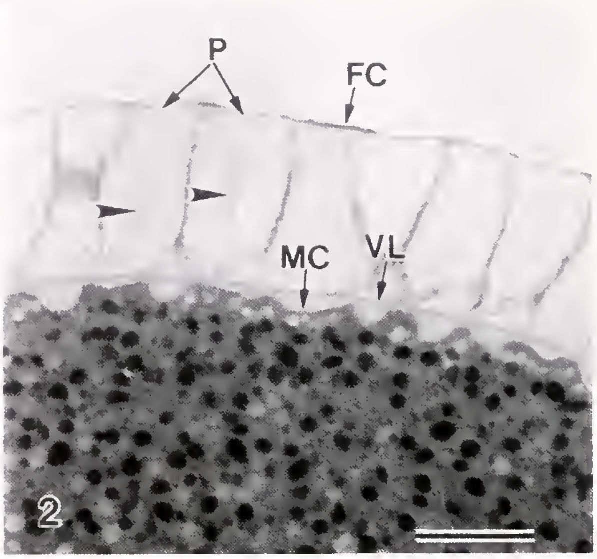
P
FC
MC
VL
2

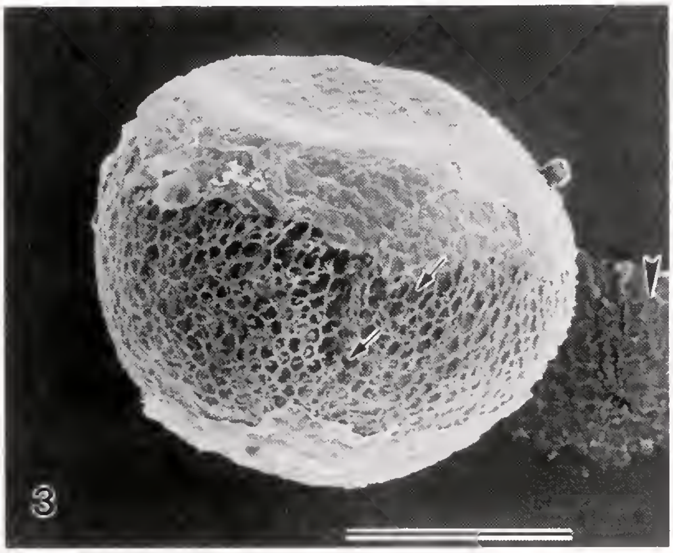
3

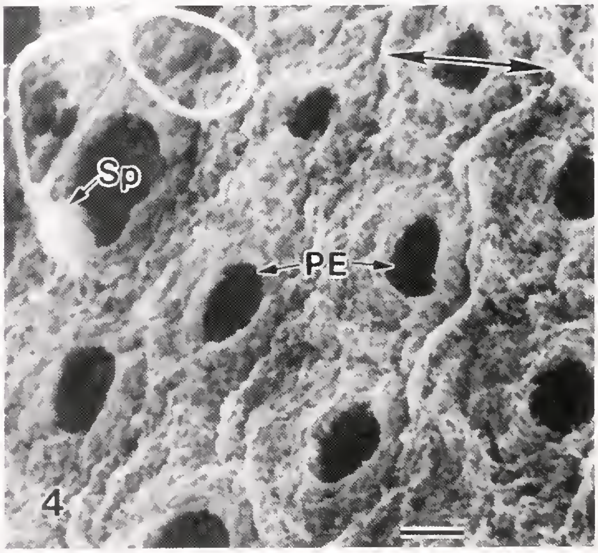
Sp
PE
4

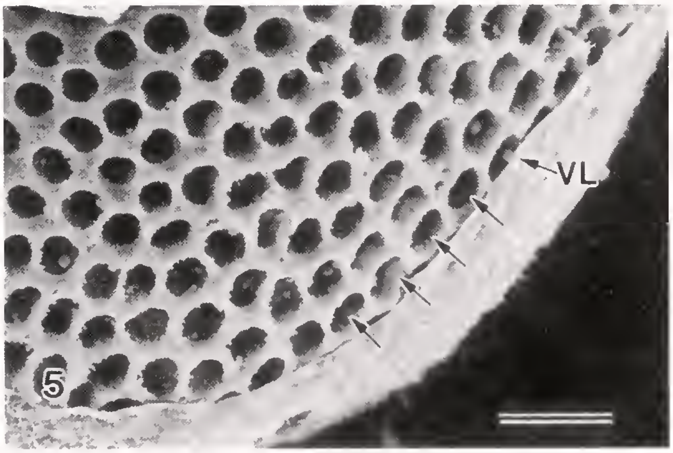
VL
5

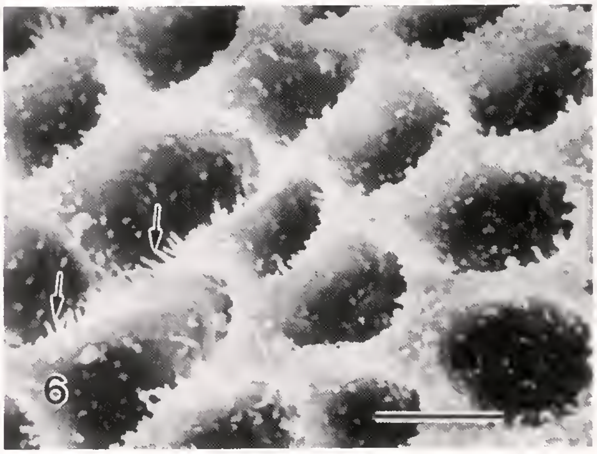
6

(Buckland-Nicks, 1993, 1995). Among Lepidopleurida, *Leptochiton asellus* has a smooth hull comprising a thick homogeneous jelly coat (Hodgson *et al.*, 1988), whereas *D. curvata* egg hulls are composed of a jelly coat that is penetrated by regularly spaced pores (Pashchenko and Drozdov, 1998). The mechanism of fertilization must be quite different in these lepidopleurids compared to Chitonina such as *Stenoplax conspicua* (Buckland-Nicks, 1995), or Acanthochitonina such as *Tonicella lineata* (Buckland-Nicks *et al.*, 1988b), because of basic differences in sperm acrosomes and egg hull structure. Sperm structure of different species has been found to be an accurate indicator of phylogenetic relationship and sometimes is used as grounds for reclassifying species to alternative taxa (Jamieson, 1987; Healy, 1988; Hodgson *et al.*, 1996).

The family Callochitonidae, although placed within the order Chitonina and regarded as "evolutionarily advanced" (Sirenko, 1997), exhibits several plesiomorphic traits (Buckland-Nicks, 1995) and is therefore one of several groups that are important to investigate in clarifying the phylogeny of chitons. This study describes in detail, for the first time in *Callochiton castaneus*, the structure of the egg hull and the mechanism of fertilization. The information gained is discussed in relation to the evolution of mechanisms of fertilization in chitons, as well as to chiton phylogeny in general.

Materials and Methods

Specimens of *Callochiton castaneus* Wood, 1815, were obtained in breeding condition from beneath intertidal rocks at East London (33° 03′ S; 28° 03′ E) and Port Alfred (33° 52′ S; 26° 53′ E), South Africa, from August to October 1999. The animals were brought back to the laboratory and placed individually in 60-mm petri dishes half-filled with 0.45-μm filtered seawater (FSW). Some individuals of each sex had spawned by the second day. Alternatively, eggs or sperm were obtained by removing the foot and digestive gland and puncturing the dorsal gonad.

If the specimen was male, the white "dry" sperm concentrate would ooze from the punctured testis and could be easily aspirated into a pipette. For a "concentrated sperm suspension," one drop of dry sperm was diluted in 5 ml of FSW. For a "dilute sperm suspension," one drop of the latter was further diluted in 5 ml of FSW. If the animal was female any free-spawned eggs were collected from the petri dish; otherwise the eggs were flushed from the ovary by aspirating a stream of FSW into the gonad. Eggs were then pipetted individually into another clean petri dish containing FSW, to reduce debris. Batches of about 50 eggs were removed into six small glass vials containing 4 ml of FSW. Two vials served as unfertilized controls. Two vials received three drops of diluted sperm suspension, and in two vials the FSW was replaced with concentrated sperm suspension. The eggs in one set of vials were transferred to primary fixative (see below) after 30 s, and the eggs in the second set of vials were fixed after 10 min.

Light microscopy

A few eggs were removed from control and experimental vials during the experiment to monitor the progress of fertilization and to be photographed using an Olympus BX50F-3 light microscope equipped with bright field and DIC optics. Slides were made by pipetting a few eggs onto a clean glass slide, placing pieces of coverslip around to make a well, then adding a whole coverslip, drying off excess water, and finally sealing the coverslip with nail varnish.

Sperm activity was noted to be highly variable. We tested the effects of serotonin (5-hydroxytryptamine) on sperm activity by mixing a drop of sperm concentrate with 1 ml of serotonin solution, to give a final concentration ranging from 1 to 10 μM serotonin. One drop of this sperm solution

---

Figures 1–6. Micrographs of unfertilized eggs of *Callochiton castaneus*.

Figure 1. Ripe egg with intact layer of follicle cells (FC) dissected from the ovary. Note regular arrangement of pores in hull (arrows) visible beneath follicle cells. Scale bar = 100 μm.

Figure 2. Light micrograph of 1-μm section of egg removed from the ovary, showing a layer of intact follicle cells (FC) and regularly spaced pores (P) in the jelly hull; the pores penetrate to the vitelline layer (VL) overlying the egg membrane cups (MC). Note meshwork of fibers (arrowheads) supporting pore structure. Scale bar = 10 μm.

Figure 3. Similar to Figure 1 except the egg has been rolled on sticky tape, which removed follicle cells and pore openings (arrowhead), thus revealing pores in the jelly hull (arrows). Scale bar = 100 μm.

Figure 4. Close-up of a spawned egg in which the follicle cells have retracted, revealing the arrangement of pores in naked jelly hull. Pore entrance (PE) is usually one-third of the diameter of the pore itself (double arrow), thus restricting sperm entry. A sperm (Sp) is visible at the entrance to one damaged pore. Scale bar = 2 μm.

Figure 5. Vitelline layer (VL) of the egg has been rolled off on sticky tape, revealing a regular series of membrane cups (arrows) that match up with pores in the hull. Scale bar = 15 μm.

Figure 6. Close-up of Figure 5, showing egg membrane cups with microvilli that are prominent on the raised edges (arrows) but sparse in the bases of cups. Scale bar = 5 μm.

was placed on a slide next to a separate drop of control sperm in filtered seawater, and observed periodically.

Electron microscopy

The primary fixative was made by mixing 1 ml of 25% glutaraldehyde with 9 ml FSW and adding this to 10 ml of 0.2 *M* Na cacodylate buffer (pH 7.4). This gave a final concentration of 2.5% glutaraldehyde in 0.1 *M* Na cacodylate buffer and FSW, to which was added 0.1 *M* sucrose. The fixative was refrigerated before use. Samples were fixed overnight and then washed in two changes of 0.1 *M* Na cacodylate buffer in FSW (pH 7.4) before post-fixing for 1 h in 1.5% osmium tetroxide in the same buffer. Fixed eggs were rinsed in distilled water and dehydrated in an ethanol series to 100%. At this stage about half of the eggs in each vial were removed to a second series of vials containing 100% ethanol for preparation for scanning electron microscopy (SEM).

In samples destined for transmission electron microscopy, ethanol was replaced with propylene oxide and then the eggs were transferred through infiltration media consisting of mixtures of propylene oxide and TAAB 812/Araldite CY212 resin (75:25, 50:50, 25:75) for 2 h in each mixture in capped vials (after Cross, 1989). Samples were exchanged into pure resin and left overnight in uncapped vials in a desiccator. The next afternoon, with the aid of a dissecting microscope, groups of five to six eggs were aspirated into BEEM capsules half filled with resin. Eggs were allowed to sink and then were arranged into the center of each mold using a stainless steel insect pin. Labels were added, and the BEEM capsules were placed in a 60°C oven for 40 h. Thick sections were cut with glass knives in an LKB 8800 ultratome, transferred to glass slides, and stained with 1% toluidine blue for about 20 s before rinsing with distilled water and air drying. Thin sections, with silver/gold interference color, were cut on a diamond knife (Diatome) and picked up on naked 150-mesh copper grids. Sections were reverse stained with aqueous lead citrate for 1 min, followed by aqueous uranyl acetate for 2 min, after the method of Daddow (1986). Stained sections were examined and photographed in a JEOL 1210 transmission electron microscope operated at 80 kV.

Samples destined for SEM were exchanged through an amyl acetate series to 100% and then aspirated under a dissecting microscope into Teflon flow-through specimen vials (Pelco) before capping and critical point drying. Subsequently, individual Teflon vials were uncapped and inverted on an SEM stub coated with a carbon sticky tab. The eggs stuck fast but could be rolled with an insect pin to remove the egg hull and expose either the vitelline layer or the egg membrane itself. Some eggs were cut in two with a Kesei microknife (Japan). Stubs prepared in this way were coated with gold in a Polaron E5100 sputter coater. Stubs were examined and photographed in a JEOL JSM 840 scanning electron microscope.

Results

Morphology of the egg

The unspawned ripe eggs of *Callochiton castaneus* are about 220 μm in diameter and surrounded by a vitelline layer and a smooth, 20-μm-thick egg hull enclosed by a single layer of follicle cells, usually hexagonally disposed (Figs. 1, 2). The egg hull is made up of a delicate jelly coat supported by a fibrous matrix that is permeated by a series of pores spaced at regular intervals of 9 μm all over the surface (Figs. 3, 4). If unspawned eggs are rolled on sticky tape to remove the follicle cells, the regular array of pores in the jelly coat becomes visible (Fig. 3). At its entrance, each pore is about 2 μm in diameter (Fig. 4), but below this the diameter enlarges to about 8 μm (Fig. 2). Furthermore, there is a network of fibers that criss-cross each pore from apex to base (Fig. 2). Opposite, but below, the point at which the pores contact the vitelline layer, the egg membrane is formed into a series of cups (Figs. 5, 6). The depression in each cup usually coincides with a pore, and the lip of each cup coincides with the division between two pores (Fig. 2). The raised edges of the cups are rich in microvilli that penetrate into the vitelline layer (Figs. 2, 6); in the base of the cups, microvilli are sparse (Fig. 7).

The mechanism of fertilization

Soon after spawned eggs contact seawater, any remaining follicle cells retract, thus exposing the pores in the hull (Figs. 4, 8). In dilute sperm suspensions, sperm quickly locate the entrance to these pores and swim down to the egg surface (Fig. 8). If a concentrated sperm suspension is used, many sperm arrive at the egg surface simultaneously, overriding any potential block to polyspermy (Fig. 9). In these cases the jellylike hull is dissolved in 1 or 2 min, leaving the exposed vitelline layer of the egg coated with thousands of penetrating sperm, many of which induce fertilization cones (Figs. 9, 10). The fragile jelly coat degenerates in about an hour even under natural conditions, and it was not preserved intact by routine fixation.

When a fertilizing sperm penetrates the vitelline layer, the needlelike nuclear filament bridges the perivitelline space and egg cup to reach and fuse with the egg membrane (Figs. 11-13). The distance between the base of each egg cup and the vitelline layer varies from 1.5 –4 μm (Fig. 2), but the elongate nuclear filament permits sperm-egg fusion up to a distance of 6 μm (Fig. 12). Contact between sperm and egg results in their fusion and the formation of a narrow tube (< 0.1 μm in diameter) through which the threadlike chromatin is injected into the egg cortex (Fig. 14). This is visible as a thin white thread when stained with Hoechst's 33358 DNA

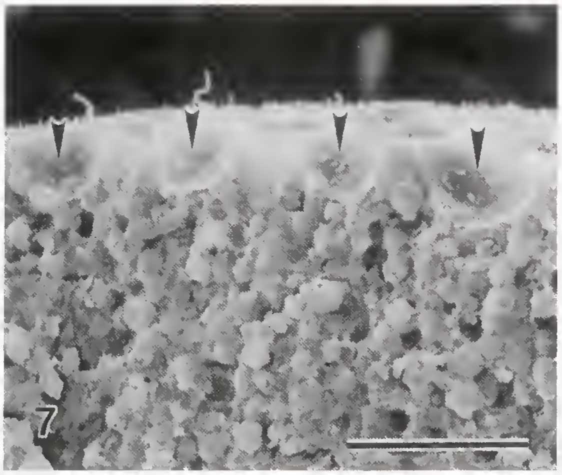

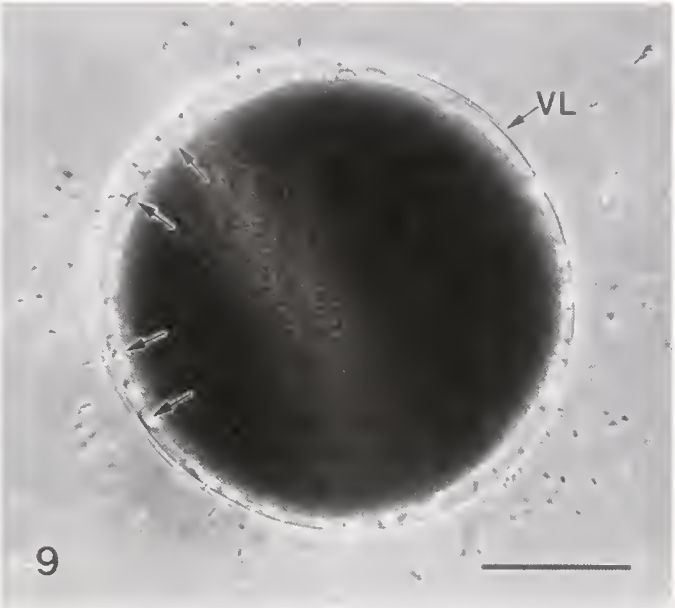

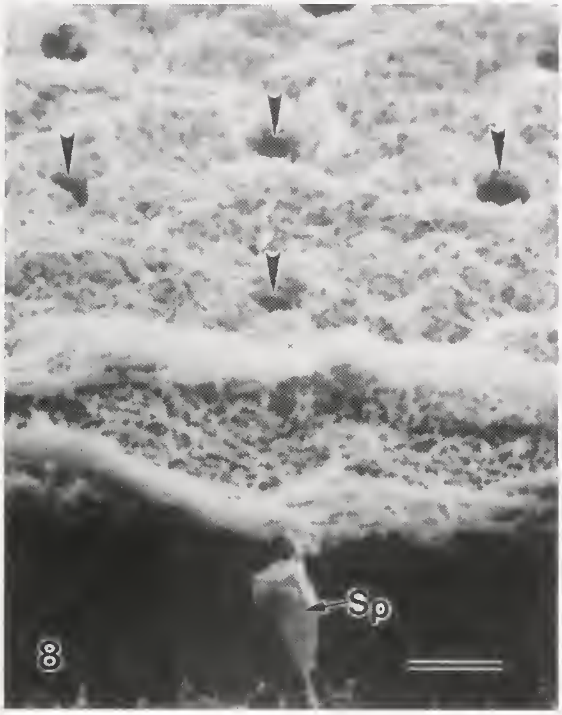

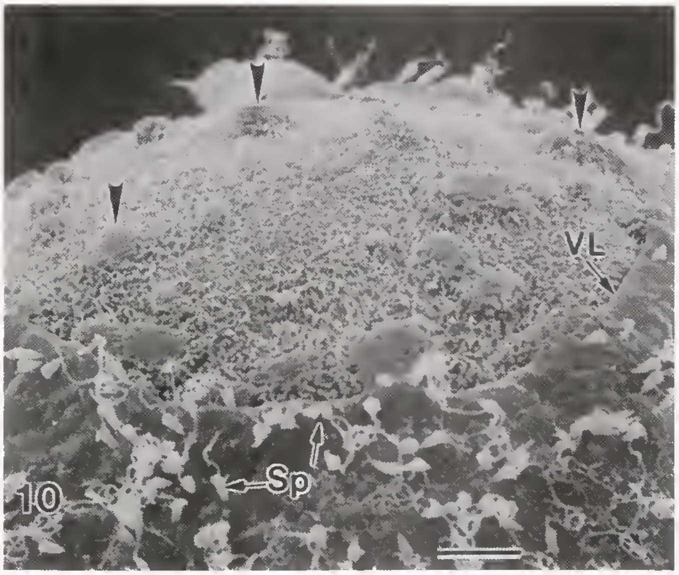

Figures 7–10. Micrographs of fertilized eggs of *Callochiton castaneus*: SEM = scanning electron micrograph; DIC LM = differential interference contrast light micrograph.

Figure 7. SEM of an unfertilized egg split in half with a Kesei microknife to show egg membrane cups (arrowheads). The vitelline layer has been removed. Scale bar = 10 μm.

Figure 8. SEM view of broken edge of the jelly hull, showing regular arrangement of pores above (arrowheads) and penetrating sperm (Sp) on vitelline layer below. Scale bar = 2 μm.

Figure 9. DIC LM of a polyspermic egg showing numerous fertilization cones (arrows) beneath the elevated vitelline layer (VL). Scale bar = 70 μm.

Figure 10. SEM of a polyspermic egg showing fertilization cones (arrowheads) beneath the vitelline layer, which has been partly removed by rolling the egg on sticky tape. Note also numerous sperm (Sp) on region of intact vitelline layer (VL). Scale bar = 10 μm.

stain and viewed under UV light (Fig. 12 inset). A fertilization cone is raised up around the penetrating nuclear filament from the surrounding egg cortex, as well as from fusion of adjacent egg microvilli (Fig. 13). However, the fertilization cone remains below the barrier of the vitelline layer and engulfs only the nuclear filament (Figs. 12, 14). The vitelline membrane raises up and forms the fertilization membrane (Figs. 9, 12). The raised edges of the egg membrane cups retract from the vitelline layer, creating a larger (6–7 μm) perivitelline space that excludes late-arriving

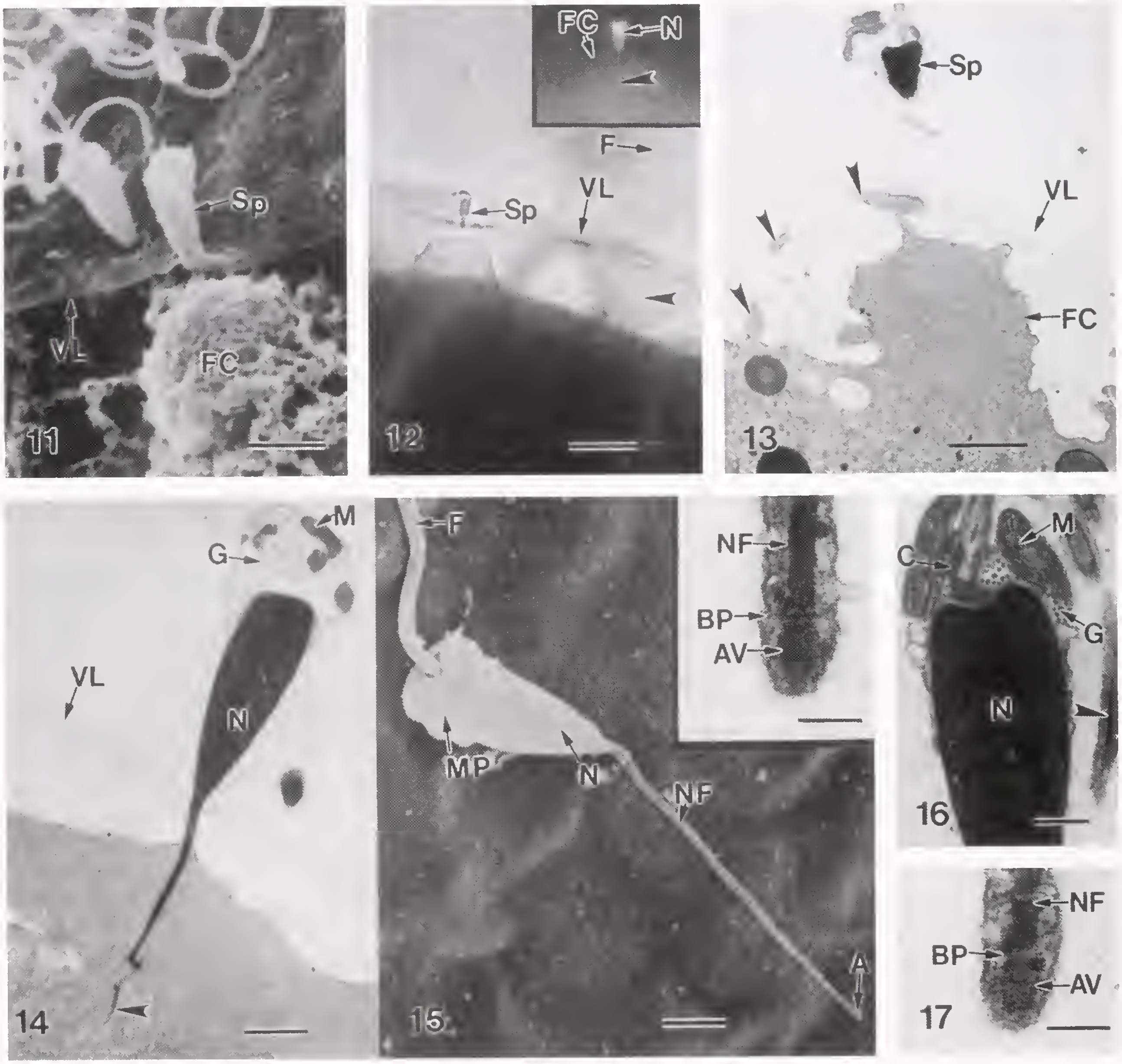

Figures 11–17. Micrographs of sperm and fertilized eggs of *Callochiton castaneus*: SEM = scanning electron micrograph; TEM = transmission electron micrograph; DIC LM = differential interference contrast light micrograph.

Figure 11. SEM of polyspermic egg that has been rolled on sticky tape, stripping the vitelline layer (VL) next to a penetrating sperm (Sp) and revealing the fertilization cone (FC) beneath it. Scale bar = 2 μm.

Figure 12. DIC LM of polyspermic egg showing one sperm (Sp) that has penetrated the vitelline layer (VL) and induced a fertilization cone, and a second, late-arriving sperm that cannot reach the egg membrane with its nuclear filament (arrowhead). Note also sperm flagellum (F) exhibiting large amplitude beat. **Inset:** Same as Figure 12 except that the penetrating sperm has been labeled with Hoechst's 33358 DNA stain and photographed under UV epifluorescence, revealing nucleus (N) injecting chromatin (arrowhead) into the egg cortex through the fertilization cone (FC). Scale bar = 6 μm.

Figure 13. TEM of a fertilization cone (FC) with part of a penetrating sperm (Sp) visible above the vitelline layer (VL). Note that the fertilization cone incorporates elevated cytoplasm as well as microvilli (arrowheads). Scale bar = 2 μm.

Figure 14. TEM of penetrating sperm injecting chromatin (arrowhead) into egg cortex. Note that the vitelline layer (VL) is intact except for a small pore through it. Sperm mitochondria (M) and remnants of glycogen (arrow) have collected in the membrane bag posterior to the nucleus (N). Compare with Figure16. Scale bar = 1 μm.

sperm (Fig. 12). The sperm organelles—including the centrioles, flagellum, and mitochondria, as well as some residual glycogen granules—collect in a bag of membranes above the fertilization membrane and do not appear to enter the egg cortex (Figs. 11, 14).

Morphology of the sperm

The sperm of *Callochiton castaneus* (described by Hodgson *et al.*, 1988) has a bullet-like nucleus extending into a long nuclear filament tipped by a minute acrosome, but it has retained a relatively unspecialized mid-piece (Figs. 15–17). Hodgson *et al.* (1988) believed that *C. castaneus* sperm did not possess an acrosome. Careful reexamination of their sections, however, revealed the presence of the minute acrosomal vesicle, which is separated from the nuclear extension by a basal plate (Figs. 15, 17). It was not possible to discern any subdivision of the acrosomal vesicle in this species. The main body of the nucleus is 3 μm long, and the nuclear filament is a further 6 μm. The mid-piece comprises five oblong mitochondria arranged fairly symmetrically around the centrioles (Figs. 15, 16).

Sperm dissected from some males were inactive even after being placed in seawater. However, all became active within 1 min following the addition of 1 *μM* serotonin. The degree of activity increased with increasing concentrations of serotonin, up to the maximum tested concentration of 10 *μM*.

Discussion

Morphology of the sperm

Except in the suborder Lepidopleurina, the acrosome of all chitons examined has been reduced to a small vesicle at the tip of a needlelike nuclear filament, which is an extension of the main body of the nucleus (see review by Buckland-Nicks, 1995). Partial reduction of the acrosome is noted among species of Lepidopleurina such as *Deshayesiella curvata* (Pashchenko and Drozdov, 1998). However, sperm of a number of families in this basal suborder have not been examined: these include Hanleyidae, Choriplacidae, and Nierstraszellidae. Acrosomes are fully reduced in Callochitonidae, although the mid-piece of sperm in this family has retained the primitive state, in which mitochondria are symmetrically disposed around the centrioles and there is no reinforcement of the flagellum (Buckland-Nicks, 1995). In most Chitonina the mitochondria are asymmetrically distributed around the centrioles and, in addition, the flagellum is reinforced near the annulus (Buckland-Nicks, 1995).

The activation of sperm by serotonin, which was observed here for *C. castaneus*, has not been previously recorded in chitons, although this response is well known from bivalves (Juneja *et al.*, 1993) and has also been noted in limpets (Buckland-Nicks and Howley, 1997; Buckland-Nicks and Hodgson, unpubl. data). In bivalves, serotonin has been shown to initiate sperm motility and egg maturation, as well as to improve fertilization success (Juneja *et al.*, 1993). This preliminary evidence for a function of serotonin in chiton reproduction brings hope that induction of spawning also may be possible. Until now, the inability to predict spawning has hampered studies of chiton reproduction.

Morphology of the egg

In Chitonida the egg hull is resilient, easily preserved, and elaborated into spines or cupules that not only slow the sinking rate but direct sperm to specific locations on the egg surface (Buckland-Nicks, 1993, 1995). The egg hulls of most Chitonina have elaborate spines with narrow bases and highly variable tips (Eernisse, 1984; Sirenko, 1993). Eernisse (1984) first suggested developing independent character sets based on hull spine structure and gill placement to test the validity of phylogenies based solely on shell valve morphology (Smith, 1960; Van Belle, 1983). Sirenko's subsequent investigations proved that these characters (1993), as well as variation in the articulamentum (1997) are useful in the analysis of chiton phylogeny. The new sperm and egg characters described here for *C. castaneus* will be important in future cladistic analyses of the Chitonina because they indicate that Callochitonidae are basal to Chitonina.

The egg hull of *C. castaneus* differs in some key respects from that of other chitons studied; in particular, it is unlike that of any other Chitonina. The vitelline layer is enclosed by a fragile, smooth jelly coat that is permeated by large pores. However, this type of hull may also occur in *Deshayesiella curvata* (Lepidopleurina); drawings of this species show a similar jelly coat containing regularly spaced pores (Pashchenko and Drozdov, 1998), although no micrographs of this feature have been published. In fertilization experiments with polyspermic eggs of *D. curvata*, it was

Figure 15. SEM of sperm, showing acrosome (A) at tip of nuclear filament (NF), main body of nucleus (N), mid-piece (MP), and flagellum (F). Scale bar = 1 μm. **Inset:** TEM of apex of sperm revealing acrosomal vesicle (AV) separated from nuclear filament (NF) by basal plate (BP). Scale bar = 0.7 μm.

Figure 16. TEM of sperm nucleus (N) and mid-piece showing mitochondria (M), centrioles (C), and glycogen granules (G). Note portion of nuclear filament (arrowhead). Scale bar = 0.7 μm.

Figure 17. TEM of apex of sperm revealing acrosomal vesicle (AV) separated from nuclear filament (NF) by basal plate (BP). Scale bar = 0.7 μm.

observed that the jelly coat disintegrated, much like that of *C. castaneus* (Buckland-Nicks and Sirenko, unpubl. results). This phenomenon of a fragile jelly coat is a plesiomorphy shared between Lepidopleurina and Callochitonidae, which excludes all other Chitonina studied thus far.

In species that have egg hulls with closed cupules, sperm penetrate the hull exclusively between the cupules, usually where their hexagonal bases meet (Buckland-Nicks, 1995). Eggs of some Acanthochitonina, such as *Lepidochitona dentiens* and *L. fernaldi*, have micropores in this region. These permit easier access to the vitelline layer, although sperm have two granules in the acrosome, suggesting that the hull may still represent a barrier (Buckland-Nicks *et al.*, 1990). *C. castaneus* appears to have a simpler acrosome structure, which would correlate with the provision of direct access to the vitelline layer by large pores in the jelly hull.

In summary, *C. castaneus* gametes and those of the Lepidopleurina share plesiomorphic characters such as a simple arrangement of mitochondria in the sperm mid-piece and a smooth egg hull. Yet *C. castaneus* shares the derived characters of nuclear extension and reduction of acrosome with all other Chitonida. A previous cladistic analysis of chitons, which was largely based on sperm and egg characters, predicted that Callochitonina was distinct from Chitonina (Buckland-Nicks, 1995). The present study corroborates this prediction and indicates that *C. castaneus* is unique and perhaps should be placed in a sister taxon to both Chitonina and Acanthochitonina.

The mechanism of fertilization in chitons

Fertilization in *C. castaneus* and other Chitonida bears some similarity to that in other molluscs, in the sense that a sperm acrosome releases enzymes that digest a pore in the egg envelope, enabling the inner acrosomal membrane to fuse with the egg membrane (Buckland-Nicks *et al.*, 1988, this study). However, in many other respects the mechanism of fertilization in these chitons is highly derived when compared with those of other molluscs and of metazoans in general.

Firstly, there is no extrusion of an acrosomal process or "perforatorium" by the polymerization of actin, as occurs throughout molluscs and other metazoan groups (see review by Tilney, 1985). Rather, in all members of Chitonida the permanent needlelike nuclear filament has replaced the perforatorium (Buckland-Nicks *et al.*, 1988b, 1990). The intermediate condition of a short nuclear extension found in *Deshayesiella curvata* (Pashchenko and Drozdov, 1998) suggests that reduction in acrosome size among lepidopleurids may be linked with an increase in the length of the nuclear filament. Furthermore, all lepidopleurids examined have a subacrosomal granule, which in other metazoans is composed of actin for extruding the perforatorium during fertilization.

A second important difference observed between Chitonida and other molluscs is that the sperm organelles, as well as most of the nuclear membrane, apparently remain on the surface of the egg (Buckland-Nicks *et al.*, 1988b; Buckland-Nicks, 1995; this study). No chiton sperm has been observed becoming completely engulfed by a fertilization cone. The probable reason for this is that the vitelline layer, disturbed only by a minute pore permitting penetration of the nuclear filament, remains a barrier to the envelopment of the sperm by the fertilization cone. In other molluscs such as bivalves, as well as in many other metazoans, the vitelline layer is breached and the fertilization cone raises up through it to engulf the entire sperm, including part of the flagellum (see reviews by Tilney, 1985; Longo, 1987). In these species there is an initial paternal contribution of centrioles and mitochondria to the egg at fertilization, although, with the exception of some bivalve molluscs (Hoeh *et al.*, 1991), the paternal mitochondria degenerate and do not contribute to the zygote. Furthermore, in sea urchins and some other metazoans, a sperm centriole contributes to the movement of the pronuclei as well as to the formation of the mitotic spindle prior to first cleavage (see review by Gilbert, 1999). Chitons may be unique among molluscs if, in addition to the exclusion of paternal mitochondria, the centrioles that form the mitotic spindle are also maternally derived. Confirmation of this derivation will require appropriate labeling of sperm centrioles and mitochondria before and after fertilization.

To better understand how the mechanism of fertilization has evolved in chitons, it will be important to examine fertilization in a species like *Leptochiton asellus*, which has a typical molluscan acrosome (Hodgson *et al.*, 1988) and perhaps a mechanism of sperm entry more similar to that of limpets or bivalves.

Acknowledgments

We thank Robin Cross and Shirley Pinchuk for assistance in setting up electron microscopes and ancillary equipment, as well as Marvin Randall for doing most of the darkroom work. We are grateful to Doug Eernisse for important and helpful criticisms. This research was supported by a Hugh Kelly Fellowship from Rhodes University and an NSERC of Canada research grant, both to J.B-N., as well as a Rhodes University research grant to A.N.H.

Literature Cited

Buckland-Nicks, J. 1993. Hull cupules of chiton eggs: parachute structures and sperm focusing devices? *Biol. Bull.* **184:** 269–276.

Buckland-Nicks, J. 1995. Ultrastructure of sperm and sperm-egg interaction in Aculifera: implications for molluscan phylogeny. Pp. 129–153 in *Advances in Spermatozoal Phylogeny and Taxonomy*, B. G. M. Jamieson, J. Ausio, and J.-L. Justine, eds. Mem. Mus. Natl. Hist. Nat. **166**, Paris.

Buckland-Nicks, J., and B. Howley. 1997. Spermiogenesis and sperm structure in relation to early events of fertilization in the limpet *Tectura testudinalis* (Muller, 1776). *Biol. Bull.* **193**: 306–319.

Buckland-Nicks, J., R. Koss, and F.-S. Chia. 1988a. The elusive acrosome of chiton sperm. *Int. J. Invertebr. Reprod. Dev.* **13:** 193–198.

Buckland-Nicks, J., R. Koss, and F.-S. Chia. 1988b. Fertilization in a chiton: acrosome-mediated sperm-egg fusion. *Gamete Res.* **21:** 199–212.

Buckland-Nicks, J., F.-S. Chia, and R. Koss. 1990. Spermiogenesis in Polyplacophora, with special reference to acrosome formation. *Zoomorphology* **109:** 179–188.

Cross, R. H. M. 1989. A reliable epoxy resin mixture and its application in routine biological transmission electron microscopy. *Micron Microsc. Acta* **20:** 1–7.

Daddow, L. Y. M. 1986. An abbreviated method of double lead stain technique. *J. Submicrosc. Cytol.* **18:** 363–372.

Eernisse, D. G. 1984. *Lepidochitona* Gray, 1821 (Mollusca: Polyplacophora), from the Pacific coast of the United States: systematics and reproduction. Ph. D. Thesis, University of California at Santa Cruz.

Eernisse, D. 1988. Reproductive patterns in six species of *Lepidochitona* (Mollusca: Polyplacophora) from the Pacific Coast of North America. *Biol. Bull.* **174:** 287–302.

Eernisse, D. J., and P. D. Reynolds. 1994. Polyplacophora. Pp. 55–110 in *Microscopic Anatomy of Invertebrates, vol 5: Mollusca 1.* Wiley-Liss, New York.

Gilbert S. F. 1999. *Developmental Biology*, 6th ed. Sinauer, Sunderland, MA. 749 pp.

Healy, J. M. 1988. Sperm morphology and its systematic importance in the Gastropoda. *Malacol. Rev. Suppl.* **4:** 251–266.

Hodgson, A. N., J. M. Baxter, M. G. Sturrock, and R. T. F. Bernard. 1988. Comparative spermatology of 11 species of Polyplacophora (Mollusca) from the suborders Lepidopleurina, Chitonina and Acanthochitonina. *Proc. R. Soc. Lond. B* **235:** 161–177.

Hodgson, A. N. , S. Ridgeway, G. M. Branch, and S. J. Hawkins. 1996. Spermatozoal morphology of 19 species of prosobranch limpets (Patellogastropoda) with a discussion of patellid relationships. *Proc. R. Soc. Lond. B.* **351:** 339–347.

Hoeh, W. R. , K. H. Blakely, and W. M. Brown. 1991. Heteroplasmy suggests limited biparental inheritance of *Mytilus* mitochondrial DNA. *Science* **251:** 1488–1490.

Jamieson, B. G. M. 1987. A biological classification of sperm types, with reference to annelids and molluscs, and an example of spermiocladistics. Pp. 311–332 in *New Horizons in Sperm Cell Research*, H. Mohri, ed. Japan Science Society, Tokyo.

Juneja, R., S. J. Segal, and S. S. Koide. 1993. Promotion of fertilizability of *Spisula* oocytes with 5-hydroxy-tryptamine. *Invertebr. Reprod. Dev.* **24:** 103–106.

Longo, F. J. 1987. *Fertilization.* Chapman and Hall, New York.

Pashchenko, S. V., and A. L. Drozdov. 1998. Morphology of gametes in five species of far-eastern chitons. *Invertebr. Reprod. Dev.* **33:** 47–56.

Richter, H. -P. 1986. Ultrastructure of follicular epithelia in the ovary of *Lepidochitona cinerea* L. (Mollusca: Polyplacophora). *Dev. Growth Differ.* **28:** 7–16.

Sirenko, B. I. 1993. Revision of the system of the order Chitonida (Mollusca: Polyplacophora) on the basis of correlation between the type of gills arrangement and the shape of the chorion processes. *Ruthenica* **3:** 93–117.

Sirenko, B. I. 1997. The importance of the development of articulamentum for taxonomy of chitons (Mollusca, Polyplacophora). *Ruthenica* **7:** 1–24.

Smith, A. G. 1960. Amphineura. Pp. 141–176 in *Treatise on Invertebrate Paleontology, Part 1, Mollusca 1*, R. C. Moore, ed. Geological Society of America, New York.

Tilney, L. G. 1985. The acrosomal reaction. Pp. 157–213 in *The Biology of Fertilization, Vol. 2,* C. Metz and A. Monroy, eds. Academic Press, New York.

Van Belle, R. A. 1983. The systematic classification of chitons (Mollusca: Polyplacophora). *Informations de la Société Belge de Malacologie. Série* **11:** 1–164.

Reference: *Biol. Bull.* **199:** 68–75. (August 2000)

Early Development of Zooxanthella-Containing Eggs of the Corals *Pocillopora verrucosa* and *P. eydouxi* with Special Reference to the Distribution of Zooxanthellae

M. HIROSE[1], R. A. KINZIE III[2], AND M. HIDAKA[1,*]

[1] *Marine Environmental Science, Department of Chemistry, Biology and Marine Science, University of the Ryukyus, Nishihara, Okinawa 903-0213, Japan; and* [2] *Department of Zoology and Hawaii Institute of Marine Biology, University of Hawaii, Honolulu, Hawaii 96822*

Abstract. Some hermatypic corals spawn eggs that contain zooxanthellae. We followed development of zooxanthella-containing eggs of two such species, *Pocillopora verrucosa* and *P. eydouxi.* We also documented changes in the distribution pattern of zooxanthellae during development. Oocytes of both species took up zooxanthellae 3 to 4 days before spawning. At first, zooxanthellae were evenly distributed in oocytes, but they later moved to the hemisphere that contained the germinal vesicle. After fertilization, early cleavage events were holoblastic, progressing by furrow formation. The first cleavage furrow started at the hemisphere that contained zooxanthellae, dividing the zooxanthellate complement of the zygote about equally into the two blastomeres. The second division divided each blastomere into one zooxanthellae-rich cell and one with few zooxanthellae. With continued cell division, blastomeres containing zooxanthellae moved into the blastocoel. The blastocoel disappeared at about 5 h after the first cleavage, and the central region of the embryo was filled with cells containing either zooxanthellae or lipid droplets, forming a stereogastrula. Our results suggest that only blastomeres that had been determined to develop into gastrodermal cells receive zooxanthellae during cleavage. This determination appears to take place, at the latest, by the second cell division at the four-cell stage.

Introduction

Reef-building corals harbor intracellular symbiotic dinoflagellates, zooxanthellae, in their endodermal cells. Some hermatypic corals acquire their symbionts from their mother colony before fertilization (Kojis and Quinn, 1981; Babcock and Heyward, 1986; Tomascik and Sander, 1987; Yeemin, 1988; Glynn *et al.,* 1991, 1994; Heyward *et al.,* 1987; Kinzie, 1993, 1996; Sier and Olive, 1994; Kruger and Schleyer, 1998). It is not known how zooxanthellae are delivered to oocytes and how their distribution relates to their eventual restriction to the endodermal cells in adults. Early development of scleractinian corals has been described in various species (*e.g.,* Szmant-Froelich *et al.,* 1980, 1985; Babcock and Heyward, 1986; Harrison and Wallace, 1990). However, early development of corals with oocytes containing zooxanthellae has been described only in the spawning species *Montipora effusa* (Yeemin, 1988) and *M. verrucosa* (Maté *et al.,* 1998) and the brooding species *Porites porites* (Tomascik and Sander, 1987).

Although zooxanthellae are generally restricted to the gastrodermis of adult corals, they are at least temporarily observed in the ectoderm of planulae of some corals and soft corals (Szmant-Froelich, 1985; Benayahu *et al.,* 1988; Benayahu, 1997; Benayahu and Schleyer, 1998; Schwarz *et al.,* 1999). This is probably because infection first occurred in the ectoderm cells of embryos or early planulae (Szmant-Froelich *et al.,* 1985) or because dividing cells of these stages transferred the multiplying symbionts to their daughter cells, including presumptive ectoderm cells (Benayahu, 1997; Benayahu and Schleyer, 1998). In these cases, zooxanthellae were transferred from ectoderm to endoderm

Received 22 October 1999; accepted 17 May 2000.

* To whom correspondence should be addressed. E-mail: hidaka@sci.u-ryukyu.ac.jp

across the mesoglea before larvae develop into mature planulae (Benayahu, 1997; Benayahu and Schleyer, 1998). Montgomery and Kremer (1995) also found that in the larvae of a scyphozoan, *Linuche unguiculata*, the algae were found mostly in the ectodermal cells, and suggested mechanisms by which zooxanthellae could be transferred from ectoderm to endoderm of planulae.

The corals *Pocillopora eydouxi* and *P. verrucosa* release zooxanthellate eggs, which display an uneven distribution of algal cells (Hirose *et al.*, unpubl. data). It is likely that, in these corals, zooxanthellae are not equally delivered to all daughter cells but go more or less exclusively to presumptive endoderm cells. If zooxanthellae become restricted to endoderm cells during the course of development, the larvae do not need to transfer the algae from ectoderm to endoderm as described in the soft corals (Benayahu, 1997).

In the present study, we followed early development of zooxanthellate eggs of the corals *P. eydouxi* and *P. verrucosa*. We studied changes in the distribution pattern of zooxanthellae during early development of the corals to determine mechanisms by which the distribution of zooxanthellae becomes localized to the endoderm of planulae.

Materials and Methods

Branches, 7–12 cm long, were collected from colonies of *Pocillopora verrucosa* a few days before the new moon and from *P. eydouxi* a few days before the full moon in June and July 1998. Colonies were collected from reefs at Sesoko Island, Okinawa. The branches were placed separately into 3-l plastic containers supplied with unfiltered running seawater. The hermaphroditic colonies of *P. verrucosa* and *P. eydouxi* spawned gametes for about 30 min in the early morning a few days after the new moon, and a few days after the full moon, respectively (Kinzie, 1993; Hirose *et al.*, unpubl. data). Both species first released sperm and then negatively buoyant eggs. To collect gametes, the supply of seawater was stopped before the expected spawning time, about 0630 h. After sperm had been shed, they were collected by sucking up seawater from the container in a large plastic pipette. The pipette was rinsed with a diluted hypochlorite solution and then with seawater to avoid contamination of gametes. Released eggs were collected by pipette from the bottom of the container and placed in a plastic beaker. Eggs were fertilized by mixing released gametes (100–300 ml suspension each) from two or three colonies in a plastic beaker. Filtered (0.45 μm) seawater was added to the beaker to make the final volume to 1 or 2 l. Fertilized eggs were kept in the seawater at a room temperature 28°–30°C. Eggs and embryos were sampled and observed under a light microscope at intervals of from 30 min to 1 h, and photomicrographs were taken with a microscope equipped with an epifluorescent system (Nikon Microphot).

Histology and transmission electron microscopy

Eggs and embryos were collected in a microtube and allowed to settle to the bottom. The supernatant was then discarded and fixative added. The specimens were fixed in 2.5% glutaraldehyde in 0.1 *M* cacodylate buffer (pH 7.4) containing 3% NaCl for 2 h or more. The specimens were rinsed in the same buffer three times and post-fixed in 1% osmium tetroxide in the same buffer for 1 h on ice, dehydrated in a graded series of acetone, immersed in *n*-butyl glycidyl ether (QY1), and embedded in Spurr's resin. For light microscopic observation, sections 0.5–1 μm thick were stained with 1% methylene blue-1% azur II in 1% borax. For electron microscopy, silver to gold sections were stained with uranyl acetate and lead citrate and observed under a JEOL JEM-2000EX electron microscope at an acceleration voltage of 100 kV.

Results

Oocytes took up zooxanthellae 3–4 days before spawning in both species. Zooxanthellae were first distributed evenly in the ooplasm (Fig. 1A, B), but later, 1–2 days before spawning, the algae became concentrated in the hemisphere that contained the germinal vesicle. The other hemisphere contained many lipid droplets of about the same size as the zooxanthellae. Although the germinal vesicle was no longer apparent by the time the eggs were spawned, the zooxanthellae remained concentrated in the hemisphere of the egg that contained the nucleus (Fig. 1C, D). At spawning, eggs of both species were about 140 μm in diameter and contained about 130 zooxanthellae (Hirose *et al.*, unpubl. data).

Cleavage took place by progressive furrow formation (Fig. 1E), at intervals of 30 to 40 min. The first cleavage furrow started at the hemisphere that contained the zooxanthellae and the oocyte nucleus, dividing the zooxanthellae equally into two blastomeres, each with a roughly equal complement of zooxanthellae still concentrated in the hemisphere containing the nucleus (Fig. 1F). At the second cleavage, each blastomere was divided into one zooxanthellae-rich blastomere and one with few zooxanthellae (Fig. 2A). By the 64- to 128-cell stage, some blastomeres in the morula contained one or sometimes more zooxanthellae, while others contained none (Fig. 2B). As cleavage proceeded, a blastocoel formed and blastomeres with zooxanthellae moved into this space (Fig. 2C, D). The outer layer of the blastula consisted of relatively large blastomeres containing no zooxanthellae. At about 5 h after fertilization, blastomeres containing zooxanthellae, lipid droplets, or both filled the blastocoel, resulting in a stereogastrula (Fig. 2E, F). Gastrulation appeared to occur by delamination rather than by invagination.

Blastomeres in the outer layer had microvilli on their outer surface and characteristic granules just below the cell membrane (Fig. 3A). Blastomeres in the outer layer were

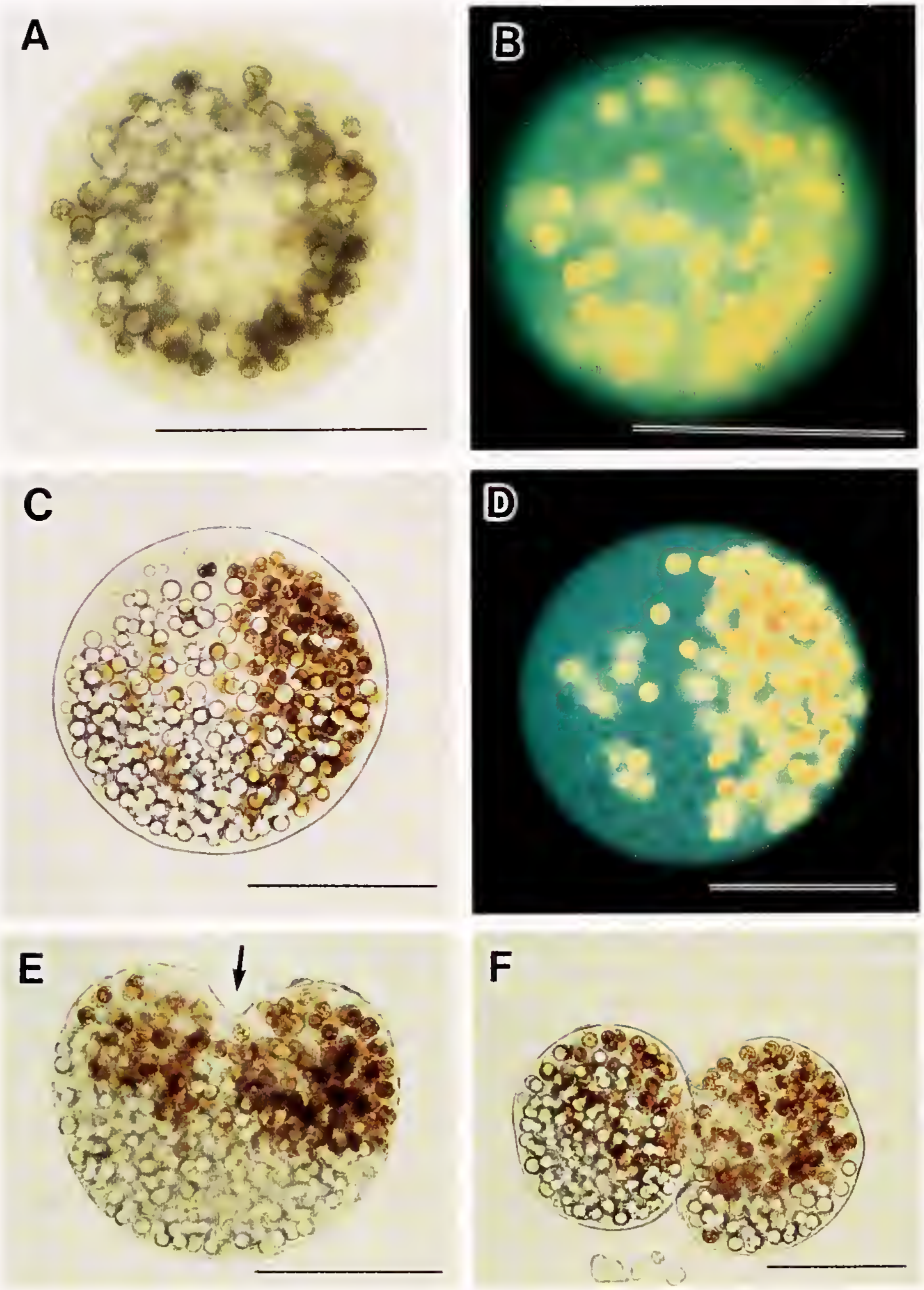

Figure 1. Early development of *Pocillopora verrucosa:* from unfertilized egg to two-cell stage. (A) Oocyte isolated from the gonad. Zooxanthellae are distributed evenly in the cytoplasm. The germinal vesicle is at the center of the oocyte. (B) Oocyte viewed under epifluorescence (BV excitation). The red fluorescence is due to algal chlorophyll. Cytoplasm of the oocyte exhibits blue-green autofluorescence. (C) Spawned egg. Zooxanthellae are mainly located in the right hemisphere and lipid droplets in the left hemisphere. (D) The same egg, observed under epifluorescence (BV excitation). (E) First cleaving stage. Cleavage furrow (arrow) starts at the hemisphere that contains the zooxanthellae. (F) Two-cell stage. Zooxanthellae are divided equally into the two blastomeres. Bars = 100 μm.

connected to each other by the contact junctions near the apical surface (Fig. 3B). In other regions of the interface, blastomeres were only loosely attached to each other or were separated by extracellular space. Villi-like cellular processes were observed in the extracellular space, and those from neighboring blastomeres were often intermingled (Fig. 3C). When blastomeres in the outer layer contained zooxanthellae, the zooxanthellae were usually at the lower or lateral margin of the blastomere. Zooxanthellae at the lateral margin of the blastomere bulged into the extra-

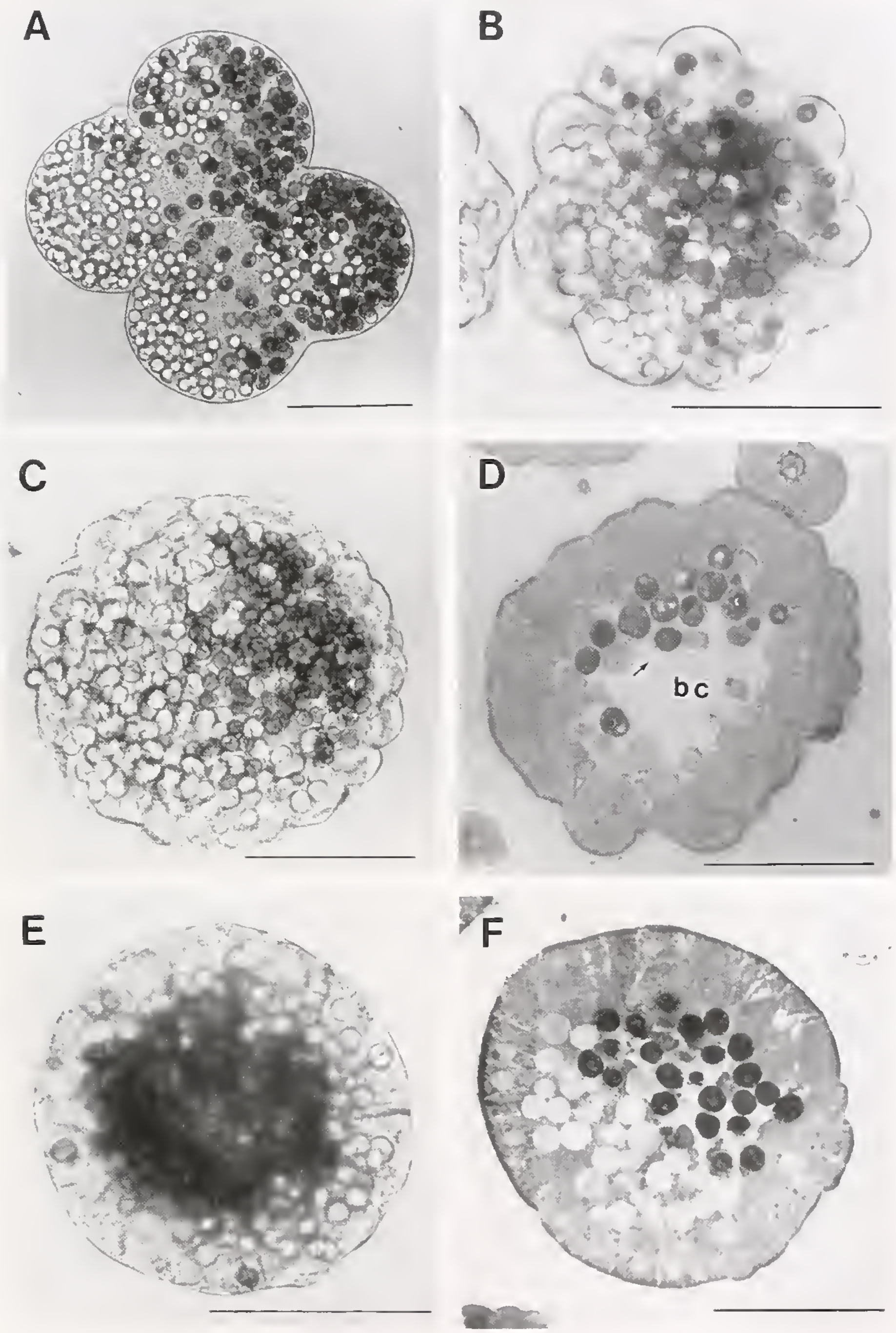

Figure 2. Early development of *Pocillopora verrucosa:* four-cell stage to gastrula. (A) Four-cell stage. The second cleavage plane was normal to the first cleavage plane, thus dividing the blastomere into a zooxanthellae-rich blastomere and a lipid-droplet-rich blastomere. (B) Morula-stage embryo. Blastomeres are round; some contain a single zooxanthellae. (C) Blastula. Zooxanthellae are still restricted to one hemisphere. (D) Section of a blastula. Blastomeres containing one or more zooxanthellae (arrow) and those containing lipid droplets are located in the blastocoel (bc), while the surface layer is composed of larger blastomeres with no algae. (E) Gastrula. The center of the gastrula appears dark due to accumulation of zooxanthella-containing blastomeres. (F) Section of a gastrula. Blastomeres containing zooxanthellae and those containing lipid droplets fill the inner space of the gastrula, forming a stereogastrula. Bars = 100 μm.

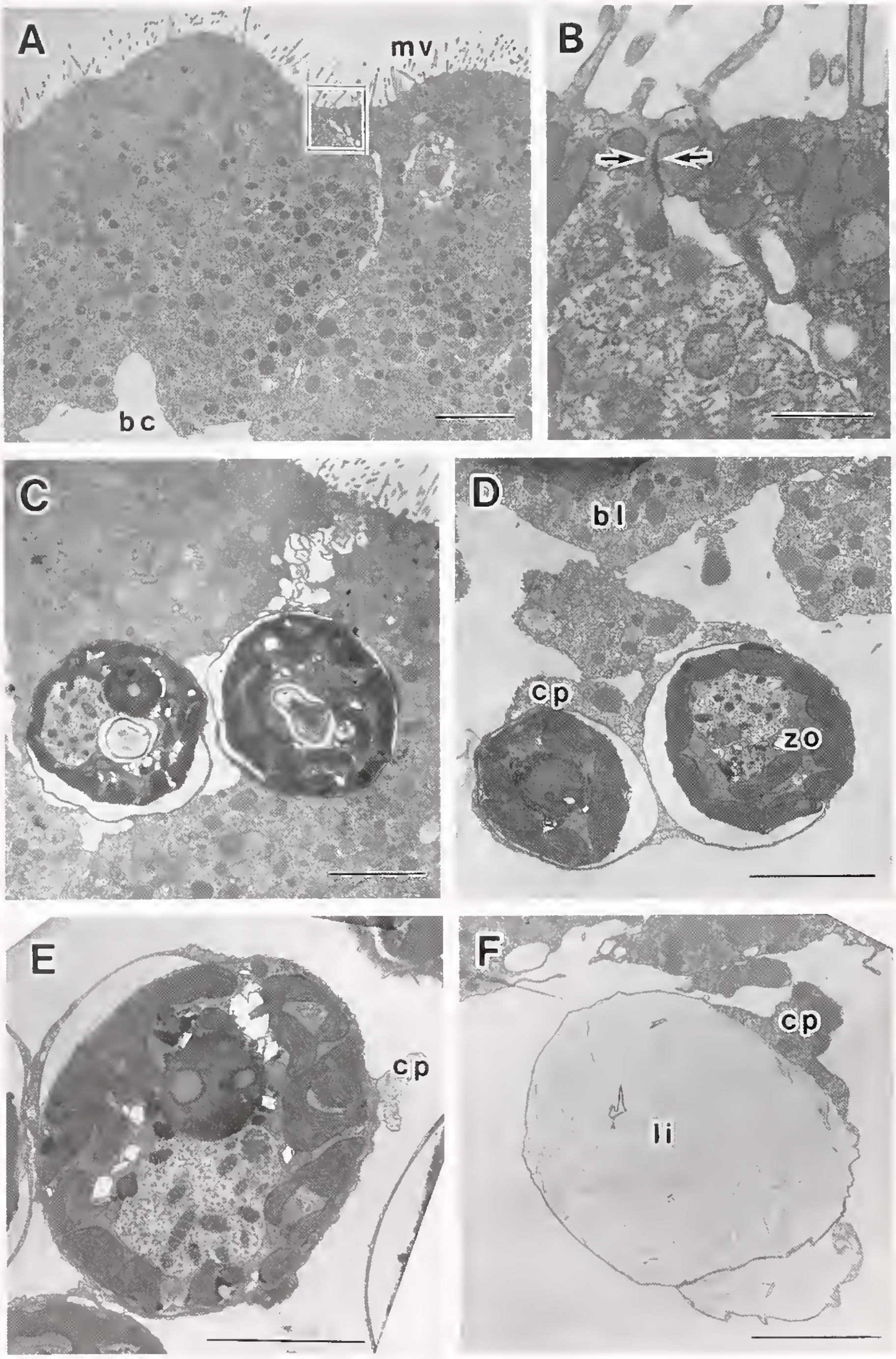

Figure 3. Electron micrographs of an early gastrula of *Pocillopora verrucosa*. (A) Blastomeres in the outer layer of an embryo. (B) Higher magnification of the boxed area in (A), showing contact junction near the apical surface (arrow). (C) Blastomere in the outer layer containing zooxanthellae. Zooxanthellae bulge into the neighboring blastomere. (D) Two zooxanthellae in a cellular process, which appears to be still connected to the outer layer blastomere. (E) Zooxanthellae surrounded by a small amount of host cytoplasm. (F) Lipid droplet surrounded by a small amount of cytoplasm. bc = blastocoel, bl = blastomere, cp = cytoplasm, li = lipid droplet, mv = microvilli, zo = zooxanthella. Bars = 5 μm except in (B), where bar = 1 μm.

cellular space and sometimes into neighboring blastomeres (Fig. 3C). Similarly, zooxanthellae or lipid droplets located at the lower margin of the blastomeres bulged into the blastocoel. In such cases, a constriction was often observed between the central cytoplasm and the protrusion containing a zooxanthella or a lipid droplet (Fig. 3D). Most zooxan-

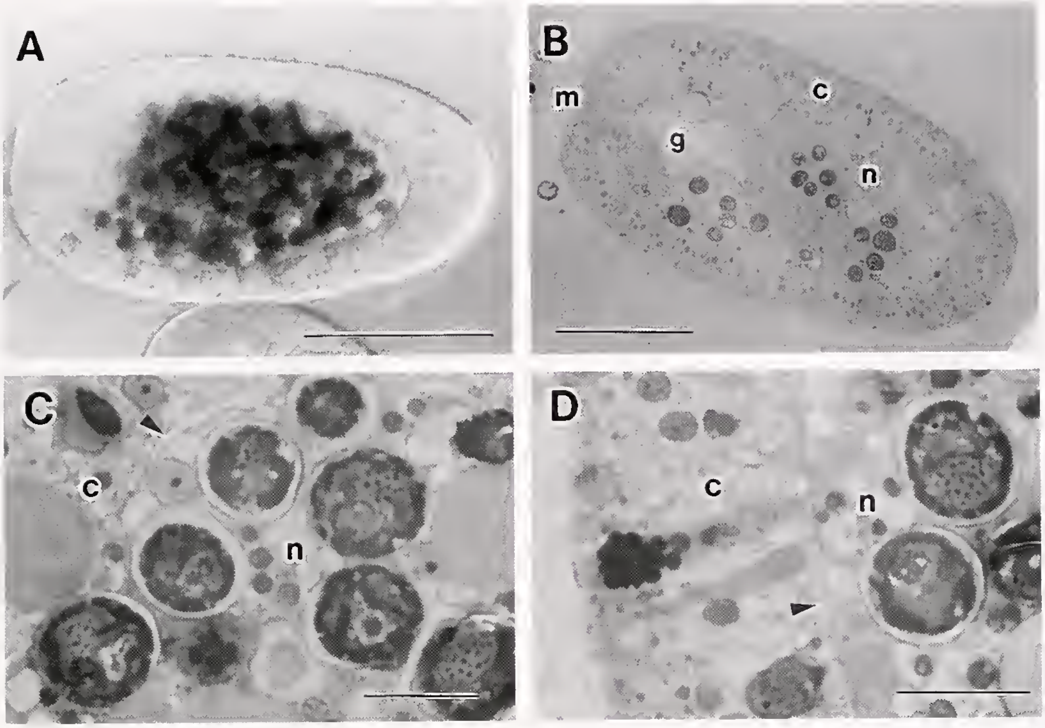

Figure 4. Planula of *Pocillopora verrucosa* 24 h after fertilization. (A) Photomicrograph of a fixed planula taken under differential interference optics. The planula is completely ciliated at this stage. (B) Histological section of a planula. Zooxanthellae and lipid droplets are in the endodermal cells. (C–D) Photomicrographs of the body wall of a planula taken under oil immersion. The ectoderm and endoderm are clearly separated by the mesoglea (arrowhead). The ectoderm consists of columnar cells. c = ectoderm, g = gastrovascular cavity, m = mouth opening, n = endoderm. Bars = 100 μm in (A) and (B), 20 μm in (C) and (D).

thellae and lipid droplets in the blastocoel were surrounded by a small amount of cytoplasm and appeared to be free—that is, detached—from blastomeres in the outer layer (Fig. 3E, F).

Spherical embryos with a smooth surface as shown in Figure 2E and F were observed 6 h after fertilization. Ciliated larvae started to swim 8 h after fertilization. The embryos became elliptical and swam spirally by 9–10 h after fertilization. An oral pore was formed by invagination of the epidermis, and a gastrovascular cavity was formed as gastrodermal cells became organized 24 h after fertilization (Fig. 4A, B). At this stage the ectodermal layer—the planula's epidermis—consisted of characteristic columnar cells, and the epidermis and gastrodermis were separated by distinct mesoglea (Fig. 4C, D). Embryos at this stage were typical planulae. Generally, only gastrodermal cells contained zooxanthellae, though a few zooxanthellae were observed in ectoderm of some planulae. Planulae 48 h old possessed some nematocysts.

Discussion

Although early development of scleractinians has been described (*e.g.*, Szmant-Froelich *et al.*, 1980, 1985; Babcock and Heyward, 1986; Harrison and Wallace, 1990), this is the first report describing the processes by which zooxanthellae become restricted to the endoderm during the course of embryogenesis. In the two *Pocillopora* species studied, regions of egg cytoplasm are differentiated and cell fates are apparently decided early in development, possibly before fertilization. Zooxanthellae moved toward the animal pole 1–2 days before spawning. The first cleavage apportioned zooxanthellae more or less equally between the first two blastomeres. At the second cleavage, however, two of the four blastomeres received almost all the zooxanthellae, while the other two had few or none. This uneven distribution of zooxanthellae persisted until the zygotes developed into gastrulae.

As cleavage progressed, relatively large blastomeres without zooxanthellae came to occupy the outer layer of the embryo as the blastocoel opened. Later, blastomeres containing zooxanthellae or lipid droplets detached from the outer layer and dropped into the blastocoel until it was filled with blastomeres containing zooxanthellae and lipid droplets. In these two species of *Pocillopora,* gastrulation may occur due to delamination rather than invagination, resulting in a stereogastrula. Gastrulation through delamination has been suggested for *Astrangia danae* (Szmant-Froelich *et al.*, 1980), *Favia fragum* (Szmant-Froelich *et al.*, 1985), and *Montipora verrucosa* (Maté *et al.*, 1998).

Titlyanov *et al.* (1996, 1998) observed degraded zooxanthellae in planulae as well as in adult polyps of hermatypic corals and suggested that digestion of zooxanthellae occurs both in planulae and in adult polyps. We saw no such degraded zooxanthellae in the surface layer of embryos or early planulae. If zooxanthellae are not digested during early development, they must be transferred from blastomeres that are determined to develop into symbiont-free ectodermal cells to blastomeres that are fated to develop into algae-bearing endodermal cells. This ontogenetic redistribution of algae might occur in several ways. One possibility is that zooxanthellae move basally within blastomeres so that subsequent horizontal cell division results in surface ectodermal cells and centrally located endodermal cells that contain zooxanthellae. Our observations suggest that zooxanthellae, along with small amounts of cytoplasm, were separated from surface cells and dropped into the blastocoel. This process is similar to the "pinching off" suggested for the transfer mechanism of zooxanthellae from follicle cells to oocytes and from ectoderm to endoderm in some soft corals (Benayahu, 1997; Benayahu *et al.*, 1992; Benayahu and Schleyer, 1998). However, the small "blastomeres" containing zooxanthellae (Fig. 3E, F) could also be produced by unequal division rather than by pinching off. If this were the case, there should be animal nuclei in these structures. These basally derived cells would then develop into gastrodermal cells. Another possibility is that ectodermal cells expel zooxanthellae by exocytosis and adjacent endodermal cells take them up by phagocytosis. The observation that zooxanthellae within vacuoles of the blastomere in the outer layer often protruded to the intercellular space, bulging into the neighboring cell, suggests that this possibility cannot be ruled out.

Few if any zooxanthellae were found in the outer layer of gastrulae or the ectoderm of planulae of the two *Pocillopora* species studied. However, zooxanthellae are sometimes found in the ectoderm of early planulae of some corals (*Favia fragum:* Szmant-Froelich *et al.*, 1985; *Fungia scutaria:* Schwarz *et al.*, 1999), soft corals (*Xenia umbellata:* Benayahu *et al.*, 1988; *Litophyton arboreum:* Benayahu *et al.*, 1992; Benayahu, 1997; *Anthelia glauca:* Benayahu and Schleyer, 1998), and the scyphozoan *Linuche unguiculata* (Montgomery and Kremer, 1995). It has been suggested that, in the early developmental stages, zooxanthellae show no specificity towards presumptive endodermal cells (Benayahu, 1997; Benayahu and Schleyer, 1998). However, as planulae develop, zooxanthellae are found increasingly in the endoderm and eventually become restricted to the gastrodermis of polyps. Several mechanisms by which the algae are translocated from ectoderm to endoderm have been suggested (Montgomery and Kremer, 1995; Benayahu, 1997; Benayahu and Schleyer, 1998). Montgomery and Kremer (1995) suggested that ectoderm cells infected by zooxanthellae may migrate to the endoderm of planulae. Benayahu (1997) and Benayahu and Schleyer (1998) observed that, in the soft corals they studied, zooxanthellae pass through temporarily opened gaps in the mesoglea towards the endoderm. Throughout the process, each zooxanthella resides within a vacuole in the detached ectodermal cytoplasm. However, we did not observe such a transfer of zooxanthellae from ectoderm to endoderm in planulae of the two *Pocillopora* species. In these corals, zooxanthellae appeared to be transferred more or less exclusively to blastomeres that were fated to develop into endodermal cells. This suggests that determination of presumptive endoderm cells and specificity of zooxanthellae towards presumptive endoderm cells occur earlier in the two *Pocillopora* species than in the soft corals studied.

We described changes in the distribution of zooxanthellae during early development as well as during final maturation of oocytes in the corals *Pocillopora verrucosa* and *P. eydouxi*. Zooxanthellae moved to the hemisphere of the oocyte that contained the germinal vesicle 1 to 2 days before spawning. Zooxanthellae moved to the lateral or basal margins of the surface blastomeres and bulged into extracellular spaces or into the blastocoel. Blastomeres containing zooxanthellae or lipid droplets along with a small amount of cytoplasm were produced, probably by unequal mitotic division, and then dropped into the blastocoel and became endodermal cells. It is not clear whether the presence of zooxanthellae affects development of the blastomere or if the fate of a blastomere is determined by the nature or quantity of its cytoplasm. Further study is necessary to understand how zooxanthellae move to a region of oocytes and to certain areas of blastomeres.

Acknowledgments

We thank the staff of Sesoko Station, Tropical Biosphere Research Center, University of the Ryukyus, where part of this study was done. Y. Nozawa, N. Takahashi, and W. Diah Permata kindly helped us. This study was partly supported by the Grant-in-Aid for Scientific Research No. 08644216 and 11694223 from the Ministry of Education, Science, Sports and Culture, Japan, and by the Sasagawa Scientific Research Grant from the Japan Science Society.

Literature Cited

Babcock, R. C., and A. J. Heyward. 1986. Larval development of certain gamete-spawning scleractinian corals. *Coral Reefs* **5:** 187–195.

Benayahu, Y. 1997. Developmental episodes in reef soft corals: ecological and cellular determinants. *Proc. 8th Int. Coral Reef Symp.* **2:** 1213–1218.

Benayahu, Y., and M. H. Schleyer. 1998. Reproduction in *Anthelia glauca* (Octocorallia: Xeniidae). II. Transmission of algal symbionts during planular brooding. *Mar. Biol.* **131:** 433–442.

Benayahu, Y., Y. Achituv, and T. Berner. 1988. Embryogenesis and acquisition of algal symbionts by planulae of *Xenia umbellata* (Octocorallia: Alcyonacea). *Mar. Biol.* **100:** 93–101.

Benayahu, Y., D. Weil, and Z. Malik. 1992. Entry of algal symbionts into oocytes of the coral *Litophyton arboreum*. *Tissue Cell* **24:** 473–482.

Glynn, P. W., N. J. Gassman, C. M. Eakin, J. Cortes, D. B. Smith, and H. M. Guzman. 1991. Reef coral reproduction in the eastern Pacific: Costa Rica, Panama, and Galapagos Islands (Ecuador). I. Pocilloporidae. *Mar. Biol.* **109:** 355–368.

Glynn, P. W., S. B. Colley, C. M. Eakin, D. B. Smith, J. Cortes, N. J. Gassman, H. M. Guzman, J. B. Del Rosario, and J. S. Feingold. 1994. Reef coral reproduction in the eastern Pacific: Costa Rica, Panama, and Galapagos Islands (Ecuador). II. Poritidae. *Mar. Biol.* **118:** 191–208.

Harrison, P. L., and C. C. Wallace. 1990. Reproduction, dispersal and recruitment of scleractinian corals. Pp. 133–207 in *Ecosystems of the World: Coral Reefs*, Vol. 25, Z. Dubinsky, ed. Elsevier, Amsterdam.

Heyward, A., K. Yamazato, T. Yeemin, and M. Minei. 1987. Sexual reproduction of corals in Okinawa. *Galaxea* **6:** 331–343.

Kinzie, R. A., III. 1993. Spawning in the reef corals *Pocillopora verrucosa* and *P. eydouxi* at Sesoko Island, Okinawa. *Galaxea* **11:** 93–105.

Kinzie, R. A., III. 1996. Modes of speciation and reproduction in Archaeocoeniid corals. *Galaxea* **13:** 47–64.

Kojis, B. L., and N. J. Quinn. 1981. Reproductive strategies in four species of *Porites* (Scleractinia). *Proc. 4th Int. Coral Reef Symp.* **2:** 145–151.

Kruger, A., and M. H. Schleyer. 1998. Sexual reproduction in the coral *Pocillopora verrucosa* (Cnidaria: Scleractinia) in KwaZulu-Natal, South Africa. *Mar. Biol.* **132:** 703–710.

Maté, T. J. L., J. Wilson, S. Field, and E. G. Neves. 1998. Fertilization dynamics and larval development of the scleractinian coral *Montipora verrucosa* in Hawai'i. *Univ of Hawaii, Hawaii Institute of Marine Biology, Technical Report* **42:** 27–39.

Montgomery, M. K., and P. M. Kremer. 1995. Transmission of symbiotic dinoflagellates through the sexual cycle of the host scyphozoan *Linuche unguiculata*. *Mar. Biol.* **124:** 147–155.

Schwarz, J. A., D. A. Krupp, and V. M. Weis. 1999. Late larval development and onset of symbiosis in the scleractinian coral *Fungia scutaria*. *Biol. Bull.* **196:** 70–79.

Sier, C. J. S., and P. J. W. Olive. 1994. Reproduction and reproductive variability in the coral *Pocillopora verrucosa* from the Republic of Maldives. *Mar. Biol.* **118:** 713–722.

Szmant-Froelich, A., P. Yevich, and M. E. Q. Pilson. 1980. Gametogenesis and early development of the temperate coral *Astrangia danae* (Anthozoa: Scleractinia). *Biol. Bull.* **158:** 257–269.

Szmant-Froelich, A., M. Reutter, and L. Riggs. 1985. Sexual reproduction of *Favia fragum* (Esper): lunar patterns of gametogenesis, embryogenesis and planulation in Puerto Rico. *Bull. Mar. Sci.* **37:** 880–892.

Titlyanov, E. A., T. V. Titlyanova, V. A. Leletkin, J. Tsukahara, R. van Woesik, and K. Yamazato. 1996. Degradation and regulation of zooxanthellae density in hermatypic corals. *Mar. Ecol. Prog. Ser.* **139:** 167–178.

Titlyanov, E. A., T. V. Titlyanova, Y. Loya, and K. Yamazato. 1998. Degradation and proliferation of zooxanthellae in planulae of hermatypic coral *Stylophora pistillata*. *Mar. Biol.* **130:** 471–477.

Tomascik, T., and F. Sander. 1987. Effects of eutrophication on reef-building corals. III. Reproduction of the reef-building coral *Porites porites*. *Mar. Biol.* **94:** 77–94.

Yeemin, T. 1988. A comparative study of reproductive biology in four congeneric species of scleractinian corals (*Montipora*) from Okinawa. Master's thesis. University of the Ryukyus, Okinawa.

Reference: *Biol. Bull.* **199:** 76–84. (August 2000)

Revised Description of the Fine Structure of *in situ* "Zooxanthellae" Genus *Symbiodinium*

TIMOTHY S. WAKEFIELD[1,*], MARK A. FARMER[2], AND STEPHEN C. KEMPF[1]

[1]*Department of Biological Sciences, Auburn University, Alabama 36849-5414; and* [2]*Center for Advanced Ultrastructural Research, University of Georgia, Athens, Georgia 30602*

Abstract. The fine structure of the symbiotic dinoflagellate genus *Symbiodinium* has been well described. All of the published descriptions are based on tissue that was fixed in standard aldehyde and osmium fixatives and dehydrated in an ethanol series before embedding. When the technique of freeze-substitution was used to fix tissue from *Cassiopeia xamachana*, *Aiptasia pallida*, and *Phyllactis flosculifera* and prepare it for embedding, thecal vesicles were revealed within the *in situ* symbionts of all three species. Although these structures have been identified in cultured symbionts, they have never been described in the *in situ* symbionts. A review of the literature has revealed several instances where thecal vesicles were either overlooked or identified incorrectly. Thus the formal description of the genus *Symbiodinium*, which describes the *in situ* symbionts, contains information that is based on artifact and should be revised. A revision of the genus is suggested, and the true nature of these structures and their significance in the symbiotic association are discussed.

Introduction

The symbiotic algae found in the tissues of numerous marine invertebrates and often called "zooxanthellae" have included members of the classes Bacillariophyceae, Cryptophyceae, Dinophyceae, and Rhodophyceae (Rowan, 1998). In recent years, common usage has relegated this term almost exclusively to the description of dinoflagellate symbionts. Loeblich and Sherley (1979) suggested that many of the taxonomically described dinoflagellate symbionts should be assigned to a new genus they termed *Zooxanthella* in recognition of very early work on dinoflagellate symbiosis by Brandt (1881). However, continued studies in symbiotic dinoflagellate taxonomy have shown that there are, in fact, many species from several genera including *Amphidinium* (Taylor, 1971a; Trench and Winsor, 1987), *Aureodinium* (Anderson and Be, 1976), *Gymnodinium* (Spero, 1987), *Gyrodinium* (Spindler and Hemleben, 1980), *Prorocentrum* (Yamasu, 1988), *Pyrocystis* (Alldredge and Jones, 1973), *Scrippsiella* and *Gloeodinium* (Banaszak *et al.*, 1993). The most frequently occurring of these is the gymnodinioid-like dinoflagellate assigned to the genus *Symbiodinium*, the alga commonly found in a variety of marine invertebrates such as tridacnid clams, certain nudibranch molluscs, reef-building corals, other anthozoans, and scyphozoans.

The first formal description of the dinoflagellate genus *Symbiodinium* was published by Hugo D. Freudenthal (1962). This work provided a detailed histological description of the species *S. microadriaticum* that had been extracted and cultured from a scyphozoan host described as *Cassiopeia* sp. In 1968 Taylor published the preliminary ultrastructural description of dinoflagellate "zooxanthellae" from *Anemonia sulcata*. The author stated that the symbionts were "akin" to *S. microadriaticum*, but that the status of any relationship would remain unknown until an ultrastructural study was performed on the symbionts of *Cassiopeia*. Kevin *et al.* (1969) provided this information in their ultrastructural examination of *S. microadriaticum* from the hosts *Cassiopeia* sp. (Scyphozoa) and *Condylactis* sp. (Anthozoa). They stated that the symbionts from these two genera were the same species as those seen by Taylor, and concluded by amending Freudenthal's formal description to include the ultrastructural data. Taylor agreed with their conclusions and later identified the dinoflagellates from several species of Tridacnidae as *S. microadriaticum* (Taylor, 1969). In 1987, Trench and Blank published the most recently amended formal description of the genus *Symbio-*

Received 27 September 1999; accepted 18 April 2000.

[*] To whom correspondence should be addressed.

dinium, and described three new species in the genus. For the most part, all four of these papers describe similar ultrastructural features. This is not surprising considering that both Kevin and Trench describe *S. microadriaticum* from its definitive host *Cassiopeia*, and that all four used a standard chemical fixation that included buffered glutaraldehyde and osmium followed by a dehydration series in preparing their tissues for the transmission electron microscope.

In the following paper, we further amend the ultrastructural description of the genus *Symbiodinium* on the basis of the use of freeze-substitution, an alternative fixation technique that provides better preservation of fine structure. The symbionts from three hosts were examined: two anthozoans—*Aiptasia pallida* (*S. bermudense*) and *Phyllactis flosculifera* (*Symbiodinium* sp.)—and the definitive scyphozoan host *Cassiopeia xamachana* (*S. microadriaticum*). This has resulted in a more clearly resolved ultrastructure revealing previously undescribed features in the *in situ* symbionts. These results suggest an alternative hypothesis for the origin of the multilayered "periplast" or "symbiosome membrane" that is prevalent around the dinoflagellate symbionts found in invertebrate hosts.

Materials and Methods

Animal collection and care

Specimens of *Cassiopea xamachana*, *Aiptasia pallida*, and a second anthozoan species identified as *Phyllactis flosculifera* (Fautin, University of Kansas, pers. comm.) were collected in the Florida Keys and transported to Auburn University, Alabama. These species were maintained in established 150-gallon aquaria filtered with both undergravel and external trickle filtration. Artificial seawater was prepared with Reef Crystals (Aquarium Systems) and deionized water at about 30 ppt. The aquaria were maintained at 25°–30° C on a 12/12 h light/dark cycle, and the animals were fed with newly hatched brine shrimp nauplii every other day.

Fixation and embedding

Anthozoan procedure. Individual specimens of *A. pallida* and *P. flosculifera* were transferred to small glass bowls containing 0.45-μm Millipore-filtered artificial seawater (MFAS) and were allowed to acclimate, attach to the glass substratum, and fully expand. Small pieces of tentacle ($<$10 mm in length, but very thin) were excised from individuals of both species and suspended from small lengths of platinum wire. The tissues were then plunge-frozen in liquid propane (Menco, 1986) and transferred to liquid nitrogen. The frozen tissues were transferred to glass vials containing a 2% osmium tetroxide-acetone solution that had been previously cooled to -80° C. The vials were held within a precooled, methanol-saturated sponge, and the tissue samples were left at -80° C for 48–72 h before being transferred to -20° C. Specimens remained at -20° C for 12–24 h and were then moved to 4° C for an additional 12–24 h before being returned to room temperature. While the specimens were being transferred from -80° C to room temperature, a gradual warming was achieved by moving the entire methanol-saturated sponge containing the vials from one environment to another. After reaching room temperature, the tissue samples were removed, and the platinum wire was discarded. Tissues were washed in 100% acetone and were either transferred to 100% propylene oxide before infiltration, or were immediately infiltrated and embedded in Poly-Bed 812 plastic.

Scyphozoan procedure. Several attempts were made to fix *Cassiopeia xamachana* symbionts *in situ* using the procedure described above, but all resulted in very poor fixation. We speculate that the copious amounts of mucus produced by the scyphozoan tissue acted as an insulator against the rapid freezing of the tissue. Thus the following, more successful, procedure was used. Six large specimens of *C. xamachana* were transferred to a large bowl of MFAS. The oral arms of each specimen were excised and discarded. With a glass slide, the external symbiotic layer of tissue from the oral side of the specimen's bell was scraped free from the underlying mesoglea and collected. The remaining mesoglea and aboral ectoderm was discarded. The collected symbiotic tissues were homogenized in MFAS using a Virtis Handishear tissue homogenizer. The tissue homogenate was centrifuged at $\sim$250 $\times$ g for 3 min to pellet the separated symbiosomes, and the supernatant was discarded. Small ($\sim$1 mm^2) samples of the pelleted symbiosomes were placed on thin strips of filter paper and then immediately plunge-frozen, fixed, and embedded in the manner described above for the anthozoan tissue.

Standard fixation and embedding. As a control for the ultra-rapid freezing and freeze-substitution fixation process, a standard aldehyde-osmium fixation at room temperature was performed on each of the three symbiotic cnidarian tissues. Briefly, small pieces ($<$10 mm in length) of tentacle from symbiotic *A. pallida* and *P. flosculifera*, as well as small portions ($<$10 mm^2) of the bell margin from *C. xamachana*, were removed from living specimens and immersed in 2.5% glutaraldehyde in 20 m*M* Millonigs phosphate buffered saline (MPBS), pH 7.6. The tissue was allowed to fix for 1 h, rinsed twice for 5 min in 20 m*M* MPBS, and then postfixed in 2% OsO_4 in 1.25% $NaHCO_3$ for 1 h. Residual OsO_4 was rinsed away in two 5-min rinses of 1.25% $NaHCO_3$. Tissues were then dehydrated in an ethanol series (30%, 50%, 70%, 85%, 90%, 95%, 3 $\times$ 100%), followed by three rinses in propylene oxide (10 min in each solution), all at room temperature. Tissues were then infiltrated and embedded in Poly-Bed 812 plastic in the same manner as the freeze-substituted tissues.

Sectioning and staining

Ultrathin sections of each kind of tissue were cut with a Reichert-Jung Ultracut E ultramicrotome and collected on Formvar-coated slot grids. Ultrathin sections were stained with lead citrate and uranyl acetate and were examined on a Zeiss EM-10 transmission electron microscope (TEM).

Measurements

Cell wall layers and thecal vesicles were measured directly from TEM negatives with a hand lens, light box, and metric ruler. A total of 100 thecal vesicles were measured for both *Symbiodinium bermudense* (*Aiptasia pallida*) and *Symbiodinium* sp. (*Phyllactis flosculifera*). In those symbionts that contained more than 10 vesicles, only 10 were measured. Other symbionts did not contain 10 clearly defined vesicles; thus a total of 15 *S. bermudense* and 13 *Symbiodinium* sp. were used to obtain the 100 total vesicles measured.

Even using the alternative method, thecal vesicle preservation for *S. microadriaticum* from *Cassiopeia xamachana* was still inferior to that of the symbionts from the other hosts. In this species, only those thecal vesicles that could be clearly identified were measured, resulting in a lower "*n*" value from 26 cells for the vesicles measured in *S. microadriaticum*. Cell wall layers (*S. bermudense*) and total cell wall thickness (all symbiont species) were measured as described above. Conversions from millimeters to micrometers or nanometers were made using a published nomogram (Ghadially *et al.*, 1981).

Results

Many aspects of the ultrastructure of freeze-substituted *in situ* symbionts show good correspondence with previously published descriptions of the genus *Symbiodinium* (Taylor, 1968, 1969; Kevin *et al.*, 1969; Trench and Blank, 1987). The multi-lobed chloroplast is peripherally located, with parallel rows of thylakoids usually arranged in groups of three. A single, stalked pyrenoid may be seen emerging from the chloroplast. Its membrane appears to be continuous with the chloroplast envelope with no invading thylakoids, and a relatively thick starch coat surrounds the entire structure. A single large, irregularly shaped, granular accumulation body is present in many cells. Typical dictyosomes and mitochondria also occur, as do many lipid vacuoles and some calcium oxalate crystals. Large, well-preserved "fibrous bodies" are present in many of the symbionts (Dodge, 1967). The nucleus of the symbionts is distinct and recognizable, but the compact spirals of chromatin typically seen in the mesokaryotic nucleus are not always visible.

The freeze-substitution process did, however, reveal some previously undescribed features of the *in situ* symbionts, as well as differences among *Symbiodinium* species. The "amorphous layer" of the periplast described by Kevin *et al.* (1969) has been correctly identified as the continuous, vegetative cell wall of the symbiont (Trench and Blank, 1987). However, our results (Fig. 1) indicate that in *Symbiodinium bermudense* this structure is in fact composed of three distinct layers: an outer layer that appears to be membranous (OL), an electron-dense middle layer (EDL), and a less dense inner layer (IL). As can be seen in Table 1, the greatest variation in layer width was seen in the IL, which ranged from 30 to 300 nm. This variation is evident in nonmitotic cells (Fig. 2), but it is most common in recently divided cells, where the OL and EDL retain similar thickness circumferentially around the divided cells, while the IL

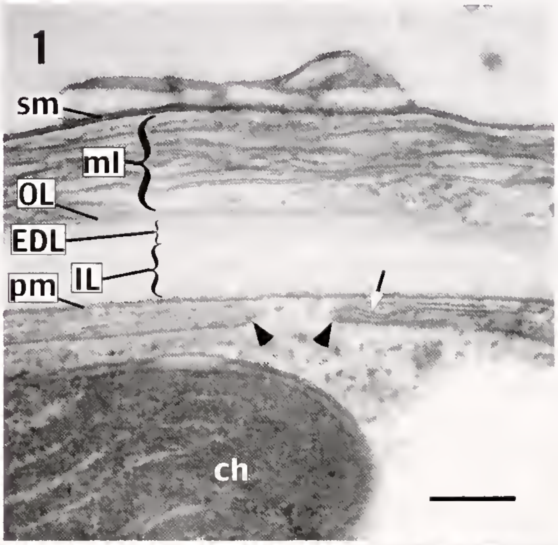

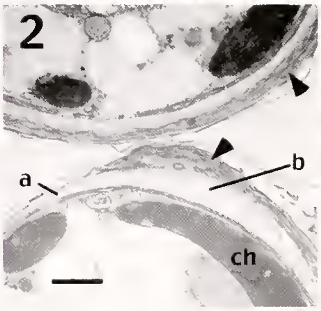

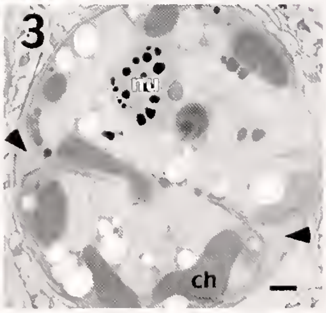

Figure 1. *Symbiodinium bermudense* within the host *Aiptasia pallida*. The cell wall of the symbiont shows three distinct regions beneath the multiple layers of membranous material that surround it. ch = chloroplast; EDL = electron dense cell wall layer; IL = inner cell wall layer; ml = multiple layers of symbiosome membrane; OL = membranous outer layer; pm = algal cell plasma membrane; sm = outer symbiosome membrane; arrow = thecal plate; arrowheads indicate thecal vesicles. Scale bar = 100 nm.

Figure 2. *Symbiodinium bermudense* within host *Aiptasia pallida*. Note the difference in thickness of the cell wall inner layer between points a and b; ch = chloroplast; arrowheads indicate accumulations of symbiosome membrane outside of vegetative cell wall. Scale bar = 500 nm.

Figure 3. Dividing *Symbiodinium bermudense* within *Aiptasia pallida*. ch = chloroplast; nu = nucleus; arrowheads indicate areas of thickening of inner layer of the cell wall along the division furrow. Scale bar = 1 μm.

Table 1

Cell wall layer thickness, total cell wall thickness, and thecal vesicle thickness (all measurements in nanometers, mean ± std. dev.)

Symbiont species	IL	EDL	OL	Total thickness (*n*)	Thecal vesicle thickness (*n*)
Symbiodinium sp.	—	—	—	137.8 ± 65.5 (100)	34.3 ± 7.8 (100)
S. microadriaticum	—	—	—	108.4 ± 37.7 (100)	38.8 ± 7.3 (50)
S. bermudense	96.7 ± 48.4	40.4 ± 7.7	10.6 ± 1.4	147.7 ± 49.9 (100)	34.9 ± 8.5 (100)

EDL = electron dense layer, IL = inner layer, OL = outer layer; — indicates no visible layers.

becomes increasingly thicker in the region of the division furrow (Fig. 3). *Symbiodinium* sp. from *P. flosculifera* and *S. microadriaticum* lacked this three-layered structure, the entire cell wall being similar in consistency to the IL layer of *S. bermudense*.

A typical multilayered symbiosome membrane could be seen around the symbionts of all three host animals, but was most prevalent around *S. bermudense* (Figs. 1, 2, 4). The membranes that completely surrounded most symbionts seemed to be distributed evenly, but in some cases a disproportionate number of membranes were located to one side of the symbiont (Figs. 2, 4).

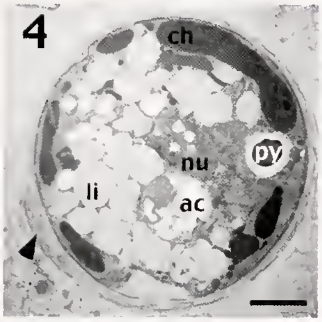

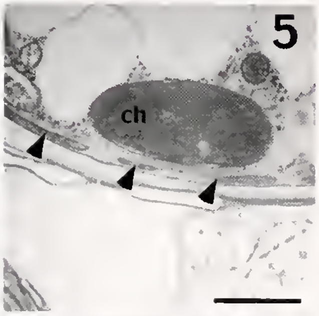

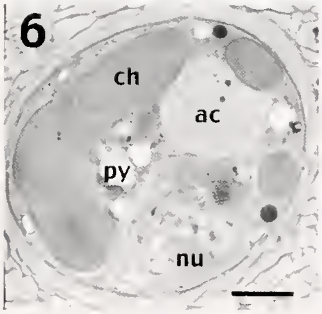

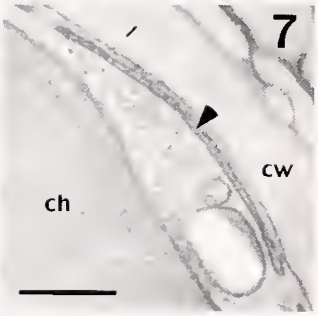

Figure 4. *Symbiodinium bermudense* within *Aiptasia pallida*. ac = accumulation body; ch = chloroplast; li = lipid vacuole; nu = nucleus; py = pyrenoid; arrowhead indicates large number of membranes on only one side of symbiont. Scale bar = 2 μm.

Figure 5. Thecal vesicles in *Symbiodinium bermudense*. ch = chloroplast; arrowheads indicate individual thecal vesicles. Scale bar = 500 nm.

Figure 6. *Symbiodinium* sp. within the host *Phylactis flosculifera*. ac = accumulation body; ch = chloroplast; nu = nucleus; py = pyrenoid. Scale bar = 1 μm.

Figure 7. Thecal vesicle in *Symbiodinium* sp. from *Phylactis flosculifera*. ch = chloroplast; cw = cell wall; arrow = algal cell plasma membrane; arrowhead = thecal vesicle. Scale bar = 300 nm.

Just inside of the cell wall is the continuous cell membrane. Below this cell membrane, the freeze-substitution process has revealed distinct thecal vesicles. These vesicles are most prominent in *Symbiodinium bermudense* (Figs. 4, 5) and the *Symbiodinium* sp. (Figs. 6, 7), but they are also present in *S. microadriaticum* (Figs. 8, 9). In TEM sections, each vesicle is membrane bound and has rounded edges at

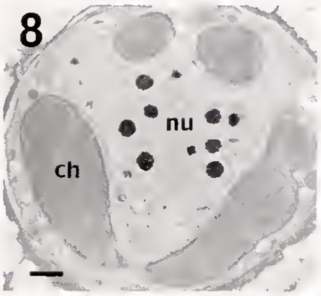

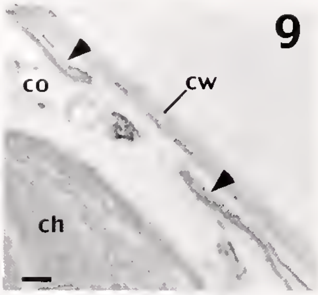

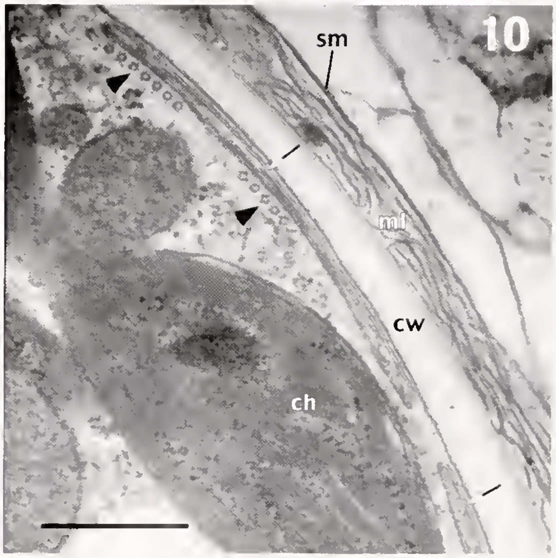

Figure 8. *Symbiodinium microadriaticum* from the host *Cassiopeia xamachana*. ch = chloroplast; nu = nucleus. Scale bar = 500 nm.

Figure 9. Thecal vesicles in *Symbiodinium microadriaticum*. ch = chloroplast; co = calcium oxalate crystal; cw = cell wall; arrowheads indicate thecal vesicles. Scale bar = 100 nm.

Figure 10. *Symbiodinium bermudense* within host *Aiptasia pallida*. ch = chloroplast; cw = cell wall; ml = multiple layers of symbiosome membrane; sm = outer symbiosome membrane; arrows identify thecal vesicles; arrowheads indicate linear array of microtubules beneath thecal vesicles. Scale bar = 300 nm.

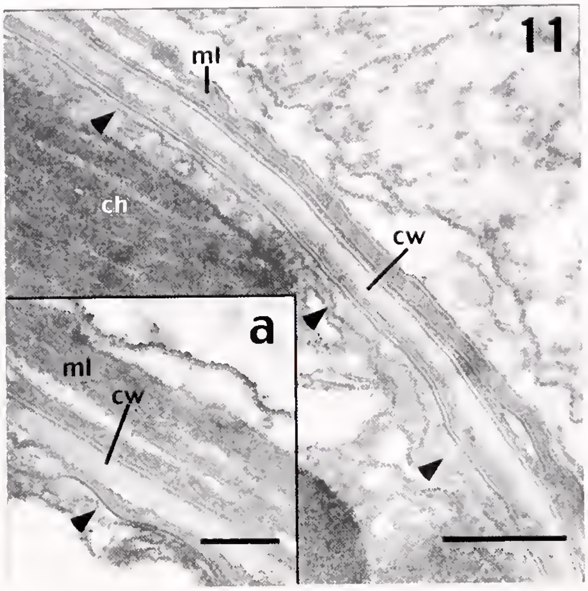

Figure 11. *Symbiodinium bermudense* within host *Aiptasia pallida*. Standard glutaraldehyde-osmium tissue fixation. Note scrolled membrane in region where thecal vesicles should be (arrowheads). ch = chloroplast; cw = cell wall; ml = multiple layers of symbiosome membrane; arrowheads identify area where thecal vesicles should be located. Scale bar = 200 nm. Inset (a) is a higher magnification of an additional symbiont showing layered membranes internal to the cell wall. Scale bar = 100 nm.

each end, with a distinct cytoplasmic separation between adjacent vesicles. Internal thecal plates were apparent within some vesicles of *S. bermudense* (Fig. 1, arrow). The enclosed thecal plate lies separate from the vesicle membrane. The overall thickness of the vesicles for each species is reported in Table 1. Since serial sections of an entire cell were not cut, we could not determine whether the differing widths of the vesicles reflect differences among species, large and small vesicles, or different vesicle profiles. In several micrographs, a linear array of microtubules was present underlying the vesicles (Fig. 10).

Standard aldehyde-osmium fixed tissues of all three species of symbiont failed to show many of the fine structures seen in the freeze-substituted tissue. The multiple-layered symbiosome membrane was apparent; but only the OL and the IL of the cell wall were seen in *S. bermudense*, and all three species failed to show any thecal vesicles or plates. Instead, there appeared to be several layers of membrane beneath the vegetative cell wall (*e.g.*, Fig. 11, 11a).

Discussion

A multiple-layered cell wall in *Symbiodinium bermudense* has been previously described by Palincsar *et al.* (1988; they identified the symbiont of *Aiptasia pallida* as *S. microadriaticum* at that time; however, the species has subsequently been redescribed as *S. bermudense* [see Trench, 1993]). The description by Palincsar *et al.* (1988) included four layers. From the inside out, the layers were described as a vesicular layer immediately outside the symbiont's plasma membrane; a thick homogeneous finely granular layer; and a "line-thin" dark layer, overlaid by an even thinner membranous layer. They also reported a wide variation in cell wall structure, with some cells displaying an almost entirely homogeneous, finely granular wall and others an almost entirely vesicular wall. The presence of multiple-layered cell walls is not surprising since similar cell wall features have been identified in other dinoflagellate species (Morrill and Loeblich, 1981). Bricheux *et al.* (1992) identified a four-layered pellicle in the free-living dinoflagellate *Glenodinium foliaceum*. The two layers immediately outside of the cell membrane (identified as the homogeneous layer and the dense layer) strongly resemble the IL and the EDL we see in species of *Symbiodinium*. The homogeneous layer in both *G. foliaceum* and *Peridinium balticum*, a symbiont-containing dinoflagellate, has been experimentally shown to contain cellulose (Morrill and Loeblich, 1981; Loeblich, 1984). However, the cellulose in this layer was assumed to be in an amorphous or low crystalline state, since no cellulose fibers have been identified with the electron microscope. On the other hand, the dense layer of *Heterocapsa niei* and other dinoflagellates has been suggested to contain sporopollenin, a very resistant plant terpenoid that has been demonstrated to be insoluble, even in hot ethanolamine (Loeblich, 1970; Morrill and Loeblich, 1981). Although the exact chemical nature of the cell wall of *Symbiodinium* is unknown, Markell *et al.* (1992) reported that the cell walls of *S. microadriaticum*, *S. kawagutii*, and *S. pilosum* did contain cellulose, an observation based on cellulase digestion of isolated cell walls. They also reported that in intact symbionts, either living or glutaraldehyde fixed, cellulase was ineffective in digesting the cell wall. If a part of *Symbiodinium*'s cell wall, such as the EDL, is composed of an extremely insoluble component, such as sporopollenin, the IL may have been unaffected by the cellulase simply because the enzyme could not penetrate to this layer in intact cells.

The current formal description of the genus *Symbiodinium* (Trench and Blank, 1987) states that the cell wall of the coccoid stage varies in thickness. It also states that this variation depends on the life history of the cell. This fact is supported by Bricheux *et al.* (1992), who found that the thickness of the cell wall of the free-living dinoflagellate *G. foliaceum* was relatively thin following ecdysis of the thecal armor; however, as the vegetative stage of the life history progressed, the cell wall became progressively thicker, with the largest amount of change seen in the inner homogeneous layer (IL). Similarly, our study has shown that, although the OL and EDL certainly contribute to the overall thickness of the cell wall, the thickness of the IL has the most variation.

The presence of the thecal vesicles within the symbionts is not in itself surprising, since Loeblich and Sherley (1979) described the thecate nature of the motile stage of *S. microadriaticum;* but this is the first report that thecal vesicles are present within *in situ* coccoid symbionts. The formal description of the genus *Symbiodinium* describes the coccoid symbionts as having a "continuous cell wall . . . underlain by a series of membranes" (Trench and Blank, 1987). We found no such membranes in our ultrastructural investigations of freeze-substituted symbionts, but instead found distinct thecal vesicles in this region. We did see apparent membranes like those described by Trench and Blank (1987) when the tissues were fixed with standard aldehyde-osmium fixations. Since thecal vesicles are well described in other dinoflagellate species (Dodge and Crawford, 1970; Bricheux *et al.*, 1992; Hohfeld and Melkonian, 1992), have been reported in *in vitro* cultured *Symbiodinium* (Taylor, 1971b; Loeblich and Sherley, 1979; Trench and Blank, 1987), and are not artifactual in nature, we conclude that the multiple membranes reported in the formal *in situ* description of the genus *Symbiodinium* (Trench and Blank, 1987) were the result of a fixation artifact.

Although this is the first report identifying the presence of thecal vesicles within the *in situ* coccoid symbionts, review of the ultrastructural literature relating to the genus *Symbiodinium* reveals apparent thecal vesicles in the figures from various published papers. In Taylor's (1968) original paper on symbiont ultrastructure, figure 3 clearly shows what appear to be thecal vesicles beneath the cell wall of the coccoid stage. However, Taylor states that the vesicles are formed in older symbionts as two of the multiple membrane layers undergo a series of infoldings to form these isolated and discrete vesicles, and he does not associate them with the thecal covering of the motile stage. Kevin *et al.* (1969) show, in their figure 5, an *in situ* symbiont that clearly has thecal vesicles beneath the plasma membrane; however, these structures are neither identified nor mentioned in the text. In 1970, Dodge and Crawford reported that two membranes, "the outer of which appear to be folded over in places," surrounded the cytoplasm of the symbionts from *Anemonia sulcata*. Their plate 7 also shows distinct thecal vesicles inside the cell wall (Dodge and Crawford, 1970). A paper by Tripodi and Santisi (1982) describes the ultrastructure of *S. microadriaticum* within the octocoral *Eunicella stricta*. In their figures 4, 5, and 6, the electron micrographs show distinct thecal vesicles beneath and adjacent to the cell membrane of the *in situ* symbionts. Their figure 8, a line drawing describing the cell covering of the symbionts, also clearly shows distinct thecal vesicles. However, the figure captions, as well as the text, describe these vesicles as profiles of the endoplasmic reticulum and once again do not associate them with the thecate motile stage.

In all of these reports, the symbiotic tissues underwent standard fixation in 3%–4% glutaraldehyde followed by post-fixation in 1%–2% osmium tetroxide. Therefore, the thecal vesicles can be visualized within the *in situ* symbionts using this type of fixation; but the results in these papers are the exception rather than the rule. It would appear that, during a standard chemical fixation, if conditions are not right (osmolality, temperature, length of fixation, age of fixative, *etc.*), the fragile thecal vesicles rupture and combine with the plasma membrane to take on the appearance of multiple or scrolled layers of membrane beneath the cell wall. Our results suggest that a more reliable way of visualizing this fine structure is by use of the freeze-substitution process.

The presence of thecal vesicles beneath the plasma membrane of the *in situ* symbionts lends further credence to an interesting hypothesis. In 1971, Taylor reported the development of flagellar structures in the *in situ* symbionts of the cnidarian *Velella velella* (pl. IIIA) and the flatworm *Amphiscolops langerhansi* (pl. IIIB). In 1980, Schoenberg and Trench also reported the presence of flagellar structures in *in situ Symbiodinium microadriaticum* from *Protopalythoa* sp. (figure 8, plate 5). They state that the sporadic appearance of these flagellar structures could represent the transient production of motile zoospores *in situ*.

The production of motile gymnodinioid zoospores is a daily occurrence in log-phase cultures of *Symbiodinium in vitro*. Within the cell wall of the vegetative mother cell, a metamorphosis occurs that results in the development of a characteristically gymnodinioid motile cell with thecae, hypocone, epicone, and longitudinal and transverse flagellae in their respective grooves or furrows (Freudenthal, 1962; Loeblich and Sherley, 1979). Motile stages often develop after the cell has divided into daughter cells, but they can also develop without any previous cell division (Schoenberg and Trench, 1980). When mature, the zoospores escape from the mother cell by some unknown mechanism to swim freely within the culture medium (Trench and Blank, 1987). After a relatively short motile stage the cells spontaneously undergo ecdysis, a process by which they shed their thecae and flagella, again by some unknown mechanism, and settle to the substratum, where they enter the longer vegetative phase of their life cycle.

The mitotic rate of *in situ* symbionts is decreased in comparison to cultured symbionts. Fitt and Trench (1983) determined that, within cultures of *Symbiodinium microadriaticum*, as many as 25% of the cells could be dividing, but Palincsar *et al.* (1988) determined the mitotic rate of *S. bermudense* within *A. pallida* to be as low as 1.2%. Although the mitotic rate *in situ* is decreased, it is not halted. We hypothesize that a similar sort of delay occurs in the ecdysis cycle and that, on a slower and perhaps irregular schedule, ecdysis continues *in situ*. This would explain the discrepancies between our cell wall description and that of Palincsar *et al.* (1988). The variations in cell wall structure that they describe (totally granular, to half granular/half vesicular, to almost completely vesicular) could be explained by symbionts caught in varying stages of the ecdysis. Similarly, such a cycle would also result in the sporadic appearance of flagella, as reported in some *in situ* symbionts (Taylor, 1971a, b; Schoenberg and Trench, 1980), and the presence of thecal vesicles, as reported in this paper.

We also suggest that the delayed ecdysis cycle could be responsible for the multiple layers of apparent membranes that are often found just outside of the vegetative cell wall of *in situ* symbionts. Unlike those of cultured symbionts, the shed thecal plates and outer plasma membrane of *in situ* symbionts would not be discarded but would accumulate inside of the symbiosome membrane (Fig. 12). Such shed plates would appear as the accumulations of the apparent membranous material (ml) that has been observed between the outer symbiosome membrane and the vegetative cell wall of the symbionts (Taylor, 1968; Kevin *et al.*, 1969; Schoenberg and Trench, 1980; Tripodi and Santisi, 1982; Colley and Trench, 1983; Blank, 1987; Trench and Blank, 1987; Trench and Winsor, 1987; Palincsar *et al.*, 1988; Rands *et al.*, 1993).

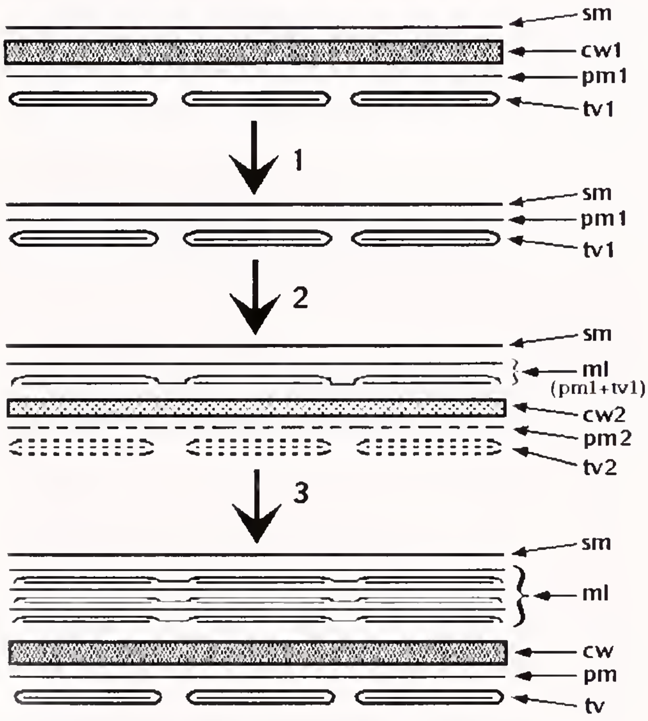

Figure 12. A hypothesis for how multiple layers of membrane could accumulate within symbiosome membrane: step 1. Vegetative cell gives rise to motile "thecate" cell; cell wall disappears. step 2. Motile cell undergoes ecdysis and sheds plasma membrane and thecal vesicles as the cell wall is reformed and new thecal vesicles form beneath it. step 3. After several cycles, accumulated material from algal plasma membrane and thecal vesicles appear as multiple membranes between the outer symbiosome membrane and the vegetative algal cell wall. cw = cell wall; ml = multiple layers of membrane; pm = symbiont plasma membrane; sm = surface of symbiosome membrane; tv = thecal vesicles. (Figure adapted from Hohfeld and Melkonian, 1992.)

These accumulations of apparently membranous material were first described by Taylor (1968), who ascribed their origin to both the algal cell and the host, but gave no specific structures from which they might arise. Later, Kevin *et al.* (1969) redefined the location of the membranes surrounding the algal cell, but once again failed to clearly state their origin. This uncertainty as to the origin of these membranes has continued throughout the literature, with some authors attributing it to the host (Tripodi and Santisi, 1982; Colley and Trench, 1983; Palincsar *et al.*, 1988; Rands *et al.*, 1993), and others to the algal cell (Schoenberg and Trench, 1980; Trench and Blank, 1987). Specifically, Trench and Blank (1987) reported that the outer layer of the cell wall is periodically "sloughed off" the surface and often produces a "scroll-like" appearance in sections. However, they do not offer any evidence to support this process as the origin of the multiple membranous layers, nor do they offer any suggestions about how this sloughed layer might be regenerated outside of the continuous cell wall. Our hypothesis of a continuing *in situ* ecdysis cycle as the origin of the apparent membranes (see Fig. 12) is based on the presence of symbiont thecal vesicles *in situ*, and on a known event within the life cycle of the symbiont. As such, it does not require the proposal of another "unknown mechanism" to explain how additional membranes would be added to those already present around the symbiont.

There is another question that must be addressed if our hypothesis is correct. If a delayed ecdysis cycle is continuing within the host cell symbiosome, then in addition to the shedding of the theca and plasma membrane, there must also be a shedding of the cell wall. If the thecal vesicles are retained within the host membrane, what happens to the cell wall material? Although this is a valid question, it is not unique to our hypothesis. The same question can be asked of mitotically active, vegetative cells *in situ*.

It has been assumed that, at the conclusion of a mitotic event, the symbiont daughter cells within the same symbiosome membrane are separated by invading extensions of symbiosome membrane and host cytoplasm (Reisser, 1992). Following division, each new daughter cell produces a new cell wall within the old cell wall of the parent cell (Taylor, 1968; Kevin *et al.*, 1969) Thus, if the "old" cell wall were not degraded in some way, each host symbiosome would contain remnants of cell wall material from previous mitotic events. Because such remnants have not been observed, the old cell wall material must be degraded, perhaps by enzymes released from the symbiont itself. As was mentioned previously, the release of motile zoospores from within the parent cell wall is controlled by an unknown mechanism, presumably enzymatic in nature. Perhaps this same mechanism is responsible for the degradation of the cell wall within the host symbiosome during the mitotic event, with the outer symbiosome membrane retaining active enzymes in the vicinity of the discarded cell wall. In the case of a retarded ecdysis cycle, if the thecal plates differ in composition from the cell wall and thus are not subject to similar enzymatic breakdown, they could accumulate as the multiple layers of membranous material found between the symbiosome membrane and symbiont cell wall *in situ*.

These membranes contribute to the membranous structure of the symbiosome and are part of the boundary between host and symbiont. All "communication" between host and symbiont, transport of gasses, and translocation of photosynthetically fixed carbon must occur through, and in conjunction with, these membranes (Rands *et al.*, 1993). Thus their origin and their role in these events is of great importance.

Acknowledgments

We thank Dr. Daphne Fautin for her aid in identifying the anthozoan species *Phyllactis flosculifera*. We also thank Dr. William Fitt and the Key Largo Marine Research Laboratory, Dr. Mike Miller and the Auburn University Biological Electron Microscope Imaging Facility, and the University of Georgia's Center for Advanced Ultrastructural Research for their assistance in this research. This work was supported by NSF #9018698 (SCK), NSF-BIR #9220230 (SCK), ONR #3231114 (SCK), and a grant from the Alabama Agricultural Experiment Station (SCK) Journal # 6-996072.

Literature Cited

Alldredge, A. L., and B. M. Jones. 1973. *Hastigerina pelagica*: foraminiferal habitat for planktonic dinoflagellates. *Mar. Biol.* **22:** 131–135.

Anderson, O. R., and A. W. H. Be. 1976. The ultrastructure of a planktonic foraminifer, *Globigerinoides sacculifer* (Brady), and its symbiotic dinoflagellates. *J. Foram. Res.* **6:** 1–9.

Banaszak, A. T., R. Iglesias-Prieto, and R. K. Trench. 1993. *Scrippsiella velellae* sp. nov. (Peridinales) and *Gloeodinium viscum* sp. nov. (Phytodiniales), dinoflagellate symbionts of two hydrozoans (Cnidaria). *J. Phycol.* **29:** 517–528.

Blank, R.J. 1987. Cell architecture of the dinoflagellate *Symbiodinium* sp. inhabiting the Hawaiian stony coral *Montipora verrucosa*. *Mar. Biol.* **94:** 143–155.

Brandt, K. 1881. Über das Zusammenleben von Thieren und Algen. *Verh. Physiologischen Ges. Berlin.* **1881–1882:** 22–26.

Bricheux, G., D. G. Mahoney, and S. P. Gibbs. 1992. Development of the pellicle and thecal plates following ecdysis in the dinoflagellate *Glenodinium foliaceum*. *Protoplasma* **168:** 159–171.

Colley, N. J., and R. K. Trench. 1983. Selectivity in phagocytosis and persistence of symbiotic algae by the scyphistoma stage of the jellyfish *Cassiopeia xamachana*. *Proc. R. Soc. Lond. B.* **219:** 61–82.

Dodge, J. D. 1967. Fine structure of the dinoflagellate *Aureodinium pigmentosum* gen. et sp. nov. *Br. Phycol. Bull.* **3:** 327–336.

Dodge, J. D., and R. M. Crawford. 1970. A survey of thecal fine structure in the Dinophyceae. *Bot. J. Linn. Soc.* **63:** 53–67.

Fitt, W. K., and R. K. Trench. 1983. The relation of diel patterns of cell division to diel patterns of motility in the symbiotic dinoflagellate *Symbiodinium microadriaticum* Freudenthal in culture. *New Phytol.* **94:** 421–432.

Freudenthal, H. D. 1962. *Symbiodinium* gen. nov. and *Symbiodinium microadriaticum* sp. nov., a zooxanthella: taxonomy, life cycle, and morphology. *J. Protozool.* **9:** 45–52.

Ghadially, F. N., P. Jackson, and J. Junor. 1981. A nomogram for electron microscopists. *J. Submicrosc. Cytol.* **13:** 95–96.

Hohfeld, I., and M. Melkonian. 1992. Amphiesmal ultrastructure of dinoflagellates: a reevaluation of pellicle formation. *J. Phycol.* **28:** 82–89.

Kevin, M. J., W. T. Hall, J. J. A. McLaughlin, and P. A. Zahl. 1969. *Symbiodinium microadriaticum* Freudenthal, a revised taxonomic description, ultrastructure. *J. Phycol.* **5:** 341–350.

Loeblich, A. R. I. 1970. The amphiesma or dinoflagellate cell covering. Pp. 867–929 in *Proceedings of the North American Paleontological Convention*, E. L. Yochelson, ed. Allen Press, Chicago.

Loeblich, A. R. I. 1984. Dinoflagellate physiology and biochemistry. Pp. 299–342 in *Dinoflagellates*, D. L. Spector, ed. Academic Press, New York.

Loeblich, A. R. I., and J. L. Sherley. 1979. Observations on the theca of the motile phase of free-living and symbiotic isolates of *Zooxanthella microadriatica* (Freudenthal) comb. nov. *J. Mar. Biol. Assoc. UK* **59:** 195–205.

Markell, D. A, R. K. Trench, and R. Iglesias-Prieto. 1992. Macromolecules associated with the cell walls of symbiotic dinoflagellates. *Symbiosis* **12:** 19–31.

Menco, B. P. M. 1986. A survey of ultra-rapid cryofixation methods with particular emphasis on applications to freeze-fracturing, freeze-etching, and freeze-substitution. *J. Electron Microsc. Tech.* **4:** 177–240.

Morrill, L. C., and A. R. I. Loeblich. 1981. The dinoflagellate pellicular wall layer and its occurrence in the division Pyrrhophyta. *J. Phycol.* **17:** 315–323.

Palincsar, J. S., W. R. Jones, and E. E. Palincsar. 1988. Effects of isolation of the endosymbiont *Symbiodinium microadriaticum* (Dinophyceae) from its host *Aiptasia pallida* (Anthozoa) on cell wall ultrastructure and mitotic rates. *Trans. Am. Microsc. Soc.* **107:** 53–66.

Rands, M. L., B. C. Loughman, and A. E. Douglas. 1993. The symbiotic interface in an alga-invertebrate symbiosis. *Proc. R. Soc. Lond. B.* **253:** 161–165.

Reisser, W. 1992. Basic mechanisms of signal exchange, recognition, specificity, and regulation in endosymbiotic systems. Pp. 657–674 in *Algae and Symbioses*, W. Reisser, ed. Biopress, Bristol, England.

Rowan, R. 1998. Diversity and ecology of zooxanthellae on coral reefs. *J. Phycol.* **34:** 407–417.

Schoenberg, D. A., and R. K. Trench. 1980. Genetic variation in *Symbiodinium* (=*Gymnodinium*) *microadriaticum* Freudenthal, and specificity in its symbiosis with marine invertebrates. II Morphological variation in *Symbiodinium microadriaticum*. *Proc. R. Soc. Lond B.* **207:** 429–444.

Spero, H. J. 1987. Symbiosis in the planktonic foraminifera, *Obulina universa*, and the isolation of its symbiotic dinoflagellate *Gymnodinium beii* sp. nov. *J. Phycol.* **23:** 307–317.

Spindler, M., and C. Hemleben. 1980. Symbionts in planktonic foraminifera (Protozoa). Pp. 133–140 in *Endocytobiology, Endosymbiosis, and Cell Biology*, W. Schwemmler and H. E. A. Schenk, eds. Walter de Gruyter, Berlin.

Taylor, D. L. 1968. *In situ* studies on the cytochemistry and ultrastructure of a symbiotic marine dinoflagellate. *J. Mar. Biol. Assoc. UK* **48:** 349–366.

Taylor, D. L. 1969. Identity of zooxanthellae isolated from some Pacific Tridacnidae. *J. Phycol.* **5:** 336–340.

Taylor, D. L. 1971a. Ultrastructure of the 'zooxanthella' *Endodinium chattonii in situ. J. Mar. Biol. Assoc. UK* **51:** 227–234.

Taylor, D. L. 1971b. On the symbiosis between *Amphidinium klebsii* (Dinophyceae) and *Amphiscolops langerhansi* (Turbellaria: Acoela). *J. Mar. Biol. Assoc. UK* **51:** 301–313.

Trench, R. K. 1993. Microalgal-invertebrate symbioses: a review. *Endocytobiosis & Cell Res.* **9:** 135–175

Trench, R. K., and R. J. Blank. 1987. *Symbiodinium microadriaticum* Freudenthal, *S. goreauii*, sp. nov., *S. kawagutii*, sp. nov., and *S. pilosum*, sp. nov.: gymnodinioid dinoflagellate symbionts of marine invertebrates. *J. Phycol.* **23:** 469–481.

Trench, R. K., and H. Winsor. 1987. Symbiosis with dinoflagellates in two pelagic flat worms *Amphiscolops* sp. and *Haplodiscus* sp. *Symbiosis* **3:** 1–22.

Tripodi, G., and S. Santisi. 1982. A study on the cell covering of *Symbiodinium*, a symbiote of the octocoral *Eunicella. J. Submicrosc. Cytol.* **14:** 613–620.

Yamasu, T. 1988. Symbiosis of marine animals and algae. *Genetics* **42:** 12–20.

Reference: *Biol. Bull.* **199:** 85–94. (August 2000)

Overgrowth Competition Between Clades: Implications for Interpretation of the Fossil Record and Overgrowth Indices

DAVID K. A. BARNES[1,*] AND MATHEW H. DICK[2]

[1] *Department of Zoology and Animal Ecology, University College Cork, Cork, Ireland; and*
[2] *Department of Biology, Middlebury College, Middlebury, Vermont 05753*

Abstract. Overgrowth interactions (2693 in total) were observed among three major groups (arguably clades) of bryozoans—cheilostomatids (57 species), ctenostomatids (3 species), and cyclostomatids (14 species). The bryozoans studied here occur in shallow water at high-temperate polar latitudes where they encrust hard substrata such as rock piles. The main study site was the intertidal and infralittoral zones of Kodiak Island, Alaska, but observations were also made in similar zones of South Georgia Island and the Falkland Islands in the South Atlantic Ocean. Cheilostomatids dominated the number of species, individuals, and interactions at all depths. Intraclade interactions formed 73.7% of the encounters for cheilostomatids, 1.6% for ctenostomatids, and 5.7% for cyclostomatids. The competitive ranking of the three clades was broadly ctenostomatids > cyclostomatids > cheilostomatids. Significantly, these results contradict all previous quantitative studies of bryozoan overgrowth, in which cheilostomatids are reported to overgrow cyclostomatids at a higher rate. From these studies and the literature, we calculated win indices to vary from 0 to 0.42 for living cyclostomatids, from 0.08 to 0.9 for living cheilostomatids, and from 0.25 to 0.75 for living ctenostomatids. The win indices of cyclostomatid and cheilostomatid clades show significantly more variation in living assemblages than in fossil assemblages. This disparity may be due to differential preservation (polar and subpolar assemblages last less than 4 years). The diversity was very high in terms of both species richness and interaction types (outcomes between competitor pairs). Comparison with the literature suggests the possibility that nearshore diversity of bryozoans may be bimodal (have two peaks) between high arctic and antarctic latitudes. Indices of success in overgrowth competition have been constructed in various ways. For cheilostomatids, the method of calculation had little influence on the ranking of representatives. In contrast, the apparent success of ctenostomatids and cyclostomatids varied hugely with how the index was calculated. This inconsistency is due to the use of very different strategies in overgrowth competition; among the two latter groups, many interactions involve tied outcomes.

Introduction

Cyclostomatida, Ctenostomatida, and Cheilostomatida are the major groups of the Phylum Bryozoa (the fourth is exclusively fresh water). For convenience, we will use the term "clade" to refer to these major groups of marine bryozoans, but this is not entirely accurate. Although the Cyclostomatida and the bulk of the Cheilostomatida probably represent monophyletic groups, or clades, Ctenostomatida is probably a paraphyletic group (Todd, 2000), better referred to as a "grade." Representatives of these groups occur together in most benthic assemblages, where frequently the encrusting members are directly competing for space and food (*e.g.*, Stebbing, 1973; Sebens, 1986; Lopez Gappa, 1989). Cheilostomatids generally dominate the bryozoan component of assemblages in space occupied, numbers of species, numbers of colonies, and overgrowth performance. As a result of such dominance, most studies of competition between encrusting benthos have either documented cheilostomatid interactions with representatives of other benthic phyla (Quinn, 1982; Sebens, 1986) or have been restricted solely to cheilostomatid-cheilostomatid interactions (*e.g.*, Jackson, 1979a; Buss, 1980; Palumbi and

Received 27 August 1999; accepted 20 April 2000.

* To whom correspondence should be addressed. E-mail: DKAB@ucc.ie

Jackson, 1983; Tanaka and Nandakumar, 1994; Barnes and Rothery, 1996). A few studies have shown that representatives of the Ctenostomatida may be high or mid-ranked in overgrowth performance against the cheilostomatid representatives (Stebbing, 1973; Turner and Todd, 1994). Cyclostomatids, in contrast, have been found to be almost always overgrown by cheilostomatids in the few studies of Recent (living) competition between the two clades (Harmelin, 1976; Buss and Jackson, 1979; Lopez Gappa, 1989; McKinney, 1992). Analysis of the fossil record has shown that competitive performance has been stable for the last 100 million years, with cheilostomatids overgrowing cyclostomatids in about 66% of encounters (McKinney, 1995a). Although broad trends have been described, many factors contribute to the outcome of interactions between any pair of competitors.

Phylum membership is the principal factor determining overgrowth ability, with ascidians > sponges > bryozoans > unitary forms such as barnacles, annelids (Buss and Jackson, 1979; Russ, 1982; Sebens, 1986). Growth form is also important, with foliaceous forms > encrusting sheets > stoloniferous types (Buss, 1979; Barnes and Rothery, 1996), and bryozoans that have the capability of frontal budding overgrowing those that lack it (Lidgard and Jackson, 1989; McKinney, 1992; 1995a). To explain the competitive advantage that cheilostomatids have over cyclostomatids, McKinney (1992; 1993; 1995a, b) has described a number of attributes, including higher growth rates and larger colonies and feeding structures. The crucial features of cheilostomatids, however, are probably (1) rapid ontogenetic development resulting in full-sized zooidal skeletons (and feeding structures) at colony margins, (2) labile morphogenetic responses at colony margins (raised growing edges, frontal budding, stolon production and others), and (3) water excurrents that leave around the colony margin, potentially into the area of uptake for a cyclostomatid competitor. These features may explain the great radiation that, since the mid-Cretaceous period, the cheilostomatids have undergone relative to the cyclostomatids (Lidgard *et al.*, 1993), or this may be due to unrelated factors such as the acquirement of planktotrophic larvae (Taylor, 1988). It seems likely that an increase in encounters with a superior competitor would contribute to the decline of cyclostomatid species richness from the end of the Cretaceous to Recent periods (Lidgard *et al.*, 1993; McKinney, 1995a; Sepkoski *et al.*, 2000).

Studies involving interpretation of competitive interactions between major groups or clades of the same phylum are rare for both living and fossil assemblages, and this is the case with the Bryozoa. Consequently, our knowledge is biased to the results of the few studies carried out and the limited distribution of the localities of these studies. Many studies are based on relatively few interactions between many species pairs and even fewer between clades, and thus a synoptic interpretation of overall outcomes is difficult. Problems of interpretation are compounded by differences in the way performance is measured (*e.g.*, wins compared to losses, or wins compared to total interactions) and by the way contact matrices are analyzed (that is, by using transitivity indices) (see Petraitis, 1979; Rubin, 1982; Tanaka and Nandakumar, 1994). Perhaps the largest barrier to meaningful comparison, though, is that the three marine bryozoan clades have not, to date, been evaluated in the same study (at a single locality).

In this study we investigate intraspecific and interspecific competitive encounters among representatives of the bryozoan clades Cyclostomatida, Ctenostomatida, and Cheilostomatida from the intertidal and infralittoral zone of Kodiak Island, Alaska. The boreal/subpolar region is unusually diverse with respect to many taxa, but particularly bryozoans (see Barnes and Dick, 2000; Dick and Ross, 1986; 1988), and provides an opportunity for comparing interactions between abundant representatives of the three clades. We compare the outcomes using different methods of competitive strength calculation, and we evaluate these methods. We also compare win indices and rankings of the clades with unpublished work involving interactions among the clades at two south Atlantic localities: the Falkland Islands and South Georgia Island. Win indices and rankings from other localities and time periods were extracted from the literature for comparisons with our results.

Materials and Methods

Study site and species

Bryozoan overgrowth interactions were analyzed on 110 rocks from 14 sites at Narrow Strait, Kodiak Island (57° 54′N, 152° 27′W) in the Alaskan boreal-Arctic (see Dick and Ross, 1988, for more detail). Four tidal levels or depths were represented by a number of rock-pile sites: upper midlittoral (2), lower midlittoral (4), upper infralittoral (3), and lower infralittoral (5). Rock surface area was measured using a nonelastic grid of square centimeters as per Barnes and Rothery (1996), but percent cover and colony size were not measured. All competitors were identified into the three orders of bryozoans present and to genus or species level where possible. Poor taxonomic resolution in the initial stages of the study led to uncertainty about the particular species involved in interactions within the genera *Caulorhamphus* (5 species), *Microporella* (4 species), *Celleporella* (2 species), and *Alcyonidium* (2 species). The cyclostomatids from Narrow Strait have not been worked up taxonomically and here were identified to ordinal level only, with the exception of a common lichenoporid designated *Lichenopora* sp.

Table 1

Mean number of species per rock and proportion of rocks (in parentheses) colonized by species occurring rarely at the study sites, Alaska

	Mean no. species per rock		
Tidal cover/depth	Cyclostomatids	Ctenostomatids	Cheilostomatids
Upper midlittoral	0	0.25 (0.13)	4.88 (0.49)
Lower midlittoral	0.88 (0.31)	0.75 (0.09)	6.81 (0.49)
Upper infralittoral	1.54 (0.72)	0.54 (0.25)	10.7 (1.00)
Lower infralittoral	4.25 (0.94)	0.73 (0.30)	13.0 (0.63)

Measurement of interactions

All colony-to-colony interactions between representatives of the three clades of bryozoans were recorded from each rock and site, along with the number of intraspecific and interspecific encounters within clades. When the growing edge of competitor A covered the apertures of competitor B, A was determined to have overgrown B. Only "frontal" overgrowth interactions between two living competitors, without direct settlement onto one of the competitors, was counted as overgrowth for the purposes of this study (see Rubin, 1982; Turner and Todd, 1994; Barnes and Rothery, 1996). The actual scores were tabulated into a competitor-contact matrix (as Turner and Todd, 1994; Barnes and Rothery, 1996). Measurements of overgrowth performance were calculated for each competitor that took part in more than 20 between-clade interactions. Various measurements of overgrowth performance were used: a score system in which a win = 3, a tied outcome = 1, and a loss = 0 (wins rated much higher than ties because ties often prevent further growth and development of colonies, see Barnes and Clarke [1998]); the number of wins divided by the total number of interactions for that competitor; the number of losses divided by the total number of interactions for that competitor; the number of wins divided by the number of losses for that competitor; and an aggregate measure in which the mean of the rankings from all methods was obtained. The rankings in Table 2 are those calculated from raw data. These may differ from true population rankings because the number of encounters with each competitor was not the same for each species, and some potential competitors did not meet. The rankings were standardized by multiplying all pairwise interactions such that each had a total value of 100, then recalculating the total wins, losses, and ties for each competitor identity.

Results

Between-species interactions

A total of 74 species of bryozoans were recorded during the study: 57 cheilostomatids, 3 ctenostomatids, and the remainder cyclostomatids (later analyzed to be 14 species). The mean number of cheilostomatid and cyclostomatid species per rock increased with depth of rocks (Table 1), the former dominating the number of species at all depths. The proportion of ctenostome species was small with respect to the total number of bryozoan species, and it varied inconsistently with depth. The mean number of interactions increased with depth for all clades (Fig. 1). Cheilostomatids were involved in 2653 interactions, of which 73.7% were within the clade; ctenostomatids were involved in 367 interactions, of which 1.6% were within the clade; and cyclostomatids were involved in 384 interactions, of which 5.7% were within the clade. All cheilostomatids that encountered ctenostomatids or cyclostomatids on more than 20 occasions are illustrated in a species-contact matrix (Table 2). The remaining cheilostomatid species are pooled because fewer than a total of 20 competitive interactions were not considered to be representative. Certain pairs of competitors had anomalously higher frequencies of encounters, such as *Alcyonidium* spp. and *Porella alba*. The cheilostomatid species *Callipora craticula* encountered only ctenostomatids and cyclostomatids, despite the overwhelming numerical dominance of cheilostomatids and being involved in 30 interspecific interactions.

Most (99.3%) of the intra-clade encounters observed were interspecific interactions. Over 80% (114) of the possible competitor-pair interactions (136 in the matrix Table 2) and 44 of the 45 between-clade interactions were observed (but these represented only a small proportion of the 74 × 74 species interactions theoretically possible). The proportion of indeterminate outcomes (neither competitor won all encounters) from competitor pairs was significantly higher within the clade of cheilostomatids (15.9%) than between cheilostomatids and other clades (5.1%) (Mann-Whitney *U* test, $P < 0.01$). The proportion of tied outcomes or standoffs in competitor pairs was significantly higher between clades than within clades (Mann-Whitney, $P < 0.001$). The proportion of ties was also significantly

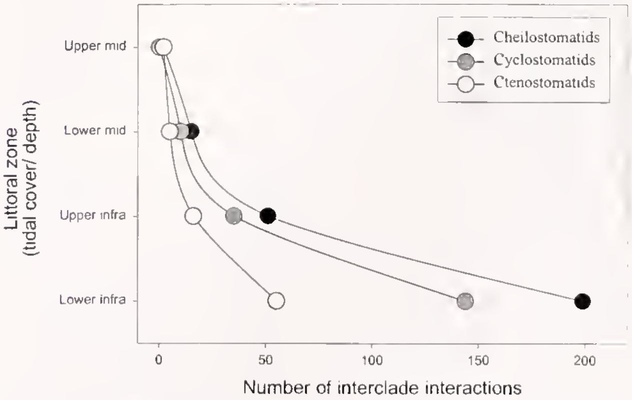

Figure 1. Mean number of interactions per clade with depth. All data are presented as mean with standard error.

Table 2

Matrix of competitive interactions for Alaskan cheilostomatid, ctenostomatid, and cyclostomatid bryozoans (latter two groups are gray shaded)

	T. armifera	*T. aquilirostris*	*M. plana*	*Caulorhamphus* sp.	*Cyclostomatids*	*M. californica*	*T. arctica*	*Lichenopora* sp.	*Cheilostomatids*	*Microporella* sp.	*C. annulata*	*P. alba*	*Alcyonidium* sp.	*Celleporella* sp.
Tegella armifera		2 5 9 16	4 3 3 10	2 1 1 4	1 2 10 13	1 0 2 3	1 1 2 4	3 0 1 4	1 3 27 31	2 2 13 17	0 1 6 7	4 3 44 51	8 1 10 19	7 25
Tegella aquilostris			0 11 8 19	0 0 1 1	2 1 4 7	1 0 1 2	0 1 6 7	2 0 2 4	1 2 16 19	2 0 6 8	2 0 3 5	3 2 24 29	8 1 7 16	5 24
Myriozoella plana				0 0 3 3	2 5 7 14	1 0 5 6	1 3 0 4	3 0 0 3	4 5 34 43	9 5 37 51	0 0 11 11	5 2 8 15	5 0 3 8	11 41
Caulorhamphus sp.					0 2 1 3	4 0 2 6	4 2 3 9	9 2 1 12	5 13 21 39	9 7 9 25	3 2 4 9	35 5 11 51	20 2 2 24	9 77
Other Cyclostomatids					4 3 3 7	1 3 2 6	1 1 2 4	6 8 1 15	12 14 16 42	14 14 20 48	6 2 5 13	6 3 10 19	3 1 3 7	8 39
Microporella californica							2 1 6 9	2 0 0 2	1 3 3 7	0 0 1 1	0 2 0 2	9 2 16 27	5 2 0 7	2 26
Tegella artica								1 1 2 4	3 3 13 19	2 5 5 12	0 0 2 2	5 3 21 29	14 0 6 20	5 21
Lichenopora sp.									11 1 5 17	6 2 7 15	7 1 3 11	8 0 5 13	4 1 0 5	16 21
Other Cheilostomatids										8 53 49 110	7 9 4 20	58 47 43 148	14 11 9 17	18 94
Microporella sp.											6 13 7 26	33 42 27 102	15 6 6 27	34 89
Cribrilina annulata												9 6 5 20	5 3 1 9	10 14
Porella alba													61 24 16 100	40 73
Alcyonidium sp.													5 1 1 6	34 39
Celleporella sp.														

Data are displayed in standard form—see Turner and Todd (1994), Barnes and Rothery (1996). If row = competitor A and columns = competitor B, for each cell the top left, top right, and bottom left data give, respectively, the number of ties between species A and B, wins by B (= losses by A) and wins by A (= losses by B). The number in the bottom right of each cell is the total number of observed interactions for that species pair.

higher in the ctenostomatids than in the non-*Lichenopora* cyclostomatids (Mann-Whitney, $P < 0.001$) but was not significantly different from that in the total cyclostomatids (Mann-Whitney, $P = 0.053$). Both clades had a significantly higher proportion of tied outcomes than did the cheilostomatids (Mann-Whitney, $P < 0.001$).

Ctenostomatids and cyclostomatids met too infrequently to assess their overgrowth performance against each other. Both of these clades, however, encountered cheilostomatids on many occasions and won more encounters than they lost. In both the midlittoral to the infralittoral, ctenostomatids won about 55% of the encounters that had a decided outcome, but the proportion of ties increased from from 4% in the midlittoral to 58% in infralittoral. Cyclostomatids were better competitors against cheilostomatids, winning 87% of midlittoral encounters and 62% of infralittoral encounters. As with ctenostomatid-cheilostomatid encounters, the proportion of tied outcomes increased from the midlittoral to the infralittoral, but less dramatically, from 31% to 35%.

The overall transitivity of the assemblage measured using the index of Tanaka and Nandakumar (1994) was 0.62. This was 25% lower than the value obtained for interactions just within the clade of cheilostomatids (0.83—Barnes and Dick, unpubl. data). This value indicates a generally hierarchical system (Buss, 1980; Russ, 1982) but, as predicted by Jackson (1979b), one that is more intransitive between clades than within the clade of cheilostomatids.

The competitors involved in interactions could be ranked in a sequence of overgrowth performance from several typically overgrown by others (cheilostomatids) to several typically overgrowing others (also cheilostomatids). Overgrowth performance can be and has been measured in a

Table 3

Ranking of competitive ability in Alaskan cheilostomatid, ctenostomatid, and cyclostomatid bryozoans (latter two clades are in bold), with names listed in descending order of initial number of wins

Taxon identity and coding		Initial	Standardized ranking Win-tie scored	W/T	L/T	W/L	Aggregate
Tegella armifera	(Ta)	Ta	Tq	Tq	Tq	Ta	Tq
Tegella aquilirostris	(Tq)	Tq	Ta	Ta	**Li**	Tq	Ta
Myriozoella plana	(Mp)	Mp	Mp	Mp	Ta	Mp	Mp
Cauloramphus sp.	(Ca)	Ca	Ca	Tr	Mp	Ca	Ca
Cyclostomatids	**(Cy)**	**Cy**	**Cy**	**Cy**	Ca	**Li**	Tr
Microporella californica	(Mc)	Mc	Tr	Ca	**A**	Tr	**Li**
Tegella arctica	(Tr)	Tr	Mc	Mc	Tr	**Cy**	**Cy**
***Lichenopora* spp.**	**(Li)**	**Li**	**Li**	M	Mc	Mc	Mc
Cheilostomatids	(C)	C	M	C	**Cy**	**A**	**A**
Microporella sp.	(M)	M	C	Cn	Cn	M	M
Cribrilina annulata	(Cn)	Cn	**A**	**Li**	Pa	C	Cn
Porella alba	(P)	P	Cn	**A**	M	Cn	C
***Alcyonidium* spp.**	**(A)**	**A**	P	Pa	C	Pa	Pa
Cylindroporella tubulosa	(Ct)	Ct	Ce	Ce	Ce	Ce	Ce
Celleporella spp.	(Ce)	Ce	Ct	Ct	Ct	Ct	Ct

Rankings are Initial (number of wins) and Standardized (multiplied up so every competitor meets each other on the same number of occasions). Standardized rankings are win-tie scored (wins score 3, ties score 1), W/T (proportion of wins over total number of interactions), L/T (proportion of losses over total number of interactions), W/L (proportion of wins over losses), and aggregate (of W/T, L/T, and W/L).

"Cheilostomatids" in the species-identity column refers to the remainder of the cheilostomatid species present but not listed.

number of ways (Table 3). A ranking based on the number of wins (actual overgrowth of the competitor) placed some cyclostomatids as intermediate competitors but others (*Lichenopora* sp.) and the ctenostomatids as poor competitors. In contrast, lichenoporid cyclostomatids and, to a lesser extent, ctenostomatids were good competitors when assessed by the ratio of losses to total interactions (they were rarely overgrown). Cheilostomatids spanned the whole range of competitor performance, but those that scored highly in the win index also scored highly on the loss index (*i.e.*, good overgrowers were rarely overgrown; poor overgrowers were usually overgrown). The average ranking change for a competitor between these different indices was 1.4 for cheilostomatids, but 6 for ctenostomatids and 6.5 for cyclostomatids. At the level of species, the performance of selected cheilostomatids against the combined representatives of each clade is illustrated in Table 4. All performed better against other cheilostomatids than against ctenostomatids or cyclostomatids, but most performed better against cyclostomatids than against ctenostomatids (*e.g.*, *Microporella californica*), although a few (*e.g.*, *Porella alba*) did the converse. A good competitor against one clade was generally a good competitor against the other, but some (*e.g.*, *Microporella californica*) had quite different performances against competitors from different clades (Table 4).

The between-clade win index of the three clades varied (Table 5) between the Alaskan site and others we analyzed from County Cork (Ireland) and the Falkland Islands and South Georgia Island (both South Atlantic). Other literature and unpublished data in Table 5 for which between-clade win scores have been calculated show the overgrowth scores of cyclostomatids in Alaska and County Cork to be the highest recorded.

Table 4

Performance of various Alaskan cheilostomatid species in overgrowth interactions with other cheilostomatids, ctenostomatids and cyclostomatids; values are the probability of a win for competitor A against competitor B

Competitor A identity	Competitor B Cheilostomatids	Ctenostomatids	Cyclostomatids
Tegella aquilostris	0.76	0.44	0.55
Tegella armifera	0.71	0.53	0.65
Myriozoella plana	0.66	0.38	0.41
Laganicella neosocialis	0.60	—	0.29
Cauloramphis spp.	0.52	0.08	0.07
Tegella arctica	0.51	0.30	0.38
Microporella californica	0.46	0.00	0.33
Cribrilina annulata	0.34	0.09	0.13
Microporella spp.	0.32	0.22	0.25
Porella alba	0.29	0.16	0.11
Celleporella spp.	0.22	0.14	0.12
Callipora craticula	—	0.06	0.14

Table 5

Between-clade overgrowth competition performance scores and rankings in the three bryozoan clades (all other rankings are cheilostomatids)

		Ctenostomatids vs. cheilostomatids		Cyclostomatids vs. cheilostomatids vs. ctenostomatids*		Cheilostomatids vs. cyclostomatids vs. ctenostomatids*
Location	Latitude	Win index	Ranking	Win index	Ranking	Win index
Alaska (USA)$^{\alpha}$	57 N	0.24	7/12	0.42 (0.25*)	6/13	0.21 (0.18*)
Scotland	56 N	0.5	5/18	—	—	(0.32*)
Ireland$^{\text{site 1}}$	51.5 N	—	—	0.41	6/8	0.56
Ireland$^{\text{site 2}}$†	51.5 N	0.56	1/6	—	—	(0.37*)
England	50 N	0.75	1/5	—	—	(0.08*)
Croatia	43 N	—	—	0.08	—	0.78
Jamaica	18 N	—	—	Low	10/10	~0.9
Mozambique†	12 S	—	—	0.2	13/15	0.60
Australia	38 S	—	—	0.0	8/8	0.74
Argentina	47 S	—	—	0.33	9/12	0.62
Falkland Is	52 S	—	—	0.32	7/10	0.44
South Georgia†	54 S	0.4	1/7	0.18 (0.08*)	6/7	0.6 (0.32*)
Signy Is†	60.5 S	—	—	0.1	22/22	0.73

Data are taken from Stebbing (1973), Buss and Jackson (1979), Russ (1982), Lopez Gappa (1989), McKinney (1992), Turner and Todd (1994), Maughan and Barnes (in press), Barnes and Lehane (unpubl. data), present study ($^{\alpha}$) and unpublished sources (†).

Discussion

Amongst the major groups of the phylum Bryozoa, cheilostomatids are generally the major space occupiers, the most speciose, and the superior overgrowth competitors (see, for example, Buss and Jackson, 1979). Sometimes they may even locally dominate the macrobenthic community—for example, on shells (Kay and Keough, 1981), on reef rubble (Jackson and Winston, 1982), on floating debris (Barnes and Sanderson, 2000), in mid-latitude shelf waters (James *et al.*, 1992), and on Antarctic shallow-water hard substratum (Barnes, 1995). When present, the rarer ctenostomatids may effectively compete against cheilostomatids (Stebbing, 1973), but cyclostomatids are typically overgrown in meetings (Buss and Jackson, 1979). Overgrowth of calcified benthos by soft-bodied forms such as ctenostomatid bryozoans or ascidians may not, however, always prove lethal to the overgrown competitor (Todd and Turner, 1988). In this study, the first to encompass all three "clades," at the same localities, cheilostomatids were the major space occupiers, were involved in most interactions, and were the most speciose of the three clades, as found elsewhere (Table 1). They were, however, outcompeted by ctenostomatids at all three localities, and at Kodiak Island, Alaska, they were uniquely outcompeted by cyclostomatids (Table 5).

McKinney analyzed living and Recent relict (1992; 1995b) and fossil (1995a) cyclostomatid and cheilostomatid interactions and found that living and Recent relict assemblages in Rovinj, Croatia, were similar to those over the last 105 million years. The win index of fossil cheilostomatids oscillated around a value of 0.66 (66% win rate), and that of cyclostomatids at around 0.29. In the Alaskan assemblage studied here the win index of cyclostomatids was nearly 1.5 times greater and the win index of cheilostomatids 3 times lower. The win index of clades varied with site (Table 5) or possibly latitude (Fig. 2). In the living assemblages studied here (from Alaska, the Falkland Islands, and South Georgia Island) and other indices taken or calculated from the literature, the win indices of cyclostomatids varied from 0 to 0.42. The win indices of living cheilostomatids varied be-

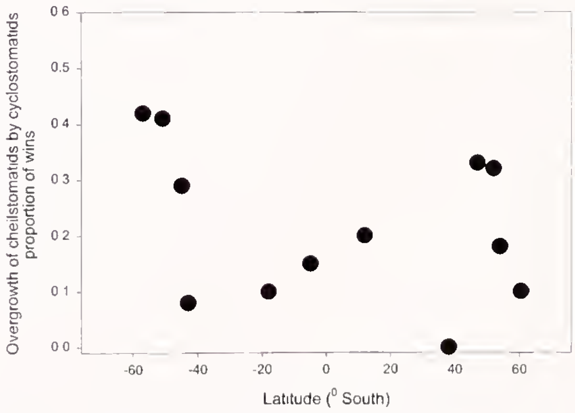

Figure 2. Magnitude of overgrowth (%) of cyclostomatids by cheilostomatids in Mesozoic and Cenozoic periods, adapted from McKinney (1995).

tween 0.08 and 0.9 and those of living ctenostomatids from 0.25 to 0.75 from the few studies carried out (Table 5). There is significantly more variation (Fig. 3) in the living assemblages that have been studied than in the fossil assemblages that have been studied in both the cyclostomatid clade (homogeneity of variance test, $F = 7.6$, $P < 0.01$) and the cheilostomatid clade ($F = 24.0$, $P < 0.01$). The sample size in both the living and fossil assemblages is reasonable (though not high in the former). McKinney (1995b) has shown that, through careful consideration of differential preservation of overgrower and overgrown, analysis of fossil assemblages probably gives an accurate representation of conditions at the time of preservation. Either there is more variation today than over the past 100 million years or we are getting some information from living assemblages that we are not getting from fossil assemblages. There is some evidence for both of these explanations.

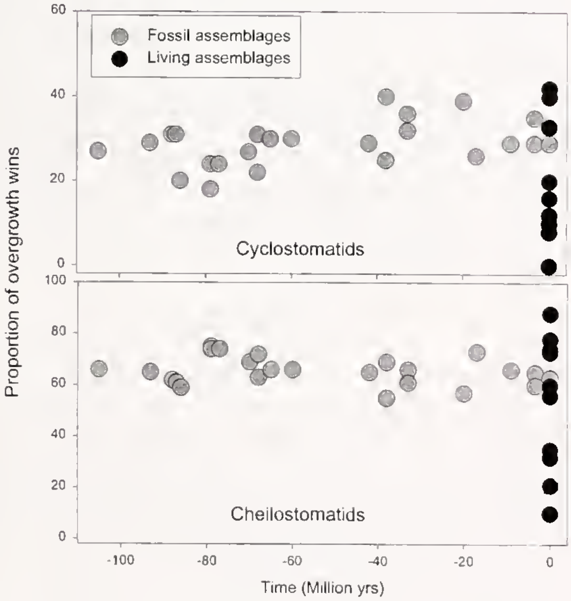

Figure 3. Non-cheilostomatid (ctenostomatid and cyclostomatid) species richness of rock-pile habitats with latitude. Data points are from Powell and Crowell (1967), Gordon (1980), Winston (1982), Cook (1985), Rao and Ganapati (1985), McKinney (1992), Barnes *et al.* (1996), Barnes and Arnold (1999), Maughan and Barnes (unpubl. data), present study, and unpublished sources.

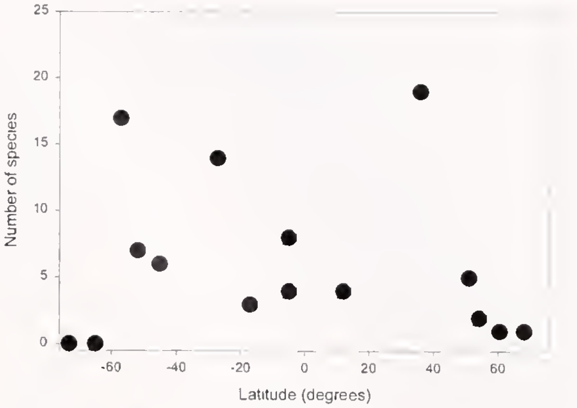

Figure 4. Cyclostomatid win index with latitude. Data points are from Buss and Jackson (1979), Russ (1982), Lopez Gappa (1989), McKinney (1992), Barnes and Rothery (1996), Maughan and Barnes (in press), present study, and unpublished sources.

The highest values of cyclostomatid win index and the lowest values of cheilostomatid win index are from high (50°–60°) latitude localities (this study and Maughan and Barnes, unpubl. data). The high values for the cheilostomatid win index are generally from studies in mid to low latitudes (and typically from more sheltered sites) (*e.g.*, Buss and Jackson, 1979; McKinney, 1992). Thus the high range of modern index values is probably partly due to the range of exposure of localities. Antarctic (high latitude) values (from data from Barnes and Rothery, 1996; Barnes, unpubl. data), however, also showed high values for the cheilostomatid win index (Fig. 4). The geologically recent succession of glaciation periods, cooling of the poles, and separation of continents has probably resulted in higher levels of disturbance through wave action and ice-scour than before. So the range of nearshore conditions may be greater than in the past 100 million years. Depth is a potential confounding factor because most interaction data that has been recorded from fossil communities is from deeper water shelf environments (see Taylor and Allison, 1998), whereas most modern data sets of similar nature are from shallow water (see Buss and Jackson, 1979; Russ, 1982; Turner and Todd, 1994; Barnes and Rothery, 1996). However, studies of fossil assemblages such as those by McKinney (1992) are largely from mid latitudes, suggesting that conditions for fossilization of communities seem to be most prevalent in mid-latitude conditions (Taylor and Allison, 1998). The survival of encrusting communities (and, more specifically, bryozoan colonies) becomes progressively shorter with increasing latitude within the Southern Ocean, such that the longest survival time of any individual (even skeletal material) at 68° S is just 4 years (Barnes and Arnold, 1999). Additional support is provided by the high win-index values, similar to those in the fossil record, of cheilostomatids in mid to low latitudes and in sheltered localities (Buss and Jackson, 1979; McKinney, 1992). Thus it is possible, and even probable, that a broad range of index values have occurred throughout the last 100 million years but have not been preserved because the very conditions that yield extreme values prevent preservation (Lescinsky, 1993; McKinney, 1995b). This situation makes judgments about the evolutionary ecology and historical position of clades and the non-escalation of competition problematical (Liddell and Brett, 1982; McKinney (1992; 1995a, b).

The diversity of the Alaskan assemblages studied here, with respect to both species richness and variety of species-pair interactions, was high—more so than at any comparable site studied to date (Barnes and Dick, 2000). The next highest value of both non-cheilostomatid and cheilostomatid species richness in intertidal or shallow subtidal rock-pile habitat is from the temperate zone of the southern hemisphere (Russ, 1982). James *et al.* (1992) have also shown bryozoan-rich carbonates peaking in mid-latitude shelf environments. This finding raises the possibility of two peaks in nearshore bryozoan species diversity centered around temperate shores (Fig. 4), though clearly more data would be needed to test this hypothesis. If such a pattern is mediated through frequency of disturbance, one would expect the peak in the northern hemisphere to be at a higher latitude than that in the south because the continental effect of Antarctica increases the range of latitude influenced by ice scour in the southern hemisphere. Species richness typically increases towards the tropics (Thorson, 1957; Kendall and Aschan, 1993), but may peak around subequatorial levels (Silva, 1992). Bryozoans (along with polychaetes) are one of the few taxa that have a diversity center in Antarctic waters (Clarke, 1992; Hayward, 1995).

The definition of a win or tie in overgrowth competition has undergone some evolution (Jackson, 1979a). A tied outcome has been found to represent a variety of situations including a cessation of growth (*e.g.*, Stebbing, 1973), minor overgrowth (Russ, 1982), mere stalling of a future win for one of the two competitors (Sebens, 1986), mutual overgrowth (McKinney, 1992), fusion of colonies (intraspecific meetings), and redirection of growth (Barnes and Rothery, 1996). Tanaka and Nandakumar (1994) argued that a tied outcome was a result equal in importance to a win or a loss and should be included in index calculations. The method of win index tabulation, analysis, and interpretation has also changed dramatically, but for bryozoans has typically been based around cheilostomatids (Petraitis, 1979; Buss and Jackson, 1979; Rubin, 1982; Tanaka and Nandakumar, 1994). In this study, the various methods of ranking competitors in overgrowth competition indicate that the type of index of success used has little influence on the relative or absolute positions of cheilostomatids. In contrast, the apparent success of ctenostomatids and cyclostomatids varies hugely with how the index is calculated because they use a very different strategy in overgrowth competition; many interactions result in tied outcomes. The strategy is essentially defensive rather than offensive, involving not many wins but not many losses. Such a strategy may pay off better where encounters and superior competitors are rare, because either a win or a tie may result in persistence, but a loss can be lethal (though not necessarily to the genet). In very exposed environments, such as that in the present study and in Antarctic assemblages, encounters and good competitors are rare due to habitat ephemerality, so even poor competitors may dominate assemblages (Barnes and Clarke, 1998). The non-lichenoporid cyclostomatids have a higher number of wins, but also a higher number of losses, than lichenoporids. Most cheilostomatids also have mostly determinate interactions, which may be a better strategy where habitats are more stable and competition is more intense. To tie with one competitor would not ensure persistence, as sooner or later an even better competitor will arrive. Although the assemblages studied here have not been followed through time, ties involving cyclostomatids cannot be considered likely to be delays on cheilostomatid wins (see Rubin, 1982; Sebens, 1986). This is partly because the majority of decided outcomes between these clades involved a win for the cyclostomatid competitor and partly because the majority of tied outcomes observed in other similarly exposed latitudes (*e.g.*, South Georgia Island [Barnes and Arnold, 1999]; Signy Island [Barnes and Rothery, 1996]) had remained as "standoffs" for a period of years. The disadvantages of cyclostomatids compared to cheilostomatids, in functional body plan and feeding or water flow dynamics (McKinney, 1992), may be reasons for achieving a defensive rather than aggressive strategy in overgrowth competition. There may, however, be other explanations, such as differential growth rates or budding patterns between environments; and other selective forces, such as the frequency of disturbance, may be more important.

Although the cyclostomatids are marginally superior to the cheilostomatids in overgrowth competition at Kodiak island, Alaska, the other study locations and literature suggest that this is atypical. The clades on aggregate are ranked ctenostomatids > cheilostomatids > cyclostomatids, but all, particularly the cheilostomatids, have a range of competitors with widely varying overgrowth strength and strategy. This study suggests, however, that locality, method of measurement, and number and identity of clades included in competition studies have important influences on and implications for the result obtained.

Acknowledgments

We thank those who assisted with data collection: Pat Chan and Clare Lehane (University College Cork) for the County Cork and Falkland Islands data; Rod Arnold (British Antarctic Survey) for the South Georgia Island data; and the Society for Environmental Exploration, FRONTIER, for the Mozambique data. We also wish to thank Irene O'Sullivan for help with preparation of Table 2.

Literature Cited

Barnes, D. K. A. 1995. Sublittoral epifaunal communities at Signy island, Antarctica: II. Below the ice foot zone. *Mar. Biol.* **121:** 565–572.

Barnes, D. K. A., and R. J. Arnold. 1999. Possible latitudinal clines in

Antarctic intertidal and subtidal zone communities encrusting ephemeral hard substrata. *J. Biogeog.* **26:** 207–213.

Barnes, D. K. A., and A. Clarke. 1998. The ecology of an assemblage dominant: the encrusting bryozoan *Fenestrulina rugula. Invertebr. Biol.* **117:** 331–340.

Barnes, D. K. A., and M. H. Dick. 2000. Overgrowth competition in encrusting bryozoan assemblages in the intertidal and infralittoral zones of Alaska. *Mar. Biol.* (in press).

Barnes, D. K. A., and P. J. Rothery. 1996. Competition in encrusting Antarctic bryozoan assemblages: outcomes, influences and implications. *J. Exp. Mar. Biol. Ecol.* **196:** 267–284.

Barnes, D. K. A., and W. G. Sanderson. 2000. Latitudinal patterns of remote island marine debris colonisation. Pp. 154–160 in 11th International Bryozoology Assoc. Conference, A. Herrera Cubilla and J. B. C. Jackson, eds. Smithsonian Tropical Research Institute, Panama City, FL.

Barnes, D. K. A., P. J. Rothery, and A. Clarke. 1996. Colonisation and development in encrusting communities from the Antarctic intertidal and sublittoral. *J. Exp. Mar. Biol. Ecol.* **196:** 251–265.

Buss, L. W. 1979. Habitat selection, directional growth and spatial refuges. Pp. 459–497 in *Biology and Systematics of Colonial Organisms,* G. P. Larwood and B. R. Rosen, eds. Academic Press, London.

Buss, L. W. 1980. Competitive intransivity and size frequency distributions of interacting populations. *Proc. Natl. Acad. Sci. USA* **77:** 5355–5359.

Buss, L. W., and J. B. C. Jackson. 1979. Competitive networks: nontransitive competitive relationships in cryptic coral reef environments. *Am. Nat.* **113:** 223–234.

Clarke, A. 1992. Is there a latitudinal diversity cline in the sea? *Trends Ecol. Evol.* **7:** 286–287.

Cook, P. L. 1985. Bryozoa from Ghana, a preliminary survey. *Zoologische Wetenschappen, Sci. Zool. Ann.* **238:** 1–315.

Dick, M. H., and J. R. P. Ross. 1986. Intertidal cheilostome bryozoans in rock pile habitat at Narrow Strait, Kodiak, Alaska. Pp. 87–93 in *Bryozoa: Ordovician to Recent,* C. Nielsen and G. P. Larwood, eds. Olsen and Olsen, Fredensborg, Denmark.

Dick, M. H., and J. R. P. Ross. 1988. Intertidal bryozoa of the Kodiak vicinity, Alaska. Center for Pacific Northwest Studies, Western Washington University, Bellingham, WA. Occasional paper **23:** 1–133.

Dick, M. H., W. E. Donaldson, and I. W. Vining. 1998. Epibionts of the tanner crab *Chionoecetes bairdi* in the region of Kodiak Island, Alaska. *J. Crustac. Biol.* **18:** 519–528.

Gordon, D. P. 1980. Bryozoa of the Cape Rodney to Okakari Point marine reserve: an identification manual. New Zealand Oceanographic Institute, Wellington. Unpublished report, 137 pp.

Harmelin, J. G. 1976. Le sous-order de Tubuliporina (Bryozoaires Cyclostomes) en Mediteranée, écologie et systématique. *Mem. Inst. Oceanogr. (Monaco)* **10:** 1–326.

Hayward, P. J. 1995. *Antarctic Cheilostomatous Bryozoa.* Oxford University Press, Oxford. 355 pp.

Jackson, J. B. C. 1979a. Overgrowth competition between encrusting cheilostome ectoprocts in a Jamaican cryptic reef environment. *J. Anim. Ecol.* **48:** 805–823.

Jackson, J. B. C. 1979b. Morphological strategies of sessile animals. Pp. 499–555 in *Biology and Systematics of Colonial Organisms,* G. P. Larwood and B. R. Rosen, eds. Academic Press, London.

Jackson, J. B. C., and J. E. L. Winston. 1982. Ecology of cryptic coral reef communities. I. Distribution and abundance of major groups of encrusting organisms. *J. Exp. Mar. Biol. Ecol.* **57:** 135–147.

James, N. P., Y. Bone, C. C. von der Borch, and V. A. Gostin. 1992. Modern carbonate and terrigenous clastic sediments on a cool water, high energy, mid-latitude shelf: Lacepede Shelf, southern Australia. *Sedimentology* **39:** 877–903.

Kay, A. M., and M. J. Keough. 1981. Occupation of patches in the epifaunal communities on pier pilings and the bivalve *Pinna bicolor* at Edithburgh, South Australia. *Oecologia* **48:** 123–130.

Kendall, M. A., and M. Aschan. 1993. Latitudinal gradients in the structure of macrobenthic communities: a comparison of Arctic, temperate and tropical sites. *J. Exp. Mar. Biol. Ecol.* **172:** 157–169.

Lescinsky, H. L. 1993. Taphonomy and paleoecology of epibionts on the scallops *Chlamys hastata* (Sowerby 1843) and *Chlamys ribida* (Hinds 1845). *Palaios* **8:** 267–277.

Liddell, W. D., and C. E. Brett. 1982. Skeletal overgrowths among epizoans from the Silurian (Wenlockian) Waldron Shale. *Paleobiology* **8:** 67–78.

Lidgard, S., and J. B. C. Jackson. 1989. Growth in encrusting cheilostome bryozoans: I. Evolutionary trends. *Paleobiology* **15:** 255–282.

Lidgard, S., F. K. McKinney, and P. D. Taylor. 1993. Competition, clade replacement, and a history of cyclostome and cheilostome bryozoan diversity. *Paleobiology* **19:** 352–371.

Lopez Gappa, J. J. 1989. Overgrowth competition in an assemblage of encrusting bryozoans settled on artificial substrata. *Mar. Ecol. Prog. Ser.* **51:** 121–130.

Maughan, B., and D. K. A. Barnes. 2000. The influence of flow rate on epilithic boulder communities of Lough Hyne MNR Co. Cork, Ireland. *J. Mar. Biol. Assoc. UK* **40** (in press).

McKinney, F. K. 1992. Competitive interactions between related clades: evolutionary implications of overgrowth interactions between encrusting cyclostome and cheilostome bryozoans. *Mar. Biol.* **114:** 645–652.

McKinney, F. K. 1993. A faster paced world? Contrasts in biovolume and life process rates in cyclostome (Class Stenolaemata) and cheilostome (Class Gymnolaemata) bryozoans. *Paleobiology* **19:** 335–351.

McKinney, F. K. 1995a. One hundred million years of competitive interactions between bryozoan clades: asymmetrical but not escalating. *Biol. J. Linn. Soc.* **56:** 465–481.

McKinney, F. K. 1995b. Taphonomic effects and preserved overgrowth relationships among encrusting marine organisms. *Palaios* **10:** 279–282.

Palumbi, S. R., and J. B. C. Jackson. 1983. Aging in modular organisms: ecology of zooid senescence in *Steginoporella* sp. (Bryozoa: Cheilostomata). *Biol. Bull.* **164:** 267–278.

Petraitis, P. S. 1979. Competitive networks and measures of intransivity. *Am. Nat.* **114:** 921–925.

Powell, N. A., and G. D. Crowell. 1967. Studies on Bryozoa (Polyzoa) of the Bay of Fundy region. I. Bryozoa from the intertidal zone of Minas Bay and Bay of Fundy. *Cah. Biol. Mar.* **8:** 331–347.

Quinn, J. F. 1982. Competitive hierarchies in marine benthic communities. *Oecologia* **54:** 129–135.

Rao, K. S., and P. N. Ganapati. 1986. Distribution pattern and abundance of Bryozoa on rocky shores at Visakhapatnam, Bay of Bengal, India. Pp. 563–578 in *Indian Ocean Biology of Benthic Marine Organisms,* M. F. Thompson, R. Sarojini, and R. Nagabhushanam, eds. Oxford and IBH Publishing, New Delhi.

Rubin, J. A. 1982. The degree of intransivity and its measurement in an assemblage of encrusting cheilostome Bryozoa. *J. Exp. Mar. Biol. Ecol.* **60:** 119–128.

Russ, G. R. 1982. Overgrowth in a marine epifaunal community: competitive hierarchies and competitive networks. *Oecologia* **53:** 12–19.

Sebens, K. P. 1986. Spatial relationships among encrusting marine organisms in the New England subtidal zone. *Ecol. Monogr.* **56:** 73–96.

Sepkoski, J. J., F. K. McKinney, and S. Lidgard. 2000. Competitive displacement among post-Paleozoic cyclostome and cheilostome bryozoans. *Paleobiology* **26.** (in press).

Silva, P. C. 1992. Geographic patterns of diversity in benthic algae. *Pac. Sci.* **46:** 429–437.

Stebbing, A. R. D. 1973. Competition for space between the epiphytes of *Fucus serratus.* L. *J. Mar. Biol. Assoc. UK* **53:** 247–261.

Tanaka, M., and K. Nandakumar. 1994. Measurement of the degree of intransitivity in a community of sessile organisms. *J. Exp. Mar. Biol. Ecol.* **182:** 85–95.

Taylor, P. D. 1988. Major radiation of cheilostome bryozoans: triggered by the evolution of a new larval type? *Hist. Biol.* **1:** 45–64.

Taylor, P. D., and A. Allison. 1998. Bryozoan carbonates through time and space. *Geology* **26:** 459.

Thorson, G. 1957. Bottom communities (sublittoral and shallow shelf). Pp. 461–534 in *Treatise on Marine Ecology and Paleoecology Vol. 1, Ecology,* J. W. Hedgpeth, ed. Geological Society of America Memoir 67, New York.

Todd, J. A. 2000. The central role of Ctenostomes in bryozoan phylogeny. Pp. 104–125 in 11th International Bryozoology Assoc. Conference, A. Herrera Cubilla and J. B. C. Jackson, eds. Smithsonian Tropical Research Institute, Panama City, FL.

Todd, C. D., and S. J. Turner. 1988. Ecology of intertidal and sublittoral cryptic epifaunal assemblages. II. Nonlethal overgrowth of encrusting bryozoans by colonial ascidians. *J. Exp. Mar. Biol. Ecol.* **115:** 113–126.

Turner, S. J., and C. D. Todd. 1994. Competition for space in encrusting bryozoan assemblages: the influence of encounter angle, site and year on outcome variability. *J. Mar. Biol. Assoc. UK* **74:** 603–622.

Winston, J. E. 1982. Marine bryozoans (Ectoprocta) of the Indian river area (Florida). *Bull. Am. Mus. Nat. Hist.* **173:** 99–176.

Marine
Biological
Laboratory
Woods Hole
Massachusetts

One Hundred and Second Report
for the Year 1999
One Hundred and Eleventh Year

Officers of the Corporation

Sheldon J. Segal, *Chairman of the Board of Trustees*
Frederick Bay, *Co-Vice Chair*
Mary J. Greer, *Co-Vice Chair*
John E. Dowling, *President of the Corporation*
John E. Burris, *Director and Chief Executive Officer*
Mary B. Conrad, *Treasurer*
Robert E. Mainer, *Clerk of the Corporation*

Contents

Report of the Director and CEO R1
Report of the Treasurer R7
Financial Statements R8
Report of the Library Director R19
Educational Programs
  Summer Courses R21
  Special Topics Courses R25
  Other Programs R32
Summer Research Programs
  Principal Investigators R35
  Other Research Personnel R36
  Library Readers R38
  Institutions Represented R39
Year-Round Research Programs R43
Honors R55
Board of Trustees and Committees R62
Administrative Support Staff R66
Members of the Corporation
  Life Members R69
  Members R70
  Associate Members R80
Certificate of Organization R84
Articles of Amendment R84
Bylaws R84
Publications R89

Photo credits:

B. Armstrong	R5, R21, R22, R23, R24, R25, R27, R30, R31, R35, R36, R37, R69, R84
J. Atema	R44
M. Dobbins	R46
M. Dornblaser	R1
L. Eckelbecker	R58
L. M. Golder	R3 (bottom)
R. Howard	R55
T. Kleindinst	R19
B. Liles	R2
G. G. Lower	R7
A. C. Maher	R43
P. Presley	R4
R. Silver	R48 (bottom)
Tsoi/Kobus	R3 (top)
L. Amaral Zettler	R62

Report of the Director and Chief Executive Officer

I am pleased to share with you this report as I have each year for the past seven years. 1999 is especially meaningful as it marks my last full year serving as Director and CEO of this wonderful institution. In August of 2000 I will leave the Laboratory to serve as the President of Beloit College, a small liberal arts institution in Wisconsin. This is an exciting opportunity for my family and me, but leaving the MBL, the community that we call home, and our friends and colleagues, will be difficult.

I have been proud to serve as Director of the Marine Biological Laboratory. The MBL is a remarkable and special place, thanks largely to the dedication and commitment of its scientists and staff. Curiosity, camaraderie, and thoughtfulness abound here. Throughout my tenure I have been impressed by the innovation and technical expertise at the Laboratory, which enables awe-inspiring advances in our knowledge.

1999 was a landmark year of growth and prosperity for the Marine Biological Laboratory. I am pleased to report that our finances are sound, our educational programs exceptional and expanding, and our research efforts increasingly exciting and novel. More and more, public awareness of the MBL's importance to biology, biomedicine, and environmental science is growing.

I am excited about what the future holds for the Marine Biological Laboratory. Thanks to the generosity of the many donors to the Discovery Campaign, we have already enhanced our educational program, strengthened our resident and summer research programs, made major strides towards building a new research facility for The Ecosystems Center, and begun shoring up our physical plant. Although we have work yet to do to complete the Campaign by December 2000, the Laboratory is now well positioned to continue its leadership role in the biomedical and environmental sciences well into the 21st Century.

The Marine Resources Center

One of the many gratifying gifts of this campaign was made recently by a long-time, dear friend of the Marine Biological Laboratory. Late in 1999, Honorary Trustee Ellen Grass made a historic gift when she endowed the director's chair of the Marine Resources Center. This is the first time in the history of the Laboratory that a research center director's chair has been endowed. This far-sighted gift will enable us to expand our research projects in the Marine Resources Center, while ensuring the MBL's ability to attract high-quality leadership for this key facility in perpetuity.

The MRC is one of the world's most advanced facilities for maintaining and culturing aquatic organisms essential for biological, biomedical, ecological and aquacultural research. As I reported last year, the Ryan-Dowling Program in Scientific Aquaculture has been established at the Marine Resources Center. We are in the final stages of conducting a national search for a scientific aquaculturist who will oversee this exciting effort.

The MRC is already actively culturing organisms for biomedical research. Currently the MRC is host to a colony of zebrafish. These tiny freshwater fish have become an exciting and important research model used by embryologists, geneticists and developmental neuroscientists. Interestingly, zebrafish and humans share much of the same genetic material. These two-inch natives of India may hold the key to understanding how all vertebrates—including humans—develop from an embryo into a whole organism. What we learn from a zebrafish ultimately may help us understand—and perhaps

treat—a wide range of birth defects, among other disorders.

MRC Director Roger Hanlon and his colleagues made substantial progress in 1999 in adapting and applying DNA fingerprints to test sexual selection processes in squid. Their results are being used by fishery managers as they decide whether to continue to allow targeted fishing on spawning squids off Cape Cod. In another area of research at the MRC, studies have progressed on understanding the mechanisms and function of polarization vision in cephalopods. MRC investigators recently found that cuttlefish are able to overcome the counter-shading camouflage of silvery fishes by detecting polarization patterns that are reflected by fish scales. The result is that cuttlefish and squid can easily detect and prey upon species that are otherwise camouflaged to most predators.

The Ecosystems Center

One of the most crucial objectives remaining to be met in our Discovery Campaign is building the new Environmental Sciences Building to house the MBL's Ecosystems Center. Founded 25 years ago, the Center is home to an interdisciplinary group of scientists whose expertise covers the fields of terrestrial and aquatic ecology, microbiology, chemistry, botany, zoology, physiology, hydrology, mathematics, and genetics. Their goal is to study the impact of humankind on the environment and discover what must be done to sustain and manage the earth's resources.

Among key environmental issues being examined are the ecological consequences of global warming, the effects of tropical deforestation, how trees in northeast forests are handling excess nitrogen, and how pollution and habitat destruction are damaging coastal ecosystems. The problems are global and so are the Center's research sites. MBL scientists have been conducting more than 30 projects around the world—in Brazil, Alaska, Sweden, Russia, and East Africa, as well as closer to home in the woods of northern New England and along coastal estuarine systems at both Plum Island, north of Boston, and here in Waquoit Bay on Cape Cod.

This summer, for example, Senior Scientist Bruce Peterson will travel to Siberia to work on the Russian-American Initiative on Land-Shelf Environments sponsored by the National Science Foundation. The goal of the project is to estimate the flux of nutrients from Eurasia to the Arctic Ocean.

Nearby on Martha's Vineyard, scientists from The Ecosystems Center are working on a pilot ecosystem restoration program. Assistant Scientists Chris Neill and Mathew Williams have begun collaborating with The Nature Conservancy on a 10-year study of how a forest functions. The project involves large-scale cutting, burning, and restoration on a track of land on the Vineyard. Pre-treatment monitoring will be conducted in 2000; cutting and burning treatments are scheduled to begin in 2001. This is a great opportunity to see how a forest works and to determine how a prior, less forested landscape functioned. Center scientists will concentrate on understanding how such treatments influence water balance, soil nitrogen cycling, and the retention and movement of nitrogen to adjacent coastal ponds. The project will also provide The Nature Conservancy with practical information on restoration design and techniques, as well as provide a place to bring people who are interested in biodiversity preservation and its connection with ecosystem functions. Center scientists see this as a pilot project for how they might eventually restore larger areas of fire-adapted ecosystems in the Vineyard State Forest and at the Massachusetts Military Reservation.

Because of the need to identify and confront real and present worldwide threats to the environment, it is not surprising that The Ecosystems Center has grown so dramatically in size, scope, and reputation. The staff has increased six-fold and the budget has more than doubled in recent years, making the Center's office and laboratory space inadequate, and forcing researchers to work at scattered locations around the MBL campus.

Soon, Ecosystems Center scientists will be in the Environmental Sciences Building on Albatross Street. This new building will have a cutting-edge geographic information systems facility, state-of-the-art laboratories for plant and soil sample analysis, a stable isotope laboratory, offices, teaching facilities, a classroom/conference room for the Semester in Environmental Science Program, ample storage areas for all equipment, and field staging areas.

To that end, the MBL has received an important challenge grant of $500,000 from The Kresge Foundation.

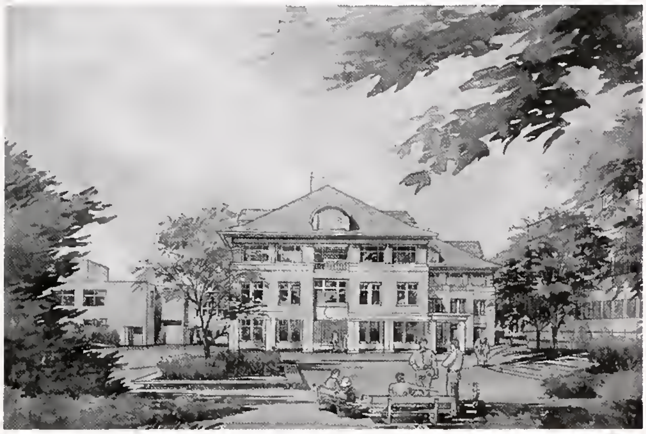

Payment of that grant is conditional upon the MBL raising an additional $2.1 million for the project. With further fundraising success, we hope to break ground for the $8 million building this spring. What a fitting way to celebrate The Ecosystem Center's 25th anniversary.

Josephine Bay Paul Center for Comparative Molecular Biology and Evolution

At the Bay Paul Center, 35 scientists and support staff continue to explore a number of aspects of molecular evolution and comparative molecular biology. Their efforts to sequence the genome of *Giardia,* a water-borne human pathogen that attacks the intestinal tract, is now more than 50 percent complete. Bay Paul Center Director Mitchell Sogin is the principal investigator on that study, which is sponsored by a major grant from the National Institutes of Health.

In 1998 the Center welcomed Dr. Michael Cummings to the scientific staff. He is currently investigating ways to accurately predict drug-resistant strains of tuberculosis by examining specific gene sequences. With a recent grant from the Alfred P. Sloan Foundation, he is also developing novel computer-based analytical procedures to study color vision.

In January 2000, Dr. Jennifer Wernegreen joined the staff as an Assistant Scientist. Dr. Wernegreen comes to the MBL from the University of Arizona where she was an NIH postdoctoral fellow in the Department of Ecology and Evolutionary Biology. Wernegreen uses comparative approaches to explore the molecular evolution of certain species of bacteria that live symbiotically with specific insects. These bacteria are thought to supplement nutritionally unbalanced diets of their hosts by providing essential amino acids, vitamins, and other nutrients.

Other Research Initiatives

Elsewhere at the MBL, scientists are working on a variety of biological and biomedical problems. Dr. David Keefe has developed a new method of non-invasively imaging the meiotic spindle of eggs during human *in vitro* fertilization at his clinic at Women and Infants Hospital in Rhode Island. This technique was developed at the MBL using the polscope designed by Dr. Rudolf Oldenbourg. Application of this exciting technology has doubled the pregnancy rates during intracytoplasmic sperm injection, and improved clinicians' ability to predict fertilization. Dr. Keefe has also been working with Dr. Peter Smith, Director of the BioCurrents Research Program at the MBL. They have developed a novel approach to measuring oxygen uptake by individual mammalian embryos using a non-invasive, self-referencing oxygen sensor. This work was recognized as one of the 50 most important biotechnology breakthroughs at a special program at the National Institutes of Health. It was also a semi-finalist for the Christopher Columbus Science Innovation Award sponsored by *Discover* magazine.

MBL Distinguished Scientist Shinya Inoué was awarded two patents in 1999 for the Slit Scan Centrifuge Microscope and the Centrifuge Microscope Capable of Realizing Polarized Light Observation. These instruments were developed in collaboration with Olympus Optical and Hamamatsu Photonics Co. Dr. Inoué has been using these and other microscopes that he has developed over the years to study several unexplored attributes of living cells. Over the past year he has taken the first measurements of crawling forces of a cell, shown how mammalian cells can be separated into fractions that only contain certain types of organelles, and recorded thin

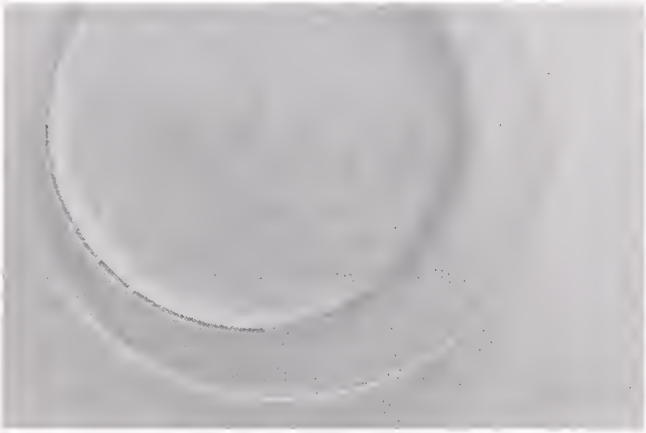

optical slices of rapid molecular changes in living cells hitherto unseen. He's been able to trace the assembly of protein filaments that move chromosomes in yeast cells and track the movement of individual protein molecules within those filaments—something thought impossible only a few years ago.

Two new resident scientists joined the MBL in 1999. Dr. Paul Colinvaux, an Adjunct Scientist, reconstructs Pleistocene climatic and environmental histories of the continents from the sediments of ancient lakes, particularly those found in the Amazon basin. Research has shown that the lowland Amazon forests persisted through glacial cycles, with some re-assortment of species as temperatures fluctuated from the last glacial maximum to the present. Although Colinvaux's research now is concentrated in the Neotropics, he maintains sites in Alaska and Russia for continued study of the paleoecology of the Arctic.

Dr. Ayse Dosemeci came to the MBL in October from the National Institutes of Health as an Adjunct Scientist. She is a neurobiologist who studies synaptic plasticity, a biological phenomenon that may be involved in learning and memory and other central nervous system functions.

Summer Research

Last summer—as has been the case for more than a century—investigators from around the world came to the Marine Biological Laboratory to do research. As always, the excitement of study, scientific exchange, and discovery was great. The 126 principal investigators came from 12 countries and represented more than 100 institutions.

One of the many highlights from last summer's research was the recent publication of a paper in *Nature* magazine by Drs. Miguel Holmgren, Jonathan Wagg, Francisco Bezanilla, Robert Rakowski, Paul De Weer, and David Gadsby. In that paper they describe their latest findings about how a specialized cellular machine, the sodium/potassium exchange pump, works. Because this pump is essential to the health of virtually every cell in all animals, including humans, scientists at the MBL have spent years studying the molecular mechanisms by which this pump transports sodium and potassium ions across cellular membranes. They use the giant nerve cell of the Woods Hole squid as a model system for their research. These investigators already knew that this pump, which is a single protein molecule, transports three sodium ions across the cell membrane at once. In the *Nature* paper they showed that three separate changes in the shape of the pump protein release the three sodium ions from the pump one at a time, in a fixed sequence. This new information will help scientists understand in greater detail how these, and other, essential ion pumps perform the crucial work that keeps all our cells alive.

Another important cellular pump, the sarcoplasmic reticulum-Ca^{2+} pump, is being studied by Dr. Larry Rome and his colleagues from the University of Pennsylvania. They are interested in learning more about how muscle design influences an organism's behavior. This past summer at the MBL they developed a new way to measure, in real time, calcium pumping and sarcoplasmic reticulum function in muscle fibers—a necessary first step in understanding the biological basis of behavior. As their model, they used the swimbladder muscle of the toadfish, the fastest known of all vertebrate fast muscle tissues. The muscles that envelop the swimbladder contract and relax at a remarkable 200 times per second, creating the animal's distinctive "boatwhistle" mating call. These muscles operate almost 100 times faster than the fish's locomotory muscles, which function just adequately to get the rather sluggish creature where it needs to go.

Among the principal summer investigators at the Laboratory last summer, 12 were awarded Grass Fellowships in neurobiology and 19 were awarded other named MBL Fellowships to conduct research on a variety of biological topics at the MBL. These scientists come from around the country and the world to work in Woods Hole for the summer. For example, Pavel Balaban of the Russian Academy of Sciences used the mollusc *Helix* to study putative command neurons that modulate

withdrawal behavior and the activities of neurons underlying this behavior. Elizabeth Jonas of Yale University School of Medicine measured ionic currents on membranes of mitochondria during neurotransmission in squid. Anthony DePass of Long Island University used sea urchins to study how calcium enters heart and nerve cells when a cell is stimulated. And David Ogden of the National Institute for Medical Research in London studied how the skate senses small electric potentials in surrounding seawater to locate prey.

Joining the annual gathering of scientists were 19 print and broadcast journalists who had been awarded MBL Science Writing Fellowships. This program offers writers the chance to step into the shoes of people they cover, to study basic biomedical and environmental science and—for some—to spend additional time doing course work in Woods Hole or research at Ecosystems Center field sites in Alaska and Brazil.

Education

It is my great pleasure to tell you that in 1999 the Howard Hughes Medical Institute awarded a new grant of $2.2 million to the MBL. The four-year award will support many of our advanced laboratory courses for graduate students, postdoctoral fellows, and university faculty members. The MBL has received $8.2 million in HHMI grants since 1988 for which we are extremely grateful. In that time, more than 4900 students have participated in courses taught by the best faculty in the world.

Last summer, the MBL offered 20 courses, involving 579 faculty and guest lecturers and 427 students. Molecular Biology of Aging and a second session of Medical Informatics were added to the course list in 1999. Also in 1999 we welcomed David Garbers (HHMI, University of Texas Southwestern Medical Center) and Randall Reed (HHMI, Johns Hopkins University School of Medicine) as new directors of the Physiology course. This past summer was also the final year in the tenures of the directors of the Neurobiology, Neural Systems & Behavior, and Microbial Diversity courses. My special thanks to retiring directors Gary Banker and Dan Madison, Janis Weeks and Harold Zakon, and Ed Leadbetter and Abigail Salyers.

Last fall, the Semester in Environmental Science Program was held at the MBL for the third time, and results again were impressive. In 1999 four new schools—Beloit College, Lawrence University, Southwestern University, and Trinity University—joined the consortium of institutions that participate in the program, bringing the total number of colleges and universities to 37. Undergraduates from a number of these small liberal arts colleges and universities around the country were immersed in a 15-week program of lectures, laboratory and fieldwork and independent research, all of this under the sponsorship of the MBL's Ecosystems Center. Students explored how human activity, such as deforestation, fisheries exploitation, changes in biodiversity, eutrophication and fossil fuel combustion alter ecological processes and ecosystem structure locally, regionally, and globally.

Trustees

The Board of Trustees elected three new members at November's meeting. Nobel Laureate Dr. Torsten I. Wiesel is President Emeritus and Vincent and Brooke Astor Professor Emeritus of The Rockefeller University. Dr. George M. Langford is the Ernest Everett Just Professor of Natural Sciences and Professor of Biological Sciences at Dartmouth College and Adjunct Professor of Physiology at Dartmouth Medical School. M. Howard Jacobson has been a Senior Advisor at Bankers Trust Private Bank since 1991. Current Board members G. William Miller, Frank Press, and Christopher M. Weld were re-appointed to the Board as members of the class of 2004. Longtime Trustee and stalwart supporter of the MBL Mary Ellen Cunningham was appointed an honorary member of the board. The Board also recognized the efforts of retiring members Alexander W. Clowes, Story C. Landis, and Irwin B. Levitan.

The Discovery Campaign

The Discovery Campaign, now in its final year, was remarkably successful in 1999, thanks to the tireless efforts of our volunteers and the generosity of donors. More than $9.9 million in private support was raised—the most ever in a single year. Our Annual Fund surpassed the half-million dollar mark last year as well, raising nearly 12 percent more than the year before.

This record support pushed the Discovery Campaign past its $25 million goal in August of 1999, an astonishing 16 months ahead of schedule. By January 1, 2000, we had raised $30 million in support of research, education, and facilities at the MBL. As I write this report, some key objectives still remain to be funded before the Campaign ends in December 2000. I am confident that we will meet, if not exceed, these important goals.

With many important gifts and the efforts of the Board's Investment Committee, the Laboratory's endowment has also grown dramatically—from $16 million when I came in 1992 to $47 million at the end of 1999.

I thank all Campaign donors and volunteers for making 1999 such a successful year. Your strong support is a testimony to your belief in the special mission of the Marine Biological Laboratory.

In Conclusion

As was noted many years ago in *Life Science in Woods Hole*, science is more than the accumulation of facts and findings and more than their interpretation. Science is, most of all, a grand collective curiosity. At the MBL, that collective curiosity is alive and well, and everyone who is touched by this place, who investigates, studies, learns and wonders is looking into the new century with hope and great expectations. I know that this place has touched me, and I will always be grateful for having been a part of it. I will miss this special institution and the many friends that I have made here. Thank you for making my tenure at the MBL such a pleasure.

—John E. Burris

Report of the Treasurer

During 1999 the Marine Biological Laboratory had an outstanding year. This was the result of favorable growth in all the areas of operating support and auspicious investment results that further strengthened the balance sheet.

All six areas of Operating Support grew by at least 6%, with double-digit growth in Government Grants (11.9%), Private Contracts (11.7%), and Fees for Conferences and Services (10.2%). The biggest change was from Contributions, which increased $3.8 million (78.8%) from 1998 levels as the Discovery Campaign hit full stride. These increases in Operating Support combined with restraining expense growth to 8% resulted in an almost sevenfold increase in the Change in Net Assets before Non-operating Activity. Also note that this included an underlying positive change in unrestricted net assets from operations of $138 thousand, the first surplus since 1994. This is particularly favorable considering these results include coverage of $1.56 million in depreciation.

Reviewing our Non-operating Activities further demonstrates positive trends. New to our presentation this year is a breakout of the Contributions to Plant, which almost tripled. We have taken this step in light of our extensive capital improvement plans for the next few years. By pulling this out of the ongoing operations we have a much more informative display that gives a better indication of how we are doing in both areas. Total Investment Income and Earnings increased sixfold and enabled us to reinvest over $4.6 million after using roughly one-fifth for Operations.

As a result, we reported for the fifth year in a row a positive Total Change in Net Assets. The increase of $11.2 million represents a very healthy 16.7% return on average net assets.

A review of the 1999 balance sheet further demonstrates the positive trends and our continued strong liquidity. The increase in Pledges and Other Receivables reflects $3 million in increased pledge receivables. The Endowment and Similar Investments increased 21.4%. Also Property, Plant and Equipment (net) increased (3%) for the first time in five years. Total Net Assets increased 18.3% during the year, with Unrestricted Net Assets increasing 7.8%.

A subsequent event, which will have a major impact on the balance sheet, occurred on March 8, 2000, when the Massachusetts Development Finance Agency issued on behalf of the Laboratory $10.2 million in variable rate revenue bonds. A portion was used to refinance the Laboratory's long-term debt at a lower interest cost. The balance of the proceeds will be used to finance capital improvements of the Laboratory's educational, research, and administrative facilities, including the Environmental Sciences Building. The leverage ratio (unrestricted & temporarily restricted net assets-to-debt) on a *pro forma* basis is an acceptable 521% and represents suitable leverage of the financial strength of the Laboratory.

In summary, the Laboratory had a very successful year of operations, fundraising, and investment performance that has greatly enhanced the financial strength of the Laboratory. The success of the Discovery Campaign and the bond financing will facilitate the upgrading of the MBL's physical plant and the continued expansion of our research and educational activities in the new millennium.

—Mary B. Conrad

PRICEWATERHOUSECOOPERS

PricewaterhouseCoopers LLP
One International Place
Boston MA 02110
Telephone (617) 478 5000
Facsimile (617) 478 3900

REPORT OF INDEPENDENT ACCOUNTANTS

To the Board of Trustees of
Marine Biological Laboratory:

In our opinion, the accompanying balance sheet of Marine Biological Laboratory (the "Laboratory") as of December 31, 1999 and the related statements of activities and of cash flows for the year then ended present fairly, in all material respects, the financial position of the Laboratory as of December 31, 1999, and the changes in its net assets and its cash flows for the year then ended in conformity with accounting principles generally accepted in the United States. These financial statements are the responsibility of the Laboratory's management; our responsibility is to express an opinion on these financial statements based on our audit. We conducted our audit in accordance with auditing standards generally accepted in the United States. Those standards require that we plan and perform the audit to obtain reasonable assurance about whether the financial statements are free of material misstatement. An audit includes examining, on a test basis, evidence supporting the amounts and disclosures in the financial statements. An audit also includes assessing the accounting principles used and significant estimates made by management, as well evaluating the overall financial statement presentation. We believe that our audit provides a reasonable basis for the opinion expressed above.

Our audit was conducted for the purpose of forming an opinion on the basic financial statements taken as a whole. The supplemental schedule of functional expenses as of December 31, 1999 is presented for the purpose of additional analysis and is not a required part of the basic financial statements. Such information has been subjected to the auditing procedures applied in the audit of the basic financial statements and, in our opinion, is fairly stated, in all material respects, in relation to the basic financial statements taken as a whole.

April 7, 2000

MARINE BIOLOGICAL LABORATORY

BALANCE SHEET

As of December 31, 1999

(with comparative totals as of December 31, 1998)

ASSETS	1999	1998
Cash and cash equivalents	$ 1,942,285	$ 1,187,954
Short-term investments, at market (Note 3)	3,182,537	3,561,544
Accounts receivable, net of allowance for doubtful accounts of $59,978 in 1999 and $34,195 in 1998	1,158,073	1,242,530
Current portion of pledges receivable (Note 8)	3,974,385	1,607,664
Receivables due for costs incurred on grants and contracts	1,380,766	1,531,083
Other assets	306,518	557,908
Total current assets	11,944,564	9,688,683
Long-term investments, at market (Notes 3 and 4)	45,001,493	37,054,120
Pledges receivable, net of current portion (Note 8)	3,498,787	2,855,352
Plant assets, net (Notes 2, 5 and 6)	20,118,725	19,536,171
Total long-term assets	68,619,005	59,445,643
Total assets	$80,563,569	$69,134,326
LIABILITIES AND NET ASSETS		
Current portion of long-term debt (Note 5)	267,404	243,274
Accounts payable and accrued expenses	1,957,508	2,057,741
Deferred income and advances on contracts	656,745	462,873
Total current liabilities	2,881,657	2,763,888
Annuities and unitrusts payable	1,460,948	1,412,200
Long-term debt, net of current portion (Note 5)	2,056,692	2,324,096
Advances on contracts	1,574,758	1,272,390
Total long-term liabilities	5,092,398	5,008,686
Total liabilities	7,974,055	7,772,574
Commitments and contingencies (Notes 5, 7, 9 and 10)		
Net assets:		
Unrestricted	19,887,437	18,451,865
Temporarily restricted	33,349,244	25,635,237
Permanently restricted	19,352,833	17,274,650
Total net assets (Note 2)	72,589,514	61,361,752
Total liabilities and net assets	$80,563,569	$69,134,326

The accompanying notes are an integral part of the financial statements.

MARINE BIOLOGICAL LABORATORY

Statement of Activities

for the year ended December 31, 1999

(with comparative totals for the year ended December 31, 1998)

	Unrestricted	Temporarily Restricted	Permanently Restricted	1999 Total	1998 Total
Operating support and revenues:					
Government grants	$12,248,442	$ —	$ —	$12,248,442	$10,943,239
Private contracts	1,819,240	—	—	1,819,240	1,629,283
Laboratory rental income	1,548,168	—	—	1,548,168	1,470,372
Tuition	537,835	—	—	537,835	489,726
Fees for conferences and services	3,765,039	—	—	3,765,039	3,415,519
Contributions	1,781,643	4,604,501	2,234,375	8,620,519	4,822,227
Investment income	705,851	1,354,627	—	2,060,478	1,955,735
Miscellaneous revenue	466,903	—	—	466,903	405,633
Present value adjustment to annuities	—	(22,680)	(7,853)	(30,533)	(76,702)
Net assets released from restrictions	3,705,796	(3,705,796)	—	—	—
Total operating support and revenues	26,578,917	2,230,652	2,226,522	31,036,091	25,055,032
Expenses:					
Research	14,147,645	—	—	14,147,645	12,666,746
Instruction	4,742,287	—	—	4,742,287	4,433,789
Conferences and services	2,252,842	—	—	2,252,842	1,999,433
Other programs (Note 2)	5,297,773	—	—	5,297,773	5,365,530
Total expenses	26,440,547	—	—	26,440,547	24,465,498
Change in net assets before nonoperating activity	138,370	2,230,652	2,226,522	4,595,544	589,534
Nonoperating revenue:					
Contributions to plant:					
Private	—	1,507,319	250,000	1,757,319	515,775
Government	198,443	—	—	198,443	—
Release from restriction	912,046	(912,046)	—	—	—
Invested in plant	1,110,489	595,273	250,000	1,955,762	515,775
Total investment income and earnings	220,372	6,116,443	(398,339)	5,938,476	819,705
Less: investment earnings used for operations	(33,659)	(1,228,361)	—	(1,262,020)	(1,246,913)
Reinvested (utilized) investment earnings	186,713	4,888,082	(398,339)	4,676,456	(427,208)
Total change in net assets	1,435,572	7,714,007	2,078,183	11,227,762	678,101
Net assets, beginning of year	18,451,865	25,635,237	17,274,650	61,361,752	60,683,651
Net assets, end of year	$19,887,437	$33,349,244	$19,352,833	$72,589,514	$61,361,752

The accompanying notes are an integral part of the financial statements.

MARINE BIOLOGICAL LABORATORY

STATEMENT OF CASH FLOWS

for the year ended December 31, 1999

(with comparative totals for the year ended December 31, 1998)

	1999	1998
Cash flows from operating activities:		
Change in net assets	$ 11,227,762	$ 678,101
Adjustments to reconcile change in net assets to net cash provided by (used in) operating activities:		
Depreciation	1,562,487	1,505,696
Unrealized (gain) loss on investments	(3,544,380)	2,755,079
Realized gain on investments	(1,639,795)	(2,805,560)
Present value adjustment to annuities and unitrusts payable	30,533	76,702
Contributions restricted for long-term investment and annuities	(2,485,624)	(682,817)
Provision for bad debt	36,968	15,771
Provision for uncollectible pledges	—	250,000
Change in certain balance sheet accounts:		
Accounts receivable	47,489	(36,520)
Pledges receivable	(3,010,156)	(255,134)
Grants and contracts receivable	150,317	(373,918)
Other assets	251,390	2,361
Accounts payable and accrued expenses	(100,233)	562,793
Deferred income and advances on contracts	193,872	78,615
Annuities and unitrusts payable	68,112	163,700
Advances on contracts	302,368	(160,818)
Net cash provided by operating activities	3,091,110	1,774,051
Cash flows from investing activities:		
Purchase of property and equipment	(2,145,041)	(1,015,287)
Proceeds from sale of investments	63,101,047	18,935,050
Purchase of investments	(65,485,238)	(19,478,036)
Net cash used in investing activities	(4,529,232)	(1,558,273)
Cash flows from financing activities:		
Payments on annuities and unitrusts payable	(49,897)	(41,785)
Receipt of permanently restricted gifts	2,438,148	653,152
Annuity and unitrusts donations received	47,476	29,665
Payments on long-term debt	(243,274)	(229,657)
Net cash provided by financing activities	2,192,453	411,375
Net increase in cash and cash equivalents	754,331	627,153
Cash and cash equivalents at beginning of year	1,187,954	560,801
Cash and cash equivalents at end of year	$ 1,942,285	$ 1,187,954

The accompanying notes are an integral part of the financial statements.

Marine Biological Laboratory

Notes to Financial Statements

1. *Background:*

The Marine Biological Laboratory (the "Laboratory") is a private, independent not-for-profit research and educational institution dedicated to establishing and maintaining a laboratory or station for scientific study and investigation, and a school for instruction in biology and natural history. The Laboratory was founded in 1888 and is located in Woods Hole, Massachusetts.

2. *Significant Accounting Policies:*

Basis of Presentation

The accompanying financial statements have been prepared on the accrual basis of accounting and in accordance with the principles outlined in the American Institute of Certified Public Accountants' Audit Guide, "Not-For-Profit Organizations." The financial statements include certain prior-year summarized comparative information in total but not by net asset class. Such information does not include sufficient detail to constitute a presentation in conformity with generally accepted accounting principles. Accordingly, such information should be read in conjunction with the Laboratory's financial statements for the year ended December 31, 1998, from which the summarized information was derived.

The Laboratory classifies net assets, revenues, and realized and unrealized gains and losses based on the existence or absence of donor-imposed restrictions and legal restrictions imposed under Massachusetts State law. Accordingly, net assets and changes therein are classified as follows:

Unrestricted

Unrestricted net assets are not subject to donor-imposed restrictions of a more specific nature than the furtherance of the Laboratory's mission. Revenues from sources other than contributions are generally reported as increases in unrestricted net assets. Expenses are reported as decreases in unrestricted net assets. Gains and losses on investments and other assets or liabilities are reported as increases or decreases in unrestricted net assets unless their use is restricted by explicit donor stipulations or law. Expirations of temporary restrictions on net assets, that is, the donor-imposed stipulated purpose has been accomplished and or the stipulated time period has elapsed, are reported as reclassifications between the applicable classes of net assets and titled "Net assets released from restrictions."

Temporarily Restricted

Temporarily restricted net assets are subject to legal or donor-imposed stipulations that will be satisfied either by the actions of the Laboratory, the passage of time, or both. These assets include contributions for which the specific, donor-imposed restrictions have not been met and pledges, annuities, and unitrusts for which the ultimate purpose of the proceeds is not permanently restricted. As the restrictions are met, the assets are released to unrestricted net assets. Also, realized/unrealized gains/losses associated with permanently restricted gifts which are not required to be added to principal by the donor are classified as temporarily restricted but maintain the donor requirements for expenditure.

Permanently Restricted

Permanently restricted net assets are subject to donor-imposed stipulations that they be invested to provide a permanent source of income to the Laboratory. These assets include contributions, pledges and trusts which require that the corpus be invested in perpetuity and only the income be made available for program operations in accordance with donor restrictions.

Nonoperating revenues include realized and unrealized gains on investments during the year as well as investment income on the master pooled investments and revenues that are specifically for the acquisition or construction of plant assets. Investment income from short-term investments and investments held in trust by others are included in operating support and revenues. To the extent that nonoperating investment income and gains are used for operations as determined by the Laboratory's total return utilization policy (see below), they are reclassified from nonoperating as "Investment earnings used for operations" to operating as "Investment income" on the statement of activities. All other activity is classified as operating revenue. The Laboratory recorded net realized gains of $1,639,795, net unrealized gains of $3,544,380 and dividend and interest income of $1,533,579 in 1999.

Cash and Cash Equivalents

Cash equivalents consist of resources invested in overnight repurchase agreements and other highly liquid investments with original maturities of three months or less.

Financial instruments which potentially subject the Laboratory to concentrations of risk consist primarily of cash and investments. The Laboratory maintains cash accounts with one banking institution.

Investments

Investments purchased by the Laboratory are carried at market value. Donated investments are recorded at fair market value at the date of the gift. For closely held non-publicly traded investments, management determines the fair value, based upon the most recent information available from the Limited Partnership. For determination of gain or loss upon disposal of investments, cost is determined based on the first-in, first-out method. Investments with an original maturity of three months to one year, or those that are available for operations within the next fiscal year, are classified as short-term. All other investments are considered long-term. Investments are maintained primarily with three institutions.

In 1924, the Laboratory became the beneficiary of certain investments, included in permanently restricted net assets, which are held in trust by others. The Laboratory has the continuing rights to the income produced by these funds in perpetuity, subject to the contractual restrictions on the use of such funds. Accordingly, the trust has established a process to conduct a review every ten years by an independent committee to ensure the Laboratory continues to perform valuable services in biological research in accordance with the restrictions placed on the funds by the agreement. The committee met in 1994 and determined that the Laboratory has continued to meet the contractual requirements. The market values of such investments are $7,275,488 and $7,673,828 at December 31, 1999 and 1998, respectively. The dividend and interest income on these investments, included in unrestricted support and revenues, totaled $221,882 and $260,805 in 1999 and 1998, respectively.

Investment Income and Distribution

For the master pooled investments, the Laboratory employs a total return utilization policy that establishes the amount of the investment return made available for spending each year. The Finance Committee of the Board of Trustees has approved a standing policy that the withdrawal will be based on a percentage of the 12 quarter average ending market values of the funds. The market value includes the principal plus reinvested income, realized and unrealized gains and losses. Spending rates in excess of 5%, but not exceeding 7%, can be utilized if approved in advance by the Finance Committee of the Board of Trustees. For fiscal 1999 and 1998, the Laboratory obtained approval to expend 6% of the latest 12 quarter average ending market values of the investments.

The net appreciation on permanently and temporarily restricted net assets is reported together with temporarily restricted net assets until such time as all or a portion of the appreciation is distributed for spending in accordance with the total return utilization policy and applicable state law.

Investment income on the pooled investment account is allocated to the participating funds using the market value unit method (Note 4).

Plant Assets

Buildings and equipment are recorded at cost. Donated facility assets are recorded at fair market value at the date of the gift. Depreciation is computed using the straight-line method over the asset's estimated useful life. Estimated useful lives are generally three to five years for equipment and 20 to 40 years for buildings and improvements. Depreciation is not recorded for those assets classified as construction-in-process as they have not yet been placed into service. Depreciation expense for the years ended December 31, 1999 and 1998 amounted to $1,562,487 and $1,505,696, respectively, and has been recorded in the statement of activities in the appropriate functionalized categories. When assets are sold or retired, the cost and accumulated depreciation are removed from the accounts and any resulting gain or loss is included in unrestricted income for the period.

Annuities and Unitrusts Payable

Amounts due to donors in connection with gift annuities and unitrusts are determined based on remainder value calculations, with varied assumptions of rates of return and payout terms.

Deferred Income and Advances on Contracts

Deferred income includes prepayments received on Laboratory publications and advances on contracts to be spent within the next year. Advances on contracts includes funding received for grants and contracts before it is earned. Long-term advances are invested in the master pooled account until they are expended.

Revenue Recognition

Sources of revenue include grant payments from governmental agencies, contracts from private organizations, and income from the rental of laboratories and classrooms for research and educational programs. The laboratory recognizes revenue associated with grants and contracts at the time the related direct costs are incurred or expanded. Recovery of related indirect costs is recorded at predetermined fixed rates negotiated with the government. Revenue related to conferences and services is recognized at the time the service is provided, while tuition revenue is recognized as classes are offered. The tuition income is net of student financial aid of $527,258 and $523,190 in 1999 and 1998, respectively. Fees for conferences and other services include the following activities: housing, dining, library, scientific journals, aquatic resources and research services.

Contributions

Contribution revenue includes gifts and pledges. Gifts are recognized as revenue upon receipt. Pledges are recognized as temporarily or permanently restricted revenue in the year pledged and are recorded at the present value of expected future cash flows, net of allowance for unfulfilled pledges. Gifts and pledges, other than cash, are recorded at fair market value at the date of contribution.

Expenses

Expenses are recognized when incurred and charged to the functions to which they are directly related. Expenses that relate to more than one function are allocated among functions based upon either modified total direct cost or square footage allocations.

Other programs expense consists primarily of fundraising, year-round labs and library room rentals, costs associated with aquatic resource sales and scientific journals. Total fundraising expense for 1999 and 1998 is $1,008,920 and $1,037,495, respectively.

Use of Estimates

The preparation of financial statements in conformity with generally accepted accounting principles requires management to make estimates and assumptions that affect the reported amounts of assets and liabilities and disclosure of contingent assets and liabilities at the date of financial statements and the reported amounts of revenues and expenses during the reporting period. Actual results could differ from those estimates.

Tax-Exempt Status

The Laboratory is exempt from federal income tax under Section 501(c)(3) of the Internal Revenue Code.

Reclassification

Certain prior year balances have been reclassified to conform with the current year presentation.

3. *Investments:*

The following is a summary of the cost and market value of investments at December 31, 1999 and 1998:

	Market		*Cost*	
	1999	*1998*	*1999*	*1998*
Certificates of deposit	$ 40,000	$ 40,000	$ 40,000	$ 40,000
Money market securities	1,781,128	1,052,276	1,781,128	1,052,276
U.S. Government securities	69,125	1,397,686	69,951	1,136,219
Corporate fixed income	2,364,068	2,504,507	2,536,808	2,472,653
Common stocks	15,665,205	5,033,704	10,608,588	4,290,581
Mutual funds	26,664,204	29,548,891	23,851,004	26,225,214
Limited partnerships	1,600,300	1,038,600	958,982	958,982
Total investments	$48,184,030	$40,615,664	$39,846,461	$36,175,925

Investment portfolios for the years ended December 31, 1999 and 1998 are as follows:

	Market		*Cost*	
	1999	*1998*	*1999*	*1998*
Short-Term Investments				
Certificates of deposit	$ 40,000	$ 40,000	$ 40,000	$ 40,000
Money market 1784 Fund	233,938	559,314	233,938	559,314
Mutal funds	2,875,480	2,955,989	2,965,273	2,940,929
Common stocks in transit	33,119	6,241	33,119	6,241
Total investments	3,182,537	3,561,544	3,272,330	3,546,484
Long-Term Investments				
Pooled investments:				
Master pooled investments	$35,354,938	$27,057,909	$27,514,505	$23,723,343
Separately invested:				
General Chase Trust	5,717,108	6,038,153	5,335,721	5,433,574
Library Chase Trust	1,558,380	1,635,675	1,448,569	1,477,462
Annuity and unitrust investments	2,371,067	2,322,383	2,275,336	1,995,062
Total	45,001,493	37,054,120	36,574,131	32,629,441
Total investments	$48,184,030	$40,615,664	$39,846,461	$36,175,925

4. *Accounting for Pooled Investments:*

Certain net assets are pooled for investment purposes. Investment income from the pooled investment account is allocated on the market value unit basis, and each fund subscribes to or disposes of units on the basis of the market value per unit at the beginning of the calendar quarter within which the transaction takes place. The unit participation of the funds at December 31, 1999 and 1998 is as follows:

	1999	*1998*
Unrestricted	8,573	4,001
Temporarily restricted	42,351	44,455
Permanently restricted	65,789	65,016
Advances on contracts	5,557	6,437
	122,270	119,909

Pooled investment activity on a per-unit basis was as follows:

	1999	*1998*
Unit value at beginning of year	$ 225.51	$ 220.30
Unit value at end of year	283.37	225.51
Total return on pooled investments	$ 57.86	$ 5.21

5. *Long-Term Debt:*

Long-term debt consisted of the following at December 31:

	1999	*1998*
Variable rate (6.3% at December 31, 1999) Massachusetts Industrial Finance Authority Series 1992A Bonds payable in annual installments through 2012	$ 890,000	$ 925,000
6.63% Massachusetts Industrial Finance Authority Series 1992B Bonds, payable in annual installments through 2012	1,175,000	1,230,000
5.8% The University Financing Foundation, Inc., payable in monthly installments through 2000	120,929	226,024
5.8% The University Financing Foundation, Inc., payable in monthly installments through 2002	138,167	186,346
	$2,324,096	$2,567,370

Subsequent to year-end, all existing debt was extinguished and new debt was issued (Note 10).

In 1992, the Laboratory issued $1,100,000 Massachusetts Industrial Finance Authority (MIFA) Series 1992A Bonds with a variable interest rate and $1,500,000 MIFA Series 1992B with an interest rate of 6.63%. Interest expense totaled $142,545 for the year ended December 31, 1999. The Series 1992 A and B Bonds mature on December 1, 2012 and are collateralized by a first mortgage on certain Laboratory property.

On March 17, 1998, the Laboratory entered into a ten-year interest rate swap contract in connection with the Series 1992A Bonds. This contract effectively fixes the interest rate at 6.30% through December 17, 2008. This contract was canceled as part of the extinguishment of debt and new debt issuance.

The agreements related to these bonds subject the Laboratory to certain covenants and restrictions. Under the most restrictive covenant of this debt, the Laboratory's operating surplus, exclusive of interest expense and depreciation expense, must be greater than or equal to 1.2 times all debt service payments, as defined by the agreement.

In 1996, the Laboratory borrowed $500,000 with an interest rate of 5.8% per annum from the University Financing Foundation, Inc. The interest expense for the year ended December 31, 1999 was $10,345. The loan matures in 2000 and is collateralized by 50,000 shares of a fixed income fund with a fair value of $576,000 at December 31, 1999.

In 1997, the MBL borrowed $250,000 with an interest rate of 5.8% per annum from the University Financing Foundation, Inc. The interest expense for the year ended December 31, 1999 was $9,541. This loan matures in 2002 and is collateralized by 19,440 shares of a fixed income mutual fund with a fair value of $223,949 at December 31, 1999.

The Laboratory has a line of credit agreement with a commercial bank from which it may draw up to $1,000,000. This line of credit has an interest rate of prime plus ½ percent. The line has no expiration date but is reviewed periodically by the bank for renewal. No amounts were outstanding under this agreement as of December 31, 1999 and 1998.

6. *Plant Assets:*

Plant assets consist of the following at December 31:

	1999	*1998*
Land	$ 702,908	$ 702,908
Buildings	33,702,485	33,082,164
Equipment	4,667,026	4,401,184
Construction in process	1,510,821	251,943
Total	40,583,240	38,438,199
Less: Accumulated depreciation	(20,464,515)	(18,902,028)
Plant assets, net	$20,118,725	$19,536,171

7. *Retirement Plan:*

The Laboratory participates in the defined contribution pension plan of TIAA-CREF (the "Plan"). The Plan is available to permanent employees who have completed two years of service. Under the Plan, the Laboratory contributes 10% of total compensation for each participant. Contributions amounted to $785,509 and $737,156 for the years ended December 31, 1999 and 1998, respectively.

8. *Pledges:*

Unconditional promises to give are included in the financial statements as pledges receivable and the related revenue is recorded in the appropriate net asset category. Unconditional promises to give are expected to be realized in the following periods:

	1999	*1998*
In one year or less	$3,974,385	$1,607,664
Between one year and five years	3,632,683	3,110,354
After five years	202,948	146,586
Total	7,810,016	4,864,604
Less: discount of $236,844 in 1999 and $301,588 in 1998 and allowance of $100,000 in 1999 and $100,000 in 1998	(336,844)	(401,588)
	$7,473,172	$4,463,016

9. *Postretirement Benefits:*

The Laboratory accounts for its postretirement benefits under Statement No. 106, "Employers' Accounting for Postretirement Benefits Other than Pensions," which requires employers to accrue, during the years that the employee renders the necessary service, the expected cost of benefits to be provided during retirement. As permitted, the Laboratory has elected to amortize the transition obligation over 20 years commencing on January 1, 1994.

The Laboratory's policy is that all current retirees and certain eligible employees who retired prior to June 1, 1994 will continue to receive postretirement health benefits. The remaining current employees will receive benefits; however, those benefits will be limited as defined by the Plan. Employees hired on or after January 1, 1995 will not be eligible to participate in the postretirement medical benefit plan.

The following tables set forth the Plan's funded status as of December 31:

	1999	*1998*
Benefit obligation at December 31	$ 2,091,057	$ 2,171,119
Fair value of plan assets at December 31	935,257	820,645
Funded status	$(1,155,800)	$(1,350,474)
Accrued benefit cost	$ (26,654)	$ (26,654)
Weighted-average assumptions as of December 31:		
Discount rate	6.75%	6.75%
Expected return on plan assets	7.25%	7.25%
Compensation increase rate	N/A	N/A
Benefit cost	209,430	210,339
Employer contribution	190,090	192,082
Benefits paid	129,589	109,404

For measurement purposes a 6.75% annual rate of increase in the per capita cost of covered health care benefits was assumed for 2000. The rate was assumed to decrease by half of 1.00% per year to 4.25% in 2006 and remain at that level thereafter. Pension plan assets consist of investment in a money market fund.

10. *Subsequent Event:*

On March 8, 2000, the Massachusetts Development Finance Agency issued on behalf of the Laboratory a series of Variable Rate Revenue Bonds (the "Bonds") in the amount of $10,200,000. The initial interest rate on the issue was 3.65% and the interest rate will be reset weekly. The bonds are scheduled to mature on February 1, 2030. The Laboratory is required to make interest payments only for the first five years. The first principal payment is due February 1, 2006 with incremental increases through maturity. The proceeds of these bonds are to be used to finance the capital improvements of the Laboratory's educational, research and administrative facilities, specifically the construction and equipping of the Environmental Sciences building. A portion of the proceeds were used to extinguish all of the Laboratory's capital obligations (Note 5).

As collateral for the bonds, the Laboratory has entered into a Letter of Credit Reimbursement Agreement which is set to expire on March 15, 2007. The Letter of Credit is in an amount sufficient to pay the aggregate principal amount of the bonds and up to forty-six days' interest.

MARINE BIOLOGICAL LABORATORY

SUPPLEMENTAL SCHEDULE OF FUNCTIONAL EXPENSES

for the year ended December 31, 1999

(with comparative totals for the year ended December 31, 1998)

	Research	*Instruction*	*Conferences*	*Other*	*Facilities Maintenance*	*Administration*	*Library Services*	*Research Services*	*Aquatic Research Services*	*1999 Total*	*1998 Total*
Salaries	$ 4,161,233	$ 430,734	$ 533,897	$ 641,771	$1,277,800	$1,818,067	$396,541	$340,938	$253,394	$ 9,854,375	$ 8,999,224
Fringe benefits	1,281,900	133,562	165,507	198,949	396,118	563,544	122,927	105,692	78,552	3,046,751	2,690,794
Professional services	130,517	314,881	6,159	37,024	16,877	192,129	7,976	8,280	—	713,843	602,815
Subcontracts	1,494,569	—	1,442,139	—	—	—	—	—	—	2,936,708	2,482,684
Equipment	464,213	43,482								507,695	804,109
Supplies	839,431	432,189	103,189	96,019	300,170	187,076	19,114	454,106	39,828	2,471,122	2,044,315
Travel	465,768	304,994	5,498	42,227	2,990	43,008	4,863	2,277	—	871,625	745,307
Serials	1,835	3,479	291	10,861	450	1,465	510,544	—	—	528,925	533,686
Utilities	1,011	366	218,766	889	635,853	134,312	—	561	1,552	993,310	1,091,602
Depreciation					1,562,487					1,562,487	1,505,696
Other	324,948	370,500	315,168	281,426	779,614	390,915	186,340	228,600	76,195	2,953,706	2,965,266
*Internal direct changes, net	424,939	978,273	(890,039)	142,303	(194,550)	32,021	42,241	(506,607)	(28,581)	—	—
Total	9,590,364	3,012,460	1,900,575	1,451,469	4,777,809	3,362,537	1,290,546	633,847	420,940	26,440,547	24,465,498
**Overhead expense allocations	4,557,281	1,729,827	352,267	3,846,304	(4,777,809)	(3,362,537)	(1,290,546)	(633,847)	(420,940)	—	—
Total expenses	$14,147,645	$4,742,287	$2,252,842	$5,297,773	—	—	—	—	—	$26,440,547	$24,465,498

*Internal direct charges are net expenses from one functional area to another based upon the actual use of goods and services.
**Overhead expense allocations include the costs allocated from the Laboratory's functional areas to the final cost objectives.

The accompanying notes are an integral part of the financial statements.

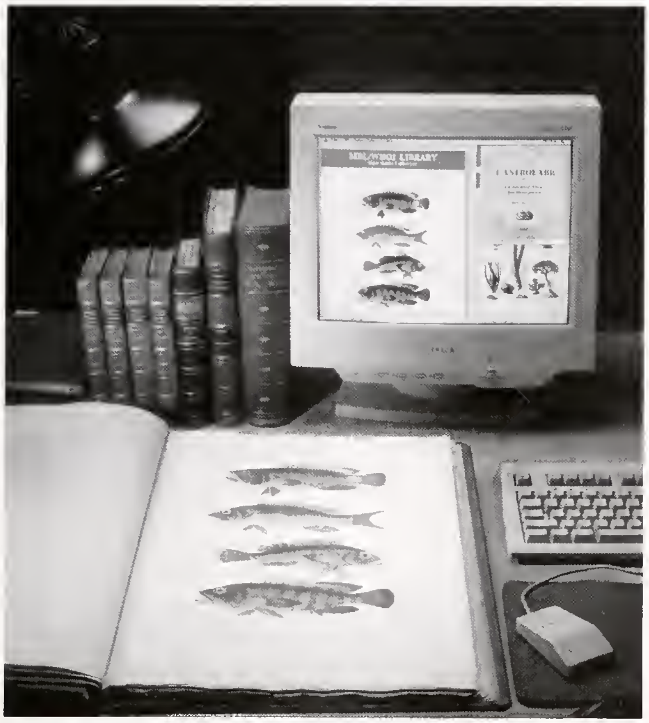

Report of the Library Director

The Library has been on the move since the fall of 1999, thanks to a long-overdue and welcome project to install air conditioning in the Library offices, reading rooms, and stacks. During the construction, each volume in the front stack was moved, alphabetized, and cleaned. When Library staff and patrons felt the first cool breezes of air conditioning in the stacks in early March, we quickly forgot about the inconveniences we encountered during this complex and time-consuming project. The construction was well worth the effort, and I am pleased to report that this summer Library patrons will find a clean, organized, and cool environment, which will be a comfort to them as well as a benefit to the collection.

The Traditional Library

At the brink of a new millennium we are focusing on the Library's traditional mission: acquiring, preserving, conserving, and distributing volumes in our collection. An article published recently in the *Library Journal* titled "Farewell to Alexandria: Not Yet!" reports on the number of publications that flow from an individual institution in relation to its library holdings, including citation productivity. The latter provides a rough measure of the scholarship quality of an individual institution. The statistics support the conclusion that the size of library holdings and institutional scholarly productivity go hand-in-hand. In this new era we need to continue to support acquisitions and preservation and conservation efforts as well as provide leadership in the creation of the new, technology-driven, scholarly environment.

Books and journals continue to be printed in numbers inconceivable even a half century ago. While the MBL/WHOI Library is providing new services and creating greater access to digital collections worldwide, we have not outlived print. Therefore, we must store it, preserve it, and make it available to our patrons.

Special Collections

The Library completed the inventory of several Special Collections in 1999. These include Charles Wilkes and his U.S. Exploring Expedition, Memoirs of the Museum of Comparative Zoology (Harvard) from 1865 to 1899, and the Harriman Alaska Expedition, the re-creation of which will become the basis of a public television special.

Science historian Dr. Garland Allen has also recently provided us with the final installment of a much-needed survey of valuable journals currently stored on the open shelves of the stacks that require preservation and secure storage.

The Journals

The Library solicited bids for a new serials vendor in 1999 and awarded the contract to RoweCom/Faxon. Our electronic resources were improved with the purchase of *Science Direct* from Elsevier. This product provides full-text access to the 107 titles that the Library subscribes to plus a transactional allowance for staff-limited access to all 1100 titles provided by Elsevier. Combined with the addition of 400 electronic journals published by Springer-Verlag, our digital library has increased substantially. We have also recently purchased *The Procaryotes*, an on-line version of the book series; *Marine Mammal Science*, volumes 1 to 13 on CD-ROM; and *Cambridge Scientific Abstracts Biological Sciences*, an interdisciplinary database offering abstracts and citations to a wide range of research in biomedicine, biotechnology, zoology, ecology, and some aspects of agriculture and veterinary science.

Harvard Depository

By early 1999, the space remaining to accommodate future growth of the journal collection in the stacks had been exhausted. This problem was further exacerbated by the installation of air conditioning ductwork in the area. Therefore, we needed to find remote storage for approximately 8000 journal volumes. Because room for collection growth was needed in the active stacks, it was decided that volumes of cancelled series in that section were prime candidates for storage. Holding records of the selected series were created for display in the on-line catalog, and an in-house inventory of each series and volume was created. By the end of the year, 5038 volumes had been prepared and shipped to the Harvard Depository for storage. An additional 3000 volumes, consisting of series for which we have purchased an online counterpart, were subsequently sent to the Depository. Although these volumes are no longer in Woods Hole, they may be retrieved within 24 hours from the Harvard Depository.

Document Delivery

A major accomplishment in Document Delivery was the creation and implementation of the web-based Inter-Library Loan (ILL) request form. Members of the Woods Hole scientific community may now request ILLs with this form rather than using the traditional paper form. Also, with the addition of full text electronic journals, desktop delivery of information is now a reality.

Cooperating Libraries

The Boston Library Consortium has received funding for a virtual catalog and interlibrary loan direct distance-borrowing project. Our Library is an early participant in the project, which will eventually make it possible for patrons to easily ascertain which of the 16 BLC Libraries has the desired material and then order it directly from that Library.

The National Library of Medicine's Medical Informatics course, sponsored by the Library, has expanded to two sessions, one in June and the other in October. The course continues to be very popular and successful with a focus on medical database design, Internet interfacing, and web page design.

The MBL/WHOI Library hosted the 25th Anniversary Conference of IAMSLIC (International Association of Aquatic and Marine Science Libraries and Information Centers) in October. The group was organized and held its first meetings in Woods Hole in 1975. Over the years it has grown from the original 25 East Coast Marine Science Librarians to the international organization of 295 members it is today.

The Library signed a new five-year contract with NOAA for the continuing operation and support of the NMFS Library at the Northeast Fisheries Center in Woods Hole and support of their serial and monograph collection held at the MBL.

Volunteers

Once again we thank Carol Winn and Millie and Bob Huettner for their tireless help and support with Rare Books and Special Collections. During 1999, more than 150 volumes were sent out for preservation under the Huettner's tutelage. Carol has provided cataloging support for esoteric material in languages from Old German to 19^{th} century Swedish.

—Catherine Norton

Bacteroides Happens
MICROBIAL DIVERSITY
1999

Educational Programs

Summer Courses

Biology of Parasitism: Modern Approaches

(June 10–August 13)

Directors

Pearce, Edward, Cornell University
Tschudi, Christian, Yale University School of Medicine

Faculty

Phillips, Meg, University of Texas Southwest, Dallas
Russell, David, Washington University Medical School
Scott, Phillip, University of Pennsylvania
Selkirk, Murray, Imperial College of Science, Technology and Medicine, United Kingdom
Sibley, David, Washington University Medical School
Ullu, Elisabetta, Yale University School of Medicine
Waters, Andrew P., University of Leiden, The Netherlands

Teaching Assistants

Appleby, Todd, Cornell University
Beatty, Wandy, Washington University Medical School
Giddings, Olivia, Washington University Medical School
Hussein, Ayman, Imperial College of Science, Technology and Medicine, United Kingdom
Kinch, Lisa, University of Texas Southwest
La Flamme, Anne Camille, Cornell University
Mair, Gunnar, Yale University School of Medicine
Mordue, Dana, Washington University Medical School
van der Wel, Annemarie, Biomedical Primate Research Centre, The Netherlands
Zaph, Colby, University of Pennsylvania

Lecturers

Andrews, Norma, Yale University School of Medicine
Bangs, James, University of Wisconsin, Madison
Beckers, Cornelis, University of Alabama, Birmingham
Beverley, Stephen, Washington University Medical School
Carucci, Daniel, Naval Medical Research Institute
Clark, Theodore, Cornell University
Cully, Doris, Merck & Co.
Day, Karen, Oxford University, United Kingdom
Dell, Anne, Imperial College of Science, Technology and Medicine, United Kingdom
Doolan, Denise, Naval Medical Research Institute
Englund, Paul, Johns Hopkins University School of Medicine
Finkelman, Fred, Veterans Administration Medical Center
Frevert, Ute, New York University Medical Center
Goldberg, Daniel, Washington University Medical School
Grencis, Richard K., University of Manchester, United Kingdom
Gull, Keith, University of Manchester, United Kingdom
Hajduk, Steve, University of Alabama, Birmingham
Hedstrom, Liz, Brandeis University
Hunter, Christopher, University of Pennsylvania
Johnson, Patricia, University of California, Los Angeles
Komuniecki, Richard, University of Toledo
Kopf, Manfred, Basel Institute for Immunology, Switzerland
Langhorne, Jean, Imperial College of Science, Technology and Medicine, United Kingdom
Long, Carol, National Institutes of Health
Matthews, Keith, University of Manchester, United Kingdom
Mottram, Jeremy, University of Glasgow, United Kingdom
Pearlman, Eric, Case Western Reserve University
Rathod, Pradip, Catholic University of America
Roos, David, University of Pennsylvania
Sacks, David, National Institutes of Health
Scherf, Artur, Institut Pasteur, France
Sher, Alan, National Institutes of Health
Sollner-Webb, Barbara, Johns Hopkins University School of Medicine
Tarleton, Rick, University of Georgia
Turco, Sam, University of Kentucky Medical Center
Ullman, Buddy, Oregon Health Sciences University
Wirth, Dyann, Harvard School of Public Health

Workshop Coordinators

Cooper, Peter, National Institutes of Health
Ealich, Steve, Cornell University
LoVerde, Philip, State University of New York, Buffalo

Course Assistants

Chapple, Taylor, Boston University
Chipperfield, Caitlin Nadine, Cornell University

Students

Angeli, Véronique, Pasteur Institute, France
Aviles, Hernan, Indiana State University
Barragan, Antonio, Karolinska Institute, Sweden
Batchelor, Adrian, Walter and Eliza Hall Institute, Australia
Bishop, Joseph, University of Alabama, Birmingham
Djimde, Abdoulaye, University of Maryland
Dobbin, Caroline, University of Technology, Sydney, Australia
Falcone, Franco, University of Edinburgh, United Kingdom

Gavrilescu, Cristina, Cornell University
Jones, Stacy, University of Virginia
Montgomery, Jacqui, Walter and Eliza Hall Institute, Australia
Santori, Isabel, University of Buenos Aires, Argentina
Sodré, Cátia, Universidade Federal do Rio de Janeiro, Brazil
Stern, Leah, University of California, San Francisco
Toe, Laurent, World Health Organization, West Africa
Wang, Zefeng, Johns Hopkins University

Embryology: Concepts and Techniques in Modern Developmental Biology

(June 13–July 24)

Directors

Bronner-Fraser, Marianne, California Institute of Technology
Fraser, Scott, California Institute of Technology

Faculty

Adoutte, Andre, University of Paris-Sud, France
Blair, Seth S., University of Wisconsin, Madison
Carroll, Sean, University of Wisconsin, Madison
Collazo, Andres, House Ear Institute
Ettensohn, Charles, Carnegie Mellon University
Harland, Richard, University of California, Berkeley
Hartenstein, Volker, University of California, Los Angeles
Henry, Jonathan, University of Illinois
Krumlauf, Robb, National Institute for Medical Research, United Kingdom
Martindale, Mark, Kewalo Marine Laboratory
Niswander, Lee, Memorial Sloan-Kettering Cancer Center
Rothman, Joel, University of California, Santa Barbara
Saunders, John Jr., Marine Biological Laboratory
Shankland, Martin, University of Texas, Austin
Wray, Gregory, State University of New York, Stony Brook
Zeller, Robert, University of California, San Diego

Teaching Assistants

Baker, Clare, California Institute of Technology
Baker, Julie, University of California, Berkeley
Georgopoulos, Katia, Harvard University
Hartenstein, Amelia, University of California, Berkeley
Kourakis, Matthew, University of Chicago
Kuhlman, Julie, Memorial Sloan-Kettering Cancer Center
Lane, Mary Ellen, University of Massachusetts Medical Center
Lartillot, Nicholas, Universite Paris-Sud, France
Maduro, Morris, University of California, Santa Barbara
Mariani, Francesca, University of California, Berkeley
Micchelli, Craig, University of Wisconsin, Madison
Ober, Elke, Max-Planck-Institute, Germany
Pepicelli, Carmen, Harvard University
Pizette, Sandrine, Memorial Sloan-Kettering Cancer Center
Trainor, Paul, Medical Research Council, United Kingdom
Wallingford, John, University of California, Berkeley
Walsh, Emily, University of California, San Francisco
Wilson, Valerie, University of Edinburgh, United Kingdom

Lecturers

Davidson, Eric, California Institute of Technology
Heasman-Wylie, Janet, University of Minnesota School of Medicine
Holland, Linda, University of California, San Diego
Hopkins, Nancy, Massachusetts Institute of Technology
Levine, Michael, University of California, Berkeley
Rosenthal, Nadia, Massachusetts General Hospital–East
Rothenberg, Ellen, California Institute of Technology
Soriano, Philippe, Fred Hutchinson Cancer Research Center
Stern, Claudio, Columbia University
Tabin, Clifford, Harvard University Medical School
Wylie, Christopher C., University of Minnesota Medical School

Course Assistants

Stringer, Kristen, Marine Biological Laboratory
Wylie, Matthew, Marine Biological Laboratory

Lab Assistant

Wylie, Sara, Marine Biological Laboratory

Students

Basch, Martin, California Institute of Technology
Casanueva, Olivia, University of Chicago
Clements, Wilson, University of Washington
Corson, Laura, Ludwig Institute for Cancer Research
Ewald, Andrew, California Institute of Technology
Freistadt, Marion, Louisiana State University Medical Center
Glavic, Alvaro, University of Chile, Chile
Gould, Thomas, Wake Forest University Medical School
Junghlut, Benno, University of Tübingen, Germany
Li, Dongling, University of Texas, Austin
Lwigale, Peter, Kansas State University
Meyers, Jason, University of Virginia
Mui, Stina, University of California, San Diego
Nance, Jeremy, University of Arizona
Panopoulou, Georgia, Max-Planck-Institute, Germany
Paul, Angelika, University of Otago, New Zealand
Pfeiffer, Sven, National Institute for Medical Research, United Kingdom
Pizer, Margaret, State University of New York, Stony Brook
Ragusa, Maria, Alberto Monroy Foundation, Italy
Robertson, Christie, University of Washington
Saúde, Leonor, National Institute for Medical Research, United Kingdom
Spengler, Tatjana, Universite Paris, France
Sumanas, Saulius, University of Minnesota
Vukovich, Wolfgang, Max-Planck-Institute, Germany
Zigler, Kirk, Duke University

Microbial Diversity *(June 13–July 29)*

Directors

Leadbetter, Edward, University of Connecticut
Salyers, Abigail, University of Illinois, Urbana

Faculty

Dawson, Scott, University of California, Berkeley
Hanselmann, Kurt, University of Zurich, Switzerland
Holmes, Dawn, University of Massachusetts, Amherst
Kenyon, Sarah, Forsyth Dental Center
Klappenbach, Joel, Michigan State University
Plugge, Caroline M., Wageningen Agricultural University, The Netherlands
Schauder, Rolf, Frankfurt, Germany

Lecturers

Blake, Ruth, Yale University
Emerson, David, ATCC
Farrand, Stephen, University of Illinois, Urbana
Fouke, Bruce, University of Illinois, Urbana
Hayes, John, Woods Hole Oceanographic Institution
Leadbetter, Jared, University of Iowa
Lovely, Derek, University of Massachusetts
Metcalf, William, University of Illinois
Newman, Dianne, Harvard University
O'Neill, Scott, Yale University
Paster, Bruce, Forsyth Dental Center
Ruby, Ned, University of Hawaii
Rummel, John, NASA
Schmidt, Thomas, Michigan State University
Shoemaker, Nadja, University of Illinois, Urbana
Sogin, Mitchell, Marine Biological Laboratory
Stein, Jeffrey, Quorum Pharmaceuticals
Teske, Andreas, Woods Hole Oceanographic Institute
Visscher, Pieter, University of Connecticut, Avery Point
Waterbury, John, Woods Hole Oceanographic Institute
Whitman, William, University of Georgia
Young, Lily, Rutgers University

Course Assistants

Ament, Nell, Marine Biological Laboratory
White, Kalina, University of Connecticut

Students

Aislabie, Jacqueline, Landcare Research, New Zealand
Bedard, Donna, General Electric Corporate Research Center
Casillas, Lilliam, Autonomous University of the State of Puebla, Mexico
Christner, Brent, Ohio State University
Chyba, Christopher, SETI Institute
Dollhopf, Sherry, Michigan State University
Gaidos, Eric, California Institute of Technology
Gillor, Osnat, The Hebrew University, Israel
Gregory, Kelvin, University of Iowa
Niggemyer, Allison, University of Idaho
Norris, Tracy, University of Oregon
Nyholm, Spencer, University of Hawaii
Pomper, Barbara, Max-Planck-Institute, Germany
Rukayadi, Yaya, Bogor Agricultural University, Indonesia
Salmassi, Tina, California Institute of Technology
Shipman, Joseph, University of Illinois, Urbana
Tuit, Caroline, Massachusetts Institute of Technology
Van Lith, Yvonne, Swiss Federal Institute of Technology, Switzerland
Warren, Lesley, McMaster University, Canada
Zopfi, Jakob, Max-Planck-Institute, Germany

Neural Systems & Behavior *(June 13–August 6)*

Directors

Weeks, Janis, University of Oregon
Zakon, Harold, University of Texas, Austin

Faculty

Barnes, Carol, University of Arizona, Tucson
Calabrese, Ronald L., Emory University
Carr, Catherine, University of Maryland
French, Kathleen, University of California, San Diego
Glanzman, David, University of California, Los Angeles
Hooper, Scott, Ohio University
Hyson, Richard, Florida State University
Kristan, William, University of California, San Diego
Levine, Richard, University of Arizona, Tucson
McNaughton, Bruce, University of Arizona, Tucson
Muir, Gillian, University of Saskatchewan, Canada
Nadim, Farzan, Rutgers University
Nusbaum, Michael, University of Pennsylvania School of Medicine
Prusky, Glen, University of Lethbridge, Canada
Roberts, William, University of Oregon
Wenning-Erxleben, Angela, Universität Konstanz, Germany
Wood, Emma, University of Edinburgh, Scotland

Teaching Assistants

Armstrong, Cecilia, University of Oregon
Blitz, Dawn Marie, University of Chicago
Bower, Mark, University of Arizona, Tucson
Chitwood, Raymond, University of Texas, San Antonio
Few, Preston, University of Texas, Austin
Gamkrelidze, Georgi, Lucent Technology
Gerrard, Jason, University of Arizona, Tucson
Golowasch, Jorge, Brandeis University
Hill, Andrew, Emory University
Lenzi, David, University of Oregon
McAnelly, Lynne, University of Texas
Melville, Johnathan, Oregon State University
Murphy, Geoffrey, University of California, Los Angeles

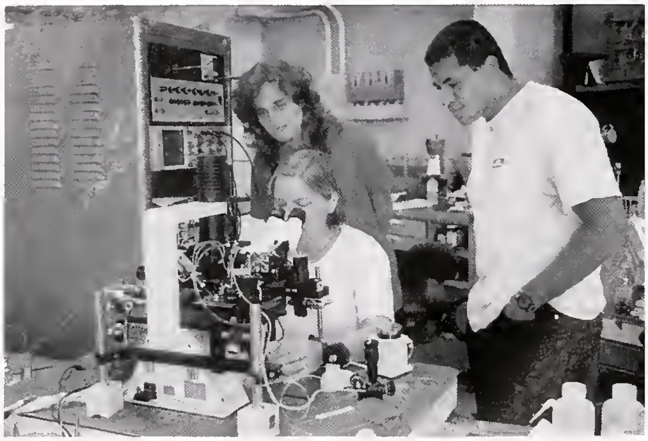

Sandstrom, David, University of Arizona, Tucson
Shaw, Brian, The Neurosciences Institute
Villareal, Greg, University of California, Los Angeles
Yong, Rocio, University of California, Los Angeles
Zee, Michelle, University of Oregon
Zirpel, Lance, University of Utah School of Medicine

Lecturers

Augustine, George, Duke University Medical Center
Barlow, Robert, State University of New York Health Science Center
Beer, Randall, Case Western Reserve University
Bodznick, David, Wesleyan University
Cohen, Avis, University of Maryland
Davis, Graeme, University of California, San Francisco
Katz, Paul, Georgia State University

Scholar-in-Residence

Abbott, Lawrence, Brandeis University
Nishikawa, Kiisa C., Northern Arizona University
Wilson, Martin, University of California, Davis

Lab Technician

Stengel, Keith, Neuralynx Inc.

Course Assistants

Almers, Lucy, Marine Biological Laboratory
Stell, Brandon, Marine Biological Laboratory

Students

Baca, Serapio, University of California, San Diego
Beenhakker, Mark, University of Pennsylvania
Cain, Shaun, University of North Carolina, Chapel Hill
Chance, Frances, Brandeis University
Coddington, Emma, Oregon State University
Crisp, Kevin, University of Minnesota
Franks, Kevin, University of California, San Diego
Greenwood, Anna, Stanford University
Hausrath, Cassandra, University of Virginia
Kao, Mimi, University of California, San Francisco
Knittel, Laura, Oregon Health Sciences University
Krieger, Patrik, Karolinska Institutet, Sweden
Maravall, Miguel, Cold Spring Harbor Laboratory
Maruska, Karen, Florida Institute of Technology
Paradis, Suzanne, University of California, San Francisco
Rao, Shankaranar, National Centre for Biological Sciences, India
Ritt, Jason, Boston University
Suadicani, Sylvia, Albert Einstein College of Medicine
Wainger, Brian, Columbia University
Wissman, Anne Marie, University of Washington

Neurobiology (June 13–August 14)

Directors

Banker, Gary, Oregon Health Sciences University
Madison, Daniel, Stanford University Medical Center

Section Directors

Greenberg, Michael, Children's Hospital
Smith, Stephen, Stanford University School of Medicine

Faculty

Delaney, Kerry, Simon Fraser University, Canada
Edmonds, Brian, University of California, Los Angeles
Feller, Marla, National Institutes of Health
Ginty, David, Johns Hopkins University School of Medicine
Griffith, Leslie, Brandeis University
Hanson, Phyllis, Washington University School of Medicine
Hart, Anne, Massachusetts General Hospital
Haydon, Philip, Iowa State University
Khodakhah, Kamran, University of Colorado School of Medicine
Reese, Thomas, National Institutes of Health
Schweizer, Felix, University of California, Los Angeles
Shamah, Steven, Children's Hospital
Smith, Carolyn, National Institutes of Health
Terasaki, Mark, University of Connecticut Health Center
Thompson, Stuart, Stanford University
Van Vactor, David, Harvard University Medical School

Teaching Assistants

Boies, Sarah, Brandeis University
Brinkhaus, Heike, Friedrich Miescher Institute, Switzerland
Imani, Farzin, University of Colorado School of Medicine
McQuiston, Rory, Duke University Medical Center
Pereda, Alberto, Allegheny University of the Health Sciences
Winters, Christine, National Institutes of Health

Lecturers

Barres, Ben, Stanford University School of Medicine
Birren, Bruce, Massachusetts Institute of Technology
Burden, Steven, New York University
Ehrlich, Barbara, Yale University School of Medicine
Ellisman, Mark, University of California, San Diego
Faber, Donald, Allegheny University of the Health Sciences
Flanagan, John, Harvard University Medical School
Greene, Lloyd, Columbia University College of Physicians and Surgeons
Hanson, Roland, Arizona State University
Heuser, John, Washington University Medical School
Lipscombe, Diane, Brown University
Llinas, Rudolfo, New York University
Nicoll, Roger, University of California, San Francisco
Ogden, David, National Institute for Medical Research, United Kingdom
Rosenberg, Robert, University of North Carolina, Chapel Hill
Li-Huei, Tsai, Harvard University Medical School
Ziff, Edward, New York University Medical Center
Zimmerberg, Joshua, National Institutes of Health
Zimmerman, Anita, Brown University

Course Assistants

Baughman, Kenneth, Boston University
Chiu, Delia, Stanford University

Students

Abenavoli, Allesandra, Scientific Institute San Raffael, Italy
Diana, Marco, Max-Planck-Institute, Germany
Haapasalo, Annakaisa, A.I. Virtanen Institute, Finland
Hrabetova, Sabina, New York University Medical Center
Matsui, Ko, University of Tokyo, Japan
Samuel, Aravinthan, Harvard University
Schmolesky, Matthew, University of Utah
Smith, Gregory, Princeton University
Spotts, James, Children's Hospital
Vollrath, Melissa, Baylor College of Medicine
Yoon, Miri, Northwestern University
Yu, Xiang, Medical Research Council, United Kingdom

Physiology: The Biochemical and Molecular Basis of Cell Signaling (June 13–July 24)

Directors

Garbers, David, University of Texas Southwestern Medical Center
Reed, Randall, Johns Hopkins University School of Medicine

Faculty

Beuve, Annie, University of Texas Southwestern Medical Center
Munger, Steven, Johns Hopkins University School of Medicine
Prasad, Brinda, Johns Hopkins University School of Medicine
Quill, Timothy A., University of Texas Southwestern Medical Center
Robinson, Susan W., University of Texas Southwestern Medical Center
Wang, Song S., Johns Hopkins University School of Medicine
Wedel, Barbara, University of Texas Southwestern Medical Center
Zhao, Haiqing, Johns Hopkins University School of Medicine
Zielinski, Raymond, University of Illinois, Urbana

Lecturers

Brady, Scott, University of Texas Southwestern Medical Center
Buck, Linda, Harvard University Medical School
Clapham, David, Harvard University Medical School
Corey, David, University of Texas Southwestern Medical Center
Devreotes, Peter, Johns Hopkins University School of Medicine
Dixon, Jack, University of Michigan Medical School
Flanagan, John, Harvard University Medical School
Furlow, John, University of California, Davis
Ginty, David, Johns Hopkins University School of Medicine
Huganir, Richard, Johns Hopkins University School of Medicine
Hurley, James, National Institutes of Health
Kirschner, Marc, Harvard University Medical School
Li, Min, Johns Hopkins University School of Medicine
Ranganathan, Rama, University of Texas Southwestern Medical Center
Yanagisawa, Masashi, University of Texas Southwestern Medical Center

Course Coordinator

Rossi, Kristen, University of Texas Southwestern Medical Center

Course Assistant

Kirby, Melissa, Marine Biological Laboratory

Students

Chen, Lihong, University of North Carolina, Chapel Hill
D'Souza, Jacinta, Tata Institute of Fundamental Research, India
van Drogen, Frank, Swiss Institute for Experimental Cancer Research, Switzerland
Duncan, Tod, Imperial Cancer Research Fund, United Kingdom
Fort, Alfredo, Albert Einstein College of Medicine
Franco, Peter, Harvard University Medical School
Ganguly, Anindita, University of Utah
Han, Qin, University of California, San Francisco
Holdaway-Clarke, Terena, University of Massachusetts, Amherst
Hom, Erik, University of California, San Francisco
Jessani, Nadim, Scripps Research Institute
Kimbell, Jennifer, University of Hawaii
Macias, Chanda, Howard University
March, Tony, University of Idaho
Mazzatenta, Andrea, University of Pisa, Italy
Narayan, Sujatha, Bryn Mawr College
Nzambi, Eduardo, Howard University
O'Neill, Forest, University of California, Santa Barbara
Purves, Dianne, California State University, Sacramento
Rao, Anita, University of Maryland
Sawai, Satoshi, Tohoku University, Japan
Sutton, Timothy, Indiana University
Tefft, Denise, University of Southern California
Tidwell, Judy, Wake Forest University
Varshney, Anurag, National Centre for Biological Sciences, India
Welman, Arkadiusz, Friedrich Miescher Institute, Switzerland
Wen, Ying, University of North Carolina, Chapel Hill
Woo, Caroline, Albert Einstein College of Medicine

Special Topics Courses

Analytical and Quantitative Light Microscopy (May 6–May 14)

Directors

Sluder, Greenfield, University of Massachusetts Medical School
Wolf, David, University of Massachusetts Medical School

Faculty

Amos, William B., Medical Research Council, United Kingdom
Cardullo, Richard, University of California, Riverside
Chaisson, Eric, Tufts University

Gelles, Jeff, Brandeis University
Hinchcliffe, Edward, University of Massachusetts Medical School
Inoué, Shinya, Marine Biological Laboratory
Lippincott-Schwartz, Jennifer, National Institutes of Health
Oldenbourg, Rudolf, Marine Biological Laboratory
Silver, Randi, Cornell University Medical College
Spring, Kenneth, National Institutes of Health
Swedlow, Jason, University of Dundee, Scotland
Tuft, Richard, University of Massachusetts Medical School

Teaching Assistant

Thompson, Christine, University of Massachusetts Medical School

Course Coordinator

Miller, Frederick, University of Massachusetts Medical School

Students

Bearman, Gregory, Jet Propulsion Laboratory
Botvinick, Elliot, University of California, San Diego
Bowden, Emma, Georgetown University
Brooks, John, Bio-Rad Microscience
Bulseco, Dylan, University of Massachusetts Medical School
Carrero, Jenny, Unilever Research U.S., Inc.
Danuser, Gaudenz, Swiss Federal Institute of Technology, Switzerland
Faulkner, Nicole, University of Massachusetts Medical School
Heynen, Susanne, University of California, San Diego
Hochegger, Helfrid, Imperial Cancer Research Fund, United Kingdom
Holbrook, Pamela, National Institutes of Health
Holz, Ronald, University of Michigan
Hughes Fulford, Millie, University of California, San Francisco
Keating, Christine, Penn State University
Koehler, Julia, Whitehead Institute
Kreitzer, Geri, Cornell University Medical College
Kwan, Kristen, Harvard University Medical School
Levin, Max, Wallenberg Laboratory for Cardiovascular Research, Sweden
Lindberg, Seth, Procter & Gamble Co.
McDonald, John, Mayo Clinic Scottsdale
Novoradovskaya, Natalia, Stratagene
Pfister, Kevin, University of Virginia
Reichelt, Stefanie, University of London, United Kingdom
Roberts, Theresa, National Institutes of Health
Rohatgi, Rajat, Harvard University Medical School
Shirani, Jamshid, Albert Einstein College of Medicine
Shonn, Marion, University of California, San Francisco
Tanphaichitr, Nongnuj, Loeb Health Research Institute, Canada
Tse, William, Children's Hospital
Van Dover, Cindy Lee, College of William and Mary
Yarovoi, Serge, University of Massachusetts Medical School

Frontiers in Reproduction: Molecular and Cellular Concepts and Applications

(May 24–July 4)

Directors

Hunt, Joan, University of Kansas Medical Center
Mayo, Kelly, Northwestern University
Schatten, Gerald, Oregon Health Sciences University

Faculty

Ascoli, Mario, University of Iowa
Bowen, Jeffery A., University of Kansas Medical Center
Camper, Sally, University of Michigan Medical School
Croy, Barbara Anne, University of Guelph, Canada
Handel, Mary Ann, University of Tennessee
Herr, John C., University of Virginia School of Medicine
Hunt, Patricia A., Case Western Reserve University
Jaffe, Laurinda, University of Connecticut Health Center
Petroff, Margaret, University of Kansas Medical Center
Shupnik, Margaret, University of Virginia Health Sciences Center
Simerly, Calvin, Oregon Regional Primate Research Center
Terasaki, Mark, University of Connecticut Health Center
Trimarchi, James, Marine Biological Laboratory
Weigel, Nancy, Baylor College of Medicine

Teaching Assistants

Aldrich, Carrie, University of Chicago
Berard, Mark, University of Michigan
Cunningham, Meghan, Georgetown University
Diekman, Alan, University of Virginia Health Sciences Center
Giusti, Andrew, University of Connecticut Health Sciences Center
Greenwood, Janice, University of Guelph, Canada
Hinkle, Beth Anne, University of Connecticut Health Sciences Center
Hodges, Craig, Case Western Reserve University
Mukherjee, Abir, Northwestern University
Nakamura, Kazuto, University of Iowa Medical School
Phillips, Teresa, University of Kansas Medical Center
Resnick, Eileen, University of Virginia Health Sciences Center
Rowan, Brian, Baylor College of Medicine
Runft, Linda, University of Connecticut Health Center
Westbrook, Anne, University of Virginia Health Sciences Center

Lecturers

Behringer, Richard, University of Texas
Campbell, Keith, PPL Therapeutics, Scotland
Carroll, David, University of California, Santa Barbara
Crowley, William, Massachusetts General Hospital
Dominko, Tanja, Oregon Regional Primate Research Center
Fazleabas, Asgi, University of Illinois
Handyside, Alan, St. Thomas' Hospital, United Kingdom
Hennighausen, Lothar, National Institutes of Health
Hewitson, Laura, Oregon Regional Primate Research Center
Johnson, Peter M., University of Liverpool Medical School, United Kingdom
Keefe, David, Marine Biological Laboratory
Kopf, Greg, University of Pennsylvania Medical Center
Ober, Carole, University of Chicago
Orth, Joanne, Temple University School of Medicine
Pederson, Roger, University of California, San Francisco
Pollard, Jeffrey W., Albert Einstein College of Medicine
Richards, JoAnne, Baylor College of Medicine
Ruderman, Joan, Harvard University Medical School
Shenker, Andrew, Children's Memorial Hospital
Tilly, Jonathan L., Massachusetts General Hospital
Wessel, Gary, Brown University
Woodruff, Teresa, Northwestern University

Course Administrator

Emme, Michelle, Oregon Health Sciences University

Chief Course Coordinator

Payne, Christopher, Oregon Health Sciences University

Course Coordinators

Daggett, Melissa, University of Kansas Medical Center
McMullen, Michelle, Northwestern University

Students

Akhmedkhanov, Arslan, New York University School of Medicine
Betts, Dean, University of Guelph, Canada
Bos-Mikich, Adriana, Fundação Universitária de Endocrinologia e Fertilidade, Brazil
Buhimschi, Irina, University of Maryland
El Guiziry, Dalal, Alexandria University, Egypt
Johanputra, Vaidehi, All India Institute of Medical Sciences, India
Johnson, Quinton, University of the Western Cape
Lue, Yanhe, Harbor-University of California, Los Angeles, Medical Center
Marín Bivens, Carrie, University of Massachusetts, Amherst
Mendeluk, Gabriela, University of Buenos Aires, Argentina
Natesampillai, Sekar, University of Virginia
Ollero, Mario, Harvard University Medical School
Paidas, Michael, New York University School of Medicine
Pritts, Elizabeth, Yale University School of Medicine
Sprague, David, Texas A&M University
Witlin, Andrea, University of Texas Medical Branch, Galveston

Medical Informatics *(May 30–June 5)*

Director

Masys, Daniel, University of California, San Diego

Faculty

Cimino, James, Columbia University
Friedman, Charles, University of Pittsburgh
Hightower, Allen, Centers for Disease Control and Prevention
Hripcsak, George, Columbia-Presbyterian Medical Center
Kingsland, Lawrence, National Library of Medicine
Landsman, David, National Library of Medicine
Lindberg, Donald D.A.B., National Library of Medicine
Safran, Charles, Center for Clinical Computing
Sengupta, Soumitra, Columbia University
Starren, Justin, Columbia University

Students

Adams, Martha, Duke University
Babbitt, Patricia, University of California, San Francisco
Barclay, Donald, Houston Academy of Medicine
Bernhard, Jeffrey, University of Massachusetts Medical School
Finley, Allen, Dalhousie University, Canada
Goldstein, Cynthia, Tulane University Medical Library
Lin, Chen-Tan, University of Colorado Health Sciences Center
Lindberg, Don, Regenstrief Institute
Lyons, Amy, University of Buffalo Health Sciences Library
Mahoney, Diane, Hebrew Rehabilitation Center for Aged
Markovitz, Barry, Washington University
McGrath, St. John, Tufts University School of Medicine
Meyers, Arlen, University of Colorado Health Sciences Center
Mullaly-Quijas, Peggy, University of Missouri, Kansas City
Pelok, Scott, University of Michigan
Pifer, Eric, University of Pennsylvania Health System
Robinson, Judith, Eastern Virginia Medical School
Rosman, Alan, Bronx Veteran's Administration Medical Center
Sack, Jean, Johns Hopkins University
Sarchet, Patricia, University of Buffalo Health Sciences Library
Seago, Brenda, Virginia Commonwealth University
Sibley, Deborah, University of Massachusetts Medical School
Stroman, Rosalie, National Institutes of Health Library
Swanson, Sandra, Cook Institute of Research and Education
Thompson, Laurie, State University of New York Health Science Center, Syracuse
Tomlinson, Louise, Morehouse School of Medicine
Travers, Robin, Boston University School of Medicine
Turman, Lynne, Virginia Commonwealth University
Volpp, Bryan, Veterans Affairs Medical Center
Warlick, Becky, Duke University Medical Center

Medical Informatics *(October 3–October 9)*

Director

Cimino, James, Columbia University

Faculty

Bakken, Suzanne, Columbia University
Canese, Kathi, National Library of Medicine
Cimino, Chris, Albert Einstein College of Medicine
Friedman, Charles, University of Pittsburgh
Hightower, Allen, Centers for Disease Control and Prevention
Jenders, Robert, Columbia University
Lindberg, Donald, National Library of Medicine
Masys, Daniel, University of California, San Diego
Safran, Charles, Center for Clinical Computing
Starren, Justin, Columbia University
Wheeler, David, National Library of Medicine

Students

Beidas, Sary, Prince George's Hospital Center
Boyle, Marian, University of Florida
Calarco, Pascal, Virginia Commonwealth University
Chong, Lisa, *Science* magazine
Cohen, Arlene, University of Guam
Coster, Trinka, US Army Medical Research Institute
Delia, Catherine, George Washington University
Dimitroff, Alexandra, University of Wisconsin–Milwaukee
Doyle, Jacqueline, Samaritan Health Systems, Phoenix
Eaton, Elizabeth, Tufts University Health Sciences Library

Feldman, Marc, University of Alabama, Birmingham
Francis, Marcia, Idaho State University
Fuller, Howard, University of California, San Francisco
Hogan, Linda, University of Pittsburgh
Hornby, Kathryn, University of British Columbia, Canada
Knight, Barbara, University of North Dakota
Kufreja, Neera, Cook County Hospital
Linton, Anne, George Washington University
Livingston, Jill, University of Connecticut Health Center
Massanari, Mike, Wayne State University
Miller, Stephen, Massachusetts General Hospital/Martha's Vineyard Hospital
Parada, Jorge, Cook County Hospital
Reilly, James, State University of New York Health Science Center, Brooklyn
Strassner, Howard, Rush-Presbyterian-St. Luke's Medical Center
Swanton, James, Harlem Hospital Center
Swiatek-Kelley, Janice, Bridgeport Hospital
Teal, Janis, University of New Mexico
Walker, James, Penn State College of Medicine
Wu, Carol, New York University School of Medicine
Wulff, Judith, University of Louisville
Yue, Cheung, MetroHealth Medical Center

Methods in Computational Neuroscience
(August 1–August 28)

Directors

Bialek, William, NEC Research Institute
van Steveninck, Rob de Ruyter, NEC Research Institute

Faculty

Abbott, Lawrence, Brandeis University
Colby, Carol, University of Pittsburgh
Dan, Yang, University of California, Berkeley
Delaney, Kerry, Simon Fraser University, Canada
Doupe, Allison, University of California, San Francisco
Ermentrout, Bard, University of Pittsburgh
Hopfield, John, Princeton University
Johnston, Daniel, Baylor College of Medicine
Kelley, Darcy, Columbia University
Kleinfeld, David, University of California, San Diego
Kopell, Nancy, Boston University
Marder, Eve, Brandeis University
Meister, Markus, Harvard University
Miller, K. D., University of California, San Francisco
Mitra, Partha, AT&T Bell Laboratories
Rieke, Fred, University of Washington
Seung, H. Sebastian, Massachusetts Institute of Technology
Sigvardt, Karen, University of California, Davis
Solla, Sara A., Northwestern University
Sompolinsky, Haim, Hebrew University of Jerusalem, Israel
Tank, David, AT&T Bell Laboratories
Tishby, Naftali, Hebrew University of Jerusalem, Israel
Zucker, Steven, Yale University

Teaching Assistants

Aguera y Arcas, B., Princeton University
Jensen, Roderick, Wesleyan University
Koberle, Roland, Universidade di Sao Paulo, Brazil
Lewen, Geoffrey David, NEC Research Institute
Nemenman, I., Princeton University
White, John, Boston University

Lecturers

Baylor, Denis, Stanford University Medical Center
Laughlin, Simon Barry, University of Cambridge, United Kingdom
Logothetis, Nikos, Max-Planck-Institute for Biological Cybernetics, Germany
Srinivasan, Mandyam V., Australian National University, Australia

Course Coordinator

Stogryn, Krista, Marine Biological Laboratory

Students

Borisyuk, Alla, New York University
Buss, Robert, McGill University, Canada
Cang, Jianhua, University of Virginia
Chechik, Gal, Hebrew University of Jerusalem, Israel
Cowen, Stephen, University of Arizona
Dumont, Sophie, Princeton University
Garcia de Polavieja, Gonzalo, University of Cambridge, United Kingdom
Jacobson, Gilad, Hebrew University of Jerusalem, Israel
Karbowski, Jan, Boston University
Kefalov, Vladimir, Boston University School of Medicine
Kozloski, James, Columbia University
Laing, Carlo, University of Pittsburgh
Mayraz, Guy, University College London, United Kingdom
Mazurek, Mark, University of Washington
Naylor, David, University of California, Los Angeles
Petersen, Ras, International School of Advanced Studies, Italy
Prescott, Steven, McGill University, Canada
Rubin, Jonathan, Ohio State University
Spence, Andrew, Cornell University
Still, Susanne, University of Zürich, Switzerland
Wittenberg, Gayle, Princeton University
Zeddies, David, Northwestern University

Microinjection Techniques in Cell Biology
(May 18–May 25)

Director

Silver, Robert B., Marine Biological Laboratory

Faculty

Cousins, Susan, Cornell University
Klaessig, Suzanne, Cornell University
Kline, Douglas, Kent State University
Mehlmann, Lisa, University of Connecticut Health Center
Shelden, Eric, University of Michigan

Teaching Assistant

Warnke, Honey, University of Maine

Students

Araujo, Loraine, State University of Rio de Janeiro, Brazil
Cohen, David, Oregon Health Sciences University
Dabrowski, Konrad, Ohio State University
James, Marianne, Massachusetts General Hospital
Koulen, Peter, Yale University
Kozek, Wieslaw, University of Puerto Rico
Kuan, Chia-Yi, Yale University
Lahti, Jill, St. Jude Children's Research Hospital
Larkin, Janet, Barnard College

Li, Bin, University of California, San Francisco
McGowan, Francis, Harvard University Medical School
Nemoto, Yasuo, Yale University
Nusser, Kevin, Oregon Regional Primate Research Center
Pai, Vinay, Florida State University
Rueda, Angélica, Centro de Investigacion y de Estudios Avanzados del I.P.N., Mexico
Wentz-Hunter, Kelly, University of Illinois, Chicago
Yu, Han-Gang, State University of New York, Stony Brook

Molecular Biology of Aging

(August 10–August 27)

Directors

Guarente, Leonard P., Massachusetts Institute of Technology
Wallace, Douglas, Emory University School of Medicine

Faculty

Aiken, Judd M., University of Wisconsin–Madison
Austad, Steven, University of Idaho
Bohr, Vilhelm A., National Institutes of Health
Campisi, Judith, Berkeley National Laboratory
Finch, Celeb, University of Southern California
Grossman, Lawrence, Johns Hopkins University
Harley, Calvin, Geron Corporation
Hekimi, Siegfried, McGill University, Canada
Johnson, Thomas, University of Colorado
Jones, Dean P., Emory University
Kenyon, Cynthia, University of California, San Francisco
Kim, Stuart, Stanford University of Medicine
Kirkwood, Tomas, University of Manchester, United Kingdom
de Lange, Titia, The Rockefeller University
Lithgow, Gordon J., University of Manchester, United Kingdom
Longo, Valter, University of Southern California
Martin, George, University of Washington School of Medicine
Melov, Simon, Buck Center for Research in Aging
Richardson, Arlan, University of Texas Health Science Center
Ruvkun, Gary, Massachusetts General Hospital
Sohal, Rajindar, Southern Methodist University
Tanzi, Rudolph E., Harvard University Medical School
Tower, John, University of Southern California
Van Voorhies, Wayne, University of Arizona, Tucson
Wright, Woodring E., University of Texas Southwestern Medical Center

Teaching Assistants

Bilger, Johannes, Emory University
Pinar, Elif, Emory University
Cottrell, Barbara, Emory University
Esposito, Luke, Emory University
Jegalian, Beatrice, Massachusetts Institute of Technology
Johnson, Brad, Massachusetts Institute of Technology
Kokoszka, Jason, Emory University
Levy, Shawn, Emory University
McNabb, David, Massachusetts Institute of Technology
Murdock, Deborah, Emory University

Course Coordinator

Burke, Rhonda E., Emory University School of Medicine

Course Assistant

Abisla, Richard, University of Chicago

Students

Ayala-Torres, Sylvette, University of Texas Medical Branch
Brown, Jeremy, Roslin Institute, Scotland
Brown-Borg, Holly, University of North Dakota
Chen, Yaohui, Yale University Medical School
Chung, Namjin, Duke University Medical Center
Crawford, Douglas, University of California, San Francisco
de Lacalle, Sonsoles, Beth Israel Deaconess Medical Center
Eshoo, Mark, Buck Center for Research in Aging
Ford, Carolyn, Northwestern University
Goto, Joy, University of California, Los Angeles
Henning, Karla, National Institutes of Health
Kennell, John, Southern Methodist University
Kukull, Walter, University of Washington
Martin, Kareen, Biological Gerontology Group, Manchester, United Kingdom
McChesney, Patricia, University of Texas Southwestern Medical Center
Merker, Robert, New York University Medical Center
Squier, Thomas, University of Kansas
Torres-Ramos, Carlos, University of Texas Medical Branch

Molecular Mycology: Current Approaches to Fungal Pathogenesis *(August 8–August 27)*

Directors

Edwards, John Jr., Harbor-UCLA Medical Center
Magee, Paul T., University of Minnesota
Mitchell, Aaron P., Columbia University

Faculty

Casadevall, Arturo, Albert Einstein College of Medicine
Cole, Gary T., Medical College of Ohio
Davidson, Robert, Duke University Medical Center
Davis, Dana, Columbia University
Filler, Scott, Harbor-UCLA Medical Center
Fonzi, William, Georgetown University Medical Center
Heitman, Joseph, Duke University Medical Center
Keath, Elizabeth, St. Louis University School of Medicine
Klein, Bruce, University of Wisconsin–Madison
Kurtz, Myra, Merck Research Lab
Kwon-Chung, June, National Institutes of Health
Lodge, Jennifer, St. Louis University School of Medicine
Murphy, Juneann, University of Oklahoma
Oliver, Brian, University of Cincinnati
Rhodes, Judith, University of Cincinnati
White, Theodore, Seattle Biomedical Research Institute
Whiteway, Malcolm, National Research Council, Canada

Course Assistant

Sandri, Brian, Marine Biological Laboratory

Students

Bammert, Gary, Pharmacia & Upjohn
Cowen, Leah, University of Toronto, Canada
Cruz, Cristina, Duke University Medical Center
de Jesús-Berríos, Marisol, University of Puerto Rico
Devasamayam, Gina, Wadsworth Center

Efimov, Vladimir, University of Medicine and Dentistry, New Jersey
Giles, Steven, University of Wisconsin–Madison
Goldstein, Alan, Duke University
Inglis, Diane, University of California, San Francisco
Kellog, Christina, Georgetown University
Latouche, Nicholas, Westmead Hospital Sydney University, Australia
Miller, Nancy, Johns Hopkins Medical Institution
Nickerson, Ken, University of Nebraska
Smith, Christina, State University of New York, Buffalo
Warenda, Amy, State University of New York, Stony Brook
Wormley, Floyd, Louisiana State University Medical Center

Neural Development and Genetics of Zebrafish (August 15–August 27)

Directors

Dowling, John E., Harvard University
Hopkins, Nancy, Massachusetts Institute of Technology

Faculty

Baker, Robert, New York University Medical Center
Collazo, Andres, House Ear Institute
Eisen, Judith S., University of Oregon
Fetcho, Joseph, State University of New York, Stony Brook
Fricke, Cornelia, University of Utah Medical Center
Hanlon, Roger, Marine Biological Laboratory
Kimmel, Charles, University of Oregon
Lin, Shuo, Medical College of Georgia
Neuhauss, Stephan, Max-Planck-Institut für Entwicklungsbiologie, Germany
Talbot, William S., Stanford University
Wilson, Stephen, University College London, United Kingdom

Teaching Assistants

Clarke, Jonathan, University College London, United Kingdom
Fadool, James, Florida State University
Granato, Michael, University of Pennsylvania
Kainz, Pamela, Harvard University
Link, Brian, Harvard University
Lorent, Kristin, University of Pennsylvania School of Medicine
Moens, Cecilia, Fred Hutchinson Cancer Research Center
Mullins, Mary, University of Pennsylvania
Sirotkin, Howard, New York University School of Medicine
Walker-Durchanek, Charline, University of Oregon

Lecturers

Astrosfky, Keith, Massachusetts Institute of Technology
Fraser, Scott, California Institute of Technology

Laboratory Technicians

Linnon, Beth, Marine Biological Laboratory
Mazanec, April, University of Oregon

Course Coordinator

Schmitt, Ellen, Harvard University

Course Assistant

Sweeney, Neal, Marine Biological Laboratory

Students

Ashworth, Rachel, University College London, United Kingdom
Bellefroid, Eric, Université Libre de Bruxelles, Belgium
Bishop, Charles, Baylor College of Dentistry
Chan, Joanne, Dana-Farber Cancer Institute
Endres, James, University of California, San Diego
Glanzman, David, University of California, Los Angeles
Levandoski, Mark, Brown University
Lightfoot, Kurt, University of the Witwatersrand, South Africa
Lunde, Karen, University of California, San Diego
Poznanski, Ann, Midwestern University
Rinkwitz, Silke, New York University Medical Center
Tong, Betty, Whitehead Institute
Vlachakis, Nikolaos, University of Massachusetts Medical Center
Waterbury, Julie, University of Pennsylvania
Wiemelt, Anthony, University of Pennsylvania
Williams, Fred, University of Toledo

Optical Microscopy and Imaging in the Biomedical Sciences (October 6–October 14)

Director

Izzard, Colin, State University of New York, Albany

Faculty

DePasquale, Joseph, New York State Department of Health
Dunn, Kenneth, Indiana University Medical Center
Hard, Robert, State University of New York, Buffalo
Herman, Brian, University of Texas Health Science Center
Murray, John, University of Pennsylvania School of Medicine
Piston, David M., Vanderbilt University
Snyder, Kenneth, State University of New York, Buffalo
Spring, Kenneth, National Institutes of Health
Swedlow, Jason, University of Dundee, Scotland

Teaching Assistants

Pierini, Lynda, Cornell University Medical College
Sigurdson, Wade, State University of New York, Buffalo

Lecturers

Hinsch, Jan, Leica, Inc.
Inoué, Shinya, Marine Biological Laboratory
Keller, H. Ernst, Zeiss Optical Systems

Students

Bhalla, Needhi, University of California, San Francisco
Biggins, Sue, University of California, San Francisco
Brotz, Tilmann, National Cancer Institute
Chien, Edward, University of Chicago
Combs, Christopher, National Institutes of Health
Cromey, Douglas, University of Arizona
Duca, Karen, University of Wisconsin
Fletcher, Tara, Albany Medical College
Gustashaw, Karen, Case Western Reserve University
Hoja, Mary-Rose, Karolinska Institute Stockholm, Sweden
Holt, Matthew, Medical Research Council, United Kingdom
Hudson, Emma, University of Dundee, Scotland
Kaplan, David, Food and Drug Administration
Lin, Keng-hui, University of Pennsylvania
Love, Dona, National Institutes of Health
Martini, Lene, University of Copenhagen, Denmark
Murnion, Mairead, University of Dundee, Scotland
Reilly, Thomas, Johns Hopkins University School of Medicine
Saslowsky, David, Virginia Tech
Shestopalov, Valery, Washington University
Silverman, Michael, Oregon Health Sciences University
Sossick, Alex, University of Cambridge, United Kingdom
Tang, Cha-Mei, Creative MicroTech, Inc.
Wallace, Wes, Brown University

Pathogenesis of Neuroimmunologic Diseases

(August 16–August 27)

Directors

Brosnan, Celia F., Albert Einstein College of Medicine
Rosenbluth, Jack, New York University School of Medicine

Faculty

Etty, Benveniste, University of Alabama, Birmingham
Berman, Joan, Albert Einstein College of Medicine
Brightman, Milton W., National Institutes of Health
Burden, Steven, New York University School of Medicine
Coyle, Patricia, State University of New York, Stony Brook
Darnell, Robert, Rockefeller University
Drachman, Daniel, Johns Hopkins University School of Medicine
Felten, David, Loma Linda University School of Medicine
Gould, Robert M., New York State Institute of Basic Research
Griffin, Diane, Johns Hopkins University
Griffin, John, Johns Hopkins University
Hickey, William, Dartmouth-Hitchcock Medical Center
Itescu, Silviu, Columbia/Presbyterian Medical Center
Kaplan, Gilla, Rockefeller University
Knopf, Paul, Brown University
Kocsis, Jeffery D., Yale University School of Medicine
Kuchroo, Vijay, Brigham and Women's Hospital
Lipton, Stuart, The Burnham Institute
Martiney, James, Picower Institute for Medical Research
McKinnon, Randall D., R. W. Johnson Medical School
Popko, Brian, University of North Carolina, Chapel Hill
Price, Donald L., Johns Hopkins University School of Medicine
Ransohoff, Richard, Cleveland Clinic Foundation
Ransom, Bruce, University of Washington School of Medicine
Reder, Anthony, University of Chicago
Salzer, James, New York University Medical Center
Saper, Clifford, Beth Israel Hospital
Shin, Moon, University of Maryland School of Medicine

Shrager, Peter, University of Rochester Medical Center
Solimena, Michele, Yale University
Sontheimer, Harald, University of Alabama, Birmingham
Sternberg, Esther, National Institutes of Health
Waksman, Byron, Foundation for Microbiology
Weiner, Howard, Harvard University Medical School

Course Coordinator

Stogryn, Krista, Marine Biological Laboratory

Students

Andjelkovic, Anuska, University of Connecticut
Brundula, Veronika, University of Calgary, Canada
D'Aversa, Teresa, Albert Einstein College of Medicine
DeFeo, Anthony, Mercy College
Dzenko, Kirk, University of Connecticut Health Center
Fischer, Falko, Harvard University Medical School
Hillert, Jan, Karolinska Institute, Sweden
Hjelmstrom, Peter, Yale University
Janson, Christopher, Thomas Jefferson University
Kuljis, Rodrigo, University of Miami
Lu, Weiquan, State University of New York, Stony Brook
Luedtke, Robert, University of North Texas
O'Brien, Nikki, Australian National University, Australia
Odyniec, Artur, Medical Academy of Lodz, Poland
Regardsoe, Emma, University of Oxford, United Kingdom
Reis, Donald, Cornell Medical College
Robichaud, Lillian, Parke-Davis Research
Salzberg, Heather, Rutgers University
Sivakumar, M. R., Apollo Hospitals, India
Troncoso, Juan, Johns Hopkins University
Vari, Gabor, Brown University
Vijayan, Shrijay, City University of New York
Woodman, Scott, Albert Einstein College of Medicine
Wu, Dona, Albert Einstein College of Medicine
Yates, Jennifer, University of North Carolina, Chapel Hill

Workshop on Molecular Evolution

(August 1–August 13)

Directors

Davison, Daniel B., Bristol-Myers Squibb PRI
Sogin, Mitchell, Marine Biological Laboratory

Faculty

Cummings, Michael, Marine Biological Laboratory
Eddy, Sean, Washington University
Edwards, Scott, University of Washington
Eisen, Jonathan, Institute for Genomic Research
Felsenstein, Joseph, University of Washington
Fitch, David H.A., New York University
Fraser, Claire M., Institute for Genomic Research
Kuhner, Mary, University of Washington
Maddison, David, University of Arizona, Tucson
Miyamoto, Michael, University of Florida
Muse, Spencer, North Carolina State University
Olsen, Gary, University of Illinois, Urbana
Pace, Norman, University of Colorado, Boulder
Pearson, William, University of Virginia Health Sciences Center
Rice, Ken, SmithKline Beecham Pharmaceuticals
Riley, Margaret, Yale University
Swofford, David, Smithsonian Institution

Teaching Assistants

Edgcomb, Virginia, Marine Biological Laboratory
MacArthur, Andrew, Marine Biological Laboratory
Thompson, Steven, Florida State University

Laboratory Technician

Holder, Michael, University of Houston

Course Coordinator

Harris, Marian, Marine Biological Laboratory

Students

Ariey, Frédéric, Institut Pasteur, France
Babin, Josephine, Louisiana State University
Baumgartner, Manuela, University Regensburg, Germany
Beati, Lorenza, Centers for Diseases Control and Prevention
Becker, Jennifer, Lehigh University
Best, Aaron, University of Illinois
Blatter, Robert, University of Basel, Switzerland
Bond, Philip, University of Wisconsin
Bouchet, Valérie, Boston University School of Medicine
Bouzat, Juan, University of Illinois
Brazeau, Dan, University of Florida
Brinkmann, Anna, University of Wisconsin–Milwaukee
Briones, Marcelo, Universidade Federal de Sao Paulo, Brazil
Carrigan, Matthew, University of Florida
Chaturvedi, Vishnu, New York State Department of Health
Chyba, Christopher, SETI Institute
Clark, Ann Marie, University of Florida
Craven, Kelly, University of Kentucky
Dacks, Joel, Dalhousie University, Canada
Dennis, Paige, University of Massachusetts, Boston
Di Meo, Carol, University of Delaware
Dimsoski, Pero, United States Environmental Protection Agency
Fitzpatrick, Jennifer, Tufts University School of Medicine
Fleming, Melissa, University of Alaska Museum
Franck, Jens, Occidental College
Freire, Nicole, University of Florida
Gasparich, Gail, Towson University
Gaucher, Eric, University of Florida
Gribaldo, Simonetta, Universita "La Sapienza," Italy
Gueneau-Novoa, Pulchérie, Instituto Venezolano Investigaciones Cientificas, Venezuela
Hansen, Jan, Technical University of Denmark, Denmark
Harbinski, Fred, Harvard University
Ho, Hoi Yan, Chinese University of Hong Kong, Hong Kong
Hurtado, Luis, Rutgers University
Inagaki, Yuji, Dalhousie University, Canada
Klingbeil, Michele, Johns Hopkins School of Medicine
Lawrence, Carolyn, University of Georgia
Liebert, Cynthia, University of Georgia
Maiwald, Matthias, Stanford University
McGraw, Beth, Yale University
Mead, Louise, University of Massachusetts
Moore, Jon, National Marine Fisheries Service
Pilcher, Carl, NASA Headquarters
Pineda, Augustin, Florida State University
Posada, David, Brigham Young University
Pritham, Ellen, University of Massachusetts, Boston
Reed, David, Louisiana State University
Richardson, Susan, Yale University/Woods Hole Oceanographic Institution
Rinke De Wit, Tobias, Ethiopian Health and Nutrition Institute, The Netherlands
Sabo, Aniko, Purdue University
Salamin, Nicolas, Université de Lausanne, Switzerland
Schreiber, Edgar, PE Applied Biosystems
Seffernick, Jennifer, University of Minnesota
Sellers, Holly, United States Department of Agriculture
Sinclair, Elizabeth, Brigham Young University
Skirnisdottir, Sigurlaug, IceTherm Inc., Iceland
Stockley, Bruce, Southampton Oceanography Centre, United Kingdom
Worapong, Jeerapun, Montana State University
Zmasek, Christian, Washington University Medical School

Other Programs

Marine Models in Biological Research Undergraduate Program *(June 8–August 6, 1999)*

Directors

Browne, Carole L., Wake Forest University
Tytell, Michael, Wake Forest University School of Medicine

Course Assistant

Begley, Gail, Marine Biological Laboratory

Faculty

Allen, Nina S., North Carolina State University
Borst, David, Illinois State University
Furie, Barbara, Harvard University
Furie, Bruce, Harvard University
Hanlon, Roger, Marine Biological Laboratory
Jonas, Elizabeth, Yale University
Laufer, Hans, University of Connecticut
Malchow, R. Paul, University of Illinois
Mensinger, Allen, Washington University
Wainwright, Norman, Marine Biological Laboratory

Seminar Speakers

Frank, Tammy, Harbor Branch Oceanographic Institution
Inoué, Shinya, Marine Biological Laboratory
Kuzirian, Alan, Marine Biological Laboratory
Reinisch, Carol, Marine Biological Laboratory
Silver, Robert, Marine Biological Laboratory

Students

Baliga, Meghan, Wake Forest University
Clifton, Christine, Mount Holyoke College
Harrist, Alexia, Yale University
Helm, Jessica, Washington and Lee University
Lassen, Kara, Wake Forest University
Mitchell, Michael, Wake Forest University
Peck, Raphaela, Reed College
Price, Nichole, Connecticut College
Ramsey, David, Harvard University
Rankin, Ellen, Colgate University
Tang, Kathleen, Washington University
Taylor, Kevin, Wake Forest University
Vasse, Aimee, Williams College

NASA Planetary Biology Internship

(June–September 1999)

Directors

Margulis, Lynn, University of Massachusetts
Dolan, Michael F., University of Massachusetts

Interns

Caylor, Kelly, University of Virginia
Chacon, Elizabeth, Universidad Nacional Autonoma de México
Franklin, Rima, University of Virginia
French, Jason, University of Alberta, Canada
Gauci, Vincent, The Open University, United Kingdom
Marx, Joseph G., International Space University, France
Omelon, Christopher, McGill University, Canada
de Peyer, Oliver, University of Reading, United Kingdom
Popa, Radu, University of Cincinnati
de Vera Gomez, Alvin, University of the Philippines
Wilson, Cindy, University of Montana

Sponsors

Cady, Sherry L., Portland State University
Des Marais, David, NASA Ames Research Center
Joyce, Gerald, Scripps Research Institute
Knoll, Andrew, Harvard University
Mancinelli, Roco, NASA Ames Research Center
Matthews, Elaine, Goddard Institute for Space Studies
Nealson, Ken, Jet Propulsion Laboratory
Privette, Jeff, NASA Goddard Space Flight Center
Rothschild, Lynn, NASA Ames Research Center
Teske, Andreas, Woods Hole Oceanographic Institution
Wheeler, Raymond, NASA Kennedy Space Center

Semester in Environmental Science

(September 5–December 17, 1999)

Administration

Hobbie, John E., Director
Foreman, Kenneth H., Associate Director
Moniz, Polly C., Administrative Assistant

Faculty

Deegan, Linda A.
Giblin, Anne E.
Hopkinson, Charles S. Jr.
Hughes, Jeffrey
Liles, George
Nadelhoffer, Knute J.
Neill, Christopher
Peterson, Bruce J.
Rastetter, Edward B.
Shaver, Gaius R.
Vallino, Joseph J.
Williams, Mathew

1999 Research and Teaching Assistants

Bahr, Michelle
Kelsey, Sam
Kwiatkowski, Bonnie
Micks, Patricia
Parker, Sophie
Tholke, Kris

1999 SES Students

Arling, Jeremy, Bowdoin College
Avery, Jennifer, Brandeis University
Butman, David, Connecticut College
Glueck, Lara, Claremont McKenna College
Greenbaum, Adena, Wellesley College
Hinckley, Eve-Lyn, Middlebury College
Horowitz, Julie, Hampshire College
Kirkby, Ryan, Harvey Mudd College
Mathrani, Vandana, Scripps College
Mathrani, Varsha, Scripps College
Mifflin, Amanda, Wellesley College
Morrisseau, Sarah, Connecticut College
Peterson, G. Gregory, Wesleyan University
Romagnano, Joseph, Worcester Polytechnic
Sohm, Jill, Harvey Mudd College
Spivak, Amanda, Bryn Mawr College
Williams, Samantha, Mount Holyoke College
Ziemann, Tori, Beloit College

SPINES—Summer Program in Neuroscience, Ethics and Survival (June 12–July 10)

Directors

Martinez, Joe L. Jr.
Townsel, James

Fellows

Herne, Moss, Boston University School of Medicine
Hubbard, Aida, University of Texas, San Antonio
McCrery, Karen, Texas Women's University
Meadows, Adimika, Boston University
Mohamed, Somaia, University of Iowa
Nelson, Rhonda, Meharry Medical College
Orfila, James, University of Texas, San Antonio
Simples, James, University of Pittsburgh
Villarreal, Julissa, University of Texas, San Antonio
Zayas, Ricardo, Tufts University

Teachers' Workshop: Living in the Microbial World (August 15–21)

Course Directors

Olendzenski, Lorraine, University of Connecticut, Storrs
Dugas, Jeff, University of Connecticut, Storrs

Curriculum Specialist

Dorritie, Barbara, Cambridge Rindge and Latin School, Cambridge, MA

Course Assistant

Wier, Andrew, University of Massachusetts, Amherst

Presenters

Margulis, Lynn, University of Massachusetts, Amherst
Guerrero, Ricardo, University of Barcelona, Spain
Knoll, Andrew, Harvard University
Edgcomb, Virginia, Marine Biological Laboratory
Gast, Rebecca, Woods Hole Oceanographic Institution
Rummel, John, National Aeronautics and Space Administration

Teacher Participants

Molyneaux, Leslie, Hanover Middle School, Hanover, MA
Buckley, Kathryn, Mashpee High School, Mashpee, MA
Henderson, Forest, Bellingham Jr./Sr. High School, Bellingham, MA
Muscatell, Gina, Bellingham Jr./Sr. High School, Bellingham, MA
Bennett, Tara, Norwell High School, Norwell, MA
Webber, Alan, Norwell High School, Norwell, MA
Yuhas, Joseph, Kennebunk High School, Kennebunk, ME
Johnston, Ross B., Nauset Regional High School, N. Eastham, MA
Albright, Lori, Nauset Regional High School, N. Eastham, MA
Carotenuto, Sheila, Quashnet River School, Mashpee, MA
Rocio, Zamaria, Horace Mann Middle School, San Diego, CA
Conn, Kathleen, West Chester Area School District, West Chester, PA
Carty, Susan, West Chester Area School District, West Chester, PA
Rutland, Susan, West Chester Area School District, West Chester, PA
Setterfield, Elena, King Ethelbert School, Kent, England
Scales, Sacha, King Ethelbert School, Kent, England
Cronin, Maureen, Nonington C.E.P. School, Kent, England
Scott, Nyree, Nonington C.E.P. School, Kent, England

Summer Research Programs

Principal Investigators

Adamo, Shelley, Dalhousie University, Canada
Armstrong, Clay, University of Pennsylvania
Armstrong, Peter B., University of California, Davis
Augustine, George J., Duke University Medical Center

Balaban, Pavel, Russian Academy of Sciences, Russia
Barlow, Robert B. Jr., State University of New York Health Science Center
Beaugé, Luis, Instituto de Investigacion Medica "Mercedes y Martin Ferreyra," Argentina
Beckman, Matthew, University of Alabama, Birmingham
Ben-Jonathan, Nira, University of Cincinnati
Bennett, Michael V. L., Albert Einstein College of Medicine
Bodznick, David, Wesleyan University
Boron, Walter, Yale University Medical School
Borst, David, Illinois State University
Boyer, Barbara, Union College
Boyle, Richard, Oregon Health Sciences University
Brady, Scott T., The University of Texas Southwestern Medical Center, Dallas
Brock, Matthew, Stanford University
Browne, Carole, Wake Forest University School of Medicine
Burger, Max M., Friedrich Miescher Institut, Switzerland

Cardullo, Richard, University of California, Riverside
Carvan, Michael, University of Cincinnati
Chappell, Richard L., Hunter College, City University of New York
Cohen, Lawrence B., Yale University School of Medicine
Cohen, William D., Hunter College, City University of New York
Crespi, Marco, Scientific Institute S. Raffaele, Italy

De Weer, Paul, University of Pennsylvania School of Medicine
DePass, Anthony, Long Island University, Brooklyn
DePina, Ana S., Dartmouth College
DiPolo, Reinaldo, Instituto Venezolano Investigaciones Cientificas, Venezula
Dodge, Frederick, State University of New York Health Science Center
Doussau, Frederic, Duke University Medical Center

Edds-Walton, Peggy, Parmly Hearing Institute
Ehrlich, Barbara, Yale University School of Medicine

Fay, Richard, Loyola University of Chicago
Field, Christine, Harvard University Medical School
Fishman, Harvey M., University of Texas Medical Branch, Galveston
Flamarique, Iñigo Novales, University of Victoria, Canada

Gadsby, David, Rockefeller University
Gerhart, John, University of California, Berkeley
Giuditta, Antonio, University of Naples, Italy
Goldman, Robert D., Northwestern University Medical School
Gould, Robert, New York State Institute for Basic Research
Groden, Joanna, University of Cincinnati

Haimo, Leah, University of California, Riverside
Han, Yi, Baylor College of Medicine
Heck, Diane, Rutgers University
Hershko, Avram, Technion-Israel Institute of Technology, Israel
Highstein, Steven M., Washington University School of Medicine
Hill, Susan Douglas, Michigan State University
Hines, Michael, Yale University School of Medicine
Hoskin, Francis, US Army Natick RD&E Center

Innocenti, Barbara, Iowa State University

Johnston, Daniel, Baylor College of Medicine
Jonas, Elizabeth, Yale University School of Medicine
Jones, Teresa, National Institutes of Health
Joye, Samantha, University of Georgia

Kaczmarek, Leonard, Yale University School of Medicine
Kaplan, Barry, National Institutes of Mental Health
Kaplan, Ilene M., Union College
Kier, William, University of North Carolina, Chapel Hill
Kirschner, Marc, Harvard University Medical School
Koulen, Peter, Yale University School of Medicine
Kuhns, William, The Hospital for Sick Children, Canada

Lafer, Eileen M., University of Texas Health Science Center
Landowne, David, University of Miami School of Medicine
Langford, George, Dartmouth College
Laskin, Jeffrey, University of Medicine and Dentistry of New Jersey
Laufer, Hans, University of Connecticut
LaVail, Jennifer, University of California, San Francisco
Lipicky, Raymond J., Food and Drug Administration
Llinás, Rodolfo R., New York University Medical Center

Magee, Jeff, Louisiana State University Medical Center
Major, Guy, Lucent Technologies
Malgaroli, Antonio, University of Milan, Italy
Martinez, Joe, University of Texas, San Antonio
McAllister, A. Kimberly, Salk Institute of Biological Studies
McNeil, Paul, Medical College of Georgia
Mensinger, Allen, Washington University School of Medicine
Metuzals, Janis, University of Ottawa Faculty of Medicine, Canada
Mitchison, Timothy, Harvard University Medical School
Miyakawa, Hiroyoshi, Tokyo University of Pharmacy and Life Science, Japan
Moore, John W., Duke University Medical Center
Mooseker, Mark, Yale University

Nasi, Enrico, Boston University School of Medicine

Ogden, David, National Institute for Medical Research
Ogunseitan, Oladele A., University of California, Irvine

Palazzo, Robert, University of Kansas
Pant, Harish, National Institutes of Health
Parysek, Linda, University of Cincinnati
Paydarfar, David, University of Massachusetts Medical School

Quigley, James P., State University of New York, Stony Brook

Rabbitt, Richard, University of Utah
Rakowski, Robert F., Finch University of Health Sciences/The Chicago Medical School
Ramus, Seth, Boston University
Ratner, Nancy, University of Cincinnati
Reese, Thomas S., National Institutes of Health
Rieder, Conly, Wadsworth Center
Ripps, Harris, University of Illinois College of Medicine
Rome, Larry, University of Pennsylvania
Russell, John M., Hahnemann University

Salmon, Edward, University of North Carolina, Chapel Hill
Siwicki, Kathleen, Swarthmore College
Sloboda, Roger D., Dartmouth College
Spiegel, Evelyn, Dartmouth College
Spiegel, Melvin, Dartmouth College
Srinivas, Miduturu, Albert Einstein College of Medicine
Standart, Nancy, University of Cambridge, United Kingdom
Steinacker, Antoinette, University of Puerto Rico
Sugimori, Mutsuyuki, New York University Medical Center
Suszkiw, Janusz, University of Cincinnati

Telzer, Bruce, Pomona College
Tilney, Lewis, University of Pennsylvania
Trinkaus, John P., Yale University
Troll, Walter, New York University Medical Center
Tytell, Michael, Wake Forest University School of Medicine

Walters, Edgar, University of Texas, Houston
Weidner, Earl, Louisiana State University

Yamaguchi, Ayako, Columbia University
Yamoah, Ebenezer, University of Cincinnati College of Medicine

Zecevic, Dejan P., Yale University School of Medicine
Zimmerberg, Joshua, National Institutes of Health
Zito, Karen, University of California, Berkeley
Zochowski, Michal, Yale University School of Medicine
Zottoli, Steven, Williams College
Zukin, R. Suzanne, Albert Einstein College of Medicine

Other Research Personnel

Adams, Curt, University of California, Riverside
Akanki, Feyisara, Williams College
Allen, Nina, North Carolina State University
Antic, Srdjan Henry, Yale University School of Medicine
Anton, Roberto, Hunter College
April, Ilana, Connecticut College
Armstrong, Clara, University of Pennsylvania
Asokan, R., University of California, Davis

Baliga, Meghna, Wake Forest University
Banini, Bubu, Swarthmore College
Bashi, Esther, Yale University
Bearer, Elaine, Brown University
Benjamins, Steven, Groningen University, The Netherlands
Bergamaschi, Andrea, Fondazione Centro San Raffaele del Moute Tabor, Italy
Berger-Sweeney, Joanne, Wellesley College
Bertetto, Lisa, Wesleyan University
Bezanilla, Francisco, University of California, Los Angeles
Billack, Blase, Rutgers University
Bingham, Eula, University of Cincinnati Medical School
Bonacci, Lisa, Hunter College
Bronner-Fraser, Marianne, California Institute of Technology
Brown, Joel, Albert Einstein College of Medicine
Bucior, Inona, Friedrich Miescher Institute, Switzerland
Burris, Jennifer, Northwestern University Medical School

Chan, Sena, Long Island University
Cho, Myoung-Soon, National Institutes of Health
Clarkson, Melissa, University of Kansas
Clifton, Christine, Mount Holyoke College
Crawford, Karen, St. Mary's College of Maryland

Davis, Bruce, Yale University
Debowy, Owen, New York University School of Medicine
Desai, Arshad, European Molecular Biology Laboratory, Germany
Detrait, Eric, University of Texas Medical Branch
Devlin, Leah, Penn State University
Doherty, Arin, Connecticut College
Dou, Hongwei, University of Cincinnati
Dumollard, Remi, Station Zoologique de Ville-Franche Sur Mer, France

Eddleman, Christopher, University of Texas Medical Branch, Austin
Escalona de Motta, Gladys, University of Puerto Rico
Eyman, Maria, University of Naples, Italy

Fakhrzadeh, Ladan, Rutgers University
Felke, Erin, University of Illinois
Fernandez-Busguets, Xavier, Friedrich Miescher Institute, Switzerland
Fraser, Scott, California Institute of Technology
Fukui, Yoshio, Northwestern University Medical School

Gainer, Harold, National Institutes of Health
Galanis, Jennifer, National Institutes of Health
Galbraith, James A., National Institutes of Health
Gallant, Paul E., National Institutes of Health

Gallo, Michael, University of Medicine and Dentistry of New Jersey
Gerosa-Erni, Daniela, Friedrich Miescher Institute, Switzerland
Gioio, Anthony, National Institutes of Mental Health
Gleeson, Richard, University of Florida
Goldman, Anne E., Northwestern University Medical School
Gomez, Maria del Pilar, Boston University School of Medicine
Gonzalez-Lima, Francisco, University of Texas, Austin
Grant, Philip, National Institutes of Health
Grassi, Daniel, Food and Drug Administration
Gyoeva, Fatima K., Institute of Protein Research, Russia

Hagar, Robert, Yale University School of Medicine
Harrington, John, University of South Alabama, Mobile
Harrist, Alexia, Yale University
Harrow, Faith, Hunter College
Harwood, Claire, University of Pennsylvania
Helfand, Brian, Northwestern University Medical School
Helm, Jessica, Washington and Lee University
Hernandez, Carlos, New York University School of Medicine
Herrick, Scott, University of California, Riverside
Hitt, James, State University of New York Health Science Center
Hiza, Nicholas, Williams College
Ho-Sang, Dwight, Williams College
Hogan, Emilia, Yale University Medical School
Holford, Kenneth, Illinois State University
Holmgren, Miguel, Harvard University Medical School
Hoof, Laura, University of Chicago

Ingrassia, Rosaria, University of Milan, Italy
Inoue, Masashi, Tokyo University of Pharmacy and Life Science, Japan
Intravaia, Anthony, NASA Ames Research Center

Janowitz, Tobias, University Hannover, Germany

Kamino, Kohtaro, Tokyo University School of Medical and Dental, Japan
Kannenberg, Kai, University of Milan, Italy
Kapoor, Turun, Harvard University Medical School
Kifaieh, Nidal, Long Island University
King, Alison Jane, Dalhousie University, Canada
Klimov, Andrei, University of Pennsylvania
Koroleva, Zoya, Hunter College
Kuner, Thomas, Duke University Medical Center

Lassen, Kara G., Wake Forest University
Lee, Kyeng Gea, Hunter College
Lee, Rosalynn, University of Georgia
Lesher, Sarah, University of Maryland
Leznik, Elena, New York University School of Medicine
Loboda, Andrey, University of Pennsylvania
Lowe, Christopher, University of California, Berkeley

Maddox, Paul, University of North Carolina, Chapel Hill
Malchow, Robert Paul, University of Illinois, Chicago
Melishchuk, Alexey, University of Pennsylvania
Mitchell, Michael, Wake Forest University
Miyake, Katsuya, Fukushima Medical College, Japan
Mohan, Nishal, Hunter College
Moir, Robert, Northwestern University
Motta, Melissa, Williams College

Nguyen, Michael P., University of Texas Medical Branch

Oegema, Karen, European Molecular Biology Laboratory, Germany
Ogan, Jeff, Illinois State University
Orfila, James, University of Texas, San Antonio

Peck, Raphaela, Reed College
Petersen, Jennifer, National Institutes of Health
Powers, Maureen, Vanderbilt University
Prahcad, Veena, Northwestern University Medical School
Prasad, Kondury, University of Texas Health Science Center
Price, Nichole, Connecticut College

Quinn, Kerry, Yale University School of Medicine

Ramsey, David, Harvard University
Rankin, Ellen, Colgate University
Reinsch, Sigrid, NASA Ames Research Center
Rhodes, Paul, New York University Medical School
Ring, Sabine, University of Frankfurt, Germany
Rosenstein, Fred, Hunter College
Ruta, Vanessa, Hunter College

Schuette, Etha, Hunter College
Schwartz, William, University of Massachusetts Medical School
Simpson, Tracy, University of Hartford
Steffen, Walter, University of Rostock, Germany
Steinacker, Antoinette, University of Puerto Rico
Stockbridge, Norman, Food and Drug Administration
Szalisznyo, Krisztina, Hungarian Academy of Science, Hungary

Tamse, Catherine, University of Rhode Island
Tan, Xiao, Williams College
Tang, Kathleen, Washington University
Taylor, Kevin, Wake Forest University
Thom, George, University of Cambridge, United Kingdom
Tokumaru, Hiroshi, Duke University Medical Center
Tokumaru, Keiko, Duke University Medical Center
Townsel, James G., Meharry Medical College
Tran, Phong, Columbia University
Twersky, Laura, Saint Peter's College

Vasse, Aimee, Williams College
Villa-Komaro, Lydia, Northwestern University

Wachowiak, Matt, Yale University School of Medicine
Ward, Rita, National Institutes of Health
Watts, Kisha, Williams College
Wen, Huajie, National Institutes of Mental Health
Wisniewski, Rachel, University of Georgia

Woellert, Torsten, University of Rostock, Germany
Wu, Samuel, Baylor College of Medicine

Yancey, Sadiga, Mass Bay Community College
Yang, Stacy, University of California, Irvine
Young, Iain, University of Pennsylvania

Zakevicius, Jane M., University of Illinois College of Medicine
Zavilowitz, Joe, Yale University

Library Readers

Abbott, Jayne, Marine Research, Inc.
Adelberg, Edward, Yale University
Ahmadjian, Vernon, Clark University
Allen, Garland, Washington University
Allen, Nina, North Carolina State University
Alliegro, Mark, Louisiana State University
Alsup, Peggy, Tennessee Department of Health
Anderson, Everett, Harvard Medical School

Barrett, Dennis, University of Denver
Barry, Susan, Mount Holyoke College
Bedard, Andre, York University
Benjamin, Thomas, Harvard Medical School
Bernhard, Jeffery, University of Massachusetts Medical School
Bernheimer, Alan, New York University School of Medicine
Borgese, Thomas, Lehman College–CUNY
Boyer, John, Union College

Campos, Ana, McMaster University
Candelas, Graciela, University of Puerto Rico
Chang, Donald, Hong Kong University
Child, Frank, Woods Hole, MA
Clark, Douglas, John Hopkins University
Clarkson, Kenneth, Lucent Technologies
Cobb, Jewel, California State University
Cohen, Seymour, Woods Hole, MA
Colinvaux, Paul, Marine Biological Laboratory
Collier, Marjorie, University of Louisiana
Cooperstein, Sherwin, University of Connecticut Health Center
Copeland, Eugene, Woods Hole, MA
Corwin, Jeffery, University of Virginia
Couch, Ernest, Texas Christian University
Cowling, Vincent, University of Florida

Duncan, Thomas K., Nichols College

Epstein, Herman, Brandeis University

Farmanfarmaian, A. Verdi, Rutgers University
Fee, Michale, Bell Laboratories
Frenkel, Krystyna, New York University School of Medicine

Gabriel, Mordecai, Brooklyn College
Galatzer-Levy, Robert, University of Chicago
German, James, Cornell University
Ginsberg, Harold, National Institutes of Health
Goldstein, Moise, Johns Hopkins University
Grossman, Albert, New York University School of Medicine
Gruner, John, Cephalon, Inc.
Guttenplan, Joseph, New York University Dental and Medical School

Haimo, Leah, University of California
Harrington, John, University of South Alabama
Hays, Thomas, University of Minnesota
Hernandez, Mari-Luz, University of Nice
Herskovits, Theodore, Fordham University
Hunter, Robert, Gartnaval Royal Hospital

Inoue, Sadayuki, McGill University

Jacobson, Allan, University of Massachusetts
Josephson, Robert, University of California

Kaltenbach, Jane, Mount Holyoke College
Kamino, Kohtaro, Tokyo Medical and Dental School of Medicine
Karlin, Arthur, Columbia University
King, Kenneth, Falmouth, MA
Klein, Donald, Colorado State University
Kornberg, Hans, Boston University
Krane, Stephen M., Harvard Medical School

Laster, Leonard, University of Massachusetts Medical Center
Lee, John, City College of CUNY
Levy, Arthur, St. Vincents Hospital
Lorand, Laszlo, Northwestern University Medical School
Luckenbill, Louise, Ohio University

MacNichol, Edward, Boston University School of Medicine
Masland, Richard, Massachusetts General Hospital
Mauzerall, David, Rockefeller University
Mitchell, Ralph, Harvard University/DEAS
Mizell, Merle, Tulane University

Nagel, Ronald, Albert Einstein College of Medicine
Narahashi, Toshio, Northwestern University Medical School
Naugle, John, National Aeronautics and Space Administration
Nicaise, Ghislain, University of Nice
Nickerson, Peter, State University of New York, Buffalo

Olds, James, George Mason University

Pappas, George, University of Illinois, Chicago
Pollen, Dan, University of Massachusetts Medical Center
Porter, Mary, University of Minnesota

Schippers, Jay, The HNG Foundation
Schuel, Herbert, University of Buffalo, SUNY
Shepro, David, Boston University
Shriftman, Molly, Woods Hole, MA
Spector, Abraham, Columbia University
Spotte, Stephen, University of Connecticut
Sundquist, Eric, U.S. Geological Survey
Sweet, Frederick, Washington University School of Medicine

Trager, William, Rockefeller University
Tweedell, Kenyon, University of Notre Dame
Tykocinski, Mark, University of Pennsylvania

Van Holde, Kensal, Oregon State University

Walton, Alan, University of Cambridge
Warren, Leonard, Wistar Institute
Weringer, Elora, Pfizer Central Research

1999 Library Room Readers

Dan Alkon
National Institute of Health

Lucio Cariello
Stazione Zoologica A. Dohrn

Giuseppe D'Alessio
University of Naples

Robert Goldman
Northwestern University Medical School

Roberto GonzalezPalaza
Northwest Indian College

Harlyn Halvorson
Marine Biological Laboratory

Michael Hines
Yale Univ. School of Medicine

Andres Kanner
Rush University

Alex Keynan
Israel Academy of Science

Kamino Kohtaro
Tokyo Medical and Dental

John W. Moore
Duke University Medical Center

Leyla Morrel
Rush University

Michael Rabinowitz
Marine Biological Laboratory

George Reynolds
Princeton University

Ann Stuart
UNC Chapel Hill

Gerald Weissmann
NYU School of Medicine

Whittaker, J. Richard, University of New Brunswick
Wolken, Jerome J., University of Pittsburgh

Yevick, George, Stevens Institute of Technology

Domestic Institutions Represented

Acorda Therapeutics
Alabama, University of, Birmingham
Alaska Museum, University of
Albany Medical College
Albert Einstein College of Medicine
Allegheny University of the Health Sciences
Arizona State University
Arizona, University of, Tucson

Barnard College
Baylor College of Dentistry
Baylor College of Medicine
Bell Laboratories
Berkeley National Laboratory
Beth Israel Hospital
Beth Israel-Deaconess Medical Center
Boston University
Boston University School of Medicine
Brandeis University
Bridgeport Hospital
Brigham and Women's Hospital
Brigham Young University
Bristol-Myers Squibb PRI
Bronx Veterans Administration Medical Center
Brown University
Bryn Mawr College
Buck Center for Research in Aging
Buffalo, University of
Burnham Institute

California Institute of Technology
California State University, Sacramento
California, University of, Berkeley
California, University of, Davis
California, University of, Irvine
California, University of, Los Angeles
California, University of, Riverside
California, University of, San Diego
California, University of, San Francisco
California, University of, Santa Barbara
Carl Zeiss, Inc.
Carnegie Mellon University
Case Western Reserve University
Catholic University of America
Center for Clinical Computing
Centers for Disease Control and Prevention
Chicago, University of
Children's Hospital, Boston
Cincinnati, University of
Cleveland Clinic Foundation
Cold Spring Harbor Laboratory
Colgate University
Colorado Health Science Center, University of
Colorado School of Medicine, University of
Colorado, University of, Boulder
Columbia University
Columbia-Presbyterian Medical Center
Connecticut College
Connecticut Health Center, University of
Connecticut, University of
Cook County Hospital
Cook Institute for Research and Education
Cornell University
Cornell University Medical Center
Cornell University Medical College
Creative Micro Tech, Inc.

Dana-Farber Cancer Institute
Dartmouth College
Dartmouth-Hitchcock Medical Center
Delaware, University of
Duke University
Duke University Medical Center

Eastern Virginia Medical School
Emory University
Emory University School of Medicine

Finch University of Health Sciences
Florida Institute of Technology
Florida State University
Florida, University of
Food and Drug Administration
Forsyth Dental Center
Foundation of Microbiology
Fred Hutchinson Cancer Research Center

General Electric Corporate Research Center
George Washington University
Georgetown University
Georgetown University Medical Center
Georgia State University
Georgia, University of
Geron Corporation
Guam, University of

Hahnemann University
Harbor-UCLA Medical Center
Harlem Hospital Center
Hartford, University of
Harvard University Medical School
Harvard School of Public Health
Harvard University
Hawaii, University of
Hebrew Rehabilitation Center for Aged
House Ear Institute
Houston Academy of Medicine
Houston, University of
Howard University
Hunter College

Idaho State University
Idaho, University of
Illinois State University
Illinois, University of, Chicago
Illinois, University of, Urbana-Champaign
Indiana State University
Indiana University
Indiana University School of Medicine
Institute for Genomic Research

Iowa State University
Iowa, University of

Jet Propulsion Laboratory
Johns Hopkins University School of Medicine

Kansas Medical Center, University of
Kansas, University of
Kent State University
Kentucky, University of
Kewalo Marine Laboratory

Lehigh University
Leica, Inc.
Loma Linda University School of Medicine
Long Island University
Louisiana State University
Louisiana State University Medical Center
Louisville, University of
Loyola University of Chicago
Lucent Technologies
Ludwig Institute for Cancer Research, San Diego

Marine Biological Laboratory
Maryland School of Medicine, University of
Maryland, University of
Mass Bay Community College
Massachusetts General Hospital
Massachusetts Institute of Technology
Massachusetts Medical School, University of
Massachusetts, University of
Mayo Clinic Scottsdale
Medical College of Georgia
Meharry Medical College
Memorial Sloan-Kettering Cancer Center
Merck & Co.
Merck Research Laboratory
Mercy College
MetroHealth Medical Center
Miami, University of
Michigan Medical School, University of
Michigan State University
Michigan, University of
Midwestern University
Minnesota School of Medicine, University of
Minnesota, University of
Missouri, University of
Montana State University
Morehouse School of Medicine
Mount Holyoke College

NASA Ames Research Center
National Cancer Institute
National Institutes of Health
National Institutes of Health Library
National Institutes of Mental Health
National Library of Medicine
National Marine Fisheries Service
Naval Medical Research Institute
Nebraska, University of
Neuralynx Inc.
Neurosciences Institute
New Jersey, University of Medicine and Dentistry
New Mexico, University of
New York and Presbyterian Hospital
New York Health Science Center, State University of
New York State Department of Health
New York State Institute for Basic Research
New York University Medical Center
New York University School of Medicine
New York, City University of
New York, State University of, Albany
New York, State University of, Buffalo
New York, State University of, Stony Brook
North Carolina State University
North Carolina, University of, Chapel Hill
North Dakota, University of
North Texas, University of
Northern Arizona University
Northwest Indian College
Northwestern University
Northwestern University Medical School

Occidental College
Ohio State University
Ohio University
Ohio, Medical College of
Oklahoma, University of
Oregon Health Science University
Oregon Regional Primate Research Center
Oregon State University
Oregon, University of

Parke-Davis Research
Parmly Hearing Institute
PE Applied Biosystems
Penn State University
Pennsylvania Health System, University of
Pennsylvania University School of Medicine
Pennsylvania, University of
Pharmacia & Upjohn
Pittsburgh, University of
Pomona College
Prince George's Hospital Center
Princeton University
Procter & Gamble
Puerto Rico, University of
Purdue University

Quorum Pharmaceuticals

Reed College
Rhode Island, University of
Rochester Medical Center, University of
Rockefeller University
Rush-Presbyterian-St. Luke's Medical Center
Rutgers University

Saint Peter's College
Samaritan Health System, Phoenix
Scripps Institution of Oceanography
Seattle Biomedical Research Institute
SETI Institute
SmithKline Beecham Pharmaceuticals
Smithsonian Institution
South Alabama, University of, Mobile
Southern California, University of
Southern Methodist University

St. Jude Children's Research Hospital
St. Louis University School of Medicine
St. Mary's College of Maryland
Stanford University
Stanford University Medical Center
Stratagene
Swarthmore College

Temple University School of Medicine
Tennessee, University of
Texas A&M University
Texas Health Science Center, University of
Texas Medical Branch, University of
Texas Southwestern Medical Center, University of
Texas Southwestern, University of
Texas, University of
Thomas Jefferson University
Toledo, University of
Towson University
Tufts University
Tufts University Health Sciences Library
Tufts University School of Medicine
Tulane University Medical Library

Unilever Research
Union College
United States Army Medical Research Institute
United States Army Natick RD&E Center
United States Department of Agriculture
United States Environmental Protection Agency
Utah Medical Center, University of
Utah, University of

Vanderbilt University
Veterans Administration Medical Center
Virginia Commonwealth University
Virginia Health Sciences Center, University of
Virginia School of Medicine, University of
Virginia Tech
Virginia, University of

Wadsworth Center for Labs and Research
Wake Forest University
Wake Forest University School of Medicine
Washington and Lee University
Washington University School of Medicine
Washington, University of
Wayne State University
Wellesley College
Wesleyan University
Western Cape, University of the
Whitehead Institute for Biomedical Research
William and Mary, College of
Williams College
Wisconsin, University of, Madison
Wisconsin, University of, Milwaukee
Woods Hole Oceanographic Institution

Yale University

Foreign Institutions Represented

Alberto Monroy Foundation Palermo, Italy
Alexandria University, Egypt
All India Institute of Medical Sciences, India
Apollo Hospitals, India
Australian National University, Australia
Autonomous University of the State of Puebla, Mexico

Basel Institute for Immunology, Switzerland
Basel, University of, Switzerland
Bio-Rad Microscience, United Kingdom
Bogor Agricultural University, Indonesia
British Columbia, University of, Canada
Bruxelles, Université Libre de, Belgium
Buenos Aires, University of, Argentina

Calgary, University of, Canada
Cambridge, University of, United Kingdom
Centro de Investigacion y de Estudios Avanzados, Mexico
Chile, University of, Chile
Copenhagen, University of, Denmark

Dalhousie University, Canada
Denmark, Technical University of, Denmark
Dundee, University of, Scotland

Edinburgh, University of, Scotland
Ethiopian Health and Nutrition Institute, The Netherlands
European Molecular Biology Laboratory, Germany

Fondazione Centro San Raffaele del Moute Tabor, Italy
Frankfurt, University of, Germany
Friedrich Meischer Institute, Switzerland
Fukushima Medical College, Japan
Fundação Universitária de Endocrinologia e Fertilidade, Brazil

Glasgow, University of, United Kingdom
Groningen University, The Netherlands
Guelph, University of, Canada

Hannover, University of, Germany
Hebrew University of Jerusalem, Israel
Hong Kong, The Chinese University of, Hong Kong
Hospital for Sick Children, Canada
Hungarian Academy of Science, Hungary

IceTherm Inc., Iceland
Imperial Cancer Research Fund, United Kingdom
Imperial College of Science, Technology and Medicine, United Kingdom
Institute of Protein Research, Russia
Instituto de Investigacion Medica "Mercedes y Martin Ferreyra," Argentina
Instituto Venezolano Investigaciones Cientificas, Venezuela
International School of Advanced Studies, Italy

Karolinska Institute Stockholm, Sweden
Konstanz, University of, Germany
Kuopio, University of, Finland

Landcare Research, New Zealand
Lausanne, University of, Switzerland
Leiden, University of, The Netherlands
Lethbridge, University of, Canada
Liverpool Medical School, University of, United Kingdom
Lodz, Medical Academy of, Poland

Loeb Health Research Institute, Canada
London, University of, United Kingdom

Manchester, University of, United Kingdom
Max-Planck-Institut, Germany
McGill University, Canada
McMaster University, Canada
Medical Research Council, United Kingdom
Melbourne, University of, Australia
Milan, University of, Italy

Naples, University of, Italy
National Centre for Biological Sciences, India
National Institute for Medical Research, United Kingdom
National Research Council, Canada

Otago, University of, New Zealand
Ottawa, University of, Canada
Oxford, University of, United Kingdom

Paris, University of, France
Pasteur Institute–Lille, France
Paterson Institute for Cancer Research, United Kingdom
Pisa, University of, Italy
PPL Therapeutics, Scotland

Regensburg, University of, Germany
Rio de Janeiro, Federal University of, Brazil
Rio de Janeiro, State University of, Brazil
Roslin Institute, Scotland
Rostock, University of, Germany
Russian Academy of Sciences, Russia

Sao Paulo, University of, Brazil
Saskatchewan, University of, Canada
Scientific Institute San Raffaele, Italy
Simon Fraser University, Canada
Southampton Oceanography Centre, United Kingdom
St. Thomas' Hospital London, United Kingdom
Station Zoologique de Ville–Franche Sur Mer, France
Swiss Federal Institute of Technology, Switzerland
Swiss Institute for Experimental Cancer Research, Switzerland
Sydney, University of Technology, Australia
Sydney, University of, Australia

Tata Institute of Fundamental Research, India
Technion-Israel Institute of Technology, Israel
Tohoku University, Japan
Tokyo University of Pharmacy and Life Science, Japan
Tokyo University School of Medical and Dental, Japan
Tokyo, University of, Japan
Toronto, University of, Canada
Tübingen, University of, Germany

Universidad Nacional Autonoma de Mexico, Mexico
Universita "La Sapienza," Italy
Université Paris-Sud, France
University College London, United Kingdom

Wageningen Agricultural University, The Netherlands
Wallenberg Laboratory for Cardio Research, Sweden
Walter and Eliza Hall Institute, Australia
Witwatersrand, University of the, South Africa
World Health Organization, West Africa

Zurich, University of, Switzerland

Year-Round Research Programs

Architectural Dynamics in Living Cells Program

Established in 1992, this program focuses on architectural dynamics in living cells—the timely and coordinated assembly and disassembly of macromolecular structures essential for the proper functioning, division, motility, and differentiation of cells; the spatial and temporal organization of these structures; and their physiological and genetic control. The program is also devoted to the development and application of powerful new imaging and manipulation devices that permit such studies directly in living cells and functional cell-free extracts. The Architectural Dynamics in Living Cells Program promotes interdisciplinary research carried out by resident core and visiting investigators.

Resident Core Investigators

Danuser, Gaudenz, Postdoctoral Fellow
Inoué, Shinya, Distinguished Scientist
Katoh, Kaoru, Postdoctoral Scientist
Oldenbourg, Rudolf, Associate Scientist

Staff

Geer, Thomas, Research Assistant
Knudson, Robert, Instrumental Development Engineer
Baraby, Diane, Laboratory Assistant
MacNeil, Jane, Executive Assistant

Staff

Arimoto, Rieko, Washington University School of Medicine
Biggs, David, AutoQuant Imaging Inc.
Desai, Arshad, EMBL, Heidelburg, Germany
Fukui, Yoshio, Northwestern University Medical School
Goda, Makoto, Kyoto University, Japan
Inoué, Theodore D., Universal Imaging Corporation
Keefe, David, Rhode Island Women and Infants Hospital
Liu, Lin, Rhode Island Women and Infants Hospital
Maddox, Paul, University of North Carolina–Chapel Hill
Matsumoto, Brian, University of California–Santa Barbara
Mitchison, Timothy J., Harvard Medical School
Murray, John M., University of Pennsylvania
Salmon, Edward D., University of North Carolina–Chapel Hill
Tran, Phong, Columbia University

The Josephine Bay Paul Center for Comparative Molecular Biology and Evolution

Major emphasis in the Josephine Bay Paul Center in Comparative Molecular Biology and Evolution is placed upon comparative/phylogenetic studies of genes and genomes, molecular microbial ecology/biodiversity and evolution of host defense mechanisms in marine invertebrates. The Center encourages studies of genotypic diversity across all phyla and promotes the use of modern molecular genetics and phylogeny to gain insights into the evolution of molecular structure and function. The Josephine Bay Paul Center is a member of NASA's Virtual Institute for Astrobiology.

Other major research programs include Mitchell Sogin's studies of molecular evolution in eukaryotes and studies of genome sequences from parasitic microorganisms, Monica Riley's metabolic database and evolutionary studies of protein sequences, Neal Cornell's comparative molecular studies of genes critical to heme biosynthesis, and Michael Cummings' studies of evolution of pathogenetic microorganisms.

Other collaborative projects include studies of P450 evolution (M. Sogin and John Stegeman's laboratory at Woods Hole Oceanographic Institution [WHOI]), a molecular ecology component of the Long Term Ecological Research project (M. Sogin's laboratory and John Hobbie of The Ecosystems Center), and studies of molecular diversity among marine protists and bacteria (with marine microbiologists at WHOI). Future recruiting efforts will focus upon molecular evolution in developmental biology and genome sciences.

The Center has excellent resources for studies of molecular evolution: automated DNA sequencing, well-equipped research laboratories, and powerful computational facilities. In addition to participating in the Parasitology and Microbial Diversity courses, the Center sponsors the Workshop in Molecular Evolution at the MBL, which has gained an international reputation for excellence. This Workshop offers 60 students a series of lectures and minisymposia that are complemented by a state-of-the-art computational facility.

The Josephine Bay Paul Center in Comparative Molecular Biology and Evolution includes the laboratories of Neal Cornell, Michael Cummings, Monica Riley, and Mitchell Sogin.

Resident Core Investigators

Sogin, Mitchell, Director and Senior Scientist
Cornell, Neal, Senior Scientist
Cummings, Michael, Assistant Scientist
Riley, Monica, Senior Scientist
Wainwright, Norman, Senior Scientist

Adjunct Scientists

Halanych, Ken, Woods Hole Oceanographic Institution
Teske, Andreas, Woods Hole Oceanographic Institution

Laboratory of Neal Cornell

Research in this laboratory is concerned with the comparative molecular biology of genes that encode the enzymes for heme biosynthesis, with particular emphasis on 5-aminolevulinate synthase, the first enzyme in the pathway. Because the ability to produce heme from common metabolic materials is a near universal requirement for living organisms, these genes provide useful indicators of molecular aspects of evolution. For example, 5-aminolevulinate synthase in vertebrate animals and simple eukaryotes such as yeast and *Plasmodium falciparum* have high sequence similarity to the enzyme from the alpha-purple subgroup of eubacteria. This supports the suggestion that alpha-purple bacteria are the closest contemporary relatives of the ancestor of eukaryotic mitochondria. The analysis also raises the possibility that plant and animal mitochondria had different origins. Aminolevulinate synthase genes in mitochondria-containing protists are currently being analyzed to obtain additional insight into endosymbiotic events. Also, genes of primitive chordates are being sequenced to gain information about the large-scale gene duplication that played a very important role in the evolution of higher vertebrates. Other studies in the laboratory have been concerned with the effects of environmental pollutants on heme biosynthesis in marine fish, and it has been shown that polychlorinated biphenyls (PCBs) enhance the expression of the gene for aminolevulinate synthase.

Staff

Cornell, Neal W., Senior Scientist
Faggart, Maura A., Research Assistant
Foster, Martin, Laboratory Assistant
Frisbee, Cameran, Laboratory Assistant

Visiting Scientist

Fox, T.O., Harvard Medical School

Laboratory of Michael P. Cummings

The research is in the area of molecular evolutionary genetics and includes the study of the mechanisms of molecular genetic processes, and uses methods from molecular biology, statistics, computer science, molecular systematics, and population genetics. The basis for much of the research is comparative, across several levels of biological organization, and involves both computer-based and empirical studies.

The major focus of research is using novel statistical methods to study relationships between genotype and phenotype. Current investigations in this area examine how gene sequence data can be used to understand and predict drug resistance in tuberculosis, variation in color vision, and basic immune system functions at the molecular level. For example, using drug resistance in *Mycobacterium tuberculosis* as a model system, we are investigating how well phenotype (level of drug resistance) can be predicted with genotype information (DNA sequence data). Drug resistance is a major problem in the treatment of infectious diseases. Understanding evolution of drug resistance, and developing accurate methods for its prediction using DNA sequence data can help in assessing potential resistance in a more timely fashion and circumvent the need for culturing bacteria, which takes several weeks in the case of tuberculosis. More generally, the relationship of genotype to phenotype is a fundamental problem in genetics, and through these investigations we hope to gain insight. The primary empirical work in the laboratory involves examination of opsins, proteins involved in color vision, from local species of Odonata (dragonflies and damselflies).

Research on evolution of pathogenic bacteria also examines species within the genus *Mycobacterium*. *Mycobacterium* provides an excellent model system for studying evolution of pathogenicity and emergent pathogens; it is a large and widely distributed group that occupies a range of habitats (*e.g.*, soil, water, skin), and exhibits a broad range of relationships with other organisms (*e.g.*, free-living, commensal, parasitic). Importantly, the group contains a number of major human pathogens (*e.g.*, those that cause tuberculosis and leprosy), including recently emerged pathogens. We are using phylogenetic analysis of DNA sequence data to study the evolutionary patterns of pathogenicity within *Mycobacterium* to discern patterns in the emergence of new pathogens. The goal of this work is to understand the origins of new pathogens and provide information that may aid in diagnosis and treatment efforts.

Staff

Cummings, Michael P., Assistant Scientist
McInerney, Laura A., Research Assistant

Visiting Scientist

Neel, Maile C., University of California, Riverside

Laboratory of Monica Riley

The genome of the bacterium *Escherichia coli* contains all of the information required for a free-living chemoautotrophic organism to live, adapt, and multiply. The information content of the genome can be dissected from the point of view of understanding the role of each gene and gene product in achieving these ends. The many functions of *E. coli* have been organized in a hierarchical system representing the complex physiology and structure of the cell. In collaboration with Dr. Peter Karp of SRI International, an electronic encyclopedia of information is being constructed on the genes, enzymes, metabolism, transport processes, regulation, and cell structure of *E. coli*. The interactive EcoCyc program is now publicly available and has graphical hypertext displays, including literature citations, on nearly all of *E. coli* metabolism, all genes and their locations, a hierarchical system of cell functions and some regulation processes. This work is continuing.

In addition, the *E. coli* genome contains valuable information on molecular evolution. We are analyzing the sequences of proteins of *E. coli* in terms of their evolutionary origins. By grouping like sequences and tracing back to their common ancestors, we learn not only about the paths of evolution for all contemporary *E. coli* proteins, but we extend even further back before *E. coli*, traversing millennia to the earliest evolutionary times when a relatively few ancestral proteins served as ancestors to all contemporary proteins of all living organisms. The complete genome sequence of *E. coli* and sophisticated sequence analysis programs permit us to identify evolutionary related protein families, determining ultimately what kinds of unique ancestral sequences generated all of present-day proteins. The data developed in the work has proven to be valuable to the community of scientists sequencing microbial genomes. *E. coli* data serve as needed reference points.

Staff

Riley, Monica, Senior Scientist
Kerr, Alastair, Postdoctoral Scientist
Liang, Ping, Postdoctoral Scientist
MacGregor, Alicia, Laboratory Clerk
Nahum, Laila, Postdoctoral Scientist
Pelegrini-Toole, Alida, Research Assistant II
Porterfield, Pamela, Laboratory Clerk
Serres, Margerethe, Postdoctoral Scientist

Program in Comparative Molecular Biology and Evolution: Laboratory of Mitchell L. Sogin

This laboratory in molecular evolution employs comparative phylogenetic studies of genes and genomes to define patterns of evolution that gave rise to contemporary biodiversity on the planet Earth. The laboratory is especially interested in discerning how the eukaryotic cell was invented as well as the identity of microbial groups that were ancestral to animals, plants, and fungi. The lab takes advantage of the extraordinary conservation of ribosomal RNAs to define phylogenetic relationships that span the largest of evolutionary distances. These studies have overhauled traditional eukaryotic microbial classifications systems. The laboratory has discovered new evolutionary assemblages that are as genetically diverse and complex as plants, fungi, and animals. The nearly simultaneous separation of these eukaryotic groups (described as the eukaryotic "Crown") occurred approximately one billion years ago and was preceded by a succession of earlier diverging protist lineages, some as ancient as the separation of the prokaryotic domains.

At the same time, this data base provides a powerful tool for the newly emerging discipline of molecular ecology. Using the ribosomal RNA data base and nucleic acid-based probe technology, it is possible to detect and monitor microorganisms, including those that cannot be cultivated in the laboratory. This strategy has uncovered new habitats and major revelations about geographical distribution of microorganisms.

The laboratory has initiated a program to sample genomic diversity from eukaryotic microorganisms that do not have mitochondria. The lab previously demonstrated that these taxa represent some of the earliest diverging lineages in the evolutionary history of eukaryotes. The objective is to develop a set of additional molecular markers for studying molecular evolution. These will be invaluable in unraveling sudden evolutionary radiations that cannot be resolved by rRNA comparisons and will provide insights into the presence or absence of important biochemical properties in the earliest ancestors common to all eukaryotic species.

More recently, we initiated a study of the complete genome of *Giardia lamblia*.

Staff

Sogin, Mitchell L., Director and Senior Scientist
Amaral-Zettler, Linda, Postdoctoral Scientist
Beaudoin, David, Research Assistant
Bressoud, Scott, Laboratory Technician
Eakin, Nora, Research Assistant
Edgcomb, Virginia, Postdoctoral Scientist
Farr, Rebecca, Research Assistant
Gao, Lingqui, Research Assistant II
Harris, Marian, Executive Assistant
Holder, Greg, Research Assistant
Kim, Ulandt, Research Assistant
Kysela, David, Research Assistant
Laan, Maris, Research Assistant II
Lim, Pauline, Executive Assistant
Luders, Bruce, Research Assistant
McArthur, Andrew, Postdoctoral Scientist
Medina, Monica, Postdoctoral Scientist
Morrison, Hilary G., Postdoctoral Scientist
Nixon, Julie, Postdoctoral Scientist
Roger, Andrew, Postdoctoral Scientist
Shakir, Muhhamed Afaq, Postdoctoral Scientist
Silberman, Jeffrey, Postdoctoral Scientist

Visiting Investigators

Bahr, Michele, The Ecosystems Center
Campbell, Robert, Serono Laboratories, Inc.
Crump, Byron, The Ecosystems Center
Weil, Jennifer, Joslin Diabetes Center

Adjunct Scientists

Halanych, Kenneth, Woods Hole Oceanographic Institution
Teske, Andreas, Woods Hole Oceanographic Institution

BioCurrents Research Center

The Biocurrents Research Center (BRC), one of the NIH National Centers for Research Resources, pioneers methods in the study of transmembrane currents and hosts numerous research pursuits. The Center provides visiting investigators access to a variety of unique technologies as well as new approaches to experimentation in the biomedical sciences.

Four systems are available at the BRC. All these probe technologies are based on the principle of a self-referencing electrode, maximizing sensitivity by noise and drift reduction. All the probes are non-invasive and generally placed in close proximity to the membrane of cells or tissues, in some cases at sub-micron distances. The two older techniques are designed to measure the movement of ions across the membranes of living tissues or cells with the minimum of disturbance. The current probe, developed in 1974, is still available for the study of external current densities resulting from the general net balance of ion transport. Most use is made of the ion-selective probes (Seris), which measure and follow the transmembrane transport of specific ions such as calcium, potassium and protons. This system also can detect non-electrogenic transporters. Two newer techniques are also available: the BioKelvin probe and the non-invasive electrochemical or polarographic probe (Serp). The BioKelvin probe measures voltages around living tissues in air. A radically different approach is being taken to the measurements of biocurrents using the electrochemical microprobes. Presently applied to molecular oxygen, such a technique offers opportunity for the study of molecular transport by using the chemical redox potential. This probe has been applied to single neurons, β-pancreatic cells, damaged neural tissues, developing embryos, and others. We are currently developing further applications of the Serp probes to measure nitric oxide, ascorbic acid, and insulin as well as the production of biosensors.

A state-of-the-art system offers non-invasive ion probes coupled with current and voltage clamp (both single, two electrode, and patch) along with ratio imaging *via* a Zeiss Attofluor system, all of which are finding uses in the hosted biomedical studies, as well as BRC research and development.

As in previous years, a wide variety of biological and biomedical subjects have been studied by BRC staff and visitors. In R&D we have continued developing the application of ion-selective and electrochemical microsensors, all applicable to single cells with square micron spatial resolution. We are currently exploring ways to combine these sensors with a variety of techniques known collectively as near field optical microscopy. In an experimental context we have advanced our technology into several fields, including reproductive physiology, diabetes research, neuroscience, development, gravitropic responses, ion transport, and homeostasis. Details of our research program and a list of publications can be found at ⟨www.mbl.edu/BioCurrents⟩.

MBL year-round laboratories with which BRC is in active collaboration are the Laboratory of Rudolf Oldenbourg and the Laboratory of Reproductive Medicine, headed by David Keefe. Dr. Keefe and Dr. Peter Smith, BRC Director, are Co-Investigators on a project to support the development of new technology to assess the developmental potential of preimplantation embryos and to study the pathophysiology of oocyte dysfunction.

Staff

Smith, Peter J.S., Director and Senior Scientist
Baikie, Iain D., Associate Scientist
Danuser, Gaudenz M., Postdoctoral Fellow
Hammar, Katherine, Research Assistant III
McLaughlin, Jane A., Research Assistant III
Porterfield, D. Marshall, Staff Scientist I
Sanger, Richard H., Research Assistant III

Part Time and Temporary Staff

Jaffe, Lionel F., Senior Scientist
Moore, Laurel, Science Reference Librarian
Pepperell, John R., Staff Scientist I

Graduate Student

Tamse, Catherine T., University of Rhode Island

Visiting Scientists and Publications

This year the Research Center hosted 47 visitors. Scientific publications during the year numbered 25.

Boston University Marine Program

Faculty

Atema, Jelle, Professor of Biology, Director
Dionne, Vincent, Professor of Biology
Golubic, Stjepko, Professor of Biology
Humes, Arthur, Professor of Biology Emeritus
Kaufman, Les, Associate Professor of Biology
Lobel, Phillip, Associate Professor of Biology
Voigt, Rainer, Research Associate Professor
Ward, Nathalie, Lecturer

Staff

Decarie, Linette, Senior Staff Coordinator
DiNunno, Paul, Research Assistant, Dionne Lab
Hall, Sheri, Program Manager
McCafferty, Michelle, Administrative Assistant
Olson, Nancy, Program Assistant
Tomasky, Gabrielle, Research Assistant, Valiela Lab
Wheatley, MaryJo, Information Officer

Postdoctoral Investigators

Basil, Jenny, Atema Laboratory
Cebrian, Just, Valiela Laboratory

Grasso, Frank, Atema Laboratory
Trott, Thomas, Atema Laboratory

Visiting Faculty and Investigators

Hanlon, Roger, Marine Biological Laboratory
Hecker, Barbara, Hecker Consulting
Margulis, Lynn, University of Massachusetts, Amherst
McFall-Ngai, Margaret, Kewalo Marine Laboratory
Moore, Michael, Woods Hole Oceanographic Institution
Nowacek, Douglas, Mote Marine Laboratory
Ruby, Edward, Kewalo Marine Laboratory
Simmons, Bill, Sandia National Laboratory
Wainwright, Norman, Marine Biological Laboratory

Other

Dolan, Mike, Visiting Teaching Assistant
Weir, Andrew, Visiting Teaching Assistant

Graduate Students

PhD Students

Existing
Cole, Marci
Dale, Jonathon
Economakis, Alistair
Hauxwell, Jennifer
Herrold, Ruth
Kroeger, Kevin
Lindholm, James
Ma, Diana
Miller, Carolyn
Oliver, Steven
Sloan, Kevin
Stieve, Erica
Zettler, Erik
Zhao, Jing
New
Dooley, Brad
Tomasky, Gabrielle
York, Joanna

Masters Students

Existing
Allen, Christel
Atkinson, Abby
Barlas, Margaret
Bentis, Christopher
Bowen, Jennifer
Cavanaugh, Joseph
Chichester, Heather
D'Ambrosio, Alison
Evgenidou, Angeliki
Ferland, Amy
Fern, Sophie
Fredland, Inga
Griffin, Martin
Homkow, Laura
Keith, Lucy
Koenig, Eduardo
Konkle, Anne
Lamb, Amy
Lawrence, David
Levine, Michael
McKenna, Ian
Neviackas, Justin
Ramon, Marina
Smith, Spence
Watson, Elise
Wright, Dana

New
Casper, Brandon
Errigo, Michael
Frenz, Christopher
Grable, Melissa
Grebner, Dawn
Kollaros, Maria
Lever, Mark
Malley, Vanessa
Martel, David
Oweke, Ojwang William
Perez, Edmundo
Pugh, Tracy
Ripley, Jennifer
Roycroft, Karen
Stueckle, Todd
Sweeny, Melissa
Tuohy-Sheen, Elizabeth
Weiss, Erica

Undergraduate Students

Spring 99
Champagne, Jaimie
Preto, Luca
Watkins, Cari
Weisbaum, Dolores

Fall 99
Burgess, Robyn
Gottlieb, Jennifer
Griggs, Ryan
Kwong, Grace
Loewensteiner, David
Matsumoto, Rae
Muhlin, Jessica
O'Connell, Timmy
Peyton, Scott
Pytel, Julie
Sarno, Jillian
Silverston, Jennifer
von Kampen, Marie
Walker, Andrew
Williams, Jade
Wingert, Sarah
Woods, Pamela

Summer 1999 Interns

Berkey, Cristin
Canfield, Susannah
Cubbage, Andrea
Hanna, John
Komarow, Sharon
McLaughlin, Leslie
Mijos, Katrin

Walters, Jennifer
Watson, Amy
Wolfe, Felisa
Young, Talia

Summer 1999 Volunteers

Hancock, Amy
Quinn, Elizabeth

Laboratory of Jelle Atema

Many organisms and cellular processes use chemical signals as their main channel of information about the environment. All environments are noisy and require some form of filtering to detect important signals. Chemical signals are transported by turbulent currents, viscous flow, and molecular diffusion. Receptor cells extract chemical signals from the environment through various filtering processes. In our laboratory, fish, marine snails, and crustacea have been investigated for their ability to use chemical signals under water. Currently, we use the lobster and its exquisite senses of smell and taste as our major model to study the signal-filtering capabilities of the whole animal and its narrowly tuned chemoreceptor cells.

Research in our laboratory focuses on amino acids, which represent important food signals for the lobster, and on the function and chemistry of pheromones used in lobster courtship. We examine animal behavior in the sea and in the lab. This includes social interactions and chemotaxis. To understand the role of chemical signals in the sea we use real lobsters and untethered small robots. Our research includes measuring and computer modeling odor plumes and the water currents lobsters generate to send and receive chemical signals. Other research interests include neurophysiology of receptor cells and anatomical studies of receptor organs and pheromone glands.

Laboratory of Vincent Dionne

How does the brain learn about an odor? This simple question frames a complex problem about how information is transferred into and within the brain. Odors are powerful stimuli. They can focus the attention, elicit behaviors, and resurrect forgotten memories. These actions depend on the initial transduction and encoding of odor signals by olfactory sensory neurons located deep in the nasal passages. Odor transduction involves a number of intracellular processes wherein odor receptors on the surfaces of olfactory receptor neurons are coupled to ion channels in the neuronal membrane through G proteins and other intracellular elements. Odors activate the transduction machinery, causing the neuron to fire a coded message carrying information that the brain is able to interpret. The information encoded after just one sniff of odor is actually carried by many olfactory neurons simultaneously, but each neuron appears to carry only part of the message. Thus encoding of odor information is a multicellular process, and different olfactory neurons can carry different pieces of the code.

We are studying the cellular processes that underlie odor transduction and encoding in aquatic salamanders and in mice. Using electrophysiological, imaging, and pharmacological tools, our goal is to learn how these most fundamental actions work, for they represent an elegant and very ancient solution to a complex problem of neural function.

Laboratory of Arthur G. Humes

Research interests include systematics, development, host specificity, and geographical distribution of copepods associated with marine invertebrates. Current research is on taxonomic studies of copepods from invertebrates in the tropical Indo-Pacific area, and poecilostomatoid and siphonostomatoid copepods from deep-sea hydrothermal vents and cold seeps.

Laboratory of Les Kaufman

Current research projects in the laboratory deal with speciation and extinction dynamics of haplochromine fishes in Lake Victoria. We are studying the systematics, evolution, and conservation genetics of a species flock encompassing approximately 700 very recently evolved taxa in the dynamic and heavily impacted landscape of northern East Africa. In the lab we are studying evolutionary morphology, behavior, and systematics of these small, brightly colored cichlid fishes.

Another area of study is developmental and skeletal plasticity in fishes. We are studying the diversity of bone tissue types in fishes, differential response to mineral and mechanical challenge, and matrophic *versus* environmental effects in the development of coral reef fishes.

We also study the biological basis for marine reserves in the New England fisheries. We are involved in collaborative research with NURC, NMFS, and others studying the relative impact on groundfish stocks of juvenile habitat destruction *versus* fishing pressure.

Laboratory of Phillip Lobel

Fishes are the most diverse vertebrate group and provide opportunities to study many aspects of behavior, ecology and evolution. We primarily study how fish are adapted to different habitats and behavioral ecology of species interactions. Current research focuses on fish acoustic communications.

We are also conducting a long-term study of the marine biology of

Johnston Atoll, Central Pacific Ocean. Johnston Atoll has been occupied continuously by the military since the 1930s and proved a unique opportunity for assessing the biological impacts of island industrialization and its effects on reefs. Johnston Atoll is the site of the US Army's chemical weapons demilitarization facility, JACADS.

Ongoing projects also include fish faunal studies in the African Congo, Belize Central America, and Wake Atoll, Pacific.

Laboratory of Ivan Valiela

A focus of our work is the link between land use on watersheds and consequences in the receiving estuarine ecosystems. The work examines how landscape use and urbanization increase nutrient loading to groundwater and streams. Nutrients in groundwater are transported to the sea, and, after biogeochemical transformation, enter coastal waters. There, increased nutrients bring about a series of changes on the ecological components. To understand the coupling of land use and consequences to receiving waters, we study the processes involved, assess ecological consequences, and define opportunities for coastal management.

A second long-term research topic is the structure and function of salt marsh ecosystems, including the processes of predation, herbivory, decomposition, and nutrient cycles.

Center for Advanced Studies in the Space Life Sciences

In 1995, the NASA Life Sciences Division and the Marine Biological Laboratory established a cooperative agreement with the formation of the Center for Advanced Studies in the Space Life Sciences (CASSLS) at MBL. The Center's overall goals are to increase awareness of the NASA Life Sciences Program within the basic science community, and to examine and discuss potential uses of microgravity and other aspects of spaceflight as probes to provide new insights to fundamental processes of basic biology and medicine.

Through symposia, workshops and seminars, CASSLS advises NASA and the biological science community on a wide variety of topics. Through fellowships, CASSLS supports summer research for investigators in areas pertinent to the aims of NASA life sciences.

Since the Center began its operations in July 1995, more than 300 people have attended the seven CASSLS workshops. Typically these workshops last for two to four days and feature an international array of scientists and NASA/International space agency staff. In many cases, workshop chairs have a long-time association with the MBL. Workshop schedules incorporate many opportunities for interaction and discussion. A major outcome for workshops is the publication of proceedings in a peer-reviewed journal. Moreover, our meetings introduce outstanding biologists to research questions and to prominent scientists involved in gravitational biology and the NASA Life Sciences Program.

The Center sponsored two workshops in 1999: Microgravity's Effects on Biological Systems and Behavior: An Integrative Approach, chaired by Richard Wassersug, Dalhousie University; and Cells in Spaceflight: Past, Present and Future, chaired by Dilip Kondepudi, Wake Forest University. The Center sponsored one Fellow during the summer of 1999: Dr. Paul McNeil of the Medical College of Georgia. Dr. McNeil used sea urchin eggs as a model system to study the subcellular and molecular basis of the cell's response to a temporary disruption in plasma membrane integrity.

Staff

Blazis, Diana E.J., Administrator
Oldham, Pamela A., Administrative Assistant

The Ecosystems Center

The Center carries out research and education in ecosystems ecology. Terrestrial and aquatic scientists work in a wide variety of ecosystems ranging from the streams, lakes and tundra of the Alaskan Arctic (limits on plant primary production) to sediments of Massachusetts Bay (controls of nitrogen cycling), to forests in New England (effects of soil warming on carbon and nitrogen cycling), and South America (effects on greenhouse gas fluxes of conversion of rain forest to pasture) and to large estuaries in the Gulf of Maine (effects on plankton and benthos of nutrients and organic matter in stream runoff). Many projects, such as those dealing with carbon and nitrogen cycling in forests, streams, and estuaries, use the stable isotopes ^{13}C and ^{15}N to investigate natural processes. A mass spectrometer facility is available. Data from field and laboratory research are used to construct mathematical models of whole-system responses to change. Some of these models are combined with geographically referenced data to produce estimates of how environmental changes affect key ecosystem indexes, such as net primary productivity and carbon storage, throughout the world's terrestrial biosphere.

The results of the Center's research are applied, wherever possible, to the questions of the successful management of the natural resources of the earth. In addition, the ecological expertise of the staff is made available to public affairs groups and governmental agencies who deal with problems such as acid rain, coastal eutrophication, and possible carbon dioxide-caused climate change.

The Semester in Environmental Science was offered again in Fall 1999. Eighteen students from 14 colleges participated in the program. There are opportunities for postdoctoral fellows.

Administrative Staff

Hobbie, John E., Co-Director
Melillo, Jerry M., Co-Director
Foreman, Kenneth H., Associate Director, Semester in Environmental Studies
Berthel, Dorothy J., Administrative Assistant
Donovan, Suzanne J., Executive Assistant
Moniz, Priscilla C., Administrative Assistant, Semester in Environmental Studies
Nuñez, Guillermo, Research Administrator
Seifert, Mary Ann, Administrative Assistant
Scanlon, Deborah G., Executive Assistant, LMER Coordination Office

Scientific Staff

Hobbie, John E., Senior Scientist
Melillo, Jerry M., Senior Scientist
Deegan, Linda A., Associate Scientist
Giblin, Anne E., Associate Scientist
Herbert, Darrell A., Staff Scientist
Holmes, Robert M., Staff Scientist
Hopkinson, Charles S., Senior Scientist
Hughes, Jeffrey E., Staff Scientist
Nadelhoffer, Knute J., Associate Scientist
Neill, Christopher, Assistant Scientist
Peterson, Bruce J., Senior Scientist
Rastetter, Edward B., Associate Scientist
Shaver, Gaius R., Senior Scientist
Steudler, Paul A., Senior Research Specialist
Tian, Hanqin, Staff Scientist
Vallino, Joseph J., Assistant Scientist
Williams, Mathew, Assistant Scientist

Educational Staff Appointments

Bovard, Brian, Postdoctoral Research Associate
Buzby, Karen, Postdoctoral Research Associate
Cieri, Matthew D., Postdoctoral Research Associate
Crump, Byron, Postdoctoral Research Associate
Garcia-Montiel, Diana C., Postdoctoral Research Associate
Hartley, Anne E., Postdoctoral Research Associate
Kappel-Schmidt, Inger, Postdoctoral Research Associate
Nordin, Annika, Postdoctoral Research Associate
Raymond, Peter, Postdoctoral Research Associate
Tobias, Craig R., Postdoctoral Research Associate

Technical Staff

Ahrens, Toby, Research Assistant
Bahr, Michele P., Research Assistant
Bettez, Neil D., Research Assistant
Byun, James P., Research Assistant
Carpino, Elizabeth, Research Assistant
Claessens, Lodevicus H. J. M., Research Assistant
Colman, Ben, Research Assistant
Downs, Martha R., Research Assistant
Fox, MaryKay, Research Assistant
Garritt, Robert H., Senior Research Assistant
Holland, Keri J., Research Assistant
Hrywna, Yarek, Research Assistant
Jablonski, Sarah A., Research Assistant
Jillson, Tracy A., Research Assistant
Kelsey, Samuel, Research Assistant
Kicklighter, David W., Senior Research Assistant
Kleinhenz, Andrew, Research Assistant
Kwiatkowski, Bonnie L., Research Assistant
Laundre, James A., Senior Research Assistant
Lux, Heidi, Research Assistant
Micks, Patricia, Research Assistant
Newkirk, Kathleen M., Research Assistant
Nolin, Amy L., Research Assistant
Nowicki, Genevieve, Research Assistant
Pan, Shufen, Research Assistant
Regan, Kathleen M., Research Assistant
Ricca, Andrea, Research Assistant
Schwamb, Carol, Research Assistant
Slavik, Karie A., Research Assistant
Thieler, Kama K., Research Assistant
Tholke, Kristin S., Research Assistant
Thomas, Suzanne M., Research Assistant
Tucker, Jane, Senior Research Assistant
Vasiliou, David S., Research Assistant
Weston, Nathaniel B., Research Assistant
Wollheim, Wilfred M., Research Assistant
Wright, Amos, Research Assistant
Wyda, Jason C., Research Assistant

Consultants

Bowles, Francis P., Research Systems Consultant
Bowles, Margaret C., Administrative Consultant

Visiting Scientists and Scholars

Banta, Gary, Roskilde University, Roskilde, Denmark
Duncan, Thomas, Nichols College
Fleischer, Dirk, Friedrich-Alexander Universität Erlangen-Nürnberg, Germany
Mondrup, Thomas, Roskilde University, Roskilde, Denmark
Moore, Marianne, SES Faculty Fellow, Wellesley College

Laboratory of Aquatic Biomedicine

Work in this laboratory centers on comparative immunopathology and molecular biology using marine invertebrates as experimental models. Examples of current research include determining the prevalence of leukemia in *Mya arenaria* (the soft shell clam) in Massachusetts. Monoclonal antibodies developed by this laboratory are being used to diagnose clam leukemia, identify and characterize a tumor-specific protein, and differentiate other leukemias in bivalve molluscs. Development and chemically induced changes in gene expression and neuronal growth are also being studied in the surf clam, *Spisula solidissima.* Work in molecular biology is creating a clearer understanding of the comparative etiology and pathogenesis of tumors, particularly in environmentally impacted aquatic animals.

Staff

Reinisch, Carol L., Senior Scientist
Jessen-Eller, Kathryn, Postdoctoral Scientist
Kreiling, Jill, Postdoctoral Scientist

Visiting Scientists

Stephens, Raymond, Boston University
Walker, Charles, Professor of Zoology, University of New Hampshire

Student

Steiger, Daniel, Tufts University School of Veterinary Medicine

Laboratory of Cell Communication

Established in 1994, this laboratory is devoted to the study of intercellular communication. The research focuses on the cell-to-cell channel, a membrane channel built into the junctions between cells. This channel provides one of the most basic forms of intercellular communication in organs and tissues. The work is aimed at the molecular physiology of this channel, in particular, at the mechanisms that regulate the communication. The channel is the conduit of growth-regulating signals. It is instrumental in a basic feedback loop whereby cells in organs and tissues control their number; in a variety of cancer forms it is crippled.

This laboratory has shown that transformed cells lacking communication channels lost the characteristics of cancer cells, such as unregulated growth and tumorigenicity, when their communication was restored by insertion of a gene that codes for the channel protein. Work is now in progress to track the channel protein within the cells from its point of synthesis, the endoplasmic reticulum, to its functional destination in the plasma membrane, the cell-to-cell junction, by expressing a fluorescent variant of the channel protein in the cells. Knowledge about the cellular regulation of this process will aid our understanding of what goes awry when a cell loses the ability to form cell-to-cell channels and thus to communicate with its neighbors, thereby taking the path towards becoming cancerous.

Another line of work is taking the first steps at applying information theory to the biology of cell communications. Here, the intercellular information spoor is tracked to its source: the macromolecular intracellular information core. The outlines of a coherent information network inside and between the cells are beginning to emerge.

Staff

Loewenstein, Werner, Senior Scientist
Rose, Birgit, Senior Scientist
Jillson, Tracy, Research Assistant

Laboratory of Paul Colinvaux

The research of this laboratory reconstructs Pleistocene climatic and environmental histories of the continents from the sediments of ancient lakes, particularly in the Amazon basin. The team has raised sediment cores from lakes in the lowland Amazon forests that span the last 30,000 years, including records of the last glacial maximum (LGM). Several of these sites were extremely remote. We use pollen analysis to reconstruct the history of vegetation around the lakes, an undertaking that required us to produce a pollen taxonomy for the diverse Amazon forests (published this year as an Amazon Pollen Manual and Atlas). The research has shown that the lowland Amazon forests persisted through glacial cycles, with some reassortment of species as temperature fluctuated from the LGM to the present. These data are useful for the calibration of global climate models and in understanding how the great diversity of the Amazon biota is maintained. Because of the variety of analytical techniques other than pollen analysis used, we organize the research in collaboration with specialized laboratories at other institutions. Although our research is now concentrated in the Neotropics we also have a continued interest in the paleoecology of the arctic, with sites in Alaska and Russia.

Staff

Colinvaux, Paul, Adjunct Scientist

Laboratory of Ayse Dosemeci

The laboratory investigates molecular processes that underlie synaptic modification. The current project is aimed at clarifying how the frequency of activation at a synapse can determine whether the synapse will be potentiated (strengthened) or depressed (weakened) through the participation of an enzyme called CaM kinase II. Self-regulatory properties of this enzyme are investigated to prove that it can respond to the temporal pattern of calcium, the intracellular signal generated upon synaptic activation. Related projects in collaboration with Dr. Thomas Reese (NIH, NINDS) involve tracing changes in the distribution of CaMKII in cultured hippocampal neurons in response to sustained glutamate receptor activation and investigating the structural plasticity of the postsynaptic density under these conditions.

Staff

Dosemeci, Ayse, Adjunct Scientist

Laboratory of Barbara Furie and Bruce Furie

γ-Carboxyglutamic acid is a calcium-binding amino acid that is found in the conopeptides of the predatory marine cone snail, *Conus*. This laboratory has been investigating the biosynthesis of this amino acid in *Conus* and the structural role of γ-carboxyglutamic acid in the conopeptides. This satellite laboratory relates closely to the main laboratory, the Center for Hemostasis and Thrombosis Research, on the Harvard Medical School campus in Boston; the main focus of the primary laboratory is the synthesis and function of γ-carboxyglutamic acid in blood clotting proteins and the role of vitamin K.

Cone snails are obtained from the South Pacific and maintained in the Marine Resources Center. Until recently, the marine cone snail had been the sole invertebrate known to synthesize γ-carboxyglutamic acid (Gla). The venomous cone snail produces neurotoxic conopeptides, some rich in Gla, which it injects into its prey to immobilize it. To examine the biosynthetic pathway for Gla, we have studied the *Conus* carboxylase which converts glutamic acid to γ-carboxyglutamic acid. This activity has an absolute requirement for vitamin K. The *Conus* carboxylase substrates contain a carboxylation recognition site on the conotoxin precursor. Given the functional similarity of mammalian vitamin K-dependent carboxylases and the vitamin K-dependent carboxylase from *Conus textile*, we hypothesized that structurally conserved regions would identify sequences critical to this common functionality. Furthermore, we examined the diversity of animal species that maintain vitamin K-dependent carboxylation to generate γ-carboxyglutamic acid. We have cloned carboxylase homologs in full length or partial form from the beluga whale (*Delphinapterus leucas*), toadfish (*Opsanus tau*), chicken (*Gallus gallus*), hagfish (*Myxine glutinosa*), horseshoe crab (*Limulus polyphemus*) and cone snail (*Conus textile*) in order to compare these structures to the known bovine, human, rat and mouse cDNA sequences. Comparison of the predicted amino acid sequences identified a highly conserved 32-amino acid residue region in all of these putative carboxylases. In addition, this amino acid motif is also present in the *Drosophila* genome and identified a *Drosophila* homolog of the γ-carboxylase. Assay of hagfish liver and *Drosophila* demonstrated carboxylase activity in these non-vertebrates. These results demonstrate the broad distribution of the vitamin K-dependent carboxylase gene, including a highly conserved motif that is likely critical for enzyme function. The vitamin K-dependent biosynthesis of γ-carboxyglutamic acid appears to be a highly conserved function in the animal kingdom.

Novel γ-carboxyglutamic acid-containing conopeptides have been isolated from the venom of *Conus textile*. The amino acid sequence, amino acid composition, and molecular weights of these peptides have been determined. For several peptides, the cDNA encoding the precursor conotoxin has been cloned. The three-dimensional structure of some of these Gla-containing conopeptides as well as conantokin G have been determined by 2D NMR spectroscopy. Complete resonance assignments were made from 2D ^{1}H NMR spectra *via* identification of intraresidue spin systems using ^{1}H-^{1}H through-bond connectivities. NOESY spectra provided $d_{\alpha N}$, d_{NN} and $d_{\beta N}$ NOE connectivities and vicinal spin-spin coupling constants $^3J_{HN\alpha}$ were used to calculate ϕ torsion angles. Structure generation based on interproton distance restraints and torsion angle measurements yield convergent structures generated using distance geometry and simulated annealing methods. The goal of this project is to determine the structural role of γ-carboxyglutamic acid in the Gla-containing conotoxins and other γ-carboxyglutamic acid-containing proteins.

Staff

Furie, Barbara C., Adjunct Scientist
Furie, Bruce, Adjunct Scientist
Stenflo, Johan, Visiting Scientist
Czerwiec, Eva, Postdoctoral Fellow
Begley, Gail, Scientist I
Rigby, Alan, Adjunct Scientist

Laboratory of Roger Hanlon

This laboratory investigates the behavior and neurobiology of cephalopods. Studies of various learning capabilities are currently being conducted, as are studies on reproductive strategies that include agonistic behavior, female mate choice, and sperm competition. The latter studies involve DNA fingerprinting to determine paternity and help assess alternative mating tactics. Currently we are studying sensory mechanisms and functions of polarization vision in cephalopods. Complementary field studies are conducted locally and on coral reefs. The functional morphology and neurobiology of the chromatophore system of cephalopods are also studied on a variety of cephalopod species, and image analysis techniques are being developed to study crypsis and the mechanisms that enable cryptic body patterns to be neurally regulated by visual input.

Staff

Hanlon, Roger, Senior Scientist
Buresch, Kendra, Research Assistant
Maxwell, Michael, Postdoctoral Scientist
Rummel, John, Visiting Scientist
Shashar, Nadav, Postdoctoral Scientist
Sussman, Raquel, Investigator

Visiting Investigators

Adamo, Shelley, Dalhousie University
Baker, Robert, New York University
Benjamins, Steven, Graduate Student, University of Groningen
Boal, Jean, Adjunct Scientist
Cavanaugh, Joseph, Graduate Student, Boston University Marine Program
Fern, Sophie, Graduate Student, Boston University Marine Program
Hatfield, Emma, Postdoctoral Fellow
Kier, William, University of North Carolina
King, Alison, Graduate Student, Dalhousie University
Milbury, Coren, Research Assistant
Ring, Sabine, Graduate Student, University of Frankfurt
Saidel, William, Rutgers University
Spotte, Stephen, University of Connecticut

Laboratory of Shinya Inoué

Scientists in this laboratory study the molecular mechanism and control of mitosis, cell division, cell motility, and cell morphogenesis, with emphasis on biophysical studies made directly on single living cells, especially developing eggs in marine invertebrates. Development of biophysical instrumentation and methodology, such as the centrifuge polarizing microscope, high-extinction polarization optical and video microscopy, digital image processing techniques including dynamic stereoscopic imaging, and exploration of their underlying optical theory are an integral part of the laboratory's efforts.

Staff

Inoué, Shinya, Distinguished Scientist
Goda, Makoto, Visiting Scientist
Baraby, Diane, Laboratory Assistant
Knudson, Robert, Instrument Development Engineer
MacNeil, Jane, Executive Assistant

Laboratory of Alan M. Kuzirian

Research in the laboratory explores the functional morphology and ultrastructure of various organ systems in molluscs. The program includes mariculture of the nudibranch, *Hermissenda crassicornis*, with emphasis on developing reliable culture methods for rearing and maintaining the animal as a research resource. The process of metamorphic induction by natural and artificial inducers is being explored in an effort to understand the processes involved and as a means to increase the yield of cultured animals. Morphologic studies stress the ontogeny of neural and sensory structures associated with the photic and vestibular systems which have been the focus of learning and memory studies, as well as the spatial and temporal occurrence of regulatory and transmitter neurochemicals. Concurrent studies detailing the toxic effects of lead on *Hermissenda* learning and memory, feeding, and the physiology of cultured neurons are also being conducted. New studies include cytochemical investigations of the Ca^{2+}/GTP binding protein, calexcitin, and its modulation with learning and lead exposure.

Collaborative research includes histochemical investigations on strontium's role in initiating calcification in molluscan embryos (shell and statoliths), immunocytochemical labelling of cell-surface antigens, neurosecretory products, second messenger proteins involved with learning and memory, as well as intracellular transport organelles using mono- and polyclonal antibodies on squid (*Loligo pealei*) giant axons and *Hermissenda* sensory and neurosecretory neurons. Additional collaborations involve studying neuronal development of myelin, myelination defects, as well as nerve regeneration and repair in phylogenetically conserved nervous systems.

Additional collaborative research includes DNA fingerprinting using RAPD-PCR techniques in preparation for isogenic strain development of laboratory-reared *Hermissenda* and hatchery produced bay scallops (*Argopectin irradians*) with distinct phenotypic markers for the rapid field identification and stock assessments. Recently obtained funding will expand this research to perform population genetic analyses of currently designated yellowtail flounder (*Limanda ferruginea*) stocks occurring in the Northeast Fisheries Region.

Systematic and taxonomic studies of nudibranch molluscs, to include molecular phylogenetics, are also of interest.

Scientific Staff

Kuzirian, Alan M., Associate Scientist

Visiting Investigators

Chikarmane, Hemant, Investigator
Clay, John R., NINDS/NIH
Gould, Robert, NYS Institute of Basic Research

Laboratory of Rudolf Oldenbourg

The laboratory investigates the molecular architecture of living cells and of biological model systems using optical methods for imaging and manipulating these structures. For imaging cell architecture non-invasively and non-destructively, dynamically and at high resolution, we have developed a new polarized light microscope (Pol-Scope). The Pol-Scope combines microscope optics with new electro-optical components, video, and digital image processing for fast analysis of specimen birefringence over the entire viewing field. Examples of biological systems currently investigated with the Pol-Scope are microtubule-based structures (asters, mitotic spindles, single microtubules); actin-based structures (acrosomal process, stress fibers, nerve growth cones); zona pellucida of vertebrate oocytes; and biopolymer liquid crystals.

Staff

Oldenbourg, Rudolf, Associate Scientist
Knudson, Robert, Instrument Development Engineer
Baraby, Diane, Laboratory Assistant

Laboratory of Michael Rabinowitz

This laboratory investigates environmental geochemistry and epidemiology. Areas of recent activity include modeling lead bioavailability, writing a history of lead biokinetic models, performing a case control survey of tea drinking and oral cancer in Taiwan, quantifying the transport and fate of various sources of residential lead exposure, and serving on several advisory boards of Superfund research projects in Boston and New York. Current activity focuses on characterizing lead paints and pigments.

Staff

Rabinowitz, Michael, Associate Scientist

Laboratory for Reproductive Medicine, Brown University and Women and Infants Hospital, Providence

Work in this laboratory centers on investigating cellular mechanisms underlying female infertility. Particular emphasis is placed on the physiology of the oocyte and early embryo, with the aim of assessing developmental potential and mitochondria dysfunction arising from mtDNA deletions. The studies taking place at the MBL branch of the Brown Laboratory use some of the unique instrumentation available through the resident programs directed by Rudolf Oldenbourg and Peter J.S. Smith. Most particularly, non-invasive methods for oocyte and embryo study are being sought. Of several specific aims, one is to use the Pol-Scope to analyze the dynamic birefringence of meiotic spindles. An additional aim is to study transmembrane ion transport using non-invasive electro-physiological techniques available at the BioCurrents Research Center. The newly developed oxygen probe offers the possibility of looking directly at abnormalities in the mitochondria arising from accumulated mtDNA damage. Our laboratory has also focused on studying the mechanism underlying age-associated infertility in terms of oocyte quality and has attempted to rescue developmentally compromised oocytes or embryos through nuclear-cytoplasmic transfer technology. We have characterized oxidative stress-induced mitochondrial dysfunctions, developmental arrest and cell death in early embryos using animal models. Ultimately, this laboratory aims to produce clinical methods for assessing preimplantation embryo viability, an advance that will significantly contribute to the health of women and children.

Staff

Keefe, David, Director
Liu, Lin, Research Scientist
Trimarchi, James, Staff Scientist

Laboratory of Osamu Shimomura

Biochemical mechanisms involved in the bioluminescence of various luminescent organisms are investigated. Based on the results obtained, various improved forms of bioluminescent and chemiluminescent probes are designed and produced for the measurements of intracellular free calcium and superoxide anion.

Staff

Shimomura, Osamu, Senior Scientist, MBL, and Boston University School of Medicine
Shimomura, Akemi, Research Assistant

Laboratory of Robert B. Silver

The members of this laboratory study how living cells make decisions. The focus of the research, typically using marine models, is on two main areas: the role of calcium in the regulation of mitotic cell division (sea urchins, sand dollars, etc.) and structure and function relationships of hair cell stereociliary movements in vestibular physiology (oyster, toadfish). Other related areas of study, *i.e.* synaptic transmission (squid), are also, at times, pursued. Tools include video light microscopy, multispectral, subwavelength, and very high speed (sub-millisecond frame rate) photon counting video light microscopy, telemanipulation of living cells and tissues, and modeling of decision processes. A cornerstone of the laboratory's analytical efforts is high performance computational processing and analysis of video light microscopy images and modeling. With luminescent, fluorescent, and absorptive probes, both empirical observation and computational modeling of cellular, biochemical, and biophysical processes permit interpretation and mapping of space-time patterns of intracellular chemical reactions and calcium signaling in living cells. A variety of *in vitro* biochemical, biophysical, and immunological methods are used. In addition to fundamental biological studies, the staff designs and fabricates optical hardware, and designs software for large video image data processing, analysis, and modeling.

Staff

Silver, Robert, Associate Scientist

Visiting Investigators

Crawford, Karen, St. Mary's College
Hummel, John, Argonne National Laboratory
Pearson, John, Los Alamos National Laboratory

Intern

Deming, Nicole A., REU Intern, St. Mary's College

Laboratory of Norman Wainwright

The mission of the laboratory is to understand the molecular defense mechanisms exhibited by marine invertebrates in response to invasion by bacteria, fungi, and viruses. The primitive immune systems demonstrate unique and powerful strategies for survival in diverse marine environments. The key model has been the horseshoe crab *Limulus polyphemus*. *Limulus* hemocytes exhibit a very sensitive LPS-triggered protease cascade which results in blood coagulation. Several proteins found in the hemocyte and hemolymph display microbial binding proteins that contribute to antimicrobial defense. Commensal or symbiotic microorganisms may also augment the antimicrobial mechanisms of macroscopic marine species. Secondary metabolites are being isolated from diverse marine microbial strains in an attempt to understand their role. Microbial participation in oxidation of the toxic gas hydrogen sulfide is also being studied.

Staff

Wainwright, Norman, Senior Scientist
Child, Alice, Research Assistant

Visiting Investigator

Anderson, Porter, University of Rochester

Laboratory of Seymour Zigman

This laboratory is investigating basic mechanisms of photooxidative stress to the ocular lens due to environmentally compatible UVA radiation. This type of oxidative stress contributes to human cataract formation. Other studies are the search for and use of chemical antioxidants to retard the damage that occurs. Cultured mammalian lens epithelial cells and whole lenses *in vitro* are exposed to environmentally compatible UVA radiation with or without previous antioxidant feeding. The following parameters of lens damage are examined: molecular excitation to singlet states *via* NADPH (the absorber); cell growth inhibition and cell death; catalase inactivation; cytoskeletal description (of actin, tubulin, integrins); and cell membrane damage (lipid oxidation, loss of gap junction integrity and intercellular chemical communications). Thus far, the most successful antioxidant to reduce these deficiencies is alpha-tocopherol (10 μg/ml) and tea polyphenols (especially from green tea). The preliminary phases of the research are usually carried out using marine animal eyes (*i.e.*, smooth dogfish) as models. Our goal is to provide information that will suggest means to retard human cataract formation.

Staff

Seymour Zigman, Laboratory Director, Professor of Ophthalmology, Boston University Medical School
Keen Rafferty, Research Associate, Boston University Medical School
Nancy S. Rafferty, Research Associate, Boston University Medical School
Bunnie R. Zigman, Laboratory Manager, Boston University Medical School

The Marine Resources Center

The Marine Resources Center (MRC) is one of the world's most advanced facilities for maintaining and culturing aquatic organisms essential to advanced biological, biomedical, and ecological research. Service and education also play an important and complementary role in the modern, 32,000-square-foot facility.

The MRC and its life support systems have already increased the ability of MBL scientists to conduct research and have inspired new concepts in scientific experiments. Vigorous research programs focusing on basic biological and biomedical aquatic models are currently being developed at the Center. The Program in Scientific Aquaculture was initiated in 1998.

In addition to research, the MRC provides a variety of services to the MBL community through its Aquatic Resources Division, the Water Quality and System Engineering Division, and the Administrative Division.

Research and educational opportunities are available at the facility to established investigators, postdoctoral fellows, graduate, and undergraduate students. Investigators and students will find that the MRC's unique life support and seawater engineering systems make this a favorable environment in which to conduct independent research and masters and doctoral theses using a variety of aquatic organisms and flexible tank space for customized experimentation on live animals. Prospective investigators and students should contact the Director of the MRC for further information.

Staff

Hanlon, Roger, Director and Senior Scientist
Buresch, Kendra, Research Assistant
Kuzirian, Alan, Associate Scientist
Maxwell, Michael, Postdoctoral Scientist
Santore, Gabrielle, Executive Assistant
Shashar, Nadav, Postdoctoral Scientist
Smolowitz, Roxanna, MBL Veterinarian
Sussman, Raquel, Investigator

Visiting Investigators

Adamo, Shelley, Dalhousie University
Baker, Robert, New York University
Benjamins, Steven, Graduate Student, University of Groningen
Boal, Jean, Adjunct Scientist
Cavanaugh, Joseph, Graduate Student, Boston University Marine Program
Fern, Sophie, Graduate Student, Boston University Marine Program
Gilland, Edwin, Staff Scientist
Hatfield, Emma, Postdoctoral Fellow
Kier, William, University of North Carolina
King, Alison, Graduate Student, Dalhousie University
Milbury, Coren, Research Assistant
Ring, Sabine, Graduate Student, University of Frankfurt
Saidel, William, Rutgers University
Spotte, Stephen, University of Connecticut

Honors

Friday Evening Lectures

June 18	Barbara and Bruce Furie, Harvard Medical School "Of Molluscs and Men: Vitamin K-dependent Synthesis of Gla, a Novel Amino Acid"
June 25	Roderick MacKinnon, Rockefeller University "Potassium Channels"
July 2	Nancy Kanwisher, Massachusetts Institute of Technology "Functional Specialization in Human Visual Cortex: Faces and Places"
July 9	Judith Kimble, University of Wisconsin, Madison "Regulation of Development of *C. elegans*—Lessons from the Gonad" (Glassman Lecture)
July 16	Eric Chivian, Harvard Medical School "The Value of Plants, Animals, and Microbes to Human Health"
July 22, 23	Marianne Bronner-Fraser and Scott E. Fraser, California Institute of Technology 1. "Formation of the Neural Crest" 2. "Working with the Wiring of the Developing Brain" (Forbes Lectures)
July 30	Dr. Bernd U. Budelmann, Marine Biomedical Institute, University of Texas "The Sensory World of Cephalopods" (Lang Lecture)
August 6	Dr. Gerald Fischbach, National Institute of Neurological Disorders and Stroke "Neuroscience at the New Millennium"
August 13	Dr. Luca Cavalli-Sforza, Stanford University School of Medicine "Crucial Times in Human Evolution"

Fellowships and Scholarships

In 1999, the MBL awarded research fellowships to 20 scientists from around the world. These fellows' research topics ranged from a study of how calcium enters heart and nerve cells when a cell is stimulated to research on how the skate senses small electric potentials in surrounding seawater to locate prey. The MBL awarded scholarships to 65 students in the MBL's summer courses as well as 11 post course research awards.

In 1999, donors provided gifts for endowed and expendable funds amounting to $103,309 in support of the research fellowships program and an additional $233,884 to provide scholarships to students im MBL courses. The individuals who received fellowships and scholarships are listed beginning on p. R56.

Robert Day Allen Fellowship Fund

Drs. Joseph and Jean Sanger

American Society for Cell Biology Scholarships

American Society for Cell Biology

Frederick B. Bang Fellowship Fund

Mrs. Betsy G. Bang

Jean and Katsuma Dan Fellowship Fund

Drs. Joseph and Jean Sanger
Mrs. Eleanor Steinbach

Bernard Davis Fellowship Fund

Mrs. Elizabeth M. Davis

Fries Fellowship

Trust of Anna B. Fries

Aline D. Gross Scholarship Fund

Dr. and Mrs. Paul R. Gross
Technic, Inc.

Keffer Hartline Fellowship Fund

Dr. Max Snodderly

E. E. Just Research Fellowship Fund

Ayco Charitable Foundation
William Townsend Porter Foundation

Fred Karush Endowed Library Readership

Dr. and Mrs. Laszlo Lorand
Dr. and Mrs. Arthur M. Silverstein

S. O. Mast Founders Endowed Scholarship Fund

Dr. and Mrs. John B. Buck
Mrs. Louise M. Specht

James A. And Faith Miller Fellowship Fund

Drs. David and Virginia Miller

Frank Morrell Scholarship Fund

Dr. Leyla de Toledo-Morrell

Emily Hartshorne Mudd Scholarship Fund

World Academy of Art and Science

Mountain Memorial Fund

Dr. and Mrs. Dean C. Allard, Jr.
Dr. and Mrs. R. Walter Schlesinger

Neural Systems & Behavior Scholarship Fund

Dr. and Mrs. Alan Gelperin
Josephine Bay Paul and C. Michael Paul Foundation
Drs. Harold Zakon and Lynne McAnelly

Nikon Fellowship Fund

Nikon, Inc.

The Ann Osterhout Edison/Theodore Miller Edison and Olga Osterhout Sears/Harold Bright Sears Endowed Scholarship Fund

Ms. Nancy Miller Arnn
Mr. and Mrs. Alan K. Karplus

Phillip H. Presley Scholarship Fund

Carl Zeiss, Inc.

William Townsend Porter Scholarship Fund for Minority Students

William Townsend Porter Foundation

The Evelyn and Melvin Spiegel Fellowship Fund

Drs. Joseph and Jean Sanger
The Sprague Foundation

H. B. Steinbach Fellowship Fund

Mrs. Eleanor Steinbach

Horace W. Stunkard Scholarship Fund

Dr. Albert Stunkard and Dr. Margaret Maurin

Eva Szent-Gyorgyi Scholarship Fund

Dr. and Mrs. Laszlo Lorand
Dr. Andrew Szent-Gyorgyi and Ms. Ursula Rowan

Selman A. Waksman Endowed Scholarship in Microbial Diversity

Foundation for Microbiology

Walter L. Wilson Endowed Scholarship

Dr. Paul N. Chervin
Mrs. Rigaumont
Mr. and Mrs. Leslie J. Wilson

Young Scholars/Fellows Program

Mr. and Mrs. David Bakalar
Mrs. LeRoy Clark
Mrs. George H. A. Clowes
Mr. and Mrs. Daniel D. Federman
Dr. and Mrs. Harold S. Ginsberg
Dr. and Mrs. Robert Haselkorn
Mr. and Mrs. Gary G. Hayward
Dr. and Mrs. John E. Hobbie
Dr. and Mrs. Edward F. MacNichol, Jr.
Mr. and Mrs. William J. Pechilis
Mrs. Atholie K. Rosett
Dr. and Mrs. Edward A. Spiegel
Mr. and Mrs. Leslie J. Wilson
Drs. Jonathan and Beatrice Wittenberg

Fellowships Awarded

MBL Summer Research Fellows

- Pavel Balaban, Ph.D., is a Professor at the Institute of Higher Nervous Activity and Neurophysiology of the Russian Academy of Sciences in Moscow. He is interested in the mechanism of post-synaptic activation potentials in connection with synaptic plasticity, using the terrestrial mollusc, *Helix*, as a model organism. Dr. Balaban studies the putative command neurons, a group of serotonin-containing cells, which modulate withdrawal behavior and the activity of neurons underlying this behavior. Spikes in these neurons do not elicit behavior, yet behavioral responses evoked by noxious stimuli are changed. Dr. Balaban was funded by the *Herbert W. Rand Fellowship*.
- Richard Cardullo, Ph.D., is an Associate Professor in the Department of Biology at the University of California, Riverside. His research project was titled: "Microscopic evaluation and functional analysis of the egg extracellular matrix." Dr. Cardullo is interested in the molecular determinants in fertilization. He uses advanced imaging technologies along with biochemical and biophysical methodologies to determine both the molecules involved in fertilization and the precise sequence of molecular events ultimately leading to the fusion of mammalian sperm and egg. Dr. Cardullo was supported by the *Lucy B. Lemann Fellowship Fund*, the *Robert Day Allen Fellowship*, the *Charles R. Crane Fellowship*, the *John O. Crane Fellowship*, and an *MBL Research Fellowship*.
- Anthony DePass, Ph.D., is an Assistant Professor in the Biology Department at Long Island University in Brooklyn, NY. His research focuses on how calcium enters heart and nerve cells when a cell is stimulated. He uses *Lytechinus pictus*, *Arbacia punctulata* (sea urchins), and *Raja arinacius* (skate) as biomedical models in this work. Specifically, he studies receptors that mediate Ca^{2+} release from intracellular stores and the second messenger pathways involved in signal transduction. Dr. DePass was a *Josiah Macy, Jr. Foundation Research Fellow*.
- Ana S. DePina is a graduate student at Dartmouth College. Her research project this summer was titled "Actin-based movement in clam oocyte extracts." She studies vesicle transport on actin filaments in clam oocyte extracts. She wants to determine the types of myosins that function as molecular motors for vesicle transport. Ms. DePina was sponsored by the *Milton L. Shifman Endowed Scholarship* and the *William Townsend Porter Fellowship*.
- Iñigo Novales Flamarique, Ph.D., is a post-doctoral fellow in the Department of Biology at the University of Victoria, British Columbia. His summer's research project was "Optical recordings of UV sensitivity in the optic tectum of rainbow trout using voltage sensitive dyes." His research focuses on the chromatic organization of neural pathways in the visual systems of vertebrates. The ultraviolet sensitive cones in the retinas of some fishes disappear and are reincorporated in the photoreceptor layer at specific stages during the animal's life. As such, the ultraviolet neural pathway is a good model to study the cellular mechanisms behind cell apoptosis and regeneration. Dr. Novales Flamarique was funded by the *Stephen W. Kuffler Fellowship*.
- Elizabeth A. Jonas, MD, is in the Department of Pharmacology at the Yale University School of Medicine in New Haven, Connecticut. Her research project was titled "Activation of conductances on intracellular organelles during synaptic transmission." She is interested in measuring ionic currents on membranes of mitochondria during neurotransmission in squid. She has found that, in addition to their role

in calcium management in cells, mitochondrial ion channels maintain electrochemical gradients that are essential to mitochondrial function as well as the regulation of the transport of peptides and metabolites between the cytosol and the inner mitochondrial matrix. Dr. Jonas was supported by the *Frank R. Lillie Fellowship Fund.*

- Samantha Joye, Ph.D., is an Assistant Professor in the Department of Marine Sciences at the University of Georgia in Athens. Her research project was titled "Denitrification of coastal marshes: relationship to nitrogen loading." Dr. Joye's research focuses on biogeochemical cycling in coastal environments and on understanding how humans impact coastal ecosystems. She examines how nitrogen and phosphorus cycles are altered by human activities, with a focus on developing critical new tools for evaluating how pristine environments might be affected by nitrogen loading. Dr. Joye was supported by the *Lucy B. Lemann Fellowship*, an *MBL Associates Fellowship*, and an *MBL Research Fellowship.*

- Eileen M. Lafer, Ph.D, is Associate Professor at the Institute of Biotechnology at the University of Texas Health Science Center in San Antonio. At the MBL she studied the molecular mechanisms that regulate neurotransmission. Her research focuses on the biochemical studies of various peptides, specifically the significance of the clathrin pathway at the squid giant synapse in an effort to understand neurotransmission in synaptic vesicles. Dr. Lafer was funded by the *Ann E. Kammer Memorial Fellowship*, the *Frederick B. Bang Fellowship*, the *Evelyn and Melvin Spiegel Fellowship*, and an *MBL Research Fellowship.*

- Jennifer LaVail, Ph.D., is a Professor of Anatomy/Ophthalmology at the University of California, San Francisco. She investigated the genetic and molecular regulation of Herpes simplex virus transport using GFP-labeled virus injected into squid axons. This movement was monitored by confocal microscopy. It is hypothesized that studying the virus transport mechanisms will shed light on transport in other classes of neurotropic viruses, and on organelle trafficking in general. Dr. LaVail was funded by the *Evelyn and Melvin Spiegel Fellowship* and the *Frederick B. Bang Fellowship.*

- Jeff Magee, Ph.D., is an Assistant Professor at the Department of Neuroscience at the Louisiana State University in New Orleans, Louisiana. His research project was titled "Mechanisms of Ca^{2+} entry into neurons." He uses optical imaging to study varying concentrations of calcium ions in hippocampal neurons. Changes in the strength of synaptic connections are thought to form the basis of memory because they ultimately lead to changes in the firing patterns of neurons. Dr. Magee was supported by an *MBL Associates Fellowship.*

- Guy Major, Ph.D., is a Research Fellow at Lucent Technologies/Bell Labs in Murray Hill, NJ. His research project was titled "Voltage-sensitive dye recordings from cortical neurons." He studies how single neurons function by means of voltage-sensitive dyes and imaging. He has been successful in measuring the spread of the action potential through the axodendritic tree of the injected cell. Dr. Major was an *MBL Associates Fellow.*

- Antonio Malgoroli, Ph.D., is a Professor in the Neurobiology of Learning Unit in the Department of Biological and Technological Research at the Scientific Institute of San Raffaele in Milan, Italy. Dr. Malgoroli studies the cellular and molecular events that form the basis of synaptic plasticity in the hippocampus, especially as it relates to learning and memory. He investigates changes in calcium concentration in the postsynaptic neuron as a function of long-term potentiation (LTP). Dr. Malgaroli is pursuing research on the nature of pre-synaptically silent synapses that are recruited into active neurotransmission during LTP. Dr. Malgoroli was supported by the *Herbert W. Rand Fellowship.*

- Paul McNeil, Ph.D., is a Professor in the Department of Cellular Biology and Anatomy at the Medical College of Georgia in Augusta. Dr. McNeil studies resealing mechanisms used in the repair of large plasma membrane disruptions. He uses the sea urchin egg as a model system to define the mechanistic basis of this fundamental cell survival response. Specifically, he investigates the calcium flows that regulate the fusion of intracellular vesicles that, in turn, fuse with the plasma membrane to reseal the disruption. Dr. McNeil was sponsored by the *NASA Life Science Program Fellowship* and the *Baxter Postdoctoral Fellowship.*

- David Ogden, Ph.D., is a Principal Investigator at the National Institute for Medical Research in London. His research project was titled "Central electrosensory processing in the skate." This summer he studied how the skate senses small electric potentials in surrounding seawater to locate prey. Specifically, he investigated the area of electroreceptors in the skin of the skate that generate sensory information that is relayed to the dorsal nucleus of the brain stem. The dorsal nucleus shows organization and structural features similar to the cerebellum and it is likely that mechanisms of plasticity will prove to be similar to mammalian cerebellar learning mechanisms. Dr. Ogden was an *M.G.F. Fuortes Memorial Fellow* and an *H.B. Steinbach Fellow.*

- Oladele A. Ogunseitan, Ph.D., is Associate Professor in the Department of Environmental Analysis and Design at the University of California, Irvine. Dr. Ogunseitan studies bacterial populations in aquatic systems because they are highly sensitive indicators of the phyiological consequences of toxic compounds, including trace metals. Molecular analyses of these natural microbial communities provide valuable ecotoxicological information, especially when coastal habitats have been affected by human habitation resulting in dynamic shifts in chemical speciation and concentration fluxes. Dr. Ogunseitan was supported by the *Josiah Macy, Jr. Foundation Research Fund.*

- David Paydarfar, Ph.D., is Associate Professor at the Department of Neurobiology at the University of Massachusetts medical School in Worcester. The title of his research project was "Can noise regulate oscillatory state? *In numero* and *in vitro* analysis of squid axon membrane." He studies how electrical nerve activity is controlled and has found that a variety of neural oscillators can exhibit abrupt and lasting transformation of activity from an oscillatory to an arrhythmic state. Dr. Paydarfar was funded by the *M.G.F. Fuortes Memorial Fellowship Fund* and the *H. Keffer Hartline Fellowship.*

- Edward Salmon, Ph.D., is Professor in the Department of Biology at the University of North Carolina, Chapel Hill. Dr. Salmon and members of the Cell Division Group investigated the protein assemblies that achieve accurate chromosome segregation in cell division using sand dollars and frogs as model systems. Using advanced imaging technology, Dr. Salmon and his colleagues studied mechanisms of chromosome segregation during meiosis and mitosis, pronuclear movement during fertilization, and cytokinesis at cell division. They were especially interested in developing experimental approaches to directly measure the magnitude and direction of forces associated with microtubule flux in mitosis in living cells. Dr. Salmon and the Cell Division Group were sponsored by the *Nikon Fellowship.*

- Edgar T Walters, Ph.D., is a Professor in the Department of Integrative Biology at the University of Texas in Houston, Texas. His research project was titled "Network representation of nociceptive memory in *Aplysia.*" He studies the primitive neural mechanisms underlying central memory of peripheral injury, using simple molluscan preparations. He uses optical recording with voltage-sensitive dyes to compare spike activity in the neurons in the abdominal ganglion of *Aplysia californica* before, during, and afer intense noxious stimulation of the siphon. Dr. Walters was funded by the *James A. and Faith Miller Fellowship Fund.*

- Ebenezer Yamoah, Ph.D., is Assistant Professor in the Department of Anatomy and Cell Biology at the University of Cincinnati College of Medicine in Cincinnati, Ohio. Dr. Yamoah's research focuses on characterizing the role of the plasma membrane calcium pump in hair cell calcium homeostasis. This work is important because the perception of sound and the ability to balance in relation to head position depend on the proper function of hair cells in the inner ear. A better understanding of the functional determinants of hair-cell sensitivity will provide rational strategies for treating hearing and vestibular disorders. Dr. Yamoah was a *Josiah Macy, Jr. Foundation Research Fellow.*

Grass Fellows

- Matthew L. Beckman, Ph.D., University of Alabama at Birmingham. Project: "Analysis of lobster serotonin transporter expression and function in *Homarus americanus.*"
- Mathew Brock, Hopkins Marine Station, Stanford University. Project: "Block of squid axon Ik by S-nitrosidithiothreitol."
- Marco Crespie, Scientific Institute S. Raffaele, Italy. Project: "Expression of LTP at CA3-CA1 hippocampal synapses: A dendritic-synaptic model to reveal contributions from recruitment of silent synapses and address spread of changes."
- Frederic Doussau, Ph.D., Laboratoire de Neurobiologie Cellulaire, France. Project: "Control of synaptic vesicle traffic by the action cytoskeleton."
- Yi Han, Ph.D., Baylor College of Medicine. Project: "Electrophysiology studies of zebrafish retinal mutants with an abnormal b-wave."
- Barbara Innocenti, Ph.D., Iowa State University. Project: "Imaging of calcium-dependent glutamate release from Müller cells."
- Peter Koulen, Ph.D., Yale University School of Medicine. Project: "Differential localization of ryanodine receptor and inositol 1,4,5-trisphospate receptor isoforms in neurons and its relationship to the regulations of intracellular calcium.
- Seth J. Ramus, Ph.D., Boston University. Project: "Learning in the Eocene ocean: The first systemic examination of learning and memory in the *Nautilus* (*Nautilus pompilius*)."
- Miduturu Srinivas, Ph.D., Albert Einstein College of Medicine. Project: "Biophysical characterization of gap junction channels in marine invertebrates."
- Ayako Yamaguchi, Ph.D., Columbia University. Project: "Neuronal coding of sexually differentiated behavior by motoneurons."
- Karen Zito, Ph.D., University of California, Berkeley. Project: "*In vitro* analysis of *Drosophila* neuromuscular development" and "Role of the adhesion molecule, Fascilin II, in synaptic function."
- Michal Zochowski, Ph.D., Yale University School of Medicine. Project: "Investigating physiological, functional and dynamical properties of synchronous oscillatory signal in turtle olfactory system using optical techniques."

MBL Science Writing Fellowships Program

Fellows

Ballingrud, David, *St. Petersburg Times*
Bates, Todd, *Asbury Park Press*
Beeman, Perry, *The Des Moines Register*
Burns, Michael K., *The Baltimore Sun*
Cohen, Nancy, Freelance reporter
Cuthbert, Lori, Discovery Channel Online
Eckelbecker, Lisa, *Worcester Telegram & Gazette*
Erickson, James, *Arizona Daily Star*
Grossman, Daniel, NPR's *Living on Earth*
Hogue, Cheryl, Bureau of National Affairs, Inc.
Lesser, Carolyn, Author of children's books
Miller, John, Freelance medical and science reporter/producer
Moran, Barbara, Freelance science writer/producer
Parks, Noreen, Freelance science writer
Pennybacker, Mindy, *The Green Guide*
Potera, Carol, Freelance writer/editor
Rogerio, Graciela, WABC-TV Eyewitness News
Schueller, Gretel, *Audubon* magazine
Witze, Alexandra, *The Dallas Morning News*

Program Directors

Goldman, Robert D., Northwestern University
Rensberger, Boyce, Knight Science Journalism Program

Hands-On Laboratory Course Directors

Chisholm, Rex, Director, Northwestern University (Biomedical)
Hobbie, John E., Co-Director, Marine Biological Laboratory (Environment)
Melillo, Jerry, Co-Director, Marine Biological Laboratory (Environment)
Palazzo, Robert, Associate Director, University of Kansas (Biomedical)

Scholarships Awarded

American Society for Cell Biology

Baca, Serapio, University of California, San Diego
Casillas, Lilliam, Autonomous University of the State of Pueblo
Jones, Stacy, University of Virginia
Macias, Chanda, Howard University
Marín Bivens, Carrie, University of Massachusetts, Amherst
Nzambi, Eduardo, Howard University
Purves, Dianne, California State University, Sacramento

Biology Club of the College of the City of New York

Suadicani, Sylvia, Albert Einstein College of Medicine

C. Lalor-Burdick Scholarship

Buhimschi, Irina, University of Maryland at Baltimore
Lwigale, Peter, Kansas State University

Burroughs Wellcome Fund Biology of Parasitism Course

Angeli, Véronique, Pasteur Institute–Lille
Aviles, Hernan, Indiana State University
Barragan, Antonio, Karolinska Institute
Dobbin, Caroline, University of Technology, Sydney
Falcone, Franco, University of Edinburgh
Gavrilescu, Cristina, Cornell University
Sodré, Cátia, Universidade Federal do Rio de Janeiro
Stern, Leah, University of California, San Francisco
Wang, Zefeng, Johns Hopkins University

Burroughs Wellcome Fund Frontiers in Reproduction Course

Betts, Dean, University of Guelph
Bos-Mich, Adriana, FUEFE-Porto Alegre-Brazil
Buhimschi, Irina, University of Maryland, Baltimore
Jobanputra, Vaidehi, All India Institute of Medical Sciences
Lue, Yanhe, Harbor-UCLA Medical Center
Marín Bivens, Carrie, University of Massachusetts, Amherst
Mendeluk, Gabriela, University of Buenos Aires
Natesampillai, Sekar, University of Virginia
Ollero, Mario, Beth Israel Deaconess Medical Center
Pritts, Elizabeth, Yale University
Sprague, David, Texas A&M

Burroughs Wellcome Fund Molecular Mycology Course

Cowen, Leah, University of Toronto
Devasamayam, Gina, Wadsworth Center
Giles, Steven, University of Wisconsin, Madison
Goldstein, Alan, Duke University Medical Center
de Jesús-Berríos, Marisol, University of Puerto Rico
Latouche, Nicholas, Sydney University
Miller, Nancy, The Johns Hopkins Medical Institute
Wormley, Floyd, Louisiana State University Medical Center

Gary N. Calkins Memorial Scholarship Fund

Li, Dongling, University of Texas

Edwin Grant Conklin Memorial Fund

D'Souza, Jacinta, Tata Institute of Fundamental Research

Contraceptive Research and Development Program

Mendeluk, Gabriela, University of Buenos Aires

William F. and Irene C. Diller Memorial Scholarship Fund

Vukovich, Wolfgang, Max-Planck-Institute of Biophysical Chemistry

Caswell Grave Scholarship Fund

Pfeiffer, Sven, National Institute for Medical Research

Daniel S. Grosch Scholarship Fund

Van Lith, Yvonne, ETH Zurich
Zopfi, Jakob, Max-Planck-Institute for Marine Microbiology

Aline D. Gross Scholarship Fund

Spengler, Tatjana, Université Paris XI

William Randolph Hearst Foundation Scholarships

Jessani, Nadium, Scripps Research Institute
Kimbell, Jennifer, University of Hawaii
March, Tony, University of Idaho

International Brain Research Organization

Ashworth, Rachel, University College, London
Bellefroid, Eric, Université Libre de Bruxelles
Lightfoot, Kurt, University of Witwaterstand
Rinkwitz, Silke, New York University Medical Center

Arthur Klorfein Scholarship and Fellowship Fund

Jungblut, Benno, University of Tübingen
Panopoulou, Georgia, Max-Planck-Institute für Molekulare Genetik
Paul, Angelika, University of Otago
Saúde, Leonor, National Institute for Medical Research

Frank R. Lillie Fellowship and Scholarship Fund

Chen, Lihong, University of North Carolina, Chapel Hill
March Tony, University of Idaho
van Drogen, Frank, ISREC
Varshney, Anurag, National Centre for Biological Sciences

Jacques Loeb Founders' Scholarship Fund

van Drogen, Frank, ISREC

Massachusetts Space Grant Consortium

Best, Aaron A., University of Illinois–Urbana
Bouchet, Valerie B., Boston University
DiMeo, Carol A., University of Delaware
Harbinski, Fred M., Harvard University
Hurtado, Luis A., Rutgers University
Mead, Louise A., University of Massachusetts
Richardson, Susan L., Yale University
Worapong, Jeerapun, Montana State University

S. O. Mast Memorial Fund

Jungblut, Benno, University of Tübingen
Spengler, Tatjana, Université Paris XI

MBL Associates Endowed Scholarship Fund

Rao, Anita, University of Maryland, College Park

MBL Pioneers Scholarship Fund

Glavic, Alvaro, University of Chile
Lwigale, Peter, Kansas State University
Pierdra, Elisa, Universidad de Cantabria, Spain
Vukovich, Wolfgang, Max-Planck-Institute of Biophysical Chemistry

Merck & Company, Inc. Scholarships

Batchelor, Adrian, Walter and Eliza Hall Institute
Bishop, Joseph, University of Alabama at Birmingham
Montgomery, Jacqui, University of Melbourne
Santori, Isabel, University of Buenos Aires
Stern, Leah, University of California, San Francisco
Toe, Laurent, World Health Organization
Wang, Zefeng, Johns Hopkins University

Charles Baker Metz and William Metz Scholarship Fund in Reproductive Biology

Betts, Dean, University of Guelph
Ollero, Mario, Beth Israel Deaconess Medical Center
Sprague, David, Texas A&M

Frank Morrell Endowed Memorial Scholarship

Matsui, Ko, University of Tokyo

Mountain Memorial Fund Scholarship

Chen, Lihong, University of North Carolina, Chapel Hill
Holdaway-Clarke, Teresa, University of Massachusetts, Amherst
Mazzatenta, Andrea, University of Pisa
Tefft, Denise, University of Southern California
Varshney, Anurag, National Centre for Biological Sciences, Bangalore

Ann Osterhout Edison/Theodore Miller Edison and Olga Osterhout Sears/Harold Bright Sears Endowed Scholarship Fund

Avery, Jennifer, Brandeis University

Pfizer Inc. Endowed Scholarship Fund

Ragusa, Maria, Alberto Monroy Foundation, Palermo

Planetary Biology Internship Awards

Van Lith, Yvonne, ETH Zurich

Phillip H. Presley Scholarship Award, Funded by Carl Zeiss, Inc.

Batchelor, Adrian, Walter and Eliza Hall Institute
Dobbin, Caroline, University of Technology, Sydney
Franco, Peter, Harvard Medical School
Krieger, Patrik, Karolinska Institute
Maruska, Karen, Florida Institute of Technology
Welman, Arkadiusz, Friedrich Miescher Institute

Herbert W. Rand Fellowship and Scholarship Fund

Duncan, Tod, Imperial Cancer Research Laboratory
Fort, Alfredo, Albert Einstein College of Medicine
Franco, Peter, Harvard Medical School
Holdaway-Clarke, Terena, University of Massachusetts
Jungblut, Benno, University of Tübingen
Mazzatenta, Andrea, University of Pisa
Sawai, Satoshi, Tohoku University
Tefft, Denise, University of Southern California
Tidwell, Judy, Wake Forest University

Ruth Sager Memorial Scholarship

Haapasalo, Annakaisa, University of Kuopio

Society for Developmental Biology Scholarships

Clements, Wilson, University of Washington
Mui, Stina, University of California, San Diego
Pizer, Margaret, State University of New York at Stony Brook
Robertson, Christie, University of Washington
Zigler, Kirk, Duke University

Society of General Physiologists' Scholarships

Diana, Marco, Max-Planck-Institute of Biophysical Chemistry
Duncan, Tod, Imperial Cancer Research Laboratory
Greenwood, Anna, Stanford University
Paul, Angelika, University of Otago

Howard A. Schneiderman Endowed Scholarship

Yu, Xiang, MRC Laboratory of Molecular Biology

Moshe Shilo Memorial Scholarship Fund

Gillor, Osnat, The Hebrew University

Marjorie W. Stetten Scholarship Fund

Yoon, Miri, Northwestern University Medical School

Horace W. Stunkard Scholarship Fund

Bos-Mikich, Adriana, FUEFE-Porto Alegre–Brazil

Surdna Foundation Scholarship

Abenavoli, Alessandra, Scientific Institute San Raffaele
Diana, Marco, Max-Planck-Institute of Biophysical Chemistry
Haapasalo, Annakaisa, University of Kuopio
Matsui, Ko, University of Tokyo
Rao, Anita, University of Maryland

William Townsend Porter Fellowship For Minority Students

Jones, Stacy, University of Virginia
Macias, Chanda, Howard University
Nzambi, Eduardo, Howard University

William Morton Wheeler Family Founders' Scholarship

Abenavoli, Alessandra, Scientific Institute San Raffaele
Yu, Xiang, MRC Lab of Molecular Biology

Walter L. Wilson Endowed Scholarship Fund

Tidwell, Judy, Wake Forest University

World Academy of Arts and Sciences Emily Mudd Scholarship

el Guiziry, Dalal, Alexandria University

Post-Course Research Awards

van Drogen, Frank, ISREC (Physiology)
Kimbell, Jennifer, University of Hawaii (Physiology)
Macias, Chanda, Howard University (Physiology)
Mazzatenta, Andrea, University of Pisa (Physiology)
Meyers, Jason, University of Virginia (Embryology)
Narayan, Sujatha, Bryn Mawr College (Physiology)
Niggemyer, Allison, University of Idaho (Microbial Diversity)
O'Neill, Forest, University of California, Santa Barbara (Physiology)
Purves, Dianne, California State University, Sacramento (Physiology)
Tidwell, Judy, Wake Forest University (Physiology)
Varshney, Anurag, National Centre for Biological Sciences (Physiology)

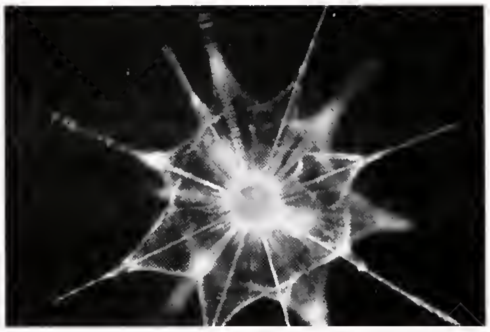

Board of Trustees and Committees

Corporation Officers and Trustees

Chairman of the Board of Trustees, Sheldon J. Segal, The Population Council
Co-Vice Chair of the Board of Trustees, Frederick Bay, Josephine Bay Paul and C. Michael Paul Foundation
Co-Vice Chair of the Board of Trustees, Mary J. Greer, New York, NY
President of the Corporation, John E. Dowling, Harvard University
Director and Chief Executive Officer, John E. Burris, Marine Biological Laboratory*
Treasurer of the Corporation, Mary B. Conrad, Fiduciary Trust International*
Clerk of the Corporation, Robert E. Mainer, The Boston Company
Chair of the Science Council, Kerry S. Bloom, University of North Carolina*

Class of 2000

Clowes, Alexander W., University of Washington School of Medicine
Landis, Story C., Case Western Reserve University
Levitan, Irwin B., Brandeis University
Miller, G. William, G. William Miller and Co., Inc.
Press, Frank, The Washington Advisory Group
Weld, Christopher M., Sullivan and Worcester, Boston

Class of 2001

Anderson, Porter W., North Miami Beach, FL
Bay, Frederick, Josephine Bay Paul and C. Michael Paul Foundation, Inc.
Cox, Martha W., Hobe Sound, FL
Greer, Mary J., New York, NY
Steere, William C. Jr., Pfizer Inc.
Weissmann, Gerald, New York University School of Medicine

Class of 2002

Cone, Sydney M. III, Cleary, Gottlieb, Steen and Hamilton
Lakian, John R., The Fort Hill Group, Inc.
Ruderman, Joan V., Harvard Medical School
Segal, Sheldon J., The Population Council
Speck, William T., New York Presbyterian Hospital
Zeien, Alfred M., The Gillette Company

Class of 2003

Kelley, Darcy Brisbane, Columbia University
Landeau, Laurie J., Marinetics, Inc.
Lee, Burton J. III, Vero Beach, FL
O'Hanley, Ronald P., Mellon Institutional Asset Mgt.
Pierce, Jean, Boca Grande, FL
Ryan, Vincent J., Schooner Capital LLC

Honorary Trustees

Cunningham, Mary Ellen, Grosse Pointe Farms, MI
Ebert, James D., Baltimore, MD
Golden, William T., New York, NY
Grass, Ellen R., The Grass Foundation

Trustees Emeriti

Adelberg, Edward A., Yale University, New Haven, CT
Buck, John B., Sykesville, MD
Cohen, Seymour S., Woods Hole, MA
Colwin, Arthur L., Key Biscayne, FL
Colwin, Laura Hunter, Key Biscayne, FL
Copeland, Donald Eugene, Woods Hole, MA
Crowell, Sears Jr., Indiana University, Bloomington, IN
Hayashi, Teru, Woods Hole, MA
Hubbard, Ruth, Cambridge, MA
Kleinholz, Lewis, Reed College, Portland, OR
Krahl, Maurice, Tucson, AZ
Prosser, C. Ladd, University of Illinois, Urbana, IL
Russell-Hunter, W.D., Syracuse University, Syracuse, NY
Saunders, John W., Waquoit, MA
Trigg, D. Thomas, Wellesley, MA
Vincent, Walter S., Woods Hole, MA

Directors Emeriti

Ebert, James D., Baltimore, MD
Gross, Paul, Falmouth, MA
Halvorson, Harlyn O., Woods Hole, MA

Executive Committee of the Board of Trustees

Segal, Sheldon J., Chair
Bay, Frederick, Co-Vice Chair
Greer, Mary J., Co-Vice Chair
Burris, John E.
Bloom, Kerry S.

---

*Ex officio

Conrad, Mary B., Treasurer
Mainer, Robert E.
Ruderman, Joan V.
Weissmann, Gerald

Science Council

Bloom, Kerry S., Chair (2000)
Burris, John E.*
Armstrong, Clay M. (2000)
Armstrong, Peter (2000)
Atema, Jelle (2001)
Barlow, Robert B. (2001)
Dawidowicz, E.A.*
Haimo, Leah (2001)
Hopkinson, Charles (2000)
Jaffe, Laurinda (2001)
Smith, Peter J.S. (2001)
Sogin, Mitchell (2000)

Standing Committees of the Board of Trustees

Development

Speck, William, Chair
Anderson, Porter W.
Barlow, Robert
Bay, Frederick
Conrad, Mary B.
Cox, Martha
Cunningham, Mary Ellen
Ebert, James D.
Grant, Philip
Lakian, John R.
Lee, Burton J.
Miller, G. William
Pierce, Jean
Steere, William C.
Weld, Christopher M.

Facilities and Capital Equipment

Ruderman, Joan, Chair
Anderson, Porter W.
Bay, Frederick
Cohen, Lawrence
Cornell, Neal
Landis, Story C.
Levitan, Irwin B.
Pierce, Jean
Press, Frank
Weld, Christopher M.

Investment

Conrad, Mary B., Chair
Cone, Sydney M.
Lakian, John R.
Mainer, Robert E.
Miller, G. William
O'Hanley, Ronald P.
Ryan, Vincent J.
Segal, Sheldon J.
Zeien, Alfred M.

Finance

O'Hanley, Ronald, Chair
Clowes, Alexander W.
Cone, Sydney M.
Conrad, Mary B.
DeHart, Donald
Kelley, Darcy Brisbane
Lakian, John R.
Landeau, Laurie J.
Loewenstein, Werner
Mainer, Robert E.
Manz, Robert
Miller, G. William
Ryan, Vincent J.
Zeien, Alfred M.

Nominating

Weissmann, Gerald, Chair
Bloom, Kerry S.
Clowes, Alexander W.
Cox, Martha W.
Greer, Mary J.
Landis, Story C.
Pierce, Jean
Segal, Sheldon J.
Speck, William T.
Steere, William C.

Standing Committees of the Corporation and Science Council

Buildings and Grounds

Cohen, Lawrence B., Chair
Boyer, Barbara C.
Cutler, Richard*
Fleet, Barry*
Hayes, Joe*
McArthur, Andrew
Peterson, Bruce J.
Tweedell, Kenyon S.
Valiela, Ivan

Ex officio

Education Committee

Dione, Vincent, Chair
Bloom, Kerry S.*
Dawidowicz, E.A.*
Dunlap, Paul
Fink, Rachel
Hanlon, Roger
Jaffe, Laurinda
Mebane, Dori Chrysler*
Mendelsohn, Michael
Venuti, Judith
Wadsworth, Patricia
Zottoli, Steve

Fellowships

Pederson, Thoru, Chair
Dawidowicz, E.A.*
Deegan, Linda
Ehrlich, Barbara
Kaufmann, Sandra* (Recording Secretary)
Lemos, Jose
Sluder, Greenfield
Smith, Peter J.S.
Treistman, Steven (Guest Member)

Housing, Food Service and Child Care

Browne, Carole, Chair
Bloom, Kerry S.*
King, LouAnn*
Malchow, Robert P.
Stuart, Ann E.
Weeks, Janis C.

Assisting
Browne, Robert (representing MBL Child Care)
Goux, Susan (Administrator)
Hinkle, Pamela Clapp (representing the MBL Club)
Cutler, Richard (representing Housing)

MBL/WHOI Library Joint Advisory Committee

Shepro, David, Chair, MBL
Ashmore, Judy,* MBL
Dow, David, NMFS
Fornari, Daniel, WHOI
Harbison, G. Richard, WHOI
Hobbie, John, MBL
Hurter, Colleen,* WHOI
Kurz, Mark, WHOI Alternate
Norton, Cathy,* MBL
Robb, James, USGS
Rose, Birgit, MBL
Smith, Peter J.S., MBL
Warren, Bruce, WHOI

Research Services and Space

Laufer, Hans, Chair
Armstrong, Peter B.
Cornell, Neal
Cutler, Richard*
Dawidowicz, E.A.*
Foreman, Kenneth
Kerr, Louis M.*
Landowne, David
Mattox, Andrew*
Melillo, Jerry
Mizell, Merle
Smith, Peter J.S.
Steudler, Paul
Valiela, Ivan

Discovery: The Campaign for Science at the Marine Biological Laboratory Steering Committee

Bay, Frederick, Campaign Chair
Golden, William T., Honorary Chair
Grass, Ellen R., Honorary Chair
Clowes, Alexander W., Vice-Chair
Cox, Martha W., Vice-Chair
Miller, G. William, Vice-Chair
Weissmann, Gerald, Vice-Chair
Anderson, Porter W
Barlow, Robert B. Jr.
Bernstein, Norman
Cobb, Jewell Plummer
Conrad, Mary B
Cunningham, Mary Ellen
Dowling, John E.
Ebert, James D.
Fischbach, Gerald D.
Goldman, Robert D.
Greer, Mary J.
Jacobson, M. Howard
Landeau, Laurie J.
Langford, George M.
Lee, Burton J. III
Pierce, Jean
Prendergast, Robert A.
Shepro, David
Speck, William T.
Steere, William C. Jr.
Weld, Christopher M.
Zeien, Alfred M.

**Ex officio*

Council of Visitors

Norman B. Asher, Esq., Hale and Dorr, Counsellors at Law, Boston, MA

Mr. Donald J. Bainton, Continental Can Co., Boca Raton, FL
Mr. David Bakalar, Chestnut Hill, MA
Mr. Charles A. Baker, The Liposome Company, Inc., Princeton, NJ
Dr. George P. Baker, Massachusetts General Hospital, Boston, MA
Dr. Sumner A. Barenberg, Bernard Technologies, Chicago, IL
Mr. Mel Barkan, The Barkan Companies, Boston, MA
Mr. Robert P. Beech, Component Software International, Inc., Mason, OH
Mr. George Berkowitz, Legal Sea Foods, Allston, MA
Mr. and Mrs. Nathaniel J. Bickford, New York, NY
Dr. Elkan R. Blout, Harvard Medical School, Boston, MA
Mr. and Mrs. Philip Bogdanovitch, Lake Clear, NY
Mr. Malcolm K. Brachman, Northwest Oil Company, Dallas, TX
Dr. Goodwin M. Breinin, NY University Medical Center, New York, NY

Mr. John Callahan, Carpenter, Sheperd & Warden, New London, NH
Mrs. Elizabeth Campanella, West Falmouth, MA
Thomas S. Crane, Esq., Mintz Levin Cohen Ferris Glovsky & Popeo, PC, Boston, MA
Dr. Stephen D. Crocker, Cyber Cash Inc., Reston, Virginia
Mrs. Lynn W. Piasecki Cunningham, Film and Videomaker, Piasecki Productions, Brookline, MA
Dr. Anthony J. Cutaia, Anheuser-Busch, Inc., St. Louis, MO

Mrs. Sara Greer Dent, Chevy Chase, MD
Mr. D. H. Douglas-Hamilton, Hamilton Thorne Research, Beverly, MA
Mr. Benjamin F. du Pont, Du Pont Company, Deepwater, NJ

Dr. Sylvia A. Earle, Founder, Deep Ocean Engineering, Oakland, CA
Mr. and Mrs. Hoyt Ecker, Vero Beach, FL
Mr. Anthony B. Evnin, Venrock Associates, New York, NY

Stuart Feiner, Esq., Inco Limited, Toronto, ON, Canada
Mrs. Hadley Mack French, Edsel & Eleanor Ford House, Grosse Pointe Farms, MI

Mr. and Mrs. Huib Geerlings, Boston, MA
Mr. William J. Gilbane, Jr., Gilbane Building Company, Providence, RI
Dr. Michael J. Goldblatt, Intelligent Biocides, Tewksbury, MA
Mr. Maynard Goldman, President, Maynard Goldman & Associates, Boston, MA

Ms. Charlotte I. Hall, Edgartown, MA
Drs. Linda Hirshman, Brandeis University, Waltham, MA, and David Forkosh, FMH Foundation
Mr. Thomas J. Hynes, Jr., Meredith & Grew, Inc., Boston, MA

Mr. M. Howard Jacobson, Bankers Trust, Westborough, MA

Mrs. Elizabeth Ford Kontulis, New Canaan, CT

Mr. and Mrs. Robert Lambrecht, Boca Grande, FL
Dr. Catherine C. Lastavica, Tufts University School of Medicine, Boston, MA
Mr. Joel A. Leavitt, Boston, MA
Mr. Stephen W. Leibholz, TechLabs, Inc., Huntingdon, PA
Mrs. Margaret Lilly, West Falmouth, MA
Mr. Richard Lipkin, ResponseLogic, Inc., New York, NY
Mr. George W. Logan, Valley Financial Corp., Roanoke, VA

Mr. Michael T. Martin, SportsMark, Inc., New York, NY
Mrs. Christy Swift Maxwell, Grosse Pointe Farms, MI
Dr. Georges de Ménil, DM Foundation, New York, NY
Mr. Ambrose Monell, G. Unger Vetlesen Foundation, Palm Beach, FL

Dr. Mark Novitch, Washington, DC

Ms. Julie Packard, Monterey Bay Aquarium, Monterey, CA
Mr. David R. Palmer, David Ross Palmer & Associates, Waquoit, MA
Dr. Roderic B. Park, Richmond, CA
Mr. Santo P. Pasqualucci, Falmouth Co-Operative Bank, Falmouth, MA
Mr. Robert Pierce, Jr., Pierce Aluminum Co., Canton, MA

Mr. Richard Reston, Vineyard Gazette, Edgartown, MA
Mr. Marius A. Robinson, Fundamental Investors Ltd., Key Biscayne, FL
John W. Rowe, M.D., Mt. Sinai School of Medicine & Mt. Sinai Medical Center, New York, NY
Mr. Edward Rowland, Tucker, Anthony, Inc., Boston, MA

Mr. Gregory A. Sandomirsky, Mintz Levin Cohen Ferris Glovsky & Popeo, PC, Boston, MA
Mrs. Mary Schmidek, Marion, MA
Dr. Cecily C. Selby, New York, NY
Mr. Robert S. Shifman, St. Simon's Island, Georgia
Mr. and Mrs. Gregory Skau, Grosse Pointe Farms, MI
Mr. Malcolm B. Smith, General American Investors Co., New York, NY
Mr. John C. Stegeman, Campus Rentals, Ann Arbor, MI
Mr. Joseph T. Stewart, Jr., Skillman, NJ
Mr. John W. Stroh, III, The Stroh Brewery Company, Detroit, MI
Mr. Gerard L. Swope, Washington, DC
Mr. John F. Swope, Concord, NH

Mr. and Mrs. Stephen E. Taylor, Milton, MA

Mrs. Donna Vanden Bosch-Flynn, Spring Lake, NJ
Mrs. Carolyn W. Verbeck, Vineyard Haven, MA

Mr. Benjamin S. Warren III, Grosse Pointe Farms, MI
Nancy B. Weinstein, R.N., The Hospice, Inc., Glen Ridge, NJ
Stephen S. Weinstein, Esq., Morristown, NJ
Mr. Frederick J. Weyerhaeuser, Beverly, MA
Mr. Tony L. White, The Perkin Elmer Corporation, Norwalk, CT
Dr. Torsten N. Wiesel, The Rockefeller University, New York, NY

Administrative Support Staff[1]

Biological Bulletin

Greenberg, Michael J., Editor-in-Chief
Hinkle, Pamela Clapp, Managing Editor
  Burns, Patricia
  Gibson, Victoria R.
  Schachinger, Carol H.

Director's Office

Burris, John E., Director and Chief Executive Officer
  Donovan, Marcia H.

Equal Employment Opportunity
MacNeil, Jane L.

Veterinarian Services
Champagne, Jaimie[2]
Reynolds, Martha[2]
Smolowitz, Roxanna
Stukey, Jetley

Ecosystems Center Administrative Staff

Berthel, Dorothy J.
Donovan, Suzanne J.
Nunez, Guillermo
Seifert, Mary Ann

External Affairs

Carotenuto, Frank C., Director
  Butcher, Valerie
  Faxon, Wendy P.
  Johnson, A. Kristine
  Martin, Theresa H.
  Patch-Wing, Dolores
  Quigley, Barbara A.
  Shaw, Kathleen L.

Associates Program
Bohr, Kendall B.
Zeida, Robert[2]

Communications Office
Hinkle, Pamela Clapp, Director
Cox, Sarah[2]
Flynn, Bridget
Furfey, Susan[2]
Joslin, Susan
Liles, Beth R.
Noonan, Ryan[2]
Schanbacher, Jennifer[2]

Financial Services Office

Lane, Homer W. Jr., Chief Financial Officer
Bowman, Richard, Controller
  Afonso, Janis
  Barry, Maureen
  Crosby, Kenneth
  Eidelman, Dana
  Lancaster, Cindy
  Livingstone, Suzanne
  McLaughlin, Rebecca Jill
  Ranzinger, Laura
  Stellrecht, Lynette

Stock Room
Schorer, Timothy M., Supervisor
Brinson, Robert[2]
Burnette, Donald
O'Connor-Lough, Susan

Purchasing
Hall, Lionel E. Jr., Supervisor
Gannon, Katherine[2]
Shamon, Lynne R.

Housing and Conferences

King, LouAnn D., Director
  Grasso, Deborah
  Hanlon, Arlene K.[2]
  Johnson-Horman, Frances N.
  Masse, Todd C.
  Perito, Diana
  Ridley, Alberta[2]

---

[1] Including persons who joined or left the staff during 1999.
[2] Summer or temporary.

Human Resources

Goux, Susan P., Director
Houser, Carmen

Josephine Bay Paul Center for Comparative Molecular Biology and Evolution Administrative Staff

Harris, Marian
Lim, Pauline

Journal of Membrane Biology

Loewenstein, Werner R., Editor
Fay, Catherine H.
Howard Isenberg, Linda L.
Lynch, Kathleen F.

Marine Resources Center

Hanlon, Roger T., Director
Santore, Gabrielle

Aquatic Resources Department
Enos, Jr., Edward G., Superintendent
Bourque, Ryan M.[2]
Chappell, P. Dreux[2]
DeGiorgis, Joseph A.[2]
Grossman, William M.
Gudas, Christopher N.[2]
Kilpatrick, Brian[2]
Klimm, Henry W. III
Reynolds, Justin[2]
Sexton, Andrew W.
Smith, Gary[2]
Sullivan, Daniel A.
Tassinari, Eugene

MRC Life Support System
Mebane, William N., Systems Operator
Carroll, James
Clark, Heidi[2]
Hanley, Janice S.
Kuzirian, Alan
Till, Geoffrey A.

MBL/WHOI Library

Norton, Catherine N., Director
Ashmore, Judith A.
Buckingham, Andrew[2]
Costa, Marguerite E.
Crocker, Daniel[2]
Deveer, Joseph M.
Farrar, Stephen R.L.
Fredericks, Julie[2]
Medeiros, Melissa
Monahan, A. Jean
Moniz, Kimberly L.
Moore, Laurel E.
Nelson, Heidi
Person, Matthew
Riley, Jacqueline
Shinkle, Chelsea[2]

Copy Center
Mountford, Rebecca J., Supervisor
Abisla, Richard L.[2]
Adams, Jessica[2]
Churchill, Elizabeth[2]
Clark, Tamara L.
Cosgrove, Nancy
Kefeauver, Lee
Mancini, Mary E.
Waterbury, Andrew[2]

Information Systems Division
Inzina, Barbara, Network Manager
Berrios, Kelly[2]
Cohen, Alex[2]
Hilliard, Channing[2]
Kokmeyer, Remmert[2]
Malchow, Robert[2]
Mountford, Rebecca J.
Moynihan, James V.
Purdy, Heather[2]
Remsen, David P.
Renna, Denis J.
Space, David B.
Wheeler, Patrick

NASA Center for Advanced Studies in the Space Life Sciences

Blazis, Diana, Administrator
Amit, Udeni P.
Golden, Catherine
Oldham, Pamela

Research Administration & Educational Programs

Dawidowicz, Eliezar A., Director
Hamel, Carol C.
Holzworth, Kelly
Kaufmann, Sandra J.
Kleinhenz, Andrea
Lynn, Rebecca
Mebane, Dorianne C.
White, Laurie

Central Microscopy Facility and General Use Rooms
Kerr, Louis M., Supervisor
Luther, Herbert
Matthews, Douglas[2]
Peterson, Martha B.

Safety Services

Mattox, Andrew H., Environmental, Health, and Safety Manager
Lingler, Nicholas[2]
Normand, Danielle[2]

Satellite/Periwinkle Children's Programs

Robinson, Paulina H.[2]
Borst, Douglas[2]
Browne, Jennifer L.[2]
Curran, Kelly[2]
David, Amy[2]

Fitzelle, Annie[2]
Gallant, Cynthia[2]
Guiffrida, Beth[2]
Halter, Sarah[2]
Hike, Kelly[2]
Mekelatos, Sharon[2]
Noonan, Brendan[2]
Robbins, Sarah[2]
Shanley, Jennifer[2]

Service, Projects and Facilities

Cutler, Richard D., Director
  Enos, Joyce B.
  Guarente, Jeffrey

Apparatus
Baptiste, Michael G.
Barnes, Franklin D.
Haskins, William A.

Building Services & Grounds
Hayes, Joseph H., Superintendent
Anderson, Lewis B.
Atwood, Paul R.
Baker, Harrison S.
Barnes, Susan M.
Beernik, Daniel
Berthel, Frederick
Billings, Julia[2]
Boucher, Richard L.
Brereton, Richard S.[2]
Callahan, John J.
Cameron, Lawrence M.[2]
Chen, Zhi Xin
Clayton, Daniel
Collins, Paul J.
Cowan, Matthew B.[2]
Cutler, Matthew D.[2]
Cutillo, David
Dimond, Jay[2]
Doherty, Garrett[2]
Dorris, John J.
Eldridge, Myles[2]
Elias, Michael
Fernandez, Peter R.[2]
Foster, Martin[2]
Gibbons, Roberto G.
Hannigan, Catherine
Illgen, Robert F.
Joyner, Matthew[2]
Ledwell, L. Patrick[2]
Lynch, Henry L.
MacDonald, Cynthia C.
Malchow, Kate[2]
McCarthy, Michael
McDonnell, Gregory
McNamara, Noreen M.
McQuillan, Jeffrey[2]
Parker, Karen[2]
Plant, Stephen W.
Pratt, Barry
Stites, Clint[2]
Thiele, Tod[2]
Ware, Lynn M.

Plant Operations and Maintenance
Fleet, Barry M., Manager
Cadose, James W., Maintenance Supervisor
Barnes, John S.
Blunt, Hugh F.
Bourgoin, Lee E.
Callahan, John
Carroll, James R.
Davis, Douglas
Fish, David L. Jr.
Fuglister, Charles K.
Goehl, George
Gonsalves, Walter W. Jr.
Hathaway, Peter J.
Henderson, Jon R.
Kelley, Kevin
L'Abbe, Robert
Langill, Richard
Lochhead, William M.
McAdams, Herbert M. III
McHugh, Michael O.
Mills, Stephen A.
Olive, Charles W. Jr.
Rattacasa, Frank[2]
Rozum, John
Schoepf, Claude
Settlemire, Donald
Shepherd, Denise M.
Toner, Michael
Wetzel, Ernest D.[2]

Members of the Corporation

Life Members

Acheson, George H., 25 Quissett Avenue, Woods Hole, MA 02543
Adelberg, Edward A., 204 Prospect Street, New Haven, CT 06511-2107
Afzelius, Bjorn, University of Stockholm, Wenner-Gven Institute, Department of Ultrastructure Research, Stockholm, Sweden
Amatniek, Ernest, (address unknown)
Arnold, John M., 329 Sippewissett Road, Falmouth, MA 02540

Bang, Betsy G., 76 F. R. Lillie Road, Woods Hole, MA 02543
Bartlett, James H., University of Alabama, Department of Physics, Box 870324, Tuscaloosa, AL 35487-0324
Berne, Robert M., University of Virginia School of Medicine, Department of Physiology, Box 1116, MR4, Charlottesville, VA 22903
Bernheimer, Alan W., New York University Medical Center, Department of Microbiology, 550 First Avenue, New York, NY 10016
Berthof, Lloyd M., Westminster Village, #2114, 2025 East Lincoln Street, Bloomington, IL 61701-5995
Bosch, Herman F., 163 Elm Road, Falmouth, MA 02540-2430
Buck, John B., Fairhaven C-020, 7200 Third Avenue, Sykesville, MD 21784
Burbanck, Madeline P., P.O. Box 15134, Atlanta, GA 30333
Burbanck, William D., P.O. Box 15134, Atlanta, GA 30333

Clark, Arnold M., 53 Wilson Road, Woods Hole, MA 02543
Clark, James M., 258 Wells Road, Palm Beach, FL 33480-3625
Cohen, Seymour S., 10 Carrot Hill Road, Woods Hole, MA 02543-1206
Colwin, Arthur L., 320 Woodcrest Road, Key Biscayne, FL 33149-1322
Colwin, Laura Hunter, 320 Woodcrest Road, Key Biscayne, FL 33149-1322
Cooperstein, Sherwin J., University of Connecticut, School of Medicine, Department of Anatomy, Farmington, CT 06030-3405
Copeland, D. Eugene, Marine Biological Laboratory, Woods Hole, MA 02543
Corliss, John O., P.O. Box 2729, Bala Cynwyd, PA 19004-2116
Costello, Helen M., Carolina Meadows, Villa 137, Chapel Hill, NC 27514-8512
Crouse, Helen, Rte. 3, Box 213, Hayesville, NC 28904

DeHaan, Robert L., Emory University School of Medicine, Department of Anatomy and Cell Biology, 1648 Pierce Drive, Room 108, Atlanta, GA 30322
Dudley, Patricia L., 3200 Alki Avenue SW, #401, Seattle, WA 98116

Edwards, Charles, 3429 Winding Oaks Drive, Longboat Key, FL 34228
Elliott, Gerald F., The Open University Research Unit, Foxcombe Hall, Berkeley Road, Boars Hill, Oxford OX1 5HR, United Kingdom

Failla, Patricia M., 2149 Loblolly Lane, Johns Island, SC 29455
Ferguson, James K. W., 56 Clarkehaven Street, Thornhill, Ontario L4J 2B4, Canada (deceased 1999)

Gabriel, Mordecai L., Brooklyn College, Department of Biology, 2900 Bedford Avenue, Brooklyn, NY 11210
Glusman, Murray, New York State Psychiatric Institute, 722 W. 168th St., Unit #70, New York, NY 10032
Graham, Herbert, 36 Wilson Road, Woods Hole, MA 02543

Hamburger, Viktor, Washington University, Department of Biology, 740 Trinity Avenue, St. Louis, MO 63130
Hamilton, Howard L., University of Virginia, Department of Biology, 238 Gilmer Hall, Charlottesville, VA 22901
Harding, Clifford V. Jr., 54 Two Ponds Road, Falmouth, MA 02540
Haschemeyer, Audrey E. V., 21 Glendon Road, Woods Hole, MA 02543-1406
Hauschka, Theodore S., 333 Fogler Road, Bremen, ME (deceased 1999)
Hayashi, Teru, 15 Gardiner Road, Woods Hole, MA 02543-1113
Hisaw, Frederick L., (address unknown)
Hoskin, Francis C. G., c/o Dr. John E. Walker, U.S. Army Natick RD&E Center, SAT NC-YSM, Kansas Street, Natick, MA 01760-5020
Hubbard, Ruth, Harvard University, Biological Laboratories, Cambridge, MA 02138
Humes, Arthur G., Marine Biological Laboratory, Boston University Marine Program, Woods Hole, MA 02543 (deceased 1999)
Hunter, W. Bruce, 305 Old Sharon Road, Peterborough, NH 03458-1736
Hurwitz, Charles, Stratton VA Medical Center, Research Service, Albany, NY 12208

Katz, George, Merck, Sharp and Dohme, Fundamental and Experimental Research Laboratory, PO Box 2000, Rahway, NJ 07065
Kingsbury, John M., Cornell University, Department of Plant Biology, Plant Science Building, Ithaca, NY 14853
Kleinholz, Lewis, Reed College, Department of Biology, 3203 SE Woodstock Boulevard, Portland, OR 97202
Kusano, Kiyoshi, National Institutes of Health, Building 36, Room 4D-20, Bethesda, MD 20892

Laderman, Ezra, Yale University, New Haven, CT 06520

LaMarche, Paul H., Eastern Maine Medical Center, 489 State Street, Bangor, ME 04401
Lauffer, Max A., Penn State University Medical Center, Department of Biophysics and Physiology, Hershey, PA 17033
Lochhead, John H., 49 Woodlawn Road, London SW6 6PS, United Kingdom
Loewus, Frank A., Washington State University, Institute of Biological Chemistry, Pullman, WA 99164
Loftfield, Robert B., University of New Mexico, School of Medicine, 915 Stanford Drive, Albuquerque, NM 87131
Lorand, Laszlo, Northwestern University Medical School, CMS Biology, Searle 4-555, 303 East Chicago Avenue, Chicago, IL 60611-3008

Malkiel, Saul, 174 Queen Street, #9A, Falmouth, MA 02540
Marsh, Julian B., 9 Eliot Street, Chestnut Hill, MA 02467-1407
Martin, Lowell V., 10 Buzzards Bay Avenue, Woods Hole, MA 02543
Mathews, Rita W., East Hill Road, P.O. Box 237, Southfield, MA 01259-0237
Moore, John A., University of California, Department of Biology, Riverside, CA 92521
Moore, John W., Duke University Medical Center, Department of Neurobiology, Box 3209, Durham, NC 27710
Moscona, Aron A., University of Chicago, Department Molecular Genetics and Cell Biology, Chicago, IL 60637
Musacchia, X. J., P.O. Box 5054, Bella Vista, AR 72714-0054

Nasatir, Maimon, P.O. Box 379, Ojai, CA 93024

Passano, Leonard M., University of Wisconsin, Department of Zoology, Birge Hall, Madison, WI 53706
Price, Carl A., 20 Maker Lane, Falmouth, MA 02540
Prosser, C. Ladd, University of Illinois, Department of Physiology, 524 Burrill Hall, Urbana, IL 61801
Prytz, Margaret McDonald, (Address unknown)

Ratner, Sarah, Public Health Research Institute, Department of Biochemistry, 455 First Avenue, New York, NY 10016 (deceased 1999)
Renn, Charles E., (Address unknown)
Reynolds, George T., Princeton University, Department of Physics, Jadwin Hall, Princeton, NJ 08544
Rice, Robert V., 30 Burnham Drive, Falmouth, MA 02540
Rockstein, Morris, 600 Biltmore Way, Apt. 805, Coral Gables, FL 33134
Ronkin, Raphael R., 3212 McKinley Street, NW, Washington, DC 20015-1635
Roslansky, John D., 57 Buzzards Bay Avenue, Woods Hole, MA 02543
Roslansky, Priscilla F., Associates of Cape Cod, Inc., P.O. Box 224, Woods Hole, MA 02543-0224

Sanders, Howard L., Woods Hole Oceanographic Institution, Woods Hole, MA 02543
Sato, Hidemi, Nagoya University, 3-24-101, Oakinishi Machi, Toba Mie 517-0023, Japan
Schlesinger, R. Walter, 7 Langley Road, Falmouth, MA 02540-1809
Scott, Allan C., Colby College, Waterville, ME 04901
Silverstein, Arthur M., Johns Hopkins University, Institute of the History of Medicine, 1900 E. Monument Street, Baltimore, MD 21205
Sjodin, Raymond A., 3900 N. Charles Street, Apt. #1301, Baltimore, MD 21218-1719
Smith, Paul F., P.O. Box 264, Woods Hole, MA 02543-0264
Speer, John W., 293 West Main Road, Portsmouth, RI 02871
Sperelakis, Nicholas, University of Cincinnati, Department of Physiology/Biophysics, 231 Bethesda Avenue, Cincinnati, OH 45267-0576
Spiegel, Evelyn, Dartmouth College, Department of Biological Sciences, 204 Gilman, Hanover, NH 03755
Spiegel, Melvin, Dartmouth College, Department of Biological Sciences, 204 Gilman, Hanover, NH 03755
Stephens, Grover C., University of California, School of Biological Sciences, Department of Ecology and Evolution/Biology, Irvine, CA 92717
Strehler, Bernard L., 42903 Moulton Parkway, #248, Laguna Hills, CA 92653-6425
Sussman, Maurice, 72 Carey Lane, Falmouth, MA 02540
Sussman, Raquel B., Marine Biological Laboratory, Woods Hole, MA 02543
Szent-Gyorgyi, Gwen P., 45 Nobska Road, Woods Hole, MA 02543

Thorndike, W. Nicholas, Wellington Management Company, 200 State Street, Boston, MA 02109
Trager, William, The Rockefeller University, 1230 York Avenue, New York, NY 10021-6399
Trinkaus, J. Philip, 870 Moose Hill Road, Guilford, CT 06437

Villee, Claude A. Jr., Harvard Medical School, Carrel L. Countway Library, 10 Shattuck Street, Boston, MA 02115
Vincent, Walter S., 16 F.R. Lillie Road, Woods Hole, MA 02543

Waterman, Talbot H., Yale University, Box 208103, 912 KBT Biology Department, New Haven, CT 06520-8103
Wigley, Roland L., 35 Wilson Road, Woods Hole, MA 02543

Members

Abt, Donald A., Aquavet, University of Pennsylvania, School of Veterinary Medicine, 230 Main Street, Falmouth, MA 02540
Adams, James A., 3481 Paces Ferry Road, Tallahassee, FL 32308
Adelman, William J., 160 Locust Street, Falmouth, MA 02540
Alkon, Daniel L., National Institutes of Health, Laboratory of Adaptive Systems, 36 Convent Drive, MSC 4124, 36/4A21, Bethesda, MD 20892-4124
Allen, Garland E., Washington University, Department of Biology, Box 1137, One Brookings Drive, St. Louis, MO 63130-4899
Allen, Nina S., North Carolina State University, Department of Botany, Box 7612, Raleigh, NC 27695
Alliegro, Mark C., Louisiana State University Medical Center, Department of Cell Biology and Anatomy, 1901 Perdido Street, New Orleans, LA 70112
Anderson, Everett, Harvard Medical School, Department of Cell Biology, 240 Longwood Avenue, Boston, MA 02115-6092
Anderson, John M., 110 Roat Street, Ithaca, NY 14850
Anderson, Porter W., 100 Bayview Drive, #2224, North Miami Beach, FL 33160
Arnett-Kibel, Christine, University of Massachusetts, Dean of Science Faculty, Boston, MA 02125
Armstrong, Clay M., University of Pennsylvania School of Medicine, B701 Richards Building, Department of Physiology, 3700 Hamilton Walk, Philadelphia, PA 19104-6085
Armstrong, Ellen Prosser, 57 Millfield Street, Woods Hole, MA 02543
Arnold, William A., Oak Ridge National Laboratory, Biology Division, 102 Balsalm Road, Oak Ridge, TN 37830
Ashton, Robert W., Bay Foundation, 17 West 94th Street, New York, NY 10025

Atema, Jelle, Boston University Marine Program, Marine Biological Laboratory, Woods Hole, MA 02543

Baccetti, Baccio, University of Sienna, Institute of Zoology, 53100 Siena, Italy
Baker, Robert G., New York University Medical Center, Department Physiology and Biophysics, 550 First Avenue, New York, NY 10016
Baldwin, Thomas O., University of Arizona, Department of Biochemistry, P.O. Box 210088, Tucson, AZ 85721-0088
Baltimore, David, California Institute of Technology, 1200 East California Boulevard, Pasadena, CA 91125
Barlow, Robert B., SUNY Health Science Center at Syracuse, 750 East Adams Street, Center for Vision Research, 3258 Weiskotten Hall, Syracuse, NY 13210
Barry, Daniel T., National Aeronautics and Space Administration, Lyn B. Johnson Space Center, 2101 NASA Road 1, Houston, TX 77058
Barry, Susan R., Mount Holyoke College, Department of Biological Sciences, South Hadley, MA 01075
Bass, Andrew H., Cornell University, Department of Neurobiology and Behavior, Seely Mudd Hall, Ithaca, NY 14853
Battelle, Barbara-Anne, University of Florida, Whitney Laboratory, 9505 Ocean Shore Boulevard, Augustine, FL 32086
Bay, Frederick, Bay Foundation, 17 W. 94th Street, First Floor, New York, NY 10025-7116
Baylor, Martha B., P.O. Box 93, Woods Hole, MA 02543
Bearer, Elaine L., Brown University, Division of Biology and Medicine, Department of Pathology, Box G, Providence, RI 02912
Beatty, John M., University of Minnesota, Department of Ecology and Behavioral Biology, 1987 Gortner, Street Paul, MN 55108
Beaugè, Luis Alberto, Instituto de Investigacion Medica, Department of Biophysics, Casilla de Correo 389, Cordoba 5000, Argentina
Begenisich, Ted, University of Rochester, Medical Center, Box 642, 601 Elmwood Avenue, Rochester, NY 14642
Begg, David A., University of Alberta, Faculty of Medicine, Department of Cell Biology and Anatomy, Edmonton, Alberta T6G 2H7, Canada
Bell, Eugene, 305 Commonwealth Avenue, Boston, MA 02115
Benjamin, Thomas L., Harvard Medical School, Pathology, D2-230, 200 Longwood Avenue, Boston, MA 02115
Bennett, Michael V. L., Albert Einstein College of Medicine, Department of Neuroscience, 1300 Morris Park Avenue, Bronx, NY 10461
Bennett, Miriam F., Colby College, Department of Biology, Waterville, ME 04901
Bennett, R. Suzanne, Albert Einstein College of Medicine, Department of Neuroscience, 1300 Morris Park Avenue, Bronx, NY 10461
Berg, Carl J. Jr., P.O. Box 681, Kilauea, Kauai, HI 96754-0681
Berlin, Suzanne T., 5 Highland Street, Gloucester, MA 01930
Bernstein, Norman, Columbia Realty Venture, 5301 Wisconsin Avenue, NW, #600, Washington, DC 20015-2015
Bezanilla, Francisco, Health Science Center, Department of Physiology, 405 Hilgard Avenue, Los Angeles, CA 90024
Biggers, John D., Harvard Medical School, Department of Physiology, Boston, MA 02115
Bishop, Stephen H., Iowa State University, Department of Zoology, Ames, IA 50010
Blaustein, Mordecai P., University of Maryland, School of Medicine, Department of Physiology, Baltimore, MD 21201
Blennemann, Dieter, 1117 East Putnam Avenue, Apt. #174, Riverside, CT 06878-1333
Bloom, George S., The University of Texas Southwestern Medical Center, Department of Cell Biology and Neuroscience, 5323 Harry Hines Boulevard, Dallas, TX 75235-9039
Bloom, Kerry S., University of North Carolina, Department of Biology, 623 Fordham Hall CB#3280, Chapel Hill, NC 27599-3280
Bodznick, David A., Wesleyan University, Department of Biology, Lawn Avenue, Middletown, CT 06497-0170
Boettiger, Edward G., 17 Eastwood Road, Storrs, CT 06268-2401
Boolootian, Richard A., Science Software Systems, Inc., 3576 Woodcliff Road, Sherman Oaks, CA 91403
Borgese, Thomas A., Lehman College, CUNY, Department of Biology, Bedford Park Boulevard, West, Bronx, NY 10468
Borst, David W. Jr., Illinois State University, Department of Biological Sciences, Normal, IL 61790-4120
Bowles, Francis P., Marine Biological Laboratory, Ecosystems Center, Woods Hole, MA 02543
Boyer, Barbara C., Union College, Biology Department, Schenectady, NY 12308
Brandhorst, Bruce P., Simon Fraser University, Institute of Molecular Biology/Biochemistry, Barnaby, B.C. V5A 1S6, Canada
Brinley, F. J. Jr., NINCDS/NIH, Neurological Disorders Program, Room 812 Federal Building, Bethesda, MD 20892
Bronner-Fraser, Marianne, California Institute of Technology, Beckman Institute Division of Biology, 139-74, Pasadena, CA 91125
Brown, Stephen C., SUNY, Department of Biological Sciences, Albany, NY 12222
Brown, William L., 80 Black Oak Road, Weston, MA 02193
Browne, Carole L., Wake Forest University, Department of Biology, Box 7325 Reynolds Station, Winston-Salem, NC 27109
Browne, Robert A., Wake Forest University, Department of Biology, Box 7325, Winston-Salem, NC 27109
Bucklin, Anne C., University of New Hampshire, Ocean Process Analysis Laboratory, 142 Morse Hall, Durham, NH 03824
Bullis, Robert A., Oceanic Institute of Applied Aquaculture, 41-202 Kalanianaole Highway, Waimanalo, HI 96795
Burger, Max M., Friedrich Miescher-Institute, P.O. Box 2543, CH-4002 Basel, Switzerland
Burgess, David R., Boston College, Bourneuf House, 84 College Road, Chestnut Hill, MA 02467-3838
Burgos, Mario H., IHEM Medical School, UNC Conicet, Casilla de Correo 56, 5500 Mendoza, Argentina
Burky, Albert, University of Dayton, Department of Biology, Dayton, OH 45469
Burris, John E., Marine Biological Laboratory, 7 MBL Street, Woods Hole, MA 02543
Burstyn, Harold Lewis, United States Air Force, Air Force Materiel Command, Rome Research Site RL/JA, 26 Electronic Parkway, Rome, NY 13441-4514
Bursztajn, Sherry, LSU Medical Center, 1501 Kings Highway, Building BRIF 6-13, Shreveport, LA 71130

Calabrese, Ronald L., Emory University, Department of Biology, 1510 Clifton Road, Atlanta, GA 30322
Callaway, Joseph C., New York Medical College, Department of Physiology, Basic Sciences Building, Valhalla, NY 10595
Cameron, R. Andrew, California Institute of Technology, Division of Biology 156-29, Pasadena, CA 91125
Campbell, Richard H., Bang-Campbell Associates, Eel Pond Place, Box 402, Woods Hole, MA 02543
Candelas, Graciela C., University of Puerto Rico, Department of Biology, P.O. Box 23360, UPR Station, San Juan, PR 00931-3360
Cariello, Lucio, Stazione Zoologica "A. Dohrn," Villa Comunale, 80121 Naples, Italy
Case, James F., University of California, Marine Science Institute, Santa Barbara, CA 93106
Cassidy, Father Joseph D., Providence College, Priory of St. Thomas Aquinas, Providence, RI 02918-0001
Cavanaugh, Colleen M., Harvard University, Biological Laboratories, 16 Divinity Avenue, Cambridge, MA 02138

Chaet, Alfred B., University of West Florida, Department of Cell and Molecular Biology, 11000 University Parkway, Pensacola, FL 32514
Chambers, Edward L., University of Miami School of Medicine, Department of Physiology and Biophysics P.O. Box 016430, Miami, FL 33101
Chang, Donald C., Hong Kong University, Science and Technology, Department of Biology, Clear Water Bay, Kowloon, Hong Kong
Chappell, Richard L., Hunter College, CUNY, Department of Biological Sciences, Box 210, 695 Park Avenue, New York, NY 10021
Child, Frank M., 28 Lawrence Farm Road, Woods Hole, MA 02543-1416
Chisholm, Rex Leslie, Northwestern University, Medical School, Department of Cell Biology, Chicago, IL 60611
Citkowitz, Elena, Hospital of St. Raphael, Lipid Disorders Clinic, 1450 Chapel Street, New Haven, CT 06511
Clark, Eloise E., Bowling Green State University, Biological Sciences Department, Bowling Green, OH 43403
Clark, Hays, 150 Gomez Road, Hobe Sound, FL 33455
Clark, Wallis H. Jr., 12705 NW 112th Avenue, Alachua, FL 32615
Claude, Philippa, University of Wisconsin, Department of Zoology, Zoology Research Building 125, 1117 W Johnson Street, Madison, WI 53706
Clay, John R., National Institutes of Health, NINDS, Building 36, Room 2-CO2, Bethesda, MD 20892
Clowes, Alexander W., University of Washington, School of Medicine, Department of Surgery, Box 356410, Seattle, WA 98195-6410
Cobb, Jewel Plummer, California State University, 5151 University Drive, Health Center 205, Los Angeles, CA 90032-8500
Cohen, Carolyn, Brandeis University, Rosenstiel Basic Medical, Sciences Research Center, Waltham, MA 02254
Cohen, Lawrence B., Yale University School of Medicine, Department of Physiology, 333 Cedar Street, New Haven, CT 06520
Cohen, Maynard M., Rush Medical College, Department of Neurological Sciences, 600 South Paulina, Chicago, IL 60612
Cohen, William D., Hunter College, Department Biological Sciences, New York, NY 10021
Coleman, Annette W., Brown University, Division of Biology and Medicine, Providence, RI 02912
Colinvaux, Paul, Marine Biological Laboratory, Woods Hole, MA 02543
Collier, Jack R., 3431 Highway, #107, P.O. Box 139, Effie, LA 71331
Collier, Marjorie McCann, 3431 Highway 107, P.O. Box 139, Effie, LA 71331
Cook, Joseph A., Edna McConnell Clark Foundation, 250 Park Avenue, New York, NY 10177-0026
Cornell, Neal W., Marine Biological Laboratory, Woods Hole, MA 02543 (deceased, 2000)
Cornwall, Melvin C. Jr., Boston University School of Medicine, Department of Physiology L714, Boston, MA 02118
Corson, D. Wesley Jr., Storm Eye Institute, Room 537, 171 Ashley Avenue, Charleston, SC 29425
Corwin, Jeffrey T., University of Virginia, School of Medicine, Department Otolaryngology and Neuroscience, Box 396, Charlottesville, VA 22908
Couch, Ernest F., Texas Christian University, Department of Biology, TCU Box 298930, Fort Worth, TX 76129
Cox, Rachel Llanelly, Woods Hole Oceanographic Institute, Biology Department, Woods Hole, MA 02543
Crane, Sylvia E., 438 Wendover Drive, Princeton, NJ 08540
Cremer-Bartels, Gertrud, Horstmarer Landweg 142, 48149 Muenster, Germany
Crow, Terry J., University of Texas Medical School, Department of Neurobiology and Anatomy, Houston, TX 77225
Crowell, Sears, Indiana University, Department of Biology, Bloomington, IN 47405
Crowther, Robert J., Shriners Hospitals for Children, 51 Blossom Street, Boston, MA 02114
Cummings, Michael P., Marine Biological Laboratory, Bay Paul Center, Woods Hole, MA 02543
Cunningham, Mary-Ellen, 62 Cloverly Road, Grosse Pointe Farms, MI 48236-3313
Cutler, Richard D., Marine Biological Laboratory, Woods Hole, MA 02543

Davidson, Eric H., California Institute of Technology, Division of Biology 156-29, 391 South Holliston, Pasadena, CA 91125
Davison, Daniel B., Bristol-Myers Squibb PRI, Bioinformatics Department, 5 Research Parkway, Wallingford, CT 06492
Daw, Nigel W., 5 Old Pawson Road, Branford, CT 06405
Dawidowicz, Eliezar A., Marine Biological Laboratory, Office of Research Administration and Education, Woods Hole, MA 02543
De Weer, Paul J., University of Pennsylvania, B400 Richards Building, Department of Physiology, 3700 Hamilton Walk, Philadelphia, PA 19104-6085
Deegan, Linda A., Marine Biological Laboratory, The Ecosystems Center, Woods Hole, MA 02543
DeGroof, Robert C., 145 Water Crest Drive, Doylestown, PA 18901-3267
Denckla, Martha Bridge, Johns Hopkins University, School of Medicine, Kennedy-Krieger Institute, 707 North Broadway, Baltimore, MD 21205
DePhillips, Henry A., Trinity College, Department of Chemistry, 300 Summit Street, Hartford, CT 06106
DeSimone, Douglas W., University of Virginia, Department of Cell Biology, Box 439, Health Sciences Center, Charlottesville, VA 22908
Dettbarn, Wolf-Dietrich, 4422 Wayland Drive, Nashville, TN 37215
Dionne, Vincent E., Boston University Marine Program, Marine Biological Laboratory, Woods Hole, MA 02543
Dowling, John E., Harvard University, Biological Laboratories, 16 Divinity Street, Cambridge, MA 02138
Drapeau, Pierre, Montreal General Hospital, Department of Neurology, 1650 Cedar Avenue, Montreal, Quebec H3G 1A4, Canada
DuBois, Arthur Brooks, John B. Pierce Foundation Laboratory, 290 Congress Avenue, New Haven, CT 06519
Duncan, Thomas K., Nichols College, Environmental Sciences Department, Dudley, MA 01571
Dunham, Philip B., Syracuse University, Department of Biology, 130 College Place, Syracuse, NY 13244-1220
Dunlap, Paul V., University of Maryland Biotechnology Institute, Center of Marine Biotechnology, Columbus Center, Suite 236, 701 East Pratt Street, Baltimore, MD 21202

Ebert, James D., The Johns Hopkins University, Department of Biology, Homewood, 3400 North Charles Street, Baltimore, MD 21218-2685
Eckberg, William R., Howard University, Department of Biology, P.O. Box 887, Administration Building, Washington, DC 20059
Edds, Kenneth T., R & D Systems, Inc., Hematology Division, 614 McKinley Place, NE, Minneapolis, MN 55413
Eder, Howard A., Albert Einstein College of Medicine, 1300 Morris Park Avenue, Bronx, NY 10461
Edstrom, Joan, 53 Two Ponds Road, Falmouth, MA 02540
Egyud, Laszlo G., Cell Research Corporation, P.O. Box 67209, Chestnut Hill, MA 02167-0209
Ehrlich, Barbara E., Yale University Medical School, Department of Pharmacology, New Haven, CT 06473

Eisen, Arthur Z., Washington University, Division of Dermatology, St. Louis, MO 63110

Eisen, Herman N., Massachusetts Institute of Technology, Center for Cancer Research, E17-128, 77 Massachusetts Avenue, Cambridge, MA 02139-4307

Elder, Hugh Young, University of Glasgow, Institute of Physiology, Glasgow G12 8QQ, Scotland

Englund, Paul T., Johns Hopkins Medical School, Department of Biological Chemistry, 725 North Wolfe Street, Baltimore, MD 21205

Epel, David, Stanford University, Hopkins Marine Station, Ocean View Boulevard, Pacific Grove, CA 93950

Epstein, Herman T., 18 Lawrence Farm Road, Woods Hole, MA 02543

Epstein, Ray L., 701 Winthrop Street, #311, Taunton, MA 02780-2187

Farb, David H., Boston University School of Medicine, Department of Pharmacology L603, 80 East Concord Street, Boston, MA 02118

Farmanfarmaian, A. Verdi, Rutgers University, Department of Biological Sciences, Nelson Biology Laboratory POB 1059, Piscataway, NJ 08855

Feldman, Susan C., University of Medicine and Dentistry, New Jersey Medical School, 100 Bergen Street, Newark, NJ 07103

Festoff, Barry William, VA Medical Center, Neurology Service (151), 4801 Linwood Boulevard, Kansas City, MO 64128

Fink, Rachel D., Mount Holyoke College, Department of Biological Sciences, Clapp Laboratories, South Hadley, MA 01075

Finkelstein, Alan, Albert Einstein College of Medicine, 1300 Morris Park Avenue, Bronx, NY 10461

Fischbach, Gerald D., National Institute of Health, Neurological Disorders and Strokes, 31 Center Drive, MSC 2540, Bldg 31, Rm 8A03, Bethesda, MD 20892-2540

Fishman, Harvey M., University of Texas Medical Branch, Department of Physiology and Biophysics, 301 University Boulevard, Galveston, TX 77555-0641

Flanagan, Dennis, 12 Gay Street, New York, NY 10014

Fluck, Richard Allen, Franklin and Marshall College, Department of Biology, Box 3003, Lancaster, PA 17604-3003

Foreman, Kenneth H., Marine Biological Laboratory, Woods Hole, MA 02543

Fox, Thomas Oren, Harvard Medical School, Division of Medical Sciences, MEC 435, 260 Longwood Avenue, Boston, MA 02115

Franzini-Armstrong, Clara, University of Pennsylvania, School of Medicine, 330 South 46th Street, Philadelphia, PA 19143

Fraser, Scott, California Institute of Technology, Beckman Institute 139-74, 1201 East California Boulevard, Pasadena, CA 91125

Frazier, Donald T., University of Kentucky Medical Center, Department of Physiology and Biophysics, MS501 Chandler Medical Center, Lexington, KY 40536

French, Robert J., University of Calgary, Health Sciences Centre, Alberta, T2N 4N1, CANADA

Fulton, Chandler M., Brandeis University, Department of Biology, MS 008, Waltham, MA 02454-9110

Furie, Barbara C., Beth Israel Deaconess Medical Center, BIDMC Cancer Center, Kirstein 1, 330 Brookline Avenue, Boston, MA 02215

Furie, Bruce, Beth Israel Deaconess Medical Center, BIDMC Cancer Center, Kirstein 1, 330 Brookline Avenue, Boston, MA 02215

Furshpan, Edwin J., Harvard Medical School, Department of Neurobiology, 220 Longwood Avenue, Boston, MA 02115

Futrelle, Robert P., Northeastern University, College of Computer Science, 360 Huntington Avenue, Boston, MA 02115

Gabr, Howaida, Suez Canal University, Department of Marine Science, Faculty of Science, Ismailia, Egypt

Gadsby, David C., The Rockefeller University, Laboratory of Cardiac Physiology, 1230 York Avenue, New York, NY 10021-6399

Gainer, Harold, National Institutes of Health, NINDS, BNP, DIR, Neurochemistry, Building 36, Room 4D20, Bethesda, MD 20892-4130

Galatzer-Levy, Robert M., 534 Judson Avenue, Evanston, IL 60202

Gall, Joseph G., Carnegie Institution, 115 West University Parkway, Baltimore, MD 21210

Garber, Sarah S., Allegheny University of the Health Sciences, Department of Physiology, 2900 Queen Lane, Philadelphia, PA 19129

Gascoyne, Peter, University of Texas, M. D. Anderson Cancer Center, Experimental Pathology, Box 89, Houston, TX 77030

Gelperin, Alan, Bell Labs Lucent, Department Biology Comp., Rm 1C464, 600 Mountain Avenue, Murray Hill, NJ 07974

German, James L. III, The New York Blood Center, Laboratory of Human Genetics, 310 East 67th Street, New York, NY 10021

Gibbs, Martin, Brandeis University, Institute for Photobiology of Cells and Organelles, Waltham, MA 02254

Giblin, Anne E., Marine Biological Laboratory, The Ecosystems Center, Woods Hole, MA 02543

Gibson, A. Jane, Cornell University, Department of Biochemistry, Biotech Building, Ithaca, NY 14850

Gifford, Prosser, Library of Congress, Madison Building LM605, Washington DC 20540

Gilbert, Daniel L., National Institutes of Health, Biophysics Sec., BNP, Building 36, Room 5A-27, Bethesda, MD 20892

Giudice, Giovanni, Universita di Palermo, Dipartimento di Biologia, Cellulare e Dello Sviluppo, I-90123 Palermo, Italy

Giuditta, Antonio, University of Naples, Department of General Physiology, Via Mezzocannone 8, Naples, 80134, Italy

Glynn, Paul, P.O. Box 6083, Brunswick, ME 04011-6083

Golden, William T., Chairman Emeritus, American Museum of Natural History, 500 Fifth Avenue, 50th Floor, New York, NY 10110

Goldman, Robert D., Northwestern University Medical School, Department of Cell and Molecular Biology, 303 E. Chicago Avenue, Chicago, IL 60611-3008

Goldsmith, Paul K., National Institutes of Health, Building 10, Room 9C-101, Bethesda, MD 20892

Goldsmith, Timothy H., Yale University, Department of Biology, New Haven, CT 06510

Goldstein, Jr., Moise H., The Johns Hopkins University, ECE Department, Barton Hall, Baltimore, MD 21218

Gould, Robert Michael, NYS Institute of Basic Research, 1050 Forest Hill Road, Staten Island, NY 10314-6399

Govind, C. K., Scarborough College, Life Sciences Division, 1265 Military Trail, West Hill, Ontario M1C 1A4, Canada

Grace, Dick, Doreen Grace Fund, The Brain Center, Promontory Point, New Seabury, MA 02649

Graf, Werner M., College of France, 11 Place Marcelin Berthelot, 75231 Paris Cedex 05, France

Grant, Philip, National Institutes of Health, NINDS\BN\DIR-Neurochemistry, Building 36, Room 4D20, Bethesda, MD 20892-4130

Grass, Ellen R., The Grass Foundation, 77 Reservoir Road, Quincy, MA 02170-3610

Grassle, Judith P., Rutgers University, Institute of Marine and Coastal Studies, Box 231, New Brunswick, NJ 08903

Graubard, Katherine G., University of Washington, Department of Zoology, NJ-15, Box 351800, Seattle, WA 98195-1800

Greenberg, Everett Peter, University of Iowa, College of Medicine, Department of Microbiology, Iowa City, IA 52242

Greenberg, Michael J., University of Florida, The Whitney Laboratory, 9505 Ocean Shore Boulevard, St. Augustine, FL 32086-8623

Greer, Mary J., 176 West 87th Street, #12A, New York, NY 10024-2902
Griffin, Donald R., Harvard University, Concord Field Station, Old Causeway Road, Bedford, MA 01730
Gross, Paul R., 123 Perkins Street, Jamaica Plain, MA 02130
Grossman, Albert, New York University Medical Center, 550 First Avenue, New York, NY 10016
Grossman, Lawrence, The Johns Hopkins University, Hygiene Building, Room W8306, Baltimore, MD 21205
Gruner, John A., Cephalon, Inc., 145 Brandywine Parkway, West Chester, PA 19380-4245
Gunning, A. Robert, P. O. Box 165, Falmouth, MA 02541
Gwilliam, G. Francis, Reed College, Department of Biology, Portland, OR 97202

Haimo, Leah T., University of California, Department of Biology, Riverside, CA 92521
Hajduk, Stephen L., University of Alabama, School of Medicine/Dentistry, Department of Biochemistry/Molecular Genetics, University Station, Birmingham, AL 35294
Hall, Linda M., Shriners Hospital for Children, 2425 Stockton Boulevard, Sacramento, CA 95817
Hall, Zach W., University of California, Department of Physiology, San Francisco, CA 94114
Halvorson, Harlyn O., University of Massachusetts, Policy Center for Marine Biosciences and Technology, 100 Morrissey Boulevard, Boston, MA 02125-3393
Haneji, Tatsuji, The University of Tokushima, Department of Histology and Oral Histology, School of Dentistry, 18-15, 3 Kuramoto-cho, Tokushima 770-8504, Japan
Hanlon, Roger T., Marine Biological Laboratory, Woods Hole, MA 02543
Harosi, Ferenc, New College of the USF, Division of Natural Sciences, 5700 North Tamiami Trail, Sarasota, FL 34243-2197
Harrigan, June F., 7415 Makaa Place, Honolulu, HI 96825
Harrington, Glenn W., Weber State University, Department of Microbiology, Ogden, UT 84408
Harrington, John P., University of South Alabama, Department of Chemistry, Mobile, AL 36688
Harrison, Stephen C., Harvard University, Department of Molecular and Cell Biology, 7 Divinity Avenue, Cambridge, MA 02138
Haselkorn, Robert, University of Chicago, Department of Molecular Genetics and Cell Biology, Chicago, IL 60637
Hastings, J. Woodland, Harvard University, The Biological Laboratories, 16 Divinity Avenue, Cambridge, MA 02138-2020
Haydon-Baillie, Wensley G., Porton Institute, 2 Lowndes Place, London SW1X 8Dd, United Kingdom
Hayes, Raymond L. Jr., Howard University, College of Medicine, 520 W Street, NW, Washington, DC 20059
Heck, Diane E., Rutgers University, Department of Pharmacology/Toxicology, 681 Frelinghuysen Road, Piscataway, NJ 08855
Henry, Jonathan Joseph, University of Illinois, Department of Cell and Structural Biology, 601 South Goodwin Avenue #B107, Urbana, IL 61801-3709
Hepler, Peter K., University of Massachusetts, Department of Biology, Morrill III, Amherst, MA 01003
Herndon, Walter R., University of Tennessee, Department of Botany, Knoxville, TN 37996-1100
Hershko, Avram, Technion-Israel Institute of Technology, Unit of Biochemistry, The Bruce Rappaport Faculty of Medicine, Haifa 31096, Israel
Herskovits, Theodore T., Fordham University, Department of Chemistry, John Mulcahy Hall, Room 638, Bronx, NY 10458
Hiatt, Howard H., Brigham and Women's Hospital, Department of Medicine, 75 Francis Street, Boston, MA 02115
Highstein, Stephen M., Washington University, Department of Otolaryngology, Box 8115, 4566 Scott Avenue, St. Louis, MO 63110
Hildebrand, John G., University of Arizona, ARL Division of Neurobiology, P.O. Box 210077, Tucson, AZ 85721-0077
Hill, Richard W., Michigan State University, Department of Zoology, East Lansing, MI 48824
Hill, Susan D., Michigan State University, Department of Zoology, East Lansing, MI 48824
Hillis, Llewellya W., Marine Biological Laboratory, Woods Hole, MA 02543
Hinchcliffe, Edward H., University of Massachusetts Medical School, Department of Cell Biology, 377 Plantation Street, Worcester, MA 01605
Hinkle, Gregory J., Bioinformatics Group, Cereon Genomics, One Kendall Square, Building 200, Cambridge, MA 02139
Hinsch, Gertrude W., University of South Florida, Department of Biology, Tampa, FL 33620
Hinsch, Jan, Leica, Inc., 110 Commerce Drive, Allendale, NJ 07401
Hobbie, John E., Marine Biological Laboratory, The Ecosystems Center, Woods Hole, MA 02543
Hodge, Alan J., 3843 Mount Blackburn Avenue, San Diego, CA 92111
Hoffman, Joseph F., Yale University School of Medicine, Cellular and Molecular Physiology, 333 Cedar Street, New Haven, CT 06520-8026
Hollyfield, Joe G., The Cleveland Clinic, Ophthalmic Research, 9500 Euclid Avenue, Cleveland, OH 44195
Holz, George G. IV, New York University Medical Center, Medical Sciences Building, Room 442, 550 First Avenue, New York, NY 10016
Hopkinson, Charles S. Jr., Marine Biological Laboratory, Woods Hole, MA 02543
Houk, James C., Northwestern University Medical School, 303 East Chicago Avenue, Ward 5-315, Chicago, IL 60611-3008
Hoy, Ronald R., Cornell University, Section of Neurobiology and Behavior, 215 Mudd Hall, Ithaca, NY 14853
Huang, Alice S., California Institute of Technology, Mail Code 1-9, Pasadena, CA 91125
Hufnagel-Zackroff, Linda A., University of Rhode Island, Department of Microbiology, Kingston, RI 02881
Hummon, William D., Ohio University, Department of Biological Sciences, Athens, OH 45701
Humphreys, Susie H., Food and Drug Administration, HFS-308, 200 C Street, SW, Washington, DC 20204-0001
Humphreys, Tom, University of Hawaii, Kewalo Marine Laboratory, 41 Ahui Street, Honolulu, HI 96813
Hunt, Richard T., ICRF, Clare Hall Laboratories, South Mimms Potter's Bar, Herts EN6-3LD, England
Hunter, Robert D., Oakland University, Department of Biological Sciences, Rochester, MI 48309-4401
Huxley, Hugh E., Brandeis University, Rosenstiel Center, Biology Department, Waltham, MA 02154

Ilan, Joseph, Case Western Reserve University, School of Medicine, Department of Anatomy, Cleveland, OH 44106
Ingoglia, Nicholas A., New Jersey Medical School, Department of Pharmacology/Physiology, 185 South Orange Avenue, Newark, NJ 07103
Inoué, Saduyki, McGill University, Department of Anatomy, 3640 University Street, Montreal, PQ H3A 2B2, Canada
Inoué, Shinya, Marine Biological Laboratory, Woods Hole, MA 02543
Isselbacher, Kurt J., Massachusetts General Hospital Cancer Center, Charlestown, MA 02129
Issidorides, Marietta Radovic, University of Athens, Department of Psychiatry, Monis Petraki 8, Athens, 140, Greece

Izzard, Colin S., SUNY–Albany, Department of Biological Sciences, 1400 Washington Avenue, Albany, NY 12222

Jacobs, Neil, Hale and Dorr, 60 State Street, Boston, MA 02109

Jaffe, Laurinda A., University of Connecticut Health Center, Department of Physiology, Farmington Avenue, Farmington, CT 06032

Jaffe, Lionel, Marine Biological Laboratory, Woods Hole, MA 02543

Jeffery, William R., University of Maryland, Department of Biology, College Park, MD 20742

Johnston, Daniel, Baylor College of Medicine, Division of Neuroscience, Baylor Plaza, Houston, TX 77030

Josephson, Robert K., University of California, School of Biological Science, Department of Psychobiology, Irvine, CA 92697

Kaczmarek, Leonard K., Yale University School of Medicine, Department of Pharmacology, 333 Cedar Street, New Haven, CT 06520

Kaley, Gabor, New York Medical College, Department of Physiology, Basic Sciences Building, Valhalla, NY 10595

Kaltenbach, Jane, Mount Holyoke College, Department Biological Sciences, South Hadley, MA 01075

Kaminer, Benjamin, Boston University Medical School, Physiology Department, 80 East Concord Street, Boston, MA 02118

Kaneshiro, Edna S., University of Cincinnati, Biological Sciences Department, JL 006, Cincinnati, OH 45221-0006

Kaplan, Ehud, Mount Sinai School of Medicine, 1 Gustave Levy Place, Box 1183, New York, NY 10029

Karakashian, Stephen J., Apartment 16-F, 165 West 91st Street, New York, NY 10024

Karlin, Arthur, Columbia University, Center for Molecular Recognition, 630 West 168th Street, Room 11-401, New York, NY 10032

Karnovsky, Morris John, Harvard Medical School, Department of Pathology, 200 Longwood Avenue, Boston, MA 02115

Keller, Hartmut Ernst, Carl Zeiss, Inc., One Zeiss Drive, Thornwood, NY 10594

Kelley, Darcy B., Columbia University, Department of Biological Sciences, 911 Fairchild, Mailcode 2432, New York, NY 10027

Kelly, Robert E., 5 Little Harbor Road, Woods Hole, MA 02543

Kemp, Norman E., University of Michigan, Department of Biology, Ann Arbor, MI 48109

Kendall, John P., Faneuil Hall Associates, 176 Federal Street, 2nd Floor, Boston, MA 02110

Kerr, Louis M., Marine Biological Laboratory, Woods Hole, MA 02543

Keynan, Alexander, Israel Academy of Science and Humanity, P.O. Box 4040, Jerusalem, Israel

Khan, Shahid M. M., Albert Einstein College of Medicine, Department of Physiology and Biophysics, 1300 Morris Park Avenue, Room U273, Bronx, NY 10461

Khodakhah, Kamran, University of Colorado School of Medicine, Department of Physiology and Biophysics, 4200 East 9th Avenue, C-240, Denver, CO 80262

Kiehart, Daniel P., Duke University Medical Center, Department of Cell Biology, Box 3709, 308 Nanaline Duke Building, Durham, NC 27710

Kleinfeld, David, University of California, Department of Physics, 0319 9500 Gilman Drive, La Jolla, CA 92093

Klessen, Rainer, (address unknown)

Klotz, Irving M., Northwestern University, Department of Chemistry, Evanston, IL 60201

Knudson, Robert A., Marine Biological Laboratory, Woods Hole, MA 02543

Koide, Samuel S., The Rockefeller University, The Population Council, 1230 York Avenue, New York, NY 10021

Kornberg, Hans, Boston University, The University Professors, 745 Commonweath Avenue, Boston, MA 02215

Kosower, Edward M., Tel-Aviv University, Department of Chemistry, Ramat-Aviv, Tel Aviv, 69978, Israel

Krahl, Maurice E., 2783 West Casas Circle, Tucson, AZ 85741

Krane, Stephen M., Massachusetts General Hospital, 55 Fruit Street, Bulf-165, Boston, MA 02114

Krauss, Robert, P.O. Box 291, Denton, MD 21629

Kravitz, Edward A., Harvard Medical School, Department of Neurobiology, 220 Longwood Avenue, Boston, MA 02115

Kriebel, Mahlon E., SUNY Health Science Center, Department of Physiology, Syracuse, NY 13210

Kristan, William B. Jr., University of California, Department of Biology 0357, 9500 Gilman Drive, La Jolla, CA 92093-0357

Kropinski, Andrew M., Queen's University, Department of Microbiology/Immunology, Kingston, Ontario K7L 3N6, Canada

Kuffler, Damien P., Institute of Neurobiology, 201 Boulevard del Valle, San Juan 00901, PR

Kuhns, William J., Hospital for Sick Children, Biochemistry Research, 555 University Avenue, Toronto, Ontario M5G 1X8, Canada

Kunkel, Joseph G., University of Massachusetts, Department of Biology, Amherst, MA 01003

Kuzirian, Alan M., Marine Biological Laboratory, Woods Hole, MA 02543-1015

Laderman, Aimlee D., Yale University, School of Forestry and Environmental Studies, 370 Prospect Street, New Haven, CT 06511

Landeau, Laurie J., Listowel, Inc., 2 Park Avenue, Suite 1525, New York, NY 10016

Landis, Dennis M. D., University Hospital of Cleveland, Department Neurology, 11100 Euclid Avenue, Cleveland, OH 44106

Landis, Story C., National Institutes of Health, Building 36, Room 5A05, 36 Convent Drive, Bethesda, MD 20892-4150

Landowne, David, University of Miami Medical School, Department of Physiology, PO Box 016430, Miami, FL 33101

Langford, George M., Dartmouth College, Department of Biological Sciences, 6044 Gilman Laboratory, Hanover, NH 03755

Laskin, Jeffrey, University of Medical and Dentistry of New Jersey, Robert Wood Johnson Medical School, 675 Hoes Lane, Piscataway, NJ 08854

Lasser-Ross, Nechama, New York Medical College, Department of Physiology, Valhalla, NY 10595

Laster, Leonard, University of Massachusetts Medical School, 55 Lake Avenue, North, Worcester, MA 01655

Laties, Alan, Scheie Eye Institute, Myrin Circle, 51 North 39th Street, Philadelphia, PA 19104

Laufer, Hans, University of Connecticut, Department of Molecular and Cell Biology, U-125, 75 North Eagleville Road Storrs, CT 06269-3125

Lazarow, Paul B., Mount Sinai School of Medicine, Department of Cell Biology and Anatomy, 1190 Fifth Avenue, Box 1007, New York, NY 10029-6574

Lazarus, Maurice, Federated Department Stores, Sears Crescent, City Hall Plaza, Boston, MA 02108

Leadbetter, Edward R., University of Connecticut, Department of Molecular and Cell Biology, U-131, Beach Hall, Room 249, 354 Mansfield Road, Storrs, CT 06269-2131

Lederberg, Joshua, The Rockefeller University, Suite 400 (Founders Hall), 1230 York Avenue, New York, NY 10021

Lee, John J., City College of CUNY, Department of Biology, Convent Avenue and 138th Street, New York, NY 10031

Lehy, Donald B., 35 Willow Field Drive, North Falmouth, MA 02556

Leighton, Joseph, Aeron Biotechnology, Inc., 1933 Davis Street #310, San Leandro, CA 94577 (deceased 1999)

Leighton, Stephen B., National Institutes of Health, Building 13, 3W13, Bethesda, MD 20892

Lemos, Jose Ramon, University of Massachusetts Medical Center, Worcester Foundation Campus, 222 Maple Avenue, Shrewsbury, MA 01545-2737

Lerner, Aaron B., Yale University School of Medicine, Department of Dermatology, P.O. Box 3333, New Haven, CT 06510

Levin, Jack, Veterans Administration, Medical Center, 111 H2, 4150 Clement Street, San Francisco, CA 94121

Levine, Michael, University of California, Department MCB, 401 Barker Hall, Berkeley, CA 94720

Levine, Richard B., University of Arizona, Division of Neurobiology, Room 611, Gould Simpson Building, PO Box 210077, Tucson, AZ 85721-0077

Levinthal, Francoise, Columbia University, Department of Biological Sciences, Broadway and 116th Street, New York, NY 10026

Levitan, Herbert, National Science Foundation, 4201 Wilson Boulevard, Room 835, Arlington, VA 22230

Levitan, Irwin B., University of Pennsylvania, School of Medicine, 218 Stemmler Hall, 3450 Hamilton Walk, Philadelphia, PA 19104-6074

Linck, Richard W., University of Minnesota School of Medicine, Cell Biology and Neuroanatomy Department, 4-135 Jackson Hall, 321 Church Street, Minneapolis, MN 55455

Lipicky, Raymond J., Food and Drug Administration, CDER/ODEI/HFD-110, 5600 Fishers Lane, Rockville, MD 20857

Lisman, John E., Brandeis University, Molecular and Cell Biology, 415 South Street, Waltham, MA 02454-9110

Liuzzi, Anthony, 180 Beacon Street, #8G, Boston, MA 02116

Llinas, Rodolfo R., New York University Medical Center, Department of Physiology/Biophysics, 550 First Avenue, Room 442, New York, NY 10016

Lobel, Phillip S., Boston University Marine Program, Marine Biological Laboratory, Woods Hole, MA 02543

Loew, Franklin M., Becker College, 61 Sever Street, Worcester, MA 01615-0071

Loewenstein, Birgit Rose, Marine Biological Laboratory, Woods Hole, MA 02543

Loewenstein, Werner R., Marine Biological Laboratory, Woods Hole, MA 02543

London, Irving M., Harvard-MIT, Division, E-25-551, Cambridge, MA 02139

Longo, Frank J., University of Iowa, Department of Anatomy, Iowa City, IA 52442

Luckenbill, Louise M., Ohio University, Department of Biological Sciences, Irvine Hall, Athens, OH 45701

Macagno, Eduardo R., Columbia University, 109 Low Memorial Library, Mail Code 4306, New York, NY 10027

MacNichol, Edward F. Jr., Boston University School of Medicine, Department of Physiology, 80 East Concord Street, Boston, MA 02118

Maglott-Duffield, Donna R., American Type Culture Collection, 12301 Parklawn Drive, Rockville, MD 20852-1776

Maienschein, Jane Ann, Arizona State University, Department of Philosophy, P.O. Box 872004, Tempe, AZ 85287-2004

Mainer, Robert E., The Boston Company, Inc., One Boston Place, OBP-15-D, Boston, MA 02108

Malbon, Craig C., SUNY, University Medical Center, Pharmacology-HSC, Stony Brook, NY 11794-8651

Malchow, Robert P., University of Illinois, Department of Ophthalmology, 1855 West Taylor Street N/C 648, Chicago, IL 60612

Manalis, Richard S., Indiana-Purdue University, Department of Biological Science, 2101 Coliseum Boulevard East, Fort Wayne, IN 46805

Manz, Robert D., 304 Adams Street, Milton, MA 02186

Margulis, Lynn, University of Massachusetts, Department of Geosciences, Morrill Science Center, Box 35820, Amherst, MA 01003-5820

Marinucci, Andrew C., 102 Nancy Drive, Mercerville, NJ 08619

Martinez, Joe L. Jr., The University of Texas, Division of Life Sciences, 6900 North Loop 1604 West, San Antonio, TX 78249-0662

Martinez-Palomo, Adolfo, CINVESTAV-IPN, Sec. de Patologia Experimental, 07000 Mexico, D.F.A.P. 140740, Mexico

Mastroianni, Luigi Jr., Hospital of University of Pennsylvania, 106 Dulles, 3400 Spruce Street, Philadelphia, PA 19104-4283

Mauzerall, David, Rockefeller University, 1230 York Avenue, New York, NY 10021

McAnelly, M. Lynne, University of Texas, Section of Neurobiology, School of Life Sciences, Austin, TX 78712

McCann, Frances V., Dartmouth Medical School, Department of Physiology, Lebanon, NH 03756

McLaughlin, Jane A., Marine Biological Laboratory, Woods Hole, MA 022543

McMahon, Robert F., University of Texas, Arlington, Department of Biology, Box 19498, Arlington, TX 76019

Meedel, Thomas, Rhode Island College, Biology Department, 600 Mount Pleasant Avenue, Providence, RI 02908

Meinertzhagen, Ian A., Dalhousie University, Department of Psychology, Halifax, NS B3H 4J1, Canada

Meiss, Dennis E., Immunodiagnostic Laboratories, 488 McCormick Street, San Leandro, CA 94577

Melillo, Jerry M., Marine Biological Laboratory, Ecosystems Center, Woods Hole, MA 02543

Mellon, DeForest Jr., University of Virginia, Department of Biology, Gilmer Hall, Charlottesville, VA 22903

Mellon, Richard P., P.O. Box 187, Laughlintown, PA 15655-0187

Mendelsohn, Michael E., New England Medical Center, Molecular Cardiology Laboratory, NEMC Box 80, 750 Washington Street, Boston, MA 02111

Mensinger, Allen F., Washington University School of Medicine, Department of Otolarynology, 4566 Scott Avenue, St. Louis, MO 63110

Merriman, Melanie Pratt, 7511 Beach View Drive, North Bay Village, FL 33141

Meselson, Matthew, Harvard University, Fairchild Biochemistry Building, 7 Divinity Avenue, Cambridge, MA 02138

Metuzals, Janis, University of Ottawa Faculty of Medicine, Department of Pathology and Laboratory Medical, 451 Smyth Road, Ottawa, Ontario K1H 8M5, Canada

Miledi, Ricardo, University of California, Irvine, Department of Psychobiology, 2205 Biology Science II, Irvine, CA 92697-4550

Milkman, Roger D., University of Iowa, Department of Biological Sciences, Biology Building, Room 318, Iowa City, IA 52242-1324

Miller, Thomas J., Analogic, 8 Centennial Drive, Peabody, MA 01960

Mills, Robert, 10315 44th Avenue, W 12 H Street, Brandenton, FL 34210

Misevic, Gradimir, University Hospital of Basel, Department of Research, Mebelstr. 20, CH-4031 Basel, Switzerland

Mitchell, Ralph, Harvard University, Division of Applied Sciences, 29 Oxford Street, Cambridge, MA 02138

Miyakawa, Hiroyoshi, Tokyo College of Pharmacy, Laboratory of Cellular Neurobiology, 1432-1 Horinouchi, Hachiouji, Tokyo 192-03, Japan

Miyamoto, David M., Drew University, Department of Biology, Madison, NJ 07940

Mizell, Merle, Tulane University, Department of Cell and Molecular, Biology, New Orleans, LA 70118

Moreira, Jorge E., National Institutes of Health, NICHD, Department of Cell and Molecular Biol., Bethesda, MD 20852

Morin, James G., Cornell University, Dept. of Ecology & Evolutionary Biology, G14 Stimson Hall, Ithaca, NY 14853-2801

Morrell, Leyla de Toledo, Rush-Presbyterian-St. Lukes Medical Center, 1653 West Congress Parkway, Chicago, IL 60612

Morse, M. Patricia, National Science Foundation, Room 885, Esie, Arlington, VA 22230

Morse, Stephen S., DARPA/DS0, 3701 North Fairfax Drive, Arlington, VA 22203-1714

Mote, Michael I., Temple University, Department of Biology, Philadelphia, PA 19122

Muller, Kenneth J., University of Miami School of Medicine, Department of Physiology and Biophysics, 1600 NW 10th Avenue, R-430, Miami, FL 33136

Murray, Andrew W., University of California, Department of Physiology, Box 0444, 513 Parnassus Avenue, San Francisco, CA 94143-0444

Nabrit, Samuel M., 686 Beckwith Street, SW, Atlanta, GA 30314

Nadelhoffer, Knute J., Marine Biological Laboratory, 7 MBL Street, Woods Hole, MA 02543

Nagel, Ronald L., Albert Einstein College of Medicine, 1300 Morris Park Avenue, Bronx, NY 10461

Naka, Ken-ichi, 2-9-2 Tatumi Higashi, Okazaki, 444, Japan

Nakajima, Yasuko, University of Illinois, College of Medicine, Anatomy and Cell Biology Department, M/C 512, Chicago, IL 60612

Narahashi, Toshio, Northwestern University Medical School, Department of Pharmacology, 303 East Chicago Avenue, Chicago, IL 60611

Nasi, Enrico, Boston University School of Medical, Department of Physiology, R-406, 80 East Concord Street, Boston, MA 02118

Neill, Christopher, Marine Biological Laboratory, 7 MBL Street, Woods Hole, MA 02543

Nelson, Leonard, Medical College of Ohio, Department of Physiology, CS 10008, Toledo, OH 43699 (deceased 1999)

Nelson, Margaret C., Cornell University, Section of Neurobiology and Behavior, Ithaca, NY 14850

Nicholls, John G., SISSA, Via Beirut 2, I-34014 Trieste, Italy

Nickerson, Peter A., SUNY at Buffalo, Department of Pathology, Buffalo, NY 14214

Nicosia, Santo V., University of South Florida, College of Medicine, Box 11, Department of Pathology, Tampa, FL 33612

Noe, Bryan D., Emory University School of Medicine, Department of Anatomy and Cell Biology, Atlanta, GA 30322

Norton, Catherine N., Marine Biological Laboratory, 7 MBL Street, Woods Hole, MA 02543

Nusbaum, Michael P., University of Pennsylvania School of Medicine, Department of Neuroscience, 215 Stemmler Hall, Philadelphia, PA 19104-6074

O'Herron, Jonathan, Lazard Freres and Company, 30 Rockefeller Plaza, 59th Floor, New York, NY 10020-1900

Obaid, Ana Lia, University of Pennsylvania School of Medicine, Neuroscience Department, 234 Stemmler Hall, Philadelphia, PA 19104-6074

Ohki, Shinpei, SUNY at Buffalo, Department of Biophysical Sciences, 224 Cary Hall, Buffalo, NY 14214

Oldenbourg, Rudolf, Marine Biological Laboratory, 7 MBL Street, Woods Hole, MA 02543

Olds, James L., George Mason University, Krasnow Institute for Advanced Studies, Mail Stop 2A1, Fairfax, VA 22030-4444

Olins, Ada L., 45 Eastern Promenade, #7-D, Portland, ME 04101

Olins, Donald E., 45 Eastern Promenade, #7-D, Portland, ME 04101

Oschman, James L., Nature's Own Research Association, P.O. Box 5101, Dover, NH 03820

Palazzo, Robert E., University of Kansas, Department of Physiology and Cell Biology, Lawrence, KS 66045

Palmer, John D., University of Massachusetts, Department of Zoology, 221 Morrill Science Center, Amherst, MA 01003

Pant, Harish C., National Institutes of Health, NINCDS, Laboratory of Neurochemistry, Building 36, Room 4D20, Bethesda, MD 20892

Pappas, George D., University of Illinois, College of Medicine, Department of Anatomy, Chicago, IL 60612

Pardee, Arthur B., Dana-Farber Cancer Institute, D810, 44 Binney Street, Boston, MA 02115

Pardy, Rosevelt L., University of Nebraska, School of Life Sciences, Lincoln, NE 68588

Parmentier, James L., AstraZeneca, 725 Chesterbrook Boulevard, Wayne, PA 19087-5677

Pederson, Thoru, University of Massachusetts Medical Center, Worcester Foundation Campus, 222 Maple Avenue, Shrewsbury, MA 01545

Perkins, Courtland D., 400 Hilltop Terrace, Alexandria, VA 22301

Person, Philip, 137-87 75th Road, Flushing, NY 11367

Peterson, Bruce J., Marine Biological Laboratory, 7 MBL Street, Woods Hole, MA 02543

Pethig, Ronald, University College of North Wales, School of Electronic Engineering, Bangor, Gwynedd, LL 57 1UT, United Kingdom

Pfohl, Ronald J., Miami University, Department of Zoology, Oxford, OH 45056

Pierce, Sidney K. Jr., University of South Florida, 4202 East Fowler Avenue, Tampa, FL 33620

Pleasure, David E., Children's Hospital, Neurology Research, 5th Floor, Ambramson Building, Philadelphia, PA 19104

Poindexter, Jeanne S., Barnard College, Columbia University, 3009 Broadway, New York, NY 10027-6598

Pollard, Harvey B., U.S.U.H.S., 4301 Jones Bridge Road, Bethesda, MD 20814

Pollard, Thomas D., Salk Institute for Biological Studies, 10010 N. Torrey Pines Road, La Jolla, CA 92037

Porter, Beverly H., 5542 Windysun Court, Columbia, MD 21045

Porter, Mary E., University of Minnesota, Department of Cell Biology and Neuroanatomy, 4-135 Jackson Hall, 321 Church Street SE, Minneapolis, MN 55455

Potter, David D., Harvard Medical School, Department of Neurobiology, 25 Shattuck Street, Boston, MA 02115

Potts, William T., University of Lancaster, Department of Biology, Lancaster, England

Powers, Maureen K., University of California, Department of Molecular & Cellular Biology, Life Sciences Addition, Berkeley, CA 94720

Prendergast, Robert A., 38 Pondlet Place, Falmouth, MA 02540

Prior, David J., Northern Arizona University, Arts and Sciences Dean's Office, Box 5621, Flagstaff, AZ 86011

Prusch, Robert D., Gonzaga University, Department of Life Sciences, Spokane, WA 99258

Purves, Dale, Duke University Medical Center, Department of Neurobiology, Box 3209, 101-I Bryan Research Building, Durham, NC 27710

Quigley, James P., The Scripps Research Institute, Department of Vascular Biology, 10550 N. Torrey Pines Road VB-1, La Jolla, CA 92037

Rabb, Irving W., 1010 Memorial Drive, Cambridge, MA 02138

Rabin, Harvey, 1102 Ralston Road, Rockville, MD 20852

Rabinowitz, Michael B., Marine Biological Laboratory, 7 MBL Street, Woods Hole, MA 02543

Rafferty, Nancy S., Marine Biological Laboratory, 7 MBL Street, Woods Hole, MA 02543

Rakowski, Robert F., Finch University of Health Sciences, The Chicago Medical School, Department of Physiology and Biophysics, 3333 Greenbay Road, N. Chicago, IL 60064

Ramon, Fidel, Universidad Nacional Autonoma de Mexico, Division EStreet Posgrado E Invest., Facultad de Medicina, 04510, D.F., Mexico

Rastetter, Edward B., Marine Biological Laboratory, The Ecosystems Center, Woods Hole, MA 02543

Rebhun, Lionel I., University of Virginia, Department of Biology, Gilmer Hall 45, Charlottesville, VA 22901

Reddan, John R., Oakland University, Department of Biological Sciences, Rochester, MI 48309-4401

Reese, Thomas S., National Institutes of Health, NINDS, Building 36, Room 2A29, Bethesda, MD 20892

Reinisch, Carol L., Marine Biological Laboratory, 7 MBL Street, Woods Hole, MA 02543

Rickles, Frederick R., 2633 Danforth Lane, Decatur, GA 30033

Rieder, Conly L., Wadsworth Center, Division of Molecular Medicine, P.O. Box 509, Albany, NY 12201-0509

Riley, Monica, Marine Biological Laboratory, 7 MBL Street, Woods Hole, MA 02543

Ripps, Harris, University of Illinois at Chicago, Department of Ophthalmology/Visual Sciences, 1855 West Taylor Street, Chicago, IL 60612

Ritchie, J. Murdoch, Yale University School of Medicine, Department of Pharmacology, 333 Cedar Street, New Haven, CT 06510

Rome, Lawrence C., University of Pennsylvania, Department of Biology, Philadelphia, PA 19104

Rosenbluth, Jack, New York University School of Medical, Department of Physiology and Biophysics, RR 714, 400 East 34th Street, New York, NY 10016

Rosenbluth, Raja, Simon Fraser University, Institute of Molecular Biology and Biochemistry, Burnaby, BC V5A 1S6, Canada

Rosenfield, Allan, Columbia University School of Public Health, 600 West 168th Street, New York, NY 10032-3702

Rosenkranz, Herbert S., 130 Desoto Street, Pittsburgh, PA 15213-2535

Ross, William N., New York Medical College, Department of Physiology, Valhalla, NY 10595

Roth, Jay S., 26 Huettner Road, P. O. Box 692, Woods Hole, MA 02543-0692

Rottenfusser, Rudi, Marine Biological Laboratory, 7 MBL Street, Woods Hole, MA 02543

Rowland, Lewis P., Neurological Institute, 710 West 168th Street, New York, NY 10032

Ruderman, Joan V., Harvard Medical School, Department of Cell Biology, 240 Longwood Avenue, Boston, MA 02115

Rummel, John D., NASA Headquarters, Office of Space Science, Washington, D.C. 20546

Rushforth, Norman B., Case Western Reserve University, Department of Biology, Cleveland, OH 44106

Russell-Hunter, William D., 711 Howard Street, Easton, MD 21601-3934

Saffo, Mary Beth, Arizona State University West, Life Science Department, MC 2352, P.O. Box 37100, Phoenix, AZ 85069-7100

Salama, Guy, University of Pittsburgh, Department of Physiology, Pittsburgh, PA 15261

Salmon, Edward D., University of North Carolina, Department of Biology, CB 3280, Chapel Hill, NC 27514

Salyers, Abigail, University of Illinois, Department of Microbiology, 407 South Goodwin Avenue, Urbana, IL 61801

Salzberg, Brian M., University of Pennsylvania School of Medicine, Department of Neuroscience, 215 Stemmler Hall, Philadelphia, PA 19104-6074

Sanger, Jean M., University of Pennsylvania School of Medicine, Department of Anatomy, 36th and Hamilton Walk, Philadelphia, PA 19104

Sanger, Joseph W., University of Pennsylvania Medical Center, Department of Cell and Developmental Biology, 36th and Hamilton Walk, Philadelphia, PA 19104-6058

Saunders, John W. Jr., P.O. Box 3381, Waquoit, MA 02536

Schachman, Howard K., University of California, Molecular and Cell Biology Department, 229 Stanley Hall, #3206, Berkeley, CA 94720-3206

Schatten, Gerald P., Oregon Health Sciences University, Oregon Regional Primate Research Center, 505 N.W. 185th Avenue, Beaverton, OR 97006

Schatten, Heide, University of Wisconsin, Department of Zoology, Madison, WI 53706

Schmeer, Arlene C., Mercenene Cancer Research Institute, 790 Prospect Street, New Haven, CT 06511

Schuel, Herbert, SUNY at Buffalo, Department of Anatomy/Cell Biology, Buffalo, NY 14214

Schwartz, James H., New York State Psychiatric Institute, Research Annex, 722 West 168th Street, 7th floor, New York, NY 10032

Schwartz, Lawrence, University of Massachusetts, Department of Biology, Morrill Science Center, Amherst, MA 01003

Schweitzer, A. Nicola, Brigham and Women's Hospital, Immunology Division, Department of Pathology, 221 Longwood Avenue, LMRC 521, Boston, MA 02115

Segal, Sheldon J., The Population Council, One Dag Hammarskjold Plaza, New York, NY 10036

Senft, Stephen Lamont, Yale University, Neuroengineering/Neuroscience Center, P.O. Box 208205, New Haven, CT 06520-8205

Shanklin, Douglas R., University of Tennessee, Department of Pathology, Room 576, 800 Madison Avenue, Memphis, TN 38117

Shashar, Nadav, The Interuniversity Institute of Eilat, P.O. Box 469, Eilat 88103, Israel

Shashoua, Victor E., Harvard Medical School, Ralph Lowell Labs, McLean Hospital, 115 Mill Street, Belmont, MA 02178

Shaver, Gaius R., Marine Biological Laboratory, The Ecosystems Center, Woods Hole, MA 02543

Shaver, John R., Michigan State University, Department of Zoology, East Lansing, MI 48824

Sheetz, Michael P., Duke University Medical Center, Department of Cell Biology, Bx 3709, 388 Nanaline Duke Building, Durham, NC 27710

Shepro, David, Boston University, CAS Biology, 5 Cummington Street, Boston, MA 02215

Shimomura, Osamu, Marine Biological Laboratory, 7 MBL Street, Woods Hole, MA 02543

Shipley, Alan M., P.O. Box 943, Forestdale, MA 02644

Silver, Robert B., Marine Biological Laboratory, 7 MBL Street, Woods Hole, MA 02543

Siwicki, Kathleen K., Swarthmore College, Biology Department, 500 College Avenue, Swarthmore, PA 19081-1397

Skinner, Dorothy M., 24 Gray Lane, Falmouth, MA 02540

Sloboda, Roger D., Dartmouth College, Department of Biological Science, 6044 Gilman, Hanover, NH 03755-1893

Sluder, Greenfield, University of Massachusetts Medical School, Room 324, 377 Plantation Street, Worcester, MA 01605

Smith, Peter J.S., Marine Biological Laboratory, 7 MBL Street, Woods Hole, MA 02543

Smith, Stephen J., Stanford University School of Medicine, Department of Molecular and Cellular Physiology, Beckman Center, Stanford, CA 94305

Smolowitz, Roxanna S., Marine Biological Laboratory, 7 MBL Street, Woods Hole, MA 02543

Sogin, Mitchell L., Marine Biological Laboratory, 7 MBL Street, Woods Hole, MA 02543

Surenson, Martha M., Cidade Universitaria-UFRJ, Department Bioquimica Medica-ICB, 21941-590 Rio de Janerio, Brazil

Speck, William T., Massachusetts General Hospital, 55 Fruit Street, Boston, MA 02114

Spector, Abraham, Columbia University, Department of Ophthalmology, 630 West 168th Street, New York, NY 10032

Speksnijder, Johanna E., University of Groningen, Department of Genetics, Kerklaan 30, 9751 NN Haren, The Netherlands

Spray, David C., Albert Einstein College of Medicine, Department of Neuroscience, 1300 Morris Park Avenue, Bronx, NY 10461

Spring, Kenneth R., National Institutes of Health, 10 Center Drive, MSC 1598, Building 10, Room 6N260, Bethesda, MD 20892-1603

Steele, John H., Woods Hole Oceanographic Institution, Woods Hole, MA 02543

Steinacker, Antoinette, University of Puerto Rico, Instituet of Neurobiology, 201 Boulevard Del Valle, San Juan, PR 00901

Steinberg, Malcolm, Princeton University, Department of Molecular Biology, M-18 Moffett Laboratory, Princeton, NJ 08544-1014

Stemmer, Andreas C., Institut für Robotik, ETH-Sentrum, 8092 Zurich, Switzerland

Stenflo, Johan, University of Lund, Department of Clinical Chemistry, Malmo General Hospital, S-205 02 Malmo, Sweden

Stetten, Jane Lazarow, 4701 Willard Avenue, #1413, Chevy Chase, MD 20815-4627

Steudler, Paul A., Marine Biological Laboratory, The Ecosystems Center, Woods Hole, MA 02543

Stokes, Darrell R., Emory University, Department of Biology, 1510 Clifton Road NE, Atlanta, GA 30322-1100

Stommel, Elijah W., Darmouth Hitchcock Medical Center, Neurology Department, Lebanon, NH 03756

Stracher, Alfred, SUNY Health Science Center, Department of Biochemistry, 450 Clarkson Avenue, Brooklyn, NY 11203

Strumwasser, Felix, P.O. Box 2278, East Falmouth, MA 02536-2278

Stuart, Ann E., 1818 North Lakeshore Drive, Chapel Hill, NC 27514

Sugimori, Mutsuyuki, New York University Medical Center, Department of Physiology and Neuroscience, Room 442, 550 First Avenue, New York, NY 10016

Summers, William C., Western Washington University, Huxley College of Environmental Studies, Bellingham, WA 982259181

Suprenant, Kathy A., University of Kansas, Department of Physiology and Cell Biology, 4010 Haworth Hall, Lawrence, KS 66045

Swenson, Katherine I., Duke University Medical Center, Department of Molecular Cancer Biology, Box 3686, Durham, NC 27710

Sydlik, Mary Anne, Hope College, Peale Science Center, 35 East 12th St./PO Box 9000, Holland, MI 49422

Szent-Gyorgyi, Andrew G., Brandeis University, Molecular and Cell Biology, 415 South Street, Waltham, MA 02454-9110

Tamm, Sidney L., Boston University, CAS Biology, 5 Cummington Street, Boston, MA 02215

Tanzer, Marvin L., University of Connecticut School of Dental Medicine, Department of Biostructure and Function, Farmington, CT 06030-3705

Tasaki, Ichiji, National Institutes of Health, NIMH, Laboratory of Neurobiology, Building 36, Room 2B-16, Bethesda, MD 20892

Taylor, D. Lansing, Carnegie Mellon University, Center for Flurorescence Research, 4400 Fifth Avenue, Pittsburgh, PA 15213

Taylor, Edwin W., University of Chicago, Department of Molecular Genetics, 920 E. 58th Street, Chicago, IL 60637

Teal, John M., Woods Hole Oceanographic Institution, Department of Biology, Woods Hole, MA 02543

Telfer, William H., University of Pennsylvania, Department of Biology, Philadelphia, PA 19104

Telzer, Bruce, Pomona College, Department of Biology, Thille Building, 175 West 6th Street, Claremont, CA 91711

Terasaki, Mark, University of Connecticut Health Center, Department of Physiology, 263 Farmington Avenue, Farmington, CT 06032

Townsel, James G., Meharry Medical College, Department of Physiology, 1005 DB Todd Boulevard, Nashville, TN 37208

Travis, David M., 19 High Street, Woods Hole, MA 02543-1221

Treistman, Steven N., University of Massachusetts Medical Center, Department of Pharmacology, 55 Lake Avenue North, Worcester, MA 01655

Trigg, D. Thomas, One Federal Street, 9th Floor, Boston, MA 02211

Troll, Walter, NYU Medical Center, Department of Environmental Medicine, 550 First Avenue, New York, NY 10016

Troxler, Robert F., Boston University School of Medicine, Department of Biochemistry, 80 East Concord Street, Boston, MA 02118

Tucker, Edward B., Baruch College, CUNY, Department of Natural Sciences, 17 Lexington Avenue, New York, NY 10010

Turner, Ruth D., Harvard University, Museum of Comparative Zoology, Mollusk Department, Cambridge, MA 02138

Tweedell, Kenyon S., University of Notre Dame, Department of Biological Sciences, Notre Dame, IN 46556-0369

Tykocinski, Mark L., Case Western Reserve University, Institute of Pathology, 2085 Adelbert Road, Cleveland, OH 44106

Tytell, Michael, Wake Forest University, Bowman Gray School of Medicine, Department of Anatomy and Neurobiology, Winston-Salem, NC 27157

Ueno, Hiroshi, Kyoto University, AGR Chemistry, Faculty of Agriculture, Sakyo, Kyoto 606-8502, Japan

Valiela, Ivan, Boston University Marine Program, Marine Biological Laboratory, Woods Hole, MA 02543

Vallee, Richard, University of Massachusetts Medical Center, Worcester Foundation Campus, 222 Maple Avenue, Shrewsbury, MA 01545

Valois, John J., 420 Woods Hole Road, Woods Hole, MA 02543

Van Dover, Cindy Lee, The College of William and Mary, Biology Department, 328 Millington Hall, Williamsburg, VA 23187

Van Holde, Kensal E., Oregon State University, Biochemistry and Biophysics Department, Corvallis, OR 97331-7503

Vogl, Thomas P., Environmental Research Institute of Michigan, 1101 Wilson Boulevard, Arlington, VA 22209

Wainwright, Norman R., Marine Biological Laboratory, 7 MBL Street, Woods Hole, MA 02543

Waksman, Byron H., New York University Medical Center, Department of Pathology, 550 First Avenue, New York, NY 10016

Wall, Betty, 9 George Street, Woods Hole, MA 02543

Wang, Hsien-Yu, State University of New York, University Medical Center, Physiology and Biophysics-HSC, Stony Brook, NY 11794-8633

Wangh, Lawrence J., Brandeis University, Department of Biology, 415 South Street, Waltham, MA 02254

Warner, Robert C., 1609 Temple Hills Drive, Laguna Beach, CA 92651

Warren, Leonard, Wistar Institute, 36th and Spruce Streets, Philadelphia, PA 19104
Waterbury, John B., Woods Hole Oceanographic Institution, Department of Biology, Woods Hole, MA 02543
Waxman, Stephen G., Yale Medical School, Neurology Department, 333 Cedar Street, P.O. Box 208018, New Haven, CT 06510
Webb, H. Marguerite, 184 Chestnut Street, Foxboro, MA 02035-1548 (deceased 1999)
Weber, Annemarie, University of Pennsylvania School of Medicine, Department of Biochemistry and Biophysics, Philadelphia, PA 19066
Weeks, Janis C., University of Oregon, Institute of Neuroscience, Eugene, OR 97403-1254
Weidner, Earl, Louisiana State University, Department of Biological Sciences, 508 Life Sciences Building, Baton Rouge, LA 70803-1715
Weiss, Alice Sara, 105 University Boulevard West, Silver Spring, MD 20901
Weiss, Dieter G., University of Rostock, Institute of Zoology, D-18051 Rostock, Germany
Weiss, Leon P., University of Pennsylvania School of Veterinary Medicine, Department of Animal Biology, Philadelphia, PA 19104
Weiss, Marisa C., Paoli Memorial Hospital, Department of Radiation Oncology, 255 W. Lancaster Avenue, Paoli, PA 19301
Weissmann, Gerald, New York University Medical Center, Department of Medicine/Division Rheumatology, 550 First Avenue, New York, NY 10016
Westerfield, Monte, University of Oregon, Institute of Neuroscience, Eugene, OR 97403
Whittaker, J. Richard, University of New Brunswick, Department of Biology, BS 4511, Frederiction, NB E3B 6E1, Canada
Wiesel, Torsten N., Rockefeller University, 1230 York Avenue, New York, NY 10021
Wilkens, Lon A., University of Missouri, Department of Biology, 8001 Natural Bridge Road, St. Louis, MO 63121-4499
Wilson, Darcy B., Torrey Pines Institute, 3550 General Atomics Court, Building 2, Room 138, San Diego, CA 92121
Wilson, T. Hastings, Harvard Medical School, Department of Physiology, 25 Shattuck Street, Boston, MA 02115
Witkovsky, Paul, NYU Medical Center, Department of Ophthalmology, 550 First Avenue, New York, NY 10016
Wittenberg, Beatrice, Albert Einstein College of Medicine, Department of Physiology and Biophysics, Bronx, NY 10461
Wittenberg, Jonathan B., Albert Einstein College of Medicine, Department of Physiology and Biophysics, Bronx, NY 10461
Wolken, Jerome J., Carnegie Mellon University, Department of Biological Sciences, 440 Fifth Avenue, Pittsburgh, PA 15213 (deceased 1999)
Wonderlin, William F., West Virginia University, Pharmacology and Toxicology Department, Morgantown, WV 26506
Worden, Mary Kate, University of Virginia, Department of Neuroscience, McKim Hall Box 230, Charlottesville, VA 22908
Worgul, Basil V., Columbia University, Department of Ophthalmology, 630 West 168 Street, New York, NY 10032
Wu, Chau Hsiung, Northwestern University Medical School, Department of Pharmacology (S215), 303 East Chicago Avenue, Chicago, IL 60611-3008
Wyttenbach, Charles R., University of Kansas, Biological Sciences Department, 2045 Haworth Hall, Lawrence, KS 66045-2106

Yeh, Jay Z., Northwestern University Medical School, Department of Pharmacology, Chicago, IL 60611

Zacks, Sumner I., 65 Saconesset Road, Falmouth, MA 02540-1851 (deceased 2000)
Zakon, Harold H., University of Texas, Section of Neurobiology, School of Life Science, Austin, TX 78712
Zigman, Seymour, Marine Park Condominiums, 174 Queen Street, Unit 10-F, Falmouth, MA 02540
Zigmond, Michael J., University of Pittsburgh, S-526 Biomedical Science Tower, 3500 Terrace Street, Pittsburgh, PA 15213
Zimmerberg, Joshua J., National Institutes of Health, LCMB, NICHD, Building 10, Room 10D14, 10 Center Drive, Bethesda, MD 20892
Zottoli, Steven J., Williams College, Department of Biology, Williamstown, MA 01267
Zucker, Robert S., University of California, Neurobiology Division, Molecular and Cellular Biology Department, Berkeley, CA 94720

MBL Associates

Executive Board

Ruth Ann Laster, President
Jack Pearce, Vice President
Kitty Brown, Treasurer
Molly Cornell, Secretary
Elizabeth Farnham, Membership Chair

Tammy Smith Amon
Duncan Aspinwall
Barbara Atwood
Kitty Brown
Julie Child
Seymour Cohen
Michael Fenlon
Sallie Giffen
Alice Knowles
Rebecca Lash
Cornelia Hanna McMurtrie
Joan Pearlman
Virginia R. Reynolds
Volker Ulbrich
John Valois

Associates Liaison/Gift Shop Coordinator

Kendall B. Bohr

Supporting Associate

Mrs. George H. A. Clowes
Dr. and Mrs. James D. Ebert
Mr. and Mrs. David Fausch
Mrs. Janet F. Gillette
Drs. Luigi and Elaine Mastroianni
Ms. Linda Sallop and Mr. Michael Fenlon
Mrs. Anne W. Sawyer
Dr. John Tochko and Mrs. Christina Myles-Tochko
Mr. and Mrs. John J. Valois
Mr. and Mrs. Leslie J. Wilson

Sustaining Associate

Dr. and Mrs. James J. Ferguson, Jr.
Mr. and Mrs. Lon Hocker

Mr. Robert A. Jaye
Dr. and Mrs. Edward F. MacNichol, Jr.

Family Membership

Dr. Frederick W. Ackroyd
Dr. and Mrs. Edward A. Adelberg
Dr. and Mrs. Dean C. Allard, Jr.
Mr. and Mrs. Douglas F. Allison
Drs. Peggy and Fred Alsup
Drs. James and Helene Anderson
Dr. and Mrs. Samuel C. Armstrong
Mr. and Mrs. Duncan P. Aspinwall
Mr. and Mrs. Donald R. Aukamp
Mr. and Mrs. John M. Baitsell
Mr. and Mrs. David Bakalar
Mr. and Mrs. William L. Banks
Dr. and Mrs. Robert B. Barlow, Jr.
Mr. and Mrs. John E. Barnes
Dr. and Mrs. Robert M. Berne
Drs. Harriet and Alan Bernheimer
Mr. and Mrs. Robert O. Bigelow
Dr. and Mrs. Edward G. Boettiger
Mr. and Mrs. Kendall B. Bohr
Dr. and Mrs. Thomas A. Borgese
Mr. and Mrs. Richard M. Bowen
Dr. and Mrs. Francis P. Bowles
Dr. and Mrs. John B. Buck
Dr. and Mrs. John E. Burris
Mr. and Mrs. William O. Burwell
Mr. and Mrs. G. Nathan Calkins, Jr.
Mr. and Mrs. D. Bret Carlson
Prof. and Mrs. James F. Case
Dr. and Mrs. Richard L. Chappell
Dr. and Mrs. Frank M. Child
Mr. and Mrs. Thomas Claflin
Dr. and Mrs. Arnold M. Clark
Mrs. LeRoy Clark
Mr. and Mrs. James Cleary
Dr. and Mrs. Laurence P. Cloud
Mr. and Mrs. Harrington T. Collins
Dr. and Mrs. Neal W. Cornell (Dr. Cornell deceased, 2000)
Mr. and Mrs. Norman C. Cross
Dr. and Mrs. John M. Cummings
Mr. and Mrs. Bruce G. Daniels
Mr. and Mrs. Joel P. Davis
Mr. and Mrs. Richard C. Dierker
Mr. and Mrs. F. Gerald Douglass
Dr. and Mrs. Arthur Brooks DuBois
Dr. and Mrs. Michael J. Fishbein
Mr. and Mrs. Harold Frank
Mr. and Mrs. Howard G. Freeman
Dr. and Mrs. Robert A. Frosch
Dr. and Mrs. John J. Funkhouser
Dr. and Mrs. Mordecai L. Gabriel
Dr. and Mrs. Sydney Gellis
Dr. and Mrs. James L. German, III
Dr. and Mrs. Harold S. Ginsberg
Dr. and Mrs. Murray Glusman
Drs. Alfred and Joan Goldberg
Mrs. Mary L. Goldman
Mr. and Mrs. Charles Goodwin, III
Dr. and Mrs. Philip Grant
Mr. and Mrs. Anthony D. Green
Dr. and Mrs. Thomas C. Gregg
Dr. Newton H. Gresser
Dr. and Mrs. Antoine F. O. Hadamard
Mr. and Mrs. Peter A. Hall
Dr. and Mrs. Harlyn O. Halvorson
Drs. Alexander and Carol Hannenberg
Dr. and Mrs. Richard Bennet Harvey
Dr. and Mrs. J. Woodland Hastings
Mr. and Mrs. Gary G. Hayward
Dr. and Mrs. Howard H. Hiatt
Mr. and Mrs. David Hibbitt
Dr. and Mrs. John E. Hobbie
Drs. Francis C. G. Hoskin and Elizabeth M. Farnham
Dr. and Mrs. Robert J. Huettner
Dr. and Mrs. Shinya Inoue
Dr. and Mrs. Kurt J. Isselbacher
Dr. and Mrs. Gary Jacobson
Mrs. Mary D. Janney
Mr. and Mrs. DeWitt C. Jones, III
Dr. and Mrs. Benjamin Kaminer
Mr. and Mrs. Paul W. Knaplund
Mr. and Mrs. A. Sidney Knowles, Jr.
Sir and Lady Hans Kornberg
Dr. and Mrs. S. Andrew Kulin
Mr. and Mrs. Trevor Lambert
Dr. and Mrs. George M. Langford
Dr. and Mrs. Leonard Laster
Dr. and Mrs. Hans Laufer
Mr. William Lawrence and Mrs. Barbara Buchanan
Dr. and Mrs. Berton J. Leach
Mr. and Mrs. Stephen R. Levy
Mr. and Mrs. Robert Livingstone, Jr.
Dr. and Mrs. Laszlo Lorand
Mr. and Dr. Bernard Manuel
Mr. and Mrs. Joseph C. Martyna
Mr. and Mrs. Frank J. Mather, III
Mr. and Mrs. John E. Matthews
Dr. and Mrs. Robert T. McCluskey
Mr. Paul McGonigle
Dr. and Mrs. Jerry M. Melillo
Mr. and Mrs. Wesley J. Merritt
Mr. and Mrs. Richard Meyers
Mr. and Mrs. Charles A. Mitchell
Dr. and Mrs. Merle Mizell
Dr. and Mrs. Charles H. Montgomery
Mr. and Mrs. Stephen A. Moore
Mr. and Mrs. Charles F. Murphy
Dr. and Mrs. John E. Naugle
Dr. Pamela Nelson and Mr. Christopher Olmsted
Mr. and Mrs. Frank L. Nickerson
Dr. and Mrs. Clifford T. O'Connell
Mr. and Mrs. James J. O'Connor
Mr. and Mrs. David R. Palmer
Mr. and Mrs. Robert Parkinson
Mr. and Mrs. Richard M. Paulson, Jr.
Dr. and Mrs. John B. Pearce
Mr. and Mrs. William J. Pechilis
Mr. and Mrs. John B. Peri
Dr. and Mrs. Courtland D. Perkins
Dr. and Mrs. Philip Person
Mr. and Mrs. Frederick S. Peters
Mr. and Mrs. George H. Plough
Dr. and Mrs. Aubrey Pothier, Jr.
Dr. and Mrs. Carl A. Price
Mr. and Mrs. Allan Putnam
Dr. and Mrs. Lionel I. Rebhun
Dr. and Mrs. George T. Reynolds
Dr. and Mrs. Harris Ripps
Ms. Jean Roberts
Drs. Priscilla and John Roslansky
Mr. and Mrs. John D. Ross
Dr. and Mrs. John W. Saunders, Jr.
Dr. and Mrs. R. Walter Schlesinger
Mr. and Mrs. Harold H. Sears
Mr. John Seder and Ms. Frances Plough
Dr. and Mrs. Sheldon J. Segal
Dr. and Mrs. David Shepro
Mr. and Mrs. Bertram R. Silver
Mr. and Mrs. Jonathan O. Simonds
Drs. Frederick and Marguerite Smith
Dr. and Mrs. William K. Stephenson
Mr. and Mrs. E. Kent Swift, Jr.
Mr. and Mrs. Gerard L. Swope, III
Mr. Norman N. Tolkan
Dr. and Mrs. Walter Troll
Mr. and Mrs. Volker Ulbrich
Ms. Susan Veeder
Drs. Claude and Dorothy Villee
Dr. and Mrs. Gerald Weissmann
Dr. and Mrs. Paul S. Wheeler
Dr. Martin Keister White
Mr. and Mrs. Geoffrey G. Whitney, Jr.
Mr. and Mrs. Lynn H. Wilke
Dr. and Mrs. T. Hastings Wilson
Mr. and Mrs. Dick Yeo
Dr. and Mrs. Sumner I. Zacks (Dr. Zacks deceased, 2000)
Dr. Linda and Mr. Erik Zettler

Individual Membership

Mrs. Jean E. Ahearn
Mr. Henry Albers
Dr. Nina S. Allen
Mrs. Tammy Amon
Mr. Dean N. Arden
Mrs. Ellen Prosser Armstrong
Mrs. Kimball C. Atwood, III
Dr. Serena Baccetti
Mr. Everett E. Bagley
Dr. Millicent Bell
Mr. C. John Berg
Dr. Thomas P. Bleck
Ms. Avis Blomberg
Mr. Theodore A. Bonn
Mr. James V. Bracchitta
Mrs. Jennie P. Brown
Mrs. M. Kathryn S. Brown
Dr. Robert H. Broyles
Ms. Henriete Bull
Dr. Alan H. Burghauser
Mrs. Barbara Gates Burwell
Mr. Bruce E. Buxton
Mr. Patrick J. Calie

Mrs. Anne M. Campbell
Dr. Graciela C. Candelas
Mr. Frank C. Carotenuto
Dr. Robert H. Carrier
Mrs. Patricia A. Case
Ms. Mia D. Champion
Dr. Sallie Chisholm
Mrs. Octavia C. Clement
Mr. Allen W. Clowes
Mrs. Margaret H. Coburn
Dr. Seymour S. Cohen
Ms. Anne S. Concannon
Prof. D. Eugene Copeland
Dr. Vincent Cowling
Mrs. Marilyn E. Crandall
Ms. Dorothy Crossley
Ms. Helen M. Crossley
Mrs. Villa B. Crowell
Mr. Norman Dana
Dr. Morton Davidson
Mrs. Elizabeth M. Davis
Ms. Carol Reimann DeYoung
Mrs. Shirley Dierolf
Mr. David L. Donovan
Ms. Suzanne Droban
Mr. Roy A. Duffus
Mrs. Charles Eastman
Dr. Frank Egloff
Mr. Raymond Eliott
Ms. Judy Ernst
Mrs. Ruth Alice Fitz
Mr. Robert Fitzpatrick
Ms. Sylvia M. Flanagan
Mr. John W. Folino, Jr.
Dr. Krystyna Frenkel
Mr. Paul J. Freyheit
Mrs. Ruth E. Fye
Mr. Joseph C. Gallagher
Miss Eleanor Garfield
Mrs. Ruth H. Garland
Mr. John Garnett
Ms. Sallie A. Giffen
Mr. Charles Gifford
Mrs. James R. Glazebrook
Mr. Michael P. Goldring
Mrs. Phyllis Goldstein
Mrs. DeWitt S. Goodman
Ms. Muriel Gould
Mrs. Rose Grant
Mrs. Jeanne B. Griffith
Mrs. Valerie A. Hall
Dr. Peter J. Hamre
Ms. Mary Elizabeth Hamstrom
Ms. Elizabeth E. Hathaway
Dr. Robert R. Haubrich
Mrs. Jane M. Heald
Mrs. Nathan Hirschfeld
Mr. Roger W. Hubbell
Miss Elizabeth B. Jackson
Mr. Raymond L. Jewett
Mrs. Barbara W. Jones
Mrs. Megan H. Jones
Mrs. Joan T. Kanwisher
Mrs. Sally Karush
Mrs. Marcella Katz
Ms. Patricia E. Keoughan
Dr. Peter N. Kivy
Dr. Bruno P. Kremer
Mr. Bernard H. Labitt
Mrs. Janet W. Larcom
Dr. Marian E. LeFevre
Dr. Mortimer Levitz
Mr. Edwin M. Libbin
Mr. Lennart Lindberg
Mrs. Barbara C. Little
Mrs. Sarah J. Loessel
Mrs. Ermine W. Lovell
Mr. Richard C. Lovering
Mrs. Victoria H. Lowell
Mrs. Margaret M. MacLeish
Ms. Anne Camille Maher
Mrs. Annemarie E. Mahler
Mr. Patrick J. Mahoney
Dr. Saul Malkiel
Ms. Diane Maranchie
Mr. Daniel R. Martin
Dr. Miriam Jacob Mauzerall
Mrs. Mary Hartwell Mavor
Mrs. Nella W. McElroy (deceased 1999)
Dr. Susan Gerbi McIlwain
Ms. Mary W. McKoan
Ms. Jane A. McLaughlin
Ms. Louise McManus
Ms. Cornelia Hanna McMurtrie
Mrs. Ellen L. Meigs
Mr. Ted Melillo
Martin Mendelson, M.D., Ph.D.
Ms. Carmen Merryman
Mrs. Grace S. Metz
Mrs. Mary G. Miles
Mrs. Florence E. Mixer
Mr. John T. Moakley
Mr. Lawrence A. Monte
Mrs. Mary E. Montgomery
Ms. Cynthia Moor
Mr. Alan F. Morrison
Dr. M. Patricia Morse
Mrs. Eleanor M. Nace
Mr. William G. Neall
Mrs. Anne Nelson
Mr. Edmund F. Nolan
Ms. Catherine N. Norton
Mr. John J. O'Connor (deceased 1999)
Dr. Renee Bennett O'Sullivan
Miss Carolyn L. Parmenter
Mrs. Dolores Patch-Wing
Ms. Joan Pearlman
Mr. Raymond W. Peterson
Ms. Victoria A. Powell
Ms. Elizabeth T. Price
Ms. Dianne Purves
Mrs. Julia S. Rankin
Mr. Fred J. Ravens, Jr.
Ms. Anecia Kathy Regis
Ms. Mary W. Rianhard
Dr. Renato A. Ricca (deceased 1999)
Dr. Mary Elizabeth Rice
Dr. Monica Riley
Master Alexander Meigs Rives
Mrs. Lola E. Robertson
Mrs. Ruth J. Robinson
Mrs. Arlene Rogers
Mrs. Wendy E. Rose
Ms. Hilde Rosenthal
Mrs. Atholie K. Rosett
Dr. Virginia F. Ross
Dr. John D. Rummel
Mr. Raymond A. Sanborn
Ms. Elaine Schott
Mrs. Elsie M. Scott
Sea Education Association, Inc.
Dr. Cecily C. Selby
Mrs. Deborah G. Senft
Mrs. Charlotte Shemin
Ms. Enid K. Sichel
Dr. Jeffrey D. Silberman
Mrs. Phyllis J. Silver
Mrs. Cynthia C. Smith
Mrs. Louise M. Specht
Dr. Guy L. Steele, Sr.
Dr. Robert E. Steele
Mrs. Eleanor Steinbach
Mrs. Jane Lazarow Stetten
Dr. Maurice Sussman
Mr. Albert H. Swain
Mr. James K. Taylor
Mr. Emil D. Tietje, Jr.
Mrs. Alice Todd
Mr. Arthur D. Traub
Mr. D. Thomas Trigg
Ms. Natalie Trousof
Mrs. Frances W. Tytell
Ms. Ciona Ulbrich
Dr. Kensal E. van Holde
Ms. Sylvia Vatuk
Mr. Lee D. Vincent
Mr. Arthur D. Voorhis
Mrs. Eve Warren
Mr. John T. Weeks
Ms. Lillian Wendorff
Dr. William M. Wheeler
Ms. Mabel Y. Whelpley
Mrs. Barbara Whitehead
Mrs. Ava Whittemore
Mrs. Joan R. Wickersham
Mrs. Clare M. Wilber
Ms. Nancy Woitkoski
Ms. Marion K. Wright
Mrs. Dorothy M. York
Mrs. Bunnie Rose Zigman
Mrs. Donald J. Zinn

MBL Gift Shop Volunteers

Marion Adelberg
Barabara Atwood
Caroline Banks
Harriet Bernheimer
Avis Blomberg
Gloria Borgese
Kitty Brown
Jewel Cobb

Janet Daniels
Carol DeYoung
Fran Eastman
Alma Ebert
Jane Foster
Becky Glazebrook
Muriel Gould
Barbara Grossman
Jean Halvorson
Hanna Hastings
Sally Karush
Marcella Katz
Alice Knowles
Evelyn Laufer
Barbara Little
Winnie Mackey
Diane Maranchie
Miriam Mauzerall
Mary Mavor
Jane McCormack
Louise McManus
Florence Mixer
Lorraine Mizell
Helen Murphy
Jack Pearce
Bertha Person
Margareta Pothier
Liz Price
Julie Rankin
Arlene Rogers
Lil Saunders
Louise Specht
Cynthia Smith
Peggy Smith
Jane Stetten
Barbara Thomson
Alice Todd
Elaine Troll
Natalie Trousof
Barbara Van Holde
Doris Van Keuren
Susan Veeder
Carol Ann Wagner
Mabel Whelpley
Clare Wilber
Betty Wilson
Grace Witzell
Bunnie Rose Zigman

MBL Summer Tour Guides

Gloria Borgese
Frank Child
Julie Child
Sears Crowell
Henry Dooley
Nancy Fraser
Sallie Giffen
Lincoln Kraeuter
Barbara Little
Steve Oliver
Julie Rankin
Lola Robertson
Arlene Rogers
Pucky Roslansky
Suzanne Thomas
Mary Ulbrich
John Valois
Margery Zinn

Certificate of Organization
Articles of Amendment
Bylaws

Certificate of Organization

(On File in the Office of the Secretary of the Commonwealth)

No. 3170

We, Alpheus Hyatt, President, William Stanford Stevens, Treasurer, and William T. Sedgwick, Edward G. Gardiner, Susan Mims and Charles Sedgwick Minot being a majority of the Trustees of the Marine Biological Laboratory in compliance with the requirements of the fourth section of chapter one hundred and fifteen of the Public Statutes do hereby certify that the following is a true copy of the agreement of association to constitute said Corporation, with the names of the subscribers thereto:

We, whose names are hereto subscribed, do, by this agreement, associate ourselves with the intention to constitute a Corporation according to the provisions of the one hundred and fifteenth chapter of the Public Statutes of the Commonwealth of Massachusetts, and the Acts in amendment thereof and in addition thereto.

The name by which the Corporation shall be known is
THE MARINE BIOLOGICAL LABORATORY.

The purpose for which the Corporation is constituted is to establish and maintain a laboratory or station for scientific study and investigations, and a school for instruction in biology and natural history.
The place within which the Corporation is established or located is the city of Boston within said Commonwealth.
The amount of its capital stock is none.
In Witness Whereof, we have hereunto set our hands, this twenty seventh day of February in the year eighteen hundred and eighty-eight, Alpheus Hyatt, Samuel Mills, William T. Sedgwick, Edward G. Gardiner, Charles Sedgwick Minot, William G. Farlow, William Stanford Stevens, Anna D. Phillips, Susan Mims, B. H. Van Vleck.
That the first meeting of the subscribers to said agreement was held on the thirteenth day of March in the year eighteen hundred and eighty-eight.
In Witness Whereof, we have hereunto signed our names, this thirteenth day of March in the year eighteen hundred and eighty-eight, Alpheus Hyatt, President, William Stanford Stevens, Treasurer, Edward G. Gardiner, William T. Sedgwick, Susan Mims, Charles Sedgwick Minot.
(Approved on March 20, 1888 as follows:
I hereby certify that it appears upon an examination of the within written certificate and the records of the corporation duly submitted to my inspection, that the requirements of sections one, two and three of chapter one hundred and fifteen, and sections eighteen, twenty and twenty-one of chapter one hundred and six, of the Public Statutes, have been complied with and I hereby approve said certificate this twentieth day of March A.D. eighteen hundred and eighty-eight

Charles Endicott
Commissioner of Corporations)

Articles of Amendment

(On File in the Office of the Secretary of the Commonwealth)

We, James D. Ebert, President, and David Shepro, Clerk of the Marine Biological Laboratory, located at Woods Hole, Massachusetts 02543, do hereby certify that the following amendment to the Articles of Organization of the Corporation was duly adopted at a meeting held on August 15, 1975, as adjourned to August 29, 1975, by vote of 444 members, being at least two-thirds of its members legally qualified to vote in the meeting of the corporation:

Voted: That the Certificate of Organization of this corporation be and it hereby is amended by the addition of the following provisions:
"No Officer, Trustee or Corporate Member of the corporation shall be personally liable for the payment or satisfaction of any obligation or liabilities incurred as a result of, or otherwise in connection with, any commitments, agreements, activities or affairs of the corporation.
"Except as otherwise specifically provided by the Bylaws of the corporation, meetings of the Corporate Members of the corporation may be held anywhere in the United States.
"The Trustees of the corporation may make, amend or repeal the Bylaws of the corporation in whole or in part, except with respect to any provisions thereof which shall by law, this Certificate or the bylaws of the corporation, require action by the Corporate Members."

The foregoing amendment will become effective when these articles of amendment are filed in accordance with Chapter 180, Section 7 of the General Laws unless these articles specify, in accordance with the vote adopting the amendment, a later effective date not more than thirty days after such filing, in which event the amendment will become effective on such later date.

In Witness whereof and Under the Penalties of Perjury, we have hereto signed our names this 2nd day of September, in the year 1975, James D. Ebert, President; David Shepro, Clerk.
(Approved on October 24, 1975, as follows:
I hereby approve the within articles of amendment and, the filing fee in the amount of $10 having been paid, said articles are deemed to have been filed with me this 24th day of October, 1975.

Paul Guzzi
Secretary of the Commonwealth)

Bylaws

(Revised August 7, 1992 and December 10, 1992)

ARTICLE I—THE CORPORATION

A. *Name and Purpose.* The name of the Corporation shall be The Marine Biological Laboratory. The Corporation's purpose shall be to establish and maintain a laboratory or station for scientific study and investigation and a school for instruction in biology and natural history.

B. *Nondiscrimination.* The Corporation shall not discriminate on the basis of age, religion, color, race, national or ethnic origin, sex or sexual preference in its policies on employment and administration or in its educational and other programs.

ARTICLE II—MEMBERSHIP

A. *Members.* The Members of the Corporation ("Members") shall consist of persons elected by the Board of Trustees (the "Board"), upon such terms and conditions and in accordance with such procedures, not inconsistent with law or these Bylaws, as may be determined by the Board At any regular or special meeting of the Board, the Board may elect new Members. Members shall have no voting or other rights with respect to the Corporation or its activities except as specified in these Bylaws, and any Member may vote at any meeting of the Members in person only and not by proxy. Members shall serve until their death or resignation unless earlier removed with or without cause by the affirmative vote of two-thirds of the Trustees then in office. Any Member who has retired from his or her home institution may, upon written request to the Corporation, be designated a Life Member. Life Members shall not have the right to vote and shall not be assessed for dues.

B. *Meetings.* The annual meeting of the Members shall be held on the Friday following the first Tuesday in August of each year, at the Laboratory of the Corporation in Woods Hole, Massachusetts, at 9:30 a.m. The Chairperson of the Board shall preside at meetings of the Corporation. If no annual meeting is held in accordance with the foregoing provision, a special meeting may be held in lieu thereof with the same effect as the annual meeting, and in such case all references in these Bylaws, except in this Article II.B., to the annual meeting of the Members shall be deemed to refer to such special meeting. Members shall transact business as may properly come before the meeting. Special meetings of the Members may be called by the Chairperson or the Trustees, and shall be called by the Clerk, or in the case of the death, absence, incapacity or refusal by the Clerk, by any other officer, upon written application of Members representing at least ten percent of the smallest quorum of Members required for a vote upon any matter at the annual meeting of the Members, to be held at such time and place as may be designated.

C. *Quorum.* One hundred (100) Members shall constitute a quorum at any meeting. Except as otherwise required by law or these Bylaws, the affirmative vote of a majority of the Members voting in person at a meeting attended by a quorum shall constitute action on behalf of the Members.

D. *Notice of Meetings.* Notice of any annual meeting or special meeting of Members, if necessary, shall be given by the Clerk by mailing notice of the time and place and purpose of such meeting at least 15 days before such meeting to each Member at his or her address as shown on the records of the Corporation.

E. *Waiver of Notice.* Whenever notice of a meeting is required to be given a Member, under any provision of the Articles or Organization or Bylaws of the Corporation, a written waiver thereof, executed before or after the Meeting by such Member, or his or her duly authorized attorney, shall be deemed equivalent to such notice.

F. *Adjournments.* Any meeting of the Members may be adjourned to any other time and place by the vote of a majority of those Members present at the meeting, whether or not such Members constitute a quorum, or by any officer entitled to preside at or to act as Clerk of such meeting, if no Member is present or represented. It shall not be necessary to notify any Members of any adjournment unless no Member is present or represented at the meeting which is adjourned, in which case, notice of the adjournment shall be given in accordance with Article II.D. Any business which could have been transacted at any meeting of the Members as originally called may be transacted at an adjournment thereof.

ARTICLE III—ASSOCIATES OF THE CORPORATION

Associates of the Corporation. The Associates of the Marine Biological Laboratory shall be an unincorporated group of persons (including associations and corporations) interested in the Laboratory and shall be organized and operated under the general supervision and authority of the Trustees. The Associates of the Marine Biological Laboratory shall have no voting rights.

ARTICLE IV—BOARD OF TRUSTEES

A. *Powers.* The Board of Trustees shall have the control and management of the affairs of the Corporation. The Trustees shall elect a Chairperson of the Board who shall serve until his or her successor is elected and qualified. They shall annually elect a President of the Corporation. They shall annually elect a Vice Chairperson of the Board who shall be Vice Chairperson of the meetings of the Corporation. They shall annually elect a Treasurer. They shall annually elect a Clerk, who shall be a resident of Massachusetts. They shall elect Trustees-at-Large as specified in this Article IV. They shall appoint a Director of the Laboratory for a term not to exceed five years, provided the term shall not exceed one year if the candidate has attained the age of 65 years prior to the date of the appointment. They shall choose such other officers and agents as they shall think best. They may fix the compensation of all officers and agents of the Corporation and may remove them at any time. They may fill vacancies occurring in any of the offices. The Board shall have the power to choose an Executive Committee from their own number as provided in Article V, and to delegate to such Committee such of their own powers as they may deem expedient in addition to those powers conferred by Article V. They shall, from time to time, elect Members to the Corporation upon such terms and conditions as they shall have determined, not inconsistent with law or these Bylaws.

B. *Composition and Election.*

(1) The Board shall include 24 Trustees elected by the Board as provided below:

(a) At least six Trustees ("Corporate Trustees") shall be Members who are scientists, and the other Trustees ("Trustees-at-Large") shall be individuals who need not be Members or otherwise affiliated with the Corporation.

(b) The 24 elected Trustees shall be divided into four classes of six Trustees each, with one class to be elected each year to serve for a term of four years, and with each such class to include at least one Corporate Trustee. Such classes of Trustees shall be designated by the year of expiration of their respective terms.

(2) The Board shall also include the Chief Executive Officer, Treasurer and the Chairperson of the Science Council, who shall be *ex officio* voting members of the Board.

(3) Although Members or Trustees may recommend individuals for nomination as Trustees, nominations for Trustee elections shall be made by the Nominating Committee in its sole discretion. The Board may also elect Trustees who have not been nominated by the Nominating Committee.

C. *Eligibility.* A Corporate Trustee or a Trustee-at-Large who has been elected to an initial four-year term or remaining portion thereof, of which he/she has served at least two years, shall be eligible for re-election to a second four-year term, but shall be ineligible for re-election to any subsequent term until one year has elapsed after he/she has last served as a Trustee.

D. *Removal.* Any Trustee may be removed from office at any time with or without cause, by vote of a majority of the Members entitled to vote in the election of Trustees; or for cause, by vote of two-thirds of the Trustees then in office. A Trustee may be removed for cause only if notice of such action shall have been given to all of the Trustees or Members entitled to vote, as the case may be, prior to the meeting at which such action is to be taken and if the Trustee to be so removed shall have been given reasonable notice and opportunity to be heard before the body proposing to remove him or her.

E. *Vacancies.* Any vacancy in the Board may be filled by vote of a majority of the remaining Trustees present at a meeting of Trustees at which a quorum is present. Any vacancy in the Board resulting from the resignation or removal of a Corporate Trustee shall be filled by a Member who is a scientist.

F. *Meetings.* Meetings of the Board shall be held from time to time, not less frequently than twice annually, as determined by the Board. Special meetings of Trustees may be called by the Chairperson, or by any seven Trustees, to be held at such time and place as may be designated. The Chairperson of the Board, when present, shall preside over all meetings of the Trustees. Written notice shall be sent to a Trustee's usual or last known place of residence at least two weeks before the meeting. Notice of a meeting need not be given to any Trustee if a written waiver of notice executed by such Trustee before or after the meeting is filed with the records of the meeting, or if such Trustee shall attend the meeting without protesting prior thereto or at its commencement the lack of notice given to him or her.

G. *Quorum and Action by Trustees.* A majority of all Trustees then in office shall constitute a quorum. Any meeting of Trustees may be adjourned by vote of a majority of Trustees present, whether or not a quorum is present, and the meeting may be held as adjourned without further notice. When a quorum is present at any meeting of the Trustees, a majority of the Trustees present and voting (excluding abstentions) shall decide any question, including the election of officers, unless otherwise required by law, the Articles of Organization or these Bylaws.

H. *Transfers of Interests in Land.* There shall be no transfer of title nor long-term lease of real property held by the Corporation without prior approval of not less than two-thirds of the Trustees. Such real property transactions shall be finally acted upon at a meeting of the Board only if presented and discussed at a prior meeting of the Board. Either meeting may be a special meeting and no less than four weeks shall elapse between the two meetings. Any property acquired by the Corporation after December 1, 1989 may be sold, any mortgage or pledge of real property (regardless of when acquired) to secure borrowings by the Corporation may be granted, and any transfer of title or interest in real property pursuant to the foreclosure or endorsement of any such mortgage or pledge of real property may be effected by any holder of a mortgage or pledge of real property of the Corporation, with the prior approval of not less than two-thirds of the Trustees (other than any Trustee or Trustees with a direct or indirect financial interest in the transaction being considered for approval) who are present at a regular or special meeting of the Board at which there is a quorum.

ARTICLE V—COMMITTEES

A. *Executive Committee.* There shall be an Executive Committee of the Board of Trustees which shall consist of not more than eleven (11) Trustees, including *ex officio* Trustees, elected by the Board.

The Chairperson of the Board shall act as Chairperson of the Executive Committee and the Vice Chairperson as Vice Chairperson. The Executive Committee shall meet at such times and places and upon such notice and appoint such subcommittees as the Committee shall determine.

The Executive Committee shall have and may exercise all the powers of the Board during the intervals between meetings of the Board except those powers specifically withheld, from time to time, by vote of the Board or by law. The Executive Committee may also appoint such committees, including persons who are not Trustees, as it may, from time to time, approve to make recommendations with respect to matters to be acted upon by the Executive Committee or the Board

The Executive Committee shall keep appropriate minutes of its meetings, which shall be reported to the Board. Any actions taken by the Executive Committee shall also be reported to the Board.

B. *Nominating Committee.* There shall be a Nominating Committee which shall consist of not fewer than four nor more than six Trustees appointed by the Board in a manner which shall reflect the balance between Corporate Trustees and Trustees-at-Large on the Board. The Nominating Committee shall nominate persons for election as Corporate Trustees and Trustees-at-Large, Chairperson of the Board, Vice Chairperson of the Board, President, Treasurer, Clerk, Director of the Laboratory and such other officers, if any, as needed, in accordance with the requirements of these Bylaws. The Nominating Committee shall also be responsible for overseeing the training of new Trustees. The Chairperson of the Board of Trustees shall appoint the Chairperson of the Nominating Committee. The Chairperson of the Science Council shall be an *ex officio* voting member of the Nominating Committee.

C. *Science Council.* There shall be a Science Council (the "Council") which shall consist of Members of the Corporation elected to the Council by vote of the Members of the Corporation, and which shall advise the Board with respect to matters concerning the Corporation's mission, its scientific and instructional endeavors, and the appointment and promotions of persons or committees with responsibility for matters requiring scientific expertise. Unless otherwise approved by a majority of the members of the Council, the Chairperson of the Council shall be elected annually by the Council. The chief executive officer of the Corporation shall be an *ex officio* voting member of the Council.

D. *Board of Overseers.* There shall be a Board of Overseers which shall consist of not fewer than five nor more than eight scientists who have expertise concerning matters with which the Corporation is involved. Members of the Board of Overseers may or may not be Members of the Corporation and may be appointed by the Board of Trustees on the basis of recommendations submitted from scientists and scientific organizations or societies. The Board of Overseers shall be available to review and offer recommendations to the officers, Trustees and Science Council regarding scientific activities conducted or proposed by the Corporation and shall meet from time to time, not less frequently than annually, as determined by the Board of Trustees.

E. *Board Committees Generally.* The Trustees may elect or appoint one or more other committees (including, but not limited to, an Investment Committee, a Development Committee, an Audit Committee, a Facilities and Capital Equipment Committee and a Long-Range Planning Committee) and may delegate to any such committee or committees any or all of their powers, except those which by law, the Articles of Organization or these Bylaws the Trustees are prohibited from delegating; provided that any committee to which the powers of the Trustees are delegated shall consist solely of Trustees. The members of any such committee shall have such tenure and duties as the Trustees shall determine. The Investment Committee, which shall oversee the management of the Corporation's endowment funds and marketable securities shall include as *ex officio* members, the Chairperson of the Board, the Treasurer and the Chairperson of the Audit Committee, together with such Trustees as may be required for not less than two-thirds of the Investment Committee to consist of Trustees. Except as otherwise provided by these Bylaws or determined by the Trustees, any such committee may make rules for the conduct of its business, but, unless otherwise provided by the Trustees or in such rules, its business shall be conducted as nearly as possible in the same manner as is provided by these Bylaws for the Trustees.

F. *Actions Without a Meeting.* Any action required or permitted to be taken at any meeting of the Executive Committee or any other committee elected by the Trustees may be taken without a meeting if all members of such committees consent to the action in writing and such written consents are filed with the records of meetings. Members of the Executive Committee or any other committee elected by the Trustees may also participate in any meeting by means of a telephone conference call, or otherwise take action in such a manner as may, from time to time, be permitted by law.

G. *Manual of Procedures.* The Board of Trustees, on the recommendation of the Executive Committee, shall establish guidelines and modifications thereof to be recorded in a Manual of Procedures. Guidelines shall establish procedures for: (1) Nomination and election of members of the Corporation, Board of Trustees and Executive Committee; (2) Election of Officers; (3) Formation and Function of Standing Committees.

ARTICLE VI—OFFICERS

A. *Enumeration.* The officers of the Corporation shall consist of a President, a Treasurer and a Clerk, and such other officers having the powers of President, Treasurer and Clerk as the Board may determine, and a Director of the Laboratory. The Corporation may have such other officers and assistant officers as the Board may determine, including (without limitation) a Chairperson of the Board, Vice Chairperson and one or more Vice Presidents, Assistant Treasurers or Assistant Clerks. Any two or more offices may be held by the same person. The Chairperson and Vice Chairperson of the Board shall be elected by and from the Trustees, but other officers of the Corporation need not be Trustees or Members. If required by the Trustees, any officer shall give the Corporation a bond for the faithful performance of his or her duties in such amount and with such surety or sureties as shall be satisfactory to the Trustees.

B. *Tenure.* Except as otherwise provided by law, by the Articles of Organization or by these Bylaws, the President, Treasurer, and all other officers shall hold office until the first meeting of the Board following the annual meeting of Members and thereafter, until his or her successor is chosen and qualified.

C. *Resignation.* Any officer may resign by delivering his or her written resignation to the Corporation at its principal office or to the President or Clerk and such resignation shall be effective upon receipt unless it is specified to be effective at some other time or upon the happening of some other event.

D. *Removal.* The Board may remove any officer with or without cause by a vote of a majority of the entire number of Trustees then in office, at a meeting of the Board called for that purpose and for which notice of the purpose thereof has been given, provided that an officer may be removed for cause only after having an opportunity to be heard by the Board at a meeting of the Board at which a quorum is personally present and voting.

E. *Vacancy.* A vacancy in any office may be filled for the unexpired balance of the term by vote of a majority of the Trustees present at any meeting of Trustees at which a quorum is present or by written consent of all of the Trustees, if less than a quorum of Trustees shall remain in office.

F. *Chairperson.* The Chairperson shall have such powers and duties as may be determined by the Board and, unless otherwise determined by the Board, shall serve in that capacity for a term coterminous with his or her term as Trustee.

G. *Vice Chairperson.* The Vice Chairperson shall perform the duties and exercise the powers of the Chairperson in the absence or disability of the Chairperson, and shall perform such other duties and possess such other powers as may be determined by the Board. Unless otherwise determined by the Board, the Vice Chairperson shall serve for a one-year term.

H. *Director.* The Director shall be the chief operating officer and, unless otherwise voted by the Trustees, the chief executive officer of the Corporation. The Director shall, subject to the direction of the Trustees, have general supervision of the Laboratory and control of the business of the Corporation. At the annual meeting, the Director shall submit a report of the operations of the Corporation for such year and a statement of its affairs, and shall, from time to time, report to the Board all matters within his or her knowledge which the interests of the Corporation may require to be brought to its notice.

I. *Deputy Director.* The Deputy Director, if any, or if there shall be more than one, the Deputy Directors in the order determined by the Trustees, shall, in the absence or disability of the Director, perform the duties and exercise the powers of the Director and shall perform such other duties and shall have such other powers as the Trustees may, from time to time, prescribe.

J. *President.* The President shall have the powers and duties as may be vested in him or her by the Board.

K. *Treasurer and Assistant Treasurer.* The Treasurer shall, subject to the direction of the Trustees, have general charge of the financial affairs of the Corporation, including its long-range financial planning, and shall cause to be kept accurate books of account. The Treasurer shall prepare a yearly report on the financial status of the Corporation to be delivered at the annual meeting. The Treasurer shall also prepare or oversee all filings required by the Commonwealth of Massachusetts, the Internal Revenue Service, or other Federal and State Agencies. The account of the Treasurer shall be audited annually by a certified public accountant.

The Assistant Treasurer, if any, or if there shall be more than one, the Assistant Treasurers in the order determined by the Trustees, shall, in the absence or disability of the Treasurer, perform the duties and exercise the powers of the Treasurer, shall perform such other duties and shall have such other powers as the Trustees may, from time to time, prescribe.

L. *Clerk and Assistant Clerk.* The Clerk shall be a resident of the Commonwealth of Massachusetts, unless the Corporation has designated a resident agent in the manner provided by law. The minutes or records of all meetings of the Trustees and Members shall be kept by the Clerk who shall record, upon the record books of the Corporation, minutes of the proceedings at such meetings. He or she shall have custody of the record books of the Corporation and shall have such other powers and shall perform such other duties as the Trustees may, from time to time, prescribe.

The Assistant Clerk, if any, or if there shall be more than one, the Assistant Clerks in the order determined by the Trustees, shall, in the absence or disability of the Clerk, perform the duties and exercise the powers of the Clerk and shall perform such other duties and shall have such other powers as the Trustees may, from time to time, prescribe.

In the absence of the Clerk and an Assistant Clerk from any meeting, a temporary Clerk shall be appointed at the meeting.

M. *Other Powers and Duties.* Each officer shall have in addition to the duties and powers specifically set forth in these Bylaws, such duties and powers as are customarily incident to his or her office, and such duties and powers as the Trustees may, from time to time, designate.

ARTICLE VII—AMENDMENTS

These Bylaws may be amended by the affirmative vote of the Members at any meeting, provided that notice of the substance of the proposed amendment is stated in the notice of such meeting. As authorized by the Articles of Organization, the Trustees, by a majority of their number then in office, may also make, amend or repeal these Bylaws, in whole or in part, except with respect to (a) the provisions of these Bylaws governing (i) the removal of Trustees and (ii) the amendment of these Bylaws and (b) any provisions of these Bylaws which by law, the Articles of Organization or these Bylaws, requires action by the Members.

No later than the time of giving notice of meeting of Members next following the making, amending or repealing by the Trustees of any Bylaw, notice thereof stating the substance of such change shall be given to all Members entitled to vote on amending the Bylaws.

Any Bylaw adopted by the Trustees may be amended or repealed by the Members entitled to vote on amending the Bylaws.

ARTICLE VIII—INDEMNITY

Except as otherwise provided below, the Corporation shall, to the extent legally permissible, indemnify each person who is, or shall have been, a Trustee, director or officer of the Corporation or who is serving, or shall have served at the request of the Corporation as a Trustee, director or officer of another organization in which the Corporation directly or indirectly has any interest as a shareholder, creditor or otherwise, against all liabilities and expenses (including judgments, fines, penalties, and reasonable attorneys' fees and all amounts paid, other than to the Corporation or such other organization, in compromise or settlement) imposed upon or incurred by any such person in connection with, or arising out of, the defense or disposition of any action, suit or other proceeding, whether civil or criminal, in which he or she may be a defendant or with which he or she may be threatened or otherwise involved, directly or indirectly, by reason of his or her being or having been such a Trustee, director or officer.

The Corporation shall provide no indemnification with respect to any matter as to which any such Trustee, director or officer shall be finally adjudicated in such action, suit or proceeding not to have acted in good faith in the reasonable belief that his or her action was in the best interests of the Corporation. The Corporation shall provide no indemnification with respect to any matter settled or comprised unless such matter shall have been approved as in the best interests of the Corporation, after notice that indemnification is involved, by (i) a disinterested majority of the Board of the Executive Committee, or (ii) a majority of the Members.

Indemnification may include payment by the Corporation of expenses in defending a civil or criminal action or proceeding in advance of the final disposition of such action or proceeding upon receipt of an undertaking by the person indemnified to repay such payment if it is ultimately determined that such person is not entitled to indemnification under the provisions of this Article VIII, or under any applicable law.

As used in the Article VIII, the terms "Trustee," "director," and "officer" include their respective heirs, executors, administrators and legal representatives, and an "interested" Trustee, director or officer is one against whom in such capacity the proceeding in question or another proceeding on the same or similar grounds is then pending.

To assure indemnification under this Article VIII of all persons who are determined by the Corporation or otherwise to be or to have been "fiduciaries" of any employee benefits plan of the Corporation which may exist, from time to time, this Article VIII shall be interpreted as follows: (i) "another organization" shall be deemed to include such an employee benefit plan, including without limitation, any plan of the Corporation which is governed by the Act of Congress entitled "Employee Retirement Income Security Act of 1974," as amended, from time to time, ("ERISA"); (ii) "Trustee" shall be deemed to include any person requested by the Corporation to serve as such for an employee benefit plan where the performance by such person of his or her duties to the Corporation also imposes duties on, or otherwise involves services by, such person to the plan or participants or beneficiaries of the plan; (iii) "fines" shall be deemed to include any excise tax plan pursuant to ERISA; and (iv) actions taken or omitted by a person with respect to an employee benefit plan in the performance of such person's duties for a purpose reasonably believed by such person to be in the interest of the participants and beneficiaries of the plan shall be deemed to be for a purpose which is in the best interests of the Corporation.

The right of indemnification provided in this Article VIII shall not be exclusive of or affect any other rights to which any Trustee, director or officer may be entitled under any agreement, statute, vote of Members or otherwise. The Corporation's obligation to provide indemnification under this Article VIII shall be offset to the extent of any other source of indemnification of any otherwise applicable insurance coverage under a policy maintained by the Corporation or any other person. Nothing contained in the Article shall affect any rights to which employees and corporate personnel other than Trustees, directors or officers may be entitled by contract, by vote of the Board or of the Executive Committee or otherwise.

ARTICLE IX—DISSOLUTION

The consent of every Trustee shall be necessary to effect a dissolution of the Marine Biological Laboratory. In case of dissolution, the property shall be disposed of in such a manner and upon such terms as shall be determined by the affirmative vote of two-thirds of the Trustees then in office in accordance with the laws of the Commonwealth of Massachusetts.

ARTICLE X—MISCELLANEOUS PROVISIONS

A. *Fiscal Year.* Except as otherwise determined by the Trustees, the fiscal year of the Corporation shall end on December 31st of each year.

B. *Seal.* Unless otherwise determined by the Trustees, the Corporation may have a seal in such form as the Trustees may determine, from time to time.

C. *Execution of Instruments.* All checks, deeds, leases, transfers, contracts, bonds, notes and other obligations authorized to be executed by an officer of the Corporation in its behalf shall be signed by the Director or the Treasurer except as the Trustees may generally or in particular cases otherwise determine. A certificate by the Clerk or an Assistant Clerk, or a temporary Clerk, as to any action taken by the Members, Board of Trustees or any officer or representative of the Corporation shall as to all persons who rely thereon in good faith be conclusive evidence of such action.

D. *Corporate Records.* The original, or attested copies, of the Articles of Organization, Bylaws and records of all meetings of the Members shall be kept in Massachusetts at the principal office of the Corporation, or at an office of the Corporation's Clerk or resident agent. Said copies and records need not all be kept in the same office. They shall be available at all reasonable times for inspection by any Member for any proper purpose, but not to secure a list of Members for a purpose other than in the interest of the applicant, as a Member, relative to the affairs of the Corporation.

E. *Articles of Organization.* All references in these Bylaws to the Articles of Organization shall be deemed to refer to the Articles of Organization of the Corporation, as amended and in effect, from time to time.

F. *Transactions with Interested Parties.* In the absence of fraud, no contract or other transaction between this Corporation and any other corporation or any firm, association, partnership or person shall be affected or invalidated by the fact that any Trustee or officer of this Corporation is pecuniarily or otherwise interested in or is a director, member or officer of such other corporation or of such firm, association or partnership or in a party to or is pecuniarily or otherwise interested in such contract or other transaction or is in any way connected with any person or person, firm, association, partnership, or corporation pecuniarily or otherwise interested therein; provided that the fact that he or she individually or as a director, member or officer of such corporation, firm, association or partnership in such a party or is so interested shall be disclosed to or shall have been known by the Board of Trustees or a majority of such Members thereof as shall be present at a meeting of the Board of Trustees at which action upon any such contract or transaction shall be taken; any Trustee may be counted in determining the existence of a quorum and may vote at any meeting of the Board of Trustees for the purpose of authorizing any such contract or transaction with like force and effect as if he/she were not so interested, or were not a director, member or officer of such other corporation, firm, association or partnership, provided that any vote with respect to such contract or transaction must be adopted by a majority of the Trustees then in office who have no interest in such contract or transaction.

Publications

Ågren, G., G. R. Shaver, and E. B. Rastetter. 1999. Nutrients: dynamics and limitations. Pp. 333–345 in *Carbon Dioxide and Environmental Stress*, Y. Luo and H. A. Mooney, eds. Academic Press, San Diego, CA.

Altamirano, A. A., G. E. Breitwieser, and J. M. Russell. 1999. Activation of Na, K, Cl cotransport in squid giant axon by extracellular ions: Evidence for ordered binding. *Biochim. Biophys. Acta* **1416:** 195–207.

Antic, S., and D. Zecevic. 1999. Imaging membrane potential changes in individual neurons. In *Fluorescent and Luminescent Probes for Biological Activity*, W. T. Mason, ed. Academic Press, London.

Antic, S., C. X. Falk, L. B. Cohen, Y. W. Lam, M. Wachowiak, D. Zecevic, and M. Zochowski. 1999. Fast multisite optical measurement of membrane potential. Three examples. *FASEB J.* **13:** S271–S276.

Antic, S., G. Major, and D. Zecevic. 1999. Fast optical recording of membrane potential changes from dendrites of pyramidal neurons. *J. Neurophysiol.* **82:** 1615–1621.

Armstrong, C. M. 1999. Distinguishing surface effects of calcium ion from pore-occupancy effects in Na^+ channels. *Proc. Natl. Acad. Sci. USA* **96:** 4158–4163.

Armstrong, C. M., and G. Cota. 1999. Calcium block of Na^+ channels and its effect on closing rate. *Proc. Natl. Acad. Sci. USA* **96:** 4154–4157.

Asokan, R., and P. B. Armstrong. 1999. Cellular mechanisms of hemolysis by the protein limulin, a sialic-acid-specific lectin from the plasma of the American horseshoe crab, *Limulus polyphemus*. *Biol. Bull.* **197:** 275–276.

Augustine, G. J., M. E. Burns, W. M. DeBello, S. Hilfiker, J. Morgan, F. E. Schweizer, H. Tokumaru, and K. Umayahara. 1999. Proteins involved in synaptic vesicle trafficking. *J. Physiol.* **520:** 33–41.

Baikie, I. D., U. Petermann, and B. Lagel. 1999. *In-situ* work function study of oxidation and thin film growth on clean surfaces. *Surfactant Sci.* **433–435:** 770–774.

Baikie, I. D., U. Petermann, and B. Lagel. 1999. UHV compatible spectroscopic scanning Kelvin probe for surface analysis. *Surfactant Sci.* **433–435:** 249–253.

Baikie, I. D., P. J. S. Smith, D. M. Porterfield, and P. J. Estrup. 1999. Multi-tip scanning Bio-Kelvin Probe. *Rev. Sci. Instrum.* **70**(3): 1842–1850.

Bearer, E. L., M. L. Schlief, X. O. Breakefield, D. E. Schuback, T. S. Reese, and J. H. LaVail. 1999. Squid axoplasm supports the retrograde axonal transport of Herpes simplex virus. *Biol. Bull.* **197:** 257–258.

Benech, J. C., M. Crispino, B. B. Kaplan, and A. Giuditta. 1999. Protein synthesis in presynaptic endings from squid brain: Modulation by calcium ions. *J. Neurosci. Res.* **55:** 776–781.

Berkey, C., and J. Atema. 1999. Individual recognition and memory in *Homarus americanus* male-female interactions. *Biol. Bull.* **197:** 253–254.

Billack, B., J. D. Laskin, M. A. Gallo, and D. E. Heck. 1999. Effects of alpha-bungarotoxin on development of the sea urchin *Arbacia punctulata*. *Biol. Bull.* **197:** 267–268.

Biswas, C., and P. B. Armstrong. 1999. Identification of a hemolytic activity in the plasma of the gastropod *Busycon canaliculatum*. *Biol. Bull.* **197:** 276–277.

Bodznick, D., J. C. Montgomery, and M. R. Carey. 1999. Adaptive mechanisms in the elasmobranch hindbrain. *J. Exp. Biol.* **202:** 1357–1364.

Burns, M. E., and G. J. Augustine. 1999. Functional studies of presynaptic proteins at the squid giant synapse. Pp. 237–264 in *Neurotransmitter Release: Frontiers in Molecular Biology*, H. Bellen, ed. Oxford University Press, New York.

Bush, K. A., J. Stenflo, D. A. Roth, E. Czerwiec, A. Harrist, G. S. Begley, B. C. Furie, and B. Furie. 1999. Hydrophobic amino acids define the carboxylation recognition site in the precursor of the gamma-carboxyglutamic acid-containing conotoxin e-TxIX from the marine cone snail *Conus textile*. *Biochemistry* **38**(44): 14,660–14,666.

Buzby, K., and L. Deegan. 1999. Retention of anchor and passive integrated transponder tags by Arctic grayling. *N. Am. J. Fish. Manage.* **19:** 1147–1150.

Buzby, K., J. Hobbie, L. Deegan, M. McDonald, and B. Peterson. 1999. Effects of fertilization on fish in Alaskan arctic tundra streams and lakes. Pp. 99–112 in *Restoration of Fisheries by Enrichment of Aquatic Ecosystems*. J. G. Stockner and G. Milbrink, eds. Uppsala University, Uppsala, Sweden.

Canfield, S., L. Claessens, C. Hopkinson Jr., E. Rastetter, and J. Vallino. 1999. Long-term effect of municipal water use on the water budget of the Ipswich River basin. *Biol. Bull.* **197:** 295–297.

Colinvaux, P., P. E. De Oliveira, and J. E. M. Patino. 1999. *Amazon Pollen Manual and Atlas*. Harwood Academic Publishers.

Créton, R., J. A. Kreiling, and L. F. Jaffe. 1999. Calcium imaging with chemiluminescence. *Microsc. Res. Tech.* **46:** 390–397.

Crump, B. C., E. V. Armbrust, and J. A. Baross. 1999. Phylogenetic analysis of particle-attached and free-living bacterial communities in the Columbia River, its estuary, and the adjacent coastal ocean. *Appl. Environ. Microbiol.* **65:** 3192–3204.

Cubbage, A., D. Lawrence, G. Tomasky, and I. Valiela. 1999. Relationship of reproductive output in *Acartia tonsa*, chlorophyll concentration, and land-derived nitrogen loads in estuaries of Waquoit Bay, Massachusetts. *Biol. Bull.* **197:** 294–295.

Cummings, M. P., S. P. Otto, and J. Wakeley. 1999. Genes and other samples of DNA sequence data for phylogenetic inference. *Biol. Bull.* **196:** 345–350.

Currie, W. S., and K. J. Nadelhoffer. 1999. Dynamic redistribution of isotopically labelled cohorts of nitrogen inputs in two temperate forests. *Ecosystems* **2:** 4–18.

Currie, W. S., K. J. Nadelhoffer, and J. D. Aber. 1999. Soil detrital processes controlling the movement of ^{15}N tracers to forest vegetation. *Ecol. Appl.* **9:** 87–102.

Danuser, G. 1999. Photogrammetric calibration of a stereo light microscope. *J. Microsc.* **193**(1): 62–83.

Davidson, Eric H., and G. Ruvkun. 1999. Themes from a NASA workshop on gene regulatory processes in development and evolution. *J. Exp. Zool.* **285:** 104–115.

Deegan, L. A., H. E. Golden, C. J. Harvey, and B. J. Peterson. 1999. Influence of environmental variability on the growth of age-0 and adult arctic grayling. *Trans. Am. Fish. Soc.* **128:** 1163–1175.

DiPolo, R., and L. Beaugé. 1999. Metabolic pathways in the regulation of invertebrate and vertebrate Na/Ca exchange. *Biochim. Biophys. Acta* **1422:** 57–71.

Downs, M. R., R. H. Michener, B. Fry, and K. J. Nadelhoffer. 1999. Routine measurement of dissolved inorganic ^{15}N in streamwater. *Environ. Monit. Assess.* **55:** 211–220.

Edds-Walton, P. L., R. R. Fay, and S. M. Highstein. 1999. Dendritic arbors and central projections of auditory fibers from the saccule of the toadfish (*Opsanus tau*). *J. Comp. Neurol.* **411**(2): 212–238.

Epstein, H. T. 1999. Stages of increased cerebral blood flow accompany stages of rapid brain growth. *Brain Dev.* **21:** 535–539.

Evgenidou, A., A. Konkle, A. D'Ambrosio, A. Corcoran, J. Bowen, E. Brown, D. Corcoran, C. Dearholt, S. Fern, A. Lamb, J. Michalowsky, I. Ruegg, and J. Cebrián. 1999. Effects of increased nitrogen loading on the abundance of diatoms and dinoflagellates in estuarine phytoplanktonic communities. *Biol. Bull.* **197:** 292–294.

Fay, R. R., and P. L. Edds-Walton. 1999. Sharpening of directional auditory input in the descending octaval nucleus of the toadfish, *Opsanus tau*. *Biol. Bull.* **197:** 240–241.

Fernandez, I. J., L. E. Rustad, M. B. David, K. J. Nadelhoffer, and M. J. Mitchell. 1999. Mineral soil and solution responses to experimental N and S enrichment at the Bear Brook Watershed in Maine (BBWM). *Environ. Monit. Assess.* **55:** 165–185.

Fukui, Y., E. L. De Hostos, S. Yumura, T. Kitanishi-Yumara, and S. Inoué. 1999. Architectural dynamics of F-actin in eupodia suggests their role in invasive locomotion in *Dictyostelium*. *Exp. Cell Res.* **249:** 33–45.

Fukui, Y., S. Engler, S. Inoué, and E. L. De Hostos. 1999. Architectural dynamics and gene replacement of coronin suggest its role in cytokinesis. *Cell Motil. Cytoskel.* **42:** 204–217.

Fukui, Y., T. Q. P. Uyeda, C. Kitayama, and S. Inoué. Migration forces in *Dictyostelium* measured by centrifuge DIC microscopy. *Biol. Bull.* **197:** 260–262.

Gould, R., C. Freund, F. Palmer, P. E. Knapp, J. Huang, H. Morrison, and D. L. Feinstein. 1999. Messenger RNAs for kinesins and dynein are located in neural processes. *Biol. Bull.* **197:** 259–260.

Hanley, J. S., N. Shashar, R. Smolowitz, W. Mebane, and R. T. Hanlon. 1999. Soft-sided tanks improve long-term health of cultured cuttlefish. *Biol. Bull.* **197:** 237–238.

Hanna, J. P., F. W. Grasso, and J. Atema. 1999. Temporal correlation between sensor pairs in different plume positions: a study of concentration information available to the American lobster, *Homarus americanus*, during chemotaxis. *Biol. Bull.* **197:** 250–251.

Harmon, M. E., K. J. Nadelhoffer, and J. M. Blair. 1999. Measuring decomposition, nutrient turnover and stores in plant litter. Pp. 202–240 in *Standard Soil Methods for Long Term Ecological Research*, G. P. Robertson, C. S. Bledsoe, D. C. Coleman, and P. Sollins, eds. Oxford University Press, New York.

Harrington, J. M., and P. B. Armstrong. A cuticular secretion of the horseshoe crab, *Limulus polyphemus:* a potential anti-fouling agent. *Biol. Bull.* **197:** 274–275.

Hartley, A. E., C. Neill, J. M. Melillo, R. Crabtree, and F. P. Bowles. 1999. Plant performance and soil nitrogen mineralization in response to simulated climate change in subarctic dwarf shrub heath. *Oikos* **86:** 331–343.

Herbert, D. A., and J. H. Fownes. 1999. Forest productivity and efficiency of resource use across a chronosequence of tropical montane soils. *Ecosystems* **2:** 242–254.

Herbert, D. A., J. H. Fownes, and P. M. Vitousek. 1999. Hurricane damage to a Hawaiian forest: nutrient supply rate affects resistance and resilience. *Ecology* **80**(3): 908–920.

Herbert, D. A., E. B. Rastetter, G. R. Shaver, and G. I. Ågren. 1999. Effects of plant growth characteristics on biogeochemistry and community composition in a changing climate. *Ecosystems* **2:** 367–382.

Hilfiker, S., and G. J. Augustine. 1999. Protein kinase C and neurotransmitter release: new insights into a familiar regulatory molecule. *J. Physiol.* **515:** 1.

Hilfiker, S., P. Greengard, and G. J. Augustine. 1999. Coupling calcium to SNARE-mediated synaptic vesicle fusion. *Nat. Neurosci.* **2:** 104–106.

Hilfiker, S., V. A. Pieribone, A. J. Czernik, H-T. Kao, G. J. Augustine, and P. Greengard. 1999. Synapsins as regulators of neurotransmitter release. *Philos. Trans. R. Soc. Lond. B* **354:** 269–279.

Hill, J. L., K. Hammar, P. J. S. Smith, and D. Gross. 1999. Stage-dependent effects of epidermal growth factor on Ca^{2+} efflux in mouse oocytes. *Mol. Reprod. Dev.* **53:** 244–253.

Hobbie, J. E., M. Bahr, N. Bettez, and P. A. Rublee. 1999. *Microbial Biosystems: New Frontiers*, C. R. Bell, M. Brylinsky, and P. Johnson-Green, eds. Proceedings of the 8th International Symposium on Microbial Ecology. Atlantic Canada Society for Microbial Ecology, Halifax, Nova Scotia.

Hobbie, J. E., M. Bahr, and P. A. Rublee. 1999. Controls on microbial food webs in oligotrophic arctic lakes. *Arch. Hydrobiol. Spec. Issues Advances Limnol.* **54:** 61–76.

Holm, I., A. Mikhailov, T. Jillson, and B. Rose. 1999. Dynamics of gap junctions observed in living cells with connexin 43-GFP chimeric protein. *Eur. J. Cell Biol.* **78:** 856–866.

Holmes, R. M., A. Aminot, R. Kérouel, B. A. Hooker, and B. J. Peterson. 1999. A simple and precise method for measuring ammonium in marine and freshwater ecosystems. *Can. J. Fish. Aquat. Sci.* **56:** 1801–1808.

Hopkinson, C. S., A. E. Giblin, J. Tucker, and R. H. Garritt. 1999. Benthic metabolism and nutrient cycling along an estuarine salinity gradient. *Estuaries* **22:** 825–843.

Hoskin, F. C. G., D. M. Steeves, and J. E. Walker. 1999. Substituted cyclodextrin as a model for a squid enzyme that hydrolyzes the nerve gas Soman. *Biol. Bull.* **197:** 284–285.

Hrywna, Y., T. V. Tsoi, O. V. Maltseva, J. F. Quensen III, and J. M. Tiedje. 1999. Construction and characterization of two recombinant bacteria that grow on ortho- and apra-substituted chlorobiphenyls. *Appl. Environ. Microbiol.* **65**(5): 2163–2169.

Inoué, S. 1999. Windows to dynamic fine structures, then and now. *FASEB J.* **13:** S185–S190.

Jaffe, L. F. 1999. Organization of early development by calcium patterns. *BioEssays* **21:** 657–667.

Jenkins, J. C., D. W. Kicklighter, S. V. Ollinger, J. D. Aber, and J. M. Melillo. 1999. Sources of variability in net primary production predictions at a regional scale: a comparison using PnET-II and TEM 4.0 in northeastern US forests. *Ecosystems* **2:** 555–570.

Jonas, E. A., J. Buchanan, and L. K. Kaczmarek. 1999. Prolonged activation of mitochondrial conductances during synaptic transmission. *Science* **286:** 1347–1350.

Kaatz, I. M., and P. S. Lobel. 1999. Acoustic behavior and reproduction of five species of *Corydoris* catfishes (Callichthyidae). *Biol. Bull.* **197:** 241–242.

Kaltenbach, J. C., W. J. Kuhns, T. L. Simpson, and M. M. Burger. 1999. Intense concanavalin A staining and apoptosis of peripheral flagellated cells in larvae of the marine sponge *Microciona prolifera:* significance in relation to morphogenesis. *Biol. Bull.* **197:** 271–273.

Kaplan, I. 1999. Suspicion, growth and co-management in the commercial fishing industry: the financial settlers of New Bedford. *Mar. Policy* **23**(3): 227–241.

Karp, P. D., M. Riley, S. M. Paley, A. Pellegrini-Toole, and M. Krummenacker. 1999. EcoCyc: Encyclopedia of *Escherichia coli* genes and metabolism. *Nucleic Acids Res.* **27:** 55–58.

Katoh, K., K. Hammar, P. J. S. Smith, and R. Oldenbourg. 1999. Arrangement of radial actin bundles in the growth cone of *Aplysia* bag cell neurons shows a short history of filopodial behavior. *Proc. Natl. Acad. Sci. USA* **96:** 7928–7931.

Katoh, K., K. Hammar, P. J. S. Smith, and R. Oldenbourg. 1999. Birefringence imaging directly reveals architectural dynamics of filamentous actin in living growth cones. *Mol. Biol. Cell* **10:** 197–210.

Kerr, L. M., P. S. Lobel, and J. M. Ingoglia. 1999. Evaluation of a reporter gene system biomarker for detecting contamination in tropical marine sediments. *Biol. Bull.* **197:** 303–306.

Kicklighter, D. W., A. Bondeau, A. L. Schloss, J. Kaduk, and A. D. McGuire. 1999. Comparing global models of terrestrial net primary productivity (NPP): Global pattern and differentiation by major biomes. *Global Change Biol.* **5:** 16–24.

King, A. J., S. A. Adamo, and R. T. Hanlon. 1999. Contact with squid egg capsules increases agonistic behavior in male squid (*Loligo pealei*). *Biol. Bull.* **197:** 256.

Koenig, E., and A. Giuditta. 1999. Protein synthesizing machinery in the axon compartment. *Neuroscience* **89:** 5–15.

Komarow, S., T. Young, L. Deegan, and R. Garritt. 1999. Influence of marsh flooding on the abundance and growth of *Fundulus heteroclitus* in salt marsh creeks. *Biol. Bull.* **197:** 299–300.

Kuhns, W. J., M. M. Burger, and E. Turley. 1999. Hyaluronic acid: a component of the aggregation factor secreted by the marine sponge, *Microciona prolifera. Biol. Bull.* **197:** 277–279.

Labedan, B., and M. Riley. 1999. Genetic inventory: *Escherichia coli* as a window on ancestral proteins. Pp. 311–329 in *Organization of the Prokaryotic Genome,* Robert Charlebois, ed. ASM Press, Washington, DC.

Lagel, B., I. D. Baikie, and U. Petermann. 1999. A novel detection system for defects and chemical contamination in semi conductors based upon the Scanning Kelvin Probe. *Surfactant Sci.* **433–435:** 622–626.

Land, S. C., D. M. Porterfield, R. H. Sanger, and P. J. S. Smith. 1999. The self-referencing oxygen-selective microelectrode: Detection of transmembrane oxygen flux from single cells. *J. Exp. Biol.* **202:** 211–218.

Lema-Foley, C., K-G. Lee, T. Parris, Z. Koroleva, N. Mohan, P. Noailles, and W. D. Cohen. 1999. Reversible alteration of morphology in an invertebrate erythrocyte: properties of the natural inducer and the cellular response. *Biol. Bull.* **197:** 395–405.

Lew, R. R. 1999. Comparative analysis of Ca^{2+} and H^{+} flux magnitude and location along growing hyphae of *Saprolegnia ferax* and *Neurospora crassa. Eur. J. Cell Biol.* **78:** 892–902.

Lewis, D. L., A. W. Garrison, K. E. Wommack, A. Whittemore, P. Steudler, and J. Melillo. 1999. Influence of environmental changes on degradation of chiral pollutants in soils. *Nature* **401:** 898–901.

Llinàs, Rodolfo R. 1999. *The Squid Giant Synapse: A Model for Chemical Transmission.* Oxford University Press.

Lobel, P. S., and L. M. Kerr. 1999. Courtship sounds of the Pacific damselfish, *Abudefduf sordidus* (Pomacentridae) *Biol. Bull.* **197:** 242–244.

Lovvorn, J. R., W. M. Wollheim, and E. A. Hart. 1999. High plains wetlands in southeast Wyoming: Salinity, vegetation, and invertebrate communities. In *Invertebrates in Freshwater Wetlands in North America.* D. B. Batzer, R. B. Rader, and S. A. Wissinger, eds. John Wiley and Sons, New York.

Maddox, P., A. Desai, E. D. Salmon, T. J. Mitchison, K. Oogema, T. Kapoor, B. Matsumoto, and S. Inoué. 1999. Dynamic confocal imaging of mitochondria in swimming *Tetrahymena* and of microtubule poleward flux in *Xenopus* extract spindles. *Biol. Bull.* **197:** 263–265.

Malchow, R. P., and D. J. Ramsey. 1999. Responses of retinal Müller cells to neurotransmitter candidates: a comparative survey. *Biol. Bull.* **197:** 229–230.

Manglapus, M. K., N. Buelow, H. Uchiyama, M. Iuvone, H. Underwood, and R. B. Barlow. 1999. Dopamine mediates a circadian rhythm in rod-cone dominance of the Japanese quail retina. *J. Neuroscience* **19:** 4132–4141.

Mass, P. A., S. J. Kleinschuster, M. Dykstra, R. Smolowitz, and J. Parent. 1999. Molecular characterization of QPX (quahog parasite unknown), a pathogen of *Mercenaria mercenaria. J. Shellfish Res.* **18:** 561–567.

McLaughlin, L. C., J. Walters, J. Atema, and N. Wainwright. 1999. Urinary protein concentration in connection with agonistic interactions in *Homarus americanus. Biol. Bull.* **197:** 254–255.

Mensinger, A. F., and S. M. Highstein. 1999. Characteristics of regenerating horizontal semicircular canal afferent and efferent fibers in the toadfish, *Opsanus tau. J. Comp. Neurol.* **410:** 653–676.

Messerli, M. A., G. Danuser, and K. R. Robinson. 1999. Pulsatile influxes of H^{+}, K^{+} and Ca^{++} lag growth pulses of *Lilium longiflorum* pollen tubes. *J. Cell Sci.* **112:** 1497–1509.

Mjos, K., F. Grasso, and J. Atema. 1999. Antennule use by the American lobster, *Homorus americanus,* during chemo-orientation in three turbulent odor plumes. *Biol. Bull.* **197:** 249–250.

Mondrup, T. 1999. Salinity effects on nutrient dynamics in estuarine sediments investigated by a plug-flux method. *Biol. Bull.* **197:** 287–288.

Montgomery, J. C., and D. Bodznick. 1999. Signals and noise in the elasmobranch electrosensory system. *J. Exp. Biol.* **202:** 1349–1355.

Moorhead, D. L., W. S. Currie, E. B. Rastetter, W. J. Parton, and M. E. Harmon. 1999. Climate and litter quality controls on decomposition: an analysis of modeling approaches. *Global Biogeochem. Cycles* **13:** 575–589.

Morgan, J., X. Zhao, M. Womack, K. Prasad, G. J. Augustine, and E. M. Lafer. 1999. A role for the clathrin assembly domain of AP180 in synaptic vesicle endocytosis. *J. Neurosci.* **19:** 10,201–10,212.

Nadelhoffer, K. J., R. D. Boone, R. D. Bowden, J. D. Canary, J. Kaye, P. Micks, A. Ricca, J. A. Aitkenhead, K. Lajtha, and W. H. McDowell. 1999. In *Forest Landscape Dynamics in New England: Ecosystem Structure and Function as a Consequence of 5000 years of Change,* D. Foster and J. Aber, eds. Synthesis Volume of the Harvard Forest LTER Program. Oxford University Press.

Nadelhoffer, K. J., M. R. Downs, and B. Fry. 1999. Sinks for ^{15}N-enriched additions to an oak forest and a red pine plantation. *Ecol. Appl.* **9:** 72–86.

Nadelhoffer, K., M. Downs, B. Fry, A. Magill, and J. Aber. 1999. Controls on N retention and exports in a forested watershed. *Environ. Monit. Assess.* **55:** 187–210.

Nadelhoffer, K. J., B. A. Emmett, P. Gundersen, O. J. Kjønaas, C. J. Koopmans, P. Schleppi, A. Tietema, and R. F. Wright. 1999. Nitrogen deposition makes a minor contribution to carbon sequestration in temperate forests. *Nature* **398:** 145–148.

Nasi, E., and M. Gomez. 1999. Divalent cation interactions with light-dependent K channels: kinetics of voltage-dependent block and requirement for an open pore. *J. Gen. Physiol.* **114:** 653–671.

Neill, C., M. C. Piccolo, J. M. Melillo, P. A. Steudler, and C. C. Cerri. 1999. Nitrogen dynamics in Amazon forest and pasture soils measured by ^{15}N pool dilution. *Soil Biol. Biochem.* **31:** 567–572.

Novales Flamarique, I., and F. I. Hárosi. 1999. Photoreceptor pigments of the blueback herring (*Alosa aestevalis*, Clupeidae) and the Atlantic silverside (*Menidia menidia*, Atherinidae). *Biol. Bull.* **197:** 235–236.

Ogunseitan, O. A., S. L. Yang, and E. Scheinbach. 1999. The δ-aminolevulinate dehydratase of marine *Vibrio alginolyticus* is resistant to lead (Pb). *Biol. Bull.* **197:** 283–284.

Oliver, S. J., and E. Watson. 1999. Threat-sensitive nest defense in domino damselfish (*Dascyllus albisella*). *Biol. Bull.* **197:** 244–246.

Palazzo, R. E. 1999. The centrosome. *Sci. Med.* **6:** 31–41.

Palazzo, R. E., and J. M. Vogel. 1999. Isolation of centrosomes from *Spisula solidissima* oocytes. In *Mitosis and Meiosis*, C. L. Rieder, ed. *Methods Cell Biol.* **61:** 36–56.

Palazzo, R. E., E. A. Vaisberg, D. G. Weiss, S. A. Kuznetsov, and W. Steffen. 1999. Dynein is required for spindle assembly in cytoplasmic lysates of *Spisula solidissima* oocytes. *J. Cell Sci.* **112:** 1291–1302.

Pease, K. M., L. Claessens, C. Hopkinson, E. Rastetter, J. Vallino, and N. Kilham. 1999. Ipswich River nutrient dynamics: preliminary assessment of a simple nitrogen-processing model. *Biol. Bull.* **197:** 289–290.

Pepperell, J. R., K. Kommineni, S. Buradagunta, P. J. S. Smith, and D. L. Keefe. 1999. Transmembrane regulation of intracellular calcium by a plasma membrane sodium/calcium exchanger in mouse oocytes. *Biol. Reprod.* **60:** 1137–1143.

Perrone-Capano, C., M. Crispino, E. Menichini, B. B. Kaplan, and A. Giuditta. 1999. Ribosomal RNAs synthesized by isolated squid nerves and ganglia differ from native ribosomal RNAs. *J. Neurochem.* **72:** 910–918.

Petermann, U., I. D. Baikie, and B. Lagel. 1999. Kelvin probe study of metastable states during initial oxygen adsorption dynamics on Si (111) 7 × 7. *Thin Solid Films* **343–344:** 492–494.

Peterson, B. J. 1999. Stable isotopes as tracers of organic matter input and transfer in benthic food webs: a review. *Acta Oecologia* **20:** 479–487.

Popescu, O., R. Interior, G. Misevic, M. M. Burger, and W. J. Kuhns. 1999. Biosynthesis of tyrosine O-sulfate by cell proteoglycan from the marine sponge, *Microciona prolifera*. *Biol. Bull.* **197:** 279–281.

Porterfield, D. M., A. Kuang, P. J. S. Smith, M. Crispi, and M. E. Musgrave. 1999. Oxygen-depleted zones inside reproductive structures of *Brassicaceae*: implications for oxygen control of seed development. *Can. J. Bot.* **77:** 1439–1446.

Price, N. N., and A. F. Mensinger. 1999. Predator-prey interactions of juvenile toadfish, *Opsanus tau*. *Biol. Bull.* **197:** 246–247.

Rainey, S. M., K. J. Nadelhoffer, W. L. Silver, and M. R. Downs. 1999. Effects of chronic nitrogen additions to understory species in a red pine plantation. *Ecol. Appl.* **9:** 949–957.

Rastetter, E. B., L. Gough, A. E. Hartley, D. A. Herbert, K. J. Nadelhoffer, and M. Williams. 1999. A revised assessment of species redundancy and ecosystem reliability. *Conserv. Biol.* **13:** 440–443.

Reilly, J., R. Prinn, J. Harnisch, J. Fitzmaurice, H. Jacoby, D. Kicklighter, J. Melillo, P. Stone, A. Sokolov, and C. Wang. 1999. Multi-gas assessment of the Kyoto Protocol. *Nature* **401:** 549–555.

Rieder, C. L., and G. Cassels. 1999. Correlative light and electron microscopy of mitotic cells in monolayer cultures. *Methods Cell Biol.* **61:** 297–315.

Rieder, C. L., and R. Cole. 1999. Chromatid cohesion during mitosis: lessons from meiosis. *J. Cell Sci.* **112:** 2607–2613.

Rigby, A., E. Lucas-Mernier, D. Kalume, E. Czerwiec, B. Hambe, I. Dahlquist, P. Fossier, G. Baux, P. Roepstorff, J. Baleja, B. C. Furie, B. Furie, and J. Stenflo. 1999. A novel *Conus textile* conotoxin, e-TxIX with unusual posttranslational modifications reduces presynaptic Ca^{2+} influx. *Proc. Natl. Acad. Sci. USA.* **96:** 5758–5763.

Riley, M. 1999. Correlates of smallest sizes for microorganisms. Pp. 21–25 in *Size Limits of Very Small Organisms: Proceedings of a Workshop*. National Academy of Sciences, Washington, DC.

Robertson, G. P., D. Wedin, P. M. Groffman, J. M. Blair, E. Holland, K. J. Nadelhoffer, and D. Harris. 1999. Soil carbon and nitrogen availability: nitrogen mineralization, nitrification, and soil respiration potentials. Pp. 258–271 in *Standard Soil Methods for Long Term Ecological Research*, G. P. Robertson, C. S. Bledsoe, D. C. Coleman, and P. Sollins, eds. Oxford University Press, New York.

Roger, A. J., H. G. Morrison, and M. L. Sogin. 1999. Primary structure and phylogenetic relationships of a malate dehydrogenase gene from *Giardia lamblia*. *J. Mol. Evol.* **48**(6): 750–755.

Ross, W. N., L. B. Cohen, and D. Zecevic. 1999. Optical recording of neuronal activity. Pp. 1542–1544 in *Encyclopedia of Neuroscience*, 2nd ed., G. Adelman, ed. Elsevier Science Publishers, Amsterdam.

Ruta, V. J., F. A. Dodge, and R. B. Barlow. 1999. Evaluation of circadian rhythms in the *Limulus* eye. *Biol. Bull.* **197:** 233–234.

Sanchez, L. B., H. G. Morrison, M. L. Sogin, and M. Muller. 1999. Cloning and sequencing of an acetyl-CoA synthetase (ADP-forming) gene from the amitochondriate protist, *Giardia lamblia*. *Gene* **233**(1–2): 224–232.

Schnackenberg, B. J., and R. E. Palazzo. 1999. Identification and function of the centrosome centromatrix. *Biol. Cell* **91:** 429–438.

Silver, R. B., and N. M. Deming. 1999. Leukotriene B_4 as calcium agonist for nuclear envelope breakdown: an enzymological survey of endomembranes of mitotic cells. *Biol. Bull.* **197:** 268–270.

Sloboda, Roger D. 1999. Membrane trafficking and the cytoskeleton: an integrated view. *EMBO J.* **18:** 5447–5452.

Smilenov, Lubomir B., A. Milhailov, R. J. Pelham Jr., E. E. Marcantonio, and G. G. Gundersen. 1999. Focal adhesion motility revealed in stationary fibroblasts. *Science* **286:** 1172–1174.

Smith, P. J. S., K. Hammar, D. M. Porterfield, R. H. Sanger, and J. R. Trimarchi. 1999. A self-referencing, non-invasive, ion-selective electrode for single cell detection of trans-plasma membrane calcium flux. *Microsc. Res. Tech.* **46:** 398–417.

Sotelo, J. R., A. Kun, J. C. Benech, A. Giuditta, J. Morillas, and C. R. Benech. 1999. Ribosomes and polyribosomes are present in the squid giant axon: an immunocytochemical study. *Neuroscience* **90:** 705–715.

Tang, K. Q., N. N. Price, M. D. O'Neill, A. F. Mensinger, and R. T. Hanlon. 1999. Temperature effects on first-year growth of cultured oyster toadfish, *Opsanus tau*. *Biol Bull.* **197:** 247–248.

Tettelback, S. T., C. Smith, R. Smolowitz, K. Tetrault, and S. Dumais. Evidence for fall spawning of northern bay scallops *Argopecten irradians* (Lamarck 1819) in New York. *J. Shellfish Res.* **18:** 47–58.

Thomas, S. M., A. H. Johnson, J. Frizano, D. R. Vann, D. J. Zarin, and A. Joshi. 1999. Phosphorus fractions in montane forest soils of the Cordillera de Piuchué, Chile: biogeochemical implications. *Plant Soil* **211:** 139–148.

Tian, H., J. M. Melillo, D. W. Kicklighter, A. D. McGuire, and J. Helfrich. 1999. The sensitivity of terrestrial carbon storage to historical climate variability and atmospheric CO_2 in the United States. *Tellus* **51B:** 414–452.

Tokumaru, H., and G. J. Augustine. 1999. UNC-13 and neurotransmitter release. *Nature Neurosci.* **2:** 929–930.

Tomasky, G., J. Barak, I. Valiela, P. Behr, L. Soucy, and K. Foreman. 1999. Nutrient limitation of phytoplankton growth in Waquoit Bay, Massachusetts, USA: a nutrient enrichment study. *Aquat. Ecol.* **33:** 147–155.

Tran, P. T., P. Maddox, F. Chang, and S. Inoué. 1999. Dynamic confocal imaging of interphase and mitotic microtubules in the fission yeast, *S. pombe*. *Biol. Bull.* **197:** 262–263.

Tucker, J., N. Sheats, A. E. Giblin, C. S. Hopkinson, and J. P. Montoya. 1999. Using stable isotopes to trace sewage-derived material through Boston Harbor and Massachusetts Bay. *Mar. Environ. Res.* **48:** 353–375.

Usdin, M. T., P. F. Shelbourne, R. M. Myers, and D. V. Madison. 1999. Impaired synaptic plasticity in mice carrying the Huntington's disease mutation. *Hum. Mol. Genet.* **8:** 839–846.

Vasse, A., A. Child, and N. Wainwright. 1999. Prophenoloxidase is not activated by microbial signals in *Limulus polyphemus*. *Biol. Bull.* **197:** 281–282.

Viscogliosi, E., V. P. Edgcomb, D. Gerbod, C. Noël, and P. Delgado-Viscogliosi. 1999. Molecular evolution inferred from small subunit rRNA sequences: what does it tell us about phylogenetic relationships and taxonomy of the parabasalids? *Parasite* **6:** 279–291.

Warner, Anne K., and Roger D. Sloboda. 1999. C-Terminal domain of the mitotic apparatus protein p62 targets the protein to the nucleolus during interphase. *Cell Motil. Cytoskeleton* **44:** 68–80.

Wassersug, Richard J. 1999. Life without gravity. *Nature* **401:** 758.

Weidner, E., and A. Findley. 1999. Extracellular survival of an intracellular parasite (*Spraguea lophii*, Microsporea). *Biol. Bull.* **197:** 270–271.

Widener, J. W., and R. B. Barlow. 1999. Decline of a horseshoe crab population on Cape Cod. *Biol. Bull.* **197:** 300–302.

Williams, M., and E. B. Rastetter. 1999. Vegetation characteristics and primary productivity along an arctic transect: Implications for scaling up. *J. Ecol.* **87:** 885–898.

Wolfe, F. L., K. D. Kroeger, and I. Valiela. 1999. Increased lability of estuarine dissolved organic nitrogen from urbanized watersheds. *Biol. Bull.* **197:** 290–292.

Wöllert, T., A. S. DePina, and G. M. Langford. 1999. Effects of vanadate on actin-dependent vesicle motility in extracts of clam oocytes. *Biol. Bull.* **197:** 265–266.

Wollheim, W. M., B. J. Peterson, L. A. Deegan, M. Bahr, J. E. Hobbie, D. Jones, W. B. Bowden, A. E. Hershey, G. W. Kling, and M. C. Miller. 1999. A coupled field and modeling approach for the analysis of nitrogen cycling in streams. *J. North Am. Benthol. Soc.* **18:** 199–221.

Wu, J-Y., L. B. Cohen, and C. X. Falk. 1999. Fast multisite optical measurement of membrane potential. With two examples. Pp. 222–237 in *Fluorescent and Luminescent Probes for Biological Activity*, 2nd ed., W. T. Mason, ed. Academic Press.

Wu, X. Y., and R. E. Palazzo. 1999. Differential regulation of paternal *vs.* maternal centrosomes. *Proc. Natl. Acad. Sci. USA* **96:** 1397–1402.

Young, T., S. Komarow, L. Deegan, and R. Garritt. 1999. Population size and summer home range of the green crab, *Carcinus maenus*, in salt marsh tidal creeks. *Biol. Bull.* **197:** 297–299.

Zecevic, D. 1999. Fast optical recordings of membrane potential changes from dendrites of pyramidal neurons. *J. Neurophysiol.* **82:** 1615–1621.

Zettler, E., and J. Atema. 1999. Chemoreceptor cells as concentration slope detectors: preliminary evidence from the lobster nose. *Biol. Bull.* **197:** 252–253.

Zigman, S., N. S. Rafferty, K. A. Rafferty, and N. Lewis. 1999. Effects of green tea polyphenols on lens photooxidative stress. *Biol. Bull.* **197:** 285–286.

Zottoli, S. J., F. R. Akanki, N. A. Hiza, D. A. Ho-Sang Jr., M. Motta, X. Tan, K. M. Watts, and E.-A. Seyfarth. 1999. Physiological characterization of supramedullary/dorsal neurons of the cunner, *Tautogolabrus adspersus*. *Biol. Bull.* **197:** 239–240.

Volume 199

Number 2

THE BIOLOGICAL BULLETIN

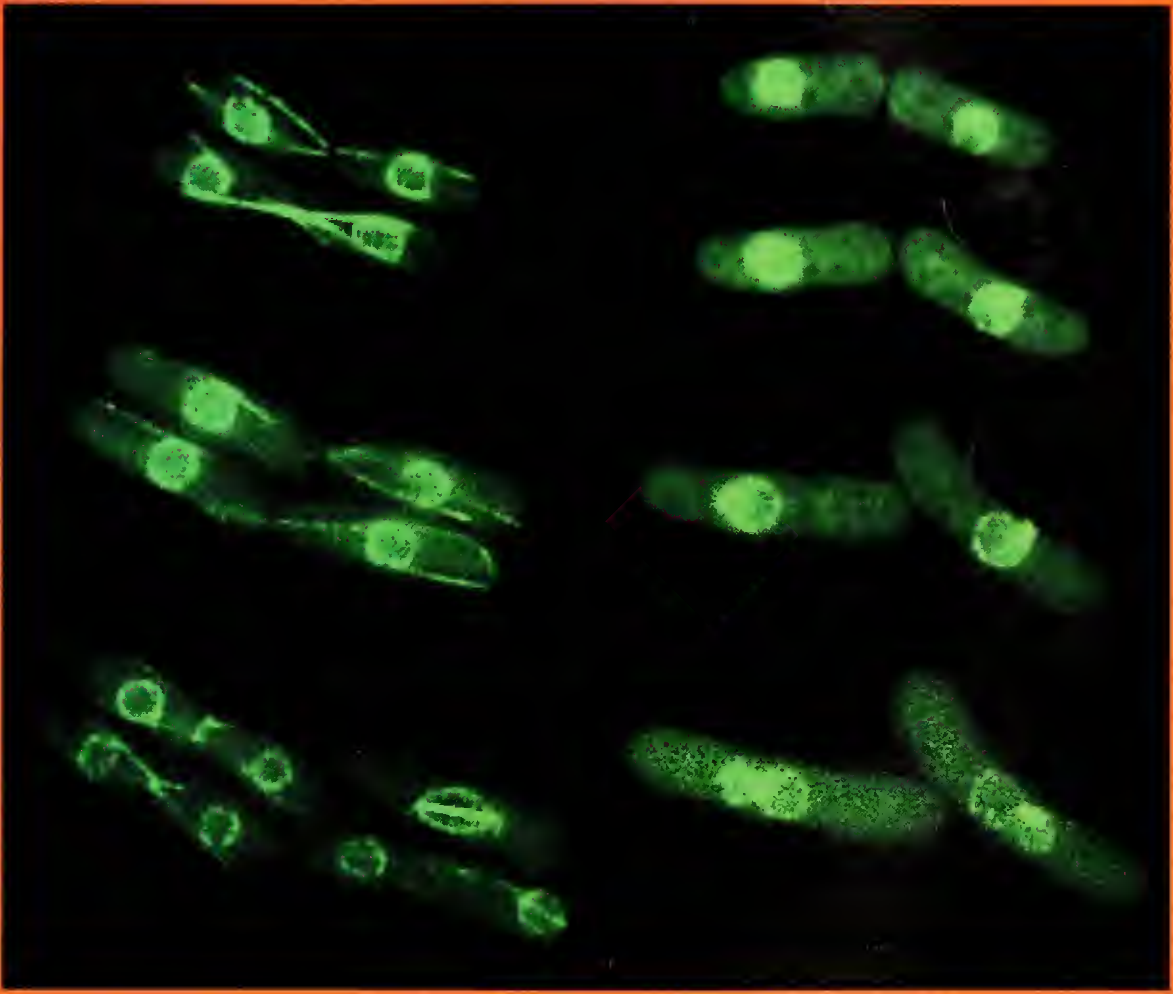

OCTOBER 2000

Published by the Marine Biological Laboratory

Thanks Galileo, Hooke and Leeuwenhoek for the incentive.

We walk in the footsteps of visionaries. And see with the eyes of disciples.

Galileo up close: astronomer, physicist, mathematician, dethroner of Aristotle, defender of Copernicus and, yes, credited with making double convex lenses and the first biological observations with a microscope. A compound microscope. In 1624.

Hooke: 43 years later, the compound microscope reveals living things are composed of cells.

Leeuwenhoek: invents the first practical microscope and discovers bacteria.

Armed with the knowledge and inspiration of these and other Olympians, secure in the history of our own accomplishments and aware that the mind's eye should always focus on challenging the enigmatic as well as the undeniable, Olympus has created the BX2 series of clinical and research microscopes, noteworthy for their enhancements in optics, imaging and ergonomics.

And each so individual, it deserves the nomenclature My Microscope.

From possibility to actuality, it is wonderful to behold.
A posse ad esse est mirabile visu.

Welcome to the next golden age of microscopy.

BX2
Microscope Series

The BX41

The new standard in laboratory microscopy vis-a-vis performance, versatility, operation.

Uncanny digitized imaging: enhanced with the **DP11 digital camera**, delivering high-resolution image recording beyond the norm.

Unusually insightful optics: observe magnifications from **1.25x to 100x without changing the condenser.** Choice of condensers includes Abbe, swing-out, phase-contrast and darkfield.

Unerringly precise-motion stage: selectable for right/left hand. Discover speed, ease, touch, comfort, and clinical accuracy.

Uncommonly easy-to-operate controls: extended fine-focus knob; forwarded-positioned illumination intensity dial; tactile X-Y control.

The BX45

The new standard in ergonomic microscopy. A dramatic metamorphosis: innovative, intelligent, insightful design improvements specifically addressing the needs of those spending hours looking through a microscope.

The **lowest low-position stage: three inches lower** than standard microscopes, offering the promise of minimum effort and hand movement when changing specimens.

The **tilting, telescoping observation tube:** a marvel of adjustability, it can be changed to accommodate any observation position. 80mm higher and 70mm closer to the operator than a conventional tilting tube. And the eyepoint can be moved forward by 45mm and inclined from 0–25 degrees.

The BX51

The new standard in research microscopy. The words "new" and "standard" really don't do it justice. How about "ingenious" or "original," "paragon" or "prototypical." Prepare yourself for a higher power.

The **6-position filter cube turret:** Not 4, not 5, but 6, so single and multi-band imaging of new fluorochromes and fluorescent proteins is faster, simpler and exclusively tailored.

The **rectangular field stop: ours alone.** By cleverly matching the camera's field of view, only the area requiring fluorescence excitation is exposed. Which means that the surrounding areas are protected from photo bleaching.

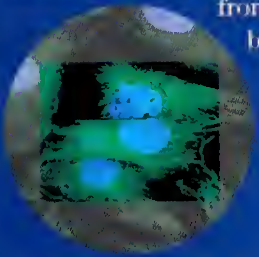

The **fluorescence excitation balancers:** another **Olympus exclusive.** A continuously variable excitation bandwidth. Visualization is enhanced, differentiation of multi-labels is immeasurably improved, capturing of images is at an unheard-of level.

Triple Labeled Specimen (l to r):

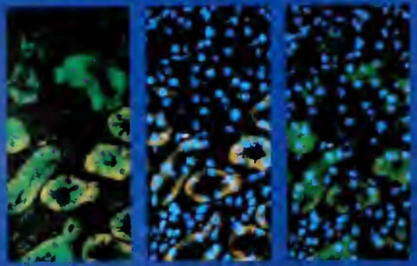

- with prevalent FITC and Cy3
- with prevalent DAPI and Cy3
- with balanced fluorescence emission

wider mirror
aspherical lens

The **aspherical collector lens:** *sui generis*, in a class by itself. Specimens appear **brighter** and **more evenly illuminated**; and achromatic performance now incorporates wavelengths from UV to IR.

The **universal condenser: with 8 positions**, it can accept optical inserts for DIC, phase, brightfield and darkfield illumination. And the advanced Nomarski DIC system has been expanded and optimized to encompass prisms for enhanced contrast and image resolution.

OLYMPUS®
FOCUS ON LIFE

Visit us at www.olympusamerica.com
or call 1-800-455-8236

© Olympus America Inc.

THE
BIOLOGICAL BULLETIN
OCTOBER 2000

Editor	Michael J. Greenberg	The Whitney Laboratory, University of Florida
Associate Editors	Louis E. Burnett	Grice Marine Biological Laboratory, College of Charleston
	R. Andrew Cameron	California Institute of Technology
	Charles D. Derby	Georgia State University
	Michael LaBarbera	University of Chicago
Section Editor	Shinya Inoué, *Imaging and Microscopy*	Marine Biological Laboratory
Online Editors	James A. Blake, *Keys to Marine Invertebrates of the Woods Hole Region*	ENSR Marine & Coastal Center, Woods Hole
	William D. Cohen, *Marine Models Electronic Record and Compendia*	Hunter College, City University of New York
Editorial Board	Peter B. Armstrong	University of California, Davis
	Ernest S. Chang	Bodega Marine Lab., University of California, Davis
	Thomas H. Dietz	Louisiana State University
	Richard B. Emlet	Oregon Institute of Marine Biology, Univ. of Oregon
	David Epel	Hopkins Marine Station, Stanford University
	Gregory Hinkle	Cereon Genomics, Cambridge, Massachusetts
	Makoto Kobayashi	Hiroshima University of Economics, Japan
	Esther M. Leise	University of North Carolina Greensboro
	Donal T. Manahan	University of Southern California
	Margaret McFall-Ngai	Kewalo Marine Laboratory, University of Hawaii
	Mark W. Miller	Institute of Neurobiology, University of Puerto Rico
	Tatsuo Motokawa	Tokyo Institute of Technology, Japan
	Yoshitaka Nagahama	National Institute for Basic Biology, Japan
	Sherry D. Painter	Marine Biomed. Inst., Univ. of Texas Medical Branch
	J. Herbert Waite	University of California, Santa Barbara
	Richard K. Zimmer	University of California, Los Angeles
Editorial Office	Pamela Clapp Hinkle	Managing Editor
	Victoria R. Gibson	Staff Editor
	Carol Schachinger	Editorial Associate
	Carol Marrama	Subscription & Advertising Secretary

Published by
Marine Biological Laboratory
Woods Hole, Massachusetts

NOV 07 2000

Cover

Fission yeast *(Saccharomyces pombe)*—in contrast to budding yeast—is a rod-shaped cell that divides by cleaving medially. The nucleus is located at the geometric center of the cell, where it is attached to multiple bundles of dynamic microtubules that push on it. As shown on the cover, both the nuclear membrane and the tubulin bundles can be visualized by fluorescence microscopy in a strain of fission yeast that expresses a pair of proteins fused to green fluorescent protein (GFP): nucleoporin-GFP and GFP-tubulin.

P.T. Tran, V. Doye, F. Chang, and S. Inoué have used this fluorescent strain of fission yeast to test the hypothesis that the microtubular bundles determine the central position of the nucleus which, in turn, determines the position of the cleavage plane and the septum that forms between the daughter cells. The details were reported at the General Scientific Meetings of the Marine Biological Laboratory in August, 2000 (see Tran *et al.*, p. 205 in this issue).

The images on the cover were produced at room temperature by time-lapse fluorescence microscopy. The panel on the left comprises successive images—taken at intervals of 2 hours—of untreated cells undergoing cell division. During interphase, the microtubules span the length of the cell. As the cells grow, the nucleus comes to lie at the center of the cell, where subsequent cell division and septation occurs, creating two daughter cells of approximately equal length. Note that, during mitosis, the interphase microtubules disappear from the cell cytoplasm, whilst the mitotic spindle appears prominently inside the cell nucleus.

The right panel on the cover shows images of cells treated with MBC, a drug that depolymerizes microtubules. Without microtubules, the nuclei are offset, the cell cycle is delayed, and no spindles form. Subsequent division planes and septa are formed at the location of the offset nuclei, creating "cut" nuclei in daughter cells of unequal length. These treated cells do not survive.

Cover design by Beth Liles

CONTENTS

Volume 199, No. 2: October 2000

RESEARCH NOTE

Hourdez, Stéphane, Jason Lamontagne, Pat Peterson, Roy E. Weber, and Charles R. Fisher
Hemoglobin from a deep-sea hydrothermal-vent copepod . . . 95

PHYSIOLOGY

Marsh, Adam G., Patrick K.K. Leong, and Donal T. Manahan
Gene expression and enzyme activities of the sodium pump during sea urchin development: implications for indices of physiological state . . . 100
Hill, Richard W., John W.H. Dacey, and Ahser Edward
Dimethylsulfoniopropionate in giant clams (Tridacnidae) . . . 108

ECOLOGY AND EVOLUTION

Baker, Shirley M., Jeffrey S. Levinton, and J. Evan Ward
Particle transport in the zebra mussel, *Dreissena polymorpha* (Pallas) . . . 116
LaJeunesse, T.C., and R.K. Trench
Biogeography of two species of *Symbiodinium* (Freudenthal) inhabiting the intertidal sea anemone *Anthopleura elegantissima* (Brandt) . . . 126

NEUROBIOLOGY AND BEHAVIOR

Rosenthal, Joshua J.C., and Francisco Bezanilla
Seasonal variation in conduction velocity of action potentials in squid giant axon . . . 135

DEVELOPMENT AND REPRODUCTION

Misamore, M.J., and J.W. Lynn
Role of the cytoskeleton in sperm entry during fertilization in the freshwater bivalve *Dreissena polymorpha* . . . 144

SHORT REPORTS FROM THE 2000 GENERAL SCIENTIFIC MEETINGS OF THE MARINE BIOLOGICAL LABORATORY

Featured Report

The Editors
Introduction to the featured report. On mapping odor quality . . . 161
Wachowiak, Matt, Michal Zochowski, Lawrence B. Cohen, and Chun X. Falk
The spatial representation of odors by olfactory receptor neuron input to the olfactory bulb is concentration invariant . . . 162

Neurobiology

Landowne, David
Heavy water (D_2O) alters the sodium channel gating current in squid giant axons . . . 164
White, Thomas H., Harris Ripps, Miduturu Srinivas, and Roberto Bruzzone
Voltage gating properties of channels formed by a skate retinal connexin . . . 165
Molina, Anthony J.A., Peter J.S. Smith, and Robert Paul Malchow
Hydrogen ion fluxes from isolated retinal horizontal cells: modulation by glutamate . . . 168
Wang, Jing W.
Odor-induced oscillatory activity in *Drosophila* CNS . . . 170
Hitt, James M., Frederick A. Dodge, Ehud Kaplan, and Robert B. Barlow
Circadian rhythms in the receptive fields of the *Limulus* lateral eye . . . 171
Fay, Richard R., and Peggy L. Edds-Walton
Frequency response of auditory brainstem units in toadfish (*Opsanus tau*) . . . 173
Yamaguchi, Ayako, Leonard K. Kaczmarek, and Darcy B. Kelley
Intrinsic membrane properties of laryngeal motoneurons that control sexually differentiated vocal behavior in African clawed frogs, *Xenopus laevis* . . . 175
Atherton, Jillian L., Matthew A. Krutky, James M. Hitt, Frederick A. Dodge, and Robert B. Barlow
Optic nerve responses of *Limulus* in its natural habitat at night . . . 176

Krutky, Matthew A., Jillian L. Atherton, Spence Smith, Frederick A. Dodge, and Robert B. Barlow
Do the properties of underwater lighting influence the visually guided behavior of *Limulus?* 178
Hale, Melina E.
Startle responses of fish without Mauthner neurons: escape behavior of the lumpfish (*Cyclopterus lumpus*) 180
Epstein, David A., Herman T. Epstein, Frank M. Child, and Alan M. Kuzirian
Memory consolidation in *Hermissenda crassicornis* ... 182
Abenavoli, A., L. Forti, and A. Malgaroli
Mechanisms of spontaneous miniature activity at CA3-CA1 synapses: evidence for a divergence from a random Poisson process 184

Physiology and Biochemistry

Novales Flamarique, Inigo, Kristiina Ovaska, and Theodore M. Davis
UV-B induced damage to the skin and ocular system of amphibians 187
Harrington, John M., and Peter B. Armstrong
Initial characterization of a potential anti-fouling system in the American horseshoe crab, *Limulus polyphemus* 189
Asokan, Rengasamy, Margaret T. Armstrong, and Peter B. Armstrong
Association of α_2-macroglobulin with the coagulin clot in the American horseshoe crab, *Limulus polyphemus:* a potential role in stabilization from proteolysis 190
Kuhns, William J., Max M. Burger, Mohan Sarker, Xavier Fernandez-Busquets, and Tracy Simpson
Enzymatic biosynthesis of N-linked glycan by the marine sponge *Microciona prolifera* 192
Armstrong, Peter B., and Rengasamy Asokan
A Ca^{+2}-independent cytolytic system from the blood of the marine snail *Busycon canaliculum* 194
Heck, Diane E., Lydia Louis, Michael A. Gallo, and Jeffrey D. Laskin
Modulation of the development of plutei by nitric oxide in the sea urchin *Arbacia punctulata* 195
Jung, Sung-Kwon, Katherine Hammar, and Peter J.S. Smith
Development of self-referencing oxygen microsensor and its application to single pancreatic HIT cells: effects of adenylate cyclase activator forskolin on oxygen consumption 197
Hanselmann, Rhea, Roxanna Smolowitz, and Daniel G. Gibson
Identification of proliferating cells in hard clams. . . 199
Brothers, Christine, Ernest Marks III, and Roxanna Smolowitz
Conditions affecting the growth and zoosporulation of the protistan parasite QPX in culture.......... 200

Cell Biology

Sandberg, Leslie, Phillip Stafford, and George M. Langford
Effects of myosin-II antibody on actin-dependent vesicle transport in extracts of clam oocytes 202
Stafford, Phillip, Jeremiah Brown, and George M. Langford
Interaction of actin- and microtubule-based motors in squid axoplasm probed with antibodies to myosin V and kinesin 203
Tran, P.T., V. Doye, F. Chang, and S. Inoué
Microtubule-dependent nuclear positioning and nuclear-dependent septum positioning in the fission yeast, *Saccharomyces pombe*..................... 205
Crawford, Karen
The role of microtubules during blastodisc formation of the squid *Loligo pealei*.................... 207
Weidner, Earl
Cytoplasmic proteins on the surface of discharged microsporidian sporoplasms 208
MacKenzie, Roger, David Newman, Max M. Burger, Rene Roy, and William J. Kuhns
Adhesion of a viral envelope protein to a non-self-binding domain of the aggregation factor in the marine sponge *Microciona prolifera*................ 209
Goda, Makoto, Mario H. Burgos, and Shinya Inoué
Fertilization-induced changes in the fine structure of stratified *Arbacia* eggs. I. Observations on live cells with the centrifuge polarizing microscope 212
Burgos, Mario H., Makoto Goda, and Shinya Inoué
Fertilization-induced changes in the fine structure of stratified *Arbacia* eggs. II. Observations with electron microscopy............................... 213
Gould, Robert M., Concetta M. Freund, John Engler, and Hilary G. Morrison
Optimization of homogenization conditions used to isolate mRNAs in processes of myelinating oligodendrocytes 215

Ecology, Biogeochemistry, and Population Biology

Kirkby, Ryan, Luc Claessens, Charles Hopkinson, Jr., Edward Rastetter, and Joseph Vallino
Modeling the effects of land-use change on nitrogen biogeochemistry in the Ipswich watershed, Massachusetts 218
Perring, Anne, Michael Williams, Charles Hopkinson, Jr., Edward Rastetter, and Joseph Vallino
Solute dynamics in storm flow of the Ipswich River Basin: effects of land use...................... 219
Westgate, Elizabeth J., Kevin D. Kroeger, Wendy J. Pabich, and Ivan Valiela
Fate of anthropogenic nitrogen in a nearshore Cape Cod aquifer 221

Denault, Michelle, Erica Stieve, and Ivan Valiela
Effects of nitrogen load and irradiance on photosynthetic pigment concentrations in *Cladophora vagabunda* and *Gracilaria tikvahiae* in estuaries of Waquoit Bay 223
Greenbaum, Adena, and Anne Giblin
Differences in properties of salt marsh sediment between hayed and reference sites 225
Chikarmane, Hemant M., Alan M. Kuzirian, Robbin Kozlowski, Mark Kuzirian, and Tony Lee
Population genetic structure of the goosefish, *Lophius americanus* 227

ORAL PRESENTATIONS

Published by title only 229

THE BIOLOGICAL BULLETIN

THE BIOLOGICAL BULLETIN is published six times a year by the Marine Biological Laboratory, 7 MBL Street, Woods Hole, Massachusetts 02543.

Subscriptions and similar matter should be addressed to Subscription Manager, THE BIOLOGICAL BULLETIN, Marine Biological Laboratory, 7 MBL Street, Woods Hole, Massachusetts 02543. Subscription per year (six issues, two volumes): $225 for libraries; $95 for individuals. Subscription per volume (three issues): $112.50 for libraries; $47.50 for individuals. Back and single issues (subject to availability): $40 for libraries; $20 for individuals.

Communications relative to manuscripts should be sent to Michael J. Greenberg, Editor-in-Chief, or Pamela Clapp Hinkle, Managing Editor, at the Marine Biological Laboratory, 7 MBL Street, Woods Hole, Massachusetts 02543. Telephone: (508) 289-7428. FAX: 508-289-7922. E-mail: pclapp@mbl.edu.

http://www.mbl.edu/BiologicalBulletin/

The home page for the electronic companion to THE BIOLOGICAL BULLETIN—*the Marine Models Electronic Record*—and other BIOLOGICAL BULLETIN publications is available on the World Wide Web at the address shown above.

THE BIOLOGICAL BULLETIN is indexed in bibliographic services including *Index Medicus* and MEDLINE, *Chemical Abstracts, Current Contents, Elsevier BIOBASE/Current Awareness in Biological Sciences,* and *Geo Abstracts.*

Printed on acid free paper,
effective with Volume 180, Issue 1, 1991.

POSTMASTER: Send address changes to THE BIOLOGICAL BULLETIN, Marine Biological Laboratory,
7 MBL Street, Woods Hole, MA 02543.

Copyright © 2000, by the Marine Biological Laboratory

Periodicals postage paid at Woods Hole, MA, and additional mailing offices.
ISSN 0006-3185

INSTRUCTIONS TO AUTHORS

The Biological Bulletin accepts outstanding original research reports of general interest to biologists throughout the world. Papers are usually of intermediate length (10–40 manuscript pages). A limited number of solicited review papers may be accepted after formal review. A paper will usually appear within four months after its acceptance.

Very short, especially topical papers (less than 9 manuscript pages including tables, figures, and bibliography) will be published in a separate section entitled "Research Notes." A Research Note in *The Biological Bulletin* follows the format of similar notes in *Nature.* It should open with a summary paragraph of 150 to 200 words comprising the introduction and the conclusions. The rest of the text should continue on without subheadings, and there should be no more than 30 references. References should be referred to in the text by number, and listed in the Literature Cited section in the order that they appear in the text. Unlike references in *Nature,* references in the Research Notes section should conform in punctuation and arrangement to the style of recent issues of *The Biological Bulletin.* Materials and Methods should be incorporated into appropriate figure legends. See the article by Lohmann *et al.* (October 1990, Vol. **179:** 214–218) for sample style. A Research Note will usually appear within two months after its acceptance.

The Editorial Board requests that regular manuscripts conform to the requirements set below; those manuscripts that do not conform will be returned to authors for correction before review.

1. ***Manuscripts.*** Manuscripts, including figures, should be submitted in quadruplicate, with the originals clearly marked. (Xerox copies of photographs are not acceptable for review purposes.) The submission letter accompanying the manuscript should include a telephone number, a FAX number, and (if possible) an E-mail address for the corresponding author. The original manuscript must be typed in no smaller than 12 pitch or 10 point, using double spacing (*including* figure legends, footnotes, bibliography, etc.) on one side of 16- or 20-lb. bond paper, 8 by 11 inches. Please, no right justification. Manuscripts should be proofread carefully and errors corrected legibly in black ink. Pages should be numbered consecutively. Margins on all sides should be at least 1 inch (2.5 cm). Manuscripts should conform to the *Council of Biology Editors Style Manual,* 5th Edition (Council of Biology Editors, 1983) and to American spelling. Unusual abbreviations should be kept to a minimum and should be spelled out on first reference as well as defined in a footnote on the title page. Manuscripts should be divided into the following components: Title page, Abstract (of no more than 200 words), Introduction, Materials and Methods, Results, Discussion, Acknowledgments, Literature Cited, Tables, and Figure Legends. In addition, authors should supply a list of words and phrases under which the article should be indexed.

2. ***Title page.*** The title page consists of a condensed title or running head of no more than 35 letters and spaces, the manuscript title, authors' names and appropriate addresses, and footnotes listing present addresses, acknowledgments or contribution numbers, and explanation of unusual abbreviations.

3. ***Figures.*** The dimensions of the printed page, 7 by 9 inches, should be kept in mind in preparing figures for publication. We recommend that figures be about 1 times the linear dimensions of the final printing desired, and that the ratio of the largest to the smallest letter or number and of the thickest to the thinnest line not exceed 1:1.5. Explanatory matter generally should be included in legends, although axes should always be identified on the illustration itself. Figures should be prepared for reproduction as either line cuts or halftones. Figures to be reproduced as line cuts should be unmounted glossy photographic reproductions or drawn in black ink on white paper, good-quality tracing cloth or plastic, or blue-lined coordinate paper. Those to be reproduced as halftones should be mounted on board, with both designating numbers or letters and scale bars affixed directly to the figures. All figures should be numbered in consecutive order, with no distinction between text and plate figures and cited, in order, in the text. The author's name and an arrow indicating orientation should appear on the reverse side of all figures.

Digital art: The Biological Bulletin will accept figures submitted in electronic form; however, digital art must conform to the following guidelines. Authors who create digital images are wholly responsible for the quality of their material, including color and halftone accuracy.

Format. Acceptable graphic formats are TIFF and EPS. Color submissions must be in EPS format, saved in CMKY mode.

Software. Preferred software is Adobe Illustrator or Adobe Photoshop for the Mac and Adobe Photoshop for Windows. Specific instructions for artwork created with various software programs are available on the Web at the Digital Art Information Site maintained by Cadmus Professional Communications at http://cjs.cadmus.com/da/home.html

Resolution. The minimum requirements for resolution are 1200 DPI for line art and 300 for halftones.

Size. All digital artwork must be submitted at its actual printed size so that no scaling is necessary.

Multipanel figures. Figures consisting of individual parts (*e.g.*, panels A, B, C) must be assembled into final format and submitted as one file.

Hard copy. Files must be accompanied by hard copy for use in case the electronic version is unusable.

Disk identification. Disks must be clearly labeled with the following information: author name and manuscript number; format (PC or Macintosh); name and version of software used.

Color: The Biological Bulletin will publish color figures and plates, but must bill authors for the actual additional cost of printing in color. The process is expensive, so authors with more than one color image should—consistent with editorial concerns, especially citation of figures in order—combine them into a single plate to reduce the expense. On request, when supplied with a copy of a color illustration, the editorial staff will provide a pre-publication estimate of the printing cost.

4. ***Tables, footnotes, figure legends, etc.*** Authors should follow the style in a recent issue of *The Biological Bulletin* in preparing table headings, figure legends, and the like. Because of the high cost of setting tabular material in type, authors are asked to limit such material as much as possible. Tables, with their headings and footnotes, should be typed on separate sheets, numbered with consecutive Roman numerals, and placed after the Literature Cited. Figure legends should contain enough information to make the figure intelligible separate from the text. Legends should be typed double spaced, with consecutive Arabic numbers, on a separate sheet at the end of the paper. Footnotes should be limited to authors' current addresses, acknowledgments or contribution numbers, and explanation of unusual abbreviations. All such footnotes should appear on the title page. Footnotes are not normally permitted in the body of the text.

5. ***Literature cited.*** In the text, literature should be cited by the Harvard system, with papers by more than two authors cited as Jones *et al.*, 1980. Personal communications and material in preparation or in press should be cited in the text only, with author's initials and institutions, unless the material has been formally accepted and a volume number can be supplied. The list of references following the text should be headed Literature Cited, and must be typed double spaced on separate pages, conforming in punctuation and arrangement to the style of recent issues of *The Biological Bulletin.* Citations should include complete titles and inclusive pagination. Journal abbreviations should normally follow those of the U. S. A. Standards Institute (USASI), as adopted by BIOLOGICAL ABSTRACTS and CHEMICAL ABSTRACTS, with the minor differences set out below. The most generally useful list of biological journal titles is that published each year by BIOLOGICAL ABSTRACTS (BIOSIS List of Serials; the most recent issue). Foreign authors, and others who are accustomed to using THE WORLD LIST OF SCIENTIFIC PERIODICALS, may find a booklet published by the Biological Council of the U.K. (obtainable from the Institute of Biology, 41 Queen's Gate, London, S.W.7, England, U.K.) useful, since it sets out the WORLD LIST abbreviations for most biological journals with notes of the USASI abbreviations where these differ. CHEMICAL ABSTRACTS publishes quarterly supplements of additional abbreviations. The following points of reference style for THE BIOLOGICAL BULLETIN differ from USASI (or modified WORLD LIST) usage:

A. Journal abbreviations, and book titles, all underlined (for *italics*)

B. All components of abbreviations with initial capitals (not as European usage in WORLD LIST *e.g., J. Cell. Comp. Physiol.* NOT *J. cell. comp. Physiol.*)

C. *All* abbreviated components must be followed by a period, whole word components *must not* (*i.e., J. Cancer Res.*)

D. Space between all components (*e.g., J. Cell. Comp. Physiol.*, not *J.Cell.Comp.Physiol.*)

E. Unusual words in journal titles should be spelled out in full, rather than employing new abbreviations invented by the author. For example, use *Rit Vísindafjélags Islendinga* without abbreviation.

F. All single word journal titles in full (*e.g., Veliger, Ecology, Brain*).

G. The order of abbreviated components should be the same as the word order of the complete title (*i.e., Proc.* and *Trans.* placed where they appear, not transposed as in some BIOLOGICAL ABSTRACTS listings).

H. A few well-known international journals in their preferred forms rather than WORLD LIST or USASI usage (*e.g., Nature, Science, Evolution* NOT *Nature, Lond., Science, N.Y.; Evolution, Lancaster, Pa.*)

6. ***Reprints, page proofs, and charges.*** Authors may purchase reprints in lots of 100. Forms for placing reprint orders are sent with page proofs. Reprints normally will be delivered about 2 to 3 months after the issue date. Authors (or delegates for foreign authors) will receive page proofs of articles shortly before publication. They will be charged the current cost of printers' time for corrections to these (other than corrections of printers' or editors' errors). Other than these charges for authors' alterations, *The Biological Bulletin* does not have page charges.

Reference: *Biol. Bull.* **199:** 95–99. (October 2000)

Hemoglobin From a Deep-Sea Hydrothermal-Vent Copepod

STÉPHANE HOURDEZ[1,*], JASON LAMONTAGNE[2], PAT PETERSON[2], ROY E. WEBER[3], AND CHARLES R. FISHER[1]

[1]*Department of Biology, 208 Mueller Lab, Pennsylvania State University, University Park, Pennsylvania 16802;* [2]*Palisades High School, 35 Church Hill Road, Kintnersville, Pennsylvania 18930; and* [3]*Center for Respiratory Adaptation, Department of Zoophysiology, University of Aarhus, 8000 Aarhus C, Denmark*

Abstract. Deep-sea hydrothermal-vent fauna live in a highly variable environment where oxygen levels can be very low, and carbon dioxide and sulfide can reach high concentrations (1). These conditions are harsh for most aerobic metazoans, yet copepods can be abundant at hydrothermal vents. Here we report the structure and functional properties of hemoglobin extracted from the copepod *Benthoxynus spiculifer,* which was found in large numbers in a paralvinellid/gastropod community collection made during a cruise to the Juan de Fuca Ridge in 1998. Although hemoglobin has been reported in some littoral copepods (2), this is the first study of the structure and functional properties of copepod hemoglobin. Hemoglobin represents about 60% of the total soluble proteins extracted from *B. spiculifer,* and although it imparts a red color to the copepod, it does not provide a significant storage pool of oxygen. It is a 208-kDa protein, composed of 14 globin chains—7 of 14.3 kDa and 7 of 15.2 kDa. The hemoglobin has a very high and temperature-sensitive oxygen affinity, with no cooperativity or Bohr effect. These properties are adaptive for an animal living in a low-oxygen environment in which the primary function of the hemoglobin is most likely oxygen acquisition to support aerobic respiration.

Copepods occur in both freshwater and marine environments that range from pelagic to benthic and littoral to deep-sea (3). Red copepods have been observed at hydrothermal vents of the Mid-Atlantic Ridge, Juan de Fuca Ridge, and East Pacific Rise (SH, pers. obs.). However, the number of animals collected has previously been too small for a study of their oxygen-binding protein. On dive 3259 of the DSRV *Alvin,* a paralvinellid (worm)/gastropod community (similar to Community III described by Sarradin *et al.* [4]) was collected from the base of the S & M chimney on the main field of the Endeavour segment of the Juan de Fuca Ridge. In that community, the animals are probably exposed to temperatures ranging from 10° to 25°C (4). The collection was made using a new device, nicknamed the Chimney Master, which is a hydraulically actuated net lined with 62-μm mesh and suspended in an aluminum frame. The 30-cm-diameter open end of the device is placed over a community to be collected, and then the net is drawn closed by a stainless steel cable while the frame is held firmly against the substrate by the submersible. In an appropriate environment, the Chimney Master removes and collects all attached and associated fauna from the substrate along with a surface layer of loose rocks and sulfides.

The collection contained many specimens of the copepod *Benthoxynus spiculifer.* Examination of the animals revealed that their deep-red color was not due to the gut content (which consisted of white filamentous material resembling bacteria) but rather to a soluble pigment distributed throughout the rest of the body. About 6000 specimens were separated from the collection, using a pipette; these were rinsed, concentrated by centrifugation, and frozen at –70°C in several cryovials.

The hemoglobin was purified from an extract of about 4000 animals that were thawed; homogenized in an extraction buffer containing 1 μM PMSF (phenylmethanesulfonyl fluoride) and 1mM EDTA in 50 mM Tris, pH 8; and then centrifuged to remove animal debris. The extract was puri-

---

Received 19 April 2000; accepted 7 July 2000.

[*] To whom correspondence should be addressed. E-mail: hourdez@sb-roscoff.fr. Portions of this work were performed at the Station Biologique de Roscoff, CNRS-UPMC, BP74, 29682 Roscoff cedex, France.

fied by size exclusion chromatography (see legend of Fig. 1). The pigment eluted as a single pink band that represented about 55% to 60% of the total soluble proteins in the extract. Using proteins of known molecular weight for calibration, we estimated the apparent native molecular weight of the pigment to be 208 kDa. This pure fraction was used for further studies.

The light absorbance spectrum of the 208-kDa fraction showed the typical peaks for oxy-hemoglobin: α, β, and δ (Soret's band) peaks at 578 and 544 and 414 nm, respectively (Fig. 1). The γ and the protein peaks were present at 348 nm and 270 nm, respectively. The absence of a methemoglobin peak at 630 nm confirmed that little or no hemoglobin had been oxidized. The ratio α/β was 0.83, smaller than unity, as reported for some other extracellular hemoglobins (see [5]). The presence of hemoglobin has previously been reported in other copepods from reduced environments by Fox (2), who detected this protein *in vivo* using a microspectrophotometer. To determine the subunit structure of the 208-kDa fraction, it was further fractionated by SDS polyacrylamide gel electrophoresis in the presence and absence of β-mercaptoethanol (Fig. 2). Two bands, of 14.3 and 15.2 kDa, were resolved under both conditions. This suggests that the native molecule is composed of monodomain globin chains that are not linked by disulfide bonds. The bands were of similar intensity, suggesting that the intact hemoglobin molecule is composed of 14 chains (7 of each type), with a calculated mass of 206.5 kDa. This agrees well with the native mass estimated by gel filtration of 208 kDa. This structure is unusual for an arthropod hemoglobin (Table 1). Insect hemoglobins are generally much smaller (15-30 kDa), whereas those of Crustacea have a high molecular weight (220-4000 kDa). The mass of *B. spiculifer* hemoglobin is at the lower limit of those observed among crustaceans. The subunits are monodomain globins and not multidomain globins as is more normal for crustaceans (Table 1). With regard to subunit mass, *B. spiculifer* hemoglobin is similar to that found in Rhizocephala, although the native mass is 5 to 20 times smaller.

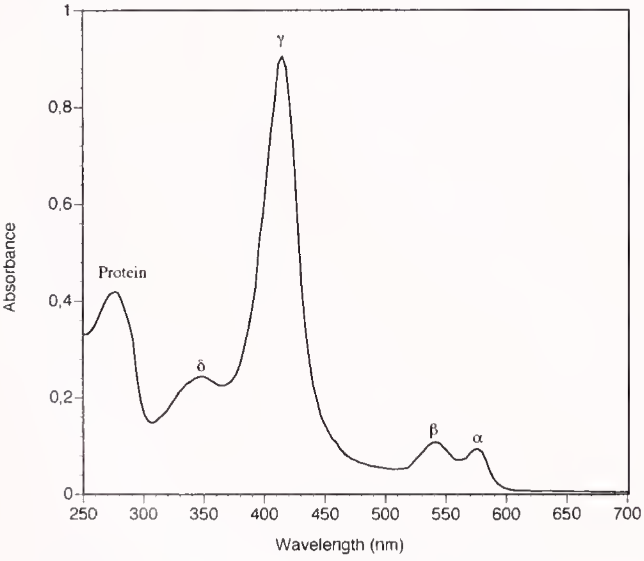

Figure 1. Absorbance spectrum of *Benthoxynus spiculifer* hemoglobin, extracted in 50 m*M* Tris pH 8, EDTA 1 m*M*, and PMSF 1 μM, and purified by FPLC on a Superose 6 column (5 to 5000 kDa mass separation range). The elution buffer contained NaCl 400 mmol l^{-1}, KCl 2.95 mmol l^{-1}, $MgSO_4$ 32 mmol l^{-1}, $CaCl_2$ 11 mmol l^{-1}, and HEPES 50 mmol l^{-1} at pH 7.0. This spectrum shows the typical Soret band at 414 nm and the α and β peaks of the liganded hemoglobin (at 578 and 544 nm, respectively).

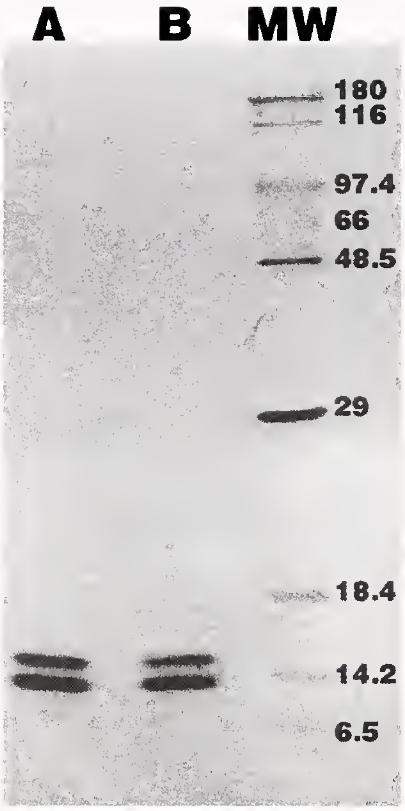

Figure 2. SDS-PAGE of *Benthoxynus spiculifer* hemoglobin. Lane A: SDS-treated sample; Lane B: SDS- and β-mercaptoethanol-treated sample. The gel was composed of a stacking gel (4% acrylamide) overlying a gradient separation gel (10% to 20% acrylamide) and was then silver-stained to reveal the presence of the proteins. The molecular weight of each subunit (14.3 and 15.2 kDa) was estimated using the Silver Staining Wide Range Molecular Weight Markers (Sigma) as calibration proteins ("MW" lane). Molecular weights are given in kilodaltons.

The functional properties of the hemoglobin were studied using the step-by-step procedure (6) in a modified diffusion chamber (7). Under the conditions we used, the oxygen affinity of the hemoglobin is extremely high, with P_{50} values at pH 7.3 of 0.05, 0.13, and 0.35 mm Hg at 10°, 20°, and 30°C, respectively (Fig. 3A). These affinities are among the highest reported for arthropod hemoglobins (8). Among the arthropods, only the conchostracan *Cyzicus hierosolymitanus* (9) has hemoglobin with higher affinity (P_{50} = 0.035 mmHg at 28°C and pH 7.2, Table 1). Both species, *B.*

Table 1

Occurrence and structural and functional characteristics of hemoglobin in arthropods

SbP	C	SbC	SpO	O	Native mass (kDa)	Subunit (kDa)	Domains/ subunit	P_{50} (Torr)	n_{50}	Bohr factor	ΔH (kJ/mol)	Reference
Uniramia												
	Hexapoda											
		Diplura			15 and 30	15	1	0.7	1	−0.15 to −0.9	−42.6	17, 18
Crustacea												
	Branchiopoda											
		Anostraca			260	130	9	1.8 to 5.3	1.6–1.9	0 to −0.21	−22.6 to −54.8	19
		Notostraca			600–800	34	2	20	2	−0.13	−30.9	20
		Cladocera			420–670	31	2	2.1 to 3.5	?	0	?	21
		Conchostraca			220–300	30	2	0.035 to 5.9	2.3–2.5	?	−20.5	9, 22
	Maxillopoda											
		Ostracoda			?	?	?	?	?	?	?	2
		Copepoda										
			Harpacticoida		?	?	?	?	?	?	?	2
			Siphonostomatoida		208	14–15	1	0.05	1	0	−68.7	This study
		Cirripedia										
			Rhizocephala		1000–4000	17	1	?	?	?	?	16
	Malacostraca											
		Eumalacostraca										
			Peracarida									
				Amphipoda	1800	175	10?	?	?	?	?	16

SbP: subphylum; C: class; SbC: subclass; SpO: superorder; O: order. Modified after Terwilliger (16). Conchastracan Hb, P_{50} measured at 28°C, all other P_{50} measured at 20°C.

spiculifer and *C. hierosolymitanus*, have P_{50} values 20 to 600 times smaller than the P_{50} values of other arthropod hemoglobins. The affinity of *B. spiculifer* hemoglobin for oxygen is also higher than that reported for the hemocyanins of other hydrothermal vent crustaceans, although their hemocyanin P_{50} values are quite low (reviewed in [10]).

Benthoxynus spiculifer hemoglobin lacks cooperativity (n_{50} = 1.0) over the range of temperature (10° to 30°C) and pH (6.7 to 8.1) examined. The hemoglobin components of *Chironomus thummi thummi* (Insecta) also lack cooperativity; however, in contrast to *B. spiculifer* hemoglobin, they are monomeric or dimeric (Table 1). The other arthropod hemoglobins are multimeric and exhibit some cooperativity (n = 1.6 to 2.3). Like the hemoglobin of most crustaceans, that of *B. spiculifer* does not exhibit a significant Bohr effect ($\Phi = +0.04$) (Table 1). However, the hemocyanins of hydrothermal vent crustaceans often show substantial Bohr effects (10), as do the hemoglobin components of the arthropod *C. thummi thummi* ($\Phi = -0.9$). *B. spiculifer* hemoglobin thus does not show any homotropic or heterotropic interactions and behaves like a myoglobin. Temperature has a strong effect on *B. spiculifer* hemoglobin, as shown by the apparent ΔH value of −69 kJ · mole^{-1} (Fig. 3B). This value is higher than that of other arthropod hemoglobins (Table 1) and is consistent with the absence of a Bohr effect (oxygenation-linked proton dissociation that is endothermic and decreases the overall exothermic heat of oxygenation) in *Benthoxynus* hemoglobin (11).

To determine the *in vivo* hemoglobin concentration, a small group of copepods (about 400 animals) was weighed and homogenized in a ground-glass tissue homogenizer, and the hemoglobin content of the homogenate was determined using the cyan-met-hemoglobin method and a millimolar absorption coefficient of 11 cm^{-1} at 540 nm (12). The estimated *in vivo* concentration of 0.95 m*M* heme explains the conspicuous red color of the animals. Large hemoglobin pools can play an important role in oxygen storage in some situations. However, assuming a respiratory rate similar to that of littoral harpacticoid copepods (13) and an abrupt switch from aerobiosis to anaerobiosis, we estimate that the quantity of hemoglobin present would support aerobic respiration for less than 2 min at 15°C and about 30 s at 25°C. Thus the hemoglobin pool is insufficient to allow the copepod to make more than short forays into anaerobic microhabitats without relying on anaerobic respiration. Another role of high affinity hemoglobins has been theorized to be detoxification of free radicals from oxygen or nitrogen monoxide (14). Although free radicals do form in sulfidic systems, and some vent animals have detoxification mechanisms (15), we consider it more likely that the hemoglobin of *B. spiculifer* functions primarily in oxygen acquisition from the environment. The other hemoglobin-containing copepods identified by Fox (2) were collected from muddy and reduced environments with low levels of oxygen and high levels of sulfide. The adaptive significance of hemoglobin for acquisition of oxygen in these environments is

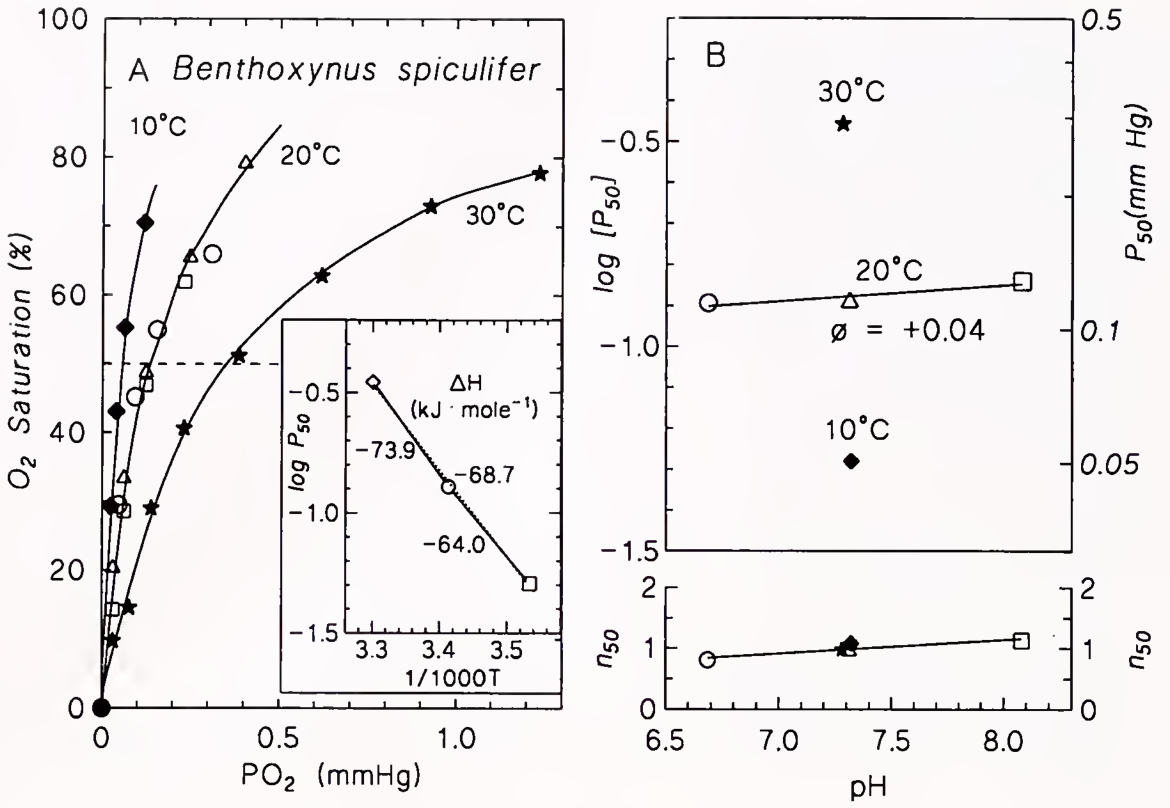

Figure 3. (A) Oxygen equilibrium curves of *Benthoxynus spiculifer* hemoglobin at 10°, 20°, and 30°C, measured as previously described (5), and (inset) arrhenius plot showing calculated values of the apparent oxygenation enthalpy values (ΔH). (B) Variation of P_{50} and n_{50} values with pH and temperature.

apparent, and the very high affinity of the hemoglobin in *B. spiculifer* probably also reflects the very low oxygen tensions this species experiences in its hydrothermal vent microhabitat. In this context it is relevant that hemoglobins or hemocyanins with high oxygen affinity characterize many hydrothermal vent animals (10).

Acknowledgments

We thank the captains, pilots, and crews of the R/V *Atlantis* and DSRV *Alvin* for their assistance at sea; Verena Tunnicliffe and Maia Tsurumi for identifying *B. spiculifer*; Anny Bang for assistance with the oxygen equilibrium experiments; and Veronique Robigou and the REVEL Project for providing science teachers with research opportunities. This project was supported by NSF OCE 9633105 and the REVEL Program (NSF OCE-9814073 to J.R. Delaney, with additional support from the Pennsylvania State University and the American Museum of Natural History).

Literature Cited

1. **Sarradin, P. M., J. C. Caprais, P. Briand, F. Gaill, B. Shillito, and D. Desbruyères. 1998.** Chemical and thermal description of the environment of the Genesis hydrothermal vent community (13 degrees N, EPR). *Cah. Biol. Mar.* 39(2): 159-167.
2. **Fox, H. M. 1957.** Haemoglobin in the Crustacea. *Nature* 179: 148.
3. **Humes, A. G. 1994.** How many copepods? *Hydrobiologia* 293: 1-7.
4. **Sarrazin, J., V. Robigou, S. K. Juniper, and J. R. Delaney. 1997.** Biological and geological dynamics over four years on a high temperature sulfide structure at the Juan de Fuca Ridge hydrothermal observatory. *Mar. Ecol. Prog. Ser.* 153: 5-24.
5. **Hourdez, S., F. H. Lallier, V. MartinJezequel, R. E. Weber, and A. Toulmond. 1999.** Characterization and functional properties of the extracellular coelomic hemoglobins from the deep-sea, hydrothermal vent scaleworm *Branchipolynoe symmytilida*. *Proteins Struct. Funct. Genet.* 34(4): 435-442.
6. **Weber, R. E. 1981.** Cationic control of O_2 affinity in lugworm erythrocruorin. *Nature* 292: 386-387.
7. **Sick, H., and K. Gersonde. 1969.** Method of continuous registration of O_2 binding curves of hemoproteins by means of a diffusion chamber. *Anal. Biochem.* 32: 362-376.
8. **Toulmond, A. 1992.** Properties and functions of extracellular heme pigments. Pp. 231-256 in *Blood and Tissues Oxygen Carriers*, C.P. Mangum, ed. Springer, Berlin.
9. **Amos, A. R., and A. Shejter. 1970.** Isolation and properties of the hemoglobin of the clam shrimp *Cyzicus* cf. *hierosolymitanus* (S. Fischer). *Comp. Biochem. Physiol.* 33: 481-490.
10. **Childress, J. J., and C. R. Fisher. 1992.** The biology of hydrothermal vent animals: physiology, biochemistry and autotrophic symbioses. *Oceanogr. Mar. Biol. Annu. Rev.* 30: 337-341.
11. **Perutz, M. 1990.** Mechanisms of cooperativity and allosteric regu-

lation in proteins. Cambridge University Press, Cambridge, UK. Pp. 1-101.

12. **Van Assendelft, O. W. 1970.** Spectrophotometry of haemoglobin derivatives. Royal Vangorcum, Assen, The Netherlands. 152 pp.
13. **Coull, B. C., and W. B. Vernberg. 1970.** Harpacticoid copepod respiration: *Enhydrosoma propinquum* and *Longipedia helgolandica. Mar. Biol.* 5: 341-344.
14. **Minning, D. M., A. J. Gow, J. Bonaventura, R. Braun, M. Dewhirst, D. E. Goldberg, and J. S. Stamler. 1999.** *Ascaris* haemoglobin is a nitric oxide-activated 'deoxygenase'. *Nature* 401: 497-502.
15. **Tapley, D. W., J. M. Shick, and G. R. Buettner. 1992.** Free radical production in hydrothermal vent invertebrates during sulfide oxidation. *Am. Zool.* 32(5): 67A.
16. **Terwilliger, N. B. 1992.** Molecular structure of the extracellular heme proteins. Pp. 87-116 in *Oxygen Carriers in Blood and Tissues, Vol. 13, Advances in Comparative and Environmental Physiology*, C.P. Mangum, ed. Springer, Berlin.
17. **Amiconi, G., E. Antonini, M. Brunori, H. Formaneck, and R. Huber. 1972.** Functional properties of native and reconstituted hemoglobins from *Chironomus thummi thummi. Eur. J. Biochem.* 31: 52-58.
18. **Weber, R. E., G. Braunitzer, and T. Kleinschmidt. 1985.** Functional multiplicity and structural correlations in the hemoglobin system of larvae of *Chironomus thummi thummi* (Insecta, Diptera): Hb components CTT I, CTT II , CTT III, CTT IV, CTT VI, CTT VIIB, CTT IX and CTT X. *Comp. Biochem. Physiol. B* 80: 747-753.
19. **D'Hondt, J., L. Moens, J. Heip, A. D'Hondt, and M. Kondo. 1978.** Oxygen-binding characteristics of three extracellular haemoglobins of *Artemia salina. Biochem. J.* 171: 705-710.
20. **Dangott, L. J., and R. C. Terwilliger. 1992.** Structural studies of a branchiopod crustacean (*Lepidurus bilobatus*) extracellular hemoglobin. Evidence for oxygen-binding domains. *Biochim. Biophys. Acta* 579: 452-461.
21. **Sugano, H., and T. Hoshi. 1970.** Purification and properties of blood hemoglobin from the fresh-water cladocera, *Moina macropopa* and *Daphnia magna. Biochim. Biophys. Acta* 229: 349-358.
22. **Dangott, L. J., and R. C. Terwilliger. 1981.** Arthropod extracellular hemoglobins: structural and functional properties. *Comp. Biochem. Physiol.B* 70: 549-557.

Reference: *Biol. Bull.* **199:** 100–107. (October 2000)

Gene Expression and Enzyme Activities of the Sodium Pump During Sea Urchin Development: Implications for Indices of Physiological State

ADAM G. MARSH*, PATRICK K.K. LEONG†, AND DONAL T. MANAHAN‡

Department of Biological Sciences, University of Southern California,
Los Angeles, California 90089-0371

Abstract. The sodium pump consumes a large portion of the metabolic energy (40%) in sea urchin larvae. Understanding the developmental regulation of ion pumps is important for assessing the physiological state of embryos and larvae. We sequenced a partial cDNA clone (1769 bp) from the sea urchin *Strongylocentrotus purpuratus* and found it to contain the C-terminal portion of an open reading frame coding for 195 amino acids that exhibited high sequence similarity (89%) to invertebrate α-subunits of the Na^+,K^+-ATPase sodium pump. Northern blots using the 3′ untranslated region of this cDNA specifically recognized a 4.6-kbp transcript under high stringency. During embryonic development, a rapid increase in levels of this mRNA transcript during gastrulation (25 h postfertilization) was paralleled by a concomitant increase in the total enzymatic activity of Na^+,K^+-ATPase. Expression of this subunit during gastrulation increased to a maximum at 36 h, followed by a rapid decline to trace levels by 60 h. The rate of removal of the transcript from the total RNA pool after 36 h closely followed a first-order exponential decay model ($r^2 = 0.988$), equivalent to a degradation rate of 7.8% h^{-1}. By 83 h, transcription of the α-subunit gene was low, yet sodium pump activity remained high. Molecular assays for the expression of this gene would underestimate sodium pump activities for assessing physiological state because of the temporal separation between maximal gene expression in a gastrula and maximal enzyme activities in the later larval stage. This finding illustrates the difficulty of using molecular probes for assessing the physiological state of invertebrate larvae.

Introduction

Maintaining Na^+ and K^+ ion gradients is one of the most energetically demanding processes of an organism's maintenance physiology. In general, animal cells routinely expend 20%–30% of their total metabolic energy on the activity of a single protein complex, the sodium pump (Na^+,K^+-ATPase; Siems *et al.*, 1982, 1992), and for adult marine invertebrates, the sodium pump can potentially account for 30%-70% of tissue metabolism (Baker and Connelly, 1966; Lucu and Pavicic, 1995). The ion gradients established by the sodium pump are critical for maintaining a cell's osmotic balance and resting membrane potential, as well as providing the electrochemical gradient necessary for the uptake of other ions, sugars, amino acids, and neurotransmitters *via* Na^+ coupled co-transporters (Blanco and Mercer, 1998).

The requirements for ion regulation change rapidly during embryonic development. The increase in cell number during early embryogenesis and the consequent increase in cellular-membrane surface area necessitates the production of more sodium pumps to regulate intracellular ion flux. The *in vivo* physiological activity of Na^+,K^+-ATPase has been characterized during early development in the sea urchins *Strongylocentrotus purpuratus* and *Lytechinus pictus* (Leong and Manahan, 1997). Using $^{86}Rb^+$ as a radioactive tracer for K^+ ion transport, Leong and Manahan (1997) described the ontogenetic changes in activity of

Received 29 February 2000; accepted 31 July 2000.

*Present address: College of Marine Studies, University of Delaware, Lewes, DE 19958.

†Present address: Department of Physiology and Biophysics, University of Southern California School of Medicine, Los Angeles, CA 90033.

‡To whom correspondence should be addressed. E-mail: *manahan@usc.edu*

Na^+,K^+-ATPase in living embryos. They found a large increase in activity—from nondetectable levels prior to fertilization to a high level accounting for 40% of total metabolic energy consumption at the pluteus larval stage (72 h postfertilization). By the same radiotracer techniques, the metabolic energy demand of Na^+,K^+-ATPase activity in the Antarctic sea urchin *Sterechinus neumayeri* was found to be as high as 80% of total metabolism at the pluteus larval stage at −1.5°C (Leong and Manahan, 1999). In the sea urchin *Hemicentrotus pulcherrimus*, the total protein activity and gene expression of Na^+,K^+-ATPase increases rapidly during gastrulation (Mitsunaga-Nakatsubo *et al.*, 1992a, b). Overall, the physiological importance of Na^+,K^+-ATPase activity during embryogenesis in sea urchins has significant implications for metabolic energy consumption during development.

This universal importance of Na^+,K^+-ATPase in animals suggests that measurements of this enzyme could be a useful indicator of physiological state. For larval stages in which direct enzyme assays are limited by the small amount of protein in an individual, measurements of gene expression might provide the sensitivity necessary to assay small amounts of tissue. Functional Na^+,K^+-ATPase pumps are a heterodimer (α, β subunits; Jorgensen and Skou, 1969), with the α-subunit possessing the ATP binding site and catalytic activity (Kyte, 1971). In this study, we describe the timing between transcription of the α-subunit and the appearance of functional sodium pumps during the development of *Strongylocentrotus purpuratus*. We also describe the ontogenetic changes in expression of the α-subunit to determine the developmental timing between increases in enzyme activity and the potential for using these measures as an index of physiological state in embryos and larvae.

Materials and Methods

Embryo cultures

Adult *Strongylocentrotus purpuratus* were induced to release gametes (injections of 0.5 *M* KCl), and fertilized eggs were divided into six 20-liter culture containers at a concentration of about 20 individuals per milliliter of filtered seawater (0.2 μm). Culture temperatures were maintained at 15°C during development. Embryos were maintained in suspension by paddles connected to slow stirring motors (~30 rpm). For the gene expression analysis, time-course samples were collected throughout development at the following times from an egg to a 4-arm pluteus larva: 0, 6, 8, 10, 12, 14, 16, 18, 20, 25, 31, 36, 42, 48, 60, 72, and 83 h postfertilization ($n = 17$). For each sample, about 100,000 embryos were removed by sieving (80-μm mesh) and pelleted by centrifugation (1000 × *g*) into 50-ml screw-cap tubes. Embryos were immediately dissolved in an acid-guanidinium buffer (4 *M* guanidinium isothiocyanate, 25 m*M* Na-citrate, 0.2% Sarkosyl and 215 m*M* β-mercaptoethanol; pH 5.2; Chomzinsky and Sacchi, 1987) and frozen at −80°C.

cDNA clone: sequencing and analysis

An expressed sequence tag (EST) library from activated coelomocytes of adult *S. purpuratus* was prepared by Smith *et al.* (1996), and a sequence fragment of one cDNA clone (#020) was found to have a high nucleotide similarity to the bovine α-subunit of Na^+,K^+-ATPase. We sequenced this clone (provided by C. L. Smith and E. H. Davidson) by random transposon insertion in a modified pBluescript (Stratagene) plasmid (pMOB; Strathmann *et al.*, 1991). The introduced transposon elements contained defined priming sites for subsequent manual sequencing of double-stranded plasmid templates using standard dideoxy termination reactions with ^{35}S-labeled dATP (Sequenase Reaction Kit, USB). Sequencing gels were visualized by autoradiography on X-ray film (Kodak, XAR 5). Nucleotide sequences were entered and edited using the software package MacVector 5.0 (Mac OS; Oxford Molecular Group), and contiguous overlaps between fragments were identified using the software package AssemblyLign 2.0 (Mac OS; Oxford Molecular Group). Both strands of the open reading frame (ORF) were sequenced by overlapping subclones so that most of the contiguous ORF sequence was assembled from three independent sequencing reactions. For phylogenetic comparisons, nucelotide and putative amino acid sequences from other animal species were structurally analyzed and aligned using the OMIGA 2.0 software package (Oxford Molecular Ltd.). Identity and similarity scores for the deduced amino acid alignments were calculated from the FASTA routine available in the GCG Wisconsin Package 8.0 (UNIX OS).

mRNA analysis: isolation and quantification

Total RNA was extracted from each sample by an acid guanidinium-phenol method (after Chomzinsky and Sacchi, 1987) and further purified by sequential precipitations in lithium chloride (4 *M* LiCl), sodium acetate (3 *M* NaOAc, pH 4.2) and ethanol (70% EtOH). After each precipitation, the RNA pellets were washed in 70% EtOH and dried under vacuum; before proceeding with the next precipitation, the pellets were resuspended in RNase-free TEN buffer (10 m*M* Tris pH 8.0, 1 m*M* EDTA and 10 m*M* NaCl). The final RNA precipitates were resuspended in RNase-free water and quantified by their optical density at 260 nm. From each developmental time point, 10 μg of total RNA was size-separated by formaldehyde gel electrophoresis and blotted overnight *via* capillary transfer onto nylon membranes. RNA on the nylon membranes was UV cross-linked (Stratalinker), and the membranes were stored dry at room temperature. A cDNA probe was generated from the 3′-untranslated region (UTR) of clone #020. The terminal 1185 bp were PCR amplified (5′- TGG GAT TGA AGG AGT CAG –3′ and T7 oligonucleotide primers) and gel purified for further use in standard Northern hybridizations (see general methods in Ausubel *et al.*, 1992). Membranes were prehybridized for several hours in 40% formamide, 25 m*M* Na_3PO_4 (pH 7.2), 5× SSC, 0.1% SDS, 5× Denhardt's, and 50 μg/ml yeast RNA at 45°C in a hybridization oven. The 3′-UTR PCR probe (1185 bp) was radiolabeled by random priming (Promega) with α-^{32}P-dCTP (3000 Ci mmol^{-1}), added to the hybridization tube with a fresh 10-ml aliquot of hybridization buffer (as above), and incubated overnight at 50°C. The blots were initially washed with 0.1× SSC, 1.0% SDS, and 0.5% $Na_4P_2O_7$ at 45°C for 1 h. Additional washes at higher temperatures (max. 55°C) were performed as necessary to further reduce the background signal. Autoradiograms (Kodak Biomax X-ray film) were digitized on a high-resolution scanner (1200 dpi), and grain densities for the signal bands were quantified using the image analysis routines in the software program PhotoShop 4.0 (Win95 OS; Adobe).

Na^+,K^+-ATPase enzyme activity

Total enzyme activity of Na^+,K^+-ATPase was measured at short intervals between 20 and 50 h postfertilization, the period during which enzyme activity increases rapidly during development in *S. purpuratus* (Leong and Manahan, 1997). Ouabain-sensitive Na^+,K^+-ATPase activity (details in Leong and Manahan, 1997) was determined in all samples on the same day with one set of standards to minimize the between-sample assay error. Total Na^+,K^+-ATPase activity was measured as the rate of hydrolysis of ATP (Esmann, 1988). Briefly, embryo tissues were thawed, sonicated, and resuspended in histidine buffer (10% sucrose, 5 m*M* EDTA and 5 m*M* histidine, pH 7.7) at a final protein concentration of 0.5 to 1.0 mg ml^{-1}. In the present study, the total Na^+,K^+-ATPase activity of the sea urchin embryos was measured as the difference in ATPase activity in the presence and absence of 2 m*M* ouabain at 25°C. A detailed consideration of the inclusion of detergents in the Na^+,K^+-ATPase assay is presented in Leong and Manahan (1997). In summary, neither deoxycholate (a common detergent used in Na^+,K^+-ATPase assays) nor alamethicin (a membrane-permeabilizing agent) had any effect on the total Na^+,K^+-ATPase activity in homogenates of *S. purpuratus* embryos, suggesting that inside-out and right-side-out vesicles are not a significant problem in assaying Na^+,K^+-ATPase activity in sea urchin embryos (Leong and Manahan, 1997). The protein content of the samples was determined by the Bradford assay with the modifications of Jaeckle and Manahan (1989).

Table 1

Comparison of nucleotide and deduced amino acid sequences for different α-subunit Na^+, K^+-ATPase

Species	GenBank accession number	Nucleotide identity (%)	Amino acid Identity (%)	Amino acid Similarity (%)
Drosophila	AF04494	69.8	73.3	89.2
Caenorhabditis	U18546	69.7	72.8	89.2
Xenopus	U49238	67.6	69.2	89.2
Artemia	X56650	65.2	72.3	89.7
Hydra	M75140	64.1	67.7	89.2

Identity and similarity to the *Strongylocentrotus purpuratus* cDNA open reading frame (clone #020) are presented as percentages determined from scoring by the GCG Wisconsin Users Group software program. Scores include only the terminal portion of the sea urchin gene's ORF: 588 base pairs (195 amino acid residues and stop codon).

Results

A partial *Strongylocentrotus purpuratus* cDNA clone (#020; Smith *et al.*, 1996) was characterized in this study and found to contain 1769 bp with the terminal portion of an ORF coding for 195 amino acids (588 bp with the stop codon). The remaining sequence (1181 bp) comprised a putative 3′ UTR domain. The clone's ORF was compared to other α-subunits of Na^+,K^+-ATPase, and the *S. purpuratus* nucelotide sequence ranged from 64% to 70% identity to these terminal ORF domains (Table 1). The deduced amino acid sequences of these organisms were aligned to the putative amino acid sequence of the *S. purpuratus* clone and evidenced a high degree of sequence conservation in this terminal domain (Table 2). When compared to the *S. purpuratus* sequence, the derived amino acid sequence was 68%–73% identical and 89%–90% similar (Table 1).

The terminal region of the ORF of known α-Na^+,K^+-ATPases is believed to contain several transmembrane domains; there is some debate over the exact number of these domains and the extra- *vs.* intracellular orientation of some of the intervening regions in α-Na^+,K^+-ATPase (Shull and Greeb, 1988; Takeyasu *et al.*, 1990; Blanco and Mercer, 1998). The hydropathy of the *S. purpuratus* sequence was estimated with Kyte-Doolittle scoring using a grouping of 11 amino acid residues (Fig. 1) and suggests a high probability of four transmembrane domains in the terminal portion of this ORF. Overlaying these domains on a structure detailed by Takeyasu *et al.* (1990) indicates that the region between the seventh and eighth transmembrane domains could have an extracellular localization. In the absence of crystallographic data, it is generally believed that most α-subunits of transmembrane ATPases (both Na^+ and Ca^{++}) are structurally similar, with 10 transmembrane do-

Table 2

Alignment of deduced amino acid sequence for the terminal 195 residues of the α-subunit of Na$^+$, K$^+$-ATPase in the sea urchin Strongylocentrotus purpuratus

```
          1
  URCHIN  SDIMKRRPRD PQNDKLVNER LISVSYGQIG MIQRSAGFFA YFVIMGENGF
     FLY  ADIMKRPPRD PFNDKLVNSR LISMAYGQIG MIQAAAGFFV YFVIMAENGF
  SHRIMP  SDIMKRRPRN PVTDKLVNER LISLAYGQIG MIQASAGFFV YFVIMAECGF
NEMATODE  SDIMKRQPRD PIRDKLVNER LISLAYGQIG MIQASAGFFT YFWIMADNGF
    FROG  SDIMKRQPRN PKTDKLVNER LISMAYGQIG MIQALGGFFT YFVILAENGF
   HYDRA  SDIMKRHPRN PIRDKLVNER LISLAYGQIG MMQATAGFFT YFIILAENGF
            ***** *      ***** * ***  ***** * *   ***  ** *    **

          51
  URCHIN  LPNDLIMLRS KWDDKAVLNV EDSYGQQWGF YQRKQLEYTC HTAFFASIVV
     FLY  LPKKLFGIRK MWDSKAVNDL TDSYGQEWTY RDRKTLEYTC HTAFFISIVV
  SHRIMP  LPWDLFGLRK HWDSRAVNDL TDSYGQEWTY DARKQLESSC HTAYFVSIVI
NEMATODE  MPWDLYQLRA QWDSRAYNNV LDSYGQEWTY ANRKILEYTC QTAYFVSIVV
    FROG  LPWTLLGIRV NWDDRWTNDV EDSYGQQWTY EQRKIVEFTC HTSFFISIVV
   HYDRA  LPSYLFGLRS QWDDMSNNNL LDSFGSEWTY FQRKEIELTC QTAFFTTIVV
           *          **         ** *  *     **  *  *  *  *  **

       101                                              150
  URCHIN  VQWADVIICK TRRNSLIHQG MNNWVLNFGL FFETALAAFL SYCPGLENGL
     FLY  VQWADLIICK TRRNSIFQQG MRNWALNFGL VFETVLAAFL SYCPGMEKGL
  SHRIMP  VQWADLIISK TRRNSVFQQG MRNNILNFAL VFETCLAAFL SYTPGMDKGL
NEMATODE  VQWADLIISK TRRNSLVQQG MSNWTLNFGL VFETALAWFM CYCPGLDNGL
    FROG  VQWADLIICK TRRNSVFQQG MKNKILIFGL FEETALAAFL SYCPGMDVAL
   HYDRA  VQWADLIISK TRRLSLFQQG MTNWFLNFGL FFETALAAFL QYTPGVNTGL
          ***** ** * *** *   ** * *    * *   ** ** *   * **    *

          151                                            195
  URCHIN  RMYPLRIGWW FVAFPFSLLI FVYDECRRFI LRHNPGGWVE LETYY↵
     FLY  RMYPLKLVWW FPAIPFALAI FIYDETRRFY LRRNPGGWLE QETYY↵
  SHRIMP  RMYPLKINWW FPALPFSFLI FVYDEARKFI LRRNPGGWVE QETYY↵
NEMATODE  RMYGLRFSWW FCALPFSILI FVYDEIRRFL IRRYPGGWVE RETYY↵
    FROG  RMYPLKPTWW FCAFPYSLII FIYDEVRKLI IRRSPGGWVE KESYY↵
   HYDRA  RLRPMNFTWW LPGLPFSLLI FVYDEIRRYL LRKNPGGWVE KETYY↵
          *       **     *    * * ***
```

The shaded blocks and bold lettering indicate the putative transmembrane domains identified by Kyte-Doolittle hydropathy scores in the sea urchin sequence (bold lettering; see Fig. 1). Genus names for the organisms and GenBank accession numbers for the sequences: urchin = *Strongylocentrotus* (this study), fly = *Drosophila* (AF04494), shrimp = *Artemia* (X56650), nematode = *Caenorhabditis* (U18546), frog = *Xenopus* (U49238), Hydra = *Hydra* (M75140); * = amino acid identity for all sequences; ↵ = termination codon.

mains and a large extracellular loop between transmembrane domains 7 and 8 (Canfield and Levenson, 1993; Blanco and Mercer, 1998).

Northern blots using the 3′ UTR of clone #020 specifically recognized a 4.5 to 4.7 kb transcript under high stringency (Fig. 2). In another sea urchin, *Hemicentrotus pulcherrimus*, the full-length α-Na$^+$,K$^+$-ATPase cDNA has been cloned and has an mRNA transcript size of 4.6 kb (Mitsunaga-Nakatsubo *et al.*, 1992a). The α-Na$^+$,K$^+$-ATPase gene is differentially expressed during development in *S. purpuratus* (Fig. 2). The level of mRNA transcripts is low during early cleavage, then rises rapidly around gastrulation (at 25–36 h postfertilization; Fig. 3). After gastrulation, mRNA returns to a low level comparable to that initially found in the egg (Fig. 3). The rapid disappearance of the α-Na$^+$,K$^+$-ATPase transcript from the total RNA pool after gastrulation closely followed a first-order exponential decay model [$f(x) = 98.512\ e^{(-0.128x)}$; $r^2 = 0.988$; Fig. 3]. The decay constant of the regression is equivalent to a degradation rate of 7.8% h^{-1} of the transcript. At 83 h, α-subunit

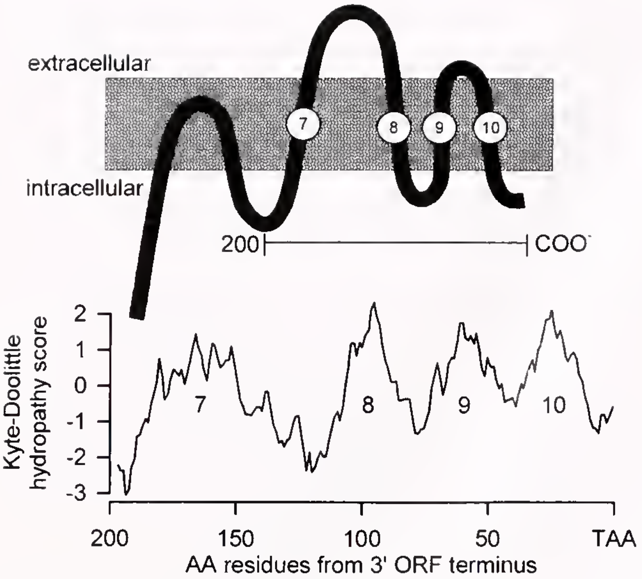

Figure 1. Secondary structure characterization for the last 195 amino acids of a putative α-Na$^+$,K$^+$-ATPase cDNA cloned from *Strongylocentrotus purpuratus*. The Kyte-Doolittle hydropathy score suggests the presence of four transmembrane domains, which match the structure of other α-Na$^+$,K$^+$-ATPase subunits (Blanco and Mercer, 1998).

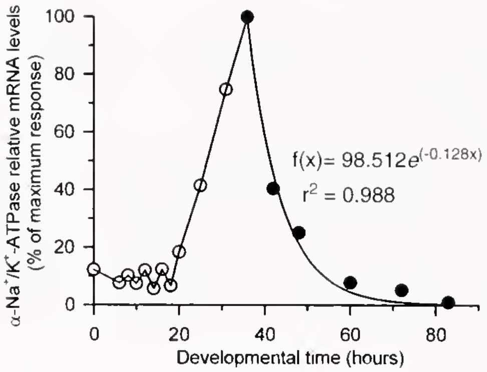

Figure 3. Relative transcript levels of the α-Na$^+$,K$^+$-ATPase cDNA during development in *Strongylocentrotus purpuratus* (quantified from Fig. 2). mRNA levels are presented relative to the maximal expression obtained at 36 h postfertilization. The rapid decline in mRNA abundance after 36 h fits a first-order exponential decay function (r^2 = 0.988; regression line plotted with shaded symbols).

transcripts were barely detectable under the conditions we used for Northern blots of total RNA.

The rapid increase in α-Na$^+$,K$^+$-ATPase mRNA transcripts during gastrulation in *S. purpuratus* was paralleled by a concomitant increase in the total activity of the sodium pump (Fig. 4). Activity levels were very low during early development in *S. purpuratus* and then increased after 20 h to a maximum level at the pluteus larval stage (Leong and Manahan, 1997). The rapid increase in activity between 20 and 40 h of development (Fig. 4) can be described by the exponential function [$f(x) = 1.167(1 + e^{[(x-x_0)/4.57]})^{-1}$; r^2 = 0.9664; maximum activity of 1.17 μmol P$_i$ h^{-1} mg^{-1} protein]. The present study resolves the increase in enzyme activity at a finer time scale (*cf.* Leong and Manahan, 1997) and reveals the close coordination between α-subunit gene transcription and the assembly of functional sodium pumps in sea urchin embryos between fertilization and gastrulation.

Discussion

It has long been a general goal of physiological ecologists to identify a sensitive biochemical indicator of an animal's physiological state or metabolic activity—for example, the ratio of RNA to DNA (Westerman and Holt, 1994) or the glycolytic enzyme activities (Childress and Somero, 1990). For developmental stages with low biochemical contents, such assays are often not possible. Molecular biological techniques have the necessary sensitivity and potentially offer an alternative for assessing physiological state in larvae and small zooplankton. Because the sodium pump consumes such a large portion of cellular energy metabolism

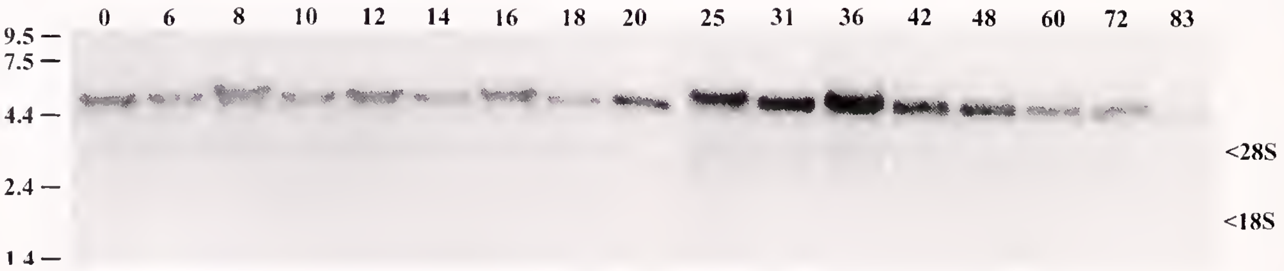

Figure 2. Northern blot hybridization of total RNA during development in *Strongylocentrotus purpuratus* using a radiolabeled probe from the 3′-untranslated domain of the α-Na$^+$,K$^+$-ATPase cDNA clone. RNA samples were collected at short time intervals during embryogenesis as shown by the hours post-fertilization at the top of each lane. Molecular size (kilobases) is indicated on the left; ribosomal RNA positions are indicated on the right. The probe recognizes a single transcript that is approximately 4.6 kb in size.

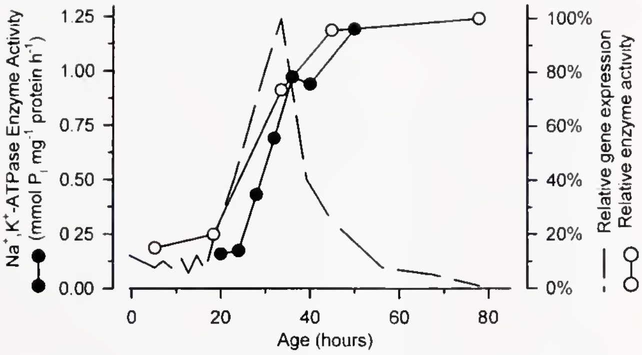

Figure 4. Total enzyme activity of Na^+,K^+-ATPase during gastrulation in *Strongylocentrotus purpuratus*. Protein-specific enzyme activity (closed circles) is plotted on the left axis; mRNA levels from Fig. 3 are overlaid (dashed line) to illustrate the temporal relationship between α-subunit gene expression and the appearance of functional sodium pump proteins. Data from Leong and Manahan (1997) are also plotted (open circles) to show the pattern of relative enzyme activities.

(*e.g.*, 40% in sea urchin larvae, Leong and Manahan 1997), it would seem to be a good candidate for such an assay, with the potential to provide sensitive information regarding rates of energy utilization in a single larva.

Several lines of evidence strongly support the conclusion that the partial cDNA clone (#020) in *Strongylocentrotus purpuratus* is the α-subunit of the sodium pump: (1) the putative amino acid sequences show a high similarity to those of other animals; (2) the 3′-UTR probe recognizes a 4.6-kb transcript, which is the full-length transcript size in other invertebrate species; (3) the ontogenetic increase in expression during gastrulation is similar to the expression pattern in another sea urchin (Mitsunaga-Nakatsubo *et al.*, 1992b); (4) total Na^+,K^+-ATPase enzyme activities show a concomitant increase as mRNA transcripts of clone #020 accumulate during gastrulation.

In the sea urchin *Hemicentrotus pulcherrimus*, the expression of the α-Na^+,K^+-ATPase gene increases rapidly during gastrulation (Mitsunaga-Nakatsubo *et al.*, 1992b). In *S. purpuratus*, the expression of the α-Na^+,K^+-ATPase gene evidences a similar pattern of ontogenetic regulation, with a sharp rise during gastrulation followed by a subsequent decline to much lower levels. In conjunction with the total Na^+,K^+-ATPase enzyme activity that is present during development (this study, Fig. 4; see also Leong and Manahan, 1997), temporal changes in both mRNA transcripts and protein activity indicate that the enzyme activity is low during early cleavage. At the point when an embryo approaches gastrulation, α-subunit gene transcription and subsequent mRNA translation increase greatly, producing a large increase in sodium pumps (Fig. 3), presumably as a necessary component of the physiological function of proliferating cells.

Once these pumps have been synthesized, mRNA transcripts for the α-Na^+,K^+-ATPase are rapidly lost. The decrease in mRNA levels over time fits a first-order exponential decay model (7.8% h^{-1}) so that by 83 h, transcription of the α-subunit gene was barely detectable (Fig. 2). At gastrulation, *S. purpuratus* appears to have synthesized most of the necessary sodium pumps. Total enzymatic activities show little increase after 50 h, further supporting this observation that the number of Na^+,K^+-ATPase ion pumps is set by the rapid transcription during gastrulation, and that once these transcripts are degraded, an early larva's sodium pump complement remains unchanged until further growth occurs, usually after feeding is initiated.

In vertebrates, the α-subunit Na^+,K^+-ATPase has several isoforms (Rossier *et al.*, 1987) that differ in many aspects, including sensitivity to proteases and cross-linking agents (Sweadner, 1979), electrophoretic mobility (Peterson *et al.*, 1982), and affinity for ouabain (Lytton *et al.*, 1985). In brine shrimp (*Artemia salina*), the α-Na^+,K^+-ATPase is present in two isoforms that are differentially expressed during early development (Peterson *et al.*, 1982). In the sea urchin *Hemicentrotus pulcherrimus*, two α-subunit isoforms are expressed during embryogenesis (Yamazaki *et al.* 1997). However, these two isoforms are encoded by a single gene and have identical sequences except for the 5′ leader sequences (Yamazaki *et al.*, 1997). If *S. purpuratus*, like *H. pulcherrimus*, has a similar isoform complement, then the cDNA probe we used for the present study (from the 3′-UTR) should hybridize to other α-subunit isoforms expressed during early development. Regardless of the mechanism, the disparity at 83 h postfertilization between the transcript measurements and the complement of active sodium pumps indicates the difficulty in isolating a single molecular factor to be used as an index for physiological rate processes.

The observation that Na^+,K^+-ATPase gene transcription and translation events are limited to a brief developmental period is intriguing. The sodium pump is considered to be a "housekeeping" protein. Consequently, for such an important physiological process, we would have expected the expression of a subunit gene to be constitutive and at a low level so that there would always be some subunit synthesis to replace any turnover in functional pump proteins. Such a continual level of replacement might have offered a sensitive assay for assessing the physiological state of individual larvae by providing a molecular index of the activity of one of the most energy-demanding cellular processes. However, this is not the case. The α-subunit expression is developmentally regulated so that gene expression is initiated rapidly at about 20 h, peaks at about 36 h, and is subsequently "turned-off." Such a temporal pattern of regulation highlights the difficulty of using molecular probes as simple indices of physiological state. Similar difficulties in the interpretation of physiological activity and expression have been found for other specific housekeeping genes (*e.g.*, Weinstein *et al.*, 1992; Yang and Somero, 1996). For the multiple enzymes in metabolic pathways, the control mechanisms at the level of genes and proteins are even more complex (Hochachka *et al.*, 1998).

Ontogenetic changes in the metabolic rates of embryos have important consequences for subsequent survival because of the finite quantity of energy reserves in an egg. During development, metabolic rates increase in embryos as their cell numbers increase (Marsh *et al.*, 1999), and the activity of the sodium pump can consume a large fraction of total metabolism in some sea urchin embryos and larvae (Leong and Manahan, 1997, 1999). Understanding ontogenetic changes in sodium pump activities is important for assessing the metabolic energy costs of development. In the pluteus larval stage of *S. purpuratus* (at 83 h postfertilization), the *in vivo* sodium pump activity consumes 40% of total metabolism, with a potential reserve activity that could increase to a maximum of 77% of metabolism (Leong and Manahan, 1997). However, α-Na$^+$,K$^+$-ATPase gene expression is barely detectable at this point in larval development (Fig. 3). Consequently, molecular assays for expression of this gene would not be informative for assessing sodium pump activity as an index of a larva's physiological state. It is likely that during development and growth many physiological processes have functional rates of protein activity that are not strictly paralleled in time by the expression of their genetic components. A knowledge of the temporal relationship between gene and enzyme activities is critical to developing a molecular genetic index of physiological state in larval forms.

Acknowledgments

We thank E. Davidson and C. Smith for providing the clone that we have characterized. D. Pace and M. Moore assisted with the culture sampling. This project was supported by California Sea Grant #R/MP-75C, and NSF #9420803.

Literature Cited

Ausubel, F. M., R. Brent, R. E. Kingston, D. D. Moore, J. G. Seidman, J. A. Smith, K. Struhl. 1992. *Short Protocols in Molecular Biology*, 2nd ed., John Wiley and Sons, New York.

Baker, P. F., and C. M. Connelly. 1966. Some properties of the external activation site of the sodium pump in crab nerve. *J. Physiol.* **185**:270–297.

Blanco, G., and R. W. Mercer. 1998. Isozymes of the α-Na$^+$,K$^+$-ATPase: heterogeneity in structure, diversity in function. *Am. J. Physiol.* **275**:F633–F650

Canfield, V. A., and R. Levenson. 1993. Transmembrane organization of the Na,K-ATPase determined by epitope addition. *Biochemistry* **32**:13782–13786.

Childress, J. J., and G. N. Somero. 1990. Metabolic scaling: a new perspective based on scaling of glycolytic enzyme activities. *Am. Zool.* **30**:161–173.

Chomzinsky, P., and N. Sacchi. 1987. Single-step method of RNA isolation by acid guanidinium thiocyanate-phenol-chloroform extraction. *Anal. Biochem.* **162**:634–647.

Esmann, M. 1988. ATPase and phosphatase activity of Na+,K+-ATPase: molar and specific activity, protein determination. *Methods Enzymol.* **156**:105–115.

Hochachka, P. W., G. B. McClelland, G. P. Burness, J. F. Staples, and R. K. Suarez. 1998. Integrating metabolic pathway fluxes with gene-to-enzyme expression rates. *Comp. Biochem. Physiol.* **120B**:17–26.

Jaeckle, W. B., and D. T. Manahan. 1989. Growth and energy imbalance during the development of a lecithotrophic molluscan larva (*Haliotis refescens*). *Biol. Bull.* **177**: 237–246.

Jorgensen, P. L., and J. C. Skou. 1969. Preparation of highly active Na$^+$,K$^+$-ATPase from the outer medulla of rabbit kidney. *Biochem. Biophys. Res. Commun.* **37**:39–47.

Kyte, J. 1971. Purification of the sodium- and potassium-dependent adenosine triphosphatase from canine renal medulla. *J. Biol. Chem.* **246**:4157–4165.

Leong, P. K. K., and D. T. Manahan. 1997. Metabolic importance of Na$^+$,K$^+$-ATPase activity during sea urchin development. *J. Exp. Biol.* **200**:2881–2892.

Leong, P. K. K., and D. T. Manahan. 1999. Na$^+$,K$^+$-ATPase activity during early development and growth of an Antarctic sea urchin. *J. Exp. Biol.* **202**:2051–2058.

Lucu, C., and D. Pavicic. 1995. Role of seawater concentration and major ions in oxygen consumption rate of isolated gills of the shore crab *Carcinus mediterraneus* Csrn. *Comp. Biochem. Physiol.* **112A**: 565–572.

Lytton, J., J. C. Lin, and G. Guidotti. 1985. Identification of two molecular forms of Na$^+$,K$^+$-ATPase in rat adipocytes. *J. Biol. Chem.* **260**:1177–1184.

Marsh, A. G., P. K. K. Leong, and D. T. Manahan. 1999. Energy metabolism during embryonic development and larval growth of an Antarctic sea urchin. *J. Exp. Biol.* **202**:2041–2050.

Mitsunaga-Nakatsubo, K., A. Fujiwara, and I. Yasumasu. 1992a. Change in the activity of Na+,K+-ATPase in embryos of the sea urchin, *Hemicentrotus pulcherrimus*, during early development. *Dev. Growth Differ.* **34**: 379–385.

Mitsunaga-Nakatsubo, K., M. Kanda, K. Yamazaki, H. Kawashita, A. Fujiwara, K. Yamada, K. Alasaka, J. Shimada, and I. Yasumasu. 1992b. Expression of Na$^+$,K$^+$-ATPase α-subunit in animalized and vegetalized embryos of the sea urchin, *Hemicentrotus pulcherrimus*. *Dev. Growth Differ.* **34**: 677–684.

Peterson, G. L., L. Churchill, J. A. Fisher, and L. E. Hokin. 1982. Structural and biosynthetic studies on two molecular forms of the (Na$^+$,K$^+$)-activated adenosine triphosphatase large subunit in *Artemia salina* nauplii. *J. Exp. Zool.* **221**:295–308.

Rossier, B. C., K. Geering, and J. P. Kraehenbül. 1987. Regulation of the sodium pump: how and why? *Trends Biochem. Sci.* **12**:483–487.

Shull, G. E., and J. Greeb. 1988. Molecular cloning of two isoforms of the plasma membrane Ca^{2+}-transporting ATPase from rat brain. Structural and functional domains exhibit similarity to Na$^+$,K$^+$- and other cation transport ATPases. *J. Biol. Chem.* **263**:8646–8657.

Siems, W., M. Müller, R. Dumdey, H.-G. Holzhütter, J. Rathmann, and S.M. Rapoport. 1982. Quantification of pathways of glucose utilization and balance of energy metabolism of rabbit reticulocytes. *Eur. J. Biochem.* **124**:567–573.

Siems, W.G., H. Schmidt, S. Gruner, and M. Jakstadt. 1992. Balancing of energy-consuming processes of K 562 cells. *Cell Biochem. Funct.* **10**:61–66.

Smith, L. C., L. Chang, R. J. Britten, and E. H. Davidson. 1996. Sea urchin genes expressed in activated coelomocytes are identified by expressed sequence tags. Complement homologues and other putative immune response genes suggest immune system homology within the deuterostomes. *J. Immunol.* **156**: 593–602.

Strathmann, M., B. A. Hamilton, C. A. Mayeda, M. I. Simon, E. M. Meyerowitz, and M. J. Palazzolo. 1991. Transposon-facilitated DNA sequencing. *Proc. Natl. Acad. Sci. USA* **88**:1247–1250.

Sweadner, K. J. 1979. Two molecular forms of (Na+K+)-stimulated ATPase in brain. Separation and difference in affinity for strophanthidin. *J. Biol. Chem.* **254**: 6060–6067.

Takeyasu, K., V. Lemas, and D. M. Fambrough. 1990. Stability of Na(+)-K(+)-ATPase alpha-subunit isoforms in evolution. *Am. J Physiol.* **259**:C619–C630.

Weinstein, S. P., and R. S. Haber. 1992. Differential regulation of glucose transporter isoforms by thyroid-hormone in rat-heart. *Biochim. Biophys. Acta* **1136**:302–308.

Westerman, M., and G. J. Holt, 1994. RNA-DNA ratio during critical period and early larval growth of the red drum *Scianeopus ocellatus*. *Mar. Biol.* **121**:1–9.

Yamazaki, K., C. Okamura, T. Ihara, and I. Yasumasu. 1997. Two types of Na^+,K^+-ATPase alpha subunit gene transcript in embryos of the sea urchin, *Hemicentrotus pulcherrimus*. *Zool. Sci.* **14**: 469-473.

Yang, T.-H., and G. N. Somero. 1996. Activity of lactate dehydrogenase but not its concentration of messenger RNA increases with body size in barred sand bass, *Paralabrax nebulifer* (Teleostei). *Biol. Bull.* **191**:155–158.

Reference: *Biol. Bull.* **199:** 108–115. (October 2000)

Dimethylsulfoniopropionate in Giant Clams (Tridacnidae)

RICHARD W. HILL[1,*], JOHN W. H. DACEY[2], AND AHSER EDWARD[3]

[1] *Department of Zoology, Michigan State University, East Lansing, Michigan 48824;* [2] *Department of Biology, Woods Hole Oceanographic Institution, Woods Hole, Massachusetts 02543; and* [3] *College of Micronesia-FSM, P. O. Box 159, Kolonia, Pohnpei, Federated States of Micronesia 96941*

Abstract. The tridacnid clams maintain symbiotic associations with certain dinoflagellates (termed zooxanthellae). Tridacnids are thus candidates to have high tissue concentrations of dimethylsulfoniopropionate (DMSP), a tertiary sulfonium compound that is not synthesized by animals but is commonly produced by dinoflagellates. This study establishes that DMSP is about an order of magnitude more concentrated in the light-exposed and shaded mantle and gills of *Tridacna maxima* and *T. squamosa* than in any other known animal tissues. The DMSP concentration in the light-exposed, siphonal mantle—the location of most zooxanthellae—is an inverse function of body size, paralleling an inverse relation between apparent density of zooxanthellae (measured as pheophytin concentration) and body size. The shaded mantle and gills are high in DMSP despite having low densities of zooxanthellae, indicating that high DMSP concentrations occur in molluscan tissue, not just in algal cells. DMSP is almost an order of magnitude less concentrated in the adductor muscle than in other tissues. The high DMSP concentrations found in tridacnids, by providing abundant substrate for formation of volatile dimethylsulfide, probably explain the peculiar tendency of tridacnids to rapidly develop offensive odors and tastes after death: a serious problem for their exploitation as food. Tridacnids are the one group of animals in which DMSP concentrations are high enough in some tissues to be in the range capable of perturbing enzyme function at high physiological temperatures. Thus, tridacnids may require enzyme forms adapted to DMSP.

Introduction

Some of the most interesting marine animals are those that maintain symbiotic associations with dinoflagellates. The symbiotic dinoflagellates are known as zooxanthellae. Included are the reef-building scleractinian corals, many alcyonarians, all of the about eight species of giant clams of the family Tridacnidae, and a few other bivalves (Maruyama *et al.*, 1998). Dinoflagellates, as a group, are noteworthy for synthesizing relatively large quantities of dimethylsulfoniopropionate (DMSP), a nonvolatile tertiary sulfonium compound that is the precursor of volatile dimethylsulfide (DMS) (Keller *et al.*, 1989a,b). DMSP is not synthesized endogenously by animals. However, the widespread synthesis of DMSP by dinoflagellates provides reason to predict accumulations of DMSP and DMS within the tissues of zooxanthellate animals. This prediction has been assessed heretofore only in reef-building scleractinians. The presence of the reduced-sulfur compounds in reef-building corals was confirmed initially by the observation of DMS release from damaged reefs (Andreae *et al.*, 1983). Later, two of us quantified DMSP and DMS in the tissues of healthy corals and in free-living dinoflagellates isolated from corals (Hill *et al.*, 1995b).

In giant clams, the zooxanthellae, which currently are assigned to two of the major subdivisions of *Symbiodinium* (Rowan, 1998), occur primarily in the siphonal mantle tissue (Norton *et al.*, 1992). This expansive tissue faces upward when the clams are in their natural orientation and is presented to the sun as a light antenna. The part of the mantle that is positioned near the downward-facing byssal opening and hinge, shaded from the sun, contains relatively few zooxanthellae (documented in this study). Similarly, zooxanthellae are sparse or absent from the adductor muscle, gills, and other tissues besides the siphonal mantle.

Received 1 December 1999; accepted 16 June 2000.

* To whom correspondence should be addressed. E-mail: hillr@msu.edu

Abbreviations: DMS, dimethylsulfide; DMSP, dimethylsulfoniopropionate.

Recent molecular evidence confirms that the giant clams are a monophyletic group (Maruyama *et al.*, 1998). This paper, based on two species, is the first to look for or quantify DMSP and DMS in the group. It is also the first to examine DMSP and DMS in zooxanthellate animals besides reef-building scleractinians.

DMSP and DMS are of current interest for several reasons. The most prominent is that atmospheric DMS originating from marine organisms affects cloud cover and climate over the oceans (Shaw, 1983; Charlson *et al.*, 1987; Falkowski *et al.*, 1992; Andreae and Crutzen, 1997). Coral reefs are sufficiently extensive that DMS from corals could be of local climatic significance (Andreae *et al.*, 1983; Hill *et al.*, 1995b). However, DMS from giant clams seems unlikely to be climatically important except as a minor component of reef-community contributions, because the clams are insufficiently abundant, especially in modern times. On the other hand, DMSP and DMS in giant clams are likely important in two major ways.

First, DMS is well known to have critical effects on taste whenever it is present in organisms used for food (Motohiro, 1962; Ackman *et al.*, 1966; Levasseur *et al.*, 1994). Giant clams have long been important sources of food and protein throughout much of the Indo-Pacific, so much so that many clam populations are decimated (Munro, 1989; Dalzell *et al.*, 1996). A problem for the indigenous and commercial exploitation of giant clams is that after death, the meat often promptly develops a strong, "unquestionably offensive" odor (Peavey and Riley, 1993, 1994), which is sometimes described as seaweed- or kelp-like (*e.g.*, Cowan, 1988). The cause has been unknown. Our experience with DMS and with the odors of the clams led us to postulate that the cause is DMS derived from the algal symbionts. If this hypothesis is confirmed, the stage will be set for a rational approach to a problem that seriously detracts from the value of the clams as sources of food in subsistence economies and as aquacultured species. Giant clams are attractive animals for aquaculture (Braley, 1988; Munro, 1989) in part because their symbionts enable them to get most of their energy for maintenance and growth from sunlight (Klumpp and Griffiths, 1994); they have been described as "the only phototrophic, and thus self-feeding, potential farm animals known to humankind" (Munro, 1989).

Second, recent research (Nishiguchi and Somero, 1992; Karsten *et al.*, 1996) has established that DMSP sometimes negatively perturbs enzyme function at high physiological temperatures. The enzyme-perturbing effects of DMSP have heretofore been considered relevant only to plants and algae, because no animals have been known to have DMSP concentrations sufficiently high to be influential. We hypothesized that the giant clams might have tissue DMSP concentrations high enough that they could potentially require biochemical adaptations to DMSP.

Materials and Methods

Tridacna maxima and *T. squamosa* were collected near Pohnpei in the Federated States of Micronesia. Two collections were made: one of six specimens of *T. maxima* (11–14 cm shell length) and four of *T. squamosa* (10–14 cm) on 13 July 1995, on the northern barrier reef of the main island of Pohnpei; the second of three specimens of *T. maxima* (16–18 cm) and nine of *T. squamosa* (14–22 cm) on 17 August 1995, in the lagoon of Ant atoll, 27 km from the first location. Collected animals were taken by boat to Kolonia, Pohnpei, where they were promptly dissected (3–4 h after collection). Samples (1–2 g) were cut from four tissues of each clam: light-exposed, siphonal mantle; shaded mantle from near the byssal opening; adductor muscle; and gill (sometimes both right and left gill sets combined). Each sample of tissue was weighed and placed into 20 ml of HPLC-grade absolute methanol in a 37-ml glass vial sealed with a Teflon-faced butyl-rubber septum (Regis Technology) secured with a crimped aluminum ring.

Samples prepared in Pohnpei were shipped in light-tight containers to Woods Hole, Massachusetts, for assay. Shipments required 6–8 days to reach Woods Hole, and assays were completed 8–10 days after collection. Vials had been filled with methanol and weighed prior to shipment to Pohnpei, and they were reweighed on return to Woods Hole as a check for leakage (none occurred).

To measure DMSP and DMS, 1.0 ml of methanol was drawn by syringe from each tissue-sample vial and placed in 25 ml of 2 N KOH in a sealed vial. Incubation in cold base quantitatively converts DMSP to DMS (Dacey and Blough, 1987). Thus, after incubation (20 h, 2°C), DMSP (plus any DMS present in the initial samples) could be measured by assaying DMS. For assay, the vials of KOH were brought to room temperature (*ca.* 22°C), and DMS was measured in head-space samples by gas chromatography, using a Chromosil 330 (Supelco) column at 54°C for separation, Sievers 350B sulfur chemiluminescence detector, and Hewlett Packard 3390A integrator. Standards were prepared in 25 ml of 2 N KOH plus 1 ml methanol using reagent grade DMS (Fluka). All measures were duplicated.

Chlorophyll in each tissue sample was measured as an index of the density of zooxanthellae. In fact, because some chlorophyll could have degraded to pheophytin during sample preparation and shipment, and because our interest was not in chlorophyll itself but in an index of relative levels of zooxanthellae, we degraded all chlorophyll by acidification (3 m*M* HCl) and used the resulting total pheopigment levels as our index (Hill *et al.*, 1995b). Chlorophyll *a* and pheopigment *a* were measured using a calibrated Turner model 10 fluorometer and standards of chlorophyll *a* from spinach (Sigma) in methanol following procedures recommended by Holm-Hansen and Reimann (1978). Aliquots of methanol drawn by syringe from tissue-sample vials were diluted in

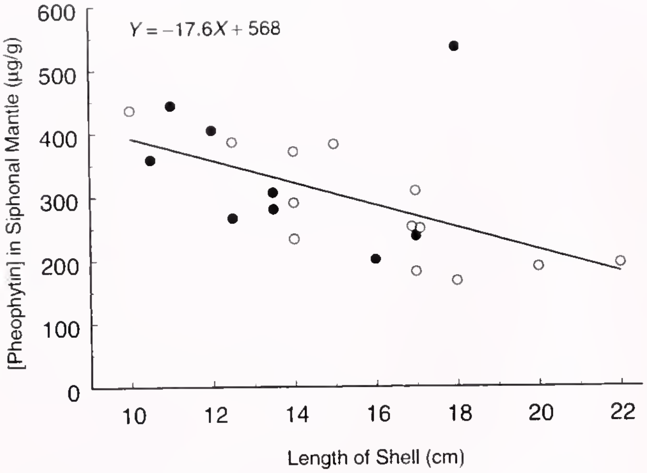

Figure 1. Pheophytin *a* per gram of siphonal mantle (wet weight) as a function of shell length in *Tridacna maxima* (filled symbols) and *T. squamosa* (open symbols). The line and equation are results of linear, least-squares regression, all data taken together. Two data points for 17-cm clams are shifted laterally for clarity.

absolute methanol to place concentrations on the linear parts of calibration curves.

In Pohnpei, tissue samples were prepared, weighed, and inserted in vials as solid blocks of tissue to minimize potential loss of DMS. To assure that extractions of DMSP, DMS, and chlorophyll from samples into methanol were complete, tissue samples were removed briefly from sample vials after completion of the measurements described above and minced with scissors into small pieces (*ca.* 1 mm greatest thickness) that fell back into the vials (the procedure required about 1 min per sample). After 24–48 h, all measurements were repeated. Chlorophyll concentrations were not altered by mincing, and concentrations of pooled DMSP and DMS (measured as earlier described) were altered little, if at all (possibly 3%–5% in the case of mantle samples). The mincing test demonstrated that extraction from whole tissue was complete or virtually complete, and all assays for a sample were averaged to obtain the results reported. A second check on our technique was to test whether the high tissue DMSP concentrations we encountered might be so high as to saturate the methanol. The highest concentration of DMSP in the methanol in any tissue-sample vial was 4.3 m*M*. Without attempting to determine the absolute solubility of DMSP in methanol, we ascertained that pure DMSP sufficient to make a solution three times as concentrated dissolved rapidly in methanol. Thus, saturation of the methanol in the sample vials did not occur.

Total amounts of pooled DMSP and DMS (in micromoles) and of pheopigment *a* (in micrograms) in tissue samples were calculated from concentrations in sample-vial methanol by multiplying by the volume of methanol (20 ml), then expressed per unit wet-weight of tissue.

Results

For simplicity of language, we express results in terms of DMSP, although we do not know what proportions of the DMS analyzed were initially in the form of DMS or DMSP. Most was probably DMSP (the nonvolatile form known to be the principal chemical species in algae; see also comparative data on molluscs presented later). Results from *Tridacna maxima* and *T. squamosa* were not statistically distinguishable and thus are generally pooled.

Pheophytin *a* per gram of siphonal (light-exposed) mantle was an inverse function of body size (analyzed by linear regression, $P = 0.008$, $r^2 = 0.30$), as shown in Figure 1. DMSP per gram of siphonal mantle was likewise an inverse function of body size ($P = 0.015$, $r^2 = 0.26$), as shown in Figure 2. The concentrations of DMSP and pheophytin in the siphonal mantle were strongly correlated ($P < 0.001$), as shown in Figure 3. The ratio of DMSP concentration to pheophytin concentration in siphonal mantle was quite consistent, the mean and standard error being 0.107 ± 0.0048 (range: 0.070–0.158) μmol/μg.

Pheophytin per gram did not show a systematic relation to body size in the byssal (shaded) mantle, adductor, or gill. Table 1 summarizes the pheophytin concentrations in these tissues. Comparison to Figure 1 shows that the concentrations were far lower than in the siphonal mantle. The simple mean concentration in the siphonal mantle, 303 μg/g, is of uncertain utility because of the regular relation between siphonal-mantle concentration and body size, but it helps bring to light that pheophytin concentrations in the byssal mantle and gill were only about 7% and 3% as high as those in siphonal mantle. Concentrations of pheophytin in the adductor approached zero.

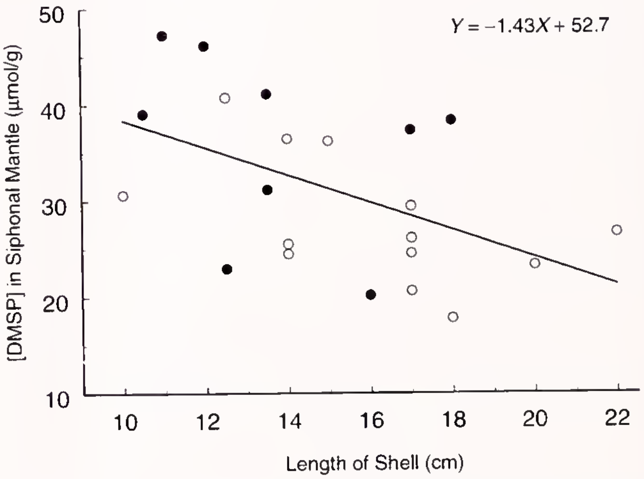

Figure 2. Concentration of dimethylsulfoniopropionate (DMSP) in siphonal mantle (wet weight) as a function of shell length in giant clams. The line and equation are results of linear, least-squares regression, all data taken together. Filled symbols, *Tridacna maxima;* open symbols, *T. squamosa.*

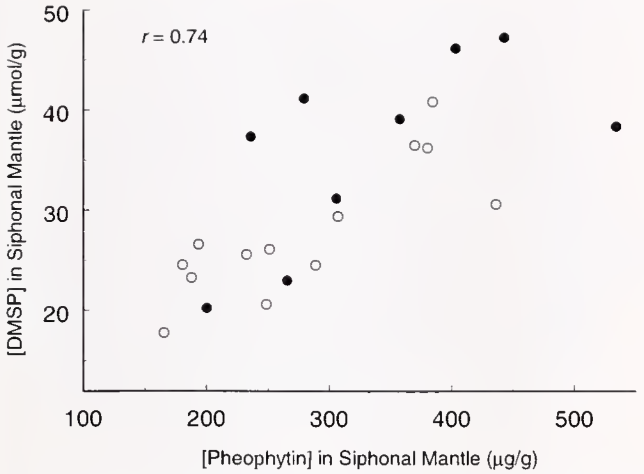

Figure 3. Correlation between concentrations of dimethylsulfoniopropionate (DMSP) and pheophytin *a* in siphonal mantle of giant clams. Filled symbols, *Tridacna maxima;* open symbols, *T. squamosa.* r = correlation coefficient.

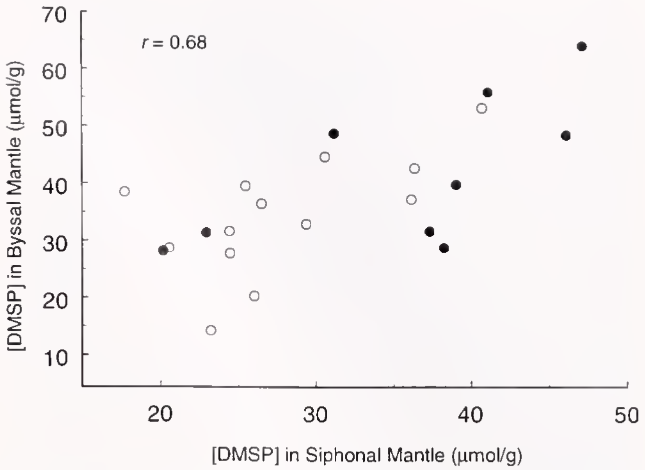

Figure 4. Correlation between concentrations of dimethylsulfoniopropionate (DMSP) in byssal and siphonal mantle in giant clams. Filled symbols, *Tridacna maxima;* open symbols, *T. squamosa.* r = correlation coefficient.

As shown in Figure 4, the concentration of DMSP in the byssal mantle tissue was strongly correlated with ($P < 0.001$) and similar to that in the siphonal mantle tissue, even though densities of zooxanthellae in the byssal tissue, as inferred from byssal pheophytin concentrations, were a small fraction of those in the siphonal tissue. Presumably because of the correlation between siphonal and byssal concentrations, the byssal DMSP concentration exhibited a regular relation to body size, similar to that in Figure 2 [linear regression: $Y(\mu\text{mol/g}) = -2.46X(\text{cm}) + 74.4$; $P = 0.001$]. Byssal DMSP concentration showed no correlation with byssal pheophytin concentration.

The DMSP concentrations in gill and adductor were unrelated to body size and uncorrelated with pheophytin concentrations in the respective tissues. The DMSP concentration in gill was positively correlated with that in mantle ($r = 0.61$, $P < 0.01$ for siphonal mantle; $r = 0.45$, $P < 0.05$ for byssal mantle), but the DMSP concentration in adductor was not correlated with that in mantle. Table 2 presents DMSP concentrations in gill and adductor. For comparison, the means in siphonal and byssal mantle were 31.2 and 37.4 μmol/g (see Fig. 4). Note that gill exhibits DMSP concentrations similar to those of mantle. In adductor, however, DMSP is almost an order of magnitude less concentrated than in mantle.

Table 1

Pheophytin a *per gram of tissue of giant clams (wet weight, species combined) in the three tissues that showed no relation between concentration and body size*

	Pheophytin *a* (μg/g)	
Tissue	Mean	Range
Byssal mantle*	22.10	1.34–86.90
Gill	10.00	0.35–31.30
Adductor muscle	0.74	0.05–3.32

Data for siphonal mantle are omitted because they are presented elsewhere (Fig. 1) and because the mean is a possibly misleading statistic for a parameter that varies systematically with body size.

* The four highest values for byssal mantle occurred in four of the smallest clams (two of each species), suggesting that the effort to keep tissue-sample size consistent might have led to the inclusion of other types of tissue in byssal-mantle samples of some small clams. If the four highest values are excluded, the mean and range for byssal mantle are 12.8 and 1.34–33.1 μg/g.

Discussion

DMSP in the mantle and gill tissues of *Tridacna maxima* and *T. squamosa* is far more concentrated than in any animal tissue heretofore known. Most comparative data in the literature represent pooled concentrations of DMSP and DMS (similar to the data we collected). In discussing the literature, we distinguish DMSP and DMS only if the orig-

Table 2

Dimethylsulfoniopropionate (DMSP) per gram of tissue of giant clams (wet weight, species combined) in the two tissues that showed no relation between concentration and body size

	DMSP (μmol/g)	
Tissue	Mean	Range
Gill	33.3	20.3–46.1
Adductor muscle	4.4	1.8–7.2

Data for mantle are omitted for reasons stated in note to Table 1.

inal investigators did. We also exclude from consideration tissues (*e.g.*, stomach) that could contain unassimilated food. Two surveys of DMSP concentrations in molluscs have been carried out. Iida and Tokunaga (1986) measured both DMS and DMSP in 11 species of bivalves and 5 of gastropods from Japanese waters. An average of 8% of the total molar amount of the two compounds was DMS and 92% was DMSP in the mantle, gill, and adductor tissues of the bivalves. The sum of the two concentrations was usually less than 0.2 μmol/g. The single highest sum was 0.9 μmol/g in adductor muscle of oysters (*Crassostrea gigas*). Ackman and Hingley (1968) reported 0–1.8 μmol/g in the tissues of 10 species of bivalves and gastropods from Canadian waters. Most values were toward the low end of the range; the highest concentrations were in adductor muscles of scallops (*Placopecten megallanicus*) and oysters (*C. virginica*). The highest concentrations observed in populations of mussels (*Mytilus edulis*) at Cape Cod, Massachusetts, were 2–4 μmol/g (Hill *et al.*, 1995a). In wild-caught fish, muscle or liver concentrations of 0.2–1.0 μmol/g (predominantly DMSP in fresh tissue) are high and commercially problematic because they cause off-flavors (see later) (Motohiro, 1962; Ackman *et al.*, 1967; Iida *et al.*, 1986; Dacey *et al.*, 1994). Even the highest tissue concentrations in fish fed DMSP supplements were only 4–8 μmol/g (Ackman *et al.*, 1966). A survey of DMS and DMSP in several species of shrimp and krill indicated that tissue concentrations are very low in most species, although pooled concentrations (predominantly DMSP) as high as 3 μmol/g are sometimes observed in muscle of *Euphausia superba* (Tokunaga *et al.*, 1977). In the context of these comparative data, the concentrations in the mantle and gill tissues of tridacnids, averaging 31–37 μmol/g, are extraordinary. The only published animal data that are at all in the same range come from a single report on pteropods (Levasseur *et al.*, 1994) in which extremes of 30–40 μmol/g were observed (calculated form published data on tissue dry weights assuming the animals to be 70% water). Such concentrations, however, are exceptional in the literature on pteropods; other reports are 0.2–3.7 μmol/g (Motohiro, 1962; Ackman and Hingley, 1968) or lower (Ackman *et al.*, 1972). Furthermore, the pteropod data are for whole animals, including digestive-tract contents. In terms of documented evidence on tissues of animals collected in the wild, the concentrations in tridacnid mantle and gill are extreme: an order of magnitude higher than the highest concentrations observed in other bivalve or gastropod molluscs, fish, crustaceans, and other animals. Other than the tridacnids, the animals mentioned acquire DMSP strictly from ingested foods.

We hypothesize that the high concentrations in tridacnids are a consequence of the production of DMSP by their algal symbionts. Three pieces of evidence support this hypothesis. First, at least in *T. squamosa*, symbiont photosynthesis supplies over 90% of all organic carbon acquired by individuals of the body sizes we studied (Klumpp and Griffiths, 1994). Thus, although the clams ingest food to some extent and could acquire DMSP from their food, the known partitioning between phototrophic and heterotrophic nutrition makes phototrophic production of DMSP the more likely source of most DMSP, especially because symbiotic dinoflagellates are documented to produce DMSP (Hill *et al.*, 1995b). Second, the sheer magnitude of the DMSP concentrations in the tridacnids points to their algal symbionts as the source, because in all the many species of studied molluscs that lack algal symbionts, even the most extreme DMSP concentrations seen do not come close to the routine concentrations seen in the tridacnids. Third, there are several reports that the density of zooxanthellae in tridacnid tissues is an inverse function of body size (*e.g.*, Fisher *et al.*, 1985; Griffiths and Klumpp, 1996), and we found evidence of this same relation in siphonal mantle (Fig. 1). If the zooxanthellae are the primary source of DMSP and if the zooxanthellae become less dense in the siphonal mantle as individuals grow, one would predict that the DMSP concentration would be an inverse function of body size. This is what we found (Fig. 2). The DMSP and pheophytin concentrations in the siphonal mantle were well correlated (Fig. 3), and the ratio of the concentrations was consistent at 0.107 ± 0.0048 (SE) μmol/μg.

If our hypothesis is correct that the zooxanthellae are the main source of DMSP in giant clams, then tissues other than the siphonal mantle must receive DMSP by internal transport from the siphonal mantle because, as our pheophytin data confirm, the zooxanthellae occur at high densities only in siphonal mantle (Table 1). Internal transport could occur by circulation of hemolymph or by transport in the zooxanthellal tubular system (Norton *et al.*, 1992). Molluscan tissues are well known to accumulate DMSP (Ackman and Hingley, 1968; Hill *et al.*, 1995a). The high concentrations of DMSP in siphonal mantle could possibly be explained by high concentrations in the algal cells only. However, the byssal mantle and gills are so low in algal cells that the high concentrations of DMSP there almost certainly demonstrate that the animal cells of giant clams can experience very high DMSP concentrations. The physiological basis for the dramatic difference in concentration between the adductor muscle and other tissues (Fig. 5) awaits study.

Whatever the cause of the high DMSP concentrations in tridacnids, the concentrations are likely to be important to the biology of the clams in two major ways. The first is taste. One of the principal conclusions of research on commercialization of giant clams is that their meat is exceptionally perishable because of the rapid development of a "particularly offensive and pervasive odor" (Peavey and Riley, 1994). Refrigeration (Peavey and Riley, 1994) or freezing in a domestic freezer (Peavey and Riley, 1993) does little to prevent this problem, even if the viscera have been removed. Comparing mantle and adductor meat, a disagree-

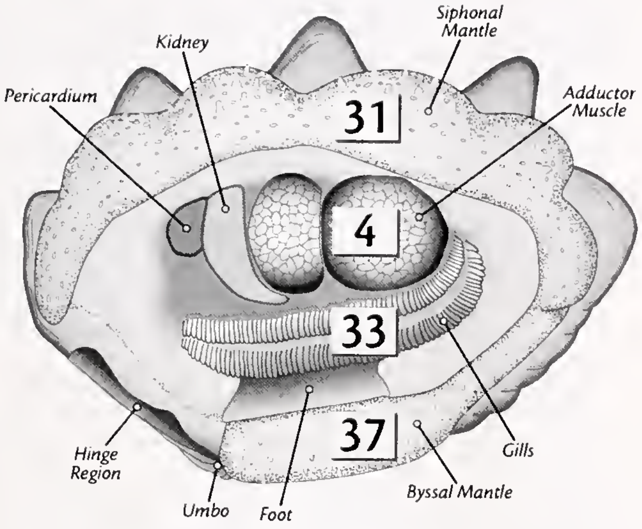

Figure 5. A giant clam in the natural orientation showing average pooled concentrations (μmol/g) of dimethylsulfoniopropionate (DMSP) and dimethylsulfide (DMS) in the four tissues studied (drawing by Jayne Doucette).

able "seaweed-like" odor has been particularly associated with the mantle (Cowan, 1988), and the mantle is far less commercially valuable than the adductor (Braley, 1988; Tisdell and Tacconi, 1993). These are serious matters in many parts of the world where giant clams occur. The clams are sources of food and protein in subsistence economies, and a number of cash-poor governments are making substantial investments in the development of giant clam aquaculture (Lucas, 1994). Partly because of preservation problems, the mantle meat may actually have a negative monetary value in commercial aquaculture (Hambrey and Gervis, 1993).

We believe we have discovered the cause of the unattractive odor and taste, thereby setting the stage for a rational approach to improvement. Although DMS has not been mentioned previously as a likely component of tridacnid tissues, it is well recognized as an important taste constituent in other seafoods. DMS produced from dietary DMSP is a negative taste factor in fish. The DMS generated during certain sorts of processing of fish meat containing as little as 0.1–1 μmol DMSP/g can cause the meat to smell "like petroleum" or taste like turnip or radish (Motohiro, 1962; Ackman *et al.*, 1966) and force catches to be discarded. On the other hand, very low concentrations of DMS are part of the valued flavor of some clams and oysters (Ackman and Hingley, 1968; Brooke *et al.*, 1968; Iida and Tokunaga, 1986). Brooke *et al.* (1968), for example, found that about 0.02 μmol/g of DMS helps impart a desirable "clamlike" odor to *Mya arenaria*, whereas more than 0.3 μmol/g of DMS is excessive.

Our data reveal that the potential for DMS formation in tridacnid tissues, particularly mantle, is enormous. We assume that in the fresh clams we studied, most of the sulfur we measured was in the form of DMSP (Iida and Tokunaga, 1986), which has unknown taste effects. After the death of the clam, DMSP is likely under many circumstances (Motohiro, 1962; Ackman *et al.*, 1966) to be broken down to DMS enzymatically (*e.g.*, by bacterial DMSP lyases; Ledyard *et al.*, 1993) or nonenzymatically (*e.g.*, Dancey and Blough, 1987). With over 30 μmol/g of DMSP present, the concentrations of DMS that could readily be formed are far in excess of ones known to make all other foods inedible. It is probably no accident that the methods devised by indigenous people to preserve tridacnid meat include acidic washes and drying (Munro, 1989; Hambrey and Gervis, 1993). Acid pHs inhibit the nonenzymatic breakdown of DMSP to DMS (Motohiro, 1962; Dacey and Blough, 1987), and because DMS is very volatile, drying would remove it from tissue. Looking to the future, it might be possible to inhibit DMS formation in a chemically specific manner or even to develop strains of zooxanthellae that produce little DMSP.

The second major way in which DMSP concentrations are potentially important to tridacnid biology is their biochemical significance. Recognizing that DMSP is employed by some organisms to help set the colligative properties of cellular solutions, Nishiguchi and Somero (1992) studied the effects of DMSP on cellular proteins. They found evidence of temperature dependence. Whereas DMSP exhibited stabilizing effects on proteins at low temperatures, it could perturb protein function at high physiological temperatures. In particular, Nishiguchi and Somero found that DMSP promotes the denaturation of glutamate dehydrogenase at 37°C in a concentration-dependent manner, with effects evident at the lowest concentration tested, 100 m*M* DMSP. Similarly, Karsten *et al.* (1996) observed a concentration-dependent suppression of activity of malate dehydrogenase at 30°C; the suppression became evident at concentrations between 19 and 75 m*M* DMSP. Such effects of DMSP have been tacitly assumed to be relevant just to plants and algae because only plants and algae have hitherto been thought to have native DMSP concentrations high enough to be in the effective range. Our results make clear that alone among animals, tridacnids can have DMSP concentrations within the range shown to have enzyme-perturbing effects. In *T. maxima* and *T. squamosa* of the sizes we studied, the mantle averages about 0.83 ml water per gram wet weight (our unpublished data). Thus, if we assume that the DMSP in mantle is entirely dissolved and distributed evenly in tissue water, the mean concentration of DMSP in the tissue water is over 40 m*M*. On the basis of the chemical structural properties of DMSP and the preferential hydration model, Nishiguchi and Somero (1992) argue that DMSP, like dimethylsulfoxide, may be toxic to cells and may denature proteins at high physiological temperatures. In warm tropical waters and especially in shallows where solar heat-ing can occur, the high DMSP concentrations of tridacnids may be stressful by-products of extreme exploitation of phototrophic nutrition (Klumpp and Griffiths, 1994). Tridacnids may require specializations of metabolic chemistry to reduce or tolerate enzyme-perturbing and other toxic effects of their high DMSP concentrations. Interspecific differences in such specializations might help explain differences in growth rates and energetics that have previously remained enigmatic (Klumpp and Griffiths, 1994).

Acknowledgments

Special thanks to Raouf Kilada for planting the seeds of this study. Thanks to Dave Kulis, Ishmael Paul, and Eric Zettler for help with sampling and chlorophyll assays. Supported by NSF OCE-9713407 and WHOI Mellon 27005129. This is Woods Hole Oceanographic Institution Contribution No. 9993.

Literature Cited

Ackman, R. G., and H. J. Hingley. 1968. The occurrence and retention of dimethyl-β-propiothetin in some filter-feeding organisms. *J. Fish. Res. Board Can.* **25:** 267–284.

Ackman, R. G., J. Dale, and J. Hingley. 1966. Deposition of dimethyl-β-propiothetin in Atlantic cod during feeding experiments. *J. Fish. Res. Board Can.* **23:** 487–497.

Ackman, R. G., J. Hingley, and A. W. May. 1967. Dimethyl-β-propiothetin and dimethyl sulphide in Labrador cod. *J. Fish. Res. Board Can.* **24:** 457–461.

Ackman, R. G., J. Hingley, and K. T. MacKay. 1972. Dimethyl sulfide as an odor component in Nova Scotia fall mackerel. *J. Fish. Res. Board Can.* **29:** 1085–1088.

Andreae, M. O., and P. J. Crutzen. 1997. Atmospheric aerosols: Biogeochemical sources and role in atmospheric chemistry. *Science* **276:** 1052–1058.

Andreae, M. O., W. R. Barnard, and J. M. Ammons. 1983. The biological production of dimethylsulfide in the ocean and its role in the global atmospheric sulfur budget. *Ecol. Bull. (Stockholm)* **35:** 167–177.

Braley, R. D. 1988. Farming the giant clam. *World Aquaculture* **20(1):** 7–17.

Brooke, R. O., J. M. Mendelsohn, and F. J. King. 1968. Significance of dimethyl sulfide to the odor of soft-shell clams. *J. Fish. Res. Board Can.* **25:** 2453–2460.

Charlson, R. J., J. E. Lovelock, M. O. Andreae, and S. G. Warren. 1987. Oceanic phytoplankton, atmospheric sulphur, cloud albedo and climate. *Nature* **326:** 655–661.

Cowan, L. 1988. Use of giant clams in Japanese cuisine. Pp. 256–257 in *Giant Clams in Asia and the Pacific*, J. W. Copland and J. S. Lucas, eds. Australian Centre for International Agricultural Research, Canberra, Australia.

Dacey, J. W. H., and N. V. Blough. 1987. Hydroxide decomposition of dimethyl-sulfoniopropionate to form dimethylsulfide. *Geophys. Res. Lett.* **14:** 1246–1249.

Dacey, J. W. H., G. M. King, and P. S. Lobel. 1994. Herbivory by reef fishes and the production of dimethylsulfide and acrylic acid. *Mar. Ecol. Prog. Ser.* **112:** 67–74.

Dalzell, P., T. J. H. Adams, and N. V. C. Polunin. 1996. Coastal fisheries in the Pacific islands. *Oceanogr. Mar. Biol. Annu. Rev.* **34:** 395–531.

Falkowski, P. G., Y. Kim, Z. Kolber, C. Wilson, C. Wirick, and R. Cess. 1992. Natural versus anthropogenic factors affecting low-level cloud albedo over the North Atlantic. *Science* **256:** 1311–1313.

Fisher, C. R., W. K. Fitt, and R. K. Trench. 1985. Photosynthesis and respiration in *Tridacna gigas* as a function of irradiance and size. *Biol. Bull.* **169:** 230–245.

Griffiths, C. L., and D. W. Klumpp. 1996. Relationships between size, mantle area and zooxanthellae numbers in five species of giant clam (Tridacnidae). *Mar. Ecol. Prog. Ser.* **137:** 139–147.

Hambrey, J., and M. Gervis. 1993. The economic potential of village based farming of giant clams (*Tridacna gigas*) in Solomon Islands. Pp. 138–146 in *The Biology and Mariculture of Giant Clams*, W. K. Fitt, ed. Australian Centre for International Agricultural Research, Canberra, Australia.

Hill, R. W., J. W. H. Dacey, D. K. D. Hill, J. E. McDowell, and D. F. Leavitt. 1995a. Accumulation and retention of dimethylsulfoniopropionate by bivalve molluscs: high and nonnormal variation. *Biol. Bull.* **189:** 233–234.

Hill, R. W., J. W. H. Dacey, and D. A. Krupp. 1995b. Dimethylsulfoniopropionate in reef corals. *Bull. Mar. Sci.* **57:** 489–494.

Holm-Hansen, O., and B. Riemann. 1978. Chlorophyll *a* determination: improvements in methodology. *Oikos* **30:** 438–447.

Iida, H., and T. Tokunaga. 1986. Dimethyl sulfide and dimethyl-β-propiothetin in shellfish. *Bull. Jpn. Soc. Sci. Fish.* **52:** 557–563.

Iida, H., J. Nakazoe, H. Saito, and T. Tokunaga. 1986. Effect of diet on dimethyl-β-propiothetin content in fish. *Bull. Jpn. Soc. Sci. Fish.* **52:** 2155–2161.

Karsten, U., K. Kück, C. Vogt, and G. O. Kirst. 1996. Dimethylsulfoniopropionate production in phototrophic organisms and its physiological function as a cryoprotectant. Pp. 143–153 in *Biological and Environmental Chemistry of DMSP and Related Sulfonium Compounds*, R. P. Kiene, P. T. Visscher, M. D. Keller, and G. O. Kirst, eds. Plenum, New York.

Keller, M. D., W. K. Bellows, and R. R. L. Guillard. 1989a. Dimethyl sulfide production in marine phytoplankton. Pp. 167–182 in *Biogenic Sulfur in the Environment*, E. S. Saltzman and W. J. Cooper, eds. American Chemical Society, Washington, DC.

Keller, M. D., W. K. Bellows, and R. R. L. Guillard. 1989b. Dimethylsulfide production and marine phytoplankton: an additional impact of unusual blooms. Pp. 101–115 in *Novel Phytoplankton Blooms*, E. M. Cosper, V. M. Bricelj, and E. J. Carpenter, eds. Springer-Verlag, New York.

Klumpp, D. W., and C. L. Griffiths. 1994. Contributions of phototrophic and heterotrophic nutrition to the metabolic and growth requirements of four species of giant clam (Tridacnidae). *Mar Ecol. Prog. Ser.* **115:** 103–115.

Ledyard, K. M., E. F. DeLong, and J. W. H. Dacey. 1993. Characterization of a DMSP-degrading bacterial isolate from the Sargasso Sea. *Arch. Microbiol.* **160:** 312–318.

Levasseur, M., M. D. Keller, E. Bonneau, D. D'Amours, and W. K. Bellows. 1994. Oceanographic basis of a DMS-related Atlantic cod (*Gadus morhua*) fishery problem: blackberry feed. *Can. J. Fish. Aquat. Sci.* **51:** 881–889.

Lucas, J. S. 1994. The biology, exploitation, and mariculture of giant clams (Tridacnidae). *Rev. Fish. Sci* **2:** 181–223.

Maruyama, T., M. Ishikura, S. Yamazaki, and S. Kanai. 1998. Molecular phylogeny of zooxanthellate bivalves. *Biol. Bull.* **195:** 70–77.

Motohiro, T. 1962. Studies on the petroleum odour in canned chum salmon. *Mem. Fac. Fish., Hokkaido Univ.* **10:** 1–65.

Munro, J. L. 1989. Fisheries for giant clams (Tridacnidae: Bivalvia) and prospects for stock enhancement. Pp. 541–558 in *Marine Invertebrate Fisheries: Their Assessment and Management*, J. F. Caddy, ed. Wiley, New York.

Nishiguchi, M. K., and G. N. Somero. 1992. Temperature- and concentration-dependence of compatibility of the organic osmolyte β-dimethylsulfoniopropionate. *Cryobiology* **29:** 118–124.

Norton, J. H., M. A. Shepherd, H. M. Long, and W. K. Fitt. 1992. The zooxanthellal tubular system in the giant clam. *Biol. Bull.* **183:** 503–506.

Peavey, S., and J. Riley. 1993. Sensory evaluation of fresh and frozen giant clams. Research Report 93-02, National Aquaculture Center, Federated States of Micronesia. 22 pp.

Peavey, S., and J. Riley. 1994. Marketing giant clams in the local foodservice industry: a case study. Research Report 94-01, National Aquaculture Center, Federated States of Micronesia. 56 pp.

Rowan, R. 1998. Diversity and ecology of zooxanthellae on coral reefs. *J. Phycol.* **34:** 407–417.

Shaw, G. E. 1983. Bio-controlled thermostasis involving the sulfur cycle. *Clim. Change* **5:** 297–303.

Tisdell, C., and L. Tacconi. 1993. Economics of giant clam production in Australia and Fiji and sensitivity factors. Pp. 133–137 in *The Biology and Mariculture of Giant Clams,* W. K. Fitt, ed. Australian Centre for International Agricultural Research, Canberra, Australia.

Tokunaga, T., H. Iida, and K. Nakamura. 1977. Formation of dimethyl sulfide in Antarctic krill, *Euphausia superba. Bull. Jpn. Soc. Sci. Fish.* **43:** 1209–1217.

Reference: *Biol. Bull.* **199:** 116–125. (October 2000)

Particle Transport in the Zebra Mussel, *Dreissena polymorpha* (Pallas)

SHIRLEY M. BAKER[1,*], JEFFREY S. LEVINTON[1], AND J. EVAN WARD[2]

[1]*Department of Ecology and Evolution, State University of New York, Stony Brook, New York 11794; and* [2]*Department of Marine Sciences, University of Connecticut, Groton, Connecticut 06340*

Abstract. The capture, transport, and sorting of particles by the gills and labial palps of the freshwater mussel *Dreissena polymorpha* were examined by endoscopy and video image analysis. More specifically, the morphology of the feeding organs in living zebra mussels was described; the mode and speeds of particle transport on the feeding organs was measured; and the sites of particle selection in the pallial cavity were identified. Particle velocities (outer demibranch lamellae, 90 μm s^{-1}; inner demibranch lamellae, 129 μm s^{-1}; marginal food groove of inner demibranchs, 156 μm s^{-1}; dorsal ciliated tracts, 152 μm s^{-1}), as well as the movement of particles on the ctenidia and labial palps of *D. polymorpha*, are consistent with mucociliary, rather than hydrodynamic, transport. Particles can be sorted on the ctenidia of zebra mussels, resulting in a two-layer transport at the marginal food groove of the inner demibranch. That is: preferred particles are transported inside the marginal groove proper, whereas particles destined for rejection are carried superficially in a string of mucus. Sorting also occurs at the ventral margin of the outer demibranch; desirable particles are retained on the outer demibranch, whereas unacceptable particles are transferred to the inner demibranch and ultimately excluded from ingestion. We suggest that the structure of homorhabdic ctenidia does not preclude particle sorting, and that some ecosystem modifications attributed to zebra mussels may ultimately be due to ctenidial sorting mechanisms.

Introduction

Many suspension-feeding organisms, including bivalves, sort food particles on the basis of size (Vahl, 1972; Stenton-Dozey and Brown, 1992; Defossez and Hawkins, 1997) and quality (MacDonald and Ward, 1994; Arifin and Bendell-Young, 1997; Ward *et al.*, 1997). Moreover, endoscopic examination and video image analysis are now frequently used to directly observe particle capture, transport, and sorting in marine bivalves (Ward *et al.*, 1991, 1998; Beninger *et al.*, 1992; Ward, 1996). With this method, pallial structures can be observed *in vivo* in relatively undisturbed specimens, so that the direction, velocity, fate, and hydrodynamic mechanisms of ciliary transport of particles within the pallial cavity can be determined directly (Ward *et al.*, 1993). The endoscope does not disturb the morphological and hydrodynamic relationships of pallial organs, an advantage over the usual techniques of excision and surgical alteration of living bivalves (Nelson, 1960; Galtsoff, 1964; Jørgensen, 1966).

In previous studies, Ward *et al.* (1998) found that particle sorting in oysters (subclass Pteriomorphia; psuedolamellibranch, heterorhabdic, plicate gills) takes place on the ctenidia; particles of differing food qualities are partitioned between the marginal groove and the dorsal ciliated tract. In contrast, the ctenidia of marine mussels (subclass Pteriomorphia; filibranch, homorhabdic, nonplicate gills) play little role in particle selection. Ward *et al.* (1998) suggested that selection by the oyster ctenidia reflects the greater complexity of those organs. (For review of bivalve gill anatomy, see Atkins, 1937a,b; Ruppert and Barnes, 1994.)

Zebra mussels [*Dreissena polymorpha* (Pallas, 1771)] are freshwater suspension-feeding bivalves in the subclass Heterodonta. Like marine mussels, zebra mussels have homorhabdic, nonplicate ctenidia. But, unlike marine mussels, they are eulamellibranchs; ctenidial filaments are connected by interfilamentous tissue junctions. This ctenidial condition is more similar to that of the pseudolamellibranch oysters in which the filaments are connected by some,

---

Received 27 October 1999; accepted 14 July 2000.

* Present address: Department of Fisheries and Aquatic Sciences, University of Florida, 7922 NW 71st Street, Gainesville, Florida 32653-3071. E-mail: smbaker@mail.ifas.ufl.edu

Abbreviations: OIT, optical insertion tube of an endoscope.

although not extensive, interfilamentous tissue junctions. An examination of zebra mussel ctenidia, therefore, might indicate whether ctenidial sorting is related to morphology or to phylogeny. Indeed, recent flow-cytometry studies by Baker *et al.* (1998) demonstrate that the zebra mussel pallial organs effectively sort particles. In this investigation, we use endoscopic examination to observe (1) the morphology of feeding organs in living zebra mussels, (2) the mode and speeds of particle transport on the feeding organs, and (3) sites of particle selection in the pallial cavity. We compare our endoscopic examination of zebra mussels with previous reports of feeding processes in both zebra mussels and marine bivalves.

Zebra mussels have invaded many freshwater localities in Europe and North America. In systems where large populations of these mussels have become established, not only has phytoplankton biomass declined (Holland, 1993; Fahnenstiel *et al.*, 1995; Caraco *et al.*, 1997), but seston composition has changed as well (Vanderploeg *et al.*, 1996; Smith *et al.*, 1998; Strayer *et al.*, 1999). Understanding the form and function of feeding structures in zebra mussels and their mechanisms of particle selection will contribute to a better understanding of these effects on ecosystems.

Materials and Methods

Phytoplankton cultures were obtained from the University of Texas Culture Collection and grown in a freshwater enrichment medium WCL1 (Guillard, 1983; Guillard and Hargraves, 1993). Cultures were grown at room temperature, under a 16:8 h light:dark regime. Species of phytoplankton that were cultured included *Cyclotella meneghiniana* (LB 2455; barrel-shaped, 18 × 6 μm) (Bacillariophyceae), *Crucigenia tetrapedia* (63; disk-shaped, 5 × 11 μm), *Scenedesmus quadricauda* (LB 614; four cells stacked, total 25 × 10 μm) (Chlorophyceae), and *Microcystis aeruginosa* (LB 2386; spherical, 4 μm) (Cyanophyceae). Cell dimensions were measured with a compound microscope and calibrated ocular micrometer.

Nonliving particles were also used in endoscopic observations. Polystyrene beads (Polysciences, Inc., Warrington, PA) of 1, 10, or 22 μm were often used as tracer particles. Dead cattail (*Typha* sp.) leaves from the previous growing season were collected for use as detrital material. The leaves were washed of debris and processed in a blender with distilled water for 5 min. The resulting suspension was sieved through a 20-μm nylon screen, and the retained particles (>20 μm) were discarded; 90% of the particles in the remaining suspension were $\leq$3.5 μm, as measured by an electronic particle counter (Coulter Electronics, Multisizer).

Specimens of *Dreissena polymorpha*, about 20 mm in length, were collected from the Hudson River at Tivoli, New York, or from the Huron River, Ann Arbor, Michigan. Mussels were maintained in 40-l aquaria at 16°C and fed a daily ration of cultured phytoplankton plus a mixture of preserved diatoms (Diet C, Coast Seafoods, Co., Quilcene, WA). Partial water changes (*ca.* 20%) were performed on alternating days; freshwater was prepared according to Sprung (1987).

We prepared zebra mussels for endoscopy by drilling a small hole (<2 mm in diameter) in one valve with a rotary tool (Dremel, Racine, WI) and cauterizing the underlying mantle tissue. The hook side of a piece of hook and loop fastener (Velcro brand) was cemented with epoxy to the valve opposite the drilled hole for later use in positioning the animal for examination. The mussels were allowed to recover for at least one day. This treatment caused no apparent adverse change in the behavior of the mussels, and shell and mantle repair at the site of the drilled hole often began within several days.

Endoscopic examinations were performed according to Ward *et al.* (1991, 1993, 1994). An endoscope (K12-09-15-53, Olympus Corp., Lake Success, NY), with an optical insertion tube (OIT) of 1.2 mm diameter, was connected to an optical zoom-adaptor (Schölly Fiberoptic, Denzlinger, Germany) and attached to a monochrome or color CCD camera (4990 or 8280, Cohu Electronics, San Diego, CA). A halogen (HLS24-0, Welch Allyn, Skaneateles Falls, NY) or xenon lamp (ALS-6250U, Olympus High Intensity Helioid Light Source) provided light to the OIT. The camera and endoscope were mounted on a macro-focusing rail, allowing fine adjustments of the OIT. Video was recorded at 30 frames s^{-1} on an sVHS videocassette recorder (VCR) (AG-1960, Panasonic Industrial Company, Secaucus, NJ).

For endoscopic examination, mussels were placed in a 500-ml plastic container set in a 15-l water bath with its temperature maintained between 16° and 18°C. A dome inside the plastic container had been covered with the loop side of Velcro-brand fastener, allowing rapid mounting and precise positioning of mussels. The OIT was inserted into the pallial cavity of the mussel through the inhalent siphon, the pedal gape, or the drilled and cauterized hole. Recordings were made after the mussel showed active feeding behavior, as indicated by extension of the mantle and siphons and by the intake of particles. Mussels were exposed to suspensions of one or two particle types at concentrations of 10^4, 10^5, and 10^6 particles ml^{-1}. Particle suspensions were delivered to the plastic container by gravity from a 4-l carboy. The container was frequently flushed to maintain particle concentration, which was also monitored with a Coulter Multisizer.

We observed and recorded the positions and movements of the ctenidia and labial palps, as well as the movement of particles on these organs. The best observations were made when the OIT was inserted into the pallial cavity through the drilled hole in the shell and mantle. In this position, the mussels fed normally, uninterrupted by movements of the OIT. Although the pallial cavity could be entered through the inhalent siphon, any movement of the OIT resulted in the cessation of feeding. And when the pallial cavity was entered through the pedal gape, the foot usually touched the OIT, coating it with mucus. Results were based on the examination of 21 mussels.

Particle velocities on feeding structures were determined from the number of video frames required for a particle to traverse a known distance. Distances were calibrated according to Ward (1996): *i.e.,* the pallial organs were dissected from several mussels, and the widths of the ctenidial filaments, palp ridges, and marginal grooves were measured with a compound microscope equipped with a calibrated ocular micrometer. Velocities (μm s^{-1}) are presented as means ± 1 standard deviation.

Results

When observed by endoscopy, the positions of the ctenidia within the pallial cavity are different from those that might be expected from dissected specimens (Fig. 1). The demibranchs are held curved towards the visceral mass, and the ventral margin of the outer demibranchs is particularly bent inward (Fig. 2). These gill postures are maintained despite variation in the overall orientation of the mussels.

Through the relatively transparent ciliated epithelia of the ctenidia, we observed internal bands of muscular cross-struts (Medler and Silverman, 1997) that are perpendicular to the ctenidial filaments and 60–80 μm apart. Ostia, located in the epithelium of the interfilamentary spaces, are lacking directly above the struts (Medler and Silverman, 1997).

The inhalent flow of suspended particles sometimes stops, or even reverses momentarily, especially under high particle concentrations. In addition, the ctenidia often contract during active feeding; the interfilamentary spaces, where the ostia are located, alternately flare and close at a rate of 1 cycle s^{-1}. The extension of the mantle and siphons, often used as an indication of steady feeding, does not change during flow cessation and reversals, or during pulsation of the ctenidia.

Particles captured by the ctenidia move smoothly along the frontal surfaces of the ctenidial filaments, and particles of different types and sizes maintain their distance from each other. Mucous strings were observed on the frontal surfaces of the filaments only when the particle concentration was extremely high.

Outer demibranchs and their ventral margins

The outer demibranchs and their ventral margins were observed in seven specimens, on 42 occasions, for 15.5 h of total observation time and 1.7 h of video recording. The outer demibranchs are held relatively straight, but with an inward bend, especially of the ascending lamella, near the ventral margin (Fig. 2). The position of the outer demibranch changes with pumping activity: the outer demibranch is positioned near the inner demibranch when inhalent flow speeds are low; as flow speeds increase, the outer demibranch moves laterally away from the inner demibranch (Fig. 1). Particles captured on the descending lamella of the outer demibranch are transported dorsally to the

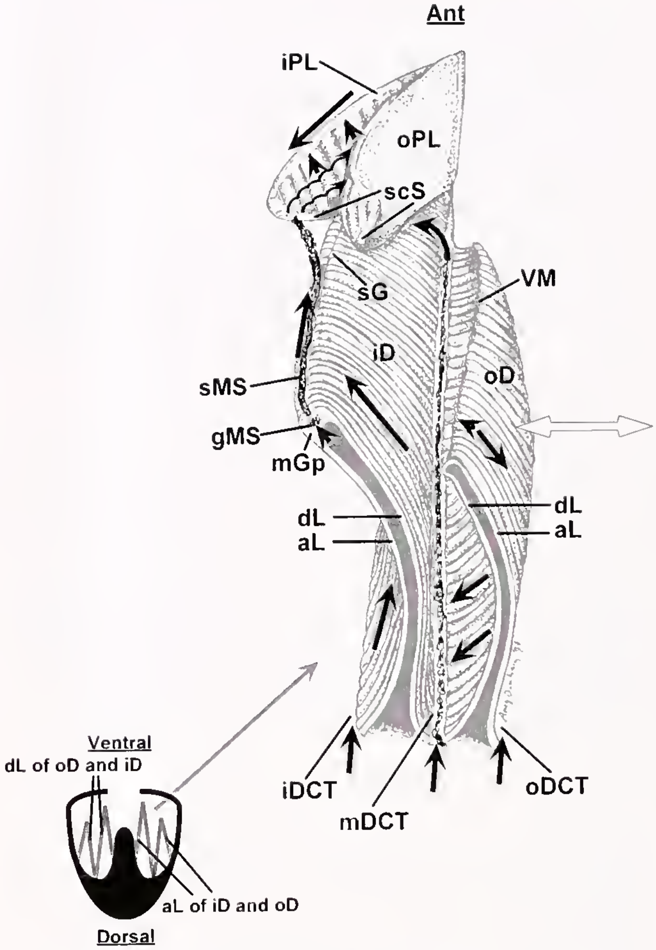

Figure 1. Diagram of labial palps and anterior portions of the inner and outer demibranchs of *Dreissena polymorpha* as observed through the endoscope (looking dorso-anteriorly). Palp lamellae are shown slightly spread apart, with the outer Palp lamella (oPL) curled back. Solid arrows indicate particle paths after capture. The white arrow indicates movement of the outer demibranch (oD). Particles in the medial dorsal ciliated tract (mDCT) are transported in mucous clumps and strings. Particles are transported at the ventral margin of the inner demibranch (iD) as both a groove mucous string (gMS) in the marginal groove proper (mGp) and as a superficial mucous string (sMS). The palps (iPL and oPL) enclose the inner demibranch only, drawing in the superficial mucous string (sMS) from the inner demibranch (iD) (see text for details). (aL = ascending lamella, Ant = anterior, dL = descending lamella, gMS = groove mucous string, iD = inner demibranch, iDCT = inner dorsal ciliated tract, iPL = inner palp lamella, mDCT = medial dorsal ciliated tract, mGp = marginal groove proper, oD = outer demibranch, oDCT = outer dorsal ciliated tract, oPL = outer palp lamella, scS = smooth ciliated surface, sG = superficial groove, sMS = superficial mucous string, VM = ventral margin.) See *Video Note,* p. 124.

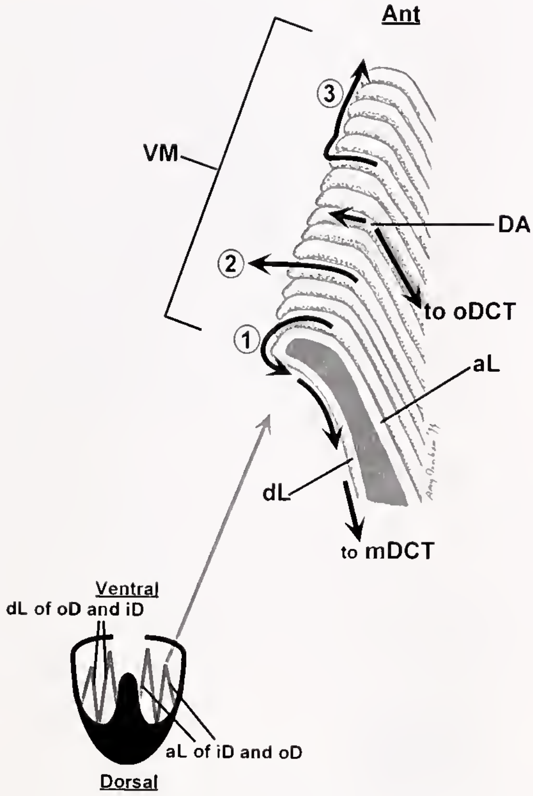

Figure 2. Diagram of the ventral margin (VM) of the outer demibranch (oD) of *Dreissena polymorpha* as observed through the endoscope (looking dorso-anteriorly). Solid arrows indicate particle paths after capture. Particles on the ascending lamella (aL) are transported either dorsally or ventrally, depending on whether they are above or below a divergence area (DA) when captured. Upon reaching the ventral margin (VM), particles traveling ventrally either (1) move over the ventral margin and proceed dorsally on the descending lamella (dL); (2) continue moving ventrally, leaving the surface of the ctenidia and becoming resuspended; or (3) make a right angle turn and begin moving anteriorly on the ventral margin (VM) (see text for details). (aL = ascending lamella, Ant = anterior, DA = divergence area, dL = descending lamella, mDCT = medial dorsal ciliated tract, oDCT = outer dorsal ciliated tract, VM = ventral margin.) See *Video Note*, p. 124.

medial dorsal ciliated tract (Fig. 2). On the ascending lamella of the outer demibranch, particles are transported either dorsally or ventrally, depending on whether they were captured above or below a divergence area located near the bend of the demibranch (Figs. 1, 2). When particles are captured directly at the divergence area, they oscillate in place for several seconds before proceeding either ventrally or dorsally. The position of the divergence area can shift ventrally or dorsally by about 1 mm. This shift does not appear to be correlated with any particular stimulus, such as particle type or concentration. Mean particle velocity on the frontal surfaces of the ascending lamella of the outer demibranch is 90 μm s^{-1} (Table 1).

Due to the bend of the outer demibranch, the ventral margin is pointed towards the inner demibranch, and the space between the two demibranchs is small (Fig. 1). Particles captured ventral to the divergence line on the ascending lamella of the outer demibranch move ventrally. Upon reaching the ventral margin, one of the following three behaviors occurs (Fig. 2): (1) The particles move over the ventral margin and proceed dorsally on the descending lamella of the demibranch. (2) The particles continue moving ventrally, leave the surface of the ctenidia, and become resuspended. Most often, these resuspended particles are then recaptured by the descending lamella of the inner demibranch and continue moving ventrally. The majority of particles that leave the ventral margin of the outer demibranch are large, like *Scenedesmus*. (3) The particles make a right angle turn and begin moving anteriorly on the ventral margin. Individual particles bounce along the ventral margin from filament to filament at a mean velocity of 65 μm s^{-1} (Table 1). At high concentrations ($>10^6$ ml^{-1}), particles are sometimes carried along the ventral margin in clumps of mucus. As a result of these three particle trajectories, desirable particles are retained on the outer demibranch, while unacceptable particles are transferred to the inner demibranch and ultimately excluded from ingestion.

Inner demibranchs and their marginal grooves

The inner demibranchs and their marginal grooves were observed in seven specimens, on 60 occasions, for 29.7 h of total observation time and 2.9 h of video. Particles captured on either descending or ascending lamellae of the inner demibranch are transported toward the ventral margin, whose mean width is 276 μm ($n = 7$; Fig. 1). Mean particle velocities on the ascending and descending lamellae of the inner demibranch are 129 μm s^{-1} (Table 1).

Material at the ventral margin of the inner demibranch is transported anteriorly in one of two channels, one deep and one superficial (Figs. 1, 3). The deep channel, the marginal groove proper, is nearly enclosed by the projection of the ventral tips of the filaments over the groove. The superficial

Table 1

Particle velocities (22-μm polystyrene beads) on the pallial organs of zebra mussels, Dreissena polymorpha, *at 18°C*

Location	Mean velocity ± SD (μm s^{-1})	Range (μm s^{-1})	*n*
Outer demibranch			
Frontal surface	90 ± 22	60–123	9
Ventral margin	65 ± 23	24–104	19
Inner demibranch			
Frontal surface	129 ± 54	42–251	33
Ventral food groove	156 ± 53	45–354	106
Dorsal ciliated tract	152 ± 62	41–305	50
Labial palps			
Frontal surfaces	94 ± 34	54–150	10
Ventral margin	54 ± 21	16–113	33

channel or groove is a depression at the center of the ventral margin, with openings between adjacent and opposite filament tips leading to the marginal groove proper (Fig. 3). The superficial groove is entirely exposed to the inhalent flow.

Particles transported in the superficial groove are embedded in a string of mucus, up to 80 μm thick (Figs. 1, 3), which moves at a mean velocity of 156 μm s^{-1} (Table 1). The presence of a superficial mucous string, as opposed to a particle slurry, was confirmed by observing the dislodgment of strings from the ventral margin when the valves were rapidly adducted, or when a jet of water was pipetted into the hole through which the OIT was inserted. After dislodgment, the superficial mucous string remains unbroken and returns to the ventral margin of the demibranch. Polystyrene spheres (1 μm) and the large green alga *Scenedesmus* are incorporated into the superficial mucous string and are eventually rejected as pseudofeces.

Particles transported anteriorly inside the marginal groove proper are also embedded in a string of mucus (Figs. 1, 3). These particles appear to be those that are eventually ingested. This observation was confirmed when specimens were fed a combination of *Microcystis*, which is preferentially ingested, and *Scenedesmus* or *Typha* detritus, which are both rejected (Baker *et al.*, 1998). The resulting colors of the mucous strings, as well as the relative particle sizes, indicate that *Microcystis* is incorporated into the groove mucous string, whereas *Scenedesmus* or *Typha* is incorporated into the superficial mucous string. Two other observations suggest that particles moving inside the marginal groove proper are also embedded in mucus. First, particles inside the marginal groove proper move at the same velocity as particles transported in the superficial mucous string. Second, particles both inside and outside the marginal groove maintain positions relative to each other as they move anteriorly. Additional observations suggest that the deep and superficial mucous strings are not continuous with each other, but are physically separate. For example, when the superficial mucous string is dislodged from the superficial groove, the groove mucous string is not disturbed and remains within the marginal groove proper.

Particles approaching the ventral margin of the inner demibranch have three potential fates (Fig. 3): (1) As particles round the crest of the ventral margin, some move anteriorly and diagonally, bouncing from filament to filament, before being entrained in the superficial mucous string. These particles join the more ventral portion of the superficial mucous string, and move in a uniform, smooth manner (Fig. 3, path 1). (2) Other particles move laterally prior to rounding the crest of the ventral margin, and enter the interfilamentary space between two adjacent filaments. Some of these particles stall, oscillate for several seconds, and then disappear from view, possibly lost to an underlying water tube through an ostial opening. Many particles, however, continue moving toward the superficial groove and became entrained in the more dorsal portion of the superficial mucous string. These particles do not move smoothly but follow the contours of the filament tips, bouncing as they move anteriorly (Fig. 3, path 2). (3) Still other particles appear to remain on the frontal surfaces of the filaments until reaching the tips, where they move laterally into the

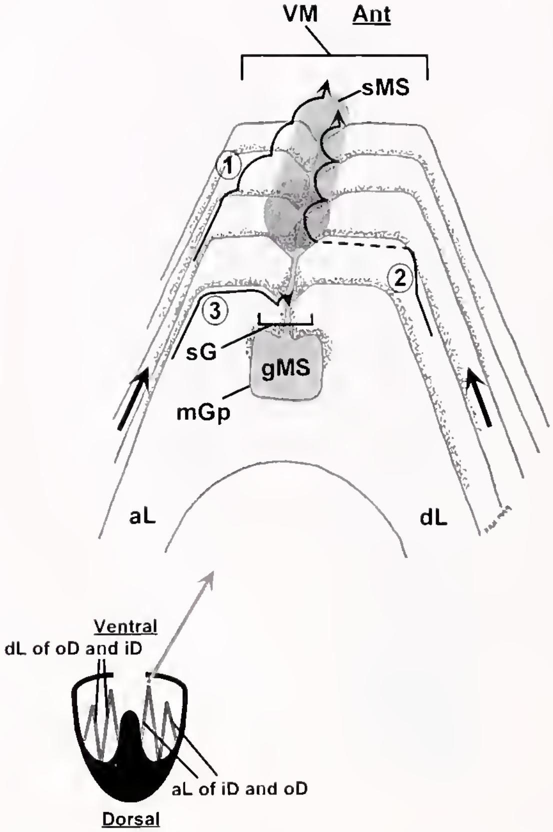

Figure 3. Diagram of the ventral margin of the inner demibranch of *Dreissena polymorpha* as observed through the endoscope (looking dorso-anteriorly). The groove mucous string (gMS) and a portion of a superficial mucous string (sMS) are shown. Solid arrows indicate particle paths after capture. Shaded arrows indicate particle paths behind a filament. Particles approaching the ventral margin (VM) of the inner demibranch (iD) enter the mucous strings in three ways: (1) As particles round the crest of the ventral margin (VM), they move anteriorly and diagonally, bouncing from filament to filament. These particles are entrained in the top (ventral side) of the superficial mucous string, where they move smoothly towards the anterior of the ctenidium. (2) Particles move laterally prior to rounding the crest of the ventral margin and enter the furrow between two adjacent filaments (dashed arrow). These particles become entrained in the bottom (dorsal side) of the superficial mucous string and follow the contours of the filament tips as they move anteriorly. (3) Particles remain on the frontal surfaces of the filaments until reaching the tips, where they move laterally and down (dorsally) into the marginal groove proper (see text for details). These particles move smoothly towards the anterior in the groove string. (aL = ascending lamella, Ant = anterior, dL = descending lamella, gMS = groove mucous string, mGp = marginal groove proper, sG = superficial groove, sMS = superficial mucous string, VM = ventral margin.) See *Video Note*, p. 124.

marginal groove proper through gaps between adjacent and opposing filament tips (Fig. 3, path 3). Those particles transported in the groove proper are alternately seen through the gaps between adjacent filament tips and, faintly, as they pass behind the relatively transparent filament tips.

Because the superficial mucous string is sometimes opaque, we were unable to observe the marginal groove proper at all particle concentrations and types. Therefore, it is unclear whether the filament tips forming the marginal groove proper flare "open" and "closed." Although the gaps through which particles enter into the marginal groove proper appear absent at times and large at others, the overall width of the superficial groove does not change markedly, ranging from 17 to 38 μm wide (n = 10).

At high particle concentrations, the ventral margin of the inner demibranch occasionally presses against the visceral mass for several seconds. In these cases, the superficial mucous string is transferred to ciliated tracts on the visceral mass and is transported posteriorly, presumably to the inhalent siphon for rejection. Movement of the mucous string inside the marginal groove proper does not appear to be interrupted.

Dorsal ciliated tracts

The dorsal ciliated tracts were observed in three specimens, on 12 occasions, for 11.4 h of total observation time and 47 min of video. There are three dorsal tracts on each side of the visceral mass: at the junction of the viscera and inner demibranch (inner dorsal ciliated tract), between the two demibranchs (medial dorsal ciliated tract), and at the junction of the outer demibranch and the mantle (outer dorsal ciliated tract) (Fig. 1). Particles enter the medial dorsal ciliated tract from the descending lamella of the outer demibranch (Figs. 1, 2); they are carried anteriorly as individuals at low particle concentrations, or in mucous clumps and discrete strings at higher concentrations (Fig. 1). Particles moving in the medial dorsal ciliated tract sometimes stop or reverse for several seconds, and this behavior is associated with extreme flaring of the interfilamentary spaces on the adjacent demibranchs. In addition, quick successive contractions by the adjacent demibranchs seem to make the mucous clumps less cohesive. At high particle concentrations, the two demibranchs occasionally contract strongly, and a slurry of particles becomes resuspended in the pallial cavity. It was not possible to determine whether these particles are recaptured. Particles in the medial dorsal ciliated tract move at a mean velocity of 152 $\mu m\ s^{-1}$ (Table 1).

A few particles are also transported anteriorly in the inner and outer dorsal ciliated tracts (Fig. 1). Particles enter these tracts not only from the demibranchs, but also from the mantle or body, suggesting that cilia on these surfaces can trap some particles.

Labial palps

The labial palps were observed in four specimens, on 14 occasions, for 11 h of total observation time and 2.2 h of video. Two pair of palp lamellae lie at the anterior end of the ctenidia, one pair on each side of the mouth. A pair of palps forms a functional unit consisting of one inner and one outer palp lamella (Figs. 1, 4). The apposing surfaces of each pair of palp lamellae are highly ciliated and folded into deep grooves and ridges (see Galtsoff, 1964; Ward *et al.*, 1994). The labial palps transport material from the ctenidia to the mouth, control the volume of food ingested, and may also

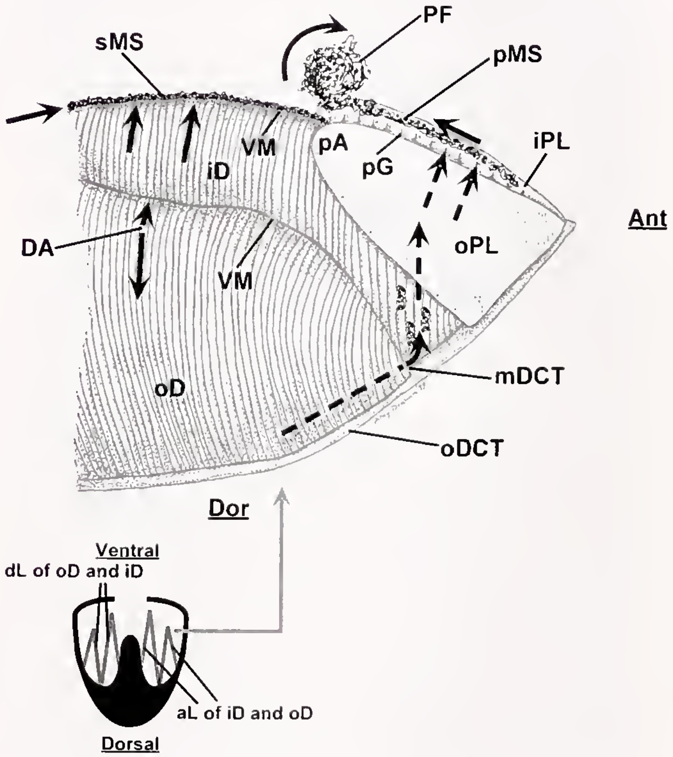

Figure 4. Diagram of the labial palps and the anterior portions of the inner and outer demibranchs of *Dreissena polymorpha* as observed through the endoscope (looking medially). Solid arrows indicate particle paths after capture. Dashed arrows indicate particle paths behind the outer demibranch (oD) and outer palp lamella (oPL). At the anterior termination of the outer demibranch (oD), mucous clumps and strings from the medial dorsal ciliated tract (mDCT) move ventrally onto the inner demibranch (iD) and enter between the palp lamellae (PL). The superficial mucous string (sMS) is drawn from the ventral margin (VM) of the inner demibranch (iD) and between the palp lamellae (PL). The material disperses on the palp lamellae (PL), and rejected particles move ventrally from the palp grooves (pG). Rejected particles are incorporated into a mucous string (pMS) that moves posteriorly and forms an irregular ball at the palp apices. This ball is expelled as pseudofeces (PF) (see text for details). (Ant = anterior, DA = divergence area, Dor = dorsal, iD = inner demibranch, iPL = inner palp lamella, mDCT = medial dorsal ciliated tract, oD = outer demibranch, oDCT = outer dorsal ciliary tract, oPL = outer palp lamella, pA = palp apex, PF = pseudofeces, pG = palp groove, pMS = palp mucous string, sMS = superficial mucous string, VM = ventral margin.) See *Video Note*, p. 124.

sort particles before ingestion (Yonge, 1926; Menzel, 1955; Newell and Jordan, 1983).

In zebra mussels, the labial palps enclose the inner demibranch only. Along the entire free dorsal edge of each palp lamella is a smooth ciliated surface that rests against the demibranch lamellae. These smooth ciliated surfaces are narrow at the distal apices of the palp lamellae and increase in width anteriorly, up to four palp ridges wide. The distal apex of the inner palp lamella often sweeps from the ascending lamella of the associated demibranch, across the superficial groove, and back, drawing in the superficial mucous string (Fig. 1).

Although the superficial mucous string is drawn between the palp lamellae at their distal apices, the superficial groove extends the entire length of the inner demibranch, ending at the oral groove between the palp pair. It was unclear whether, or at what point, the mucous string is removed from the marginal groove proper. This material may remain within the marginal groove proper to be deposited directly into the oral groove, without processing by the palps.

At the anterior terminus of the outer demibranch, mucous clumps and discrete strings from the medial dorsal ciliated tract move ventrally on the filaments of the descending lamella of the inner demibranch (Figs. 1, 4). The superficial mucous string is drawn between the palp lamellae at a point posterior to this location (Fig. 1). Rather than proceeding anteriorly in the superficial groove, the mucous clumps from the dorsal tract continue moving in a ventral direction, entering between the labial palp lamellae.

Mucous strings or clumps from the superficial groove or the dorsal ciliated tract disperse on the palp lamellae. Individual particles bounce anteriorly over the ridges of the palps, slowing in the grooves and moving more quickly over the ridges to the next groove (Fig. 1); the mean velocity is 94 μm s^{-1} (Table 1). The palp lamellae alternate between being spread slightly apart and being closely appressed. When the palp lamellae part slightly, particles remain close to one or the other lamella and continue their bouncing motion. Occasionally, the palp lamellae spread wide apart, and particles can be seen suspended between the apposing palp surfaces and moving posteriorly. This material may include particles that are moving ventrally from the dorsal ciliated tract. When appressed, the lamellae rub together with an anterior-posterior displacement of the width of one to two palp ridges (one palp ridge = 125 μm), and the smooth outer surfaces of the palp lamellae undulate in waves from dorsal to ventral.

Rejected particles move ventrally from the palp grooves (Figs. 1; 4). At the ventral margins of the palp lamellae, these particles form a mucous string which then moves posteriorly at a mean velocity of 54 μm s^{-1} (Table 1). The palp mucous string moves toward the distal apices of the palps, where it forms an irregular ball (Fig. 4). Once the ball of mucus and particles reaches a particular size, the palps push or "clap" the ball away. In this manner, the ball is transferred to ciliated tracts on the mantle, presumably to be expelled from the inhalent siphon or pedal gape as pseudofeces. Sometimes the palp mucous strings are transferred to the mantle before reaching the palp apices.

During exposure to high particle concentrations (10^6 ml^{-1}), the processing of particles by the labial palps changes according to the acceptability of the particles. When mussels were fed high concentrations of a combination of both desirable and unacceptable particles (*Microcystis* and *Scenedesmus*), the ball of mucus that forms near the palp apices was drawn back between the palp lamellae and once again dispersed. We observed mucous balls being reprocessed by the palps up to four times before finally being rejected. In contrast, when mussels were fed high concentrations of primarily unacceptable particles (*Scenedesmus* alone), the superficial mucous string from the inner demibranch sometimes by-passed processing by the labial palps. In this case, the superficial mucous string does not disperse on the ridged surfaces of the palp lamellae but is transferred from the marginal groove of the inner demibranch directly to the palp apices by the extreme posterior section of the smooth ciliated surface (see Fig 1). At the palp apices, the material is formed into a mucous ball and rejected.

Discussion

The observations reported here explain the efficient selection of particles measured in our previous work (Baker *et al.*, 1998) with *Dreissena polymorpha.* Particles are sorted on the ctenidia of zebra mussels, and more specifically, at the marginal food groove of the inner demibranch. We observed a two-layer transport at the marginal food groove: desirable particles appear to be transported inside the groove proper, while unacceptable particles are carried superficially. We also observed sorting at the ventral margin of the outer demibranch: desirable particles are retained on the outer demibranch, while unacceptable particles are transferred to the inner demibranch and ultimately rejected. Here, we compare and contrast our observations with previous reports of feeding processes in both zebra mussels and marine bivalves. We suggest that the structure of homorhabdic ctenidia does not preclude particle sorting, and that the changes in seston composition attributed to zebra mussels may ultimately be due to the ctenidial sorting mechanisms observed in this study.

Foster-Smith (1975) proposed that three conditions must be met for particle selection to take place at the marginal groove of bivalve ctenidia (*i.e.*, in *Mytilus edulis, Cerastoderma edule, Venerupis pullastra*): (1) some particles must be able to enter the deep area of the marginal groove; (2) particles in the deep area of the marginal groove must be physically separate from the superficial material; and (3) the superficial material must be rejected, while the material in the deeper area of the marginal groove is accepted. The two-layer transport that we observed at the marginal groove of zebra mussels meets these requirements for particle selection.

Two-layer transport has previously been described for filibranchs and pseudolamellibranchs, but does not necessarily indicate the capacity for particle selection. Foster-Smith (1975) reported two-layer transport in *M. edulis* (filibranch), with the particles in the deep region of the marginal groove tending to be small, and those in the superficial material tending to be larger. But the two layers are contiguous, precluding particle selection. In *M. edulis*, partitioning between the two layers may be temporal, rather than physical. Jørgensen (1975) reported that particles arriving at the marginal groove might either enter the groove between the bases of the filament tips or pass outside, depending on whether the groove is open or closed. We never observed the marginal groove in zebra mussels to be "open" with filament tips flared, as Jørgensen (1975) illustrated for *M. edulis*, although our observations suggest that there may be some regulation of the amount of material allowed to enter the marginal groove proper.

Two-layer transport at the marginal groove, in combination with particle sorting, has previously been reported only for pseudolamellibranchs. Atkins (1937a) described both two-layer transport and the potential for size sorting at the marginal groove in *Pinna fragilis* and several *Pinna*-like species (pseudolamellibranchs). In these species, which have plicate heterorhabdic ctenidia, fine particles transported by the principal filaments are deposited into the depth of the marginal groove proper, while coarse particles transported by the ordinary filaments are deposited outside the groove and are usually rejected (Atkins, 1937a). Although the mode of particle introduction to the marginal groove of *D. polymorpha* differs from that observed in *Pinna* sp. due to the nonplicate nature of the zebra mussel ctenidia, the marginal groove appears to function similarly in both species.

Previous feeding studies have indicated that, in addition to selection by particle size in *D. polymorpha*, a chemical mechanism of selection is also present (Ten Winkel and Davids, 1982; Baker *et al.*, 1998). In the present study, the disparate sizes of particle types embedded in the superficial mucous string in *D. polymorpha* suggest that some factor other than size is important in the shunting of particles either to the marginal groove proper or to the superficial groove. The superficial mucous string is picked up by the apices of the palps, and much of the material is rejected. The arrangement of the ctenidium/palp junction suggests that material within the marginal groove proper may be transported to the anterior portion of the labial palps or directly to the oral groove. The differing degree to which the two mucous strings are processed by the palps suggests that the material in the superficial mucous string is of lower quality than that in the groove string. This two-layer transport at the marginal groove could potentially increase the rate of processing and decrease the possibility of sorting mistakes at the palps. Microscopic examination of the structure and function of cilia at the marginal groove may help elucidate the sorting mechanisms.

The labial palps of zebra mussels function very similarly to those of other bivalves, despite differences in demibranch structure and function. Zebra mussels have a smooth ciliated surface along the free dorso-posterior edge of the labial palp lamellae, similar to that of oysters (Ward *et al.*, 1994). Our observations of mucous ball formation near the apices of the labial palps are similar to those described for both oysters (Menzel, 1955; Galtsoff, 1964; Ward *et al.*, 1994) and marine mussels (Beninger and St-Jean, 1997a). As in oysters, *D. polymorpha* palp lamellae alternate between being appressed and being slightly separated. When separated, we observed off-surface posterior movements of particles like those reported by Galtsoff (1964) and Ward *et al.* (1994) for oysters. Ward *et al.* (1994) speculated that the posterior movement allows the particles to be cycled through the palps several times before being rejected or ingested. In addition to this type of reprocessing, we observed a second recycling method: the mucous ball forming near the palp apices is sometimes re-engulfed by the palps up to four times before finally being rejected.

Video endoscopy allowed us to observe, *in situ*, the position of the feeding organs within the pallial cavity of living zebra mussels. These observations build on previous reports of feeding organ functioning based on dissected specimens of zebra mussels (Atkins, 1937b; Morton, 1969). For example, like Atkins (1937b) and Morton (1993), we observed particles passing off the outer demibranch at the ventral margin and being transferred to the inner demibranch. Dissected preparations, however, did not allow the authors of previous studies to observe the bend in the outer demibranch and the curvature of the inner demibranch that occurs under natural feeding conditions. Our observations suggest that maintenance of the ctenidia in these positions may facilitate particle recapture; this natural ctenidial morphology enhances the transfer of some particles from the outer demibranch to the inner demibranch.

Our observations of particle transport in zebra mussels contradict some previous observations and corroborate others. For example, Atkins (1937b) described rare filaments of the descending lamella of the outer demibranch that transport particles ventrally; these particles are then passed to normal filaments that transport them dorsally. During our observations of this area (five specimens on 14 occasions, for 8.2 h total observation time), all filaments of the descending lamella of the outer demibranch transported particles dorsally. In addition, Atkins (1937b) did not report any anteriorly directed movement on the ventral margin of the outer demibranch, such as we occasionally observed. That anterior movement is, however, similar to that of mucous-particle masses on the ventral bend of *Placopecten magellanicus* ctenidia, which also lack a ventral groove (Beninger *et al.*, 1992).

In greater contrast, both Atkins (1937b) and Morton (1969) reported ventral movement of particles on the ascending lamella of the outer demibranch, whereas we observed dorsally directed movement, above a divergence area. Atkins (1937b) reported dorsally directed currents on the ascending lamella of the outer demibranch of the Unionidae, another unrelated group of freshwater bivalves.

The dorsally directed movement on the ascending lamella of the outer demibranch allows some proportion of material to be directed to the outer dorsal tract, rather than to the medial dorsal ciliated tract between the two demibranchs, perhaps preventing overloading of the latter tract. Both Atkins (1937b) and Morton (1993) described the anterior movement in the dorsal tract at the junction of the mantle and ascending lamella of the outer demibranch as well; Atkins (1937b) noted that anterior movement in this outer tract usually occurs only in bivalves with heterorhabdic ctenidia. Partitioning material between two dorsal tracts may increase the rate of total particle transport.

Particle velocities, as well as the movement of particles on the ctenidia and labial palps of *D. polymorpha*, are consistent with mucociliary, rather than hydrodynamic, transport (Ward *et al.*, 1993; Beninger and St-Jean, 1997b). The velocities of particles transported on the frontal surfaces of the demibranchs overlap the ranges reported for *M. edulis* and for the plical crests of *C. virginica* (Ward *et al.*, 1993). In addition, the superficial mucous string at the marginal groove moves at a rate similar to the mucous strings observed in *C. virginica, M. edulis, Mya arenaria,* and *Placopecten magellanicus* (Ward *et al.*, 1993, 1994). Material in the dorsal ciliated tract, however, travels at a rate many times slower than it does in *C. virginica* or *P. magellanicus.* In *D. polymorpha,* material at the dorsal ciliated tract is embedded in mucous clumps and trains, but in the oyster and scallop, the material is in a slurry (Ward *et al.*, 1993). Transport rate is generally inversely correlated with the viscosity of the mucus (Menzel, 1955; Winet and Blake, 1980), and therefore, material in a slurry moves at a faster rate than material in more cohesive mucous clumps. The lack of hydrodynamic transport in zebra mussels may reflect a dorsal tract that is smaller and less well developed than that in oysters and scallops.

Zebra mussels have had major impacts on the freshwater systems in which they have become established. Because of the high clearance rates of these mussels, phytoplankton biomass has decreased by more than 60% in many of the invaded systems (Morton, 1971; Kryger and Riisgård, 1988; Holland, 1993; Fahnensteil *et al.*, 1995). In addition, seston composition has changed in some systems, including the Hudson River, New York, where the phytoplankton community has shifted from a prevalence of cyanobacteria to diatoms (Vanderploeg *et al.*, 1996; Smith *et al.*, 1998). Recent studies using flow cytometry (Baker *et al.*, 1998) have shown that zebra mussels can very effectively sort particles and preferentially accept the cyanobacterium *Microcystis.* In the present study we found that accepted particles were directed to the inside of the marginal groove of the inner demibranch and appear to be transported directly to the mouth for ingestion.

In summary, we observed pallial organ morphology, particle transport, and particle sorting in zebra mussels by using video endoscopy. These observations contribute to a growing body of information on the feeding dynamics of bivalves and suspension-feeding invertebrates. More importantly, our results suggest that particle sorting occurs on zebra mussel ctenidia, despite their homorhabdic nature and their lack of adjacent tracks of frontal cilia beating in opposing directions. Our direct observations of zebra mussel ctenidia provide an explanation for the efficient selection of particles measured by Baker *et al.* (1998) and, ultimately, for the role of zebra mussels in ecosystem modification. The role of ctenidial morphology in particle selection by zebra mussels exemplifies the direct link between the functioning of individual bivalves and ecosystem-level processes.

Acknowledgments

This paper is dedicated to the memory of Dr. James H. Crichton, uncle and mentor (SMB). We thank the following persons: C. Nieder, New York State Department of Environmental Conservation, and H. Roditi, SUNY at Stony Brook, provided zebra mussels. Amy Dunham, SUNY at Stony Brook, and Heather Herb, University of Florida, drew the illustrations. J. Kurdziel and P. Baker, SUNY at Stony Brook, provided assistance during all aspects of this study. Comments from two reviewers improved this manuscript. This study was supported by grants from the Hudson River Foundation (01096A and 00798A) and the National Science Foundation (OCE9811380).

Video Note

Supplementary video clips are available for viewing on *The Biological Bulletin* Website at ⟨http://www.mbl.edu/BiologicalBulletin/VIDEO/BB.video.html⟩.

Literature Cited

Arifin, Z., and L. I. Bendell-Young. 1997. Feeding response and carbon assimilation by the blue mussel *Mytilus trossulus* exposed to environmentally relevant seston matrices. *Mar. Ecol. Prog. Ser.* **160:** 241–253.

Atkins, D. 1937a. On the ciliary mechanisms and interrelationships of lamellibranchs. Part II: Sorting devices on the gills. *Q. J. Microsc. Sci.* **79:** 339–373.

Atkins, D. 1937b. On the ciliary mechanisms and interrelationships of lamellibranchs. Part III: Types of lamellibranch gills and their food currents. *Q. J. Microsc. Sci.* **79:** 375–421.

Baker, S. M., J. S. Levinton, J. P. Kurdziel, and S. E. Shumway. 1998. Selective feeding and biodeposition by zebra mussels and their relation to changes in phytoplankton composition and seston load. *J. Shellfish Res.* **17:** 1207–1213.

Beninger, P. G., and S. D. St-Jean. 1997a. Particle processing on the labial palps of *Mytilus edulis* and *Placopecten magellanicus* (Mollusca: Bivalvia). *Mar. Ecol. Prog. Ser.* **147:** 117–127.

Beninger, P. G., and S. D. St-Jean. 1997b. The role of mucus in particle processing by suspension-feeding marine bivalves: unifying principles. *Mar Biol.* **129:** 389–397.

Beninger, P. G., J. E. Ward, B. A. MacDonald, and R. J. Thompson. 1992. Gill function and particle transport in *Placopecten magellanicus* (Mollusca: Bivalvia) as revealed using video endoscopy. *Mar. Biol.* **114:** 281–288.

Caraco, N. G., J. J. Cole, P. A. Raymond, D. L. Strayer, M. L. Pace, S. E. G. Findlay, and D. T. Fischer. 1997. The zebra mussel invasion in a large, turbid river: phytoplankton response to increased grazing. *Ecology* **78:** 588–602.

Defossez, J.-M., and A. J. S. Hawkins. 1997. Selective feeding in shellfish: size-dependent rejection of large particles within pseudofeces from *Mytilus edulis, Ruditapes philippinarum* and *Tapes decussatus. Mar. Biol.* **129:** 139–147.

Fahnenstiel, G. L., G. A. Lang, T. F. Nalepa, and T. H. Johengen. 1995. Effects of the zebra mussel (*Dreissena polymorpha*) colonization on water quality parameters in Saginaw Bay, Lake Huron. *J. Gt. Lakes Res.* **21:** 435–448.

Foster-Smith, R. L. 1975. The role of mucus in the mechanism of feeding in three filter-feeding bivalves. *Proc. Malacol. Soc. Lond.* **41:** 571–588.

Galtsoff, P. S. 1964. The American oyster, *Crassostrea virginica* (Gmelin). *Fishery Bull. Fish. Wildl. Serv. US* **64:** 1–480.

Guillard, R. R. L. 1983. Culture of phytoplankton for feeding marine invertebrates. Pp. 108–132 in *Culture of Marine Invertebrates, Selected Readings.* C. J. Berg, Jr., ed. Huchison Ross Publishing, Stroudsberg, PA.

Guillard, R. R. L., and P. E. Hargraves. 1993. *Stichochrysis immobilis* is a diatom, not a chrysophyte. *Phycologia* **32:** 234–236.

Holland, R. E. 1993. Changes in planktonic diatoms and water transparency in Hatchery Bay, Bass Island area, western Lake Erie since the establishment of the zebra mussel. *J. Gt. Lakes Res.* **19:** 617–624.

Jørgensen, C. B. 1966. *Biology of Suspension Feeding.* Pergamon Press, New York. 357 pp.

Jørgensen, C. B. 1975. On gill function in the mussel *Mytilus edulis* L. *Ophelia* **13:** 187–232.

Kryger, J., and H. U. Riisgård. 1988. Filtration rate capacities in 6 species of European freshwater bivalves. *Oecologia* **77:** 34–38.

MacDonald, B. A., and J. E. Ward. 1994. Variation in food quality and particle selectivity in the sea scallop *Placopecten magellanicus* (Mollusca: Bivalvia). *Mar. Ecol. Prog. Ser.* **108:** 251–264.

Medler, S., and H. Silverman. 1997. Functional organization of intrinsic gill muscles in zebra mussels, *Dreissena polymorpha* (Mollusca: Bivalvia), and response to transmitters *in vitro. Invertebr. Biol.* **116:** 200–212.

Menzel, R. W. 1955. Some phases of the biology of *Ostrea equestris* Say and a comparison with *Crassostrea virginica* (Gmelin). *Inst. Mar. Sci.* **4:** 69–153.

Morton, B. 1969. Studies on the biology of *Dreissena polymorpha* Pall. I. General anatomy and morphology. *Proc. Malacol. Soc. Lond.* **38:** 301–321.

Morton, B. 1971. Studies on the biology of *Dreissena polymorpha* Pall. V. Some aspects of filter-feeding and the effect of micro-organisms upon the rate of filtration. *Proc. Malacol. Soc. Lond.* **39:** 289–301.

Morton, B. 1993. The anatomy of *Dreissena polymorpha* and the evolution and success of the heteromyarian form in the Dreissenoidea. Pp. 185–215 in *Zebra Mussels: Biology, Impacts, and Control,* T. F. Nalepa and D. W. Schloesser, eds. Lewis Publishers, Boca Raton, FL.

Nelson, T. C. 1960. The feeding mechanism of the oyster. II. On the gills and palps of *Ostrea edulis, Crassostrea virginica* and *C. Angulata. J. Morphol.* **107:** 163–203.

Newell, R. I. E., and S. J. Jordan. 1983. Preferential ingestion of organic material by the American oyster, *Crassostrea virginica. Mar. Ecol. Prog. Ser.* **13:** 47–53.

Ruppert, E. E., and R. D. Barnes. 1994. Evolution of bivalve feeding. Pp. 426–435 in *Invertebrate Zoology,* 6th ed. Saunders College Publishing, Orlando, FL.

Smith, T. E., R. J. Steverson, N. F. Caraco, and J. J. Cole. 1998. Changes in phytoplankton community structure during the zebra mussel (*Dreissena polymorpha*) invasion of the Hudson River (New York). *J. Plankton Res.* **20:** 1567–1579.

Sprung, M. 1987. Ecological requirements of developing *Dreissena polymorpha* eggs. *Arch. Hydrobiol. (Suppl.)* **79:** 69–86.

Stenton-Dozey, J. M. E., and A. C. Brown. 1992. Clearance and retention efficiency of natural suspended particles by the rock-pool bivalve *Venerupis corrugatus* in relation to tidal availability. *Mar. Ecol. Prog. Ser.* **82:** 175–186.

Strayer, D. L., N. F. Caraco, J. J. Cole, S. Findlay, and M. L. Pace. 1999. Transformation of the Hudson River ecosystem by the invasion of the zebra mussel (*Dreissena polymorpha*). *Bioscience* **49:** 19–27.

Ten Winkel, E. H., and C. Davids. 1982. Food selection by *Dreissena polymorpha* Pallas (Mollusca: Bivalvia). *Freshwater Biol.* **12:** 553–558.

Vahl, O. 1972. Efficiency of particle retention in *Mytilus edulis* L. *Ophelia* **10:** 17–25.

Vanderploeg, H. A., T. H. Johengen, J. R. Strickler, J. R. Liebig, and T. F. Nalepa. 1996. Zebra mussels may be promoting *Microcystis* blooms in Saginaw Bay and Lake Erie. *Bull. North Am. Benthol. Soc.* **13:** 181–182.

Ward, J. E. 1996. Biodynamics of suspension-feeding in adult bivalve molluscs: particle capture, processing, and fate. *Invertebr. Biol.* **115:** 218–231.

Ward, J. E., P. G. Beninger, B. A. MacDonald, and R. J. Thompson. 1991. Direct observations of feeding structures and mechanisms in bivalve molluscs using endoscopic examination and video image analysis. *Mar. Biol.* **111:** 287–291.

Ward, J. E., B. A. MacDonald, R. J. Thompson, and P. G. Beninger. 1993. Mechanisms of suspension feeding in bivalves: resolution of current controversies by means of endoscopy. *Limnol. Oceanogr.* **38:** 265–272.

Ward, J. E., R. I. E. Newell, R. J. Thompson, and B. A. MacDonald. 1994. *In vivo* studies of suspension-feeding processes in the eastern oyster, *Crassostrea virginica* (Gmelin). *Biol. Bull.* **186:** 221–240.

Ward, J. E., J. S. Levinton, S. E. Shumway, and T. Cucci. 1997. Direct identification of the locus of particle selection in a bivalve mollusk. *Nature* **390:** 131–132.

Ward, J. E., J. S. Levinton, S. E. Shumway, and T. Cucci. 1998. Particle sorting in bivalves: *in vivo* determination of the pallial organs of selection. *Mar. Biol.* **131:** 283–292.

Winet, H., and J. R. Blake. 1980. On the mechanics of mucociliary flows. I. Observation of a channel model. *Biorheology* **17:** 135–150.

Yonge, C. M. 1926. Structure and physiology of the organs of feeding and digestion in *Ostrea edulis. J. Mar Biol. Assoc. UK* **14:** 295–386.

Reference: *Biol. Bull.* **199:** 126–134. (October 2000)

Biogeography of Two Species of *Symbiodinium* (Freudenthal) Inhabiting the Intertidal Sea Anemone *Anthopleura elegantissima* (Brandt)

T. C. LaJEUNESSE* AND R. K. TRENCH

Department of Ecology, Evolution and Marine Biology, University of California at Santa Barbara, Santa Barbara, California 93106

Abstract. We have analyzed the genetic profiles of dinoflagellate populations obtained from the Pacific coast sea anemone *Anthopleura elegantissima* (Brandt) at collection sites from Washington to California. Genetic differences within the symbiont populations of California anemones have been uncovered by restriction length polymorphism (RFLP) analysis of the small subunit (SSU) and large subunit (LSU) ribosomal RNA genes, and by denaturing gradient gel electrophoresis (DGGE) of the internal transcribed spacer region 2 (ITS 2). The existence of two *Symbiodinium* species is substantiated by sequence analysis of the variable regions V1, V2, and V3 of the SSUrDNA, which also establishes their phylogenetic relatedness to other members of the genus *Symbiodinium*. Anemones from Washington and Oregon harbor a single dinoflagellate species, for which we propose the name *S. muscatinei* sp. nov. At these northern locations, *S. muscatinei* either exists alone or co-occurs with the *Chlorella*-like green algal symbiont. Our results indicate that *S. muscatinei* co-occurs with a second dinoflagellate, *S. californium*, in mixed populations in central and southern California. We suggest that the geographic distribution of these dinoflagellates is related to the temperature cline created by latitude.

Introduction

Intertidal anemones of the genus *Anthopleura* are abundant along the Pacific coast of North America (Hand, 1955). *A. elegantissima*, the most common and wide ranging species, is distributed along the rocky intertidal from Alaska to central Baja California (Hand, 1955; Francis, 1979; McFadden *et al.*, 1997). Throughout its geographical range this species harbors intracellular dinoflagellates of the genus *Symbiodinium*. Anemones in regions north of California may also host a *Chlorella*-like (Chlorophyta) alga alone or in mixed populations with the dinoflagellate (Muscatine, 1971). Whether a particular algal symbiont occurs in an anemone, and whether it is present alone or in mixed populations are phenomena believed to be influenced by physical parameters. Relative sensitivities to light and temperature appear to be most significant in regulating the distribution of algal populations. Anemones in warm, bright habitats typically possess the dinoflagellate symbiont, whereas anemones in cool, shadier habitats contain the green alga (Secord, 1995; Saunders and Muller-Parker, 1997).

Environmental parameters have also been implicated in modulating *Symbiodinium* populations in some tropical symbioses. The Caribbean reef-building corals *Montastraea annularis* and *M. faveolata* either host a single algal taxon or have mixed algal populations with patterns of distribution and relative abundance that may be in response to irradiance and temperature (Rowan and Knowlton, 1995; Rowan *et al.*, 1997). Continued analyses of *Symbiodinium* populations in scleractinians are resolving greater diversity within individual hosts than previously recognized (Baker and Rowan, 1997; Baker *et al.*, 1997; Baker, 1999). Restriction fragment length polymorphism (RFLP) analysis of the large subunit (LSU) ribosomal DNA from 107 Pacific and Caribbean corals (Baker, 1999) identified 69 species that harbored a single algal taxon; 13 other species harbored more than one *Symbiodinium* taxon, but not in the same colony, and 25 species sometimes harbored more than one algal taxon within the same colony. Depth (and thus reduced light) was

---

Received 2 February 2000; accepted 17 July 2000.

* To whom correspondence should be addressed. E-mail: lajeunes@lifesci.ucsb.edu

Abbreviations: DGGE, denaturing gradient gel electrophoresis; ITS 2, internal transcribed spacer region 2; LSU, large subunit; RFLP, restriction fragment length polymorphism; SSU, small subunit.

regarded as the most significant factor regulating the distribution of a particular alga.

Previous studies conducted on algae isolated from *A. elegantissima* collected in Washington and California showed marked differences in mitotic indices (Wilkerson *et al.*, 1983) and carbon translocation (Shick and Dykens, 1984; Verde and McCloskey, 1996). The possibility that these differences reflect different *Symbiodinium* species has been suggested (Verde and McCloskey, 1996), but has not been empirically tested. A limited genetic study was conducted by Rowan and Powers (1991) on symbiont populations collected from Pacific Grove, California. Their RFLP and partial small subunit (SSU) ribosomal DNA sequence analyses from cloned amplification products detected only one dinoflagellate taxon belonging to lineage B *Symbiodinium* (*sensu* Rowan and Powers, 1991). It is now recognized that analyses based on the conserved SSUrRNA gene underestimate genetic diversity (Rowan, 1998). Furthermore, sampling from a single collection site would not necessarily identify symbiont diversity in a host with a range of thousands of kilometers.

The extensive geographic range of *A. elegantissima*, its occupancy of diverse intertidal habitats, its occurrence in two different growth forms—solitary and clonal—which may represent two distinct species (McFadden *et al.*, 1997), and its ability to harbor symbionts from different algal divisions suggest that *A. elegantissima* may harbor more than one taxon of symbiotic dinoflagellate. This possibility is strengthened by the finding that different *Symbiodinium* spp. are adapted to different regimes of light (Iglesias-Prieto and Trench, 1994, 1997b) and temperature (Warner *et al.*, 1996). To test the hypothesis that different dinoflagellate taxa may co-occur in *Anthopleura*, anemones were collected from intertidal habitats along a latitudinal gradient ranging from Puget Sound in Washington to San Diego in Southern California. A genetic examination, using traditional RFLP analyses of the SSUrDNA and LSUrDNA, and analyses of partial SSUrDNA sequences were conducted on *Symbiodinium* populations isolated from these anemones. Denaturing gradient gel electrophoresis (DGGE; Myers *et al.*, 1985; Abrams and Stanton, 1992) is a technique frequently used to characterize and compare genetic diversity in complex microbial assemblages from samples collected over spatial and temporal scales (Muyzer *et al.*, 1993; Muyzer and Smalla, 1998). This technique was used here to analyze the variable internal transcribed spacer region 2 (ITS 2), and thus to visualize and identify the occurrence of more than one algal taxon within a host.

Materials and Methods

Anemone collections

Specimens of symbiotic *Anthopleura elegantissima* were collected from rocky intertidal locations along the Washington, Oregon, and California coastlines. Between February 1997 and August 1998, collections were conducted at Anaco Beach, Fidalgo Island, Washington (48°29′; 122°42′); Coos Bay, Charleston, Oregon (43°34′; 124°33′); Carmel, California (36°55′; 121°92′); Cayucos, California (35°44′; 120°88′); Ellwood Beach and Campus Point, Santa Barbara, California (34°43′; 119°83′); and Swami's Beach, Cardiff-by-the-Sea (Encinitas), California (33°04′; 117°29′). Symbiotic *A. xanthogrammica* were collected only from Cayucos. Individual anemones were collected from a range of habitats, from exposed upper intertidal to shaded lower intertidal locations. Aposymbiotic *A. elegantissima* were obtained from drainage sluice-ways beneath the wet lab facilities of the Marine Science Institute of the University of California, Santa Barbara, California.

Isolation of algal cells from tissues of host anemones

Oral discs and tentacles from anemones were macerated in a Tenbroek tissue grinder. This step was followed by a 5-min centrifugation at about 800 × *g* in a Dynac II bench-top centrifuge. The pellets containing the algal cells were resuspended and further homogenized with a Tissue Tearor (Model 985-370) to dissociate most of the remaining animal cellular debris. After a second centrifugation, the algal pellets were resuspended in Millipore-filtered (porosity 0.22 μm) seawater, centrifuged, and resuspended two or three times to remove most of the animal debris from the algal cell preparation.

The cultured *Symbiodinium californium* (#383, Banaszak *et al.*, 1993) was originally isolated, in 1989, from a solitary form of *A. elegantissima* by using a technique developed by Polne-Fuller (1991). The isolate was grown in 1 l of ASP-8A (Blank, 1987) for 2 months at 17°C, illuminated by banks of VitaLite fluorescent tubes delivering 80 μmol quanta $m^{-2}s^{-1}$ photosynthetically active radiation on a 14:10 (light:dark) photoperiod. Algae were harvested by centrifugation at 9000 × *g* in a Sorvall RC-5B centrifuge.

DNA extraction, amplification, RFLP

Symbiodinium populations were isolated from 64 specimens of *A. elegantissima* (37 clonal and 27 solitary) and three of *A. xanthogrammica*. DNA was extracted from about 25 mg of algal material by using a proteinase digestion and spin-column separation protocol described in the QIAamp Tissue kit (Qiagen Corporation, Santa Clarita, CA). From the spin-column eluate, 1 μl of product was used as a template to amplify the small-subunit ribosomal RNA gene (SSUrDNA) and part of the large subunit ribosomal RNA gene (LSUrDNA) (Lenaers *et al.*, 1989). SSUrDNA was amplified on a Perkin-Elmer thermal cycler 2400 using primers of Rowan and Powers (1991), and under the following conditions: an initial denaturing step of 3 min at 92°C followed by 35 cycles of 30 s at 92°C, 40 s at 52°C, and 30 s at 72°C, followed by a single cycle of 5 min at 72°C. A fragment corresponding to a region between 28 bp and 929 bp of the *Prorocentrum micans* LSU rRNA gene containing the variable portions D1–D3 (Lenaers *et al.*, 1989; Wilcox, 1998) was amplified using primers described by Wilcox (1998) with the same protocol used for the SSUrDNA, but with an optimal annealing temperature of 48°C.

Restriction digests were performed by incubating amplified products with 1–5 units of Taq I (New England BioLabs, Beverly, MA) at 65°C for 3 to 5 h or with 1–5 units of Dpn II (New England BioLabs) for 4 to 5 h at 37°C. Products of the digests were separated by electrophoresis in a 2.5% high-melt agarose gel at a constant 70 V for 3 h.

Denaturing gradient gel electrophoresis (DGGE)

Primers for polymerase chain reaction (PCR)-DGGE analyses were designed to amplify the variable internal transcribed spacer region II (ITS 2), producing a fragment size of 330–360 bp. ITS and 5.8S rDNA sequence data (unpublished) from cultured *Symbiodinium* spp. isolated from various cnidarian and molluscan hosts were compared to identify conserved regions. An internal primer "ITSint-for2" (5′GAATTGCAGAACTCCGTG-3′) was designed from this analysis, and it anneals to a conserved region of the 5.8S rDNA. Primer ITS-Reverse (Coleman *et al.*, 1994) was modified with a 40-bp GC clamp (Sheffield *et al.*, 1989) and is referred to as "ITS2CLAMP" (5′CGCCCGCCG-CGCCCCGCGCCCGTCCCGCCGCCCCCGCCCGGGA-TCCATATGCTTAAGTTCAGCGGGT-3′). A "touch-down" amplification (Don *et al.*, 1991) protocol was used to ensure specificity. Initial annealing conditions began 10°C above the final annealing temperature of 52°C. Every two cycles, the annealing temperature was decreased one degree. After 20 cycles the annealing temperature was held, and remained at 52°C for another 15 cycles. Reaction products were loaded onto an 8% acrylamide denaturing gradient gel (a 40% to 75% gradient, 100% consists of 7 *M* urea and 40% deionized formamide). PCR products were loaded on the gel with a 2% Ficoll loading buffer (2% Ficoll-400, 10 m*M* Tris-HCl pH 7.8, 1 m*M* EDTA, 1% bromophenol blue) and separated by electrophoresis for 22 h at 90 V at a constant temperature of 60°C. The gel was then stained in a 1X TAE and 5 μg/ml ethidium bromide solution for 15 min, washed in deionized water for 15 min and photographed.

DNA sequencing, alignment, and analysis

Partial sequences of the SSUrDNA and the ITS spacer (ITS 1 and 2 and 5.8 rRNA gene) were obtained from direct cycle sequencing of amplified products. Cycle sequencing of amplified SSUrDNA products was accomplished using Rowan and Power's (1991) forward primer and an internal primer (Anderson *et al.*, 1993), which permitted sequence reads spanning the V1, V2, and part of the V3 variable regions (Sogin and Gunderson, 1987; as described in Rowan and Knowlton, 1995). Reagents were supplied and reaction conditions specified in the ABI Prism Big Dye Terminator Cycle Sequencing Ready Reaction Kit (PE Applied Biosystems, Foster City, CA). Reaction products were analyzed on an Applied Biosystems 310 Genetic Analyzer (Division of Perkin Elmer, Foster City, CA). The resulting chromatograms were checked and edited using Sequence Navigator, version 1.0, software (ABI, Division of Perkin Elmer, Foster City, CA). Sequence composites of the SSUrDNA were assembled and, including gaps, totaled 375 nucleotides. Partial sequences from the two algal types identified in our RFLP and DGGE analyses were then aligned by eye with published *Symbiodinium* sequences obtained from Genbank; they included *S. corculorum*, *S. microadriaticum*, *S. pilosum*, *S. pulchrorum*, *Gymnodinium varians*, *G. simplex*, *Porocentrum micans*, and four *Symbiodinium* spp. symbiotic with the coral *Montastraea annularis*. Cladistic analyses, by the method of parsimony, were conducted on the aligned data set using PAUP 4.0b4 software under default settings (Swofford, 1993). A bootstrap analysis was conducted on the most parsimonious tree to assess relative support for each branch (Felsenstein, 1985).

Results

Anemones collected from high and low intertidal habitats at each study site contained the same *Symbiodinium* populations. We found no indication, based on our molecular analyses, that the *Symbiodinium* populations in *A. elegantissima* are influenced by the local environmental differences within the littoral zone. However, we found significant differences between the algal populations in anemones collected from Washington and Oregon, and those collected at lower latitudes in California. Figure 1 summarizes the findings from our RFLP and DGGE analyses that detected a single genetic entity in northern anemones and at least two genetic entities in southern anemones.

Taq I digests of the SSUrDNA amplified from northern populations of *Symbiodinium* exhibited a characteristic "clade B" restriction pattern (Rowan and Power, 1991) (Fig. 1A, lane 1). The same analysis conducted on southern populations produced a mixed pattern consisting of the "clade B" type with a second undescribed pattern (Fig. 1C, lane 1). We have identified this latter pattern as diagnostic of a second algal type. It is identical to the restriction pattern of cultured *S. californium*, whose SSUrDNA does not yield a classical "clade A, B, or C" pattern (Fig. 1C, lane 2) (*cf.* RFLP type "T6" in Darius *et al.*, 1998). This new pattern results from the loss of a restriction site at approximately position 1500 and the gain of a restriction site at position 870 of the amplified 1785 bp product, as determined from the entire SSUrDNA sequence of *S. californium* (GenBank

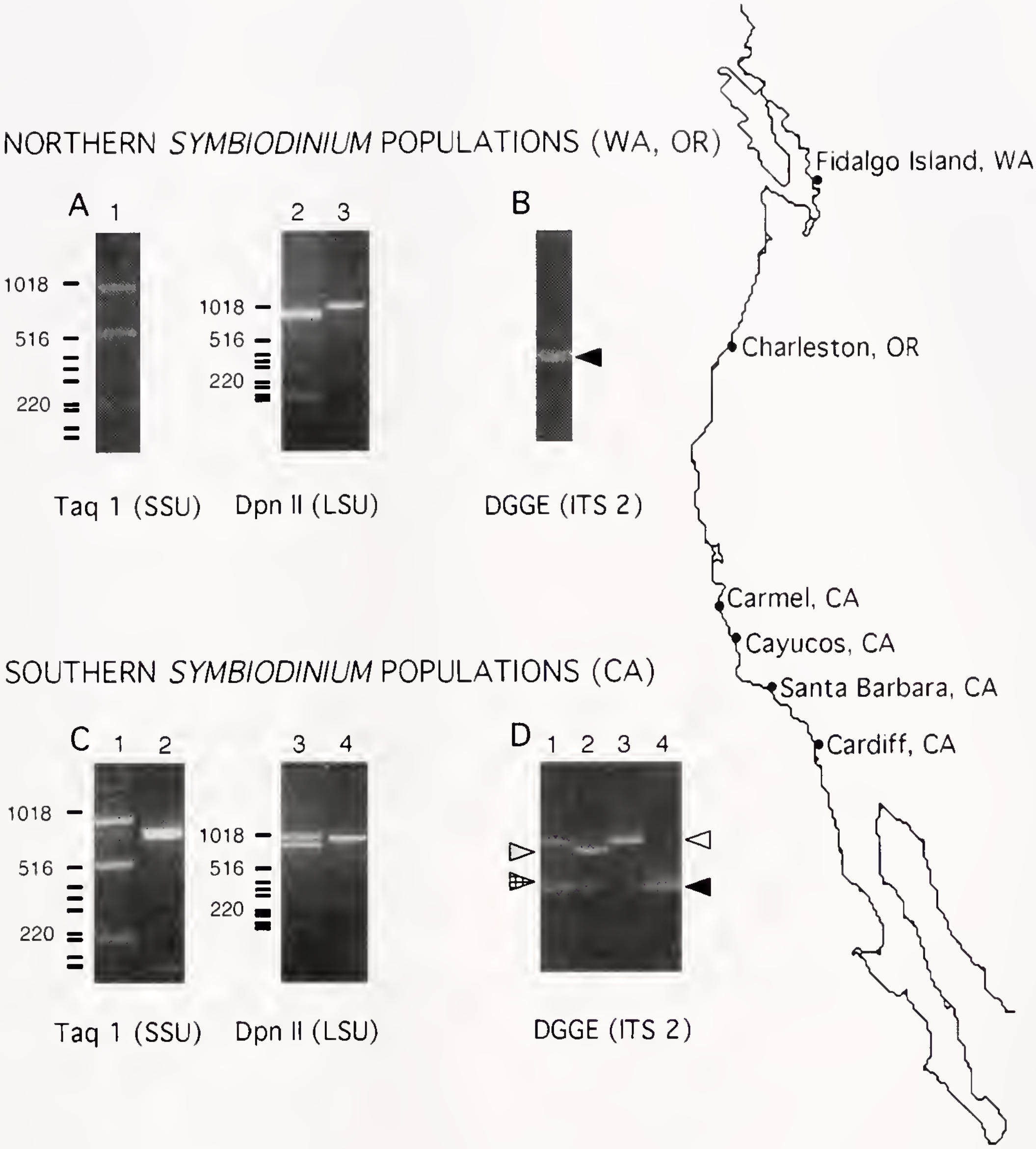
NORTHERN *SYMBIODINIUM* POPULATIONS (WA, OR)
A 1
2 3
B
1018
516
220
1018
516
220
Taq 1 (SSU)
Dpn II (LSU)
DGGE (ITS 2)
SOUTHERN *SYMBIODINIUM* POPULATIONS (CA)
C 1 2
3 4
D 1 2 3 4
1018
516
220
1018
516
220
Taq 1 (SSU)
Dpn II (LSU)
DGGE (ITS 2)
Fidalgo Island, WA
Charleston, OR
Carmel, CA
Cayucos, CA
Santa Barbara, CA
Cardiff, CA

Figure 1. Pacific coastline of North America depicting collection sites and genetic analyses of northern and southern *Symbiodinium* populations. ITS 2, internal transcribed spacer region 2; LSU, large subunit; SSU, small subunit. (A) RFLP analysis of the SSUrDNA and LSUrDNA from northern algal populations. Lane 1, Taq 1 digest of SSUrDNA indicative of lineage B *Symbiodinium* (Rowan and Powers, 1991); lane 2, Dpn II digest of the D1–D3 variable region of the LSUrRNA gene; and for comparison, in lane 3, Dpn II digest of the same region from *S. californium* (#383). (B) DGGE gel of the ITS 2 depicting a single ITS signature (black arrow). (C) RFLP analysis of the ribosomal repeat from southern algal populations; lane 1, Taq 1 digest of SSUrDNA showing the lineage B *Symbiodinium* co-occurring with a second pattern not belonging to any of the described "clades" (*sensu* Rowan and Powers, 1991); lane 2, Taq 1 digest of SSUrDNA of #383, a pattern identical to the undescribed RFLP profile in lane 1. Lanes 3 and 4 are Dpn II digest on LSUrRNA gene amplified from natural populations and the cultured clonal isolate #383 respectively; indicates more than one algal taxon in southern populations. (D) DGGE gel showing three representative profiles of ITS 2 signatures from natural populations, lanes 1, 2, and 4; and for comparison, lane 3 depicts the ITS signature for #383 (white arrow). (See text for further explanation.)

accession #AF225965). The poor amplification of the SSUrDNA from *S. californium* in mixed populations may explain why the smallest fragment (130 bp) appears to be absent from RFLPs on natural samples (Fig. 1C, lane 1). Dpn II restriction digests of SSUrDNA from both freshly isolated northern and southern algal samples and cultured *S.*

californium produced a single restriction pattern characteristic of "clade B" *Symbiodinium* (Rowan and Powers, 1991) (data not shown). The utility of RFLP analyses of the SSUrDNA in distinguishing sequence variation, especially among congeneric members, has limitations. The more variable gene regions and more informative techniques were therefore employed to achieve a better resolution of the variation detected by the Taq I enzyme.

An 850-bp fragment of the LSUrRNA gene was examined by restriction analysis in an attempt to measure the extent of the genetic varitation observed in our RFLP analysis of the small subunit and to uncover possible variation not resolved by the SSUrRNA gene (Baker *et al.*, 1997; Wilcox, 1998). Dpn II restriction digests of LSUrDNA amplified from all northern *Symbiodinium* populations produced the fragment pattern in Figure 1A, lane 2. A restriction site exists at one end of the amplified product and produces two bands, one 740 bp, the other about 70–80 bp. A Dpn II digest of the LSUrDNA from *S. californium* lacks a restriction site for this enzyme, and a single band is depicted (Fig. 1A, lane 3, and also 1C, lane 4). RFLPs conducted on algal populations from southern anemones always contained a nondigested fragment, as observed for *S. californium,* as well as two fragments identical to those observed in restriction patterns from the northern algal populations. This indicates the presence of two different gene sequences in the same amplification product—one with and one without a restriction site for Dpn II. These data are consistent with our results from the SSUrDNA digests. Taq I digests of the LSUrDNA (data not shown) also showed the presence of a single type in northern populations and two types in southern populations of *A. elegantissima.* The same two algal types were also found in *A. xanthogrammica* from Cayucos.

The ITS region has historically been useful in resolving species-level differences (Gonzalez *et al.*, 1990; Coleman *et al.*, 1994; Goff *et al.*, 1994; Larsen and Medlin, 1997). Among dinoflagellates, it has been used to resolve differences between closely related species within the genus *Alexandrium* (Adachi *et al.*, 1996) and to assess intraspecific variation in *Gymnodinium catenatum* (Adachi *et al.*, 1997). Hunter *et al.* (1997), in their preliminary study, reported that the ITS is potentially a good marker for interspecific comparisons between *Symbiodinium* taxa. In this study, a region encompassing the ITS 2 and a portion of the 5.8S was chosen for DGGE analyses.

DGGE separates amplification products by differences in sequence composition and nucleotide order. The results are therefore a qualitative assessment of the entire sequence. Application of DGGE has permitted the rapid assessment of complex microbial populations and identification of specific microbes from marine, aquatic, and terrestrial samples (Muyzer and Smalla, 1998). This analysis, applied to *Symbiodinium* populations, has verified the existence of a single *Symbiodinium* species in anemones collected from northern locations (Washington and Oregon) (Fig. 1B, black arrow). In contrast, at least two algal species were identified in populations of *Anthopleura* from California.

In southern populations, the algal ITS "signature" found in northern anemone populations (black arrow) is often associated with an ITS signature consistent with *S. californium* (white arrow; Fig. 1D, lanes 1 and 3 respectively). An unidentified ITS type was observed (light gray arrow; Fig. 1D, lane 2) but is believed to be a variant of *S. californium* based on our findings from the RFLP data on the LSUrDNA. In our analyses of southern populations, a fourth ITS type (hatched arrow), although sometimes appearing faint, is always associated with the most common ITS type (black arrow). This is believed to either be a DGGE artifact or to represent fixed variation within the ribosomal repeat.

An inferred phylogeny (Fig. 2) reconstructed from partial SSUrDNA sequences shows the relationships between the algae identified in *A. elegantissima* and those from tropical hosts. The algal species found throughout northern and southern anemone populations is a member of the B lineage found by Rowan and Powers (1991). Here, we propose the name *Symbiodinium muscatinei* sp. nov. to refer to the dinoflagellate symbiotic with *A. elegantissima* from Washington to California. (A morphological description must

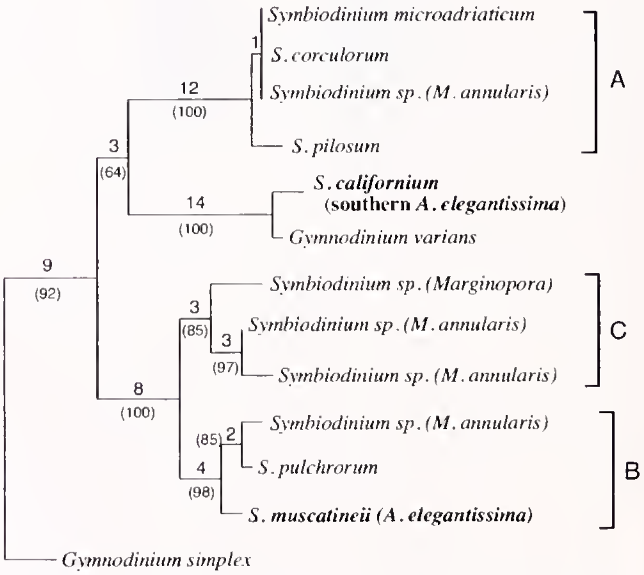
Symbiodinium microadriaticum
1
S. corculorum
12
(100)
Symbiodinium sp. (M. annularis)
S. pilosum
A
3
(64)
S. californium
(southern A. elegantissima)
14
(100)
Gymnodinium varians
9
(92)
Symbiodinium sp. (Marginopora)
3
(85)
Symbiodinium sp. (M. annularis)
3
(97)
Symbiodinium sp. (M. annularis)
C
8
(100)
(85)
2
Symbiodinium sp. (M. annularis)
S. pulchrorum
4
(98)
S. muscatineii (A. elegantissima)
B
Gymnodinium simplex

Figure 2. Phylogenetic reconstruction of the *Symbiodinium* lineage by the method of parsimony using a 375-bp composite of the SSUrRNA gene spanning the V1, V2, and V3 variable region. *S. californium* is closely related to *Gymnodinium varians* and forms a separate lineage. *S. muscatinei* groups with members of the B lineage and is probably the same taxa identified in the study by Rowan and Powers (1991). Numerals above branch segments indicate number of base pair changes; numbers in parentheses below show bootstrap consistency based on 1000 replicates. For simplicity, the out group, *Prorocentrum micans,* is not shown.

await achieving axenic culture, but the partial sequence of the SSUrDNA has been given the GenBank accession numbers AF228362 and AF228363 for the V1, and V2 and V3 regions of the SSUrDNA, respectively.) *S. californium*, identified in anemones from California only, is closely related to *Gymnodinium varians*; together they form a lineage separate from the described "clades A, B, and C" (bracketed). Sequence differences between the SSUrDNA from *S. muscatinei* and *S. californium* are significantly greater than differences observed between described species. The entire ITS region was sequenced from each alga and compared (data not shown). No reliable alignment was possible due to extreme sequence divergence. The ITS sequence of *S. muscatinei* was aligned and compared with sequences from several other lineage B *Symbiodinium*. Results indicated a level of divergence many times greater (12%) than interspecific variation observed among other dinoflagellates (Adachi *et al.*, 1997). These data collectively indicate the presence of two distinct dinoflagellate species.

Animal DNA isolated from aposymbiotic *A. elegantissima* was used to determine whether host material would be a source of contamination in freshly isolated algal samples. Amplification was never achieved with the primers and reaction conditions used for the amplification of LSUrDNA and SSUrDNA. However, the ITS 2 primers designed for DGGE amplified host DNA, but only rarely when algal DNA was present.

Cloned *S. californium* (#383) served as a control, so we could ascertain the presence of pseudogenes or natural variation in ribosomal repeats within a single genome. Ribosomal pseudogenes have been observed in some dinoflagellates (Scholin *et al.*, 1993; Adachi *et al.*, 1996). Although none have been reported in *Symbiodinium*, their presence cannot be discounted. The DGGE analysis on *S. californium* (#383) repeatedly identified a single type with no obvious intragenomic variation.

Discussion

The molecular methods employed in this study demonstrate that there are two distantly related species of *Symbiodinium* in populations of *Anthopleura elegantissima* along the Pacific coast of the United States. Evidence based on RFLP, DGGE, and sequence analysis indicates the presence of a single *Symbiodinium* species, designated here as *S. muscatinei*, in northern populations. This is consistent with previous reports that many hosts harbor a single population of algae (Schoenberg and Trench, 1980a; Baker and Rowan, 1997; Bythell *et al.*, 1997; Billinghurst *et al.*, 1997; Stochaj and Grossman, 1997). Our analyses also show that anemones from southern latitudes in California harbor a mixed dinoflagellate population consisting of two congeneric species: *S. muscatinei* identified from northern anemones, and *S. californium*.

It has been recognized for some time that some invertebrate taxa may simultaneously harbor more than one algal taxon (Muscatine, 1971; Trench and Winsor, 1987). The coexistence of two or more *Symbiodinium* taxa in the same host was first described by Rowan and Knowlton (1995) in the Caribbean reef building corals *Montastrea annularis* and *M. faveolata*. Since then, more than one *Symbiodinium* taxon has been identified in populations of certain other coral species. Furthermore, some individual colonies have been shown to harbor mixed symbiont taxa (Baker and Rowan, 1997; Darius *et al.*, 1998; Baker, 1999; Carlos *et al.*, 1999; Banaszak *et al.*, 2000). From the data of Baker (1999), about 23% of the total coral taxa sampled may have mixed symbiont populations, indicating that the presence of more than one symbiont simultaneously is not uncommon.

Environmental parameters have been hypothesized to regulate the distribution and population dynamics of each symbiont in hosts that harbor more than one algal species (Rowan *et al.*, 1997; Baker, 1999). The patterns of these distributions are specific and correlate closely with environmental gradients. *Symbiodinium* species examined in culture and *in hospite* show species-specific physiological adaptations to photosynthetically active radiation and temperature (Chang *et al.*, 1983, Iglesias-Prieto and Trench, 1994, 1997a, b; Warner *et al.*, 1996, 1999). Algal species better adapted for a particular environment will out-compete those less suited (Schoenberg and Trench, 1980b; Rowan *et al.*, 1997; Saunders and Muller-Parker, 1997).

Previous studies have focused primarily on the reef-wide distribution of symbioses involving more than one algal taxon, but very little is known about the biogeography of algal symbionts and about how the distribution of algal species in geographically widespread hosts may be influenced by differences in environment. Ultimately, the problem revolves around the determination of the species of algae involved in the associations. The difficulty in delineating species has been a long-standing problem for oceanographers studying phytoplankton biogeography (Round, 1981). With regard to *Symbiodinium*, one example is the coral *Plesiastrea versipora*, which has an unusually broad latitudinal distribution along the east coast of Australia. On the tropical Great Barrier Reef it forms a symbiosis with *Symbiodinium* sp. of the C lineage, while in cooler temperate waters off Sydney it harbors a *Symbiodinium* sp. from the B lineage (Baker, 1999).

Temperature and irradiance are the most significant environmental variables that change predictably with latitude. Within the tropics, among coral species with more than one algal taxon, the algae exhibit ecological zonation that correlates with irradiance (Rowan and Knowlton, 1995; Baker, 1999). Irradiance in temperate regions is less consistent and may not be an important parameter regulating the distribution of *S. californium*. When compared to California, Washington and Oregon have longer periods of daylight during the summer, but experience shorter periods in the winter. Assessment of the influence of light as an environmental factor that regulates algal distribution is further complicated because anemones act to control irradiance levels impinging on the algae by covering their surfaces with fragments of rock and shell (Dykens and Shick, 1984).

Temperature is an environmental factor that regulates species distributions along the coast of California (Newman, 1979), and it probably governs the distribution of *S. californium*. Collection sites from Oregon and Washington routinely experience colder temperatures than locations in California (Fig. 3), particularly in winter. In addition, northern anemones experience greater annual temperature fluctuations, which may also be of selective importance. Low temperature extremes, like high temperatures, may result in the loss of symbionts from hosts (Muscatine *et al.*, 1991). Temperature as a selective force is supported by the observation that, in northern anemone populations that harbor *S. muscatinei* and the green Chlorella-like alga, symbiont growth rates are more strongly affected by temperature than by irradiance (Saunders and Muller-Parker, 1997). Temperature changes associated with increased latitude may also influence the competitive balance between *S. californium* and *S. muscatinei* by affecting their relative growth rates. We also suggest the possibility that low temperatures found in the north exclude *S. californium*; in the south, *S. californium* and *S. muscatinei* coexist because the latter species may have a wider temperature tolerance. Because attempts to culture *S. muscatinei* were unsuccessful, controlled physiological comparisons were not possible.

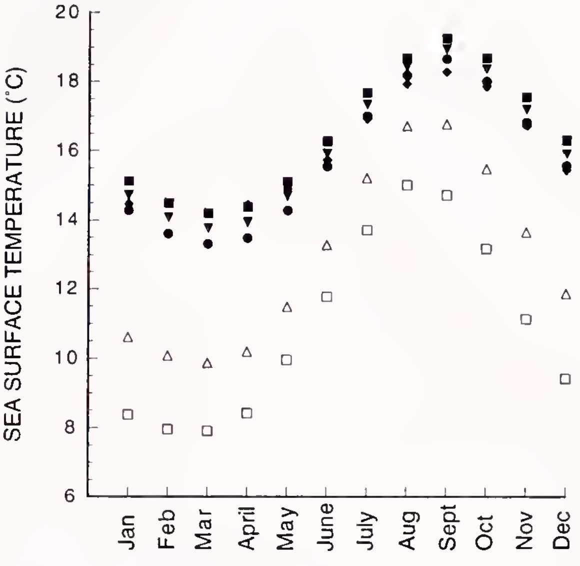

Figure 3. Average coastal sea surface temperature data from the Comprehensive Ocean-Atmosphere Data Set (COADS) monthly climatology records (1946–1989). Graph compares the seasonal fluctuation of sea surface temperature in degrees Celsius at collection sites in Washington (open square), Oregon (open triangle), and from central and southern California (Carmel, solid circle; Cayucos, solid triangle; Santa Barbara, solid square; Cardiff-by-the-Sea (Encinitas), solid diamond). The locations are shown on the map in Figure 1. The southern locations in California have similar seasonal temperatures and are always 1° to 6°C warmer than northern locations depending on the time of year. The range in temperature fluctuation between March (lowest yearly temperature) and September (highest) is greater for Washington and Oregon (*ca.* 7°C) than for locations in California (*ca.* 4°–5°C).

The nonrandom sorting or specificity of algal-invertebrate symbioses is contingent on the interplay of multiple factors (Trench *et al.*, 1981; Trench, 1988, 1997), and is not expressed as one alga for one host (Schoenberg and Trench, 1980b). Cnidarian hosts are symbiotic with selectively few microalgal taxa (Trench, 1997), yet they are exposed to hundreds and possibly thousands of "free-living" microalgal species. The "complementariness of the dynamically interacting attributes" (Dubos and Kessler, 1963) of both symbiont and host substantially limits possible symbiotic combinations. The extent to which a host shows specificity for one or more algal species depends ultimately on the poorly understood cellular and molecular processes that may take place during initial intracellular contact, and possibly also after the association is established (Colley and Trench, 1983; Trench, 1993). In those hosts harboring more than one algal taxon, symbiont distributions are strongly influenced by changes in the physical environment over both local (Rowan and Knowlton, 1995; Secord, 1995) and geographic sales (Baker, 1999). Because the influence of environment on host-symbiont dynamics can be variously interpreted, further experimental analyses are needed to explain the mechanisms that result in these observed patterns (Saunders and Muller-Parker, 1997). For example, it is unclear whether changes in the physical environment have an intrinsic or extrinsic effect on the biology of the symbiosis. Changes in the environment might modify the physiological integration of the symbiotic partners so that they are no longer compatible. Finally, differential changes in symbiont growth rates may, and can, cause competitive exclusion of one algal species over another (Provasoli *et al.*, 1968). Progress in elucidating these mechanisms should provide a more accurate description of host symbiont interactions and specificity.

Acknowledgments

We thank Drs. Ed Delong and Scott Hodges for use of their lab facilities. We thank Dr. Gisele Muller-Parker for collecting specimens from Anacortes, Washington; Dr. Jeff Goddard for collecting anemones in Coos Bay, Oregon, and Dr. Shana Goffriedi and Victoria Orphan for collections at Cardiff-by-the-Sea, near Encinitas, California. Dr. Robert A. Andersen and Dr. Craig Bailey at the Center for Culture of Marine Phytoplankton, Bigelow Laboratory for Ocean Sciences, and Dr. Lynda Goff and Dr. Deb Moon at the University of California, Santa Cruz, are greatly appreciated for their assistance in sequencing. We especially thank Dr. Alison Murray for her advice, invaluable technical guidance on DGGE analysis, and comments on an early draft of this paper.

Literature Cited

Abrams, E. S., and V. P. Stanton, Jr. 1992. Use of denaturing gradient gel electrophoresis to study conformational transitions in nucleic acids. *Methods Enzymol.* **212:** 71–104.

Adachi, M., Y. Sako, and Y. Ishida. 1996. Analysis of *Alexandrium* (Dinophyceae) species using sequences of the 5.8S ribosomal DNA and internal transcribed spacer regions. *J. Phycol.* **32:** 424–432.

Adachi, M., Y. Sako, and Y. Ishida. 1997. Analysis of *Gymnodinium catenatum* Dinophyceae using sequences of the 5.8S rDNA-ITS regions and Random Amplified Polymorphic DNA. *Fish. Sci.* **63:** 701–707.

Andersen, R. A., G. W. Saunders, M. P. Paskind, and J. P. Sexton. 1993. The ultrastructure and 18s rRNA gene sequence for *Pelagomonas calceolata* gen. et sp. nov., and the description of a new algal class, the Pelagophyceae Class nov. *J. Phycol.* **29:** 701–705.

Baker, A. C. 1999. The symbiosis ecology of reef-building corals. Ph.D. dissertation, University of Miami, Miami, FL. 120 pp.

Baker, A. C., and R. Rowan. 1997. Diversity of symbiotic dinoflagellates (zooxanthellae) in scleractinian corals of the Caribbean and eastern Pacific. *Proc 8th Int. Coral Reef Symp.* **2:** 1301–1306.

Baker, A. C., R. Rowan, and N. Knowlton. 1997. Symbiosis ecology of two Caribbean acroporid corals. *Proc 8th Int. Coral Reef Symp.* **2:** 1295–1300.

Banaszak, A. T., R. Iglesias-Prieto, and R. K. Trench. 1993. *Scrippsiella velellae* sp. nov. (Peridiniales) and *Gloeodinium viscum* sp. nov. (Phytodiniales), dinoflagellate symbionts of two hydrozoans (Cnidaria). *J. Phycol.* **29:** 517–528.

Banaszak, A. T., T. C. LaJeunesse, and R. K. Trench. 2000. The synthesis of mycosporine-like amino acids (MAAs) by cultured symbiotic dinoflagellates. *J. Exp. Mar. Biol. Ecol.* **249:** 219–233.

Billinghurst, Z., A. E. Douglas, and H. G. Trapido-Rosenthal. 1997. On the genetic diversity of the symbiosis between the coral *Montastraea cavernosa* and zooxanthellae in Bermuda. *Proc. 8th Coral Reef Symp.* **2:** 1291–1294.

Blank, R. J. 1987. Cell architecture of the dinoflagellate *Symbiodinium* inhabiting the Hawaiian stony coral *Montipora verrucosa*. *Mar. Biol.* **94:** 143–155.

Bythell, J. C., A. E. Douglas, V. A. Sharp, J. B. Searle, and B. E. Brown. 1997. Algal genotype and photoacclimatory responses in natural populations of the symbiotic sea anemone *Anemonia viridis*. *Proc. R. Soc. Lond. B.* **264:** 1277–1282.

Carlos, A. A., B. K. Baillie, K. Brett, M. Kawaguchi, and T. Maruyama. 1999. Phylogenetic position of *Symbiodinium* (Dinophyceae) isolates from tridacnids (Bivalvia), cardiids (Bivalvia), a sponge (Porifera), a soft coral (Anthozoa), and a free-living strain. *J. Phycol.* **35:** 1054–1062.

Chang, S. S., B. B. Prézelin, and R. K. Trench. 1983. Mechanisms of photoadaptation in three strains of the symbiotic dinoflagellate *Symbiodinium microadriaticum*. *Mar. Biol.* **76:** 219–231.

Coleman, A. W., A. S. Suarez, and L. J. Goff. 1994. Molecular delineation of species and syngens in volvocacean green algae (Chlorophyta). *J. Phycol.* **30:** 80–90.

Colley, N. J., and R. K. Trench. 1983. Selectivity in phagocytosis and persistence of symbiotic algae by the scyphistoma stage of the jellyfish *Cassiopeia xamachana*. *Proc. R. Soc. Lond. B* **219:** 61–82.

Darius, H. T., C. Dauga, P. A. D. Grimont, C. Chungue, and P. M. V. Martin. 1998. Diversity in symbiotic dinoflagellates (Pyrrhophyta) from seven scleractinian coral species: restriction enzyme analysis of small subunit ribosomal RNA genes. *J. Eukaryot. Microbiol.* **45:** 619–627.

Don, R. H., P. T. Cox, B. J. Wainwright, K. Baker, and J. S. Mattick. 1991. "Touchdown" PCR to circumvent spurious priming during gene amplification. *Nucleic Acids Res.* **19:** 4008.

Dubos, R., and A. Kessler. 1963. Integrative and disintegrative factors in symbiotic associations. *Symp. Soc. Gen. Microbiol.* **13:** 1–11.

Dykens, J. A., and J. M. Shick. 1984. Photobiology of the symbiotic sea anemone, *Anthopleura elegantissima*: defenses against photodynamic effects, and seasonal photoacclimatization. *Biol. Bull.* **167:** 683–697.

Felsenstein, J. 1985. Confidence limits on phylogenies: an approach using the bootstrap. *Evolution* **39:** 783–791.

Francis, L. 1979. Contrast between solitary and clonal lifestyles in the sea anemone *Anthopleura elegantissima*. *Am. Zool.* **19:** 669–681.

Goff, L. J., D. A. Moon, and A. W. Coleman. 1994. Molecular delineation of species and species relationships in the red algal agarophytes *Gracilariopsis* and *Gracilaria* (Gracilariales). *J. Phycol.* **30:** 521–537.

Gonzales, I. L., J. E. Sylvester, T. F. Smith, D. Stambolian, and R. D. Schmickel. 1990. Ribosomal RNA gene sequences and hominoid phylogeny. *Mol. Biol. Evol.* **7:** 203–219.

Hand, C. 1955. The sea anemones of central California. Part II. The endomyarian and mesomyarian anemones. *Wasmann J. Biol.* **13:** 37–99.

Hunter, C. L., C. W. Morden, and C. M. Smith. 1997. The utility of ITS sequences in assessing relationships among zooxanthellae and corals. *Proc. 8th Int. Coral Reef Symp.* **2:** 1599–1602.

Iglesias-Prieto, R., and R. K. Trench. 1994. Acclimation and adaptation to irradiance in symbiotic dinoflagellates. I. Responses of the photosynthetic unit to changes in photon flux density. *Mar. Ecol. Prog. Ser.* **113:** 163–175.

Iglesias-Prieto, R., and R. K. Trench. 1997a. Photoadaptation, photoacclimation and niche diversification in invertebrate-dinoflagellate symbioses. *Proc. 8th Int. Coral Reef Symp.* **2:** 1319–1324.

Iglesias-Prieto, R., and R. K. Trench. 1997b. Acclimation and adaptation to irradiance in symbiotic dinoflagellates. II. Response of chlorophyll-protein complexes to different photon-flux densities. *Mar. Biol.* **130:** 23–33.

Larsen, A., and L. K. Medlin. 1997. Inter- and intraspecific genetic variation in twelve *Prymnesium* (Haptophyceae) clones. *J. Phycol.* **33:** 1007–1015.

Lenaers, G., L. Maroteax, B. Michot, and M. Herzog. 1989. Dinoflagellates in evolution. A molecular phylogenetic analysis of large subunit ribosomal RNA. *J. Mol. Evol.* **29:** 40–51.

McFadden, C. S., R. K. Grosberg, B. B. Cameron, D. P. Karlton, and D. Secord. 1997. Genetic relationships within and between clonal and solitary forms of the sea anemone *Anthopleura elegantissima* revisited: evidence for the existence of two species. *Mar. Biol.* **128:** 127–139.

Muscatine, L. 1971. Experiments with green algae coexistent with zooxanthellae in sea anemones. *Pac. Sci.* **25:** 13–21.

Muscatine, L., D. Grossman, and J. Doino. 1991. Release of symbiotic algae by tropical sea anemones and corals after cold shock. *Mar. Ecol. Prog. Ser.* **77:** 233–243.

Muyzer, G., and K. Smalla. 1998. Application of denaturing gradient gel electrophoresis (DGGE) and temperature gradient gel electrophoresis (TGGE) in microbial ecology. *Antonie Leeuwenhoek* **73:** 127–141.

Muyzer, G., E. De Waal, and A. G. Uitterlinden. 1993. Profiling of complex microbial populations by denaturing gradient gel electrophoresis analysis of polymerase chain reaction-amplified genes coding for 16S rRNA. *Appl. Environ. Microbiol.* **59:** 695–700.

Myers, R. M., S. G. Fischer, L. S. Lerman, and T. Maniatis. 1985. Nearly all single base substitutions in DNA fragments joined to a GC-clamp can be detected by gradient gel electrophoresis. *Nucleic Acid Res.* **13:** 3131–3145.

Newman, W. A. 1979. California transition zone: significance of short-range endemics. Pp. 399–416 in *Historical Biogeography, Plate Tectonics and the Changing Environment*. J. Gray and A. J. Boucot, eds. Oregon State University Press, Corvallis.

Polne-Fuller, M. 1991. A novel technique for preparation of axenic cultures of *Symbiodinium* (Pyrrophyta) through selective digestion by amoebae. *J. Phycol.* **27:** 552–554.

Provasoli, L., T. Yamasu, and I. Manton. 1968. Experiments on the resynthesis of symbiosis in *Convoluta roscoffensis* with different flagellate cultures. *J. Mar. Biol. Assoc. UK* **48:** 465–479.

Round, F. E. 1981. *The Ecology of Algae*. Cambridge University Press, Cambridge. 653 pp.

Rowan, R. 1998. Diversity and ecology of zooxanthellae on coral reefs. *J. Phycol.* **34:** 407–417.

Rowan, R., and N. Knowlton. 1995. Intraspecific diversity and ecological zonation in coral-algal symbiosis. *Proc. Natl. Acad. Sci. USA* **92:** 2850–2853.

Rowan, R., and D. A. Powers. 1991. A molecular genetic classification of zooxanthellae and the evolution of animal-algal symbiosis. *Science* **251:** 1348–1351.

Rowan, R., N. Knowlton, A. Baker, and J. Jara. 1997. Landscape ecology of algal symbionts creates variation in episodes of coral bleaching. *Nature* **388:** 265–269.

Saunders, B. K., and G. Muller-Parker. 1997. The effects of temperature and light on two algal populations in the temperate sea anemone *Anthopleura elegantissima* (Brandt, 1835). *J. Exp. Mar. Biol. Ecol.* **211:** 213–224.

Schoenberg, D. A., and R. K. Trench. 1980a. Genetic variation in *Symbiodinium* (= *Gymnodinium*) *microadriaticum* Freudenthal, and specificity in its symbiosis with marine invertebrates. I. Isoenzyme and soluble protein patterns of axenic cultures of *S. microadriaticum*. *Proc. R. Soc. Lond. B* **207:** 405–427.

Schoenberg, D. A., and R. K. Trench. 1980b. Genetic variation in *Symbiodinium* (= *Gymnodinium*) *microadriaticum* Freudenthal, and specificity in its symbiosis with marine invertebrates. III. Specificity and infectivity of *S. microadriaticum*. *Proc. R. Soc. Lond. B* **207:** 445–460.

Scholin, C. A., D. M., Anderson, and M. L. Sogin. 1993. Two distinct small subunit RNA genes in the North American toxic dinoflagellate *Alexandrium fundyense* (Dinophyceae). *J. Phycol.* **29:** 209–216.

Secord, D. L. 1995. Host specificity and symbiotic interactions in sea anemones. Ph.D. dissertation, University of Washington, Seattle, WA. 88 pp.

Sheffield, V. C., D. R. Cox, L. S. Lerman, and R. M. Myers. 1989. Attachment of a 40-base-pair G + C-rich sequence (GC-clamp) to genomic DNA fragments by the polymerase chain reaction results in improved detection of single-base changes. *Proc. Natl. Acad. Sci. USA* **86:** 232–236.

Shick, J. M., and J. A. Dykens. 1984. Photobiology of the symbiotic sea anemone *Anthopleura elegantissima*: photosynthesis, respiration, and behavior under intertidal conditions. *Biol. Bull.* **166:** 608–619.

Sogin, M. L., and J. H. Gunderson. 1987. Structural diversity of eukaryotic small subunit ribosomal RNAs: evolutionary implications. *Ann. NY Acad. Sci.* **503:** 125–139.

Stochaj, W. R., and A. R. Grossman. 1997. Differences in the protein profiles of cultured and endosymbiotic *Symbiodinium* sp. (Pyrrophyta) from the anemone *Aiptasia pallida* (Anthozoa). *J. Phycol.* **33:** 44–53.

Swofford, D. L. 1993. PAUP, Phylogenetic Analysis Using Parsimony, Version 4.0b2, program and documentation. Illinois Natural History Survey, University of Illinois, Champaign.

Trench, R. K. 1988. Specificity in dinomastigote-marine invertebrate symbioses: an evaluation of hypotheses of mechanisms involved in producing specificity. Pp. 325–346 in *Cell to Cell Signals in Plant, Animal and Microbial Symbiosis*, NATO Advanced Workshop. S. Scannerini, D. C. Smith, P. Bonfante-Fasolo, and V. Gianinazzi-Pearson, eds. Springer Verlag, Berlin.

Trench, R. K. 1993. Microalgal-invertebrate symbioses: A review. *Endocytobiosis Cell Res.* **9:** 135–175.

Trench, R. K. 1997. Diversity of symbiotic dinoflagellates and the evolution of microalgal-invertebrate symbioses. *Proc. 8th Int. Coral Reef Symp.* **2:** 1275–1286.

Trench, R. K., and H. Winsor. 1987. Symbiosis with dinoflagellates in two pelagic flat-worms *Amphiscolops* sp. and *Haplodiscus* sp. *Symbiosis* **3:** 1–22.

Trench, R. K., N. J. Colley, and W. K. Fitt. 1981. Recognition phenomena in symbioses between marine invertebrates and zooxanthellae: uptake, sequestration and persistence. *Ber. Dtsch. Bot. Ges.* **94:** 529–545.

Verde, E. A., and L. R. McCloskey. 1996. Photosynthesis and respiration of two species of algal symbionts in the anemone *Anthopleura elegantissima* (Brandt) (Cnidaria, Anthozoa). *J. Exp. Mar. Biol. Ecol.* **195:** 187–202.

Warner, M. E., W. K. Fitt, and G. W. Schmidt. 1996. The effects of elevated temperature on the photosynthetic efficiency of zooxanthellae *in hospite* from four different species of reef coral: a novel approach. *Plant Cell Environ.* **19:** 291–299.

Warner, M. E., W. K. Fitt, and G. W. Schmidt. 1999. Damage to Photosystem II in symbiotic dinoflagellates: a determinant of coral bleaching. *Proc. Natl. Acad. Sci. USA* **96:** 8007–8012.

Wilcox, T. 1998. Large-subunit ribosomal RNA systematics of symbiotic dinoflagellates: morphology does not recapitulate phylogeny. *Mol. Phylogenet. Evol.* **10:** 436–448.

Wilkerson, F. P., G. Muller-Parker, and L. Muscatine. 1983. Temporal patterns of cell division in natural populations of endosymbiotic algae. *Limnol. Oceanogr.* **28:** 1009–1014.

Reference: *Biol. Bull.* **199:** 135–143. (October 2000)

Seasonal Variation in Conduction Velocity of Action Potentials in Squid Giant Axons

JOSHUA J. C. ROSENTHAL AND FRANCISCO BEZANILLA*

Departments of Physiology and Anesthesiology, UCLA School of Medicine,
Los Angeles, California 90095

Abstract. To determine whether the electrical properties of the squid giant axon are seasonally acclimated, action potentials, recorded at different temperatures, were compared between giant axons isolated from *Loligo pealei* caught in May, from relatively cold waters (~10°–12°C), and in August, from relatively warm waters (~20°C). Parameters relating to the duration of the action potential (*e.g.*, maximum rate of rise, maximum rate of fall, and duration at half-peak) did not change seasonally. The relationship between conduction velocity and temperature remained constant between seasons as well, in spite of the fact that May axons were significantly larger than August axons. When normalized to the fiber diameter, mean May conduction velocities were 83% of the August values at all temperatures tested, and analysis of the rise time of the action potential foot suggested that a change in the axoplasmic resistivity was responsible for this difference. Direct measurements of axoplasmic resistance further supported this hypothesis. Thus seasonal changes in the giant axon's size and resistivity are not consistent with compensatory thermal acclimation, but instead serve to maintain a constant relationship between conduction velocity and temperature.

Introduction

Signal transduction in the nervous system is profoundly temperature sensitive. Acclimation of higher order nervous function to variation in environmental temperature has been the subject of many investigations (see Prosser and Nelson, 1981); however, the precise mechanisms of such acclimations are not well understood. Do they involve changes at the level of the action potential, the synapse, or both? Action potential duration and propagation are strongly influenced by acute temperature changes (Hodgkin and Katz, 1949), largely due to temperature sensitivity of the underlying ion channels (Hodgkin *et al.*, 1952). If action potentials themselves are a common target for thermal acclimation, which properties are affected? In the giant nerve fibers of earthworms, cold acclimation speeds the action potential duration, conduction velocity, and refractory period *vs.* temperature relationship, but not to the extent that, when measured at rearing temperatures, the kinetics of cold- and warm-acclimated worms are equivalent (Lagerspetz and Talo, 1967; Talo and Lagerspetz, 1967). In goldfish cardiac muscle cells, the action potential's duration is reduced in cold-acclimated fish (Ganim *et al.*, 1998). In certain *Aplysia* neurons, however, early potassium current kinetics are not affected by rearing temperature (Treistman and Grant, 1993).

The squid giant axon, long a model for understanding the basic physiology of voltage-dependent ion channels, is, for a variety of reasons, an excellent system for examining temperature-dependent acclimation of the action potential. First, its output participates in a known function—the jet-propelled escape response (Prosser and Young, 1937; Young, 1938; Otis and Gilly, 1990)—and presumably it is advantageous for this response to be rapid. Second, the dimensions of the giant axon permit action potentials, macroscopic ionic currents, gating currents, and single-channel currents to be measured from the same preparation (Hodgkin and Huxley, 1952; Armstrong and Bezanilla, 1973; Conti and Neher, 1980; Bezanilla, 1987). Third, Na and K currents, which underlie the action potential, have been extensively characterized in this system (see Gilbert *et al.*, 1990). Fourth, giant axon Na and K channels have been

---

Received 3 March 2000; accepted 7 July 2000. E-mail: fbezanil@UCLA.edu

* To whom correspondence should be addressed.

Abbreviations: C_m, membrane capacitance; MRF, maximum rate of fall; MRR, maximum rate of rise; R_e, external resistivity; R_i, internal resistivity; r_e, external resistance; r_i, internal resistance.

defined on a molecular level (Rosenthal and Gilly, 1993; Rosenthal *et al.*, 1996). Finally, and perhaps most important, squid of the genus *Loligo* (and other genera that contain "giant" axons) inhabit a wide variety of thermal environments.

Squid of the species *Loligo pealei* live off the eastern seaboard of North America, where inshore water temperatures undergo large seasonal fluctuations. By examining the axons from these squid in both May and August, the present study seeks to identify those properties of the action potential that change on a seasonal basis.

Materials and Methods

Squid collection and water temperatures

Adult specimens of *Loligo pealei* were collected from the waters surrounding Woods Hole, Massachusetts, in 1997 and 1998 during May and August. In May, specimens were jigged from the town dock, and in August they were caught by trawls in Vineyard Sound. During two trawls, water temperature was measured at the net opening with a data logger. Daily temperatures, recorded near the Marine Biological Laboratory (MBL) seawater intake system at a depth of 15 feet, were kindly furnished by Janice Hanley, MBL water quality technician. Data used in Figure 2 were recorded by the National Oceanic and Atmospheric Administration (NOAA) at the Woods Hole Oceanographic Institution pier (tide station number 8447930, available on the NOAA website). Squid were maintained in flowing seawater, whose temperature was kept within 1 degree of the intake temperature, and were used within 2 days of capture. Animals were killed by rapid decapitation, and hindmost stellar nerves were removed and carefully cleaned of small fibers in seawater. All experiments, unless otherwise specified, were performed in 10 K^+ artificial seawater (ASW; composition in millimoles: 430 NaCl, 10 KCl, 50 $MgCl_2$, 10 $CaCl_2$, 10 HEPES, pH 7.5, 970 mOsm).

Action potential measurements

Propagated action potentials were measured by mounting a freshly dissected axon (4–6 cm) in a long, rectangular glass chamber filled with 10 K^+ ASW. Temperature was regulated using two Peltier units mounted under the chamber and was measured with a hand-held thermocouple positioned directly adjacent to the axon. After equilibration of the chamber, temperatures at all points along the axon were within ±0.5°C of the recorded temperature. Action potentials were stimulated intracellularly at one end of the axon using brief current pulses (2–20 μA for 200–400 μs) administered through a 0.4–0.6 MΩ micropipette filled with 3 *M* KCl, and connected to the output of the online D/A converter. Stimuli, which varied from axon to axon, were the minimum required to produce a consistent action potential. Voltage signals were recorded at two points along the axon using two additional micropipettes (3 *M* KCl, 1–3 MΩ) connected to two high-impedance, capacitance-compensated electrometers. The chamber was grounded using two Ag^+/AgCl coils embedded in 10 K^+ ASW + 3% agarose and connected to virtual ground. Signals were collected using software written in-house and a PC44 (Innovative Technologies) signal processor board connected to a PC compatible computer. Sampling rates varied between 200 kHz and 1 MHz, depending on the temperature, and signals were filtered at 1⁄10 of the sampling rate. Axon diameters and distances between micropipettes were measured with an eyepiece micrometer. Data were analyzed only from electrode impalements with resting potentials more hyperpolarized than −55 mV.

Capacitance and resistance measurements

Membrane capacitance was measured in the voltage-clamp configuration as previously described (Bezanilla *et al.*, 1982a, b) with minor modifications. Signals were collected as described in the previous section. A 75-μm platinum wire for passing current and an internal measuring electrode consisting of an 80-μm glass capillary filled with 0.6 *M* KCl and containing a floating 25-μm platinum wire were inserted into the axon in a piggy-back configuration (Hodgkin *et al.*, 1952). A wide-aperture glass capillary filled with 10 K^+ ASW + 3% agar was used as an external reference. Capacity transients were generated by brief pulses from a holding potential of −80 mV to −90 mV. The average of 10 such records was used for analysis. Data were collected at 500 kHz and filtered at 50 kHz. For resistance measurements, axons were carefully cleaned of all adhering accessory fibers and placed on a platform of clear acrylic plastic. The axon ends were then cut and dipped into two pools containing 500 m*M* K-glutamate, 10 HEPES, 5 EGTA, pH 7.5. These pools were voltage clamped, and signals were collected, as described above. In all cases, data were analyzed using in-house software. Error bars represent the standard error of the mean (SEM), and a Student's *t* test was used where probabilities are indicated in the text.

Results

In the giant axon, action potential duration and conduction velocity are strongly affected by temperature (Hodgkin and Katz, 1949; Chapman, 1967). Figure 1A shows three action potentials, recorded at different temperatures, from a single electrode inserted into a giant axon. Clearly, the durations of the rising and falling phase both increase as the temperature is decreased. The half-width of the action potential recorded at 20°C is 365 μs. This number increases to 850 μs at 10.2°C, and to 2400 μs at 1.8°C. Furthermore, the conduction velocity shows a similar temperature dependence. In Figure 1B, action potentials, evoked by a single

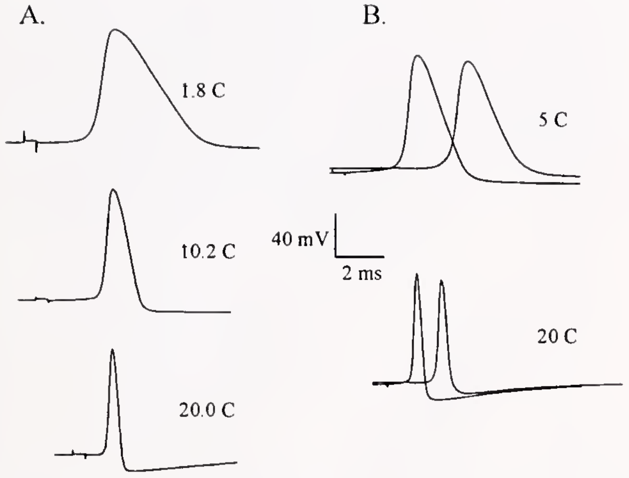

Figure 1. Action potentials recorded at different temperatures. (A) Propagated action potentials from a single position in a single giant axon measured at three temperatures. (B) Propagated action potentials recorded at two positions in a single axon measured at two temperatures. Axons were bathed in 10 K$^+$ artificial seawater. Brief transients at the beginning of records are stimulus artifacts.

stimulus, are recorded at two points, separated by 19.6 mm, along the same axon. From this experiment the conduction velocity is calculated to be 9.56 m/s at 5°C and 18.94 m/s at 20°C. The axons used in this figure were dissected from a squid captured in May.

Water temperatures in the Woods Hole Passage and in Vineyard Sound, where squid for these studies were captured, change dramatically between the spring and summer. In May, squid were collected by jigging from waters directly measured to be 10°–12°C. In late August, squid were captured by trawling, and on two trawls the average temperature at the net opening was recorded to be 20.4°C and 21.2°C. Figure 2 shows hourly water temperatures recorded by the NOAA tidal monitoring station (adjacent to the Woods Hole Oceanographic Institution pier in the Woods Hole Passage) between April and October, 1997 and 1998. During May, water temperatures vary between about 10° and 12°C. In August they average slightly greater than 20°C. These values are corroborated by daily temperature records taken near the MBL seawater intake system at a depth of 15 feet. In 1998, May and August average temperatures (±SD) were 12.4°C ± 1.2 and 21.8°C ± 0.49, respectively. The few data points available for this site in 1997 are similar to the 1998 values (10.2°C on May 5, 12.8°C on May 28, 22.0°C on August 8, and 21.1°C on August 26). Thus, water temperatures during the study period in both 1997 and 1998 changed by about 10°C. Acute temperature changes of this magnitude would clearly affect the giant axon's electrical properties (see Fig. 1). Do these properties change to compensate for seasonal temperature variation?

To answer this question, action potentials were compared between squid captured in May and in late August. Figure 3 compares maximal rates of rise (MRR) and fall (MRF) of the action potential, at various temperatures, for May and August squid. No significant difference exists for either measurement between groups. MRRs have a nearly linear

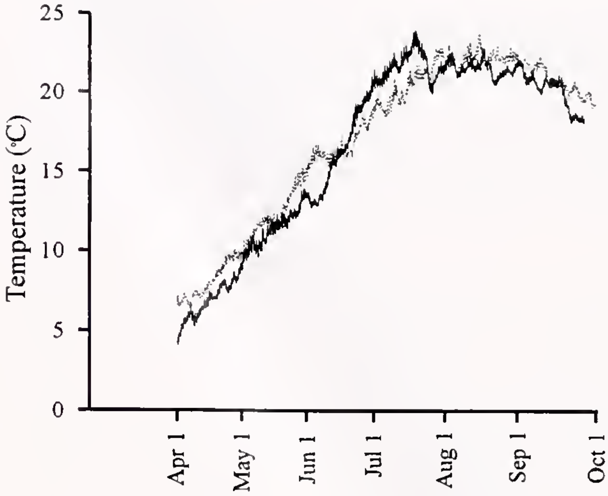

Figure 2. Seasonal temperature variation in the Woods Hole Passage. Hourly temperature records from April through September for 1997 (solid line) and 1998 (dotted line). Temperatures were taken from NOAA station number 8447930 located at the Woods Hole Oceanographic Institution at 41° 31.5' N, 70° 40.3' W.

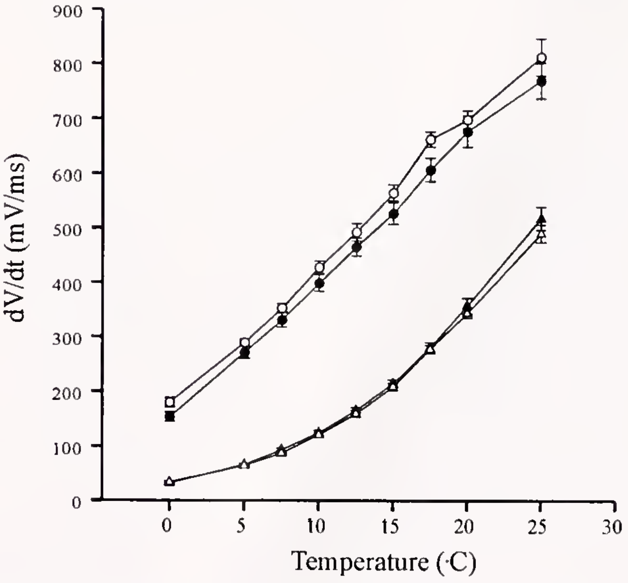

Figure 3. Action potential maximum rates of rise and fall do not change seasonally. Action potential records from squid in May (filled symbols) and August (open symbols) were differentiated numerically, and maximum values (rates of rise; circles) and minimum values (rates of fall, absolute values; triangles) were plotted against temperature. Action potentials were recorded at two positions along an axon. Error bars represent the standard error of the mean; n = 10 records (5 axons) for May and 11 records (6 axons) for August.

temperature relationship, while that of the MRFs is exponential. In addition, the MRFs have a higher temperature coefficient. Q_{10} values for the MRF are 3.7 and 2.5 for the temperature ranges 0°–12.5°C and 12.5°–25°C, respectively. For the same intervals, Q_{10}'s for the MRR are 2.4 and 1.5. Other measurements relating to the action potential duration (*e.g.*, rise time, fall time, and duration at half-peak amplitude) also showed no seasonal difference.

In contrast, resting potentials and conduction velocities did exhibit significant seasonal variation. Figure 4A compares the resting potential *vs.* temperature relationship for May and August axons. Between 0° and 15°C, both groups

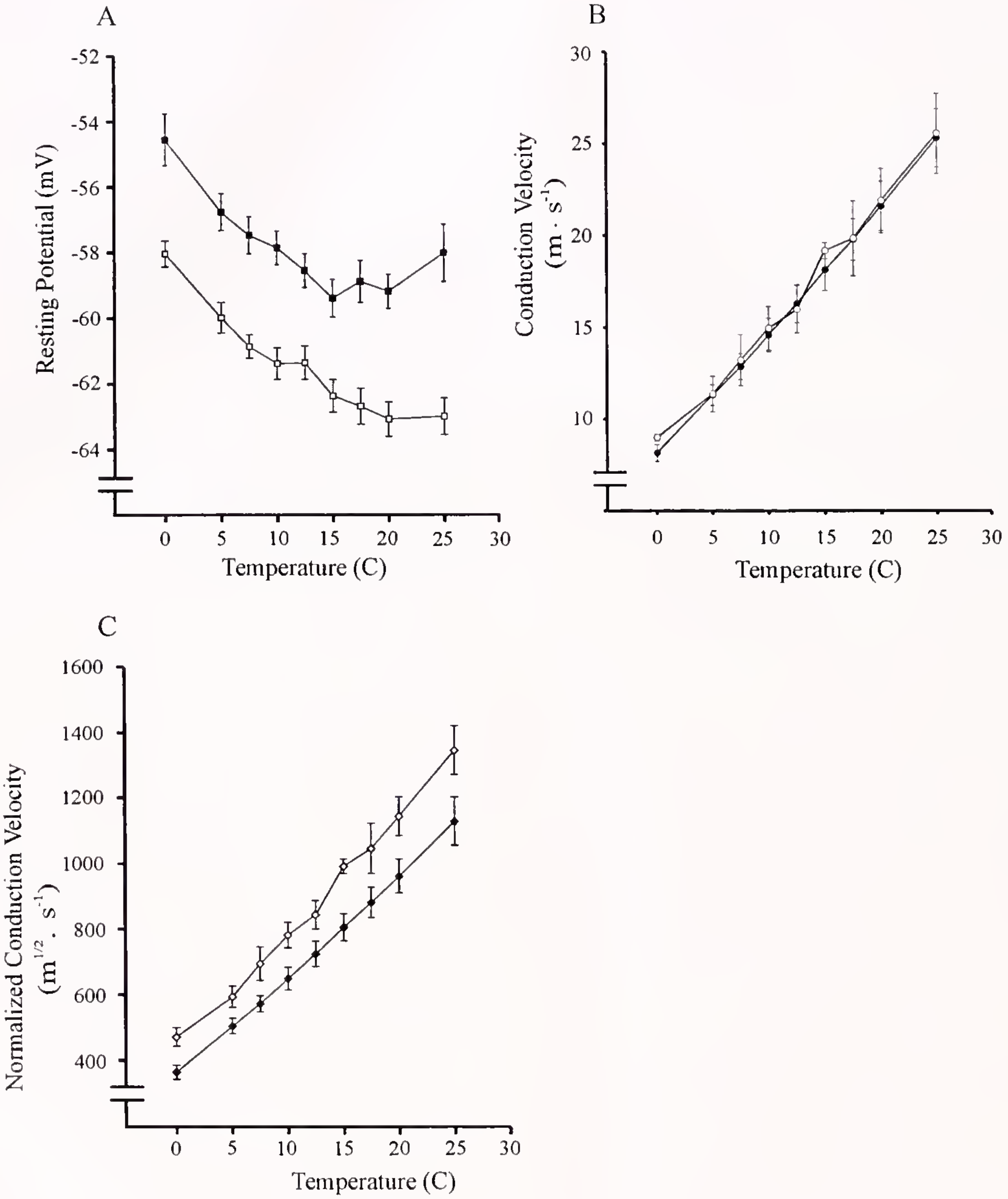

Figure 4. Resting potentials and conduction velocities change seasonally. (A) Resting potential *vs.* temperature relationship for May axons (filled symbols) and August axons (open symbols). Error bars represent the standard error of the mean (SEM); n = 10 for each season. (B) Conduction velocities *vs.* temperature for May and August axons (same symbol convention) as in A. (C) Conduction velocities, normalized to the square root of the diameter, *vs.* temperature for May and August axons (same symbol convention). Error bars represent SEM; n = 6 for each season for both B and C.

become more hyperpolarized as the temperature is raised. In this temperature range, the May axons are on average ~3 mV more depolarized. At temperatures greater than 15°C, May axons become progressively more depolarized, while August axons continue to hyperpolarize until approximately 20°C, after which they level out. Thus at 25°C the resting potential disparity reaches ~5 mV.

Figures 4B and 4C show the relationship between conduction velocity and temperature. Absolute (non-normalized) conduction velocities were equivalent between May and August squid (4B) at all temperatures tested. Interestingly, May axons had significantly larger diameters (506 ± 26.8 μm; mean ± SEM) than those in August (383 ± 14.68 μm; mean ± SEM). Conduction velocity in the giant axon is proportional to the square root of the axon diameter, a relationship originally established by Hodgkin and Huxley (1952) and verified by many other groups (Chapman, 1967; Taylor, 1963). Taking this into account, normalized conduction velocities are plotted *vs.* temperature in Figure 4C. Conduction velocities from May axons are relatively slow, being on average 83% ± 2.5% (SD) of the August values. In both seasons the Q_{10} values were equivalent (1.5 between 10° and 20°C).

The fact that normalized conduction velocity values changed from May to August, but the MRR and MRF did not, suggested that the passive electrical properties of the axon had also changed. The action potential's initial rate of rise, or "foot," can be used to extract information related to the axon's cable properties by the following relationship:

$$C_m(r_i + r_e) = 1/\tau\theta^2$$

where C_m is membrane capacitance, r_i is internal resistance, r_e is external resistance, τ is the time constant of the rise time of the action potential foot, and θ is the conduction velocity (Taylor, 1963). Figure 5A shows an example of an exponential fit to the foot of an action potential recorded at 10°C from a May axon. In this case, τ was 210 μs, θ was 12.45 m/s, and therefore $C_m(r_i + r_e)$ was 30.7 Ω*F*cm. Similar analysis was extended to action potentials from May and August, and all data were normalized to account for axons of different diameters (Fig. 5B). At all temperatures, normalized $C_m(r_i + r_e)$ was greater in May than in August axons. On average, May values were 31.7% ± 6% (SD) greater.

The preceding analysis indicated that the product of resistance and capacitance was variable between seasons; however, it did not identify which property changed. To accomplish this, capacitance and resistance were measured independently. Capacitance was measured at a variety of temperatures using a conventional axial wire voltage clamp. A Q_{10} of 1.06 was determined for the relationship between capacitance and temperature in two axons (data not shown). This number agrees well with previously published data from squid (Taylor *et al.*, 1962) and was used to extrapolate all experimental values to 15°C. For May and August axons, mean capacitance was determined to be 1.03 ± 0.039 μF/cm^2 (SEM, $n = 6$) and 0.96 ± 0.027 μF/cm^2 (SEM, $n = 6$), respectively. A statistical difference between these means is not well supported ($P = 0.18$). Thus differences in capacitance are not sufficient to account for the $C_m(R_i + R_e)$ data from the previous section.

Axoplasmic resistance was measured directly in dissected axons. Axons were blotted dry and placed on an acrylic plastic platform; their ends were cut and dipped into two reservoirs containing internal solution (Fig. 6A). The reservoirs were then voltage clamped, and after transients had subsided, the current flow through the axon was measured and normalized to the axon's cross sectional area and length. All measurements were conducted at room temperature (about 20°C). The results from a typical axon segment of 404 μm diameter and 3.65 cm length are shown in Figure 6B. In this case, the voltage between the reservoirs and the current flow through the axon were 107.3 mV and 1.24 μA. Thus the resistance ($r_i + r_e$) for this axon was calculated to be 86.5 kΩ, and the specific resistance ($R_i + R_e$) was 30.3 Ω*cm. As expected, the current voltage relationship at a variety of test potentials is linear (Fig 6C). A series of axons from May and August were analyzed in a similar manner and their specific resistivities were found to differ. Mean $R_i + R_e$ was measured to be 35.2 ± 1.3 Ω*cm (± SEM, $n = 6$) and 28.4 ± 2.5 (± SEM, $n = 6$; $P = 0.05$) in May and August, respectively. Thus on average, May values are 22% greater than August values.

Discussion

The present investigations were initiated to identify seasonal changes in the giant axon's electrical properties, and to address whether these changes could compensate for seasonal temperature variability. Implicit in these studies is that the squid do in fact experience seasonal temperature variability. Temperature data from all sources, taken at various depths, all show a temperature profile similar to that in Figure 2 (*i.e.*, an approximate 10°C difference between May and August). The recorded spring temperatures are probably maximum values and thus are a conservative estimate of the squid's environment. Summer temperatures reported in this paper are probably representative for Vineyard Sound and the Woods Hole Passage, the locations where the squid used for these experiments were captured. Turbulence, created by large tidal flows, prevents the formation of thermoclines in these shallow areas, and temperatures are uniform throughout the water column. Other papers have come to a similar conclusion about mixing and report summer temperatures as high as 23°C (Summers, 1968; McMahon and Summers, 1971). Outside of the Vineyard Sound, temperatures are likely to be significantly

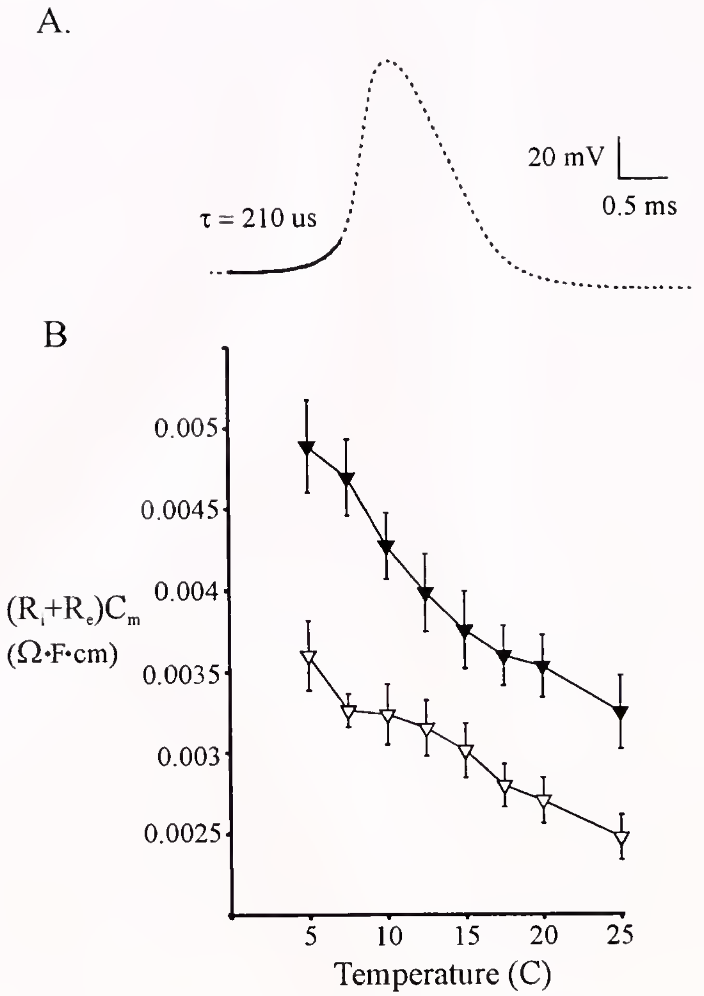

Figure 5. Product of resistance and capacitance changes seasonally. (A) Example of measurement. Dotted line is an action potential recorded at 10°C from a May axon; solid line is an exponential fit to the action potential foot. (B) Values of $(R_i + R_e)C_m$ *vs.* temperature for May (filled triangles) and August (open triangles) axons. See text for derivation of $(R_i + R_e)C_m$. Error bars represent the standard error of the mean; $n = 6$ for May and 5 for August.

lower. Schopf (1967) reports the presence of thermoclines and maximum annual bottom-water temperatures of 13°C in the waters off Nantucket.

The migration patterns of *Loligo pealei* are not well understood. On a seasonal basis this species is reported to winter near the break of the continental shelf where it can avoid temperatures below 8°C (Summers, 1969). In the spring these squid move inshore when waters warm past about 10°C (Summers, 1969; Mesnil, 1977). The first group to arrive are the 2-year-olds, normally in early May, followed by the 1-year-olds in June (Summers, 1971). This sequence of events probably explains the larger diameter of the May axons. Migration on a shorter time scale has not been reported for this species, and therefore it is unknown whether these squid migrate to colder oceanic waters on a daily basis. We consider such a migration unlikely for two reasons. First a substantial horizontal shift would be required to reach deep oceanic waters (depending on the point of departure in Vineyard Sound). Second, the August squid were routinely captured during the day. In other cephalopods, daily migrations involve a nocturnal shift to shallow waters (Boyle, 1983; Hanlon and Messenger, 1996). Therefore it is likely that the squid spend a significant portion of their time at the water temperatures specified in this report. Various reports document the presence of *L. pealei* in yet warmer waters (*e.g.*, 22°–29°C in the Gulf of Mexico; see Boyle, 1983).

This study presents no evidence for a seasonal compensation in the propagated action potential's duration, as there is no change in the curve of MRR or MRF *vs.* temperature. These data also suggest that the properties of the underlying ionic current do not change, and studies using voltage-clamped giant axons support this conjecture (data not shown). Therefore it is predicted that *in vivo*, the duration of

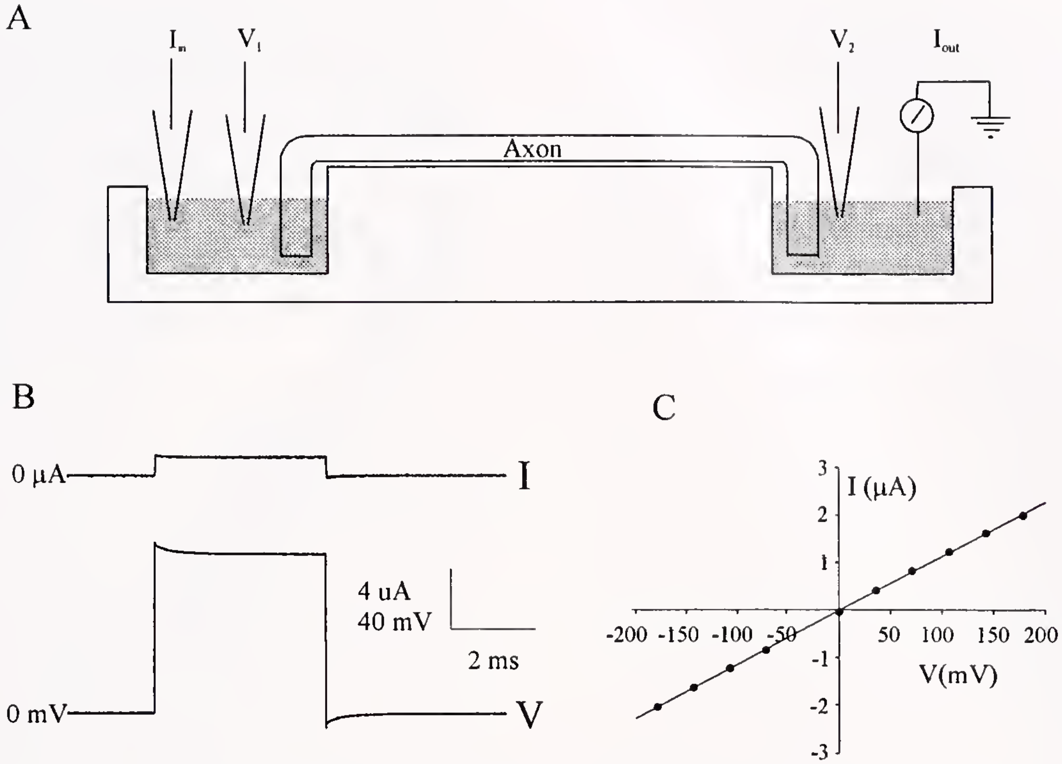

Figure 6. Direct resistance measurements. (A) Schematic of experimental setup. A defined length of axon was placed on a clear plastic platform, and each end was cut and placed in a bath containing internal solution (in m*M*: 500 K-glutamate, 10 HEPES, 2.5 EGTA, pH 7.5). The interbath voltage was clamped using a home-built squid axon apparatus, and the resulting current was measured. (B) An example of the current resulting from a 100-mV voltage step (May axon). (C) Current-voltage relationship from the same axon. All experiments performed at temperatures between 18° and 20°C.

the action potential in May squid is over twice as long as it is in August squid (see Fig. 1 for examples of action potentials recorded at 10°C and 20°C). Unlike the action potential duration, the conduction velocity does appear to be regulated between seasons. However, the direction of the change is not consistent with a compensatory thermal acclimation: despite a seasonal disparity in axon diameter, the relationship between conduction velocity and temperature remains constant, due mostly to resistive changes in the axon. Computer simulations of conduction velocities using the Hodgkin and Huxley equations (Hodgkin and Huxley, 1952) support this assertion. By substituting the May and August values for $C_m(R_i + R_e)$, determined by fits to the action potential foots (32.4 ΩF and 42.7 ΩF, respectively, at 10°C), there is a 14.2% increase in conduction velocity. The difference determined from direct measurements of conduction velocities in May and August axons at 10°C was 14.6%.

Fits to the action potential foot predicted that the product of $(R_t + R_e)$ and C_m increased by approximately 30% between August and May. This is in reasonable agreement with direct measurements of $(R_i + R_e)$ for the same seasons, which increased by 22%. Capacitive changes were not found to be statistically significant. It is probable that resistive changes are due to changes in R_t, as the contribution of R_e to our measurements is expected to be very small. Great care was taken to blot the axon's external surface prior to recording, thus the layer of adhering seawater would be quite small compared to the cross-sectional area of the axon. Cole and Hodgkin, who employed a similar experimental setup, came to the same conclusion (Cole and Hodgkin, 1939). In addition, our reported values of $R_i + R_e$, particularly those for August (28.7 Ω•cm), are consistent with previously reported values of R_i. Cole and Hodgkin reported 29 Ω•cm (Cole and Hodgkin, 1939) and in a separate report, Cole reported the resistivity of extruded axoplasm to be 28 Ω•cm (Cole, 1975). Using two internal microelectrodes, Carpenter *et al.* (1975) reported it to be 31 Ω•cm. It is unclear during which season these studies were conducted.

Seawater, which is isosmotic with axoplasm (Gilbert *et al.*, 1990), has a specific resistivity of only 20 Ω•cm (Cole and Hodgkin, 1939). Why is axoplasm a relatively poor conductor? First, unlike seawater, axoplasm contains mostly large organic anions that have lower mobilities than chloride. In addition, our measurements of resistivity consider the axon as a conducting cylinder, and do not take into account the organelles, which occupy an unknown percentage of the volume. Finally, axoplasm contains a good deal of immobile protein. We observed that axoplasm appears gelatinous in May, whereas in August it is considerably more liquid, possibly due to a decrease in the order of the underlying cytoskeletal proteins. Differences in any of these parameters could underlie the seasonal differences in axoplasmic resistivity.

In the absence of a seasonal acclimation, giant axon action potentials would travel much faster in August than in May. The resistive changes discussed in this paper would not help compensate for temperature changes in conduction velocity and therefore they do not contribute to a compensatory acclimation. However, the giant axon is clearly a part of a larger motor system, the pieces of which do not have equal temperature sensitivities. Perhaps thermal acclimation involves maintaining specific ratios between the rates of processes. For example, the temperature dependence of the giant synapse is steep compared to the various properties related to the action potential discussed in this paper (see Llinas, 1999). Between 10° and 20°C, synaptic delay at the giant synapse has a Q_{10} of 3.8 (Llinas *et al.*, 1987) as compared with the Q_{10} of 1.5 measured for action potential conduction velocity in this work. Therefore the ratio of synaptic transmission to conduction velocity, which may be important for integration in the nervous system, would be greater in August than in May. The resistive changes discussed in this paper would help to maintain a more similar ratio between seasons. In support of this conjecture it is noteworthy that the non-normalized relationship between conduction velocity and temperature did not vary between May and August, in spite of the fact that August axons were significantly smaller.

Acknowledgments

We thank Drs. David Gadsby, Paul De Weer, Robert Rakowski, and Barbara Ehrlich for generously sharing laboratory space at the Marine Biological Laboratory; Roger Hanlon for help procuring and maintaining squid; and Janice Hanley, Dr. George Hampson, and John Valois for providing temperature data. This work was supported by a National Institute of Health Grant (GM 30376) and a National Institute of Health NRSA postdoctoral training grant (NS 07101-18-19) for Dr. Joshua Rosenthal.

Literature Cited

Armstrong, C. M., and F. Bezanilla. 1973. Currents related to movement of the gating particles of the sodium channels. *Nature* **242:** 459–461.

Bezanilla, F. 1987. Single sodium channels from the squid giant axon. *Biophys. J.* **52:** 1087–1090.

Bezanilla, F., R. E. Taylor, and J. M. Fernández. 1982a. Distribution and kinetics of membrane dielectric polarization. 1. Long-term inactivation of gating currents. *J. Gen. Physiol.* **79:** 21–40.

Bezanilla, F., J. Vergara, and R. E. Taylor. 1982b. Voltage clamping of excitable membranes. *Meth. Exp. Phys.* **20:** 445–511.

Boyle, P. R. 1983. *Cephalopod Life Cycles.* Academic Press, London.

Carpenter, D. O., M. M. Hovey, and A. F. Bak. 1975. Resistivity of axoplasm. II. Internal resistivity of giant axons of squid and *Myxicola. J. Gen. Physiol.* **66:** 139–148.

Chapman, R. A. 1967. Dependence on temperature of the conduction velocity of the action potential of the squid giant axon. *Nature* **213:** 1143–1144.

Cole, K. S. 1975. Resistivity of axoplasm. I. Resistivity of extruded squid axoplasm. *J. Gen. Physiol.* **66:** 133–138.

Cole, K. S., and A. L. Hodgkin. 1939. Membrane and protoplasm resistance in the squid giant axon. *J. Gen. Physiol.* **22:** 671–687.

Conti, F., and E. Neher. 1980. Single channel recordings of K^+ currents in squid axons. *Nature* **285:** 140–143.

Ganim, R. B., E. L. Peckol, J. Larkin, M. L. Ruchhoeft, and J. S. Cameron. 1998. ATP-sensitive K^+ channels in cardiac muscle from cold-acclimated goldfish: characterization and altered response to ATP. *Comp. Biochem. Physiol. A* **119:** 395–401.

Gilbert, D. L., W. J. Adelman, and J. M. Arnold. 1990. *Squid as Experimental Animals.* Plenum Press, New York.

Hanlon, R. T., and J. B. Messenger. 1996. *Cephalopod Behaviour.* Cambridge University Press, Cambridge.

Hodgkin, A. L., and A. F. Huxley. 1952. A quantitative description of membrane current and its application to conduction and excitation in nerve. *J. Physiol.* **117:** 500–541.

Hodgkin, A. L., and B. Katz. 1949. The effect of temperature on the electrical activity of the giant axon of the squid. *J. Physiol.* **109:** 240–249.

Hodgkin, A. L., A. F. Huxley, and B. Katz. 1952. Measurement of current-voltage relations in the membrane of the giant axon of *Loligo. J. Physiol.* **116:** 424–448.

Lagerspetz, K. Y. H., and A. Talo. 1967. Temperature acclimation of the functional parameters of the giant nerve fibers in *Lumbricus terrestris:* I. Conduction velocity and the duration of the rising and falling phase of action potential. *J. Exp. Biol.* **47:** 471–480.

Llinas, R. R. 1999. *The Squid Giant Synapse: a Model for Chemical Transmission.* Oxford University Press, Oxford. Pp. 48–54.

Llinas, R., M. Sugimori, and K. Walton. 1987. Further studies on depolarization release coupling in squid giant synapse. *Adv. Exp. Med. Biol.* **221:** 1–17.

McMahon, J. J., and W. C. Summers. 1971. Temperature effects on the developmental rate of squid (*Loligo pealei*) embryos. *Biol. Bull.* **141:** 561–567.

Mesnil, B. 1977. Growth and life cycle of squid, *Loligo pealei* and *Illex illecebrosus,* from the northwest Atlantic. *Int. Comm. Northwest Atl. Fish. Sel. Pap.* **2:** 55–69.

Otis, T. S., and W. F. Gilly. 1990. Jet-propelled escape in the squid *Loligo opalescens:* concerted control by giant and non-giant motor axon pathways. *Proc. Natl. Acad. Sci. USA* **87:** 2911–2915.

Prosser, C. L., and D. O. Nelson. 1981. The role of nervous systems in temperature adaptation of poikilotherms. *Annu. Rev. Physiol.* **43:** 281–300.

Prosser, C. L., and J. Z. Young. 1937. Responses of muscles of the squid to repetitive stimulation of the giant nerve fibers. *Biol. Bull.* **73:** 237–241.

Rosenthal, J. J., and W. F. Gilly. 1993. Amino acid sequence of a putative sodium channel expressed in the giant axon of the squid *Loligo opalescens. Proc. Natl. Acad. Sci. USA* **90:** 10026–10030.

Rosenthal, J. J., R. G. Vickery, and W. F. Gilly. 1996. Molecular identification of SqKv1A. A candidate for the delayed rectifier K channel in squid giant axon. *J. Gen. Physiol.* **108:** 207–219.

Schopf, T. J. M. 1967. Bottom-water temperatures on the continental shelf off New England. *Geol. Surv. Res.* **575-D:** D192–D197.

Summers, W. C. 1968. The growth and size distribution of current year class *Loligo pealei. Biol. Bull.* **135:** 366–377.

Summers, W. C. 1969. Winter population of *Loligo pealei* in the mid-Atlantic Bight. *Biol. Bull.* **137:** 202–216.

Summers, W. C. 1971. Age and growth of *Loligo pealei,* a population study of the common Atlantic coast squid. *Biol. Bull.* **141:** 189–201.

Talo, A., and K. Y. H. Lagerspetz. 1967. Temperature acclimation of the functional parameters of the giant nerve fibers in *Lumbricus terrestris:* II. The refractory period. *J. Exp. Biol.* **47:** 481–484.

Taylor, R. E. 1963. Cable theory. Pp. 219–262 in *Physical Techniques in Biological Research.* Academic Press, New York.

Taylor, R. E., W. K. Chandler, and W. Knox. 1962. Effect of temperature on squid axon membrane capacity. *Biophys. Soc. Abstr.* TD1.

Treistman, S. N., and A. J. Grant. 1993. Increase in cell size underlies neuron-specific temperature acclimation in *Aplysia. Am. J. Physiol.* **264:** C1061–C1065.

Young, J. Z. 1938. The functioning of the giant nerve fibres of the squid. *J. Exp. Biol.* **15:** 170–185.

Reference: *Biol. Bull.* **199:** 144–156. (October 2000)

Role of the Cytoskeleton in Sperm Entry During Fertilization in the Freshwater Bivalve *Dreissena polymorpha*

M. J. MISAMORE* AND J. W. LYNN†

Department of Biological Sciences, Louisiana State University, Baton Rouge, Louisiana 70803

Abstract. The present study examined the role of the cytoskeleton in sperm entry and migration through the egg cytoplasm during fertilization in the zebra mussel, *Dreissena polymorpha* (Bivalvia: Veneroida: Dreissenidae). Fertilization in this freshwater bivalve occurs outside the mantle cavity, permitting detailed observations of fertilization. After its initial binding to the egg surface, the sperm is incorporated in two stages: (1) a gradual incorporation of the sperm nucleus into the egg cortex, followed by (2) a more rapid incorporation of the sperm axoneme, and translocation of the sperm head through the egg cytoplasm. Initial incorporation into the egg cortex was shown to be microfilament dependent. Microfilaments were found in the sperm's preformed acrosomal filament, the microvilli on the egg surface, and in an actin-filled insemination cone surrounding the incorporating sperm. Treatment of eggs with cytochalasin B inhibited sperm entry in a dose- and time-dependent manner. Microtubule polymerization was not necessary for initial sperm entry.

Following incorporation of the sperm head, the flagellar axoneme entered the egg cytoplasm and remained active for several minutes. Associated with the incorporated axoneme was a flow of cytoplasmic particles originating near the proximal end of the flagella. Inhibition of microtubule polymerization prevented entry of the sperm axoneme, and the subsequent cytoplasmic current was not observed. After sperm incorporation into the egg cortex, no appreciable microfilaments were associated with the sperm nucleus. A diminutive sperm aster was associated with the sperm nucleus during its decondensation, but no obvious extension toward the female pronucleus was observed. The sperm aster was significantly smaller than the spindle associated with the female pronucleus, suggesting a reduced role for the sperm aster in amphimixis.

Introduction

During fertilization in the freshwater zebra mussel, *Dreissena polymorpha* (Bivalvia: Veneroida: Dreissenidae), gametes are spawned directly into the water column, where gamete binding occurs. External fertilization is common among marine bivalves but is unusual among freshwater bivalves, in which fertilization and larval development typically occur in the mantle cavity (Burky, 1983). Broadcast spawning of gametes, the relative ease of inducing spawning (Ram *et al.*, 1993), and the highly transparent nature of the egg cytoplasm make zebra mussels a good model system for studying early fertilization events.

Sperm entry into the egg cytoplasm during fertilization is a two-step process (Misamore *et al.*, 1996). During the initial phase, the sperm head and midpiece are gradually (10 μm/min) incorporated into the egg cortex. Following sperm binding, an insemination cone forms on the egg surface and envelopes the fertilizing sperm head as it passes through the egg plasma membrane. Once inside the egg cortex, the sperm rotates 180° and "drifts" laterally along the egg cortex. During the second phase of sperm entry, most of the sperm axoneme is incorporated into the egg cytoplasm, and the sperm head may be rapidly (1 μm/s) translocated through the egg cytoplasm. The amount of translocation apparently depends on the position of the female genome in relation to the site of sperm entry (M. Misamore, unpubl.

Received 16 May 2000; accepted 5 July 2000.

*Present address: Dept. Cell Biology, Univ. of Texas–Southwestern Medical Center, 5323 Harry Hines Blvd., Dallas, TX 75235-9039. E-mail: michael.misamore@email.swmed.edu

† To whom correspondence should be addressed. E-mail: zolynn @lsu.edu

Abbreviations: CB, cytochalasin B; MF, microfilament; MT, microtubule; Pt, post insemination; PW, pondwater.

results). After axonemal incorporation and nuclear translocation, the sperm chromatin decondenses and is encompassed by a membrane forming the male pronucleus. Concurrent with sperm fusion, meiosis is reinitiated from metaphase I arrest, polar bodies form, and the female pronucleus develops. Pronuclear fusion and cleavage occur by 60–70 min postinsemination (PI).

The gradual incorporation of the sperm head in *D. polymorpha* displays similarities to early sperm entry in other invertebrate species (Longo and Anderson, 1968; Schatten and Mazia, 1976; Longo, 1973b). In these systems, microfilaments are believed to play a critical role in sperm incorporation into the egg cortex (Longo, 1980; Tilney and Jaffe, 1980; Cline *et al.,* 1983; Cline and Schatten, 1986). This theory is supported by the localization of microfilaments both in egg microvilli (Burgess and Schroeder, 1977; Spudich and Amos, 1979; Tilney and Jaffe, 1980) and in sperm acrosomes (Tilney, 1975, 1978; Tilney *et al.,* 1973); by the fertilization modifications of microfilament distribution, particularly in fertilization cones (Longo, 1978b, 1980; Tilney and Jaffe, 1980; Schatten and Schatten, 1980; Cline and Schatten, 1986); and by the blockage of fertilization by the inhibition of microfilament polymerization using cytochalasins (Gould-Somero *et al.,* 1977; Longo, 1978a; Byrd and Perry, 1980; Schatten and Schatten, 1980). Movement of the sperm nucleus, or subsequent pronucleus, through the egg cortex in most invertebrate and mammalian systems is attributed primarily to the formation of a microtubule-containing sperm aster. However, many bivalve species produce only a rudimentary sperm aster.

The objective of this study was to determine the role of microfilaments and microtubules in the two-step incorporation of sperm into the egg cytoplasm in *Dreissena polymorpha.* The initial, gradual incorporation of the sperm into the egg cortex required microfilament polymerization, whereas the rapid translocation of the sperm nucleus through the egg cytoplasm was microfilament independent but could be inhibited by preventing flagellar incorporation into the egg. Furthermore, a flow of cytoplasmic particles was observed to be associated with the sperm axoneme, which remained active following entry into the egg.

Materials and Methods

Collection of gametes

Specimens of *Dreissena polymorpha* were collected from the Mississippi River near Baton Rouge, Louisiana, or from Portage Lake near Ann Arbor, Michigan, and maintained at 9°C. Animals were individually isolated overnight in artificial pondwater (PW) (Dietz *et al.,* 1994) to avoid cross-contamination of gametes prior to use. Spawning was induced by external exposure of animals to 2×10^{-4} *M* serotonin (5-hydroxytryptamine) for 12 min. Animals were washed twice with PW. At the start of spawning, females were transferred to 50-ml crystalizing dishes to complete spawning. Eggs were inseminated with about 300 sperm per egg.

Three preparation and fixation protocols were used. For light microscopy, eggs were fixed in 3.2% paraformaldehyde in mussel buffer (5 m*M* TAPS, 0.8 m*M* NaCl, 0.145 m*M* KCl, 1.8 m*M* Na_2SO_4, 0.887 m*M* $MgSO_4 \cdot 7H_2O$, 1.32 m*M* $NaHCO_3$, 1.19 m*M* $CaCl_2 \cdot 7H_2O$, pH = 7.6) for 3 h followed by two washes in mussel buffer. Eggs for antibody labeling were permeabilized in an extraction buffer (1.0 m*M* TAPS, 5 m*M* KCl, 0.5 m*M* $MgCl_2$, 1.0 m*M* EGTA, 0.05% Nonidet P-4O, 1% glycerol, pH = 7.6) for 5 min, followed by fixation in 3.2% paraformaldehyde in a low-Ca^{2+} mussel buffer (3 m*M* EGTA, 10 m*M* TAPS, 3 m*M* NaCl, 0.01 m*M* KCl, 1.5 m*M* $MgSO_4$, 0.01% sodium azide, pH = 7.6) for 3 h, followed by two washes in phosphate buffered saline (PBS) (8.1 m*M* sodium phosphate dibasic, 1.8 m*M* sodium phosphate monobasic, 25 m*M* NaCl, 25 m*M* KCl, pH = 7.8) with 0.5% bovine serum albumin. Electron microscopy samples were fixed in 2.5% glutaraldehyde in mussel buffer, washed twice with 30 m*M* sodium cacodylate buffer, postfixed in 0.5% osmium tetroxide for 1 h, dehydrated through a graded acetone series, and embedded in a modified Spurr's medium (Spurr, 1969).

Microscopy

For real-time observations, either a Nikon Optiphot with phase contrast and epifluorescence optics or a Nikon Diaphot with differential interference contrast (DIC) was used. Confocal imaging was performed on a Noran Instruments (Madison, WI) argon laser confocal microscope with Intervision Software. A JEOL 100CX transmission electron microscope was used for high-magnification observations.

Eggs were stained with 1 μg/ml Hoechst 33342 for 8 min to label DNA. To distinguish sperm bound to the egg surface from sperm incorporated into the egg cytoplasm, a dual-labeling procedure was used. Briefly, inseminated eggs were fixed and dual-labeled with Hoechst 33342 and FITC-conjugated wheat germ agglutinin (WGA) (Sigma Chemicals, St. Louis). Hoechst 33342 labeled sperm and egg DNA; WGA-FITC labeled sperm and egg surfaces (Kreimborg and Lynn, 1996). Sperm bound to the surface were labeled with both fluorochromes; incorporated sperm were labeled only with Hoechst. To label microfilaments, samples were stained with 1 μg/ml FITC-conjugated phalloidin (Sigma Chemicals) for 10 min then washed twice with mussel buffer. To label egg microtubules (MTs), permeabilized samples were exposed to a monoclonal antibody to yeast α-tubulin (Accurate Antibodies MAS-077, Westbury, NY) at 1:20 dilution for 45 min, followed by a FITC-conjugated secondary antibody. A monoclonal antibody to acetylated α-tubulin (Sigma Chemicals) at 1:100 dilution for 1 h was used to selectively label sperm axonemes. This

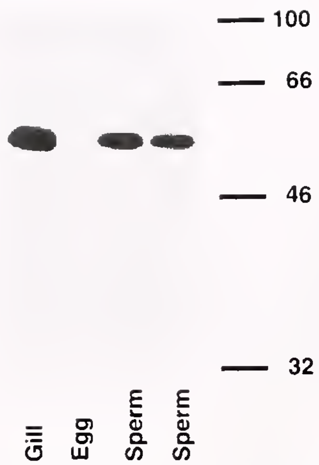

Figure 1. The monoclonal antibody against acetylated α-tubulin recognizes microtubules associated with the sperm but not the egg. Western blot analysis against whole-cell sperm (Sp) or Eggs (E) labeled a 55-Kd band in sperm that was not present in eggs.

antibody selectively labeled sperm axonemal MTs but not egg MTs (Fig. 1) (L'Hernault and Rosenbaum, 1983; L'Hernault and Rosenbaum, 1985; Fechter *et al.*, 1996).

Inhibition experiments

Prior to exposure to the inhibitors, eggs were treated with 0.005% sodium periodate for 2 min to increase permeability through the extracellular coats of the eggs. This pretreatment does not significantly impact sperm binding or fertilization (Misamore, unpubl. results). Eggs from one spawn were aliquoted into the various treatment groups.

Cytochalasin B (CB) (Sigma Chemicals, St. Louis, MO) was used to inhibit microfilament (MF) polymerization during fertilization. Microtubule polymerization was inhibited with colchicine and colcemid, which form complexes with tubulin on MT ends, preventing further polymerization; or with nocodazole, a synthetic benzimidazole that promotes MT depolymerization (Bray, 1992).

To determine the dose-dependent effects of the inhibitors on fertilization, periodate-treated eggs were incubated in the inhibitors (final concentrations: CB—6.2, 12.4 μM in 0.6% DMSO; colchicine—50 to 200 μM; colcemid—51 μM in 0.4% DMSO; nocodazole—0.1, 50 μM) or the appropriate PW control (with or without DMSO) for 10 min prior to insemination. Eggs were inseminated in the presence of the inhibitors without washing. Real-time observations were captured using video microscopy from 30 s to 40 min PI. Samples were fixed at 10 and 30 min PI and dual-stained with Hoechst 33342 and WGA-FITC. Stained eggs (n = 100) were scored to determine sperm entry, number of bound sperm, meiotic stage of female DNA, and presence of polar bodies. To determine whether the effects of the inhibitors are reversible, eggs were incubated in the inhibitors for 10 min, washed twice with PW, and inseminated.

Based on preliminary findings, a time-exposure series was also performed to determine the temporal effect of CB on early sperm entry. Cytochalasin B (12.4 μM) was added to periodate-treated eggs at the following time points: 10 min before insemination or 0 min, 2 min, or 4 min PI. Control eggs were incubated in 0.6% DMSO 10 min prior to insemination.

Statistical analysis

For each trial, eggs from a single female were divided into the treatment groups. From each treatment, 100 eggs were scored for incorporated sperm nuclei and polar body formation. Replicate trials (n = 5) for the dose-dependent and time-dependent experiments were performed, and means of numbers of eggs with incorporated sperm were calculated for all treatments. A two-way analysis of variance (ANOVA) blocking for variability between trials (*i.e.*, different batches of eggs) as one factor and treatment as the second factor was performed using SigmaStat software, version 2.0 (SPSS Science, Chicago, IL). Tukey multiple comparisons were performed if significant differences (α = 0.05) were found.

Results

Morphology

As background pertinent to the results, an expanded description of the basic gamete morphology is presented here. Additional descriptions of *Dreissena polymorpha* gametes are given by Franzén (1983), Denson and Wang (1994), Misamore *et al.* (1996), and Walker *et al.* (1996). The acrosome of *D. polymorpha* sperm contains four distinct regions, including an axial rod 1.4 μm in length. The filaments composing the axial rod are about 6 nm in diameter (Fig. 2) and extend from the apex of the acrosome to the anterior margin of the nucleus (Misamore *et al.*, 1996). FITC-phalloidin labeling was localized to a spike-like structure in the acrosomal region of both bound and acrosome-reacted sperm (Fig. 2, inset).

The surface of spawned eggs is uniformly covered in microvilli at an estimated density of 50 microvilli/μm^2 over the entire egg surface. The microvilli are 0.8 μm in length and 0.07 μm in diameter (Misamore *et al.*, 1996). The internal core of the microvilli consists of 5-nm parallel fibers perpendicular to the egg cortex. The distal tips of the microvilli have many tufts of filamentous material perpendicular to the long axis of the microvilli (Fig. 3).

Initial sperm entry

Shortly after sperm binding, the sperm acrosome opened, exposing the membrane-bound axial rod. The preformed

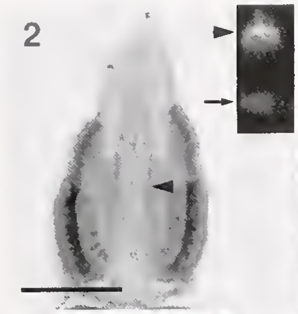

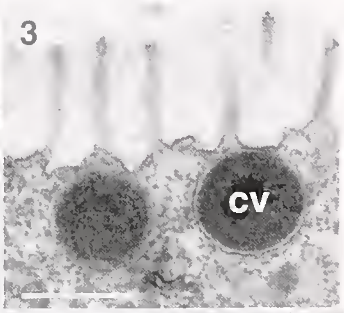

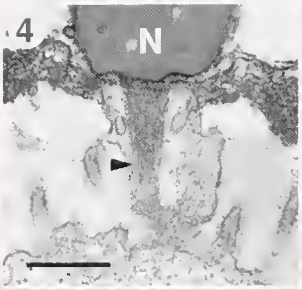

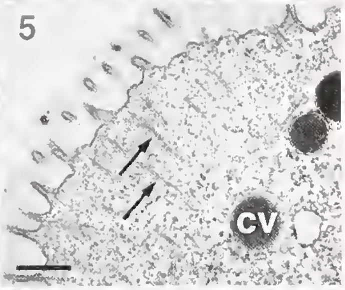

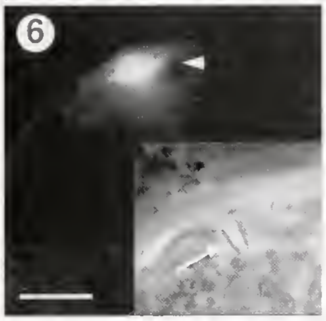

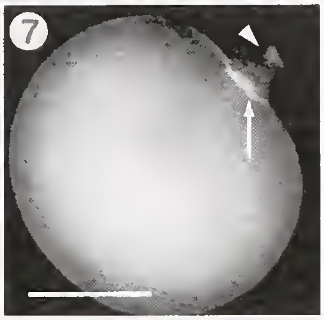

Figure 2. Transmission electron micrograph (TEM) of a cross section through the sperm acrosome. The central axial rod (arrowhead) extended the length of the acrosome and consisted of numerous 6-nm filaments. Inset: Fluorescent micrograph of a spontaneously acrosome-reacted sperm stained with the fluorochrome phalloidin-FITC. Intense fluorescent localization occurred with the anterior portion of the sperm nucleus and the axial rod (arrowhead). Additional localization was observed at the basal region of the sperm nucleus (arrow). Bar = 0.5 μm.

Figure 3. TEM of the egg cortex exhibiting numerous microvilli embedded in a 0.7-μm-thick extracellular coat. The distal tips of the microvilli were bulbous and possessed minuscule, fibrous lateral projections. The microvilli were 0.8 μm in length, 0.07 μm in diameter, and had an internal core of 5-nm parallel fibers perpendicular to the egg surface. CV—cortical vesicle. Bar = 1 μm.

Figure 4. TEM of the sperm axial rod spanning the extracellular matrix and contacting the egg plasma membrane. The axial rod (arrowhead) did not elongate following binding with the egg surface. N—sperm nucleus. Bar = 0.5 μm.

Figure 5. Numerous bundles 60 nm in diameter consisting of 6-nm filaments (arrows) extended the length of the insemination cone perpendicular to the plasma membrane in this TEM. Cortical vesicles (CV) were not exocytosed following egg activation and remained subjacent to the insemination cone. Bar = 1 μm.

Figure 6. Epifluorescent micrograph of an inseminated egg labeled with the actin-specific fluorochrome phalloidin-FITC. A fluorescing region (arrowhead) corresponded to the insemination cone. Inset: Phase micrograph of the insemination cone showing the position of the sperm nucleus (arrow) within the insemination cone. Dual labeling with the DNA-specific fluorochrome Hoechst 33342 confirmed the position of the nucleus within the phalloidin localization (data not shown). Bar = 10 μm.

axial rod was long enough to traverse the egg investment coat to the egg surface (Fig. 4). No additional polymerization or elongation of the axial rod was observed. Microvilli directly subjacent to the open acrosome remained perpendicular to the egg surface. Small fibrous structures positioned peripheral to bound sperm and angled toward the bound sperm were observed with scanning electron microscopy (Misamore *et al.*, 1996). However, no reorientation of microvilli toward the sperm was discernible. The filamentous tufts of the distal microvillar tips did not appear to be associated with a specific region of the acrosome. No change in microvilli length was observed up to 10 min PI.

About 2–3 min PI, an insemination cone formed on the egg surface. As the sperm passed through the oolemma, the cone initially appeared as a conical structure about 1.6 μm in diameter and 2.7 μm in length. Once the sperm head reached the egg cortex, the distal end of the cone became pointed as the egg cytoplasm closed around the sperm head. Filaments 6 nm in diameter extend the length of the fertilization cone in the egg cytoplasm (Fig. 5). FITC-phalloidin labeled the fertilization cone as a well-defined region on the oolemma surrounding the sperm nucleus (Fig. 6). After the sperm had entered the egg cortex, no definitive phalloidin labeling was associated with the sperm head; however, high background fluorescence may have obscured minimal labeling.

About 5–7 min PI, the first polar body began to form. There was a clearing of cortical vesicles and a reduction in microvilli length associated with the site of polar body extrusion. When the egg stained with phalloidin-FITC, a brightly fluorescing region was seen on the surface where the polar body first emerged (Fig. 7). After expulsion of the female dyad, a cleavage furrow formed, separating the polar body cytoplasm from the remaining egg cytoplasm. This polar body furrow corresponds with a fluorescing ring at the base of the first polar body (Fig. 7).

This initial passage of the sperm through the insemination cone into the egg cortex was blocked by inhibiting microfilament polymerization with CB in a dose-dependent manner (Fig. 8). In the presence of CB, sperm were able to bind to the egg surface but did not enter into the egg cytoplasm. When eggs were exposed to 12.4 μM CB, sperm entry was completely inhibited, whereas exposure to 6.2 μM CB significantly reduced the number of eggs with incorporated sperm relative to the control ($P < 0.001$) (Fig. 8; Fig. 9B′, C′). Polar body formation was completely inhibited by both 6.2 and 12.4 μM CB. The female chromosomes were positioned at the egg periphery and persisted through anaphase

Figure 7. Actin localization with phalloidin-FITC produced a highly fluorescing region associated with the polar bodies in this fertilized egg. The actin-containing region was associated with the margins separating the first and second polar bodies (arrowhead) and the second polar body and egg surface (arrow). Bar = 25 μm.

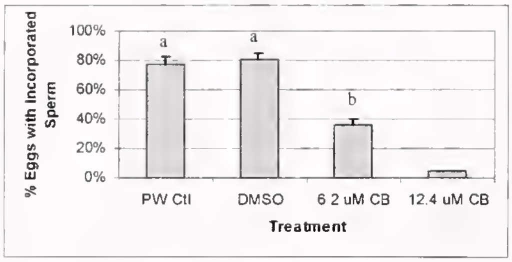

Figure 8. Dose-dependent effects of cytochalasin B on sperm entry into the egg cortex during fertilization. Eggs were exposed to two concentrations of the microfilament inhibitor cytochalasin B (CB). Unfertilized eggs were pretreated with periodic acid, then transferred to a solution of either 6.2 μM CB or 12.4 μM CB in 0.6% DMSO or to a control of either artificial pondwater (PW Ctl) or 0.6% DMSO. Eggs were incubated 10 min and inseminated directly in the egg-inhibitor solution. Eggs were fixed at 10 min PI and scored for number of incorporated sperm (n = 100/trial). Values are mean ± standard error (n = 5). Letters indicate statistically significant differences based on a two-way ANOVA and Tukey multiple comparisons ($P < 0.05$).

(Fig. 9). Although a brief extrusion of cytoplasm was observed during the period of normal polar body formation (5 min PI), no cytoplasmic separation occurred and the extrusion was reabsorbed by 10 min PI.

Sperm entry into the egg cortex was not affected by inhibition of MT polymerization. In both normal (control) fertilizations and fertilizations in the presence of MT inhibitors, *D. polymorpha* sperm bound to the egg surface within 30 s of insemination, and an insemination cone formed by 3 min PI. The insemination cones of both control and MT-inhibited trials were morphologically similar, and the sperm head and mitochondria passed through the oolemma and entered the egg cytoplasm within 4 min of binding (Fig. 9D, D′). Compared to the control, there was no significant difference (Fig. 10) in the numbers of eggs exhibiting sperm entry in the samples treated with colchicine (P = 0.935) or nocodazole (P = 0.774). Colcemid did significantly decrease sperm entry relative to controls (P = 0.032); however, greater than 68% of the eggs had sperm incorporated. While not affecting sperm entry, the MT inhibitors disrupted the first meiotic spindle, and female chromosomes appeared scattered and did not reach anaphase I (Fig. 9D, D′). Subsequent polar body formation was likewise prevented.

Sperm translocation through egg cytoplasm

Following incorporation into the egg cortex, the sperm head passed through the insemination cone, rotated 180° in the egg cortex—positioning its basal end toward the egg center, and moved laterally along the egg cortex (Fig. 11A–D; Fig. 12A–C). The direction of lateral movement was towards the quadrant of the egg containing the female genome. Following rotation, most of the axoneme entered the egg cytoplasm. During the initial axonemal incorporation when the sperm head was immediately (≤10 μm) subjacent to the cortex, the sperm head frequently pivoted around the entry point through angles exceeding 90° (Fig.

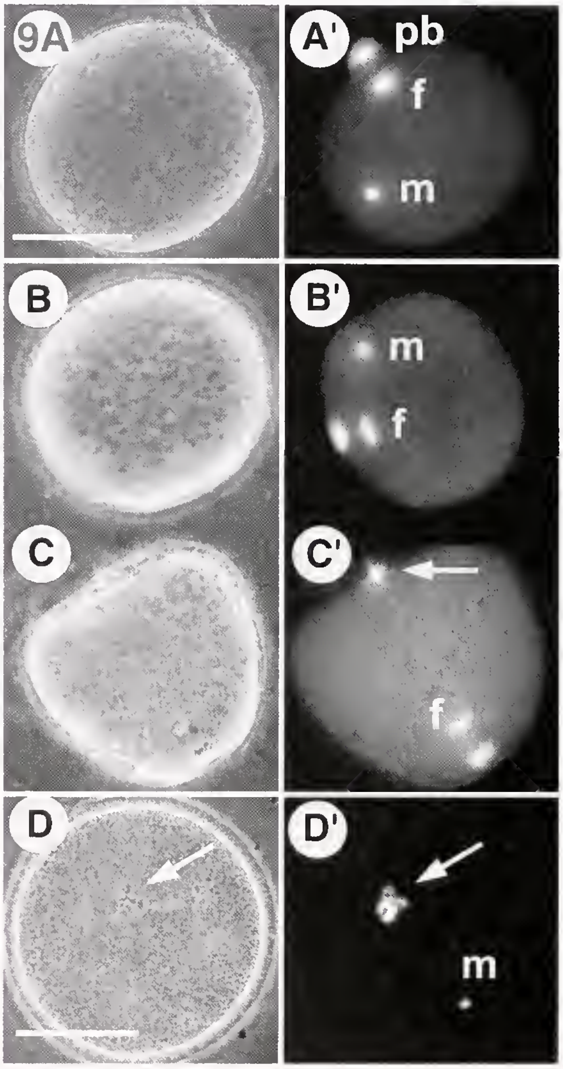

Figure 9. Complementary phase (A, B, C, D) and epifluorescent (A′, B′, C′, D′) micrographs of eggs incubated in various treatments for 10 min prior to insemination. (A, A′) Control fertilization of eggs incubated in 0.6% DMSO. The female chromatin (f) was positioned subjacent to the first polar body (pb) following meiosis I. The male chromatin (m) was seen decondensing in the egg cytoplasm. (B, B′) Egg incubated in 6.2 μM cytochalasin B prior to insemination. Sperm entered the egg cytoplasm and began chromatin decondensation (m). Egg activation occurred, as evident by resumption of meiosis. The female chromatin (f) separated in anaphase I, but polar body formation was inhibited. (C, C′) Egg incubated in 12.4 μM cytochalasin B for 10 min prior to insemination. Sperm bound to the egg surface (arrow) but were not incorporated into the egg cytoplasm. Female chromatin separated (f), but polar body formation was inhibited. (D, D′) Egg treated with 50 mM colcemid. Sperm entered the egg cytoplasm and began chromatin decondensation (M). The female chromatin appeared scattered and not arranged in either the arrested (metaphase) or activated (anaphase) orientation. Eggs were fixed 10 min PI and stained with the DNA-specific fluorochrome Hoechst 33342. Bar = 25 μm.

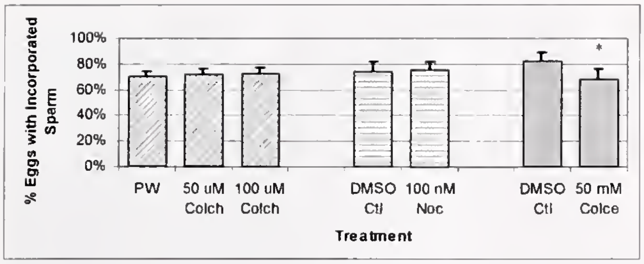

Figure 10. The effect of the microtubule inhibitors on sperm entry. Unfertilized eggs were pretreated with periodic acid, then incubated in various inhibitors or their respective control solutions. Eggs were incubated 10 min and inseminated directly in the egg-inhibitor solution. Eggs were fixed at 10 min postinsemination and scored for incorporated sperm (n = 100/trial). Values are mean percentage of eggs with incorporated sperm ± standard error for 5 replicate trials. PW Ctl—eggs incubated with pondwater, DMSO Ctl—control eggs incubated in 0.6% DMSO, Colch—eggs incubated in either 50 μM or 100 μM colchicine, Noc—eggs incubated in 100 mM nocodazole in 0.6% DMSO, Colcemid—eggs incubated in 50 nM colcemid in 0.6% DMSO. No statistically significant difference was detected between inhibitor treatments and their respective controls ($P > 0.78$) except colcemid ($P = 0.032$). *—indicates significant difference.

13). As more of the axoneme entered the cytoplasm, the axoneme extended deeper into the egg cortex relative to the sperm head, which remained near the egg cortex (Fig. 14A, A′). Once the bulk of the axoneme passed through the oolemma, the sperm head frequently moved rapidly through the egg cytoplasm. This movement did not occur in the sinusoidal pattern typical of sperm swimming. Rather, a portion of the axoneme extended ahead of the trailing sperm head along the direction of movement.

Although they did not impact entry of the sperm head into the egg cortex, MT inhibitors suppressed the rotation and lateral movement of the sperm head along the cortex. Furthermore, MT inhibitors prevented the incorporation of the sperm axoneme into the egg cortex (Figs. 12A–C; 14B, B′; 15; 16). Under these conditions, the sperm heads exhibited rapid, sporadic oscillations immediately subjacent to the insemination cone for several minutes after passage through the cone. This sporadic oscillation seen in the presence of MT inhibitors corresponded temporally to the period of expected axoneme incorporation in control fertilizations. In most inhibitor observations, the sperm remained immediately subjacent to the cone up to 7 min PI and the axoneme ultimately fractured, allowing the sperm nucleus to move deeper into the ooplasm—although more slowly than in controls (Fig. 12). During this period the sperm flagellum remained outside the egg, extending out through the insemination cone. On occasion, the unincorporated portion of the flagellum detached from the egg surface and remained active for several minutes. In contrast to control observations, probing MT-inhibited eggs with the flagellar monoclonal antibody failed to label an axoneme associated with decondensing sperm nuclei (Fig. 14B, B′).

Once sperm passed through the egg cortex, inhibition of MF polymerization did not affect sperm head or axoneme incorporation or subsequent nuclear decondensation. Exposure of eggs to 12.6 μM CB at various times pre- and postinsemination showed a temporal effect of CB on insemination ($P < 0.001$) (Fig. 17). Eggs incubated in CB 10 min prior to insemination showed no sperm incorporation or polar body formation (see Fig. 8). Eggs exposed immediately prior to insemination (0 min) showed almost complete

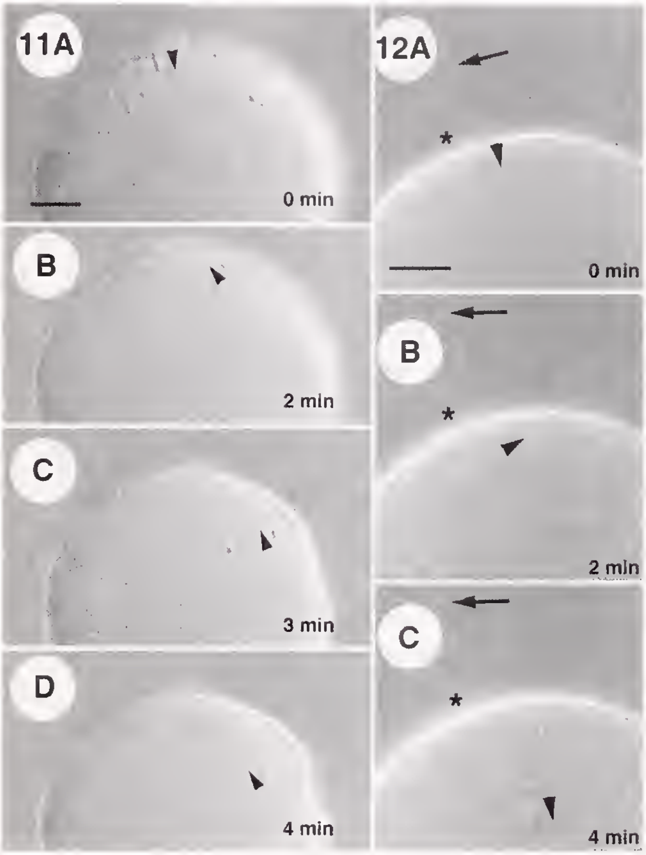

Figure 11. DIC microscopy Time series, in differential interference contrast (DIC) microscopy, of captured video images showing the incorporation of the sperm head during a normal (control) fertilization. The arrowhead parallels the left side of the sperm and illustrates the orientation of the sperm head with the apex of the arrowhead corresponding to the anterior end of the sperm nucleus. (A) Sperm head immediately subjacent to insemination cone. (B–D) Sperm head rotated and was laterally displaced along the egg cortex. Notice the rotation and lateral displacement of the sperm nucleus along the egg cortex relative to the insemination cone. Times indicate elapsed time from initial frame (A). Bar = 20 μm.

Figure 12. DIC microscopy time series of captured video images showing the incorporation of the sperm head into eggs exposed to 100 nM nocodazole. The arrowhead parallels the left side of the sperm and illustrates the orientation of the sperm head, with the apex of the arrowhead corresponding to the anterior end of the sperm nucleus. (A) Sperm head immediately subjacent to insemination cone (*). (B) Sperm head remained subjacent to insemination cone, did not undergo rotation or lateral displacement. (C) Sperm head separated from the attached flagellum and moved deeper into the egg. The arrow marks a particle adhering to the flagellum. Notice that the flagellum remains external to the egg. Times indicate elapsed time from initial frame (A). Bar = 20 μm.

blockage of sperm entry and were not significantly different from the preincubation trial ($P < 0.05$). Addition of CB at 2 min PI significantly reduced sperm entries ($P < 0.05$) relative to controls but did not cause complete inhibition (Fig. 17). Sperm entry was not significantly different from controls when CB was added 4 min PI. Sperm entry and rotation in the egg cytoplasm occurred in eggs treated at 4 min PI with CB. At about 3 min PI, sperm-head translocation and axoneme incorporation were observed. The presence of the axoneme in the egg cytoplasm was verified using the monoclonal antibody to acetylated α-tubulin.

At about 8 min PI, sperm nuclei began to decondense in control (Fig. 18) and MF and MT inhibitor trials. Sperm mitochondria separated from the nucleus and moved away from the nucleus concurrent with the decondensation of the sperm chromatin. At the same time, or immediately afterward, a small sperm aster started to develop (Fig. 19). The aster formed at the base of the decondensing sperm head and was only detectable with the monoclonal yeast α-tubulin antibody, visualized with confocal microscopy. In contrast, the female meiotic spindle and astral array were clearly discernible with light microscopy. In control fertilizations, the sperm aster was detectable as a diminutive structure as late as 40 min PI. During this period the female aster and associated bundle were substantially larger (Fig. 19) (Walker, 1996). Colchicine-treated eggs exhibited no obvious sperm aster, and the female meiotic spindle was not observed. Since egg activation was determined based on the resumption of meiosis as visualized by movement of chromosomes into anaphase I, disruption of the meiotic spindle made the status of egg activation in MT inhibitor treatments difficult to ascertain.

Flow of cytoplasmic particles

Concurrent with axoneme entry, sporadic "vibrations" were observed in the egg cytoplasm between the sperm head and the sperm entry site near the expected position of the axoneme. A directed flow of cytoplasmic particles was similarly observed originating near the base of the sperm

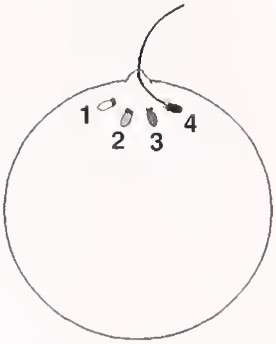

Figure 13. A diagrammatic representation of the oscillations exhibited by a single sperm head following its passage through the insemination cone. Once the sperm head had entered the egg cortex there was a coordinated flexing of the internal and external portions of the flagellum. This movement resulted in oscillation of the sperm head (1 ↔ 4) within the egg cortex.

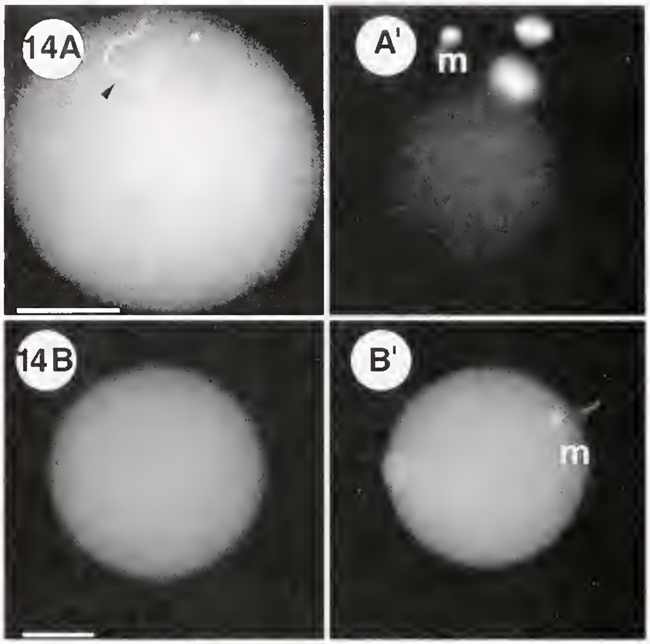

Figure 14. Complementary epifluorescent micrographs of the incorporated sperm dual-labeled for flagella (A, B—a monoclonal antibody to acetylated tubulin) and sperm nucleus (A', B'—Hoechst 33342). (A, A') Control fertilization—The sperm axoneme (arrowhead) extended deeper into the egg cytoplasm relative to the peripherally positioned sperm nucleus (m). (B, B') Eggs pretreated with colchicine prior to insemination. No incorporated axoneme (B) was observed in association with fertilizing sperm nuclei (m) seen in (B'). These findings support real-time observations that the sperm axoneme was not incorporated in the presence of MT inhibitors. 10 min PI. Bar = 25 μm.

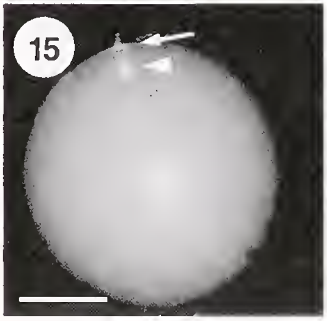

Figure 15. Epifluorescent micrograph of an colchicine-treated egg fertilized with a sperm dual-labeled with FITC-WGA (arrow) and Hoechst 33342 (arrowhead) prior to insemination. The sperm nucleus (arrowhead) was incorporated into the egg cytoplasm and began decondensing. Colchicine inhibited the incorporation of the sperm flagellum, which was visualized by the FITC-WGA labeling of the sperm plasma membrane (arrow). Bar = 25 μm.

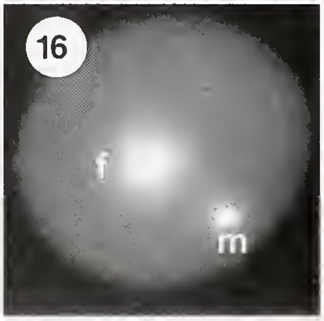

Figure 16. Epifluorescent micrograph of Hoechst-stained eggs inseminated and exposed to 12.4 μM cytochalasin B 4 min PI. By 10 min PI, sperm entered into the egg cortex and began decondensing. The incorporated sperm nucleus (m) was clearly identified by the less intensely fluorescing halo formed by the dispersing chromatin. Polar body formation was inhibited. f—female chromatin.

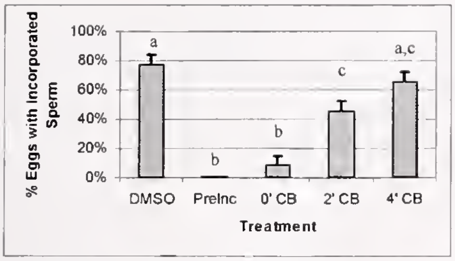

Figure 17. Temporal effects of cytochalasin B (CB) on sperm entry following the addition of the microfilament inhibitor at various time points pre- and postinsemination (PI). CB was added to sodium periodate-treated eggs at 12.4 μM. Treatments were (DMSO), Control of 0.6% DMSO at 10 min preinsemination; (PreInc), CB added 10 min preinsemination; (0′ CB), immediately following insemination; (2′ CB), 2 min PI; and (4′ CB), 4 min PI. Eggs were fixed at 10 min PI and scored for the number of eggs with incorporated sperm. Values are mean ± standard error ($n = 5$). Letters indicate statistically significant differences based on a two-way ANOVA and Tukey multiple comparisons ($P < 0.05$).

head and penetrating as deep as 10 μm into the ooplasm (http://www.mbl.edu/BiologicalBulletin/VIDEO/BB.video.html). The vibrations in the egg cytoplasm began shortly after rotation and lateral displacement of the sperm head, lasted from 1–3 min, and ceased shortly before the sperm nucleus began to decondense. Although the extent varied between fertilizations, this cytoplasmic flow was evident in greater than 70% of the 20–30 similar filmed observations and on about 80 more unfilmed occasions. These observations are the norm rather than the exception in the hundreds of fertilizations observed during several reproductive seasons. Furthermore, polyspermic eggs exhibited multiple currents associated with the polynumery sperm. When flagellar incorporation was inhibited, no flow of cytoplasmic particles was observed in eggs. Similarly, the flow of cytoplasmic particles was also observed in eggs exposed to MT inhibitors followed by washing prior to insemination.

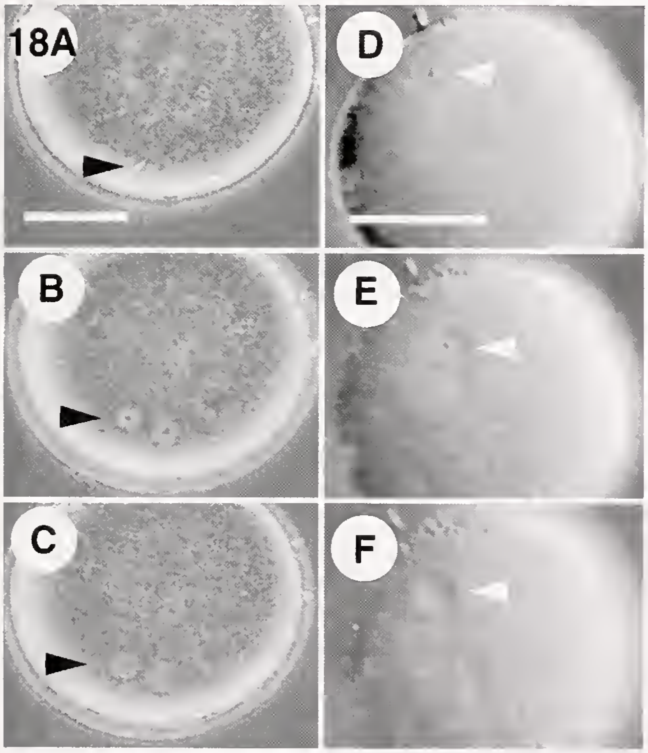

Figure 18. Phase-micrograph time series of video-captured images showing the sperm decondensation and pronuclear formation. Sperm nucleus (arrowhead) was visible in the egg cortex by 4 min PI. (B) Sperm chromatin (arrowhead) decondensation occurred by 10 min PI. (C) Sperm pronuclear (arrowhead) formation began by 30 min PI. Similar results were observed in eggs incubated in 100 μM colchicine prior to insemination (D–G) or in 12.4 μM cytochalasin B at 4 min PI (not shown). Note multiple decondensing sperm pronuclei, indicating polyspermic eggs. Bar = 25 μm.

Discussion

Initial sperm entry

The incorporation of the sperm components through the oolemma into the egg cortex in *Dreissena polymorpha* occurs in two morphologically distinct steps (Misamore *et al.*, 1996). During the initial incorporation, the sperm head and midpiece gradually enter into the egg cortex at a rate of 1 μm/min (Misamore *et al.*, 1996). A distinct, cylindrical insemination cone encompasses the sperm as it passes through the oolemma. The insemination cone of *D. polymorpha* consisted of many 6-nm-thick filaments (Fig. 5) and labeled with FITC-phalloidin (Fig. 6), suggesting the presence of microfilaments. The cone assumed a more pyramidal configuration once the sperm entered the egg cortex. This is similar to morphological changes in the insemination cone of sea urchins, in which an initially rounded cone becomes a "spike-like" cone following sperm entry (Tilney and Jaffe, 1980; Cline and Schatten, 1986). When treated

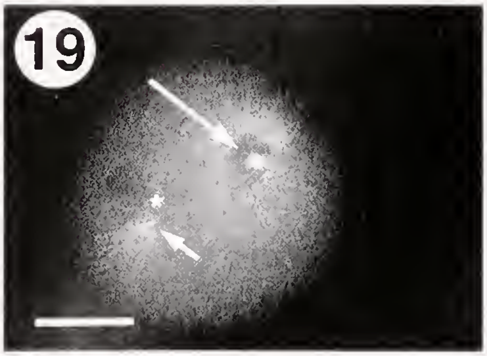

Figure 19. Laser scanning confocal image of a diminutive sperm aster in an egg. The 30-min PI egg was labeled with a monoclonal antibody to yeast α-tubulin. Notice the relatively small size of the male aster (small arrow) in relation the large microtubule array (large arrow) associated with the female pronucleus and polar body. The asterisk (*) indicates the relative position of the sperm nucleus dual-labeled with Hoechst 33342 (not shown). Bar = 25 μm.

with the inhibitor to MF polymerization, cytochalasin B, this initial sperm entry was blocked (Fig. 9C, C′), and no fertilization cone formed. These findings suggest that the initial incorporation of the sperm into the egg cortex was dependent on the polymerization of MFs.

Although the critical involvement of microfilaments in sperm incorporation has been reported for many marine invertebrates (Gould-Somero *et al.*, 1977; Longo, 1978a, 1980; Byrd and Perry, 1980; Schatten and Schatten, 1980; Cline and Schatten, 1986; Schatten *et al.*, 1986) and the present freshwater model, exactly how sperm pass through the oolemma is not well understood. Microfilaments are associated with several processes during fertilization in *D. polymorpha* that could potentially account for the inhibition of initial sperm entry. The major sites of polymerized MFs include the sperm acrosome, the egg microvilli, and the fertilization cone. Furthermore, MFs are critical for cytokinesis during polar body formation (Longo, 1972; Longo *et al.*, 1993).

The sperm of several marine bivalves including *Spisula* and *Mytilus* possess preformed acrosomal processes that do not undergo a polymerization-driven elongation (Hylander and Summers, 1977; Longo, 1978a). Following activation, *Mytilus* sperm extend a preformed acrosomal process without the polymerization of new MFs (Dan, 1967; Longo, 1977, 1983). Like these marine bivalves, *D. polymorpha* has sperm that possess a preformed acrosomal process (Fig. 2) that does not elongate and is apparently insensitive to CB treatments at the dosages tested. Although it was not possible to expose only sperm to CB because washing disrupted the fragile acrosomes, polymerization of sperm MFs is not believed to be the critical component in sperm entry. This conclusion is based on several pieces of evidence. First, no elongation of the acrosomal process was observed during fertilization in *D. polymorpha*. Second, several studies in which washing of sperm was possible have shown that CB does not affect the fertilization capability of sperm (Sanger and Sanger, 1975; Longo, 1978a; Byrd and Perry, 1980). Third, the relative polarity of MFs in sperm acrosomes and egg microvilli is inappropriate to allow a myosin-actin ratcheting mechanism to draw the sperm into the egg in urchins (Tilney, 1978), and this is presumably the case for *D. polymorpha* as well. Finally, the addition of CB at 2 min PI allowed sufficient time for the sperm binding to occur prior to inhibition; however, sperm entry was still suppressed, suggesting MF involvement at a stage later than sperm binding.

The involvement of microvilli in sperm entry varies greatly between species, but a role has been suggested in hamsters (Yanagimachi and Noda, 1970), urchins (Tilney and Jaffe, 1980), annelids (Anderson and Eckberg, 1983), and bivalves (Longo, 1987). Furthermore, Wilson and Snell (1998) propose that microvillus-like structures may be essential for most types of cell-cell fusion events. Hylander and Summers (1977) proposed a generalized model of fertilization in Mollusca. According to their model, sperm binding occurs between an inner acrosomal region of the sperm and microvilli tufts. Similar microvillar tufts were observed in *D. polymorpha;* however, no obvious association between these tufts and the inner acrosomal membrane was observed. Furthermore, microvilli appeared to remain perpendicular to the egg surface and did not reorient toward bound sperm as reported for *Spisula* (Longo and Anderson, 1970; Hylander and Summers, 1977). Misamore *et al.* (1996) reported extracellular fibers extending toward attached sperm; however, these fibers are substantially smaller than the egg microvilli.

Microfilament presence in insemination cones has been well documented. In urchins, insemination cones may form from the fusion of microvilli (Schatten and Schatten, 1980), and MFs in the cones are polymerized into discrete bundles (Tilney and Jaffe, 1980) from monomeric actin in the egg cortex (Spudich and Amos, 1979). Molluscan insemination cones are markedly smaller than urchin cones and MFs are not consistently reported in the cones (Longo, 1983). As in *Mytilus* and *Spisula* (Longo and Anderson, 1970; Longo, 1983), in *D. polymorpha* MFs in fertilization cones run the length of the ooplasmic projection, but not in discrete bundles as observed in urchins (Fig. 5). While the exact mechanisms involved remain unclear, insemination cones are implicated in sperm entry (Longo, 1980). The inhibition of sperm entry by CB also suppresses the formation of insemination cones (Longo, 1980; Schatten and Schatten, 1980, 1981).

Cytochalasin B was shown to have a reversible, dose-dependent effect on fertilization: partial inhibition occurred at 6.2 μM CB and complete inhibition at 12.4 μM. Byrd and Perry (1980) reported similar dose-dependent findings in two urchin species, *Strongylocentrotus purpuratus* and *Lytechinus pictus.* Sperm entry was decreased at 2.5 μg/ml (5 μM) CB in the former species and at 5 μg/ml (10 μM) in the latter; inhibition was complete at 5 μg/ml (10 μM) and 10 μg/ml (20 μM) respectively. Gould-Somero *et al.* (1977) found that slightly lower levels of CB partially (1 μM) or completely (2 μM) blocked sperm entry. That the dose-dependent responses are similar is somewhat remarkable considering the variability in the gametes, extracellular coats, and fertilization mechanisms between these diverse species.

Sperm entry was effectively blocked when CB addition preceded or was concomitant with insemination (Fig. 17). Addition of CB at 2 min PI resulted in fewer eggs exhibiting sperm penetration, but at 4 min PI sperm entry was not significantly affected. These findings suggest that CB was able to rapidly (within 1–2 min) block sperm entry, and that the period of susceptibility to CB inhibition was completed by 4 min PI. The first 4 min PI during *D. polymorpha* fertilization corresponds to the 1 μm/min gradual-incorporation phase into the egg cortex. After 4 min PI, CB was unable to inhibit sperm-axoneme incorporation, mitochondria detachment, or male-chromatin decondensation and pronuclear formation. CB impact on fertilization is limited to the first 6 min PI in several urchin species (Longo, 1980; Byrd and Perry, 1980; Schatten and Schatten, 1980), and echiuroid worms (Gould-Somero *et al.*, 1977). The restriction of MF involvement in sperm incorporation to the first 6 min following insemination applies across a wide taxonomic range.

Unlike MF polymerization, MT polymerization was not required for the initial incorporation of the sperm nucleus into the egg cortex in *D. polymorpha*. Initial entry of sperm into eggs in marine invertebrates (Schatten and Schatten, 1981; Schatten *et al.*, 1982, 1989) and algae (Swope and Kropf, 1993) also does not require MTs. Sperm were able to enter the egg cortex in MT inhibitors at a rate (1 μm/min) similar to that observed in normal fertilizations. MT inhibitors were able to penetrate the egg and were effective at disrupting the meiotic spindle, thereby preventing polar body formation. Furthermore, no MT array was observed to be associated with entering sperm nuclei when α-tubulin monoclonal antibody was used to label fertilized eggs.

Sperm nuclear translocation and flagellar incorporation

After passing through the fertilization cone and entering the egg cortex, *D. polymorpha* sperm rotated 180°, positioning the basal end of the nucleus centrad (Fig. 11). The first fluorochrome-detectable MTs associated with entering sperm were the diminutive sperm asters adjacent to decondensing sperm chromatin (Fig. 19). Small sperm asters have been reported for other bivalve species (Longo and Anderson, 1969, 1970; Longo *et al.*, 1993). In contrast, the sperm aster is significantly larger in most invertebrate and mammalian systems and is believed to be responsible for the migration of the male and female pronuclei during syngamy. For example, in sea urchins the sperm aster extends toward the female pronucleus and is thought to effect the migration of the two pronuclei (Zimmerman and Zimmerman, 1967; Longo and Anderson, 1968; Longo, 1976; Schatten, 1981; Bestor and Schatten, 1981; Sluder *et al.*, 1985). The role of the sperm aster in *D. polymorpha* is not fully understood as it does not extend toward the female pronucleus.

A markedly larger MT array is associated with the female chromatin in *D. polymorpha* (Walker, 1996). A dense bundle of MTs is observed immediately subjacent to the polar bodies. Emanating from the MT bundle toward and surrounding the female pronucleus is a prominent cone-shaped array of MTs. This MT bundle is believed to anchor the female pronucleus and guide its centrad movement into the egg (Walker, 1996). The large female aster is also believed to play an important role in movement of the male pronucleus. An analogous structure may also be present in both *Spisula* and *Mytilus* (Longo, 1973a). Furthermore, as has been found in urchins (Zimmerman and Zimmerman, 1967), colcemid prevents pronuclear migration in *D. polymorpha* (Walker, 1996).

Following sperm rotation, most of the sperm axoneme was incorporated into the egg cytoplasm and the sperm head often was rapidly (1 μm/s) translocated through the egg cytoplasm (Misamore *et al.*, 1996). Microfilament polymerization appeared to play little or no role in the second stage of sperm entry. Addition of CB after initial sperm entry (4 min PI trials) failed to prevent the rapid translocation of the sperm nucleus or the incorporation of the flagella. Furthermore, no obvious association of MFs and incorporated sperm was observed using epifluorescence or electron microscopy.

Conversely, MT polymerization played a prominent, yet somewhat unconventional, role in sperm nuclear translocation and flagellar incorporation. Following entry of the sperm head into the cortex, the bulk of the sperm axoneme was incorporated into the egg cytoplasm in *D. polymorpha*. During this incorporation, dramatic movements of the sperm head were observed, as well as a lateral migration of the sperm head along the egg cortex. These movements may be analogous to "jerking" movements exhibited by urchin sperm during axoneme incorporation (Schatten, 1981). Schatten (1981) suggests that the continued movement of the sperm tail may be involved in its movement through the fertilization cone and into the cytoplasm proper. In *D. polymorpha*, there is an obvious correlation between movements of the flagellum as it enters the egg cytoplasm and movements exhibited by the sperm head in the egg cortex. The exact mechanisms involved in flagellar incorporation are not known. Video microscopic observations of both urchins (Schatten, 1981) and zebra mussels (this study) suggest that flagellar movement may be involved. Furthermore, flagellar incorporation in *D. polymorpha* was blocked by MT inhibitors. Microtubule polymerization appears to be essential for flagellar incorporation in *D. polymorpha*. This finding is in contrast to the results of studies with urchins, in which nocodazole did not inhibit axoneme incorporation (Schatten and Schatten, 1981; Fechter *et al.*, 1996). Furthermore, the exaggerated movement of the sperm head immediately subjacent to the insemination cone during the inhibited axoneme incorporation further supports the concept that flagellar movement takes part in axoneme incorporation.

In contrast, Epel *et al.* (1977) reported that deflagellated sperm heads were able to bind and enter sea urchin eggs. Attempts to duplicate those experiments with *D. polymorpha* in the present investigations were unsuccessful. Finally, Schatten and Schatten (1981) reported that MT inhibitors increased the lateral displacement of the sperm head along the cortex and that the formation of the sperm aster may signal the end of this lateral movement (Schatten, 1982). In

D. polymorpha, lateral displacement of the sperm head was restrained by the attached yet unincorporated flagellum. Once the flagellum was severed, however, lateral displacement and decondensation were observed.

Following axonemal incorporation and quiescence, the sperm mitochondria separated from the nucleus as it began to decondense. As in other invertebrate species (Schatten and Schatten, 1981), sperm decondensation in *D. polymorpha* was not affected by either MF or MT inhibitors. In zebra mussels, nuclear decondensation and mitochondrial separation are apparently unaffected by MT inhibitors, suggesting that flagellar detachment is also unaffected. In sea urchins, microtubules appear to be essential for detachment of the sperm tail, its migration toward the female pronucleus, and its disassembly (Schatten and Schatten, 1981; Fechter *et al.,* 1996). Similarly, activation of *D. polymorpha* eggs by sperm was unaffected by the presence of either MF or MT inhibitors. Several studies have shown that early egg activation occurs during fertilization even in the presence of CB (Byrd and Perry, 1980; Schatten and Schatten, 1980; Dale and DeSantis, 1981; Lynn, 1989). In these studies, initiation of the cortical granule release or an electrophysiological response were used as indicators of egg activation. Like those of most molluscs (Humphreys, 1967; Longo, 1983), the eggs of *D. polymorpha* do not release cortical granules immediately following egg activation. Since *D. polymorpha* eggs are inseminated at metaphase I arrest, the resumption of meiosis can serve as an indicator of egg activation (Longo, 1972, 1978a; Longo *et al.,* 1993). In this study, *D. polymorpha* sperm readily bound to the egg surface in the presence of MF or MT inhibitors and apparently induced the resumption of meiosis, since eggs devoid of bound sperm remained in metaphase arrest.

Flow of cytoplasmic particles

During axoneme incorporation, a significant cytoplasmic movement was noted in the region of the axoneme. Flows of cytoplasmic particles were observed in numerous regions near the site of sperm entry and conspicuously originating at the basal region of the sperm head. The impetus or functional significance of this flow remains in question. Two possible mechanisms for generating these currents include beating by a functional axoneme displacing the particles or plus-end-directed transport along axonemal MTs by motor proteins associated with either the cytoplasmic particles or the sperm axoneme.

There appear to be few, if any, reported instances where flagella retain dynamic function once incorporated into the egg cytoplasm (Schatten, 1981; 1982). The last movement typically associated with flagellar bending occurs shortly after sperm binding, and movement of the sperm nucleus once inside the egg is typically associated with cytoskeletal elements, specifically the sperm aster (Schatten, 1982; Longo, 1987). Technical limitations make it difficult to isolate movements attributed to incorporated axonemes from egg-derived events; nevertheless, several pieces of evidence support the concept of an active axoneme inside the egg.

First, the sperm axoneme retains the ability to generate movement following demembranation during incorporation. Active movement by isolated, demembraned sperm axonemes has been demonstrated in other species (Bray, 1992). Second, video microscopy of mechanically-ruptured, fertilized *D. polymorpha* eggs revealed incorporated sperm vigorously moving within the collapsing egg membrane (Misamore, pers. obs.). Third, there is an apparent alteration of the flagellar beat pattern in incorporated sperm. During the rapid translocation of the sperm through the egg cytoplasm (Misamore *et al.,* 1996), the sperm head trails the proximal portion of the axoneme. The proximal third of the axoneme becomes the leading portion of the moving sperm cell. Similar types of flagella-driven movement can be seen in other systems. For example, the single-celled flagellate *Euglena* moves *via* a singular flagellum that extends slightly more anterior than the cell body before bending posteriorly (Bray, 1992). Helical waves running the length of the flagellum propel the cell forward, resulting in a rotational movement to the cell body. Hamster sperm exhibit a pronounced change in beat pattern upon entry into the dense cumulus oophorous surrounding the egg. Penetrating sperm frequently progress with the proximal portion of the flagellum extending slightly forward, with the head ratcheting through the dense cumulus oophorous (Yanagimachi, 1994). The change in flagellar beating seen in *D. polymorpha* may be attributable to the greater viscosity of the egg cytoplasm relative to the external milieu.

A second potential source of the observed cytoplasmic flow could result from active movement of particles down the exposed axoneme MTs by molecular motors. The plus-end-directed flow of particles suggests the presence of a kinesin or kinesin-like motor. Initial attempts to label incorporated axonemes with kinesin antibodies have been unsuccessful (data not shown); however, support for this hypothesis is as follows. Microtubule motors are relatively abundant in the egg cytoplasm. Gilksman and Salmon (1993) reported substantial MT gliding along surfaces coated with an ooplasm extract. Scholey *et al.* (1985) have isolated a kinesin from urchin eggs. Porter *et al.* (1987) showed that this egg kinesin exhibited plus-end movement along isolated axonemes, and kinesin-coated beads translocate along centrosome MTs. Furthermore, Kozminski *et al.* (1995) found that a flagellar kinesin, FLA10, facilitated movement of intraflagellar particles, or rafts, along the length of the axoneme of *Chlamydomonas* flagella. Clearly, more detailed testing of this hypothesis is needed.

Finally, no flow of cytoplasmic particles was observed in *D. polymorpha* zygotes when axoneme incorporation was blocked with MT inhibitors. The observed flow is either directly, or at least indirectly, related to the incorporated flagellum. The significance of this particle flow down the axoneme remains an intriguing question.

In summary, initial sperm entry into the egg cortex is a gradual, MF-dependent process, while subsequent flagellar incorporation is MT dependent. Dynamic movement of the incorporated sperm head and flagella is observed inside the egg cytoplasm, and a flow of cytoplasmic particles associated with the incorporated axoneme was observed. *D. polymorpha* serves as a good model for studying fertilization and exhibits many similarities to other fertilization models. However, as demonstrated in this study, its remarkably transparent cytoplasm allows extremely detailed observations of the intracellular interactions between eggs and their incorporated sperm, revealing previously undescribed phenomena that warrant further study in both this and other systems.

Acknowledgments

We gratefully acknowledge the following individuals for their invaluable contributions to this research: Susan J. Nichols, J. Rachel Walker, Katie Kreimborg, Steven Smith, Thomas Dietz, and the staff of the M.D. Socolofsky Microscopy Center. This research was funded in part by a grant from Sea Grant of Louisiana NOAA grant #46RG00960, project R/ZMM-2.

Literature Cited

Anderson, W. A., and W. R. Eckberg. 1983. A cytological analysis of fertilization in *Chaetopterus pergamentaceus*. *Biol. Bull.* **165:** 110–118.

Bestor, T., and G. Schatten. 1981. Anti-tubulin immunofluorescence microscopy of microtubules present during the pronuclear movements of sea urchin fertilization. *Dev. Biol.* **88:** 80–91.

Bray, D. 1992. *Cell Movements.* Garland Publishing, New York.

Burgess, D. R., and T. E. Schroeder. 1977. Polarized bundles of actin filaments within microvilli of fertilized sea urchin eggs. *J. Cell Biol.* **74:** 1032–1037.

Burky, A. J. 1983. Physiological ecology of freshwater bivalves. Pp. 281–327 in *The Mollusca, Vol. 6, Ecology*, W. D. Russel-Hunter, ed. Academic Press, New York.

Byrd, E. W., and G. Perry. 1980. Cytochalasin B blocks sperm incorporation but allows activation of the sea urchin egg. *Exp. Cell Res.* **126:** 333–342.

Cline, C. A., and G. Schatten. 1986. Microfilaments during sea urchin fertilization: fluorescence detection with rhodaminyl phalloidin. *Gamete Res.* **14:** 277–291.

Cline, C. A., H. Schatten, R. Balczon, and G. Schatten. 1983. Actin-mediated surface motility during sea urchin fertilization. *Cell Motil.* **3:** 513–524.

Dale, B., and A. DeSantis. 1981. The effect of cytochalasin B and D on the fertilization of sea urchins. *Dev. Biol.* **83:** 232–237.

Dan, J. C. 1967. Acrosome reaction and lysins. Pp. 237–294 in *Fertilization*, C. B. Metz and A. Monroy, eds. Academic Press, New York.

Denson, D. R., and S. Y. Wang. 1994. Morphological differences between zebra and quagga mussel spermatozoa. *Am. Malacol. Bull.* **11:** 79–81.

Dietz, T. H., D. Lessard, H. Silverman, and J. W. Lynn. 1994. Osmoregulation in *Dreissena polymorpha:* the importance of Na, Cl, K and particularly Mg. *Biol. Bull.* **187:** 76–83.

Epel, D., N. L. Cross, and N. Epel. 1977. Flagellar motility is not involved in the incorporation of the sperm into the egg at fertilization. *Dev. Growth Differ.* **19:** 15–21.

Fechter, A., A. Schöneberg, and G. Schatten. 1996. Excision and disassembly of sperm tail microtubules during sea urchin fertilization: requirements for microtubule dynamics. *Cell Motil. Cytoskeleton.* **35:** 281–288.

Franzén, A. 1983. Ultrastructural studies of spermatozoa in three bivalve species with notes on evolution of elongated sperm nucleus in primitive spermatozoa. *Gamete Res.* **7:** 199–214.

Gilksman, N. R., and E. D. Salmon. 1993. Microtubule-associated motility in cytoplasmic extracts of sea urchin eggs. *Cell Motil. Cytoskel.* **24:** 167–178.

Gould-Somero, M., L. Holland, and M. Paul. 1977. Cytochalasin B inhibits sperm penetration into eggs of *Urechis caupo* (Echiura). *Dev. Biol.* **58:** 11–22.

Humphreys, W. J. 1967. The fine structure of cortical granules in eggs and gastrulae of *Mytilus edulis*. *J. Ultrastruct. Res.* **17:** 314–326.

Hylander, B. L., and R. G. Summers. 1977. An ultrastructural analysis of the gametes and early fertilization in two bivalve molluscs, *Chama macerophylla* and *Spisula solidissima* with special reference to gamete binding. *Cell Tissue Res.* **182:** 469–489.

Kozminski, K. G., P. L. Beech, and J. L. Rosenbaum. 1995. The Chlamydomonas kinesin-like protein FLA10 is involved in motility associated with the flagellar membrane. *J. Cell Biol.* **131:** 1517–1527.

Kreimborg, K. M., and J. W. Lynn. 1996. Lectin binding affinities of egg coats and sperm of *Dreissena polymorpha*. *Am. Zool.* **36:** 103a.

L'Hernault, S. W., and J. L. Rosenbaum. 1983. *Chlamydomonas* α-tubulin is posttranslationally modified in the flagella during flagellar assembly. *J. Cell Biol.* **97:** 258–263.

L'Hernault, S. W., and J. L. Rosenbaum. 1985. Reversal of the posttranslational modification on *Chlamydomonas* flagellar α-tubulin occurs during flagellar resorption. *J. Cell Biol.* **100:** 457–462.

Longo, F. J. 1972. The effects of cytochalasin B on the events of fertilization in the surf clam, *Spisula solidissima*. I. Polar body formation. *J. Exp. Zool.* **182:** 321–344.

Longo, F. J. 1973a. An ultrastructural analysis of polyspermy in the surf clam, *Spisula solidissima*. *J. Exp. Zool.* **183:** 153–180.

Longo, F. J. 1973b. Fertilization: a comparative ultrastructural review. *Biol. Reprod.* **9:** 149–215.

Longo, F. J. 1976. Sperm aster in rabbit zygotes: its structure and function. *J. Cell Biol.* **69:** 539–547.

Longo, F. J. 1977. An ultrastructural study of cross-fertilization (*Arbacia* × *Mytilus*). *J. Cell Biol.* **73:** 14–26.

Longo, F. J. 1978a. Effects of cytochalasin B on sperm-egg interactions. *Dev. Biol.* **67:** 249–265.

Longo, F. J. 1978b. Surface alterations of fertilized surf clam (*Spisula solidissima*) eggs induced by concanavalin A. *Dev. Biol.* **68:** 422–439.

Longo, F. J. 1980. Organization of microfilaments in sea urchin (*Arbacia punctulata*) eggs at fertilization: effects of cytochalasin B. *Dev. Biol.* **74:** 422–433.

Longo, F. J. 1983. Meiotic maturation and fertilization. Pp. 49–89 in *The Mollusca, Vol. 3, Development*, N. H. Verdonk and J. A. M. Van Den Biggelaar, eds. Academic Press, New York.

Longo, F. J. 1987. *Fertilization*, Chapman and Hall, New York.

Longo, F. J., and E. Anderson. 1968. The fine structure of pronuclear development and fusion in the sea urchin, *Arbacia punctulata*. *J. Cell Biol.* **39:** 339–368.

Longo, F. J., and E. Anderson. 1969. Cytological aspects of fertilization in the Lamellibranch, *Mytilus edulis.* II. Development of the male pronucleus and the association of the maternally and paternally derived chromosomes. *J. Exp. Zool.* **172:** 97–120.

Longo, F. J., and E. Anderson. 1970. An ultrastructural analysis of fertilization in the surf clam, *Spisula solidissima.* II. Development of the male pronucleus and the association of the maternally and paternally derived chromosomes. *J. Ultrastruct. Res.* **33:** 515–527.

Longo, F. J., L. Mathews, and D. Hedgecock. 1993. Morphogenesis of maternal and paternal genomes in fertilized oyster eggs (*Crassostrea gigas*): effects of cytochalasin B at different periods during meiotic maturation. *Biol. Bull.* **185:** 197–214.

Lynn, J. W. 1989. Correlations between time-dependent and cytochalasin B affected sperm entry in voltage-clamped sea urchin eggs. Pp. 43–60 in *Mechanisms of Egg Activation,* R. Nuccitelli, G. N. Cherr, and W. H. Clark, Jr., eds. Plenum Press, New York.

Misamore, M., H. Silverman, and J. W. Lynn. 1996. Analysis of fertilization and polyspermy in serotonin-spawned eggs of the zebra mussel, *Dreissena polymorpha. Mol. Reprod. Devel.* **43:** 205–216.

Porter, M. E., J. M. Scholey, D. L. Stemple, G. P. A. Vigers, R. D. Vale, M. P. Sheetz, and J. R. McIntosh. 1987. Characterization of the microtubule movement produced by sea urchin egg kinesis. *J. Biol. Chem.* **262:** 2794–2802.

Ram, J. L., G. W. Crawford, J. U. Walker, J. J. Mojares, N. Patel, P. P. Fong, and K. Kyozuka. 1993. Spawning in the zebra mussel (*Dreissena polymorpha*): activation by internal or external application of serotonin. *J. Exp. Zool.* **265:** 587–598.

Sanger, J. W., and J. M. Sanger. 1975. Polymerization of sperm actin in the presence of cytochalasin-B. *J. Exp. Zool.* **193:** 441–447.

Schatten, G. 1981. Sperm incorporation: The pronuclear migrations and their relation to the establishment of the first embryonic axis: Time-lapse video microscopy of the movements during fertilization of the sea urchin *Lytechinus variegatus. Dev. Biol.* **86:** 426–437.

Schatten, G. 1982. Motility during fertilization. *Int. Rev. Cytol.* **79:** 59–163.

Schatten, G., and D. Mazia. 1976. The penetration of the spermatozoon through the sea urchin egg surface at fertilization. *Exp. Cell Res.* **98:** 325–337.

Schatten, G., and H. Schatten. 1980. Surface activity at the egg plasma membrane during sperm incorporation and its cytochalasin B sensitivity. *Dev. Biol.* **78:** 435–499.

Schatten, G., and H. Schatten. 1981. Effects of motility inhibitors during sea urchin fertilization. *Exp. Cell Res.* **135:** 311–330.

Schatten, G., H. Schatten, T. Bestor, and R. Balczon. 1982. Taxol inhibits the nuclear movements during fertilization and induces asters in unfertilized sea urchin eggs. *J. Cell Biol.* **94:** 455–465.

Schatten, G., H. Schatten, I. Spector, C. A. Cline, N. Paweletz, C. Simerly, and C. Petzelt. 1986. Latrunculin inhibits the microfilament-mediated processes during fertilization, cleavage and early development in sea urchins and mice. *Exp. Cell Res.* **166:** 191–208.

Schatten, H., C. R. Simerly, G. Maul, and G. Schatten. 1989. Microtubule assembly is required for the formation of the pronuclei, nuclear lamin acquisition, and DNA synthesis during mouse, but not sea urchin, fertilization. *Gamete Res.* **23:** 309–322.

Scholey, J. M., M. E. Porter, P. M. Grissom, and J. R. McIntosh. 1985. Identification of kinesin in sea urchin eggs, and evidence for its localization in the mitotic spindle. *Nature* **318:** 483-486.

Sluder, G., C. L. Rieder, and F. J. Miller. 1985. Experimental separation of pronuclei in fertilized sea urchin eggs: chromosomes do not organize a spindle in the absence of centrosomes. *J. Cell Biol.* **100:** 897–903.

Spudich, J. A., and L. A. Amos. 1979. Structure of actin filament bundles from microvilli of sea urchin eggs. *J. Mol. Biol.* **129:** 319–331.

Spurr, A. R. 1969. A low viscosity epoxy resin embedding medium for electron microscopy. *J. Ultrastruct. Res.* **26:** 31–43.

Swope, R. E., and D. L. Kropf. 1993. Pronuclear positioning and migration during fertilization in *Pelvetia. Dev. Biol.* **157:** 269–276.

Tilney, L. G. 1975. Actin filaments in the acrosomal reaction of *Limulus* sperm. *J. Cell Biol.* **64:** 289–310.

Tilney, L. G. 1978. The polymerization of actin V. A new organelle, the actomere, that initiates the assembly of actin filaments in *Thyone* sperm. *J. Cell Biol.* **77:** 551–564.

Tilney, L. G., and L. A. Jaffe. 1980. Actin, microvilli, and the fertilization cone of sea urchin eggs. *J. Cell Biol.* **87:** 771–782.

Tilney, L. G., S. Hatano, H. Ishikawa, and M. S. Mooseker. 1973. The polymerization of actin: its role in the generation of the acrosomal process of certain echinoderm sperm. *J. Cell Biol.* **59:** 109–126.

Walker, J. R. 1996. Functional roles of cytoskeletal proteins during precleavage developmental events in the egg of *Dreissena polymorpha.* Master's Thesis, Louisiana State University, Baton Rouge, LA.

Walker, G. K., M. K. Black, and C. A. Edwards. 1996. Comparative morphology of zebra (*Dreissena polymorpha*) and quagga (*Dreissena bugensis*) mussel sperm: light and electron microscopy. *Can. J. Zool.* **74:** 809–815.

Wilson, N. F., and W. J. Snell. 1998. Microvilli and cell-cell fusion during fertilization. *Trends Cell Biol.* **8:** 93–96.

Yanagimachi, R. 1994. Mammalian fertilization. Pp. 189–317 in *The Physiology of Reproduction,* E. Knobil and J. D. Neill, eds. Raven Press, New York.

Yanagimachi, R., and T. D. Noda. 1970. Ultrastructural changes in the hamster sperm head during fertilization. *J. Ultrastruct. Res.* **31:** 465–485.

Zimmerman, A. M., and S. Zimmerman. 1967. Action of colcemid in sea urchin eggs. *J. Cell Biol.* **34:** 483–488.

Reports of Papers Presented at THE GENERAL SCIENTIFIC MEETINGS OF THE MARINE BIOLOGICAL LABORATORY, Woods Hole, Massachusetts

14 to 16 August 2000

Program Chairs:

BARBARA BOYER, Union College
WILLIAM ECKBERG, Howard University
CHARLES HOPKINSON, Ecosystems Center, MBL
ROBERT PAUL MALCHOW, University of Illinois at Chicago

Each of these reports was reviewed by two members of a special editorial board drawn from the research community of Woods Hole, Massachusetts. Reviewers included scientists from THE MARINE BIOLOGICAL LABORATORY, THE WOODS HOLE OCEANOGRAPHIC INSTITUTION, AND THE NATIONAL MARINE FISHERIES SERVICE.

SHORT REPORTS FROM THE 2000 GENERAL SCIENTIFIC MEETINGS OF THE MARINE BIOLOGICAL LABORATORY

Featured Report

The Editors
Introduction to the featured report. On mapping odor quality 161
Wachowiak, Matt, Michal Zochowski, Lawrence B. Cohen, and Chun X. Falk
The spatial representation of odors by olfactory receptor neuron input to the olfactory bulb is concentration invariant 162

Neurobiology

Landowne, David
Heavy water (D_2O) alters the sodium channel gating current in squid giant axons 164
White, Thomas H., Harris Ripps, Miduturu Srinivas, and Roberto Bruzzone
Voltage gating properties of channels formed by a skate retinal connexin 165
Molina, Anthony J.A., Peter J.S. Smith, and Robert Paul Malchow
Hydrogen ion fluxes from isolated retinal horizontal cells: modulation by glutamate 168
Wang, Jing W.
Odor-induced oscillatory activity in *Drosophila* CNS . . . 170
Hitt, James M., Frederick A. Dodge, Ehud Kaplan, and Robert B. Barlow
Circadian rhythms in the receptive fields of the *Limulus* lateral eye 171
Fay, Richard R., and Peggy L. Edds-Walton
Frequency response of auditory brainstem units in toadfish (*Opsanus tau*) 173
Yamaguchi, Ayako, Leonard K. Kaczmarek, and Darcy B. Kelley
Intrinsic membrane properties of laryngeal motoneurons that control sexually differentiated vocal behavior in African clawed frogs, *Xenopus laevis* 175
Atherton, Jillian L., Matthew A. Krutky, James M. Hitt, Frederick A. Dodge, and Robert B. Barlow
Optic nerve responses of *Limulus* in its natural habitat at night 176
Krutky, Matthew A., Jillian L. Atherton, Spence Smith, Frederick A. Dodge, and Robert B. Barlow
Do the properties of underwater lighting influence the visually guided behavior of *Limulus*? 178
Hale, Melina E.
Startle responses of fish without Mauthner neurons: escape behavior of the lumpfish (*Cyclopterus lumpus*) 180
Epstein, David A., Herman T. Epstein, Frank M. Child, and Alan M. Kuzirian
Memory consolidation in *Hermissenda crassicornis* . . . 182
Abenavoli, A., L. Forti, and A. Malgaroli
Mechanisms of spontaneous miniature activity at CA3-CA1 synapses: evidence for a divergence from a random Poisson process 184

Physiology and Biochemistry

Novales Flamarique, Inigo, Kristiina Ovaska, and Theodore M. Davis
UV-B induced damage to the skin and ocular system of amphibians 187
Harrington, John M., and Peter B. Armstrong
Initial characterization of a potential anti-fouling system in the American horseshoe crab, *Limulus polyphemus* 189
Asokan, Rengasamy, Margaret T. Armstrong, and Peter B. Armstrong
Association of α_2-macroglobulin with the coagulin clot in the American horseshoe crab, *Limulus polyphemus:* a potential role in stabilization from proteolysis 190
Kuhns, William J., Max M. Burger, Mohan Sarker, Xavier Fernandez-Busquets, and Tracy Simpson
Enzymatic biosynthesis of N-linked glycan by the marine sponge *Microciona prolifera* 192
Armstrong, Peter B., and Rengasamy Asokan
A Ca^{+2}-independent cytolytic system from the blood of the marine snail *Busycon canaliculum* 194
Heck, Diane E., Lydia Louis, Michael A. Gallo, and Jeffrey D. Laskin
Modulation of the development of plutei by nitric oxide in the sea urchin *Arbacia punctulata* 195
Jung, Sung-Kwon, Katherine Hammar, and Peter J.S. Smith
Development of self-referencing oxygen microsensor and its application to single pancreatic HIT cells: effects of adenylate cyclase activator forskolin on oxygen consumption 197
Hanselmann, Rhea, Roxanna Smolowitz, and Daniel G. Gibson
Identification of proliferating cells in hard clams. . . 199

Brothers, Christine, Ernest Marks III, and Roxanna Smolowitz
Conditions affecting the growth and zoosporulation of the protistan parasite QPX in culture. 200

Cell Biology

Sandberg, Leslie, Phillip Stafford, and George M. Langford
Effects of myosin-II antibody on actin-dependent vesicle transport in extracts of clam oocytes 202
Stafford, Phillip, Jeremiah Brown, and George M. Langford
Interaction of actin- and microtubule-based motors in squid axoplasm probed with antibodies to myosin V and kinesin 203
Tran, P.T., V. Doye, F. Chang, and S. Inoué
Microtubule-dependent nuclear positioning and nuclear-dependent septum positioning in the fission yeast, *Saccharomyces pombe*. 205
Crawford, Karen
The role of microtubules during blastodisc formation of the squid *Loligo pealei*. 207
Weidner, Earl
Cytoplasmic proteins on the surface of discharged microsporidian sporoplasms 208
MacKenzie, Roger, David Newman, Max M. Burger, Rene Roy, and William J. Kuhns
Adhesion of a viral envelope protein to a non-self-binding domain of the aggregation factor in the marine sponge *Microciona prolifera*. 209
Goda, Makoto, Mario H. Burgos, and Shinya Inoué
Fertilization-induced changes in the fine structure of stratified *Arbacia* eggs. I. Observations on live cells with the centrifuge polarizing microscope 212
Burgos, Mario H., Makoto Goda, and Shinya Inoué
Fertilization-induced changes in the fine structure of stratified *Arbacia* eggs. II. Observations with electron microscopy. 213
Gould, Robert M., Concetta M. Freund, John Engler, and Hilary G. Morrison
Optimization of homogenization conditions used to isolate mRNAs in processes of myelinating oligodendrocytes 215

Ecology, Biogeochemistry, and Population Biology

Kirkby, Ryan, Luc Claessens, Charles Hopkinson, Jr., Edward Rastetter, and Joseph Vallino
Modeling the effects of land-use change on nitrogen biogeochemistry in the Ipswich watershed, Massachusetts 218
Perring, Anne, Michael Williams, Charles Hopkinson, Jr., Edward Rastetter, and Joseph Vallino
Solute dynamics in storm flow of the Ipswich River Basin: effects of land use. 219
Westgate, Elizabeth J., Kevin D. Kroeger, Wendy J. Pabich, and Ivan Valiela
Fate of anthropogenic nitrogen in a nearshore Cape Cod aquifer 221
Denault, Michelle, Erica Stieve, and Ivan Valiela
Effects of nitrogen load and irradiance on photosynthetic pigment concentrations in *Cladophora vagabunda* and *Gracilaria tikvahiae* in estuaries of Waquoit Bay. 223
Greenbaum, Adena, and Anne Giblin
Differences in properties of salt marsh sediment between hayed and reference sites 225
Chikarmane, Hemant M., Alan M. Kuzirian, Robbin Kozlowski, Mark Kuzirian, and Tony Lee
Population genetic structure of the goosefish, *Lophius americanus*. 227

Oral Presentations

Published by title only. 229

Reference: *Biol. Bull.* **199:** 161. (October 2000)

Introduction to the Featured Report
On Mapping Odor Quality

In vertebrate olfactory systems, the coding of odor quality by the brain is constrained by four considerations. Three of these suggest that the code is specific: *i.e.*, about 1000 genes encode olfactory receptors; every primary olfactory receptor neuron expresses only one of those genes; and the axons of all of the neurons expressing a particular gene project to the same glomerulus (a synaptic exchange site in the olfactory bulb). The fourth consideration suggests that coding lacks specificity, for single receptor neurons respond, though not always with the same potency, to a variety of odor molecules. Thus, the recognition of a chemically pure odor cannot be restricted to its effect on a single specific set of receptor neurons and their common glomerulus. Rather, odor quality must be identified by some array or pattern of inputs induced in diverse neurons and glomeruli.

Many previous experiments show that these patterns of response or input vary with concentration. On the other hand, psychophysical experimentation—as well as common experience—tells us that recognition of an odor is not confounded by even enormous differences in concentration.

Matt Wachowiak and his colleagues point, in their brief report, to a resolution of this paradox. They fill the olfactory nerve terminals of the three-toed box turtle with a fluorescent dye, apply pulses of odor, and produce a map representing the location of the glomeruli responding to the odor, as well as the amplitude of the response. With this preparation, the variation in the pattern of olfactory receptor neuron inputs to the olfactory bulb can be measured as a function of concentration. In fact, the experiments confirm that the absolute size of the response to an odor increases with concentration. But if the responses are normalized, the resulting maps are virtually invariant with concentration. Wachowiak *et al.* conclude that—if higher olfactory centers receive and can analyze normalized maps of the input to the olfactory bulb—then odor recognition, independent of concentration, would be possible.

—The Editors
August 2000

Reference: *Biol. Bull.* **199:** 162–163. (October 2000)

The Spatial Representation of Odors by Olfactory Receptor Neuron Input to the Olfactory Bulb is Concentration Invariant

Matt Wachowiak, Michal Zochowski, Lawrence B. Cohen, and Chun X. Falk (Department of Cellular and Molecular Physiology, Yale University School of Medicine, New Haven, Connecticut 06520)

We wish to understand how odorants are distinguished and how one odorant is recognized as the same across a concentration range of several orders of magnitude. To this end we have measured the spatial pattern of the olfactory receptor neuron input to the olfactory bulb in the three-toed box turtle (*Terepene triunguis*).

To monitor the input to the bulb we labeled the nerve terminals of the olfactory receptor neurons with Calcium Green-1 dextran 10 kD (Molecular Probes) following the method developed by Friedrich and Korsching (1). We then formed a magnified (4×) image of the bulb on an 80 × 80 CCD camera (NeuroCCD; RedShirtImaging, LLC, Fairfield, CT) and recorded the changes in fluorescence that resulted from a 2-s odorant pulse delivered to the nose. The signals we measured had approximately the same time-course everywhere in the bulb, and we therefore characterized the response by the amplitude of the signal as a function of its position on the bulb.

Figure 1 shows three pseudocolor representations of activity in response to the odorant, hexanone. Red represents a large signal in each measurement and blue represents a signal 30% as large. The left-hand image shows the response to hexanone at a concentration that was 0.3% of saturation. The largest signal in the response was colored red (normalized scaling). Both right-hand images show the

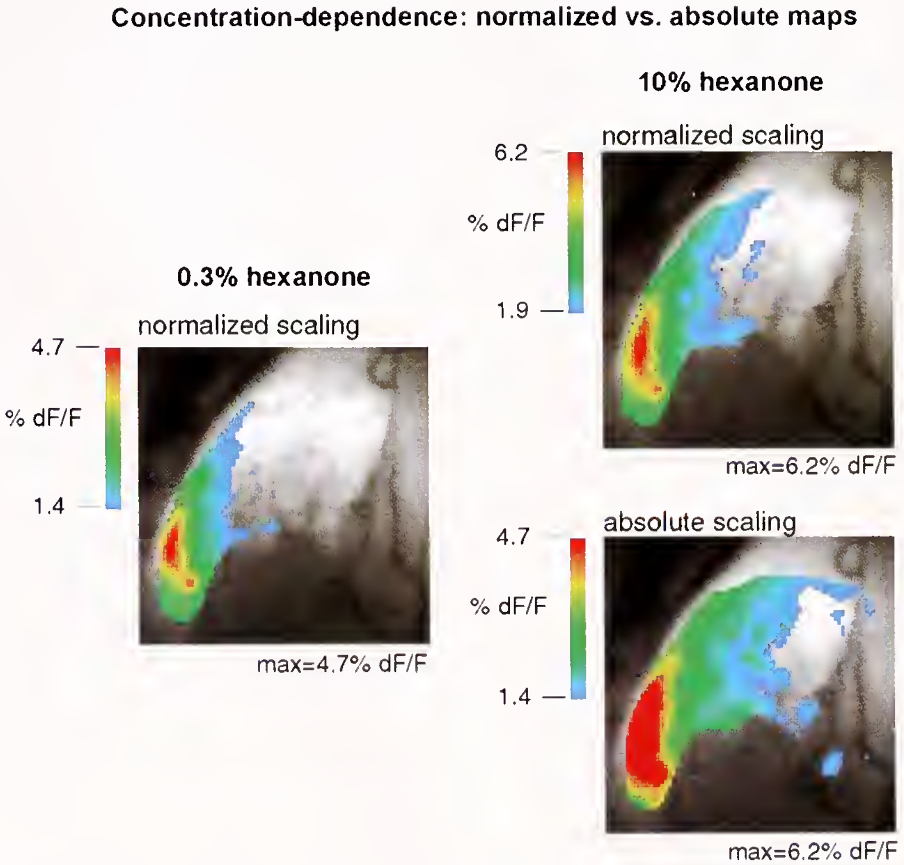

Figure 1. *Normalized maps of receptor neuron input to the turtle olfactory bulb are concentration-invariant. The left panel shows a pseudocolor map of the response to a 0.3% dilution of saturated vapor of 2-hexanone. The map is normalized to the maximum signal amplitude for this trial. The right panels show pseudocolor maps of the response to a 10% dilution of 2-hexanone. The map on the top is normalized to its maximum signal amplitude. The map on the bottom (absolute scaling) shows the same data using the same scaling as for the 0.3% hexanone trial. The figure shows a concentration-dependent increase in the number of glomeruli activated above a given absolute level, but shows concentration-invariance in the relative levels of input to all glomeruli activated by an odorant. 4× image magnification. The field of view is approximately 4 mm × 4 mm.*

response to 10% hexanone using two different scaling procedures. The bottom image shows the response using the same scale as that used for the response to 0.3% hexanone (absolute scaling). This image is qualitatively different from the 0.3% image. In contrast, the top image shows the response using normalized scaling. Again, the largest signal was colored red. This image is essentially identical to the image on the left, even though the concentration of odorant differed by a factor of 30. Thus, normalized maps of input to the olfactory bulb appear to be concentration invariant.

We hypothesize that concentration invariant odorant identification could be achieved if higher olfactory centers "read" the normalized maps of the input to the olfactory bulb.

Supported by NINDS Grant, NS08437 and an NRSA fellowship, DC 00378.

Literature Cited

1. **Friedrich, R., and S. Korsching. 1997.** *Neuron* **18:** 737–752.

Reference: *Biol. Bull.* **199:** 164–165. (October 2000)

Heavy Water (D_2O) Alters the Sodium Channel Gating Current in Squid Giant Axons

David Landowne (University of Miami, Miami, Florida 33101)

When nerve axon membranes are abruptly depolarized, a small outward displacement current precedes the sodium current that underlies the propagated nerve impulse. This displacement current is asymmetric; it does not appear in a symmetrical hyperpolarization. It was named "gating current" by earlier workers because of its association with the opening of the activation gates of the sodium channels. The gating currents were isolated by replacing permeant ions with impermeant ones, thus reducing ionic currents, subtracting away symmetrical currents and, in most cases, blocking the ionic sodium current with tetrodotoxin (1, 2).

Replacing the H_2O in solutions with D_2O slows many chemical and biological reactions including the squid axon action potential (3), ionic currents (4), and the sodium pump (5). However, Meves (6) reported that D_2O had no significant effect on the asymmetry currents of squid axons. This result was confirmed in *Myxicola* (7) and crayfish (8) axons. Most measurements were made at voltages less than +20 mV, which would not be expected to open all of the channels, and in the presence of tetrodotoxin. Both the ionic and gating currents can be recorded if the experiments are carried out in solutions with low sodium content (9). When this is done, D_2O can be seen to reduce the amplitude of the gating currents at more positive potentials.

Segments of squid axons were bathed in an artificial seawater containing 44 m*M* NaCl, 396 m*M* tetramethylammonium (TMA) chloride, and 2 m*M* TMA Hepes, pH 7.4; and the internal Cs perfusion fluid contained 150 m*M* Cs glutamate, 50 m*M* CsF, 750 m*M* sucrose, and 40 m*M* Cs Hepes, pH 7.4. Solutions were made up with either H_2O or 99.8% D_2O. The axons were voltage-clamped at a −70 mV holding potential. Gating currents were recorded with a p/8 protocol, as follows: the holding potential was shifted to −140 mV, and 8 small "subtraction" pulses, ⅛ the amplitude of the test pulse, were applied and their currents summed. Then the potential was shifted back to −70 mV, and a single test pulse was applied. This procedure was repeated every two seconds. Currents were filtered at 40 kHz and sampled at 100 kHz. The records presented are the difference between the test current and the summed subtraction currents averaged over 64 cycles. Experiments were performed at 3°–4°C.

The figure shows records made with pulses to +25 and +50 mV. The effect of D_2O (filled symbols) is to reduce the initial outward gating current by about 30%, to increase the time to peak inward current to about 1.4 times its value in H_2O, and to slow the decline of inward current associated with inactivation of the sodium channels. The sodium conductance was reduced by about 35%. The changes in ionic currents are similar to those previously described (3, 6, 7). In 56 measurements at 0 to +75 mV on 11 axons in the absence of tetrodotoxin, D_2O reduced the peak of the

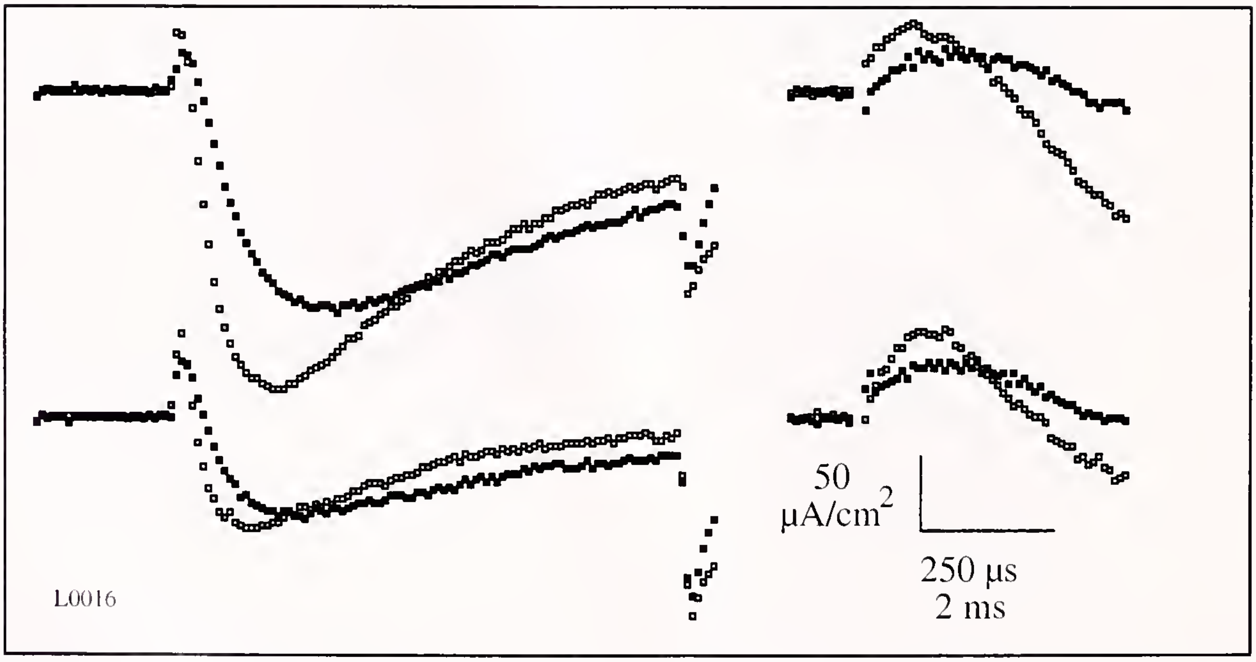

Figure 1. *D_2O alters gating and ionic currents. Open symbols are currents in H_2O-based solutions; filled symbols indicate D_2O-based solutions. The records are for a steps from a −70 mV holding potential. The upper records are to +25 mV; the lower, to +50 mV. The records on the right are shown at the expanded timebase.*

initial outward gating current to 0.70 ± 0.02 times its value in H_2O.

The simplest interpretation of these results is that D_2O slowed the rate of the conformational change by 30%, thus reducing the amplitude of the gating current and increasing the time required to open the channels. This could occur by changing the channels or changing the environment in which they operate. The viscosity of D_2O is larger than that of H_2O, and in fact, the reduction of gating and the slowing of ionic currents described above are qualitatively similar to those seen in solutions with a viscosity that has been increased with non-electrolytes (10). On the other hand, the D_2O effect seems larger than predicted by viscosity alone. Perhaps D_2O alters the gating machinery. About 40% of the amide protons of the *Streptomyces lividans* K+ channel exchange within 3 minutes of D_2O exposure accompanied by subtle structural changes (11). To test between these two possibilities, currents were recorded during the transition from 0 m*M* sodium H_2O seawater into 44 m*M* sodium D_2O seawater. In the 0 m*M* Na H_2O solution, there was no inward sodium current. By 90 s after beginning the switch into the 44 m*M* Na D_2O solution, the inward current appeared—but in the H_2O pattern, similar to the open symbols in Figure 1. Over the next 3 min the current pattern switched to the D_2O pattern, similar to the filled symbols. This suggests that the D_2O effect involves changes in channel structure.

I thank Dr. R. J. Lipicky and the Howard Gilman Foundation for encouragement and support.

Literature Cited

1. **Armstrong, C. M., and F. Bezanilla. 1973.** *Nature (Lond.)* **242:** 459–461.
2. **Keynes, R. D., and E. Rojas. 1973.** *J. Physiol. (Lond)* **233:** 28P–30P.
3. **Thies, R. E., and F. D. Carlson. 1955.** *Biol. Bull.* **111:** 295.
4. **Conti, F., and G. Palmieri. 1968.** *Biophysik.* **5:** 71–77.
5. **Landowne, D. 1987.** *J. Membr. Biol.* **96:** 277–281.
6. **Meves, H. 1974.** *J. Physiol. (Lond)* **243:** 847–867.
7. **Schauf, C. L., and J. O. Bullock. 1979.** *Biophys. J.* **27:** 193–208.
8. **Alicata, D. A., M. D. Rayner, and J. G. Starkus. 1990.** *Biophys. J.* **57:** 745–758.
9. **Bezanilla, F., and C. M. Armstrong. 1974.** *Science* **183:** 753–754.
10. **Kukita, F. 1997.** *J. Physiol. (Lond.)* **498:** 109–133.
11. **Tatulian, S. A., D. M. Cortes, and E. Perozo. 1998.** *FEBS Lett.* **423:** 205–212.

Reference: *Biol. Bull.* **199:** 165–168. (October 2000)

Voltage Gating Properties of Channels Formed by a Skate Retinal Connexin

Thomas W. White[1], *Harris Ripps*[2], *Miduturu Srinivas*[3], *and Roberto Bruzzone*[4]
(Marine Biological Laboratory, Woods Hole, Massachusetts 02543)

Gap junctions provide pathways for electrical and chemical communication between networks of coupled cells. They act as simple electrical synapses, and also synchronize and regulate a broad range of cellular activities. The structural proteins constituting gap-junctional channels in vertebrates are the connexins, members of a multigene family that exhibit a common topology: four transmembrane domains separating two well-conserved extracellular loops and three cytoplasmic domains. Six connexin polypeptides oligomerize to form a membrane hemichannel or connexon, clusters of which join with the connexons of adjacent cells to create the gap junction. Once assembled, the gap-junctional channel consists of an aqueous pore that allows the cell-to-cell diffusion of ions, second-messenger molecules, and small metabolites. Different cell types contain connexins that are unique to their special needs, and variations in the molecular structure of the individual connexins determine the gating properties, voltage dependence and cellular interactions of their gap-junctional channels (1).

The vertebrate retina is a useful model with which to study the diversity of electrical coupling in nervous tissue. Diverse experimental approaches have shown that virtually every class of retinal neuron and glial cell makes gap junctions with neighboring cells of similar type, and in some cases with cells of another type (2, 3). Moreover, coupling between different cell types appears to be mediated by gap junctions that exhibit asymmetric dye transfer, as well as distinct pharmacological properties (4, 5). Although there is abundant evidence that the electrical synapses formed by gap junctions affect every aspect of retinal function, relatively little is known about the connexins mediating these effects. The situation has been changed by the identification of a distinct subgroup (γ) of the connexin family that shows a pattern of expression restricted to the retina and the central nervous system (6–11). The first member to have been discovered, Cx35, was cloned from a skate retinal cDNA library (6), and some of its functional characteristics were examined in the *Xenopus* oocyte expression system (12). In the present study, we have extended these observations to analyze more fully the voltage sensitivity and kinetics of the gap junctions formed by Cx35 in paired oocytes. In addition, we have investigated the properties of the non-junctional hemichannels formed in single oocytes, and have compared the effects of quinine on the kinetics of the tail currents evoked at the termination of voltage pulses.

The procedures for preparing cRNA, and its analysis in *Xenopus* oocytes have been described previously (12). Oocytes were isolated by enzymatic digestion and injected with either an antisense oligonucleotide (3 ng/cell) to suppress the endogenous *Xenopus*

---

[1] Department of Neurobiology, Harvard Medical School, Boston, MA 02115.

[2] Department of Ophthalmology and Visual Sciences, UIC College of Medicine, Chicago, IL 60612.

[3] Department of Neuroscience, Albert Einstein College of Medicine, Bronx, NY 10461.

[4] Départment de Virologie, Institut Pasteur, 75015 Paris, France.

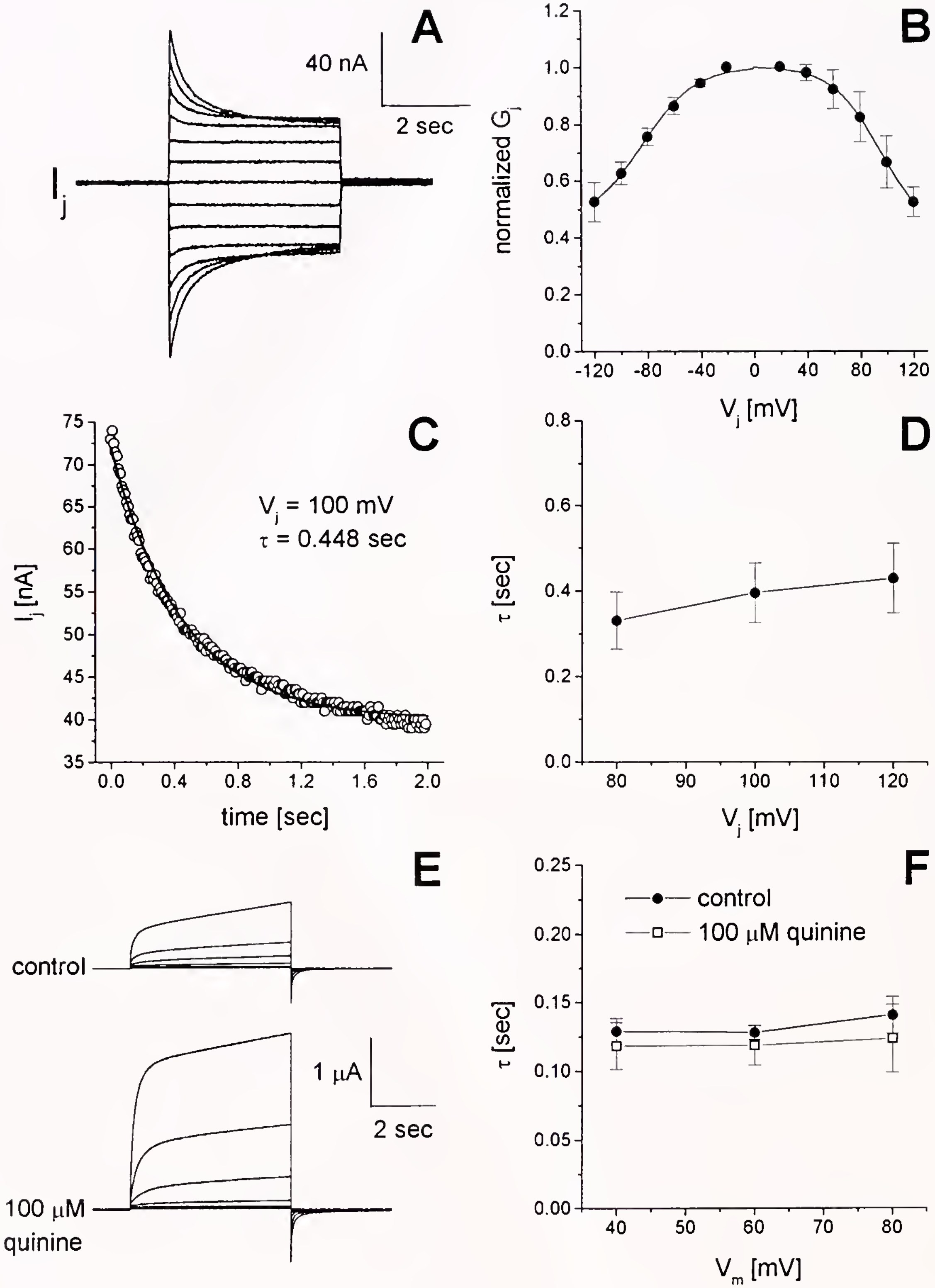

Figure 1. *Voltage gating of channels in* Xenopus *oocytes expressing skate Cx35. (A) Gap junctional currents (I_j) were elicited by transjunctional voltage (V_j) steps, 4 s in duration, applied in ±20 mV increments from a holding potential of −40 mV. (B) Plotting steady state junctional conductance (G_{jss}, normalized to the values measured at ±20 mV) vs. V_j shows that, even at the extremes of ΔV_j (±120 mV), the residual conductance is equal to about half the initial value; data are the means (±SD) of 4 cell pairs. Curves drawn through the data were derived from the Boltzmann equation in which the parameters for positive values of V_j were A = 0.06; V_o = 95; G_{jmax} = 1; and G_{jmin} = 0.40. For negative values of V_j, the corresponding values were 0.05,*

Cx38 (13), or a combination of antisense (as above) plus Cx35 RNA (5 ng/cell). To study intercellular channels, oocytes were stripped of their vitelline membranes and brought into contact at their vegetal poles for 48 h before electrophysiological analysis. This step was omitted to explore hemichannel activity, which was recorded 48–72 h after RNA injection.

Intercellular communication was quantified by dual cell voltage clamp (12, 14). To determine the voltage-gating properties of the intercellular channels, transjunctional potentials (V_j) of opposite polarity were generated by hyperpolarizing or depolarizing one cell in 20 mV steps (over a range of ±120 mV), while clamping the second cell at −40 mV. Currents were measured 4 s after the onset of the voltage pulse, at which time they approached steady state (I_{jss}), and the macroscopic conductance (G_{jss}) was calculated by dividing I_{jss} by V_j. G_{jss} was then normalized to the values determined at ±20 mV, and plotted against V_j. Data describing the relationship of G_{jss} as a function of V_j were fit to a Boltzmann relation (14) of the form: $G_{jss} = \{(G_{jmax} - G_{jmin})/(1 + \exp[A(V_j - V_o)]\} + G_{jmin}$, where G_{jss} is the steady-state junctional conductance, G_{jmax} (normalized to unity) is the maximum conductance, G_{jmin} is the residual conductance at large values of V_j, and V_o is the transjunctional voltage at which $G_{jss} = (G_{jmax} - G_{jmin})/2$. The constant A ($=nq/kT$) represents the voltage sensitivity in terms of gating charge as the equivalent number (n) of electron charges (q) moving through the membrane, k is the Boltzmann constant, and T is the absolute temperature. The time constants (τ) of voltage-dependent transitions of junctional conductance were calculated using data-fitting functions in Microcal Origin. To characterize the hemichannel activity of connexons, non-junctional current recordings were obtained from single oocytes with a two-electrode voltage-clamp procedure. Cells were clamped at −40 mV, and whole cell currents recorded in response to depolarizing voltage steps (from −20 to +80 mV in 20-mV intervals) imposed for 5 s.

In a previous study (12), we restricted our observations of voltage gating to transjunctional potentials of ±80 mV and did not quantify voltage dependence. In the current study, we have extended this analysis to much larger values of V_j and have quantified the degree and kinetics of voltage gating. Figure 1A illustrates a family of gap-junctional currents elicited at transjunctional voltage steps up to ±120 mV in oocyte pairs expressing Cx35. Voltage gating occurred symmetrically at the higher values of V_j (80–120 mV), and the current decay approached steady-state levels by the end of the imposed step. Quantitative analysis (Fig. 1B) indicated that a large residual conductance, equivalent to approximately half of the initial value, was still present at the extremes of the voltage range tested. Fitting the G_j vs. V_j relationship to the Boltzmann equation yielded V_o values > 80 mV (see figure legend) confirming the relatively weak V_j gating described earlier. Thus, voltage is not likely to be a primary modulator of Cx35-mediated intercellular communication in retinal neurons.

The voltage gating characteristics of Cx35 were further explored by analyzing the kinetics of channel closure for values of $V_j \geq 80$ mV, *i.e.*, sufficient to consistently induce current decay. Figure 1C illustrates results obtained from one cell pair in response to a transjunctional voltage step of +100 mV. The time-dependent decline in I_j was well fit by a single exponential function with a time constant (τ) of 0.448 s. Interestingly, the mean values of τ, obtained both for different values of V_j, as well as for positive and negative voltage steps, hovered about 0.4 s and showed no significant change as a function of either the polarity or the magnitude of V_j (Fig. 1D). These data are in sharp contrast to kinetic analyses of many other connexins, where τ values decreased with increasing driving force (15, 16). This feature is shared by another γ connexin, mouse Cx36 (data not shown), and illustrates further the unique properties of this subgroup.

The ability of connexins to form hemichannels in *Xenopus* oocytes, a property reminiscent of membrane currents observed in some retinal neurons (17, 18), prompted us to investigate the kinetics of Cx35 hemichannel closure by analyzing tail currents. As we showed previously, quinine-sensitive hemichannel currents can be recorded from oocytes expressing skate Cx35 (12). This is confirmed in Figure 1E, which shows the increase in the outward (non-junctional) current recorded from a single oocyte in response to depolarizing voltage increments ≥ 40 mV, and the current enhancement produced by the addition of 100 μM quinine to the normal bath solution. To determine whether quinine exerted an effect on the gating properties of the hemichannels, we measured the kinetics of the tail currents recorded at the termination of the voltage step. Figure 1F shows that the mean of the time constants of the single exponential decay functions describing the data for the return of V_m to −40 mV from values of +40 to +80 mV were unaffected by quinine. However, the hemichannel time constants are not directly comparable to the intercellular channel τ values, as the ionic strength of control bath solution is greatly reduced in comparison to ooplasm, and K^+ is replaced by Na^+ as the principal cation. Further studies are required to determine the precise relationship between hemichannel and intercellular channel gating, and to clarify the mechanism whereby quinine markedly increases Cx35 mediated hemichannel currents.

The authors thank Jane Zakevicius for technical help and Marco White for assistance with the animal care. This work was supported by National Eye Institute grants (EY-13163 to TWW and EY-06516 to HR), by the Association RETINA France (to RB) and by MBL fellowships (to TWW, MS, and RB).

84, 1, and 0.45, respectively. The slight asymmetry in Boltzmann values implies a small degree of dependence of G_{jss} on V_m. (C) In response to a +100 mV voltage step, the transjunctional current decayed toward a steady state level along a single exponential with a time constant (τ) of 0.448 s. (D) The values of τ remained relatively constant for voltage steps ranging from ±80 to ±120 mV and were not dependent on the polarity of V_j; data are the means (±SD) of 8 experiments. (E) Hemichannel activity of Cx35 recorded from single oocytes expressing Cx35. With the cells clamped at −40 mV, non-junctional currents were elicited by depolarizing voltage steps (from −20 to +80 mV in 20 mV intervals) imposed for a duration of 5 s. When bathed in control solution, progressively larger currents were obtained as the depolarizing voltage step exceeded +20 mV. With the addition of 100 μM quinine, activation of hemichannel activity occurred over the same voltage range, but the magnitudes of the outward currents were greatly enhanced. (F) Tail currents measured at the end of the voltage pulses were well fit by single exponentials having τ values of ~0.125 s. Quinine had no significant effect on the gating kinetics of Cx35 hemichannels; data are the means (±SD) of 6 experiments.

Literature Cited

1. **Bruzzone, R., T. W. White, and D. L. Paul. 1996.** *Eur. J. Biochem.* **238:** 1–27.
2. **Vaney, D. I. 1994.** *Prog. Ret. Eye Res.* **13:** 301–353.
3. **Becker, D. L., V. Bonness, and P. Mobbs. 1998.** *Cell. Biol. Int.* **22:** 781–792.
4. **Mills, S. L., and S. C. Massey. 1995.** *Nature* **377:** 734–737.
5. **Newman, E. A., and K. R. Zahs. 1997.** *Science* **275:** 844–847.
6. **O'Brien, J., M. R. Al-Ubaidi, and H. Ripps. 1996.** *Mol. Biol. Cell* **7:** 233–243.
7. **O'Brien, J., R. Bruzzone, T. W. White, M. R. Al-Ubaidi, and H. Ripps. 1998.** *J. Neurosci.* **18:** 7625–7637.
8. **Condorelli, D. F., R. Parenti, F. Spinella, A. T. Salinaro, N. Belluardo, V. Cardile, and F. Cicirata. 1998.** *Eur. J. Neurosci.* **10:** 1202–1208.
9. **Söhl, G., J. Degen, B. Teubner, and K. Willecke. 1998.** *FEBS Lett.* **428:** 27–31.
10. **Srinivas, M., R. Rozental, T. Kojima, R. Dermietzel, M. Mehler, D. F. Condorelli, J. A. Kessler, and D. C. Spray. 1999.** *J. Neurosci.* **19:** 9848–9855.
11. **Al-Ubaidi, M. R., T. W. White, H. Ripps, I. Poras, P. Avner, D. Gomès, and R. Bruzzone. 2000.** *J. Neurosci. Res.* **59:** 813–826.
12. **White, T. W., M. R. Deans, J. O'Brien, M. R. Al-Ubaidi, D. A. Goodenough, H. Ripps, and R. Bruzzone. 1999.** *Eur. J. Neurosci.* **11:** 1883–1890.
13. **Bruzzone, R., J.-A. Haefliger, R. L. Gimlich, and D. L. Paul. 1993.** *Mol. Biol. Cell* **4:** 7–20.
14. **Spray, D. C., A. L. Harris, and M. V. L. Bennett. 1981.** *J. Gen. Physiol.* **77:** 77–93.
15. **Barrio, L. C., J. Capel, J. A. Jarillo, C. Castro, and A. Revilla. 1997.** *Biophys. J.* **73:** 757–769.
16. **White, T. W., R. Bruzzone, D. A. Goodenough, and D. L. Paul. 1992.** *Mol. Biol. Cell* **3:** 711–720.
17. **DeVries, S. H., and E. A. Schwartz. 1992.** *J. Physiol. (Lond.)* **445:** 201–230.
18. **Malchow, R. P., H. Qian, and H. Ripps. 1993.** *J. Neurosci. Res.* **35:** 237–245.

Reference: *Biol. Bull.* **199:** 168–170. (October 2000)

Hydrogen Ion Fluxes from Isolated Retinal Horizontal Cells: Modulation by Glutamate

Anthony J. A. Molina (Department of Biological Sciences, University of Illinois at Chicago, Chicago, Illinois 60607), Peter J. S. Smith[1]*, and Robert Paul Malchow*[2]

Retinal horizontal cells are second order neurons that receive direct input from photoreceptors. These cells are believed to play a crucial role in the formation of the surround aspect of the classic center-surround receptive fields of visual neurons. Debate still persists as to the molecular mechanisms used by horizontal cells to establish the surround portion of these receptive fields. One hypothesis, promulgated recently by Kamermans and colleagues (1), suggests that horizontal cells may exert their lateral inhibitory actions by modulating the calcium flux into the synaptic terminals of photoreceptors, thus altering the release of the photoreceptor neurotransmitter. Hydrogen ions are among several agents that have been proposed to act in this modulatory role (2), and in fact, the responses to light by second order retinal neurons are very sensitive to changes in extracellular pH (3, 4). In an elegant series of experiments, Barnes and coworkers (5) demonstrated that this pH-dependent modulation of synaptic transmission was due to the marked sensitivity of calcium channels in the photoreceptors to extracellular hydrogen ions. These investigators found that elevated concentrations of H^+ shifted the voltage-dependence of the calcium current activation curve of the photoreceptors to more depolarized levels and also reduced the calcium conductance. Moreover, small light-induced changes in extracellular pH within the intact retina have been reported by Oakley and Wen (6).

Horizontal cells could thus exert their inhibitory influences by modifying the concentration of hydrogen ions in the external milieu. In the present work, we have used pH-selective microelectrodes to monitor the flux of hydrogen ions surrounding isolated retinal horizontal cells. In particular, we examined whether the amino acid glutamate could alter the flux of hydrogen ions recorded from these cells. We reasoned that, if the release of hydrogen ions from horizontal cells is indeed a key factor in the creation of the surround portion of retinal receptive fields, then such a flux should be modified by glutamate, the neurotransmitter believed to be released by vertebrate photoreceptors (7).

The pH-selective electrodes were used in a self-referencing mode (8), which greatly enhances their signal sensitivity and stability, eliminating much of the electrical noise and drift inherent in such electrodes. In this format, the electrode is first placed just adjacent to the membrane of the cell, and a reading taken; the electrode is then moved a set distance away (typically 30 μm), and a second reading taken. The difference between the voltage readings at the two positions reflects differences in the free hydrogen activity at the two locations. This method allowed us to measure the small hydrogen ion fluxes that would otherwise have been lost in the noise of the recordings.

pH selective electrodes were prepared by pulling thin-walled glass capillary tubing (o.d. 1.5 mm) to a tip diameter of 2–4 μm. The pipettes were silanized and back-filled with 100 m*M* potassium chloride, and the fluid was forced to the tip of the pipette by air pressure applied to the back of the pipette from a syringe. The pipette tip was then filled with a pH-selective resin (hydrogen ionophore 1-Cocktail B, Fluka Chemica); the tip was placed in contact with a source pipette containing the resin, and about 50 μm of the resin was then drawn up by suction on the back of the pipette. The resin employed here has a particularly high selectivity for hydrogen ions, and is reported to be more than 10^9 times more sensitive to hydrogen ions than to either sodium or potassium ions (9). Isolated retinal horizontal cells were obtained by enzymatic dissociation of the retina of the skate (*Raja erinacea* or *R. ocellata*) as described in Malchow *et al.* (10). Briefly, the animals were chilled in ice, cervically transected, and double pithed. The eyes were removed, and the retinas were isolated and placed for 45 min under gentle agitation into a skate-modified L-15 culture medium containing 2 mg/ml papain and 1 mg/ml cysteine. The retinas were then rinsed 8 times in media lacking papain and cysteine, and then mechanically agitated through a 5-ml graduated glass pipette. Single drops of this cellular suspension were placed in 35-mm plastic culture dishes that had previously been coated with 1% protamine sulfate and 0.1% concanavalin A. Cells were stored at 14°C for up to 4 days before use. Recordings were made in a skate Ringer's solution containing 2 m*M* of the pH buffer HEPES and no added bicarbonate. A 5 m*M* glutamate stock solution was prepared in skate Ringer and adjusted to pH 7.6 with 1 *M* NaOH. Glutamate was applied by adding 1 ml of the 5 m*M* glutamate solution to 4 ml of Ringer already present in the culture dish, resulting in a final concentration of 1 m*M* glutamate.

---

[1] BioCurrents Research Center, Marine Biological Laboratory, Woods Hole, MA.

[2] Departments of Biological Sciences and Ophthalmology, University of Illinois at Chicago, Chicago, IL.

Under these conditions, a steady differential signal was obtained from horizontal cells indicative of a higher concentration of hydrogen ions near the membranes of the cells. The size of this signal decreased as the concentration of the pH buffer HEPES was increased, consistent with the hypothesis that the signal detected indeed reflected hydrogen ions. Moreover, as shown in Figure 1, the application of 1 m*M* glutamate resulted in a marked decrease in the size of the differential signal. A differential signal of approximately 100 μV was initially recorded from this cell. The actual proton flux represented by this differential voltage can be calculated using an equation derived by D. M. Porterfield [in prep.: see also (12)] as follows:

$$J = -D(\Delta[H^+] + [\text{Buffer}] * 0.25\Delta[H^+] * K_a^{-1}) * \Delta r^{-1}$$

Where J is the flux, D is the diffusion coefficient for hydrogen ions, $\Delta[H^+]$ the change in hydrogen ion activity between the two poles of measurement, [Buffer] is the buffer concentration expressed in moles per cm^{-3}, K_a is the pK_a of the buffer expressed in cm^{-3}, and Δr is the distance in cm between the two measuring positions of the probe. Taking into account a small loss of the signal within the electronics of the amplification system (8), under our experimental conditions the 100 μV signal we observe is then estimated to be indicative of a proton flux of ~75 p*M* cm^{-2} s^{-1}. In 6 cells studied in this fashion, 1 m*M* glutamate reliably reduced the differential signal by an average of 60%.

We thus conclude that glutamate, the presumed neurotransmitter from vertebrate photoreceptors, can indeed alter the flux of hydrogen ions from horizontal cells. In this context, it is interesting to note that glutamate has previously been reported to promote an acidification of the internal milieu of catfish retinal horizontal cells as measured using the pH-indicator dye BCECF (11). We hypothesize that glutamate may shut down the transport of hydrogen ions from horizontal cells, thus trapping hydrogen ions in the interior of the cell. This would account for the increased intracellular acidity and the alkalinization of the extracellular milieu that we have observed. The alteration in extracellular pH induced by glutamate may be important in modifying signaling within the outer plexiform layer of the retina. Indeed, extracellular alkalinizations induced by neuronal activity occur in several other regions of the nervous system (reviewed by Chesler (13)), and excitatory amino acid receptors have been implicated in the generation of these phenomena. Thus, modulation of extracellular pH within the CNS by glutamate may be a common means by which synaptic activity is altered. Future experiments are planned in which specific pharmacological agents will be used to determine which transporter or transporters may be involved in the glutamate-induced changes in extracellular hydrogen ion concentrations.

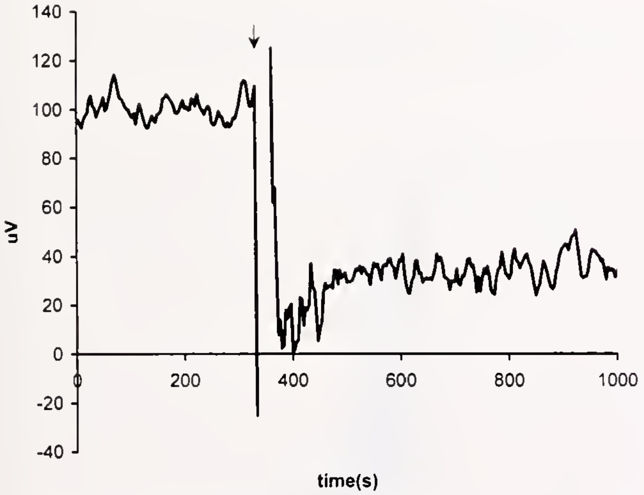

Figure 1. *Effects of glutamate on the hydrogen ion flux recorded from a single isolated retinal horizontal cell. The differential voltage recorded from a pH-selective electrode is plotted as a function of time. Before the application of glutamate, a differential signal indicative of a higher concentration of hydrogen ions near the membrane of the cell is observed. At the arrow, glutamate was added such that the final concentration in the dish was 1 mM. A marked decrease in the differential signal recorded by the pH-selective electrode was observed.*

We are grateful to Kasia Hammar for her generous assistance with electrode preparation and cell culture, Naomi Rosenkranz for help preparing isolated cells, and Richard H. Sanger for electronic and computer assistance. This work was supported by grants EYO9411 from the National Eye Institute, P41 RR01394 from the National Center for Research Resources, and a grant from the Campus Research Board of the University of Illinois at Chicago.

Literature Cited

1. **Verweij, J., M. Kamermans, and H. Spekreijse. 1996.** *Vision Res.* **36:** 3943–3953.
2. **Kamermans, M., and H. Spekreijse. 1999.** *Vision Res.* **39:** 2449–2468.
3. **Kleinschmidt, J. 1991.** *Ann. N.Y. Acad. Sci.* **635:** 468–470.
4. **Harsanyi, K., and S. C. Mangel. 1993.** *Vis. Neurosci.* **10:** 81–91.
5. **Barnes, S., V. Merchang, F. Mahmud. 1993.** *Proc. Natl. Acad. Sci. U.S.A.* **90:** 10081–10085.

6. **Oakley, B. and R. Wen. 1989.** *J. Physiol. (Lond)* **419:** 353–378.
7. **Copenhagen, D. R., and C. E. Jahr. 1989.** *Nature* **341:** 536–539.
8. **Smith, P. J. S., K. Hammar, D. M. Porterfield, R. H. Sanger, and J. R. Trimarchi. 1999.** *Microsc. Res. Tech.* **46:** 398–417.
9. **Flnka, 1991.** *Selectophore, Ionophores for Ion-Selective Electrodes and Optrodes.* Fluxa Chemie A. G. Ronkonkoma, New York.
10. **Malchow, R. P., H. Qian, H. Ripps, and J. E. Dowling. 1990.** *J. Gen. Physiol.* **95:** 177–188.
11. **Dixon, D. B., K-I. Takahashi, and D. R. Copenhagen. 1993.** *Neuron* **11:** 267–277.
12. **Smith, P. J. S. and J. Trimarchi. 2000.** *Am. J. Physiol.* (in press.)
13. **Chesler, M. 1990.** *Progr. Neurobiol.* **34:** 401–427.

Reference: *Biol. Bull.* **199:** 170–171. (October 2000)

Odor-induced Oscillatory Activity in *Drosophila* CNS

Jing W. Wang (Department of Biochemistry and Molecular Biophysics, Howard Hughes Medical Institute, Columbia University, New York, New York 10032)

In mammals and the fruit fly, the vast array of odors in the environment is discriminated by a large number of receptor molecules (1, 2, 3). Individual olfactory sensory neurons express only one of the many receptor genes (1, 2, 3). Neurons expressing the same receptor gene project to the same glomerulus (4, 5, 6), providing the anatomical evidence for a spatial coding mechanism. Electrophysiological recordings from olfactory neurons suggest that the temporal pattern of their responses can also convey information about odor quality (7). Odor-induced oscillatory activity, an indication of synchrony, has been observed in phylogenetically different species, including molluscs, insects, and mammals (7, 8, 9, 10, 11, 12).

The adult *Drosophila* antennal lobe, organized in spheroidal subcompartments termed glomeruli, receives about 1200 olfactory afferents from the antenna and 120 afferent fibers from the maxillary palp (13). Although the fly and mammals share the similarity that receptor neurons expressing the same receptor gene project to one or two glomeruli in a stereotypic manner (4, 5, 6), there are only 60 receptor genes and 43 glomeruli in *Drosophila*, in contrast to the 1000 receptor genes and 1800 glomeruli within the olfactory bulb of mammals (1, 2, 3). The lower complexity in anatomy and the rich behavioral repertoire in *Drosophila* makes it an attractive system with which to study olfaction. Moreover, sophisticated genetic tools and behavioral mutants can now also be used to study the olfactory system in *Drosophila*. Nevertheless, understanding mechanisms of odor discrimination in the CNS of the fly has been difficult due to a lack of physiological tools for functional studies.

Odor-induced oscillations have been observed in several insect species, including the locust, cockroach, honeybee, bumblebee, and wasp (7). Local field potential (LFP) recordings show odor-induced oscillation at ~10 Hz which typically lasts for the duration of odor stimulation. I have investigated this phenomenon in the *Drosophila* CNS. LFPs were recorded with glass electrodes (tip, 5 μm) that were filled with *Drosophila* HL3 saline and

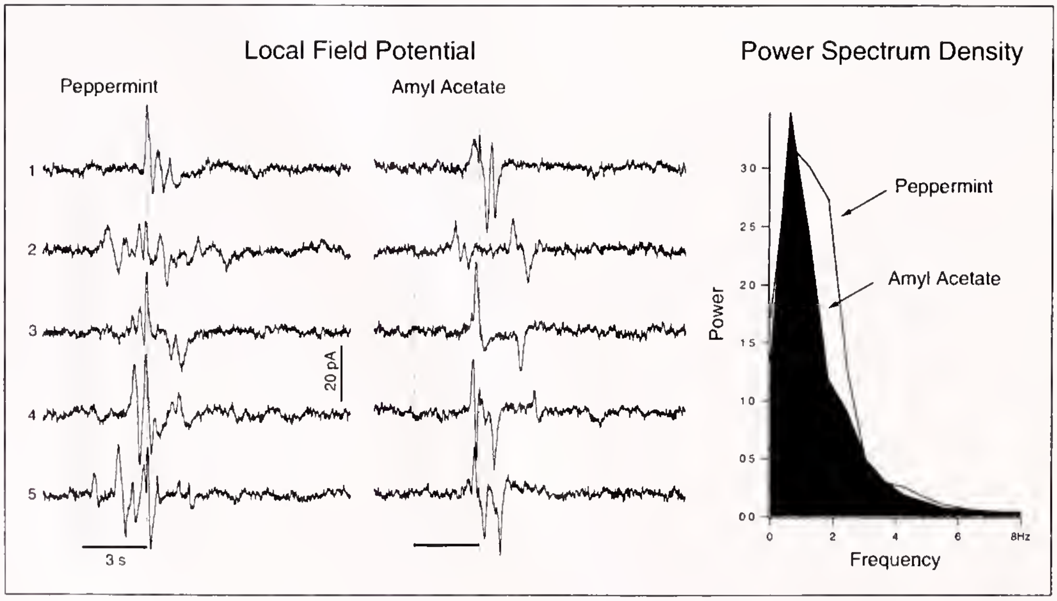

Figure 1. *Local field potential recordings of odor-induced oscillation in the CNS of* Drosophila. *The left panel shows five sequential responses to peppermint stimulation recorded from the same preparation. Responses to amyl acetate from the same preparation are shown in the middle panel. Averaged power spectrum density from the five trials is shown in the right panel. The LFP response to peppermint appears to have a higher density at 2 Hz than the response to amyl acetate.*

positioned with a motorized manipulator (MP285, Sutter). A patch clamp amplifier (EPC 7, Heka) was used, and the signal was filtered (band pass at 0.1 to 20 Hz) with a signal conditioner (CyberAmp, Axon Instruments) and recorded with software (AxoScope, Axon Instruments) run on a PC. Adult flies (less than a week after eclosion) were lightly anesthetized with CO_2 and decapitated. The heads were immobilized with wax on a microscope slide with the antennae pointing upward. A small opening was made on the dorsal cuticle for the extracellular recording.

Figure 1 shows LFP recordings from the CNS of the Canton-S wild-type fly that reveal an odor-induced oscillation. This phenomenon was confirmed in 6 preparations. A power spectrum analysis indicates that the major frequency components are less than 4 Hz (Fig. 1). This LFP oscillation signal appears to be sensitive to the position of the electrode, and the coordinates taken from the manipulator suggest that the recordings may have originated in the antennal lobe. Future experiments with GFP-labeled antennal lobe may help in identifying the sources of the oscillatory activity. The patterns of oscillation in response to the same odor appear to be roughly similar in sequential recordings from the same animal. The LFP patterns generated in response to peppermint (from McCormick) and amyl acetate (from Sigma) were distinguishable by eye. Moreover, the power spectrum analysis indicates that peppermint generates slightly more high frequency components.

This is the first LFP recording from the *Drosophila* CNS. The preliminary results presented here show that odor-induced oscillation occurs in *Drosophila;* this finding suggests that a temporal coding mechanism may be employed by the fly, and that the power of genetics may be applied in the future to decipher the physiological significance of the odor-induced oscillation.

I would like to thank Alan Gelperin for his generous support, Leonardo Belluscio for critical comments on the manuscript, and Carl Zeiss, Inc., and Axon Instruments, Inc., for providing equipment. This research was carried out in the Grass Laboratory at the Marine Biological Laboratory, Woods Hole, Massachusetts, and was supported by the Grass Foundation.

Literature Cited

1. **Buck, L., and R. Axel. 1991.** *Cell* **65:** 175–187.
2. **Clyne, P. J., C. G. Warr, M. R. Freeman, D. Lessing, J. Kim, and J. R. Carlson. 1999.** *Neuron* **22:** 327–338.
3. **Vosshall, L. B., H. Amrein, P. S. Morozov, A. Rzhetsky, and R. Axel. 1999.** *Cell* **96:** 725–736.
4. **Gao, Q., B. Yuan, and A. Chess. 2000.** *Nature Neurosci.* **3:** 780–785.
5. **Vosshall, L. B., A. M. Wong, and R. Axel. 2000.** *Cell* **102:** 147–159.
6. **Ressler, K. J., S. L. Sullivan, and L. B. Buck. 1994.** *Cell* **79:** 1245–1255.
7. **Stopfer, M., M. Wehr, K. MacLeod, and G. Laurent. 1999.** Pp. 163–180 in *Insect Olfaction*, B. S. Hansson, ed. Springer, Berlin.
8. **Adrian, E. D. 1942.** *J. Physiol. Lond.* **100:** 459–473.
9. **Delaney, K. R., and J. B. Hall. 1995.** *J. Neurosci. Methods* **68:** 193–202.
10. **Gray, C. M. 1994.** *Neurosci.* **1:** 11–38.
11. **Tank, D. W., A. Gelperin, and D. Kleinfeld. 1994.** *Science* **265:** 1819–1820.
12. **Lam, Y.-W., L. B. Cohen, M. Wachowiak, and M. R. Zochowski. 2000.** *J. Neurosci.* **20:** 749–762.
13. **Stocker, R. F., and V. Rodrigues. 1999.** Pp. 283–314 in *Insect Olfaction*, B. S. Hansson, ed. Springer, Berlin.

Reference: *Biol. Bull.* **199:** 171–173. (October 2000)

Circadian Rhythms in the Receptive Fields of the *Limulus* Lateral Eye

James M. Hitt (Marine Biological Laboratory, Woods Hole, Massachusetts 02543),
Frederick A. Dodge, Ehud Kaplan, and Robert B. Barlow

Hartline found that in the frog "a given optic nerve fiber responds to light only if a particular region of the retina receives illumination." He called the region the receptive field of that fiber (1). Continuing Hartline's study of the frog retina, H. B. Barlow detected an inhibitory influence surrounding the excitatory region of the receptive field (2). In the lateral eye of the horseshoe crab *Limulus polyphemus,* the receptive fields of single ommatidia have both excitatory centers and inhibitory surrounds. The field of view of a single ommatidium defines the narrow excitatory center, whereas the neural network connecting neighboring ommatidia (~200) generates the wide inhibitory surround. A circadian clock in the animal's brain transmits signals to the lateral eye at night, changing its structure and function to increase the retinal sensitivity (3) so that the animal can detect mates nearly as well at night as it can during the day (4). Several mechanisms underlying the remarkable nighttime sensitivity have been identified: they are increased photoreceptor gain, decreased photoreceptor noise, decreased lateral inhibition, and increased photon catch as a consequence of an increased acceptance angle for each ommatidium (3).

High retinal sensitivity at night is associated with highly variable ("noisy") optic nerve responses, which result from random photon events at low nighttime levels of illumination. Such noisy neural responses hinder our efforts to measure properties of the nighttime state of the eye and, thus, our development of an accurate cell-based model of retinal function. Our goal is to understand the neural code the eye sends to the brain at night as we have already done for the daytime state of the eye (5, 6). Here we report an analysis of retinal receptive fields and demonstrate how their properties change from day to night.

Our method takes advantage of the remarkable linearity of the responses of the lateral eye to small modulations of the visual input. We employ time-varying sinusoidal stimuli and linear systems analysis. Modulated square patterns are presented on a TV monitor having a grey background, with nighttime stimuli attenuated by a 4.25 log unit neutral density filter. After isolating the response of a single optic nerve fiber, we align the animal so that the optic axis of the recorded ommatidium views the center of the pattern. We use animals that had been entrained to the natural lighting cycle, taking daytime measurements before 1730 h and nighttime measurements from 2200 to 0100. The square pattern is modulated ±10% relative to the background at 1 Hz. Using a strategy previously developed for studying retinal receptive fields in the frog (2), we measured the width of the excitatory center by illuminating the eye with square stimuli of increasing size. Because the inhibitory surround extends into the excitatory center, responses are a mixture of excitatory and inhibitory inputs; but the responses to the smallest square stimuli are predominantly excitatory.

Figure 1A plots the amplitude of modulated optic nerve responses as a function of the visual angle of the square stimuli during the day (gray points) and night (black points). For each data set, the ordinate scale ranges from no response (0%), to the theoretical maximum excitatory response (100%) that would be achieved in the absence of inhibition. The points plotted in Figure 1A show an increase in response for increasing stimulus size, up to 24° of visual angle, beyond which responses decrease because more of the inhibitory surround is illuminated by the square stimulus. The growth of the responses to expanding stimuli (smooth curves) are estimated from the responses to the smallest square stimuli, because the small stimuli minimally activate the inhibitory surround. Assuming that the excitatory center can be well represented by a two-dimensional gaussian function (3), the "pure" excitatory response is proportional to the volume of the excitatory center surface covered by a stimulus. Using this relationship, we estimated the size of the excitatory center based on the recorded responses to the four smallest square stimuli and extrapolated the theoretical maximum response of the excitatory center (100% on the ordinate in Figure 1A; E_p in Equation [1]). The smooth curves plot the theoretical responses, yielding excitatory centers with half-maximal width of 12° during the day (gray curve) and 16° at night (black curve). Because the size of the excitatory center increased at night, the recorded response reached only 85% of its maximum theoretical value before decreasing as a result of surround inhibition. Although the inhibitory surround overlaps the excitatory center, the effects of surround inhibition are minimal for small squares. We therefore attribute the observed changes in Figure 1A to an expanded excitatory field width at night, arising from circadian changes in ommatidial structure, that is, a shift of photoreceptor position and migration of pigmented cells (3).

The vectors in Figure 1B plot the modulated optic nerve response in terms of its phase and amplitude relation to the stimulus—a sine wave with a direction of 0° (vertical) and a length of 1.0. To measure the strength of the inhibitory surround, we first determine the maximal excitatory response, as described above, and plot it as a vector in Figure 1B (open circles). We next determine the response vector for full-field stimulation by modulating the entire TV monitor with a ±10% contrast at 1 Hz (open squares); this vector represents the summed response of excitatory and inhibitory inputs. Finally, we measure the response vector for inhibition by modulating the surround while holding constant the stimulus to the center (crosses). Because the *Limulus* eye responds linearly to small amplitude stimulation, the effects of excitation and inhibition superimpose; *i.e.*, the sum of center and surround response vectors should equal the full-field response. The vector sum of excitatory and inhibitory responses during the day is plotted as a thin line that lies adjacent to the vector for the full-field response (open square) and thus confirms response linearity. We attribute the discrepancy between the vectors at night to response noise at low nighttime light levels caused by random photon events.

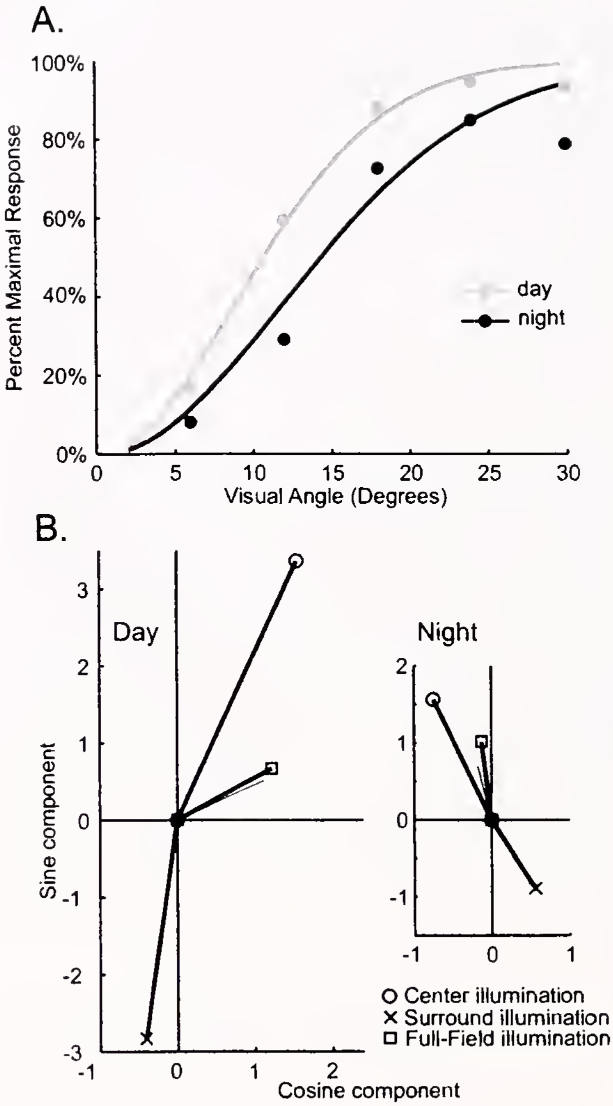

Figure 1. *A: Plot of the response of a single optic nerve (ordinate) as a function of the size of the centrally located visual stimulus (abscissa). Daytime (gray points) and nighttime (black points) responses are normalized to their respective theoretical maximum excitatory response. As expected, the response increases with the size of the stimulus. Solid lines show the growth of the response calculated on the basis of a gaussian-shaped excitatory center. B: Vector plots of responses to illumination of the center (unfilled circle), surround (crosses), and full-field (squares) stimulation. Vectors are plotted relative to the sine wave stimulus, which has an angle of 0° and a length of 1. As explained in the text, responses to center and surround alone predict with reasonable accuracy the response to full-field stimulation, which drives both the excitatory center and the inhibitory surround. Such vector addition confirms the linear properties of the* Limulus *lateral eye. The nighttime vectors show a reduction in the difference between excitation and full-field responses, indicating a decrease in the strength of the inhibitory surround.*

From the Hartline-Ratliff formulations of lateral inhibitory interactions in the retina (7), the firing rate of the p^th^ ommatidium (R_p) equals its pure excitatory response (E_p) minus the sum of inhibitory influences from its neighbors; the inhibition delivered from the j^th^ ommatidium equals the strength of its inhibitory coupling to the p^th^ ommatidium (K_{pj}) multiplied by the response of the j^th^ ommatidium. These relationships can be expressed as:

$$R_p = E_p - \Sigma K_{pj} \times R_j. \qquad (1)$$

For the case of full-field illumination (8), all ommatidia in the eye receive the same illumination and thus respond at the same rate: $R_p = R_j = R$. Equation (1) thus simplifies to:

$$R = E_p - K_{total} \times R, \qquad (2)$$

where K_{total} is the summed total strength of inhibition in the surround, and E_p is the theoretical, maximum response of pure excitation. All responses are measured to stimuli modulated at 1 Hz. Rearranging Equation (2) gives:

$$K_{total} = (E_p - R)/R. \qquad (3)$$

where R is the magnitude of the vector for full-field illumination (square), and E_p is the magnitude of the vector for center modulation (circle). From the data in Figure 1, $K_{total} = 2.2$ during the day, and $K_{total} = 0.8$ at night.

In Figure 1B, the nighttime vector set shows a counterclockwise shift and a reduction in the modulated response amplitudes. The reduction in nighttime vector lengths does not represent a diminution of sensitivity to light, but rather a decreased modulated response to sinusoidal stimulation at 1 Hz. The reduced amplitude and phase shift of the nighttime response vectors result from circadian changes in adaptation and the temporal response properties of the retina.

We conclude, first, that the excitatory center of the receptive field in the lateral eye increases at night. Second, we conclude that the total strength of inhibition in the eye decreases by more than 50% at night. Whether the nighttime decrease in the strength of inhibition also includes a decrease in the size of the inhibitory surround is not yet known, but these results point to a circadian modulation of the synaptic mechanisms that mediate lateral inhibition.

Supported by the National Institute of Mental Health, National Science Foundation, National Eye Institute, Research to Prevent Blindness, and the Central Lions of New York.

Literature Cited

1. **Hartline, H. K. 1940.** *Am. J. Physiol.* **130:** 690–699.
2. **Barlow, H. B. 1953.** *J. Physiol.* **119:** 69–88.
3. **Barlow, R. B., S. C. Chamberlin, and J. Z. Levinson. 1980.** *Science* **210:** 1037–1039.
4. **Barlow, R. B., L. C. Ireland, and L. Kass. 1982.** *Nature* **296:** 65–66.
5. **Passaglia, C. L., F. A. Dodge, E. H. Herzog, S. Jackson, and R. B. Barlow. 1997.** *Proc. Natl. Acad. Sci. USA* **94:** 12649–12654.
6. **Passaglia, C. L., F. A. Dodge, and R. B. Barlow. 1998.** *J. Neurophysiol.* **80:** 1800–1815.
7. **Ratliff, F. 1974.** *Studies of Excitation and Inhibition in the Retina.* Rockefeller University Press, New York.
8. **Barlow, R. B., and D. A. Quarles. 1975.** *J. Gen. Physiol.* **65:** 709–730.

Reference: *Biol. Bull.* **199:** 173–174. (October 2000)

Frequency Response of Auditory Brainstem Units in Toadfish (*Opsanus tau*)

Richard R. Fay and Peggy L. Edds-Walton (Loyola University Chicago, Chicago, Illinois 60611)

Toadfish are vocal teleosts. Both males and females produce a pulsed grunt in agonistic contexts. In addition, male toadfish call during courtship, using a "boatwhistle" sound to attract females to the nest. This sound consists of rapidly repeated pulses having a fundamental frequency (F_0) of about 130 to 220 Hz in the Woods Hole area, and several higher harmonics up to about 800 Hz (1; Edds-Walton, Mangiamele, and Rome, unpub. obs.). These and other sounds are thought to be detected by the sacculi, which respond to the particle motion component of underwater sound (2). Previous studies (2, 3) showed that primary saccular afferents respond in a phase-locked and directional manner to particle motions as small as 0.1 nm in the frequency range from below 50 Hz to above 200 Hz. One goal of this work is to understand the brain's representations of the boatwhistles that these fish use during the breeding season. The present study focused on the range of frequencies represented in the brainstem, including the descending octaval nucleus of the medulla (DON), and the torus semicircularis (TS) of the midbrain. The DON is one of the medullary nuclei that receives input from saccular afferents and is known to be a site of auditory processing (4). Previous work has also shown that toadfish DON cells project to the TS, primarily contralaterally (5).

Extracellular recordings were made from single units of the left side of the brain, at 20–22°C, as they responded to oscillatory motion at a range of frequencies between 50 and 303 Hz. Recording electrodes were either metal-filled glass pipettes with tip diameters of about 10 μm (6), or 3 *M* NaCl, 4% neurobiotin-filled pipettes with tip diameters of 3–7 μm. For medullary recordings, the DON was sampled between the entrances of cranial nerves VIII and IX. For midbrain recordings, electrodes were advanced through the optic tectum to the TS. Stimuli were created with a three-dimensional shaker system, described previously (2, 7), as linear oscillations at −30° azimuth (to the left front and right rear) in the horizontal plane, and at 0° elevation [the best direction for a majority of saccular afferents (2, 4)]. Tone bursts (500 ms in duration, including 20-ms rise-fall times) were presented at equal displacement levels, eight times each, at 50, 65, 84, 100, 141, 185, 244, and 303 Hz. Average spike rate was plotted as a function of tone frequency to define the frequency response areas. Frequency response areas were typically determined at four or more stimulus

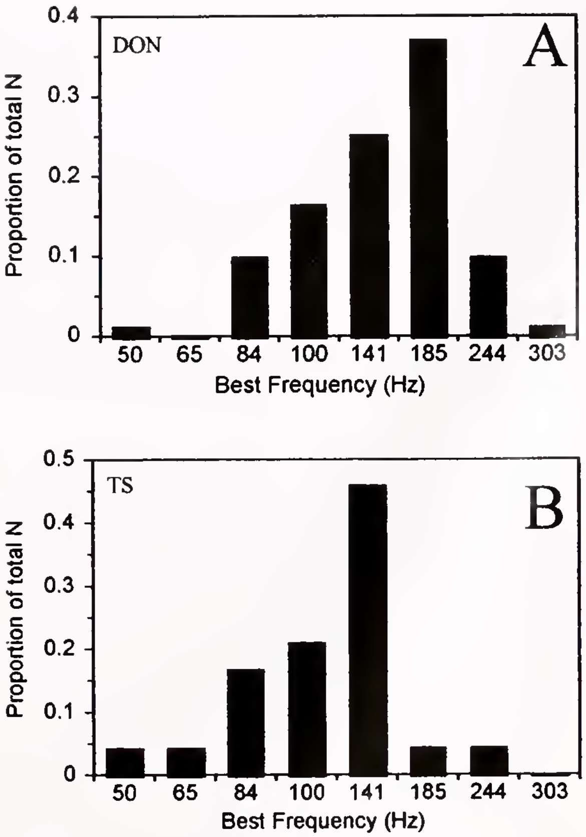

Figure 1. *Frequency distributions of single unit best frequencies (BF) for units recorded in the descending octaval nucleus (DON, A:* n = *92) and the torus semicircularis (TS, B:* n = *24) of the toadfish. The numbers along the abscissa give the stimulus tone frequencies used, and the abscissa is approximately logarithmically scaled.*

levels within a unit's dynamic range (generally between −10 and 30 dB re: 1 nanometer, root mean square). Ninety-two units of the DON (23 animals, 6 of which were females), and 24 units of the TS (12 animals, 3 of which were females) have been successfully characterized. A unit's best frequency, or BF, was defined as the stimulus frequency producing the greatest spike rate at the approximate center of the unit's dynamic range. Frequency response range was defined as the frequency range within which the unit responded at or above 50% of the maximum spike rate (at BF).

Figure 1 shows frequency distributions of BF for the DON units (A-top) and TS units (B-bottom). The lowest BF was 50 Hz (or less), and the highest was 303 Hz (or more). Most BFs were between 100 and 185 Hz. The mode for BF was 185 Hz for DON cells, and 141 Hz for TS cells. There were no differences in the range of BFs for males *versus* females. The single animal with a BF of 303 was male. While the distributions for both recording sites overlap substantially, relatively fewer units with BFs above 141 Hz were found in the TS. This could be due to sampling error, or it might have resulted from a nonhomogeneous spatial distribution of BF within the TS, which was not explored as systematically as the DON. Frequency response area widths averaged 64 Hz for TS and 117 Hz for DON. This difference probably reflects the lower mean BF for the TS distribution.

Because the fundamental frequency of the boatwhistles recorded in the Woods Hole area varies between 130 and 220 Hz, these results indicate that most, but not all, auditory brainstem cells of the toadfish represent F_0. Thus, contrary to a previous report (8), there is a good "match" between the fundamental frequency of the vocalization and the response of the auditory portions of the brain. In addition, because the highest BF is about 303 Hz, the higher harmonics of the boatwhistle (first harmonic at 360 to 440 Hz), so evident in field recordings (at 19°–22°C; Edds-Walton, Mangiamele, and Rome, unpub. obs.), are probably not represented by the brain, and thus may play no role in boatwhistle perception or other behaviors. The neural representations of the boatwhistle encode the fundamental frequency only. Although not demonstrated experimentally as yet, this frequency is probably equivalent to the rate at which muscular contractions to the swimbladder occur during generation of the sound.

Supported by an R01 grant from NIH, NIDCD to R.R.F.

Literature Cited

1. **Watkins, W. A. 1967.** Pp. 15–43 in *Marine Bioacoustics*. W. N. Tavolga, ed. Pergamon Press, New York.
2. **Fay, R. R., and P. L. Edds-Walton. 1997.** *Hear. Res.* **111:** 1–21.
3. **Fay, R. R., and P. L. Edds-Walton. 1997.** *Hear. Res.* **113:** 235–246.
4. **Edds-Walton, P. L., R. R. Fay, and S. M. Highstein. 1999.** *J. Comp. Neurol.* **411:** 212–238.
5. **Edds-Walton, P. L. 1998.** *Hear. Res.* **123:** 41–54.
6. **Dowben, R. M., and J. D. Rose. 1953.** *Science* **118:** 22.
7. **Fay, R. R. 1984.** *Science* **225:** 951–954.
8. **Fine, M. 1981.** Pp. 257–263 in *Hearing and Sound Communication in Fishes*, W. N. Tavolga, A. N. Popper, and R. R. Fay, eds. Springer-Verlag, New York.

Reference: *Biol. Bull.* **199:** 175–176. (October 2000)

Intrinsic Membrane Properties of Laryngeal Motoneurons that Control Sexually Differentiated Vocal Behavior in African Clawed Frogs, *Xenopus laevis*

Ayako Yamaguchi, Leonard K. Kaczmarek[1]*, and Darcy B. Kelley (Department of Biological Sciences, Columbia University, Sherman Fairchild, MailCode 2430, New York, New York 10027)*

Males and females behave differently during reproduction. Although sexually differentiated patterns of behavior in vertebrates are clearly regulated by the action of gonadal steroids, the neural mechanisms underlying the expression of sex-specific behavior are largely unknown.

Male and female African clawed frogs (*Xenopus laevis*) produce sexually distinct vocalizations composed of a series of clicks. The fundamental difference between male and female calls is the rate at which the clicks are repeated (reviewed in 1); male calls cover a wide range of click repetition rates (8 to 80 Hz), whereas female calls contain only slow repetition rates (2 to 20 Hz). This behavioral difference can conveniently be reduced to the sexual difference in contraction rate of laryngeal muscle (2), which, in turn, is determined by the sexually distinct firing patterns of laryngeal motoneurons (3). Thus, there is a direct correspondence between the sexually dimorphic patterns of vocalization and the activity of motoneurons.

How, then, do male and female laryngeal motoneurons produce sex-specific patterned activity? While the overall pattern is probably produced by a pattern generator upstream of the motoneurons, the motoneurons themselves may have intrinsic membrane properties that differ between male and female *Xenopus*. Testing this possibility was the goal of this study.

Whole-cell patch clamp recordings were used to characterize the membrane properties of laryngeal motoneurons in n.IX-X of adult male and female *Xenopus*. A thick brain slice preparation of *Xenopus* hindbrain was developed, and the neurons were visualized by IR/DIC microscopy. To facilitate identification, the motoneurons were retrogradely labeled with fluorescent dye (AlexaFluor 594 biocytin, Molecular Probes, Eugene, OR) before the brain was sliced. Responses to hyperpolarizing and depolarizing current steps (200 ms long) by 6 male and 10 female motoneurons (3 male and 6 female frogs), were recorded in current clamp mode. The resting membrane potential, threshold, spike amplitude, and spike half-width were directly measured from voltage traces. The membrane time constant was determined by fitting single exponential curves to hyperpolarizing voltage responses. Input resistance was calculated from the steady-state membrane potential in response to different hyperpolarizing current pulses. The capacitance of the cell was calculated from input resistance and time constant. The peak firing rate was determined by measuring the interval between the first two action potentials in response to the largest depolarizing current (1.5–2nA) applied to each neuron.

Membrane properties of male and female motoneurons are summarized in Table I. All the properties measured are statistically similar in the two sexes except for the input resistance and the cell capacitance; input resistance is significantly lower, and the cell capacitance is significantly higher in male motoneurons than in female motoneurons. These differences predict that male motoneurons are larger than female motoneurons. A previous study has shown that the dendrites of male n.IX-X neurons are longer than those of female n.IX-X neurons, although the somal size is similar in the two sexes (4). The difference in the dendritic arborization may account for the differences in input resistance and cell capacitance in the two sexes. Functionally, sexual differences in the input resistance imply that the male and female motoneurons exhibit different responsiveness to synaptic input.

At depolarized membrane potentials, all the motoneurons showed repeated action potential firing that accommodated over a time course of 100 ms. The peak firing rates, determined by the first two spikes in response to depolarizing currents, were well over 100 Hz in both sexes. To determine whether the neurons could maintain this rapid firing frequency for more than two spikes, four female and two male motoneurons were stimulated with trains of depolarizing pulses at various rates (0.5 ms, 7–10 V, 10 to 300 Hz). Both male and female motoneurons could follow the depolarizing pulses at frequencies of at least 90 Hz. Although the maximum click rate of female vocalizations is 20 Hz, and that of male calls is 80 Hz, the motoneurons of both sexes can fire at a much higher frequency than is required for call production.

Taken together, the results suggest that the laryngeal motoneurons of *Xenopus* do not limit the click repetition rate, and that the motoneurons may be sexually differentiated in their responsiveness to synaptic input.

Table I

Basic membrane properties of male and female laryngeal motoneurons of adult Xenopus laevis

Membrane properties	Male (n = 6)	Female (n = 10)	P-value
Resting membrane potential (mV)	−49.1 ± 1.2	−48.1 ± 2.5	n.s.
Time constant (ms)	9.15 ± 0.91	11.46 ± 1.44	n.s.
Input resistance (MΩ)	69.4 ± 3.9	182.4 ± 25.7	$P < 0.01$
Cell capacitance (nF)	0.148 ± 0.017	0.066 ± 0.009	$P < 0.01$
Spike amplitude (mV)	35.56 ± 3.81	35.94 ± 4.30	n.s.
Spike half-width (ms)	0.69 ± 0.10	0.67 ± 0.11	n.s.
Threshold (mV)	−29.11 ± 10.25	−36.14 ± 3.12	n.s.
Highest firing frequency (Hz)	192.17 ± 29.47	257.40 ± 25.86	n.s.

---

[1] Department of Pharmacology, Yale University School of Medicine, 333 Cedar Street, New Haven, CT 06520.

Literature Cited

1. **Kelley, D. B. 1996.** Pp. 143–176 in *Biology of Xenopus*, R. C. Tinsley, and H. R. Kobel, eds. Clarendon Press, Oxford.
2. **Tobias, M., and D. B. Kelley. 1987.** *J. Neurosci.* **7:** 3191–3197.
3. **Yamaguchi, A., and D. B. Kelley. 2000.** *J. Neurosci.* **20:** 1559–1567.
4. **Kelley, D. B., S. Fenstemaker, P. Hannigan, and S. Shih. 1988.** *J. Neurobiol.* **19:** 413–429.

Reference: *Biol. Bull.* **199:** 176–178. (October 2000)

Optic Nerve Responses of *Limulus* in its Natural Habitat at Night

Jillian L. Atherton[1], Matthew A. Krutky[2], James M. Hitt[3], Frederick A. Dodge, and Robert B. Barlow
(Marine Biological Laboratory, Woods Hole, Massachusetts 02543)

What information does the eye send to the brain when an animal sees? We are exploring this question with the relatively simple visual system of the horseshoe crab, *Limulus polyphemus*. By combining cell-based computational models of the retina with single-cell electrophysiology, we have examined the optic nerve code underlying *Limulus* vision during the day in the animal's natural habitat (1).

Field studies during the animals' mating season show that male horseshoe crabs use vision to find mates and do so about equally well day and night (2). We attribute their remarkable nighttime vision to a circadian modulation of the sensitivity of their lateral eyes (3). At night, efferent optic nerve fibers carry signals from the circadian clock in the animal's brain to its eyes, increasing nighttime retinal sensitivity as much as 1,000,000 times. The increased sensitivity nearly compensates for the average 1,000,000-fold decrease in ambient light intensity after sundown. Here we investigate optic nerve activity recorded from the animal in its habitat, both day and night, with emphasis on signals that convey information about potential mates at night.

A convenient method for recording what the horseshoe crab sees underwater is to mount a miniature video camera, "CrabCam," on the animal (1). This documents the crab's eye view during the day, but not at night when light levels fall below the camera's sensitivity. To investigate the optic nerve responses of an animal in its natural habitat at night, we used a repetitive, artificial stimulus that simulates the movement of a potential mate within the animal's visual field. The stimulus is a rotating grey cylinder (30 cm in diameter, 15 cm in height) with a black sector (30 cm in width) that simulates the size of a typical female horseshoe crab. The cylinder was placed 1 m from the crab and rotated by hand (4–8 rpm), moving the black sector horizontally at 7–13 cm/s, which simulates the average speed of a horseshoe crab. Our strategy is as follows: first, during the day and under water, we record the optic nerve response of a stationary crab to the rotating cylinder while simultaneously videotaping the eye's input with the shell-mounted CrabCam. This allows us to document the visual input when ambient light levels are sufficient for CrabCam operation. We then leave the animal and cylinder in place underwater until after sundown, when we repeat the experiment carried out during the day, but of course without the Crabcam. This method allows us to record the response of the eye to a known visual stimulus at night in the animal's natural habitat.

We recorded the response of single optic nerve fibers following a procedure developed in this laboratory (1). In brief, we trephine a hole in the carapace about 2 cm anterior to the right lateral eye, expose the optic nerve trunk, and draw it into a chamber that is then attached to the carapace. We tease away a single active optic nerve fiber corresponding to a single ommatidium and pull it into a micro-suction electrode. The chamber is sealed to make it water tight, and then a small point light source is used to locate the optic axis of the recorded ommatidium. We then mount the CrabCam on the carapace and align it in the direction of view of the recorded ommatidium. The CrabCam (72° by 54° field of view) encompasses about a quarter of the hemispheric view of the lateral eye, which is seen by about 250 ommatidia, each viewing about a 6° region during the day and about a 12° at night (4). The animal is firmly attached to a weighted platform that is placed on the sandy bottom of the animal's habitat and oriented so that the optic axis of the recorded ommatidium intersects the axis of rotation of the cylinder located about 1 m away. Experiments were carried out at depths of 0.5–1 m in estuaries near the Marine Biological Laboratory in Massachusetts. Signals from the microsuction electrode and the CrabCam are led *via* shielded cables (13 m in length) to a portable camcorder on shore or in a nearby boat.

Figure 1 (right) shows two video frames taken with the CrabCam during the day. These frames show the rotating cylinder at two distances (.87 m and 1 m) from the horseshoe crab. On the left are 14 s samples ("Day") of the responses of a single optic nerve fiber to rotations of the cylinder at the two distances from the crab. The video frames were taken 6 s after the beginning of the response records (arrows), when the grey-black edge of the cylinder began to enter the field of view of the recorded ommatidium from the right. In both cases, the black sector evoked clear decreases in response, with the larger decrease recorded when the cylinder was closer to the animal and water turbidity was minimal. The top "Day" response was recorded at 1630 h and the second was recorded at 1800 h. In both cases, the setup was bathed in direct sunlight. After the second record was recorded, the animal and cylinder were left underwater as nightfall approached.

The experiment was then repeated several hours later after sundown (2030–2100 h) but without CrabCam recordings because of insufficient lighting. Figure 1 ("Night") displays the responses of the same single optic nerve fiber to nine sequential rotations of the cylinder (thin black traces). The heavy black trace gives the average of the nine responses. Note that the individual responses

---

[1] Allegheny College, Meadville, PA.

[2] Syracuse University, Syracuse, NY.

[3] Upstate Medical University, Syracuse, NY.

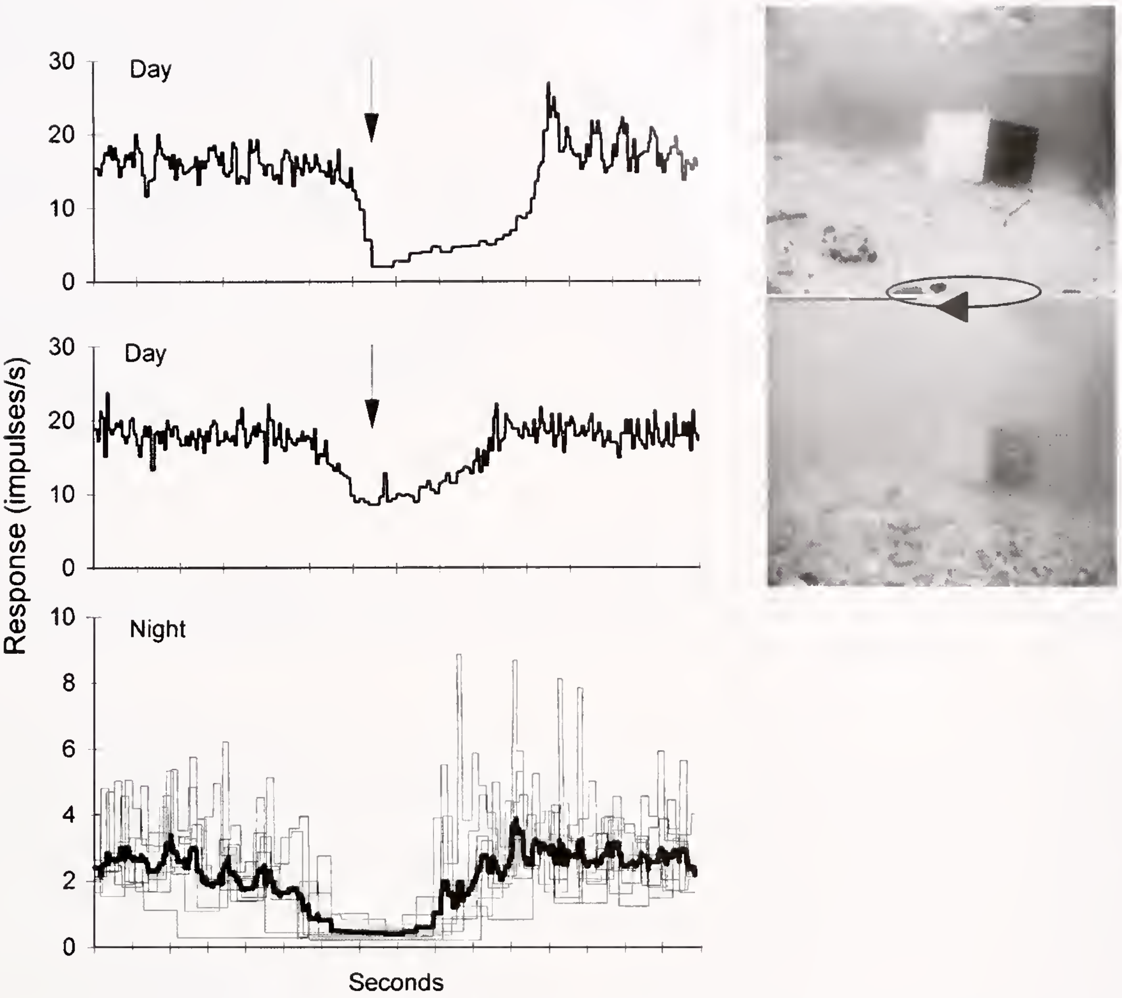

Figure 1. *The responses of a single ommatidium to an underwater rotating visual stimulus. The records on the left plot the instantaneous frequency (reciprocal of the interval between adjacent optic nerve impulses) as a function of the rotation of the stimulus shown on the right. The speed of rotation is approximately the same for all records. The visual stimulus is aligned so that the optic axis of the recorded ommatidium is centered on the rotating cylinder with its field of view lying within the black sector. At a distance of 1 m the black sector intercepts the optic axis of about 9 ommatidia. The "Day" responses were recorded between 1630 and 1800 h, and the "Night" responses were recorded between 2030 and 2100 h. The top video frame was taken in the clear water of Great Harbor, Woods Hole, Massachusetts, where the grey/black sectors of the cylinder had a contrast of 69% [contrast =* $(L_{Grey} - L_{Black})/(L_{Grey} + L_{Black})$*]. The second video frame was taken near Stoney Beach, Woods Hole, where turbid water reduced the contrast of the grey/black sectors to 26%. Arrows indicate the times at which the underwater scenes to the right were videotaped. At these times the black sector begins to enter the field of view of the recorded ommatidium, reducing its response rate. The "Day" records are responses to a single rotation of the cylinder in a right to left direction (loop with arrow). The "Night" records show responses to nine consecutive rotations of the cylinder (thin black traces; period of rotation ~ 16 s) and their average (thick black trace). The peaks and valleys of the thin black traces reflect the highly variable rate of discharge of the single optic nerve fiber under low nighttime levels of illumination.*

are highly variable relative to those recorded during the day, and that the average response rate to the grey sector is about 3 impulses/s which is 6-fold lower than the mean daytime response rate of about 18 impulses/s (middle trace). We attribute the highly variable response rates to random photon events occurring at the very low nighttime levels of illumination. The nighttime sky during this experiment was heavily overcast and lacked moonlight. From radiometric measurements we estimate that ambient light decreased by about 10^6 to 10^7 relative to daytime levels. The circadian increase in lateral eye sensitivity cited above nearly compensates for such large reductions in ambient lighting. Experiments in the laboratory (R. Barlow and F. Dodge, unpub. obs.) indicate that the average response to the grey sector of ~3 impulses/s is about 50% lower than expected for the low nighttime levels of illumination. The surgery performed to isolate the single optic nerve fiber may have partially damaged the fragile efferent fibers that carry the circadian clock's signal from the brain to the eye; as a consequence, the lateral eye may not have received the normal efferent input and thus the retina may not have shifted completely to its fully sensitive nighttime state. Nevertheless the eye's circadian increase in sensitivity was sufficient to detect the rotating black sector of the cylinder, which mimics a moving mate.

Computational analyses of visual processing in the *Limulus* brain indicate that retinal inputs may sum at the first synaptic level

(5). Spatial summation across a matrix of 5–10 ommatidia significantly increases the signal-to-noise properties of responses recorded at night. Indeed summing seven sequential optic nerve responses to the rotating cylinder yielded a relatively noise-free response.

These experiments represent our first attempts to analyze lateral-eye responses of *Limulus* at night in the animal's natural habitat. The use of a periodic stimulus obviated the need for video documentation of the visual stimulus, which is not feasible under nighttime lighting conditions. With this technique, we successfully recorded visual responses in the animal's habitat and found that the lateral eye transmits information to the brain about mate-like objects at night under dark overcast skies. Under such conditions *Limulus* could see what we could not.

Supported by the National Science Foundation, National Institute of Mental Health, National Eye Institute, Research to Prevent Blindness, and the Central Lions of New York.

Literature Cited

1. **Passaglia, C., F. Dodge, E. Herzog, S. Jackson, and R. Barlow. 1997.** *Proc. Natl. Acad. Sci.* **94:** 12649–12654.
2. **Barlow, R. B., L. C. Ireland, and L. Kass. 1982.** *Nature* **296:** 65–66.
3. **Barlow, R. B. 1983.** *J. Neuroscience* **3:** 856–870.
4. **Barlow, R. B., S. C. Chamberlain, and S. C. Levinson. 1980.** *Science* **210:** 1037–1039.
5. **Hitt, J., C. Passaglia, F. Dodge, and R. Barlow. 2000.** *Ninth Annual Computational Neuroscience Meeting.* Brugge, Belgium. p. 75.

Reference: *Biol. Bull.* **199:** 178–180. (October 2000)

Do the Properties of Underwater Lighting Influence the Visually Guided Behavior of Limulus?

Matthew A. Krutky[1], *Jillian L. Atherton*[2], *Spence Smith, Frederick A. Dodge and Robert B. Barlow*
(Marine Biological Laboratory, Woods Hole, Massachusetts 02543)

In the spring, horseshoe crabs, *Limulus polyphemus,* migrate to the water's edge along the East coast of the United States to pair off and build nests (1). As they enter a nesting area, males use their lateral eyes to locate mates both day and night (2). They approach females and objects resembling them, such as rocks, patches of seaweed, or mate-like objects. What does a male see in a female? Her size and contrast are two important factors. Males are attracted to objects that approximate the size of females. They orient toward mate-like objects at distances up to 1.2 meters, detecting higher contrast objects better than lower contrast ones (3). How do the properties of underwater lighting in the animal's natural habitat influence whether a crab finds a mate during the day or at night? The approximate 1,000,000-fold reduction in ambient lighting after sundown has no appreciable effect. Their remarkable visual performance results in part from a circadian increase in lateral eye sensitivity of as much as 1,000,000 times at night (4). In this paper we consider another property of the animal's underwater habitat, termed "strobic lighting."

In the shallow waters of nesting areas, overhead waves act like lenses, creating moving beams of sun- and moonlight that reflect off the sandy bottom and submerged objects. On average, the peak intensity of these beams is about three times that of ambient illumination. The fields of view of single ommatidia are wider than the moving beams of light. Because ommatidia sum the illumination within their field of view, the amplitude of modulation of the light beams reaching the underlying photoreceptor cells decreases to about 70% contrast. The strobic illumination by the beams strongly modulates the firing rate of an ommatidium, with peak firing rates reaching three times the mean (5). Such strobic illumination might be expected to enhance the detectability of underwater objects, such as potential mates. Indeed, an earlier study suggested that strobic conditions enhance the visibility of low contrast mate-like objects, and that without strobing, *Limulus* is attracted to higher contrast objects (6). We have further explored the influence of strobic lighting by carrying out more field studies and combining the results with those collected over the past five years.

We investigated the visual performance of *Limulus* during their springtime mating seasons at Mashnee Dike, Bourne, and North Monomoy Island, Chatham, both located in Massachusetts. Our study and those of previous years were carried out day and night under various weather conditions ranging from dense cloud cover to clear skies, yielding 10^5 to 10^7-fold diurnal changes in the intensity of ambient illumination, with an average change of about 10^6. In all our studies, a modified two-alternative forced choice technique adapted from human psychophysics was used (7). As shown in Figure 1, we placed on the sandy bottom a clear Plexiglas chute with a funnel at one end and a narrow chute at the other. Crabs entered the funnel and, upon exiting the chute, were presented with the choice of a black or gray female-sized object; these were located 1 m from the exit of the chute and 1 m from each other, creating an equilateral triangle. The objects were either a hemisphere (diameter of 0.3 m) or a cylinder (height of 0.15 m; diameter of 0.3 m), both approximating the size of an adult female horseshoe crab. The objects were switched periodically during an observation period to avoid any effects of directional bias in behavior. Their black and gray tones represent the greatest range of contrast of the female carapace (8). The black object has a negative contrast of 37% against the background of sand and seawater, and the gray object has a positive contrast of 35%. Animals exiting the chute either approached and contacted one of the two targets or swam by them. In 1999 and 2000, about 60% of animals exiting the chute did not approach or contact either submerged object. The animals passing by both objects were not recorded in the years

---

[1] Syracuse University, Syracuse, New York.

[2] Allegheny College, Meadville, Pennsylvania.

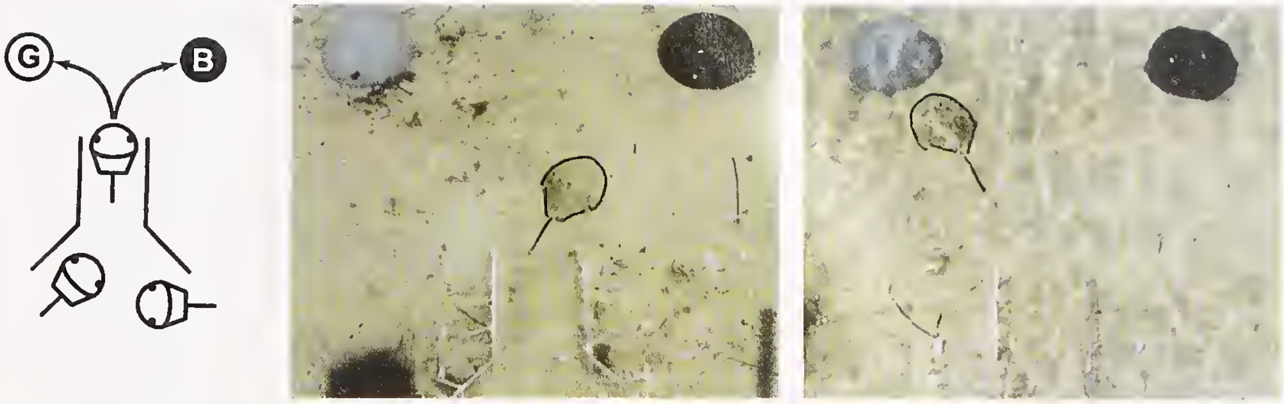

Figure 1. *Left: Diagram of field experiment.* Limulus *approaches the Plexiglas chute and exits toward gray (G) and black (B) mate-like objects located 1 m from the opening and 1 m from each other. Middle: Photograph taken under nonstrobic conditions showing an animal (outlined) exiting the chute and oriented toward the black object. Right: Photograph taken under strobic conditions showing an animal approaching the gray object which is highlighted by bright beams of light. Only the chute and part of the funnel are visible in the photos. Nonstrobic conditions occurred when either no sun or moon was visible, when the wind was calm, or when overhead waves were blocked by a clear-bottom Plexiglas box.*

preceding 1999. More than 99% of the animals studied were males, because animals in amplexus were prevented from entering the funnel, and <1% of single animals in nesting areas are females (1). We could not determine whether a specific male crab passed through the chute more than once in a single observation period, but since animals in nesting areas are abundant, such events are unlikely to have occurred. When an animal exited the chute, observers noted whether the lighting conditions were strobic or nonstrobic. In 1995 through 1998, nonstrobic conditions occurred naturally day and night, under cloudy skies or in calm water. In 1999 and 2000, we controlled strobing by placing a clear-bottomed box on the surface of the water above both targets. The Plexiglas bottom of the box prevented rippling wave action, thereby eliminating strobic lighting of the underwater scene (See Fig. 1).

Table 1 summarizes the data collected in 2000 and during the five previous years. Taken together, the data for all six years ("Total" in Table 1) indicate that, under nonstrobic conditions, there is no significant difference between the number of animals attracted to the two objects day or night (P-values of 0.76 and 0.077 respectively, as determined by the χ^2 test). Under strobic conditions, significantly more animals, 69 or 24% more, approached the gray object during the day ($P < 0.00005$). The greater number of animals, 12, attracted to the gray target at night under strobic conditions, was not significant ($P > 0.4$).

These field studies show that when the distribution of illumination in the animal's natural habitat is uniform (nonstrobic conditions), the animals detect black and gray mate-like objects about equally well day and night. This is understandable because the black and gray objects have about the same absolute contrast, 37% and 35% respectively, against the underwater background. Under strobic conditions, significantly more animals are attracted to the gray object during the day, but not at night. This is also understandable because, as described above, the moving, underwater light beams increase the contrast of the gray object, but not the black one. Indeed optic nerve recordings in the animals' natural habitat reveal bursts of activity in response to gray objects illuminated by strobic light (5). Why the gray objects are not more attractive under strobic conditions at night is not understood. The highly variable optic nerve discharge resulting from random photon events at low levels of nighttime illumination (9) might be masking the bursts of activity generated by strobic lighting. We conclude that the properties of ambient lighting can affect an animal's vision in its natural habitat, particularly during the day. *Limulus* is not unique. Strobic lighting appears to have a prominent role in the visual performance of other marine animals (10, 11).

Supported by the National Science Foundation, National Institute of Mental Health, National Eye Institute, Research to Prevent

Table 1

Number of crabs that exited the chute and hit black or grey targets in the 1995–2000 mating seasons

		Strobic		Nonstrobic	
Year	Time	Black	Gray	Black	Gray
1995	Day	3	7	0	0
	Night	13	10	13	1
1996	Day	16	25	44	41
	Night	16	36	8	2
1997	Day	0	0	17	10
	Night	33	35	10	12
1998	Day	11	13	21	18
	Night	6	9	54	48
1999	Day	30	76	63	87
	Night	28	22	15	16
2000	Day	44	48	193	190
	Night	4	2	5	11
Total	Day	107	176	338	346
	Night	100	112	139	111

Hits were divided into strobic and nonstrobic categories depending on the underwater lighting conditions when an animal left the chute. Strobic refers to moving beams of sun- and moonlight that reflect off the sandy bottom and submerged objects, whereas nonstrobic refers to the absence of this phenomenon.

Blindness, and the Central Lions of New York. Special thanks to Lori Broderick, Hoyt and Deborah Ecker, Elizabeth Flynn, Jason Friedenfelds, Son Gibson, Carrie McGuinnes, Michelle Parshley, and Vanessa Ruta, and the Monomoy National Wildlife Refuge, U.S. Dept. of Interior, Chatham, MA.

Literature Cited

1. **Barlow, R. B., M. K. Powers, H. Howard, and L. Kass. 1986.** *Biol. Bull.* **171:** 310–329.
2. **Barlow, R. B., L. C. Ireland, and L. Kass. 1982.** *Nature* **296:** 65–66.
3. **Herzog, E. D., M. K. Powers, and R. B. Barlow. 1996.** *Visual Neurosci.* **13:** 31–41.
4. **Barlow, R. B. 1983.** *J. Neuroscience.* **3:** 856–870.
5. **Passaglia, C. L., F. A. Dodge, E. Herzog, and R. B. Barlow. 1997.** *Proc. Natl. Acad. Sci. USA.* **94:** 12,649–12,654.
6. **Passaglia, C. L., M. E. McSweeny, K. M. Stewart, E. Kim, E. J. Mole, M. K. Powers, and R. B. Barlow. 1997.** *Biol. Bull.* **193:** 205–207.
7. **Teller, D. Y. 1979.** *Infant Behav. and Dev.* **2:** 135–153.
8. **Herzog, E. D., and R. B. Barlow. 1992.** *Visual Neurosci.* **9:** 571–580.
9. **Atheron, J. L., M. A. Krutky, J. Hitt, F. Dodge, and R. B. Barlow. 2000.** *Biol. Bull.* **199:** 176–178.
10. **Loew E. R., and W. N. McFarland. 1990.** Pp. 1–40 in *Visual System of Fish.* R. H. Douglas and M. B. A. Djagmoz, eds. Chapman and Hall, London.
11. **Glantz, R. M., and A. Bartels. 1994.** *J. Neurophysiol.* **71:** 2168–2182.

Reference: *Biol. Bull.* **199:** 180–182. (October 2000)

Startle Responses of Fish Without Mauthner Neurons: Escape Behavior of the Lumpfish (*Cyclopterus lumpus*)

Melina E. Hale (Dept. of Neurobiology and Behavior, SUNY Stony Brook, Stony Brook, New York 11794-5230 and Grass Foundation Fellow, Marine Biological Laboratory, Woods Hole, Massachusetts 02543)

Fast start escape responses are the primary behaviors used by fishes to avoid an attacking predator. Of particular importance is the C-start type of fast start (reviewed by 1, also see 2, 3). During a C-start the fish rapidly turns away from a threatening stimulus into a "C" shaped body bend, called stage 1. Frequently, stage 1 is followed by a tail stroke to the opposite side of the body, stage 2, which propels the fish away from the stimulus. The C-start is initiated by the Mauthner cells, a pair of large reticulospinal interneurons (4, 5). Each M-cell has a large axon that crosses the body midline and extends the length of the spinal cord, exciting motoneurons that innervate the lateral muscle. In response to a stimulus from the right side of the body, the right M-cell fires an action potential that propagates rapidly down the axon to cause nearly simultaneous contraction of muscle on the opposite side of the body from the M-cell soma and the "C" bend away from the stimulus (6, 7).

Although Mauthner cells have been identified in a large number of taxa broadly representing the phylogenetic diversity of actinopterygian fishes, a few species appear to lack these neurons (8). This study examines the startle behavior of one such species, the lumpfish (*Cyclopterus lumpus*). Two specific questions are addressed. First, do lumpfish have a startle response that is distinct from routine swimming? If so, how does the behavioral pattern and performance compare with the M-cell initiated C-start of other fishes?

The startle response was examined in larval lumpfish rather than in mature individuals. The larval lumpfish have a more generalized morphology than mature lumpfish, and so it was thought that the response of the larvae to a startle stimulus may be more easily compared to other species. Additionally, it seemed that if the lumpfish were to have high performance behavioral responses to predation, it would be seen in the larvae because of greater vulnerability to predators due to less developed morphological defenses. It is possible that M-cells are present in larval lumpfish and are reduced or lost during development; however, morphological examination of the reticulospinal neurons of the larval lumpfish ($n = 30$) with retrograde labeling has not identified Mauthner neurons or homologous cells.

For studies of behavior, lumpfish ($n = 12$; 6.2 ± 1.0 mm, total length) were hatched from eggs collected off the coast of Gloucester, Massachusetts, at approximately 6 m depth. Eggs and larvae were maintained in a 10-gallon aquarium with flow-through seawater chilled to 11°C. Behavioral trials were conducted within a week of hatching. A tactile stimulus—touching the head with a fine gauge wire—was used to elicit startle behavior which was filmed in a small petri dish (3.5 cm diameter). The responses were captured on high-speed video (1000 Hz) taken with an EG&G Reticon digital camera imaging through a Zeiss Stemi SR microscope. Three trials from each fish (36 total trials) were analyzed with Microsoft Excel 98 and Scion Image 1.6. Parameters examined were the angles of head movement during stage 1 and stage 2, the latency between stimulus and response, and the durations of stages 1 and 2.

The larval lumpfish respond to the stimulus with a C-start behavior pattern (Fig. 1A). Fish turned tightly away from the stimulus direction in stage 1 [Fig. 1A, left column (0–24 ms)] with an average stage 1 angle of 146° ± 23°C degrees. Stage 1 was consistently followed by a stage 2 tail stroke [Fig. 1A, right column (24–56 ms)] and movement away from the stimulus. The stage 2 angle, generally in the opposite direction of the stage 1

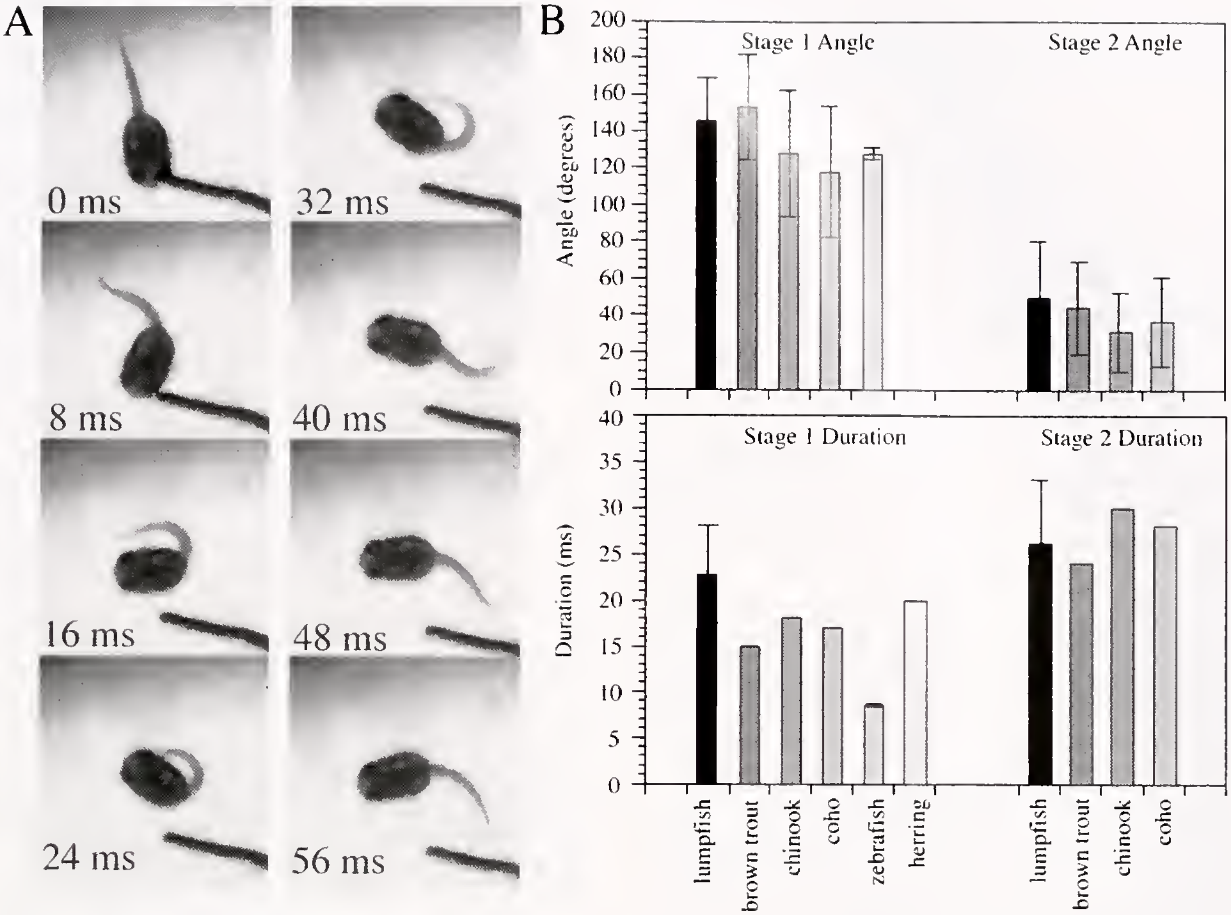

Figure 1. *A. A typical startle response of larval lumpfish (*Cyclopterus lumpus*). Stage 1, the tight "C" bend away from the stimulus, lasts 24 ms (column 1) and stage 2, the first propulsive tail stroke, follows from 24 to 56 ms (column 2). Data for the angle of movement and kinematic stage durations are shown in B, with comparative data from brown trout (*Salmo trutta*), chinook salmon (*Oncorhynchus tshawytscha*), coho salmon (*Oncorhynchus kiisutch*) (10, minimum values in scaling relationships), zebrafish (*Danio rerio*) (9), and herring (*Clupea harengus*) (12).*

turn, was consistently smaller than that of stage 1 (stage 2 angle = 50° ± 30°). The movement angles made by larval lumpfish during the C-start are comparable to those of other species (Fig. 1B; *e.g.* 9, 10, 12, 13).

Several important fast start performance variables are the latency of response to the stimulus and the duration of the kinematic stages. The latency between stimulus and initiation of movement of an M-cell initiated startle can take less than 4 ms (9) and the duration of the response is generally less than 100 ms (1). The latency of the lumpfish, recorded for a subset of the trials (one from each of 10 individuals) was 9 ± 2.1 ms. It was considerably longer than that of the larval zebrafish (3.9 ± 0.2 ms) (9). The duration of stage 1 of the larval lumpfish was 22.8 ± 5.2 ms, and the duration of stage 2 was 26.3 ± 6.8 ms. Because the duration of the fast-start stages changes with size (11) and developmental stage (10), direct comparisons among species are difficult. Still, the durations of kinematic stages 1 and 2 of the larval lumpfish are in the same range of values as other immature fishes; all under 5 cm (Fig. 1B; 9, 10, 12). The total duration of the fast start (stages 1 and 2) for the larval lumpfish is shorter than the fast start duration of most larger fishes (reviewed in 1).

Although the lumpfish has a longer response latency to a startle stimulus than zebrafish larvae, the C-start of the larval lumpfish—in pattern and in the duration of response—has the characteristics of the M-cell initiated C-start. One explanation for the similarities in the startle response among taxa is that the Mauthner cell and its homologs are present in the larval lumpfish but have not yet been identified. Another is that alternative neural circuits can generate rapid C-start behavior and that the Mauthner cell and its homologs are most critical for rapid initiation of movement. If so, such mechanisms may be taxon specific since ablating the Mauthner cell and its homologs in the larval zebrafish results in a significant decrease in performance (9). The presence of a rapid C-start type escape behavior in the lumpfish, a species that appears to generate the fast start behavior without the Mauthner cell system, provides an exciting opportunity for comparative examination of an evolutionarily conserved neural and behavioral system.

I thank S. Van Sant and J. Fetcho for their contributions of fish and equipment, respectively. Thanks to S. Zottoli and M. Westneat for helpful discussion and advice on this paper and to the reviewers of this paper for their comments. This project was supported by a Grass Foundation Fellowship and a NIH NRSA fellowship (MH 11861).

Literature Cited

1. **Domenici, P., and R. W. Blake. 1997.** *J. Exp. Biol.* **200:** 1165–1178.
2. **Weihs, D. 1973.** *J. Theor. Biol.***106:** 189–206.
3. **Webb, P. W. 1976.** *J. Exp. Biol.* **65:** 157–177.
4. **Hackett, J. T., and D. S. Faber. 1983.** *Neuroscience* **8:** 317–331.
5. **Eaton, R. C., R. DiDomenico, and J. Nissanov. 1991.** *Brain Behav. Evol.* **37:** 272–285.
6. **Foreman, M. B., and R. C. Eaton. 1993.** *J. Neurosci.* **13:** 4101–4133.
7. **Jayne, B. C., and G. V. Lander. 1993.** *J. Comp. Physiol. A.* **173:** 495–508.
8. **Zottoli, S. J. 1978.** *J. Comp. Neurosci.* **178:** 741–758.
9. **Liu, K. S., and J. R. Fetcho. 1999.** *Neuron* **23:** 325–335.
10. **Hale, M. E. 1999.** *J. Exp. Biol.* **202:** 1465–1479.
11. **Webb, P. W. 1978.** *J. Exp. Biol.* **74:** 211–226.
12. **Blaxter, J. H. S., and R. S. Batty, 1985.** *J. Mar. Biol. Assoc. U.K.* **65:** 737–750.

Reference: *Biol. Bull.* **199:** 182–183. (October 2000)

Memory Consolidation in *Hermissenda crassicornis*

David A. Epstein, Herman T. Epstein, Frank M. Child, and Alan M. Kuzirian
(Marine Biological Laboratory, Woods Hole, Massachusetts 02543)

Experiments with shell-less molluscs (*Aplysia* and *Hermissenda*) have revealed a number of processes that underlie learning by these organisms and also by some vertebrates. *Hermissenda*, for example, shows significant Pavlovian conditioning capabilities (1). Follow-up investigations on these molluscs dealt with the sensory stimuli needed for short-term memory (STM) and long-term memory (LTM) (2). The relationship of the two memories with *in vitro* changes in excitatory post-synaptic potentials (EPSPs) have also been investigated in the neural networks of these organisms (3). Many studies of the molecular aspects of these two different memory regimes have led to quite detailed descriptions of the events (4, 5, 6).

Both *Aplysia* and *Hermissenda* have been tested for their recall of induced behavioral modifications after one, two, or many conditioning events (CEs). In *Aplysia*, the EPSP component of learning produced by 1 CE was compared to that produced by 5 CEs (3). In *Hermissenda*, the comparison was made between 2 CEs and 9 CEs (2). Five to ten minutes after finishing one or two conditioning events, both animals exhibited significant behavioral recall (*i.e.* STM); but there was no recall after an hour or more (*i.e.* no LTM). The larger numbers of CEs, however, did induce LTM in both species.

Since STM and LTM are clearly responding to a different set of conditions, we focused first on what might inhibit or block STM. This problem was partially anticipated in 1900, according to McGaugh (7) who cited Muller and Pilzecker as having found that "memory of newly learned information was disrupted by the learning of other information shortly after the original learning" (8).

This concept led us to test, in *Hermissenda*, whether STM recall (at 5 min) might be blocked simply by the input of additional information (*i.e.* extraneous sensory stimuli) if the latter were applied within the first 5 min after conditioning. The initial results of the blocking experiments, which showed that the simple sensory inputs blocking STM also blocked LTM, then led to the hypothesis that temporal consolidation of LTM could be detected by measuring when the blocking sensory input was no longer effective.

Hermissenda (Sea Life Supply, Sand City, CA) were tested with 2 and 9 paired CEs for induction of STM and LTM. Conditioning events consisted of exposing the animals to 6 s of bright, white light (CS) explicitly paired with 4 s of strong orbital agitation (US) following a 2-s onset delay with an inter-trial interval of 1 min. Recall of the behavioral modification induced by associative conditioning was assessed by recording the animal's change in foot length when presented with 6 s of light alone. The conditioned response (CR) was foot contraction, the unconditioned response (UR) was foot elongation (9). Two paired conditioning events initiated behavioral recall after 5 min but not after 90 min; the LTM input of 9 pairings was recalled at both 5 and 90 min (Fig. 1A). The small and non-overlapping S.E.Ms for each point indicate statistical significance ($P = <0.01$, $t = 3.18$).

After giving the animals the paired CS and US stimuli leading to STM, we tested two simple paradigms of blocking sensory stimuli. The first was a modification of the conditioning stimuli: dim orange light and very slow orbital rotation. The second blocking stimulus tested consisted of rotating the tray containing the animals upside down and, after 5 s, rotating it upright again (rotational block). Both experimental paradigms blocked STM and LTM (Fig. 1B).

To determine the temporal specificity of LTM in *Hermissenda*, the following experiments were done. Animals were trained with 9 CEs, and the CR was measured at the usual 90 min. However, at selected time intervals (2, 25, 50, 55, 60, 65 min) post-conditioning, the animals were rotationally blocked. Control animals received only the 9 paired CEs. When the animals' behavior was plotted, a clear and decisive LTM consolidation interval in *Hermissenda* appeared; consolidation occurred between 55 and 60 min (Fig. 1C). Presentations of rotational blocking prior to 55 min totally blocked memory consolidation. However, the stimulus given after 60 had no blocking effects, and the animals demonstrated the CR. The consistency of and surprisingly little variability in the response among the majority of the animals indicated the robustness of the paradigm. When the data were analyzed with t-test and F-test statistics, they were found to be highly significant, whether compared between data points or to zero ($P = <0.001$, $t = 15.24$; F-value, inf).

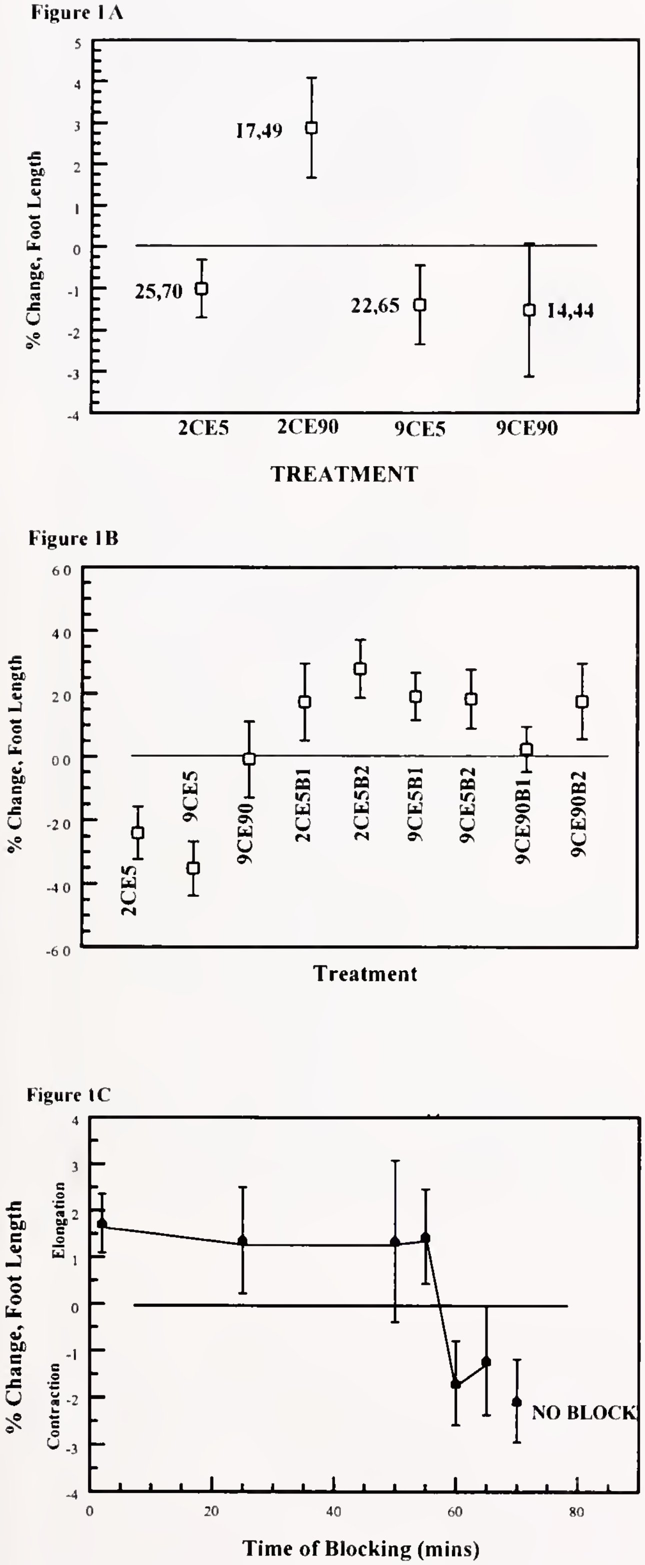

Figure 1. (A) *The typical percent changes in foot lengths of* Hermissenda *after 2 and 9 paired conditioning events (CEs) measured 5 min and 90 min after completing training (e.g. 2CE5). A positive value indicates elongation of the animal's foot, the (non-learned) unconditioned response (UR). Negative values indicate foot contraction and a positive conditioned response (CR). The numbers beside the points (e.g. 25,70) signify the number of animals measured, and observational differences averaged.* (B) *The effects of the two experimental blocking stimuli applied during the first 5 min after training and tested for inhibition of short-term memory (STM) and long-term memory (LTM). Designations are as in Figure 1A with the addition of B1, first blocking sensory stimuli (dim light plus slow agitation); B2, second blocking stimulus consisting of vertically rotating the animals upside down for 5 s, then re-righting them. Both blocking paradigms interfered with STM and LTM. Weakened conditioning response of 9CE90 was due to the blockade of memory induced by handling.* (C) *Temporal specificity of memory consolidation in* Hermissenda. *Percent foot changes measured 90 min after training with 9 CEs, but with the second blocking stimulus (B2, vertical rotation) applied at designated times after the end of training. Memory consolidation appeared to occur between 55 and 60 min. Statistical analyses using t-tests and F-tests were highly significant* ($P = <0.001$).

As a secondary result of these experiments, we could assess the degree to which an animal's training is modified by extraneous handling. The less than optimal (non-significant) training results of animals given 9 CEs and tested after 90 min (*i.e.* 9CE90 animals; Fig. 1B) could be directly attributable to the effects of handling. In future behavioral experimental protocols, as well as in routine animal training procedures, the potential for introducing extraneous blocking stimuli that could confound results must be eliminated.

Memory consolidation has long been recognized to depend on the species being studied, the nature and the frequency of the instructional inputs, and the kind of blocking activity used to determine when the consolidation is completed (7). Our results thus far apply only to the simplest of conditioning stimuli. However, if the concept of consolidation time applies to humans, then awareness of it could help with schooling in two ways: by alerting teachers to the possible blocking of learning by presenting unrelated materials too close to the main point, or by wakening teachers to the need for waiting past the consolidation time before asking complex questions about what had just been presented to the students. Our best estimate, derived from the literature, is that human consolidation time for simple inputs is about 6 to 10 min (10).

The authors acknowledge Dr. Daniel Alkon, Laboratory of Adaptive Systems, NINDS-NIH, Bethesda, MD, for his support and for providing *Hermissenda* for these experiments.

Literature Cited

1. **Alkon, D. L. 1974.** *J. Gen. Physiol.* **64:** 70–84.
2. **Ramirez, R. R., C. C. Gandhi, I. A. Muzzio, and L. D. Matzel. 1998.** *Learn. Mem.* **4:** 462–477.
3. **Montarolo, P. G., P. Goelet, V. F. Castellucci, J. Morgan, E. R. Kandel, and S. A. Schacher. 1986.** *Science* **234:** 1249–1254.
4. **Bailey, C. H., D. Bartsch, and E. R. Kandel. 1996.** *Proc. Nat. Acad. Sci.* **93:** 13445–13452.
5. **Muzzio, I. A., A. C. Talk, and L. D. Matzel. 1998.** *Neuroreport* **11:** 1625–1631.
6. **Izquierdo, I., J. H. Medina, M. R. M. Vianna, L. A. Izquierdo, and D. M. Barros. 1999.** *Behav. Brain Res.* **103:** 1–11.
7. **McGaugh, J. L. 2000.** *Science* **287:** 248–251.
8. **Muller, G. E., and A. Pilzecker. 1900.** *Z. Psychol.* Suppl. 1–288.
9. **Kuzirian, A. M., H. T. Epstein, T. J. Nelson, N. S. Rafferty, and D. L. Alkon. 1998.** *Biol. Bull.* **195:** 198–201.
10. **Lechner, H. A., L. R. Squire, and J. H. Byrne. 1999.** *Learn. Mem.* **2:** 77–87.

Reference: *Biol. Bull.* **199:** 184–186. (October 2000)

Mechanisms of Spontaneous Miniature Activity at CA3-CA1 Synapses: Evidence for a Divergence From a Random Poisson Process

A. Abenavoli, L. Forti[1]*, and A. Malgaroli (Unit of Neurobiology of Learning, Università San Raffaele, Milano, Italy and Marine Biological Laboratory, Woods Hole, Massachusetts 02543)*

Most of the CNS synapses investigated so far release quanta in a spontaneous manner. Since the pioneering work of Fatt and Katz (1), spontaneous release of synaptic quanta is considered a probabilistic process where each quantum is randomly discharged at individual release sites. Release sites are assumed to behave independently and discharge quanta at a very low and stable rate. This hypothesis has been confirmed by a large number of observations at the neuromuscular junction and at other peripheral terminals (1–2). Regrettably, it is unclear that such a description of the release process applies to small CNS synapses. To investigate this problem, we used whole-cell recordings to study the stochastic properties of spontaneous release at hippocampal synapses. In these experiments, clustering of miniature events (minis) was a consistent observation. In about 60% of the experiments, multiple decaying exponentials were required for best fit of interval distributions, and this facilitatory behavior—which could not be accounted for by random coincidences—was independent of calcium elevations in the cytosol. For these experiments, postnatal CA3-CA1 hippocampal cultures were prepared from P4-5 neonatal rats essentially as previously described (3). Neurons were used for synaptic experiments 10–21 days after plating. Whole-cell recordings of miniature currents were also made, as previously described (3).

Hippocampal neurons were continuously perfused with a bath solution containing (in m*M*): NaCl 119, KCl 5, $CaCl_2$ 2, $MgCl_2$ 2, HEPES 25, glucose 30, picrotoxin 100 μM (Sigma), APV (D-2-amino-phosphonovalerate) 25-100 μM, tetrodotoxin 0.5 μM, adjusted to 305 mOsm and pH 7.4. Patch electrodes (2–5 MΩ) contained (in m*M*): Cs-gluconate 110, $MgCl_2$ 5, NaCl 10, EGTA or BAPTA 0.6–10, ATP 2, GTP 0.2, HEPES 49, adjusted to pH 7.2 and 290 mOsm. Current traces were digitized off-line from the magnetic tape at 10–70 KHz after low-pass filtering at 3–5 KHz. Miniature events were detected semiautomatically (3). Intervals between events were log-binned and plotted on a log-log scale: the bin content was normalized for the bin width (4). The resulting histograms were fitted with nested models made by the sum of exponentials with a Simplex algorithm and a maximum likelihood estimator. The minimum number of exponential components was chosen using the log-likelihood-ratio test. Averaged values are reported as the mean ± s.e.m., and statistical comparisons were obtained using an independent Student's *t* test, unless otherwise indicated. In these conditions, when the occurrence of spontaneous events was analyzed, clusters of minis (*i.e.*, very brief episodes with a few consecutive quantal releases) were found to be a very consistent observation. The statistical significance of this finding can be tested by analyzing the distributions of inter-event intervals from large data sets. According to predictions from Poisson's law, a frequency distribution of random intervals should display a mono exponential profile:

$$F(x) \propto exp(-\lambda x)$$

where $F(x)$ is the probability of having an interval greater than x, and λ is the mean mini frequency. Log-binned frequency distributions of mini-intervals indicated (4) that in most cases ($n = 14/24$; $P < 0.05$, log-likelihood ratio test), multiple decaying exponentials are required for optimal fit of interval distributions. This indicates a clear divergence of spontaneous exocytosis from a random Poisson process (Fig. 1, A-B). The best fit of the interval distributions indicated that the area underneath the fast or bursting component (a_{fast}) could be as high as 66% or as low as 3% (mean $a_{fast} = 12 \pm 4\%$; $n = 14$) (Fig. 1, A-B). Since miniature events arise from a large population of independent synapses, could this divergence arise simply from the temporal averaging? The answer is "No," according to the following argument. If each synapse generates spontaneous events according to a Poisson process, then the probability of finding *k* events in the time interval Δt is:

$$P(k) = \frac{\exp(-\mu_i \cdot \Delta t) \cdot \mu_i^k}{k!}$$

where μ_i is the mean Poisson rate at the ith synapse. With a population of N independent synapses, the occurrence of minis at the soma will also be a Poisson process with a single parameter μ which is just the sum of the individual parameters:

$$\mu = \sum_{i=1}^{N} \mu_i$$

Therefore, based on these simple mathematical considerations, if every synapse made onto an individual neuron is releasing in a random manner, whole-cell mini interval distributions should display a single exponential component. Moreover, this conclusion would also be valid in the presence of a large variability in spontaneous quantal rates at different synapses, as previously reported in the same system (5). In agreement with these expectations we have used a technique that permits to us record minis from individual hippocampal synapses and have found that, even at the level of a single terminal, the generation of quanta diverges from a random memory-less Poisson process (Abenavoli *et al.*, unpub.).

A transient up-modulation of quantal discharges, such as the

---

[1] Present Address: Dipartimento di Fisiologia, Università di Pavia, Via Forlanini 6, I-27100 Pavia, Italy.

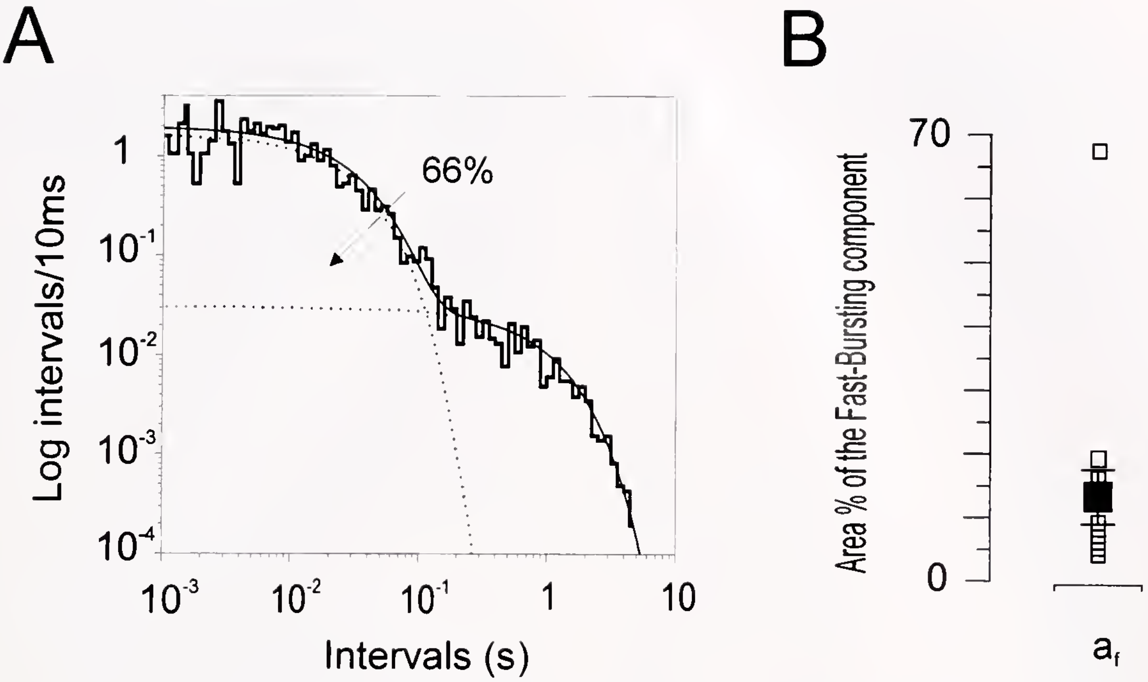

Figure 1. *Distribution of intervals between minis at hippocampal synapses. A) Minis were acquired in voltage clamp using the Whole-cell recording configuration. Short trains of minis could be seen consistently under these conditions. In these experiments multiple exponentials were always required for best fit of mini-interval distributions indicating a divergence from Poisson's statistics. The histogram presented was best fitted by the sum (solid line) of two decaying exponentials (dotted lines). B) Summary data for the area* (a_f) *of the short-interval component (range* a_f *= 3–66%, mean value = 12 ± 4%; range* τ_f *= 1.56 – 48.64 ms, mean value 20.37 ± 4.07 ms).*

one observed in the fast component of mini interval distributions, might result from some sort of transient change in presynaptic Ca^{2+} levels (see ref. 6 for review). We have therefore tested the effects of cadmium (50 μM), a broad spectrum Ca^{2+} channel blocker. When cadmium was applied, no effects on mini frequency and mini amplitude were detected. In 9 cells, the average mini frequency in control conditions was 2.51 ± 0.75 Hz, and it was 2.56 ± 0.74 Hz after the application of cadmium. In these experiments, when log-binned distributions of mini-intervals were constructed, if multiple decaying exponentials were required for optimal fit in control conditions, they were also required in the presence of Cd^{2+} (n = 4/4; $P < 0.01$). We also examined the effects of BAPTA, a high affinity, fast-binding Ca^{2+} chelator (7). BAPTA was introduced in all synaptic terminals impinging upon a postsynaptic neuron by perfusing those neurons with the membrane permeable analog BAPTA-AM while recording synaptic events. Long-term application of BAPTA (>20 min) (in the presence of tetrodotoxin) produced no significant effect on mini frequency ($<f_{ctr}> =$ 2.14 ± 1.30 Hz, $<f_{Bapta}> =$ 1.74 ± 1.56, mean ± sd; n = 7). Importantly, interval-distributions of minis displayed no detectable change after the BAPTA treatment (n = 3/3; $P < 0.05$; $a_{fControl}$ = 8 ± 3%; a_{fBAPTA} = 8 ± 3%). Taken together, these observations rule out a role in the divergence from a random Poisson process for a brief elevation in presynaptic Ca^{2+}, whether from an influx through the plasma membrane or release from internal stores. Our electrophysiological recordings revealed that the dynamics of spontaneous quanta is more complex than previously thought and cannot be simply predicted by applying the Poisson theorem (1–2). This is because short epochs of multiple quanta releases were consistently present in the recordings. The genesis of this phenomenon is independent of Ca^{2+} elevation in the presynaptic terminals. Our relative ignorance about the molecular organization of release sites precludes any deeper understanding of this synaptic behavior. Nonetheless, we can speculate that, since minis keep occurring in the absence of any incoming electrical activity, trophic support through minis would circumvent requirements for Hebbian mechanisms to maintain some forms of synaptic plasticity (8). In particular, the rapid discharge within a burst would certainly lead to a temporal summation in the postsynaptic spine and dramatically increase the probability of calcium influx through postsynaptic NMDA channels. The input-output properties of CNS synapses are an additional consideration.

The results presented might also be relevant to the hypothesis that the release of multiple vesicles is happening under some conditions and in some neuronal systems during spontaneous and evoked exocytosis (9–12). Regardless of the frequency of multivesicular exocytosis, this could certainly have an impact on the synaptic input-output characteristics of hippocampal synapses, since glutamate AMPA receptors are not saturated by the content of a single vesicle (3).

A. Abenavoli was a recipient of an Armenise-Harvard fellowship. This research was supported by a Rand award, Telethon, Human Frontier and MURST grants to A.M.

Literature Cited

1. **Fatt, P., and B. Katz. 1952.** *J. Physiol. (Lond.)* **117:** 109–128.
2. **Rotshenker, S., and R. Rahamimoff. 1970.** *Science* **170:** 648–649.
3. **Forti, L., M. Bossi, A. Bergamaschi, A. Villa, and A. Malgaroli. 1997.** *Nature* **388:** 874–878.
4. **McManus, O. B., A. L. Blatz, and L. Magleby. 1987.** *Pflügers Arch.* **410:** 530–533.
5. **Malgaroli, A., A. E. Ting, B. Wendland, A. Bergamaschi, A. Villa, R. W. Tsien, and R. H. Scheller. 1995.** *Science* **268:** 1624–1628.
6. **Augustine, G. J., M. P. Charlton, and S. J. Smith. 1987.** *Annu. Rev. Neurosci.* **10:** 633–693.
7. **Adler, E. M., G. J. Augustine, S. N. Duffy, and M. P. Charlton. 1991.** *J. Neurosci.* **11:** 1496–1507.
8. **Bliss, T. V. P., and G. L. Collingridge. 1993.** *Nature* **361:** 31–39.
9. **Korn, H., C. Sur, S. Charpier, P. Legendre, and D. S. Faber. 1994.** Pp. 301–322 in *Molecular and Cellular Mechanisms of Neurotransmitter Release,* L. Stjarne *et al.,* eds. Raven Press, New York.
10. **Auger, C., S. Kondo, and A. Marty. 1998.** *J. Neurosci.* **18:** 4532–4547.
11. **Tong, G., and C. E. Jahr. 1994.** *Neuron* **12:** 51–59.
12. **Ryan T. A., H. Reuter, and S. J. Smith. 1997.** *Nature* **388:** 478–482.

Reference: *Biol. Bull.* **199:** 187–188. (October 2000)

UV-B Induced Damage to the Skin and Ocular System of Amphibians

Iñigo Novales Flamarique (Department of Biological Sciences, Simon Fraser University, 888 University Drive, Burnaby, British Columbia, V5A 1S6, Canada), Kristiina Ovaska, and Theodore M. Davis

The depletion of stratospheric ozone and the consequential increase in ultraviolet (UV-B) radiation reaching the Earth's surface may be partly responsible for the recent declines in some amphibian populations (1). Present or predicted UV-B levels for the next decades in northern latitudes can cause pronounced mortalities in amphibians during early development both under laboratory and semi-natural conditions (2–6). However, except for limb and spinal malformations (7, 8), observable damage at the systems level has been seldom described. Here, we report on the incidence of skin burns and eye cataracts in tadpoles exposed to enhanced UV-B levels under semi-natural conditions.

The tadpoles examined in this study originated from experiments carried out in a forest clearing near Victoria (British Columbia, Canada) using containers filled with pond water (4). Two species of frogs (*Hyla regilla* and *Rana aurora*) were raised from eggs under one of three light regimes: (1) ambient sunlight, (2) sunlight blocked for UV wavelengths less than 450 nm (control), or (3) sunlight enhanced from 4.8% to 23% UV-B (280–320 nm) over ambient levels at noon, depending on atmospheric conditions (from sunny to overcast days, respectively [5]). The enhanced UV-B treatment was obtained by placing fluorescent UV-B lamps, with peak output in the range of 280–315 nm, over the appropriate containers. These lamps were on from 0900–1700 h each day, resulting in a mean hourly increase of approximately 30% UV-B radiation per day over ambient levels for the duration of the study. Tadpoles were collected from each treatment during weeks 3 and 4 after hatching and examined under a dissecting microscope for damage to the lens (*i.e.*, presence of lens opacities) and to the skin (*i.e.*, integument burns). To assess damage to retinal photoreceptors, the retinas from five animals collected during week 4 were prepared for electron microscopy. This procedure involved enucleation of the eyecup and fixation in primary fixative (2.5% glutaraldehyde, 1% paraformaldehyde in 0.06 *M* phosphate buffer, pH 7.3); post-incubation of extracted retinas in secondary fixative (1% osmium tetroxide) for 1 h at 4°C; dehydration of the tissue through a series of ethanol solutions of increasing concentration; and embedding in Epon plastic. Thin (75 nm) radial sections were cut, exposing photoreceptors from the centroventral part of the retina along their lengths. These sections were mounted on copper grids, stained with uranyl acetate and lead citrate, and examined with the transmission electron microscope.

The numbers of dead embryos and larvae were monitored throughout the study (4). Mortalities during the study can be summarized as follows. Although significantly higher egg mortality was observed in the enhanced UV-B treatment for *R. aurora* only, tadpoles of both species suffered high mortality in the enhanced treatment: only 2.6% of *R. aurora* and 18.4% of *H. regilla* survived 1 month after hatching, compared to 55% and 51.7% in the ambient treatment, and 43.8% and 65% in the control.

In the control and ambient treatments, the majority of animals had clear lenses (Fig. 1a). Of the controls, only 3 of 10 *R. aurora* and 2 of 10 *H. regilla* tadpoles examined during weeks 3 and 4 after hatching showed signs of lens opacities. The extent of these opacities was smaller than that presented in Figure 1b. In the ambient treatment, 3 of 9 *R. aurora* and 1 of 10 *H. regilla* showed similar small lens opacities. In the enhanced UV-B treatment, however, 16 of 20 *R. aurora* and 12 of 16 *H. regilla* tadpoles showed prominent lens opacities. Thus, for both species, more tadpoles raised under the enhanced UV-B treatment showed lens opacities than did those from the control or ambient treatments (*R. aurora* $\chi^2 = 11.4$, df = 2, $P < 0.005$; *H. regilla* $\chi^2 = 13.4$, df = 2, $P < 0.005$). Large opacities, a sign of advanced cataracts, were particularly visible among *R. aurora* tadpoles (Fig. 1c). Substantial skin burns were also present in 6 *H. regilla* and 9 *R. aurora* tadpoles from the enhanced UV-B treatment (Fig. 1d); however, this skin damage may have been amplified by fungal infections (9). No skin sores were found in tadpoles from the ambient and control treatments.

Electron micrographs revealed single cones that were similar in all animals irrespective of treatment (Fig. 1e). The outer segments of cones (Fig. 1f), which contain the light-sensitive visual pigments, were not appreciably different from those of fish at early developmental stages (personal observation). Our data, therefore, suggests that the damage from enhanced UV-B radiation to the ocular system of amphibians occurs primarily in the lens. It may be that the early onset of lens opacities prevents substantial levels of UV-B radiation from reaching the photoreceptor layer of the retina and disrupting cell structure. However, other explanations, including the involvement of repair mechanisms, may also account for these results.

The incidence of skin sores and cataracts, as observed in our UV-B enhanced treatment, can have important consequences for tadpoles in nature. Animals with cataracts are incapable of forming a clear image in the retina due to scattering of light within the lens, hence their foraging and predator avoidance capabilities are greatly reduced. In addition, the skin sores can be infected by parasites, thereby further increasing tadpole mortality (9).

In many regions of the world, the removal of riparian vegetation and creation of large clearcuts increases the exposure of small water bodies, used by amphibians for oviposition, to UV-B and total radiation levels (10). Tadpoles developing in such habitats might be exposed to UV-B levels sufficient to cause the type of damage reported here. Monitoring the incidence of cataracts in clearcuts and forest pools could potentially be used as an indicator of biological effects of increased UV-B radiation.

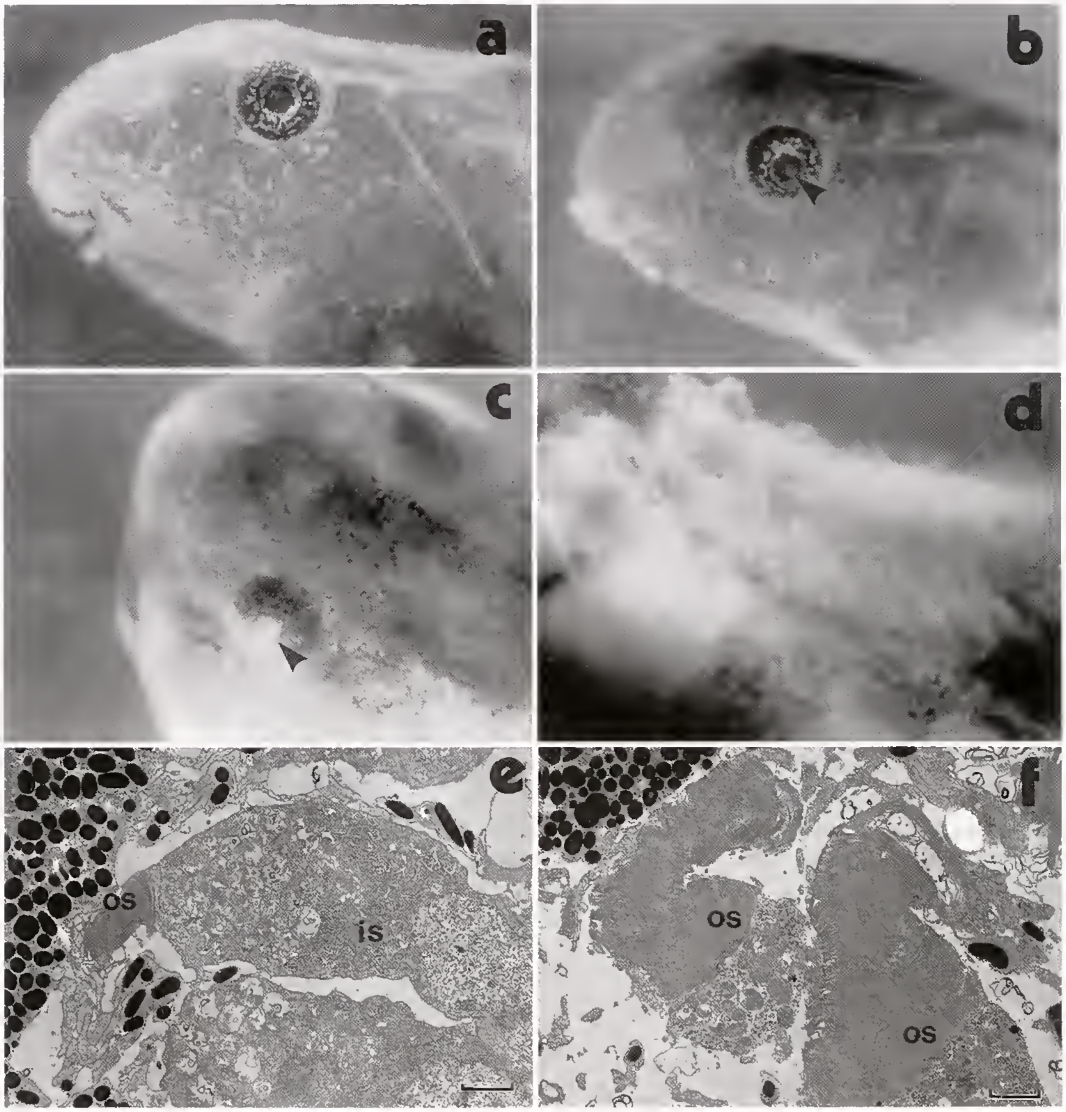

Figure 1. *Photographs of (a)* Hyla regilla *tadpole with clear lens; (b)* H. regilla *tadpole with lens opacity (arrowhead); (c)* Rana aurora *tadpole showing extensive cataracts (arrowhead); (d) lesion area of* R. aurora *tadpole exposing dorsal musculature; (e)* R. aurora *cone photoreceptor showing normal inner and outer segments (is and os respectively), bar = 1.2 μm; and (f) details of two cone outer segments, bar = 0.6 μm. No damage was readily apparent in the photoreceptor layer of tadpole retinas from any of the treatments.*

Literature Cited

1. **Blaustein, A. R., P. D. Hoffman, D. G. Hokit, J. M. Kiesecker, S. C. Walls, and J. B. Hays. 1994.** *Proc. Natl. Acad. Sci. USA* **91:** 1791–1795.
2. **Blaustein, A. R., B. Edmond, J. M. Kiesecher, J. J. Beatty, and D. G. Hokit. 1995.** *Ecol. Appl.* **5:** 740–743.
3. **Grant, K. P., and L. E. Licht.** 1995. *Can. J. Zool.* **73:** 2292–2301.
4. **Ovaska, K., T. M. Davis, and I. Novales Flamarique. 1997.** *Can. J. Zool.* **75:** 1081–1088.
5. **Ovaska, K., T. M. Davis, and I. Novales Flamarique. 1998.** *Can. J. Zool.* **76:** 1797.
6. **Anzalone, P. G., L. B. Kats, and M. S. Gordon. 1998.** *Conserv. Biol.* **12:** 646–653.
7. **Blaustein, A. R., J. M. Kiesecker, D. P. Chiversand, and R. G. Anthony. 1997.** *Proc. Natl. Acad. Sci. USA* **94:** 13,735–13,737.
8. **Ankley, G. T., J. E. Tietge, D. L. DeFoe, K. M. Jensen, G. W. Holcombe, E. J. Durhan, and S. A. Diamond. 1998.** *Environ. Toxicol. Chem.* **17:** 2530–2542.
9. **Kiesecker, J. M., and A. R. Blaustein. 1995.** *Proc. Natl. Acad. Sci. USA* **92:** 11,049–11,052.
10. **Novales Flamarique, I., and W. Harrower. 1999.** *Environ. Biol. Fishes* **55:** 279–293.

Reference: *Biol. Bull.* **199:** 189–190. (October 2000)

Initial Characterization of a Potential Anti-fouling System in the American Horseshoe Crab, *Limulus polyphemus*

John M. Harrington (Biological Sciences Department, University of South Alabama, Mobile, Alabama 36688) and Peter B. Armstrong[1]

Although the surfaces of most solid objects are rapidly colonized by sessile fouling organisms within a short time after immersion in the ocean, macroscopic fouling organisms are surprisingly sparse on the cuticle of healthy adults of the American horseshoe crab, *Limulus polyphemus*. One of the major identified causes of mortality of adult horseshoe crabs is the erosion of the cuticle that follows its colonization by green or blue-green algae (1). Thus it is in the interest of the animal to maintain the cuticle clear of fouling species. The mechanism(s) responsible for keeping the cuticle clean in an environment liberally stocked with fouling species have not been identified. One likely candidate is a mucous secretion from the hypodermal glands, a system of glands that discharge onto the surface of the cuticle (2). Here we show that this secretion has antibiological activities that may contribute to its ability to deter the colonization of the cuticle of *Limulus* by fouling organisms.

The cuticular secretion can be provoked by housing healthy adults in the presence of decaying fish (3). The secretion from the hypodermal glands was scraped from the dorsal cuticle of the *Limulus* shell with a rubber scraper and stored at 4°C in the presence of 0.2 mg/ml NaN_3 to prevent bacterial contamination. Antibodies to whole cuticular secretion were prepared in rabbits. Immunostaining utilized a 1:1000 dilution of the primary antiserum, a 1:1000 dilution of HRP-anti rabbit IgG, and 4-chloronaphthol using standard methods for staining Western and dot blots (4).

Stimulated animals renewed the layer of cuticular secretion within 1–2 h after the cuticle had been scraped clean. Although most of the animals in the Marine Resources Center of the Marine Biological Laboratory, which are collected from the pristine waters of Pleasant Bay, lacked the thick layer of cuticular secretion of the pollution-challenged animal, the secretion was present as a thin layer on their surfaces as well. Anti-cuticular secretion antisera specifically immunostained swipes of the surface of the cephalothorax of these animals, indicating the presence of the secreted products of the hypodermal glands. Control swipes immunostained with non-immune rabbit IgG in place of immune serum failed to stain.

It has been proposed that the cuticular secretion contains the secreted products of the *Limulus* blood cells (2). This apparently is not true because the principal secreted product of the blood cells, the clotting protein coagulogen, is absent from the secretion. Antibodies to coagulogen failed to immunostain dot blots of cuticular secretion, and the anti-cuticular secretion antiserum failed to stain coagulogen or the collective secretion of the blood cells. This latter material was prepared as described previously (5, 6). The anti-coagulogen antiserum did stain dot blots of coagulogen, and the anti-cuticular secretion antiserum did stain dot blots of cuticular secretion. The cuticular secretion showed 15 protein bands by SDS-PAGE (reducing conditions, silver-staining) in the molecular mass range of 143–20 kDa.

The anti-biological activity of the cuticular secretion was tested by its cytolytic actions on target cells. Cuticular secretion hemolysed sheep red blood cells at a 1:16 dilution in a standard hemolysis assay (7) (Fig. 1A). Hemolysis was judged to be divalent cation-dependent because the divalent cation chelator, ethylenediaminetetraacetic acid, reduced hemolysis (Fig. 1A). The macromolecular osmolites dextran-8 (Mr 8–12 kDa) and, to a lesser extent, dextran-4 (Mr 4–6 kDa) reduced the extent of hemolysis (Fig. 1B). This suggests that hemolysis is the result of hydrophilic membrane channels established in the plasma membrane of the target red blood cell by the hemolytic protein of the cuticular secretion. Protection by the dextrans is suggested to result from their ability to balance the osmotic pressure across the permeabilized cell membrane, which will reduce the flow of water through the hemolytic pore and into the cell and will prevent swelling and lysis (8). It is difficult to envision ways for macromolecular osmolites to protect the cell if the hemolytic process featured such other possible mechanisms as phospholipase action or detergent-mediated membrane reorganization.

It is proposed that the cuticular secretion is one agent that helps maintain the cleanliness of the cuticle of *Limulus*. Its

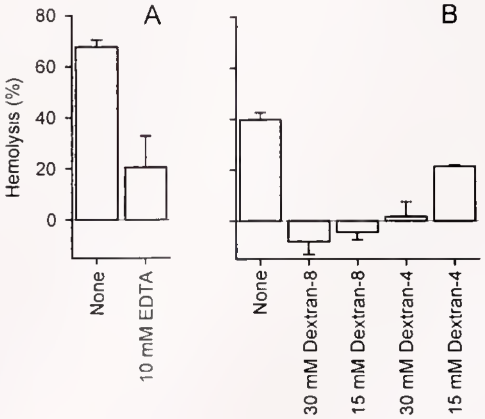

Figure 1. *Hemolytic activity of the cuticular secretion from* Limulus polyphemus *to rabbit red cells. All samples contain a 1:16 dilution of the cuticular secretion, with the indicated additions. The hemolysis buffer is 0.25* M *NaCl, 0.01* M Ca^{+2}*, 0.14* M *dextrose, 0.01* M *Tris, pH 7.3. Added EDTA (10 mM) reduces hemolysis (Fig. 1A). Dextran-8 and dextran-4 reduce hemolysis (Fig. 1B).*

---

[1] Molecular and Cellular Biology, University of California, One Shields Avenue, Davis, CA 95616, (pbarmstrong@ucdavis.edu).

anti-biological activity, exemplified by its ability to lyse foreign cells such as mammalian erythrocytes, may contribute to this activity. Under normal conditions, the volume of cuticular secretion is low, but it can be detected by immunological assays. Under conditions of challenge by a polluted environment, the volume of the secretion is augmented. In addition to its anti-biological activity, the continuous production of the cuticular secretion can be expected to exert a mechanical action, entrapping and sweeping potential fouling organisms away from the solid surface of the cuticle. Contrary to previous suggestions (2), the cuticular secretion does not contain secretion products of the blood cells.

Supported by Grant No. MCB-97-26771 from the National Science Foundation. We thank Ms. Yvonne Coursey for the anti-coagulogen antiserum.

Literature Cited

1. **Leibovitz, L., and G. A. Lewbart. 1987.** *Biol. Bull.* **173:** 430 (abstr.).
2. **Stagner, J. I., and J. R. Redmond. 1975.** *Mar. Fish. Rev.* **37:** 11–19.
3. **Harrington, J. M., and P. B. Armstrong. 1999.** *Biol. Bull.* **197:** 274–275.
4. **Harlow, E., and D. Lane. 1988.** *Antibodies, A Laboratory Manual.* Cold Spring Laboratory, New York. 726 pp.
5. **Armstrong, P. B., and J. P. Quigley. 1985.** *Biochim. Biophys. Acta* **827:** 453–459.
6. **Armstrong, P. B., J. P. Quigley, and F. R. Rickles. 1990.** *Biol. Bull.* **178:** 137–143.
7. **Swarnakar, S., R. Asokan, J. P. Quigley, and P. B. Armstrong. 2000.** *Biochem. J.* **347:** 679–685.
8. **Hatakeyama, T., H. Nagatomo, and N. Yamasaki. 1995.** *J. Biol. Chem.* **270:** 3560–3564.

Reference: *Biol. Bull.* **199:** 190–192. (October 2000)

Association of α_2-Macroglobulin with the Coagulin Clot in the American Horseshoe Crab, *Limulus polyphemus:* A Potential Role in Stabilization from Proteolysis

Rengasamy Asokan (Molecular and Cellular Biology, University of California, Davis, California 95616), Margaret T. Armstrong[1], *and Peter B. Armstrong*[2]

The blood clot of the horseshoe crab is established by the proteolytic conversion of the soluble clotting protein, coagulogen, into the form (coagulin) that polymerizes to establish a fibrillar extracellular clot (1). The coagulin clot functions in hemostasis (2), wound repair (3), and entrapment of bacteria invading through wounds in the cuticle. Bacteria entrapped in the coagulin clot are so strongly held that they fail even to show Brownian motion (2). Entrapment reduces the systemic dissemination of invading bacteria to locations far from the wound and its coagulin clot.

Secreted proteases serve important roles in parasitic virulence, and protease inhibitors of the plasma and blood cells of the host play a substantial role in immunity by the inactivation and clearance of the foreign proteases of invading parasites (4). In the present context, if entrapped bacteria were able to proteolyze the coagulin clot, then the period of entrapment would be reduced and the systemic dissemination of the invading bacteria would be facilitated. The sole protease inhibitor of the plasma of the horseshoe crab is α_2-macroglobulin (α_2M) (5). The blood cells also secrete α_2M when activated (6). Here we investigate the potential role of α_2M in the protection of the coagulin clot from proteolysis.

Limulus α_2M was purified as described previously (7). Coagulogen was purified as described by Srimal (8). Antibodies to *Limulus* α_2M and coagulogen were produced in rabbits. Western and dot blotting were conducted using standard methods and controls (9). Specimens for immunohistochemistry were fixed in 4% paraformaldehyde in seawater, quenched in 0.1 *M* glycine, blocked with 5% serum albumin, and stained with rabbit first antibodies and fluoresceinated goat anti-rabbit IgG. Affinity resins were prepared by coupling purified protein to CNBr-activated Sepharose 4B using standard methods (10). Extracts subjected to affinity chromatography were first exposed to large volumes of plain Sepharose and were then exposed to Sepharose conjugated to the desired target protein, washed with high-salt buffer (containing 0.5 *M* NaCl, 10 m*M* Ca^{+2}, 10 m*M* Tris, pH 7.3), and finally eluted with a buffer containing the Ca^{+2} chelator, ethylenediaminetetraacetic acid (EDTA).

Biochemical evidence for the specific binding of coagulogen to *Limulus* α_2M was provided by our ability to isolate coagulogen from detergent extracts of *Limulus* blood cells by affinity chromatography over *Limulus* α_2M-Sepharose. The protein that was eluted following removal of Ca^{+2} was identified as coagulogen by molecular mass (~21 kDa) and reactivity with anti-coagulin antibodies (Western blotting and dot blotting). Coagulogen was by far the most abundant protein eluted from the α_2M affinity column.

Immunohistochemical and biochemical approaches were used to investigate the binding of α_2M to the coagulin clot. Blood clots were prepared *in vitro* by collecting 0.3 ml of whole blood into 90-mm petri dishes containing 10 ml of sterile, cell-free *Limulus* plasma. The cells that attach to the surface of the petri dish flatten and degranulate, and the coagulogen that is released from the secretory granules polymerizes into a fibrillar coagulin clot situated above the cell layer (11). These fibrils immunostain specifically with antisera directed against coagulogen (Fig. 1A), showing their similarity to the fibrils of the blood clot that forms *in situ* at the locations of wounds to the cuticle of the animal. When treated with an affinity-purified antibody to *Limulus* α_2M, the clot fibrils also stain brightly for *Limulus* α_2M (Fig. 1B). Treatment of the clot with 50 m*M* EDTA prior to fixation and processing for immunohistochemistry reduced but did not eliminate staining with

---

[1] Molecular and Cellular Biology, University of California, One Shields Avenue, Davis, CA 95616, (mtarmstrong@ucdavis.edu).

[2] Molecular and Cellular Biology, University of California, One Shields Avenue, Davis, CA 95616, (pbarmstrong@ucdavis.edu).

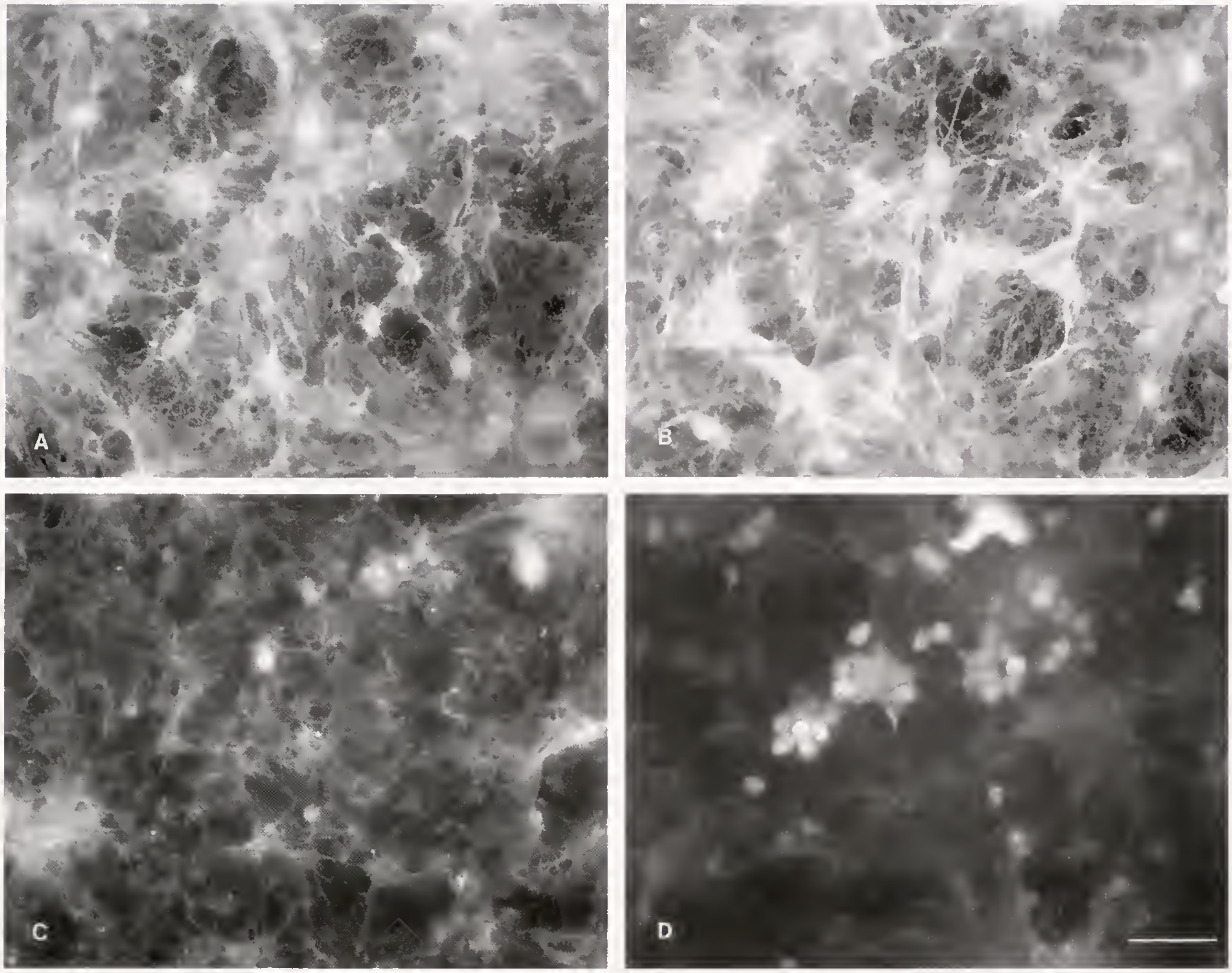

Figure 1. *Immunofluorescent demonstration of the decoration of the coagulin fibrils of the blood clot by* Limulus *α_2M. Blood cells were allowed to attach to microscope coverglasses in numbers sufficient to produce a confluent monolayer. The attached cells degranulate and produce a fibrillar coagulin clot that lies above the cell layer and stains with antibodies against coagulin (panel A, top left). The clot stains intensely with an affinity-purified antibody against* Limulus *α_2M (panel B, top right), indicating the presence of α_2M attached to the clot fibrils. Most, but not all, of the α_2M is removed by treatment with 50 mM EDTA prior to fixation (panel C, bottom left). The specimen treated with non-immune serum failed to stain (panel D, bottom right). Photomicrographs B, C, and D were exposed identically to permit comparison of differing fluorescent intensities. Although most of the blood cells attach to the glass and degranulate, a few cells migrate to the top of the clot. These fail to degranulate and show as cells with autofluorescent granules in all pictures. Scale bar (Fig. 1D) = 50 μm.*

anti-*Limulus* α_2M antibodies (Fig. 1C). A similar pattern of decoration of clot fibrils by α_2M was found in clots extracted with 0.5% Triton X-100. Control specimens treated with non-immune rabbit IgG failed to show staining of the fibrillar elements of the coagulin clot (Fig. 1D). This indicates that α_2M does indeed decorate the coagulin fibrils of the clot and that the binding is largely Ca^{+2}-dependent. It is possible that the EDTA-insensitive α_2M is covalently linked *via* transglutaminase-catalyzed isopeptide bonds. The *Limulus* clot does contain such protein-protein bonds (12) and human α_2M is a substrate for transglutaminase crosslinking.

Additional evidence for α_2M binding was provided by the characterization of the proteins that co-purify with the blood clot. For this, the clots formed *in vitro* were washed exhaustively with high-salt buffers (0.5 *M* NaCl, 10 m*M* $CaCl_2$, 10 m*M* Tris, pH 7.3) and detergent (0.5% Triton-X 100), and were then scraped from the petri dish and transferred to microcentrifuge tubes, where they were compressed by centrifugation, washed further, and finally eluted by removal of Ca^{+2} with 0.1 *M* EDTA. The coagulin clot was not solubilized by this treatment. The supernatant fraction contained substantial quantities of α_2M, as shown by Western blotting and dot blotting using an affinity-purified antibody to *Limulus* α_2M.

This study provides evidence that α_2M binds selectively to coagulogen and coagulin in a Ca^{+2}-dependent fashion. We suggest that this serves the important function of positioning α_2M from the plasma onto the fibrils of the blood clot, where it is perfectly situated to protect the clot from microbial proteolysis and the consequent compromise of the clot's function as a device that immobilizes entrapped bacteria.

Supported by Grant No. MCB-97-26771 from the National Science Foundation. We thank Ms. Yvonne Coursey for the anticoagulogen antiserum.

Literature Cited

1. **Iwanaga, S., T. Miyata, F. Tokunaga, and T. Muta. 1992.** *Thromb. Res.* **68:** 1–32.
2. **Bang, F. B. 1979.** Pp. 109–123 in *Biomedical Applications of the Horseshoe Crab (Limulidae)*, E. Cohen, ed. Alan R. Liss, New York.
3. **Bursey, C. R. 1977.** *Can. J. Zool.* **55:** 1158–1165.
4. **Armstrong, P. B., and J. P. Quigley. 2000.** *Phylogenetic Perspectives on the Vertebrate Immune System*, G. Beck, ed. Plenum Publishing, New York.
5. **Quigley, J. P., and P. B. Armstrong. 1983.** *J. Biol. Chem.* **258:** 7903–7906.
6. **Armstrong, P. B., J. P. Quigley, and F. R. Rickles. 1990.** *Biol. Bull.* **178:** 137–143.
7. **Armstrong, P. B., R. Melchior, and J. P. Quigley. 1996.** *J. Insect Physiol.* **42:** 53–64.
8. **Srimal, S., T. Miyata, S. Kawabata, and S. Iwanaga. 1985.** *J. Biochem. (Tokyo)* **98:** 305–318.
9. **Harlow, E., and D. Lane. 1988.** *Antibodies, a Laboratory Manual.* Cold Spring Laboratory, New York. Pp. 1–726.
10. *Pharmacia Fine Chemicals. Affinity Chromatography.* **1979.** Uppsala, Sweden, Pharmacia Fine Chemicals.
11. **Armstrong, P. B., and F. R. Rickles. 1982.** *Exp. Cell Res.* **140:** 15–24.
12. **Wilson, J., F. R. Rickles, P. B. Armstrong, and L. Lorand. 1992.** *Biochem. Biophys. Res. Commun.* **188:** 655–661.

Reference: *Biol. Bull.* **199:** 192–194. (October 2000)

Enzymatic Biosynthesis of N-Linked Glycan by the Marine Sponge *Microciona prolifera*

William J. Kuhns[1], *Max M. Burger*[2], *Mohan Sarkar*[1], *Xavier Fernandez-Busquets*[3], *and Tracy Simpson*[4]
(Marine Biological Laboratory, Woods Hole, Massachusetts 02543)

Complex carbohydrates occur in and on practically all cell types and in cellular secretions. They participate in a multitude of functions, such as fertilization, development and differentiation, cell sorting, motility, signal transduction and phagocytosis (1, 2). The *Microciona* aggregation factor (MAF) is a highly glycosylated compound that is involved in such functions. Glycosylation of carbohydrates proceeds enzymatically by the stepwise addition of single activated sugars to a growing sugar chain. The products may consist entirely of sugars, *i.e.*, polysaccharides, or they may be linked to lipids or proteins. There are two types of protein-sugar binding structures: O-linked serine or threonine and N-linked asparagine. Favored N-glycosylation sites possess a characteristic asn-x-ser/thr tripeptide sequence (3). The protein expressed from the cDNA that encodes MAF contains many of these tripeptide motifs (4). Moreover, when MAF is treated with specific glycosidases, sugars known to be present in complex N-glycans, *i.e.*, mannose, *N*-acetylglucosamine (GlcNAc), fucose and galactose (5) appear as products. Confirmatory studies have demonstrated GlcNAc, mannose, fucose and galactose lectin binding to sponge cell membranes (6).

Here we report for the first time that tissues of *Microciona* appear to contain an enzyme activity, here named *N*-acetyl glucosaminyltransferase I or GnT I, that processes N-linked glycans. This activity is part of a series of enzymatic events that begin in the cytoplasm where an oligosaccharide-linked dolichol phosphate is transported to the lumen of the endoplasmic reticulum whence it continues to the Golgi. During the process, the sugar is transferred from the dolichol to a tripeptide (see above) and is modified further by processing enzymes (7; Fig. 1a). N-glycosylation and complex glycan synthesis can be inhibited by specific compounds such as tunicamycin and swainsonine (8).

Assays for sponge GnT I were performed using as a source of enzyme fresh-packed sponge cells extracted in 1% Triton X-100 and buffered in 100 m*M* Tris at pH 7.4. The substrate was a synthetic compound, trimannosyl octyl, which has proved useful as an alternate to natural substrates in which the octyl group is replaced by two GlcNAc residues (9). The co-substrate and active glycosyl donor was a ^{14}C-labeled uridine diphosphate *N*-acetylglucosoamine (UDP-^{14}C-GlcNAc), with a specific activity of 7.1 m*M* and 7402 dpm/nmol. Replicate tubes containing these compounds were added to a buffered cocktail that consisted of 25 m*M* adenosine monophosphate, 0.5 *M* *N*-acetylglucosamine, 0.2% Triton X-100, bovine serum albumin 2 mg/ml, 40 m*M* MnCl$_2$, and 0.2 *M* 2-(N-morpholino) ethanesulfonic acid pH 6.1 in a total volume of 62.5 μl. After incubation for 1 h at 37°C, the reaction was terminated by the addition of 20 μl of 2% sodium borate in 20 m*M* EDTA. Separation of unreacted UDP-^{14}C-GlcNAc from glycosylated radioactive product was accomplished by passing the reaction mixture through an AG1-X8 (BioRad) ion exchange column. Additional purification of the reaction product could be achieved by HPLC with C18 matrix that binds the hydrophobic product. Following a wash with deionized water, the purified radioactive product was eluted with methanol and the eluate was placed in vials for determination of counts. The average figures for product yield, expressed as nanomoles per hour per milligram of protein (nm/h/mg), were derived from duplicate counts from which were subtracted nanomoles present in endogenous assays lacking acceptor.

In a series of assays to determine acceptor-product ratios, the amount of trimannosyl substrate was increased over a fourfold range. A straight line relationship was demonstrated over a quantity of acceptor ranging from 2.5 to 10.0 μl (12.5 to 50 nmol) (Fig.

---

[1] Hospital for Sick Children, Toronto, Ontario, Canada.

[2] Friedrich Miescher Institute, Basel, Switzerland.

[3] Department de Bioquimica i Biologia Molecular, Facultat de Farmacia, Universitat de Barcelona, Barcelona, Spain.

[4] Department of Biology, University of Hartford, Hartford, CT.

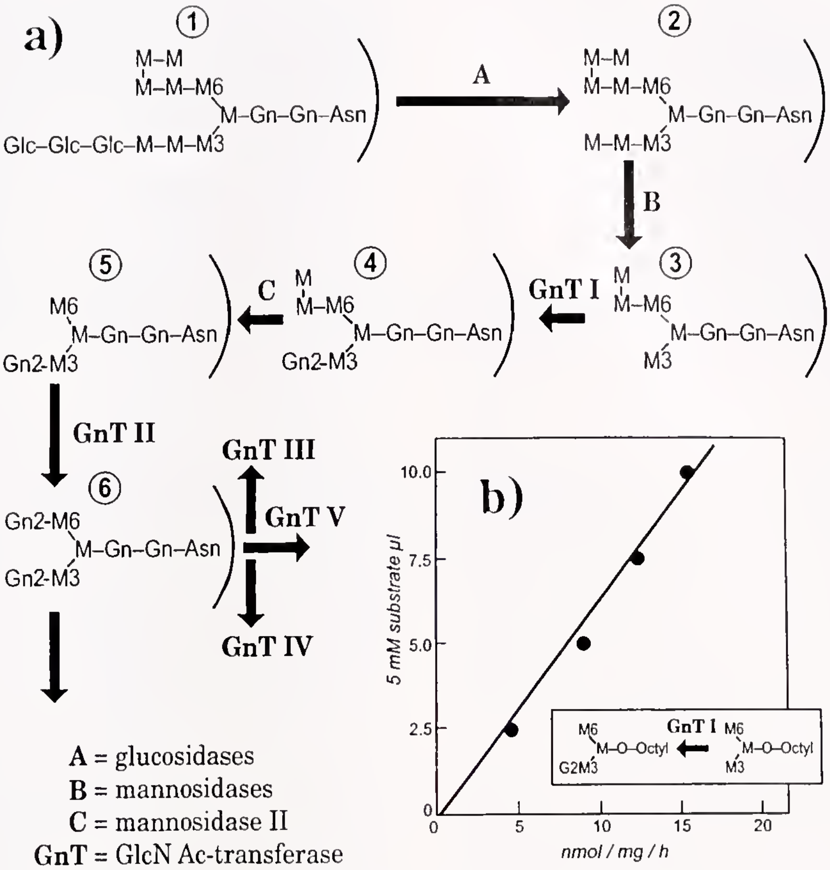

Figure 1. *(a) Biosynthesis of N-linked glycans. Encircled numbers 1–6 designate structural formulae for glycopeptides resulting from sequential enzyme activities (A–C) and of GnTs (I, II). Briefly, compound 1 is acted upon by glycosidases (A), which remove glucose (Glc) to produce compound 2. This is modified by mannosidases (B) to yield the M5 structure (3), which in turn becomes a substrate for steps 4–5 after the additional removal of mannose residues by another mannosidase (C). Compound 6 results from GnT II activity upon the GnT I product. Succeeding structures are enriched, one GlcNAc at a time, by the actions of GnT III, IV, and V. This scheme is practically universal as inferred from many species studied, including lower invertebrates (7). (Fig. 1a adapted from ref. 2). (b) The results of trimannosyl substrate-product assays are presented for substrate concentrations ranging from 12.5 to 50 nanomoles. A straight line relationship was observed. The inset (lower right) represents the biosynthetic activity presumed to occur when GnT I converts trimannosyloctyl substrate into GlcNAc 2-trimannosyloctyl product.*

1b). This relationship established GlcNAc-trimannosyl octyl as the presumed product catalyzed by sponge lysate GnT I activity. The specificity of this synthetic acceptor substrate has been confirmed using a wide range of Gn-T I compounds, including cell lysate from vertebrate and non-vertebrate sources, as well as the cloned and expressed rabbit, human, and mouse Gn-T I gene product (9). Final confirmation of the GlcNAc-trimannosyl link requires additional detailed NMR and spectroscopic analysis of scaled-up purified product.

The finding of a GnT I activity in the sponge raises the prospect of manipulating sponge N-glycan structures by the use of specific GlcNAc enzyme inhibitors. Gray cells, regarded as the immunocytes of the sponge (10), bear the highly N-glycosylated CD44 surface antigen (T. Simpson and W. Kuhns, unpub. data) that may be an appropriate substrate for such chemical interventions. CD44 is likely to be involved in allograft rejection events (11), and if so, alterations in its structure by de-N-glycosylation may play a role as biological response modifiers. In summary, GnT I enzyme activity appears to function in a manner very much like its counterpart in higher species. Since the sponges are the most ancient eukaryotes with a multicellular lineage, the occurrence of cellular GnT I speaks to its importance in cell functions and to its remarkable conservation over time.

Literature Cited

1. **Drickamer, K., and J. Carver. 1992.** *Curr. Opin. Struct. Biol.* **2:** 653.
2. **Brockhausen, I., and W. J. Kuhns. 1997.** *Glycoproteins and Human Disease.* R. G. Landes, Austin, TX.
3. **Schachter, H., and I. Brockhausen. 1993.** Pp. 263–332 in *Glycoconjugates, Composition, Structure and Function.* H. Allen and E. Kisailus, eds. Marcel Dekker, New York.
4. **Jarchow, J., J. Fritz, D. Anselmetti, A. Calabro, V. Hascall, D. Gerosa, M. Burger, and X. Fernandez-Busquets. 2000.** *J. Struct. Biol.* (in press).
5. **Misevic, G., J. Finne, and M. Burger. 1987.** *J. Biol. Chem.* **262:** 5870–5877.

6. **Kaltenbach, J., K. Hudock, M. Burger, G. Misevic, and W. J. Kuhns. 1996.** *Biol. Bull.* **191:** 296–297.
7. **Kornfeld, S., and R. Kornfeld. 1985.** *Annu. Rev. Biochem.* **54:** 631–664.
8. **Kaushal, G., and A. Elhein. 1994.** *Methods Enzymol.* **230:** 316–320.
9. **Reck, F., M. Springer, H. Paulson, I. Brockhausen, M. Sarkar, and H. Schachter. 1994.** *Carbohydr. Res.* **259:** 93–101.
10. **Humphreys, T., and E. Reinherz. 1994.** *Immunol. Today* **15:** 316–320.
11. **Fernandez-Busquets, X., and M. Burger. 1999.** *Microsc. Res. Tech.* **44:** 204–218.

Reference: *Biol. Bull.* **199:** 194–195. (October 2000)

A Ca^{+2}-Independent Cytolytic System from the Blood of the Marine Snail, *Busycon canaliculum*

Peter B. Armstrong[1] *and Rengasamy Asokan (Molecular and Cellular Biology, University of California, Davis, California 95616)*

The immune system is the ensemble of cell-based and humoral agents that protect the organism against parasites that have gained access to the internal milieu. One of the important immune activities for a variety of animals is the outright lysis of foreign cells that contact the blood (1). Cytolytic systems are frequently explored as if they were hemolytic systems, where the foreign cell that is destroyed is the mammalian erythrocyte. The red cell is convenient for the assay of cytolysis because its hemolysis is easily quantified by the release of hemoglobin into the bathing medium. Here we report the presence of a hemolytic system in the plasma of the marine snail, *Busycon.*

Blood was obtained as follows. The foot of the adult whelk was wounded, and the blood flowing from the wound was collected and then immediately centrifuged to remove the cells. Hemocyanin was removed from the plasma by centrifugation (40,000 RPM, 4 h). The hemocyanin-free plasma was dialyzed into Tris-buffered saline (0.15 *M* NaCl, 50 m*M* Tris, pH 7.3). Hemolysis was assayed with rabbit red cells as described previously (2).

The hemolytic activity of hemocyanin-depleted *Busycon* plasma is shown in Figure 1. Hemolysis is progressive, requiring 4 h for completion. The hemolytic activity is unaffected by the inclusion of EDTA in the hemolysis assay, and thus is independent of divalent cations. The lack of a Ca^{+2} dependence distinguishes this hemolytic system from one reported previously in *Busycon* (3). Hemolysis is reduced at low ionic strength, showing a broad activity maximum in buffers containing in excess of 0.2 *M* NaCl. The hemolytic activity is inactivated by trypsin treatment of the plasma, indicating a proteinaceous character to the hemolytic system. The hemolytic activity of plasma is thermolabile, showing complete inactivation by treatment of plasma at 40°C for 0.5 h. The hemolytic protein(s) are retained by a PM30 Amicon filter and pass through a YM100 filter, indicating a molecular mass between 30 and 100 kDa. The hemocyanin-free plasma shows 13 distinct protein bands in this interval by SDS-PAGE, with prominent bands at 78, 55, 43, 35, and 34 kDa.

At least three mechanisms can be envisioned for hemolysis: the insertion of the hemolytic protein into the lipid phase of the plasma membrane to create a hydrophilic trans-membrane pore, the enzymatic modification of the lipid head groups by a phospholipase, and the initiation of membrane-lipid phase-transitions by a detergent-like, or a surface-active protein (4). To test the first possibility, we determined the effects of macromolecular osmolites. The macromolecular osmolite dextran-4 (Mr 4–6 kDa) reduced hemolysis significantly (from 57.0 ± 2.0% to 8.0 ± 2.3% in one trial). This suggests that hemolysis in the present system is produced by insertion of the hemolytic protein into the plasma membrane, generating hydrophilic channels that allow water to flow into the cell in response to the high internal concentration of macromolecular osmolites, principally the protein hemoglobin. The presence of osmolites in the external milieu larger than the channel pore size (*e.g.,* dextran-4), at concentrations sufficient to balance the osmotic pressure of hemoglobin in the cell, would protect the cell from osmotic rupture (5). The molecular size of dextran-4 is approximately 1.7 nm (6), indicating an effective pore size for the membrane-associated hemolytic protein as no larger than this value.

The hemolytic system of *Busycon* is sensitive to the presence of lipopolysaccharide (LPS) from the cell wall of gram-negative bacteria (Fig. 1B). The reduction in the hemolytic action at higher concentrations of LPS may derive from the binding of the hemolytic agent to this important signature molecule of the gram-negative bacterium, reflective of an anti-bacterial action

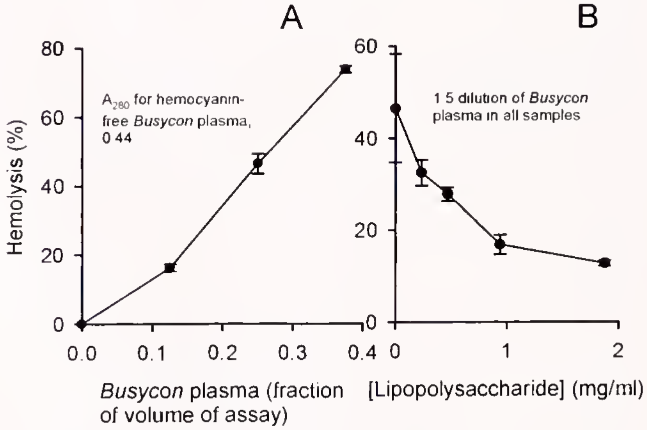

Figure 1. *Hemolytic activity from the plasma of* Busycon canaliculatum. *Hemocyanin was removed by ultracentrifugation, and the supernatant was dialyzed into Tris-buffered saline (0.15* M *NaCl, 50* mM *Tris, pH 7.3). Figure 1A, dependence of hemolysis on the presence of hemocyanin-free* Busycon *plasma. Figure 1B, sensitivity of hemolysis to lipopolysaccharide.*

---

[1] Molecular and Cellular Biology, University of California, One Shields Avenue, Davis, CA 95616, (pbarmstrong@ucdavis.edu).

of the hemolytic agent. Although the concentrations of LPS used for Figure 1B are high, the actual concentration of LPS at the surface of the bacterium is far higher than the solution concentrations used in this trial. The possibility that the hemolytic agent does bind to gram-negative bacteria deserves further investigation.

The ability to destroy foreign cells that come in contact with the blood is an important defense strategy for a variety of animals. In mammals, the cytolysis of foreign cells is conducted by the complement system, a multi-component ensemble of plasma proteins whose membrane attack elements are activated by a proteolytic cascade that, itself, is initiated by a variety of stimuli indicative of parasitic invasion (7). The complement system is found only in the deurostomate animals (*i.e.*, the echinoderms and the chordates) and is absent from protostomate animals (8, 9). In the latter, the relatively few cytolytic systems that have been characterized are less complex than the vertebrate complement system, with some the province of a single protein that both recognizes and binds to the foreign cell and mediates its cytolytic destruction (5, 10). Only a few cytolytic systems have been reported in the plasma of molluscs (11, 12), and we have not found any reports for gastropods. The systems reported from bivalves (11, 12) are Ca^{+2}-dependent, suggesting that they are based on different effector molecules than the system described here from *Busycon*.

Supported by Grant No. MCB-97-26771 from the National Science Foundation.

Literature Cited

1. **Canicatti, C. 1990.** *Experientia (Basel)* **46:** 239–244.
2. **Swarnakar, S., R. Asokan, J. P. Quigley, and P. B. Armstrong. 2000.** *Biochem. J.* **347:** 679–685.
3. **Biswas, C., and P. B. Armstrong. 1999.** *Biol. Bull.* **197:** 276–277.
4. **Oliver, A. E., F. Tablin, N. J. Walker, and J. H. Crowe. 1999.** *Biochim. Biophys. Acta* **1416:** 349–360.
5. **Hatakeyama, T., H. Nagatomo, and N. Yamasaki. 1995.** *J. Biol. Chem.* **270:** 3560–3564.
6. **Scherrer, R., and P. Gerhardt. 1971.** *J. Bacteriol.* **107:** 718–735.
7. **Law, S. K., and K. B. M. Reid. 1988.** *Complement.* IRL Press, Oxford.
8. **Smith, L. C., L. Chang, R. J. Britten, and E. H. Davidson. 1996.** *J. Immunol.* **156:** 593–602.
9. **Al-Sharif, W. Z., J. O. Sunyer, J. D. Lambris, and L. C. Smith. 1998.** *J. Immunol.* **160:** 2983–2997.
10. **Armstrong, P. B., S. Swarnakar, S. Srimal, S. Misquith, E. A. Hahn, R. T. Aimes, and J. P. Quigley. 1996.** *J. Biol. Chem.* **271:** 14,717–14,721.
11. **Anderson, R. S. 1981.** *Dev. Comp. Immunol.* **5:** 575–585.
12. **Yoshino, T., and T.-L. Tuan. 1985.** *Dev. Comp. Immunol.* **9:** 515–522.

Reference: *Biol. Bull.* **199:** 195–197. (October 2000)

Modulation of the Development of Plutei by Nitric Oxide in the Sea Urchin *Arbacia Punctulata*

Diane E. Heck, Lydia Louis, Michael A. Gallo and Jeffrey D. Laskin (Departments of Pharmacology and Toxicology, Rutgers University, and Environmental and Community Medicine, UMDNJ Robert Wood Johnson Medical School, Piscataway, New Jersey 08854)

Nitric oxide, a reactive free radical, has recently been identified as a key mediator of intercellular signaling in numerous species (1). It is produced enzymatically from l-arginine by the nitric oxide synthase family of oxidoreductases (2). Nitric oxide regulates a variety of physiological functions including relaxation of vascular smooth muscle, long-term potentiation, tumor cell apoptosis, and cytostasis (3). In addition, inappropriate or excessive production of nitric oxide has been implicated in tissue injury (4). Nitric oxide is known to initiate biochemical effects through binding to iron and iron-sulfur-containing proteins and modulating their activity (5). Nitric oxide can also modify DNA and is known to alter growth factor-mediated transcription processes (5). At the present time, no clear role for this free radical species in regulating development has been defined.

We have previously reported that nitric oxide synthase inhibitors alter fertilization and differentiation of sea urchin eggs (6). In the present studies, we examined the direct effects of nitric oxide on the development of the sea urchin *Arbacia punctulata*. For these studies, fertilized eggs were prepared from sea urchins, as described by Hinegardner (7), and maintained at 24°C. Embryos were exposed to S-nitroso-N-acetylpenicillamine (SNAP, Molecular Probes, Eugene, OR), an agent that spontaneously releases nitric oxide, for 1 h at various developmental stages. These stages included: immediately after fertilization, following the first and fifth divisions, the morula and prism stages, and at two points in pluteal development, *i.e.*, 24 and 48 h after fertilization. Treated embryos and untreated controls were further evaluated at regular intervals for 72 h. Both morphological abnormalities and transient delays in development were observed, but particular effects were dependent on the developmental stage at the time of treatment. Morphological abnormalities were quantified at the morula, prism, and pluteus stages.

In initial experiments, we determined the effects of a range of concentrations of SNAP (2 n*M*–2 μ*M*) applied to sea urchin eggs immediately after fertilization. Embryo mortality with little cell division was observed when embryos were treated with concentrations of SNAP in excess of 200 n*M*. However, both transient and permanent developmental changes were found after treatment with lower concentrations of the nitric oxide releasing agent (see further below). For our studies, we used 20 n*M* SNAP; at this concentration, prominent morphological alterations occurred without significant toxicity.

Developmental lesions are often induced by temporally restricted biochemical changes that eliminate critical downstream events or cause them to occur inappropriately. The resulting aberrant development reflects a stage-specific sensitivity to a pharmacological agent or event. To determine the developmental stages at which sea urchin embryos are sensitive to nitric oxide, we next exposed fertilized eggs to SNAP during various stages of development. Following fertilization, sea urchin eggs divide synchronously until the fifth division. At this stage, the embryo is designated a morula, and the uniformly distributed pigment granules become unevenly distributed to specific cells, with most going to the 8 macromere cells. When SNAP was applied after fertilization or first division, we observed no morphological alterations in the morula. Both drug-treated embryos and controls contained 2–4 darkly pigmented cells.

Sea urchin embryos hatch and become free-swimming shortly after the initiation of motility. Later, about 18 h after fertilization, the free-swimming sea urchin embryos become pyramidal, and enter the prism stage. When such embryos were exposed to SNAP, no anatomical aberrations were observed. However, embryos treated with SNAP at any stage prior to hatching exhibited delays in development (Table 1). Thus, 18 h after fertilization, embryos treated with SNAP prior to the morula stage had not progressed beyond the blastula stage. In addition, embryos exposed to SNAP before hatching contained fewer than the 6–8 darkly pigmented cells observed in controls.

Developing sea urchins generally progress to the pluteus by about 24 h after fertilization. At this stage, plutei that had been treated with SNAP immediately after fertilization, or the first division, exhibited gross morphological alterations. Additionally, the pigment cells aggregated and were fewer in number (Table 1; Fig. 1, compare panels A and B; other data not shown). This effect was associated with fewer animals progressing through development. Those that did develop further exhibited diminished arm extension when evaluated 48 h after fertilization (Fig. 1, compare panels C and D and not shown). As these plutei continued to develop, the poorly extended arms were often oriented 90° to the longitudinal axis rather than parallel to it. Aberrant morphology was less pronounced in embryos exposed to nitric oxide after division 5. In addition, when evaluated 24 h after fertilization, the number of pigment cells remained unchanged in embryos treated with SNAP before division 5, while about 4 times as many darkly pigmented cells were identified in untreated embryos.

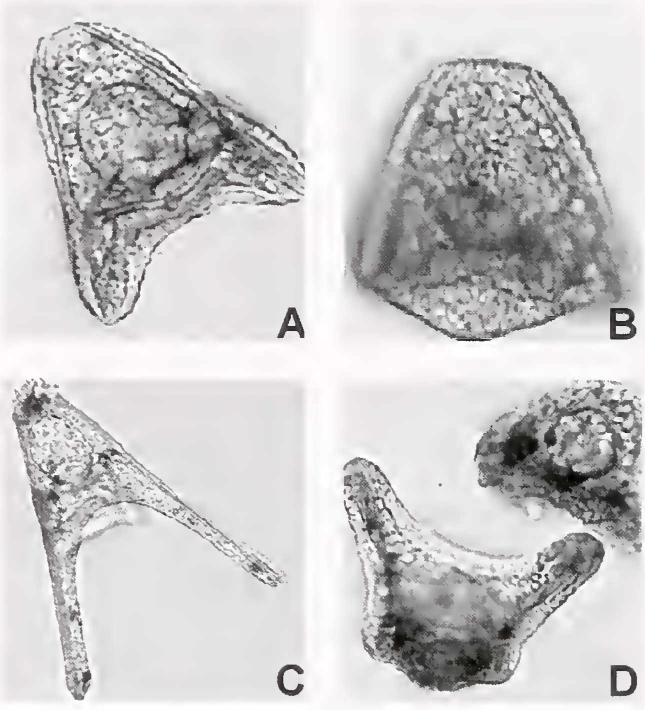

Figure 1. *Effect of nitric oxide on the development of sea urchin eggs. Immediately following fertilization, sea urchin eggs were treated with 20 nM SNAP. After 1 h the embryos were washed and allowed to develop. Panels A and B are sea urchin embryos 24 h after fertilization; panels C and D show embryos 48 h after fertilization. Panels A and C are control embryos; panels B and D are embryos that have been treated with SNAP.*

Table 1

Changes in sea urchin embryo development in response to treatment with SNAP

Developmental stage at treatment	Developmental stage 24 hours after fertilization (embryos/50 μl)		
	Morula	Prism	Pluteus
Untreated	1 ± 2.3	0 ± 0.6	13 ± 3.9
Following fertilization[1]	24 ± 6.1	7 ± 3.2	0 ± 0.3
First Division	27 ± 0.6	14 ± 2.3	1 ± 3.3
Division 5	19 ± 4.0	10 ± 1.9	0 ± 3.4
Morula	1 ± 4.3	4 ± 0.8	9 ± 2.3
Prism	0 ± 3.4	0 ± 0.9	21 ± 4.5
Pluteus	2 ± 3.3	1 ± 0.3	13 ± 2.6

[1] Approximately 10^5 embryos were suspended in 10 ml of sea water supplemented with 20 n*M* SNAP at the indicated developmental stages. After 1 h, embryos were transferred into 100 ml of SNAP-free sea water. Embryos were then evaluated for progress through development at 24 h after fertilization. Each point represents the average number of embryos in each stage of development for 5 experiments ± SEM.

When observed 24 h after fertilization, delayed development was again evident in embryos treated with SNAP at all stages prior to hatching. However, following exposure to SNAP at the morula stage, embryos appeared normal in development by 48–72 h after fertilization. No effects on morphology or development were observed in embryos exposed to nitric oxide at the prism stage or as plutei either 24 or 48 h after fertilization (not shown). Anatomical changes resulting from exposure to nitric oxide were preceded by an apparent inhibition of pigment cell division. These results indicate that sea urchin embryos exposed to nitric oxide before their development into morula show permanent morphological changes, whereas exposure at later stages has no apparent permanent effects.

Taken together, our results demonstrate that brief exposure of sea urchin embryos to nitric oxide during early development causes irreversible abnormalities in plutei, including skeletal aberrations and changes in the proliferation and migration of pigment cells. The effects of nitric oxide applied at later stages are reversible. We speculate that nitric oxide may act as a negative regulator of pigment cell division and skeletal extension *in vivo*.

Literature Cited

1. **Hobbs, A. J., A. Higgs, and S. Moncada. 1999.** *Annu. Rev. Pharmacol. Toxicol.* **39:** 191–220.
2. **Hemmens, B., and B. Mayer. 1998.** *Methods Mol. Biol.* **100:** 1–32.
3. **Moncada, S. 1999.** *J. R. Soc. Med.* **92:** 164–169.
4. **Laskin, J. D., D. E. Heck, and D. L. Laskin. 1994.** *Trends Endocrinol. Metab.* **5:** 377–382.
5. **Lane, P., and S. Gross. 1999.** *Semin. Nephrol.* **19:** 215–229.
6. **Heck, D. E., J. D. Laskin, S. Zigman, and W. Troll. 1994.** *Biol. Bull.* **187:** 248–249.
7. **Hindgardner, R. 1975.** Pp. 10–25 in *The Sea Urchin Embryo, Biochemistry and Morphogenesis*, G. Czihak, ed. Springer-Verlag, Berlin.

Reference: *Biol. Bull.* **199:** 197–198. (October 2000)

Development of Self-Referencing Oxygen Microsensor and its Application to Single Pancreatic HIT Cells: Effects of Adenylate Cyclase Activator Forskolin on Oxygen Consumption

Sung-Kwon Jung, Katherine Hammar, and Peter J. S. Smith (BioCurrents Research Center, Marine Biological Laboratory, Woods Hole, Massachusetts 02543)*

Information about oxygen dynamics is valuable for evaluating the metabolic activity of pancreatic β cells, which contribute to the regulation of glucose homeostasis in the blood. When glucose, the key secretagogue, is metabolized in β cells, intracellular messengers such as ATP are formed. ATP-sensitive potassium channels (K_{ATP}) then close, which depolarizes the cell, leading to Ca^{2+} entry and stimulation of insulin secretion by exocytosis (1, 2). The relationships between metabolism, oxygen consumption, insulin secretion, and other biochemical changes in pancreatic islets have been examined (3–5). In the present investigation, we focused on the relationship between altered cAMP levels and oxygen consumption. According to Ammala *et al.*, insulin release by intracellular cAMP is calcium-independent (6). But exocytosis is metabolically driven, and intracellular calcium levels are tightly correlated with oxygen consumption (3). Therefore, we need to study the oxygen dynamics of β cells, but at the level of a single cell, because pancreatic islets are composed of four distinct cell types. However, such studies with single β cells are very difficult, primarily because single cells generate very small changes in oxygen level during respiration. Often, therefore, the electrochemical drift of an oxygen sensor dwarfs such small changes, so interpretation of the data is difficult. We have now developed a self-referencing oxygen microsensor with a tip diameter $< 3\ \mu$m and have measured the oxygen consumption of single pancreatic HIT cells.

The self-referencing technique has been successfully used to measure selected ion and oxygen fluxes at single cell levels by minimizing the impact of sensor drift and noise (7, 8). The technique is based on the translational movements of a microprobe between two points in the concentration gradient that extends outward from the cell membrane. The difference in the values measured at two points provides information about the gradient. The oxygen sensor used in the current study was designed to have the characteristics required for the self-referencing technique, such as minimal convection perturbation and a response time <1 s. The sensor has an etched Pt wire electrochemically recessed inside a pulled glass micropipette, which was coated with cellulose acetate (9).

To validate the applicability of the self-referencing oxygen sensor to flux measurements, an oxygen gradient was artificially generated and measured (Fig. 1A). The apparent oscillation of the DC trace is the result of sensor relocations in the oxygen gradient. The translational frequency was optimized for maximal sensitivity (0.2 Hz). For example, as observed in Figure 1A, the signal rapidly equilibrated as the sensor was repeatedly brought to a new position in the self-referencing mode compared to the stationary mode. IonView (a product of BioCurrents Research Center, Marine Biological Laboratory, Woods Hole, MA) automatically subtracts current values at the far position from those at the near position. The first half of the values at each position were discarded to eliminate the artifacts from sensor motion and response time; the second half were sampled for mathematical subtraction (7). The resulting data, designated as AC, are used for calculating oxygen flux according to the Fick equation:

$$J = -D_o(\Delta C/\Delta r), \tag{1}$$

where J is flux (mol cm^{-2} s^{-1}), D_o is the diffusion coefficient of oxygen (2.6×10^{-5} cm^2 s^{-1}), and ($\Delta C/\Delta r$) is the concentration difference divided by the translational distance (*i.e.*, the concentration gradient).

We applied the self-referencing oxygen sensor to single pancreatic HIT cells. Oxygen consumption was significantly decreased upon the injection of rotenone, an inhibitor of mitochondrial respiration (Fig. 1B). Based on equation 1, the oxygen flux with a Δr of 30 μm at 25 μm from the plasma membrane of single cells was 640 ± 40 fmol/cm^2/s (mean ± SEM, $n = 5$) at 11 mM glucose, which is then converted into a consumption (3.2 fmol/cell/min) by taking the geometric surface area into account. After rotenone injection, the oxygen flux significantly decreased to 97 ± 15 fmol/cm^2/s (mean ± SEM, $n = 5$), a consumption of 0.4 fmol/

---

* Corresponding author: sjung@mbl.edu

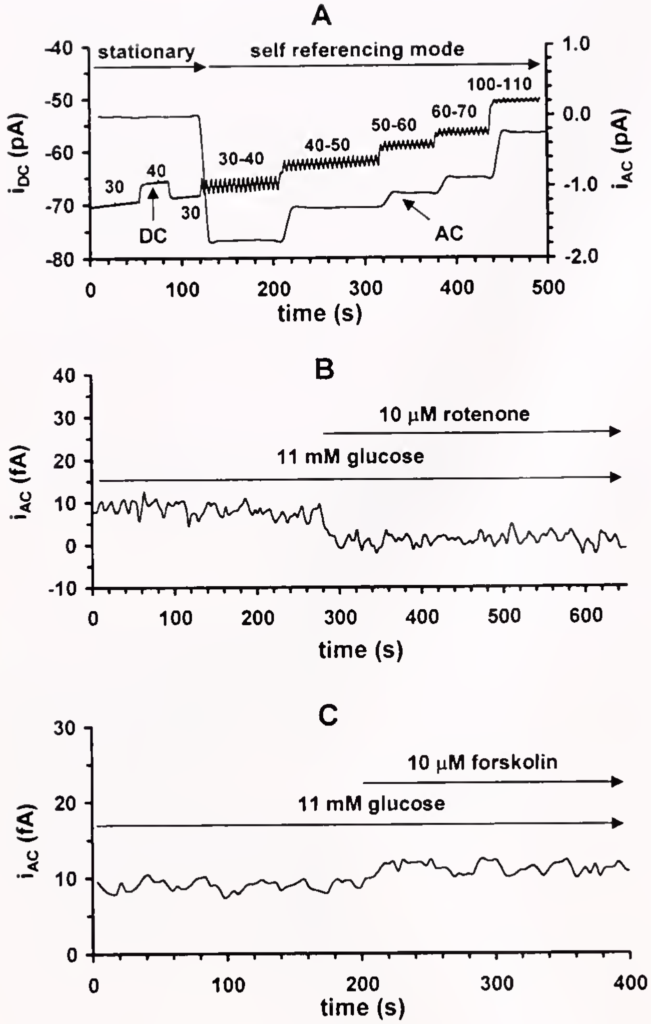

Figure 1. *(A) Real time trace (DC) and IonView processed trace (AC) of oxygen current as a function of distance from an oxygen source (diameter ~ 10 μm) measured with a stationary and a self-referencing oxygen microsensor. In the self-referencing mode, the oxygen sensor was oscillated within a 10-μm excursion at a frequency of 0.2 Hz. The numbers are the relative distance from the oxygen source in microns. (B) Influence of rotenone on oxygen consumption by a single pancreatic HIT cell. The trace is a representative of five measurements. (C) Influence of forskolin on oxygen consumption by a single pancreatic HIT cell. The trace is a representative of four measurements. There is a significant difference in oxygen consumption after forskolin treatment ($P < 0.01$). In the above single cell measurements, the oxygen sensor was positioned 10 μm from the plasma membrane of the cell and oscillated between 10 and 40 μm (a 30-μm excursion) at a frequency of 0.2 Hz. A potential of −600 mV vs. Ag/AgCl was applied to the oxygen sensor in a modified HEPES buffer at 37°C for all experiments.*

cell/min ($P < 0.001$ according to two-tailed Student's t tests). This decrease (~88%) is presumably due to the inhibition of NADH-dependent respiration. We injected forskolin, a specific activator of adenylate cyclase, to elevate cAMP level and observed a flux of 0.76 ± 0.07 pmol/cm^2/s (mean ± SEM, $n = 4$), a consumption of 4.0 fmol/cell/min (see Fig. 1C). The oxygen consumption after forskolin treatment was significantly higher than before ($P < 0.01$). This increase (~19%) may account for the ATP demand in insulin secretion.

Calcium ions may have a role in the response of HIT cells to adenylate cyclase activation. Oxygen dynamics and intracellular Ca^{2+} ([Ca^{2+}]$_i$) are well correlated in islet cells, in that increases in oxygen consumption closely follow increases in [Ca^{2+}]$_i$, according to the observation by Jung *et al.* (3). The activation of adenylate cyclase will lead to a decrease in ATP levels unless ATP is rapidly replenished. Therefore, we postulate that the forskolin-induced increase in oxygen consumption reflects the release of Ca^{2+} from subcellular organelles, a notion supported by the finding that blockage of sarco-endoplasmic reticulum Ca^{2+}-ATPase (SERCA) pumps by thapsigargin abolishes transient increase in [Ca^{2+}]$_i$ induced by forskolin (10). On the other hand, cAMP could directly deinhibit the activity of phosphofructokinase, a controlling enzyme of glycolysis, resulting in NADH elevation and then an increase in oxygen consumption. The above intertwined relationships could be explained by a recent report suggesting that, while Ca^{2+} may activate respiration, its entry into β cells has a net effect of decreasing the ATP/ADP ratio resulting from the activation of numerous ATP consuming processes, such as insulin secretion and ion-pumping (11).

In conclusion, the development of a self-referencing oxygen microsensor and its application to single HIT cells hold promise for the elucidation of the relationship between oxygen dynamics and the role of cAMP in exocytosis. Further use of the self-referencing oxygen sensor will include correlated measurements with [Ca^{2+}]$_i$, ATP/ADP and insulin secretion at the single cell level.

We thank Richard Sanger for technical assistance. This work was supported by the NIH Grant NCRR P41 RR01395 to PJS Smith.

Literature Cited

1. **Asfari, M., D. Janjic, P. Meda, G. Li, P. A. Halban, and C. B. Wollheim. 1992.** *Endocrinol.* **130:** 167–178.
2. **Bergsten, P., E. Grapengiesser, E. Gylfe, A. Tengholm, and B. Hellman. 1994.** *J. Biol. Chem.* **269:** 8749–8753.
3. **Jung, S.-K., L. M. Kauri, W.-J. Qian, and R. T. Kennedy. 2000.** *J. Biol. Chem.* **275:** 6642–6650.
4. **Corkey, B. E., K. Tornheim, J. T. Deeney, M. C. Glennon, J. C. Parker, F. M. Matschinsky, N. B. Ruderman, and M. Prentki. 1988.** *J. Biol. Chem.* **263:** 4254–4258.
5. **Larsson, O., H. Kindmark, R. Branstrom, B. Fredholm, and P.-O. Berggren. 1996.** *Proc. Natl. Acad. Sci. USA* **93:** 5161–5165.
6. **Ammala, C., F. M. Ashcroft, and P. Rorsman. 1993.** *Nature* **363:** 356–358.
7. **Smith, P. J. S., K. Hammar, D. M. Porterfield, R. H. Sanger, and J. R. Trimarchi. 1999.** *Microsc. Res. Tech.* **46:** 398–417.
8. **Land, S. C., D. M. Porterfield, R. H. Sanger, and P. J. S. Smith. 1999.** *J. Exp. Biol.* **202:** 211–218.
9. **Jung, S.-K., W. Gorski, C. A. Aspinwall, L. M. Kauri, and R. T. Kennedy. 1999.** *Anal. Chem.* **71:** 3642–3649.
10. **Liu, Y.-J., E. Grapengiesser, E. Gylfe, and B. Hellman. 1996.** *Arch. Biochem. Biophys.* **334:** 295–302.
11. **Detimary, P., P. Gilon, and J. C. Henquin. 1998.** *Biochem. J.* **333:** 269–274.

Reference: *Biol. Bull.* **199:** 199–200. (October 2000)

Identification of Proliferating Cells in Hard Clams

Rhea Hanselmann[1], *Roxanna Smolowitz (Marine Biological Laboratory, Woods Hole, Massachusetts), and Daniel Gibson*[1]

The origin of hemocytes, the circulating "blood cells" of bivalve molluscs, including hard clams (*Mercenaria mercenaria*) has not been identified (1, 2). Proliferation of hemocytes, however, can be recognized through their increased numbers in diseased animals. Proliferating cell nuclear antigen (PCNA), or cyclin, is a protein produced during the late G1 and S phases of the cell cycle (3, 4). Using antibodies that recognize PCNA in mice, we attempted to identify the origin of hemocytes in the hard shell clams. Quahog parasite unknown (QPX) is a protist that causes severe inflammation and mortality in infected clams (5, 6). We attempted to induce hemocyte proliferation by exposing clams to QPX in a 10-l water column in which 12 ml of undiluted QPX culture (at a concentration of $7*10^6$ cells/ml) were added every 10 days; by injecting QPX between the membranous mantles and the right valves, 3 cm ventral anterior to the siphon and into the pericardial cavities (0.25 ml of undiluted QPX culture); and by injecting an inert particle (India ink, 1:10 dilution in sterile seawater [7, 8]) into the pericardial cavities. The controls consisted of two groups of clams. One group was injected with sterile seawater in the pericardial cavities; the other was untreated. Groups were sampled at 24 h, and at 1, 4, and 8 weeks after the start of the experiment. At sampling, the animals were shucked, fixed in 10% neutral buffered formalin (NBF) for 24 h, and embedded in paraffin. Sections were cut (4–6 μm), mounted onto positively charged slides (Fisherbrand, Superfrost/Plus and ProbeOn Plus slides) and stained either with hematoxylin and eosin (H&E) (9) or with anti-PCNA with a hematoxylin counterstain (Zymed, PCNA Staining Kit).

Clams injected with QPX in the pericardial cavities showed mild focal inflammation associated with viable and necrotic QPX organisms. At 2 months post-injection, viable QPX organisms were no longer identified. QPX organisms and associated inflammation were not observed in clams injected in the mantle cavity. After 2 months of water column exposure, only very rare infection by QPX organs with minimal inflammation was observed in mantle tissue. India ink injection caused a minimal inflammatory response. Pools of injected ink in the tissues and vascular spaces were either engulfed by individual hemocytes or surrounded and sequestered by hemocytes (encapsulation), forming thin-walled granulomas (6, 10). Numerous individual hemocytes containing India ink were eliminated from the clams by diapedesis over lumenal epithelial surfaces (Fig. 1A). Thick-walled granulomas (6, 10) were also identified in the gills, pericardial sacs, and other

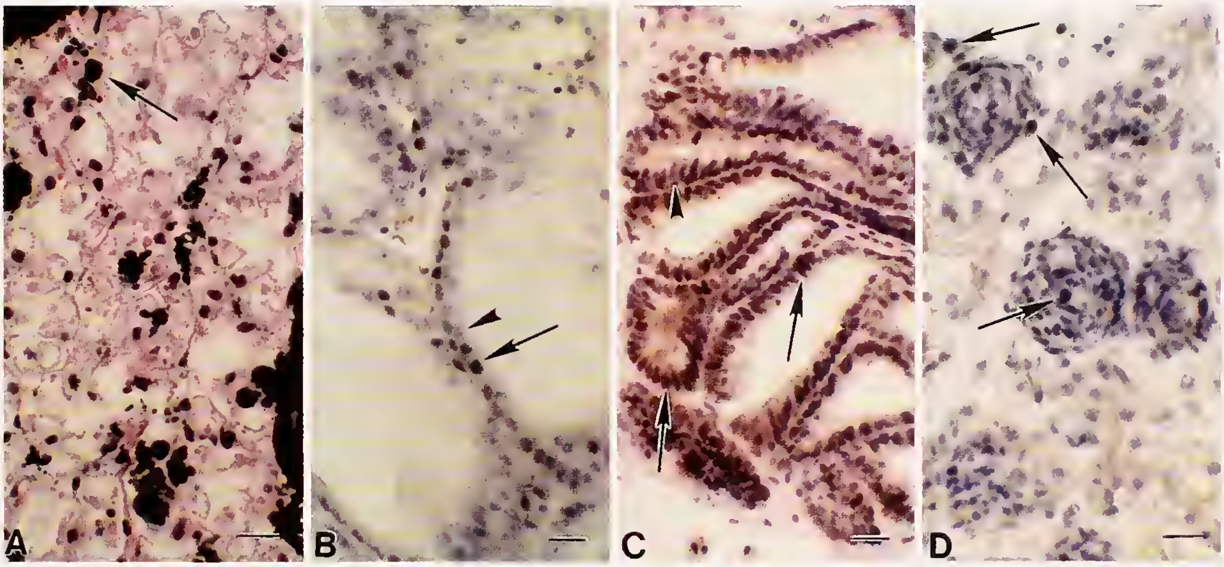

Figure 1. *Proliferating epithelial cells and hemocytes of* Mercenaria mercenaria *stained with anti-Mouse Proliferating Cell Nuclear Antigen (PCNA). (A) India ink is phagocytized and eliminated by diapedesis of India ink-filled hemocytes (arrow) into the renal tubular lumens (H&E, bar = 13 μm). (B) Nuclei of proliferating reserve cells of the digestive gland's tubular epithelia stained black (arrow) with anti-PCNA. PCNA negative nuclei stain blue (arrowhead) (hematoxylin counterstain, bar = 13 μm). (C) Strong PCNA nuclear staining is present in the proliferating nuclear epithelial cells at the base of the gills (arrows). PCNA negative nuclei stain blue (arrowhead) (hematoxylin counterstain, bar = 13 μm). (D) Nuclei of some hemocytes in thick-walled granulomas in the kidney tissue of clams are positive for PCNA stain (arrows) and present evidence for the proliferation of hemocytes directly at the inflammatory site (hematoxylin counterstain, bar = 13 μm).*

---

[1] Worcester Polytechnic Institute, Worcester, MA.

organs of saline-injected animals, indicating that the injection may not have been sterile.

Using the anti-mouse PCNA, areas of abundant PCNA staining (black-stained nuclei), indicating areas of marked cell proliferation, were identified in the reserve cells of the digestive gland (Fig. 1B), the proliferative epithelial cells of the gill base (2) (Fig. 1C), and in early proliferative phases of reproductive epithelium. As expected, cells of other tissues throughout the body also stained positive for PCNA (*i.e.*, epithelium of the intestine, foot and body wall, and gill plical epithelium), but in much lower numbers. Proliferating hemocytes were identified in the inflammatory cells forming the thick-walled granulomas (Fig. 1D) and rarely in adjacent non-inflammatory cells. In no other areas examined were proliferating hemocytes identified.

These results demonstrate that the epitopes associated with PCNA are conserved between the clam and the mouse, as shown by the positive staining of known proliferative cells in the clam body. Previous studies have shown that hemocytes appear to migrate to areas of infection in bivalves (2, 6). In diseased bivalves, hemocyte numbers appear to increase; the site of origin of these hemocytes has never been determined (2). This study provides evidence that the hemocytes of the hard clam proliferate directly at the inflammatory site, as opposed to a possible bone marrow-like area in the body of the clam, with subsequent migration of hemocytes to sites of infections, as seen in vertebrates.

This work was supported, in part, by a NOAA Sea Grant Award to the Woods Hole Oceanographic Institution Sea Grant Program, Grant No. NA86RG0075, Project Number R/A-39.

Literature Cited

1. **Moore, C. A., and A. F. Eble. 1977.** *Biol. Bull.* **152:** 105–119.
2. **Cheng, T. C. 1996.** Pp. 631–642 and 299–333 in *The Eastern Oyster,* Crassostrea virginica. V. S. Kennedy, R. I. E. Newell, and A. F. Eble, eds. Maryland Sea Grant College Publication UM-SG-TS-96-01.
3. **Waseem, N. H., and D. P. Lane. 1990.** *J. Cell. Sci.* **96:** 121.
4. **Ogata, K., Y. Ogata, R. M. Nakamura, and E. M. Tan. 1985.** *J. Immunol.* **135:** 2623.
5. **Kleinschuster, S. J., R. Smolowitz, and J. Parent. 1998.** *J. Shellfish Res.* **17:** 75–78.
6. **Smolowitz, R., D. Leavitt, and Frank Perkins. 1998.** *J. Invertebr. Pathol.* **71:** 9–25.
7. **Stauber, L. A. 1950.** *Biol. Bull.* **98:** 227–241.
8. **Tripp, M. R. 1960.** *Biol. Bull.* **119:** 273–282.
9. **Humanson, G. L. 1997.** Pp. 101–118 in *Humanson's Animal Tissue Techniques,* 5th ed. J. K. Presnell and M. P. Schreibman, eds. The John Hopkins University Press, Baltimore, MD.
10. **Eble, A. F., and R. Scro. 1996.** Pp. 25–30 in *The Eastern Oyster,* Crassostrea virginica. V. S. Kennedy, R. I. E. Newell, and A. F. Eble, eds. Maryland Sea Grant College Publication UM-SG-TS-96-01.

Reference: *Biol. Bull.* **199:** 200–201. (October 2000)

Conditions Affecting the Growth and Zoosporulation of the Protistan Parasite QPX in Culture

Christine Brothers[1], *Ernest Marks III*[2], *and Roxanna Smolowitz*
(Marine Biological Laboratory, Woods Hole, Massachusetts 02543)

Quahog Parasite Unknown (QPX) is a protistan disease of hard clams (*Mercenaria mercenaria*). The QPX organism has been classified in the phylum Labyrinthomorpha (1, 2). Disease resulting from QPX infection has been identified in New Brunswick and Prince Edward Island, Canada; Barnegat Bay, New Jersey; Chatham, Duxbury, and Provincetown, Massachusetts; and three locations in Virginia (1, 2). Mortality from QPX can be severe, with losses especially high in clams just under market size (about 2 years old). An important clinical sign of infection is the occurrence of QPX-infected inflammatory nodules in the mantle.

Whyte *et al.* (3) isolated QPX cells from infected clams; when placed in artificial seawater, these cells produced sporangia and zoospores. Kleinschuster and Smolowitz (2) recently described continuous *in vitro* culture of QPX. QPX was isolated from inflamed mantle nodules and cultured in modified MEM medium at pH 7.2 at 22°C. Mature cultures (after 5 to 10 days) showed thalli, immature sporangia, and mature sporangia containing endospores. Organisms in these stages ranged from 5 to 120 μm in diameter. Endospores released from mature sporangia became the new thalli. Cultured QPX organisms produced, and were embedded in, a thick mucoid material that could be removed intact from the remaining unused culture medium. When placed into sterile seawater, QPX produced motile zoospores within 4 days.

The effects of different environmental conditions on the occurrence of QPX and the resulting disease in the field are unknown. Determination of how environmental parameters affect cultured QPX may help in understanding the pathogenesis of the disease in the field. In this study, the environmental effects of temperature, pH, and salinity were investigated on QPX cells in culture.

Medium (pH 7.2 and salinity 40 ppt) was prepared using the standard methods (2). Modified medium (40 ppt) was prepared at pH 6.0, 7.0, and 8.0 by adjusting pH with 2 *M* HCl and 2 *M* NaOH. Modified medium (pH 7.2) was also prepared at 20, 28, and 34 ppt by proportionally reducing the salt content of the medium and monitoring the resulting solutions with a refractometer. All media were filter sterilized. To test the effects of pH and salinity on the proliferation of QPX in culture, 0.4 ml of two QPX subcultures was placed in a culture flask with 10 ml of each of the three pH variations or four (including standard) salinity variations. Fourteen cultures were created (seven of each subculture). These cultures were incubated for 10 days at 22°C. To test the effects of temperature on QPX growth in culture, the same procedure was followed

---

[1] Falmouth High School, 874 Gifford St., Falmouth, Massachusetts 02540.

[2] Barnstable County AmeriCorps Cape Cod, PO Box 427, Barnstable, MA 02630.

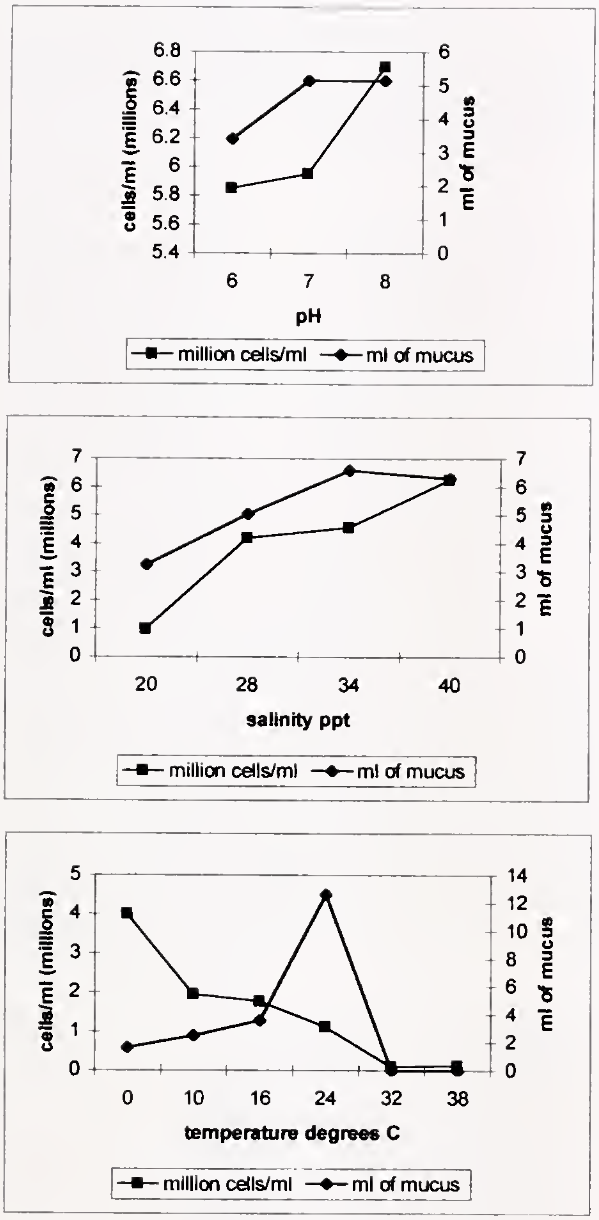

Figure 1. *Growth of QPX as a function of pH, salinity, and temperature as measured by cell count (millions of cells per ml) and volume of mucoid containing QPX material produced (ml of mucus).*

using 10 ml of standard medium to create a total of 12 cultures. One flask of each subculture was incubated at six temperatures (0°, 10°, 16°, 22°, 32°, 38°C) for 10 days.

Concentrations of the mucus containing QPX from each of the four initial subcultures, as well as from the 26 experimental cultures at the end of the 10-day incubation, were determined. The QPX-containing mucus was extracted from the culture medium and measured using a 10-ml pipette. Concentrations of QPX organisms were measured by counting the number of cells per milliliter of a 1:10 saline dilution of the mucus, using a hemocytometer. Initial concentrations of QPX averaged 1.4 million cells per milliliter (range = 1.1 to 1.8 million). Final concentrations and volumes are shown in Figure 1.

QPX concentrations per milliliter and volume of mucus produced both increased with increasing pH and increasing salinity. In culture, the modified MEM medium becomes more acidic as the culture matures. This lower pH may inhibit further growth of the culture. At low salinities, QPX thalli have previously been observed lysing, which may explain the lower cell concentrations at 20 ppt. The cell concentration was highest at 0°C and decreased with increasing temperature. This may represent a thinning out and spreading of the mucus containing the cells with increasing temperature. However, the total number of QPX organisms and total mucus production was greatest at 24°C. The volume of mucus containing QPX produced was low from 0° to 16°C, peaked at 24°C, then declined with increasing temperature. Above 32°C, there was no growth of QPX and no mucus production. Whether QPX will grow above pH 8.0 and above 40 ppt should be investigated.

Proliferation of cultured QPX is best at a temperature of 24°C, pH 7 to 8, and salinities of 28 ppt and above. Such findings are consistent with the field observation of increased infection in the summer and occurrence of QPX disease primarily in high-salinity waters.

Conditions affecting the zoosporulation of QPX were also investigated. Seawater (pH 8.0, salinity 30 ppt) was adjusted to pHs of 6.0, 7.0, and 9.0 (using 2 *M* HCl and 2 *M* NaOH) and to salinities of 20 and 40 ppt (by dilution with distilled water or addition of NaCl), then filter sterilized. Concentrations of 1% and 10% QPX in seawater of each pH and salinity were placed in replicates in a 24-well sterile plate. The plates were incubated at 10°, 16°, 22°, 32°, and 38°C and examined daily for 5 days.

Other researchers (2, 3) have reported zoosporulation in QPX; however, there is reason to believe these may not have been from pure cultures of QPX. This study attempted to replicate those findings; however, no zoospores were observed in repeated trials, even in normal sterile seawater. Whether in fact QPX produces zoospores, as not all members of the phylum do, and under what conditions it does so are important both in the further classification of the organism and in studying transmission of the disease. Therefore, this question deserves further investigation.

This work was supported, in part, by a NOAA Sea Grant Award to the Woods Hole Oceanographic Institution Sea Grant Program, Grant No. NA86RG0075, project number R/A-39.

Literature Cited

1. **Smolowitz, R., D. Leavitt, and F. Perkins. 1998.** *J. Invert. Path.* **71:** 9–25.
2. **Kleinschuster, S. J., R. Smolowitz, and J. Parent. 1998.** *J. Shellfish Res.* **17:** 75–78.
3. **Whyte, S. K., R. J. Cawthorn, and S. E. McGladdery. 1994.** *Dis. Aquat. Org.* **19:** 129–136.

Reference: *Biol. Bull.* **199:** 202–203. (October 2000)

Effects of Myosin-II Antibody on Actin-Dependent Vesicle Transport in Extracts of Clam Oocytes

Leslie Sandberg, Phillip Stafford and George M. Langford
(Dartmouth College, Hanover, New Hampshire 03755)

The movement of vesicles and organelles in cells has been shown to occur on both microtubules and actin filaments (1, 2). The transport of vesicles on microtubules permits movement over long distances in cells, while the short-range transport of vesicles on actin filaments produces the fine and precise movements required to position vesicles at membrane sites for capture, docking, or fusion (3, 4). The transport of vesicles on actin filaments requires vesicle-associated myosins, some of which have been identified. Myosin V, for example, transports endoplasmic reticulum (ER) vesicles (5–7) and synaptic vesicles (8) in neurons and is involved in the capture of melanosomes at the tips of mouse melanocytes (9). In addition, myosin V is involved in the transport of lysosomes in some cells (10), secretory vesicles in yeast (11), and melanosomes in *Xenopus* melanophores (12).

Myosin II, also known as conventional myosin, is vesicle-associated in extracts of clam (*Spisula solidissima*) oocytes (4, 13). In addition, myosin II was reported to be associated with Golgi vesicles (14), but the antibody used in these studies cross-reacts with coatomer proteins on Golgi-derived vesicles (15–17). Therefore, the role of myosin II in vesicle transport remains controversial. In this study we performed antibody-inhibition experiments with extracts of clam oocytes to provide additional evidence that myosin II is a vesicle motor. Clam oocyte extracts are well characterized and have been used extensively to study cell cycle events including cyclin synthesis and degradation, as well as ubiquitin-mediated proteolysis of cyclins (18).

Extracts were prepared from quiescent oocytes by the method of Ruderman *et al.*, (18) with slight modifications. Fluorescence microscopy was used to view rhodamine-phalloidin stained actin filaments in the extracts, and AVEC-DIC microscopy was used to assay vesicle transport on actin filaments. Motile activity in extracts was determined by counting the number of vesicles moving per minute per field (v/m/f). Antibody-inhibition experiments were performed with an antibody made to oocyte myosin II. The myosin II in oocyte extracts was precipitated with ammonium sulfate, dissolved in buffer (20 mM Tris pH 7.2, 1 mM EDTA-K, 0.2 mM $CaCl_2$, 1 mM DTT), and dialyzed overnight at 4°C. The pure fraction of the myosin II was prepared by running the solubilized fractions on SDS-gels and eluting the myosin II heavy chain band. The eluted protein was used for antibody production in rabbit. The serum of the immunized rabbit was collected, and the polyclonal antibody (αp-205) was purified on protein A beads.

The antibody (αp-205) recognized a single band at 205 kD on western blots of oocyte extracts (Fig. 1A) and in myosin II-enriched fractions (Fig. 1B). The protein recognized by αp-205 was also recognized by a myosin II antibody, M2.42 (Fig. 1A), produced to a peptide in the head domain of *Acanthamoeba*

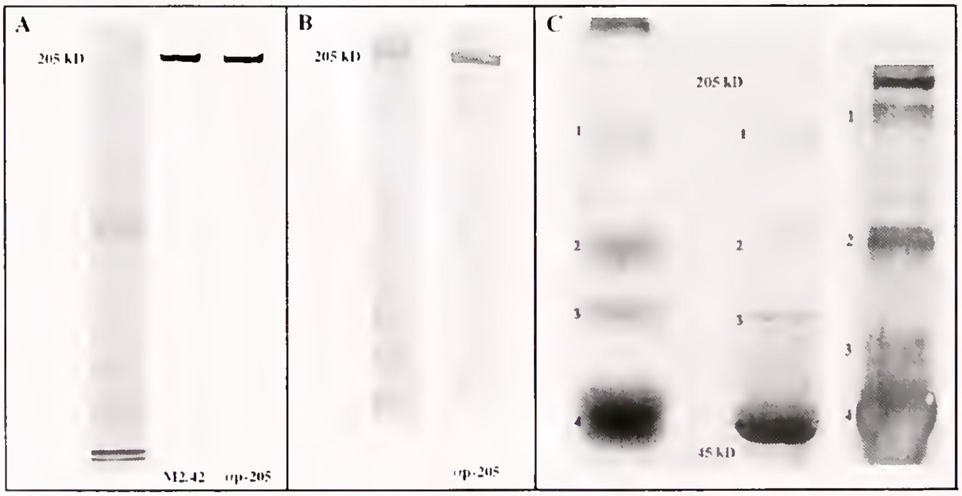

Figure 1. *Panel A: Lane 1 is a coomassie blue stained SDS-PAGE gel of an oocyte extract. Lane 2 is a western blot of the same extract probed with M2.42, a myosin II antibody, showing a single band at 205 kD. Lane 3 is a western blot probed with αp-205 showing a single band at 205 kD. Panel B: Lane 1 is coomassie blue stained SDS-PAGE gel showing a myosin II-enriched fraction prepared from clam oocytes. Lane 2 is the corresponding western blot of the fraction probed with αp-205 and showing a single band at 205 kD. Panel C: Lane 1 is a gel of protein-A purified αp-205 showing at least four bands: the antibody at 55 kD and three serum proteins that co-purify with the antibody. Lane 2 shows an immunoprecipitation with αp-205. Six proteins are seen: the four serum proteins, myosin II at 205 kD, and actin at 45 kD. Lane 3 is the corresponding western blot probed with αp-205; the antibody recognizes the four serum proteins and myosin II.*

myosin II (gift of Donald Kaiser). Therefore, the αp-205 antibody exhibited high affinity and specificity for clam myosin II. In immuno-precipitation (IP) experiments with αp-205, proteins of 205 and 45 kD, the respective molecular weights of myosin II and actin, were present in the precipitate (Fig. 1C, lane 2). A blot of the αp-205 immuno-precipitate probed with αp-205 (Fig. 1C, lane 3) identified the 205 kD band as myosin II, and a blot with an antibody to actin identified the 45 kD band as actin (data not shown). The 4 additional bands seen on both the gel and blot were present in the protein A-purified antibody (Fig. 1C, lane 1); therefore, they represent serum proteins rather than proteins in the oocyte extracts. The IP data provided evidence that the antibody binds to native myosin II and may serve as a function-blocking antibody. We therefore examined the effects of the αp-205 antibody on actin-dependent vesicle transport.

The protein-A purified αp-205 antibody was concentrated to 3 mg/ml and buffer-exchanged into vesicle motility buffer (T buffer, pH 7.2) for antibody-inhibition experiments. An antibody (αQLLQ) made to squid myosin V (5) that does not detect oocyte proteins on western blots was used as the control. Extracts were prepared for motility assays with either 0.38 or 1.0 mg/ml of αp-205, and a control sample was prepared at the same time with αQLLQ. The motile activity was determined in the control and the treated samples at regular intervals for a period of 1.5 hours. Motile activity in the control remained at 412 ± 96 vesicles/minute/field (v/m/f) for the observation period, while the extracts treated with 0.38 mg/ml αp-205 decreased to 232 ± 51 v/m/f (43% inhibition). At 1.0 mg/ml αp-205, motile activity decreased to 199 ± 58 v/m/f, while the control remained at 363 ± 71 v/m/f (45% inhibition). These data showed that αp-205 inhibited 40% to 45% of the motile activity in clam oocyte extracts. We plan to use affinity-purified αp-205 to determine whether motile activity is inhibited completely.

In summary, the inhibition of vesicle transport by a myosin II-specific antibody provides evidence in support of the conclusion that myosin II in clam oocytes functions as a vesicle motor. The lack of 100% inhibition by αp-205 may suggest the involvement of other myosin motors in actin-based vesicle transport in oocytes. The vesicles in these extracts are probably ER-derived, and myosin II may therefore be involved in the transport of ER vesicles during the early events of fertilization and embryonic development.

Supported by NSF grants DCB 9974709 and DBI-9977613 and an MBL fellowship sponsored by the Josiah Macy, Jr. Foundation.

Literature Cited

1. **Kuznetsov, S. A., G. M. Langford, and D. G. Weiss. 1992.** *Nature* **356:** 725–727.
2. **Langford, G. M. 1995.** *Curr. Opin. Cell Biol.* **7:** 82–88.
3. **Langford, G. M., and B. J. Molyneaux. 1998.** *Brain Res. Rev.* **28:** 1–8.
4. **DePina, A. S., and G. M. Langford. 1999.** *Microsc. Res. Tech.* **47:** 93–106.
5. **Tabb, J. S., B. J. Molyneaux, D. L. Cohen, S. A. Kuznetsov, and G. M. Langford. 1998.** *J. Cell Sci.* **111:** 3221–3234.
6. **Dekker-Ohno, K., S. Hayasaka, Y. Takagishi, S. Oda, and N. Wakasugi. 1996.** *Brain Res.* **714:** 226–230.
7. **Takagishi, Y., S. Oda, S. Hayasaka, K. Dekker-Ohno, T. Shikata, M. Inouye, and H. Yamamura. 1996.** *Neurosci. Lett.* **215:** 169–172.
8. **Prekeris, R., and D. M. Terrian. 1997.** *J. Cell Biol.* **137:** 1589–1601.
9. **Wu, X., B. Bowers, Q. Wei, B. Kocher, and J. A. Hammer 3rd. 1997.** *J. Cell Sci.* **110:** 847–859.
10. **Hill, K. L., N. L. Catlett, and L. S. Weisman. 1996.** *J. Cell Biol.* **135:** 1535–1549.
11. **Govindan, B., R. Bowser, and P. Novick. 1995.** *J. Cell Biol.* **128:** 1055–1068.
12. **Rogers, S. L., and V. I. Gelfand. 1998.** *Curr. Biol.* **8:** 161–164.
13. **Woellert, T., A. S. DePina, and G. M. Langford. 1999.** *Biol. Bull.* **197:** 41–42.
14. **Stow, J. L., K. R. Fath, and D. R. Burgess. 1998.** *Trends Cell Biol.* **8:** 138–141.
15. **Ikonen, E., J. B. de Almeid, K. F. Fath, D. R. Burgess, K. Ashman, K. Simons, and J. L. Stow. 1997.** *J. Cell Sci.* **110:** 2155–2164.
16. **Musch, A., D. Cohen, and E. Rodriguez-Boulan. 1997.** *J. Cell Biol.* **138:** 291–306.
17. **Buss, F., J. Kendrick-Jones, C. Lionne, A. E. Knight, G. P. Cote, and J. P. Luzio. 1998.** *J. Cell Biol.* **143:** 1535–1545.
18. **Ruderman, J. V., V. Sudakin, and A. Hershko. 1997.** *Methods Enzymol.* **283:** 614–622.

Reference: *Biol. Bull.* **199:** 203–205. (October 2000)

Interaction of Actin- and Microtubule-Based Motors in Squid Axoplasm Probed with Antibodies to Myosin V and Kinesin

Phillip Stafford, Jeremiah Brown and George M. Langford
(Dartmouth College, Hanover, New Hampshire 03755)

Myosin V, an actin-dependent molecular motor highly expressed in neurons, transports ER vesicles on actin filaments in the giant axon of the longfin squid, *Loligo pealei* (1). The amino acid sequence of squid brain myosin V is similar to those of mouse and human myosin Va (2). In a recent study, Huang *et al.* (3) showed that the rod-tail domain of ubiquitous kinesin (aa680 to aa1100) and the AF6/cno globular tail domain of MyoV (aa1643 to aa1800) bind to each other. This led to the hypothesis that the two motors form a complex on vesicles through tail-tail interaction. The direct interaction of these motors could provide a mechanism by which vesicles move efficiently from microtubules to actin filaments, as postulated in the dual filament model of vesicle transport (4–7).

In this study, we used antibodies raised to squid brain myosin V (αQLLQ) and squid brain kinesin (H2 antibody provided by

Dr. S. Brady) to determine whether kinesin binds to myosin V in squid neurons. In addition, we used recombinant tail fragments of mouse MyoV and mouse kinesin (constructs provided by Dr. Huang) to test whether these fragments form heterologous complexes with squid brain kinesin and myosin V, respectively. The plasmids containing the glutathione S-transferase (GST)-labeled mouse AF6/cno tail-globular-domain (GST-MyoV-tail aa1569 to aa1768 without the coiled medial tail domain) and the histidine (His)-labeled, kinesin-tail fragment of mouse ubiquitous kinesin (aa763-856) were expressed in *E. coli.* The bacterially expressed mouse GST- or His-tagged fragments were purified on affinity columns and used in binding assays of squid brain extracts.

The specificity of αQLLQ and H2 was determined by probing blots of squid brain extracts with the two antibodies. αQLLQ recognized a single protein of 196 kD in blots of squid brain extracts (Fig. 1A, lane 2), and H2 recognized a single protein of 120 kD (Fig. 1A, lane 3). These antibodies were then used in immunoprecipitation experiments to determine whether myosin V and kinesin interact directly. Squid brain extracts were incubated with the αQLLQ and then with protein-A beads. The precipitate was collected by centrifugation and run on a SDS-PAGE gel (Fig. 1B, lane 1). Proteins in the 50–55 kD range representing the antibody were the primary components in the precipitate. A blot of the immuno-precipitate probed with αQLLQ showed a myosin-V band at 196 kD, protein bands at 50–55 kD representing the antibody, and one unknown protein at about 100 kD. The unknown protein may represent a serum protein that binds to the antibody during protein-A purification or a breakdown product of myosin V. A blot of the immunoprecipitate was probed with H2, and a protein of 120 kD representing kinesin was revealed (Fig. 1B, lane 3). Therefore, these data support the hypothesis that kinesin is a binding partner of myosin V and the interaction may function to regulate the motor activity of myosin V.

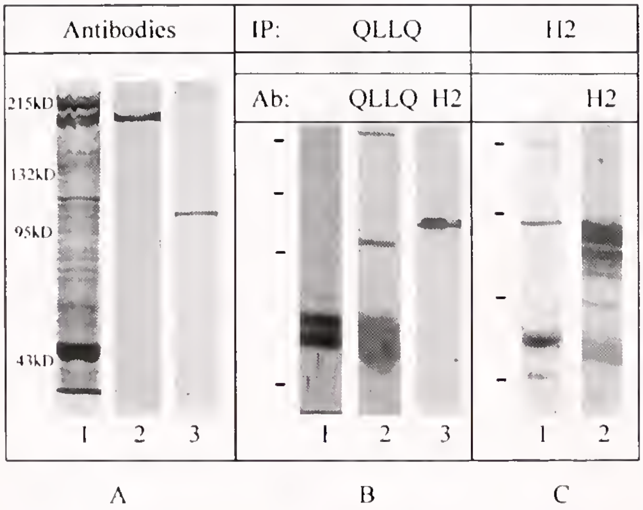

Figure 1. *Protein size marker is listed on the left, dashes indicate the corresponding sizes on the gels to the right. Panel A: Lane 1 is a coomassie-stained SDS-PAGE gel showing total squid optic lobe homogenate, lane 2 is an immunoblot using an antibody to the MyoV tail, QLLQ, lane 3 is the same blot probed with H2, an antibody against the kinesin heavy chain (provided by Dr. Scott Brady). Panel B: Lane 1 shows a gel of an immunoprecipitation using QLLQ to pull down MyoV from squid optic lobes. Lane 2 is a western probed with QLLQ showing MyoV at 196 kD and the QLLQ antibody at ~50 kD and a possible MyoV-tail breakdown product at ~100 kD. Lane 3 is a western probed with H2. Panel C: Lane 1 shows a gel from an immunoprecipitation using H2 to pull down kinesin. Lane 2 is a western probed with H2.*

In corollary experiments, squid brain extracts were incubated with the kinesin antibody H2 followed by incubation with protein-A beads. The precipitate was collected by centrifugation and analyzed by SDS-PAGE. Multiple bands were observed, including a protein of 120 kD and one of 200 kD (Fig. 1C, lane 1). The antibody (50 kD) was the other major band on the gel. The 120 kD protein was shown to be kinesin by probing a blot with H2 (Fig. 1C, lane 2). The H2 antibody recognized several other unknown proteins. These results complement those obtained with αQLLQ and support the conclusion that kinesin and myosin V bind to each other in neurons.

The purified mouse GST-MyoV-tail fragment and the His-labeled kinesin-tail fragment were analyzed by SDS-PAGE, transferred to nitrocellulose, and probed with αQLLQ and H2. αQLLQ and H2, respectively (data not shown), did not detect the GST-MyoV-tail fragment and the His-kinesin-tail fragment. The αQLLQ antibody was made to a 14-amino acid synthetic peptide in the AF6/cno domain of squid myosin V (8), so its failure to recognize the mouse protein fragment was not surprising. Affinity isolation experiments were performed to determine whether the GST-MyoV-tail fragment binds to squid brain kinesin. Squid brain extracts were incubated with the GST-MyoV-tail fragment and then with glutathione beads. The beads were washed 5× with PBS and eluted by the addition of 3 bead-volumes of 1× glutathione, then analyzed by SDS-PAGE. A blot of the precipitate probed with an antibody to squid brain kinesin (H2) did not show kinesin as one of the proteins in the complex (data not shown). In a similar experiment, purified mouse His-kinesin-tail fragment was analyzed for its ability to interact with squid brain myosin V. Squid brain extracts were incubated with the His-labeled kinesin fragment followed by incubation with the His-antibody. The antibody kinesin-fragment was precipitated with protein A-Sepharose beads and analyzed on SDS-gels. Blots of the immuno-precipitate probed with an antibody to squid brain myosin V (αQLLQ) did not show myosin V as one of the proteins in the complex. Therefore, these data suggested that heterologous complexes do not form between the mouse MyoV-tail and native squid kinesin and between mouse kinesin-tail and native squid myosin V.

In summary, these experiments demonstrate that squid brain myosin V and squid brain kinesin are binding partners in neurons. The mouse recombinant fragments and squid native proteins did not form complexes that could be detected on blots. Therefore we plan to produce squid recombinant proteins to determine whether vesicle transport is inhibited in axoplasm. The inhibition of vesicle transport by tail fragments of myosin V and kinesin has been shown in cells grown in culture (9, 10) but has not been demonstrated *in vitro.*

Supported by NSF grants DCB 9974709 and DBI-9977613 and an MBL fellowship sponsored by the Josiah Macy, Jr. Foundation.

Literature Cited

1. **Tabb, J. S., B. J. Molyneaux, D. L. Cohen, S. A. Kuznetsov, and G. M. Langford. 1998.** *J. Cell Sci.* **111:** 3221–3234.

2. **Molyneaux, B. J., M. K. Mulcahey, P. Stafford, and G. M. Langford. 2000.** *Cell Motil. Cytoskeleton* **46:** 108–115.
3. **Huang, J. D., S. T. Brady, B. W. Richards, D. Stenoien, J. H. Resau, N. G. Copeland, and N. A. Jenkins. 1999.** *Nature* **397:** 267–270.
4. **Langford, G. M. 1995.** *Curr. Opin. Cell Biol.* **7:** 82–88.
5. **Langford, G. M., and B. J. Molyneaux. 1998.** *Brain Res. Rev.* **28:** 1–8.
6. **Langford, G. M. 1999.** *FASEB J.* **13** Suppl 2:S248–250.
7. **DePina, A. S., and G. M. Langford. 1999.** *Microsc. Res. Tech.* **47:** 93–106.
8. **Molyneaux, B. J., and G. M. Langford. 1997.** *Biol. Bull.* **193:** 222–223.
9. **Wu, X., B. Bowers, K. Rao, Q. Wei, and J. A. Hammer, 3rd. 1998.** *J. Cell Biol.* **143:** 899–918.
10. **Wubbolts, R., M. Fernandez-Borja, L. Jordens, E. Reits, S. Dusseljee, C. Echeverri, R. B. Vallee, and J. Neefjes. 1999.** *J. Cell Sci.* **112:** 785–795.

Reference: *Biol. Bull.* **199:** 205–206. (October 2000)

Microtubule-Dependent Nuclear Positioning and Nuclear-Dependent Septum Positioning in the Fission Yeast *Saccharomyces pombe*

P. T. Tran[1], *V. Doye*[2], *F. Chang*[1], *and S. Inoué*
(Marine Biological Laboratory, Woods Hole, Massachusetts 02543)

The correct placement of the cell division plane is important for cell shape, size, and orientation, and for the proper partition of cellular determinants for development. The position of the division plane has been shown to be dependent on microtubules in many organisms (1). What molecular mechanism of the fission yeast ensures that the division plane and septum will be properly positioned?

Fission yeast is a rod-shaped cell that divides by medial cleavage. The nucleus is located at the geometric center of the cell, attached to multiple bundles of dynamic, anti-parallel microtubules that push on the nucleus (2–4; our unpublished results). The position of the division plane and septum coincides with the position of the interphase nucleus (5). By examining the effect of depolymerizing microtubules within the cell, we tested the hypothesis that microtubules dictate the central position of the nucleus; and the position of the nucleus, in turn, dictates the future position of the septum.

A wild-type fission yeast strain (h^- leu1-32 nup107-GFP nmt-GFP-atb2), expressing (1) fusion of a nuclear pore protein to the green fluorescent protein and (2) fusion of the green fluorescent protein to tubulin, was used to visualize both the nucleus and the microtubules. For imaging, cells grown to mid-log phase in liquid yeast media (EMM + 5 μg/ml thiamine) at room temperature (21°–23°C) were mounted between a coverslip- and slide-sealed chamber containing a thin pad of 2% agarose and yeast media (YE5S). Methyl-2-benzimidazole-carbamate (MBC), a potent inhibitor of microtubule polymerization, was used from fresh stock (100× in DMSO) at the final concentration of 25 μg/ml to depolymerize the microtubules. Time-lapsed images (1-h interval, 1-s exposure time) were digitally acquired at room temperature (21°–23°C) with Metamorph Software (Universal Imaging Corp.) controlling a CCD digital camera (Orca-1, Hamamatsu Corp.), attached to a Leica DMRX microscope stand equipped with DIC optics, as well as with a PL Fluotar 100×/1.3NA oil-immersion objective (Leica Corp.) and a mercury arc lamp for wide-field epi-fluorescent microscopy.

To determine whether microtubules play a role in the placement of the nucleus at the cell center, we used time-lapse microscopy to examine the position of the nucleus in interphase cells treated with the microtubule-depolymerizing drug MBC. Nuclear position in a cell can be expressed as the ratio of two lengths: the length from the center of the nucleus to the shorter cell tip (L_{short}), and the length from the center of the nucleus to the opposite longer cell tip (L_{long}). The ratio $L_{short}/L_{long} = 1$ when the nucleus is exactly at the cell geometric center, and $L_{short}/L_{long} < 1$ when the nucleus is off-center. MBC-treated cells, which have no microtubules and ultimately die, continued to lengthen for several hours at a rate similar to that of control cells, ~1.5 μm/h. During a 2-h period, the control cells grew from an average length of 9.16 ± 1.04 μm to 12.16 ± 1.47 μm ($N = 23$ cells). Almost all nuclei were positioned in the middle of the cell, with an average L_{short}/L_{long} ratio of 0.96 ± 0.03; and ~96% of cells had better than 0.90 ratio. In contrast, MBC-treated cells grew from an average length of 8.73 ± 1.55 μm to 11.45 ± 2.01 μm ($N = 40$ cells), with many offset nuclei, an average L_{short}/L_{long} ratio of 0.80 ± 0.15; and only ~28% of cells had better than 0.90 ratio (Fig. 1A). Clearly, while MBC did not affect the cell growth rate, the proper central positioning of the nucleus was dependent on microtubules.

To test whether the position of the nucleus dictates the position of the division plane and septum, we examined the position of the septum in MBC-treated cells, which have off-center nuclei. Lacking microtubules, MBC-treated cells showed a delay in the cell cycle, and a curvilinear or "bent" growth pattern (6, 7). Whereas control cells exhibited a cell cycle time of ~4 h, the cell cycle in MBC-treated cells was significantly delayed to ~6–8 h. However, MBC-treated cells attempted to divide at the end of the cell cycle delay, and eventually each cell formed a septum at the site of the offset nucleus that "cut" the nucleus. The new daughter cells subsequently died. Figure 1(B, C) illustrates the formation and position of the septum in control and MBC-treated cells, respectively. Thus, the septum formed at the position of the nucleus, even when the nucleus was not at the center of the cell.

Our preliminary results are consistent with our hypothesis that the central position of the nucleus is dependent on microtubules, and that the position of the nucleus, in turn, may dictate the position of the plane of cell division and the septum. Cells which have lost their microtubule cytoskeleton can continue to grow, and can undergo septation and cytokinesis after a cell cycle delay.

---

[1] Columbia University, New York, NY 10032.

[2] Institute Curie, Paris, France.

Our results are consistent with phenotypes seen in studies of tubulin mutants (7). However, our experimental conditions ensure an almost complete loss of the microtubule cytoskeleton; and our time-lapse microscopy allows long-term viewing of the development of phenotypes.

It has been proposed that cytokinesis factors may be localized to the nuclear region by association or movements on microtubules (8). However, our studies suggest that microtubules may not be strictly required for the assembly or localization of the ring at the nucleus.

P.T.T. thanks Dr. Rudolf Oldenbourg for generously providing lab space and equipment during this study. This work was funded in part by NIH and March of Dimes grants to P.T.T. and F.C.

Literature Cited

1. **Field, C., R. Li, and K. Oegema. 1999.** *Curr. Opin. Cell Biol.* **11:** 68–80.
2. **Drummond, D. R., and R. A. Cross. 2000.** *Curr. Biol.* **10:** 766–775.
3. **Hagan, I. 1998.** *J. Cell Sci.* **111:** 1603–1612.
4. **Tran, P. T., P. Maddox, F. Chang, and S. Inoué. 1999.** *Biol. Bull.* **197:** 262–263.
5. **Chang, F., and P. Nurse. 1996.** *Cell* **84:** 191–194.
6. **Sawin, K. E., and P. Nurse. 1998.** *J. Cell Biol.* **142:** 457–471.
7. **Toda, T., K. Umesomo, A. Hirata, and M. Yanagida. 1983.** *J. Mol. Biol.* **168:** 251–270.
8. **Chang, F. 1999.** *Curr. Biol.* **9:** 849–852.

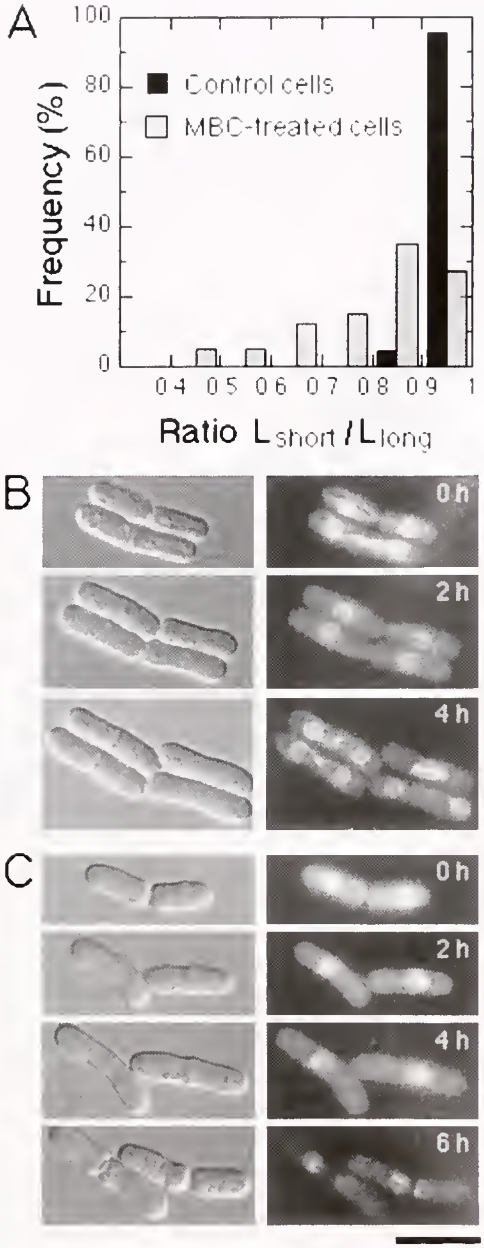

Figure 1. *Cells treated with MBC exhibit a misplaced nucleus and septum. Fission yeast cells expressing nucleoporin-GFP and GFP-tubulin were imaged at room temperature (21°–23° C) with time-lapse fluorescence microscopy. (A) Plot of distribution frequency of nuclear positions expressed as the ratio* L_{short}/L_{long}, *where* L_{short} *is the length from the center of the nucleus to the short cell tip and* L_{long} *is the length from the center of the nucleus to the opposite long cell tip. (B) Wild-type cells through one cell cycle. Left panels are DIC images showing septum formation at the middle of the cell (at 0 h and later at 4 h). Right panels are fluorescent images of nuclear membrane and microtubules. Microtubules span the length of the cell during interphase. As the cell grew, nuclei were positioned by dynamic microtubules at the center of the cells where subsequent cell division and septation occurred, creating two daughter cells of approximately equal length. Note the disappearance of interphase microtubules in the cell cytoplasm and the appearance of the mitotic spindle inside the cell nucleus during mitosis (at 4 h). (C) MBC-treated cells through one cell cycle. No microtubules were present in MBC-treated cells. Without microtubules, the nuclei were offset, the cell cycle was delayed, no spindles were formed, and subsequent division planes and septum were also offset, creating "cut" nuclei and daughter cells of unequal length. The DIC panels from 0–4 h show a cell with a "birth scar," not to be confused with the septum. Bar = 10 µm.*

Reference: *Biol. Bull.* **199:** 207–208. (October 2000)

The Role of Microtubules During Blastodisc Formation of the Squid, *Loligo pealei*

Karen Crawford (Department of Biology, St. Mary's College of Maryland, St. Mary's City, Maryland 20686)

After fertilization, cytoplasm streams from the vegetal region of the squid egg towards the animal cap to form a blastodisc where meroblastic cleavage will occur (1, 2). This process begins at fertilization, accelerates after second polar body formation (90 min, at 20°C), and continues through third cleavage (6.5–7.0 h). A blastodisc cap is formed, although at a slower rate, in eggs that have been artificially activated with 10 μg/ml A23187 (Molecular Probes) (3). To explore the role of the cytoskeleton in this process, *in vitro* fertilized (4) or activated embryos were placed in small petri dishes lined with 0.2% agarose (Sigma, Type II) and filled with 20°C Millipore-filtered seawater (MFSW). The dishes were placed on ice and cooled to 4°C. Exposure to cold was chosen to perturb cytoplasmic movements targeting microtubules (5), so that the effect on the embryos could be easily reversed. Cold treatment periods were selected to include the first and second polar body meiotic divisions (20 min and 1.5 h respectively), and the first (3.5 h), second (4.0 h) and third (6.5 h) cleavage events. Treatment periods were 20 min to 3 h, 3 to 4 h, 4 to 5 h, 5 to 6 h and 6 to 7 h of development. After treatment, dishes of embryos were removed from the ice and allowed to return to room temperature (20°C). Embryos were compared to control embryos for blastodisc formation, the presence of polar bodies, and cleavage pattern. Cleavage in squid is bilateral (Fig. 1a). First cleavage occurs along the line between the polar bodies and the apex of the embryo where the male pronucleus enters the egg. Second cleavage occurs perpendicular to this, and third cleavage is unequal and distinguishes the future right and left sides of the developing embryo.

Exposure to cold inhibited blastodisc cap formation in all embryos treated prior to cytoplasmic streaming; it also arrested streaming in embryos treated after second polar body formation. Twenty minutes after removal from cold exposure, precleavage stage embryos develop a blister-like swelling of clear cytoplasm surrounding the male pronucleus. Activated eggs do not form blisters of cytoplasm when removed from cold treatment, although a small crescent of cytoplasm may form over the female pronucleus after 50 minutes. Over this same period of time, the polar bodies that are present swell to more than 4 times their normal diameter of 10 μm and then slowly return to normal size. Over the next 20 min the blister of cytoplasm around the male pronucleus relaxes into a small but growing blastodisc cap that resembles a normal cap in most (95%) cases. Abnormal cap formation was observed in about 5% of the embryos examined and included displacement of the cytoplasm to one side of the animal pole or splitting of the cap at the apex into two regions. Normal cleavage did not occur in these cases. In contrast to control squid embryos, which form two polar bodies, *in vitro* fertilized embryos treated during polar body formation possessed one (59/73, 37%) or two (3/73, 4%) and more frequently no (43/73 or 59%) polar bodies. Similar results were observed in activated eggs treated with cold during polar body formation. Fertilized embryos that failed to complete their meiotic divisions often possessed three nuclei at the apex of the blastodisc cap prior to cleavage, indicating that cold shock at this early stage induces polyploidy. These embryos seldom underwent normal cleavage. Interestingly, in contrast to the 2%–10% of control-activated eggs that underwent a cleavage event, 60% (79/132) of activated eggs treated with cold during their meiotic divisions possessed cleavage furrows. Embryos treated with cold from 3 to 4 h, the time when control embryos undergo first cleavage, possessed two polar bodies (as did all other embryos treated at later times), formed normal blastodisc caps, and cleaved normally. In contrast, even though first cleavage begins at 3.5 h, embryos treated from 4 to 5 h of development and returned

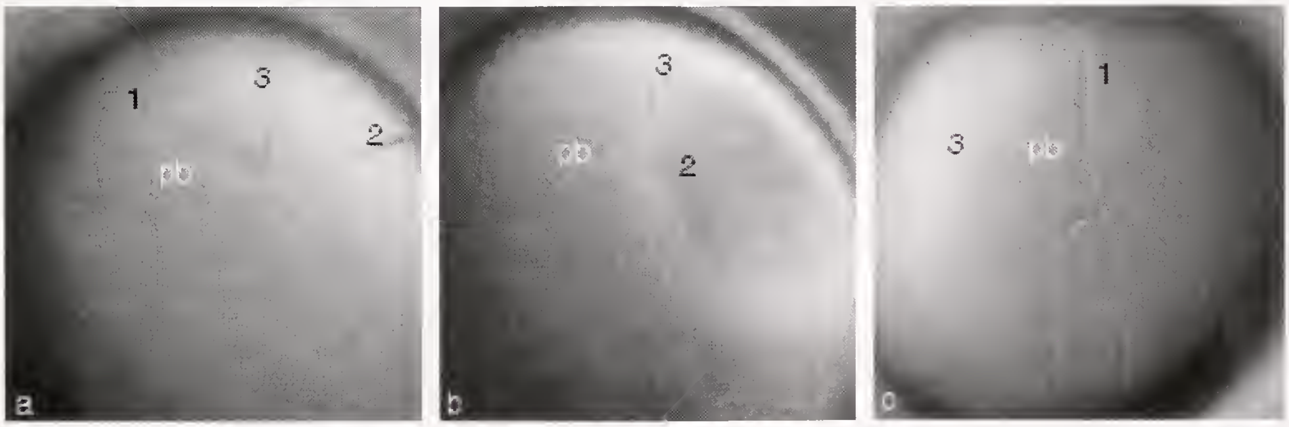

Figure 1. *Cold exposure inhibits specific cleavage furrows in the squid embryo. Individual furrows are numbered in order of their appearance. (a) Control third cleavage stage embryo, animal pole view. Note that third cleavage is unequal and that the polar bodies (pb) lie adjacent to the first cleavage furrow, which marks the midline body axis. (b) Embryo treated with cold exposure from 4 to 5 h after fertilization. The first cleavage furrow is missing, and third cleavage is equalized. (c) Embryo treated with cold exposure from 5 to 6 h after fertilization. The second cleavage furrow is missing in this embryo, while first and third cleavage furrows are present and normal. Images magnified 650×.*

to room temperature failed to retain their first cleavage furrow (Fig. 1b) in 90% of the cases examined (36/40). In these embryos, because the polar bodies mark the region through which first cleavage will form, it is possible to determine that second cleavage occurred normally, while third cleavage—which is normally unequal—was equalized to mirror the cells in the future dorsal region of the embryo. Most embryos treated between 5 and 6 h of development retained a reduced first cleavage furrow at the center of the blastodisc and formed normal second and third cleavage furrows (76/89 or 85%), while other embryos from this group developed without a second cleavage furrow (Fig. 1c). This pattern was also observed in embryos treated between 6 and 7 h. Surprisingly, most of the embryos from all treatment groups continue to develop and at 48 h appeared fairly normal, although they often possessed clumps of large cells, uneven blastoderm yolk boarders, and regions where cell layers appeared thicker than controls.

These results suggest that the ordered movement of cytoplasm, which forms the blastodisc in the squid, is disturbed by cold treatment. Cold exposure also induced polyploidy and perturbed cleavage furrows. The failure to retain or create specific cleavage furrows may be due to the direct action of cold on the microfilaments responsible for furrow formation, cell membranes, or specific factors that regulate mitosis. However, the formation of the blister-like swellings of cytoplasm around the male pronucleus, likely initiated by the sperm centriole to form microtubule arrays, suggests that cytoplasmic movements are rapidly resuming and may disturb the previously formed or forming microfilaments responsible for cleavage. That the polar bodies, which are little more than unwanted chromosomes and microtubules, swell rapidly during this same period further suggests that microtubules may be partially responsible for these events, although this does not rule out the possibility that cold exposure results in destabilization of membranes in these cells. Microtubules originating from the sperm pronucleus are crucial for the reorganization of cytoplasm after fertilization in frog eggs (6). The result that cold exposure can equalize third cleavage in squid embryos is nearly identical to what was reported when squid embryos were treated with the microfilament inhibitor cytochalasin B, although first cleavage furrows were still present in some of those embryos (7). To address the importance of microtubules and microfilaments alone and in concert to blastodisc formation and cleavage in the squid, it will be necessary to selectively challenge each element with specific inhibitors and characterize their appearance over time with immunohistochemistry.

This work was supported by a Research Opportunity Award from the National Science Foundation to Karen Crawford.

Literature Cited

1. **Brooks, W. K. 1880.** *Anniv. Mem. Boston Soc. N.H.* 1–22.
2. **Arnold, J. M. 1968.** *Dev. Biol.* **18:** 180–197.
3. **Crawford, K. 1985.** *Biol. Bull.* **169:** 540.
4. **Klein, K. C., and L. A. Jaffe. 1984.** *Biol. Bull.* **167:** 518.
5. **Yahara, I., and F. Kakimoto-Sameshima. 1978.** *Cell* **15:** 251–259.
6. **Elinson, R. P., and B. Rowning. 1988.** *Dev. Biol.* **128:** 185–197.
7. **Arnold, J. M., and L. D. Williams-Arnold. 1974.** *J. Embryol. Exp. Morphol.* **31:** 1–25.

Reference: *Biol. Bull.* **199:** 208–209. (October 2000)

Cytoplasmic Proteins on the Surface of Discharged Microsporidian Sporoplasms

Earl Weidner (Biology, Louisiana State University, Baton Rouge, Louisiana)

The spore cell of an intracellular microsporidian parasite is a missile which, when activated, explosively discharges an invasion tube. The spore contents (sporoplasm) pass through the invasion tube and are introduced into a target cell. Evidence reported earlier indicates that the membrane surrounding the newly discharged sporoplasm cell is derived in part from the polaroplast organelle of the spore (1). An early accepted model for microsporidian sporoplasm discharge held that the membrane everts with the cytoplasmic face shifting outward during extrusion (2). If this is what happens, it would seem that cytoplasmic proteins might remain attached to this membrane and end up on the surface of the discharged sporoplasm. Evidence presented here indicates that cytoplasmic tubulin and dynactin proteins are on the surface of discharged microsporidian sporoplasms, thus supporting the idea of membrane eversion during spore extrusion.

In this study, proteins were identified from the sporoplasms discharged from spores of the microsporidian, *Spraguea lophii*. The protocol for isolating the sporoplasms was reported earlier (3). Sporoplasms examined immunocytochemically for surface tubulin (using IgG monoclonal or polyclonal primary antibody, with fluorescein-coupled secondary antibody) revealed an even, but sometimes patchy labeling (Fig. 1A). Similar results were found when sporoplasms were tested with fluorescein-labeled colchicine. In a follow-up experiment, sporoplasms were incubated in tubulin assembly medium with fluorescein-coupled tubulin. The results showed a preferential bordering of the labeled tubulin around the sporoplasms (Fig. 1B).

The *S. lophii* sporoplasms were also tested for surface dynactin proteins by using antibodies for p150$^{\text{glued}}$, dynein intermediate chains, and dynein heavy chains. The site of binding was visualized with colloidal gold or fluorescein-coupled secondary antibody. The results showed some uneven labeling for p150$^{\text{glued}}$ (Fig. 1C) and dynein light chains, but no dynein heavy-chain labeling was apparent. Western blot analyses revealed substantial levels of p150$^{\text{glued}}$ and dynein light-chain proteins. The positioning of these proteins onto the sporoplasm surface suggests that the sporoplasm membrane at first faces the cytoplasm within the spore, but shifts to the outside during spore discharge.

Surface dynactin is an important component in the movement of membranous structures within cells. Recall, moreover, that *S.*

lophii parasitizes the central nervous system of different species of angler fish of the genus *Lophius*, the infections being particularly evident in the cranial ganglia, dorsal root ganglia, and the supramedullary neurons. Surface dynactin, therefore, is probably involved in positioning the microsporidian parasites in neuronal cell bodies within the central nervous system of their piscine hosts (4).

Literature Cited

1. **Weidner, E., W. Byrd, A. Scarborough, J. Pleshinger, and D. Sibley. 1984.** *J. Protozool.* **31:** 195–198.
2. **Lom, J., and J. Vavra. 1963.** *Acta Protozool.* **1:** 279–283.
3. **Weidner, E., and A. Findley. 1999.** *Biol. Bull.* **197:** 270–271.
4. **Weidner, E., and T. King. 1998.** *Biol. Bull.* **195:** 229–228.

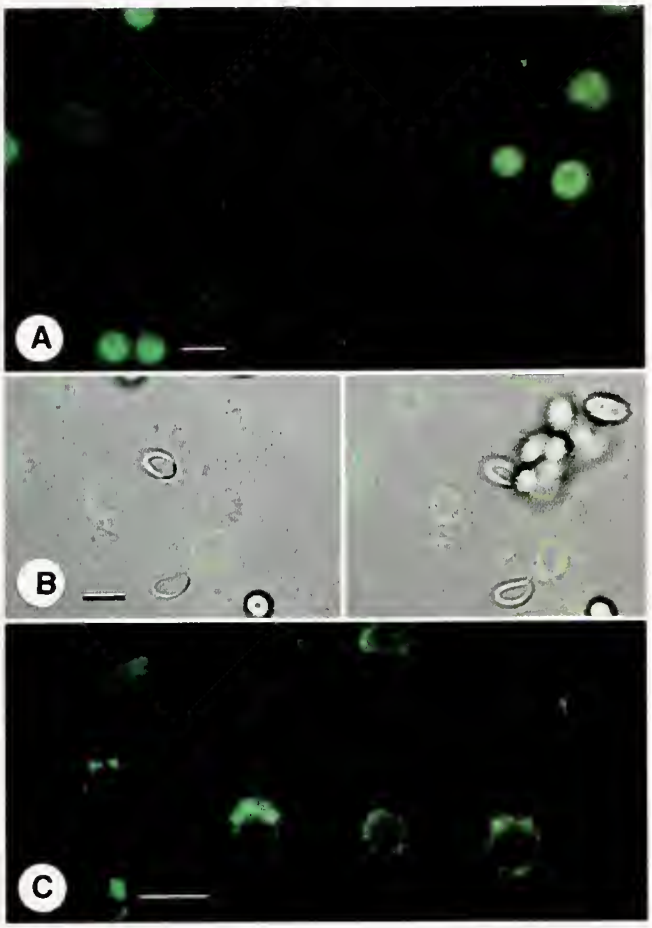

Figure 1. Spraguea lophii *sporoplasms with tubulin labeling. (A) Anti-tubulin fluorescence confined to sporoplasm surface. (B) Time-interval recordings of fluorescein-coupled tubulin bordering spherical sporoplasms. (C) Anti-dynactin* $p150^{glued}$ *label with patchy positioning on sporoplasms. All scale bars represent 5 μm.*

Reference: *Biol. Bull.* **199:** 209–211. (October 2000)

Adhesion of a Viral Envelope Protein to a Non-Self-Binding Domain of the Aggregation Factor in the Marine Sponge *Microciona prolifera*

Roger MacKenzie[1], *David Newman*[2], *Max M. Burger*[3], *Rene Roy*[4], *and William J. Kuhns*[5]
(Marine Biological Laboratory, Woods Hole, Massachusetts 02543)

Studies of the *Microciona* aggregation factor (MAF) have thus far been focused upon its self-binding characteristics. This study demonstrates for the first time an MAF non-self-binding domain. The purpose of this study has been two-fold: (a) to purify the binding motif as a potential pharmacoactive microbicide; and (b) to characterize non-self adhesins as participants in the cross-species binding of microbes to sponge cells. Cell-cell aggregation in *Microciona prolifera* is mediated by its aggregation factor, a species-specific compound exhibiting a unique sunburst structure at high magnifications, with a molecular weight of 2×10^7 Da (1, 2). There is a bracelet-like protein core composed of multiple beads, each attached to a protein-carbohydrate arm. Multiple anionic glycans on the arms polymerize to form a viscous gel in the presence of calcium. A sulfate disaccharide and a pyruvate trisaccharide mediate self-binding to adjacent arms and to cell membranes (3, 4). A hyaluronic acid (HA)-like compound stabilizes the core-arm connections (5). Binding inhibition studies of MAF

---

[1] Institute for Biological Sciences, National Research Council of Canada, Ottawa, Ontario.

[2] Natural Products Branch, National Cancer Institute, Frederick, MD.

[3] Friedrich Miescher Institute, Basel, Switzerland.

[4] Department of Chemistry, University of Ottawa, Ottawa, Ontario, Canada.

[5] Hospital for Sick Children, Toronto, Ontario, Canada.

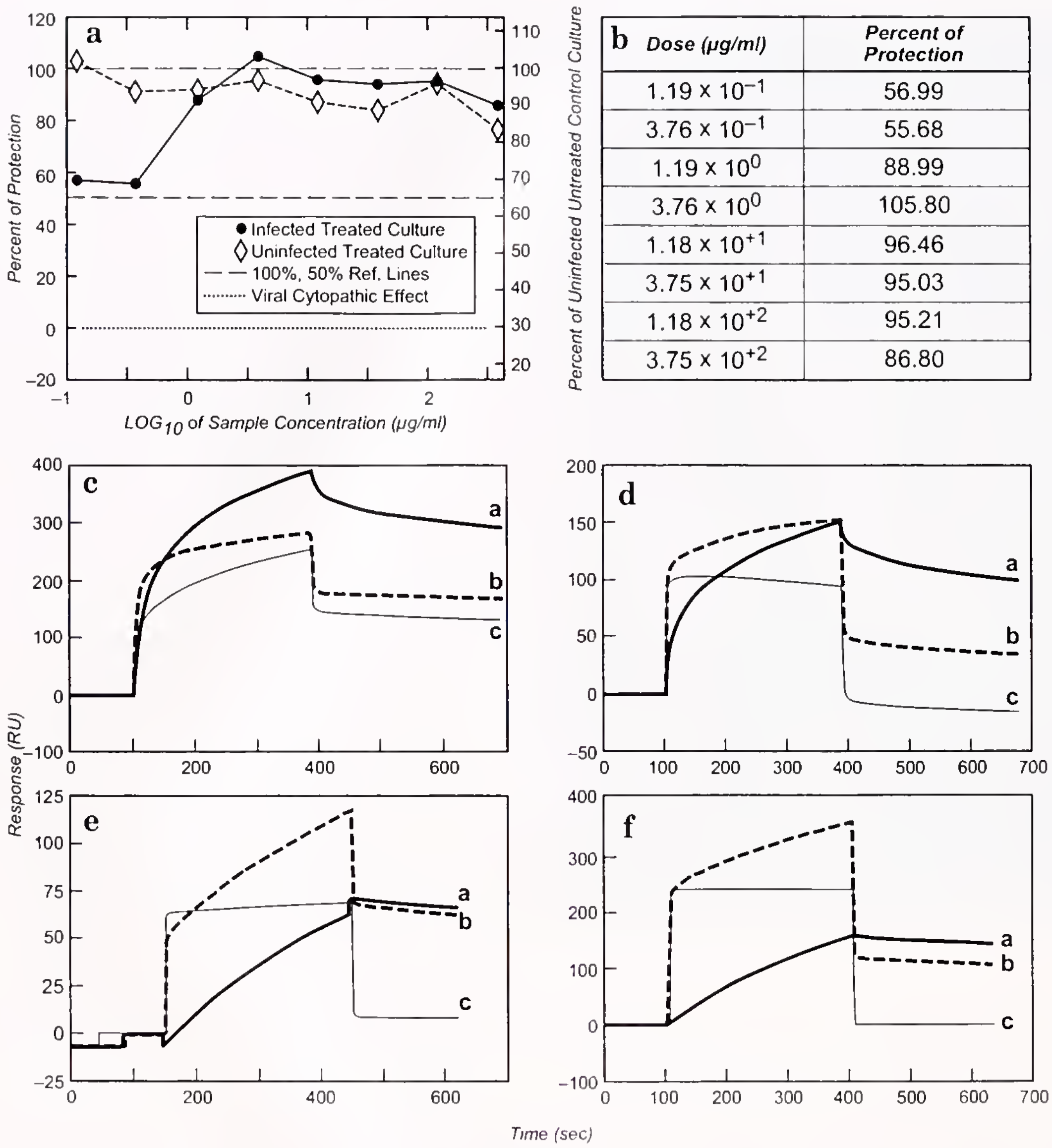

b Dose (µg/ml)	Percent of Protection
1.19×10^{-1}	56.99
3.76×10^{-1}	55.68
1.19×10^{0}	88.99
3.76×10^{0}	105.80
$1.18 \times 10^{+1}$	96.46
$3.75 \times 10^{+1}$	95.03
$1.18 \times 10^{+2}$	95.21
$3.75 \times 10^{+2}$	86.80

Figure 1. *Summary of the antiviral property of MAF in CEM lymphoblastoid cells infected with human immunodeficiency virus (HIV-1) (a, b). Sensorgrams indicate MAF inhibition of rgp120-rCD4 binding by MAF (c, d), whereas synthetic sulfated and pyruvylated constructs show no inhibition (e, f). (a, b) Results of formazan XTT assays for viral inhibitory properties of MAF derivatives. Round black dots and diamonds depict infected treated culture and uninfected treated culture respectively. MAF gave >50% protection at a dose as low as 0.1 µg/ml (EC50), while demonstrating little or no toxic effects. Lower dotted line demonstrates viral pathogenic effect in infected untreated culture. Straight dashes are 50% and 100% reference lines. (c–f) Sensorgrams which schematize the relative binding affinities of self and non-self MAF binding epitopes. The small letters that accompany each set of curves represent the following: a = rpg120 − rCD4 binding, b = rpg120 + putative inhibitor − rCD4 interaction, c = putative inhibitor − rCD4 reaction. The constants for these reactions are given by the terms k_a and k_d, where k_a refers to the association constant and k_d describes the dissociation constant. The values for rpg120 at the stated concentration were 1.2×10^4 and 3.3×10^{-4} respectively and indicated a strong binding affinity between rpg120 and rCD4 (a curves). The reactions did not differ appreciably when gp120 was in mixture with the sulfate or pyruvylated compounds (b curves). However, both MAF1 and MAF ds were reactive as inhibitory compounds. MAF1 also possessed a strong affinity for rCD4, as indicated by the c curve shown on the left middle drawing.*

fractions were carried out using as a binding model recombinant (r) gp120 human immunodeficiency virus (HIV-1) envelope protein and lymphocyte rCD4 protein receptor.

MAF was prepared from cuttings of sponge branches and processed as described elsewhere (6). The clear gel derived from cesium chloride gradient ultracentrifugation was dialyzed repeatedly against 200× volume de-ionized water and then lyophilized (MAF-I). The result was a truncated molecule, as shown by electron microscopy—one having morphologically intact bracelets, but lacking arms (7). Low molecular weight anionic glycans were prepared from MAF-I by ethanol precipitation (8) followed by recovery and lyophilization of the ethanolic supernatant (MAF-ds).

Compositional analyses of MAFds demonstrated a high sulfate and carbohydrate content; spectroscopic analysis showed a major peak that had a mass/charge ratio of 3 kDa and represented about 60% of the solids in the dried sample. Neither fraction was active in aggregation assays at levels above 20 μg/ml, although freshly derived MAF was active at a level of 0.5 μg/ml.

Binding of the HIV-1 envelope protein gp120 to target lymphocytes *via* CD4 peptide is necessary for syncytium formation and viral entry and multiplication in target cells (9). Inhibition of gp120-CD4 binding by MAF fractions was evaluated using surface plasmon resonance as the detection principle for molecular interaction analysis (10). Instrumentation provided by BIACORE Company (Piscataway, New Jersey) permits ligands to be immobilized on a gold sensor chip upon which a light beam is directed. A continuous flow system permits injection of binding compounds alone or in mixture with inhibitors over the ligands. Binding causes a change in the angle of the light beam, with an association phase beginning at analyte injection and a dissociation phase at the end of injection. The changes are recorded as a sensorgram. The inhibition of HIV-1 by MAF compounds was assayed in infected lymphoblastoid cells by using a colorimetric method in which a colorless compound (formazan XTT) is metabolically converted by healthy cells, but not dead cells, to an orange-colored derivative (11).

The results of MAF titrations for two MAF fractions in formazan assays indicated that amounts as low as 0.1 μg conferred protection on more than 50% of the cells (EC50) while simultaneously showing little or no toxic effects toward non-infected cells (Fig. 1a, b). Data for the binding of recombinant rgp120 to rCD4 gave a dissociation constant of 17 n*M*, which agrees well with the value of 19 n*M* previously reported by Wu *et al.* (12). At concentrations of 0.75 mg/ml, both MAF derivatives inhibited binding (Fig. 1c, d). Tests for binding inhibition using synthetic constructs and polymers of the MAF self-binding epitopes sulfated disaccharide and pyruvylated trisaccharide were completely negative (Fig. 1e, f). Of the four compounds, only MAF-1 showed any binding to rCD4 at the end of the injection cycle, while MAF-ds was bound to rgp120, but not to rCD4.

In summary, a partially purified MAF derivative (MAFds) inhibited the replication of the human immunodeficiency virus (HIV) by specific gp120 binding and interfering with syncytium formation between the viral gp120 envelope protein and the lymphocyte CD4 antigen. Thus, in pure form, it will qualify at a clinical level as a microbicide or as a microbistatic agent, similar in its chemical properties to HIV-inhibitory products derived from some other marine invertebrates (13). Although it seems unlikely that *Microciona* would encounter the HIV virus in its natural surrounding, we propose that this model typifies cross-species binding (as demonstrated by a non-self adhesin unrelated to the known self-binding epitopes), and it may provide the sponge with a means of immobilizing symbionts or other forms that are required for nutrition or for disposal by macrophages.

Literature Cited

1. **Humphreys, S., T. Humphreys, and J. Sano. 1977.** *J. Supramol. Struct.* **7:** 339–351.
2. **Fernandez-Busquets, X., and M. M. Burger. 1999.** *Microsc. Res. Tech.* **44:** 204–218.
3. **Spillmann, D., J. Thomas-Oates, J. van Kuik, J. Vliegenthart, G. Misevic, M. Burger, and J. Finne. 1995.** *J. Biol. Chem.* **270:** 5089–5097.
4. **Spillmann, D., K. Hard, J. Thomas-Oates, J. Vliegenthart, G. Misevic, M. M. Burger, and J. Finne. 1993.** *J. Biol. Chem.* **268:** 13378–13387.
5. **Jarchow, J., J. Fritz, D. Anselmetti, A. Calabro, V. Hascall, D. Gerosa, M. M. Burger, and X. Fernandez-Busquets. 2000.** *J. Struct. Biol.* (In press).
6. **Misevic, G., J. Finne, and M. M. Burger. 1987.** *J. Biol. Chem.* **262:** 5870–5877.
7. **McLaurin, J., T. Franklin, W. Kuhns, and P. Fraser. 1999.** *Amyloid. Int. J. Exp. Clin. Invest.* **6:** 233–243.
8. **Cardellina, J., R. Munro, K. Fuller, T. Manfredi, M. McKee, H. Tischler, K. Bokesch, J. Gustafson, J. Beutler, and M. Boyd. 1993.** *J. Nat. Prod.* **56:** 1123–1129.
9. **Chimule, N., and S. Phawa. 1996.** *Microbiol. Rev.* **60:** 386.
10. **Inagawa, J., J. Okazaki, K. Morimoto, and S. Hashimoto. 2000.** Pp. 37–57 in *Real Time Analysis of Biomolecular Interactions. Applications of BIOCORE.* K. Nagata and H. Handa, eds. Springer Verlag, Tokyo.
11. **Weislow, O., R. Kiser, D. Fine, J. Bader, R. Shoemaker, and M. Boyd. 1989.** *J. Natl. Cancer Inst.* **81:** 577–586.
12. **Wu, H., D. Myszka, S. Tendian, C. Brouillette, R. Sweet, I. Chaiken, and W. Hendrickson. 1996.** *Proc. Natl. Acad. Sci. USA* **93:** 15030–15035.
13. **Beutler, J., T. McKee, R. Fuller, M. Tischler, J. Cardellina, K. Snader, T. McCloud, and M. Boyd. 1996.** *Antivir. Chem. Chemother.* **4:** 83–88.

Reference: *Biol. Bull.* **199:** 212–213. (October 2000)

Fertilization-induced Changes in the Fine Structure of Stratified *Arbacia* Eggs. I. Observations on Live Cells with the Centrifuge Polarizing Microscope

Makoto Goda[1], *Mario H. Burgos*[2], *and Shinya Inoué (Marine Biological Laboratory, Woods Hole, Massachusetts)*

Eggs of the sea urchin (*Arbacia punctulata*), when suspended in isopicnic seawater and subjected, by centrifugation for several minutes, to a gravitational field a few thousand times greater than the earth's, stratify into several layers. As shown earlier by Harvey, who used supra vital dyes (1), the layers are, from top (centripetal pole) to bottom: oil cap, a large clear zone immediately below the oil cap containing the nucleus, the mitochondrial layer, yolk granules, and the pigment granule layer.

Observing this phenomenon with a recently developed centrifuge polarizing microscope (CPM) (2, 3), we find that centrifugation introduces to the upper part of the clear zone a negatively birefringent curtain of material that drapes down from the oil cap and surrounds the isotropic nucleus (Fig. 1A, B). The negative birefringence increases with both time and speed of centrifugation. The negative sign of birefringence (larger refractive index perpendicular to the texture), fluorescence staining with brefeldin A, and electron microscopy of fixed cells (5) suggest that this negatively birefringent material is a pleated series of endoplasmic reticular membranes, stratified and oriented by the centrifugation.

When a stratified egg is fertilized, the birefringence, viewed with the CPM, disappears in a few seconds, a surprising observation (Fig. 1C–E). Furthermore, the egg concurrently starts floating up in the Percoll-seawater density gradient (Fig. 1F–H). As the egg floats up, the fertilization envelope rises and its positive birefringence increases over the next 3 to 4 min. In the next 10 or so min, the negative birefringence below the oil cap

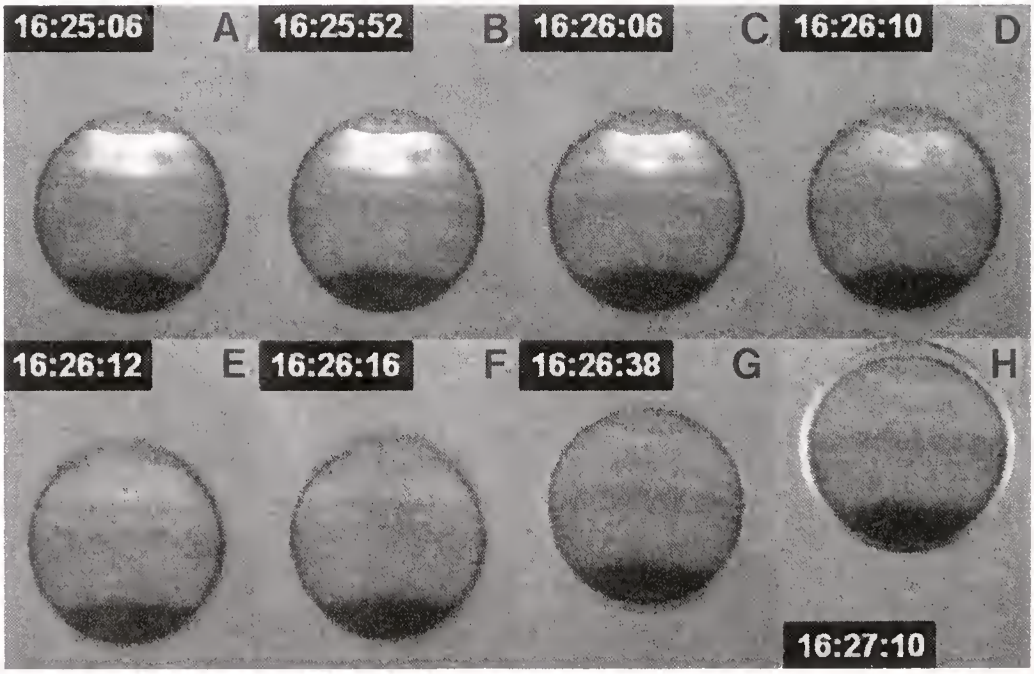

Figure 1. *Fertilization of sea urchin egg observed with the CPM. After the unfertilized* Arbacia *eggs were centrifugally stratified at 3000 × g for about 15 min, the CPM was stopped, and a drop of sperm suspension was placed on the wall of the specimen chamber above the Percoll seawater containing the eggs. Upon re-starting the CPM, the sperm suspension crept down and fused with the egg suspension. Sperm then swam and reached the eggs (at about 16:26:00), which were still stratified, but had rounded up during the few minutes that the CPM was stopped. (A, B): Negatively birefringent curtain of material shows in the upper region of the clear zone surrounding the nucleus of unfertilized eggs. (C–E): During about the first 10 s after fertilization, the negative birefringence disappears. (F–H): The egg starts to float as the (positively birefringent) fertilization envelope gradually rises. Time of day in h:min:s. Egg diameter: about 75 μm. In 1952, McCulloch observed negative birefringence in the upper region of the clear zone in* Arbacia *eggs examined after centrifugation but not the changes we saw after fertilization (4). He attributed the birefringence to cytoplasmic fibrils, and with the fixatives available in those days, he was unable to discern any ultrastructure in the clear zone using an electron microscope, the only exception being the annulate lamellae, which he interpreted to be "coarse fibrous components."*

---

[1] Kyoto University, Japan

[2] IHEM, UNC-CONICET, Argentina

gradually returns again, but with a much more complex alignment of material.

To test whether these changes reflect a rise in cytosolic Ca^{2+} (released from the endoplasmic reticulum [ER], an intracellular Ca^{2+} storage organelle), we observed the responses of unfertilized stratified eggs to the calcium ionophore A-23187 (6). Whether in normal or Ca^{2+}-free seawater, the eggs indeed responded exactly as when fertilized. We surmise that elevation of cytosolic Ca^{2+} in the seconds immediately following fertilization (7) is correlated with the transient breakup of the ER (8, 9), and that this breakup is manifested as the rapid loss of birefringence. As the Ca^{2+} level drops again, the ER must re-assemble into large layered sheets since the negative birefringence reappears. In control experiments, inactivated eggs, that had received the identical history of centrifugation, retain their negative birefringence for more than 30 min.

Following fertilization, the egg may become less dense due to exocytosis and swelling of the cortical granules, or by uptake of water by the egg or the egg jelly. While not observed when stratified eggs were fertilized in normal, Ca^{2+}-containing seawater, eggs activated with the Ca^{2+} ionophore suddenly fall in the density gradient after steadily rising for several minutes. Since this fall is accompanied by a sudden release of diffuse material surrounding the fertilization envelope, swelling of the egg jelly may be primarily responsible for the increased buoyancy of the egg following its activation.

Support of research by Hamamatsu Photonics KK, Olympus Optical Company, Kyoto University, and the Marine Biological Laboratory is gratefully acknowledged. We thank Drs. B. Kaminer and M. Terasaki for extensive discussions of their work relating to changes in cytosolic Ca^{2+} and ER organization following fertilization.

Literature Cited

1. **Harvey, E. B. 1941.** *Biol. Bull.* **81:** 114–118.
2. **Inoué, S., R. A. Knudson, K. Suzuki, N. Okada, H. Takahashi, M. Iida, and K. Yamanaka. 1997.** *Microsc. Microanal.* **4:** 36–37.
3. **Inoué, S. 1999.** *FASEB J. (Suppl.)* **13:** s185–s190.
4. **McCulloch, D. 1952.** *J. Exp. Zool.* **119:** 47–65.
5. **Burgos, M. H., M. Goda, and S. Inoué. 2000.** *Biol. Bull.* **199:** 213–214.
6. **Steinhardt, R. A., and D. Epel. 1974.** *Proc. Natl. Acad. Sci. USA* **71:** 1915–1919.
7. **Gilkey, J. C., L. F. Jaffe, E. B. Ridgeway, and G. T. Reynolds. 1978.** *J. Cell Biol.* **76:** 448–466.
8. **Henson, J. H., D. A. Begg, S. M. Beaulieu, D. J. Fishkind, E. M. Bonder, M. Terasaki, D. Lebeche, and B. Kaminer. 1989.** *J. Cell Biol.* **109:** 149–161.
9. **Terasaki, M., and L. A. Jaffe. 1991.** *J. Cell Biol.* **114:** 929–940.

Reference: *Biol. Bull.* **199:** 213–214. (October 2000)

Fertilization-induced Changes in the Fine Structure of Stratified *Arbacia* Eggs. II. Observations with Electron Microscopy

Mario H. Burgos[1], *Makoto Goda*[2], *and Shinya Inoué*
(Marine Biological Laboratory, Woods Hole, Massachusetts)

Unfertilized *Arbacia* eggs are stratified by centrifugation; the centripetal pole is occupied by an oil cap, which crowns a large clear zone containing the nucleus (1). When such eggs are observed with the centrifuge polarizing microscope (CPM), a curtain of negatively birefringent material, draping down from the oil cap, is introduced to the upper part of the clear zone (2). When stratified eggs are fertilized or activated by the Ca^{2+} ionophore A23187, this birefringence disappears within a few seconds—even before the fertilization envelope starts to elevate. Its sign, and the fluorescent staining by brefeldin A, suggest that the negative birefringence is due to a stack of membranes, stratified and aligned by centrifugation, and oriented more or less parallel to the direction of the centrifugal force.

To evaluate this proposal further, we investigated the birefringent region of the egg by electron microscopy. We used 2% glutaraldehyde in phosphate-buffered saline made up into 700-m*M* sucrose to prevent swelling of the *Arbacia* egg. Eggs placed in fixative without sucrose swelled up to about eight times the volume of the unfixed egg, lost their microvilli, and (reversibly) lost their negative birefringence.

Thin sections of stratified non-activated eggs, fixed with sucrose-glutaraldehyde, retained their negative birefringence and revealed that the birefringent region is occupied by stacks of smooth and rough endoplasmic reticulum (ER; Fig. 1A). The ER surrounded the nucleus and was aligned more or less parallel to the axis of centrifugation. A small number of Golgi membrane stacks were found amidst the ER, but with random orientation. At the lower region of the ER, we found stacks of annulate lamellae (3,4). These are most likely the refractile rod- and plate-like structures that are seen in centrifuged eggs by light microscopy, especially clearly in DIC. They tended, at first, to lie parallel to the axis of centrifugation, but changed their orientation as time elapsed after the centrifuge was stopped.

In centrifugally stratified eggs fixed about 5 min after fertilization—well after the negative birefringence had disappeared, but before it re-appeared—the distribution of the Golgi and annulate-lamellar material was basically unchanged. However, the ER was no longer in large sheets oriented along the centrifugal axis; rather, the sheets had fragmented into smaller vesicles (Fig. 1B), as was anticipated from their loss of bire-

[1] IHEM, UNC-CONICET, Argentina

[2] Kyoto University, Japan

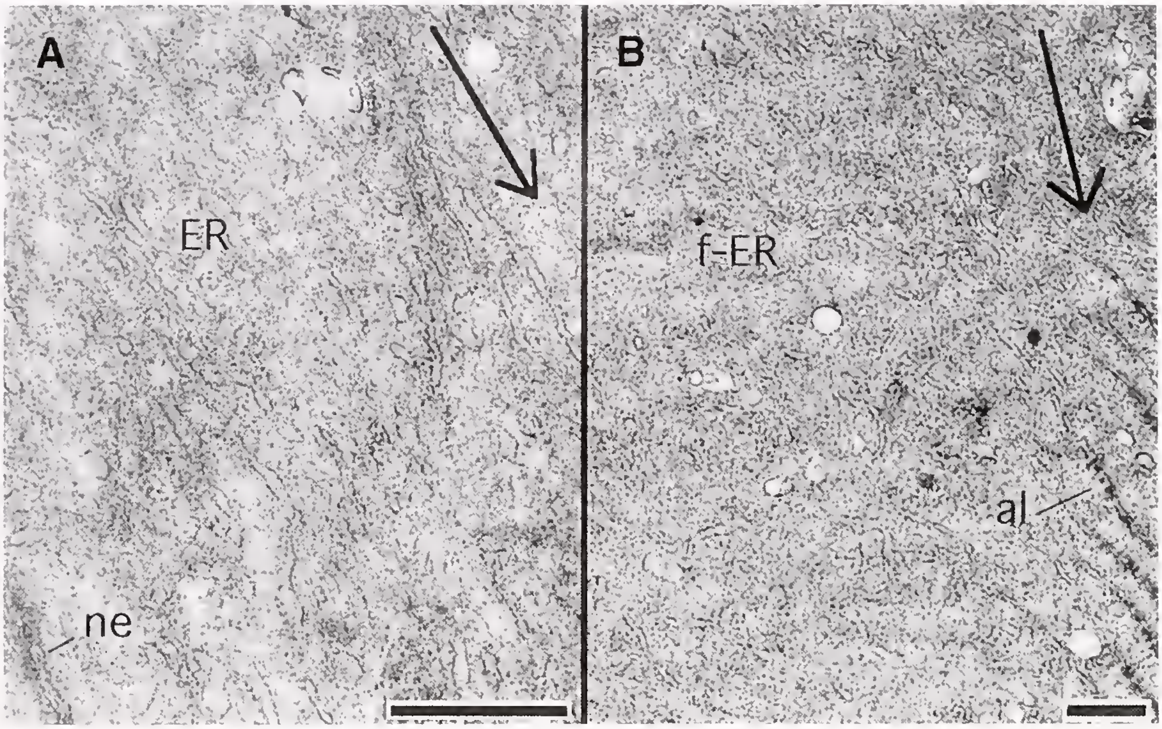

Figure 1. *Ultrastructure of upper clear zone in centrifugally stratified* Arbacia *egg. A. Unfertilized; B. fixed about 5 min after fertilization. After centrifugation on a Percoll-seawater density gradient for about 30 min (A), and after an additional 5 min centrifugation following fertilization (B), the eggs were fixed in 2% glutaraldehyde phosphate buffer made up in 700-mM sucrose solution. After confirming, with 1-μm sections of the unfertilized eggs, that the negative birefringence in the upper part of the clear zone remained intact, the cells were post fixed with osmium, dehydrated, embedded in Epon, and sectioned for electron microscopy. In A, the upper region of the clear zone contains a dense stack of ER, oriented more or less in the direction of the centrifugal force (long arrow). In B, only small pieces of ER remain, consistent with the (transient) loss of the negative birefringence. al: annulate lamellae. ER: endoplasmic reticulum. f-ER: fragmented ER. ne: nuclear envelope. Scale bars 0.5 μm.*

fringence. Because the birefringence of activated live eggs does return in the upper half of the clear zone after about 10 min, albeit with less ordered alignment of the birefringence axes, the EM of cells fixed at that stage would be expected to again show stacks of large ER membrane sheets, but with the stacks oriented along less uniform axes.

These observations suggest that the birefringence observed in live eggs with the CPM is a good indicator of membrane anisotropy, distribution, and especially their dynamic changes. In addition, centrifugally fragmented mini-cells could well prove to be a useful source for several isolated membrane components of the cells.

We thank Hamamatsu Photonics KK, Olympus Optical Company, Kyoto University, and the Marine Biological Laboratory for support of this project. We also thank Louis Kerr and Christina Stamper of the MBL Central Microscope Facility for their cooperative help with electron microscopy. M.B. was supported by an MBL Chairman of the Board Fellowship.

Literature Cited

1. **Harvey, E. B. 1941.** *Biol. Bull.* **81:** 114–118.
2. **Goda, M., M. H. Burgos, and S. Inoué. 2000.** *Biol. Bull.* **199:** 212–213.
3. **Afzelius, B. 1955.** *Exp. Cell Res.* **8:** 147–158.
4. **Swift, H. 1956.** *J. Biophys. Biochem. Cytol. (Suppl.)* **2:** 415–418 and 4 plates.

Reference: *Biol. Bull.* **199:** 215–217. (October 2000)

Optimization of Homogenization Conditions Used to Isolate mRNAs in Processes of Myelinating Oligodendrocytes

Robert M. Gould[1], *Concetta M. Freund*[1], *John Engler*[2], *and Hilary G. Morrison*[3]

Many of us visualize the myelinated nervous system from light microscope (LM) images. Almost all white matter space is occupied by myelinated fibers, each sheath having a thickness that relates to the caliber of its axon. Myelin sheaths are made by oligodendrocytes during nervous system development. The enormous space occupied by myelinated fibers leaves oligodendrocytes so far apart that it is impossible to see connections between cell bodies and myelin sheaths in adult tissue sections.

A picture of how myelin sheaths form comes from reconstructions of morphological images. Oligodendrocyte precursors migrate to each of the regions where axons are developing. When they arrive, they replicate and send out processes, which select, ensheath, and myelinate axons that have reached a certain size. Each process must successfully compete for the axon segment that it myelinates and then produce and maintain a sheath of identical dimensions to its neighbors. This morphological picture represents a multitude of complex process that requires coordinated expression of many gene products. At present only a very small number of these genes are known. The immediate goal of our research program is to identify new genes involved in myelination and determine their contributions.

As a first step we developed a method to identify a population of mRNAs that are important for myelination in rat brain. This mRNA population is selectively translated near sites where myelin sheaths assemble. Myelin basic protein, a dominant myelin protein, is selectively synthesized in these sites, for unlike other myelin proteins, MBP enters myelin within minutes of its synthesis. For MBP to enter myelin so rapidly, not only MBP mRNA, but also all other components needed for its translation, must be transported from the oligodendrocyte soma to each myelin sheath assembly site. We reasoned that the capacity to synthesize proteins at sites distant from the oligodendrocyte soma would not be limited to a single protein. Furthermore, as we identified other proteins synthesized near to where myelin basic protein was incorporated into myelin, we would broaden our understanding of how myelin sheaths are assembled.

David Colman and his collaborators (1, 2) provided a starting point for our studies. They showed that MBP mRNA behaves differently from mRNAs for other myelin proteins when brain samples are subjected to subcellular fractionation. MBP mRNA purifies in myelin vesicles whereas mRNAs for other known myelin-related proteins do not. We used rat brain myelin mRNA as starting material and suppression subtractive hybridization to isolate cDNAs that represent mRNAs which colocalize with MBP mRNA in myelin sheath assembly sites. In the initial study (3), we compared two different homogenization media, one isoosmotic (0.32 *M* sucrose) and one hypertonic (0.85 *M* sucrose). Although we obtained more myelin RNA from samples homogenized in hypertonic sucrose, we worried that this RNA had higher levels of contaminating RNA than samples obtained from tissue homogenized in isoosmotic sucrose. We thus conducted most (2 of 3) suppression subtractive hybridization studies with myelin RNA prepared from isoosmotic homogenates (4). However, when we counted the novel mRNAs obtained in screens with samples prepared under each condition, we found a far more diverse population was obtained when samples homogenized in 0.85 *M* sucrose were used (4). Some of the mRNAs with particular relevance to myelin sheath biogenesis, SH3p13 or endophilin 3 (5) and dynein light intermediate chain (6) were obtained from the screen with the hypertonic sample (4).

During the summer of 2000, we analyzed 90 (25 were sequenced) subtraction products prepared from samples homogenized in 0.32 *M* sucrose and 90 subtraction products (46 were sequenced) prepared from samples homogenized in 0.85 *M* sucrose. We used colony hybridization and hybridization of inserts prepared from mini-prep samples to identify cDNAs derived from MBP and MOBP (myelin-associated oligodendrocytic basic protein) mRNAs. These RNAs are known to be located in oligodendrocyte processes (7), since these were highly enriched in myelin (3; Fig. 1). The remaining cDNAs were sequenced in the Bay Paul Center sequencing facility at the Marine Biological Laboratory in Woods Hole, Massachusetts. Confirming results from our recent study (4), we found that far more (30 *versus* 13) novel cDNAs were obtained from myelin prepared in 0.85 *M* sucrose. Most of these cDNAs relate to known mRNAs (Table 1). A significant portion of the mRNAs generate proteins involved in regulating protein synthesis, namely eukaryotic translation elongation factors alpha and delta and ribosomal proteins L7a and L21. A few, kinesin light chain, rab7 and evectin, increase the number of proteins with recognized functions in membrane trafficking and biogenesis. We have analyzed four cDNAs from the 0.32 *M* sucrose subtraction product and six cDNAs from the 0.85 *M* sucrose subtraction product by northern blot comparisons (starting material RNA *versus* myelin RNA). All of them have mRNAs that are highly enriched in myelin. Among the known mRNAs analyzed so far were ferritin light chain, eukaryotic elongation factor alpha-1 and kinesin light chain.

Future studies aim to locate the mRNAs and proteins in myelinating tissue. In addition, we will use this approach to identify mRNAs located in myelin sheath assembly sites in spiny dogfish.

---

[1] N. Y. S. Institute for Basic Research in Developmental Disabilities, Staten Island, NY.

[2] Dept. of Biology, North Carolina State University, Raleigh, NC.

[3] Bay Paul Center for Molecular Biology and Evolution, Marine Biological Laboratory, Woods Hole, MA.

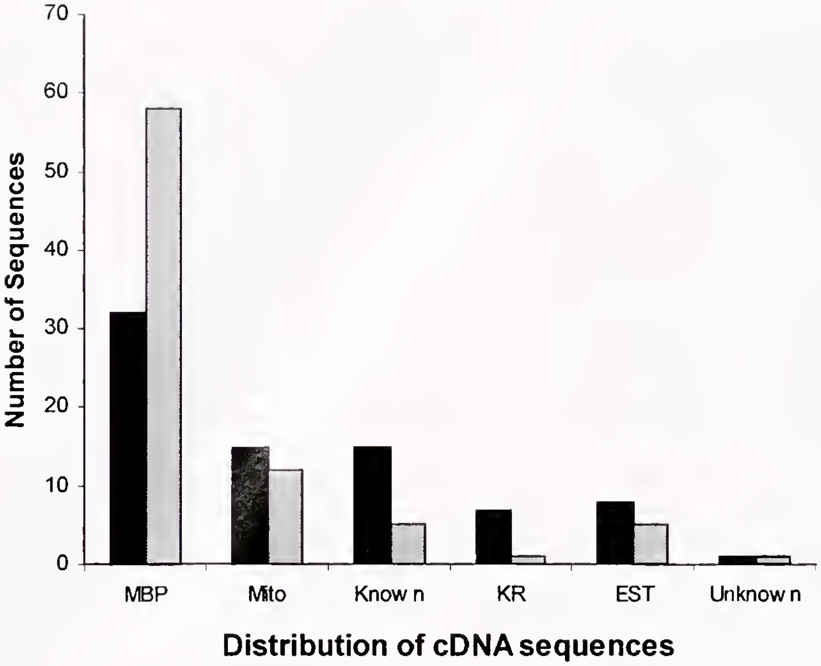

Figure 1. *Number and distribution of cDNAs obtained from subtractive hybridization studies with rat brain samples homogenized in 0.85* M *sucrose (black bars) or 0.32* M *sucrose (gray bars). Clearly larger numbers of novel (30 vs. 13) cDNAs, many of which are related to known mRNAs (see Table 1), are obtained in the sample homogenized in 0.85* M *sucrose. This difference is mainly due to the higher numbers (58 vs. 33) of cDNAs derived from myelin basic protein (MBP) or myelin-associated oligodendrocytic basic protein (MOBP) mRNAs in the 0.32* M *sucrose sample. Other abbreviations: Mito, sequences related to the mitochondrial genome; Known, sequences in the non-redundant GenBank database; KR, sequences related to known GenBank sequences but with less than 50% of the sequence matching the known; EST, sequences in the GenBank EST database; Unknown, sequences unrelated to sequences in either the non-redundant or EST databases.*

The results of this study will, in particular, help us to select appropriate conditions to homogenize dogfish brain, which exists in an environment of far higher tonicity (approximately 1 *M*) than mammalian brain.

This work was funded by the National Multiple Sclerosis Society grant RG2944 (RMG) and the G. Unger Vetlesen Foundation (HGM). Funds for John Engler were from the Marine Models in Biological Research Program (NSF grant, DBI-9912287). We

Table 1

Identities of "known" mRNAs obtained in this study

Name	Accession*	Size (region)†	Homogenization
Astrocytic phosphoprotein	AJ243949	1565–2073 (2341)	0.85 *M*
Phosphodiesterase I	D28560	2282–2898 (3216)	0.85 *M*
Ferritin light chain	NM_008064	605–886 (886)**	0.85 *M*
Glial maturation factor	NM_004124	6–291 (4131)	0.85 *M*
Eukaryotic translation elongation factor α1	X63561	584–1449 (1714)	0.85 *M*
Eukaryotic translation elongation factor δ1	NM_001960	37–281 (991)	0.85 *M*
Rab7	NM_009005	1179–1361 (2089)	0.85 *M*
Ribosomal protein L7a	X15013	417–838 (851)**	0.85 *M*
Ribosomal protein L21	X15212	268–543 (554)**	0.85 *M*
RANP-1	D50559	1237–1540 (1712)	0.85 *M*
Zinc finger homeodomain enhancer protein	U51583	1172–2094 (3403)	0.85 *M*
Kinesin light chain A, B, C	M75146	1322–1705 (2308)	0.32 *M*
KPL-1, evectin	AF081582	933–1411 (1903)	0.32 *M*
Lens epithelial protein	U20525	660–705 (2308)	0.32 *M*

* GenBank accession number.

† Size refers to the nucleotide sequence in the known that matches the cDNA sequence we obtained. The size of the known is in parentheses.

** Highly related to known mRNAs—there are differences evident in comparison of aligned sequences.

would like to thank Dr. Mitchell Sogin for the generous use of the Bay Paul sequencing facility.

Literature Cited

1. **Colman, D. R., G. Kreibich, A. B. Frey, and D. D. Sabatini. 1982.** *J. Cell Biol.* **95:** 598–608.
2. **Gillespie, C. S., L. Bernier, P. S. Brophy, and D. R. Colman. 1990.** *J. Neurochem.* **54:** 656–661.
3. **Gould, R. M., C. M. Freund, and E. Barbarese. 1999.** *J. Neurochem.* **73:** 1913–1924.
4. **Gould, R. M., C. M. Freund, F. Palmer, and D. L. Feinstein. 2000.** *J. Neurochem.* (in press).
5. **Ringstad, N., Y. Nemoto, and P. De Camilli. 1997.** *Proc. Natl. Acad. Sci. USA* **94:** 8569–8574.
6. **Hughes, S. M., K. T. Vaughan, J. S. Herskovits, and R. B. Vallee. 1995.** *J. Cell Sci.* **108:** 17–24.
7. **Holz, A. *et al.* 1996.** *J. Neurosci.* **16:** 467–477.

Reference: *Biol. Bull.* **199:** 218–219. (October 2000)

Modeling the Effects of Land-Use Change on Nitrogen Biogeochemistry in the Ipswich Watershed, Massachusetts

Ryan Kirkby, Luc Claessens, Charles Hopkinson Jr., Edward Rastetter, and Joseph Vallino
(The Ecosystems Center, Marine Biological Laboratory, Woods Hole, Massachusetts 02543)

The Ipswich River Basin, which is located in northern Massachusetts and drains into the Plum Island Sound Estuary, covers a 400-km^2 area composed of forest, wetlands, open and agricultural land, and a gradient of low- to high-density residential and commercial land (1). Over the last century, population growth and land-use changes in the basin have altered the land cover of the watershed. The United States Geological Survey (USGS) has recently modeled the hydrology of the Ipswich River Basin using a precipitation-runoff model called Hydrological Simulation Program-Fortran (HSPF) (2). Their intent was to develop a better understanding of the effects of water withdrawal on the water budget of the river basin (1). In addition to the hydrological data that has been collected by the USGS, we have monitored nutrient loading to build a better picture of the effects of land-use change on nutrient biogeochemistry in the Ipswich river basin. To further investigate nutrient processing in the watershed, the USGS HSPF model (1) was modified to include simulation of nutrient processing on land and in the Ipswich River and tributaries. Considering the projections that have been made for urban development in the Ipswich watershed, the ability to accurately model the resulting changes in nutrient processing may be an important tool in understanding the health of the Ipswich ecosystem. It could also become an important aid in planning future development that minimizes harmful effects to the watershed.

HSPF, in addition to simulating hydrology, is capable of simulating nutrient processing, sediment transport, pH and gasses, phytoplankton, and algae dynamics in a watershed. Nitrate-processing components for stream reaches and land areas were added to the HSPF model. Initial values required by the model were obtained from a database (3) which contains parameter values used in similar HSPF projects in the northeastern United States. Nitrate processing and output from different land types was further calibrated using an empirical relationship between fractional cover of agricultural and forested land in small catchments *versus* nitrate concentration in the streams into which they drain (Fig. 1A, B). In this calibration, the only nitrate input was atmospheric deposition; so the differences in nitrate output between the two land types (Fig. 1B) represent the different values chosen for constants in equations governing the simulation of nutrients in the two land-use types. A more rigorous calibration of the model, which is in progress, will include comparing simulated data on nitrate concentration in the Ipswich River with data we are collecting. All simulations run on the model were driven by meteorological input for the years 1989 to 1993, but future work on the model will include adding more recent meteorological data. The base simulation was run using 1991 land-use data for the watershed; other land-use change scenarios were run by modifying the areas of different land types in certain parts of the river basin.

Calibration of the model resulted in simulated nitrate output from forest and from open plus agricultural land (Fig. 1B) that coincided with the empirical relationship for fractional cover *versus* nitrate concentration (Fig. 1A). The base concentration of nitrate in first-order streams draining only forested lands was approximately 10 μM, whereas the value for streams fed by agricultural and open pasture land was closer to 70 μM (Fig. 1B). Modeled nitrate transects along the main stem of the Ipswich River show a strong trend of decreasing concentration near the head of the river, followed by a slowly decreasing concentration toward the Ipswich dam (Fig. 1C). This same general trend is seen in data collected for the same month, although in a different year (Fig. 1C). Stream-flow data along the Ipswich River reveal the opposite trend: a quick increase in flow near the head of the river, followed by a slower increase moving towards the mouth of the Ipswich River (Fig. 1C). Seasonally, nitrate concentrations at the mouth of the Ipswich River reach a peak during winter and spring (Fig. 1D). Similarly, river flow at the mouth has its highest peak in the spring and another, smaller peak in the winter (Fig. 1D). Data we have collected show similar correlation between peak discharge and peak nitrate concentrations (4).

The opposite trends in stream flow and nitrate concentration along transects from the head to the mouth of the Ipswich River suggest that the decreasing nitrate concentration may be due, at least partially, to a dilution effect. The other factors contributing to diminishing nitrate concentration in the river are in-stream processes, such as denitrification and uptake by plants and algae, that can be examined using the model. One purpose of continuing to examine nutrient processing with this model is to help determine what processes are the most important contributors to the trends that have been observed and modeled.

The HSPF model can be used to examine different scenarios for land use by modifying the areas of different land types in the basin. A 12-km^2 residential development was modeled at different locations in the watershed. The results from those scenarios indicated that nitrate concentration would increase at the mouth of the river, and that the increase would be greater the closer the development is to the mouth of the river. The model predicts that urbanization in the watershed will have a smaller effect if it occurs farther upstream and on tributaries, as opposed to farther downstream and on the main stem of the river. One simulation of two different scenarios showed that a 12-km^2 residential area built in the lower watershed on the main stem would increase nitrate concentrations at the mouth of the river by approximately 5 μM, but an identical development on a tributary feeding into the main stem at the same location would produce roughly baseline conditions at the mouth. The model can be used to look more closely at the sources and sinks of nitrate in the river basin to better characterize the processing of nitrogen and other nutrients in the watershed.

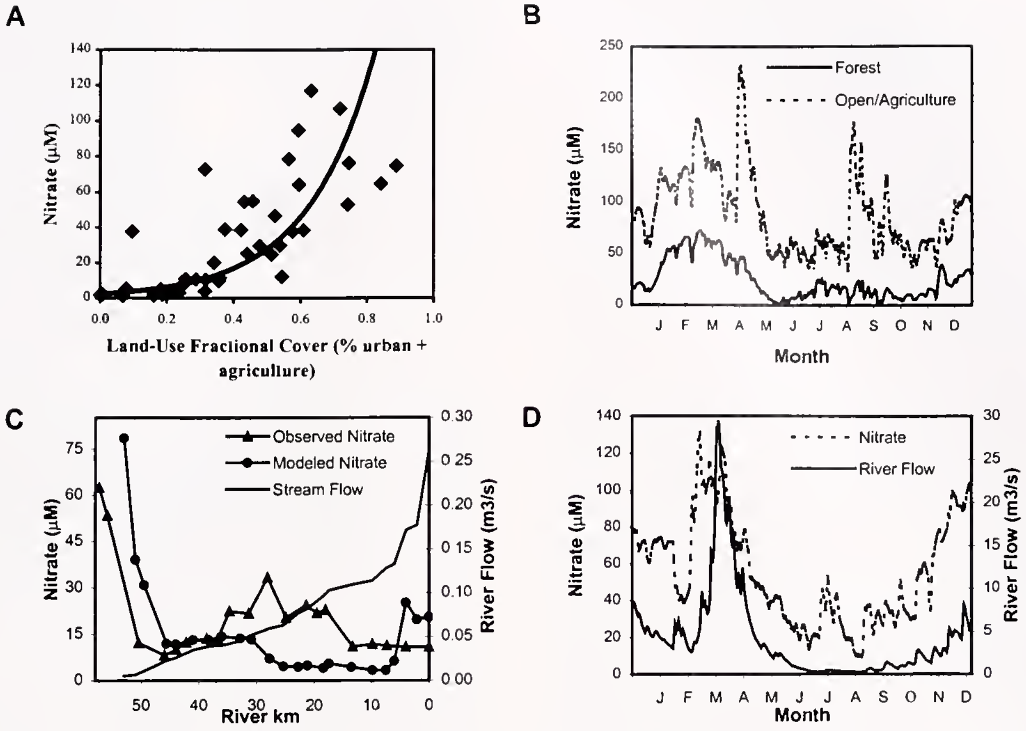

Figure 1. *(A) An empirical relationship between the forest cover in a catchment and the nitrate concentration in streams draining the catchment. (B) Modeled nitrate concentration timeseries in first-order streams with all forest and all open plus agriculture contributing land area. (C) Modeled nitrate concentration and stream flow transect along the main stem of the Ipswich River in July 1993, and observed nitrate data from July 1998. (D) Modeled nitrate concentration and river flow at the mouth of the Ipswich River over the course of 1993.*

This research was funded through the NSF-EPA Water and Watersheds program DEB-9726862.

Literature Cited

1. **Zarriello, P., and K. Ries. 2000.** *A Precipitation-Runoff Model for Analysis of the Effects of Water Withdrawals on Streamflow, Ipswich River Basin, Massachusetts.* United States Geological Survey, Denver, CO.
2. **Bicknell, B. R., J. C. Imhoff, J. L. Kittle, A. S. Donigian, and R. C. Johanson. 1993.** *Hydrologic Simulation Program—FORTRAN (HSPF): User's manual for release 10.0.* EPA 600/3-84-066. U.S. Environmental Protection Agency, Environmental Research Laboratory, Athens, GA.
3. **EPA HSPFParm site.** http://www.epa.gov/docs/ostwater/BASINS/support.htm [21 Aug. 2000].
4. **The Ecosystems Center Plum Island Estuary data.** http://ecosystems.mbl.edu/pie [21 Aug. 2000].

Reference: *Biol. Bull.* **199:** 219–221. (October 2000)

Solute Dynamics in Storm Flow of the Ipswich River Basin: Effects of Land Use

Anne Perring, Michael Williams, Charles Hopkinson Jr., Edward Rastetter, and Joseph Vallino
(The Ecosystems Center, Marine Biological Laboratory, Woods Hole, Massachusetts 02543)

The Ipswich River in northeastern Massachusetts has supplied surrounding suburban communities with water since the 1800s. With current projections of increased urbanization in the watershed (1), solute fluxes from developed areas may have an impact on the ecology of the Ipswich River. Solute fluxes from storm flow are particularly important since storms commonly flush solutes from storage reservoirs, thereby increasing the mass transfer of solutes to the aquatic system (2). The objectives of this study were to observe solute dynamics in storm flow in three first-order catchments of the Ipswich River basin to infer how increased development will affect the aquatic system.

The three catchments were selected to represent the end-members of different land-use areas commonly found in the Ipswich River basin. The catchments represent predominately urban (URB), agricultural (AG) and forested (FOR) areas. The baseline discharges were 100, 0.4 and 10 l/s at the URB, AG and FOR sites, respectively. Rain volume at each site was measured using manual rain gauges, and samples for chemical analyses were collected.

Baseline samples of stream water were collected before and after a storm that occurred 15–16 June, 2000. Each hour during the storm, filtered and unfiltered samples of stream water were collected and stage measurements were taken. Discharge was estimated from stage measurements. Stream water and rain samples were filtered immediately with glass-fiber filters, stored on ice in the field, and refrigerated at the laboratory until analysis. All filtered samples were analyzed for NH_4 colorimetrically, for Cl, NO_3, and SO_4 using ion chromatography, and for Na, K, Ca, and Mg by atomic absorption. Unfiltered samples were analyzed for acid neutralizing capacity (ANC) and pH.

Total rainfall at the sites ranged from 19 to 46 mm. Maximum stage observed was 25, 12, and 3 cm above base flow at the URB, AG and FOR sites, respectively; maximum discharges were 400, 140, and 70 l/s. Solute concentrations in rain were similar among all sites and much lower than those found in stream water. Base flow values for all solutes were lower at the FOR site than at the other, more developed sites. Sodium and Cl concentrations were high at the URB site, probably because of salting roadways in winter months. Calcium concentrations were high in the AG site, perhaps due to the addition of lime to agricultural fields. During the storm, solute concentrations in stream water of the FOR site were relatively invariant compared to the URB and AG sites (Fig. 1a–c). Concentrations of NH_4 and NO_3 increased at the beginning of the storm, and trends were similar at the AG and URB sites (Fig. 1a). Concentrations of other solutes at the URB and AG sites decreased with the onset of the storm (Figs. 1b, c). After the storm, solute concentrations at the AG site increased rapidly toward base flow values (Figs. 1b, c). Stream water discharge from the URB site was the highest of the three catchments, as was the net flux of solutes measured (Fig. 1d).

The variations in solute concentrations observed are primarily due to site-specific differences in the relative proportions of groundwater and overland flow inputs to the stream. The proportion of these inputs is commonly regulated by the type and amount of ground cover in a particular catchment. The lack of forest cover in agricultural areas and impermeable surfaces in urban settings increase overland flow inputs to streams during storms (3). In forested catchments, runoff is typically smaller than in more developed catchments because soil and vegetation allow much of the precipitation to percolate slowly to the groundwater table. In contrast, soils in predominately agricultural catchments can become quickly saturated during storms, causing larger inputs of water to enter a stream in the form of overland flow and diluting solute concentrations. As a storm subsides, solute concentrations in stream water will typically return to base flow levels as the ratio of groundwater inputs to overland flow increases. Urban settings characteristically have large amounts of impervious ground cover preventing rain from percolating to groundwater reservoirs, thereby increasing the proportion of overland flow (urban runoff) to the stream. Hence, the large decreases in solute concentrations observed at the AG and URB sites during a storm are probably due to a larger overland flow component in these catchment streams. In contrast, the increases of NH_4 and NO_3 concentrations at these sites must be due to strong sources of nitrogen in overland flow and groundwater at the beginning of a storm that may be linked to the application of fertilizers in developed settings.

Our results show that there are marked differences in the solute dynamics of storm flow among streams in areas characterized by different land uses. Because anthropogenic inputs of nitrogen are associated with the eutrophication of receiving waters, further study is required to determine the impact of increased NH_4 and NO_3 export from urban and agricultural catchments on the aquatic ecology of the Ipswich River.

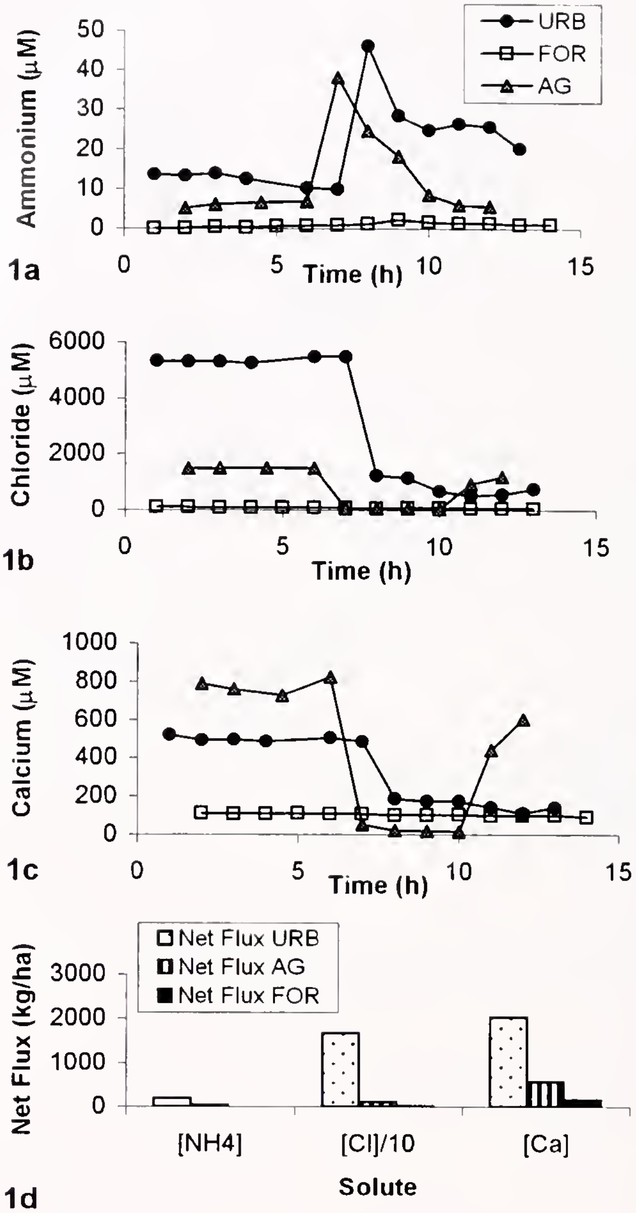

Figure 1. *Concentrations of ammonium (A), chloride (B), and calcium (C) plotted against time. Relative fluxes of ammonium, chloride (divided by 10) and calcium at the three study sites (D).*

Literature Cited

1. Pontius, R. G. Jr., L. Claessens, C. S. Hopkinson, Jr., A. Marzouk, E. B. Rastetter, L. C. Schneider, and J. Vallino. 2000. In

Proceedings of the 4^{th} International Conference on Integrating GIS and Environmental Modeling (GIS/EM4): Problems, Prospects and Research Needs. Banff, Alberta, Canada, 2–8 September 2000. (In press).

2. **Wood, E. F., M. Sivapalan, and K. Beven. 1990.** *Reviews of Geophysics.* **28:** 1–18.
3. **Jordan, T. E., D. L. Correll, and D. E. Weller. 1997.** *J. Environ. Qual.* **26:** 836–848.

Reference: *Biol. Bull.* **199:** 221–223. (October 2000)

Fate of Anthropogenic Nitrogen in a Nearshore Cape Cod Aquifer

Elizabeth J. Westgate[1], *Kevin D. Kroeger, Wendy J. Pabich, and Ivan Valiela*
(Boston University Marine Program, Marine Biological Laboratory, Woods Hole, Massachusetts 02543)

Nitrogen loading from land is a principal cause of eutrophication of shallow estuaries (1, 2, 3). In regions such as Cape Cod, Massachusetts, which are underlain by unconsolidated sands, the major mechanism that transports nitrogen to estuaries is groundwater flow, and the major nitrogen source (primarily in the form of nitrate, NO_3) is often wastewater from septic systems (1, 2, 3). Wastewater nitrate concentrations decrease during travel in groundwater due to dilution with clean groundwater and to loss by denitrification (4). The loss of nitrogen during flow between a septic tank and receiving estuary can be calculated by determining the reduction in concentration of dissolved inorganic nitrogen relative to the change in concentration of a passive tracer that accounts for dilution.

We investigated losses of nitrate for a domestic septic system in the watershed of Quashnet River, Cape Cod. Effluent from septic systems moves downgradient within plumes containing high concentrations of nitrate. In addition, the study area has plumes derived from fertilized turf or fields. To sort out the different plumes, we measured boron (B, a passive tracer derived from laundry detergents and associated with wastewater sources [5, 6, 7]) and potassium (K, associated with both wastewater and fertilizer sources [8, 9]) in the samples of groundwater.

To calculate loss of nitrate along the plumes, we collected samples from nine wells downgradient from the septic system. Each well was furnished with 14 ports that allowed us to sample groundwater at intervals of 1–2 m. We collected 300 ml of water from 129 ports during June and July 2000 and measured concentrations of nitrate ($NO_3 + NO_2$) and ammonium (NH_4) using colorimetric and fluorometric techniques, respectively. We selected samples with nitrate concentrations above 8 μM and conductivities less than 4,000 μS/cm for measurements of B and K. These samples were analyzed by Ward Laboratories (Kearney, NE).

Examination of vertical and horizontal profiles of nitrate and ammonium suggested that there were three distinct plumes within our well field (Fig. 1). The upper plume moved along near the surface of the water table and contained the highest nitrate concentration of the three plumes; at nearly 3000 μM, it was similar to literature values (8) for septic effluent that has just left the leaching field. The nitrate, B, and K concentrations in this plume differed considerably from those of the other plumes (Fig. 2, A and B).

In contrast, the lower plume showed no increase in nitrate relative to increase in B (Fig. 2, A). It did, however, show a positive relationship to K, and at a given K concentration had a much higher nitrate concentration than did the upper plume (Fig. 2, B). This evidence suggests that the lower plume might be due to fertilizer use upgradient of our septic system.

The middle plume had no significant relationships between nitrate and B or K, perhaps because of the small number of samples and the low concentrations. The concentrations of nitrate, B, and K from the middle plume do, however, fit on the lower portions of the curves for the upper plume (Fig. 2, A and B). These circumstances lead us to think that the middle plume was probably the leading edge of a plume from a septic system located farther upgradient from our septic system. We therefore used data for the upper and middle plumes in our examination of the fate of septic system nitrogen in this watershed.

Concentrations of nitrate and B diminished as water parcels aged (age, Fig. 2, C and D, calculated from Vogel equations [10] that predict time since recharge as a function of depth in aquifer). To allow for dilution, we normalized the data by expressing concentrations as NO_3/B (Fig. 2, E). We estimated the NO_3/B in the effluent that had just left the septic system (age 0) by using a literature value (8) (Fig. 2, E, upper dashed line). The NO_3/B values we used came from a Cape Cod site near our study area, and the data dated from 1992, only a 7–8 year difference from our date of collection. We presume that differences in B were therefore a reasonable proxy for those in our study system. We calculated losses of NO_3 as the difference between the age 0 nitrate concentration, allowing for dilution, and the measured nitrate concentration.

Losses of nitrate in excess of dilution were quite rapid, with rates reaching 50% loss at 0.2 years (Fig. 2, F). The loss rates diminished with time, which suggests that, if these data are representative of losses elsewhere, N losses by denitrification and retention take place primarily near the septic system source. Extrapolating the curve of Figure 2 (F), we find that near-complete losses may be reached at 4.8 years, which is equivalent to 480–730 m from the septic system, assuming a travel rate of 100–150 m per year (11).

As a minimum estimate of loss, we also calculated loss relative to our highest measured NO_3/B ratio (Fig. 2, E, lower dashed line). If our initial NO_3/B ratio were closer to this measured value, our estimate of time to 50% NO_3 loss would increase to 0.6 years; but the estimate of time to 100% loss was not affected. The extrapolation to 100% loss assumes that the relationship between percent loss NO_3 and age continues to hold beyond our oldest sample. This would not be the case if the availability of labile organic carbon were to limit NO_3 loss before 100% loss is achieved.

---

[1] Lafayette College, Easton, PA 18042.

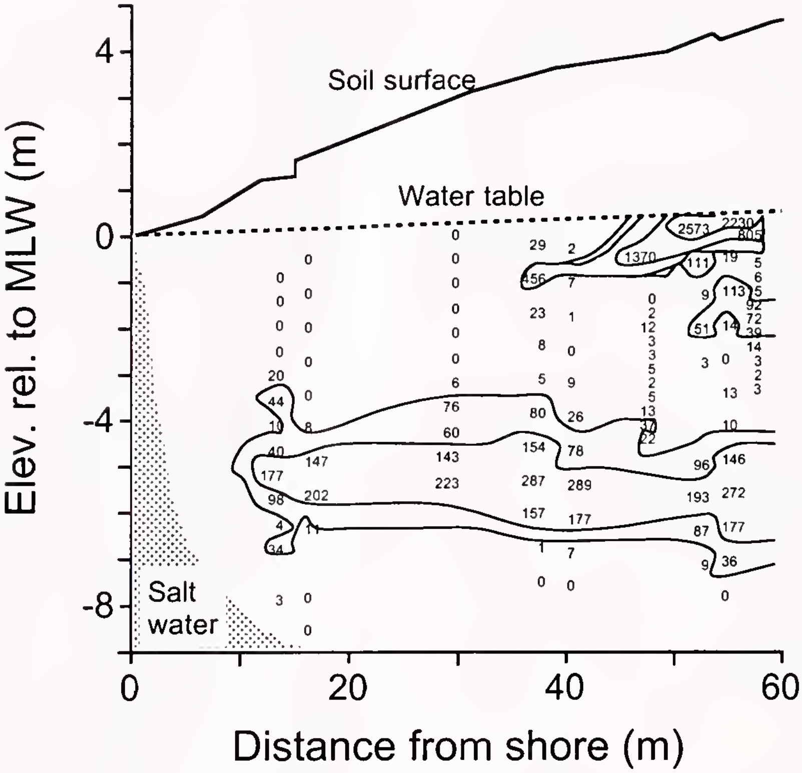

Figure 1. *Vertical cross section from the soil surface, water table, and aquifer through our field of multiple sampling wells (elevation relative to mean low water [MLW]). The numbers are concentrations of NO_3 (μM) for water samples collected from each of the 14 ports in each of the 9 wells. Although the wells were not all in one plane, for simplicity they are shown as if they were. Contour lines are drawn to indicate NO_3 concentrations of 32, 128, 512, and 2048 μM. Position of salty water determined from salinity of water samples.*

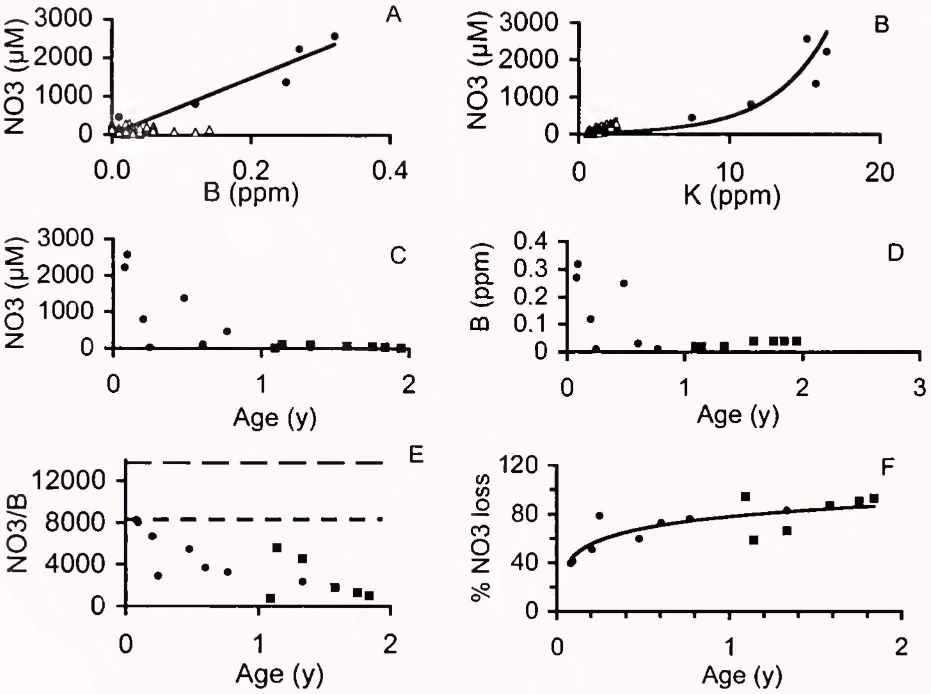

Figure 2. *A: NO_3 concentration versus B concentration for samples collected from upper (●), middle (■), and lower (△) plumes. B: NO_3 concentration* versus *K concentration for all three plumes. C: NO_3 concentration* versus *age for upper and middle plumes. D: B concentration* versus *age for upper and middle plumes. E: NO_3 to B ratio* versus *age for upper and middle plumes. F: Percent loss of NO_3* versus *age for upper and middle plumes.*

If coastal zone managers wish to regulate septic nitrogen loads, they could concentrate on management of septic systems that lie within 480–730 m of the shore, since these appeared to be the major contributors of nitrate to receiving estuaries. Septic sources farther upgradient probably contribute less significantly.

This research was supported by an internship from the Woods Hole Marine Science Consortium to Elizabeth Westgate, an MIT Sea Grant (#65591) awarded to Ivan Valiela and Harold Hemond, and National Estuarine Research Reserve Fellowships to Kevin Kroeger and Wendy Pabich.

Literature Cited

1. **Valiela, I., *et al.* 1992.** *Estuaries* **15:** 443–457.
2. **Valiela, I., *et al.* 1997.** *Ecol. Appl.* **7:** 358–380.
3. **Valiela, I., *et al.* 2000.** *Biogeochemistry* **49:** 277–293.
4. **Wilhelm, S. R., S. L. Schiff, and J. A. Cherry. 1994.** *Ground Water* **32:** 905–916.
5. **Barth, S. 1998.** *Water Res.* **32:** 685–690.
6. **LeBlanc, D. R. 1984.** U.S. Geological Survey Water-Supply Paper 2218. 28 pp.
7. **Barber, L. B. II, E. M. Thurman, M. P. Schroeder, and D. R. LeBlanc. 1988.** *Environ. Sci. Technol.* **22:** 205–211.
8. **DeSimone, L. A., P. M. Barlow, and B. L. Howes.** Open-File Rep.–U.S. Geol. Surv. 1995, No. 95-290.
9. **Bjerg, P. L., and T. H. Christensen. 1992.** *J. Hydrol.* **131:** 133–149.
10. **Vogel, J. C. 1967.** Pp. 355–369 in *Isotopes in Hydrology,* Proceedings of IAEA-SM-83/24, Vienna.
11. **LeBlanc, D. R., *et al.* 1991.** *Wat. Res.* **27:** 895–910.

Reference: *Biol. Bull.* **199:** 223–225. (October 2000)

Effects of Nitrogen Load and Irradiance on Photosynthetic Pigment Concentrations in *Cladophora vagabunda* and *Gracilaria tikvahiae* in Estuaries of Waquoit Bay

Michelle Denault[1], *Erica Stieve, and Ivan Valiela*
(Boston University Marine Program, Marine Biological Laboratory, Woods Hole, Massachusetts 02543)

Two major controls of activity and standing crop in macroalgae are nitrogen supply and irradiance (1). Increased nitrogen loads increase production (2) and biomass of macroalgae such as *Cladophora vagabunda* and *Gracilaria tikvahiae* (E. Stieve, unpub. data). Lower light availability lowers growth rates of macroalgae, although this effect varies among species (3). Because of exponential attenuation and self shading within algal mats, the irradiance available for benthic algae depends on water depth (1). Supply as well as storage of nitrogen and photons affect the concentration of photosynthetic components in macroalgae (1, 4). Photosynthetic pigments such as phycoerythrin also act as nitrogen pools, and macroalgae acclimate to different irradiance regimes by changing pigment concentrations (5).

To examine the effects of different nutrient supplies on photosynthetic pigment concentrations in a green and a red alga, we collected samples of *Cladophora vagabunda* (L.) van den Hoek and *Gracilaria tikvahiae* McLachlan from five estuaries within Waquoit Bay (Childs River, Eel River, Quashnet River, Sage Lot Pond, and Timms Pond) that are exposed to different nitrogen loads (6). To study the effect of irradiance on pigment concentration we collected samples at a range of depths (80 to 210 cm). Irradiance at each sampling depth was measured using a spherical underwater sensor attached to a Li-Cor DataLogger LI-1000. Samples were collected during one day in early June.

At each site, six samples of benthic macroalgal material were collected and sorted to isolate fronds of *C. vagabunda* and *G. tikvahiae.* The samples were sorted by species. Chlorophyll *a*, *b*, and carotenoids were extracted as described by Figueroa *et al.* (7); phycobiliproteins were extracted as described by Beer and Eshel (8). Pigments were extracted within 36 h of collecting and were kept at 5°C until extraction to avoid pigment degradation. Concentrations of pigments were determined by use of a Perkin Elmer UV/VIS spectrophotometer (8, 9, 10). Chlorophyll *a* and carotenoid concentrations were measured in both *C. vagabunda* and *G. tikvahiae.* Chlorophyll *b* concentrations were measured in *C. vagabunda.* Phycoerythrin concentrations were measured in *G. tikvahiae.* To further ascertain the internal storage of nitrogen and carbon under different nitrogen and irradiance regimes, we dried macroalgal samples and measured percent nitrogen and percent carbon in a Perkin Elmer elemental analyzer according to the manufacturer's instructions.

Concentrations of chlorophyll *a* (Fig. 1A) and carotenoids (Fig 1B) in both species of macroalgae increased as nitrogen load to the estuaries increased. There was no consistent difference between upstream and downstream sites within the estuaries, and there was no apparent effect of different salinities at the sites of collection (range of 10‰ to 32‰) on pigment concentrations (data not shown), so data were pooled within each estuary. Concentrations of chlorophyll *a* and carotenoids in *C. vagabunda* and *G. tikvahiae* are within the range found in other published literature (5); more importantly, the nitrogen loads increase pigment concentrations from values characteristic of nitrogen-poor waters to those of nitrogen-rich estuaries (Fig. 1A, B) (5). The response of *C. vagabunda* to nitrogen supply was more pronounced than that of *G. tikvahiae* (Fig. 1A, B).

These results suggest that nitrogen supply has important effects on pigment concentrations and nitrogen content of fronds, and that the response depends on the species. Surprisingly, concentrations of phycoerythrin in *G. tikvahiae* did not increase as nitrogen load

---

[1] Brown University, Providence, RI 02912.

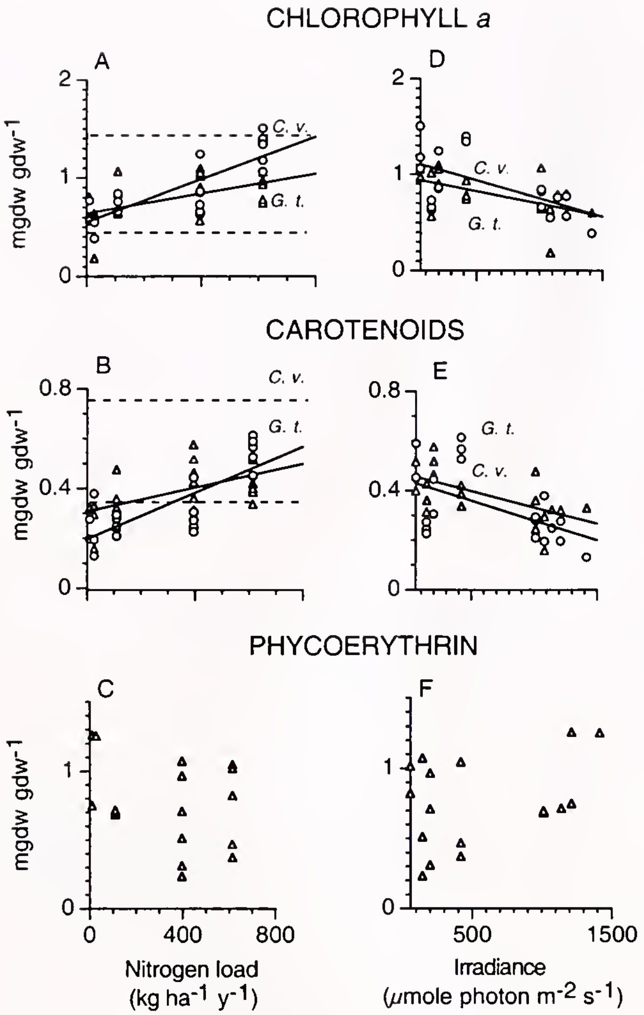

Figure 1. *Milligrams dry weight of pigments per gram dry weight of macroalgae are shown versus nitrogen load (left column) and* versus *irradiance (right column). (A) Chlorophyll* a (C. vagabunda, $F = 32.83$, $P < 0.001$; G. tikvahiae, $F = 6.86$, $P < 0.05$), *(B) carotenoid* (C. vagabunda, $F = 26.88$, $P < 0.001$; G. tikvahiae, $F = 6.61$, $P < 0.05$), *and (C) phycoerythrin (ns) concentrations* versus *nitrogen load. The dotted lines show published (5) pigment concentrations ranges for macroalgae in nitrogen-poor waters (lower dotted lines) and nitrogen-rich water (upper dotted lines). (D) Chlorophyll* a (C. vagabunda, $F = 8.52$, $P < 0.01$; G. tikvahiae, $F = 7.50$, $P < 0.05$), *(E) carotenoids* (C. vagabunda, $F = 6.71$, $P < 0.05$; G. tikvahiae, $F = 10.60$, $P < 0.01$) *and (F) phycoerythrin (ns) concentrations* versus *irradiance.*

increased (Fig. 1E), even though this pigment is known to function as a nitrogen reserve (11). *G. tikvahiae* may not be nitrogen-limited in these estuaries, an inference that we base on both the relatively low response of chlorophyll *a* (Fig. 1A) and carotenoid (Fig. 1B) concentrations, and the lack of response of phycoerythrin concentrations (Fig. 1C) to nitrogen load. We also measured concentrations of chlorophyll *b*, which showed a positive response to nitrogen load (data not shown). Curiously, concentrations of chlorophyll *b* responded more strongly to increased nitrogen supply than did chlorophyll *a* concentrations (Fig. 2A). We have no explanation for this response.

Concentrations of chlorophyll *a* (Fig. 1D) and carotenoids (Fig. 1E) in both species of algae decreased similarly and significantly at lower irradiance. These results suggest that the mechanism of response to irradiance is similar for both species of algae. Phycoerythrin concentrations (Fig. 1F) did not change with differences in irradiance. The percent N content of *C. vagabunda*, but not of *G. tikvahiae*, increased in parallel to nitrogen load (Fig. 2B, C). The increase in nitrogen content in *C. vagabunda* is even more striking in view of the decrease of carbon content in *C. vagabunda* as nitrogen load increased (Fig. 2B). Percent nitrogen in *G. tikvahiae* fronds did not increase significantly with nitrogen load, in agreement with the results of Figure 2C.

Increased nitrogen loads were paralleled by significant increases in photosynthetic pigments in *C. vagabunda* and *G. tikvahiae* as well as by an increase in percent N in *C. vagabunda*, but not in *G. tikvahiae*. These results suggest that the supply of nitrogen may be sufficient to support growth in *G. tikvahiae*, but that *C. vagabunda* is nitrogen-limited in those estuaries of Waquoit Bay that receive the lowest nitrogen load from land. This conclusion is verified by biomass data (E. Stieve, unpub. data) that show that the response of standing crop of *C. vagabunda* is a function of nitrogen load, and that

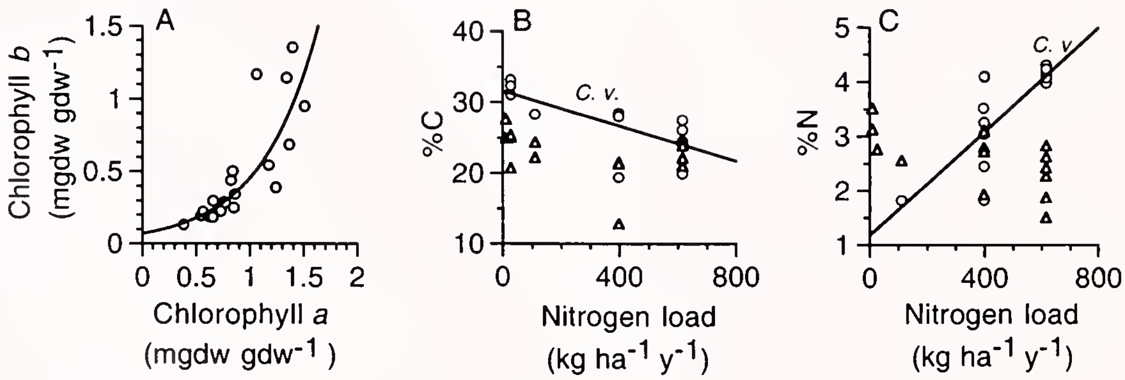

Figure 2. *(A) Chlorophyll* b *concentration* versus *chlorophyll* a *concentration* ($r^2 = 0.785$). *(B) Percent carbon* (C. vagabunda, $F = 19.17$, $P < 0.01$; G. tikvahiae, $F = 3.00$, *ns) and (C) percent nitrogen* (C. vagabunda, $F = 34.56$, $P < 0.001$; G. tikvahiae, $F = 0.99$, *ns*) versus *nitrogen load.*

standing crop of *G. tikvahiae* responds less to nitrogen supply than to seasonal changes in light availability. The increase of chlorophyll *a* and carotenoid concentrations in *C. vagabunda* and *G. tikvahiae* in response to high irradiance is paralleled by biomass data taken from the estuaries (E. Stieve, unpub. data). The biomass of *G. tikvahiae* was greater than that of *C. vagabunda* in low-nitrogen estuaries that also furnished high irradiance to algae.

The physiological changes in photosynthetic pigments and nitrogen concentrations created by increased loads suggest increased growth of at least the green alga *C. vagabunda.* Increased nitrogen load may also increase phytoplankton standing crop, increasing light attenuation in the water column and therefore decreasing the growth of light-limited benthic algae. On balance, the growth-stimulating effect of increased nutrients seems to more than compensate for the detrimental effect of light attenuation from the influence of phytoplankton shading at the time of sampling; and *C. vagabunda,* in particular, proliferates and causes macroalgal blooms in nitrogen enriched estuaries.

This research was supported by the Woods Hole Marine Science Consortium. Special thanks to Jennifer Hauxwell for help with algae and Jennifer Bowen for her endless patience.

Literature Cited

1. **Ruecker, J., J. Kohl, and K. Kaiser. 1995.** *Arch. Hydrobiol. (Suppl.)* **108:** 51–65.
2. **Peckol, P., and J. Rivers. 1996.** *Estuarine Coastal Shelf Sci.* **43:** 311–325.
3. **Peckol, P., and J. Rivers. 1995.** *J. Phycol.* **31:** 229–232.
4. **Peckot, P., B. DeMeo-Anderson, J. Rivers, I. Valiela, M. Maldonado, and J. Yates. 1994.** *Mar. Biol.* **121:** 175–185.
5. **Bird, K., C. Habig, and T. DeBusk. 1982.** *J. Phycol.* **18:** 344–348.
6. **Valiela, I., K. Foreman, M. LaMontagne, D. Hersh, J. Costa, P. Peckol, B. DeMeo-Anderson, C. D'Avanzo, M. Babione, C.-H. Sham, J. Brawley, and K. Lajtha. 1992.** *Estuaries* **15:** 443–457.
7. **Figueroa, F., S. Soluna, J. Aguilera, C. Jiménez, J. Mercado, B. Viñegla, A. Flores-Moya, and M. Altamirano. 1997.** *Mar. Ecol. Prog. Ser.* **151:** 81–90.
8. **Beer, S., and A. Eshel. 1985.** *Aust. J. Mar. Freshw. Res.* **36:** 785–792.
9. **Jeffrey, S., and G. Humphrey. 1975.** *Biochem. Physiol. Pflanz.* **167:** 191–194.
10. **Dawes, C. 1998.** Pp. 380–382 in *Marine Botany.* John Wiley, New York.
11. **Lapointe, B. 1985.** *J. Exp. Mar. Biol. Ecol.* **93:** 211–222.

Reference: *Biol. Bull.* **199:** 225–226. (October 2000)

Differences in Properties of Salt Marsh Sediment Between Hayed and Reference Sites

Adena Greenbaum (Wellesley College) and Anne Giblin[1]

The practice of haying salt marsh grasses began in colonial times. Early settlers began harvesting marsh grasses for fodder, and the practice has continued to the present (1). Current haying techniques remove more than 90% of aboveground plant biomass, and could have a number of effects on processes within the marsh. Salt marsh food webs are based on detritus, so it can be hypothesized that removal of plant biomass could alter food webs. Nutrient cycles, benthic algal biomass, microbial processes, and species composition could also be affected (2, 3). This study examined the effect of detritus removal on several sediment properties to assess the long-term effects of haying.

Sediment cores were taken from Plum Island Sound intertidal marsh, a long-term ecological research site located in northeastern Massachusetts. To study the effects of detritus removal, we measured several characteristics of sediment in areas where the marsh grass is hayed by commercial farmers. We compared the results to those of reference areas, which are not hayed. We sampled two areas that are hayed every other year, a practice the commercial farmers recognized produced the highest hay yield.

Duplicate cores were taken from each of two hayed and reference sites. All cores were taken from high marsh areas that were heavily dominated by *Spartina patens.* Measurements of the following sediment characteristics were taken at 2 cm intervals above 10 cm and 5 cm intervals below 10 cm, to a depth of at least 25 cm. Bulk density, a measure of soil density, was expressed as ratio between the weight and volume of sediment; percent organic matter was measured by loss of ignition; total sulfur was measured using a LECO sulfur analyzer; sedimentation rates were calculated using Pb profiles (4); and total phosphorus was measured using the technique of Krom and Berner (5). These properties were measured to examine sediment composition.

There was no significant difference in bulk density between surface sediments in the hayed and reference sites (Fig. 1). Bulk densities for both the hayed and reference areas decreased from a range of 0.37 to 0.34 g cm^{-3} at the surface to 0.22 g cm^{-3} at 12.5 cm. Below this depth, there was a slight difference in bulk density values. The hayed areas increased to a maximum of 0.34 g cm^{-3} at 23 cm. However, the bulk density of the reference sites remained around 0.23 g cm^{-3}. Judging from surface values for bulk density, current haying practices apparently do not compact the sediments.

Percent organic matter was similar between the managed and natural areas to a depth of 12.5 cm. Values ranged from 31.7% to 44.5% organic matter. Deeper sediment samples of reference plots had a slightly higher percent organic matter than the hayed sites, but the difference between them was not significant. This indicated that the removal of biomass from the hayed sites does not affect organic matter content.

Haying did not appear to affect the total sulfur content in the sediment. In both hayed and reference areas, total sulfur increased from about 0.65% at the surface to a maximum of 2.2% between 17 and 22 cm, and then decreased to about 1.55% at a depth of 30 cm.

---

[1] Ecosystems Center, Marine Biological Laboratory, Woods Hole, MA.

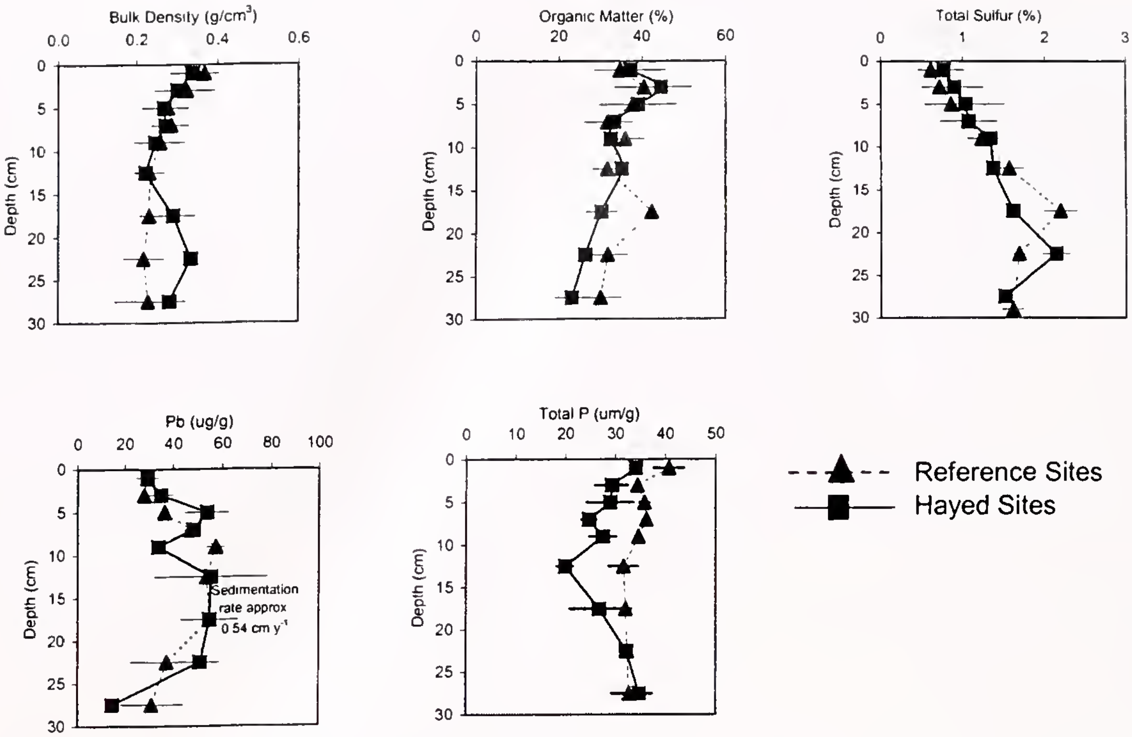

Figure 1. *Measures of bulk density, percent organic matter, total sulfur, sedimentation rate, and total phosphorus in hayed and reference sites of salt marsh sediment in Plum Island Estuary.*

Values between hayed and reference sites for percent total sulfur, along with bulk density and percent organic matter deviated slightly below 12.5 cm. This sediment was deposited more than 25 years ago, and since land practices before this time are unknown, it is difficult to hypothesize reasons for the deviation.

Sedimentation rates can be estimated by using stable lead profiles to approximate dates of deposition. The lead profiles for hayed and reference areas were not significantly different. Although the cores were not deep enough to reach pre-industrial background values, we used a previous study to establish background levels (Schmitt, unpub. data). Using both sets of data, we calculated a sedimentation rate of 0.54 cm y^{-1} for both the reference and the hayed areas. The lack of differentiation in sedimentation between the hayed and natural marsh is surprising given that the haying process removes a large portion of the aboveground biomass. One possible explanation is that most of the organic matter making up the peat comes from other sources. Belowground biomass could contribute significant amounts of organic matter to detritus, especially since a large percent of biomass in a salt marsh could be below ground. Organic matter washed in with the tide could settle as detritus as well. The profile for the hayed sites was more variable than that of the reference site. Perhaps the tractor and trailer used for haying disturbs the surface sediment as it travels over the marsh.

There was a significant difference between total phosphorus measured in hayed and reference sites. The hayed areas had less total phosphorus than the reference sites from the surface until 22.5 cm deep in the sediment, where the values for the two areas converged. One explanation is that the input of phosphorus to the marshes of the area is very low, and the periodic removal of biomass from the system eventually leads to a measurable loss in phosphorus.

Of the sediment properties we examined—bulk density, percent organic matter, total sulfur, sedimentation rate, and total phosphorus—only the last was affected by harvesting the aboveground biomass every other year. Current haying practices on the marsh did not significantly alter most of the properties we measured. However, other processes in the marsh could be affected by the decrease in phosphorus, and other systems could respond differently to comparable practices.

This research was supported by the Plum Island Sound LTER and a Research Experience for Undergraduates NSF fellowship. Thanks to Linda Deegan, Hap Garritt, and Nat Weston for advice and assistance with sampling.

Literature Cited

1. **Teal, J., and M. Teal. 1969.** *Life and Death of the Salt Marsh.* Pp. 21, 183.
2. **Knapp, A. K., and T. R. Seastedt. 1986.** *Bioscience* **36:** 662–668.
3. **Bouchard, V., and J. Lefeuvre. 2000.** *Aquat. Bot.* **67:** 23–42.
4. **Ng, A., and C. Patterson. 1982.** *Geochem. Cosmochim. Acta* **48:** 2307–2321.
5. **Krom, M. D., and R. A. Berner. 1981.** *Geochem. Cosmochim. Acta* **45:** 207–216.

Reference: *Biol. Bull.* **199:** 227–228. (October 2000)

Population Genetic Structure of the Goosefish, *Lophius americanus*

Hemant M. Chikarmane, Alan M. Kuzirian (Marine Biological Laboratory, Woods Hole, Massachusetts), Robbin Kozlowski[1], *Mark Kuzirian,*[2] *and Tony Lee*[3]

Lophius americanus Cuvier & Valenciennes 1837 (1), the goosefish, anglerfish, or monkfish, is common in coastal waters of the northeastern United States. Its geographic range extends from the northern Gulf of St. Lawrence south to Cape Hatteras, North Carolina (2, 3). The highest fish concentrations are found along the shallower depths of the shelf from 70 to 100 m, but there is also a significant deep-water population below 190 m. Adult fish migrate seasonally in response to spawning, food availability, and optimal temperatures (3°–9°C) (2). The species is also dispersed through the drifting of egg rafts. Total dispersal time from embryonic development through larval and juvenile stages can extend to several months until benthic recruitment occurs. Sexual maturity is reached between 3 and 4 years of age (3).

Goosefish is the fourth largest commercial species in the U.S. fishery, and number one in demersal species landings. Goosefish landings have risen steeply through the 1980s, reaching approximately 28,800 mt ($35 million) for 1997 (4). Since the 1980s, the Canadian contribution to the fishery has declined precipitously, and now the major landings occur in the southern regions of the species range. In their autumn survey data, the Northeast Fisheries Science Center, Woods Hole, Massachusetts, has documented recent sharp declines in goosefish abundance, from 2.24 kg/tow in 1986 to 0.74 kg/tow in 1996. The New England and Mid-Atlantic Fishery Management Councils (NEFMC and MAFMC) consequently designated goosefish as overexploited and at low abundance (5). The 23rd Stock Assessment Workshop at the Northeast Fisheries Science Center concluded that it was not possible to delineate the stock structure for goosefish because of the lack of genetic, tagging, or migration studies. Nevertheless, the Councils divided the coastal population into northern and southern stocks (41°N latitude) for stock management purposes. This formula led to fishing restrictions being placed geographically, and made certain areas uneconomical to fish. Because of the lack of definitive stock data for goosefish (5), we undertook a population genetic study of goosefish in eastern waters from the Canadian border to North Carolina. We used random amplification of polymorphic DNA and PCR (RAPD-PCR) (6) to analyze the genetic structure of the sampled populations.

Eight representative sampling sites were chosen, extending from Maine (42°40′ N, 68°20′ W) to North Carolina (35°40′, 75°00′), from depths to about 300 m. Fish were collected from September 1999 to June 2000. Up to 45 fish were sampled at each location. Tissue samples were collected in tissue preservation buffer (7). Genomic DNA was purified by standard phenol-chloroform procedures, and was finally dissolved in Tris-EDTA (TE) buffer (8). DNA fingerprinting was performed by RAPD-PCR (6), using 10 μl per reaction. Amplification products were separated by electrophoresis on 1.2% agarose gels in 0.5x TBE (8). Gels were stained with ethidium bromide and photographed under UV light. The presence or absence of amplification products was scored manually. Cluster analysis was performed with the RAPDistance package (9).

Six fish, three each from Georges Bank and New York/New Jersey sites were first screened with the seven primers shown in Table I. As expected, the number of amplification products per primer varied, ranging from 2 to 9, and very few bands were polymorphic (Table I). On the basis of the initial screening, a subset of 6–8 DNA samples from each site was analyzed, using primers 101 and 103; Figure 1 shows data for primer 103.

There appeared to be no significant differences between individuals or between populations, with either primer. Polymorphic bands were present in a minority of individuals, usually one or two. A set of eight fish collected off Martha's Vineyard, Massachusetts, by the Marine Biological Laboratory, was examined with an additional set of primers (115, 119, 130, and 143). Again, the band distribution was very homogeneous (data not shown). Of the 22 identifiable bands produced by these primers, 21 were present at a frequency of 100%. Band 22 was present at a frequency of 58%. All the MBL samples were clustered as one group by the RAPDistance package. These results taken together imply that the fish populations are relatively homogeneous genetically across all geographic sampling sites, the level of polymorphism **within** populations being as low as that **between** populations. Fish caught at shallower (<200 m) depths could not be differentiated from those at lower (>200 m) depths, neither could those collected north or south of the 41°N line. For the primers tested, there was no amplification product (or the absence of one) that uniquely characterized a particular population. The trend in the data is clear even though only a subset of samples was analyzed with two primers. We are currently examining the entire sample set with more primers to reinforce the validity of our results.

Table I

RAPD primer sequences and polymorphic bands for Lophius americanus

Primer	Sequence	Number of bands	Polymorphic bands
101	GCGGCTGGAG	9	1
103	GTGACGCCGC	7	2
104	GGGCAATGAT	3	0
105	CTCGGGTGGG	8	1
106	CGTCTGCCCG	8	1
107	CTGTCCCTTT	2	2
108	GTATTGCCCT	7	1

The primer numbering system and sequence is from the University of British Columbia RAPD primer kits (10).

---

[1] Cape Cod Community College, W. Barnstable, MA.

[2] University of Rhode Island, Kingston, RI.

[3] Duke University, Durham, NC.

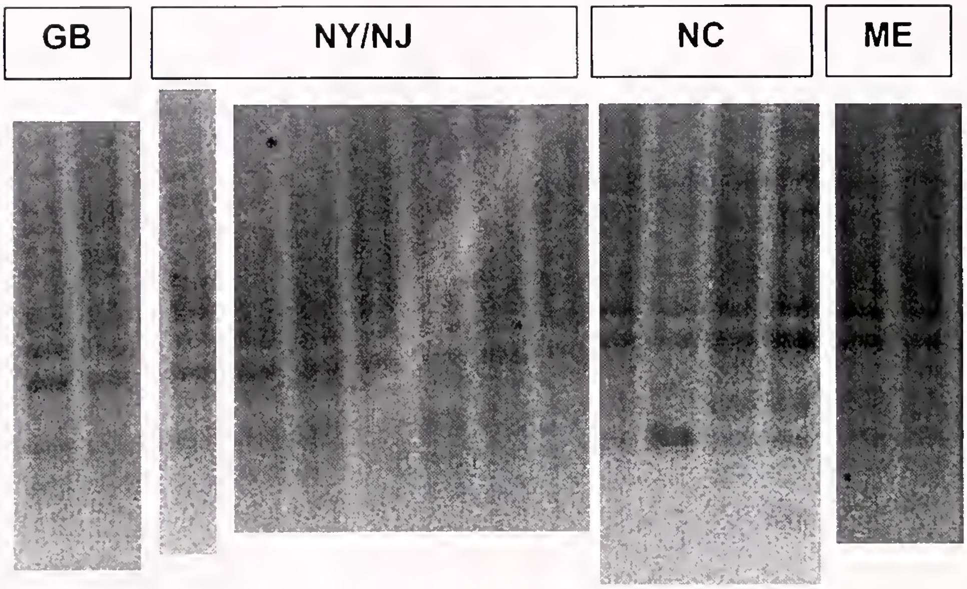

Figure 1. *Representative RAPD-PCR profiles with Primer 103 for individual goosefish samples from indicated locations. GB–Georges Bank, NY/NJ–New York/New Jersey, NC–North Carolina, ME–Maine.*

The homogeneity of the goosefish populations off the eastern coastline of the United States suggests that there is unrestricted gene flow across the region. This is very plausible considering the preferred temperature profile and migratory patterns of the adults, and the long dispersal times of the embryos, larvae, and postlarval juveniles (2, 3). These data will have serious implications for management of the goosefish fishery. The study results run counter to the current NEFMC/MAFMC policy of dividing the fishery into northern and southern stocks. Any management plan will be difficult to implement because the spawning stock biomass is unknown. More data is also needed to determine the location of the standing reproductive population, and to assemble specific temporal data on when spawning occurs over the fish's geographic range. Integration of the published data on seasonal abundances (NMFS Spring/Autumn Bottom Trawl Surveys) with yearly temperature profiles along the coastlines might suggest some possible avenues to pursue these answers. Such data will assist in defining the natural and fishing mortality rates (F) and what the $F_{\text{threshold}}$ should realistically be for this commercially important species.

This work was supported in part by the Monkfish Defense Fund. H.M.C. and A.M.K. are indebted to Kathy Downey of the MDF for acquainting them with the problems of the goosefish fishery, and for organizing the fishermen for sample collection. We thank the Aquatic Resources Division, MBL, for collecting some goosefish used in this study.

Literature Cited

1. **Cuvier, G., and A. Valenciennes. 1837.** *Histoire Naturelle des Poissons.* 12. Bertrand, Paris.
2. **Grosslein, M. D., and T. R. Azarovitz. 1982.** *MESA New York Bight Atlas Monograph.* N.Y. Sea Grant Institute, Albany, NY.
3. **Bigelow, H. B., and W. C. Schroeder. 1953.** *Fish. Bull.* **74:** 53.
4. **NOAA technical memo. 1999.** *Our Living Oceans. Report on the Status of U.S. Living Marine Resources.* U.S. Department of Commerce, National Oceanic and Atmospheric Administration, National Marine Fisheries Service. Washington, DC.
5. **Idoine, J. 1998.** Pp. 88–89 in *Status of Fishery Resources off the Northeastern United States for 1998.* S. H. Clark, ed. U.S. Department of Commerce, National Marine Fisheries Service, Woods Hole, MA.
6. **Williams, J. G. K., A. R. Kubelik, K. J. Livak, J. A. Rafalski, and S. V. Tingey. 1990.** *Nucl. Acids Res.* **18:** 6531–6535.
7. **Asahida, T., T. Kobayashi, K. Saitoh, and I. Nakayama. 1996.** *Fish. Sci.* **62:** 727–730.
8. **Sambrook, J., E. F. Fritsch, and T. Maniatis. 1989.** *Molecular Cloning. A Laboratory Manual.* Cold Spring Harbor Press, Cold Spring Harbor, NY.
9. **Armstrong J. S., A. J. Gibbs, R. Peakall, and G. Weiller. 1994.** *The RAPDistance Package.* ftp://life.anu.edu.au/pub/RAPDistance [21 Aug. 2000].
10. *Primer Kits.* NAPS Unit, University of British Columbia Biotechnology Laboratory. http://www.biotech.ubc.ca/services/naps/primers.html [21 Aug. 2000].

Published by Title Only

Bewley, Arnaud
Variations in white and black oaks as a function of their distance from the coast.

Chiao, Chuan-Chin, and Roger Hanlon
Visual mechanism of body patterning in young cuttlefish, *Sepia pharaonis.*

Dayel, Mark
Analysis of keratocyte motility and fine structure.

Haines, Jamie, Matthew Cieri, and Linda Deegan
Food choice convergence of benthic and pelagic fishes along an estuarine gradient.

Hinckley, Eve-Lyn
From forest to shore: the path of total dissolved nitrogen in a pristine coastal system, Martha's Vineyard, Massachusetts.

Horowitz, Julie, Linda Deegan, and Robert Garritt
Stable isotope analysis of detrital food webs in hayed and unhayed salt marsh.

Janowitz, Tobias, P. Koulen, and B. E. Ehrlich
Characterization of ryanodine receptors from zebrafish skeletal muscle.

Kreitzer, Matthew, Naomi Rosenkranz, and Robert Paul Malchow
Effects of extracellular ATP on skate retinal horizontal cells.

Schwartz, Jesse, and Les Kaufman
Mechanistic mass-balance models and community ecology.

Sergeant, Kara, Matthew Cieri, and Linda Deegan
Bivalve grazing pressure on primary producers in a New England estuary.

Silver, Robert B., and Steven A. Farber
Calcium-independent perinuclear phospholipase A_2 and leukotriene B_4 regulate the calcium signal required for nuclear envelope breakdown in sand dollar (*Echinaracnius parma*) cells.

Wolf, Amelia, Craig Tobias, and Bruce Peterson
Dissolved inorganic nitrogen uptake kinetics and relative preference indices for estuarine primary producers.

THE BIOLOGICAL BULLETIN
2001 SUBSCRIPTION FORM
(VOLUMES 200-201, 6 ISSUES)

(please print)

NAME: ______________________________

INSTITUTION: ______________________________

ADDRESS: ______________________________

CITY: ______________ STATE: ______________

POSTAL CODE: ______________ COUNTRY: ______________

TELEPHONE: ______________ FAX: ______________

E-MAIL ADDRESS ______________________________

All subscriptions run on the calendar year

☐ Please send me a 2001 subscription to The Biological Bulletin at the rate indicated below:

☐ Individual: $95.00 (6 ISSUES) ☐ Institutional : $235.00 (6 ISSUES)

☐ Individual: $47.50 (3 ISSUES) ☐ Institutional : $117.50 (3 ISSUES)

Check one: ☐ February April June or ☐ August October December

☐ Please send me the following back issue(s): ______________________________

☐ Individual: at $20.00 (PER ISSUE) ☐ Institutional : at $40.00 (PER ISSUE)

Delivery Options

______ Surface Delivery (Surface delivery is included in the subscription price.)
______ Air delivery (Please add the correct amount to your payment.)

☐ U.S. and Canada: $25.00 ☐ Mexico: $60.00 ☐ All other locations: $100.00

Payment Options

______ Enclosed is my check or U.S. money order for $ ______
made payable to The Marine Biological Laboratory

______ Please charge my ☐ VISA, ☐ MasterCard ☐ Discover Card $__________

______ Please send me an invoice. (Note: Payment must be received before subscription commences.)

Account No.: ______________________________ Exp. Date: ______________

Signature: ______________________________ Date: ______________

Return this form with your check or credit information to:

Marine Biological Laboratory
Subscription Office ◆ The Biological Bulletin ◆ 7 MBL Street ◆ Woods Hole, MA 02543-1015

THE BIOLOGICAL BULLETIN

2001 Subscription Rates
Volumes 200-201

	Institutional*	**Individual***
One year subscription (6 issues - 2 volumes)	$235.00	$95.00
Single volume (3 issues)	$117.50	$47.50
Single Issues	$ 40.00	$20.00

*Surface delivery included in above prices.
For prompt delivery, we encourage subscribers outside the U.S. to request airmail service.

Airmail Delivery Charge

U.S. and Canada:	$ 25.00
Mexico:	$ 60.00
All other locations:	$100.00

Orders Must Be Prepaid in U.S. Dollars, Check Payable to The Marine Biological Laboratory

About *The Biological Bulletin*
ISSN: 0006-3185
Frequency: Bimonthly
Number of issues per year: 6
Months of Publication: February, April, June, August, October, December
Subscriptions entered for calendar year
Volume indexes contained in June and December issues
Annual report of the Marine Biological Laboratory contained in August issue
Most back issues available
Claims handled upon receipt
No agency discounts
Internet: http://www.mbl.edu/BiologicalBulletin/

Please address orders to:
Carol Marrama
Subscriptions
The Biological Bulletin
Marine Biological Laboratory
7 MBL Street
Woods Hole, MA 02543-1015 U.S.A.
Fax: 508-289-7922 Telephone: 508-289-7402

Published by the Marine Biological Laboratory
Woods Hole, Massachusetts, 02543 U.S.A.

It's Worth A Closer Look

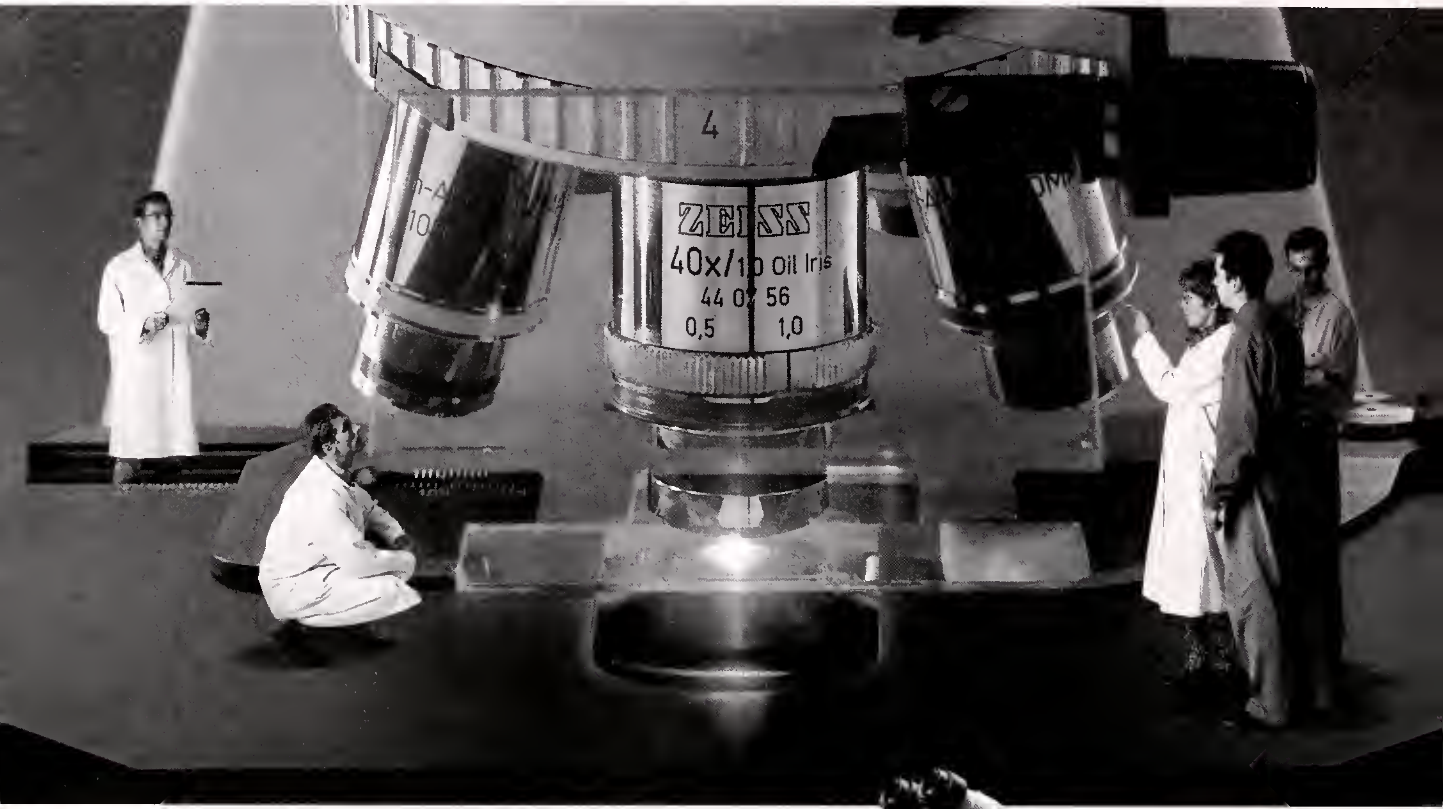

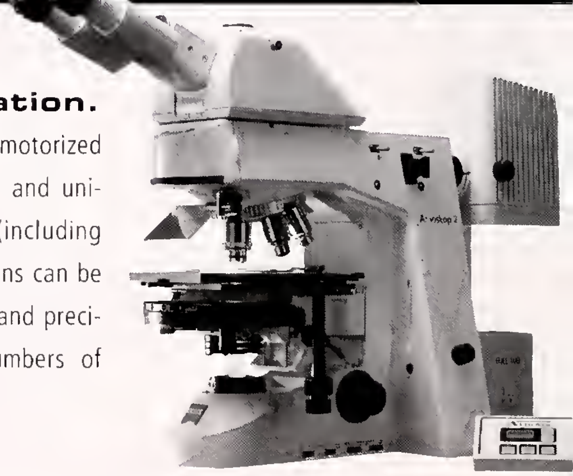

Brilliant and easy.

The **Axioskop 2** is the microscope that brings new levels of comfort and productivity to biomedical research. Renowned ICS infinity optics provide top quality images, and its operating convenience adds extra efficiency to your work.

Fluorescence 4-fold.

Carry out demanding fluorescence applications with flexibility and optimal illumination. Reflector turret for 4 fluorescence modules, 6-place excitation filter slide, plus the power of 100 watts.

Motorized automation.

In the **Axioskop 2 MOT** option, motorized functions include stage focusing and universal condenser setting (including Koehler). These and other functions can be automated for high productivity and precision when examining large numbers of specimens.

*Contact Zeiss today for the full story on the **Axioskop 2**.*

It's smart microscopy made easy.

Carl Zeiss, Inc.
Microscopy & Imaging Systems
One Zeiss Drive
Thornwood, NY 10594

800.233.2343
Fax 914.681.7446
micro@zeiss.com
www.zeiss.com

ZEISS

Volume 199

Number 3

THE BIOLOGICAL BULLETIN

DECEMBER 2000

Published by the Marine Biological Laboratory

Thanks Galileo, Hooke and Leeuwenhoek for the incentive.

We walk in the footsteps of visionaries.
And see with the eyes of disciples.

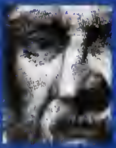

Galileo up close: astronomer, physicist, mathematician, dethroner of Aristotle, defender of Copernicus and, yes, credited with making double convex lenses and the first biological observations with a microscope. A compound microscope. In 1624.

Hooke: 43 years later, the compound microscope reveals living things are composed of cells.

Leeuwenhoek: invents the first practical microscope and discovers bacteria.

Armed with the knowledge and inspiration of these and other Olympians, secure in the history of our own accomplishments and aware that the mind's eye should always focus on challenging the enigmatic as well as the undeniable, Olympus has created the BX2 series of clinical and research microscopes, noteworthy for their enhancements in optics, imaging and ergonomics.

And each so individual, it deserves the nomenclature My Microscope.

From possibility to actuality, it is wonderful to behold.
A posse ad esse est mirabile visu.

Welcome to the next golden age of microsopy.

BX2
Microscope Series

The BX41

The new standard in laboratory microscopy vis-a-vis performance, versatility, operation.

Uncanny digitized imaging: enhanced with the **DP11 digital camera**, delivering high-resolution image recording beyond the norm.

Unusually insightfu optics: observe magnifications from **1.25x to 100x without changing the condenser.** Choice of condenser includes Abbe, swing out, phase-contrast and darkfield.

Unerringly precise-motion stage: selectable for right/ left hand. Discover speed, ease, touch, comfort, and clinical accuracy.

Uncommonly easy-to-operate controls: extended fine-focus knob; forwarded-positioned illumination intensity dial; tactile X-Y control.

The BX45

The new standard in ergonomic microscopy. A dramatic metamorphosis: innovative, intelligent, insightful design improvements specifically addressing the needs of those spending hours looking through a microscope.

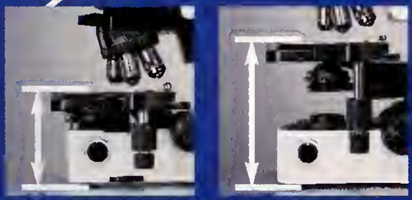

The **lowest low-position stage: three inches lower** than standard microscopes, offering the promise of minimum effort and hand movement when changing specimens.

The **tilting, telescoping observation tube:** a marvel of adjustability, it can be changed to accommodate any observation position. 80mm higher and 70mm closer to the operator than a conventional tilting tube. And the eyepoint can be moved forward by 45mm and inclined from 0–25 degrees.

The BX51

The new standard in research microscopy. The words "new" and "standard" really don't do it justice. How about "ingenious" or "original," "paragon" or "prototypical." Prepare yourself for a higher power.

The **6-position filter cube turret:** Not 4, not 5, but 6, so single and multi-band imaging of new fluorochromes and fluorescent proteins is faster, simpler and exclusively tailored.

2
4
5
6
5
6
WIG
WIY

The **rectangular field stop: ours alone**. By cleverly matching the camera's field of view, only the area requiring fluorescence excitation is exposed. Which means that the surrounding areas are protected from photo bleaching.

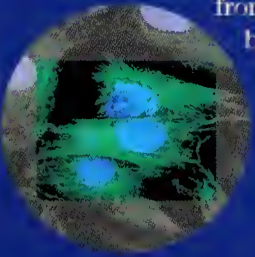

The **fluorescence excitation balancers:** another **Olympus exclusive**. A continuously variable excitation bandwidth. Visualization is enhanced, differentiation of multi-labels is immeasurably improved, capturing of images is at an unheard-of level.

Triple Labeled Specimen (l to r):

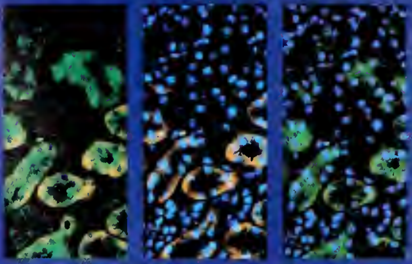

- with prevalent FITC and Cy3
- with prevalent DAPI and Cy3
- with balanced fluorescence emission

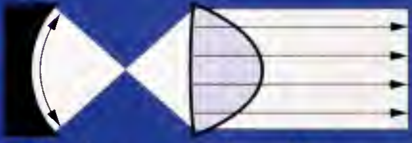

The **aspherical collector lens:** *sui generis*, in a class by itself. Specimens appear **brighter** and **more evenly illuminated**; and achromatic performance now incorporates wavelengths from UV to IR.

The **universal condenser: with 8 positions**, it can accept optical inserts for DIC, phase, brightfield and darkfield illumination. And the advanced Nomarski DIC system has been expanded and optimized to encompass prisms for enhanced contrast and image resolution.

OLYMPUS®

FOCUS ON LIFE

Visit us at www.olympusamerica.com
or call 1-800-455-8236

© Olympus America Inc.

THE
BIOLOGICAL BULLETIN

DECEMBER 2000

Editor	Michael J. Greenberg	The Whitney Laboratory, University of Florida
Associate Editors	Louis E. Burnett	Grice Marine Biological Laboratory, College of Charleston
	R. Andrew Cameron	California Institute of Technology
	Charles D. Derby	Georgia State University
	Michael LaBarbera	University of Chicago
Section Editor	Shinya Inoué, *Imaging and Microscopy*	Marine Biological Laboratory
Online Editors	James A. Blake, *Keys to Marine Invertebrates of the Woods Hole Region*	ENSR Marine & Coastal Center, Woods Hole
	William D. Cohen, *Marine Models Electronic Record and Compendia*	Hunter College, City University of New York
Editorial Board	Peter B. Armstrong	University of California, Davis
	Ernest S. Chang	Bodega Marine Lab., University of California, Davis
	Thomas H. Dietz	Louisiana State University
	Richard B. Emlet	Oregon Institute of Marine Biology, Univ. of Oregon
	David Epel	Hopkins Marine Station, Stanford University
	Gregory Hinkle	Cereon Genomics, Cambridge, Massachusetts
	Makoto Kobayashi	Hiroshima University of Economics, Japan
	Esther M. Leise	University of North Carolina Greensboro
	Donal T. Manahan	University of Southern California
	Margaret McFall-Ngai	Kewalo Marine Laboratory, University of Hawaii
	Mark W. Miller	Institute of Neurobiology, University of Puerto Rico
	Tatsuo Motokawa	Tokyo Institute of Technology, Japan
	Yoshitaka Nagahama	National Institute for Basic Biology, Japan
	Sherry D. Painter	Marine Biomed. Inst., Univ. of Texas Medical Branch
	J. Herbert Waite	University of California, Santa Barbara
	Richard K. Zimmer	University of California, Los Angeles
Editorial Office	Pamela Clapp Hinkle	Managing Editor
	Victoria R. Gibson	Staff Editor
	Carol Schachinger	Editorial Associate
	Carol Marrama	Subscription & Advertising Secretary

Published by
Marine Biological Laboratory
Woods Hole, Massachusetts

JAN 5 2001

Cover

The sacculinid rhizocephalans are parasitic crustaceans related to barnacles (class Cirripedia); their hosts are primarily decapod crustaceans. The image on the cover shows a portunid crab (*Charybdis longicollis,* Leene) on its back; and protruding into the space under the crab's ventrally recurved abdomen are six young externae of the sacculinid *Heterosaccus dollfusi* Boschma. For such a large number of parasites to inhabit a single host is unusual, since a mature externa can be 2 cm long, and the maximum width of the crab is 6.6 cm. The specimen was collected off the Mediterranean coast of Israel at a depth of 35 m, but both species – the host and the parasite – are invaders from the Red Sea. The photograph was taken by B. Galil and D. Friedman, both affiliated with the National Institute of Oceanography in Haifa.

The protruding externa is the only externally visible part of the parasite and is its reproductive component; when young, it contains the female gonad and two empty sperm sacs. The externa is produced by the interna, a mass of rootlets that ramify throughout the body of the host, obtaining nutrition for the parasite. The adult sacculinid has virtually no arthropod-like features, and its relationship with free-living barnacles is based largely on a common larval stage – the cypris, which develops from a pelagic nauplius larva. If she settles on a crab, a female cypris larva metamorphoses into a device that injects a mass of undifferentiated cells into the body of the host; the interna develops from these cells. Once the externa appears, two male cypris larvae may settle on it, each entering a sperm sac to form a testis, enabling fertilization. The ramifying rootlets of the interna also modify the morphology, physiology, and behavior of the host. In particular, the abdomen of male crabs becomes broader like that of a female, providing protection for the externa; and both male and female crabs are sterilized. A parasitized crab of either sex ventilates and grooms the externae under its abdomen as it would its own eggs, and assists in the dispersion of the sacculinid's nauplius larvae when they are released after fertilization.

The extravagant life history of the sacculinid rhizocephalans is one of a series of case studies that illustrate B. Rinkevich's reevaluation of the "unit of selection" (UOS) in this issue (p. 231). The concept that natural selection operates upon a particular biological entity or entities – the UOS – is straightforward, but attempts to identify these entities unambiguously have led to controversy. In his essay, Rinkevich adopts the principle that any biological entity, regardless of its morphological level of organization, can constitute all, or even a part, of a UOS. The sacculinids, comprising three allogeneic units of selection (two males and a female), are used to argue that multiple conspecific UOSs can, together, constitute a new morphological unit.

CONTENTS

Volume 199, No. 3: December 2000

EVOLUTION

Rinkevich, B.
A critical approach to the definition of Darwinian units of selection 231

NEUROBIOLOGY AND BEHAVIOR

Leise, Esther M., and Michael G. Hadfield
An inducer of molluscan metamorphosis transforms activity patterns in a larval nervous system 241
Finley, Luke, and David Macmillan
The structure and growth of the statocyst in the Australian crayfish *Cherax destructor* 251
Jury, Steven H., and Winsor H. Watson III
Thermosensitivity of the lobster, *Homarus americanus*, as determined by cardiac assay 257
Cromarty, S. I., J. Mello, and G. Kass-Simon
Molt-related and size-dependent differences in the escape response and post-threat behavior of the American lobster, *Homarus americanus* 265

CELL BIOLOGY

Baghdasarian, Garen, and Leonard Muscatine
Preferential expulsion of dividing algal cells as a mechanism for regulating algal-cnidarian symbiosis. 278

DEVELOPMENT AND REPRODUCTION

Kominami, Tetsuya, and Hiromi Takata
Cellular basis of gastrulation in the sand dollar *Scaphechinus mirabilis* 287
Vickery, Minako S., and James B. McClintock
Effects of food concentration and availability on the incidence of cloning in planktotrophic larvae of the sea star *Pisaster ochraceus* 298
Dickinson, Amanda J. G., Roger P. Croll, and Elena E. Voronezhskaya
Development of embryonic cells containing serotonin, catecholamines, and FMRFamide-related peptides in *Aplysia californica*. 305

RESEARCH NOTE

Takeda, Naokuni
Development of a penis from the vestigial penis in the female apple snail, *Pomacea canaliculata* 316

* * *

Index for Volume 199 321

THE BIOLOGICAL BULLETIN

THE BIOLOGICAL BULLETIN is published six times a year by the Marine Biological Laboratory, 7 MBL Street, Woods Hole, Massachusetts 02543.

Subscriptions and similar matter should be addressed to Subscription Manager, THE BIOLOGICAL BULLETIN, Marine Biological Laboratory, 7 MBL Street, Woods Hole, Massachusetts 02543. Subscription per year (six issues, two volumes): $225 for libraries; $95 for individuals. Subscription per volume (three issues): $112.50 for libraries; $47.50 for individuals. Back and single issues (subject to availability): $40 for libraries; $20 for individuals.

Communications relative to manuscripts should be sent to Michael J. Greenberg, Editor-in-Chief, or Pamela Clapp Hinkle, Managing Editor, at the Marine Biological Laboratory, 7 MBL Street, Woods Hole, Massachusetts 02543. Telephone: (508) 289-7428. FAX: 508-289-7922. E-mail: pclapp@mbl.edu.

http://www.mbl.edu/BiologicalBulletin/

The home page for the electronic companion to THE BIOLOGICAL BULLETIN—*the Marine Models Electronic Record*—and other BIOLOGICAL BULLETIN publications is available on the World Wide Web at the address shown above.

THE BIOLOGICAL BULLETIN is indexed in bibliographic services including *Index Medicus* and MEDLINE, *Chemical Abstracts, Current Contents, Elsevier BIOBASE/Current Awareness in Biological Sciences,* and *Geo Abstracts.*

Printed on acid free paper,
effective with Volume 180, Issue 1, 1991.

POSTMASTER: Send address changes to THE BIOLOGICAL BULLETIN, Marine Biological Laboratory,
7 MBL Street, Woods Hole, MA 02543.

Copyright © 2000, by the Marine Biological Laboratory

Periodicals postage paid at Woods Hole, MA, and additional mailing offices.
ISSN 0006-3185

INSTRUCTIONS TO AUTHORS

The Biological Bulletin accepts outstanding original research reports of general interest to biologists throughout the world. Papers are usually of intermediate length (10–40 manuscript pages). A limited number of solicited review papers may be accepted after formal review. A paper will usually appear within four months after its acceptance.

Very short, especially topical papers (less than 9 manuscript pages including tables, figures, and bibliography) will be published in a separate section entitled "Research Notes." A Research Note in *The Biological Bulletin* follows the format of similar notes in *Nature.* It should open with a summary paragraph of 150 to 200 words comprising the introduction and the conclusions. The rest of the text should continue on without subheadings, and there should be no more than 30 references. References should be referred to in the text by number, and listed in the Literature Cited section in the order that they appear in the text. Unlike references in *Nature,* references in the Research Notes section should conform in punctuation and arrangement to the style of recent issues of *The Biological Bulletin.* Materials and Methods should be incorporated into appropriate figure legends. See the article by Lohmann *et al.* (October 1990, Vol. **179:** 214–218) for sample style. A Research Note will usually appear within two months after its acceptance.

The Editorial Board requests that regular manuscripts conform to the requirements set below; those manuscripts that do not conform will be returned to authors for correction before review.

1. ***Manuscripts.*** Manuscripts, including figures, should be submitted in quadruplicate, with the originals clearly marked. (Xerox copies of photographs are not acceptable for review purposes.) The submission letter accompanying the manuscript should include a telephone number, a FAX number, and (if possible) an E-mail address for the corresponding author. The original manuscript must be typed in no smaller than 12 pitch or 10 point, using double spacing (*including* figure legends, footnotes, bibliography, etc.) on one side of 16- or 20-lb. bond paper, 8 by 11 inches. Please, no right justification. Manuscripts should be proofread carefully and errors corrected legibly in black ink. Pages should be numbered consecutively. Margins on all sides should be at least 1 inch (2.5 cm). Manuscripts should conform to the *Council of Biology Editors Style Manual,* 5th Edition (Council of Biology Editors, 1983) and to American spelling. Unusual abbreviations should be kept to a minimum and should be spelled out on first reference as well as defined in a footnote on the title page. Manuscripts should be divided into the following components: Title page, Abstract (of no more than 200 words), Introduction, Materials and Methods, Results, Discussion, Acknowledgments, Literature Cited, Tables, and Figure Legends. In addition, authors should supply a list of words and phrases under which the article should be indexed.

2. ***Title page.*** The title page consists of a condensed title or running head of no more than 35 letters and spaces, the manuscript title, authors' names and appropriate addresses, and footnotes listing present addresses, acknowledgments or contribution numbers, and explanation of unusual abbreviations.

3. ***Figures.*** The dimensions of the printed page, 7 by 9 inches, should be kept in mind in preparing figures for publication. We recommend that figures be about 1 times the linear dimensions of the final printing desired, and that the ratio of the largest to the smallest letter or number and of the thickest to the thinnest line not exceed 1:1.5. Explanatory matter generally should be included in legends, although axes should always be identified on the illustration itself. Figures should be prepared for reproduction as either line cuts or halftones. Figures to be reproduced as line cuts should be unmounted glossy photographic reproductions or drawn in black ink on white paper, good-quality tracing cloth or plastic, or blue-lined coordinate paper. Those to be reproduced as halftones should be mounted on board, with both designating numbers or letters and scale bars affixed directly to the figures. All figures should be numbered in consecutive order, with no distinction between text and plate figures and cited, in order, in the text. The author's name and an arrow indicating orientation should appear on the reverse side of all figures.

Digital art: The Biological Bulletin will accept figures submitted in electronic form; however, digital art must conform to the following guidelines. Authors who create digital images are wholly responsible for the quality of their material, including color and halftone accuracy.

Format. Acceptable graphic formats are TIFF and EPS. Color submissions must be in EPS format, saved in CMKY mode.

Software. Preferred software is Adobe Illustrator or Adobe Photoshop for the Mac and Adobe Photoshop for Windows. Specific instructions for artwork created with various software programs are available on the Web at the Digital Art Information Site maintained by Cadmus Professional Communications at http://cjs.cadmus.com/da/home.html

Resolution. The minimum requirements for resolution are 1200 DPI for line art and 300 for halftones.

Size. All digital artwork must be submitted at its actual printed size so that no scaling is necessary.

Multipanel figures. Figures consisting of individual parts (*e.g.*, panels A, B, C) must be assembled into final format and submitted as one file.

Hard copy. Files must be accompanied by hard copy for use in case the electronic version is unusable.

Disk identification. Disks must be clearly labeled with the following information: author name and manuscript number; format (PC or Macintosh); name and version of software used.

Color: The Biological Bulletin will publish color figures and plates, but must bill authors for the actual additional cost of printing in color. The process is expensive, so authors with more than one color image should—consistent with editorial concerns, especially citation of figures in order—combine them into a single plate to reduce the expense. On request, when supplied with a copy of a color illustration, the editorial staff will provide a pre-publication estimate of the printing cost.

4. ***Tables, footnotes, figure legends, etc.*** Authors should follow the style in a recent issue of *The Biological Bulletin* in preparing table headings, figure legends, and the like. Because of the high cost of setting tabular material in type, authors are asked to limit such material as much as possible. Tables, with their headings and footnotes, should be typed on separate sheets, numbered with consecutive Roman numerals, and placed after the Literature Cited. Figure legends should contain enough information to make the figure intelligible separate from the text. Legends should be typed double spaced, with consecutive Arabic numbers, on a separate sheet at the end of the paper. Footnotes should be limited to authors' current addresses, acknowledgments or contribution numbers, and explanation of unusual abbreviations. All such footnotes should appear on the title page. Footnotes are not normally permitted in the body of the text.

5. ***Literature cited.*** In the text, literature should be cited by the Harvard system, with papers by more than two authors cited as Jones *et al.*, 1980. Personal communications and material in preparation or in press should be cited in the text only, with author's initials and institutions, unless the material has been formally accepted and a volume number can be supplied. The list of references following the text should be headed Literature Cited, and must be typed double spaced on separate pages, conforming in punctuation and arrangement to the style of recent issues of *The Biological Bulletin*. Citations should include complete titles and inclusive pagination. Journal abbreviations should normally follow those of the U. S. A. Standards Institute (USASI), as adopted by BIOLOGICAL ABSTRACTS and CHEMICAL ABSTRACTS, with the minor differences set out below. The most generally useful list of biological journal titles is that published each year by BIOLOGICAL ABSTRACTS (BIOSIS List of Serials; the most recent issue). Foreign authors, and others who are accustomed to using THE WORLD LIST OF SCIENTIFIC PERIODICALS, may find a booklet published by the Biological Council of the U.K. (obtainable from the Institute of Biology, 41 Queen's Gate, London, S.W.7, England, U.K.) useful, since it sets out the WORLD LIST abbreviations for most biological journals with notes of the USASI abbreviations where these differ. CHEMICAL ABSTRACTS publishes quarterly supplements of additional abbreviations. The following points of reference style for THE BIOLOGICAL BULLETIN differ from USASI (or modified WORLD LIST) usage:

A. Journal abbreviations, and book titles, all underlined (for *italics*)

B. All components of abbreviations with initial capitals (not as European usage in WORLD LIST *e.g., J. Cell. Comp. Physiol.* NOT *J. cell. comp. Physiol.*)

C. *All* abbreviated components must be followed by a period, whole word components *must not* (*i.e., J. Cancer Res.*)

D. Space between all components (*e.g., J. Cell. Comp. Physiol.*, not *J.Cell.Comp.Physiol.*)

E. Unusual words in journal titles should be spelled out in full, rather than employing new abbreviations invented by the author. For example, use *Rit Vísindafjélags Islendinga* without abbreviation.

F. All single word journal titles in full (*e.g., Veliger, Ecology, Brain*).

G. The order of abbreviated components should be the same as the word order of the complete title (*i.e., Proc.* and *Trans.* placed where they appear, not transposed as in some BIOLOGICAL ABSTRACTS listings).

H. A few well-known international journals in their preferred forms rather than WORLD LIST or USASI usage (*e.g., Nature, Science, Evolution* NOT *Nature, Lond., Science, N.Y.; Evolution, Lancaster, Pa.*)

6. ***Reprints, page proofs, and charges.*** Authors may purchase reprints in lots of 100. Forms for placing reprint orders are sent with page proofs. Reprints normally will be delivered about 2 to 3 months after the issue date. Authors (or delegates for foreign authors) will receive page proofs of articles shortly before publication. They will be charged the current cost of printers' time for corrections to these (other than corrections of printers' or editors' errors). Other than these charges for authors' alterations, *The Biological Bulletin* does not have page charges.

CONTENTS
for Volume 199

No. 1, August 2000

RESEARCH NOTE

Bolton, Toby F., Florence I. M. Thomas, and Celere N. Leonard
Maternal energy investment in eggs and jelly coats surrounding eggs of the echinoid *Arbacia punctulata* 1

PHYSIOLOGY

Johnson, M. L., P. M. J. Shelton, E. Gaten, and P. J. Herring
Relationship of dorsoventral eyeshine distributions to habitat depth and animal size in mesopelagic decapods 6
Dietz, T. H., A. S. Udoetok, J. S. Cherry, H. Silverman, and R. A. Byrne
Kidney function and sulfate uptake and loss in the freshwater bivalve *Toxolasma texasensis* 14
Vollmer, Steven V., and Peter J. Edmunds
Allometric scaling in small colonies of the scleractinian coral *Siderastrea siderea* (Ellis and Solander) 21

DEVELOPMENT AND REPRODUCTION

Torrado, Mario, and Alexander T. Mikhailov
Frog Lim-1-like protein is expressed predominantly in the nervous tissue, gonads, and early embryos of the bivalve mollusc *Mytilus galloprovincialis* 29
Gibson, Glenys D., and Jennifer M. L. Harvey
Morphogenesis during asexual reproduction in *Pygospio elegans* Claparede (Annelida, Polychaeta) 41
Watson, G. J., F. M. Langford, S. M. Gaudron, and M. G. Bentley
Factors influencing spawning and pairing in the scale worm *Harmothoe imbricata* (Annelida: Polychaeta) . . . 50
Buckland-Nicks, John, and Alan N. Hodgson
Fertilization in *Callochiton castaneus* (Mollusca) 59
Hirose, M., R. A. Kinzie III, and M. Hidaka
Early development of zooxanthella-containing eggs of the corals *Pocillopora verrucosa* and *P. eydouxi* with special reference to the distribution of zooxanthellae 68

CELL BIOLOGY

Wakefield, Timothy S., Mark A. Farmer, and Stephen C. Kempf
Revised description of the fine structure of *in situ* "Zooxanthellae" genus *Symbiodinium* 76

ECOLOGY AND EVOLUTION

Barnes, David K. A., and Mathew H. Dick
Overgrowth competition between clades: implications for interpretation of the fossil record and overgrowth indices 85

* * *

Annual Report of the Marine Biological Laboratory R1

No. 2, October 2000

RESEARCH NOTE

Hourdez, Stéphane, Jason Lamontagne, Pat Peterson, Roy E. Weber, and Charles R. Fisher
Hemoglobin from a deep-sea hydrothermal-vent copepod 95

PHYSIOLOGY

Marsh, Adam G., Patrick K.K. Leong, and Donal T. Manahan
Gene expression and enzyme activities of the sodium pump during sea urchin development: implications for indices of physiological state 100
Hill, Richard W., John W.H. Dacey, and Ahser Edward
Dimethylsulfoniopropionate in giant clams (Tridacnidae) 108

ECOLOGY AND EVOLUTION

Baker, Shirley M., Jeffrey S. Levinton, and J. Evan Ward
Particle transport in the zebra mussel, *Dreissena polymorpha* (Pallas) 116

LaJeunesse, T.C., and R.K. Trench
Biogeography of two species of *Symbiodinium* (Freudenthal) inhabiting the intertidal sea anemone *Anthopleura elegantissima* (Brandt) 126

NEUROBIOLOGY AND BEHAVIOR

Rosenthal, Joshua J.C., and Francisco Bezanilla
Seasonal variation in conduction velocity of action potentials in squid giant axon. 135

DEVELOPMENT AND REPRODUCTION

Misamore, M.J., and J.W. Lynn
Role of the cytoskeleton in sperm entry during fertilization in the freshwater bivalve *Dreissena polymorpha* 144

SHORT REPORTS FROM THE 2000 GENERAL SCIENTIFIC MEETINGS OF THE MARINE BIOLOGICAL LABORATORY

Featured Report

The Editors
Introduction to the featured report. On mapping odor quality. 161

Wachowiak, Matt, Michal Zochowski, Lawrence B. Cohen, and Chun X. Falk
The spatial representation of odors by olfactory receptor neuron input to the olfactory bulb is concentration invariant. 162

Neurobiology

Landowne, David
Heavy water (D_2O) alters the sodium channel gating current in squid giant axons 164

White, Thomas H., Harris Ripps, Miduturu Srinivas, and Roberto Bruzzone
Voltage gating properties of channels formed by a skate retinal connexin. 165

Molina, Anthony J.A., Peter J.S. Smith, and Robert Paul Malchow
Hydrogen ion fluxes from isolated retinal horizontal cells: modulation by glutamate 168

Wang, Jing W.
Odor-induced oscillatory activity in *Drosophila* CNS . . . 170

Hitt, James M., Frederick A. Dodge, Ehud Kaplan, and Robert B. Barlow
Circadian rhythms in the receptive fields of the *Limulus* lateral eye. 171

Fay, Richard R., and Peggy L. Edds-Walton
Frequency response of auditory brainstem units in toadfish (*Opsanus tau*). 173

Yamaguchi, Ayako, Leonard K. Kaczmarek, and Darcy B. Kelley
Intrinsic membrane properties of laryngeal motoneurons that control sexually differentiated vocal behavior in African clawed frogs, *Xenopus laevis* 175

Atherton, Jillian L., Matthew A. Krutky, James M. Hitt, Frederick A. Dodge, and Robert B. Barlow
Optic nerve responses of *Limulus* in its natural habitat at night. 176

Krutky, Matthew A., Jillian L. Atherton, Spence Smith, Frederick A. Dodge, and Robert B. Barlow
Do the properties of underwater lighting influence the visually guided behavior of *Limulus*?. 178

Hale, Melina E.
Startle responses of fish without Mauthner neurons: escape behavior of the lumpfish (*Cyclopterus lumpus*) 180

Epstein, David A., Herman T. Epstein, Frank M. Child, and Alan M. Kuzirian
Memory consolidation in *Hermissenda crassicornis* . . . 182

Abenavoli, A., L. Forti, and A. Malgaroli
Mechanisms of spontaneous miniature activity at CA3-CA1 synapses: evidence for a divergence from a random Poisson process 184

Physiology and Biochemistry

Novales Flamarique, Inigo, Kristiina Ovaska, and Theodore M. Davis
UV-B induced damage to the skin and ocular system of amphibians 187

Harrington, John M., and Peter B. Armstrong
Initial characterization of a potential anti-fouling system in the American horseshoe crab, *Limulus polyphemus* 189

Asokan, Rengasamy, Margaret T. Armstrong, and Peter B. Armstrong
Association of α_2-macroglobulin with the coagulin clot in the American horseshoe crab, *Limulus polyphemus:* a potential role in stabilization from proteolysis. 190

Kuhns, William J., Max M. Burger, Mohan Sarker, Xavier Fernandez-Busquets, and Tracy Simpson
Enzymatic biosynthesis of N-linked glycan by the marine sponge *Microciona prolifera* 192

Armstrong, Peter B., and Rengasamy Asokan
A Ca^{+2}-independent cytolytic system from the blood of the marine snail *Busycon canaliculum* 194

Heck, Diane E., Lydia Louis, Michael A. Gallo, and Jeffrey D. Laskin
Modulation of the development of plutei by nitric oxide in the sea urchin *Arbacia punctulata* 195

Jung, Sung-Kwon, Katherine Hammar, and Peter J.S. Smith
Development of self-referencing oxygen microsensor and its application to single pancreatic HIT cells: effects of adenylate cyclase activator forskolin on oxygen consumption 197

Hanselmann, Rhea, Roxanna Smolowitz, and Daniel G. Gibson
Identification of proliferating cells in hard clams. . . 199

Brothers, Christine, Ernest Marks III, and Roxanna Smolowitz
Conditions affecting the growth and zoosporulation of the protistan parasite QPX in culture. 200

Cell Biology

Sandberg, Leslie, Phillip Stafford, and George M. Langford
Effects of myosin-II antibody on actin-dependent vesicle transport in extracts of clam oocytes 202

Stafford, Phillip, Jeremiah Brown, and George M. Langford
Interaction of actin- and microtubule-based motors in squid axoplasm probed with antibodies to myosin V and kinesin 203

Tran, P.T., V. Doye, F. Chang, and S. Inoué
Microtubule-dependent nuclear positioning and nuclear-dependent septum positioning in the fission yeast, *Saccharomyces pombe*. 205

Crawford, Karen
The role of microtubules during blastodisc formation of the squid *Loligo pealei*. 207

Weidner, Earl
Cytoplasmic proteins on the surface of discharged microsporidian sporoplasms 208

MacKenzie, Roger, David Newman, Max M. Burger, Rene Roy, and William J. Kuhns
Adhesion of a viral envelope protein to a non-self-binding domain of the aggregation factor in the marine sponge *Microciona prolifera*. 209

Goda, Makoto, Mario H. Burgos, and Shinya Inoué
Fertilization-induced changes in the fine structure of stratified *Arbacia* eggs. I. Observations on live cells with the centrifuge polarizing microscope 212

Burgos, Mario H., Makoto Goda, and Shinya Inoué
Fertilization-induced changes in the fine structure of stratified *Arbacia* eggs. II. Observations with electron microscopy. 213

Gould, Robert M., Concetta M. Freund, John Engler, and Hilary G. Morrison
Optimization of homogenization conditions used to isolate mRNAs in processes of myelinating oligodendrocytes 215

Ecology, Biogeochemistry, and Population Biology

Kirkby, Ryan, Luc Claessens, Charles Hopkinson, Jr., Edward Rastetter, and Joseph Vallino
Modeling the effects of land-use change on nitrogen biogeochemistry in the Ipswich watershed, Massachusetts 218

Perring, Anne, Michael Williams, Charles Hopkinson, Jr., Edward Rastetter, and Joseph Vallino
Solute dynamics in storm flow of the Ipswich River Basin: effects of land use. 219

Westgate, Elizabeth J., Kevin D. Kroeger, Wendy J. Pabich, and Ivan Valiela
Fate of anthropogenic nitrogen in a nearshore Cape Cod aquifer 221

Denault, Michelle, Erica Stieve, and Ivan Valiela
Effects of nitrogen load and irradiance on photosynthetic pigment concentrations in *Cladophora vagabunda* and *Gracilaria tikvahiae* in estuaries of Waquoit Bay. 223

Greenbaum, Adena, and Anne Giblin
Differences in properties of salt marsh sediment between hayed and reference sites 225

Chikarmane, Hemant M., Alan M. Kuzirian, Robbin Kozlowski, Mark Kuzirian, and Tony Lee
Population genetic structure of the goosefish, *Lophius americanus*. 227

Oral Presentations

Published by title only. 229

No. 3, December 2000

EVOLUTION

Rinkevich, B.
A critical approach to the definition of Darwinian units of selection 231

NEUROBIOLOGY AND BEHAVIOR

Leise, Esther M., and Michael G. Hadfield
An inducer of molluscan metamorphosis transforms activity patterns in a larval nervous system 241

Finley, Luke, and David Macmillan
The structure and growth of the statocyst in the Australian crayfish *Cherax destructor*. 251

Jury, Steven H., and Winsor H. Watson III
Thermosensitivity of the lobster, *Homarus americanus*, as determined by cardiac assay 257
Cromarty, S. I., J. Mello, and G. Kass-Simon
Molt-related and size-dependent differences in the escape response and post-threat behavior of the American lobster, *Homarus americanus* 265

CELL BIOLOGY

Baghdasarian, Garen, and Leonard Muscatine
Preferential expulsion of dividing algal cells as a mechanism for regulating algal-cnidarian symbiosis. 273

DEVELOPMENT AND REPRODUCTION

Kominami, Tetsuya, and Hiromi Takata
Cellular basis of gastrulation in the sand dollar *Scaphechinus mirabilis* 287
Vickery, Minako S., and James B. McClintock
Effects of food concentration and availability on the incidence of cloning in planktotrophic larvae of the sea star *Pisaster ochraceus* 298
Dickinson, Amanda J. G., Roger P. Croll, and Elena E. Voronezhskaya
Development of embryonic cells containing serotonin, catecholamines, and FMRFamide-related peptides in *Aplysia californica*. 305

RESEARCH NOTE

Takeda, Naokuni
Development of a penis from the vestigial penis in the female apple snail, *Pomacea canaliculata* 316

* * *

Index for Volume 199 321

ERRATA

The Biological Bulletin Volume **199**, Number 2

In the article by P. T. Tran, V. Doye, F. Chang, and S. Inoué, which appeared on pages 205 to 206, the genus name *Saccharomyces* is in error. The correct genus name, in all instances, is *Schizosacchromyces*.

Cover legend: The organism described as *Saccharomyces pombe* should be *Schizosacchromyces pombe*.

The editors regret these errors.

Notice to Subscribers

2001 SUBSCRIPTION RATES FOR *THE BIOLOGICAL BULLETIN*

	Libraries	**Individuals**
Per year (six issues, two volumes):	$235.00	$95.00
Per volume (three issues):	$117.50	$47.50
Back and single issues: (subject to availability)	$ 40.00	$20.00

For additional information, please contact our subscription manager at the Marine Biological Laboratory, 7 MBL Street, Woods Hole, MA 02543; tel: (508) 289-7402; e-mail: cmarrama@mbl.edu.

Reference: *Biol. Bull.* **199:** 231–240. (December 2000)

A Critical Approach to the Definition of Darwinian Units of Selection

B. RINKEVICH

Israel Oceanographic and Limnological Research, National Institute of Oceanography, P.O. Box 8030, Haifa 31080, Israel

Abstract. What are the biological units of selection? In fact, the notion of "unit of selection" (UOS) is blurred by ambiguity and controversy. To further evaluate the biological entities that are the objects of natural selection, three novel conceptual criteria (holism, minimalism, functionalism) are critically applied; they reveal, in addition to the self-evident case of the "individual," at least six distinct types of UOSs. These UOSs do not always have a defined structural organization; they can be parts of a living organism, a cohesive group of conspecifics, a multiunit entity, a totipotent cell, a DNA fragment, or a whole organism. UOS types diversify by amalgamation or parcelation processes of apparent entities. Therefore, previous attempts to characterize the UOSs solely on some morphological levels (gene, individual, group) without applying stringent criteria have failed to cope with the structural variations of natural phenomena and have led to the ambiguity of terms used.

Introduction

Much of the ambiguity, confusion, and controversy engendered by the concept of the "unit of selection" (UOS) seem to arise from a failure to identify the biological entities upon which natural selection operates (Sober and Wilson, 1994; Mayr, 1997; Gould and Lloyd, 1999, and literature therein). Along with the debates about the three to four possible organizational levels of selection (gene, individual, group, and metapopulation), the objections to the hierarchical theory of selection (Wilson and Sober, 1994; Michod, 1997; Gould, 1998; Gould and Lloyd, 1999), and the distinction between transmitted units and those which transmit (Wynne Edwards, 1962; Lewontin, 1970; Mayr, 1970, 1997; Dawkins, 1976; Hull, 1980; Gliddon and Gouyon, 1989; Sober and Wilson, 1994; Wilson and Sober, 1994; Williams, 1996; Gould, 1998), "metaphors have replaced the empirical world as foci for discussion while precise meanings and derivatives have been forgotten in the process" (Slobodkin, 1986). Even the basic term "unit of selection" is under dispute (Wilson and Sober, 1994), bearing polemic aspects (Mayr, 1997) as do other terms in this discipline (Gould and Lloyd, 1999).

One approach to clarifying such an ambiguous field is a critical evaluation of the arguments and definitions used (Hull, 1980; Sober and Wilson, 1994; Mayr, 1997; Gould and Lloyd, 1999). Such a reevaluation process might germinate a novel idea or might help dispel excessive ambiguity. On the other hand, anathematized concepts could reappear, revealing further ill-considered definitions (Gould and Lloyd, 1999) or adding additional ambiguities. An alternative approach is to envisage the main controversial issues through an untraditional analysis. In this essay, such an untraditional approach is used to examine the biological entities that are the objects of natural selection. By adapting the unbiased principle that any living thing can be all or part of a potential UOS, we can critically evaluate organisms—regardless of their level of morphological organization—on the basis of a few conceptual criteria.

Criteria for Analysis of UOSs

Three conceptual criteria guide this examination:

Holism

Genes and soma are not necessarily independent. The distinction between the terms "interactor" and "vehicle," as opposed to "replicator" and "gene" (Dawkins, 1976; Hull, 1980) is central in the debate over UOSs (Hull, 1980; Sober and Wilson, 1994; Mayr, 1997). The use of these terms to

Received 17 August 1999; accepted 11 September 2000.
E-mail: buki@ocean.org.il

identify different units of selection evolved from the *a priori* rationale that living organisms are made of at least two distinct types of evolutionarily selected units. Additionally, the notion of the UOS has become ambiguous because it was used to refer to either replicators or vehicles, depending on the choice of the author (Wilson and Sober, 1994). I suggest that this rationale is false and misleading, that it artificially distinguishes between "genes," "information," and "replication" on the one hand, and "soma," "vehicle," and "interactor" on the other (Lewontin, 1970; Dawkins, 1976; Hull, 1980; Buss, 1982; Gliddon and Gouyon, 1989; Sober and Wilson, 1994; Mayr, 1997). The genes in any organism have a fate in common with their amalgamated soma (Sober and Wilson, 1994, and literature therein). They are part of a whole; they are not completely independent (with the exception of specific cases as outlined in the next section), but rather functionally integrated within the soma. In physics, light and mass are regarded as two facets of energetic matter. Similarly, in biology, genes and soma should be regarded as two facets of an organic entity that constitutes a living organism. Even the term "unit" (Oxford Dictionary) embraces this metaphysical concept of holism. A unit is a thing (individual, person, group, etc.) that is complete or distinctive and that has the characteristics of the complex whole. Following this rationale, the so-called replicators and interactors of each entity are intermingled to form, for each UOS, its idiographic (its own peculiar) entity, which is presented to natural selection as a coherent whole. This is in contrast to the acknowledgement of recent years that interactors, not replicators, constitute the causal unit of selection" (Gould and Lloyd, 1999).

Minimalism

Ignore complex cases; choose the simplest ones. Additional ambiguity is caused by different hypotheses for the UOS that deliver opposing predictions about the traits that have evolved (Sober and Wilson, 1994; Wilson and Sober, 1994). In such cases, a search for the simplest manifestation of the system, the minimalist approach (Slobodkin, 1986), has been suggested to be the most useful in maintaining clarity. This approach has been characterized as "the process of deliberately choosing to work in the simplest possible mode that is still recognizable as part of an existing professional field." Slobodkin (1986) has also discussed the main objection against this approach as the claim for uncritical acceptance of standards. However, this objection may not be the case in the controversy over the UOS, where metaphors, rather than empirical themes, dominate the scientific discipline (Wilson and Sober, 1994; Gould and Lloyd, 1999). When employing the minimalist approach (Slobodkin, 1986), or the very similar "back to basics" (Sober and Wilson, 1994) treatment, complex cases (such as the situations illustrated in Wynne Edwards, 1962) are left aside for future analyses when the field will presumably be more formally organized. Therefore, we must accept the idea that the UOS theory, almost three decades after it was first elaborated (Lewontin, 1970), should still be conceptualized through the clearest examples.

Functionalism

UOSs function *in vivo*. A unit of biological organization upon which selection might act should be both an autonomous functional entity and physically and structurally coherent, even if it is in the form of a gene. It cannot be in the form of "information" or "avatar" (Gliddon and Gouyon, 1989; Tuomi and Vuorisalo, 1989a) or "anything in the universe of which copies are made" (Dawkins, 1989). A UOS must function, because functionalism is the primary focus of natural selection. Functionalism, therefore, does not rest upon an active maintenance of distinctive properties (Gould, 1998), but evaluates the general sum of independent activities presented by a UOS. At this point, the existence of only a single functional level or of several functional levels (in hierarchical order, Tuomi and Vuorisalo, 1989a; Gould and Lloyd, 1999; or not) will not be discussed. Only a holistic unit (possessing cohesive structural and information properties) may reveal the capacity for functionalism. Therefore, previously distinguished UOSs such as replicators, interactors, vehicles, memes, etc., that are literally not holistic, are excluded from being real UOSs. They remain as highly justified theoretical paradigms that characterize only components of holistic and functional units of selection.

The three conceptual criteria (holism, minimalism, functionalism) provide enormous flexibility for analysis and circumvent the use of ill-defined issues and debatable arguments. These criteria have been used to scrutinize different potential types of UOSs that are presented by a variety of organismal entities. The term "organism" refers here to "any biological entity whose parts have evolved to function in a harmonious and coordinated fashion" (Wilson and Sober, 1994). This analysis has revealed several types of UOSs; of these, one traditional and six new characteristic types (Table 1, Nos. 1–7) are briefly described below.

Seven Types of Units of Selection

I am—and part of me is it

Molecular sequences may themselves be UOSs. "Doctor there is a fly in my genome" was the title chosen by the journal *New Scientist* (Vol. 149, p. 16, 1996) for an article about a tiny fragment of an insect genome (called *mariner*, a jumping gene first discovered in the fruit fly *Drosophila*) that is embedded in human chromosome 17. This location directly coincides with a recombination hot spot and has been associated with distinct hereditary neurological syndromes (Reiter *et al.*, 1996). This is only one of an enor-

The Biological Bulletin

First-Time Subscribers — *Receive the December 2000 issue FREE when you order a 2001 subscription!*

☐ I would like to order a 2001 subscription ☐ Please send me the December 2000 issue

Name ______
Institution ______
Department ______
Address ______
City ______ State______ Zip ______ Country ______
2001 Subscription Prices *(includes surface delivery)*: ☐ **Individual $95** ☐ **Institution $235**
Enclosed is my check or US money order for $ ______
Charge my ☐ VISA ☐ MasterCard ☐ Discover Card
Card # ______ Exp. Date______
Signature ______

Mail this form along with your check or payment information to:
Marine Biological Laboratory, *The Biological Bulletin*
7 MBL Street, Woods Hole, MA 02543-1015

espeare, *King Lear*, Act 1, Scene 4

Examples

ic DNA in eukaryotic and
ıomes

ı and mosaicism
tism
e-body chimerism and invertebrate
ı
ɔed organisms, monozygotic twins,

ripedia
anisms

mous number of documentations that eukaryotic and prokaryotic cells carry foreign DNA molecules of various types (plasmids, B chromosomes, t haplotypes, retroviruses, and more), as well as diverse mobile DNA sequences (such as transposons, retrotransposons, LINEs, SINEs, mobile introns) that are transmitted vertically or horizontally within genomes (Zeyl and Bell, 1996; Flavell, 1999) and may be regarded as real UOSs. These DNA sequences have functional and holistic properties; they are characterized by a discrete organismal realm, function in a coordinated fashion, and are clearly subject to natural selection forces. Many examples now point to real UOSs situated within the genomes of other UOSs. A few will be outlined below.

One well-studied group is the B-chromosomes, a variety of germ-line parasites described from more than a thousand species of plants and animals. These small chromosomes do not contribute to the regular functions of the host, and their numbers per cell vary even within the same host organism. More important, although they share the same nucleus with regular chromosomes, they have evolved peculiar characteristics of their own. By various non-Mendelian systems of biased transmission and by their ability to move specifically to one of the two products of the first meiosis division (such as by avoiding penetration into the polar body during oogenesis), they increase their representation in the germ-line nuclei. The B-chromosomes in the wasp *Nasonia*, which are transmitted solely through sperm, are a representative case. The entire parental set of chromosomes in an infected zygote becomes condensed and is lost, leaving a haploidized animal that develops as a male, transmitting the B-chromosome to all its gametes (citations in Bell and Burt, 1990). Such functionalism of the parasitic entity reveals distinct host and parasitic units of selection. Within this context, I am reluctant to consider the B-chromosomes as selfish chromosomes. They are distinct molecular UOSs.

The mouse t haplotypes (each extending over the proximal half of chromosome 17) also have developed the ability to propagate at the expense of the wild-type homolog from heterozygous males. These entities probably evolved from a wild-type form of chromosome 17. Genes that were recruited later on, together with the addition of accompanying inversions, all increased the survival rates of the t haplotypes, until finally these entities started "taking on a life of their own" (reviewed in Silver, 1993).

Not only a whole piece of chromosome may be counted as a UOS; even transposable genetic elements, gene size segments of DNA, may be so considered. This field is too broad to be even partially covered here, so only the most relevant features of these mobile elements will be discussed. Many transposable elements have the ability to jump from place to place on the chromosomes; they can behave like new introns creating novel intron processing patterns; they may spread vertically and horizontally within host organisms; and they can promote their own replication (the functionalism component). With time, the mobile elements become domesticated through full integration into the host's genome. A good example is the *mariner* which, by being functional in both germ lines and somatic cell lines, could infect many organisms, crossing several phyletic borders (arthropods, platyhelminths, nematodes, chordates), probably by splicing into viral or other pathogenic genomes. During each introduction into a new host species, the *mariner* transposon was probably highly mobile and significantly disruptive. With time, more and more defecting transposons with mutations that disabled the cut-and-paste enzyme were accumulated, littering eukaryotic genomes

identify different units of
priori rationale that living
two distinct types of evoluti
ally, the notion of the UOS
it was used to refer to either
ing on the choice of the autl
suggest that this rationale
artificially distinguishes be
and "replication" on the on
and "interactor" on the otl
1976; Hull, 1980; Buss, 19
Sober and Wilson, 1994; M
organism have a fate in cc
soma (Sober and Wilson, 19
are part of a whole; they a
(with the exception of speci
section), but rather function
In physics, light and mass
energetic matter. Similarly, in biology, genes and soma should be regarded as two facets of an organic entity that constitutes a living organism. Even the term "unit" (Oxford Dictionary) embraces this metaphysical concept of holism. A unit is a thing (individual, person, group, etc.) that is complete or distinctive and that has the characteristics of the complex whole. Following this rationale, the so-called replicators and interactors of each entity are intermingled to form, for each UOS, its idiographic (its own peculiar) entity, which is presented to natural selection as a coherent whole. This is in contrast to the acknowledgement of recent years that interactors, not replicators, constitute the causal unit of selection" (Gould and Lloyd, 1999).

Minimalism

Ignore complex cases; choose the simplest ones. Additional ambiguity is caused by different hypotheses for the UOS that deliver opposing predictions about the traits that have evolved (Sober and Wilson, 1994; Wilson and Sober, 1994). In such cases, a search for the simplest manifestation of the system, the minimalist approach (Slobodkin, 1986), has been suggested to be the most useful in maintaining clarity. This approach has been characterized as "the process of deliberately choosing to work in the simplest possible mode that is still recognizable as part of an existing professional field." Slobodkin (1986) has also discussed the main objection against this approach as the claim for uncritical acceptance of standards. However, this objection may not be the case in the controversy over the UOS, where metaphors, rather than empirical themes, dominate the scientific discipline (Wilson and Sober, 1994; Gould and Lloyd, 1999). When employing the minimalist approach (Slobodkin, 1986), or the very similar "back to basics" (Sober and Wilson, 1994) treatment, complex cases (such as the situations illustrated in Wynne Edwards, 1962) are left activities presented by a UOS. At this point, the existence of only a single functional level or of several functional levels (in hierarchical order, Tuomi and Vuorisalo, 1989a; Gould and Lloyd, 1999; or not) will not be discussed. Only a holistic unit (possessing cohesive structural and information properties) may reveal the capacity for functionalism. Therefore, previously distinguished UOSs such as replicators, interactors, vehicles, memes, etc., that are literally not holistic, are excluded from being real UOSs. They remain as highly justified theoretical paradigms that characterize only components of holistic and functional units of selection.

The three conceptual criteria (holism, minimalism, functionalism) provide enormous flexibility for analysis and circumvent the use of ill-defined issues and debatable arguments. These criteria have been used to scrutinize different potential types of UOSs that are presented by a variety of organismal entities. The term "organism" refers here to "any biological entity whose parts have evolved to function in a harmonious and coordinated fashion" (Wilson and Sober, 1994). This analysis has revealed several types of UOSs; of these, one traditional and six new characteristic types (Table 1, Nos. 1–7) are briefly described below.

Seven Types of Units of Selection

I am—and part of me is it

Molecular sequences may themselves be UOSs. "Doctor there is a fly in my genome" was the title chosen by the journal *New Scientist* (Vol. 149, p. 16, 1996) for an article about a tiny fragment of an insect genome (called *mariner*, a jumping gene first discovered in the fruit fly *Drosophila*) that is embedded in human chromosome 17. This location directly coincides with a recombination hot spot and has been associated with distinct hereditary neurological syndromes (Reiter *et al.*, 1996). This is only one of an enor-

Table 1

Who is it that can tell me who I am?

—Shakespeare, *King Lear*, Act 1, Scene 4

No.	Type of unit of selection	Organizational level on which selection acts	Examples
1	I am—and part of me is it	On a molecular level, a piece of DNA, usually not larger than a single chromosome (B-chromosomes, however, can pair among themselves to form a chiasmata)	Symbiotic/parasitic DNA in eukaryotic and prokaryotic genomes
2	I am—and part of me is he	On a whole organismal level	Natural chimerism and mosaicism
3	I am—and this is actually he	On a cellular level	Germ cells parasitism
4	I am—and this is actually we	On groups of conspecifics that intermingled together	Mammalian whole-body chimerism and invertebrate multichimerism
5	I am—and this is actually only part of me	On different ramets of the same genet	Asexually developed organisms, monozygotic twins, polyembryony
6	We are—and this is actually me	On multiunit entities	Rhizocephalen cirripedia
7	I am—that I am (Exodus 3:14)	On the whole organismic level	Many unitary organisms

mous number of documentations that eukaryotic and prokaryotic cells carry foreign DNA molecules of various types (plasmids, B chromosomes, t haplotypes, retroviruses, and more), as well as diverse mobile DNA sequences (such as transposons, retrotransposons, LINEs, SINEs, mobile introns) that are transmitted vertically or horizontally within genomes (Zeyl and Bell, 1996; Flavell, 1999) and may be regarded as real UOSs. These DNA sequences have functional and holistic properties; they are characterized by a discrete organismal realm, function in a coordinated fashion, and are clearly subject to natural selection forces. Many examples now point to real UOSs situated within the genomes of other UOSs. A few will be outlined below.

One well-studied group is the B-chromosomes, a variety of germ-line parasites described from more than a thousand species of plants and animals. These small chromosomes do not contribute to the regular functions of the host, and their numbers per cell vary even within the same host organism. More important, although they share the same nucleus with regular chromosomes, they have evolved peculiar characteristics of their own. By various non-Mendelian systems of biased transmission and by their ability to move specifically to one of the two products of the first meiosis division (such as by avoiding penetration into the polar body during oogenesis), they increase their representation in the germ-line nuclei. The B-chromosomes in the wasp *Nasonia*, which are transmitted solely through sperm, are a representative case. The entire parental set of chromosomes in an infected zygote becomes condensed and is lost, leaving a haploidized animal that develops as a male, transmitting the B-chromosome to all its gametes (citations in Bell and Burt, 1990). Such functionalism of the parasitic entity reveals distinct host and parasitic units of selection. Within this context, I am reluctant to consider the B-chromosomes as selfish chromosomes. They are distinct molecular UOSs.

The mouse t haplotypes (each extending over the proximal half of chromosome 17) also have developed the ability to propagate at the expense of the wild-type homolog from heterozygous males. These entities probably evolved from a wild-type form of chromosome 17. Genes that were recruited later on, together with the addition of accompanying inversions, all increased the survival rates of the t haplotypes, until finally these entities started "taking on a life of their own" (reviewed in Silver, 1993).

Not only a whole piece of chromosome may be counted as a UOS; even transposable genetic elements, gene size segments of DNA, may be so considered. This field is too broad to be even partially covered here, so only the most relevant features of these mobile elements will be discussed. Many transposable elements have the ability to jump from place to place on the chromosomes; they can behave like new introns creating novel intron processing patterns; they may spread vertically and horizontally within host organisms; and they can promote their own replication (the functionalism component). With time, the mobile elements become domesticated through full integration into the host's genome. A good example is the *mariner* which, by being functional in both germ lines and somatic cell lines, could infect many organisms, crossing several phyletic borders (arthropods, platyhelminths, nematodes, chordates), probably by splicing into viral or other pathogenic genomes. During each introduction into a new host species, the *mariner* transposon was probably highly mobile and significantly disruptive. With time, more and more defecting transposons with mutations that disabled the cut-and-paste enzyme were accumulated, littering eukaryotic genomes with foreign elements in varying stages of decay (Zeyl and Bell, 1996; Flavell, 1999), and blurring the boundaries (Dawkins, 1990) between two distinct units of selection. Many of the mobile elements constitute a significant portion of host genomes. The *Alu* elements (the largest family of SINEs in humans) represent in excess of 5×10^6 copies per haploid genome, and constitute about 5% of the human genome. The chloroplast genome of *Euglena gracilis* possesses at least 155 mobile introns, making up 39% of the genome by forming complex nested structures of introns within introns (literature cited in Zeyl and Bell, 1996).

From highly functional to nonfunctional: natural selection has shaped foreign DNA elements between these two extreme levels of activity. With respect to the UOS paradigm, elements with well-distinguished sequences and with high activity levels of their own (even if they are the size of a single gene) can be regarded as units of selection. Natural selection may act on them independent of their host, and may especially act on those elements that move between different organisms (Flavell, 1999). Other elements that are completely integrated in the host's genome, replicating when the entire collective of genes reproduce and contributing to basic functions and processes derived by the host cells (such as the LINE elements that preserve the telomeres of *Drosophila;* literature cited in Flavell, 1999), are clearly not UOSs.

I am—and part of me is he

In chimeras or mosaics, two or more UOSs amalgamated to form a single distinct UOS. Genetically nonhomogenous entities can be established by chimerism (a situation where an organism possesses cells simultaneously derived from at least two genetically distinct conspecifics) or by a mosaicism (production of an organism with genetically different cells that derived from a single zygote lineage). Both phenomena have been widely documented: chimeric entities in nature have been recorded from a variety of protists, plants, and animals, distributed over nine phyla (Buss, 1982); and a number of factors may produce mosaicism in almost any living organism (Benirshke, 1981; Hall, 1988; Gill *et al.*, 1995). Clear distinctions between chimeras and mosaics are often not available in reported cases because an insufficient number of genetic characters were employed (Benirshke, 1981). Although, in many cases, a chimera or mosaic seems to represent a single UOS, this "single organism" actually consists of two or more distinct embedded units of selection upon which natural selection acts. This type of "blurring of the boundaries" between the interacting entities (*sensu* Dawkins, 1990) obliges us to develop epistemological tools with which we may distinguish between false UOSs and real ones whose existence does not depend upon the researcher's perception.

Mosaic, sectorial, and cytomictial (mixed-cell) chimeras often occur after allogeneic encounters in a variety of colonial marine invertebrates (Rinkevich, 1996a). Participants in such chimeras are sometimes so intermingled that the death of one of them (*e.g.*, from senescence) results in chimeric death (Rinkevich and Weissman, 1989; Rinkevich *et al.*, 1992). The evolutionary significance of chimerism has been evaluated by comparing (Buss, 1982; Grosberg and Quinn, 1986; Rinkevich and Weissman, 1987a; Rinkevich, 1996a) the fitness cost-benefit ratio of the chimera with that of the genetically homogenous UOS. Several classes of benefits, including the increase of genetic variability, improvements in growth rates, reproduction or survivorship, and developmental synergism (citations in Buss, 1982; Rinkevich and Weissman, 1987a; Rinkevich, 1996a), have been attributed to chimeric states. Costs are the threats of somatic and germ-cell parasitism (next section) and, within chimerical selection, towards the more heterogeneous partner (Rinkevich, 1996b). If the outcome is a state of chimerical improvement, each UOS participating in it gains. Biological and environmental factors may directly affect just one UOS within a chimerical entity or may influence the chimera as a whole.

Vertebrates also exhibit a variety of naturally occurring chimeras, mostly in the form of dizygotic twin bone-marrow transplantation and as diseases like choriocarcinomas (Benirshke, 1981; Tippet, 1984; Benirshke and Kaufman, 1990). These and other types (whole body and germ cell chimerism, which will be discussed in the next two sections) are much more common than is usually believed.

Studies on cattle, sheep, goats, pigs, horses, humans, rodents, deer, mink, birds, and other vertebrates (Benirshke, 1981; Benirshke and Kaufman, 1990) have unequivocally established the occurrence of placental (when applicable) or vascular anastomoses between dizygotic twins. Hematopoietic precursor cells are then frequently exchanged during early embryonic periods; and by virtue of acquired tolerance, they may continue to propagate throughout life in the new host. The new UOS, thus formed at one higher level entity, also bears evolutionary relevance in at least two types of phenomena. The first type comprises resultant costs such as freemartinism (masculinization of the female twin, resulting in sexual reproductive sterility; Benirshke, 1981) and a high frequency of malignancy (Picus *et al.*, 1985). The second type—more interesting, but sporadically observed—is gonadal chimerism (literature cited in Benirshke, 1981). In this phenomenon, primordial germ cells may reach the gonads of the other partner through early vascular anastomoses. Since a mammalian XY germ cell, for example, has the capacity to develop into an oocyte (Evans *et al.*, 1977), it is possible that even in twins of different sexes moving germ cells may become functional, giving an evolutionary significance to both genotypes in the chimera.

Genetic heterogeneities are also frequently developed as single-gene, chromosomal, and germ-cell mosaicisms (Benirshke, 1981; Hall, 1988; Gill *et al.*, 1995), and are also recorded in human monozygotic twins (Ford, 1969). This scientific field is too broad to be even partly covered here. As UOSs, however, many mosaic cases have evolutionary relevance because they are hereditarily transmitted and may manifest a variety of costs (Benirshke, 1981; Hall, 1988; Gill *et al.*, 1995; Rinkevich, 1996a). Studies of human syndromes in offspring have shown that somatic mutations of the germ line may occur in phenotypically normal parents (Hall, 1988). These mutations probably evolved from a germ-line cell or its precursors, before the meiotic event. The same holds for plants and for at least nine different animal phyla in which a variety of organisms develop by somatic embryogenesis (where at least one cell lineage remains totipotent throughout the whole life cycle) or epigenetic development (where sequestration of germ cells is made late in the life span; refs. in Buss, 1982; Gill *et al.*, 1995). Somatic mutations in those organisms not only provide the variation necessary to deal with fluctuating environments (Gill *et al.*, 1995), they also create new entities that may maintain and inherit the genetic heterogeneities through the colonial expansion of viable mutated cells.

I am—and this is actually he

Phenotypically expressed entities can serve as "incubators" for the germ line of other conspecific entities. For example, a detailed and very thorough study (Mayr *et al.*, 1979) reported the case of a human female chimera detectable only by investigation of her progeny. None of the four children fitted genetically with their mother, and none of the 21 unique genetic markers found in the children could be detected in the woman. The possibility of any type of somatic mutation was ruled out, as was the least probable hypothesis that all four children had been interchanged. The conclusion of this study was that this female possessed two populations of allogeneic cells, one in the soma and the second in her gonads. An extreme somatic clearance process was suggested for this case, occurring either in a dispermic chimera or after the fusion of two embryos into one entity (see next section), with only the germ line to be left from one partner.

Colonies of the cosmopolitan urochordate *Botryllus schlosseri* may undergo natural transplantation reactions upon allogenic contacts between their peripheral blood vessels. They may develop cytotoxic lesions in contact zones or form vascular parabionts (review in Weissman *et al.*, 1990; Rinkevich, 1992). This histocompatibility discrimination resides in a single highly polymorphic fusibility-histocompatibility (Fu/HC) locus (Weissman *et al.*, 1990). Allogeneic fusions occur between colonies that share at least one Fu/HC allele; rejecting partners share no Fu/HC allele. After fusion, all modular units (zooids) from one partner in the chimera are resorbed by massive phagocytosis, leaving the zooid of the other colony intact, a phenomenon called colony resorption (Rinkevich and Weissman, 1987b). In three clear, independent studies (Pancer *et al.*, 1995; Stoner and Weissman, 1996; Stoner *et al.*, 1999), polymorphic molecular markers were used to demonstrate somatic and germ-cell parasitism of the inferior partners in the resorption phenomenon. Of special interest are the cases where the soma were cleared of foreign cells, but the only foreign partner's cells were found in the gonads. This unilateral germ-cell parasitism (Pancer *et al.*, 1995; Stoner and Weissman, 1996; Stoner *et al.*, 1999) documents another example of an incubator that carries and successfully delivers the genetic material of an allogeneic partner to the next generation (Stoner *et al.*, 1999).

Incubated entities, as in the above cases, are the evolutionarily successful UOSs, whereas the *incubator* entities are those with the role of directly interacting with the environment. In such unique cases, natural selection therefore operates with consequences that do not fit the accepted dogma (Lewontin, 1970), because the positively selected organisms inherit different, nonrelated sets of genetic material. The intimate relationships between the incubator entities (which cannot be regarded as valid UOSs and better fit the notion of the "extended phenotype"; Dawkins, 1989) and the incubated UOSs are still unknown. Moreover, without discussing, at this point, the conflicts of interests between the genes of the incubated and the incubator entities, it is evident that the physically blended incubated entities blur the conventional practical divisions between one organism and the other. The perception of a UOS as a group of dispersed stem cells raises the conceptual dilemma of a physically noncoherent UOS.

I am—and this is actually we

Whole body chimerism—a complete integration of two or more genetically different conspecifics into a single unified entity, with a shared participation in the soma and the germ line—creates another type of self-maintaining UOS. Such a new form may bear specific properties, different from those expressed by each of the components. Natural selection may act simultaneously on each component and on each of the chimeric entities as a whole. In some chimeric entities, the physical boundaries between the different units are so blurred that a morphological separation between the components is not possible. The literature reveals instances where such a blending is beneficial to the original components, and others that are characterized by malformations or a variety of costs (such as higher rates of malignancy and other pernicious phenomena). Both situations will be discussed here, since successful sexual reproduction has been recorded even by malformed entities.

Colonies of *Botryllus schlosseri* may also form natural multichimeras (multiple partners; more than two fused genotypes) that result from an aggregated co-settlement of Fu/HC compatible colonies (Rinkevich, 1996b). When compared with bichimeras, multichimeras grow faster; reach larger sizes; do not fragment; have lower frequencies of colony resorption cases; and like more equilibrated entities, show other features that increase robustness (Rinkevich and Shapira, 1999). In these "monsters," the various costly intraspecific conflicts between the participant genotypes neutralize each other, generating an improved entity. In such an instance, natural selection may act on the "group" level (the chimera as a whole; Rinkevich, 1996b; Rinkevich and Shapira, 1999). The increase in fitness of the multichimeric entity, a new higher level of UOS, eventually increases the individual fitness of each UOS within this chimeric alliance. Therefore, even less adapted genotypes may survive and propagate.

A whole-body chimerism in mammals is a state in which the entire body consists of cells with at least two genetic lineages that are derived from separate fertilization products (Benirshke and Kaufman, 1990). Two types of genetic chimerism are of interest here: the early fusion of two embryos into one entity and the case of dispermic-chimerism, simultaneous fertilization of an ovum and the polar body by two spermatoza (Bernishke, 1981; Tippet, 1984; Bernishke and Kaufman, 1990). Both conditions are characterized by uniform dissemination, throughout the chimeral body, of the different cell lineages in the admixture, and they are found frequently in a variety of animals (Benirshke, 1981), including humans (Tippet, 1984; Benirshke and Kaufman, 1990). In some cases, due either to limited background information or complexity, the two conditions cannot be easily distinguished. One such example (summarized in Tippet, 1984) is a case of a monozygous pair of male twins identical in chromosome markers, HLA, isozymes and serum proteins, both XX/XY in the blood, but differing in other organs sampled such as skin and secretory tissues. One explanation for the unusual chimerism was that two embryos started to develop as XY monozygotic twins. One continued in the normal way, whereas the second fused with a dead XX triplet embryo which was completely adsorbed. In humans, many of such whole-body chimerisms are characterized by sexual reproductive sterility and a variety of tumors, but some of them are fertile (Tippet, 1984). One of the most interesting examples is a report (Talerman *et al.*, 1990) of a 29-year-old phenotypic female, a true hermaphrodite with bilateral ovotestes, a 46XX/46XY karyotype, and a successful pregnancy (before the development of a dysgerminoma, a germ-cell tumor). Several XX/XY male phenotypic dispermic chimeras have been recorded as sexually normal by having children (Tippet, 1984), but there is yet no study that analyzes the possible activation of both germ lines in the gonads, or the genetic constituents of the offspring in fertile cases.

Whole-body chimerism, and even true hermaphroditism, were recorded in a variety of vertebrates, most commonly in cats, but also in dogs, mink, horses, pigs, cattle, sheep, goats, deer, rabbits, rodents, chickens, and primates. In humans, as in other animals, XX/XY dispermic chimeras tend to be phenotypically males (Tippet, 1984), a phenomenon which further simplifies sexual reproduction. It is also possible that many cases of dispermic chimeras, even XX/XY ones, may remain undisclosed (Tippet, 1984) as long as they are healthy and remain fit.

I am—and this is actually only part of me

The same UOS may replicate endlessly to produce multiple identical copies. When addressing the issue of the unit at which selection acts, most biologists take into consideration only a simple list of basic biological organizations (*e.g.*, genes, cells, organisms, group). Most discussions (but see Tuomi and Vuorisale, 1989a, b) eschew conceptually challenged phenomena, such as modular organisms (which consist of repeated morphological units) and organisms that propagate similar, but morphologically independent, structures through a variety of processes, wrongly subsumed under the title of "asexual reproduction." The fuzzy boundaries of terms like "individual," "colony," and "clonal organism" (Michod, 1997) become even more apparent when they emerge in evolutionary concepts, in our case the concept UOS. For example, what are the levels of structural organization and what is the UOS of a stand of 47,000 aspen trees covering 100 ha of land, all produced from a single founder tree by "asexual" reproduction process (Gill *et al.*, 1995)? Or of a large branching coral colony that, during an episodic storm, is broken into fragments which are "replanted" and grow separately in different microhabitats? Or where a larva of an ophiuroid echinoderm produces secondary larval clones (Balser, 1998)? Numerous sessile marine organisms can generate detached fragments that by different mechanisms are dispersed before establishing themselves as independent colonies (Highsmith, 1982; Wulff, 1991). Following that, even the analysis for fragment size may reveal a whole range of controversial aspects, since a variety of life history patterns—such as growth rates, partial or whole fragment mortalities, and fecundity—are directly correlated with size rather than, for example, with the classical evaluated trait of "age" in unitary organisms (Hughes and Connell, 1987).

For this consideration of the UOS issue and evaluation of organismal body constructions, we shall deliberately treat "asexual reproduction" and "modularity" in the wider sense. No consideration will be given to the order of integration in modular organisms, to the physiological or morphological aspects, or to life history parameters. Consequently, it is not important for this discussion whether modules emerge spontaneously by self-organization, are developmentally controlled by a genetic mechanism, or are the products of environmental or biological causes that affect different conspecifics at random. All that matters is that when separation occurs, the original organism and the fragments continue to survive.

Three classes of "modularity," in which independent separated units (Harper, 1977) are produced, if taken together, may characterize another UOS prototype: a single entity that occurs simultaneously in several places, all distant from each other. The first class includes numerous colonial and clonal organisms (such as plants or marine invertebrates) that divide by fission (spontaneously, or under genetic control) to produce autonomous ramets. The second class includes unitary and clonal organisms (invertebrates, plants) that can, by budding, produce many similar modules that separate from their point of origin upon morphological completion. A well-known example is the freshwater hydra, a small carnivorous organism that, under normal conditions, shows no evidence of aging and continuously buds off unlimited numbers of "copies" of entirely comparable units (Slobodkin, 1986). Bosch *et al.* (1989) further described a dramatic mode of cloning by fission in the planktotrophic larvae of a sea star. The great multiplicative potential of this species prolongs the pelagic life of a genet and enhances its chances for recruitment into benthic adult populations. The third class includes mammalian monozygotic twins (two normally developed organisms that share the same genetic constituents) and polyembryony, in which the division of a single fertilized egg produces several to hundreds of similar genetic larvae. Polyembryony occurs in invertebrates and vertebrates and appears to be a paradox of evolution because it clones more of an unproven genotype at the expense of genetic diversity in a clutch of eggs (Craig *et al.*, 1997).

The above three classes of modular organisms share one basic life history trait, the production and dispersal of somatic individuals, the ramets. Each single genotype is therefore represented by more than one ramet. In ecological terms, each ramet could be regarded as an individual (Harper, 1977); from the perspective of the UOS, the whole genet constitutes a single unit of selection (assuming that no somatic mutation or any other type of somatic mosaicism is taking place). Among modular organisms, each unit of selection may be found simultaneously under different environmental conditions and exposed to a variety of selection pressures that sometimes oppose each other. Under these conditions, some ramets will die, while others will survive, which provides the option for each specific genet to "exercise" its phenotypic potentiality.

We are—and this is actually me

Several genets may form one coherent whole. The situation wherein several conspecific UOSs combine to form a morphologically new structure is best represented by certain primitive crustaceans (order Rhizocephala in the subclass Cirripedia, the barnacles). The rhizocephalans are mostly known for the genera *Sacculina* and *Peltogaster* (Hoeg and Rybakov, 1992; Glenner and Hoeg, 1995), which are parasitic, almost exclusively on decapod crustaceans, and are structurally unique. The "adults" have neither appendages nor segmentation, in contrast to all other arthropods, and their massive body is fastened to the host by a stalk from which "roots" proceed into the host tissues. These creatures also have neither an alimentary canal nor a mouth.

The life history of these parasitic crustaceans (Hoeg and Rybakov, 1992; Glenner and Hoeg, 1995) reveals a unique type of UOS. The cypris larva develops from a nauplius stage (both larval types are characteristic of primitive crustaceans). When the cypris is attached to the host crab, remarkable changes occur: the whole trunk of the parasite is discarded and a hollow, dart-like organ is formed. This organ is thrust into the crab's body cavity and the remnant of the cypris, a mass of undifferentiated cells enclosed within a thin ectodermal layer, is injected. The cell mass travels through the host's body cavity, attaches itself to the intestine, and anchors there by rootlets. Recent studies (Glenner and Hoeg, 1995) have further documented that the injected parasite has the form of a motile vermiform body that splits up into a number of naked, motile amoeboid cells. Each cell has the potential to develop into an adult parasite. A globular mass begins to develop. This structure will develop only the female gonads. Meanwhile, other cypris larvae attach themselves to the body of the juvenile parasite and inject their cellular contents into its mantle cavity. Only the first two will be successful in this enterprise. The cells from each such larva migrate and eventually enter one of the two "testes" (a better term would be spermatheca); there they develop into spermatozoa. Additional larvae attached to the parasite will be rejected. Reproduction is internal and within each parasitic unit.

Each single rhizocephalen organism is therefore an amalgamated structure, consisting of three distinct conspecific UOSs (two form only spermatozoa, one the soma and eggs). Together they participate in forming a different adult structural organism and a new unit of selection at a higher level. Selection acts only on this adult structure.

Epilogue

Thompsonia, another rhizocephalan parasite, is an extreme case; this crustacean has degenerated to the level of a fungus with rootlets that diffuse throughout the host crab. The rootlets branch off numerous sacs on small stalks, each sac contains one ovum per sac. The structureless parasite has no testes, ganglia, alimentary canal, or appendages, and there is no evidence of segmentation. It is believed that ova develop into cypris larvae by parthenogenesis, escaping the sacs through small openings (Lützen, 1992), although recent studies have challenged this hypothesis.

What is the unit of selection in this example? ("selection of?" *sensu* Sober, 1984). It is only one out of many cases where the data are insufficient for such analysis. However, the six types of UOSs characterized in this essay, in addition to the whole organismic level as a UOS (No. 7 in Table 1; not discussed here), indicate that a multiplicity of patterns are shaped by selective forces. The examples raised here symbolize the failure of many biologists and theoreticians to grasp the rich diversity of UOSs imposed upon the endless variety of adaptive structures found among living organisms. That many of the UOSs described in this essay are unconventional was therefore to have been expected, when the three novel conceptual criteria were applied to the analysis.

The concept of UOS is variously defined by different authors. Former attempts to identify the particular entities that are the targets of natural selection (Wynne-Edwards, 1962; Lewontin, 1970; Mayr, 1970, 1997; Dawkins, 1976, 1989; Hull, 1980; Buss, 1982; Gliddon and Gouyon, 1989; Sober and Wilson, 1994; Wilson and Sober, 1994; Williams, 1996; Michod, 1997; Gould, 1998; Gould and Lloyd, 1999) have suggested three or four potentially "structural" UOSs—the gene, the individual, the group, and the metapopulation—but there has been no consensus. Some (Kitcher *et al.*, 1990) have even argued that there are no "things" like UOSs, stating that "asking about the real unit of selection is an exercise in muddled metaphysics." However, I completely agree with the notion that "if selection is real, then so are units of selection" (Shanahan, 1997).

Kitcher *et al.* (1990), on the other hand, have correctly pointed to a major pitfall in the concept of the UOS by advocating that biologists "assume that for each selection episode, there is a unique account that will identify the level of selection." When the descriptions of UOSs in the literature are aligned with the organizational levels, they fail, in many cases, to grasp the structural comprehensiveness of other UOSs and no consistency emerges (Hull, 1980; Kitcher *et al.*, 1990; Sober and Wilson, 1994; Mayr, 1997; Shanahan, 1997). For example, the argument for the "gene," allegedly the most appropriate UOS (the reductionist approach), does not hold if we consider the changes that genes may go through during development (structurally and functionally). One such change is gene methylation. A methylated gene must be demethylated before it can be transcribed (Cedar, 1988). Another example is the changes that occur in the maturation of the mammalian immune system: the T and B cell genome rearrangement, the reshuffling of DNA fragments like a kaleidoscope to generate enormous genetic recombination patterns. Within a single individual, no two B cells, of more than 10^8 produced, are alike. In such situations, a single gene on its own may be regarded as only a tiny information fragment, a fraction within the organismal machinery that cannot produce anything unless it is in the right internal environment. With all its biological importance, a single gene cannot be termed a UOS (except in UOS type 1; Table 1).

In this essay, I have focused on the argument that real UOSs should evince a kind of holism and should possess the properties of independent functionalism. I have also eliminated cases that fail to comply with Slobodkin's (1986) minimalistic approach; thus I have omitted symbiosis (Nardon, 1999) and complicated cases such as symbiotic-parasitic relationships between a virus, an algal chloroplast, and a sea slug (Pierce *et al.*, 1999). Following from this analysis, six new types of UOSs were discussed (Table 1, Nos. 1–6), in addition to the self-evident case (Table 1, no. 7) of the "individual" (but see the search for several kinds of individuals based on characterizations of genetic uniqueness, genetic homogeneity, and autonomy; Santelices, 1999), which was not discussed here.

All UOSs differ from each other in substantial ways, and the characteristic properties of any one of them cannot be imposed on others. The analysis further revealed that neither the morphology nor the structural organization of a UOS is always orthodox. UOSs can also be blended morphologically into the somatic background of other conspecifics or different organisms. The blurred boundaries between organisms and colonies may raise a new theoretical question about the definition of "an organism." We find here that UOSs are associated with a variety of structural organizations, ranging from a DNA fragment (No. 1 in Table 1), to cells (No. 3), part of an organism (No. 5), whole organisms (Nos. 2, 7; that differ in the contents of the entity), a group of conspecifics (No. 4), and finally to a multiunit level entity (No. 6). The UOSs discussed here are, variously, based on one or a mixture of conspecific entities (Nos. 2–7), or on an association between several biological species (No. 1). There are probably other UOSs belonging to other biological organizations, even where the dividing line between components is not blurred; one good example is the existence of symbiotic unicellular algae within animal cells. Since these types of UOSs are more complicated, they were not analyzed here. In any event, all of the above UOSs bear in common their holistic character and their functionalism. All multiply through a variety of reproductive activities.

This essay reveals that a unit of selection can be a part of a biological organization, or can be an integration of several such organizations. It is not necessarily related to any conventional biological organization. Different selective forces operating on different levels of biological organizations may account for the diversification of UOSs by processes of integration (Nos. 1–4, 6; Table 1) or parcelation (No. 5). The simple characterization of the UOS on the basis of pure morphological level (gene, individual, group) may lead to unsatisfactory results. An entity like a single "individual" organism may represent a group of conspecifics that are intermingled (No. 4 in Table 1), only a part of a larger UOS (No. 5), an entity that possesses other types of UOSs (No.

1), another conspecific UOS (No. 3), a conglomerate of two units (No. 2), more than the sum of several conspecific UOSs (No. 6), or simply the traditional "individual" as the unit of selection (No. 7). Using an unprejudiced analysis on biological phenomena, we seem able to slip from the biased thinking of UOSs as being fixed entities, into an understanding that a UOS is the existence at a specific time point of a holistic and functional entity. Points of disagreement with traditional opinions always arise from the plurality in nature.

Acknowledgments

This study is part of the research carried out in the Minerva Center for Marine Invertebrate Immunology and Developmental Biology. Thanks are due to T. Newberry, K. Wasson, and three anonymous referees for critically reading the manuscript.

Literature Cited

Balser, E. J. 1998. Cloning by ophiuroid echinoderm larvae. *Biol. Bull.* **194:** 187–193.

Bell, G., and A. Burt. 1990. B-chromosomes: germ-line parasites which induce changes in host recombination. *Parasitology* **100:** S19–S26.

Benirshke, K. 1981. Hermaphrodites, freemartins, mosaics and chimeras in animals. Pp. 421–463 in *Mechanisms of Sex Differentiation in Animals and Man,* C. R. Austin and R. G. Edwards, eds. Academic Press, London.

Benirshke, K., and P. Kaufman. 1990. *Pathology and the Human Placenta.* Springer-Verlag, New York.

Bosch, I., R. B. Rivkin, and S. P. Alexander. 1989. Asexual reproduction by oceanic planktotrophic echinoderm larvae. *Nature (Lond.)* **337:** 169–170.

Buss, L. W. 1982. Somatic cell parasitism and the evolution of somatic tissue compatibility. *Proc. Natl. Acad. Sci. USA* **79:** 5337–5341.

Cedar, H. 1988. DNA methylation and gene activity. *Cell* **53:** 3–4.

Craig, S. F., L. B. Slobodkin, G. A. Wray, and C. H. Biermann. 1997. The 'paradox' of polyembryony: a review of the cases and a hypothesis for its evolution. *Evol. Ecol.* **11:** 127–143.

Dawkins, R. 1976. *The Selfish Gene.* Oxford University Press, Oxford.

Dawkins, R. 1989. *The Extended Phenotype.* Oxford University Press, Oxford.

Dawkins, R. 1990. Parasites, desiderata lists and the paradox of the organism. *Parasitology* **100:** S63–S73.

Evans, E. P., C. E. Ford, and M. F. Lyon. 1977. Direct evidence of the capacity of the XY germ cell in the mouse to become an oocyte. *Nature (Lond.)* **267:** 430–431.

Flavell, A. J. 1999. Long terminal repeat retrotransposons jump between species. *Proc. Natl. Acad. Sci. USA* **96:** 12211–12212.

Ford, C. E. 1969. Mosaics and chimaeras. *Br. Med. Bull.* **25:** 104–109.

Gill, D. E., L. Chao, S. L. Perkins, and J. B. Wolf. 1995. Genetic mosaicism in plants and clonal animals. *Annu. Rev. Ecol. Syst.* **26:** 423–444.

Glenner, H., and J. T. Hoeg. 1995. A new motile, multicellular stage involved in host invasion by parasitic barnacles (Rhizocephala). *Nature (Lond.)* **377:** 147–150.

Gliddon, C. J., and P. H. Gouyon. 1989. The units of selection. *Trends Ecol. Evol.* **4:** 204–208.

Gould, S. J. 1998. Gulliver's further travels: the necessity and difficulty of a hierarchical theory of selection. *Philos. Trans. R. Soc. Lond. B* **353:** 307–314.

Gould, S. J., and E. A. Lloyd. 1999. Individuality and adaptation across levels of selection: How shall we name and generalize the unit of Darwinism? *Proc. Natl. Acad. Sci. USA* **96:** 11904–11909.

Grosberg, R. K., and J. F. Queen. 1986. The genetic control and consequences of kin recognition by the larvae of a colonial marine invertebrate. *Nature (Lond.)* **322:** 456–459.

Hall, J. G. 1988. Review and hypotheses: somatic mosaicism. Observations related to clinical genetics. *Am. J. Hum. Genet.* **43:** 355–363.

Harper, J. L. 1977. *Population Biology of Plants.* Academic Press, London.

Highsmith, R. C. 1982. Reproduction by fragmentation in corals. *Mar. Ecol. Prog. Ser.* **7:** 207–226.

Hoeg, J. T., and A. V. Rybakov. 1992. Revision of the Rhizocephala Akentrogonida (Cirripedia), with a list of all the species and a key to the identification of families. *J. Crustac. Biol.* **12:** 600–609.

Hughes, T. P., and J. H. Connell. 1987. Population dynamics based on size or age? A reef-coral analysis. *Am. Nat.* **129:** 818–829.

Hull, D. L. 1980. Individuality and selection. *Annu. Rev. Ecol. Syst.* **11:** 311–332.

Kitcher, P., K. Sterelny, and C. K. Waters. 1990. The illusory riches of Sober's monism. *J. Philos.* **87:** 158–161.

Lewontin, R. C. 1970. The units of selection. *Annu. Rev. Ecol. Syst.* **1:** 1–18.

Lützen, J. 1992. Morphology of *Thompsonia reinhardi,* new species (Cirripedia: Rhizocephala), parasitic on the north-east Pacific hermit crab *Discorsopagurus schmitt* (Stevens). *J. Crustac. Biol.* **12:** 83–93.

Mayr, E. 1970. *Populations, Species and Evolution.* Harvard University Press, Cambridge, MA.

Mayr, E. 1997. The objects of selection. *Proc. Natl. Acad. Sci. USA* **94:** 2091–2094.

Mayr, W. R., V. Pausch, and W. Schnedl. 1979. Human chimaera detectable only by investigation of her progeny. *Nature (Lond.)* **277:** 210–211.

Michod, R. E. 1997. Cooperation and conflict in the evolution of individuality. I. Multilevel selection of the organism. *Am. Nat.* **149:** 607–645.

Nardon, P. 1999. Symbiosis as an example of an acquired character: Neo-Lamarckism or Darwinism? *Bull. Soc. Zool. Fr.* **124:** 39–52.

Pancer, Z., H. Gershon, and B. Rinkevich. 1995. Coexistence and possible parasitism of somatic and germ cell lines in chimeras of the colonial urochordate *Botryllus schlosseri. Biol. Bull.* **189:** 106–112.

Picus, J., W. R. Aldrich, and N. L. Letvin. 1985. A naturally occurring bone-marrow-chimeric primate. I. Integrity of its immune system. *Transplantation* **39:** 297–303.

Pierce, S. K., T. K. Maugel, M. E. Rumpho, J. J. Hanten, and W. L. Mondy. 1999. Annual viral expression in a sea slug population: life cycle control and symbiotic chloroplast maintenance. *Biol. Bull.* **197:** 1–6.

Reiter, L. T., T. Murakami, T. Koeuth, L. Pentao, D. M. Muzny, R. A. Gibbs, and J. R. Lupski. 1996. A recombination hotspot responsible for two inherited peripheral neuropathies is located near a mariner transposon-like element. *Nature Genetics* **12:** 288–296.

Rinkevich, B. 1992. Aspects of the incompatibility nature in botryllid ascidians. *Anim. Biol.* **1:** 17–28.

Rinkevich, B. 1996a. Immune responsiveness in marine invertebrates revisited: the concourse of puzzles. Pp. 55–90 in *New Directions in Invertebrate Immunology.* K. Söderhäll, S. Iwanaga, and G. R. Vasta, eds. SOS Publications, Fair Haven, NJ.

Rinkevich, B. 1996b. Bi- *vs.* multi-chimerism in colonial urochordates: a hypothesis for links between natural tissue transplantation allogenetics and evolutionary ecology. *Exp. Clin. Immunogenet.* **13:** 61–69.

Rinkevich, B., and M. Shapira. 1999. Multi-partner urochordate chimeras outperform two-partner chimerical entities. *Oikos* **87:** 315–320.

Rinkevich, B., and I. L. Weissman. 1987a. Chimeras in colonial invertebrates: a synergistic symbiosis or somatic and germ parasitism? *Symbiosis* **4:** 117–134.

Rinkevich, B., and I. L. Weissman. 1987b. A long-term study of fused subclones of a compound ascidian. The resorption phenomenon. *J. Zool.* **213:** 717–733.

Rinkevich, B., and I. L. Weissman. 1989. Variation in the outcomes following chimera formation in the colonial tunicate *Botryllus schlosseri. Bull. Mar. Sci.* **45:** 213–227.

Rinkevich, B., R. J. Lauzon, B. W. N. Brown, and I. L. Weissman. 1992. Evidence for a programmed lifespan in a colonial protochordate. *Proc. Natl. Acad. Sci. USA* **89:** 3546–3550.

Santelices, B. 1999. How many kinds of individual are there? *Trends Ecol. Evol.* **14:** 152–155.

Shanahan, T. 1997. Pluralism, antirealism and the units of selection. *Acta Biotheor.* **45:** 117–126.

Silver, L. M. 1993. The peculiar journey of a selfish chromosome: mouse t haplotypes and meiotic drive. *Trends Genet.* **9:** 250–254.

Slobodkin, L. B. 1986. The role of minimalism in art and science. *Am. Nat.* **127:** 257–265.

Sober, E. 1984. *The Nature of Selection: Evolutionary Theory in Philosophical Focus.* MIT Press, Cambridge, MA.

Sober, E., and D. S. Wilson. 1994. A critical review of philosophical work on the units of selection problem. *Philos. Sci.* **61:** 534–555.

Stoner, D., and I. L. Weissman. 1996. Somatic and germ cell parasitism in a colonial ascidian: possible role for a highly polymorphic allorecognition system. *Proc. Natl. Acad. Sci. USA* **93:** 15254–15259.

Stoner, D., B. Rinkevich, and I. L. Weissman. 1999. Heritable germ and somatic cell lineage competitions in chimeric colonial protochordates. *Proc. Natl. Acad. Sci. USA* **96:** 9148–9153.

Talerman, A., M. S. Verp, E. Senekjian, T. Gilewski, and N. Vogelzang. 1990. True hermaphrodite with bilateral ovotestes, bilateral gonadoblastomas and dysgerminomas, 46, XX/46, XY karyotype, and a successful pregnancy. *Cancer* **66:** 2668–2672.

Tippet, P. 1984. Human chimeras. Pp. 165–178 in *Chimeras in Developmental Biology,* N. Le Douarin and A. McLaren, eds. Academic Press, London.

Tuomi, J., and T. Vuorisalo. 1989a. Hierarchical selection in modular organisms. *Trends Ecol. Evol.* **4:** 209–213.

Tuomi, J., and T. Vuorisalo. 1989b. What are the units of selection in modular organisms? *Oikos* **54:** 227–233.

Weissman, I. L., Y. Saito, and B. Rinkevich. 1990. Allorecognition histocompatibility in a protochordate species: Is the relationship to MHC semantic or structural? *Immunol. Rev.* **113:** 227–241.

Williams, G. C. 1996. *Adaptation and Natural Selection.* Princeton University Press, Princeton, NJ.

Wilson, D. S., and E. Sober. 1994. Reintroducing group selection to the human behavioral sciences. *Behav. Brain Sci.* **17:** 585–654.

Wulff, J. L. 1991. Asexual fragmentation, genotype success and population dynamics of erect branching sponges. *J. Exp. Mar. Biol. Ecol.* **149:** 227–247.

Wynne Edwards, V. C. 1962. *Animal Dispersion in Relation to Social Behavior.* Oliver and Boyd, Edinburgh.

Zeyl, C., and G. Bell. 1996. Symbiotic DNA in eukaryotic genomes. *Trends Ecol. Evol.* **11:** 10–15.

Reference: *Biol. Bull.* **199:** 241–250. (December 2000)

An Inducer of Molluscan Metamorphosis Transforms Activity Patterns in a Larval Nervous System

ESTHER M. LEISE[1,2,*] AND MICHAEL G. HADFIELD[1]

[1]*Kewalo Marine Laboratory, Pacific Biomedical Research Center, University of Hawaii, 41 Ahui Street, Honolulu, Hawaii 96813; and* [2]*Department of Biology, University of North Carolina Greensboro, Greensboro, North Carolina 27402-6174*

Abstract. Larvae of the nudibranch mollusc *Phestilla sibogae* metamorphose in response to a small organic compound released into seawater by their adult prey, the scleractinian coral *Porites compressa.* The transformations that occur during metamorphosis, including loss of the ciliated velum (swimming organ), evacuation of the shell, and bodily elongation, are thought to be controlled by a combination of neuronal and neuroendocrine activities. Activation of peripheral chemosensory neurons by the metamorphosis-inducing compound should therefore elicit changes within the central nervous system. We used extracellular recording techniques in an attempt to detect responses of neurons within the larval central ganglia to seawater conditioned by *P. compressa,* to seawater conditioned by the weakly inductive coral *Pocillopora damicornis,* and to non-inductive seawater controls. The activity patterns within the nervous systems of semi-intact larvae changed in response to both types of coral exudates. Changes took place in two size classes of action potentials, one of which is known to be associated with velar ciliary arrests.

Introduction

For a number of molluscan larvae, specific chemical compounds from the juvenile environment can act as chemosensory cues and trigger metamorphosis. For example, inductive compounds may be given off by the adult prey (Hadfield and Karlson, 1969; Hadfield, 1977, 1978; Chia and Koss, 1978, 1988; Lambert and Todd, 1994; Avila *et al.,* 1996; Lambert *et al.,* 1997), by adult conspecifics (Pechenik, 1980; McGee and Targett, 1989; Pechenik and Gee, 1993), by bacteria associated with adult conspecifics (Fitt *et al.,* 1990; Tamburri *et al.,* 1992), and by the algal food of the juveniles (Scheltema, 1961; Kriegstein *et al.,* 1974; Switzer-Dunlap and Hadfield, 1977; Morse *et al.,* 1979; Levantine and Bonar, 1986; Morse, 1990; Boettcher and Targett, 1996; Leise *et al.,* 1996). In gastropods, sensory neurons that may mediate the induction of settlement and metamorphosis occur on the head, between the ciliated velar lobes (Bonar, 1978; Chia and Koss, 1982, 1984; Wodicka and Morse, 1991; Baxter and Morse, 1992; Uthe, 1995; Marois and Carew, 1997; Kempf *et al.,* 1997), and on the foot (Chia and Koss, 1989). Our understanding of how these neurons function is still limited. Observations of Morse and colleagues (Trapido-Rosenthal and Morse, 1985; Baxter and Morse, 1987, 1992; Morse, 1990; Wodicka and Morse, 1991) strongly imply that receptors for lysine, an amino acid that modifies inducer reception, lie on chemosensory cilia in the apical sensory organ of larval abalone. If pre-competent nudibranch and abalone larvae are exposed to an inducer substance, they display habituation—that is, decreased rates of metamorphosis—when they reach competency (Hadfield, 1980; Hadfield and Scheuer, 1985; Trapido-Rosenthal and Morse, 1986; Avila *et al.,* 1996). Habituation is thus a phenomenon associated with the morphogenetic pathway that directly initiates metamorphosis.

More recent studies are beginning to elucidate further internal mechanisms that are downstream from the chemosensory processes. These include changes in gene expression (Degnan and Morse, 1993, 1995; Degnan *et al.,* 1997), protein synthesis, and second messenger levels (Inestrosa *et*

Received 18 January 2000; accepted 7 September 2000.

* To whom correspondence should be addressed. Present address: Department of Biology, University of North Carolina Greensboro, Greensboro, NC 27402-6174. E-mail: Esther_Leise@uncg.edu

Abbreviations: ASW, artificial seawater; CAS, ciliary arrest spike; CNS, central nervous system; FSW, 0.2-μm-filtered natural seawater; ISW, *Porites*-conditioned seawater; PSW, *Pocillopora*-conditioned seawater; SU, smaller units.

al., 1993). Although the cellular circuitry that actually drives metamorphosis is still unknown, recent pharmacological studies have revealed some attributes of this pathway. Serotonin, which occurs widely in larval molluscan nervous systems (Goldberg and Kater, 1989; Marois and Carew, 1997; Kempf *et al.*, 1997), apparently acts as a neurotransmitter or neuromodulator that promotes metamorphosis in the mud snail *Ilyanassa obsoleta* (Couper and Leise, 1996). The neurotransmitter dopamine appears to be necessary for metamorphorphosis in the nudibranch *Phestilla sibogae* and the slipper limpet *Crepidula fornicata*, whereas norepinephrine may endogenously inhibit this process in *Crepidula* (Pires *et al.*, 1996, 2000). Nitric oxide appears to be yet another endogenous inhibitor of metamorphosis, as shown by studies on *Ilyanassa* (Froggett and Leise, 1999). Yet, even with these recent advances, we still have much to learn about the integrative mechanisms that follow the reception of chemosensory information to produce, ultimately, a juvenile organism.

Electrophysiological studies conducted on a variety of molluscan veligers have also provided some insight into their neural activities. Rapid and coordinated velum-wide ciliary arrests are driven by action potentials in the ciliated cells of the preoral band (Mackie *et al.*, 1976; Arkett *et al.*, 1987), and ramp depolarizations can slow ciliary beating on a more localized level (Arkett *et al.*, 1987). Thus, metachronal beating appears to be controlled by the relative depolarization of the ciliated cells and is modulated by excitatory neuronal input, presumably from the brain ganglia (Carter, 1926; Mackie *et al.*, 1976; Arkett *et al.*, 1987). These mechanisms are likely to be involved in the cessation of ciliary beating that accompanies larval settlement and crawling, behaviors that often precede metamorphosis. Barlow (1990) demonstrated that the ciliated velar cells in abalone larvae change their spiking activity only as an indirect response to the presence of the inducer substance. They do not act as sensory receptor cells. Arkett *et al.* (1989) recorded depolarizing receptor potentials from sensory neurons in nudibranch larvae in response to a settlement-inducing substance, although the use of cobalt anesthetic in their experiments limits the conclusions that can be drawn from their electrophysiological traces. Larvae of several molluscan species can be induced to metamorphose by an increase in external potassium ion concentration (Baloun and Morse, 1984; Yool *et al.*, 1986; Pechenik and Heyman, 1987; Todd *et al.*, 1991; Inestrosa *et al.*, 1992; Pechenik and Gee, 1993), a classical method for depolarizing nerve cells (Nicholls *et al.*, 1992), which again suggests that the peripheral nervous system, the larval central nervous system (CNS), or both are active during the initial phases of metamorphosis. If so, changes in the activity of central neurons, as well as in peripheral sensory receptors, should be detectable as they respond to a natural inducing substance.

The full range of metamorphic phenomena will most likely be controlled by neuroendocrine products as well as by classical synaptic interactions (Scheltema, 1974; Schacher *et al.*, 1979), but molluscan metamorphosis includes at least two relatively rapid events that may be under direct neuronal control. These are loss of the velum, a process common to all molluscan veliger larvae, and shell dehiscence, which occurs in many opisthobranchs (Bonar and Hadfield, 1974; Hadfield, 1978). These events, in addition to the chemosensory initiation of metamorphosis, could involve neuronal networks within the CNS that drive appropriate effector organs. Indeed, Hadfield (1978) summarized data in support of the hypothesis that the nervous system was the most likely and sufficient regulatory system underlying all facets of metamorphosis in molluscs.

To learn more about the role played by the nervous system during the metamorphosis of marine invertebrates, we used larvae of a nudibranch mollusc, *Phestilla sibogae*, to study the response of the CNS to a natural metamorphosis-inducing compound. The scleractinian coral *Porites compressa* is the major prey for adult *P. sibogae* in Hawaii. A small organic compound that is a natural exudate from live *P. compressa* induces metamorphosis in developmentally competent larvae (Hadfield and Karlson, 1969; Hadfield, 1977; Hadfield and Pennington, 1990). Our extracellular recordings from the exposed dorsal surface of the brain ganglia provide evidence that activity patterns in the CNS change in the presence of the coral extract. We propose that the electrical changes we observed are associated with the initiation of metamorphosis, and that some of them are specific responses to larval exposure to *P. compressa*.

Materials and Methods

Veliger larvae of the nudibranch *Phestilla sibogae* Bergh were cultured in the laboratory in 0.2-μm-filtered natural seawater (FSW) using previously described methods (Miller and Hadfield, 1986; Pires and Hadfield, 1991). During initial experiments, insufficient electrical activity was recorded from the epidermal surfaces of intact larvae, so we used an *in vitro* reduced preparation to maximize our ability to record spiking activity. To facilitate access to the larval brain, larvae without shells were used in all electrophysiological experiments. Deshelled larvae settle and metamorphose normally, although they do not undergo shell dehiscence (Pennington and Hadfield, 1989). Larval shells were decalcified by culturing about 100 larvae in a stender dish in 30 ml of artificial seawater (ASW) (Cavanaugh, 1956) lacking the usual 2.14×10^{-3} *M* sodium bicarbonate and buffered instead with 0.01 *M* Tris to pH 7.0 (Pires and Hadfield, 1993). Nine-day-old larvae were kept in ASW overnight so that metamorphically competent, shell-less, 10-day-old larvae were available as experimental subjects. About 70% of larvae cultured in this fashion had no shells 14 h after immersion. Deshelled larvae were rinsed in six changes of FSW over the following 2 h to reacclimate them to normal seawater (pH 8.3) before experimentation began.

Isolated larval heads (Fig. 1) were produced by chilling 20–25 individuals in FSW in a small petri dish in an ice water bath. Larvae became immobile as the FSW temperature approached 0°C. Small knives made from broken razor blades (Pires and Hadfield, 1993) were used to remove the visceral mass and foot from these cold, anesthetized larvae. This cut (line A in Fig. 1A) exposed the dorsal surface of the brain for extracellular recording, although it may have also eliminated part of the pedal ganglia. The eyes and statocysts remained in this isolated head preparation.

We also conducted experiments on animals from which only the visceral mass was removed (head-foot preparations). Results were similar, but we have chosen to leave those data unreported because fewer controls were conducted. Initial activity patterns in all experiments were somewhat varied (Fig. 3A, C, E, G), so data from different dissected veliger heads were not pooled.

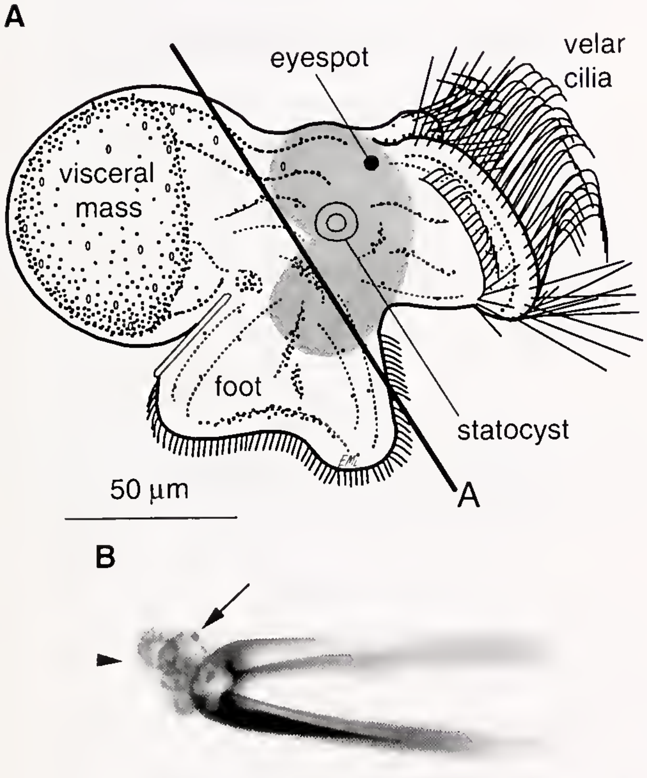

Figure 1. (A) Drawing of a deshelled larva (after Rasmussen, 1944) showing approximate location of the cut used to remove the visceral mass and foot from the head. Grey area represents approximate extent of the brain. The upper lobe containing the eyespot is likely to be a fusion product of the cerebral and pleural ganglia and may also contain elements of the parietal and buccal ganglia (Tardy, 1970). The region below the statocyst corresponds to the pedal ganglion. (B) Isolated head on the end of a suction electrode. The micropipette tip shown here is smaller than that typically used for recording purposes, to make the head more visible. The left eyespot is at arrow; right eyespot is visible through the transparent neural tissue within the open tip of the electrode. Velum is at arrowhead. For recording purposes, micropipettes were sized appropriately so that the entire cut surface could be contained by the electrode. ×178

Immediately after being cut, the chilled, isolated heads were transferred to fresh FSW at room temperature, whereupon they recovered normal metachronal beating of the velar cilia. Electrical recordings were made with a fire-polished glass micropipette suction electrode with an inner tip diameter of 40 to 50 μm. The suction electrode was appressed to the exposed dorsal surface of the brain and gentle suction was applied to maintain contact between the electrode and the larval tissue.

Larvae were exposed to one of three experimental solutions: FSW, FSW containing the natural metamorphosis-inducing compound produced by *Porites compressa* Dana (ISW), or a similar exudate from the relatively non-inductive coral *Pocillopora damicornis* (PSW). PSW induces less than 30% metamorphosis compared to 90% induced by ISW (Hadfield, 1977). Adult *P. sibogae* do not use *Pocillopora* as prey (Hadfield, 1977). ISW and PSW were prepared by placing about 22 g of living coral into 250 ml of aerated seawater in a covered beaker. Coral tips were used to maximize the ratio of living tissue to skeleton. The coral was removed after 48 h and the resulting conditioned seawater passed through a 1.2-μm filter. ISW and PSW were stored in the refrigerator and used within 48 h of production. Freshly made ISW normally induces more than 92% of 10-day-old intact larvae to metamorphose within 24 h. If the coral showed signs of ill health during preparation of ISW or PSW, the coral and solutions were discarded. Assays for the metamorphosis-inducing capabilities of ISW and PSW were compared to FSW controls and conducted with intact larvae as previously described (Pennington and Hadfield, 1989). Assays were examined at 24 and 48 h and scored for number of larvae, juveniles, and empty shells. We also tested 34 isolated heads for their ability to metamorphose. These heads were cultured under sterile conditions for 48 h as previously described (Pires and Hadfield, 1993), then examined for loss of ciliated velar cells.

Electrophysiological data were recorded for 5–10 min before and after the addition of experimental solutions. The decision to expose each head to control or experimental solutions was made before recordings were initiated. Experiments were conducted in 35 × 10 mm plastic petri dishes in about 6 ml of FSW. Changes to bath solutions were made manually; 4 ml of the bath solution were exchanged four times over the course of 1–3 min, during which time recording continued. Solution changes sometimes introduced mechanical artifacts, so results are reported for spiking activity occurring after solution changes were complete. Changes in spiking activity typically began 2–3 min after solutions first contacted the larval head. Data were collected from a new isolated head for each experiment, amplified through a differential AC amplifier (A-M Systems, Inc.), and recorded in digital format on videocas-

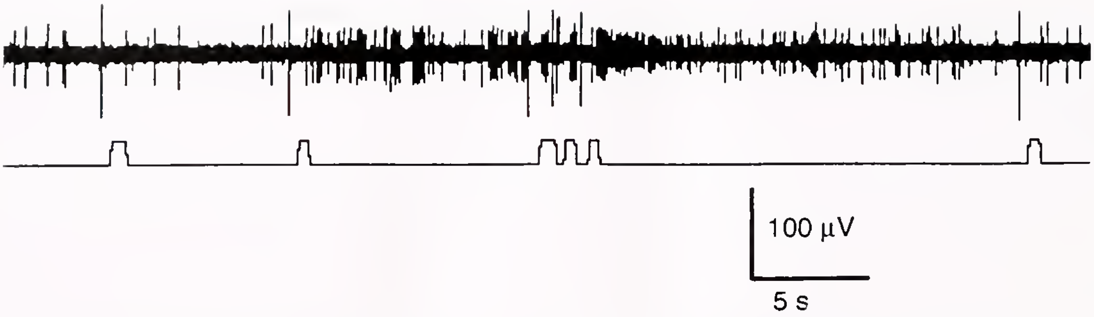

Figure 2. Representative trace from an isolated head in FSW. Large spikes are truncated and correlate with spontaneous velar ciliary arrest. No stimulus was used to elicit these large ciliary arrest spikes. Bottom trace is manually controlled cue (event marker) on the PCM data recorder. Cue was depressed, yielding an upward deflection, whenever spontaneous velar cilia were observed to cease beating. Audio monitor was turned off to avoid biasing the observer. Cessation of ciliary beating coincides with the largest spikes.

sette tape through an Instrutech VR-100 PCM (pulse code modulation) device. This device has a manually operated event marker, or "cue" switch. When depressed, a positive 2.5-V deflection from ground is recorded on a separate channel on the videotape. Data were played back directly onto a Western Graphtek thermal chart recorder or, alternatively, collected on a 486 Insight computer and analyzed with the Enhanced Graphics Acquisition and Analysis (EGAA) software programs, ver. 3.50.02 (RC Electronics, Goleta, CA). Action potentials of different magnitudes were identified and counted using the EGAA Waveshape Recognition program, which stores start and stop times in digital data files. As necessary, files were converted to standard ASCII text format and analyzed further with Microsoft Excel 97 (Microsoft Corp.). Traces with relatively few spikes were analyzed directly from chart recorder records or the EGAA display screens. Two-sample analyses (two-tailed t tests) were conducted with Statgraphics Plus ver. 7.1 (Manugistics, Inc., Rockville, MD) or GB-STAT 6.0 (Dynamic Microsystems, Silver Spring, MD). Results were graphed with DeltaGraph 4.0 (SPSS, San Francisco, CA).

Results

Extracellular recordings from the dorsal surfaces of brains in isolated heads of competent veliger larvae displayed two general sizes of spiking units in FSW (Fig. 2). Continuous recordings were made while the preparations were exposed to the various experimental solutions. The largest spikes, between 200 and 500 μV, were associated with partial or velum-wide ciliary arrests that occurred spontaneously in all preparations (Figs. 2, 3; Mackie *et al.*, 1976; Arkett *et al.*, 1987). No stimulation was needed to elicit this activity. Initial patterns of activity in FSW were varied, but we recorded spontaneous ciliary arrest spikes (CASs) in all preparations (Fig. 3A, C, E, G). CAS activity typically occurred tonically, as relatively regular trains of single action potentials at 1 Hz or less. Spikes from smaller

Figure 3. Representative 64-s traces, taken about 3 min before (A, C, E, G) and 1 min after (B, D, F, H) addition of experimental solutions, demonstrate induced changes in spiking activity. Traces A, C, E, and G, under the heading "before," all illustrate activity in filtered seawater (FSW). Trace B, a sham experiment, shows activity after the addition of FSW. Traces D and F show activity in seawater conditioned by the presence of the inductive coral *Porites compressa* (ISW), while trace H shows activity after the addition of seawater conditioned by the presence of *Pocillopora damicornis* (PSW). In all traces, most velar ciliary arrest spikes (CASs) are truncated and were maximally 200 μV in C and D and 500 μV in all other traces. Traces A and B from Expt. 90-60b, traces C and D from expt. 91-21, traces E and F from expt. 90-61, traces G and H from expt. 91-22. (A) Note relative lack of activity in small units (SU). (B) Addition of FSW did not significantly change the firing rates of CASs when averaged over 5 min ($[|t| = 0.80] < t_{0.05(2),8} = 2.31$). Low activity levels in SUs were likewise unaffected (Figs. 4A, 5A). (C) Note the variable firing patterns of SUs in FSW. (D) Addition of ISW (arrow) significantly increased activity of SUs ($[|t| = 3.14] > t_{0.05(2),14} = 2.15$, Fig. 5B), but did not affect activity of velar arrest spikes (Fig. 4B). (E) Note variable firing pattern of SUs. (F) In this experiment, addition of ISW did not significantly change activity in large or small units (Figs. 4B, 5B), but produced a qualitative change in the firing pattern of CASs. We recorded short bursts of 2–4 spikes during the 10 min after ISW addition. Longer bursts, with spike frequencies at or above 1 Hz (asterisks), coincided with a contraction of the velar lobes and cessation of ciliary beating. (G) Note variable firing patterns of SUs. (H) Addition of PSW again produced no significant changes in average number of spikes/minute in large or small units, but induced an increased variability in the firing pattern of CASs (Figs. 4C, 5C).

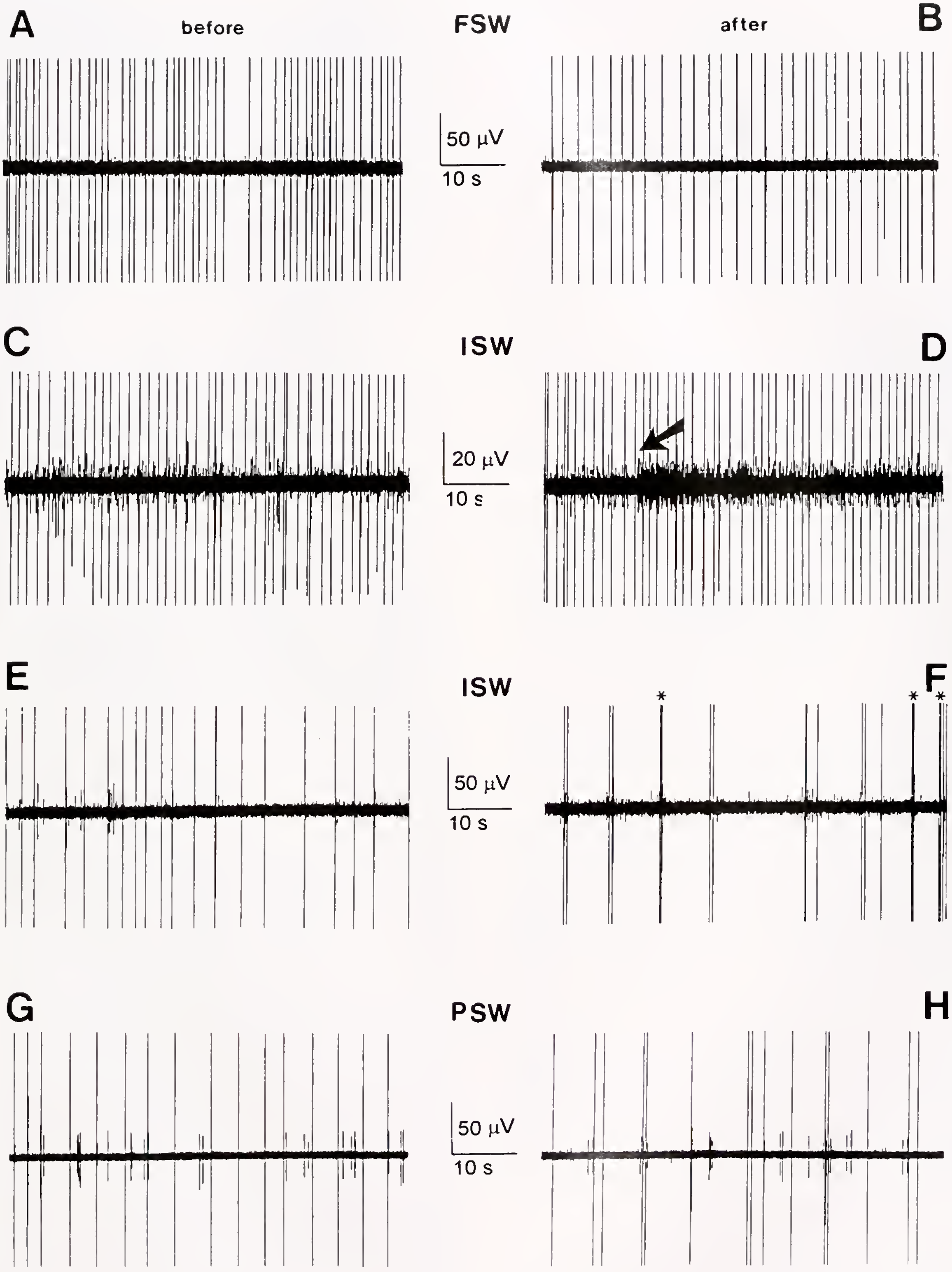
A
before
FSW
after
B
50 µV
10 s
C
ISW
D
20 µV
10 s
E
ISW
F
*
*
*
50 µV
10 s
G
PSW
H
50 µV
10 s

units (20–100 μV) also occurred spontaneously, but with less regularity (Fig. 3A, C, E, G).

Ciliary arrest was often accompanied by a contraction of the entire velar lobe; during prolonged arrest periods the cilia and velar tissue were held in an upright position. At CAS frequencies below 1 Hz, velar cilia resumed beating between arrest spikes (Figs. 2; 3A, B). During spiking activity at frequencies above 1 Hz, cilia remained relatively motionless (Fig. 3F).

We compared firing rates of CASs and the smaller units (SUs) before and after addition of experimental and control solutions to 13 isolated heads. In one experiment, addition of FSW elicited statistically significant changes in firing frequencies of both CASs and small spikes (Figs. 4A, 5A). In the remaining two experiments, as expected, no statistically significant differences were seen in spiking activity after the addition of FSW (Figs. 3A, B; 4A; 5A).

In contrast to larval heads that were exposed to FSW, those exposed to ISW exhibited some type of statistically significant change in firing pattern, in either CASs, SUs, or both, in 6 of 7 experiments (Figs. 4B, 5B). In only one experiment, #90-61 (Fig. 3E, F), did we fail to observe any statistically significant differences in spiking activity in response to ISW. However, in this experiment, after the addition of ISW, CASs tended to occur in short bursts of 2–4 spikes (Fig. 3F). Short bursts of spikes elicited longer periods of ciliary arrest than did single CASs, and were often accompanied by contractions of the velar lobes. We observed similar results from preparations with an intact foot on several occasions (data not shown). In 4 of the 7 experiments, addition of ISW elicited a significant decrease in the frequency of CASs (Fig. 4B) and a change in the spiking activity of SUs (Fig. 5B).

The addition of PSW to isolated heads elicited no statistically significant changes in firing rates (Figs. 4C, 5C), but in all cases, PSW elicited a qualitative change in CAS activity. With PSW, the firing pattern of the CASs became irregular (Fig. 3H), which accounted for the significant increase in variance that occurred in all experiments (Fig. 4C). No such increase in variance was detected for the firing rates of small spikes.

Finally, we tested 34 isolated heads for their ability to metamorphose. The results were equivocal: four (12%) lost velar cilia, suggesting that isolated heads may be able to detect and respond to ISW, depending, perhaps, upon the amount of intact central nervous tissue. Because a large proportion (56%) died within 48 h, we cannot make a definitive conclusion about the metamorphic capabilities of isolated heads.

Discussion

Metamorphosis in the nudibranch *Phestilla sibogae* is triggered by a chemosensory event, namely, the perception by a competent larva of a small organic compound given off by its adult prey, the coral *Porites compressa* (Hadfield and Scheuer, 1985; Hadfield and Pennington, 1990). In 6 of 7 experiments, we recorded statistically significant changes in electrical activity from *in vitro* heads of larval *P. sibogae* shortly after the addition of a metamorphic inducer. In 3 of the 4 experiments in which spiking activity in small units changed, activity increased. In 4 of the 7 experiments with ISW, firing rates of velar ciliary arrest spikes decreased. Although we did not record consistent responses from all preparations, it is clear that long-lasting changes in electrical activity are initiated within minutes of initial exposure to the coral inducer.

Competent larvae of *P. sibogae* display a rapid behavioral response to ISW that can be reliably observed under laboratory conditions (Koehl and Hadfield, unpubl. obs.). These larvae, which are negatively buoyant, stop swimming and rapidly sink when encountering ISW (Hadfield, unpubl. data). In the field, such a response would increase the chances of a larva contacting its adult food source. External signs of metamorphosis occur only 18–20 h after larvae have been exposed to an inducer substance for at least 4–6 h (Hadfield, 1977; Hadfield and Pennington, 1990). During this delay period, crucial physiological transformations and biochemical pathways must be activated as a prelude to the more obvious morphological transformations of metamorphosis.

The reduced preparation that we used may have produced neural activity different from that which occurs in an intact organism. The isolated heads retained most of the brain ganglia as well as intact velar lobes, eyespots, and statocysts. However, central circuits may have been damaged by a loss of ganglionic tissue, resulting in decreased connectivity and insufficient afferent information. This in turn may have led to unusual patterns of activity. Because we are reporting results from a relatively small number of experiments with a limited number of controls, we cannot fully explain the variability in endogenous activity, nor the variability in our results. The responses to *Porites compressa* that we recorded in four experiments would lead to an increase in larval sinking, but not to a complete cessation of ciliary beating, as seen in the behavioral responses mentioned above. This suggests that the isolated heads are not responding in a completely normal fashion.

Larval *Phestilla* can apparently differentiate between their adult prey and at least one other coral species in their reef habitat. In addition to positive metamorphic responses, negative responses to unfavorable or even potentially lethal juvenile environments have been reported for other invertebrates, including several polychaete species (Woodin, 1986, 1991; Woodin *et al.*, 1993; Walters *et al.*, 1996), bryozoan larvae (Walters *et al.*, 1996), and veligers of the gastropod *Ilyanassa obsoleta* (Leise *et al.*, 1996). The ability of *Phestilla* larvae to respond differentially to species of

Porites and *Pocillopora* is thus not without precedent. How many coral species these small larvae can distinguish remains to be investigated.

Beat frequency of the velar cilia is modulated by excitatory neural input in veliger larvae of the snails *Mangelia nebula* (Mackie *et al.*, 1976) and *Calliostoma ligatum* (Arkett *et al.*, 1987) and the abalone *Haliotis rufescens* (Barlow, 1990). Velum-wide ciliary arrests are caused by an action potential that propagates throughout the velar ciliated cells. The large action potentials we recorded were always associated with ciliary arrests and were smaller than, but similar to, the signals recorded from the velum of *Mangelia* and *Calliostoma* (Mackie *et al.*, 1976; Arkett *et al.*, 1987). The exact origin of the large spikes in *Phestilla* is unclear: they may be the propagated action potentials of the ciliated cells, or a combination of these spikes plus the summed output of central activity that drives ciliary arrests. In her work with larval abalone, Barlow (1990) found that exposure to an inducer substance increased the likelihood and duration of ciliary arrests. In our experiments, we mostly observed a decrease in firing frequency of the CASs, which

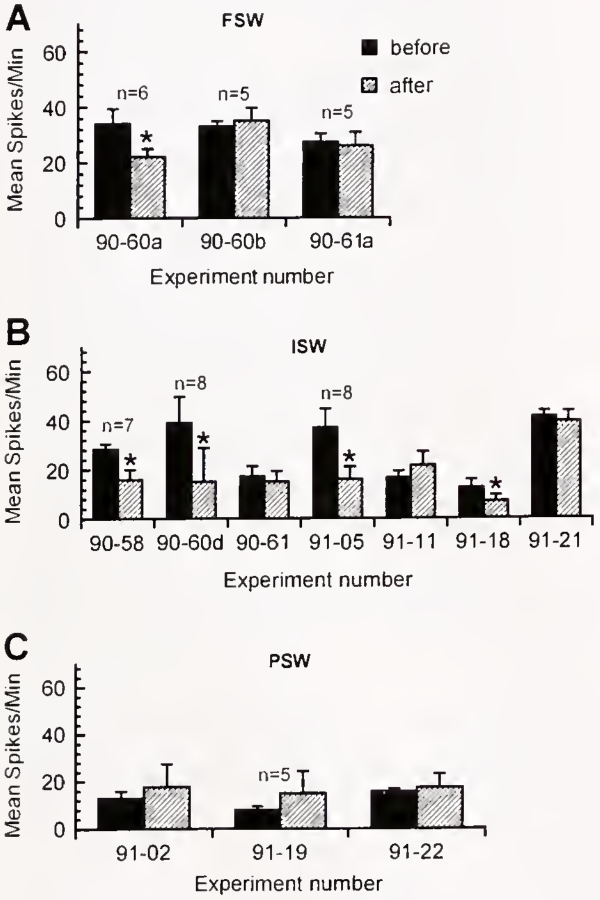

Figure 4. Mean number of velar ciliary arrest spikes recorded per minute before and after addition of experimental solutions, ± one standard deviation. Asterisks (*) indicate mean firing rate is significantly different from initial conditions ($P < 0.05$) after addition of control or experimental solution. Experiments 90-60 (a, b) incorporated different isolated heads. Means were averaged from 10 min of continuous recordings whenever possible. Exceptions are noted on graphs as $n = x$ number of minutes. (A) In one experiment, addition of FSW elicited a significantly slower rate of firing of CASs ($[|t| = 4.85] > t_{0.05(2),12} = 2.18$). (B) Addition of ISW elicited a significant decrease in the firing rate of CASs by 40% or more in 4 of the 7 experiments (*e.g.*, expt 91-18, $[|t| = 4.16] > t_{0.05(2),18} = 2.10$). (C) No change in mean number of arrest spikes per minute was recorded from isolated heads after addition of PSW (*e.g.*, expt 91-19, $[|t| = 1.96] < t_{0.05(2),8} = 2.30$). However, addition of PSW elicited a significant increase in the variance in all experiments (*e.g.*, expt 91-22, $[F = 11.4] > F_{0.05(2),9,9} = 4.03$).

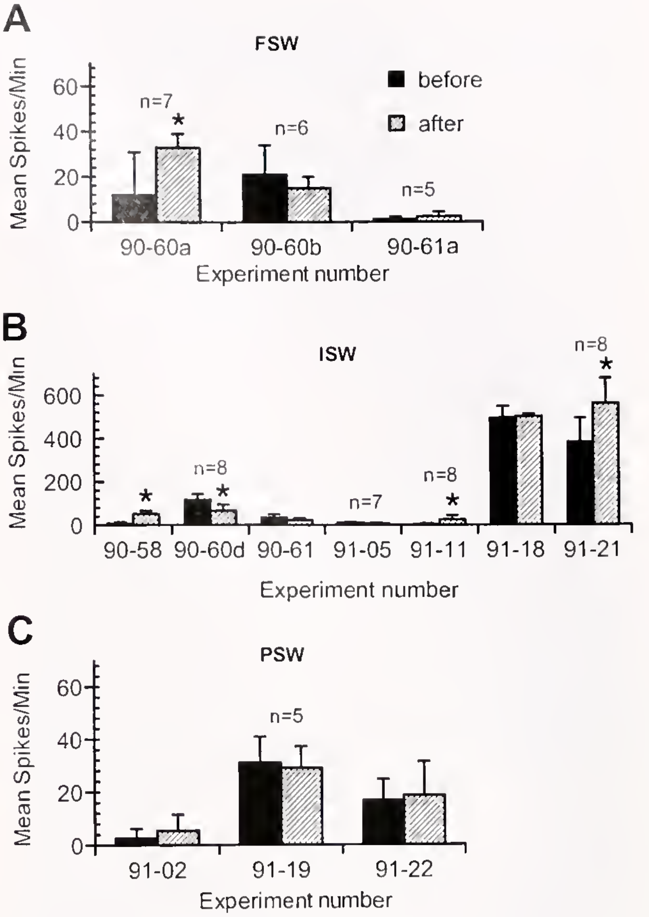

Figure 5. Mean number of spikes per min recorded from smaller units before and after addition of experimental solutions, ± standard deviation. Means calculated from 10 min before and after addition of experimental solutions, except as indicated on graph ($n = x$ number of minutes). Asterisks (*) indicate that mean firing rates before and after addition of experimental solution were significantly different. (A) Addition of FSW in one experiment elicited a significant increase in the number of SUs ($[|t| = 4.16] > t_{0.05(2),18} = 2.10$). (B) Activity levels of SUs were highly variable both before and after addition of ISW. Firing rate of SUs increased significantly after addition of ISW in three experiments (*e.g.*, expt 91-21, $[|t| = 3.13] > t_{0.05(2),14} = 2.15$), but decreased in one experiment. (C) Addition of PSW elicited no change in firing rates of SUs. Variances were similar in all of these experiments, both before and after PSW addition (*cf.* Fig. 4C).

would lead to fewer, not more, ciliary arrests. Only the qualitative change to short bursts of CASs, as seen in some experiments (*e.g.*, #90-61) would lead to longer ciliary arrests.

The behavioral relevance of the spiking activity in the smaller-sized units is unknown. We do not know if their activity arises from circuits that detect environmental odorants or drive motor activities, such as crawling or changes in swimming speed or direction. As elicited by ISW, the bursts of smaller action potentials are irregular, unlike bursts from any of the well-known molluscan motor systems (*e.g.*, Getting and Dekin, 1985) or recently described olfactory circuits (Gelperin and Tank, 1990; Gelperin *et al.*, 1993, 1996; Laurent and Davidowitz, 1994; Laurent *et al.*, 1996; Delaney *et al.*, 1994). Activity in the smaller larval units was also quite variable, with firing rates ranging from a few spikes per minute to hundreds per minute. We have no explanation for such variability, beyond suggesting that the amount of SU activity may reflect the amount of tissue lost during dissection. We also have no explanation for the increase in SU activity seen in one control experiment (Fig. 5A). Extracellular recordings from distal stumps of either the rhinophoral or oral-tentacle nerves of adult *P. sibogae* display changes in firing activity of small units in response to *Porites compressa* that are similar to the changes we record from SUs in response to ISW (Boudko and Hadfield, unpubl. data). We can only speculate that the SUs recorded from larval *P. sibogae* might indicate olfactory activity.

The high mortality rate that occurred in experiments on the metamorphic capabilities of isolated heads does not allow us to make a definitive statement about their ability to metamorphose. Isolated velar lobes do not metamorphose—that is, they retain their ciliated velar cells in the presence of ISW—but such lobes lack the neural apparatus that can respond to a metamorphic inducer (Pires and Hadfield, 1993). Although our results support the idea that larval perception of an inducer substance depends upon peripheral chemosensory neurons and central processing circuitry, an additional caveat is warranted. Suction electrodes do not provide a tight seal against passage of fluid between the bathing medium and the core of the electrode. Thus, in our experiments, ISW in the bath seawater could have been interacting directly with neurons of the CNS as well as with epidermal sensory neurons. Thus, the neural activity we recorded in response to ISW may or may not duplicate neural activity occurring within intact larvae at the initiation of metamorphosis. Still, the responses we recorded suggest that the beginning of this process in *Phestilla sibogae* is accompanied by lasting changes in central neural activity.

Acknowledgments

We would like to acknowledge the late Dr. Robert Kane for many constructive discussions. We also thank Dr. Anthony Pires for advice, important technical suggestions, and help in conducting the *in vitro* induction experiments. Dr. Stephen Kempf for his critique of an earlier version of this manuscript, Dr. Louise Page for neuroanatomical insights, and Bryan Turner for technical assistance. This work was supported by ONR grant N00014-91-J-1533 and NSF grants DCB-8903800 to M.G.H. and IBN-9604516 to E.M.L. We are also grateful to UNCG for providing equipment and a Research Assignment award to E.M.L.

Literature Cited

Arkett, S. A., G. O Mackie, and C. L. Singla. 1987. Neuronal control of ciliary locomotion in a gastropod veliger (*Calliostoma*). *Biol. Bull.* **173:** 513–526.

Arkett, S. A., F.-S. Chia, J. I. Goldberg, and R. Koss. 1989. Identified settlement receptor cells in a nudibranch veliger respond to specific cue. *Biol. Bull.* **176:** 155–160.

Avila, C., C. T. Tamse, and A. M. Kuzirian. 1996. Induction of metamorphosis in *Hermissenda crassicornis* larvae (Mollusca: Nudibranchia) by GABA, choline and serotonin. *Invertebr. Reprod. Devel.* **29:** 127–141.

Baloun, A. J., and D. E. Morse. 1984. Ionic control of settlement and metamorphosis in larval *Haliotis rufescens* (Gastropoda). *Biol. Bull.* **167:** 124–138.

Barlow, L. A. 1990. Electrophysiological and behavioral responses of larvae of the red abalone (*Haliotis rufescens*) to settlement-inducing substances. *Bull. Mar. Sci.* **46:** 537–554.

Baxter, G., and D. E. Morse. 1987. G protein and diacylglycerol regulate metamorphosis of planktonic molluscan larvae. *Proc. Natl. Acad. Sci. USA* **84:** 1867–1870.

Baxter, G. T., and D. E. Morse. 1992. Cilia from abalone larvae contain a receptor-dependent G protein transduction system similar to that in mammals. *Biol. Bull.* **183:** 147–154.

Boettcher, A. A., and N. M. Targett. 1996. Induction of metamorphosis in queen conch, *Strombus gigas* Linnaeus, larvae by cues associated with red algae from their nursery grounds. *J. Exp. Mar. Biol. Ecol.* **196:** 29–52.

Bonar, D. B. 1978. Ultrastructure of a cephalic sensory organ in larvae of the gastropod *Phestilla sibogae* (Aeolidacea, Nudibranchia). *Tissue Cell* **10:** 153–165.

Bonar, D. B., and M. G. Hadfield. 1974. Metamorphosis of the marine gastropod *Phestilla sibogae* Bergh (Nudibranchia: Aeolidacea). I. Light and electron microscopic analysis of larval and metamorphic stages. *J. Exp. Mar. Biol. Ecol.* **16:** 227–255.

Carter, G. S. 1926. On the nervous control of velar cilia of the nudibranch veliger. *J. Exp. Biol.* **4:** 1–26.

Cavanaugh, G. M. 1956. *Formulae and Methods VI of the Marine Biological Laboratory Chemical Room*, Marine Biological Laboratory Press, Woods Hole, MA. Pp. 1–84.

Chia, F.-S., and R. Koss. 1978. Development and metamorphosis of the planktotrophic larvae of *Rostanga pulchra* (Mollusca: Nudibranchia). *Mar. Biol.* **46:** 109–119.

Chia, F.-S., and R. Koss. 1982. Fine structure of the larval rhinophores of the nudibranch, *Rostanga pulchra*, with emphasis on the sensory receptor cells. *Cell Tissue Res.* **225:** 235–248.

Chia, F.-S., and R. Koss. 1984. Fine structure of the cephalic sensory organ in the larva of the nudibranch *Rostanga pulchra* (Mollusca, Opisthobranchia, Nudibranchia). *Zoomorphology* **104:** 131–139.

Chia, F.-S., and R. Koss. 1988. Induction of settlement and metamorphosis of the veliger larvae of the nudibranch, *Onchidoris bilamellata*. *Int. J. Invertebr. Reprod. Dev.* **14:** 53–70.

Chia, F.-S., and R. Koss. 1989. The fine structure of the newly discovered propodial ganglia of the veliger larva of the nudibranch *Onchidoris bilamellata. Cell Tissue Res.* **256:** 17–26.

Couper, J. M., and E. M. Leise. 1996. Serotonin injections induce metamorphosis in larvae of the gastropod mollusc *Ilyanassa obsoleta. Biol. Bull.* **191:** 178–186.

Degnan, B. M., and D. E. Morse. 1993. Identification of eight homeobox-containing transcripts expressed during larval development and at metamorphosis in the gastropod mollusc *Haliotis rufescens. Mol. Mar. Biol. Biotechnol.* **2:** 1–9.

Degnan, B. M., and D. E. Morse. 1995. Developmental and morphogenetic gene regulation in *Haliotis rufescens* larvae at metamorphosis. *Am. Zool.* **35:** 391–398.

Degnan, B. M., S. M. Degnan, G. Fentenany, and D. E. Morse. 1997. A Mox homeobox gene in the gastropod mollusc *Haliotis rufescens* is differentially expressed during larval morphogenesis and metamorphosis. *FEBS Lett.* **411:** 119–122.

Delaney, K. R., A. Gelperin, M. S. Fee, J. A. Flores, R. Gervais, D. W. Tank, and D. Kleinfeld. 1994. Waves and stimulus-modulated dynamics in an oscillating olfactory network. *Proc. Natl. Acad. Sci. USA* **91:** 669–673.

Fitt, W. K., S. L. Coon, M. Walch, R. M. Weiner, R. R. Colwell, and D. B. Bonar. 1990. Settlement behavior and metamorphosis of oyster larvae (*Crassostrea gigas*) in response to bacterial supernatants. *Mar. Biol.* **106:** 389–394.

Froggett, S. J., and E. M. Leise. 1999. Metamorphosis in the marine snail *Ilyanassa obsoleta*, yes or NO? *Biol. Bull.* **196:** 57–62.

Gelperin, A., and D. W. Tank. 1990. Odour-modulated collective network oscillations of olfactory interneurons in a terrestrial mollusc. *Nature* **345:** 437–440.

Gelperin, A., L. D. Rhines, J. Flores, and D. W. Tank. 1993. Coherent network oscillations by olfactory interneurons: modulation by endogenous amines. *J. Neurophysiol.* **69:** 1930–1939.

Gelperin, A., D. Kleinfeld, W. Denk, and I. R. C. Cooke. 1996. Oscillations and gaseous oxides in invertebrate olfaction. *J. Neurobiol.* **30:** 110–122.

Getting, P. A., and M. S. Dekin. 1985. *Tritonia* swimming: a model system for integration within rhythmic motor systems. Pp. 3–20 in *Model Neural Networks and Behavior,* A. I. Selverston, ed. Plenum Press, New York.

Goldberg, J. I., and S. B. Kater. 1989. Expression and function of the neurotransmitter serotonin during development of the *Helisoma* nervous system. *Dev. Biol.* **131:** 483–495.

Hadfield, M. G. 1977. Chemical interactions in larval settling of a marine gastropod. Pp. 403–413 in *Marine Natural Products Chemistry,* D. J. Faulkner and W. H. Fenical, eds. Academic Press, New York.

Hadfield, M. G. 1978. Metamorphosis in marine molluscan larvae: an analysis of stimulus and response. Pp. 165–175 in *Settlement and Metamorphosis of Marine Invertebrate Larvae,* F. S. Chia and M. Rice, eds. Elsevier/North Holland Biomedical Press, New York.

Hadfield, M. G. 1980. Habituation in metamorphic induction of larvae of *Phestilla sibogae* (Gastropoda). *Am. Zool.* **20:** 955.

Hadfield, M. G., and R. H. Karlson. 1969. Externally induced metamorphosis in a marine gastropod. *Am. Zool.* **9:** 317.

Hadfield, M. G., and J. T. Pennington. 1990. Nature of the metamorphic signal and its internal transduction in larvae of the nudibranch *Phestilla sibogae. Bull. Mar. Sci.* **46:** 455–464.

Hadfield, M. G., and D. Scheuer. 1985. Evidence for a soluble metamorphic inducer in *Phestilla:* ecological, chemical, and biological data. *Bull. Mar. Sci.* **37:** 556–566.

Inestrosa, N. C., E. O. Campos, and M. González. 1992. Inducción de metamorfosis en larvas de *Concholepas concholepas* por el ión K^+. *Bolet. Red Regional Acuicult. Amer. Lat.* **6:** 16–19.

Inestrosa, N. C., M. González, and E. O. Campos. 1993. Molecular changes induced by metamorphosis in larvae of the prosobranch *Concholepas concholepas* Bruguiere (Mollusca: Gastropoda: Muricidae). *J. Exp. Mar. Biol. Ecol.* **168:** 205–215.

Kempf, S. C., L. Page, and A. Pires. 1997. The development of serotonin-like antigenicity in the embryos and larvae of nudibranch molluscs with emphasis on the apical sensory organ. *J. Comp. Neurol.* **386:** 507–528.

Kriegstein, A. R., V. Castellucci, and E. R. Kandel. 1974. Metamorphosis of *Aplysia californica* in laboratory culture. *Proc. Natl. Acad. Sci. USA* **71:** 3654–3658.

Lambert, W. J., and C. D. Todd. 1994. Evidence for a water-borne cue inducing metamorphosis in the dorid nudibranch mollusc *Adalaria proxima* (Gastropoda: Nudibranchia). *Mar. Biol.* **120:** 265–271.

Lambert, W. J., C. D. Todd, and J. D. Hardege. 1997. Partial characterization and biological activity of a metamorphic inducer of the dorid nudibranch *Adalaria proxima* (Gastropoda: Nudibranchia). *Invertebr. Biol.* **116:** 71–81.

Laurent, G., and H. Davidowitz. 1994. Encoding of olfactory information with oscillating neural assemblies. *Science* **265:** 1872–1875.

Laurent, G., M. Wehr, K. MacLeod, M. Stopfer, B. Leitch, and H. Davidowitz. 1996. Dynamic encoding of odors with oscillating neuronal assemblies in the locust brain. *Biol. Bull.* **191:** 70–75.

Leise, E. M., J. E. Nearhoof, S. J. Froggett, and L. B. Cahoon. 1996. Benthic diatoms induce metamorphosis in larvae of the caenogastropod mollusc *Ilyanassa obsoleta. Am. Zool.* **36:** 107A.

Levantine, P. L., and D. B. Bonar. 1986. Metamorphosis of *Ilyanassa obsoleta:* natural and artificial inducers. *Am. Zool.* **26:** 14A.

Mackie, G. O., C. L. Singla, and C. Thiriot-Quievreux. 1976. Nervous control of ciliary activity in gastropod larvae. *Biol. Bull.* **151:** 182–199.

Marois, R., and T. J. Carew. 1997. Fine structure of the apical ganglion and its serotonergic cells in the larva of *Aplysia californica. Biol. Bull.* **192:** 388–398.

McGee, B. L., and N. M. Targett. 1989. Larval habitat selection in *Crepidula* (L.) and its effect on adult distribution patterns. *J. Exp. Mar. Biol. Ecol.* **131:** 195–214.

Miller, S. E., and M. G. Hadfield. 1986. Ontogeny of phototaxis and metamorphic competence in larvae of the nudibranch *Phestilla sibogae* Bergh (Gastropoda: Opisthobranchia). *J. Exp. Mar. Biol. Ecol.* **97:** 95–112.

Morse, D. E. 1990. Recent progress in larval settlement and metamorphosis: closing the gaps between molecular biology and ecology. *Bull. Mar. Sci.* **46:** 465–483.

Morse, D. E., N. Hooker, H. Duncan, and L. Jensen. 1979. γ-Aminobutyric acid, a neurotransmitter, induces planktonic abalone larvae to settle and begin metamorphosis. *Science* **204:** 407–410.

Nicholls, J. G., A. R. Martin, and B. G. Wallace. 1992. *From Neuron to Brain.* Sinauer, Sunderland, MA. Pp. 70–71.

Pechenik, J. A. 1980. Growth and energy balance during the larval lives of three prosobranch gastropods. *J. Exp. Mar. Biol. Ecol.* **44:** 1–28.

Pechenik, J. A., and C. C. Gee. 1993. Onset of metamorphic competence in larvae of the gastropod *Crepidula fornicata* (L.), judged by a natural and an artificial cue. *J. Exp. Mar. Biol. Ecol.* **167:** 59–72.

Pechenik, J. A., and W. D. Heyman. 1987. Using KCl to determine size at competence for larvae of the marine gastropod *Crepidula fornicata* (L.). *J. Exp. Mar. Biol. Ecol.* **112:** 27–38.

Pennington, J. T., and M. G. Hadfield. 1989. A simple nontoxic method for the decalcification of living invertebrate larvae. *J. Exp. Mar. Biol. Ecol.* **130:** 1–7.

Pires, A., and M. G. Hadfield. 1991. Oxidative breakdown products of catecholamines and hydrogen peroxide induce partial metamorphosis in the nudibranch *Phestilla sibogae* Bergh (Gastropoda: Opisthobranchia). *Biol. Bull.* **180:** 310–317.

Pires, A., and M. G. Hadfield. 1993. Responses of isolated vela of nudibranch larvae to inducers of metamorphosis. *J. Exp. Zool.* **266:** 234–239.

Pires, A., J. A. Skiendzielewiski, and J. V. Mitten. 1996. Depletion of norepinephrine and metamorphosis in a gastropod. *Am. Zool.* **36:** 13A.

Pires, A., R. P. Croll, and M. G. Hadfield. 2000. Catecholamines modulate metamorphosis in the opisthobranch gastropod *Phestilla sibogae*. *Biol. Bull.* **198:** 319–331.

Rasmussen, E. 1944. Faunistic and biological notes on marine invertebrates I. The eggs and larvae of *Brachystomia rissoides* (Hanl.), *Eulimella nitidissima* (Mont.), *Retusa truncatula* (Brug.) and *Embletonia pallida* (Alder and Hancock), (Gastropoda marina). *Vidensk. Medd. Dan. Naturhist. Foren.* **107:** 207–233.

Schacher, S., E. R. Kandel, and R. Woolley. 1979. Development of neurons in the abdominal ganglion of *Aplysia californica* II. Nonneural support cells. *Dev. Biol.* **71:** 176–190.

Scheltema, R. S. 1961. Metamorphosis of the veliger larvae of *Nassarius obsoletus* (Gastropoda) in response to bottom sediment. *Biol. Bull.* **120:** 92–109.

Scheltema, R. S. 1974. Biological interactions determining larval settlement of marine invertebrates. *Thalassia Jugosl.* **10:** 263–296.

Switzer-Dunlap, M., and M. G. Hadfield. 1977. Observations on development, larval growth and metamorphosis of four species of aplysiidae (Gastropoda: Opisthobranchia) in laboratory culture. *J. Exp. Mar. Biol. Ecol.* **29:** 245–261.

Tamburri, M. N., R. K. Zimmer-Faust, and M. L. Tamplin. 1992. Natural sources and properties of chemical inducers mediating settlement of oyster larvae: a re-examination. *Biol. Bull.* **183:** 327–338.

Tardy, J. 1970. Contribution a l'étude des métamorphoses chez les nudibranches. *Ann. Sci. Nat. Zool. Paris.* **12:** 299–370.

Todd, C. D., M. G. Bentley, and J. N. Havenhand. 1991. Larval metamorphosis of the opisthobranch mollusc *Adalaria proxima* (Gastropoda: Nudibranchia): the effects of choline and elevated potassium ion concentration. *J. Mar. Biol. Assoc. UK* **71:** 53–72.

Trapido-Rosenthal, H. G., and D. E. Morse. 1985. L-α,ω-Diamino acids facilitate GABA induction of larval metamorphosis in a gastropod mollusc. *J. Comp. Physiol. B* **155:** 403–414.

Trapido-Rosenthal, H. G., and D. E. Morse. 1986. Regulation of receptor-mediated settlement and metamorphosis in larvae of a gastropod mollusc (*Haliotis rufescens*). *Bull. Mar. Sci.* **39:** 383–392.

Uthe, D. 1995. Fine structure of the cephalic sensory organ in veliger larvae of *Littorina littorea*, (L.) (Mesogastropoda, Littorinidae). *Hydrobiologia* **39:** 45–52.

Walters, L. J., M. G. Hadfield, and C. M. Smith. 1996. Waterborne chemical compounds in tropical macroalgae: positive and negative cues for larval settlement. *Mar. Biol.* **126:** 383–393.

Wodicka, L. M., and D. E. Morse. 1991. cDNA sequences reveal mRNAs for two Gα signal transducing proteins from larval cilia. *Biol. Bull.* **180:** 318–327.

Woodin, S. A. 1986. Settlement of infauna: larval choice? *Bull. Mar. Sci.* **39:** 401–407.

Woodin, S. A. 1991. Recruitment of infauna: positive or negative cues? *Am. Zool.* **31:** 797–807.

Woodin, S. A., R. L. Marinelli, and D. E. Lincoln. 1993. Allelochemical inhibition of recruitment in a sedimentary assemblage. *J. Chem. Ecol.* **19:** 517–530.

Yool, A. J., S. M. Grau, M. G. Hadfield, R. A. Jensen, D. A. Markell, and D. E. Morse. 1986. Excess potassium induces larval metamorphosis in four marine invertebrate species. *Biol. Bull.* **170:** 255–266.

Reference: *Biol. Bull.* **199:** 251–256. (December 2000)

The Structure and Growth of the Statocyst in the Australian Crayfish *Cherax destructor*

LUKE FINLEY AND DAVID MACMILLAN*

Department of Zoology, University of Melbourne, Parkville, Victoria 3052, Australia

Abstract. The morphology of the statocyst of the Australian crayfish *Cherax destructor* was examined using scanning electron microscopy. It resembles in general structure, size, and position the statocysts of crayfish described previously, and the size and distribution of the fields of setae on the floor of the capsule are similar but not the same. Over the size range examined, the relationship between the carapace length, the length of the basal antennular segment, the diameter of the statocyst capsule, and the total number of setae are all linear. The number and position of setae on the floor of the statocyst capsule were mapped for animals in two size classes (small, *ca.* 20 mm; large, *ca.* 50 mm) to test for changes in their arrangement during growth. The change in the ratio of setal number to statocyst size between the two size classes was about three times greater for the anterior setal field than for the other fields. We propose that differential development of the setal fields may be related to changes in the force-monitoring requirements of the animals as they increase in size, but this remains to be experimentally tested.

Introduction

Many decapod crustaceans have paired equilibrium organs called statocysts in the basal segment of each antennule. Statocysts monitor spatial orientation and movement (Cohen, 1955; Schöne and Neil, 1977; Sekiguchi and Terazawa, 1997). Each statocyst is a sac-like epidermal invagination of cuticle with a number of mechanosensory setae inside, mainly on the ventral floor. These are typically associated with a dense mass of sand, the statolith. The setae can be adjacent to the statolith and free to move, adjacent and touching, or cemented to the sand grains of the statolith. When the statolith deflects a seta it stimulates the neurons innervating it, and setae can differ in their physiological responses to stimulation (Cohen, 1955, 1960; Breithaupt and Tautz, 1988; Cate and Roye, 1997). The position and movement of the animal determine the pattern of setal stimulation, which in turn determines the form of compensatory movements made by the appendages and body (Sandeman and Okajima, 1972; Schöne and Neil, 1977; Patton and Grove, 1992b).

The morphology and spatial arrangement of setae within the statocyst vary between species (Cohen, 1955; Kovalev and Kharkeevich, 1993; Sekiguchi and Terazawa, 1997), and it has been suggested that groups of features may be associated with higher taxonomic groupings (Sekiguchi and Terazawa, 1997). In the statocyst of the crayfish *Orconectes limosus*, Hertwig *et al.* (1991) identified four separate fields of innervated setae: a lateral group of two semicircles, an approximately fusiform medial group with its axis roughly parallel to the long axis of the statocyst, and a single row of proximal setae. These setae appeared to be morphologically identical internally, but they differed in length and diameter in different parts of the field. Whether they differ in their physiological responses has not been tested.

Although both structure and function of crustacean statocysts are well understood, their growth has not been described as it has for other cuticular sensors on the crayfish and lobster tailfan (Letourneau, 1976; Schmitz, 1992; Stuart and Macmillan, 1997) and other appendages (Sandeman and Sandeman, 1996; Macmillan *et al.*, 1998; Steullet *et al.*, 2000). Growth in crustaceans occurs by periodic shedding of the cuticle, a process known as ecdysis, or molting, the body increasing in size with each molt. As the body grows, the sensory representation from the integument may need to change to maintain appropriate sensory input and function. As new sensory structures can only be added to the cuticle when the animal molts, a comparison of sensory structures

Received 14 October 1999; accepted 31 August 2000.

* To whom correspondence should be addressed. E-mail: d.macmillan@zoology.unimelb.edu.au

in sequential molt stages reveals the order in which elements develop. Because of their accessibility, setae on the telson have been the subject of a number of developmental studies based on this principle. Letourneau (1976) found, for example, that the order of addition of sensory setae to the telson of *Procambarus clarkii* is a function of the growth of the animal. Schmitz (1992) described four functionally distinct setal types that are added at different rates. "Short smooth hairs" and "guard hairs" increase rapidly in number throughout development, whereas the number of two types of "feathered hydrodynamic hairs" remains relatively constant.

We describe here the basic structure of the statocyst in the Australian crayfish *C. destructor*, and the relationship between body size, basal antennal segment size, and statocyst capsule size over the size range of animals examined. We report the first data on the pattern of addition of setae within the capsule as the animal grows by comparing the statocysts from small and large individuals.

Materials and Methods

Individuals of *Cherax destructor* were obtained from a commercial hatchery at Bendigo, Victoria, Australia. They were kept in 50 × 20 × 120 cm aquaria under constant temperature with a normal 12-hour light/dark cycle, and were fed dried pellet food weekly.

Specimens with carapace lengths from 20 to 50 mm were examined. The animals were anesthetized by chilling in crushed ice for 30 min and were then decapitated. Statocysts were dissected from the dorsal surface of the basal segment of the antennules, and any extraneous tissue or adhesions were removed from around the cuticle of the statocyst with a fine paintbrush. The preparations were dehydrated in a series of ethanol solutions before being transferred to 100% ethanol for 12 h. After an additional 24 h in a desiccator, conducting graphite paint was used to glue the preparations to a scanning electron microscope stub. They were sputter coated with gold, and examined with a Phillips 505 scanning electron microscope. The images were processed using Adobe Photoshop Version 4.0. Measurements of carapace, basal segment of the antennule, and statocyst diameter were recorded for body index relationships, and comparisons were made using SYSTAT 6.0 for Windows.

Results

Location and general structure of the statocyst

The statocysts of *Cherax destructor* are in the dorsal region of the basal segment within the antennules (= first antennae; Fig. 1A, B). The statocyst is a cup-like invagination of the cuticle forming a cavity with a triangular, anteriorly facing opening on the dorsal surface. The opening is covered with a dense mat of setae that prevents entry of large foreign particles, effectively forming a closed capsule (Fig. 1B). The cavity itself is oval and slightly pointed posteriorly (Figs. 1C, 2A). The ventral floor of the cavity has an oval depression (Fig. 2A, B), and setae project dorsally through the cuticle adjacent to this. A statolith composed of fused sand grains sits in the depression (Fig. 2C).

Relationships between size of animal and size of antennule and cavity

The length of the basal segment of the antennule correlates closely with the carapace length ($n = 39$; $R^2 = 0.9711$; $P < 0.001$; Fig. 3A), so we were able to collect data on both body size and statocyst parameters from scanning micrographs of the local area. The length of the statocyst capsule increases linearly as a function of the size of the basal segment of the antennule ($n = 26$, $R^2 = 0.9546$; $P < 0.001$; Fig. 3A) and hence of the size of the animal.

Arrangement of setae and changes in distribution during growth

All of the setae on the base of the statocyst capsule of *C. destructor*, except those in the anterior part of the anterior setal field, are bound to the statolith (Fig. 2C). All setae that could be seen in scanning micrographs, because they were not obscured by the statolith, appeared to have the same external morphology (Fig. 2E), even though they varied in size. Because of the close association between the setae and the statolith, the process of removing it to examine the base of the capsule usually removed not only the setae but all associated tissues, including the tissues passing through the holes in the floor of the capsule. Remnants of these remained in a number of our preparations, however; these demonstrated that at least some of the setae are innervated through the holes in the base of the capsule (Fig. 2F). The presumption is that the holes represent innervation channels, as they do in other species (Hertwig *et al.*, 1991). The holes indicate the precise position of each seta on the floor of the capsule (Fig. 2A, B). Their disposition around the depression that normally holds the statolith resembles that in *Orconectes limosus* (Hertwig *et al.*, 1991), and direct correspondence with three of the four setal fields they described and named is apparent. A curved field made up of an inner double row and an outer single row forms a semicircle around the medial and posterior rim of the central depression. On the lateral side, this merges into the narrow end of a large triangle of setae occupying the area lateral to the rim of the depression. Opposite this large field, on the medial side of the depression, is a smaller triangular field. In an adult animal of around 50-mm carapace length, these fields are composed of about 68, 135, and 36 setae, respectively (Fig. 2D, Fig. 4) The total number of setae increases

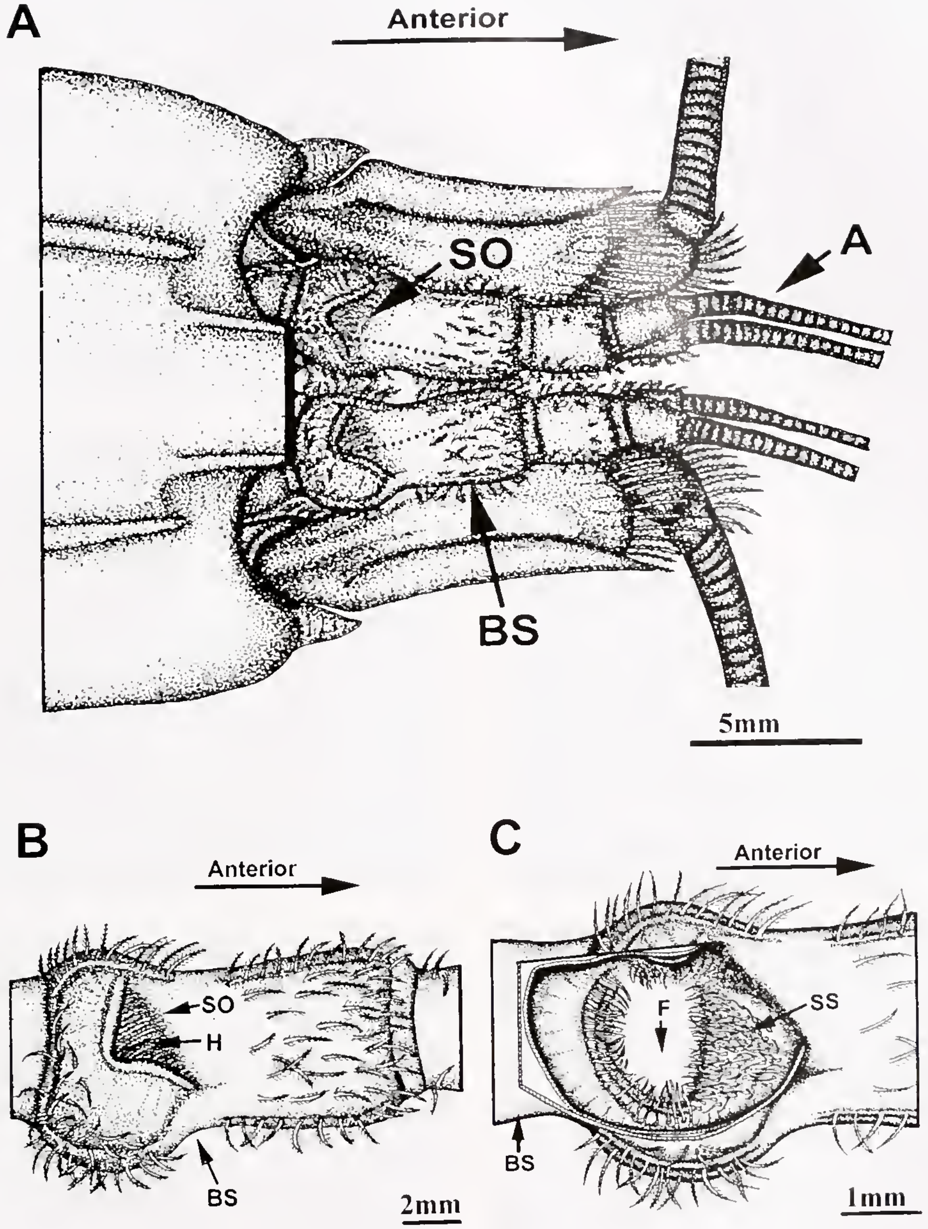

Figure 1. Morphology of antennular region and statocyst of the crayfish *Cherax destructor*. (A) Dorsal view of the basal segment (BS) of the antennule, and the location of the statocyst opening (SO). The rostrum and eyes have been removed. The position occupied by the rostrum is indicated by dotted lines. (B) Higher magnification of the basal segment (BS) of the antennule showing the dense screen of setae (H) that covers the statocyst opening (SO). (C) The statocyst capsule viewed through a window cut in the dorsal cuticle of the basal segment (BS) of the antennule to reveal the setae (SS) projecting upwards from the ventral floor (F) of the capsule. The statolith, with which all but the anterior setae make contact, has been removed.

linearly with the size of the animal ($n = 24$; $R^2 = 0.8663$; $P < 0.005$; Fig. 3B).

To examine the way in which this increase occurs, we counted the number of setae in a group of animals with a basal antennule length of 1.97 mm (SD = 0.19) ("small") and compared the result with a sample of animals with a basal antennule length of 5.75 mm (SD = 0.27) ("large"). The results of the survey are shown in Figure 4. A two-factor analysis of variance on the data testing for setal field type and size of animals showed that the large animals have significantly more setae in each field than the small animals ($F_{(1,50)} = 322.6$, $P < 0.01$), the number of setae in the three fields is significantly different ($F_{(2,50)} = 848.9$, $P < 0.01$), and the size of the difference varies between fields

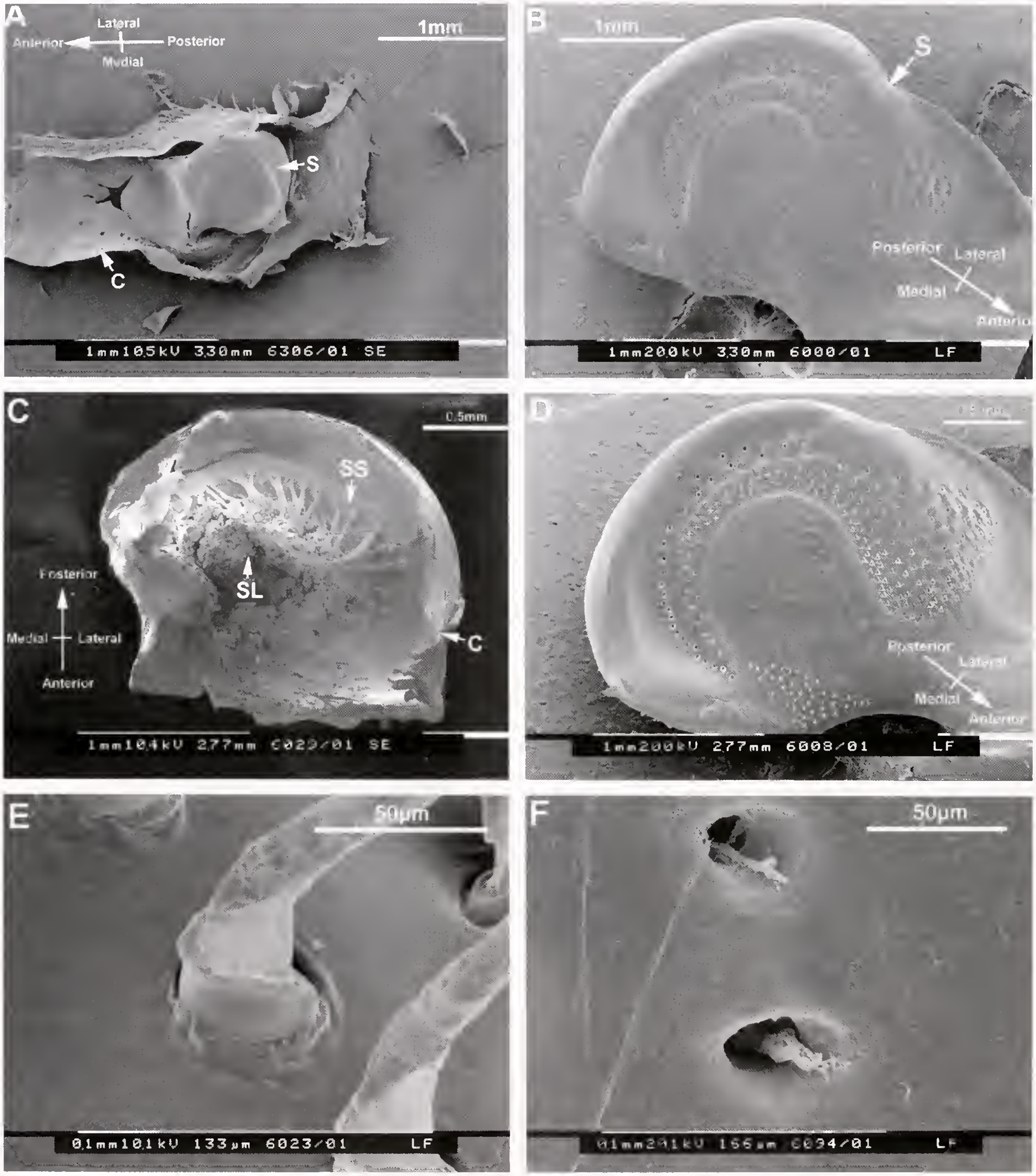
A
Lateral
Anterior
Posterior
Medial
1mm
S
C
1mm10.5kV 3.30mm 6306/01 SE
B
1mm
S
Posterior
Lateral
Medial
Anterior
1mm20.0kV 3.30mm 6000/01 LF
C
0.5mm
SS
SL
Posterior
Medial
Lateral
Anterior
C
1mm10.4kV 2.77mm 6029/01 SE
D
0.5mm
Posterior
Lateral
Medial
Anterior
1mm20.0kV 2.77mm 6008/01 LF
E
50µm
0.1mm10.1kV 133µm 6023/01 LF
F
50µm
0.1mm20.1kV 166µm 6034/01 LF

Figure 2. Scanning electron micrographs showing the statocyst of the crayfish *Cherax destructor.* (A) Dorsal view of the right antennule of an animal from the "small" group with part of the dorsal cuticle (C) cut away to reveal the floor of the capsule of the statocyst (S). The basal segment of this animal was 1.99 mm long. (B) Dorsal view of the floor of the statocyst (S) from the left antennule of an animal from the "large" group. The basal segment of this animal was 5.7 mm long. The magnification is the same in A and B so that the large increase in the number of setae in the anterior field is readily apparent. (C) Dorsal view of the statocyst capsule with part of the dorsal cuticle (C) removed to reveal the sensory setae (SS) in contact with the statolith (SL). Note that many of the setae in the anterior field do not contact the statolith. (D) Dorsal view of the ventral floor of the statocyst showing position of setae. The fields have been marked to correspond with the classification used previously in *Orconectes limosus.* △ Large anterior field (139 setae); curved field (69 setae): ○, outer row (29 setae); + inner rows (40 setae); ×, small field (46 setae). (E) High magnification view of base of a seta from the outer curved field viewed from the dorsal aspect. (F) High magnification view of the ventral surface of the same statocyst base as in E, showing holes beneath each seta and remnants of the mechanical and neural connections broken during the statocyst removal and preparation process.

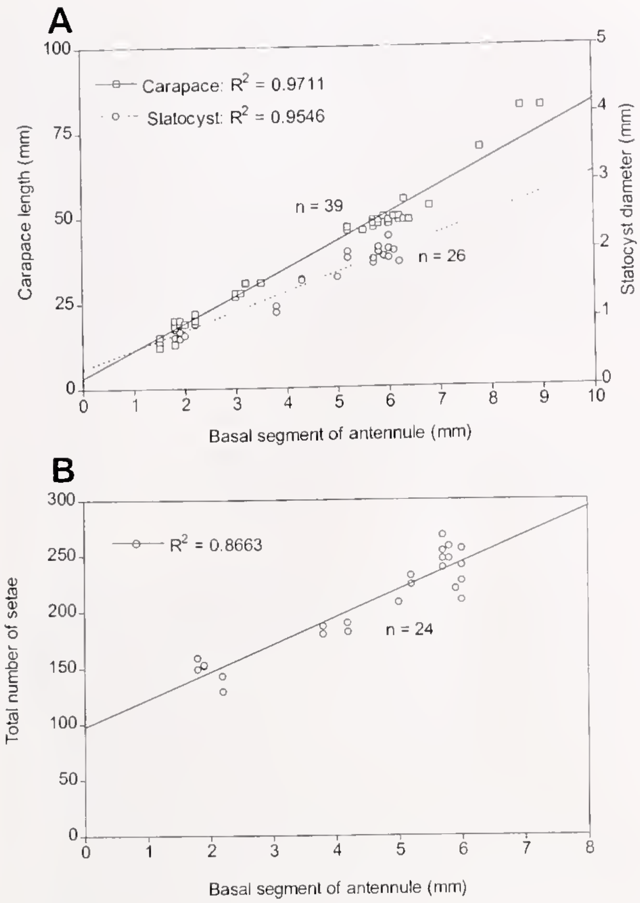

Figure 3. Statocyst size relationships. (A) Relationship between statocyst diameter, carapace length, and length of the basal segment of the antennule. The bold and dotted lines are the linear regression lines. Note the high correlation for both body measurement indices. (B) Relationship between length of basal segment of antennule and total number of setae within the statocysts. Note the high level of correlation between the base of the antennule (and hence body size) and the number of setae.

($F_{(2,50)} = 69.2$, $P < 0.01$). Tukey-Kramer pairwise comparisons between the three fields in both large and small animals showed that the number of setae is different in the three fields at the $P < 0.01$ significance level.

Discussion

The outcome of this work is straightforward. The result is a description of statocyst morphology in a previously undescribed crayfish species which permits some species comparisons to be made. In addition, this is the first report on changes in the size and setal arrangements of the statocyst with changing body size. The results therefore have implications for comparative and developmental questions.

In a mini-review, Sekiguchi and Terazawa (1997) compared information on statocysts across a range of crustacean species and found considerable morphological variation between taxonomic groupings but some evidence of consistency within them. The number of examples available, however, is probably not yet sufficient for a firm conclusion on this issue. The general morphology of the statocyst of *Cherax destructor* does appear, however, to be closely similar to that of other crayfish species examined (*Procambarus clarkii:* Takahata and Hisada, 1979; *Orconectes limosus:* Hertwig *et al.*, 1991). Because they used transmission electron microscopy as well as scanning electron microscopy, Hertwig *et al.* (1991) were able to show that all the setae on the floor of the statocyst capsule in *O. limosus* are morphologically identical. The external morphology of the setae in *C. destructor* suggests that they too may be of one type and probably even are closely similar to those in *O. limosus*. This does not, of course, mean that they are uniform in their physiological responses, because setae that appear closely similar may differ in their responses (Patton and Grove, 1992a). Irrespective of the way in which they transduce the detected forces into electrical signals, the positioning of different setae relative to the statolith must reflect the displacement forces that they can monitor (Cohen, 1955, 1960); thus the results suggest that further comparison of the arrangement of these elements across a range of species with differing lifestyles has the potential to reveal principles of statocyst structure and function.

Fortuitously, we were able to select specimens with a mean basal antennal segment length of 5.75 mm, which is close to the 5-mm length of *O. limosus* used by Hertwig *et al.* (1991), making comparisons between the fields in the two species less likely to be confounded by a size factor. They found four distinct groups of setae in *O. limosus*. Of these, three are clearly present in *C. destructor* and, in two cases, in comparable numbers: the curved field (*O. limosus: C. destructor* = 60:68), the large anterolateral field (135:<60), and the smaller medial field (30:36). The posterior line of 8 setae is not evident in *C. destructor*, but it is possible that they are part of the outer curved group but less

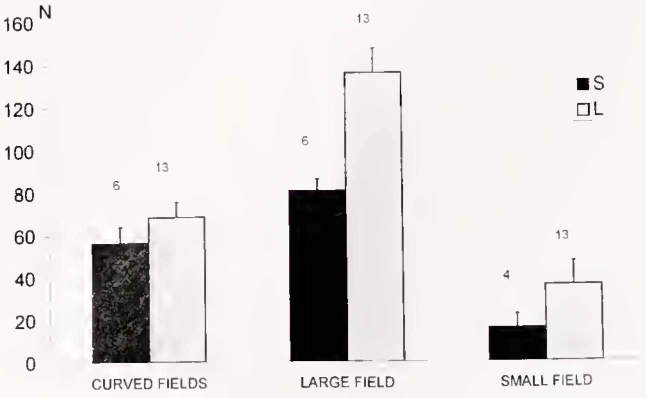

Figure 4. Comparison of the number of setae (N) in the different fields (curved, large, small) in a sample of small animals (S, mean basal antennal segment of 1.97 mm) and large animals (L, mean basal antennal segment of 5.75 mm).

distinctly separate than they are in *O. limosus*. If this were the case, the two species would both have about the same number of setae (*ca.* 68) in the posterolateral complex formed by these adjacent groups. In other decapod species studied, behavioral responses to stimulation of setae were found to correlate with the spatial location within the statocyst (Ozeki *et al.*, 1978; Kovalev and Kharkeevich, 1993). The curved and small fields occupy roughly the same position relative to the statolith in *O. limosus* and *C. destructor* and have approximately the same number of setae, all of which are attached to the statolith, an arrangement Cohen (1955) suggested as indicative of a prescribed output. It is therefore probable that they serve similar functions in terms of the requirements of the two species for positional information during behavior. In the lobster, setae in the lateral, posterior field respond to body roll, whereas setae anteriorly respond mostly to acceleration (Cohen, 1960). Although the argument rests on a body of cross-species data, it is likely that the body roll monitoring systems of *O. limosus* and *C. destructor* are similar. This then raises the interesting question of why the number of setae in the large anterior field differs so significantly between the two species.

In both *O. limosus* and *C. destructor*, the large anterior field differs from the other fields because many of the setae do not make contact with the statolith. Hertwig *et al.* (1991) argue that setae that are free of the statolith are most suited for detecting angular accelerations, an observation supported by behavioral observations in other species (Cohen, 1960; Patton and Grove, 1992a). The comparison of setal numbers in the different fields in the two size classes examined in our experiments showed that the ratio of change in the anterior free-field was about three times that seen in the small medial and the curved groups. Their rapid differential growth is therefore likely to correlate with the interaction between increasing body size and particular behavioral activities that involve a high degree of body mobility—activities such as three-dimensional movements in the water column or escape. The precise relationship between these behavioral considerations and the development of the statocyst remains to be determined.

Acknowledgments

We thank Dr. Jeremy Sullivan for suggesting this project and for advice on statocyst dissection and preparation. We thank Ms. Joan Clark for advice and assistance with the scanning electron microscopy, Dr. Zen Faulkes for assistance in preparing the figures, and Dr. Jo Drummond for suggestions and critical advice on late drafts of the manuscript. Supported by an Australian Research Council Grant to D. Macmillan.

Literature Cited

Breithaupt, T., and J. Tautz. 1988. Vibration sensitivity of the crayfish statocyst. *Naturwissenschaften* **75:** 310–312.

Cate, H. S., and D. B. Roye. 1997. Ultrastructure and physiology of the outer row statolith sensilla of the blue crab *Callinectes sapidus*. *J. Crustac. Biol.* **17:** 398–411.

Cohen, M. J. 1955. The function of receptors in the statocyst of the lobster *Homarus americanus*. *J. Physiol.* **130:** 9–34.

Cohen, M. J. 1960. The response patterns of single receptors in the crustacean statocyst. *Proc. R. Soc. Lond. B* **152:** 30–49.

Hertwig, I., H. Schneider, and J. Hentschel. 1991. Light- and electron microscopic analysis of the statocyst of the American crayfish *Orconectes limosus* (Crustacea, Decapoda). *Zoomorphology* **110:** 189–202.

Kovalev, V. A., and T. A. Kharkeevich. 1993. Studies on morphological and functional organisation of the statocyst receptor macula in the crayfish *Procambrus cubensis*. *J. Evol. Biochem. Physiol.* **29:** 117–119.

Letourneau, J. G. 1976. Addition of sensory structures and associated neurons to the crayfish telson during development. *J. Comp. Physiol.* **110:** 13–23.

Macmillan, D. L., T. Stuart, and M. Thomas. 1998. Development of a proprioceptive organ on the walking legs of rock lobsters (*Jasus edwardsii*) occurs by ordered addition and deletion of receptor elements. *J. Crustac. Biol.* **18:** 1–9.

Ozeki, M., T. Takahata, and H. Mituhiko. 1978. Afferent response patterns of the crayfish statocyst with ferrite grain statolith to magnetic field stimulation. *J. Comp. Physiol.* **123:** 1–10.

Patton, M. L., and R. F. Grove. 1992a. The response of statocyst receptors of the lobster *Homarus americanus* to movements of statolith hairs. *Comp. Biochem. Physiol.* **101A:** 249–257.

Patton, M. L., and R. F. Grove. 1992b. Statolith hair movements and the regulation of tonic gravity reflexes in the lobster *Homarus americanus*. *Comp. Biochem. Physiol.* **101A:** 259–268.

Sandeman, D. C., and A. Okajima. 1972. Statocyst-induced eye movements in the crab *Scylla serrata*. *J. Exp. Biol.* **57:** 187–204.

Sandeman, D. C., and R. E. Sandeman. 1996. Pre- and postembryonic development, growth and turnover of olfactory neurones in crayfish antennules. *J. Exp. Biol.* **199:** 2409–2418.

Schmitz, B. 1992. Post embryonic development of the crayfish *Procambarus clarkii* and its tailfan mechanosensory system. Pp. 69–90 in *Nervous Systems: Principles of Design and Function*, P. N. Singh, ed. Wiley Eastern, New Delhi.

Schöne, H., and D. M. Neil. 1977. The integration of leg position-receptors and their interaction with statocyst inputs in spiny lobsters. *Mar. Behav. Physiol.* **5:** 45–49.

Sekiguchi, H., and T. Terazawa. 1997. Statocyst of *Jasus edwardsii* pueruli (Crustacea, Palinuridae), with a review of crustacean statocysts. *Mar. Freshwater Res.* **48:** 715–719.

Steullet, P., H. S. Cate, and C. D. Derby. 2000. A spatio-temporal wave of turnover and functional maturation of olfactory receptor neurons in the spiny lobster, *Panulirus argus*. *J. Neurosci.* **20:** 3282–3294.

Stuart, T., and D. L. Macmillan. 1997. Development of sensory hairs on the telson of the Rock Lobster *Jasus edwardsii*. *Aust. J. Zool.* **45:** 307–315.

Takahata, M., and M. Hisada. 1979. Functional polarization of statocyst receptors in the crayfish *Procambarus clarkii* Girard. *J. Comp. Physiol.* **130:** 201–207.

Reference: *Biol. Bull.* **199:** 257–264. (December 2000)

Thermosensitivity of the Lobster, *Homarus americanus*, as Determined by Cardiac Assay

STEVEN H. JURY* AND WINSOR H. WATSON III

Zoology Department and Center for Marine Biology, University of New Hampshire, Durham, New Hampshire 03824

Abstract. It is generally accepted that crustaceans detect, and respond to, changes in water temperature, yet few studies have directly addressed their thermosensitivity. In this investigation a cardiac assay was used as an indicator that lobsters (*Homarus americanus*) sensed a change in temperature. The typical cardiac response of lobsters to a 1-min application of a thermal stimulus, either warmer (n = 19) or colder (n = 17) than the holding temperature of 15 °C, consisted of a short bradycardia (39.5 ± 8.0 s) followed by a prolonged tachycardia (188.2 ± 10.7 s). Lobsters exposed to a range of rates of temperature change (0.7, 1.4, 2.6, 5.0 °C/min) responded in a dose-dependent manner, with fewer lobsters responding at slower rates of temperature change. The location of temperature receptors could not be determined, but lesioning of the cardioregulatory nerves eliminated the cardiac response. Although the absolute detection threshold is not known, it is conservatively estimated that lobsters can detect temperature changes of greater than 1 °C, and probably as small as 0.15 °C. A comparison of winter and summer lobsters, both held at 15 °C for more than 4 weeks, revealed that although their responses to temperature changes were similar, winter lobsters (n = 18) had a significantly lower baseline heart rate (34.8 ± 4.4 bpm) and a shorter duration cardiac response (174 s) than summer lobsters (n = 18; 49.9 ± 5.0 bpm, and 320 s respectively). This suggests that some temperature-independent seasonal modulation of cardiac activity may be occurring.

Introduction

Temperature is one of the most important and pervasive environmental influences on the American lobster, *Homarus americanus* (Cobb and Phillips, 1980; Aiken and Waddy, 1986; Factor, 1995). It is generally accepted that locomotory activity in this species is temperature dependent (McLeese and Wilder, 1958; Reynolds and Casterlin, 1979; Haakonsen and Anoruo, 1994) and that it carries out seasonal inshore to offshore migrations to gain the developmental benefits of warmer coastal temperatures in the spring and summer (Cooper and Uzmann, 1971; Pezzack and Duggan, 1986; Karnofsky *et al.*, 1989; Haakonsen and Anoruo, 1994; Factor, 1995; Watson *et al.*, 1999). Laboratory studies have demonstrated that *H. americanus* has a thermal preference of about 16 °C (Reynolds and Casterlin, 1979; Crossin *et al.*, 1998), and it has been proposed that behavioral thermoregulation may allow members of the species to occupy thermal niches which maximize their metabolic or behavioral efficiency. The behavioral responses of lobsters to thermal gradients suggest they have some mechanism to *sense* temperature so that they may effectively respond to the thermal properties of their environment.

Thermosensitivity in lobsters may be mediated by distinct thermoreceptors or thermosensitive neurons as in some other invertebrates (Prosser and Nelson, 1981; Mori and Ohshima, 1995). Although behavioral studies strongly suggest that *H. americanus* can sense temperature (Reynolds and Casterlin, 1979; Crossin *et al.*, 1998), to our knowledge only one study has addressed how neurons respond to changes in temperature in this species. In that study, firing of cells associated with thoracic ganglia connectives generally showed no spontaneous activity below 14 °C, but most became spontaneously active above this temperature. Interestingly, these cells "cycle reversibly from silent to continuously active to bursting and back as the temperature is

---

Received 22 March 1999; accepted 14 August 2000.

*Present address: Caribbean Marine Research Center, Tequesta, FL 33469. E-mail: sjury@cmrc.org increased and decreased" (Konishi and Kravitz, 1978). Other than these cells, which may or may not play a role in thermally guided behaviors, we know little about the location of putative thermoreceptors, or the mechanisms used to detect temperature, in lobsters and most other crustaceans (Dorai Raj and Murray, 1962; Ache, 1982).

In situations where the precise receptors have not been identified, or are not readily accessible to electrophysiological investigation, cardiac assays are a valuable tool for preliminary investigations of sensory capabilities (Larimer, 1964; Offutt, 1970; Florey and Kriebel, 1974; Dufort, 1997). For example, many crustaceans exhibit a drop in heart rate in response to novel stimuli (Maynard, 1960; Larimer, 1964; McMahon and Wilkens, 1972; DeWachter and McMahon, 1996). This cardiac response has been used to measure the ability of *H. americanus* to detect sound (Offutt, 1970) and salinity (Dufort, 1997). Although a number of studies have addressed the effect of temperature on decapod heart rates at time scales ranging from hours to days (Ahsanullah and Newell, 1971; Florey and Kriebel, 1974; DeFur and Magnum, 1979; DeWachter and McMahon, 1996; DeWachter and Wilkens, 1996; Hokkanen and Demont, 1997), few have characterized the initial response (*i.e.*, <5 min.) to brief changes in water temperature. The present study used a cardiac assay to demonstrate that American lobsters are consistently capable of sensing increases or decreases in temperature that are greater than 1 °C. The typical response elicited by both cold and warm stimuli was a brief slowing of the heart rate, followed by prolonged cardioacceleration. Winter and summer lobsters responded somewhat differently to thermal stimuli, suggesting some type of seasonal temperature-independent modulation of their responsiveness to thermal stimuli.

Materials and Methods

Animals

Adult (82–92 mm carapace length), intermolt lobsters were held at 15 ± 1 °C (salinity 30 ± 1 ppt) for more than 4 weeks prior to use, and experiments were initiated at this temperature. All lobsters were captured from coastal New Hampshire waters, and experiments were conducted at the University of New Hampshire, Durham, New Hampshire. Experiments were carried out in both summer and winter under ambient light conditions. In the summer, the thermosensitivity of 18 lobsters was determined (cold stimuli, n = 9; warm stimuli, n = 9); in the winter, lobsters kept at the same temperature (15 °C) as summer lobsters were used in identical experiments (cold stimuli, n = 8; warm stimuli, n = 10).

Recording of temperature and heart activity

Small wire electrodes were inserted through the dorsal carapace above the heart and used with a UFI impedance converter (model #2991) to record heart rate (Dyer and Uglow, 1970). Because the impedance recording technique can be sensitive to temperature, the method was verified by using a second pair of electrodes and a Grass model 7D polygraph to simultaneously monitor the electrical activity associated with lobster heart contractions (see Watson and Wyse, 1978; Watson, 1980). External temperature was recorded using a small (3 mm × 1 mm) thermistor (C & B Sciences/iWorx, Inc., Dover, NH) placed on the dorsal carapace. The thermistor was calibrated weekly over the range of temperatures used in the experiments. The time constant of the thermistor was 2.0 s (time to achieve 67% of the final response). The absolute resolution of the thermistor was ±0.15 °C, but it could accurately detect *changes* in temperature as small as 0.01 °C. However, because of turbulent mixing within the recording chamber, the slight time delay due to the time constant of the thermistor (Fig. 1), and the unknown location of temperature-sensitive neural elements relative to the location of the thermistor, it was not possible to assess the thermal detection threshold with great accuracy. All temperatures presented are those recorded by the externally located thermistor above the dorsal carapace. These should be interpreted conservatively, in the context of the methods used and the unknown location of the sensory receptors.

Experimental chamber

After insertion of the electrodes, lobsters were placed in a recording chamber consisting of an 18-cm-diameter PVC pipe covered on the top and bottom by perforated plates through which seawater (temperature 15 ± 1 °C) continuously flowed (Fig. 1). This arrangement kept lobsters relatively immobile and ensured that changes in temperature within the recording chamber were rapid and relatively homogeneous. The chamber was placed in an acrylic plastic insert (30 × 30 × 30 cm) that was immersed in a temperature-controlled 120-l aquarium (the ambient bath). Ambient seawater was continuously pumped (2 l/min) from the aquarium through the recording chamber, into the insert, and back to the aquarium. Thermal stimuli were delivered by switching the source of seawater from the ambient bath to the stimulus bath. This switching was accomplished by turning a stopcock and was considered the initiation of the stimulus (see arrows in Fig. 2). The stimulus bath was filled from the ambient bath to minimize novel chamber chemosensory cues (Fig. 1) and brought to the appropriate experimental temperature using aquarium heaters or cooling coils. The recording chamber was covered with black plastic to minimize visual disturbance, and the lobster was left in the experimental apparatus overnight before an experiment. Lobsters are much more sensitive to stimuli if allowed to recover from electrode insertion and become accustomed to the recording chamber (Larimer, 1964; Dufort, 1997).

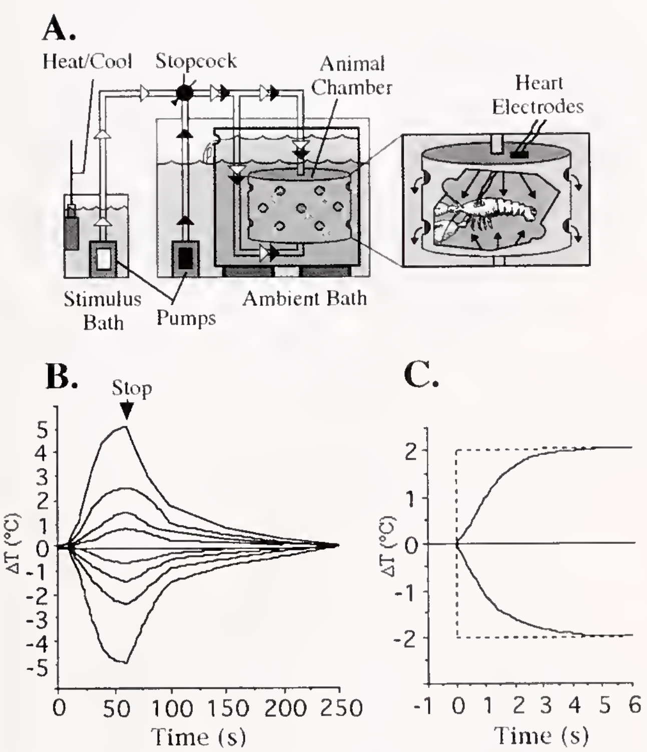

Figure 1. Experimental apparatus used to record lobster cardiac responses to changes in temperature. (A) Seawater (15 °C) flows continuously from the ambient bath into the animal chamber through perforated plates located above and below the lobster (direction of flow indicated by dark arrows). Heart rate is recorded before, during, and after exposure to a temperature stimulus. Switching the stopcock changes the source of seawater from the ambient bath to seawater from the stimulus bath (direction of flow indicated by white arrows). A thermistor on the dorsal carapace is used to monitor temperature during each trial. (B) Rates of temperature change in a typical experiment in response to 1 min stimuli (turned on at time = 0 and off at arrow) of ± 0.7, 1.4, 2.6, and 5.0 °C warmer or colder than the ambient temperature. (C) Time constant of the thermistor when exposed to a step change in temperature of ± 2 °C (dotted line). The estimated time to achieve 67% of final temperature is 2.0 s.

The following day, after basal heart rate was measured for at least 30 min, each animal was exposed for 1 min to a warm or cold stimulus that changed the temperature in the recording chamber at a rate of ±0.7 °C/min. This was followed by stimuli delivered at targeted rates of ±1.5 °C/min, ±2.5 °C/min, and ±5.0 °C/min for 1 min. Temperature was allowed to return to ambient (Fig. 2) between each treatment. Treatments were separated by at least 30 min. The temperature in the recording chamber was monitored with the dorsally located thermistor, and the actual mean rates achieved were 0.72 ± 0.04, 1.37 ± 0.06, 2.61 ± 0.10, and 4.95 ± 0.16 °C/min. Thus, the average maximum warm stimuli after 60 s were 15.7, 16.4, 17.6, and 20.0 °C, and the maximum cold stimuli were 14.3, 13.6, 12.4, and 10.0 °C.

Which stimulus (warm or cold) was tested on the first day was assigned randomly, and the other set of stimuli (warm or cold) were tested on the following day. A 25% change in heart rate—bradycardia (decrease) or tachycardia (increase)—was used as an indicator that lobsters sensed a change in water temperature (Offutt, 1970; Dufort, 1997). All records were digitized using a MacLab system (C & B Sciences/iWorx, Inc.) and were analyzed to determine the following: (1) delay to a response; (2) duration of bradycardia, tachycardia, or both; (3) heart rate (bpm) during bradycardia; and (4) heart rate (bpm) during tachycardia. In addition, thermosensitivity thresholds were estimated from the water temperature measured above the dorsal carapace at the time of the initial cardiac response. Controls were conducted before any thermal stimuli were applied; the same protocol described above was followed, but without changing the temperature in the stimulus bath.

Localization of putative temperature receptors

In an attempt to localize regions with putative temperature receptors, lobsters missing antennae ($n = 4$) or missing antennae and antennules ($n = 4$) were tested for a response to a temperature change of +2.5 °C/min. Antennae or antennules were removed bilaterally at their base, the wounds were sealed with wax to prevent blood loss, and the lobsters were allowed more than 24 h to recover.

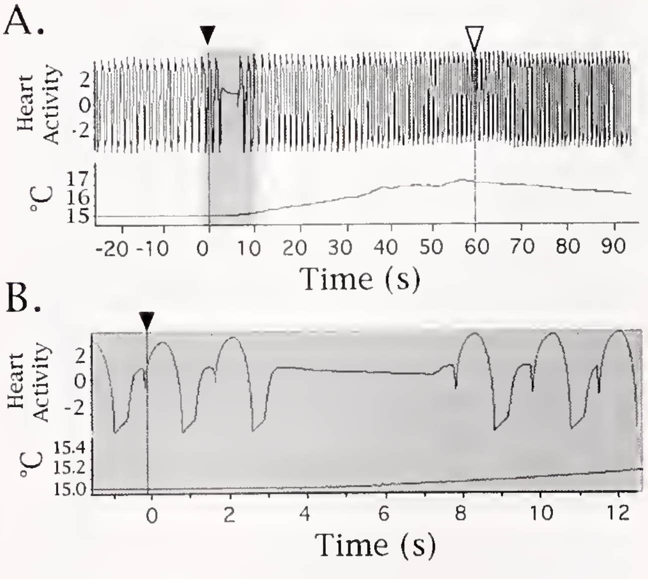

Figure 2. Typical cardiac response to a change in temperature. (A) The top trace shows the typical response to a +1.4 °C/min stimulus; the lower trace is a plot of the temperature change during the 60-s trial. The dark closed arrow shows when the stimulus flow was turned on, and the white open arrow shows when it was turned off. (B) An enlargement of the highlighted area from (A), showing the time course of the bradycardia and associated temperature change. Note that the rapid response may be a result of the combination of the location of the thermistor relative to the location of the unknown temperature sensitive receptors and the slight delay due to the time constant of the thermistor. There was no response to controls when the flow was switched but the temperature was not changed.

To determine whether changes in cardiac activity were mediated by the cardioregulatory nerves, responses to thermal stimuli were measured before and after nerve lesions (n = 5). Changes in heart rate were initially recorded in response to thermal stimuli of +1.5 °C/min and −1.5 °C/min. Then the cardioregulatory nerves were cut, and lobsters were allowed at least 2 days to recover. Finally their cardiac responses were measured again in response to the same stimuli that were applied before the lesions. Lesions were made as described in Guirguis and Wilkens (1995). A small (3-cm^2) rectangular piece of dorsal carapace just above the heart was removed, and superficial cuts were made with fine scissors through the connective tissue along the border of the opening. The shell was then replaced and fastened in place with tape. Sham-operated control animals (n = 4) were treated in the same manner except that no cuts were made in the connective tissue.

Statistical analysis

Throughout the text, variation is presented as standard error of the mean (*i.e.*, mean ± SEM). A P value of <0.05 was considered to be significant for all statistical tests.

Results

Typical response to a change in temperature

The typical cardiac response to both warm and cold stimuli consisted of a short bradycardia (39.5 ± 8.0 s), followed by a significantly (paired t test) longer tachycardia (188.2 ± 10.7 s; Fig. 2). In general, changes in heart activity were similar in response to both warm (n = 19) and cold (n = 17) stimuli. Although the intensity and duration of cardiac responses were similar for all temperatures tested (ANOVA, $P > 0.05$), some lobsters did not respond to slower rates of change (0.7 and 1.4 °C/min), whereas almost all lobsters responded to the maximum rate of change (5.0 °C/min; Fig. 3). There was no cardiac response in control trials (n = 36), where temperature was not changed but ambient water was pumped through the chamber from the stimulus bath (Fig. 4).

Sensitivity to warm and cold stimuli

Lobsters were extremely sensitive to both warm and cold stimuli (Fig. 3). For example, when subjected to a +2.6 °C/min stimulus, lobsters responded after just 3.8 ± 0.5 s, when the temperature in the chamber had changed by only 0.09 ± 0.04 °C. Lobsters exposed to the −2.6 °C/min stimulus responded after a drop of only 0.13 ± 0.09 °C, and the latency to respond (4.6 ± 1.8 s) was not significantly different (paired t test) than during a warm stimulus (Fig. 3).

Temperature change measured at the initiation of a cardiac response by individual lobsters ranged from 0.01 to 0.79 °C. There were no significant differences (unpaired t test) between the sexes in the temperature change at initial response; when lobsters responded, they exhibited comparable thresholds, at all measured rates of change (Fig. 3, Kruskal-Wallis test). The average temperature-detection threshold, for all trials in which animals responded, was 0.15 ± 0.03 °C. This is considered to be only an estimate because of the inherent time constant and resolution of the thermistor, the flow of water in the chamber, and the location of the thermistor relative to the still *unknown* location of the receptors mediating the response. Nonetheless, this assay demonstrates that lobsters are sensitive to very small changes in temperature.

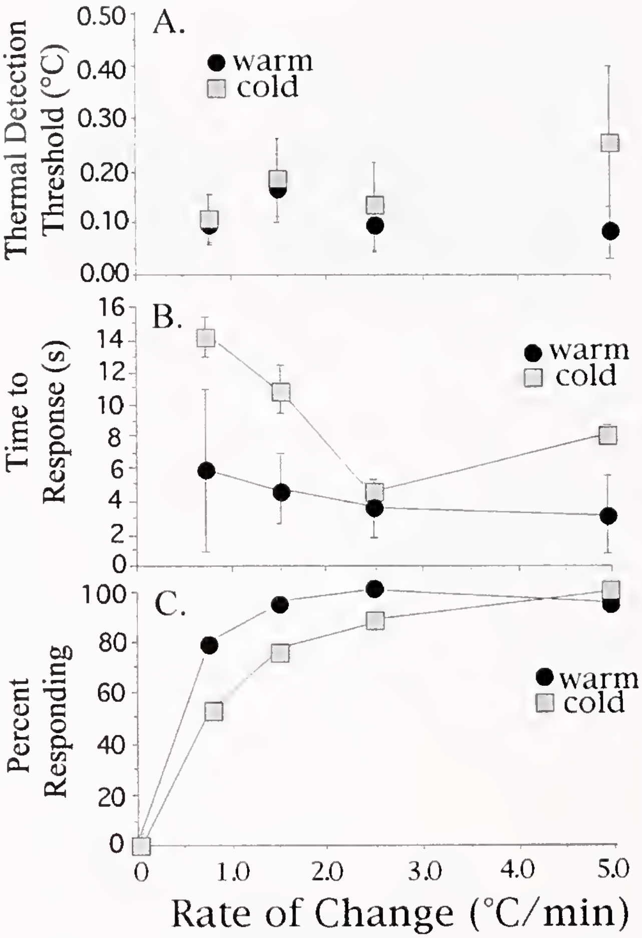

Figure 3. Responses to thermal stimuli at different rates of change. (A) The thermal detection threshold, or the amount of temperature change required to elicit a cardiac response, was similar even when hot and cold stimuli were applied at different rates. (B) When thermal stimuli were applied at slow rates of change, the delay to respond was longer, especially in the case of cold stimuli. (C) Although lobsters responded similarly to thermal stimuli applied at fast and slow rates of change, some animals did not respond at all to slow rates of change, while all animals responded to higher rates of change.

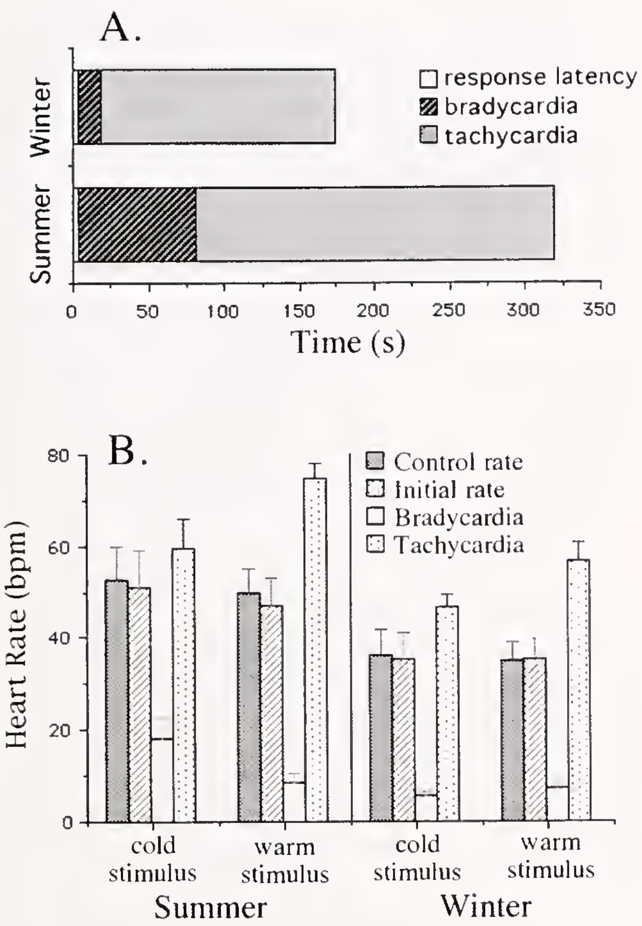

Figure 4. Responses to cold and warm stimuli by summer and winter animals. (A) The mean response latency, duration of bradycardia, and duration of tachycardia in response to ± 2.6 °C/min stimuli in both summer and winter lobsters. While the latency to respond, and thus thresholds, were similar between seasons, the duration of both bradycardia and tachycardia responses tended to be longer in summer animals. (B) Differences in the responsiveness of summer and winter lobsters. For all treatments, an application of control 15 °C stimuli to lobsters held at 15 °C did not cause a statistically significant change in heart rate. Lobsters in both seasons responded to ± 2.6 °C/min stimuli with a short bradycardia followed by a longer tachycardia. The major difference between summer and winter lobsters, other than the duration of responses shown in A, was that animals in the winter had significantly lower initial heart rates. Thus, although all animals were held at 15 °C, there appears to be some temperature-independent seasonal modulation of heart rate.

Localization of receptors

All lobsters with ablated antennae ($n = 4$) or ablated antennae and antennules ($n = 4$) showed typical responses to a stimulus of +2.5 °C/min. There was no significant difference (unpaired t tests) in the duration of bradycardia and tachycardia, the thermosensitivity threshold, or the baseline heart rate when compared to intact lobsters ($n = 18$).

Prior to cardioregulatory nerve lesions, lobsters ($n = 5$) had a mean heart rate of 41 ± 2.9 bpm. Following recovery, their heart rate increased to 70 ± 5.3 bpm, which was significantly higher (paired t test) than the basal rate. This increase may not have been due solely to the lesion of the cardioregulatory nerves: sham-operated controls ($n = 4$) also had heart rates (48 ± 9.4 bpm) that were slightly higher than their pre-operation baselines (37 ± 5.4 bpm), although that difference was not significant (paired t test). In response to a hot or cold stimulus, all lobsters exhibited typical bradycardia and tachycardia responses before cardioregulatory nerve lesioning. However, after lesioning none of the lobsters showed an increase or decrease in heart rate in response to thermal stimuli. In contrast, all of the sham-operated lobsters showed typical responses (100% showed both bradycardia and tachycardia) when exposed to identical thermal stimuli. These data indicate that the change in heart rate elicited by warm and cold stimuli is mediated by the cardioregulatory nerves and not by the direct influence of temperature on the heart itself.

The influence of season

The characteristic cardiac response of lobsters to a change in temperature (a short bradycardia followed by a longer tachycardia) was similar for lobsters tested in the winter and those tested in the summer. However, the following differences were apparent: (1) the mean baseline heart rate was significantly lower (unpaired t test) in winter lobsters (34.8 ± 4.4 bpm) than in summer lobsters (49.9 ± 5.0 bpm; Fig. 4); (2) the duration of bradycardia and tachycardia responses tended to be shorter in the winter lobsters (unpaired t tests, $P < 0.1$); and (3) winter lobsters tended to respond to temperature changes with both tachycardia (83%) and bradycardia (72%), whereas only 50% of the summer lobsters responded with tachycardia, but 94% showed bradycardia. Thus, even though winter and summer lobsters were both held at 15 °C for at least one month and tested with identical warm and cold stimuli, they responded differently. This difference may be related to the observed seasonal differences in basal physiological state (Fig. 4).

Discussion

This study supports the findings of two previous behavioral studies which infer that American lobsters can sense changes in temperature (Reynolds and Casterlin, 1979; Crossin *et al.*, 1998). Assuming that the initiation of a cardiac response indicates detection of an environmental change, our conservative estimate is that lobsters can sense both increases and decreases in water temperature of greater than 1 °C (Fig. 3) and probably as small as 0.15 °C. Similar thermal sensitivity has been documented in a number of terrestrial arthropods (Murphy and Heath, 1983; Altner and Loftus, 1985). For example, the spider *Cupiennius salei* has a warm receptor with a detection threshold between 0.08

and 0.6 °C (Ehn and Tichy, 1996). Studies of thermoreception in aquatic species are fewer, but are consistent with our findings. For example, Forward (1990) found that crab larvae (*Rhithropanopeus harrisii* and *Neopanope sayi*) ascend or descend in a water column in response to absolute temperature changes of 0.29–0.49 °C, as long as the rate of change is fast enough (0.06–0.24 °C/min, depending on larval stage and species). Thus, the American lobster is probably not unusual in its ability to detect small changes in temperature, although the extent to which this level of thermosensitivity exists in other crustaceans remains to be investigated.

Although several behavioral studies indicate that crustaceans are quite sensitive to changes in temperature, little is known about thermosensitivity in this large group of primarily aquatic invertebrates. A study of the thermal sensitivity of the dactyl receptors of *Cancer antennarius*, *C. anthonyi*, and *Panulirus interruptus* strongly suggests that they possess a thermal sensory system capable of integrating temperature information for use in thermally cued behavior (Cook, 1984). However, the actual thermoreceptors have not been identified in these species. In lobsters, a number of neurons change their rate of firing in response to shifts in temperature, but it is not clear if these cells are actually serving the function of thermoreceptors. For example, intracellular recordings from cells of the thoracic ganglia connectives of *H. americanus* show firing patterns that reversibly change from silent to continuously active to bursting over the range of 10–17 °C (Konishi and Kravitz, 1978). This is within the normal ecological range for this species, and while it is unknown what physiological or motor output results from this neuronal property, the correspondence to the behaviorally determined preferred temperature (16 °C; Crossin *et al.*, 1998) for this species is intriguing. In the spiny lobster, *Panulirus japonicus*, ligamental nerves innervating the pericardial organ have also been reported to increase their firing in response to cold stimulation (Kuramoto and Tani, 1994). Once again, temperature stimuli were shown to have a direct physiological effect *in vitro*, but it is unknown how, or if, this effect is related to the existence of thermoreceptors or behavioral thermoregulation. Ablation studies indicate that lobsters missing antennae or antennules respond to temperature just like intact animals, suggesting that while these appendages may or may not contain thermosensitive elements, they are not necessary in order for lobsters to exhibit a cardiac response to temperature. Thus, while localization of receptors and mechanisms of thermoreception are beginning to be elucidated in some invertebrates (Mori and Ohshima, 1995; Komatsu *et al.*, 1996; McCleskey, 1997), it remains unclear exactly where and how crustaceans are sensing temperature (Ache, 1982).

Although gradual changes in temperature have a profound, well-documented influence on the metabolism and cardiovascular function of lobsters (Mercaldo-Allen and Thurberg, 1987; McMahon, 1995; Whiteley *et al.*, 1995; DeWachter and McMahon, 1996), brief decreases in heart rate following acute temperature changes are also common in lobsters and many crustaceans (McMahon and Wilkens, 1972; McMahon, 1995; DeWachter and McMahon, 1996). It is unlikely that these acute responses are due to a direct impact of temperature on the heart for the following reasons: (1) lobsters with cut cardioregulatory nerves do not change their heart rate in response to acute temperature changes; (2) Q_{10} values for heart rates of intact lobsters generally range from 1.5 to 2.5 (Mercaldo-Allen and Thurberg, 1987; Schreiber *et al.*, 1998), but excised lobster hearts are not very sensitive to changes in temperature over the range of 12 to 19 °C, and they generally have lower Q_{10} values than intact lobsters over the same range (Schreiber *et al.*, 1998; Jury, unpublished data); (3) the initiation of a cardiac response is immediate and robust, and the response extends well beyond the duration of a temperature stimulus (Fig. 2); and (4) the response is similar (*i.e.*, bradycardia followed by tachycardia) whether warm or cool stimuli are applied (Fig. 3). Therefore, although temperature can have a long-term, direct influence on heart rate and cause release of modulatory substances from the pericardial organs of lobsters (Kuramoto and Tani, 1994), all current data strongly suggest that in lobsters some type of thermosensitive mechanism senses a change in temperature, and this leads to a change in heart rate through activation of inhibitory or excitatory cardioregulatory nerves.

Lobsters do not appear to have seasonal differences in their ability to detect temperature. However, winter lobsters have lower basal heart rates and respond to temperature somewhat differently than summer lobsters. These differences suggest the presence of some type of seasonal modulation of the lobster cardiovascular system, similar to the actions of thyroid hormones in frogs (Miller and Mizell, 1972). Biogenic amines, such as serotonin and octopamine, have been shown to increase cardiac output. Seasonal changes in circulating levels of these, or similar, neuromodulators might increase basal heart rates in the summer or alter how the heart responds to input from cardioregulatory nerves (Fingerman *et al.*, 1994; Wood *et al.*, 1995; Weiger, 1997). This type of seasonal modulation is likely to influence responses to a variety of stimuli, in addition to temperature. The precise mechanisms underlying these seasonal changes in the cardiovascular system of crustaceans remain to be resolved. A recent study of blue crabs, *Callinectes sapidus*, which documented seasonal differences in their behavioral responses to injected biogenic amines and proctolin (Wood *et al.*, 1995), suggests that seasonal variability in the expression of receptors may be the mechanism.

The rate of temperature change may be an important variable in detection of thermal shifts in the environment. The lobsters in this study responded to rates as low as 0.7

°C/min, and there was no statistically significant difference between the thermal-detection thresholds obtained over the range of rates tested. We did not attempt to determine the slowest rate of change they were able to detect, but we did find that some lobsters did not respond at all to the slower rates of change used in our experiments (0.7–1.4 °C/min). Florey and Kriebel (1974) found that in *Cancer* species, the rate of change must be greater than 0.33 °C/min to "avoid hysteresis effects." This is interpreted as meaning that acute bradycardias or tachycardias were seen at rates of change faster than this, but only long-term changes in heart rate were observed at slower rates. Crab larvae (*R. harrisii*) descend in the water column when the temperature is elevated at rates ranging from 0.07 to 0.24 °C/min, and they ascend when the temperature decreases at rates of 0.06 to 0.1 °C/min. However, "the average absolute amounts of temperature change needed to evoke a response was independent of the rate of change at rates above threshold and ranged from 0.29 to 0.49 °C" (Forward, 1990). Seasonal changes in water temperature in some lobster habitats (*e.g.*, coastal New Hampshire) can range from 0 to 25 °C, but rates of change may be too slow to directly stimulate putative lobster thermoreceptors. However, tidal changes or thermoclines may change fast enough to be detected. We have measured rates of temperature change as high as 0.33 °C/min in the Great Bay estuary, although average rates are about 0.004 °C/min (based upon hourly Licor CTD readings, R. Langan, University of New Hampshire, Durham, unpublished data). Some studies have also found lobsters to aggregate at thermoclines (Ennis, 1984; Estrella and Morrissey, 1997). Movement of a lobster (or an appendage) within a thermally heterogeneous habitat may increase the realized rate of change to the point at which temperatures fall within the detection range. In addition, movement of water (*i.e.*, a current) past a stationary or moving lobster could also increase the rate of change if the water was thermally heterogeneous. Thus, under appropriate conditions, the combination of mobility and sensitivity to small temperature changes may provide lobsters with sufficient information to behaviorally thermoregulate in their natural habitat in the same manner observed in small thermal gradient tanks (Crossin *et al.*, 1998). Nonetheless, although lobsters can apparently use temperature as a cue in habitat selection (Reynolds and Casterlin, 1979; Crossin *et al.*, 1998), the neural mechanisms giving rise to thermally guided movements are unknown.

In this study we used changes in heart rate to determine the sensitivity of lobsters to thermal stimuli. While this assay is useful for determining an animal's ability to sense small changes in temperature, it is not known whether lobsters exhibit similar changes in heart rate when they encounter thermal shifts in their natural habitat. Crustaceans held for more than12 h in a state of "sensory deprivation" have been reported to be much more responsive to a variety of environmental stimuli (Offutt, 1970; Florey and Kriebel, 1974); thus, the sensitivity of lobsters to temperature may have been enhanced in our experiments. In contrast, lobsters that are not given time to recover from handling have high basal heart rates and often do not exhibit typical responses to environmental stimuli. Thus, although lobsters in their natural habitat can probably sense very small changes in water temperature, these thermal stimuli may not always lead to the types of cardiac responses observed in quiescent laboratory animals. This hypothesis is being tested by recording from freely moving lobsters subjected to acute changes in temperature as they move spontaneously through thermal gradients.

Acknowledgments

We thank the following people for helping to make this project possible: Heather Jury, Chris Dufort, Jim Newcomb, Paul Bartell, Christina Rockel, and Glen Crossin. Special thanks to Dan O'Grady for conducting the cardioregulatory nerve lesion experiments; Hunt Howell at the UNH Coastal Marine Lab for supplying animals; Rich Langan at the UNH Jackson Estuarine Lab for housing animals; Dan Reves for drawings; and Cliff Bredneberg and Ashish More of C & B Sciences, Inc., for technical assistance. This work was supported by USDA (Hatch) and NOAA (Sea Grant) grants to WHW and by UNH Graduate student enhancement and Center for Marine Biology Grants to SHJ. This study was part of the doctoral dissertation research of SHJ. This manuscript was greatly improved by the comments of three anonymous reviewers. This is contribution #355 of the UNH Center for Marine Biology Series.

Literature Cited

Ache, B. W. 1982. Chemoreception and thermoreception. Chapter 8, pp. 390–391, in D. Bliss, ed., *The Biology of Crustacea. Neurobiology: Structure and Function, Vol. 3.* Academic Press, New York.

Ahsanullah, M., and R. C. Newell. 1971. Factors affecting the heart rate of the shore crab *Carcinus maenas (L.). Comp. Biochem. Physiol.* **39A:** 277–287.

Aiken, D. E., and S. L. Waddy. 1986. Environmental influence on recruitment of the American lobster, *Homarus americanus:* a perspective. *Can. J. Fish. Aquat. Sci.* **43(11):** 2258–2270.

Altner, H., and R. Loftus. 1985. Ultrastructure and function of insect thermo- and hygroreceptors. *Annu. Rev. Entomol.* **30:** 273–295.

Cobb, J. S., and B. F. Phillips. 1980. *The Biology and Management of Lobsters, Vol. 1. Physiology and Behavior.* Academic Press, New York.

Cook, D. P. 1984. Chemoreception, thermoreception and osmoreception in three marine decapod crustaceans. Ph.D. dissertation. University of California, Santa Barbara. 140 pp.

Cooper, R. A., and J. R. Uzmann. 1971. Migrations and growth of deep-sea lobsters, *Homarus americanus. Science* **171:** 288–290.

Crossin, G., S. A. Al-Ayoub, S. H. Jury, W. H. Howell, and W. H. Watson III. 1998. Behavioral thermoregulation in the American lobster (*Homarus americanus*). *J. Exp. Biol.* **201:** 365–374.

deFur, P. L., and C. P. Magnum. 1979. The effects of environmental variables on the heart rates of invertebrates. *Comp. Biochem. Physiol.* **62A:** 283–294.

DeWachter, B., and B. R. McMahon. 1996. Temperature effects on heart performance and regional hemolymph flow in the crab, *Cancer magister. Comp. Biochem. Physiol.* **114A(1):** 27–33.

DeWachter, B., and J. L. Wilkens. 1996. Comparison of temperature effects on heart performance of the Dungeness crab, *Cancer magister, in vitro* and *in vivo. Biol. Bull.* **190:** 385–395.

Dorai Raj, B. S., and R. W. Murray. 1962. Non-myelinated nerves as a model for thermoreceptors. *Comp. Biochem. Physiol.* **5:** 311–317.

Dufort, C. 1997. Detection of salinity by the American lobster, *Homarus americanus.* M.S. Thesis. University of New Hampshire, Durham.

Dyer, M. F., and R. F. Uglow. 1970. On a technique for monitoring heart and scaphognathite activity in Natantia. *J. Exp. Mar. Biol. Ecol.* **27:** 117–124.

Ehn, R., and H. Tichy. 1996. Response characteristics of a spider warm cell: temperature sensitivities and structural properties. *J. Comp. Physiol. A* **178:** 537–542.

Ennis, G. P. 1984. Small-scale seasonal movements of the American lobster *Homarus americanus. Trans. Am. Fish. Soc.* **113:** 336–338.

Estrella, B. T., and T. D. Morrissey. 1997. Seasonal movement of offshore American lobster, *Homarus americanus,* tagged along the eastern shore of Cape Cod, Massachusetts. *Fish. Bull.* **95:** 466–476.

Factor, J. R. (ed.). 1995. *Biology of the Lobster* Homarus americanus. Academic Press, San Diego, CA.

Fingerman, M., R. Nagabhushanam, R. Sarojini, and P. S. Reddy. 1994. Biogenic amines in crustaceans: identification, localization, and roles. *J. Crustac. Biol.* **14:** 413–437.

Florey, E., and M. E. Kriebel. 1974. The effects of temperature, anoxia and sensory stimulation on the heart rate of unrestrained crabs. *Comp. Biochem. Physiol.* **48A:** 285–300.

Forward, R. B. 1990. Behavioral responses of crustacean larvae to rates of temperature change. *Biol. Bull.* **178:** 195–204.

Guirgis, M. S., and J. L. Wilkens. 1995. The role of the cardioregulatory nerves in mediating heart rate responses to locomotion, reduced stroke volume and neurohormones in *Homarus americanus. Biol. Bull.* **188:** 179–185.

Haakonsen, H. O., and A. O. Anoruo. 1994. Tagging and migration of the American lobster *Homarus americanus. Rev. Fish. Sci.* **2(1):** 79–93.

Hokkanen, J. E. I., and M. E. DeMont. 1997. Complex dynamics in the heart of the lobster *Homarus americanus. Can. J. Zool.* **75:** 746–754.

Karnofsky, E. B., J. Atema, and R. H. Elgin. 1989. Natural dynamics of population structure and habitat use of the lobster, *Homarus americanus,* in a shallow cove. *Biol. Bull.* **176:** 247–256.

Komatsu, H., I. Mori, H-S. Rhee, N. Akaike, and Y. Ohshima. 1996. Mutations in a cyclic nucleotide-gated channel is required for sensory development and function in *C. elegans. Neuron* **17:** 695–706.

Konishi, S., and E. A. Kravitz. 1978. The physiological properties of amine-containing neurones in the lobster nervous system. *J. Physiol.* **279:** 215–229.

Kuramoto, T., and M. Tani. 1994. Cooling-induced activation of the pericardial organs of the spiny lobster, *Panulirus japonicus. Biol. Bull.* **186:** 319–327.

Larimer, J. L. 1964. Sensory induced modifications of ventilation and heart rate in crayfish. *Comp. Biochem. Physiol.* **12:** 25–36.

Maynard, D. M. 1960. Circulation and heart function. Pp. 161–226 in *The Physiology of Crustacea, Vol. 1.* Academic Press, New York.

McCleskey, E. W. 1997. Thermoreceptors: recent heat in thermosensation. *Curr. Biol.* **7(11):** 679–681.

McLeese, D. W., and D. G. Wilder. 1958. The activity and catchability of the lobster (*Homarus americanus*) in relation to temperature. *J. Fish. Res. Board Can.* **15:** 1345–1354.

McMahon, B. R. 1995. The physiology of gas exchange, circulation, ion regulation, and nitrogenous excretion: an integrative approach. Pp. 497–517 in *Biology of the Lobster* Homarus americanus, J. R. Factor, ed. Academic Press, San Diego, CA.

McMahon, B. R., and J. L. Wilkens. 1972. Simultaneous apnoea and bradycardia in the lobster *Homarus americanus. Can. J. Zool.* **50:** 165–170.

Mercaldo-Allen, R., and F. Thurberg. 1987. Heart and gill ventilatory activity in the lobster, *Homarus americanus,* at various temperatures. *Fish. Bull.* **85(3):** 643–644.

Miller, L. C., and S. Mizell. 1972. Seasonal variation in heart rate response to core temperature changes. *Comp. Biochem. Physiol.* **42A:** 773–779.

Mori, I., and Y. Ohshima. 1995. Neural regulation of thermotaxis in *Caenorhabditis elegans. Nature* **376:** 344–348.

Murphy, B. F., and J. E. Heath. 1983. Temperature sensitivity in the prothoracic ganglion of the cockroach, *Periplaneta americana,* and its relationship to thermoregulation. *J. Exp. Biol.* **105:** 305–315.

Offutt, G. C. 1970. Acoustic stimulus perception by the American lobster, *Homarus americanus* (Decapoda). *Experientia* **26:** 1276–1278.

Pezzack, D. S., and D. R. Duggan. 1986. Evidence of migration and homing of lobsters (*Homarus americanus*) on the Scotian Shelf. *Can. J. Fish. Aquat. Sci.* **43:** 2206–2211.

Prosser, C. L., and D. O. Nelson. 1981. The role of nervous systems in temperature adaptation of poikilotherms. *Annu. Rev. Physiol.* **43:** 281–300.

Reynolds, W. W., and M. E. Casterlin. 1979. Behavioral thermoregulation and activity in *Homarus americanus. Comp. Biochem. Physiol.* **64A:** 25–28.

Schreiber, S., S. Krull, S. H. Jury, and W. H. Watson. 1998. Effects of temperature on the heart rate and locomotion of the American lobster (*Homarus americanus*). *Am. Zool.* **37(5):** 147A.

Watson, W. H. 1980. *Limulus polyphemus* gill cleaning behavior. *J. Comp. Physiol.* **141:** 67–75.

Watson, W. H., and G. A. Wyse. 1978. The coordination of heart and gill rhythms in *Limulus polyphemus. J. Comp. Physiol.* 124: 267–275.

Watson, W. H. III, A. Vetrovs, and W. H. Howell. 1999. Lobster movements in an estuary. *Mar. Biol.* **134:** 65–75.

Weiger, W. A. 1997. Serotonergic modulation of behavior: a phylogenetic overview. *Biol. Rev.* **72:** 61–95.

Whiteley, N. M., A. H. Al-Wassia, and E. W. Taylor. 1995. The effects of sudden changes in temperature on aquatic and aerial respiration in the lobster, *Homarus gammarus* (L.). *Mar. Freshw. Behav. Phys.* **27(1):** 13–28.

Wood, D. E., R. A. Gleeson, and C. D. Derby. 1995. Modulation of behavior by biogenic amines and peptides in the blue crab, *Callinectes sapidus. J. Comp. Physiol. A* **177:** 321–333.

Reference: *Biol. Bull.* **199:** 265–277. (December 2000)

Molt-Related and Size-Dependent Differences in the Escape Response and Post-Threat Behavior of the American Lobster, *Homarus americanus*

S. I. CROMARTY,* J. MELLO, AND G. KASS-SIMON†

Biological Sciences Department, University of Rhode Island, Kingston, Rhode Island 02881

Abstract. Videotaped recordings of adult lobsters of different molt stages were analyzed. The escape response of adults was compared with that of juveniles recorded in an earlier study.

Juvenile lobsters always respond to a threat with escape behavior irrespective of their molt stage, but in adults the probability of eliciting a response was a function of molt stage: more hard-shelled (intermolt stage C) and (premolt stage D) animals tailflipped than did soft-shelled (postmolt stages A and B) animals.

The number, frequency, and duration of tailflips, and the average distance swum by animals in each molt stage were measured for the entire escape response, for the initial power swim, and for the subsequent swims. These measurements were used to compute several parameters: velocity, acceleration, force, and work; average distance traveled in a tailflip for each kilogram of body weight (distance/kg/tailflip); and average distance traveled for each bodylength (distance/bodylength).

Among adults, intermolt (stage C) lobsters traveled significantly farther and faster than postmolt animals (stages A and B). Among juveniles, late postmolt (stage B) animals traveled farther. Among adults, although the total number of tailflips and the duration of the response were not significantly different among molt stages, the number of tailflips/second (frequency) and distance traveled/kg/tailflip were greater for intermolt animals. In juvenile intermolts, however, frequency and distance/kg/tailflip were markedly lower than in the premolt stages. Although values were lower than intermolts and premolts, postmolt adults sustained their swimming frequency, distance/kg/tailflip, and distance/bodylength for the entire escape distance (as did postmolt juveniles). These parameters then dropped off sharply for both adult and juvenile intermolt and premolt animals in the second half of the escape distance.

Post-threat behaviors reveal that stage D animals have the highest aggression index and often attack the presented stimulus, whereas stage A animals are the least likely to approach the stimulus and typically back away in a non-aggressive posture.

Thus, although effects of the molt cycle on adult and juvenile escape behavior are similar in some ways, other physical characteristics of adults, such as weight, allometry, and physiology, seem to become important in determining the likelihood of escape behavior and the characteristics of the escape swim in each molt stage.

Introduction

The behavior of the American lobster, *Homarus americanus,* varies (both in the laboratory and in the field) with sex and reproductive state (Cowan and Atema, 1990; Figler *et al.,* 1997, 1998; Cromarty *et al.,* 1998; Mello *et al.,* 1999), relative size (Scrivener, 1971; Lang *et al.,* 1977), time in residence (O'Neill and Cobb, 1979; Peeke *et al.,* 1998; Cromarty *et al.,* 1999), and dominance (Karnofsky and Price, 1989; Huber and Kravitz, 1995). However, molt-cycle-related behaviors have been rarely been studied—probably because the long-term approaches and experimental designs needed are complex.

The physiological transformations that occur in decapod crustaceans over the molt cycle are clearly profound; they include a variety of metabolic, neuroendocrine, and neuro-

---

Received 22 October 1999; accepted 7 July 2000.

* Present address: Department of Natural Sciences, Assumption College, 500 Salisbury Street, Worcester, MA 01609-1296. E-mail: scromart@eve.assumption.edu

† To whom correspondence should be addressed. Biological Sciences Department, University of Rhode Island, 100 Flagg Rd., Kingston, RI 02881-0816. E-mail: Kass.Simon@uri.edu

physiological changes (Knowles and Carlisle, 1956; Passano, 1960; Kleinholz and Keller, 1979; Quackenbush, 1986) that could manifest themselves in distinctive molt-stage-related behavioral modifications. Specifically, the escape response behavior in decapod crustaceans is ideally suited for modulation because it is composed of multiple tailflips, or swims. The escape response consists of an initial power swim followed by a series of subsequent swims; in crayfish, the initial power swim is elicited by visual and tactile excitation in the front of the animal which is mediated by the medial giant neuronal system, while tactile excitation of the telson at the rear of the animal is mediated by the lateral giant system. The subsequent swims immediately following the power swim are mediated by the non-giant system, which innervates the phasic flexor abdominal musculature (Wine and Krasne, 1972, 1982). Although the physiology of tailflip escape circuits has not yet been fully described in lobsters, the close similarity between the two species suggests that the innervation is similar.

While studying confrontations between juvenile American lobsters, Tamm and Cobb (1978) identified an increased *probability* of eliciting an escape response in early postmolt stages (stages A and B). In contrast, the frequency of aggressive behaviors, in particular the meral spread, increased during mid-premolt stages (stages D_1 and D_2). Hard-shelled lobsters tend to be aggressive, but soft-shelled lobsters tend to avoid confrontations. Stomatopods exhibit similar behavioral differences (Steger and Caldwell, 1983). These differences are understandable in view of the fact that in their postmolt, soft-shelled state, these animals are much more vulnerable to predation by predators and conspecifics than are hard-shelled animals, and they are less able to fend off attacks with aggressive behaviors, so that when threatened, they are forced to try to escape instead of mounting a defense (Tamm and Cobb, 1978; Atema and Cobb, 1980; Atema and Voigt, 1995).

One might expect that a newly molted animal would have difficulty doing much of anything until the exoskeleton hardens. Although this is true for lobsters in very early stage A, our studies revealed subtle differences in escape behavior among juvenile lobsters over the molt cycle (Cromarty *et al.*, 1991; Cromarty, 1995). We found that overall, postmolt lobsters produced the more effective escape behavior. Soft-shelled, postmolt juvenile lobsters (stage B) traveled farther, produced more tailflips, and swam longer, at sustained velocity, than did premolt lobsters. Earliest postmolt (stage A) juveniles swam at a higher frequency. In contrast, premolt juveniles produced a quick, forceful initial power swim, followed by subsequent swims that rapidly decreased in velocity, acceleration, force, and work output (Cromarty *et al.*, 1991).

The above studies focused on juvenile lobsters; even less information exists on molt-related changes in escape behavior in adult or larger animals. We know that the escape response occurs more frequently among juveniles and smaller adults than among large adults (Lang *et al.*, 1977), and that the conduction time of medial giant impulses from the brain to the sixth abdominal ganglion increases greatly, causing an increase in the latency of the response. The relative ratio of abdomen length to carapace length decreases with increased size, forcing the abdominal flexing muscles to propel a larger body mass (mostly claws). As with crayfish (Krasne and Wine, 1975), removal of the claws of a large lobster increases its propensity to tailflip (Lang *et al.*, 1977), as we have also observed in these experiments. Since large lobsters are less apt to be preyed upon than small ones (Atema and Voigt, 1995), it is expected that large soft- and hard-shelled adult lobsters would exhibit different but unique escape behaviors from one another.

Because of the physical and behavioral differences between adults and juveniles, on the one hand, and the physiological and behavioral differences among animals of different molt stages, on the other, we wished to investigate whether *adults* and *juveniles* in the *same* molt stage differed in the measurable characteristics of the escape response. We therefore examined the escape response of adult male lobsters of different molt stages in an experiment similar to the one we had designed for juvenile lobsters (Cromarty *et al.*, 1991). We measured distance traveled (m); number of tailflips (Tf); duration of the response (s); frequency of tailflips (Tf/s); velocity (m/s), acceleration (m/s/s), force (N; kg · m/s/s) and work (J) of each tailflip; distance traveled in each tailflip for each unit of body weight (m/kg/Tf); distance traveled in each tailflip for each unit of bodylength (distance/bodylength); and distance traveled in each tailflip for each unit of body weight (m/kg). In addition, we compared the escape thresholds of juveniles and adults.

Our earlier work indicated that lobsters could show significant differences in post-stimulus behaviors towards the threatening object, as well as in the characteristics of the escape behavior itself (Cromarty *et al.*, 1999). Thus we also analyzed post-stimulus agonistic behaviors and now present evidence that these behaviors—like escape behavior—differ significantly from one molt stage to another: premolt lobsters are more likely than postmolt animals to attack a threatening stimulus, and postmolt animals are more likely to back away from a stimulus with no display of aggression.

Materials and Methods

Procedures and experimental protocols are essentially the same as those described elsewhere (Cromarty *et al.*, 1991, 1998, 1999), but are summarized again here with relevant differences included.

Animals

Adult American lobsters (carapace length 74 to 90 mm) were obtained and housed as described previously (Cromarty *et al.*, 1999). Twenty-four hours prior to an experiment, an animal was moved to the Kingston campus of the University of Rhode Island, where it was placed in a holding tank (30 cm^3) and was not fed during this acclimation and experimental period. Isolation periods in the holding tank were identical for all experimental animals. The tank had its own air supply. To avoid possible sex-related effects, only males were used in this study. Ten lobsters from each molt stage (A, B, C, and D) were randomly selected as they entered the stage. Lobsters weighed (in grams) an average of 451.4 ± 69.6 (mean ± SD) and had an average carapace length (in millimeters) of 81.3 ± 4.7 (mean ± SD).

The experiments were performed randomly so that no molt-stage clustering occurred. A correlation statistic was run to check for molt stage and date of experiment. No correlation was found between the animals' molt stage, the time between the animals' capture and their use in the experiment, and the sequence of experiments ($R^2 < 0.18$, $F > 0.05$).

Lobsters were presented with the stimulus only once and were immediately sacrificed for identification of possible molt-related differences in the phasic flexor musculature system that is responsible for the escape response behavior. This required that over 200 animals be individually housed so that lobsters entering different molt stages could be selected.

Freshly caught lobsters were continually added to the holding population to reduce "inactivity" and potential for increasing aggressive behavior (Cromarty *et al.*, 1999). Because of possible seasonal differences in physiology and morphology such as those described in crayfish (Lnenicka and Zhao, 1991), experiments were conducted between June and October when Rhode Island waters maintain temperatures between 18°C and 23°C and similar conditions can be maintained in the indoor holding tanks. Again, no correlation was found between any of the significant parameters and the date of experiment.

Experiments

Each experiment was run between 1200 and 1500 hours in a 4000-l tank filled with filtered recirculated seawater. The large amount of seawater held in the experimental tank made it impractical to drain the tank after each experiment, but carbon filters were continuously used throughout this experimental period to remove possible recognition odors originating from the lobsters' urine. Nevertheless, a correlation statistic was run to check for success of tailflipping and lobster order. No correlation was found between the order of experiments and the animals' success and failure of tailflipping ($R^2 < 0.13$, $F > 0.05$).

Salinity was kept between 29‰ and 33‰, and adjustments (if any) were made before each experiment. One hour before an experiment, the physical condition of each animal was checked. Animals were used only if they moved around the tank or exhibited antennule flicking.

Water temperature in the experimental tank was maintained between 18°C and 20°C by a chiller. The experimental area consisted of an open-ended tank (1.0-m L × 0.3-m W × 0.3-m H) immersed in a larger main tank (2.2-m L × 0.75-m W × 0.91-m H). A weighted wooden partition with a pulley acted as a blind (and separation to the main tank) at the open side of the experimental tank (Fig. 1A).

The experimental tank was designed with an open end so that a threatening stimulus could be introduced at that end. To ensure that lobsters were initially at the closed, non-stimulus end, a light was placed at the open end of the tank. The partition was raised once the lobster had reached the closed end. The light was then placed over the closed, non-stimulus end. This served to "push" the animal back towards the open (stimulus) end. Because adult lobsters did not respond to the stimulus that was used to induce an escape response in juveniles (a flat shiny and reflective mirror, 0.1 m^2, housed in a wooden frame attached to a dowel stick), a piece of PVC tubing (15-cm L × 10-cm W) weighted with pebbles weighing 1.45 kg served as the threatening stimulus. The stimulus was raised above the open end, as depicted in Figure 1A, and was released into the water at a preset distance of 10 cm (measured from the open edge of the tank to the lobster's rostrum) whenever a lobster approached the open end of the tank.

Cameras were placed in horizontal and vertical positions so that the experiments were simultaneously recorded on two video recording systems. Video recordings of each lobster were analyzed frame-by-frame. To measure distance traveled, a metric grid divided into 0.5-cm units was painted onto the side of the experimental tank. Distance traveled along the length of the tank was measured using the position of the tip of the lobster's rostrum as the point of reference. Time was automatically recorded on the videotape, and numbers of tailflips were counted in subsequent viewing of the recordings.

After each experiment, the animal's molt stage was determined by examining cuticular and setal development in the pleopods (Aiken, 1973). Because animals become progressively harder after ecdysis (stage E), we also determined postmolt periods by testing various carapace areas for rigidity (Aiken, 1980). Experimental animals were placed in the following categories: intermolt (stage C); premolt (stages D_0, D_1, D_2, or D_3); and postmolt (stage A up to 48 h following ecdysis and stage B from 48 to 96 h after ecdysis).

Probabilities of an escape response were determined for each molt stage ($n = 10$) and statistically compared. The

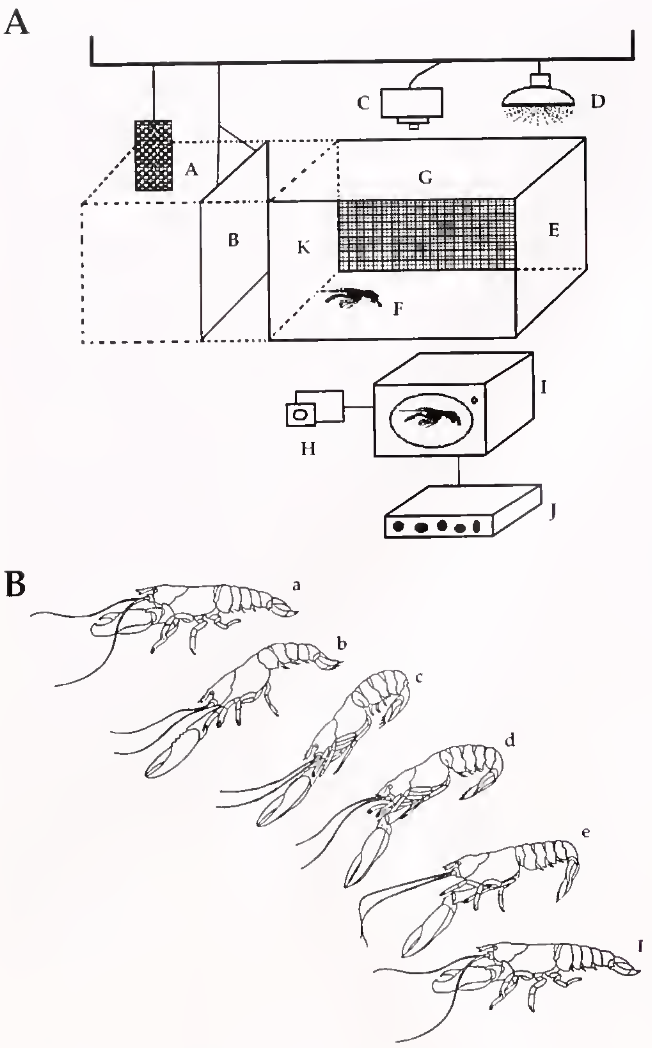

Figure 1. (A) Diagram of the experimental tank (E). The stimulus was a weighted piece of PVC tubing filled with pebbles (A); the screen (B) was lifted while the lobster (F) was at the opposite end of the tank. A light (D) at the closed end of the tank caused the animal to move towards the darker open end (K). The escape behavior of each lobster was recorded against a 0.5-cm metrically divided grid (G). The recording system consisted of vertical (C) and horizontal (H) cameras, a monitor (I), and a time-lapse VCR (J). (B) Schematic breakdown of a single tailflip as it was seen in the video analysis: (a) = beginning of swim; (f) = end of a single tailflip. (Drawings by K. Davignon, Graphics specialist, URI.) Previously published in *The Biological Bulletin* (Cromarty *et al.*, 1998).

other characteristics of the escape response of animals that escaped were analyzed as in our earlier study of juvenile escape behavior (Cromarty *et al.*, 1991, 1998, 1999).

Videotape analysis

Each of the escape parameters was analyzed for (1) the entire escape response; (2) the initial power swim; (3) the subsequent swims over the entire subsequent swimming distance; and (4) the subsequent swims in each half of that distance, since earlier experiments showed that there were differences in the total subsequent swimming distance traveled by lobsters. We therefore divided the distance traveled in the subsequent swims by half and analyzed each half (Cromarty *et al.*, 1991, 1998, 1999). Because the distances differed and because each distance was divided equally in half for each escape sequence for each animal, no data are available to compare distance traveled between the two halves of the subsequent swims for each molt stage. (A complete tailflip, or swim, is defined as beginning immediately after the start of abdominal flexion and ending at abdominal extension [Fig. 1B: sequence a through f].) The following characteristics of the escape response were analyzed for each lobster: distance traveled (m), number of tailflips (Tf), duration of the response (s), frequency of tailflips (Tf/s), velocity (m/s), acceleration (m/s/s), force [N; (kg · m/s/s)], work (J), distance traveled/weight/tailflip (m/kg/Tf), distance traveled/weight (m/kg), and distance traveled/lobster bodylength. The latter two parameters were calculated to determine whether individual lobster variability in weight and size altered the relative significance of a parameter. Velocity, acceleration, force, and work are all initially calculated from the distance that the individual tailflipped divided by the length of time the animal spent tailflipping. Calculations were based on the distance measured on the video records for the total escape response, the power stroke, and the subsequent swims. Therefore, because of small differences in each measurement due to the finite resolution of the number of frames per second of the video camera, the added mean values of the power stroke and subsequent swims are slightly different from the mean values of the total escape response. (The analysis of the escape response is meant to reflect relative changes in lobster escape behavior and not kinematic relationships such as those investigated by other researchers [Batchelor, 1967; Daniel and Meyhöfer, 1989; Nauen and Shadwick 1999].)

To quantify the degree of "aggression" in the post-stimulus behavior of each animal, we ordered the behavior towards the stimulus and then subjectively ranked an animal's post-stimulus threat behavior on a scale of 0 to 6 (Cromarty *et al.*, 1999):

0 = back away, never approach
1 = approach but remain more than one bodylength away
2 = approach within one bodylength
3 = approach, touch
4 = approach, touch, grasp
5 = approach, touch, grasp, and tug or pull
6 = approach, touch and grasp, tug or pull and, execute an offensive tailflip

Statistical analysis

Molt stage versus probability of escape: Fisher's exact probability tests (FEPs) were used to determine differences in probabilities of an escape response over the molt stages. Because of the small number of stage A and B lobsters (4 out of our original sample of 20 animals) that tailflipped ($n = 4$), the two molt stages were collapsed into a single sample to represent postmolt, soft-shelled lobsters. Stage C animals were classified as intermolts, and stage D lobsters were classified as premolts.

Comparison of weight and carapace length versus *molt stage:* Weight and carapace length among the molt stages were compared in a one-way analysis of variance (ANOVA) with a *post-hoc* Scheffé test to compare means of the planned comparisons. Weights of animals that escaped within each molt stage were compared to those that did not in a Mann-Whitney *U* test (MW).

Characteristics of the escape response: Linear regressions were performed on all escape parameters against weight to double-check weight influence. Due to a non-normal distribution of data, Kruskal-Wallis tests (KWs) were used for all the escape parameters except for the comparison of the first and second halves of the subsequent swims, where a multiple analysis of variance (MANOVA) with a one-way repeated measures follow-up test was used to compare the two halves of the subsequent swims.

Post-threat behaviors: Post-threat behaviors were quantified according to the "aggression index" and were compared in a one-way analysis of variance (ANOVA) with a *post-hoc* Scheffé test used to compare means of the planned comparisons.

KWs, ANOVAs, MANOVAs, and Scheffé tests were run using the University of Rhode Island mainframe computer (IBM ES/9000) and SPSS 6.1 software (SPSS Inc., Chicago) for the Macintosh G3 computer. Values for all tests were considered significant at $P \leq 0.05$, while trends were considered at ($0.05 \leq P \leq 0.10$).

Results

Comparison of adult and juvenile escape probabilities

The data are summarized in Figure 2. In contrast to our earlier studies on small juveniles (±14 g) in which 100% of the 36 juvenile lobsters tailflipped (9 in each of the four stages; Cromarty *et al.*, 1991), none of the larger juvenile (≥150 g) or adult (≥450 g) lobsters responded to the stick stimulus, regardless of size class or molt stage (see Fig. 2). Various stimuli (water injection over the lobster, a larger conspecific lobster, a predator (tautog), and bubbles blown over the lobster) also failed to elicit an escape response. However, a 15-cm-long piece of PVC tubing weighted with pebbles, dropped suddenly from above as the lobster approached, caused both larger juvenile (±150 g) and adult (±450 g) lobsters to tailflip (Fig. 2). In the large-juvenile size class, 23 out of 34 tailflipped (stage A: 4 of 8; stage B: 1 of 8; stage C: 9 of 9; stage D: 9 of 9). In the large-adult size class, 15 out of 40 tailflipped (stage A: 2 of 10; stage B: 2 of 10; stage C: 5 of 10; stage D: 6 of 10) or 20% of soft-shelled (stages A and B) and 55% of hard-shelled lobsters (stages C and D; FEP, $P = 0.01$). When comparing the probability of eliciting an escape response for soft-shelled (stages A and B) *versus* hard-shelled (stages C and D) lobsters, soft-shelled postmolt lobsters were significantly

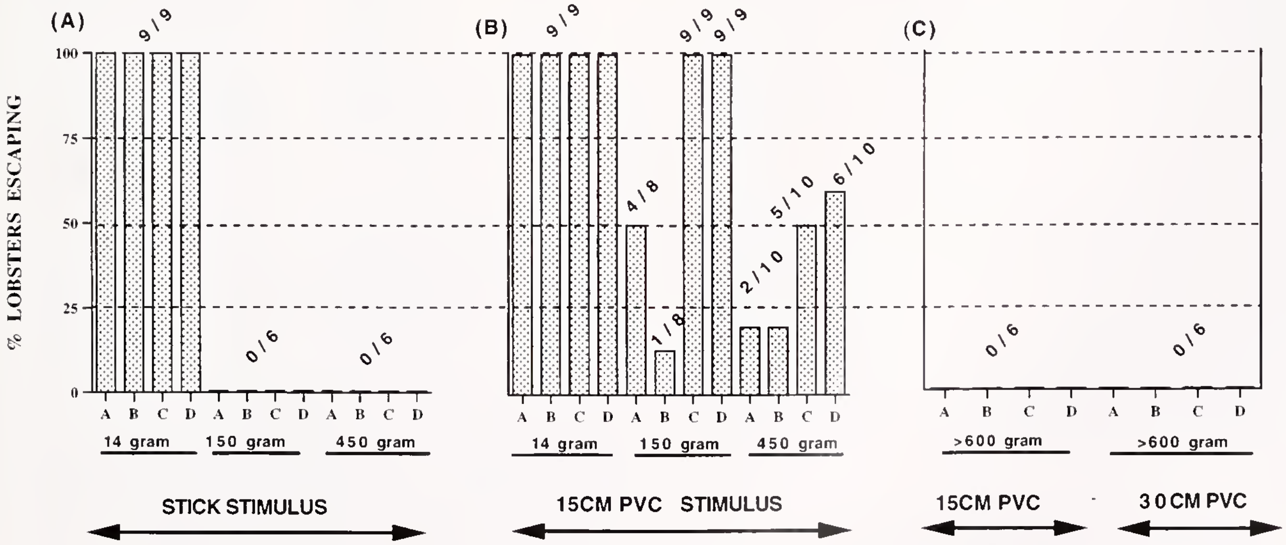

Figure 2. Percentage (%) of lobsters escaping at each weight and molt stage in response to stimuli of different sizes. The stimulus was (A) a stick to which a mirror was attached; (B) a 15-cm length of PVC weighted with stone weighing 1.45 kg; (C) two pieces of PVC tubing, one was 15 cm in length and weighing 1.45 kg, and the other 30 cm in length and weighing 2.45 kg (animals heavier than 600 g did not respond to the two stimuli). Molt stages, weights of animals, and types of stimuli are below the x-axis. Ratios at top of each bar are the number of lobsters escaping to the total number of animals presented with the stimulus.

less likely to tailflip than hard-shelled premolt lobsters: 20% (4 of 20) compared to 55% (11 of 20) (FEP, $P = 0.01$). Adult lobsters larger than 600 g did not tailflip, even when the size of the PVC tubing was increased from 15-cm L × 10-cm W, 1.45 kg, to 30-cm L × 10-cm W, 2.45 kg.

Analysis of escape behavior in adults

A. Effect of weight on escape response in the various molt stages

As had been shown by Lang *et al.* (1977), size and weight have significant effects on a lobster's propensity to exhibit an escape response.

Among the groups of animals tested, there were significant differences in weights (Table 1a). Stage B lobsters weighed significantly more than either stages C or D (ANOVA, $F(3, 36) = 7.42$, $P = 0.0005$). Stage B lobsters also had significantly larger carapace lengths than either stages C or D (ANOVA, $F(3, 36) = 15.69$, $P = 0.0001$).

To determine whether any of the characteristics of the escape response were correlated with weight, linear regressions were calculated in which each of the following seven parameters were evaluated against weight, irrespective of molt stage: (1) probability of tailflipping; (2) duration of escape swimming; (3) tailflip frequency, (4) velocity, and (5) acceleration of the total escape swim; (6) force exerted during the swim; and (7) work performed. No correlation was found between the animals' weights and any of the parameters tested ($R^2 < 0.20$; $F > 0.05$).

Of the animals tested, only 15 out of 40 tailflipped. When the weights of animals that tailflipped (Table 1b) were compared, there were *no* significant differences *among* the four molt stages (ANOVA, $F(3, 11) = 2.61$, $P = 0.11$). These animals were therefore subsequently used to analyze the characteristics of the escape response with respect to weight and molt stage.

Among the animals that did *not* tailflip (Table 1c), there were significant molt-stage differences in the weights of the animals. Stages A and B weighed significantly more than stages C and D (ANOVA, $F(3, 21) = 4.22$, $P = 0.002$). More soft-shelled lobsters (16 out of 20) than hard-shelled animals (9 out of 20) did not tailflip, suggesting that size in this weight class could determine whether an animal will tailflip; possible reasons for this are detailed in the discussion.

B. Parameters of the adult escape response

A summary of all the parameters tested, with means and standard deviations for each molt stage, are summarized in Table 2. Precision of measurements is a function of the number of video frames per second; therefore, since the power stroke and subsequent swims were separately analyzed, their mean values are not additive.

Table 1

Weight (in grams) for adult lobsters in the four molt stages; values are mean ± standard error of the mean

Softshelled premolt		Hardshelled intermolt	Premolt
STAGE A	STAGE B	STAGE C	STAGE D
(a) Combined weights of all lobsters irrespective of escape behavior			
514.3	595.1	420.3	372.1
474.2	512.1	421.0	403.4
470.0	582.0	373.0	440.2
592.2	358.6	456.0	326.2
401.0	544.2	435.6	424.5
497.0	441.4	417.4	484.9
400.0	487.6	438.7	396.0
535.1	438.0	390.6	360.4
476.2	513.4	433.5	378.0
420.8	596.3	369.0	465.1
478.1 ± 19.3	506.9 ± 24.6	415.5 ± 9.2	405.1 ± 15.5
(b) Animals that tailflipped			
470.0	441.4	420.3	403.4
420.8	513.4	421.0	326.2
		456.0	484.9
		435.6	396.0
		438.7	360.4
			378.0
445.4 ± 24.6	477.4 ± 36.0	434.3 ± 6.6	391.5 ± 21.8
(c) Animals that did not escape			
514.3	595.1	373.0	372.1
474.2	512.1	417.4	440.2
592.2	358.6	390.6	424.5
401.0	544.2	433.5	465.1
497.0	582.0	369.0	
400.0	487.6		
535.1	438.0		
476.2	596.3		
486.3 ± 22.9	514.2 ± 29.7	396.7 ± 12.6	425.5 ± 19.7

1. Total escape response (initial power swim plus subsequent swims)

Intermolt (stage C) animals tailflipped farther than either postmolt (stages AB) or premolt (stage D) animals (KW, $\chi^2 = 5.42$, $P = 0.046$; Fig. 3A). Although the total time spent in the escape response was not significantly different among the three molt stages (KW, $\chi^2 = 2.58$, $P = 0.28$; Fig. 3B), the velocity (distance/time) of the swim was also significantly higher for intermolt animals than for postmolt lobsters (KW, $\chi^2 = 5.94$, $P = 0.041$; Fig. 3C). Although the apparently shorter duration of the swim for premolts was not significant, when time was used to calculate acceleration (velocity/time), the resulting value became significantly greater for premolt (stage D) lobsters (KW, $\chi^2 = 6.76$, $P = 0.034$; Fig. 3D). Neither the force (weight × acceleration) exerted nor the work (force × distance) performed proved to be significantly different for the three molt stages

Table 2

Summary of significant differences among all components analyzed over the escape response

Component	Molt stage	Total escape response	Initial power swim	Total subsequent swims	Subsequent swims 1 (SS1)	Subsequent swims 2 (SS2)	SS1 *vs.* SS2
Distance (m)		$\boxed{C > (AB = D)}$	$\boxed{C > (AB = D)}$	$\boxed{C > (AB = D)}$	NA	NA	NA
	AB	0.29 ± 0.27	0.06 ± 0.01	0.25 ± 0.23			
	C	0.71 ± 0.10	0.17 ± 0.02	0.64 ± 0.08			
	D	0.39 ± 0.05	0.08 ± 0.02	0.35 ± 0.23			
Duration (s)		NS	NS	NS	NS	NS	NS
	AB	1.08 ± 0.53	0.29 ± 0.23	1.03 ± 0.47	0.35 ± 0.24	0.70 ± 0.39	
	C	1.32 ± 0.29	0.13 ± 0.04	1.08 ± 0.39	0.38 ± 0.10	0.86 ± 0.16	
	D	0.81 ± 0.58	0.21 ± 0.13	0.75 ± 0.62	0.29 ± 0.25	0.61 ± 0.38	
Velocity (m/s)		$\boxed{C > (AB = D)}$	NS	NS	NS	NS	NS
	AB	0.28 ± 0.22	0.63 ± 0.24	0.65 ± 0.26	0.90 ± 0.29	0.38 ± 0.08	
	C	0.56 ± 0.14	0.33 ± 0.26	0.28 ± 0.28	0.51 ± 0.33	0.25 ± 0.18	
	D	0.35 ± 0.12	0.44 ± 0.46	0.37 ± 0.09	0.64 ± 0.29	0.27 ± 0.04	
Acceleration (m/s/s)		$\boxed{D > (AB) = C}$	NS	$\boxed{D > (AB) = C}$	NS	NS	NS
	AB	0.27 ± 0.19	2.87 ± 3.06	0.22 ± 0.16	1.77 ± 1.00	0.38 ± 0.26	
	C	0.46 ± 0.20	5.64 ± 3.16	0.36 ± 0.12	2.66 ± 1.42	0.47 ± 0.18	
	D	0.55 ± 0.20	4.12 ± 4.1	0.50 ± 0.18	3.27 ± 1.79	0.66 ± 0.49	
Force [N; (kg · m/s/s)		NS	NS	NS	NS	NS	NS
	AB	0.14 ± 0.11	1.56 ± 1.66	0.10 ± 0.06	1.02 ± 0.61	0.22 ± 0.16	
	C	0.17 ± 0.07	2.00 ± 0.88	0.14 ± 0.04	0.95 ± 0.39	0.18 ± 0.07	
	D	0.22 ± 0.09	1.51 ± 1.39	0.20 ± 0.06	1.23 ± 0.69	0.25 ± 0.20	
Work (J)		NS	NS	NS	NS	NS	NS
	AB	0.06 ± 0.09	0.16 ± 0.12	0.05 ± 0.04	0.04 ± 0.02	0.02 ± 0.01	
	C	0.12 ± 0.05	0.20 ± 0.06	0.11 ± 0.06	0.09 ± 0.04	0.02 ± 0.03	
	D	0.05 ± 0.03	0.15 ± 0.07	0.04 ± 0.07	0.03 ± 0.06	0.01 ± 0.03	
Number of tailflips (Tf)		NS	NA	NS	NS	NS	NS
	AB	3.5 ± 1.9		2.5 ± 1.5	1.8 ± 0.9	0.9 ± 0.3	
	C	5.8 ± 1.8		4.8 ± 1.8	3.6 ± 1.0	1.3 ± 0.4	
	D	3.5 ± 3.1		2.5 ± 2.7	2.0 ± 2.0	1.6 ± 0.8	
Frequency (Tf/s)		$\boxed{(C = D) > AB}$	NA	$\boxed{(C = D) > AB}$	$\boxed{(C = D) > AB}$	NS	$\boxed{C1 > C2}$
	AB	3.05 ± 1.08		6.96 ± 1.69	3.63 ± 3.17	3.33 ± 2.59	$\boxed{D1 > D2}$
	C	4.52 ± 1.34		10.52 ± 4.17	8.40 ± 3.54	2.12 ± 0.91	
	D	3.94 ± 1.02		10.78 ± 1.02	9.13 ± 2.40	1.65 ± 1.94	
Distance/Weight (m/kg)		NS	NS	NS	NA	NA	NA
	AB	0.52 ± 0.46	0.10 ± 0.03	0.41 ± 0.50			
	C	1.67 ± 0.16	0.17 ± 0.03	1.52 ± 0.11			
	D	0.84 ± 0.72	0.21 ± 0.07	0.61 ± 0.72			
Distance/Weight/Tailflip (m/kg/Tf)		$\boxed{C > (AB = D)}$	NS	$\boxed{C > (AB = D)}$	NA	NA	NA
	AB	0.14 ± 0.07	0.10 ± 0.03	0.12 ± 0.05			
	C	0.41 ± 0.09	0.17 ± 0.03	0.38 ± 0.06			
	D	0.23 ± 0.07	0.21 ± 0.07	0.19 ± 0.05			
Distance/Bodylength		$\boxed{C > (AB = D)}$	NS	$\boxed{C > (AB = D)}$	NA	NA	NA
	AB	3.5 ± 1.9	0.13 ± 0.03	3.1 ± 1.6			
	C	5.8 ± 1.8	0.10 ± 0.02	5.4 ± 1.7			
	D	3.5 ± 3.1	0.15 ± 0.03	3.1 ± 2.8			

A, B, C, and D represent the four molt stages. Mean ± SD of all components analyzed for three molt stages. Significant differences are indicated in boxes at the top of each column. Stages equated with those in the parentheses are not significantly different from them.

AB, results of experiments with stages A and B were pooled due to only 4 animals that tailflipped.

SS1, first half of the subsequent swimming distance; SS2, second half of the subsequent swimming distance.

SS1 *versus* SS2 compares the component in the two halves of the subsequent swimming distance.

NA, not analyzed due to the experimental design (see methods).

NS, no significant difference.

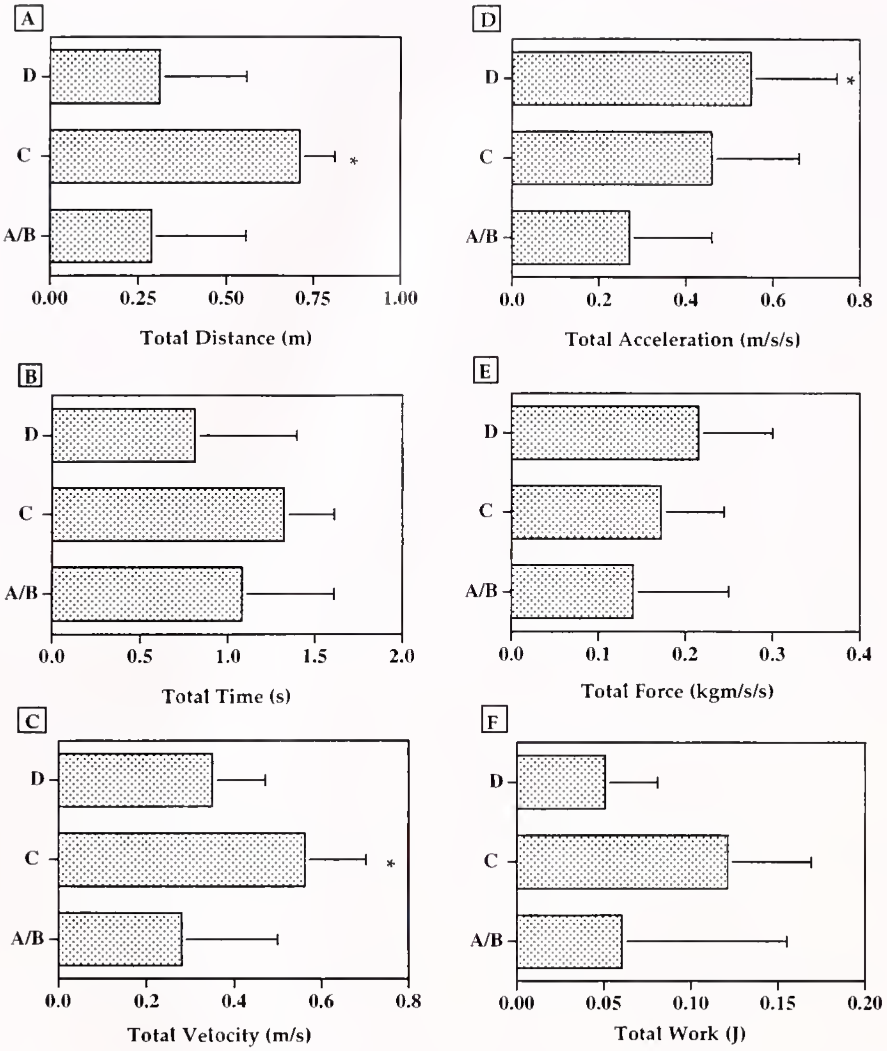

Figure 3. Parameters of the total escape response (initial power swim plus subsequent swims) for adult lobsters in all three molt stages. An asterisk (*) indicates significant differences. (A) Distance traveled in meters (m). (B) Time spent escaping in seconds (s). (C) Velocity of tailflips in meters/second (m/s). (D) Acceleration in meters/second/second (m/s/s). (E) Force of tailflips in newtons (kg · m/s/s). (F) Work produced (force × distance) is measured in joules (J).

(KW, $\chi^2 = 4.98$, $P = 0.083$ and $\chi^2 = 2.15$, $P = 0.16$; Fig. 3E and 3F, respectively).

Although the total number of tailflips and the total time were not significantly different (KW, $\chi^2 = 4.20$, $P = 0.123$ and $\chi^2 = 2.58$, $P = 0.275$, respectively), swim frequency was significantly higher for intermolt and premolt lobsters, with stage C and D lobsters performing more tailflips per second than AB animals (KW, $\chi^2 = 6.93$, $P = 0.048$; Fig. 4A). Distance traveled per lobster weight per tailflip was greater for intermolt (stage C) animals than for the other molt stages (C > (AB = D); KW, $\chi^2 = 5.98$, $P = 0.046$, Fig. 4D), and distance traveled per bodylength was also greater for intermolt animals than for the other molt stages (stages (C > (AB = D); KW, $\chi^2 = 5.36$, $P = 0.047$, Fig. 4F).

2. *Initial power swim*

Except for distance traveled, none of the parameters were significantly different for the three molt stages at $P \leq 0.05$, no doubt because of the large variability among the animals that exhibited an escape response. However, trends in the tests suggest that intermolt and premolt lobsters executed a faster, more accelerating, and more forceful power swim than postmolt animals ($0.05 \leq P \leq 0.10$; KW).

3. *Subsequent swims*

a. *Entire subsequent swim*

Of the original 15 animals that responded to the stimulus with escape swimming, only 12 executed subsequent swims. Of these, 3 were postmolts (stages A and B), 5 were intermolts (stage C), and 4 were premolts (stage D). The following parameters were statistically different: the fre-

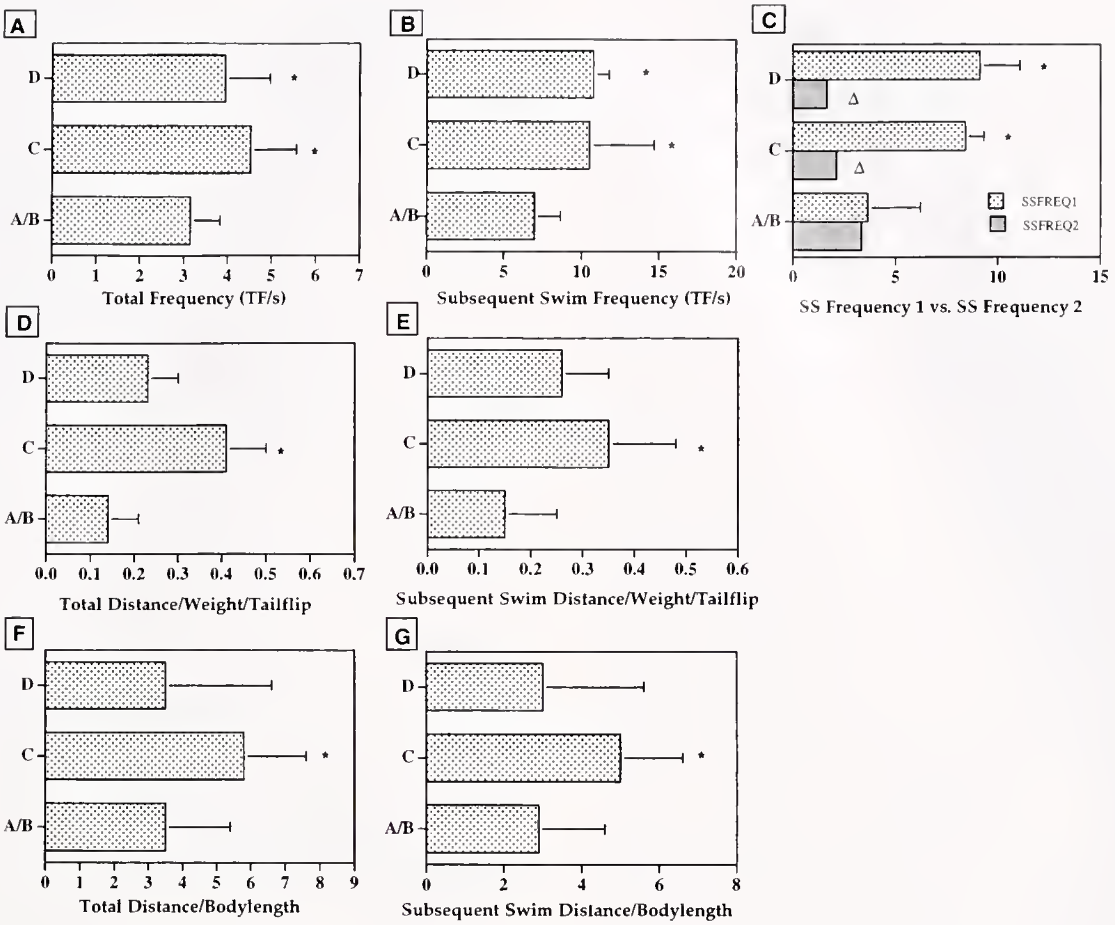

Figure 4. Mean frequency of tailflips (Tf/s) for adult lobsters for (A) total swim sequence; (B) the total subsequent swims frequency, and (C) the subsequent swims of both the first and second halves. Mean distance per weight per tailflip (m/kg/Tf) for the total swim sequence (D) and for the total subsequent swims—that is, minus the power stroke (E). Mean distance per bodylength for total distance of swim sequence per bodylength (F) and for the total subsequent swims distance per bodylength (G). Stage AB (n = 3), stage C (n = 5), and stage D (n = 4). An asterisk (*) indicates significant differences among the molt stages; a triangle (△) indicates significant differences between the two halves of the subsequent swims.

quency of swimming was higher for stages C and D (KW χ^2 = 7.92, P = 0.037; Fig. 4B); the distance swum per weight per tailflip was higher in intermolt (stage C) animals (KW, χ^2 = 8.01, P = 0.028, Fig. 4E); and distance per bodylength was greater for intermolt (Stage C) animals than for the other molt stages (KW, χ^2 = 6.46, P = 0.046, Fig. 3G).

b. Comparisons of SS1 and SS2

As in the previous study (Cromarty *et al.*, 1991), the total distance traveled by each animal during the entire subsequent escape swims was divided in half and then the swimming parameters were compared for each of the two halves across the molt stages and between the two halves of the swimming distance within each molt stage. SS1 = the first half of the distance; SS2 = the second half.

Comparison of SS1 across molt stages. In the first half of the subsequent swims, stage C and D lobsters swam at a higher frequency than stages A and B (MANOVA, F(1, 9) = 23.18, P = 0.014; Fig. 4C).

Comparison of SS2 across molt stages. No significant differences were found in any of the parameters for the second half of the subsequent swims among the molt stages (Table 2).

Comparison of SS1 and SS2 (SS_1 vs. SS_2) within each molt stage. For the following parameters—subsequent swimming distance, duration, velocity, acceleration, force, work output, number of tailflips—no significant differences were found between the two halves of the subsequent swims within each molt stage. There was a significant drop-off in the frequency of swims between the first to the second halves of the subsequent swims for hard-shelled (stages C and D), while no differences between SS1 and SS2 were observed for soft-shelled (stages A and B) lobsters (MANOVA $F(1, 9)$, $P \leq 0.003$; Fig. 4C).

Comparison of SS1 and SS2 across molt stages. Frequency of swimming was significantly different among the three molt stages (MANOVA, $P \leq 0.026$). Among hard-shelled lobsters (stages C and D), the frequency of swimming was greatly reduced in the latter half of the escape swims (Fig. 4C).

C. Post-threat behavior

There was a gradual increase in the aggression index of all lobsters in the experiment, such that stage A had an index value of 0.3 ± 0.5, while stage D had a value of 2.2 ± 1.4. The values for stage D were significantly greater than for molt stages A, B, and C (ANOVA $F(3, 39)$, $P \leq 0.0012$; Fig. 5A). This is especially interesting given that stage B animals were significantly larger than stages C and D (see section A above), yet the post-threat aggression of the smaller hard-shelled lobsters was significantly higher.

Among the animals that tailflipped, there were significant differences in the aggression index among the four molt stages (ANOVA $F(3, 11)$, $P \leq 0.02$): soft-shelled lobsters (stages A and B) had very low or zero aggression towards the stimulus, whereas hard-shelled lobsters (stages C and D) had an overall aggression index of 1.4 ± .09 (Fig. 5B). Importantly, no weight differences were observed among the molt stages for the animals that did tailflip.

When the post-threat behaviors of lobsters that did *not* tailflip were compared over the molt stages, a progression in the index was observed: starting with a value of 0.4 ± 0.5 for stage A lobsters, the index gradually increased until the index for stage D animals was 3.3 ± 0.5. Stage D lobsters had a significantly higher aggression index than molt stages A, B, and C (ANOVA $F(3, 21)$, $P \leq 0.0001$; Fig. 5C). Although the soft-shelled animals were significantly larger than the hard-shelled ones (see section A), the smaller hard-shelled lobsters were more aggressive in their post-threat behaviors.

Discussion

In this study, we show that, like juveniles, adult male lobsters display significant molt-related differences in escape behavior. However, the escape behavior of adults, unlike that of juveniles (weight less than 100 g), is also influenced by physical factors.

Thus, we have found that among animals that *did not* respond to a threat with an escape response, soft-shelled adults weighed significantly more than hard-shelled adults. This suggests that an animal's weight begins to modify the molt-dependent swimming response to threat.

In our earlier experiments, all juvenile animals (both soft and hard-shelled; ±14 g) responded to a stimulus threat with escape swimming (Cromarty *et al.*, 1991). No adults responded to the same stimulus that induced 14-g juveniles to swim. Indeed, adults failed to respond to a number of other stimuli (such as air bubbles, water injection, larger conspecifics) that were presented to them and ultimately responded only to a heavy weight (PVC tubing filled with pebbles and weighing 1.45 kg) dropped suddenly in their paths.

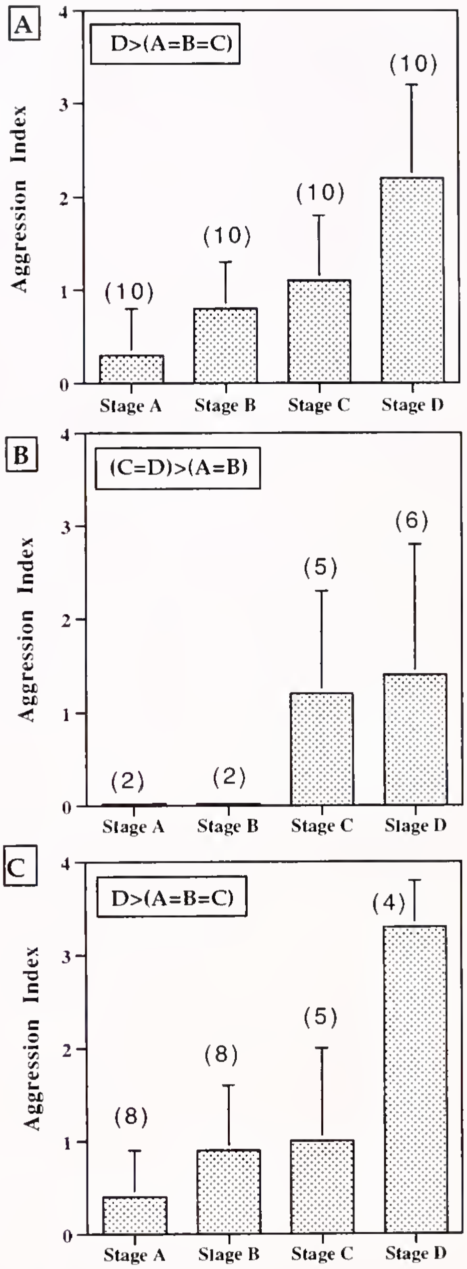

Figure 5. Mean aggression index for post-threat behavior of adult lobsters for (A) all lobsters regardless of tailflipping; (B) lobsters that did tailflip; and (C) lobsters that did not tailflip. The numbers in parentheses represent the number of individuals in each molt stage; the statistical differences are displayed in a box in the upper left-hand corner of each graph.

There seems to be an inverse relationship between the probability of eliciting an escape response and the weight of an animal: 14-g juveniles tailflipped with a 100% probability; 450-g adults tailflipped with a probability of 50%, and 600-g adults failed to tailflip even when the stimulus size was doubled. Other workers have shown that lobsters weighing more than 600 g could be induced to tailflip only if their claws were autotomized (Lang *et al.*, 1977), as we also have observed.

It appears, therefore, that the effects of molt stage—that is, an animal's physiological condition, characterized by the hardness of its shell (Aiken, 1973; 1980), the flaccidity of its muscles (Passano, 1960), and the titers of its hormones (Stevenson *et al.*, 1979; Fadool *et al.*, 1989; Snyder and Chang, 1991a, b)—begin to be modified by size and weight.

That size and weight begin to modulate the molt-determined characteristics of escape swimming can be seen if all our findings are taken into account. Among adults, as among juveniles, there was a significant drop off in the frequency and distance traveled/weight/tailflip during the second half of the subsequent swims for premolt hard-shelled animals, but not for postmolt animals. This suggests that escape swimming may have evolved as the primary survival strategy among soft-shelled juvenile animals, and that this strategy is retained in adults even as they become heavier; however, fewer large animals were likely to tailflip, perhaps because swimming becomes less energy-efficient (the heavier the animal, the more work is involved).

Although size and weight appear to modulate the effects of molt stage on escape swimming, with larger adult soft-shelled animals not tailflipping, an inverse relationship to weight became apparent in the *post-threat behaviors* of our experimental animals. Regardless of whether the animals had tailflipped—and even when weight was taken into account—the indices of aggression of the post-threat behaviors increased incrementally from stages A and B (the largest animals) to stages C and D (the smallest animals). Weight and size appears to be of secondary importance in post-threat aggression; indeed, changes in aggression over the molt stages were the deciding factor, with the lobsters responding to a threat in accordance with the expected molt-related changes in aggressive behaviors (Tamm and Cobb, 1978). Undue significance should not be given to the inverse relationship of weight and size on aggression in general, however. In confrontations between lobsters in the same molt stage, the size of an opponent significantly affected the outcome of a bout (Scrivener, 1971; Mello *et al.*, 1999; Bolingbroke and Kass-Simon, 2000).

Overall, we found that among juveniles, soft-shelled animals were better swimmers than their hard-shelled counterparts, but among adults, hard-shelled premolt and intermolt lobsters were the best swimmers. Thus juveniles of stage B outperformed stage C and D animals in the following parameters: distance traveled, number of tailflips produced, distance/tailflip, time spent swimming, and velocity (Cromarty *et al.*, 1991). In contrast, among adults, hard-shelled premolt and intermolt animals outperformed soft-shelled animals in distance traveled, velocity, acceleration, frequency and distance traveled/lobster weight/tailflip. This would suggest that molt stage is the predominant determinant of the characteristics of escape behavior in smaller animals, while other physical factors such as weight and claw size may begin to dominate among adults.

The physiological bases for the differences in adult and juvenile escape behavior over the molt cycle are likely to be manifold and varied. In addition to probable differences within the central nervous system, differences in endocrine, sensory, and motor systems are certain to exist.

With regard to sensory systems (Watson, 1992), synaptic modulation has been described for mechanoreceptors (Pasztor and Bush, 1987) and stretch receptors (El Manira *et al.*, 1991). Studies by Coulter (1988) indicate that lobsters in stages C and D responded (with a meral spread) at different speeds to the presentation of an expanding black disc. Increases in lobster size have been correlated with a decrease in the speed of an action potential traveling from the sensory system to the central nerve cord (Lang *et al.*, 1977). It is possible that juvenile and adult lobsters perceive and respond to stimuli differently due to inherent age-related differences in sensory functioning.

Other factors such as central (Kravitz *et al.*, 1984; Kravitz, 1988; Yeh *et al.*, 1996, 1997; Hörner *et al.*, 1997) and peripheral modulations (Kravitz *et al.*, 1980; Kravitz, 1990; Schwanke *et al.*, 1990) are likely to affect molt-cycle behavior. We have recently found that 20-hydroxyecdysone (20-HE), the active steroid regulating the molt, also alters the neuromuscular properties of the claw-opener and phasic flexor systems in intermolt animals (Cromarty, 1995; Cromarty and Kass-Simon, 1998), in a way that is consistent with molt-determined behavioral differences (Tamm and Cobb, 1978; Cromarty *et al.*, 1991). Our findings are consistent with the rise in the blood titer of 20-HE (Snyder and Chang, 1991a, b) when lobster aggression is beginning to peak. In our 20-HE experiments we found that 20-HE increases the size of the excitatory junctional potential (EJP) in the claw opener muscle, which is used in threat displays, and decreases the EJP amplitude in the abdominal phasic flexor, which is used in escape behavior. In crayfish, Cooper and Ruffner (1998) have found that EJP amplitude in the opener muscle of the walking legs is reduced; this keeps the dactyl from splaying and allows the animal to stand tall, as has been observed in dominant lobster displays (for recent review on modulation of aggressive behavior, see Kravitz, 2000). The effects of 20-HE on these above-mentioned tissues are consistent with the functions attributed to them during agonistic behavior. Our recent studies also show that when 20-HE is directly injected into the lobsters' hemolymph, aggressive behavior increases dramatically during agonistic encounters, although the probability of eliciting escape swimming is unaltered (Bolingbroke and Kass-Simon, 2000).

The sexual status of an American lobster may also alter its use of escape behavior. Intermolt gravid females that are presented with a startle stimulus do not tailflip, whereas intermolt males and non-gravid females tailflip readily (Cromarty *et al.*, 1998); gravidity did not appear to affect escape behavior during a confrontation, but caused an increase in aggressive tail flipping (Mello *et al.*, 1999). It remains to be seen whether neuromuscular properties are modulated to reflect these sex-related behavioral differences.

Among juveniles, we have found that EJPs in the distal region of the muscle in soft-shelled stage B animals are larger and have a greater amplitude-duration integral than those of hard-shelled D stage animals (Cromarty *et al.*, 1995). Earlier studies by Schwanke *et al.* (1990) also found molt-related differences in the dactyl opener muscle. These findings correspond with the fact that stage B juveniles swim greater distances by covering more distance in each swim than do hard-shelled (stage C and D) juveniles. Further, although EJPs continue to be produced at frequencies up to 6 Hz in stage A and B juveniles, they begin to fail at 4 Hz in stage C and D animals. This also correlates with the fact that stage B juveniles swim longer and cover more ground, and that stage A animals are able to sustain swimming longer and at a higher frequency than stage C or D animals (Cromarty *et al.*, 1991; Cromarty *et al.*, 1995).

Among adults, EJPs were found to fail at 4 Hz in soft-shelled postmolts but continued to 6 Hz in intermolt and premolt animals (Cromarty and Kass-Simon, 1994). As in juveniles, in adults, EJPs were largest and longest lasting in the distal region of soft-shelled postmolts. We have also found that EJPs in the proximal region of the abdominal phasic flexor muscles, the anchorage or insertion region of the contracting muscle, are significantly greater in adult C and D stages than in juvenile C and D stages (Cromarty and Kass-Simon, 1994). This coincides with their greater swimming ability and supports our present finding that escape swimming is used less as the animal grows, although hard-shelled animals retain it longer than soft-shelled animals do. This might be because escape swimming would be less effective in large soft-shelled animals—not only because of the large mass that would need to be propelled by the still-flaccid muscles, but also because the large transmitter output required by these muscles might not be sustainable for long periods at higher frequencies.

Acknowledgments

The authors thank Bill MacElroy for allowing us to collect animals while he was fishing offshore, and Tom Angell of the Rhode Island Department of Environmental Management for supplying us with additional lobsters. Thanks to Dr. Mike Clancy and Kathy Castro for help in lobster collection and maintenance. Drs. Stanley Cobb and Frank Heppner kindly provided laboratory space and equipment. We also thank Malia Schwartz for critiquing an earlier draft of the manuscript. This research was supported by a Whitehall Foundation grant to G.K-S. Grant-in Aid of Research from Sigma Xi and Lerner Gray Grants for Marine Research to S.I.C.

Literature Cited

Aiken, D. E. 1973. Proecdysis, setal development, and molt prediction in the American lobster (*Homarus americanus*). *J. Fish. Res. Board Can.* **30:** 1334–1337.

Aiken, D. E. 1980. Molting and growth. Pp. 91–163 in *The Biology and Management of Lobsters*, vol. 1, J. S. Cobb and B. F. Phillips, eds. Academic Press, New York.

Atema, J., and J. S. Cobb. 1980. Social behavior. Pp. 409–450 in *The Biology and Management of Lobsters*, Vol. 1, J. S. Cobb and B. F. Phillips, eds. Academic Press, New York.

Atema, J., and R. Voigt. 1995. Behavior and sensory biology. Pp. 313–348 in *The Biology of the Lobster*, Homarus americanus. J. Factor, ed. Academic Press, New York.

Batchelor, G. K. 1967. *An Introduction to Fluid Dynamics*. Cambridge University Press, London.

Bolingbroke, M. B., and G. Kass-Simon. 2000. Increased aggressiveness in female American lobsters caused by 20-hydroxyecdysone. *Soc. Neurosci. Abstr.* **26:** 368.5.

Cooper, R. L., and M. E. Ruffner. 1998. Depression of synaptic efficacy at intermolt in crayfish neuromuscular junctions by 20-hydroxyecdysone, a molting hormone. *J. Neurophysiol.* **79:** 1931–1941.

Coulter, D. 1983. Analysis of a visually-evoked aggressive display in the American lobster, *Homarus americanus*. MS Thesis, University of Rhode Island, Kingston, RI.

Cowan, D. C., and J. Atema. 1990. Moult staggering and serial monogamy in American lobsters, *Homarus americanus*. *Anim. Behav.* **39:** 1199–1206.

Cromarty, S. I. 1995. Neuroethology of the escape behavior in the American lobster, *Homarus americanus*, over the molt cycle. Ph.D. dissertation, University of Rhode Island, Kingston, RI.

Cromarty, S. I., and G. Kass-Simon. 1994. Plasticity of the non-giant phasic flexor neuromuscular junctions in the adult American lobster, *Homarus americanus*, over the molt cycle. *Soc. Neurosc. Abstr.* **20:** 331.

Cromarty, S. I., and G. Kass-Simon. 1998. Differential effects of a molting hormone, 20-hydroxyecdysone, on the neuromuscular junctions of the claw opener and abdominal flexor muscles of the American lobster. *Comp. Biochem. Physiol.* **120(2): 289–300.**

Cromarty, S. I., J. S. Cobb, and G. Kass-Simon. 1991. Behavioral analysis of the escape response in juvenile American lobsters, *Homarus americanus* over the molt cycle. *J. Exp. Biol.* **158:** 565–581.

Cromarty, S. I., J. S. Cobb, and G. Kass-Simon. 1995. Adult and juvenile lobsters (*Homarus americanus*) differ markedly in the neuromuscular physiology and behavior of the escape response over the molt cycle. *Soc. Neurosc. Abstr.* **21:** 72.12.

Cromarty, S. I., J. Mello, and G. Kass-Simon. 1998. Comparative analysis of escape behavior in male, and gravid and non-gravid, female lobsters. *Biol. Bull.* **194:** 63–71.

Cromarty, S. I., J. Mello, and G. Kass-Simon. 1999. Time in residence affects escape and agonistic behavior in adult male American lobsters. *Biol. Bull.* **196:** 105–112.

Daniel, T. L., and E. Meyhöfer. 1989. Size limits in escape locomotion of caridean shrimp. *J. Exp. Biol.* **143:** 245–265.

El Manira, A., C. Rossi-Durand, and F. Clarac. 1991. Serotonin and proctolin modulate the response of a stretch receptor in crayfish. *Brain Res.* **541:** 157–162.

Fadool, D. A., P. R. Brown, J. S. Cobb, and G. Kass-Simon. 1989. HPLC analysis of lobster haemolymph over the molt cycle. *Comp. Biochem. Physiol.* **93C:** 225–230.

Figler, M. H., H. V. S. Peeke, and E. S. Chang. 1997. Maternal aggression in American lobsters (*Homarus americanus* Milne Edwards): shelter-related encounters against non-maternal conspecifics. *Mar. Freshw. Behav. Physiol.* **30:** 267–274.

Figler, M. H., H. V. S. Peeke, and E. S. Chang. 1998. Shelter-related aggression between adult male conspecific intruders and resident maternal American lobsters (*Homarus americanus*) with eggs at different stages of embryogenesis. *Mar. Freshw. Behav. Physiol.* **31:** 151–166.

Huber, R., and E. A. Kravitz. 1995. A quantitative analysis of agonistic behavior in juvenile American lobsters (*Homarus americanus* L.). *Brain. Behav. Evol.* **46:** 72–83.

Hörner, M., W. Weiger, D. H. Edwards, and E. A. Kravitz. 1997. Excitation of identified serotonergic neurons by escape command neurons in lobsters. *J. Exp. Biol.* **200:** 2017–2033.

Karnofsky, E. B., and H. J. Price. 1989. Dominance, territoriality and mating in the lobster, *Homarus americanus*: a mesocosm study. *Mar. Behav. Physiol.* **15:** 101–121.

Kleinholz, L. H., and R. Keller. 1979. Endocrine regulation in Crustacea. Pp. 159–214 in *Hormones and Evolution*. J. W. Barrington, ed. Academic Press, New York.

Knowles, F. G. W., and D. B. Carlisle. 1956. Endocrine control in the Crustacea. *Biol. Revs. Cambr. Philos. Soc.* **31:** 396–473.

Krasne, F. B., and J. J. Wine. 1975. Extrinsic modulation of crayfish escape behaviour. *J. Exp. Biol.* **63:** 433–450.

Kravitz, E. A. 1988. Hormonal control of behavior: amines and the biasing of behavioral output in lobsters. *Science* **241:** 1775–1781.

Kravitz, E. A. 1990. Hormonal control of behavior: amines as gain-setting elements that bias behavioral output in lobsters. *Am. Zool.* **30:** 595–608.

Kravitz, E. A. 2000. Serotonin and aggression: insights gained from a lobster model system and speculations on the role of amine neurons in a complex behavior like aggression. *J. Comp. Physiol. A.* **186:** 221–238.

Kravitz, E. A., S. Glusman, R. M. Harris-Warrick, M. S. Livingstone, T. Schwarz, and M. F. Goy. 1980. Amines and a peptide as neurohormones in lobster: actions on neuromuscular preparations and preliminary behavioral studies. *J. Exp. Biol.* **89:** 159–175.

Kravitz, E. A., B. Beltz, S. Glusman, M. Goy, R. Harris-Warrick, M. Johnston, M. Livingstone, and T. Schwarz. 1984. The well-modulated lobster: the roles of serotonin, octopamine and proctolin in the lobster nervous system. *Pestic. Biochem. Physiol.* **22:** 133–147.

Lang, F., C. K. Govind, W. J. Costello, and S. I. Greene. 1977. Developmental neuroethology: changes in escape and defensive behavior during growth of the lobster. *Science* **197:** 682–684.

Lnenicka, G. A., and Y. Zhao. 1991. Seasonal differences in the physiology and morphology of crayfish motor terminals. *J. Neurobiol.* **22:** 561–569.

Mello, J., S. I. Cromarty, and G. Kass-Simon. 1999. Increased aggressiveness in gravid female American lobsters, *Homarus americanus*. *Aggressive. Behav.* **25:** 451–472.

Nauen, J. C., and R. E. Shadwick. 1999. The scaling of acceleratory aquatic locomotion: body size and tail-flip performance of the California spiny lobster *Panulirus interruptus*. *J. Exp. Biol.* **202:** 3181–3193.

O'Neill, D. J., and J. S. Cobb. 1979. Some factors influencing the outcome of shelter competition in lobsters (*Homarus americanus*). *Mar. Behav. Physiol.* **6:** 33–45.

Passano, L. M. 1960. Molting and its control. Pp. 473–536 in *The Physiology of Crustacea*, Vol. 1, T. H. Waterman, ed. Academic Press, New York.

Pasztor, V. M., and B. M. H. Bush. 1987. Peripheral modulation of mechanosensitivity in primary afferent neurons. *Nature* **326:** 793–795.

Peeke, H. V. S., M. H. Figler, and E. S. Chang. 1998. Sex differences and prior resident effects in shelter competition in juvenile lobsters, *Homarus americanus* Milne Edwards. *J. Exp. Mar. Biol. Ecol.* **229:** 149–156.

Quackenbush, L. S. 1986. Crustacean endocrinology, a review. *Can. J. Fish. Aquat. Sci.* **43:** 2271–2282.

Schwanke, M. L., J. S. Cobb, and G. Kass-Simon. 1990. Synaptic plasticity and humoral modulation of neuromuscular transmission in the lobster claw opener during the molt cycle. *Comp. Biochem. Physiol.* **97C:** 143–149.

Scrivener, J. C. E. 1971. Agonistic behavior of the American lobster, *Homarus americanus* (Milne-Edwards). *Fish. Res. Board Can., Tech. Report.* **235:** 1–128.

Snyder, M. J., and E. S. Chang. 1991a. Ecdysteroids in relation to the molt cycle of the American lobster, *Homarus americanus*. I. Hemolymph titers and metabolites. *Gen. Comp. Endocrinol.* **81:** 113–145.

Snyder, M. J., and E. S. Chang. 1991b. Ecdysteroids in relation to the molt cycle of the American lobster, *Homarus americanus*. II. Excretion of metabolites. *Gen. Comp. Endocrinol.* **83:** 118–131.

SPSS Inc. 1988. *SPSS User's Guide*. SPSS Inc., Chicago.

Steger, R., and R. L. Caldwell. 1983. Intraspecific deception by bluffing: a defense strategy of newly moulted stomatopods. *Science* **221:** 79–81.

Stevenson, J. R., P. W. Armstrong, E. S. Chang, and J. D. O'Connor. 1979. Ecdysone titers during the molt cycle of the crayfish *Orconectes sanborni*. *Gen. Comp. Endocrinol.* **39:** 20–25.

Tamm, G. R., and J. S. Cobb. 1978. Behavior and the crustacean molt cycle: changes in aggression of *Homarus americanus*. *Science* **200:** 79–81.

Watson, A. H. D. 1992. Presynaptic modulation of sensory afferents in the invertebrate and vertebrate nervous system. *Comp. Biochem. Physiol.* **103A:** 227–239.

Wine, J. J., and F. B. Krasne. 1972. The organization of escape behavior in the crayfish. *J. Exp. Biol.* **56:** 1–18.

Wine, J. J., and F. B. Krasne. 1982. The cellular organization of crayfish escape behavior. Pp. 241–292 in *The Biology of Crustacean Neurobiology: Structure and Function*, Vol. 3, D. E. Bliss, ed. Academic Press, New York.

Yeh, S. R., R. A. Fricke, and D. H. Edwards. 1996. The effect of social experience on serotonergic modulation of the escape circuit of crayfish. *Science* **271:** 366–369.

Yeh, S. R., B. E. Musolf, and D. H. Edwards. 1997. Neuronal adaptations to changes in the social dominance status of the crayfish. *J. Neurosci.* **17:** 697–708.

Reference: *Biol. Bull.* **199:** 278–286. (December 2000)

Preferential Expulsion of Dividing Algal Cells as a Mechanism for Regulating Algal-Cnidarian Symbiosis

GAREN BAGHDASARIAN* AND LEONARD MUSCATINE

Department of Organismic Biology, Ecology, and Evolution, University of California, Los Angeles, Los Angeles, California 90095-1606

Abstract. A wide range of both intrinsic and environmental factors can influence the population dynamics of algae in symbiosis with marine cnidarians. The present study shows that loss of algae by expulsion from cnidarian hosts is one of the primary regulators of symbiont population density. Because there is a significant linear correlation between the rate of algal expulsion and the rate of algal division, factors that increase division rates (*e.g.*, elevated temperature) also increase expulsion rates. Additionally, ^{3}H-thymidine is taken up to a greater extent by algae destined to be expelled than by algae retained in the host cnidarians. Taken together, data for rates of expulsion, rates of division at different temperatures, and uptake of ^{3}H-thymidine suggest that dividing algal cells are preferentially expelled from their hosts. The preferential expulsion of dividing cells may be a mechanism for regulation of algal population density, where the rate of expulsion of algae may be an inverse function of the ability of host cells to accommodate new algal daughter cells. This kind of regulation is present in some cnidarian species (*e.g., Aiptasia pulchella, Pocillopora damicornis*), but not in all (*e.g., Montipora verrucosa, Porites compressa*, and *Fungia scutaria*).

Introduction

Algal-cnidarian symbioses are characterized by long-term stability wherein neither partner outgrows the other, and where algal population densities remain relatively constant (Drew, 1972; Pardy, 1974; Davies, 1984). During repopulation of aposymbiotic sea anemones (recovery from bleaching), symbiotic dinoflagellates grow at relatively high rates normally associated with log phase growth in culture (Berner *et al.*, 1993). If these high growth rates are sustained, host fitness is reduced (Smith, 1992), leading to the eventual breakdown of the symbiosis (Neckelmann and Muscatine, 1983; Taylor *et al.*, 1989). Instead, as the size of the algal population reaches some optimum level, its growth rate decreases by a factor of 20 (Kinzie, 1974; Kinzie and Chee, 1979; Berner *et al.*, 1993), and a "steady state" is achieved, in which the growth rates of the algae and the host cells are in dynamic equilibrium. Clearly, regulation of symbiont population density is essential in maintaining a stable symbiosis, yet little is known of the cellular mechanisms involved.

A number of intrinsic and environmental factors can potentially regulate algal cell division and population growth. These factors could act pre- or post-mitotically (Hoegh-Guldberg and Smith, 1989); that is, population growth rate could be regulated either before or after algal cell division. Algal numbers could be regulated pre-mitotically by limited nutrient availability (see, for example, Blank and Muscatine, 1987; Kolber *et al.*, 1988; Falkowski *et al.*, 1993; Hoegh-Guldberg, 1994; Muller-Parker *et al.*, 1994; Snidvongs and Kinzie, 1994); by density-dependent negative feedback by the algae themselves (Muscatine and Pool, 1979; McAuley and Darrah, 1990); by host-induced release of photosynthate from the algae (Muscatine, 1967; Cook, 1983; Douglas and Smith, 1984; Sutton and Hoegh-Guldberg, 1990; McAuley, 1992; Gates *et al.*, 1995); or by factors manifested by the host cells that inhibit the algal cell cycle (Smith and Muscatine, 1999). Algal numbers could also be regulated postmitotically by degradation of algae *in situ* (Muscatine and Pool, 1979; Titlyanov *et al.*, 1996; Jones and Yellowlees, 1997), by direct expulsion of excess algae (Hoegh-Guldberg and Smith, 1989; Stimson and Kinzie, 1991; McCloskey *et al.*, 1996; Jones and Yellowlees, 1997), or by accommodation of excess algae by division of host cells (Muscatine and Pool, 1979; Neckelmann and

Received 2 August 1999; accepted 25 September 2000.

* To whom correspondence should be addressed.

Muscatine, 1983; Smith and Muscatine, 1986; Titlyanov *et al.*, 1996).

Whereas previous studies have addressed pre-mitotic control of algae in symbiotic cnidarians, there is little information on mechanisms involved in post-mitotic regulation, especially relating to loss of algae by expulsion. Jones and Yellowlees (1997) showed that the combined effect of changes in rates of algal division and loss are involved in repopulation of bleached corals and in the eventual regulation of steady-state algal-cnidarian symbioses. In a previous study, we observed that the Hawaiian sea anemone *Aiptasia pulchella* maintained in the laboratory expels algae at a rate of about 0.046 d^{-1} (Baghdasarian and Muscatine, unpubl. data), a value high enough to be a major factor in regulating algal densities. Studies of other cnidarians report not only that algae are lost by expulsion, but also that the expelled algae have higher mitotic indices than algae retained by the host (Suharsono and Brown, 1992; McCloskey *et al.*, 1996). It has been hypothesized that the higher mitotic indices of expelled algae are due to release from some regulatory constraint by the hosts. In this study we test an alternative hypothesis, that higher mitotic indices of expelled algae are the result of preferential expulsion of dividing cells. It is important to note here that the release mechanism probably entails detachment of host cells (Gates *et al.*, 1992), their disintegration, and release of algae. Whereas the mechanism of preferential detachment of host cells remains to be addressed, here we focus on algal parameters.

Materials and Methods

Collection and maintenance of organisms

Specimens of the sea anemone *Aiptasia pulchella* Carlgren (1943) symbiotic with the dinoflagellate *Symbiodinium pulchrorum* were collected from Kaneohe Bay, Oahu, Hawaii (spring and fall 1995/1996). The animals were transferred by air to the University of California, Los Angeles, and maintained in natural seawater in 1.5-liter glass bowls in a Percival model I-35VL incubator at 25°C on a 12-h light/dark cycle at irradiance levels of 80–100 μmole photons m^{-2} s^{-1}, from two Rainbow Lifeguard 40-watt Primetinic and two General Electric 40-watt Cool White light sources. The animals were fed twice a week in the evenings on *Artemia* sp. The morning after every feeding, the bowls were cleaned using cotton swabs, and the seawater, collected from Redondo Beach, California, was replaced. Prior to the experiments, sea anemones were starved for 24 h under the light and temperature conditions described above.

The symbiotic corals *Porites compressa* Dana 1846, *Montipora verrucosa* Lamarck 1816, *Pocillopora damicornis* Linnaeus 1758, and *Fungia scutaria* Lamarck 1801 were collected from Kaneohe Bay, Oahu, Hawaii (October/November 1996). The corals were transferred to the laboratory of the Hawaii Institute of Marine Biology, and were maintained in running seawater and exposed to natural light levels. All experiments were performed within 24 h of the collections.

Mitotic index of algae

Five *A. pulchella* were homogenized individually and their symbiotic algae isolated by repetitive centrifugation and resuspension (Steen, 1987). The technique was applied rigorously to eliminate the possibility of inclusion of algae still within host cells. The algal mitotic index (MI), defined as the percentage of cells with division plates (Wilkerson *et al.*, 1983) was determined by examination of at least 1000 algal cells under 400× magnification using an Olympus BH-2 microscope. All additional microscopic observations were made under the same specifications.

Incorporation of ^{3}H-thymidine by algae in situ

Each of five *A. pulchella* specimens was incubated individually in 4 ml of a 2-μCi/ml solution of ^{3}H-thymidine (Sigma Chemical Company; Sp. act. 50 Ci per mmol) in filtered seawater (FSW) for 24 h under the same maintenance conditions as the stock animals. The sea anemones were then washed serially 10 times in FSW to remove unincorporated ^{3}H-thymidine. Each wash consisted of adding fresh FSW, irrigating the coelenteron with a Pasteur pipette, and then waiting 3 min before changing the water again. Seven to nine washes were sufficient to remove unincorporated ^{3}H-thymidine from the sea anemones and the incubation medium. Algae expelled during the labeling period were discarded. ^{3}H-thymidine-labeled sea anemones were then incubated in FSW for an additional 15.5 h at 25°C in the light. At the end of the incubation period, both the algae released and those remaining in the hosts were isolated (using techniques described above on ice), adjusted to known volumes, and counted with a hemacytometer (Fisher Scientific). One-hundred-microliter samples of algae, along with 5 ml of Bio-Safe II biodegradable counting cocktail, were then added to plastic scintillation vials, and the incorporation of ^{3}H-thymidine by the algae was determined using an LKB Wallac 1214 Rackbeta liquid scintillation counter. Results were expressed as DPM $*$ $(10^6 \text{ algae})^{-1}$. To determine whether the incorporation of ^{3}H-thymidine was by the algae or by host cells that contain the algae and may have been released along with them, techniques described in Gates and Muscatine (1992) were used to stain cells with Hoechst 33258 to check for the occurrence of host cell nuclei.

Rates of expulsion of algae

Fourteen sea anemones were allowed to settle in 4 ml of FSW in 15-ml test tubes. Six of the sea anemones were incubated for 15.5 h at 25°C in the light, and the other eight were incubated for 15.5 h at 27.5°C in the light. After the incubation, algae in the incubation medium were recovered by centrifugation and set aside for analysis. Algae remaining in the animals were isolated by homogenization and centrifugation (Steen, 1987). Both the algae expelled into the medium and those retained by the hosts were counted, and the MI of the expelled algae was determined (Hoegh-Guldberg *et al.*, 1987).

Mitotic index and rate of expulsion of algae in corals

Mitotic indices and rates of algal expulsion were also established for four species of scleractinian corals commonly found in Kaneohe Bay, Oahu, Hawaii. Six pieces of each coral type from different colonies (*P. compressa, M. verrucosa, P. damicornis,* and in the case of *F. scutaria,* entire corals) were incubated in 30 ml of FSW at 27°C (seawater temperature in Kaneohe Bay) for 15.5 h. Next, to determine the effect of slight elevations of temperature on MI values and algal expulsion rates, six additional pieces from each coral type were incubated at 29.5°C for the same length of time. At the end of the incubation period, the corals were removed from the seawater. The released algae were collected by high-speed centrifugation of the incubation medium using a Damon IEC clinical centrifuge, followed by resuspension in 5 ml of fresh FSW. Algae remaining in the corals were removed with a toothbrush. The product was collected in FSW. The algae were then cleaned of mucus and animal tissue by centrifugation and resuspension in 20 ml of FSW, and MI values and rates of algal expulsion were determined using the techniques described above.

Results

Mitotic index of algae: natural expulsion vs. *mechanical isolation*

Algae naturally expelled from *A. pulchella* have a higher MI than the algae remaining in the hosts (Fig. 1; Wilcoxon signed rank nonparametric test: $P = 0.001$). To determine if the higher MI of the expelled algae is due to the absence of host-related regulation, algae were mechanically isolated from the sea anemones, and the MI was measured immediately and after a 15.5-h incubation at 25°C in the light. No significant changes in MI were observed following the 15.5-h incubation period (Wilcoxon signed rank nonparametric test: $P = 0.593$). These data suggest that the higher MI of algae expelled by *A. pulchella* is not necessarily due to release from putative host-related regulation.

Incorporation of ^{3}H-thymidine by algae in situ

To determine if the higher MI of expelled algal cells is due to preferential expulsion of dividing algae, sea anemones were incubated with ^{3}H-thymidine for 24 h, rinsed free of unincorporated ^{3}H-thymidine, and then incubated in FSW for 15.5 h. Algae expelled and algae retained in the hosts were then assayed for incorporation of ^{3}H-thymidine. Expelled algae had incorporated significantly higher levels of ^{3}H-thymidine than cells remaining in the hosts (Fig. 2; Wilcoxon signed rank nonparametric test: $P = 0.043$). Because released algae are often contained within host cells (Gates *et al.*, 1992), it was important to determine whether the ^{3}H was associated with the algae or with the nuclei of host cells. This question was investigated by staining samples of retained and released algae with Hoechst 33582 to detect host cell nuclei that might be associated with the algae. Using epifluorescence microscopy to analyze the cells (Gates *et al.*, 1992), we found no evidence of host cell nuclei (*i.e.*, host nuclear DNA contamination). Taken together, these data suggest that the host preferentially expels algal cells that have entered S-phase of the cell cycle.

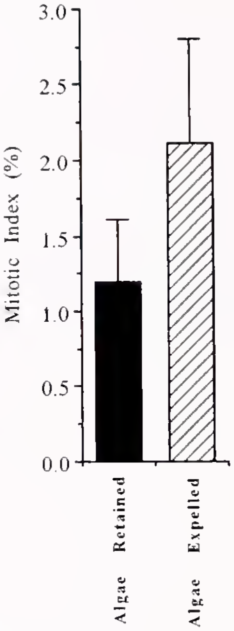

Figure 1. Mitotic index of the symbiotic alga *Symbiodinium pulchrorum* after a 15.5-h incubation of the host sea anemone, *Aiptasia pulchella*, at 25°C. Comparison between expelled algae (▨) and algae retained by the host (■). Error bars represent standard deviations of the mean.

Mitotic index and rate of expulsion of algae

The correlation between the MI of the expelled algae and the rate of expulsion of these cells from the host could distinguish between expulsion of algae in random phases of the cell cycle *versus* expulsion of algae in a preferred phase of the cell cycle. If expulsion of algae from the host is random, then there should be no correlation between division rate of the expelled algae (*i.e.*, MI) and rate of expulsion. If, however, expulsion of algae is a function of cell cycle phase (more specifically, preferential release during late G_2 or M phases), then a positive correlation between the two parameters would be expected, as illustrated

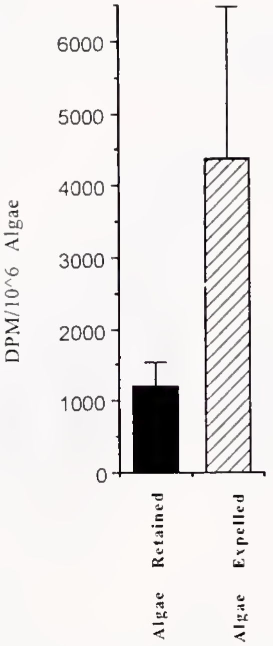

Figure 2. ^{3}H-Thymidine incorporation by the symbiotic alga *Symbiodinium pulchrorum* after a 15.5-h incubation of the host sea anemone, *Aiptasia pulchella*, in filtered seawater. Comparison between expelled algae (▨) and algae retained by the host (■). Sea anemones were initially incubated in a 2-μCi/ml solution of ^{3}H-thymidine for 24 h. Error bars represent standard deviations of the mean.

theoretically in Figure 3. Figure 4 shows that there is a positive linear correlation between expulsion rate of algae and their MI.

Effect of temperature on rate of algal expulsion

If expulsion of algae is affected by algal division rate, then environmental factors (such as slight increases in seawater temperature) that increase algal division rate (and hence MI) should also increase rate of expulsion of algae. Slightly elevated temperatures resulted in higher MI and expulsion rates (Fig. 5; Wilcoxon signed rank nonparametric test; Expulsion rate: $P = 0.034$, MI: $P = 0.050$). Further, the ratio of algal expulsion to MI at 25°C = 2.2, and at 27.5°C = 2.4. The similarity of these two ratios suggests that the higher MI values due to slight elevations in temperature are concomitant with higher algal expulsion rates. Finally, at 27.5°C, the observed changes in rates of algal division and expulsion follow the same positive linear correlation associated with preferential algal expulsion as a function of their MI (Fig. 6).

Rates of algal expulsion in corals

The relation between algal expulsion rate and division rate was investigated in four species of Hawaiian corals. In general, the released algae had a higher MI than did the algae remaining in the hosts (Fig. 7; Wilcoxon signed rank nonparametric test; significant differences seen in *Pocillopora damicornis, Montipora verrucosa, Fungia scutaria*: $P = 0.028$, but not in *Porites compressa*: $P = 0.249$). However, the linear correlation between algal

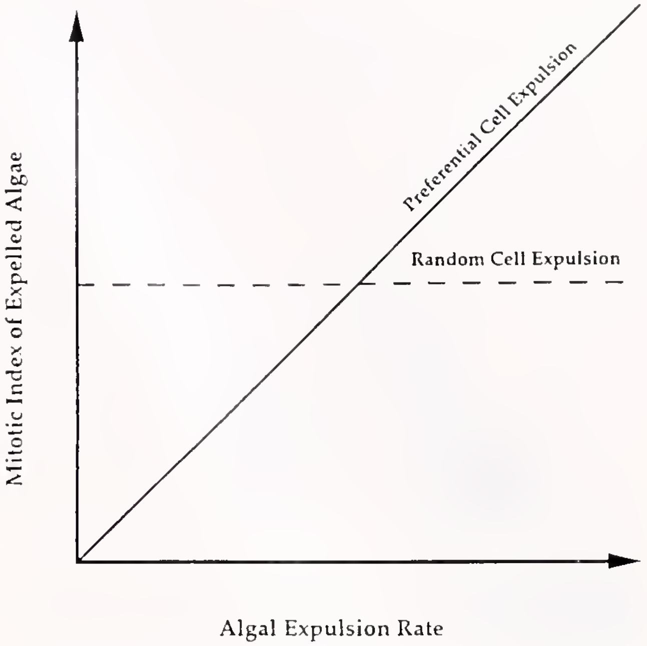

Figure 3. Hypothetical correlation between mitotic index of expelled symbiotic algae and their rate of expulsion from the hosts under conditions of preferential versus random cell expulsion.

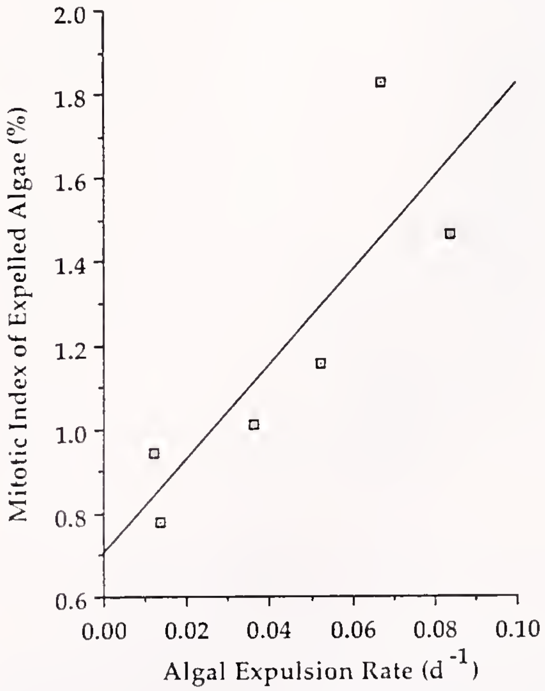

Figure 4. Correlation between mitotic index and rate of expulsion of *Symbiodinium pulchrorum*. $Y = 0.69971 + 11.185X$; $R^2 = 0.711$.

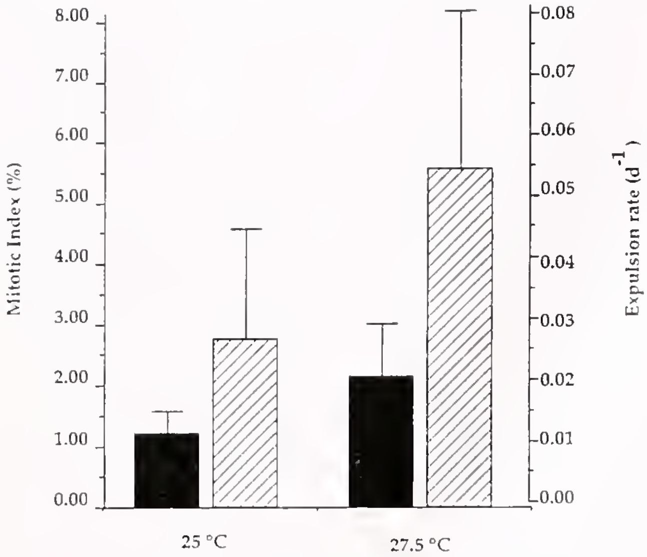

Figure 5. Effect of a 2.5°C temperature increase on rate of expulsion (▨) and mitotic index (■) of *Symbiodinium pulchrorum* released from the symbiotic system. Error bars represent standard deviations of the mean.

expulsion rate and MI, observed in *A. pulchella,* appears to hold only for *P. damicornis* (Fig. 8a); it does not hold for *P. compressa, M. verrucosa,* or *F. scutaria* (Fig. 8b, c, d).

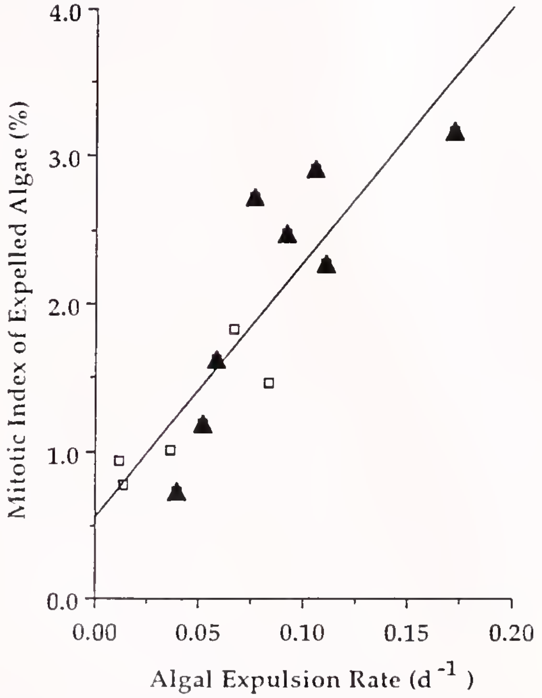

Figure 6. Correlation between mitotic index and rate of expulsion of *Symbiodinium pulchrorum* under control and elevated temperatures. 25°C control (☐), 27.5°C experimental (▲). $Y = -0.53328 + 17.244X$; $R^2 = 0.771$.

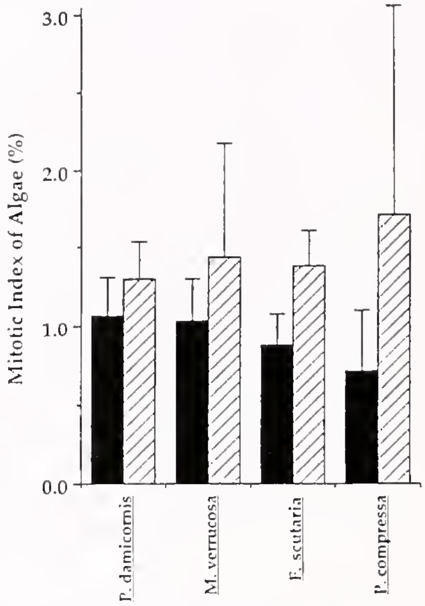

Figure 7. Mitotic indices of expelled algae (▨) and algae remaining within host tissues (■) of different corals, following a 15.5-h incubation at 27°C. Error bars represent standard deviations of the mean.

Discussion

In algal-cnidarian symbioses, regulation of algal numbers is an essential part of the symbiotic relationship, both during "steady state" (Muscatine *et al.,* 1975a, b; Trench, 1987) and during recovery of cnidarians from "bleaching events" (Gates, 1990; Hayes and Bush, 1990; Fitt *et al.,* 1993; Jones and Yellowlees, 1997). The present study has established that preferential expulsion of dividing algae contributes to regulation of algal-cnidarian symbiosis. If dividing algal cells are more likely to be expelled from the host, net algal population growth (within their hosts) will be effectively regulated.

Mitotic index of algae expelled naturally versus *isolated mechanically*

Algae naturally expelled from *Aiptasia pulchella* and other Hawaiian marine cnidarians have a higher MI than the algae remaining in their hosts (Figs. 1, 7). Suharsono and Brown (1992) and McCloskey *et al.* (1996) have also observed this phenomenon in other cnidarian species. Citing the most parsimonious explanation, these studies suggested that the increase in algal division rates is perhaps due to a lack of host regulation in the released algae. The present study tests this hypothesis by addressing an alternative hypothesis—that the higher MI of the released algae could be explained by preferential expulsion of dividing algal cells. These two possibilities were tested by separating the algae from the host and observing any changes in the algal MI. If the increase in MI is simply a function of a lack of host regulation, then artificially releasing the algae should result in an increase in MI. However, algae artificially

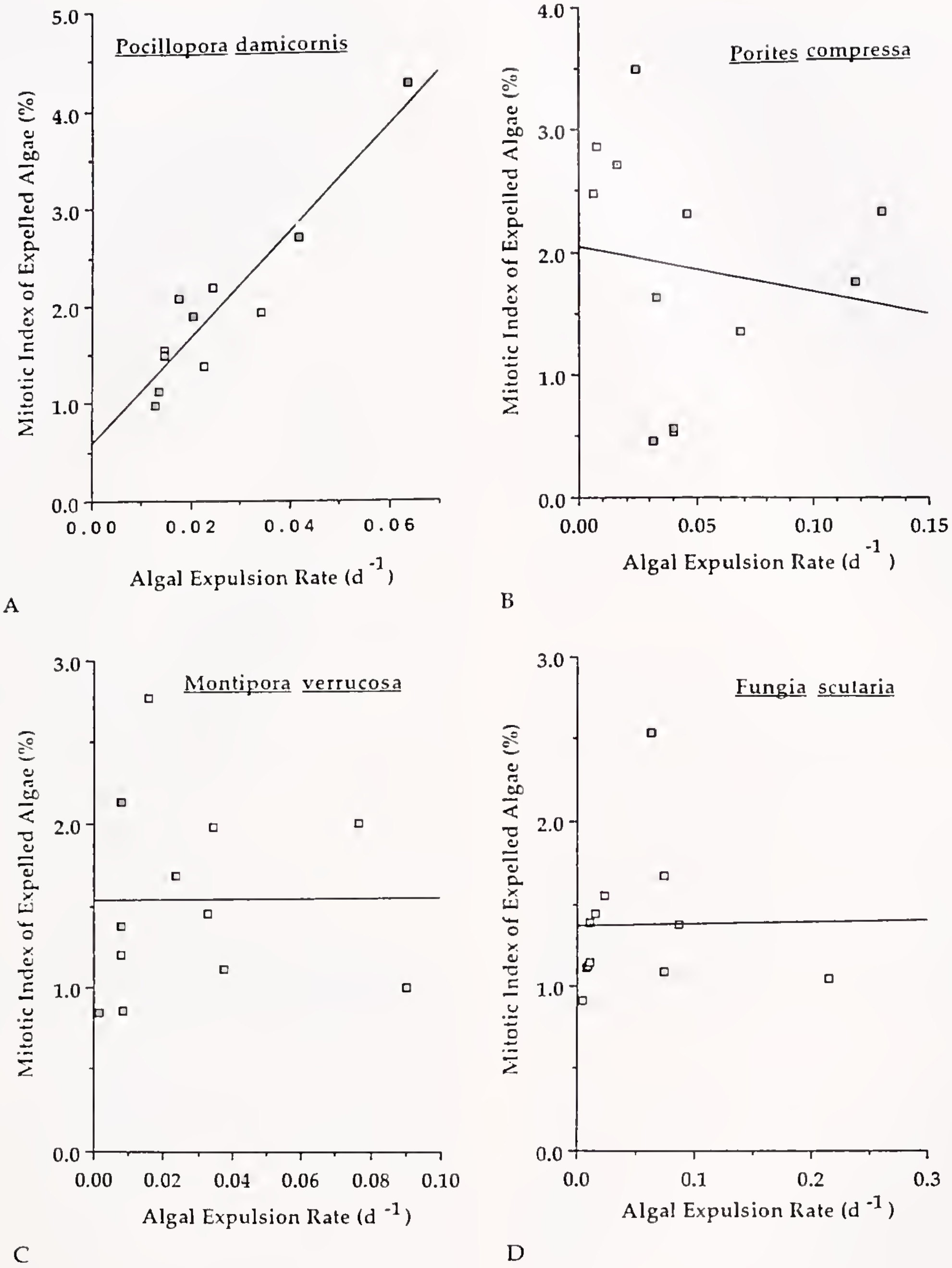

Figure 8. Correlation between mitotic index and rates of expulsion for various hermatypic corals from Kaneohe Bay, Oahu, Hawaii. (A) *Pocillopora damicornis* ($Y = 0.57457 + 54.019X$; $R^2 = 0.869$). (B) *Porites compressa* ($Y = 2.0435 - 3.7634X$; $R^2 = 0.023$). (C) *Montipora verrucosa* ($Y = 1.5287 + 0.12587X$; $R^2 = 0.000$). (D) *Fungia scutaria* ($Y = 1.3582 + 0.11192X$; $R^2 = 0.000$).

released from their host sea anemones (*A. pulchella*) in this study showed no increase in MI.

Incorporation of ^{3}H-thymidine by algae in situ

Uptake and incorporation of ^{3}H-thymidine is an indicator of cells advancing through S-phase of the cell cycle. In *A. pulchella*, cells naturally lost from the symbiosis (following a preincubation in ^{3}H-thymidine) incorporate more ^{3}H-thymidine (just prior to release) than did cells remaining in the hosts (Fig. 2). These data suggest that the released algae had been in S-phase during the ^{3}H-thymidine incubation and, by inference, were growing and dividing. Therefore, it can be concluded that dividing cells are preferentially expelled from the population.

This is the first study to successfully employ ^{3}H-thymidine as an indicator of algal division in symbiotic dinoflagellates. Cheney (1974) observed uptake of ^{3}H-thymidine by the host cells of the coral *Pocillopora damicornis*, but not by the symbiotic algae. Absence of ^{3}H-thymidine in the algae may have been due to (1) very low growth rates of the resident algae, resulting in minimal uptake of the ^{3}H-thymidine; (2) uptake and retention of the ^{3}H-thymidine by the host, thus minimizing availability of ^{3}H-thymidine to the algae; or (3) a high percentage of substitution of the base thymine by 5-hydroxymethyluracil in the algal DNA (Blank *et al.*, 1988; Taylor, 1990), resulting in low affinity for the ^{3}H-thymidine molecules in *P. damicornis*. The success of the present experiment may be attributed, in part, to the application of longer incubation times or higher doses of ^{3}H-thymidine. ^{3}H-thymidine is a tool that, in parallel with more classic approaches, may be useful in studying regulation of algal-cnidarian symbiosis; in this case, it has provided evidence for preferential loss of dividing algae from symbiotic cnidarians.

Mitotic index, algal expulsion, and effect of temperature

Figure 4 shows a direct linear correlation between expulsion and division rates of algae. That is, higher rates of division translate into greater expulsion of algae, supporting our suggestion of preferential loss of dividing cells (Fig. 3). Further, small increases in temperature, which result in slightly higher rates of division, also result in greater expulsion of algae (Fig. 5). This increased expulsion follows the same linear correlation patterns (relative to division rate) observed previously (Fig. 6). The data therefore strongly support the interpretation that expulsion of algae is preferential and related to the position of the algal cells within the cell cycle.

Expulsion of algae as a mechanism for regulating algal-cnidarian symbiosis

The mechanism involved in preferential expulsion of dividing cells is not clear, but appears to be related to the host's ability to accommodate algal growth. Whereas the expulsion rate of algae from *A. pulchella* in "steady-state" symbiosis is about 0.046 d^{-1}, expulsion of algae from re-infected aposymbiotic anemones during log phase repopulation is negligible (pers. obs.), confirming a previous study on repopulation of bleached individuals of the coral *Acropora formosa* (Jones and Yellowlees, 1997). Therefore, it appears that algal cells are primarily expelled from the system when the host cells can no longer accommodate them. This process can act as a "fine tuning" mechanism for regulating a steady-state symbiosis, where expulsion of algae may be viewed as an inverse function of the host's ability to accommodate new algal cells. Further, this mechanism could explain the differential expulsion of algae from tentacle *versus* body regions of the cnidarians, where differences in MI and algal densities would require different rates of expulsion from those regions (Muller-Parker and Pardy, 1987).

Preferential expulsion of dividing cells can also play a stabilizing role in algal-cnidarian symbiosis by dampening the effects of environmental conditions that can influence algal division rates. For example, whereas large increases in temperature can lower algal photosynthetic capacities, small increases in temperature may increase algal photosynthesis, metabolism, and thus growth and rates of division (Iglesias-Prieto *et al.*, 1992). However, if rates of algal expulsion vary as a function of the environmentally induced changes in rates of division (Fig. 6), then effectively, by releasing the "excess" cells, the total number of algae within the host will be regulated.

Preferential expulsion of dividing cells is not, however, the only means of regulating algal-cnidarian symbiosis. In case of the green hydra symbiosis, studies have already shown that algal ejection is not the normal mechanism for regulating population densities (McAuley, 1982), probably because of the higher numbers and growth rates of algae per host cell. Among Hawaiian anthozoans, although *A. pulchella* and *P. damicornis* do use preferential expulsion of dividing cells as a regulatory mechanism, other cnidarian species, such as *P. compressa, M. verrucosa*, and *F. scutaria*, may not (Fig. 8). This interspecific variability could be a function of the magnitude of "normal" algal growth rates at steady-state for each of the different species considered. Species with higher steady-state growth rates might be more likely to depend on a system of preferential expulsion of dividing cells for regulating their symbiosis. In contrast, among species that have very low daily rates of algal expulsion (such as *Xenia macrospiculata, Heteroxenia fuscescens, Stylophora pistillata*, and *Millepora dichotoma*; Hoegh-Guldberg *et al.*, 1987), the incidence of expulsion of algae would not significantly affect the regulation of population dynamics. Another possibility is that cnidarians with different algal clades may have evolved different mechanisms of regulation based on sensitivity to environmental factors or on the physiology of their hosts (Rowan *et al.*, 1997). In the case of *M. verrucosa, P. compressa*, and *F. scutaria*, the higher MI values of the expelled algae relative to those remaining in the hosts (Fig. 7) may simply be due to a lack of host regulation of division following algal release (Suharsono and Brown, 1992; McCloskey *et al.*, 1996).

A complete understanding of the role of expulsion of algal cells in regulating algal-cnidarian symbiosis requires further research into the release mechanisms involved. This study has shown that at least some symbiotic cnidarians preferentially expel dividing algal cells. In combination with other regulatory factors, this pattern of cell loss can play a major role in regulating algal-cnidarian symbiosis in steady state.

Acknowledgments

This research was partially funded by various National Science Foundation grants to L.M. We thank two anonymous reviewers for their comments on this work.

Literature Cited

Berner, T., G. Baghdasarian, and L. Muscatine. 1993. Repopulation of a sea anemone with symbiotic dinoflagellates: analysis by *in vivo* fluorescence. *J. Exp. Mar. Biol. Ecol.* **170:** 145–158.

Blank, R. J., and L. Muscatine. 1987. How do combinations of nutrients cause symbiotic *Chlorella* to overgrow hydra? *Symbiosis* **3:** 123–134.

Blank, R. J., V. A. R. Huss, and W. Kersten. 1988. Base composition of DNA from symbiotic dinoflagellates: a tool for phylogenetic classification. *Arch. Microbiol.* **149:** 515–520.

Cheney, D. P. 1974. The influence of temperature, dose level and morphology on the uptake of ^{3}H-thymidine by reef corals. *Proceedings of the Second International Coral Reef Symposium 1. Great Barrier Reef Committee,* Brisbane, Australia.

Cook, C. B. 1983. Metabolic interchange in algae-invertebrate symbiosis. *Int. Rev. Cytol. Suppl.* **14:** 177–210.

Davies, P. S. 1984. The role of zooxanthellae in the nutritional energy requirements of *Pocillopora eydouxi. Coral Reefs* **2:** 181–186.

Douglas, A., and D. C. Smith. 1984. The green hydra symbiosis VIII. Mechanisms in symbiont regulation. *Proc. R. Soc. Lond. B.* **221:** 291–319.

Drew, E. A. 1972. The biology and physiology of algae-invertebrate symbiosis II. The density of symbiotic algal cells in a number of hermatypic hard corals and alcyonarians from various depths. *J. Exp. Mar. Biol. Ecol.* **9:** 71–75.

Falkowski, P. G., Z. Dubinsky, L. Muscatine, and L. McCloskey. 1993. Population control in symbiotic corals. Ammonium ions and organic materials maintain the density of zooxanthellae. *BioScience* **43(9):** 606–611.

Fitt, W. K., H. J. Spero, J. Halas, M. W. White, and J. W. Porter. 1993. Recovery of the coral *Montastrea annularis* in the Florida Keys after the 1987 Caribbean "bleaching event." *Coral Reefs* **12:** 57–64.

Gates, R. D. 1990. Sea water temperature and sublethal coral bleaching in Jamaica. *Coral Reefs* **8:** 193–197.

Gates, R. D., and L. Muscatine. 1992. Three methods for isolating viable anthozoan endoderm cells with their intracellular symbiotic dinoflagellates. *Coral Reefs* **11:** 143–145.

Gates, R. D., G. Baghdasarian, and L. Muscatine. 1992. Temperature stress causes host cell detachment in symbiotic cnidarians: implications for coral bleaching. *Biol. Bull* **182:** 324–332.

Gates, R. D., O. Hoegh-Guldberg, M. J. McFall-Ngai, K. Y. Bil, and L. Muscatine. 1995. Free amino acids exhibit anthozoan "host factor" activity: They induce the release of photosynthate from symbiotic dinoflagellates *in vitro. Proc. Natl. Acad. Sci. USA* **92:** 7430–7434.

Hayes, R. L., and P. G. Bush. 1990. Microscopic observations of recovery in the reef-building scleractinian coral, *Montastrea annularis,* after bleaching on a Cayman reef. *Coral Reefs* **8:** 203–209.

Hoegh-Guldberg, O. 1994. Population dynamics of symbiotic zooxanthellae in the coral *Pocillopora damicornis* exposed to elevated ammonium [$(NH_4)_2SO_4$] concentrations. *Pac. Sci.* **48:** 263–272.

Hoegh-Guldberg, O., and G. J. Smith. 1989. Influence of the population density of zooxanthellae and supply of ammonium on the biomass and metabolic characteristics of the reef corals *Seriatorpora hystrix* and *Stylophora pistillata. Mar. Ecol. Prog. Ser.* **57(2):** 173–186.

Hoegh-Guldberg, O., L. R. McCloskey, and L. Muscatine. 1987. Expulsion of zooxanthellae by symbiotic cnidarians from the Red Sea. *Coral Reefs* **5:** 201–204.

Iglesias-Prieto, R., J. L. Matta, W. A. Robins, and R. K. Trench. 1992. Photosynthetic response to elevated temperature in the symbiotic dinoflagellate *Symbiodinium microadriaticum* in culture. *Proc. Natl. Acad. Sci. USA* **89:** 10302–10305.

Jones, R. J., and D. Yellowlees. 1997. Regulation and control of intracellular algae (equals zooxanthellae) in hard corals. *Philos. Trans. R. Soc. Lond. B* **352(1352):** 457–468.

Kinzie, R. A., III. 1974. Experimental infection of aposymbiotic gorgonian polyps with zooxanthellae. *J. Exp. Mar. Biol. Ecol.* **15:** 335–345.

Kinzie, R. A., III, and G. S. Chee. 1979. The effect of different zooxanthellae on the growth of experimentally reinfected hosts. *Biol. Bull.* **156:** 315–327.

Kolber, Z. S., J. Zehr, and P. G. Falkowski. 1988. Effects of growth irradiance and nitrogen limitation on photosynthetic energy conversion in photosystem II. *Plant Physiol.* **88:** 923–929.

McAuley, P. J. 1982. Temporal relationships of host cell and algal mitosis in the green hydra symbiosis. *J. Cell Sci.* **58:** 423–431.

McAuley, P. J. 1992. The effect of maltose release on growth and nitrogen metabolism of symbiotic *Chlorella. Br. Phycol. J.* **27:** 417–422.

McAuley, P. J., and P. R. Darrah. 1990. Regulation of numbers of symbiotic *Chlorella* by density-dependent division. *Philos. Trans. R. Soc. B* **329:** 55–63.

McCloskey, L. R., T. G. Cove, and E. A. Verde. 1996. Symbiont expulsion from the sea anemone *Anthopleura elegantissima* (Brandt) (Cnidaria; Anthozoa). *J. Exp. Mar. Biol. Ecol.* **195:** 173–186.

Muller-Parker, G., and R. L. Pardy. 1987. The green hydra symbiosis: analysis of a field population. *Biol. Bull.* **173:** 367–376.

Muller-Parker, G., L. R. McCloskey, O. Hoegh-Guldberg, and P. J. McAuley. 1994. Effect of ammonium enrichment on animal algal biomass of the coral *Pocillopora damicornis. Pac. Sci.* **48:** 273–283.

Muscatine, L. 1967. Glycerol excretion by symbiotic algae from corals and *Tridacna,* and its control by the host. *Science* **156:** 516–519.

Muscatine, L., and R. R. Pool. 1979. Regulation of numbers of intracellular algae. *Proc. R. Soc. Lond. B* **204:** 131–139.

Muscatine, L., C. B. Cook, R. L. Pardy, and R. R. Pool. 1975a. Uptake, recognition, and maintenance of symbiotic *Chlorella* by *Hydra viridis. Symp. Soc. Exp. Biol.* **29:** 175–203.

Muscatine, L., R. R. Pool, and R. K. Trench. 1975b. Symbiosis of algae and invertebrates: aspects of the symbiont surface and the host-symbiont interface. *Trans. Am. Microsc. Soc.* **94(4):** 450–469.

Neckelmann, N., and L. Muscatine. 1983. Regulatory mechanisms maintaining the *Hydra-Chlorella* symbiosis. *Proc. R. Soc. Lond. B* **219:** 193–210.

Pardy, R. L. 1974. Some factors affecting the growth and distribution of the algal endosymbionts of *Hydra viridis. Biol. Bull.* **147:** 105–118.

Rowan, R., N. Knowlton, A. Baker, and J. Java. 1997. Landscape ecology of algal symbionts creates variation in episodes of coral bleaching. *Nature* **388:** 265–269.

Smith, D. C. 1992. The symbiotic condition. *Symbiosis* **14:** 3–15.

Smith, G. J., and L. Muscatine. 1986. Carbon budgets and regulation of the population density of symbiotic algae. *Endocyt. Cell Res.* **3:** 213–238.

Smith, G. J., and L. Muscatine. 1999. Cell cycle of symbiotic dinoflagellates: variation in G1 phase-duration with anemone nutritional status and macronutrient supply in the *Aiptasia pulchella—Symbiodinium pulchrorum* symbiosis. *Mar. Biol.* **134:** 405–418.

Snidvongs, A., and R. A. Kinzie. 1994. Effect of nitrogen and phosphorus enrichment on *in vivo* symbiotic zooxanthellae of *Pocillopora damicornis*. *Mar. Biol.* **118:** 705–711.

Steen, R. G. 1987. Evidence for facultative heterotrophy in cultured zooxanthellae. *Mar. Biol.* **95:** 15–23.

Stimson, J., and R. K. Kinzie III. 1991. The temporal pattern and rate of release of zooxanthellae from the reef coral *Pocillopora damicornis* (Linnaeus) under nitrogen-enrichment and control conditions. *J. Exp. Mar. Biol. Ecol.* **153:** 63–74.

Suharsono, R. K., and B. E. Brown. 1992. Comparative measurements of mitotic index in zooxanthellae from a symbiotic cnidarian subject to temperature increase. *J. Exp. Mar. Biol. Ecol.* **158:** 179–188.

Sutton, D. C., and O. Hoegh-Guldberg. 1990. Host-zooxanthella interactions in four temperate marine invertebrate symbioses: assessment of effect of host extracts on symbionts. *Biol. Bull.* **178:** 175–186.

Taylor, C. E., L. Muscatine, and D. R. Jefferson. 1989. Maintenance and breakdown of the *Hydra-Chlorella* symbiosis: a computer model. *Proc. R. Soc. Lond. B* **238:** 277–289.

Taylor, F. J. R. 1990. Phylum Dinoflagellata. Pp. 419–437 in *Handbook of Protoctista*, L. D. Margulis, J. O. Corliss, M. Melkonian, and D. J. Chapman, eds. Jones and Bartlett, Boston.

Titlyanova, E. A., T. V. Titlyanova, V. A. Leletkin, J. Tsukahara, R. van Woesik, and K. Yamazato. 1996. Degradation of zooxanthellae and regulation of their density in hermatypic corals. *Mar. Ecol. Prog. Ser.* **139:** 167–178.

Trench, R. K. 1987. Dinoflagellates in non-parasitic symbiosis. Pp. 530–570 in *The Biology of Dinoflagellates*, F. J. R. Taylor, ed. Blackwell, Oxford.

Wilkerson, F. P., G. Muller-Parker, and L. Muscatine. 1983. Temporal patterns of cell division in natural populations of endosymbiotic algae. *Limnol. Oceanogr.* **28:** 1009–1014.

Reference: *Biol. Bull.* **199:** 287–297. (December 2000)

Cellular Basis of Gastrulation in the Sand Dollar *Scaphechinus mirabilis*

TETSUYA KOMINAMI* AND HIROMI TAKATA

Department of Biology and Earth Sciences, Faculty of Science, Ehime University, 2-5 Bunkyo-Cho, Matsuyama, 790-8577, Japan

Abstract. The processes of gastrulation in the sand dollar *Scaphechinus mirabilis* are quite different from those in regular echinoids. In this study, we explored the cellular basis of gastrulation in this species with several methods. Cell-tracing experiments revealed that the prospective endodermal cells were convoluted throughout the invagination processes. Histological observation showed that the ectodermal layer remained thickened, and the vegetal cells retained an elongated shape until the last step of invagination. Further, most of the vegetal ectodermal cells were skewed or distorted. Wedge-shaped cells were common in the vegetal ectoderm, especially at the subequatorial region. In these embryos, unlike the embryos of regular echinoids, secondary mesenchyme cells did not seem to exert the force to pull up the archenteron toward the inner surface of the apical plate. In fact, the archenteron cells were not stretched along the axis of elongation and were in close contact with each other. Here we found that gastrulation was completely blocked when the embryos were attached to a glass dish coated with poly-L-lysine, in which the movement of the ectodermal layer was inhibited. These results suggest that a force generated by the thickened ectoderm, rather than rearrangement of the archenteron cells, may play a key role in the archenteron elongation in *S. mirabilis* embryos.

Introduction

The processes of gastrulation in sea urchin embryos have been divided into two phases, known as primary and secondary invagination (Dan and Okazaki, 1956; Gustafson and Kinnander, 1956). During primary invagination, the thickened vegetal plate buckles into the blastocoel and gives rise to a short stub-like gut rudiment. After a couple of hours, the gut rudiment begins to elongate, and its tip reaches the inner wall of the apical plate. After secondary invagination, the gut rudiment results in a slender tube-like archenteron.

Primary invagination is autonomous, because the excised vegetal plate can still undergo morphological changes similar to those in the intact embryo (Moore and Burt, 1939; Ettensohn, 1984). One of the driving forces for primary invagination seems to be generated by bottle cells (Nakajima and Burke, 1996; Kimberly and Hardin, 1998). Wedge-shaped cells, which are frequently observed in the vegetal ectodermal layer, may produce another motive force for primary invagination (Burke *et al.*, 1991). During secondary invagination, a population of secondary mesenchyme cells (SMCs) connect the archenteron tip to the inner surface of the apical plate and exert the force to pull up the archenteron (Dan and Okazaki, 1956; Hardin, 1988). Rearrangement of the archenteron cells is an important cellular basis for elongation of the gut rudiment (Ettensohn, 1985; Hardin and Cheng, 1986; Hardin, 1989).

However, these mechanisms apply mainly to the regular echinoids and cannot fully explain the processes of gastrulation in a variety of sea urchins (Ettensohn, 1999). The embryos of a primitive sea urchin, *Eucidaris tribuloides*, show a different manner of gastrulation (Schroeder, 1981; Hardin, 1989); SMCs are not formed, but the embryos gastrulate. Even in the so-called "Regularia," some species of embryos do not show a typical manner of gastrulation (Amemiya *et al.*, 1982a, b). In a previous study, we indicated that the processes of gastrulation in the sand dollar *Scaphechinus mirabilis* (Clypeasteroida) were different from those reported in regular echinoids (Kominami and Masui, 1996). The processes of gastrulation could not be divided into two phases, because invagination proceeded at

---

Received 9 September 1999; accepted 10 August 2000.

* To whom correspondence should be addressed. E-mail: tkom@sci.ehime-u.ac.jp

a constant rate from beginning to end. Unlike the SMCs of regular echinoids, those of *S. mirabilis* did not form long filopodia. Moreover, the number of archenteron cells observed in cross sections remained unchanged, suggesting the absence of cell rearrangement in the archenteron.

One of the ways to a full understanding of the mechanisms of gastrulation in a species is to study the processes of gastrulation in a variety of related species. A less important factor in one species may be crucial in another species. The purpose of this study is to elucidate the cellular basis of gastrulation in *S. mirabilis* embryos. Changes in the morphology of gastrulating embryos were quantified. To clarify the movements of vegetal cells during gastrulation, cell-tracing experiment was undertaken. The shapes of constituent cells were observed on scanning electron micrographs and in immunostained specimens. To examine whether the ectodermal layer plays a role in archenteron elongation, the movement of the layer was inhibited by attaching the embryos to a glass dish coated with poly-L-lysine. Some of the results are compared with those obtained in the sea urchin *Hemicentrotus pulcherrimus* (Echinida), which shows a typical pattern of sea urchin gastrulation.

Materials and Methods

Animals

Adults of the sand dollar *Scaphechinus mirabilis* and the sea urchin *Hemicentrotus pulcherrimus* were collected and kept in aquaria supplied with circulating cold seawater (18°C for *S. mirabilis* and 15°C for *H. pulcherrimus*). Gametes of both species were handled as previously described (Kominami and Masui, 1996). Millipore-filtered seawater (MFSW) supplemented with 100 units/ml penicillin and 50 μg/ml streptomycin (Meiji Seika, Tokyo) was used throughout the experiments. Embryos of both species were cultured at 18 ± 1°C.

Histological observation

Gastrulating embryos were fixed with 1% glutaraldehyde dissolved in MFSW at room temperature for 2 h. After two rinses with MFSW, an aliquot of fixed embryos was dehydrated with an acetone series and mixed with Spurr resin. A drop of the mixture was mounted on a glass slide, sealed with coverslips, and polymerized. These specimens were for measurements of the thickness of the blastocoel wall, which cannot be obtained accurately in living embryos, because of optical reflections through the ectodermal layer.

Another aliquot of specimens was post-fixed with 1% OsO_4 dissolved in MFSW for 1 hr. The embryos were dehydrated with an ethanol series and critical-point dried (Hitachi, HCP-1, Tokyo). The specimens were adhered to the stub with a piece of double-sided transparent tape, and were fractured with a fine tungsten needle under a dissecting microscope. These specimens were coated with gold and platinum (Eiko, IB-3, Tokyo), and observed under a scanning electron microscope (Hitachi, S-450DX).

Cell contours were traced on scanning electron micrographs using transparent sheets. Shapes of cells were classified into four types according to the criteria described in Burke *et al.* (1991): columnar, cells longer than wide and rectangular in outline; wedge-shaped, apical surface broader than basal surface; skewed, the apex of the cell deviates from the apical basal axis; and others. The frequency of the appearance of these types of cells was obtained by examining between 4 and 19 SEM images at each observation point. Degree of archenteron invagination was obtained according to the method described in the previous report (Kominami and Masui, 1996). More than 20 embryos were measured at each observation point.

Cell tracing

The vegetal blastomeres of the 8-cell-stage embryos of *S. mirabilis* were somewhat smaller than those in the animal hemisphere. This morphological characteristic was used to orient the 8-cell-stage embryos so that Lucifer yellow CH (Sigma, St. Louis, MO) could be injected into one of the vegetal blastomeres. An experimental setup for iontophoretic injection of the dye was previously described (Kominami, 1988). The dye-injected embryos were observed under an epifluorescence microscope (Olympus, BH-RFL, Tokyo), and photographed.

Immunofluorescence

Gastrulating embryos were fixed successively with cold methanol and ethanol (−20°C), 20 min in each. Fixed embryos were embedded in polyester wax (BDH Laboratory Supplies, Poole, England) and sectioned (6 μm). After removal of the wax with absolute ethanol, specimens were rinsed twice with phosphate-buffered saline (PBS), and were reacted with a monoclonal antibody (VE10) that recognizes the carbohydrates at the cell surface. After the primary reaction, the specimens were rinsed twice with PBS, and then reacted with FITC-conjugated goat anti-mouse IgG (Sigma) for 1 h. The immunostained sections were mounted on a glass slide with a small amount of glycerol.

Attaching the embryos to the glass dish

The cleaned glass dish was soaked overnight in 1 mg/ml poly-L-lysine (Sigma) dissolved in distilled water. After the solution was removed, the glass dish was rinsed three times with distilled water and air-dried. A micropipette was used to attach the gastrulating embryos to the bottom of the glass dish; in some cases, the embryos were pressed against the bottom of the dish with a fine glass needle, to ensure

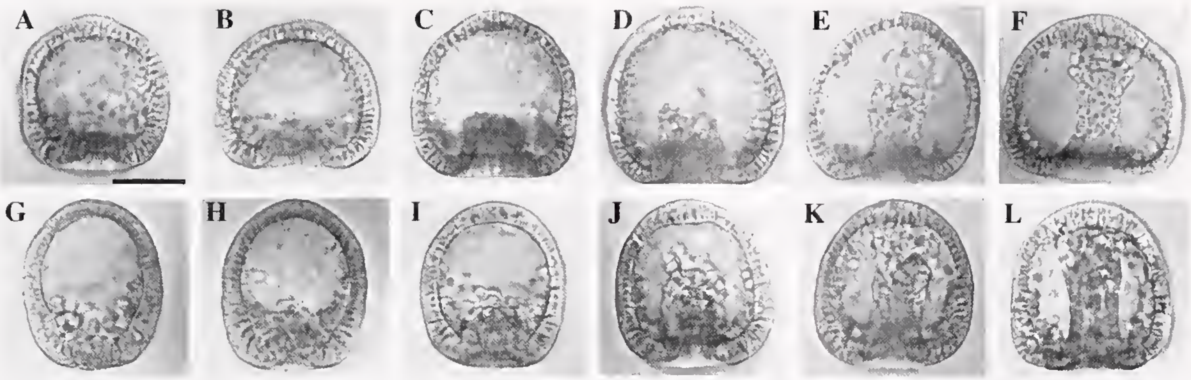

Figure 1. Processes of gastrulation in *Hemicentrotus pulcherrimus* and *Scaphechinus mirabilis*. Embryos of both species were cultured at 18°C and observed hourly. Embryos were embedded in Spurr resin. (A–F) *H. pulcherrimus*, 17–22 h. (G–L) *S. mirabilis*, 14–19 h. In *H. pulcherrimus* embryos, the primary and secondary invagination is clearly distinguished by the presence of a pause in the archenteron elongation (C–D, 1–2 hours). After the occurrence of the secondary invagination, the archenteron became slender. In *S. mirabilis* embryos, the archenteron invaginated continuously, and the diameter of the archenteron remained unchanged during gastrulation. The scale bar indicates 50 μm.

attachment. The processes of gastrulation were photographed at intervals of 10 min.

Results

Morphological changes during gastrulation

Figure 1 shows the processes of gastrulation in embryos of *H. pulcherrimus* (A–F) and *S. mirabilis* (G–L) kept at 18°C. In a regular echinoid, *H. pulcherrimus*, primary (Fig. 1A–C) and secondary invagination (Fig. 1D–F) were clearly distinguished by the presence of a time lag in archenteron elongation (1–2 h, Fig. 1C–D). On the other hand, the archenteron of *S. mirabilis* embryos elongated at a constant rate during the course of invagination (Fig. 1G–L).

Besides archenteron elongation, several differences were noticed in the morphology of the embryos of these two species. In *H. pulcherrimus*, the height of the embryo increased to some extent during primary invagination. After the onset of secondary invagination, the embryos were shortened along the animal-vegetal axis (Fig. 2A). The width of the embryos increased as gastrulation progressed (Fig. 2B). This was caused by the expansion of the ectodermal layer, especially at the lateral blastocoel wall (Fig. 2C). In contrast, *S. mirabilis* embryos became shorter as invagination progressed (Fig. 2D). Though their width increased to some extent (Fig. 2E), the expansion of the ectodermal layer was not so conspicuous as in *H. pulcherrimus* (Fig. 2F).

Tracing of the vegetal blastomeres

The dye-injected *S. mirabilis* embryos were examined to learn how vegetal cells move toward the blastopore during gastrulation (Fig. 3). Before the initiation of invagination, the boundary between labeled and nonlabeled cells was at about 50% of the distance from the vegetal pole to the animal pole (Fig. 3A, A′). The boundary gradually shifted toward the vegetal pole side as invagination progressed (Fig. 3B, B′, C, C′, D, D′). At the end of invagination, the

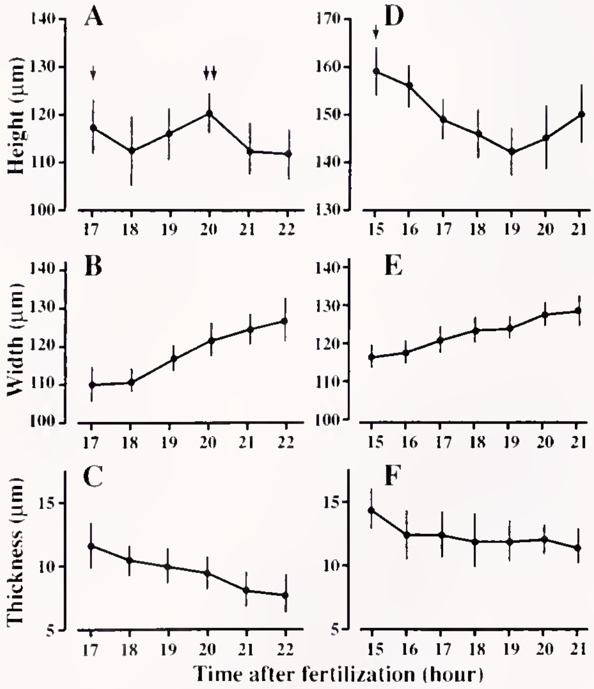

Figure 2. Change in the height and width of the embryos, and in the thickness of the blastocoel wall (the lateral part of the embryo) during gastrulation. (A–C) *Hemicentrotus pulcherrimus*. (D–F) *Scaphechinus mirabilis*. Single arrows indicate the time of the initiation of gastrulation. Double arrows indicate the time of the onset of the secondary invagination in *H. pulcherrimus* embryos. Changes in the height of the embryo (A, D) show different patterns. In both species, the width of the embryo increased as invagination progressed (B, E). This is more evident in *H. pulcherrimus* than in *S. mirabilis*. The thickness of the blastocoel wall decreases during gastrulation, but the change is not conspicuous in *S. mirabilis* (C, F).

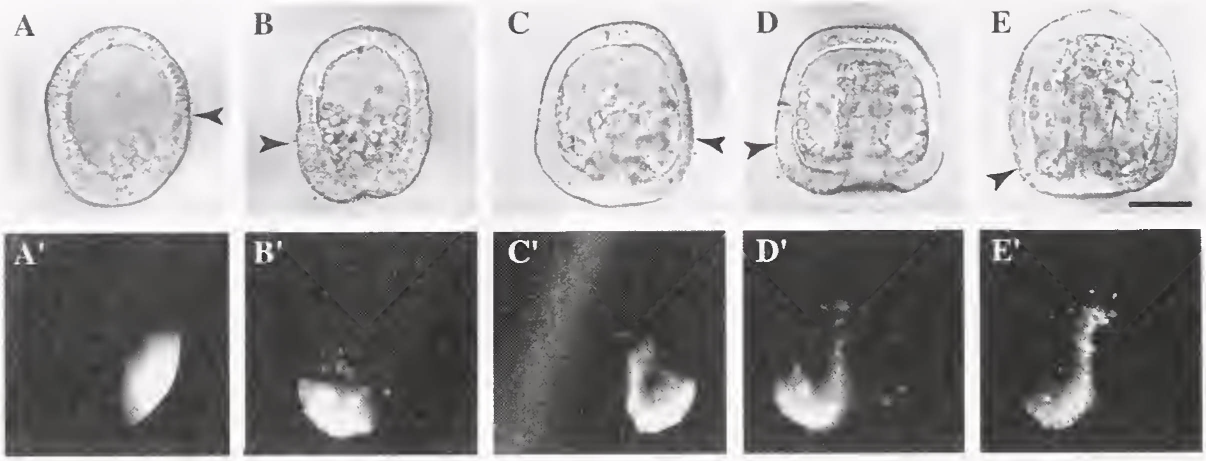

Figure 3. Movement of vegetal cells during gastrulation in *Scaphechinus mirabilis* embryos: bright-field images (A–E); fluorescence images (A′–E′). (A, A′) 14 h. (B, B′) 16 h. (C, C′) 17 h. (D, D′) 18 h. (E, E′) 20 h. Distribution of labeled cells in invaginating gastrulae, which had been injected with Lucifer yellow CH into one of vegetal blastomeres at the 8-cell stage, was examined. As gastrulation proceeds, the boundary between labeled and nonlabeled cells moves downward. Arrowheads in A–E demarcate the boundary observed on fluorescent images. The scale bar indicates 50 μm.

boundary was located at 10%–15% of the embryo length from the vegetal pole (Fig. 3E, E′). This value corresponds to the thickness of the anal plate ectoderm. The relationship between the degree of invagination and the position of the boundary is shown in Figure 4. During the early stages of invagination, the position of the boundary shifted rapidly to the vegetal pole; during the later stages, the rate of the movement decreased gradually. The result clearly indicates that the involution of cells through the blastopore continues until the archenteron tip reaches the apical plate.

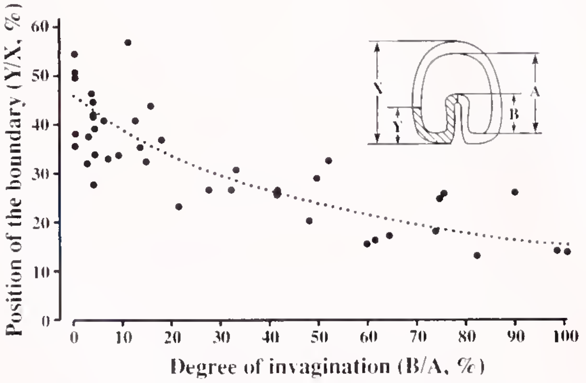

Figure 4. Change in the position of the boundary between animal and vegetal ectoderm during gastrulation. The degree of invagination (%) and the position of the boundary along the embryo axis (%) were sought using the parameters shown in the inset. The most fitting hyperbolic curve is also shown. The movement of the vegetal cells toward the vegetal pole continues throughout the invagination processes, though the rate of the movement changes.

Shapes of the ectodermal cells during early stages of gastrulation

The shapes of the ectodermal cells during early stages of gastrulation were examined with SEM (Fig. 5). The cells were classified as columnar, skewed, wedge-shaped, and other, as described in the Materials and Methods. Among these types, wedge-shaped cells showed differences in their distribution between the two species of embryos. In *H. pulcherrimus,* two to three wedge-shaped cells were observed just at the bending point of the ectodermal epithelium (Fig. 5A–D, arrowheads). In *S. mirabilis,* such wedge-shaped cells were distributed more broadly apart from the blastopore (Fig. 5E–H, arrowheads). In addition, the number of wedge-shaped cells was larger than in *H. pulcherrimus.* At the beginning of invagination, bottle-shaped (apically constricted and basally rounded-up) cells were frequently observed in the bending vegetal plate (arrows indicate bottle cells in Fig. 5D [*H. pulcherrimus*] and 5G [*S. mirabilis*]).

Figure 6 shows the change in the ratio of these three types of cells during early stages of gastrulation. In both species, it takes 3–4 h to give rise to a short, stub-like gut rudiment after the first sign of invagination. These stages were divided hourly and designated Stages I–IV. In the animal halves, columnar and skewed cells were abundant (Fig. 6A, *H. pulcherrimus; 6C, S. mirabilis*). In both species, the ratio of columnar cells increased as gastrulation progressed. In contrast, most cells in the vegetal half were skewed or distorted (Fig. 6B, *H. pulcherrimus; 6D, S. mirabilis*). In *H. pulcherrimus,* wedge-shaped cells occupied nearly 40% of the total at the initial stage of invagination, but decreased to

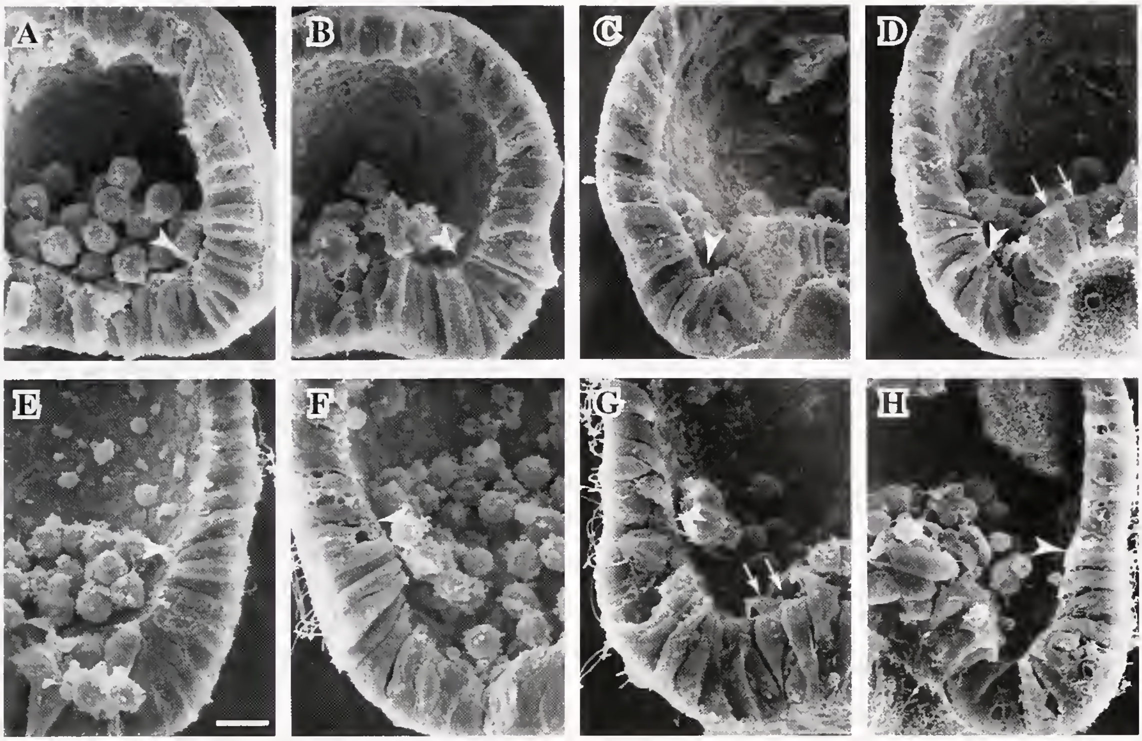

Figure 5. Scanning electron micrographs of the cells in the ectoderm and invaginated archenteron during early stages of gastrulation: *Hemicentrotus pulcherrimus* (A–D); *Scaphechinus mirabilis* (E–H). In A–D, arrowheads indicate the bending point; in E–H they indicate the boundary between animal and vegetal cells. Arrows in D and G indicate bottle cells. Ectodermal cells of *S. mirabilis* (F–H) were more elongated in the apico-basal direction than those of *H. pulcherrimus* (B–D). Columnar and skewed cells were frequently observed in both species. Wedge-shaped cells were also observed in both species, especially in the vegetal half. In *H. pulcherrimus*, two to three wedge-shaped cells were observed just at the bending point of the epithelium (B, C). Such wedge-shaped cells are distributed more broadly apart from the blastopore in *S. mirabilis* (F, G). The scale bar indicates 10 μm.

about 20% as invagination progressed; in *S. mirabilis*, the ratio remained constant at a rather higher level. Columnar cells were barely observed in *S. mirabilis* (Fig. 6D), whereas this type of cell increased in *H. pulcherrimus* at the end of primary invagination (Fig. 6B).

Secondary mesenchyme cells at the archenteron tip

Figure 7 shows the secondary mesenchyme cells observed at the archenteron tip of the midgastrulae. In *H. pulcherrimus*, these cells were globular and formed long thin filopodia. Several SMCs were located between the archenteron tip and the future oral opening region. In *S. mirabilis*, SMCs were flattened to some extent and formed broad ruffled membranes. No cells were observed between the archenteron tip and the future oral opening region. Although more than 200 gastrulating *S. mirabilis* embryos were examined, an image that showed direct contact between the filopodia of the SMCs and the inner surface of the apical plate could not be obtained.

Shape of archenteron cells during later stages of invagination

Figure 8 shows cross fractures of the archenteron at later gastrula stages. SEM images of the archenteron at three levels along its axis (top, middle and bottom) are shown. The cells in the archenteron of *H. pulcherrimus* were cuboid and loosely in contact with each other (Fig. 8A–C). The numbers of cells observed in cross fractures increased from top (6–7) to bottom (about 12) of the archenteron. The archenteron cells had a rounded basal surface. In contrast, cells in the archenteron of *S. mirabilis* embryos were elongated along the apico-basal direction (Fig. 8D–F). The numbers of cells observed in cross fractures were almost the same at the top (14–15), middle (13), and bottom (13) levels of the archenteron.

As gastrulation proceeded, it became difficult to crack the archenteron along its long axis. The shapes of cells in the embryos at later stages of invagination were examined on histological sections. The stages shown in Figure 9 correspond to the secondary invagination in *H. pulcherrimus* embryos. As clearly shown, the cells in the archenteron of

H. pulcherrimus embryos were stretched along the axis of the archenteron (Fig. 9A–D). After the completion of the secondary invagination, the cells resumed a cuboid shape (Fig. 9E–F). In contrast, the cells in the archenteron of *S. mirabilis* embryos were not stretched at any stage of later invagination (Fig. 9G–L). It should be noted that the cells near the blastopore were elongated along their apico-basal direction through all the stages examined.

These changes in cell shape were quantified according to the methods described by Hardin (1988); two ratios, *Y/X* (ratio of lengths along and perpendicular to the axis of the archenteron) and *L/W* (ratio of cell length and width) were obtained (Fig. 10). Both *Y/X* and *L/W* increased during the secondary invagination in *H. pulcherrimus* embryos, and decreased to the initial level at the end of secondary invagination (Fig. 10A). On the other hand, the ratios did not change in *S. mirabilis* embryos through these stages of invagination (Fig. 10B). The result clearly shows that the archenteron cells in *S. mirabilis* embryos were not stretched along the axis of the archenteron.

Attaching embryos to a glass dish coated with poly-L-lysine

The obtained results suggest the ectodermal layer plays a role in the invagination process in *S. mirabilis* embryos. If

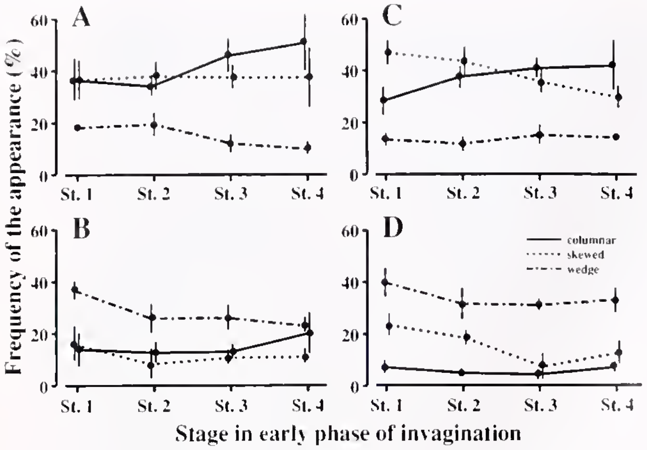

Figure 6. Frequency of the appearance of columnar, skewed, and wedge-shaped cells during gastrulation: *Hemicentrotus pulcherrimus* (A, B); *Scaphechinus mirabilis* (C, D). (A, C) Animal hemisphere. (B, D) Vegetal hemisphere. Columnar cells (solid lines) are more abundant in the animal hemisphere. Skewed cells (dotted lines) were observed more frequently in *S. mirabilis*. In both species, the population of columnar cells increased as the gastrulation proceeded (A, C). Wedge-shaped cells (broken lines) appear sparsely in the animal hemisphere. In contrast, the most abundant type of cells are wedge-shaped cells in the vegetal halves (B, D). Columnar cells were rarely observed in *S. mirabilis*, but such cells increased in *H. pulcherrimus* after the secondary invagination had started.

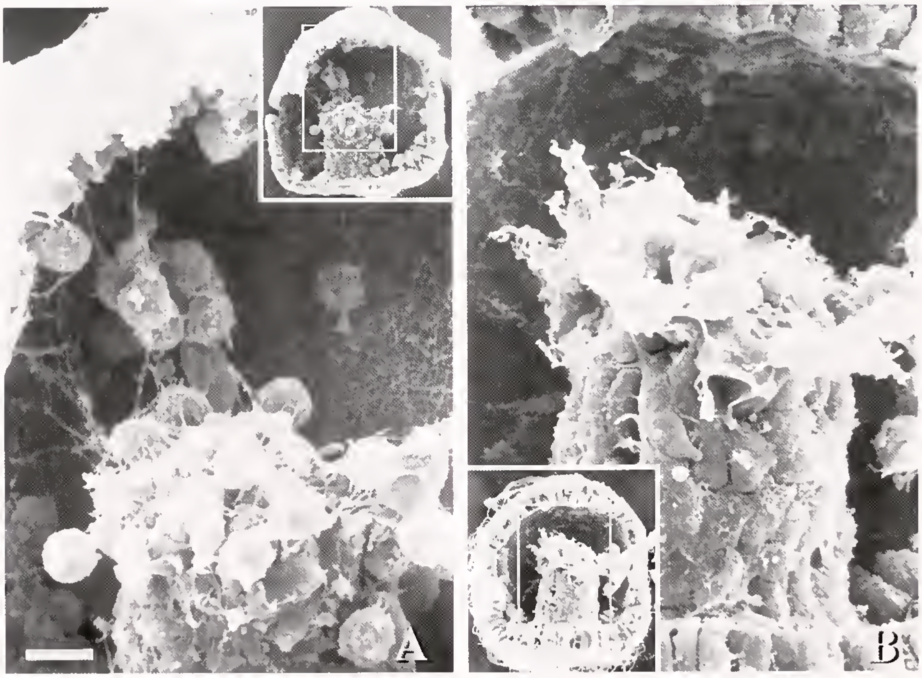

Figure 7. Scanning electron micrographs of the secondary mesenchyme cells at the archenteron tip. *Hemicentrotus pulcherrimus* (A); *Scaphechinus mirabilis* (B). Insets in A and B show whole view of the mid-gastrula. Secondary mesenchyme cells in *H. pulcherrimus* are globular in shape and form long thin filopodia. Several secondary mesenchyme cells (SMCs) are located between the archenteron tip and the inner surface of the future oral opening region. In contrast, SMCs are flattened and form ruffled membranes in *S. mirabilis* gastrulae. No SMCs were observed between the archenteron tip and the future oral opening region. The scale bar indicates 10 μm.

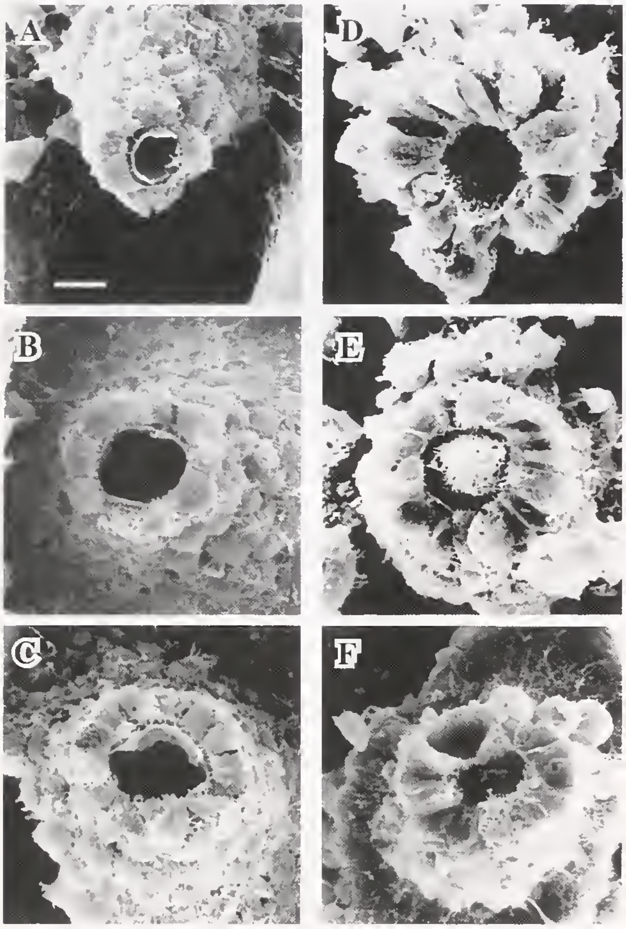

Figure 8. Scanning electron micrographs of the cells in the archenteron after the completion of invagination: *Hemicentrotus pulcherrimus* (A–C); *Scaphechinus mirabilis* (D–F). Top (A, D), middle (B, E), and bottom (C, F) levels of the archenteron are shown. The cells in the archenteron of *H. pulcherrimus* are cuboid, while those in *S. mirabilis* are elongated along the apico-basal direction. Note that the wall of the archenteron is thicker in *S. mirabilis* than in *H. pulcherrimus*. The scale bar indicates 10 μm.

this is the case, immobilization of the ectodermal layer should affect the invagination process. To test this possibility, the change in the length of the archenteron was monitored in gastrulating embryos attached to a glass dish coated with poly-L-lysine.

H. pulcherrimus gastrulae attached to the poly-L-lysine coated glass dish (Fig. 11A). If the embryos had been undergoing primary invagination when attached, the invagination was slowed and tip of the archenteron could not reach the apical plate. However, the embryos gastrulated almost normally if they had been attached after primary invagination. In these cases, the rate of archenteron elongation was not different from that in control embryos (Fig. 11B).

In contrast, the invagination process was greatly affected in *S. mirabilis* embryos. If the embryos were not pressed against the bottom of the glass dish using a glass needle, they did not firmly attach to the glass dish. Embryo II shown in Figure 12 loosely attached to the glass dish, so that its position changed during observation. In this embryo, invagination occurred almost normally. On the other hand, embryos I, III, and IV were rather firmly attached to the glass dish. In these embryos, invagination of the gut rudiment was considerably delayed. Nonetheless, embryos III and IV restarted invagination when they detached from the glass dish (Fig. 12F and H, respectively). Embryos that were firmly attached to the glass dish could not gastrulate at all, irrespective of the degree of invagination at attachment (Fig. 13A and B). In addition, the contour of the embryos was distorted during prolonged observation.

Discussion

Involution of the vegetal cells continues during gastrulation

Endodermal tissue in sea urchin embryos had been thought to be exclusively derived from the veg_2 tier of blastomeres formed at the 60-cell stage (Hörstadius, 1973; Cameron *et al.*, 1987, 1991; Ruffins and Ettensohn, 1996). More recently, it has been shown that the descendants of the veg_1 tier of blastomeres also participate in the formation of the digestive tract (McClay and Logan, 1996; Logan and McClay, 1997). The recruitment of the veg_1-derived cells seems to occur only after the tip of the archenteron reaches the apical plate (Martins *et al.*, 1998; Piston *et al.*, 1998; Ransick and Davidson, 1998). The mechanisms of such late ingression of endodermal cells are, however, unknown. Here we focus on the invagination processes that occur before and around the time that the archenteron tip reaches the inner surface of the apical plate.

In embryos of an irregular echinoid, *S. mirabilis*, some unique aspects of gastrulation were elucidated from the measurement of the size of the gastrulating embryos. As is well known, the embryos of regular echinoids expand considerably during gastrulation (Fig. 1A–F). This expansion was caused by thinning of the ectoderm (Fig. 2C). In contrast, the thinning of the blastocoel wall was not so conspicuous in *S. mirabilis* (Fig. 2F). Although the width of the embryos became somewhat larger, their height became smaller as invagination progressed (Fig. 1G–L). This implies a physical continuity between endodermal and ectodermal epithelia during invagination. In fact, convolution of the vegetal cells continued until the archenteron tip reached the apical plate (Figs. 3, 4), whereas such convolution terminates at the end of primary invagination in regular echinoids (Burke *et al.*, 1991).

In *H. pulcherrimus* embryos, invagination was partially inhibited if the embryos just undergoing primary invagination were attached to a glass dish coated with poly-L-lysine (Fig. 11, embryos III and IV). However, the archenteron elongated almost normally if the embryos

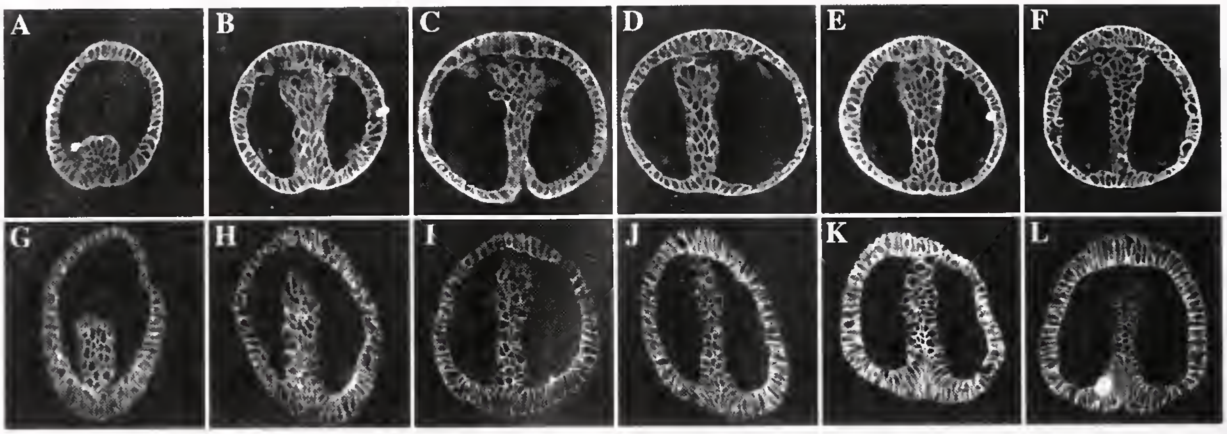

Figure 9. Change in the contour of cells during later stages of invagination as seen in immunostained histological sections. (A–F) *Hemicentrotus pulcherrimus* embryos at 19, 20, 22, 24, 26, and 28 h, respectively. (G–L) *Scaphechinus mirabilis* embryos at 17, 18, 19, 20, 21, and 22 h, respectively. The ectodermal cells in *H. pulcherrimus* embryos were initially elongated along the apico-basal direction (A), and became cuboid with the progress of gastrulation. The archenteron cells were stretched along the axis of the archenteron (B–D or E), and resumed a cuboid shape (F). In contrast, both the ectodermal and endodermal cells in *S. mirabilis* embryos remained elongated along the apico-basal direction during the later stages of invagination (G–L).

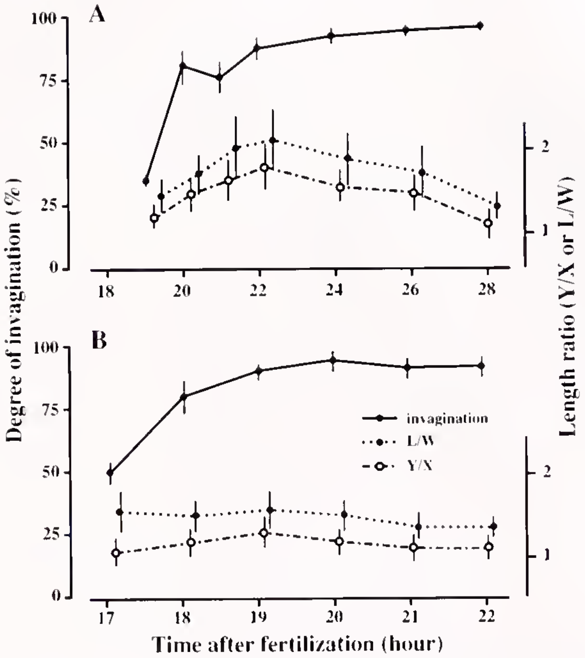

Figure 10. Change in the shape of the archenteron cells during later stages of gastrulation: *Hemicentrotus pulcherrimus* (A); *Scaphechinus mirabilis* (B). Shape was expressed as two ratios: *Y/X* (length along the archenteron axis to length perpendicular to the axis) and *L/W* (cell length to width). In *H. pulcherrimus* embryos, both ratios increased as secondary invagination progressed, up to at least 22 h. Then the ratios decreased to about 1.0. In *S. mirabilis* embryos, the ratios did not change significantly, though the degree of invagination increased. The *Y/X* ratio remained about 1.0, which indicates that the archenteron cells are not stretched along the axis of the archenteron.

had finished primary invagination when attached (Fig. 11, embryos I and II). This suggests that the vegetal ectodermal layer moves toward the blastopore during primary invagination, and that the layer loses physical continuity from the gut rudiment after the completion of primary invagination. On the other hand, elongation of the archenteron was completely blocked in *S. mirabilis* if the embryos were attached to a coated glass dish, irrespective of the degree of invagination (Fig. 13). This inhibitory effect of poly-L-lysine cannot be ascribed solely to the chemical toxicity of the drug, because the embryos restarted gastrulation soon after they detached from the glass dish (Fig. 12). We suppose that the ectodermal epithelium and the invaginated archenteron are physically continuous during the invagination processes and that the blockage of invagination is mainly due to physical constraint of the ectodermal layer attached to the glass dish.

The precise mechanism by which elongation of the gut rudiment is blocked in *S. mirabilis* embryos is unknown. The ectodermal layer seems to be more rigid in *S. mirabilis* embryos than in those of *H. pulcherrimus*, because the former is thicker (Fig. 2F). In addition, *S. mirabilis* embryos retained normal configuration after they were fixed with 10% formaline, while the ectodermal layer of *H. pulcherrimus* embryos was severely distorted when the fixative was applied. The ectodermal cells in *S. mirabilis* embryos are probably tightly connected with each other, forming a rigid structure over the entire vegetal ectoderm. Even if embryos are attached to the glass dish on one side of the body, such a rigid structure may be destroyed totally, resulting in a blockage of archenteron elongation.

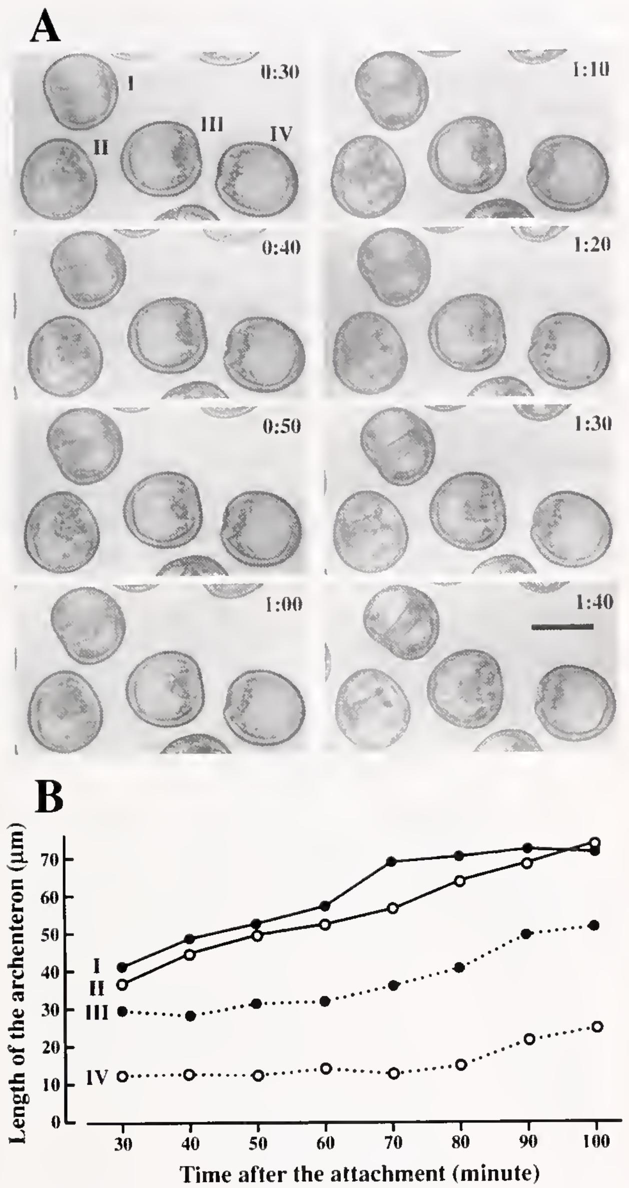

Figure 11. Adhesion of *Hemicentrotus pulcherrimus* embryos to the glass dish coated with poly-L-lysine. The numeral at the top right corner in each photograph in A indicates the time after the attachment to the glass dish. Roman numerals (I–IV) in A and B indicate the same embryos. The embryos gastrulated almost normally if they had been attached after the primary invagination (embryo I and II). If the embryos had been just in the primary invagination when attached, the rate of elongation of the archenteron was slowed and the archenteron could not reach the apical plate (embryo III and IV). The scale bar indicates 100 μm.

The initial phase of gastrulation

In both species of embryos, bottle cells (Nakajima and Burke, 1996) were observed in the vegetal plate (Fig. 5D, G, arrows). The appearance of bottle cells in the vegetal plate may lead to the first step of invagination, if the archenteron cells retain the monolayer arrangement (Gustafson and Wolpert, 1963, 1967). Unlike the archenteron cells in *H. pulcherrimus* embryos (Fig. 5C, D), those in *S. mirabilis* embryos were variable in shape and were not organized into a complete monolayer sheet (Fig. 5G, H). As a result, the force produced by bottle cells does not necessarily cause the bending of the vegetal plate. Other forces seem to be necessary to produce the invagination of the vegetal plate cells in *S. mirabilis* embryos.

In this study, several types of cells were observed on SEM images. The role of each type of cell is unknown. If cells are pulled apically or basally, they should become skewed, because cells are connected with extracellular matrix (Wessel and McClay, 1987; Burke *et al.*, 1991; Berg *et al.*, 1996). If a monolayer cell sheet is bent, wedge-shaped cells should appear at the bending point. Thus, the shapes of cells are signs of the existence of the forces generated by surrounding tissues or by the cells themselves. In both species of embryos, the ratio of columnar cells in the animal hemisphere increased as invagination progressed (Fig. 6A, C). On the other hand, most cells in the vegetal hemisphere were distorted (Fig. 6B, D). Especially in *S. mirabilis* embryos, columnar cells were barely observed through the stages examined. These results imply that

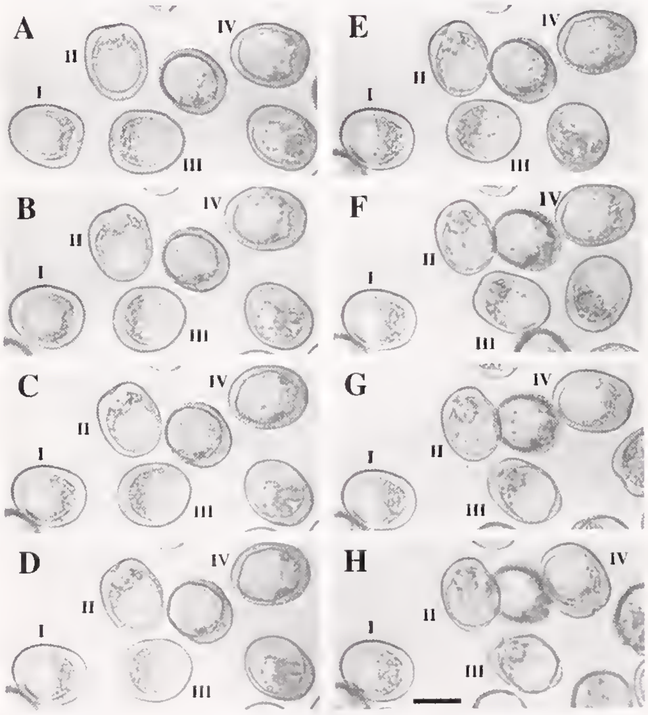

Figure 12. Adhesion of the *Scaphechinus mirabilis* embryos to the glass dish coated with poly-L-lysine. Embryo II was loosely attached to the glass dish, because its position changed during observation. In this embryo, invagination occurred almost normally. On the other hand, embryos I, III, and IV were rather firmly attached to the glass dish and invagination of the gut rudiment were considerably delayed. Nonetheless, embryos III and IV reinitiated invagination when they detached from the glass dish. The scale bar indicates 100 μm.

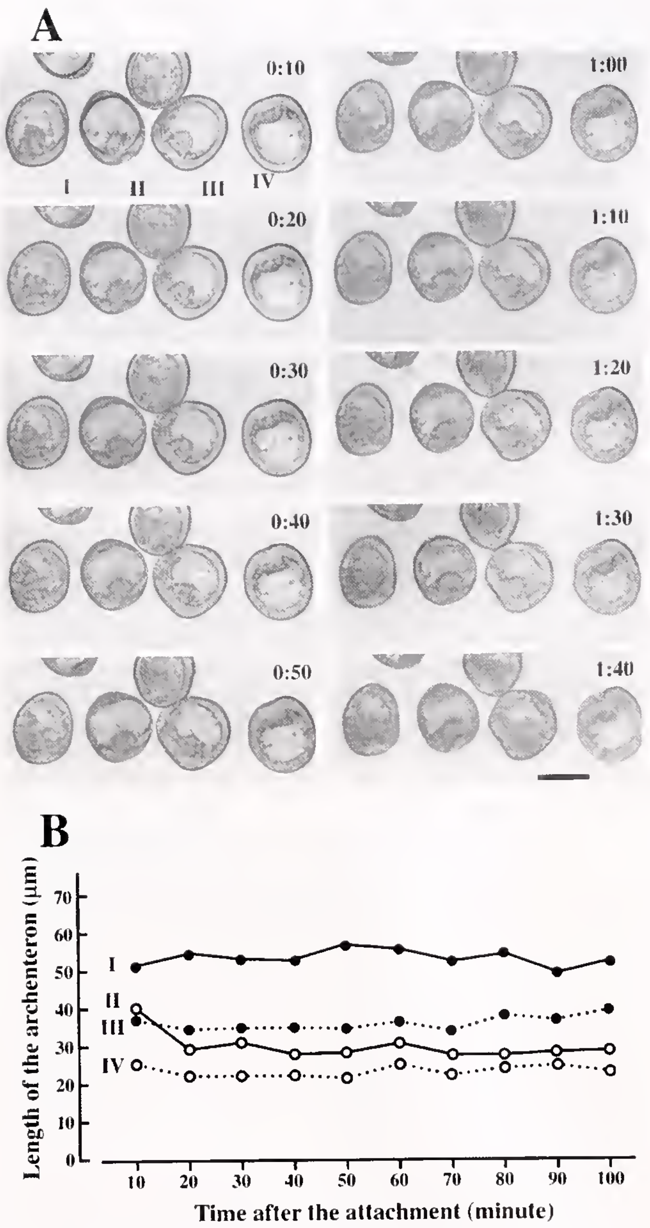

Figure 13. Adhesion of the *Scaphechinus mirabilis* embryos to the glass dish coated with poly-L-lysine. The numeral at the top right corner in each photograph in A indicates the time after the attachment to the glass dish. Roman numerals (I–IV) in A and B indicate the same embryos. *S. mirabilis* embryos could not gastrulate at all, irrespective of the degree of invagination. The scale bar indicates 100 μm.

some forces continue to operate in the vegetal hemisphere of *S. mirabilis* embryos.

Elongation of the archenteron

It is well-established that SMCs pull up the gut rudiment during secondary invagination in some sea urchins (Dan and Okazaki, 1956; Gustafson and Kinnander, 1956; Hardin, 1988; Hardin and McClay, 1990). In *H. pulcherrimus* embryos, a chain of SMCs was observed to connect the archenteron tip and the apical plate (Fig. 7A). The height of the embryos became shortened after the onset of secondary invagination (Fig. 2A). This shortening could be caused by contraction of the SMCs' pseudopodia, which connect the archenteron tip and the apical plate across the blastocoel. The contraction of pseudopodia should stretch the archenteron. In fact, the archenteron cells in *H. pulcherrimus* embryos were stretched along the axis of the archenteron during secondary invagination (Fig. 9B–D, Fig. 10A). On the other hand, the SMCs of *S. mirabilis* embryos did not connect the archenteron tip and the site of the future oral opening (Fig. 7B). Although it is possible that the connecting filopodia were broken by fixation, the archenteron cells in *S. mirabilis* embryos were not stretched throughout the invagination processes (Fig. 9G–L, Fig. 10B). Thus, unlike the SMCs in regular echinoids, those in *S. mirabilis* embryos may not pull up the archenteron.

Rearrangement of archenteron cells is another cellular basis of the extension of the gut rudiment during secondary invagination (Ettensohn, 1985; Hardin and Cheng, 1986; Hardin, 1989). The archenteron cells of *H. pulcherrimus* embryos were cuboid, with rounded basal surfaces (Fig. 8A–C). In contrast, the archenteron cells in *S. mirabilis* embryos were elongated—a configuration that should be brought about by close contact between cells. In fact, the archenteron cells of *S. mirabilis* embryos looked closely compacted (Fig. 7B). It is unlikely that these cells change their position freely in the archenteron. Moreover, the numbers of cells observed in the cross fractures of the archenteron were almost the same at any level along the axis of the archenteron (Fig. 8D–F). Thus, rearrangement of the archenteron cells is not a major cellular basis of archenteron elongation in *S. mirabilis*.

Motive force for the elongation of the archenteron

During the early stages of invagination, prospective endodermal cells are elongated and concentrated in the vegetal plate in both species of embryos. This configuration of cells may be brought about by an increase in cell adhesiveness or by lateral pressure generated by the surrounding tissues. In *S. mirabilis* embryos, cells near the blastopore were elongated throughout the invagination processes (Fig. 9G–L). On the other hand, vegetal cells regained cuboid shape after the completion of primary invagination in *H. pulcherrimus* (Fig. 9A–F). The archenteron cells in *S. mirabilis* embryos were also elongated along the apico-basal direction (Fig. 8, 9). These cell shapes suggest the existence of the lateral pressure in the thickened vegetal plate and the archenteron.

Wedge-shaped cells observed in the thickened vegetal ectoderm are one possible source of such pressure. Appearance of the wedge-shaped cell in a monolayer cell sheet should produce a bending force, although such a shape of cells is merely a result of a bending of the cell sheet. In both species of embryos, wedge-shaped cells appeared in the thickened vegetal plate prior to invagination (Fig. 5A, E). It should be noted that a mass of wedge-shaped cells is found at the subequatorial region (corresponds to the boundary between the descendants of an_2 and veg_1) in *S. mirabilis* embryos, but is located just at the bending point (boundary between veg_1 and veg_2) around the vegetal plate in *H. pulcherrimus*. Wedge-shaped cells should be formed by constriction of the basally distributed microfilaments. Microfilaments play a key role in generating the motive force for invagination (Lane *et al.*, 1993; Nakajima and Burke, 1996), whereas the elongation of the archenteron is independent of microtubules (Hardin, 1987). The precise distribution of microfilaments, especially in wedge-shaped cells, remains to be examined in *S. mirabilis* embryos.

Acknowledgments

We thank the staff of Tateyama Marine Biological Laboratory for collecting animals and for their hospitality.

Literature Cited

Amemiya, S., K. Akasaka, and H. Terayama. 1982a. Scanning electron microscopy of gastrulation in a sea urchin (*Anthocidaris crassispina*). *J. Embryol. Exp. Morphol.* **67:** 27–35.

Amemiya, S., K. Akasaka, and H. Terayama. 1982b. Scanning electron microscopical observation on the early morphogenetic processes in developing sea urchin embryos. *Cell Differ.* **11:** 291–293.

Berg, L. K., S. W. Chen, and G. M. Wessel. 1996. An extracellular matrix molecule that is selectively expressed during development is important for gastrulation in the sea urchin embryo. *Development* **122:** 703–713.

Burke, R. D., R. L. Myers, T. L. Sexton, and C. Jackson. 1991. Cell movements during the initial phase of gastrulation in the sea urchin embryo. *Dev. Biol.* **146:** 542–557.

Cameron, R. A., B. R. Hough-Evans, R. J. Britten, and E. H. Davidson. 1987. Lineage and fate of each blastomere of the eight-cell sea urchin embryo. *Genes Dev.* **1:** 75–84.

Cameron, R. A., S. Fraser, R. J. Britten, and E. H. Davidson. 1991. Macromere cell fates during sea urchin development. *Development* **113:** 1085–1091.

Dan, K., and K. Okazaki. 1956. Cyto-embryological studies of sea urchins. III. Role of the secondary mesenchyme cells in the formation of the primitive gut in sea urchin larvae. *Biol. Bull.* **110:** 29–42.

Ettensohn, C. A. 1984. Primary invagination of the vegetal plate during sea urchin gastrulation. *Am. Zool.* **24:** 571–588.

Ettensohn, C. A. 1985. Gastrulation in the sea urchin embryo is accompanied by the rearrangement of invaginating epithelial cells. *Dev. Biol.* **112:** 383–390.

Ettensohn, C. A. 1999. Cell movement in the sea urchin embryo. *Curr. Opin. Genet. Dev.* **9:** 461–465.

Gustafson, T., and H. Kinnander. 1956. Micro-aquaria for time-lapse cinematographic studies of morphogenesis in swimming larvae and observation on gastrulation. *Exp. Cell Res.* **11:** 36–51.

Gustafson, T., and L. Wolpert. 1963. The cellular basis of morphogenesis and sea urchin development. *Int. Rev. Cytol.* **15:** 139–214.

Gustafson, T., and L. Wolpert. 1967. Cellular movement and cell contact in sea urchin morphogenesis. *Biol. Rev. Camb. Philos. Soc.* **42:** 442–498.

Hardin, J. D. 1987. Archenteron elongation in the sea urchin embryo is a microtubule-independent process. *Dev. Biol.* **121:** 253–262.

Hardin, J. D. 1988. The role of secondary mesenchyme cells during sea urchin gastrulation studied by laser ablation. *Development* **103:** 317–324.

Hardin, J. D. 1989. Local shifts in position and polarized motility drive cell rearrangement during sea urchin gastrulation. *Dev. Biol.* **136:** 430–445.

Hardin, J. D., and L. Y. Cheng. 1986. The mechanisms and mechanics of archenteron elongation during sea urchin gastrulation. *Dev. Biol.* **115:** 490–501.

Hardin, J. D., and D. R. McClay. 1990. Target recognition by the archenteron during sea urchin gastrulation. *Dev. Biol.* **142:** 86–102.

Hörstadius, S. 1973. *Experimental Embryology of Echinoderms.* Clarendon Press, Oxford.

Kimberly, E. L., and J. Hardin. 1998. Bottle cells are required for the initiation of primary invagination in the sea urchin embryo. *Dev. Biol.* **204:** 235–250.

Kominami, T. 1988. Determination of dorso-ventral axis in early embryos of the sea urchin, *Hemicentrotus pulcherrimus. Dev. Biol.* **127:** 187–196.

Kominami, T., and M. Masui. 1996. A cyto-embryological study of gastrulation in the sand dollar, *Scaphechinus mirabilis. Dev. Growth Differ.* **38:** 129–139.

Lane, M. C., M. A. R. Koehl, F. Wilt, and R. Keller. 1993. A role for regulated secretion of apical extracellular matrix during epithelial invagination in the sea urchin. *Development* **117:** 1049–1060.

Logan, C., and D. R. McClay. 1997. The allocation of early blastomeres to the ectoderm and endoderm is variable in the sea urchin embryo. *Development* **124:** 2213–2223.

Martins, G. G., R. G. Summers, and J. B. Morrill. 1998. Cells are added to the archenteron in the sea urchin *Lytechinus variegatus. Dev. Biol.* **198:** 330–342.

McClay, D. R., and C. Y. Logan. 1996. Regulative capacity of the archenteron during gastrulation in the sea urchin. *Development* **122:** 607–616.

Moore, A. R., and A. S. Burt. 1939. On the locus and nature of the forces causing gastrulation in the embryos of *Dendraster excentricus. J. Exp. Zool.* **82:** 159–171.

Nakajima, Y., and R. D. Burke. 1996. The initial phase of gastrulation in sea urchins is accompanied by the formation of bottle cells. *Dev. Biol.* **179:** 436–446.

Piston, D. W., R. G. Summers, S. M. Knobel, and J. B. Morrill. 1998. Characterization of involution during sea urchin gastrulation using two-photon excited photorelease and confocal microscopy. *Microsc. Microanal.* **4:** 404–414.

Ransick, A., and E. H. Davidson. 1998. Late specification of veg_1 lineages to endodermal fate in the sea urchin embryo. *Dev. Biol.* **195:** 38–48.

Ruffins, S. W., and C. A. Ettensohn. 1996. A fate map of the vegetal plate of the sea urchin (*Lytechinus variegatus*) mesenchyme blastula. *Development* **122:** 253–263.

Schroeder, T. E. 1981. Development of a "primitive" sea urchin (*Eucidaris tribuloides*): irregularities in the hyaline layer, micromeres, and primary mesenchyme. *Biol. Bull.* **161:** 141–151.

Wessel, G. M., and D. R. McClay. 1987. Gastrulation in the sea urchin embryo requires the deposition of cross-linked collagen within the extracellular matrix. *Dev. Biol.* **121:** 149–165.

Reference: *Biol. Bull.* **199:** 298–304. (December 2000)

Effects of Food Concentration and Availability on the Incidence of Cloning in Planktotrophic Larvae of the Sea Star *Pisaster ochraceus*

MINAKO S. VICKERY* AND JAMES B. McCLINTOCK

Department of Biology, University of Alabama at Birmingham, Birmingham, Alabama 35294-1170

Abstract. A decade ago, cloning was first observed in the planktotrophic larvae of sea stars obtained from plankton tows. However, no controlled experimental studies have investigated what factors may regulate this remarkable phenomenon. In the present study we offer the first documentation of cloning in the planktotrophic larvae of *Pisaster ochraceus* from the northern Pacific coast. This species was used as a model system to investigate three factors that may influence the incidence of asexual reproduction (cloning) in planktotrophic sea star larvae. In an initial experiment, larvae were reared under nine combinations of three temperatures and three food (phytoplankton) concentrations. Larvae reared at 12–15°C and fed the highest food concentrations grew larger than the other larvae and produced significantly more clones. In a second experiment, qualitatively different algal diets were fed to larvae reared under the conditions found to be optimal in the initial experiment. Up to 24% of the larvae consuming a mixed phytoplankton diet of *Isochrysis galbana, Chaetocerous calcitrans,* and *Dunaliella tertiolecta* cloned, and significantly more clones were produced by these larvae than by those fed monospecific diets. Our experiments indicate that cloning generally occurs after larvae have attained asymptotic body length and only when food is abundant and of high quality. Since larval mortality is considered to be extremely high for marine invertebrates with planktotrophic larvae, production of clones under optimal conditions of temperature and food may serve to increase larval populations when the environment is most conducive to larval growth.

Introduction

Asexual reproduction and regeneration of missing body parts are well-known phenomena in adult sea stars (Anderson, 1956; Emson and Wilkie, 1980; Shirai and Walker, 1988; Mladenov *et al.*, 1989; Mladenov and Burke, 1994). The capacity for asexual reproduction (cloning) in sea star larvae was first suggested over 60 years ago from observations of the bipinnaria larvae of *Luidia sarsi* (Tattersall and Sheppard, 1934), but subsequent laboratory experiments indicated that these larvae were incapable of asexual reproduction (Wilson, 1978). Only recently has cloning and regeneration of missing body parts been confirmed in planktotrophic larvae of sea stars (Bosch *et al.*, 1989; Rao *et al.*, 1993; Jaeckle, 1994; Vickery and McClintock, 1998; Kitazawa and Komatsu, 2000).

Cloning in the bipinnaria larvae of the sea star *Luidia* sp. was first documented from plankton samples collected in the Sargasso Sea in which clones were observed to develop from buds that formed on the larval arms (Bosch, 1988; Bosch *et al.*, 1989). Shortly thereafter, two additional reports confirmed the occurrence of cloning in the natural environment in two unidentified species of planktotrophic sea star larvae also obtained from plankton samples (Rao *et al.*, 1993; Jaeckle, 1994). In addition to the budding process described above (Bosch, 1988; Bosch *et al.*, 1989), autotomy of the anterior portions of larvae was also observed in one of these studies (Jaeckle, 1994). Recently, brachiolaria larvae of the sea star *Distolasterias brucei* have been reported to undergo cloning in laboratory cultures (Kitazawa and Komatsu, 2000) in a manner identical to that described in previous reports (budding and autotomy). Moreover, cloning in laboratory cultures of the planktotrophic larvae of the brittle star *Ophiopholis aculeata* from the northern Pacific has been reported (Balser, 1998). We reported regen-

Received 29 February 2000; accepted 21 August 2000.

* To whom correspondence should be addressed: E-mail: vickerym@uab.edu

eration in planktotrophic larvae of the sea stars *Luidia foliolata* and *Pisaster ochraceus* (Vickery and McClintock, 1998). In addition, we observed similar regenerative capacity in planktotrophic echinopluteus larvae of the sea urchins *Dendraster excentricus* and *Lytechinus variegatus* (Vickery and McClintock, 1999). Thus, among Echinodermata, regenerative capacity in planktotrophic larvae has been demonstrated in sea stars, brittle stars, and sea urchins.

The existence of cloning and regenerative capacity among echinoderms with planktotrophic modes of reproduction suggests that there may be selective and adaptive advantages associated with such life history traits. These processes presumably operate under a suite of energetic constraints and trade-offs, whereby only larvae exposed to the most appropriate conditions would be expected to undergo clonal and regenerative events.

To date, no experimental studies have investigated the factors that regulate cloning in planktotrophic marine invertebrate larvae. Larval development, growth, and survivorship are particularly influenced by temperature and food availability (*e.g.*, George, 1994; Fenaux *et al.*, 1994). These may also be important factors affecting rates of larval cloning (Levitan, 1995; Morgan, 1995). In the present study we offer the first confirmed report of cloning in the planktotrophic larvae of the sea star *P. ochraceus*. We also examined the effects of temperature and both food concentration and availability on growth and cloning in *P. ochraceus* larvae.

Materials and Methods

Larval culturing

Pisaster ochraceus is commonly found in intertidal and shallow subtidal habitats of the U.S. Pacific Northwest. The breeding season of *P. ochraceus* is in the late spring and early summer months in the vicinity of Puget Sound, Washington (Strathmann, 1987). Adult specimens were collected during late spring months in 1997 (for temperature-food experiment) and 1998 (for food availability experiment) from rocky substrates along the shore of East Sound, Orcas Island, and transported to Friday Harbor Laboratories, San Juan Island, Washington. Ovaries and testes were dissected from sexually mature specimens (a single female and a single male). Fertilizable ova were obtained by treating excised ovaries with 1-methyladenine (10^{-4} *M*) (Kanatani, 1969), and sperm were diluted in filtered seawater prior to fertilization. During fertilization, ova were rinsed in filtered seawater to remove excess sperm. Embryos and larvae were reared in 2.5-liter glass jars. The cultures were gently stirred and the seawater was changed every 3 days following the methods outlined by Strathmann (1987). The single-celled algae *Chaetocerous calcitrans*, *Dunaliella tertiolecta*, and *Isochrysis galbana* were selected for larval diets (Strathmann, 1987). Observations and photographs of larvae were made with both a Wild M-5 dissecting microscope and a Nikon Optiphot-2 compound microscope.

Combined temperature and food-level experiments

Once the bipinnaria larvae developed functional digestive systems they were separated into nine experimental treatments (3 × 3 factorial design) to examine the effects of temperature and food level on rates of cloning. Each experimental treatment combining temperature and food level was replicated three times, and each consisted of about 2400 larvae held in 2.5 l of seawater in a glass jar (approx. 1 larva/ml). Ambient spring seawater temperatures (12–15°C) were bracketed in increments of about 5°C to yield treatment groups of low (7–10°C), medium (12–15°C), and high (17–20°C) temperature. Ambient seawater temperatures along the northern Pacific coast generally fall within the middle temperature range (12–15°C) throughout the year, but it is likely that larvae encounter lower temperatures (7–10°C) at the northern limit of their biogeographic range and in deeper water, or during the late winter months (Cannon, 1978). Similarly, larvae may encounter higher temperatures (17–20°C) at the southern limits of their biogeographic distribution, or in surface waters during the early summer months (Cannon, 1978; Strathmann, 1987).

Three levels of food composed of equal cell numbers (as determined using a hemocytometer) of the phytoplankton species *Chaetocerous calcitrans, Dunaliella tertiolecta,* and *Isochrysis galbana* were proffered to larvae in each treatment. The three concentrations of mixed algal cells were 5×10^2, 5×10^3, and 5×10^4 cells/ml (modified after Basch, 1996; Fenaux *et al.*, 1994). The nine experimental treatments combining temperature and food level were therefore as follows: high temperature and high food (HT-HF), high temperature and medium food (HT-MF), high temperature and low food (HT-LF), medium temperature and high food (MT-HF), medium temperature and medium food (MT-MF), medium temperature and low food (MT-LF), low temperature and high food (LT-HF), low temperature and medium food (LT-MF), and low temperature and low food (LT-LF). Subsamples of larvae in each experimental treatment ($n = 200$) were examined every 3 days under a dissecting microscope. The numbers of clones and of larvae undergoing clonal reproduction as evidenced by budding were recorded. The lengths of the larvae in each subsample of each experimental treatment and of all larvae in the process of cloning were measured along the larval axis (George, 1994). Clones and larvae undergoing cloning were placed in separate containers and monitored every 3 days to determine whether clones successfully developed into normal functional larvae and metamorphosed into juveniles. Larval lengths were compared within temperature and food-level experiments using analysis of variance. Only probability levels where $P \leq 0.05$ were considered statistically significant.

Food-availability experiment

To examine the effects of food availability (phytoplankton type) on the rate of cloning, simulating conditions in which nutrient diversity might be limited, larvae of *Pisaster ochraceus* were obtained as described above using ova and sperm from a different set of parent sea stars than those used for the combined temperature and food-level experiment. The larvae were cultured at 12–15°C at a density of about 2400 larvae per 2.5-l of seawater. Larvae were fed 5×10^4 cells/ml of either a monospecific diet of *Chaetocerous calcitrans, Dunaliella tertiolecta,* or *Isochrysis galbana* or a mixed diet composed of an equal cell number of these three algae. Each of the four experimental treatments was replicated three times. Subsamples of larvae ($n = 200$) were examined every 3 days under a dissecting microscope and analyzed using the same methods as for the combined temperature and food-level experiment. Larval lengths were compared within food availability experiments using analysis of variance. Only probability levels where $P \leq 0.05$ were considered statistically significant.

Results

Combined temperature and food-level experiments

Bipinnaria larvae exposed to seawater temperatures of 12–15°C and fed the highest food level (MT-HF) attained lengths significantly greater than those of larvae in any other experimental treatment (Fig. 1). Moreover, cloning occurred only in this experimental treatment (Fig. 2). Thirty-four days after fertilization, larval clones were first observed in the MT-HF bipinnaria culture (1.2%, Fig. 2). Subsequently, small numbers of additional larval clones were observed. Once bipinnaria in this treatment had doubled in length while developing into brachiolaria larvae (at about day 45), a fivefold increase was observed in the incidence of cloning (6%, Fig. 2).

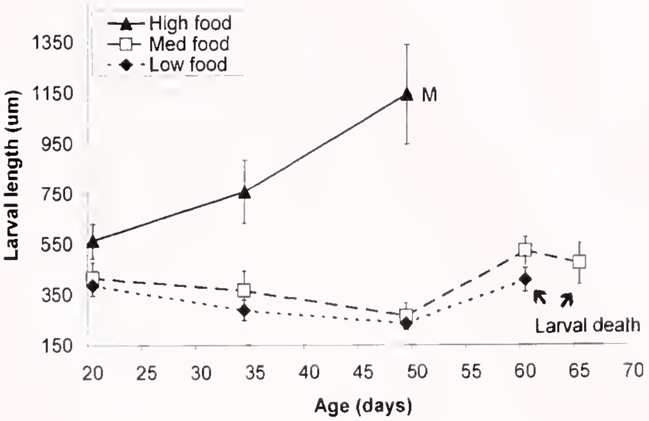

Figure 1. Growth of larvae of *Pisaster ochraceus* (measured as changes in length) reared at 12–15°C and fed low, medium, and high levels of mixed phytoplankton. M indicates stage at which brachiolaria larvae developed an adult rudiment and a decrease in length of the larval body (indicating metamorphic competence). Larvae that reached metamorphic competence were later observed to complete the metamorphosis to juveniles. Error bars represent mean values ±1 SD.

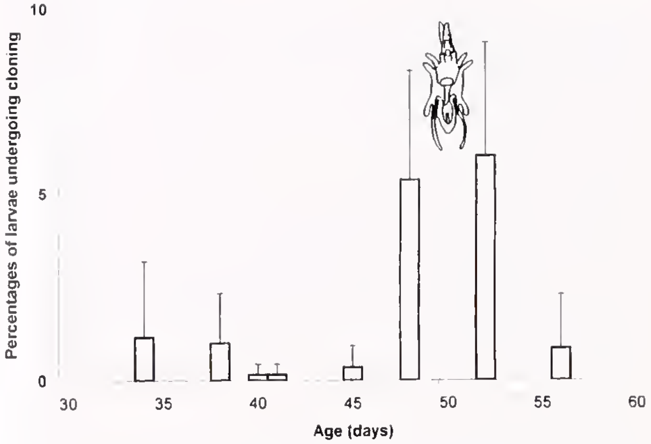

Figure 2. Percentages of larvae of *Pisaster ochraceus* undergoing cloning when reared at 12–15°C and fed high levels of mixed phytoplankton. Diagram indicates approximate onset of brachiolaria stage. Error bars represent mean values ±1 SD.

Larval clones obtained from the MT-HF cultures were isolated and their development was followed through metamorphosis. The clones produced resulted from the regeneration of anterior and posterior portions of bipinnaria and brachiolaria larvae (Fig. 3A, B) by processes that closely resembled those described in detail by Vickery and McClintock (1998). After about 2 weeks, fully developed clonal larvae were functionally and morphologically indistinguishable from larvae in the cultures from which they were originally isolated. A number of bipinnaria and brachiolaria larvae in the MT-HF cultures had missing larval arms or were missing small fragments of the larval body. Some larvae with missing larval arms were in the process of cloning, as evidenced by the development of projections or buds, which later became functional larvae, at the site of the missing fragment (Fig. 3C). However, some larvae with missing larval arms did not form projections or buds, but instead regenerated the larval arm. In addition, some small fragments of larval body parts, including severed larval arms, were observed in the MT-HF cultures, presumably the result of damage incurred when the water in the larval culture was changed. A number of these fragments, including severed arms, were separated from the cultures and observed for 2 weeks. During this time the fragments neither grew nor formed clones, although no mortality was observed.

Those bipinnaria larvae exposed to the highest temperature treatments (HT-LF, HT-MF, and HT-HF) all died

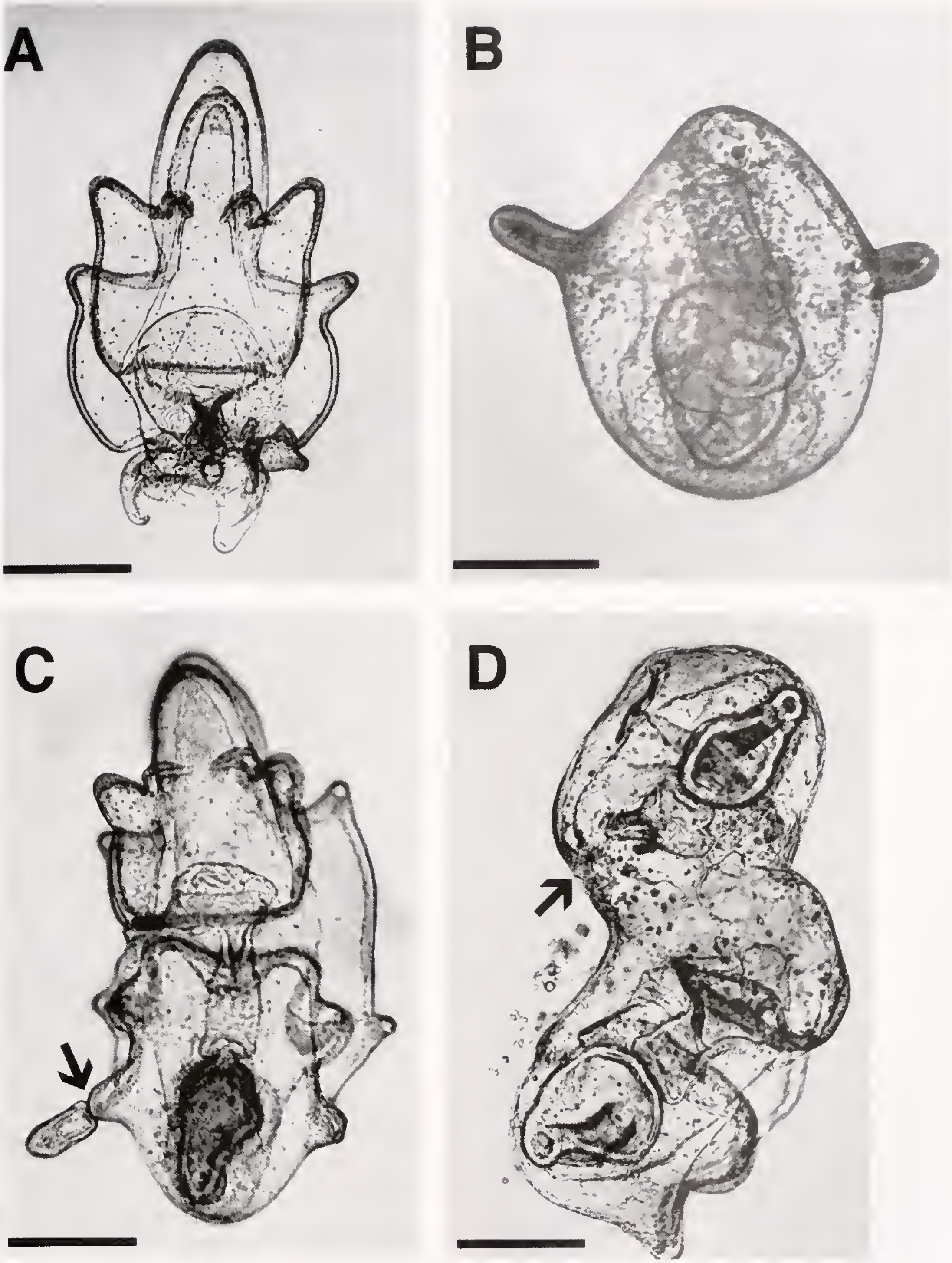

Figure 3. Light photomicrographs of clonal larvae of *Pisaster ochraceus* including the anterior (A) and posterior (B) portion of bipinnaria larvae. (C) Bipinnaria larva in the process of budding (see arrow). The bud later formed an early bipinnaria stage larva and subsequently detached (similar to that described by Bosch *et al.*, 1989). (D) Bipinnaria larva in the process of autotomization by fission. This larva was observed for about 2 weeks, during which the secondary larva (see arrow) detached and became functionally and morphologically indistinguishable from the primary larva in a manner similar to that described by Jaeckle (1994). We have observed this type of autotomy in several other species of planktotrophic larvae (pers. obs., M. Vickery). Scale bars = 200 μm.

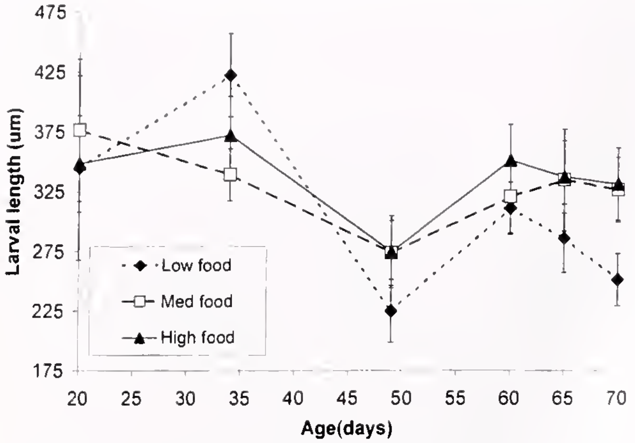

Figure 4. Growth of larvae of *Pisaster ochraceus* (measured as changes in length) reared at 7–10°C on low, medium, and high levels of mixed phytoplankton. Error bars represent mean values ±1 SD.

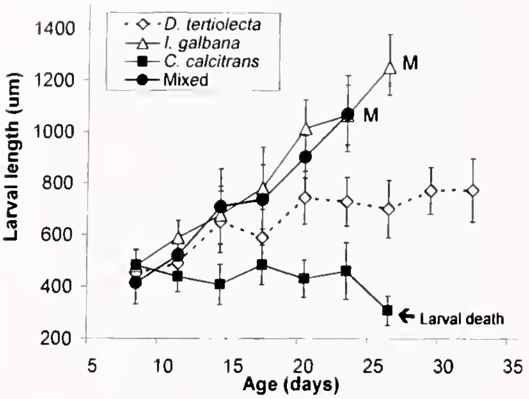

Figure 5. Growth of larvae of *Pisaster ochraceus* (measured as changes in length) reared at 12–15°C and fed high levels of four different phytoplankton diets. M indicates stage at which brachiolaria larvae developed an adult rudiment and a decrease in length of the larval body (indicating metamorphic competence). Larvae that reached metamorphic competence were later observed to complete the metamorphosis to juveniles. Error bars represent mean values ±1 SD.

within one week; no cloning occurred in the short period before mortality. Unlike larvae held at mid-range temperatures, bipinnaria larvae reared at low temperatures (7–10°C) and fed any of the three levels of food (LT-LF, LT-MF, and LT-HF) never developed into brachiolaria larvae over a 70-day period. They remained morphologically identical to early-stage bipinnariae. Moreover, no clones were produced. Larvae presented any food level at low temperature did not increase in length. In fact, they were slightly reduced in length by the end of the 70-day observation period (Fig. 4). Considerable larval mortality occurred throughout the experiment in all low-temperature treatment groups.

Food availability experiment

Bipinnaria larvae in experimental treatments fed a monospecific diet of *I. galbana* or an equivalent density of a mixture of equal cell numbers of *C. calcitrans, D. tertiolecta*, and *I. galbana* grew significantly larger than larvae fed monospecific diets of *C. calcitrans* or *D. tertiolecta* (Fig. 5). The incidence of cloning was greatest (24%) on a mixed diet during and after the transformation from the bipinnaria to the brachiolaria stage (Fig. 6). Although temperature and food concentration were similar in this treatment and in the MT-HF treatment group of the combined temperature and food-level experiment (Figs. 1, 2), growth was more rapid, and cloning began earlier and was more frequent. This might be attributed to the high variability in larval development rate in batches of larvae of *P. ochraceus* (Strathmann, 1978). Also, larvae used for this experiment were the offspring of a different set of parents than those used in the previous experiments.

Discussion

Cloning and regenerative capacity in echinoderm larvae has only recently been documented (Bosch, 1988; Bosch *et al.*, 1989; Rao *et al.*, 1993; Jaeckle, 1994; Balser, 1998; Vickery and McClintock, 1998, 1999; Kitazawa and Komatsu, 2000). In the present study we provide the first documentation of cloning in the planktotrophic larvae of *Pisaster ochraceus*. The results of our bifactorial analysis indicated that both seawater temperature and food level are important factors affecting growth and survival—and therefore cloning—of *P. ochraceus* larvae. Simulated environmental conditions that produced normal development and optimal larval growth generated the greatest number of clones. Larvae reared at temperatures (12–15°C) with the most abundant food exhibited normal development and positive growth, which resulted in the highest survival, with the greatest incidence of cloning. Although we observed rapid larval growth in the high-temperature treatment (15–17°C), none of the larvae survived beyond one week. One possible

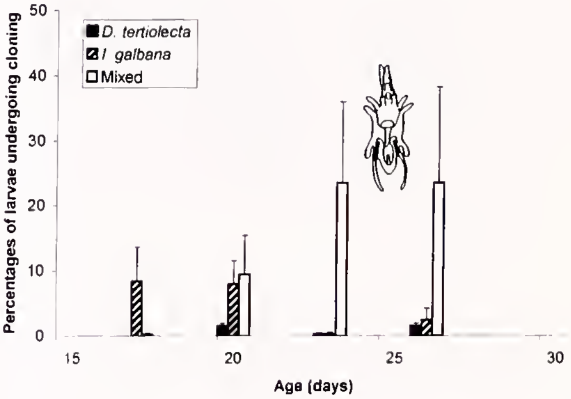

Figure 6. Percentages of larvae of *Pisaster ochraceus* undergoing cloning when reared at 12–15°C and fed high levels of four different phytoplankton diets. Error bars represent mean values ±1 SD.

explanation for the high mortality is that the higher temperatures triggered an increase in bacterial and microalgal growth in the cultures.

In contrast, sea star larvae reared in the low-temperature treatments (7–10°C) showed no net positive growth, and in most cases, decreased in length, regardless of food availability. These larvae also failed to attain the brachiolaria stage of development. It is unlikely these larvae would eventually become clonal because they continued to shrink in length over the course of the experiment. Decreased rates of growth and development at low temperatures may be related to decreased rates of larval metabolism (Boidron-Métairon, 1995). While low seawater temperatures have been suggested as an indirect cause of mortality in marine invertebrate larvae (Thorson, 1950), no studies of larval culturing have shown that low temperature can actually lead to a decrease in larval length as seen in the present study.

The production of larval clones was greatest during phases of rapid larval growth in MT-HF condition. As *P. ochraceus* in the North Pacific spawns in the late spring, larvae typically encounter moderate seawater temperatures (12–15°C) and high phytoplankton availability (Cannon, 1978). Such conditions could be expected to enhance *in situ* rates of larval cloning. Further analysis indicated that presenting larvae with different levels and types of food under an optimal regime of seawater temperature had a pronounced effect on the initiation and rate of larval clone production.

The greatest numbers of clones were produced by larvae in cultures presented a mixture of three single-celled algae. Although monospecific patches of single-celled algae are unlikely to exist in the natural environment, our use of monospecific algal diets simulated conditions in which nutrient diversity might be limited. Thus some of the observed differences in growth (and cloning) rates among the larvae fed monoalgal diets may have resulted from differences in the nutrient content of the food rather than in the type of food, since the larvae were fed equal cell numbers of algae, not an equal nutritional content (Pechenik and Fisher, 1979). However, the amount of nutrients actually consumed by the larvae does not necessarily have any correlation with the nutrient content of the food presented, as some food types may be more palatable to the larvae than others. Future studies may shed more light on this subject. The important information gained from the food-availability experiment is that nutrient availability may be an important factor affecting larval growth and therefore the rate of cloning, as evidenced by the fact that growth rates among larvae fed a monoalgal diet of *Isochrysis galbana* were similar to those fed a diet of mixed algae, yet the larvae fed the mixed diet produced far more clones.

In adult echinoderms, cloning (fission) is common and has been well described (Emson and Wilkie, 1980). Seasonal fluctuations in the incidence of cloning in adult sea stars, especially a high incidence in summer months, have been related to periods of maximum growth (Emson and Wilkie, 1980). This suggests that suitable biotic and environmental conditions such as abundant food and moderate temperatures may trigger cloning processes in adults just as they did in the larvae studied here. In some instances, more than 50% of the adults in a population were observed undergoing cloning (fission) when conditions were optimal (Emson and Wilkie, 1980).

Cloning may serve as a mechanism to enhance recruitment in *P. ochraceus* and perhaps in other marine invertebrates with planktotrophic modes of reproduction. Larvae dispersed across significant distances are likely to encounter a variety of environmental and biotic conditions, and our results suggest that those larvae encountering favorable conditions may be stimulated to reproduce by cloning, thereby possibly increasing the probability of successful larval metamorphosis and juvenile recruitment. Future studies of the effects of larval cloning on larval survivalship and recruitment will provide more insight into the true impact of this phenomenon on the life history of sea stars with planktotrophic larvae.

Acknowledgments

We thank Dennis Willows and Richard Strathmann of Friday Harbor Laboratories, University of Washington, for use of laboratory facilities and technical support. We are grateful to Al Schuetz of Johns Hopkins University for providing ovaries from *Pisaster ochraceus*. We thank Michael Vickery for his assistance in collection and maintenance of larval cultures. Our appreciation is also extended to Asim Bej, Thane Wibbels, and Daniel Jones for their support. Funding for this research was provided by Sigma-Xi, The Alabama Academy of Science, and The University of Alabama at Birmingham.

Literature Cited

Anderson, J. M. 1956. Observation on autotomy in the starfish, *Asterias forbesi*. *Biol. Bull.* **111:** 297.

Balser, E. J. 1998. Cloning by ophiuroid echinoderm larvae. *Biol. Bull.* **194:** 187–193.

Basch, L. V. 1996. Effects of algal and larval densities on development and survival of asteroid larvae. *Mar. Biol.* **126:** 693–701.

Boidron-Métairon, I. F. 1995. Larval nutrition. Pp. 223–248 in *Ecology of Marine Invertebrate Larvae*, L. R. McEdward, ed. CRC Press, New York.

Bosch, I. 1988. Replication by budding in natural populations of bipinnaria larvae of the sea star genus *Luidia*. P. 728 in *Echinoderm Biology*, R. D. Burke, P. V. Mladenov, P. Lambert, and R. L. Parsley, eds. A. A. Balkema, Rotterdam.

Bosch, I., R. B. Rivkin, and S. P. A. Alexander. 1989. Asexual reproduction by oceanic planktotrophic echinoderm larvae. *Nature* **337:** 169–170.

Cannon, G. A. 1978. Circulation in the Strait of Juan de Fuca: some recent oceanographic observations. *NOAA Tech Rep.* U.S. Dept. Commerce: ERL 399-PMEL 29:1–49.

Emson, R. H., and I. C. Wilkie. 1980. Fission and autotomy in echinoderms. *Oceanogr. Mar. Biol. Annu. Rev.* **18:** 155–250.

Fenaux, L., M. F. Strathmann, and R. R. Strathmann. 1994. Five tests of food-limited growth of larvae in coastal waters by comparisons of rates of development and form of echinoplutei. *Limnol. Oceanogr.* **39(1):** 84–98.

George, S. B. 1994. Phenotypic plasticity in the larvae of *Luidia foliolata* (Echinodermata: Asteroidea). Pp. 297–307 in *Echindoerms Through Time*, B. David, A. Guille, J. Feral, and M. Roux, eds. Balkema, Rotterdam.

Jaeckle, W. B. 1994. Multiple modes of asexual reproduction by tropical and subtropical sea star larvae: an unusual adaptation for genet dispersal and survival. *Biol. Bull.* **186:** 62–71.

Kanatani, H. 1969. Inducing of spawning and oocyte maturation by 1-methyladenine in starfishes. *Exp. Cell. Res.* **57:** 333–337.

Kitazawa, C., and M. Komatsu. 2000. Larval development and asexual development of the sea star, *Distolasterias nipon.* Programme and Abstracts. 10th International Echinoderm Conference, Dunedin, New Zealand, 123.

Levitan, D. R. 1995. The ecology of fertilization in free-spawning invertebrates. Pp. 123–156 in *Ecology of Marine Invertebrate Larvae,* L. R. McEdward, ed. CRC Press, New York.

Mladenov, P. V., and R. D. Burke. 1994. Echinodermata: asexual propagation. Pp. 339–383 in *Reproductive Biology of Invertebrates,* K. G. Adiyodi and R. G. Adiyodi, eds. Oxford and IBH Publishing, New Delhi.

Mladenov, P. V., S. Igdoura, S. Asotra, and R. D. Burke. 1989. Purification and partial characterization of an autotomy-promoting factor from the sea star *Pycnopodia helianthoides. Biol. Bull.* **176:** 169–175.

Morgan, S. G. 1995. Life and death in the plankton: larval mortality and adaptation. Pp. 279–322 in *Ecology of Marine Invertebrate Larvae.* L. R. McEdward, ed. CRC Press, New York.

Pechenik, J. A., and N. S. Fisher. 1979. Feeding assimilation and growth of mud snail larvae, *Nassarius obsoletus* (Say) on three different algal diets. *J. Exp. Mar. Biol. Ecol.* **37:** 57–80.

Rao, P. S., K. H. Rao, and K. Shyamasundari. 1993. A rare condition of budding in bipinnaria larva (Asteroidea). *Curr. Sci.* **65(10):** 792–793.

Shirai, H., and C. W. Walker. 1988. Chemical control of asexual and sexual reproduction in echinoderms. Pp. 453–476 in *Endocrinology of Selected Invertebrate Types,* H. Laufer and R. G. H. Downer, eds. Alan Liss, New York.

Strathmann, R. R. 1978. Length of pelagic period in echinoderms with feeding larvae from the northeast Pacific. *J. Exp. Mar. Biol. Ecol.* **34:** 23–27.

Strathmann, M. F. 1987. *Reproduction and Development of Marine Invertebrates of the Northern Pacific Coast.* University of Washington Press, Seattle. 670 pp.

Tattersal, W. M., and E. M. Sheppard. 1934. Observation of the bipinnaria of the asteroid genus *Luidia.* Pp. 35–61 in *James Johnstone Memorial Volume.* R. J. Daniel, ed. University Press of Liverpool, Liverpool.

Thorson, G. 1950. Reproduction and larval ecology of marine bottom invertebrates. *Biol. Rev.* **25:** 1–45.

Vickery, M. S., and J. B. McClintock. 1998. Regeneration in metazoan larvae. *Nature* **394:** 140.

Vickery, M. S., and J. B. McClintock. 1999. Regeneration in echinoid larvae. *Am. Zool.* **39(5):** 50A.

Wilson, D. P. 1978. Some observations on bipinnaria and juveniles of the starfish genus *Luidia. J. Mar. Biol. Assoc.* UK **58:** 467–478.

Reference: *Biol. Bull.* **199:** 305–315. (December 2000)

Development of Embryonic Cells Containing Serotonin, Catecholamines, and FMRFamide-Related Peptides in *Aplysia californica*

AMANDA J. G. DICKINSON[1,*], ROGER P. CROLL[1], AND ELENA E. VORONEZHSKAYA[2]

[1] *Department of Physiology and Biophysics, Faculty of Medicine, Dalhousie University, Halifax, Nova Scotia, B3H 4H7, Canada; and* [2] *Institute of Developmental Biology, Russian Academy of Sciences, 117808 Moscow, Russia*

Abstract. This study demonstrates the presence of a relatively extensive but previously unrecognized nervous system in embryonic stages of the opisthobranch mollusc *Aplysia californica.* During the trochophore stage, two pairs of cells were observed to be reactive to antibodies raised against the neuropeptides FMRFamide and EFLRIamide. These cells were located in the posterior region of the embryo, and their anterior projections terminated under the apical tuft. As the embryos developed into veliger stages, serotonin-like immunoreactive (LIR) cells appeared in the apical organ and were later observed to innervate the velum. Also, aldehyde-induced fluorescence indicative of catecholamines was present in cells in the foot, oral, and possibly apical regions during late embryonic veliger stages. Just before the embryo hatches as a free-swimming veliger, additional FMRFamide-LIR and catecholamine-containing cells appeared in regions that correspond to the ganglia of what will become the adult central nervous system (CNS). Neurons and connectives that will contribute to the adult CNS appear to develop along the pathways that are pioneered by the earliest posterior FMRFamide-LIR cells. These observations are consistent with the hypothesis that, besides their presumed roles in the control of embryonic behaviors, some elements may also guide the development of the CNS. Embryonic nervous systems that develop prior to and outside of the adult CNS have also been reported in pulmonate and prosobranch species of molluscs. Therefore, the demonstration of early developing neurons and their transmitter phenotypes in *A. californica* presents new opportunities for a better understanding of the ontogeny and phylogeny of both behavioral and neuronal function in this important model species.

Introduction

The opisthobranch gastropod *Aplysia californica,* which has been studied extensively as a model for understanding the neuronal underpinnings of behavior (for review see Kandel [1979]), has also become an important model in the study of molluscan neurodevelopment. The development of the ganglia that constitute the central nervous system (CNS) has been studied in detail (Kriegstein, 1977; Schacher *et al.,* 1979; Kandel *et al.,* 1981; Jacob, 1984), but more recent studies also report the presence of nerve cells that exist outside the boundaries of the developing ganglia that will constitute the adult CNS. For example, in an early embryonic veliger stage, three serotonin-like immunoreactive (LIR) cells exist in the anterior apical organ: an unpaired median cell and a bilateral pair of cells (Croll and Voron-

---

Received 24 January 2000; accepted 2 October 2000.

* To whom correspondance should be addressed. E-mail: ajdickin@is2.dal.ca

Abbreviations: ACP, 35 amino acid acidic peptide; CC-1, catecholaminergic central cell one; CC-2, catecholaminergic central cell two; CC-3, catecholaminergic central cell three; CNS, central nervous system; EFLRIamide, Glu-Phe-Leu-Arg-Ile-NH_2; EDTA, ethylenediaminetetraacetic acid; FC-1, FMRFamide central cell one; FC-2, FMRFamide central cell two; FC-3, FMRFamide central cell three; FITC, fluorescein isothiocyanate; F-*l*1, left FMRFamide-LIR posterior cell one; F-*l*2, left FMRFamide-LIR posterior cell two; F-*r*1, right FMRFamide-LIR posterior cell one; F-*r*2, right FMRFamide-LIR posterior cell two; FMRFamide, Phe-Met-Arg-Phe-NH_2; LIR, like-immunoreactive; PBS, phosphate-buffered saline; SEEPLY, 22 amino acid peptide SEQPDVDDYLRDVVLQSEEPLY; S-*l*1, left serotonin-LIR bilateral cell one; S-*l*2, left serotonin-LIR bilateral cell two, S-*r*1, right serotonin-LIR bilateral cell one; S-*r*2, right serotonin-LIR bilateral cell two; SUM, serotonin-LIR unpaired median cell.

ezhskaya, 1995; Croll and Voronezhskaya, 1996b; Marois and Carew, 1997a, b, c). Soon afterwards, these three cells are joined by another more lateral pair of apical serotonin-LIR cells. By the end of the embryonic period, as the veliger is about to hatch as a free-swimming larva, serotonin-LIR projections extend into the velar lobes, foot, and abdominal and visceral regions (Marois and Carew, 1997a, b, c). Kempf *et al.* (1997) showed that such apical cells and processes appear to be general features of opisthobranch larvae. Similarly shaped and positioned apical cells have also been reported in larvae of other molluscan species (Bonar, 1978; Kulakovskiy and Flyachinskaya, 1994; Raineri and Ospovat, 1994; Raineri, 1995; Leise, 1996; Lin and Leise, 1996a, b; Dickinson *et al.*, 1999; Voronezhskaya *et al.*, 1999; Parries, 2000).

In addition to the cells of an apical organ, other neuronal elements have been observed outside the boundaries of the developing adult CNS. Croll and Voronezhskaya (1996b) reported preliminary observations of elements containing peptides related to Phe-Met-Arg-Phe-NH_2 (FMRFamide) in posterior regions of embryonic *A. californica*. Recent studies also indicate the presence of similar neuronal elements in other molluscan species. For example, Croll and Voronezhskaya (1995; 1996a) identified neuronal elements in what corresponds to the trochophore or early veliger stage (Mescheryakov, 1990) of the pulmonate *Lymnaea stagnalis*, using antibodies raised against FMRFamide. These FMRFamide-LIR cells develop in posterior regions of the embryo and send anterior projections that terminate in the regions of the future cerebral and pedal ganglia. A posterior FMRFamide-LIR cell has also been observed in the early developmental stages of the prosobranch *Crepidula fornicata* (Dickinson *et al.*, 1999). As in *L. stagnalis*, this posterior FMRFamide-LIR cell also sends anterior projections that terminate in the region of the future cerebral and pedal ganglia. Therefore, cells expressing FMRFamide-like immunoreactivity appear to develop in a posterior-to-anterior sequence rather than the anterior-to-posterior development of the ganglia. In addition, these FMRFamide-LIR cells and their fibers seem to mark the pathways along which the adult ganglia and connectives develop, and therefore they may be involved in guiding the developing CNS.

Additional peripherally located neurons in the foot and surrounding the mouth were revealed in the gastropods *L. stagnalis* (Voronezhskaya *et al.*, 1999), *C. fornicata* (Dickinson *et al.*, 1999), and *Phestilla sibogae* (Pires *et al.*, 2000) and the bivalve *Mytilus edulis* (Croll *et al.*, 1997), using techniques to localize catecholamines.

The above descriptions of neurodevelopment in representative species suggest the presence of a primary larval nervous system that appears earlier than and outside of the developing adult CNS. Morphological descriptions in other species also indicate that components of such primary larval nervous systems may either be incorporated into the adult ganglia or disappear. The present study investigated the early development of neurons that may compose a primary larval nervous system in *A. californica*, starting at the trochophore stage and continuing until the embryo hatches as a free-swimming veliger. We used immunocytochemical techniques to study the first cells expressing FMRFamide and related peptides, and we provide details of the morphology of these cells and the timing of their appearance, with comparisons to the earliest cells exhibiting serotonin-like immunoreactivity. We additionally used aldehyde-induced fluorescence, which has been previously applied to molluscan tissues (Croll *et al.*, 1997, 1999; Smith *et al.*, 1998), to examine cells containing catecholamines. This study shows that, as in these other molluscs, *A. californica* also has a nervous system first present in early embryonic stages. Furthermore, these observations suggest several new hypotheses regarding the mechanism shaping the ontogeny of the nervous system in this well-studied species.

Materials and Methods

Animals

Adult specimens of *Aplysia californica* were purchased from the Aplysia Resource Facility of the University of Miami and maintained in a salt-water aquarium. Egg masses were collected soon after oviposition and kept in separate containers of artificial salt water (Crystal Sea, Baltimore, MD) at 20°–22°C. Under these conditions, embryos required about 9–10 days to develop from first cleavage to hatching. The hatched veliger required another few weeks before becoming competent to metamorphose into juvenile sea slugs (Kandel, 1979; Kandel *et al.*, 1981; Marois and Croll, 1992; Marois and Carew, 1997b).

The developmental stages of *A. californica* were described previously (Kriegstein, 1977; Kandel, 1979; Kandel *et al.*, 1981; Marois and Croll, 1992; Marois and Carew, 1997b). In the present study, morphological and behavioral features were examined on each day from first cleavage to hatching, and the embryonic development was divided into three stages. During the trochophore stage (days 2.5–4) the embryo had a distinct apical tuft and a shell gland and began to move using the prototrochal cilia. On day 4 the body began to change shape as the rudiments of a velum, foot, and shell were observed. During the early embryonic veliger stage (days 5–7) the velum became bilobate and possessed long cilia along its edge. During the late embryonic veliger stage (days 8–10) the velum, foot, and shell enlarged and differentiated.

Immunocytochemistry

Immunohistological procedures were performed according to Marois and Croll (1992) and Marois and Carew (1997b). Egg ribbons were fixed in 4% paraformaldehyde in phosphate-buffered saline (PBS; 50 m*M* $Na_2HPO_4 \cdot 7H_2O$ and 140 m*M* NaCl in distilled water adjusted to pH 7.2) for 1–4 h at room temperature. Then embryos were removed from the capsules, washed in PBS, and stored in 70% ethanol at −18°C until further processing. For immunohistochemical processing, the stored embryos were first given two to three 5-min washes in PBS. The shells of older embryos (>day 4) were then decalcified with 10% ethylenediaminetetraacetic acid (EDTA) (Sigma Chemical Co., Mississauga, ON) in PBS for 30–45 min. Embryos were next washed for 2–3 h in 4% Triton X-100 in PBS. The embryos were then incubated in antibodies raised against FMRFamide, serotonin (both obtained from Diasorin, Stillwater, MI), or antibodies (gifts from Dr. P. R. Benjamin, University of Sussex) against three FMRFamide gene encoding peptides: the pentapeptide Glu-Phe-Leu-Arg-Ile-NH_2 (EFLRIamide), the 22-amino-acid peptide SEQPDVDDYLRDVVLQSEEPLY (SEEPLY), and a 35-amino-acid acidic peptide, SDPFFRFGKQQVATDDSGELDDEILSRVSDDDKNI (ACP) (Santama *et al.*, 1996). All these antibodies except anti-SEEPLY were diluted 1:500–1:1000 in PBS with the addition of 1.0% normal goat serum and 1.0% Triton X-100. The SEEPLY antibody was diluted 1:200 in a solution of 50 m*M* Tris base, 150 m*M* NaCl, pH 7.6, containing 0.25% w/v gelatin and 1% v/v Trition X-100 (Santama *et al.*, 1993). Incubation periods lasting 48 h at 4°C or 12 h at room temperature gave comparable results. The embryos were next rinsed three times (5 min each) with PBS and given a final wash for 1 h before incubating for 24–48 h in goat anti-rabbit antibodies conjugated to fluorescein isothiocyanate (FITC) or rhodamine (Bio/Can Scientific, Mississauga, Ontario) and diluted 1:50 in PBS with the addition of 1.0% Triton X-100.

To localize FMRFamide-like immunoreactivity relative to external morphological structures at the trochophore stage, some embryos were double-labeled with monoclonal antibodies against ∝-tubulin (DM1A clone from Sigma Chemical Co., Mississauga, ON) (Jackson *et al.*, 1995). These embryos were first labeled, as described above, for FMRFamide-like immunoreactivity, then rinsed three times (5 min each) in PBS. Next, the embryos were incubated in anti-∝tubulin (diluted 1:500 in PBS) for 12 h at room temperature. The embryos were washed again three times in PBS before incubating in sheep anti-mouse serum conjugated to FITC or rhodamine for 12 h at room temperature. These secondary antibodies were diluted 1:50 in PBS and 1% Triton X-100.

Embryos processed for immunocytochemistry were mounted on glass slides in a 3:1 mixture of glycerol to PBS for viewing on a Leitz Aristoplan microscope equipped for epifluorescence. FITC fluorescence was viewed using a 450–490-nm excitation filter and a 525/20-nm barrier filter; rhodamine fluorescence was viewed using a 530–560-nm excitation filter and 580-nm long-pass barrier filter. Embryos processed for FMRFamide- and ∝-tubulin-like immunoreactivity were also viewed on a Zeiss Axiovert microscope equipped for confocal laser scanning (model LSM 410).

As negative controls, embryos were processed without incubation in primary antibody; such specimens exhibited no detectable fluorescence. Positive controls involved parallel processing of embryonic *L. stagnalis* that exhibited typical staining, as described elsewhere for serotonin and FMRFamide (Marois and Croll, 1992; Croll and Voronezhskaya, 1995; Croll and Voronezhskaya, 1996a).

Catecholamine histofluorescence

The formaldehyde glutaraldehyde technique of Furness *et al.* (1977) was used to localize catecholamines. Embryos were incubated for at least 12 h in a solution consisting of 4% paraformaldehyde, 0.5% glutaraldehyde, and 35% sucrose in PBS. Similar results were also obtained when the embryos were stored in this solution for several weeks. The fixed embryos were decalcified in 10% EDTA in PBS for 45 min. Embryos were then placed on glass slides, air dried for several hours, and then mounted in a 3:1 mixture of glycerol and PBS. These embryos were viewed and photographed through the Leitz compound microscope equipped with a 355–425-nm excitation filter and 460-nm long-pass barrier filter. Positive controls involved parallel processing of embryonic *L. stagnalis* that exhibited typical blue-green fluorescent staining, as described elsewhere for catecholamines (Voronezhskaya *et al.*, 1999). Negative controls were performed by omitting the glutaraldehyde from the formaldehyde glutaraldehyde solution, thus eliminating the characteristic fluorescent staining.

Photography

Most histological preparations were photographed on the Leitz compound microscope using Kodak TMAX 100 film; the negatives were digitally scanned. Photographs from the Zeiss confocal microscope were produced by superpositioning stacks of 10–15 images obtained through stepped sequences of focal planes at intervals of 1–2 μm. All the images were then assembled into plates and labeled using Photoshop 5.0 (Adobe Systems, Inc., San Jose, CA). Contrast and brightness of the images were adjusted to provide consistency within plates.

Results

Trochophore stage (days 2.5–4)

Halfway through day 2, two bilaterally symmetrical pairs of FMRFamide-LIR posterior cells were observed (Figs. 1A, 2A). Fibers projected ipsilaterally and anteriorly from each cell on the right (F-*r*1 and F-*r*2) and the left (F-*l*1 and F-*l*2) (Fig. 1A). By day 3 these fibers terminated in a plexus

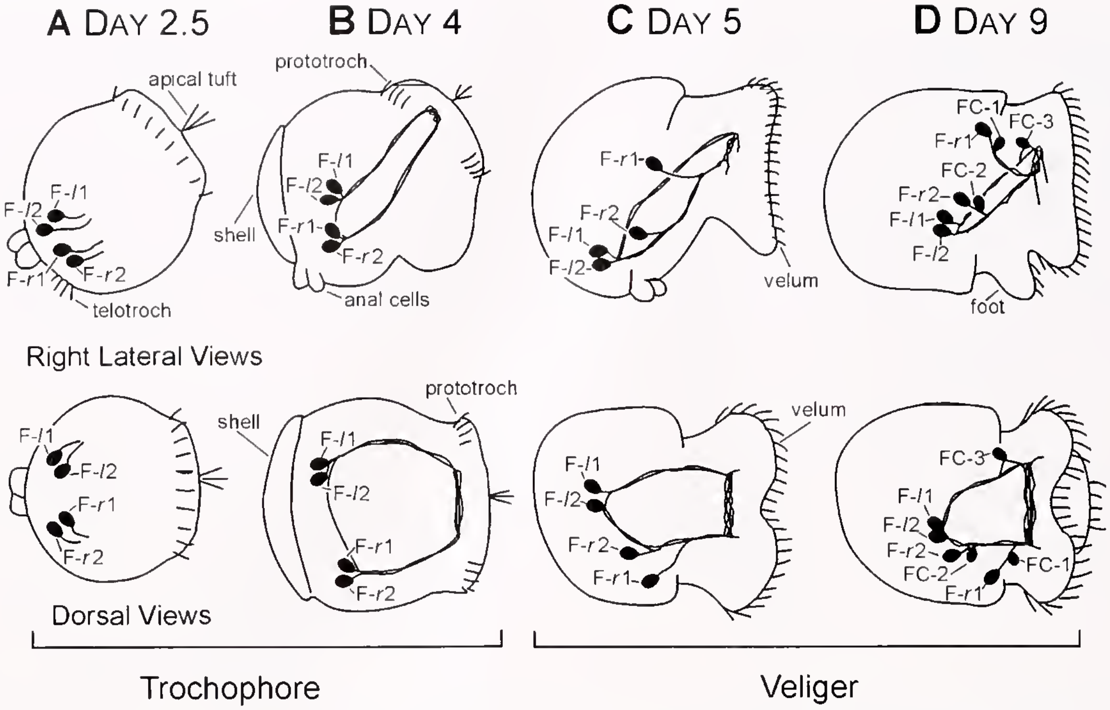

Figure 1. Schematic representations of FMRFamide-LIR cells and fibers in embryos of *Aplysia californica*. Top row: views from the right side and slightly superior to give a three-dimensional perspective; bottom row: dorsal views. Anterior is to the right in each figure. (A) Two pairs of posteriorly located FMRFamide-LIR cells with anterior projections observed on day 2.5. (B) FMRFamide-LIR cells and their processes observed on day 4. The FMRFamide-LIR processes reached the anterior region, where they formed a plexus under the apical tuft. (C) FMRFamide-LIR cells were no longer symmetrical by day 5; the cells (*l*1 and *l*2) on the left appeared in a ventral position, and the cells on the right (*r*1 and *r*2) appeared more dorsally. (D) On day 9 additional FMRFamide-LIR cells (FC-1, FC-2, FC-3) appeared in the anterior region.

of FMRFamide-LIR processes in the region beneath the apical tuft (see day 4, Figs. 1B, 2B, D). Also by day 3, one to two additional FMRFamide-LIR fibers extended across the midline of the body just anterior to the somata of the FMRFamide-LIR posterior cells (See day 4, Figs. 1B, 2D). Initially the pairs of FMRFamide-LIR cells were positioned symmetrically within the embryo, but they gradually became displaced and by the end of day 4 had all moved to the right side of the body (Fig. 1C). The FMRFamide-LIR cells and processes were also identified using antibodies against EFLRIamide (Fig. 2C). No immunoreactivity was detected during the trochophore stage or any later stages with antibodies against SEEPLY and ACP.

Early embryonic veliger stage (days 5–7)

By day 5 the FMRFamide-LIR cells had assumed more anterior positions in the embryo. F-*r*1 and F-*r*2 moved apart from each other, with F-*r*1 occupying a more dorsal location. F-*l*1 and F-*l*2 remained close to each other and together assumed a central and ventral position (Figs. 1C, 3A). Their anteriorly projecting fibers crossed the midline and formed a commissure in the anterior region. All cells and processes listed above were also identified using antibodies against EFLRIamide (Fig. 3B).

Also by day 5, a serotonin-LIR unpaired median cell (SUM; see Marois and Carew [1997b]) appeared beneath the apical tuft. Soon afterwards, a pair of vase-shaped serotonin-LIR cells (S-*r*1 and S-*l*1) were observed to the left and right of SUM. Short serotonin-LIR fibers projected ventrally from the SUM, S-*r*1, and S-*l*1 to form a plexus in the same region as the FMRFamide-LIR commissure (see day 9, Figs. 4A, 5A, B, also see Marois and Carew [1997b]).

By day 7 the three serotonin-LIR cells (SUM, S-*r*1, and S-*l*1) were joined by a new pair of serotonin-LIR cells (S-*r*2 and S-*l*2) located slightly posteroventrally to S-*r*1 and S-*l*1 on either side of the plexus (see day 9, Figs. 4A, 5A, B).

Late embryonic veliger or prehatching stage (days 8–10)

By day 8 the posterior FMRFamide-LIR cells and their fibers appeared just anterior to the midpoint along the anteroposterior axis. F-*l*1 and F-*l*2 together assumed a ventral and central position, while F-*r*1 and F-*r*2 each assumed more dorsal positions than previously (see day 9, Figs. 1D, 3C). FMRFamide-LIR fibers extended ventrally from the

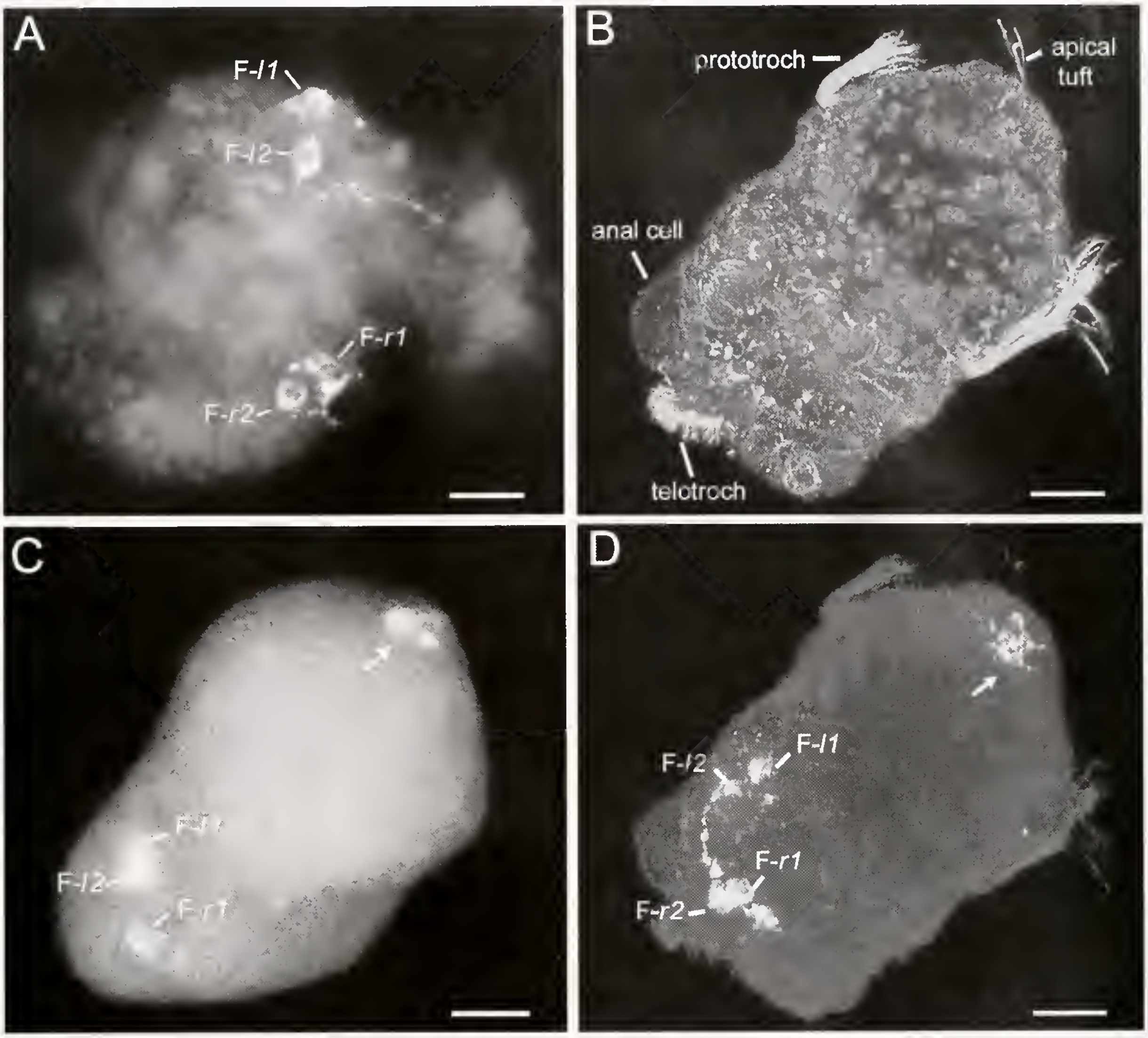

Figure 2. *Aplysia californica* during trochophore stages. Anterior is to the right in each figure. (A) Dorsal view of an embryo on day 2.5 showing the two pairs of posteriorly located FMRFamide-LIR cells with anterior projections. Scale bar = 20 μm. (B) Right lateral view of an embryo showing immunoreactivity for α-tubulin on day 3. Displays the locations of the apical tuft, prototroch, telotroch, and anal cell in the trochophore. Scale bar = 25 μm. (C) EFLRIamide-like immunoreactivity observed on day 3, showing F-*r*1, F-*l*1 and -*l*2 (which are not in focus), and the plexus under the apical tuft (arrow). Scale bar = 25 μm. (D) FMRFamide-like immunoreactivity observed in the same embryo as 2B showing F-*r*1, -*r*2, -*l*1 and -*l*2, and plexus under the apical tuft. Scale bar = 25 μm. C and D demonstrate the similar pattern of immunoreactivity for EFLRIamide and FMRFamide.

apical commissure toward the foot. Also by day 8, formaldehyde glutaraldehyde-induced fluorescence, indicative of catecholamine-containing cells, was observed in the foot region. The catecholamine-containing foot cells were vase-shaped and appeared in two bilaterally symmetric groups of two to three cells on each side (see day 9, Figs. 4B, 6A, B).

By day 9 additional FMRFamide-LIR cells were observed in positions consistent with the locations previously identified as the developing cerebral, pedal, and pleural ganglia of the future adult CNS in *A. californica* (Kriegstein, 1977; Marois and Carew, 1990; Marois and Carew, 1997b) and other opisthobranchs (Kempf *et al.*, 1997a). One of these FMRFamide central cells (FC-1) appeared near F-*r*1, another (FC-2) was located near F-*r*2, and a third (FC-3) was observed to the left of the apical commissure (Figs. 1D, 3C). Also by day 9, the number of catecholamine-containing cells increased to four to five cells on each side of the foot (Figs. 4B, 6A, 6B). Another pair of catecholamine-containing cells was located in the oral region. Catecholamine-containing fibers also extended from each

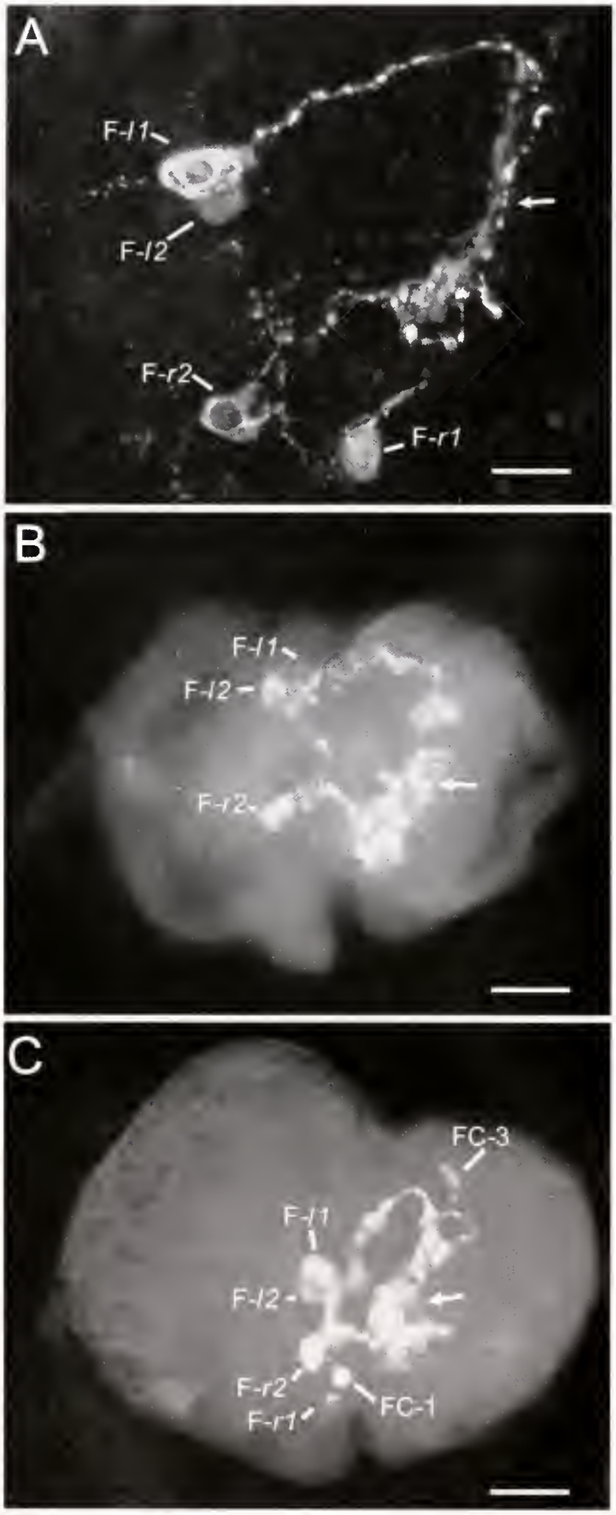

Figure 3. FMRFamide- and EFLRIamide-LIR cells and fibers in representative embryonic veliger stages of *Aplysia californica.* Anterior is to the right in each figure. Arrows indicate the FMRFamide-LIR plexus. (A) FMRFamide-like immunoreactivity observed on day 5, showing the asymmetry of F-*l*1, F-*l*2, F-*r*1, and F-*r*1. Scale bar = 15 μm. (B) Montage of two photographs showing the EFLRIamide-LIR cells and fibers on day 7. Scale bar = 28 μm. (C) FMRFamide-like immunoreactivity on day 9. Two additional cells, FC-1 and FC-3, are shown in this focus. Scale bar = 28 μm.

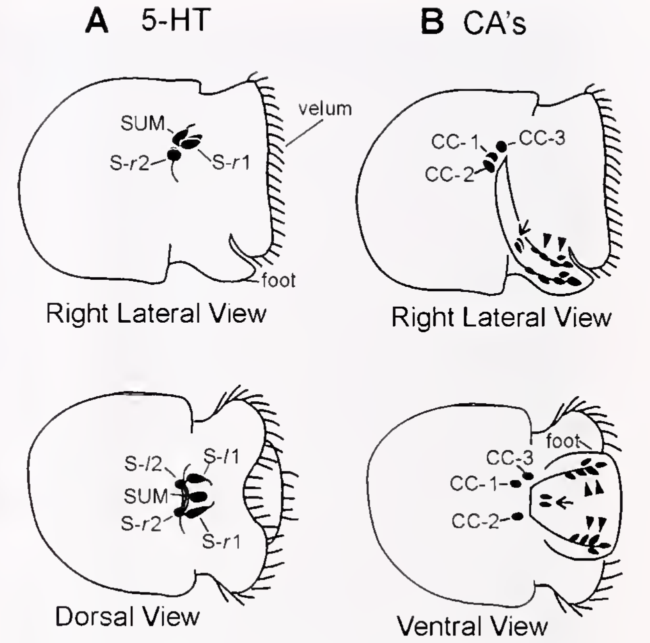

Figure 4. Schematic representations of serotonin-LIR and catecholamine-containing neurons in *Aplysia californica* during day 9. Top row: views from the right side and slightly superior to give a three-dimensional perspective. Anterior is to the right in each figure. (A) Serotonin-LIR cells (S-*l*1, S-*l*2, S-*r*1, S-*r*2, SUM) and fibers in the apical organ. Bottom row: dorsal view. (B) Cells and fibers containing catecholamines were located in the foot (arrow heads), oral region (arrow), and the region of the future CNS (CC-1, CC-2, CC-3). Bottom row: ventral view.

group of foot cells toward the region below the apical tuft where the FMRFamide-LIR apical commissure and serotonin-LIR plexus were located. In this region, three catecholamine-containing central cells were observed (Fig. 6B); two of these cells (CC-1, CC-2) were located on the right and another cell (CC-3) on the left. Unfortunately, the formaldehyde glutaraldehyde technique resulted in high background fluorescence, making it difficult to determine whether these cells were located in the apical organ or the developing cerebral or pedal ganglia of the future adult CNS. Also by this time, serotonin-LIR fibers could be seen projecting toward the velum, foot, and posterior region (Figs. 4A, 5A).

Discussion

The current study offers evidence that a relatively extensive nervous system forms during embryonic development of the opisthobranch gastropod *Aplysia californica.* The early nervous system includes posterior FMRFamide-LIR cells that first appear during the trochophore stage. By the veliger stage, serotonin-LIR cells appear in the apical organ (Marois and Carew, 1997a, b, c), and shortly before hatching catecholamine-containing cells appear around the mouth and in the foot. The first neurons within the developing

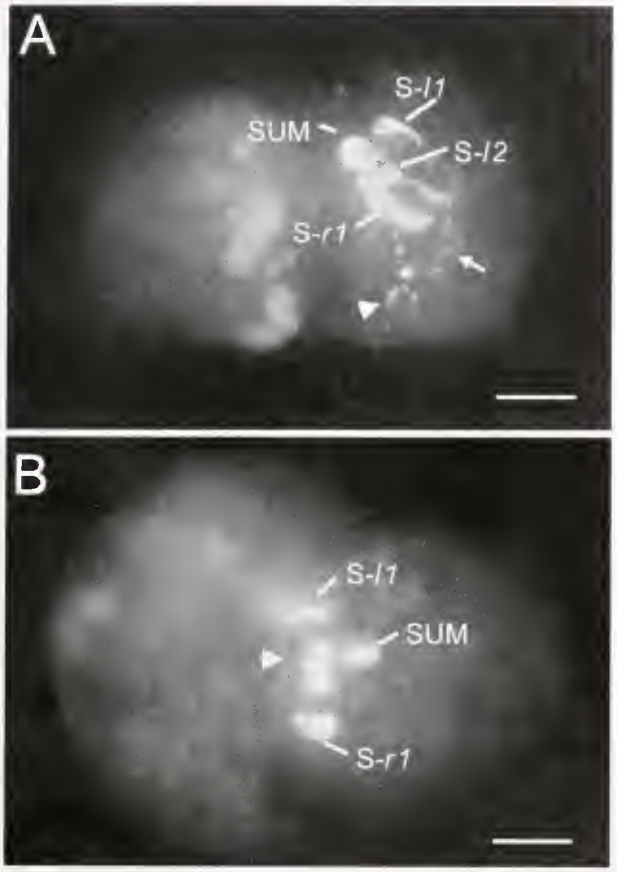

Figure 5. Serotonin-LIR cells and fibers in *Aplysia californica* during days 8–9. Anterior is to the right in each figure. (A) Right lateral view of an embryo on day 9 showing serotonin-LIR cells in the apical organ (S-*l*1, S-*l*2, S-*r*1, SUM) and fibers projecting into the foot (arrowhead) and velum (arrow). Scale bar = 30 μm. (B) Dorsal view of an embryo on day 8 showing three of the serotonin-LIR cells (S-*l*1, S-*r*1, SUM) of the apical organ. The apical commissure is indicated by the arrowhead. Scale bar = 28 μm.

ganglia, which will eventually constitute the adult CNS, only begin to appear during late embryonic stages (Schacher *et al.*, 1979). Such an arrangement of neuronal cells and fibers is similar to that found in representative pulmonate and prosobranch gastropod species (Croll and Voronezhskaya, 1996a; Dickinson *et al.*, 1999).

Posterior FMRFamide-LIR cells

Two pairs of FMRFamide-LIR cells appear in posterior regions and project anteriorly directed fibers in early trochophore stages of *A. californica*. FMRFamide-like immunoreactivity has also been observed posteriorly in early embryos of the other gastropod molluscs; however, differences were observed in the number and precise positions of these cells. *Lymnaea stagnalis* (Croll and Voronezhskaya, 1995, 1996a) and *Crepidula fornicata* (Dickinson *et al.*, 1999) each possess a single medial FMRFamide-LIR cell in posterior regions near the shell gland. No such cell was observed during embryonic development in *A. californica*. Nevertheless, it could have been missed if it was present only for a very brief period of development and if it did not exhibit reactivity to the anti-FMRFamide antibodies used in this study. During early veliger stages of *L. stagnalis*, additional FMRFamide-LIR posterior cells exist on the left and right fibers projecting from the most posterior medial cell (Croll and Voronezhskaya, 1995, 1996a). The location of these left and right cells in *L. stagnalis* may correspond to the left and right pairs of FMRFamide-LIR posterior cells in *A. californica*. FMRFamide-LIR cells in such lateral regions were not detected in *C. fornicata* (Dickinson *et al.*, 1999).

Despite variations in the number and position of posterior FMRFamide-LIR cells in the different species, they all share certain features. In all three species, the posterior

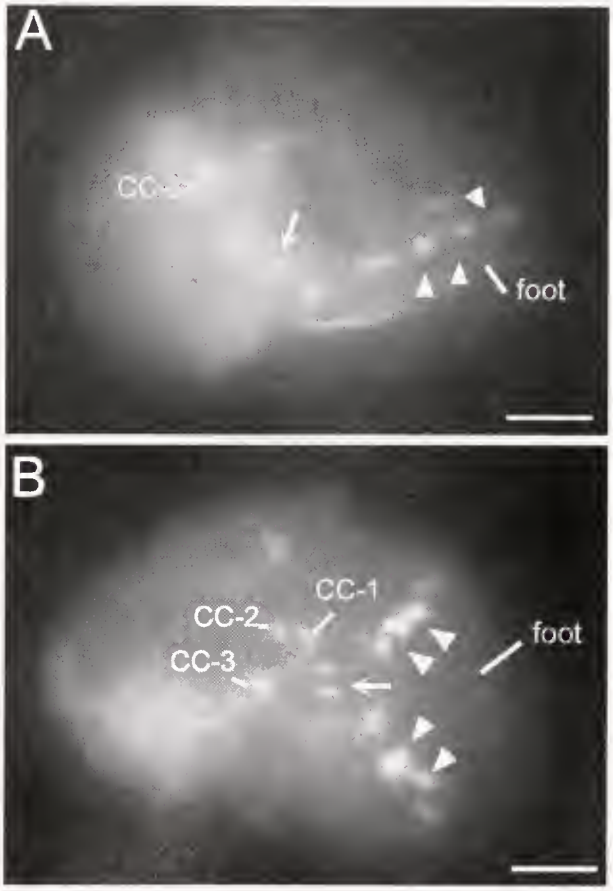

Figure 6. Catecholamine-containing cells and fibers in *Aplysia californica* during day 9. Anterior is to the right in each figure. (A) Right lateral view of an embryo showing catecholamine-containing cells in the foot (arrowheads), oral region (arrows), and apical region or region corresponding to the future ganglia of the adult CNS (CC-3). Scale bar = 28 μm. (B) Ventral view montage showing cells containing catecholamines. Cells are shown in the foot (arrowheads), oral region (arrows), and apical region or region corresponding to the future ganglia of the adult CNS (CC-1, CC-2, CC-3). Scale bar = 28 μm.

FMRFamide-LIR cells appear before any other nerve cells are detected. Also, the posterior FMRFamide-LIR cells all extend anteriorly directed axons that pass through the region in which the cerebral ganglia will later develop, and they eventually terminate in a region of the future pedal ganglia. FMRFamide-LIR fibers also appear under the apical tuft during trochophore stages of both *A. californica* and *C. fornicata*. This region later develops into the apical sensory organ, the underlying cerebral commissure, or both (Marois and Carew, 1997a, c). The plexus of immunoreactive fibers is extensive in this region, even at very early developmental stages. Although no other immunoreactive somata were detected at these stages, we cannot exclude the possibility that at least some fibers may derive from sources other than the posterior cells. In fact, FMRFamide-LIR fibers also branched repeatedly under the apical plate in early embryonic stages of *L. stagnalis*, but these fibers originate from nearby somata that exhibit little or no immunoreactivity (Croll and Voronezhskaya, 1996a).

Similarity also exists in the patterns of expression of the FMRFamide-related peptides in two species of molluscs. In both *L. stagnalis* and *A. californica*, the cells and fibers expressing FMRFamide- and EFLRIamide-like immunoreactivity are similar (Voronezhskaya and Elekes, 1997). The FMRFamide antiserum is immunoreactive to several FMRFamide-related peptides (Gaus *et al.*, 1993), whereas the EFLRIamide antiserum is immunoreactive only to EFLRIamide and FMRFamide itself (Santama *et al.*, 1995a, b, 1996). Our results thus indicate that immunoreactivity in early stages of *A. californica* is due to the presence of FMRFamide and EFLRIamide and not to the exclusive presence of other FMRFamide-related peptides. Antibodies against SEEPLY and the acidic peptide (ACP) that are processed from the FMRFamide precursor protein of *L. stagnalis* are not immunoreactive in embryonic *A. californica*. The sequence of SEEPLY is identical in *L. stagnalis* and *A. californica* (Greenberg and Price, 1992), but consistent with our findings in *A. californica*, Voronezhskaya and Elekes (1997) reported no detectable occurrence of this peptide in FMRFamide-LIR cells during embryonic stages of *L. stagnalis*. Conversely, ACP has not been isolated in *A. californica*. Therefore, the lack of positive immunoreaction for this latter peptide may be attributed to species-specificity of the amino acid sequence.

The aim of the present study was to examine the ontogeny of the nervous system during embryonic development, thus representing times much earlier than typically examined in *A. californica*. Since we did not examine later stages, the fates of the FMRFamide-LIR cells are unclear. It seems possible, however, that at least some of these FMRFamide-LIR cells and fibers later become incorporated in the ganglia and connectives of the CNS. The regions where the ganglia of the adult CNS are located have been previously identified in later veliger stages of *A. californica* (Kriegstein, 1977; Marois and Carew, 1990, 1997b). In the present study, FMRFamide-LIR cells can be observed in positions that correspond to these regions. For example, F-*l*1 and F-*l*2 seem to lie in positions that correlate to the future site of the left abdominal ganglia. F-*r*2 appears in the region where the osphradium will develop, whereas FC-2 seems to lie in a position that corresponds to the location of the right abdominal ganglia. F-*r*1, FC-1, and FC-3 appear in regions where the pleural or pedal ganglia will develop. Confirmation of the locations of these FMRFamide-LIR cells within the CNS must, however, await additional histological examination to identify the boundaries of the developing central ganglia. Although our work may have tentatively identified individual central neurons at earlier stages than previously demonstrated, the findings are still consistent with other descriptions of gangliogenesis. The presence of cerebral and pedal cells has been previously reported in hatchlings of *A. californica* (Kriegstein, 1977; Marois and Carew, 1997b) and other gastropods (D'Asaro, 1969; Page, 1992a, b; Lin and Leise, 1996b; Dickinson *et al.*, 1999). Anlagen of the visceral loop ganglia have also been identified in hatching stages of *A. californica* (Schacher *et al.*, 1979).

It is also possible that at least some posterior FMRFamide-LIR cells lie outside the developing ganglia and transiently express their transmitter phenotype during a short phase of embryogenesis. Such a fate for the early posterior FMRFamide-LIR cells has been shown in the developing embryos of *L. stagnalis* (Croll and Voronezhskaya, 1995; Voronezhskaya and Elekes, 1996).

Whatever the exact locations and fates of the various somata, FMRFamide-LIR fibers clearly mark pathways that span the length and breadth of the embryos in *A. californica*, and they may play a role in pioneering the various commissures and connectives of the adult nervous system. Such a role for early FMRFamide-LIR cells and fibers has been suggested in other molluscs such as *L. stagnalis* (Croll and Voronezhskaya, 1995, 1996a) and *C. fornicata* (Dickinson *et al.*, 1999) and is consistent with hypothesized roles of early developing fibers in other invertebrate groups such as insects (Bate, 1976; Caudy and Bentley, 1986; Goodman and Shatz, 1993) and annelids (Lacalli, 1981, 1982). The necessity of such pioneering fibers for the normal development of the CNS in gastropods must be tested in future experiments.

Serotonergic apical cells

The serotonin-LIR cells in the apical organ of *A. californica* have been previously described in detail (Croll and Voronezhskaya, 1995; Marois and Carew, 1997a, b, c). A similar arrangement of serotonin-LIR cells was also reported in other opisthobranchs (Kempf *et al.*, 1997a), prosobranchs (Dickinson *et al.*, 1999), and bivalves (Croll *et al.*, 1997).

The apical organ in molluscs and other invertebrate larvae may control larval behaviors such as swimming, feeding, and crawling (Leise, 1996; Lin and Leise, 1996a, b). Morphological evidence supports such hypothesized functions since serotonin-LIR cells of the apical organ innervate the velum in *A. californica* (Marois and Carew, 1997b, c) and other molluscs (Kulakovskiy and Flyachinskaya, 1994; Croll *et al.,* 1997; Kempf *et al.,* 1997; Dickinson *et al.,* 1999). Such velar innervation probably controls locomotion and feeding currents generated by cilia, which are responsive to serotonin in both adult forms (Audesirk *et al.,* 1979; Murakami, 1987; Syed and Winlow, 1989) and larval stages (Koshtoyants *et al.,* 1961; Beiras and Widdows, 1995). The apical organ is also thought to control the transduction of the metamorphic signal (Hirata and Hadfield, 1986; Couper and Leise, 1996; Hadfield *et al.,* 2000) and possibly to influence subsequent development of the adult CNS (Lacalli, 1981, 1994; Marois and Carew, 1997c).

Although non-serotonergic apical cells were not identified in the present study, other neurons in the apical organ of *A. californica* were previously identified using electron microscopy (Marois and Carew, 1997b). Flask-shaped, FMRFamide-LIR cells have also been observed in the apical region of the pulmonate *L. stagnalis* (Croll and Voronezhskaya, 1996a), the prosobranch *C. fornicata* (Dickinson *et al.,* 1999), and the opisthobranch *Phestilla sibogae* (Kempf *et al.,* 1992). It is possible that apical somata exhibit other transmitters or peptides in later stages of development in *A. californica.*

Anterior catecholaminergic cells

Catecholamine-containing cells exist in the foot region of *A. californica.* Similar cells also appeared in the foot of the gastropods *L. stagnalis* (Voronezhskaya *et al.,* 1999) and *C. fornicata* (Dickinson *et al.,* 1999), and in the bivalves *Mytilus edulis* and *Placopecten magellanicus* (Croll *et al.,* 1997). Such cells may be involved in metamorphosis, because catecholamines were found to modulate or induce metamorphosis in both gastropods (Pires *et al.,* 2000) and bivalves (Coon and Bonar, 1986). Similarly located cells have also been found to be responsive to the chemical cues inducing metamorposis in the opisthobranch *Onchidoris bilamellata* (Arkett *et al.,* 1989).

Catecholamine-containing cells are also found near the mouth of embryonic *A. californica,* consistent with similar cells reported in pulmonates, prosobranchs, and bivalves (Croll *et al.,* 1997; Dickinson *et al.,* 1999; Voronezhskaya *et al.,* 1999). The role for these cells is also unknown, although it is tempting to suggest that they might influence feeding behavior, which already displays a significant degree of sophistication within larval stages of molluscs (Baldwin and Newell, 1995).

We suggest that at least some other catecholamine-containing cells found in later larval stages might lie within the developing central ganglia, consistent with previous discussions of other central neurons in this paper. Confirmation of the locations of these cells must, however, await further experimentation to identify the boundaries of the developing central ganglia during embryonic stages.

Torsion and neurodevelopment

It was previously hypothesized that the opisthobranch nervous system lacks chiastoneury, or the twisting of the visceral loop into a figure-eight pattern, because neurodevelopment begins after torsion (Kandel *et al.,* 1981). However, the present study shows posterior neurons and fibers before the onset of torsion in *A. californica,* and if such neurons are later incorporated in the developing ganglia, a reevaluation of this hypothesis may be necessary. In early stages of the prosobranch *C. fornicata,* chiastoneury was observed in a figure-eight pattern of the FMRFamide-LIR fibers (Dickinson *et al.,* 1999). In corresponding stages of *A. californica,* such a figure-eight pattern did not exist, probably due to the different degrees of torsion in the two groups: 120-degree rotation in the opisthobranchs compared with the 180-degree rotation in the prosobranchs (Kandel, 1979; Kandel *et al.,* 1981). Cells and fibers may also be positioned more anteriorly and the connectives between ganglia may be shorter in opisthobranchs than in prosobranchs. Detorsion in opisthobranchs (Kandel, 1979; Kandel *et al.,* 1981) presumably eliminates much of the remaining evidence of twisting of the neural pathways.

Conclusion

The present study provides morphological evidence of neuronal elements that appear earlier in development than any previously identified neural structure, including the apical organ, in *A. californica.* Many catecholamine-containing cells are also identified in anterior regions of early embryonic stages. Together these elements (posterior cells, apical organ, and anterior catecholaminergic cells) may compose a distinct, primary larval nervous system that may be responsible for the control of several embryonic and larval behaviors such as swimming, feeding, and metamorphosis. The fate of such a primary larval nervous system is unknown, but evidence suggests that some neurons and connectives may be incorporated into the adult CNS while other cells disappear. Other invertebrate larvae from taxa such as polychaetes, nemertines, echinoderms, and phoronids have embryonic nervous systems that are very similar to those of molluscs (Hay-Schmidt, 1990a, b, c; 1995).

This report also suggests the possibility that the larval nervous system may form a scaffold along which the adult nervous system develops. Such a hypothesis is consistent with the suggested role of FMRFamide-LIR cells and processes in corresponding stages of other gastropods and other invertebrate groups. The demonstration of early developing neurons and their transmitter phenotypes in *A. californica* opens new opportunities for a deeper understanding of the ontogeny and phylogeny of both behavior and neuronal function in this important model species.

Acknowledgments

We thank J. Nason for technical assistance and L. Nezlin for critical readings of this manuscript. Funding was provided by grants from the Natural Sciences and Engineering Research Council of Canada (NSERC) to R.P.C. (grant number: OGP0038863) and from the Russian Fund for Basic Research (RFBR) to E.E.V. (grant number 99-04-48415).

Literature Cited

Arkett, S. A., F.-S. Chia, J. I. Goldberg, and R. Koss. 1989. Identified settlement receptor cells in a nudibranch veliger respond to specific cue. *Biol. Bull.* **176:** 155–160.

Audesirk, G., R. E. McCaman, and A. O. D. Willows. 1979. The role of serotonin in the control of pedal ciliary activity by identified neurons in *Tritonia diomedea. Comp. Biochem. Physiol.* **62:** 87–91.

Baldwin, N. S., and R. I. E. Newell. 1995. Feeding rate responses of oyster larvae (*Crassostrea virginica*) to seston quantity and composition. *J. Exp. Mar. Biol. Ecol.* **189:** 77–91.

Bate, C. M. 1976. Pioneer neurons in an insect embryo. *Nature* **260:** 54–55.

Beiras, R., and J. Widdows. 1995. Effects of the neurotransmitters dopamine, serotonin and norepinephrine on the ciliary activity of mussel (*Mytilis edulis*) larvae. *Mar. Biol.* **122:** 597–603.

Bonar, D. B. 1978. Ultrastructure of a cephalic sensory organ in larva of the gastropod *Phestilla sibogae* (Aeolidacea, Nudibranchia). *Tissue Cell* **10:** 153–165.

Caudy, M., and D. Bentley. 1986. Pioneer growth cone steering along a series of neuronal and non-neuronal cues of different affinities. *J. Neurosci.* **6:** 1781–1795.

Coon, S. L., and D. B. Bonar. 1986. Norepinephrine and dopamine content of larvae and spat of the Pacific oyster, *Crassostrea gigas. Biol. Bull.* **171:** 632–639.

Couper, J. M., and E. M. Leise. 1996. Serotonin injections induce metamorphosis in larvae of the gastropod mollusc *Ilyanassa obsoleta. Biol. Bull.* **191:** 178–186.

Croll, R. P., and E. E. Voronezhskaya. 1995. Early FMRFamide-like immunoreactive cells in gastropod neurogenesis. *Acta Biol. Hung.* **46:** 295–303.

Croll, R. P., and E. E. Voronezhskaya. 1996a. Early elements in gastropod neurogenesis. *Dev. Biol.* **173:** 344–347.

Croll, R. P., and E. E. Voronezhskaya. 1996b. Early neurodevelopment in *Aplysia, Lymnaea* and *Helisoma. Soc. Neurosci. Abstr.* **22:** 1948.

Croll, R. P., D. L. Jackson, and E. E. Voronezhskaya. 1997. Catecholamine-containing cells in larval and postlarval bivalve molluscs. *Biol. Bull.* **193:** 116–124.

Croll, R. P., E. E. Voronezhskaya, L. Hiripi, and K. Elekes. 1999. Development of catecholaminergic neurons in the pond snail, *Lymnaea stagnalis* II: Postembryonic development of central and peripheral cells. *J. Comp. Neurol.* **404:** 285–296.

D'Asaro, C. N. 1969. The comparative embryogenesis and early organogenesis of *Bursa corrugata* Perry and *Distorsio clathrata* (Gastropoda: Prosobranchia). *Malacologia* **9:** 349–389.

Dickinson, A. J. G., J. Nason, and R. P. Croll. 1999. Histochemical localization of FMRFamide, serotonin and catecholamine in embryonic *Crepidula fornicata* (Prosobranchia: Gastropoda). *Zoomorphology* **119:** 49–62.

Furness, J. B., M. Costa, and A. J. Wilson. 1977. Water-stable fluorophores, produced by reaction with aldehyde solutions, for the histochemical localization of catechol- and indolethylamines. *Histochemistry* **52:** 159–170.

Gaus, G., K. E. Doble, D. A. Price, M. J. Greenberg, T. D. Lee, and B.-A. Battle. 1993. The sequences of five neuropeptides isolated from *Limulus* using antisera to FMRFamide. *Biol. Bull.* **184:** 322–329.

Goodman, C. S., and C. J. Shatz. 1993. Developmental mechanisms that generate precise patterns of neuronal connectivity. *Cell* **72:** 77–98.

Greenberg, M. J., and D. A. Price. 1992. Relationships among the FMRFamide-like peptides. *Prog. Brain Res.* **92:** 25–37.

Hadfield, M. G., E. A. Meleshkevitch, and D. Y. Boudko. 2000. The apical sensory organ of a gastropod veliger is a receptor for settlement cues. *Biol. Bull.* **198:** 67–76.

Hay-Schmidt, A. 1990a. Distribution of catecholamine-containing, serotonin-like and neuropeptide FMRFamide-like immunoreactive cells and processes in the nervous system of the pilidium larva (Nemertini). *Zoomorphology* **109:** 231–244.

Hay-Schmidt, A. 1990b. Distribution of catecholamine-containing, serotonin-like and neuropeptide FMRFamide-like immunoreactive neurons and processes in the nervous system of the actinotroch larva of *Phoronis muelleri* (Phoronida). *Cell Tissue Res.* **259:** 105–118.

Hay-Schmidt, A. 1990c. Distribution of catecholamine-containing, serotonin-like and neuropeptide FMRFamide-like immunoreactive neurons and processes in the nervous system of the early actinotroch larva of *Phoronis vancouverensis* (Phoronida): distribution and development. *Can. J. Zool.* **68:** 1525–1536.

Hay-Schmidt, A. 1995. The larval nervous system of *Polygodius lacteus* Schiender, 1868 (Polygordiidae, Polychaeta): Immunocytochemical data. *Acta Zool. (Stockholm)* **76:** 121–140.

Hirata, K. Y., and M. G. Hadfield. 1986. The role of choline in metamorphic induction of *Phestilla* (Gastropoda, Nudibranchia). *Comp. Biochem. Physiol.* **84:** 15–21.

Jackson, A. R., T. W. MacRae, and R. P. Croll. 1995. Unusual distribution of tubulin isoforms in the snail *Lymnaea stagnalis. Cell Tissue Res.* **281:** 507–516.

Jacob, M. H. 1984. Neurogenesis in *Aplysia californica* resembles nervous system formation in vertebrates. *J. Neurosci.* **4:** 1225–1239.

Kandel, E. R. 1979. *Behavioral Biology of* Aplysia. W. H. Freeman, San Francisco.

Kandel, E. R., A. Kriegstein, and S. Schacher. 1981. Development of the central nervous system of *Aplysia* in terms of the differentiation of its specific identifiable cells. *Neuroscience* **5:** 2033–2063.

Kempf, S. C., G. V. Chun, and M. G. Hadfield. 1992. An immunocytochemical search for potential neurotransmitters in larvae of *Phestilla sibogae* (Gastropoda, Opisthobranchia). *Comp. Biochem. Physiol.* **101C:** 299–305.

Kempf, S. C., L. R. Page, and A. Pires. 1997. Development of serotonin-like immunoreactivity in the embryos and larvae of nudibranch mollusks with emphasis on the structure and possible function of the apical sensory organ. *J. Comp. Neurol.* **386:** 507–528.

Koshtoyants, K. S., G. A. Buznikov, and B. N. Manukhin. 1961. The possible role of 5-hydroxy-tryptamine in the motor activity of embryos of some marine gastropods. *Comp. Biochem. Physiol.* **3:** 20–26.

Kriegstein, A. R. 1977. Development of the nervous system of *Aplysia californica. Proc. Natl. Acad. Sci. USA* **74:** 375–378.

Kulakovskiy, E. Y., and L. P. Flyachinskaya. 1994. Formation of elements of the regulatory systems in larval development of *Mytilus edulis. Hydrobiol. J.* **30:** 85–94.

Lacalli, T. C. 1981. Structure and development of the apical organ in trochophores of *Spirobranchus polycerus, Phyllodoce maculata* and *Phyllodoce mucosa* (Polychaeta). *Proc. R. Soc. Lond. B* **212:** 381–402.

Lacalli, T. C. 1982. The nervous system and ciliary band of Muller's larva. *Proc. R. Soc. Lond. B* **217:** 37–58.

Lacalli, T. C. 1994. Apical organs, epithelial domains and origin of the chordate central nervous system. *Am. Zool.* **34:** 533–541.

Leise, E. M. 1996. Selective retention of the fluorescent dye DASPEI in a larval gastropod mollusc after paraformaldehyde fixation. *Micro. Res. Tech.* **33:** 496–500.

Lin, M., and E. M. Leise. 1996a. NADPH-Diaphorase activity changes during gangliogenesis and metamorphosis in the gastropod mollusc *Ilyanassa obsoleta. J. Comp. Neurol.* **374:** 194–203.

Lin, M.-F., and E. M. Leise. 1996b. Gangliogenesis in the prosobranch gastropod *Ilyanassa obsoleta. J. Comp. Neurol.* **374:** 180–193.

Marois, R., and T. J. Carew. 1990. The gastropod nervous system in metamorphosis. *J. Neurobiol.* **7:** 1053–1071.

Marois, R., and T. J. Carew. 1997a. Fine structure of the apical ganglion and its serotonergic cells in the larva of *Aplysia californica. Biol. Bull.* **192:** 388–398.

Marois, R., and T. J. Carew. 1997b. Ontogeny of serotonergic neurons in *Aplysia californica. J. Comp. Neurol.* **386:** 477–490.

Marois, R., and T. J. Carew. 1997c. Projection patterns and target tissues of serotonergic cells in larval *Aplysia californica. J. Comp. Neurol.* **386:** 491–506.

Marois, R., and R. P. Croll. 1992. Development of serotonergic cells within the embryonic central nervous system of the pond snail, *Lymnaea stagnalis. J. Comp. Neurol.* **322:** 255–265.

Mescheryakov, V. N. 1990. The common pond snail *Lymnaea stagnalis* L. Pp. 69–132 in *Animal Species for Developmental Studies*, D. A. Dettlaff and S. G. Vassetzky, eds. Plenum Press, New York.

Murakami, A. 1987. Control of ciliary beat frequency in the gill of *Mytilus. Comp. Biochem. Physiol.* **86C:** 273–279.

Page, L. R. 1992a. New interpretation of a nudibranch central nervous system based on ultrastructural analysis of neurodevelopment in *Melibe leonina.* I. Cerebral and visceral loop ganglia. *Biol. Bull.* **182:** 348–365.

Page, L. R. 1992b. New interpretation of a nudibranch central nervous system based on ultrastructural analysis of neurodevelopment in *Melibe leonina.* II. Pedal, pleural, and labial ganglia. *Biol. Bull.* **182:** 366–381.

Page, L. R., and S. C. Parries. 2000. Comparative study of the apical ganglion in planktotrophic caenogastropod larvae: ultrastructure and immunoreactivity to serotonin. *J. Comp. Neurol.* **418:** 383–401.

Pires, A., R. P. Croll, and M. G. Hadfield. 2000. Catecholamines modulate metamorphosis in the opisthobranch gastropod, *Phestilla sibogae. Biol. Bull.* **198:** 319–331.

Raineri, M. 1995. Is a mollusc an evolved bent metatrochophore? A histochemical investigation of neurogenesis in *Mytilus* (Mollusca:Bivalvia). *J. Mar. Biol. Assoc. U.K.* **75:** 571–592.

Raineri, M., and M. Ospovat. 1994. The initial development of gangliar rudiments in a posterior position in *Mytilus galloprovincialis* (Mollusca: Bivalvia). *J. Mar. Biol. Assoc. U.K.* **74:** 73–77.

Santama, N., K. W. Li, K. E. Bright, M. Yeoman, W. P. Geraerts, P. R. Benjamin, and J. F. Burke. 1993. Processing of the FMRFamide precursor protein in the snail *Lymnaea stagnalis:* characterization and neuronal localization of a novel peptide, "SEEPLY." *Eur. J. Neurosci.* **5:** 1003–1016.

Santama, N., P. R. Benjamin, and J. F. Burke. 1995a. Alternative RNA splicing generates diversity of neuropeptide expression in the brain of the snail *Lymnaea: in situ* analysis of mutually exclusive transcripts of the FMRFamide gene. *Eur. J. Neurosci.* **7:** 65–76.

Santama, N., C. H. Wheeler, D. R. Skingsley, M. S. Yeoman, K. Bright, I. Kaye, J. F. Burke, and P. R. Benjamin. 1995b. Identification, distribution and physiological activity of three novel neuropeptides of *Lymnaea:* EFLRIamide and pQFYRIamide encoded by the FMRFamide gene, and a related peptide. *Eur. J. Neurosci.* **7:** 234–246.

Santama, N., K. W. Li, W. P. Geraerts, P. R. Benjamin, and J. F. Burke. 1996. Post-translational processing of the alternative neuropeptide precursor encoded by the FMRFamide gene in the pulmonate snail, *Lymnaea stagnalis. Eur. J. Neurosci.* **8:** 968–977.

Schacher, S., E. R. Kandel, and R. Woolley. 1979. Development of neurons in the abdominal ganglion of *Aplysia californica* I. Axosomatic synaptic contacts. *Dev. Biol.* **71:** 176–190.

Smith, S. A., J. Nason, and R. P. Croll. 1998. Distribution of catecholamines in the sea scallop, *Placopecten magellanicus. Can. J. Zool.* **76:** 1254–1262.

Syed, N. I., and W. Winlow. 1989. Morphology and electrophysiology of neurons innervating the ciliated locomotor epithelium in *Lymnaea stagnalis* (L.). *Comp. Biochem. Physiol.* **93A:** 633–644.

Voronezhskaya, E. E., and K. Elekes. 1996. Transient and sustained expression of FMRFamide-like immunoreactivity in the developing nervous system of *Lymnaea stagnalis. Cell Mol. Neurobiol.* **16:** 661–676.

Voronezhskaya, E. E., and K. Elekes. 1997. Expression of FMRFamide gene neuropeptides is partly different in the embryonic nervous system of the pond snail, *Lymnaea stagnalis* L. *Neurobiology* **5:** 91–93.

Voronezhskaya, E. E., L. Hiripi, K. Elekes, and R. P. Croll. 1999. Development of catecholaminergic neurons in the pond snail, *Lymnaea stagnalis* I: Embryonic development of dopaminergic neurons and dopamine-dependent behaviors. *J. Comp. Neurol.* **404:** 297–309.

Reference: *Biol. Bull.* **199**: 316–320. (December 2000)

Development of a Penis from the Vestigial Penis in the Female Apple Snail, *Pomacea canaliculata*

NAOKUNI TAKEDA

Brainway Group, Brain Science Institute, The Institute of Physical and Chemical Research,
2-1 Wako, Saitama 351-0198, Japan

In the apple snail (Pomacea canaliculata), *females have an undifferentiated mass of tissue near the anus. Although this mass is called the vestigial penis, there are no signs of a hermaphroditic gonad or any structure that represents a transition from one sex to the other. Based on considerations of the steroid hormone theory of reproduction and in view of disruption of endocrine systems in molluscs by organotins, a study was made of the effects of tributyltin on female snails. Exposure to tributyltin resulted in the so-called imposex phenomenon, and both a penis and a penis sheath were newly generated from the so-called vestigial penis. The same phenomenon was also induced by testosterone. Thus the vestigial penis, named more than one hundred years ago, has been demonstrated for the first time to be a rudiment of the penis itself.*

The Ampullariidae (Gastropoda, Prosobranchia, Architaenioglossa) is a family of freshwater prosobranchs that are widely distributed in Asia, Africa, and South America (1). It is well known that some molluscs exhibit unusual sexual diversity and hermaphroditism (2, 3). One of the most interesting features of members of the Ampullariidae is that females in 5 of the 10 genera—namely, *Pila* (4, 5, 6, 7, 8, 9, 10, 11, 12), *Pomacea* (13, 14, 15, 16), *Lanistes* (13, 17, 18), *Afropomus* (19), and *Turbinicola* (13)—have a so-called vestigial penis in addition to the normal reproductive system (Fig. 1). The vestigial penis was first described by Bouvier (4, 5), a skilled neuroanatomist, in *Ampullaria (Pila) polita* more than 100 years ago. Since then, many molluscan researchers have used that term for this tissue without further explanation. The question examined here is this: Is the organ historically described as a vestigial penis a remnant of a penis—a degenerate structure that lacks the capacity to develop further—or is it a rudiment, or precursor—an incipient structure that, under the proper conditions, could develop into a penis?

The vestigial penis is a tongue-like structure lying inside the elevated mantle skirt, near the anus (Fig. 2A). Histologically, it consists of connective tissue, and no differentiation of the structure is apparent during the life cycle of the female (Fig. 2B).

To my knowledge, no experimental evidence has been presented to justify the designation of the elevated tissue near the anus in some female snails as a "vestigial penis" (4, 5). No clear evidence of hermaphroditism has yet been shown in any extant species of Ampullariidae. In *Pomacea canaliculata*, the apple snail, the positions of the gonads are basically different: the testis is located at the tip of the spiral, and the ovary is spread over the surface of the hepatopancreas at a location similar to that of the testis. It has also been confirmed that there is no apparent precursor or vestige of a hermaphroditic condition in any part of the reproductive system throughout the life history. As Andrews (13) stated, the copulatory apparatus appears to develop at the same rate in both sexes until the gonad becomes active, when its growth is arrested in the female. Andrews hypothesized that the gonad might produce a hormone responsible for the cessation of growth, but in the early 1960s, when this work was published, the chemical nature of reproductive hormones in molluscs had not yet been established. In 1991, Berthold (20) proposed that the so-called vestigial organ be designated an "oriment"—a term implying that the tissue is a precursor with the potential to develop into an adult organ. The question then arose as to whether such a designation might be appropriate. As a basis for such a designation, at the very least, some experiments involving implantation of testes into females should be performed to determine whether a true penis might develop from the tissue mass.

Received 7 December 1999; accepted 10 August 2000.
E-mail: takeda@brainway.riken.go.jp

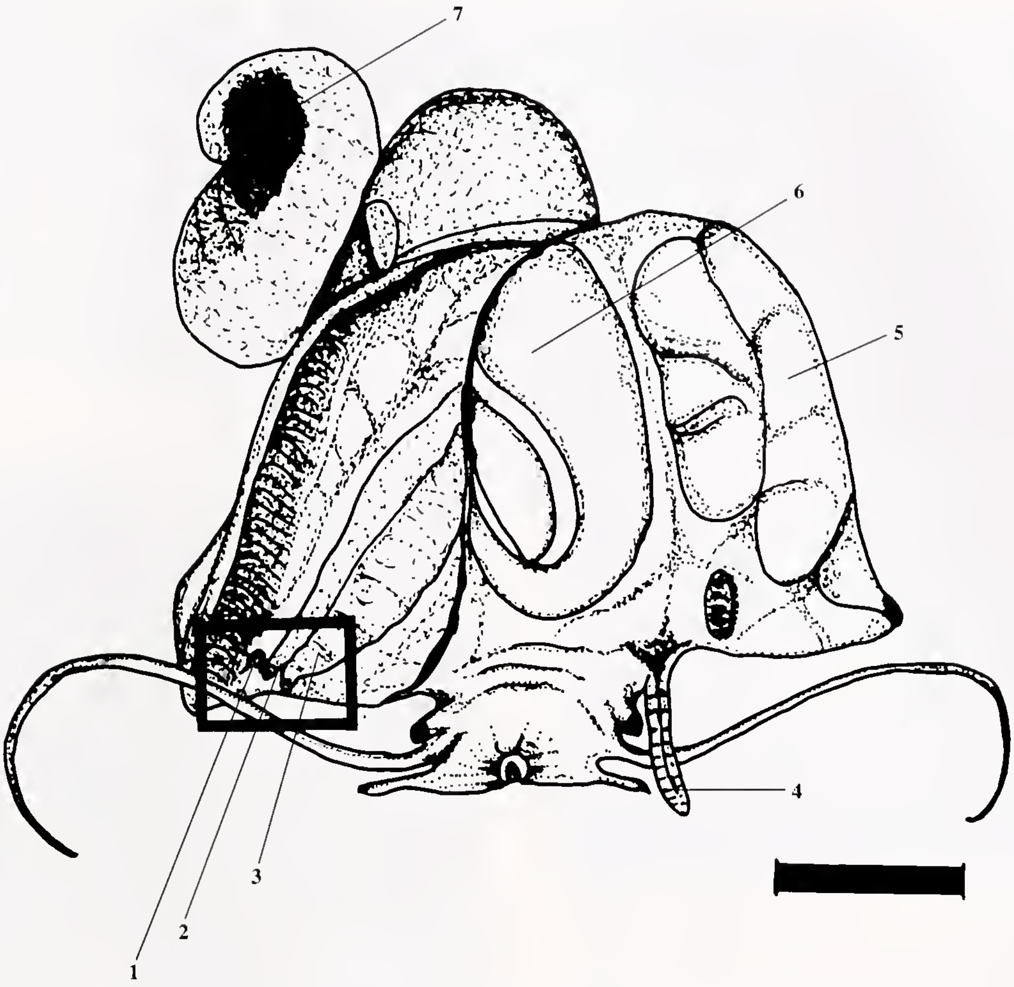

Figure 1. General appearance of the vestigial penis in a female apple snail (*Pomacea canaliculata*). The shell was removed and the region to the left of the head was dissected to reveal the vestigial penis (1), rectum (2), and oviduct (3), which are enclosed in a square. The siphon (4), pulmonary sac (5), albumen gland (6), and ovary (7) are also indicated. Scale bar represents 1 cm.

As an approach to this problem, I examined the effects of an endocrine disruptor that appears to be associated with as yet unresolved environmental problems. Organotins, and in particular tributyltin, which is a component of some antifouling paints, induce a condition known as "imposex" in prosobranch gastropods. Imposex, in which a penis and vas deferens develop in females (21), has been widely observed in marine snails that belong to the Caenogastropoda; *Nucella* and *Littorina* are common examples (22). Females of these species lack a vestigial penis, but the capacity exists for induction of a penis and vas deferens. *Pomacea canaliculata* has been proposed as a potential bioindicator for tributyltin (22), which is used as a biocidal agent against molluscs, in fungicides (23) and in anti-fouling paints in freshwater environments. Anticipating possible endocrine disruption by tributyltin, I examined its effects to see whether the vestigial penis in this species might develop further after female snails were exposed to this compound and, if such a penis did develop, how would it differentiate?

Female specimens of *P. canaliculata* were reared in water that contained 30 ng/l tributyltin. About 3 months after the start of treatment, the outside of the elevated tissue of the vestigial penis began to form a long process that resembled a penis, and its interior developed as a thick mass. These structures grew gradually and reached a maximum size after about 6 months of treatment with tributyltin (Fig. 3A). Histological staining revealed that the inside tissue mass contained a penis; the cross section of a penis was also found within the tissue mass (Fig. 3B). Thus, the outside structure appeared to be a penis sheath. Within about one further month, a complete penis had developed from the tissue of the vestigial penis (Fig. 4).

In *P. canaliculata*, the copulatory system of the male consists of a stout penis sheath and a long, slender penis

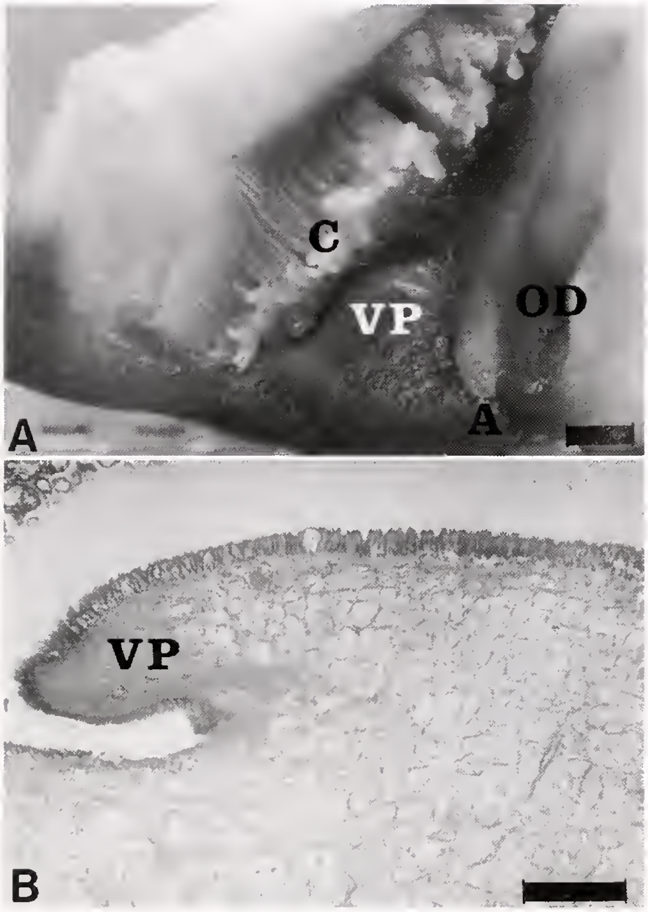

Figure 2. (A) General appearance of the vestigial penis in a female apple snail (*Pomacea canaliculata:* control) reared by artificial mass culture. Scale bar represents 1 mm. (B) Histological appearance of the vestigial penis in A. The regions containing a vestigial penis were fixed in Bouin's fluid and embedded in paraffin wax by the standard method. Sections were stained with hematoxylin and eosin. Scale bar represents 200 μm. A, anus; C, ctenidium; OD, oviduct; VP, vestigial penis.

within it (24). The penis and the penis sheath are located together to the left of the extreme right margin of the mantle cavity. In treated females, the arrangement of these male copulatory organs was similar but differed in the distance between the penis sheath and the penis: the penis sheath in females was located at the edge of the ctenidium at the mantle skirt, at a distance from the penis.

It has been suggested that tributyltin inhibits cytochrome P450 aromatase, which converts testosterone to estradiol in females (25, 26). Inhibition of aromatase activity thus increases levels of testosterone which induces imposex, with the development of male copulatory organs. Development of the imposex phenomenon in *P. canaliculata* was also confirmed by direct treatment with testosterone. Female snails reared in water that contained 500 ng/l testosterone exhibited changes similar to those induced by tributyltin, including the development of a penis sheath and a penis. Therefore, these observations support the proposed mechanism of action of tributyltin.

It is difficult to explain the unusual phenomenon of a rudimentary penis in females; however, I propose the following hypothesis. In the early stages of development, both sexual rudiments develop as an undifferentiated tissue mass. Once the sex of the snail is determined genetically (27), however, these rudiments differentiate in response to the secretion of specific sex steroid hormones. The undifferentiated tissue mass that develops into a penis in males is left as an arrested rudiment in females. The vestigial penis develops into a complete copulatory organ only if the anlage of the gonad becomes a testis.

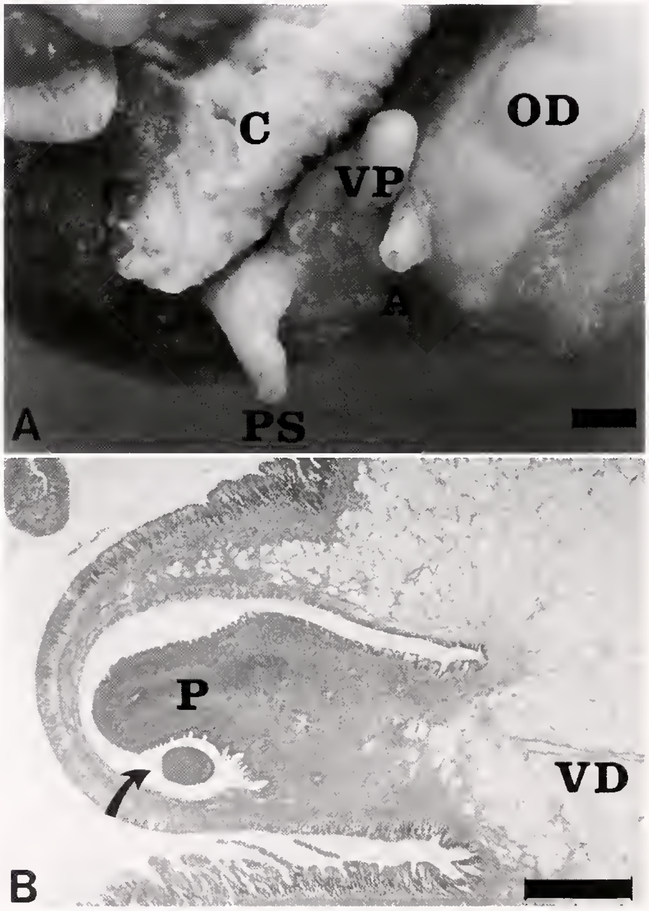

Figure 3. (A) Morphology of the imposex induced by tributyltin in a female apple snail (*Pomacea canaliculata*). Female snails (n = 100) for experiments were reared in a freshwater tank that contained tributyltin (Tokyo Kasei, Co. Ltd., Tokyo, Japan) at 30 ng/l for about 6 months. The state of imposex was checked at weekly intervals. Scale bar represents 1 mm. Similar results were also obtained in female snails (n = 100) reared with testosterone (Wako, Co. Ltd., Osaka, Japan) at 500 ng/l for about 7 months. (B) Histological appearance of the vestigial penis in A. The arrowhead indicates the cross section of a penis. Hematoxylin and eosin stain. See legend to Fig. 2B for methods. Scale bar represents 200 μm. P, penis; PS, penis sheath; VD, vas deferens (see legend to Fig. 2 for other abbreviations).

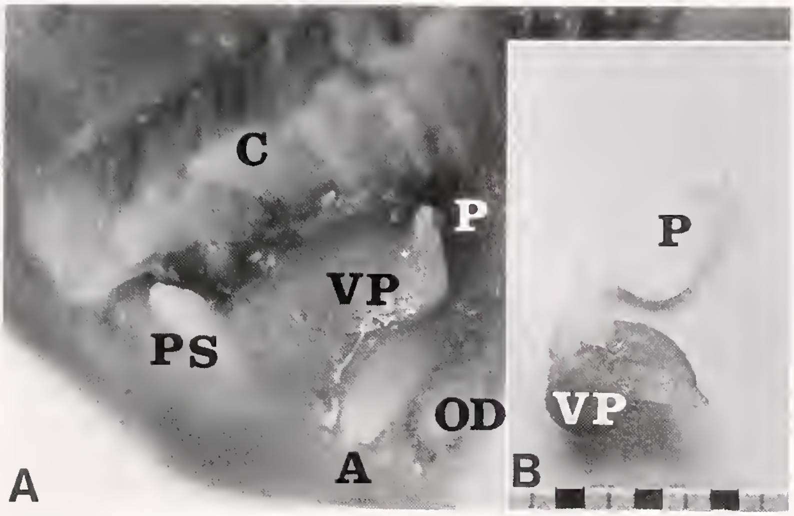

Figure 4. (A) A penis that arose from the vestigial penis of a female apple snail (*Pomacea canaliculata*) after treatment with tributyltin for about 7 months. The same phenomenon was also seen in female snails reared with testosterone for about 8 months. See legend to Fig. 3A for methods. (B) The extirpated penis from the vestigial penis. See legends to Fig. 2 and 3 for other abbreviations. Scale represents 1 mm.

The "steroid hormone theory," which I proposed previously (28, 29) for the reproduction of terrestrial pulmonates, apparently also applies to prosobranch snails. This theory states basically that the development of accessory sex organs is controlled by steroid hormones secreted by the gonad. This concept of the effects of hormones on snail reproduction, together with the effects of endocrine disruption in molluscs, allowed me to demonstrate, for the first time, that the so-called "vestigial penis," named more than one hundred years ago (4, 5), is a rudiment of the penis itself.

Literature Cited

1. **Perera, G., and J. G. Walls. 1996.** *Apple Snails in the Aquarium*, T. F. H. Publications, Jersey City, NJ. 121 pp.
2. **Fioroni, P., J. Oehlmann, and E. Stroben. 1991.** The pseudohermaphroditism of prosobranchs: morphological aspects. *Zool. Anz.* **226:** 1–26.
3. **Takeda, N. 2000.** Mollusca. Pp. 93–147 in *Reproductive Biology of Invertebrates, Vol. 10, Part A, Progress in Developmental Endocrinology*, A. Dorn, ed. John Wiley, New York.
4. **Bouvier, E. L. 1888.** Sur l'anatomie de l'Ampullaire. *Bull. Soc. Philom. Paris* **12:** 5–70.
5. **Bouvier, E. L. 1888.** Étude sur l'organisation des Ampullaires. *Mem. Soc. Philom. Paris* (centenary vol.) 63–85.
6. **Sachwatkin, V. A. 1920.** Das Urogenitalsystem von *Ampullaria gigans* Spix. *Acta Zool. (Stockh.)* **1:** 67–130.
7. **Hagler, K. 1923.** Anatomie von *Pachylabra (Ampullaria) cinerea* (Reeve). 1. Teil. Mit Einsch ass einer burzen Besprechung der wichtigsten Literatur über die Ampullariidae. *Acta Zool. (Stockh.)* **4:** 314–410.
8. **Franc, A. 1968.** Sous-classe des Prosobranches (Prosobranchia Milne Edwards 1848 = Streptoneura). Pp. 40–324 in *Traite de Zoologie V (III)*, P.-P. Grasse, ed. Masson, Paris.
9. **Kaewjam, R. S. 1987.** The apple snails of Thailand: aspects of comparative anatomy. *Malacol. Rev.* **20:** 69–89.
10. **Keawjam, R., and E. S. Upatham. 1990.** Shell morphology, reproductive anatomy and genetic patterns of three species of apple snails of the genus *Pomacea* in Thailand. *J. Med. Appl. Malacol.* **2:** 45–57.
11. **Prashad, B. 1925.** Anatomy of the common Indian apple-snail, *Pila globosa*. *Mem. Indian Mus.* **8:** 91–154.
12. **Scott, M. I. H. 1957.** Estudio morfologica y taxonomica de los Ampullaridos de la Republica Argentina. *Rev. Mus. Argent. Cienc. Nat. (Zool).* **3:** 233–333.
13. **Andrews, E. B. 1964.** The functional anatomy and histology of the reproductive system of some pilid gastropod molluscs. *Proc. Malacol. Soc. Lond.* **36:** 121–140.
14. **Thiengo, S. C. 1987.** Observations on the morphology of *Pomacea lineata* (Spix, 1827) (Mollusca: Ampullariidae). *Mem. Inst. Oswaldo Cruz Rio J.* **82:** 563–570.
15. **Thiengo, S. C. 1989.** On *Pomacea sordida* (Swaison, 1823) (Prosobranchia, Ampullariidae). *Mem. Inst. Oswaldo Cruz Rio J.* **84:** 351–355.
16. **Thiengo, S. C., C. E. Borda, and J. L. Barros Araujo. 1993.** On *Pomacea canaliculata* (Lamarck, 1822) (Mollusca; Pilidae: Ampullariidae). *Mem. Inst. Oswaldo Cruz Rio J.* **88:** 67–71.
17. **Aboul-Ela, I. A., and E. A. Beddiny. 1969.** Morphological and histological studies on the genitalia of *Lanistes bolteni* Chemnitz, 1786. *Ain Shams Sci. Bull.* **13:** 145–176.
18. **Berthold, T. 1990.** Phylogenetic relationships, adaptations and biogeographic origin of the Ampullariidae (Mollusca, Gastropoda) endemic to Lake Malawi, Africa. *Abh. Naturwiss. Ver. Hamburg* **31/32:** 47–84.
19. **Berthold, T. 1988.** Anatomy of *Afropomus balanoideus* (Mollusca, Gastropoda, Ampullariidae) and its implications for phylogeny and ecology. *Zoomorphology* **108:** 149–159.
20. **Berthold, T. 1991.** Vergleichende Anatomie, Phylogenie und historische Biogeographie der Ampullariidae (Mollusca, Gastropoda). *Abh. Naturwiss. Ver. Hamburg.* **29:** 1–256.
21. **Matthiessen, P., and P. E. Gibbs. 1998.** Critical appraisal of the evidence for tributyltin-mediated endocrine disruption in mollusks. *Environ. Toxicol. Chem.* **17:** 37–43.
22. **Takeda, N. 2000.** Endocrine disruption of reproduction by organotins. Pp. 259–285 in *Reproductive Biology of Invertebrates, Vol.*

10, Part A, Progress in Developmental Endocrinology, A. Dorn, ed. John Wiley, New York.

23. **Duncan, J. 1980.** The toxicology of molluscicides. The organotins. *Pharmacol. Ther.* **10:** 407–429.
24. **Takeda, N. 1999.** Histological studies on the maturation of the reproductive system in the apple snail, *Pomacea canaliculata. J. Anal. Biosci.* **22:** 425–432.
25. **Spooner, N., P. E. Gibbs, G. W. Bryan, and L. J. Goad. 1991.** The effects of tributyltin upon steroid titres in the female dogwhelk, *Nucella lapillus*, and the development of imposex. *Mar. Environ. Res.* **32:** 37–49.
26. **Bettin, C., J. Oehlmann, and E. Stroben. 1996.** TBT-induced imposex in marine neogastropods is mediated by an increasing androgen level. *Helgol. Meeresunters.* **50:** 299–317.
27. **Brand, E., T. Yokosawa, and Y. Fujio. 1990.** Chromosome analysis of apple snail *Pomacea canaliculata. Tohoku J. Agric. Res.* **40:** 81–89.
28. **Takeda, N. 1983.** Endocrine regulation of reproduction in the snail, *Euhadra peliomphala*. Pp. 106–110 in *Molluscan Neuro-Endocrinology*, J. Lever and H. H. Boer, eds. North-Holland, Amsterdam.
29. **Takeda, N. 1989.** Hormonal control of reproduction in land snails. *Venus* **48:** 99–139.

INDEX

A

Abenavoli, A., L. Forti, and A. Malgaroli, Mechanisms of spontaneous miniature activity at CA3-CA1 synapses: evidence for a divergence from a random Poisson process, 184
Actin, 202, 203
Action potential, 135
Adenylate cyclase, 197
Adhesion of a viral envelope protein to a non-self binding domain of the aggregation factor in the marine sponge *Microciona prolifera*, 209
Adhesive proteoglycans, 192
Aggregation factor, 192, 209
Aggression, 265
Aiptasia, 76
Allometric scaling in small colonies of the scleractinian coral *Siderastrea siderea* (Ellis and Solander), 21
Allometry, 21
cAMP, 197
Amphibian, 187
An inducer of molluscan metamorphosis transforms activity patterns in a larval nervous system, 241
Annual Report of the Marine Biological Laboratory, v. 199 (1), R1
Anuran, 187
Apical organ, 305
Aplysia, 305
Arbacia eggs, 212, 213
Armstrong, Margaret T., see Rengasamy Asokan, 190
Armstrong, Peter B., and Rengasamy Asokan, A Ca^{+2}-independent cytolytic system from the blood of the marine snail *Busycon canaliculum*, 194
Armstrong, Peter B., see John M. Harrington, 189; Rengasamy Asokan, 190
Asokan, Rengasamy, Margaret T. Armstrong, and Peter B. Armstrong, Association of α_2-macroglobulin with the coagulin clot in the American horseshoe crab, *Limulus polyphemus:* a potential role in stabilization from proteolysis, 190
Asokan, Rengasamy, see Peter B. Armstrong, 194
Association of α_2-macroglobulin with the coagulin clot in the American horseshoe crab, *Limulus polyphemus:* a potential role in stabilization from proteolysis, 190
Asteroidea, 298
Atherton, Jillian L., Matthew A. Krutky, James M. Hitt, Frederick A. Dodge, and Robert B. Barlow, Optic nerve responses of *Limulus* in its natural habitat at night, 176
Atherton, Jillian L., see Matthew A. Krutky, 178
Axonal transport, 202, 203
Axoplasm, 203

B

Baghdasarian, Garen, and Leonard Muscatine, Preferential expulsion of dividing algal cells as a mechanism for regulating algal-cnidarian symbiosis, 278
Baker, Shirley M., Jeffrey S. Levinton, and J. Evan Ward, Particle transport in the zebra mussel, *Dreissena polymorpha* (Pallas), 116
Barlow, Robert B., see James M. Hitt, 171; Jillian L. Atherton, 176; Matthew A. Krutky, 178
Barnes, David K. A., and Matthew H. Dick, Overgrowth competition between clades: implications for interpretation of the fossil record and overgrowth indices, 85
Bentley, M. G., see G. J. Watson, 50
Bezanilla, Francisco, see Joshua J. C. Rosenthal, 135
Biogeochemistry, 218
Biogeography, 126
Biogeography of two species of *Symbiodinium* (Freudenthal) inhabiting the intertidal sea anemone *Anthapleura elegantissima* (Brandt), 126
Biosynthesis, 192
Birefringence, 212
Bivalve, 29, 116, 144, 199
Blood clotting, 190
Boatwhistle, 173
Bolton, Toby F., Florence I. M. Thomas, and Celere N. Leonard, Maternal energy investment in eggs and jelly coats surrounding eggs of the echinoid *Arbacia punctulata*, 1
Boron, 221
Brothers, Christine, Ernest Marks iii, and Roxanna Smolowitz, Conditions affecting the growth and zoosporulation of the protistan parasite QPX in culture, 200
Brown, Jeremiah, see Phillip Stafford, 203
Bruzzone, Roberto, see Thomas H. White, 165
Bryozoan, 85
Buckland-Nicks, John, and Alan N. Hodgson, Fertilization in *Callochiton castaneus* (Mollusca), 59
Burger, Max M., see William J. Kuhns, 192; Roger MacKenzie, 209
Burgos, Mario H., Makoto Goda, and Shinya Inoué, Fertilization-induced changes in the fine structure of stratified *Arbacia* eggs. II. Observations with electron microscopy , 213
Burgos, Mario H., see Makoto Goda, 212
Byrne, R. A., see T. H. Dietz, 14

C

Ca^{2+}, 212
A Ca^{+2}-independent cytolytic system from the blood of the marine snail *Busycon canaliculum*, 194
Cable properties, 135
Calcium imaging, 162
Camouflage, 6
Carotenoid, 223
Cassiopeia, 76
Cataract, 187
Catecholamines, 305
Cell
  contact, 287
  motility, 202, 203
  movement, 287
  proliferating, 199
Cellular basis of gastrulation in the sand dollar *Scaphechinus mirabilis*, 287
Centrifugation, 212, 213
Centrifuge polarizing microscope, 212
Chang, F., see P. T. Tran, 205
Channel, 165
Cherax destructor, 251
Cherry, J. S., see T. H. Dietz, 14
Chikarmane, Hemant M., Alan M. Kuzirian, Robbin Kozlowski, Mark Kuzirian, and Tony Lee, Population genetic structure of the goosefish, *Lophius americanus*, 227
Child, Frank M., see David A. Epstein, 182
Chimerism, 231
Chlorophyll, 223
Circadian rhythms in the receptive fields of the *Limulus* lateral eye, 171
Clades, 85
Cladophora vagabunda, 223
Claessens, Luc, see Ryan Kirkby, 218

Cleavage, 207
Cnidaria, 68, 278
Cohen, Lawrence B., see Matt Wachowiak, 162
Colony, 231
Conditions affecting the growth and zoosporulation of the protistan parasite QPX in culture, 200
Conduction velocity, 135
Connexin, 165
Copepod, 95
Coral, 21, 68
Crawford, Karen, The role of microtubules during blastodisc formation of the squid *Loligo pealei*, 207
Crayfish, 251
A critical approach to the definition of Darwinian units of selection, 231
Croll, Roger P., see Amanda J. G. Dickinson, 305
Cromarty, S. I., J. Mello, and G. Kass-Simon, Molt-related and size-dependent differences in the escape response and post-threat behavior of the American lobster, *Homarus americanus*, 265
Crustacea, 265
Cytoplasmic streaming, 207
Cytoskeleton, 144, 202, 203

D

Dacey, John W. H., see Richard W. Hill, 108
Davis, Theodore M., see Inigo Novales Flamarique, 187
Denaturing gradient gel electrophoresis, 126
Denault, Michelle, Erica Stieve, and Ivan Valiela, Effects of nitrogen load and irradiance on photosynthetic pigment concentrations in *Cladophora vagabunda* and *Gracilaria tikvahiae* in estuaries of Waquoit Bay, 223
Denitrification, 221
Descending octaval nucleus, 173
Detritus, 225
Development, 68, 195
Development of a penis from the vestigial penis in the female apple snail, *Pomacea canaliculata*, 316
Development of embryonic cells containing serotonin, catecholamines, and FMFRamide-related peptides in *Aplysia californica*, 305
Development of self-referencing oxygen microsensor and its application to single pancreatic HIT cells; effects of adenylate cyclase activator forskolin on oxygen consumption, 197
Dick, Matthew H., see David K. Barnes, 85
Dickinson, Amanda J. G., Roger P. Croll, and Elena E. Voronezhskaya, Development of embryonic cells containing serotonin, catecholamines, and FMFRamide-related peptides in *Aplysia californica*, 305
Dietz, T. H., A. S. Udoetok, J. S. Cherry, H. Silverman, and R. A. Bryne, Kidney function and sulfate uptake and loss in the freshwater bivalve *Toxolasma texasensis*, 14
Differences in properties of salt marsh sediment between hayed and reference sites, 223
Differentiation, 41
Dimethylsulfoniopropionate, 108
Dimethylsulfoniopropionate in giant clams (Tridacnidae), 108
Disease, 199
Do the properties of underwater lighting influence the visually guided behavior of *Limulus*?, 178
Dodge, Frederick A., see James M. Hitt, 171; Jillian L. Atherton, 176; Matthew A. Krutky, 178
Doye, V., see P. T. Tran, 205
Dreissena, 116, 144
Drosophila, 170

E

Early development of zooxanthella-containing eggs of the corals *Pocillopora verrucosa* and *P. eydouxi* with special reference to the distribution of zooxanthellae, 68
Echinodermata, 298
Echinoid, 1
Edds-Walton, Peggy L., see Richard R. Fay, 173
Edmunds, Peter J., see Steven V. Vollmer, 21
Edward, Ahser, see Richard W. Hill, 108
Effects of food concentration and availability on the incidence of cloning in planktotrophic larvae of the sea star *Pisaster ochraceus*, 298
Effects of myosin-II antibody on actin-dependent vesicle transport in extracts of clam oocytes, 202
Effects of nitrogen load and irradiance on photosynthetic pigment concentrations in *Cladophora vagabunda* and *Gracilaria tikvahiae* in estuaries of Waquoit Bay, 223
Electron microscopy, 213
Embryo, 305
Embryogenesis, 29
Endocrine disruption, 316
Endoplasmic reticulum, 212, 213
Endoscopy, 116
Engler, John, see Robert M. Gould, 215
Enzymatic biosynthesis of N-linked glycan by the marine sponge *Microciona prolifera*, 192
Enzyme activity, 100
Epstein, David A., Herman T. Epstein, Frank M. Child, and Alan M. Kuzirian, Memory consolidation in *Hermissenda crassicornis*, 182
Epstein, Herman T., see David A. Epstein, 182
ER transport, 202, 203
Escape response, 265
Eye, 171, 176
Eyeshine, 6

F

Factors influencing spawning and pairing in the scale worm *Harmothoe imbricata*, 50
Falk, Chun X., see Matt Wachowiak, 162
Farmer, Mark A., see Timothy S. Wakefield, 76
Fate of anthropogenic nitrogen in a nearshore Cape Cod aquifer, 221
Fay, Richard R., and Peggy L. Edds-Walton, Frequency response of auditory brainstem units in toadfish *Opsanus tau*, 173
Fernandez-Busquets, Xavier, see William J. Kuhns, 192
Fertilization, 59, 144, 212, 213
Fertilization in *Callochiton castaneus* (Mollusca), 59
Fertilization-induced changes in the fine structure of stratified *Arbacia* eggs. I. Observations on live cells with the centrifuge polarizing microscope, 212
Fertilization-induced changes in the fine structure of stratified *Arbacia* eggs. II. Observations with electron microscopy, 213
Finley, Luke, and David Macmillan, The structure and growth of the statocyst in the Australian crayfish *Cherax destructor*, 251
Fish, startle response, 180
Fisher, Charles R., see Stéphane Hourdez, 95
FMRFamide, 305
Forskolin, 197
Forti, L., see A. Abenavoli, 184
Fouling organism, 189
Freeze substitution, 76
Frequency response of auditory brainstem units in toadfish *Opsanus tau*, 173
Freund, Concetta M., see Robert M. Gould, 215
Frog Lim-1-like protein is expressed predominantly in the nervous tissue, gonads, and early embryos of the bivalve mollusc *Mytilus galloprovincialis*, 29

G

Gallo, Michael A., see Diane E. Heck, 195
Gastropod, 241
Gastrulation, 287
Gaten, E., see M. L. Johnson, 6
Gating current, 164
Gaudron, S. M., see G. J. Watson, 50
Gene, 231
  activity, 100
  expression, 215

Gene expression and enzyme activities of the sodium pump during sea urchin development: implications for indices of physiological state, 100
Giant axon, squid, 135
Giblin, Anne, see Adena Greenbaum, 223
Gibson, Daniel G., see Rhea Hanselmann, 199
Gibson, Glenys D., and Jennifer M. L. Harvey, Morphogenesis during asexual reproduction in *Pygospio elegans* Claparede (Annelida, Polychaeta), 41
Goda, Makoto, Mario H. Burgos, and Shinya Inoué, Fertilization-induced changes in the fine structure of stratified *Arbacia* eggs. I. Observations on live cells with the centrifuge polarizing microscope, 212
Goda, Makoto, see Mario H. Burgos, 213
Gonad, 29
Gould, Robert M., Concetta M. Freund, John Engler, and Hilary G. Morrison, Optimization of homogenization conditions used to isolate mRNAs in processes of myelinating oligodendrocytes, 215
Gracilaria tikvahiae, 223
Greenbaum, Adena, and Anne Giblin, Differences in properties of salt marsh sediment between hayed and reference sites, 223
Groundwater, 221
Growth, 251

H

Hadfield, Michael G., see Esther M. Leise, 241
Hale, Melina E., Startle responses of fish without Mauthner neurons: escape behavior of the lumpfish *(Cyclopterus lumpus)*, 180
Hammar, Katherine, see Sung-Kwong Jung, 197
Hanselmann, Rhea, Roxanna Smolowitz, and Daniel G. Gibson, Identification of proliferating cells in hard clams, 199
Hard clam, 199
Harmothoe imbricata, 50
Harrington, John M., and Peter B. Armstrong, Initial characterization of a potential anti-fouling system in the American horseshoe crab, *Limulus polyphemus*, 189
Harvey, Jennifer M. L., see Glenys D. Gibson, 41
Haying, 225
Hearing, 173
Heart rate, 257
Heavy water, 164
Heavy water (D_2O) alters the sodium channel gating current in squid giant axons, 164
Heck, Diane E., Lydia Louis, Michael A. Gallo, and Jeffrey D. Laskin, Modulation of the development of plutei by nitric oxide in the sea urchin *Arbacia punctulata*, 195
Hemocyte proliferation, 199
Hemoglobin, 95
  functional properties, 95
  structure, 95
Hemoglobin from a deep-sea hydrothermal-vent copepod, 95
Hemolysis, 194
Hermissenda, 182
Herring, P. J., see M. L. Johnson, 6
Hidaka, M., see M. Hirose, 68
Hill, Richard W., John W. H. Dacey, and Ahser Edward, Dimethylsulfoniopropionate in giant clams (Tridacnidae), 108
Hippocampus, 184
Hirose, M., R. A. Kinzie III, and M. Hidaka, Early development of zooxanthella-containing eggs of the corals *Pocillopora verrucosa* and *P. eydouxi* with special reference to the distribution of zooxanthellae, 68
Hitt, James M., see Jillian L. Atherton, 176
Hitt, James M., Frederick A. Dodge, Ehud Kaplan, and Robert B. Barlow, Circadian rhythms in the receptive fields of the *Limulus* lateral eye, 171
Hodgson, Alan N., see John Buckland-Nicks, 59
Homarus, 257, 265
Hopkinson, Charles, Jr., see Ryan Kirkby, 218; Anne Perring, 219
Horizontal cell, 168
Hourdez, Stéphane, Jason Lamontagne, Pat Peterson, Roy E. Weber, and Charles R. Fisher, Hemoglobin from a deep-sea hydrothermal-vent copepod, 95
Human immunodeficiency virus, 209
Hydrogen ion fluxes from isolated retinal horizontal cells, modulation by glutamate, 168

I

Identification of proliferating cells in hard clams, 199
Immunity, innate, 189, 190, 194
Imposex, 316
Individual, 231
Initial characterization of a potential anti-fouling system in the American horseshoe crab, *Limulus polyphemus*, 189
Inoué, Shinya, see P. T. Tran, 205; Makoto Goda, 212; Mario H. Burgos, 213
Interaction of actin- and microtubule-based motors in squid axoplasm probed with antibodies to myosin V and kinesis, 203
Intercellular communication, 165
Intrinsic membrane properties of laryngeal motoneurons that control sexually differentiated vocal behavior in African clawed frogs, *Xenopus leavis*, 175
Ipswich, 218
Irradiance, 223

J

Jelly coat, 1
Johnson, J. L., P. M. J. Shelton, E. Gaten, and P. J. Herring, Relationship of dorsoventral eyeshine distributions to habitat depth and animal size in mesopelagic decapods, 6
Jung, Sung-Kwon, Katherine Hammar, and Peter J. S. Smith, Development of self-referencing oxygen microsensor and its application to single pancreatic HIT cells; effects of adenylate cyclase activator forskolin on oxygen consumption, 197
Jury, Steven H., and Winsor H. Watson III, Thermosensitivity of the lobster, *Homarus americanus*, as determined by cardiac assay, 257

K

Kaczmarek, Leonard K., see Ayako Yamaguchi, 175
Kaplan, Ehud, see James M. Hitt, 171
Kass-Simon, G., see S. I. Cromarty, 265
Kelley, Darcy B., see Ayako Yamaguchi, 175
Kempf, Stephen C., see Timothy S. Wakefield, 76
Kidney function, 14
Kidney function and sulfate uptake and loss in the freshwater bivalve *Toxolasma texasensis*, 14
Kinesin, 203
Kinzie, R. A., III, see M. Hirose, 68
Kirkby, Ryan, Luc Claessens, Charles Hopkinson, Jr., Edward Rastetter, and Joseph Vallino, Modeling the effects of land-use changes on nitrogen biogeochemistry in the Ipswich watershed, Massachusetts, 218
Kominami, Tetsuya, and Hiromi Takata, Cellular basis of gastrulation in the sand dollar *Scaphechinus mirabilis*, 287
Kozlowski, Robbin, see Hemant M. Chikarmane, 227
Kroeger, Kevin D., see Elizabeth J. Westgate, 221
Krutky, Matthew A., Jillian L. Atherton, Spence Smith, Frederick A. Dodge, and Robert B. Barlow, Do the properties of underwater lighting influence the visually guided behavior of *Limulus?*, 178
Krutky, Matthew A., see Jillian L. Atherton, 176
Kuhns, William J., Max M. Burger, Mohan Sarker, Xavier Fernandez-Busquets, and Tracy Simpson, Enzymatic biosynthesis of N-linked glycan by the marine sponge *Microciona prolifera*, 192
Kuhns, William J., see Roger MacKenzie, 209
Kuzirian, Alan M., see David A. Epstein, 182; Hemant M. Chikarmane, 227
Kuzirian, Mark, see Hemant M. Chikarmane, 227

L

Labyrinthomorpha, 200
LaJeunesse, R. C., and R. K. Trench, Biogeography of two species of *Symbiodinium* (Freudenthal) inhabiting the intertidal sea anemone *Anthopleura elegantissima* (Brandt), 126
Lamontagne, Jason, see Stéphane Hourdez, 95
Landowne, David, Heavy water (D_2O) alters the sodium channel gating current in squid giant axons, 164
Langford, F. M., see G. J. Watson, 50
Langford, George M., see Leslie Sandberg, 202; Phillip Stafford, 203
Laskin, Jeffrey D., see Diane E. Heck, 195
Learning, human, 182
Lee, Tony, see Hemant M Chikarmane, 227
Leise, Esther M., and Michael G. Hadfield, An inducer of molluscan metamorphosis transforms activity patterns in a larval nervous system, 241
Leonard, Celere N., see Toby F. Bolton, 1
Leong, Patrick K. K., see Adam G. Marsh, 100
Levinton, Jeffrey S., see Shirley M. Baker, 116
Lim-1 protein, 29
Limulus, 171, 176, 178, 189, 190
Lobster, 257, 265
Loligo, 135
Lophius americanus, 227
Louis, Lydia, see Diane E. Heck, 195
Lynn, J. W., see M. J. Misamore, 144

M

MacKenzie, Roger, David Newman, Max M. Burger, Rene Roy, and William J. Kuhns, Adhesion of a viral envelope protein to a non-self-binding domain of the aggregation factor in the marine sponge *Microciona prolifera*, 209
MacMillan, David, see Luke Finley, 251
Macroalgae, 223
$\alpha_2$macroglobulin, 190
Malchow, Robert Paul, see Anthony J. A. Molina, 168
Malgaroli, A., see A. Abenavoli, 184
Manahan, Donal T., see Adam G. Marsh, 100
Marine Biological Laboratory
  Annual Report, v. 199 (1), R1
  General Scientific Meetings, Short Reports, 157
Marine invertebrate reproduction, 1
Marks, Ernest, III, see Christine Brothers, 200
Marsh, Adam G., Patrick K. K. Leong, and Donal T. Manahan, Gene expression and enzyme activities of the sodium pump during sea urchin development: implications for indices of physiological state, 100
Maternal energy investment in eggs and jelly coats surrounding eggs of the echinoid *Arbacia punctulata*, 1
Maternal investment, 1
Mauthner neuron, 180
MBL
  Annual Report, v. 199 (1), R1
  General Scientific Meetings, Short Reports, 157
McClintock, James B., see Minako S. Vickery, 298
Mechanisms of spontaneous miniature activity at CA3-CA1 synapses: evidence for a divergence from a random Poisson process, 184
Mello, J., see S. I. Cromarty, 265
Memory
  blocking, 182
  long-term, 182
  short-term, 182
  consolidation, 182
Memory consolidation in *Hermissenda crassicornis*, 182
MEPSC, 184
Mesopelagic ecology, 6
Microciona, 192, 209
Microsporidian, 208
Microtubule, 205, 207
Microtubule-dependent nuclear positioning and nuclear-dependent septum positioning in the fission yeast, *S. pombe*, 205
Mikhailov, Alexander T., see Mario Torrado, 29
Misamore, M. J., and J. W. Lynn, Role of the cytoskeleton in sperm entry during fertilization in the freshwater bivalve *Dreissena polymorpha*, 144
Modeling the effects of land-use changes on nitrogen biogeochemistry in the Ipswich watershed, Massachusetts, 218
Modular organisms, 21
Modulation of the development of plutei by nitric oxide in the sea urchin *Arbacia punctulata*, 195
Molina, Anthony J. A., Peter J. S. Smith, and Robert Paul Malchow, Hydrogen ion fluxes from isolated retinal horizontal cells, modulation by glutamate, 168
Mollusc, 59, 194, 241
Molt cycle, 265
Molt-related and size-dependent differences in the escape response and post-threat behavior of the American lobster, *Homarus americanus*, 265
Monkfish, 227
Morphogenesis, 287
Morphogenesis during asexual reproduction in *Pygospio elegans* Claparede (Annelida, Polychaeta), 41
Morphology, 251
Morrison, Hilary G., see Robert M. Gould, 215
Mosaic, 231
Motoneuron, 175
mRNA transport, 215
Muscatine, Leonard, see Garen Baghdasarian, 278
Myelination, 215
Myosin, 202, 203

N

Nervous ganglion, 29
Newman, David, see Roger MacKenzie, 209
Nitrate, 221
Nitric oxide, 195
Nitrogen, 223
  processing, 218
Novales Flamarique, Inigo, Kristiina Ovaska, and Theodore M. Davis, UV-B-induced damage to the skin and ocular system of amphibians, 187
Nuclear positioning, 205
Nudibranch, 241

O

Odor recognition, 162
Odor-induced oscillatory activity in *Drosophila* CNS, 170
Olfaction, 170
Olfactory bulb, input to, 162
Oocyte, 202
Opisthobranch, 241
Optic nerve, 176
Optic nerve responses of *Limulus* in its natural habitat at night, 176
Optimization of homogenization conditions used to isolate mRNAs in processes of myelinating oligodendrocytes, 215
Organotin, 316
Oscillation, 170
Ovaska, Kristiina, see Inigo Novales Flamarique, 187
Overgrowth competition, 85
Overgrowth competition between clades: implications for interpretation of the fossil record and overgrowth indices, 85
Oxygen
  consumption, 197
  microsensor, 197

P

Pablich, Wendy J., see Elizabeth J. Westgate
PAH clearance, 14

Pancreatic HIT cell, 197
Particle selection, 116
Particle transport in the zebra mussel, *Dreissena polymorpha* (Pallas), 116
Passive tracer, 221
PCNA, 199
PEG clearance, 14
Perring, Anne, Michael Williams, Charles Hopkinson, Jr., Edward Rastetter, and Joseph Vallino, Solute dynamics in storm flow of the Ipswich River Basin: effects of land use, 219
Peterson, Pat, see Stéphane Hourdez, 95
pH, 200
Pheromone, 50
Phycoerythrin, 223
Pigment, 223
Pigment cell, 195
Planula, 68
Plume, 221
Polychaete, 41, 50
Polyplacophora, 59
Pomacea canaliculata, 316
Population, 227
Population genetic structure of the goosefish, *Lophius americanus*, 227
Preferential expulsion of dividing algal cells as a mechanism for regulating algal-cnidarian symbiosis, 278
Protease inhibitor, 190
Protein synthesis, 215
Proteoglycans, 192, 209

Q

QPX, 199, 200
Quanta, spontaneous release, 184

R

RAPD, 227
Rastetter, Edward, see Ryan Kirkby, 218; Anne Perring, 219
Regeneration, 41
Relationship of dorsoventral eyeshine distributions to habitat depth and animal size in mesopelagic decapods, 6
Renal clearance, 14
Reproduction, 50
Retina, 165, 168
Revised description of the fine structure of *in situ* "Zooxanthellae" genus *Symbiodinium*, 76
Rinkevich, B., A critical approach to the definition of Darwinian units of selection, 231
Ripps, Harris, see Thomas H. White, 165
The role of microtubules during blastodisc formation of the squid *Loligo pealei*, 207
Role of the cytoskeleton in sperm entry during fertilization in the freshwater bivalve *Dreissena polymorpha*, 144
Rosenthal, Joshua J. C., and Francisco Bezanilla, Seasonal variation in conduction velocity of action potentials in squid giant axon, 135
Roy, Rene, see Roger MacKenzie, 209

S

Salinity, 200
Salt marsh, 225
Sandberg, Leslie, Phillip Stafford, and George M. Langford, Effects of myosin-II antibody on actin-dependent vesicle transport in extracts of clam oocytes, 202
Sarker, Mohan, see William J. Kuhns, 192
Scaling, 21
Sea star larval cloning, 298
Sea urchin, 195, 287
  development, 100
Seasonal variation in conduction velocity of action potentials in squid giant axon, 135
Segmentation, 41
Self-referencing, 197
Septic, 221
Septum positioning, 205
Serotonin, 305
Sex steroid hormone, 316
Sexual differences, 175
Shelton, P. M. J., see M. L. Johnson, 6
Silverman, H., see T. H. Dietz, 14
Simpson, Tracy, see William J. Kuhns, 192
Size-dependent behavior, 265
Skate, 168
Smith, Peter J. S., see Anthony J. A. Molina, 168; Sung-Kwong Jung, 197
Smith, Spence, see Matthew A. Krutky, 178
Smolowitz, Roxanna, see Rhea Hanselmann, 199; Christine Brothers, 200
SO_4 clearance, 14
Sodium
  channel, 164
  pump, 100
Solute dynamics, 219
Solute dynamics in storm flow of the Ipswich River Basin: effects of land use, 219
The spatial representation of odors by olfactory receptor neuron input to the olfactory bulb is concentration invariant, 162
Spawning, 50
Species diversity, 126
Sponge, 192, 209
Sporoplasm, 208
Squid, 135, 164, 207
Srinivas, Miduturu, see Thomas H. White, 165
Stafford, Phillip, Jeremian Brown, and George M. Langford, Interaction of actin- and microtubule-based motors in squid axoplasm probed with antibodies to myosin V and kinesis, 203
Stafford, Phillip, see Leslie Sandberg, 202
Startle responses of fish without Mauthner neurons: escape behavior of the lumpfish *(Cyclopterus lumpus)*, 180
Statocyst, 251
Stem cell, 231
Stieve, Erica, see Michelle Denault, 223
The structure and growth of the statocyst in the Australian crayfish *Cherax destructor*, 251
Sulfate transport, 14
Suppression subtractive hybridization, 215
Surface motor proteins, 192
Symbiodinium, 76, 108, 126
Symbiosis, 76, 126, 278
Symbiotic dinoflagellate, 278
Synapse, 184
Synchrony, 170

T

Tail flip, 265
Takata, Hiromi, see Tetsuya Kominami, 287
Takeda, Naokuni, Development of a penis from the vestigial penis in the female apple snail, *Pomacea canaliculata*, 316
Temperature, 200, 257
  acclimation, 135
Thermosensitivity, 257
Thermosensitivity of the lobster, *Homarus americanus*, as determined by cardiac assay, 257
Thomas, Florence I. M., see Toby F. Bolton, 1
Torrado, Mario, and Alexander T. Mikhailov, Frog Lim-1-like protein is expressed predominantly in the nervous tissue, gonads, and early embryos of the bivalve mollusc *Mytilus galloprovincialis*, 29
Torus semicircularis, 173
Tran, P. T., V. Doye, F. Chang, and S. Inoué, Microtubule-dependent nuclear positioning and nuclear-dependent septum positioning in the fission yeast, *S. pombe*, 205
Transitivity index, 85
Trench, R. K., see R. C. LaJeunesse, 126
Tridacnidae, 108

3583

U

Udoetok, A. S., see T. H. Dietz, 14
Ultrastructure, 76
Unionid, 14
Unit of selection, 231
UV-B radiation, 187
UV-B-induced damage to the skin and ocular system of amphibians, 187

V

Valiela, Ivan, see Elizabeth J. Westgate, 221; Michelle Denault, 223
Vallino, Joseph, see Ryan Kirkby, 218; Anne Perring, 219
Veliger, 241, 305
Vesicle transport, 202, 203
Vestigial penis, 316
Vickery, Minako S., and James B. McClintock, Effects of food concentration and availability on the incidence of cloning in planktotrophic larvae of the sea star *Pisaster ochraceus*, 298
Viral envelope, 209
Vision, 6, 171, 176, 178
Vocal behavior, 175
Vollmer, Steven V., and Peter J. Edmunds, Allometric scaling in small colonies of the scleractinian coral *Siderastrea siderea* (Ellis and Solander), 21
Voltage gating properties of channels formed by a skate retinal connexin, 165
Voronezhskaya, Elena E., see Amanda J. G. Dickinson, 305

W

Wachowiak, Matt, Michal Zochowski, Lawrence B. Cohen, and Chun X. Falk, The spatial representation of odors by olfactory receptor neuron input to the olfactory bulb is concentration invariant, 162
Wakefield, Timothy S., Mark A. Farmer, and Stephen C. Kempf, Revised description of the fine structure of *in situ* "Zooxanthellae" genus *Symbiodinium*, 76
Wang, Jin W., Odor-induced oscillatory activity in *Drosophila* CNS, 170
Ward, J. Evan, see Shirley M. Baker, 116
Wastewater, 221
Watershed modeling, 218
Watson, G. J., F. M. Langford, S. M. Guadron, and M. G. Bentley, Factors influencing spawning and pairing in the scale worm *Harmothoe imbricata*, 50
Watson, Winsor H., III, see Steven H. Jury, 257
Weber, Roy E., see Stéphane Hourdez, 95
Weidner, Earl, Cytoplasmic proteins on the surface of discharged microsporidian sporoplasms, 208
Westgate, Elizabeth J., Devin D. Kroeger, Wendy J. Palich, and Ivan Valiela, Fate of anthropogenic nitrogen in a nearshore Cape Cod aquifer, 221
White, Thomas H., Harris Ripps, Miduturu Srinivas, and Roberto Bruzzone, Voltage gating properties of channels formed by a skate retinal connexin, 165
Williams, Michael, see Anne Perring, 219

Y

Yamaguchi, Ayako, Leonard K. Kaczmarek, and Darcy B. Kelley, Intrinsic membrane properties of laryngeal motoneurons that control sexually differentiated vocal behavior in African clawed frogs, *Xenopus leavis*, 175

Z

Zebra mussel, 116, 144
Zochowski, Michal, see Matt Wachowiak, 162
Zooxanthella, 68, 76, 108, 126, 278

THE BIOLOGICAL BULLETIN

2001 Subscription Rates
Volumes 200-201

	Institutional*	**Individual***
One year subscription (6 issues - 2 volumes)	$235.00	$95.00
Single volume (3 issues)	$117.50	$47.50
Single Issues	$ 40.00	$20.00

*Surface delivery included in above prices.
For prompt delivery, we encourage subscribers outside the U.S. to request airmail service.

Airmail Delivery Charge

U.S. and Canada:	$ 25.00
Mexico:	$ 60.00
All other locations:	$100.00

Orders Must Be Prepaid in U.S. Dollars, Check Payable to The Marine Biological Laboratory

About *The Biological Bulletin*
ISSN: 0006-3185
Frequency: Bimonthly
Number of issues per year: 6
Months of Publication: February, April, June, August, October, December
Subscriptions entered for calendar year
Volume indexes contained in June and December issues
Annual report of the Marine Biological Laboratory contained in August issue
Most back issues available
Claims handled upon receipt
No agency discounts
Internet: http://www.mbl.edu/BiologicalBulletin/

Please address orders to:
Carol Marrama
Subscriptions
The Biological Bulletin
Marine Biological Laboratory
7 MBL Street
Woods Hole, MA 02543-1015 U.S.A.
Fax: 508-289-7922 Telephone: 508-289-7402

Published by the Marine Biological Laboratory
Woods Hole, Massachusetts, 02543 U.S.A.

THE BIOLOGICAL BULLETIN
2001 SUBSCRIPTION FORM
(VOLUMES 200-201, 6 ISSUES)

(please print)

NAME: ______________________________

INSTITUTION: ______________________________

ADDRESS: ______________________________

CITY: ______________ STATE: ______________

POSTAL CODE: __________ COUNTRY: ______________

TELEPHONE: ______________ FAX: ______________

E-MAIL ADDRESS ______________________________

All subscriptions run on the calendar year

☐ Please send me a 2001 subscription to The Biological Bulletin at the rate indicated below:

☐ Individual: $95.00 (6 ISSUES) ☐ Institutional : $235.00 (6 ISSUES)

☐ Individual: $47.50 (3 ISSUES) ☐ Institutional : $117.50 (3 ISSUES)

Check one: ☐ February April June or ☐ August October December

☐ Please send me the following back issue(s): ______________________

☐ Individual: at $20.00 (PER ISSUE) ☐ Institutional : at $40.00 (PER ISSUE)

Delivery Options

_____ Surface Delivery (Surface delivery is included in the subscription price.)
_____ Air delivery (Please add the correct amount to your payment.)

☐ U.S. and Canada: $25.00 ☐ Mexico: $60.00 ☐ All other locations: $100.00

Payment Options

_____ Enclosed is my check or U.S. money order for $ _______
made payable to The Marine Biological Laboratory

_____ Please charge my ☐ VISA, ☐ MasterCard ☐ Discover Card $________

_____ Please send me an invoice. (Note: Payment must be received before subscription commences.)

Account No.: ______________________ Exp. Date: ______________

Signature: ______________________ Date: ______________

Return this form with your check or credit information to:
Marine Biological Laboratory
Subscription Office ◆ The Biological Bulletin ◆ 7 MBL Street ◆ Woods Hole, MA 02543-1015

It's Time To Make
A New Discovery

Axiovert 200. The New Standard In Inverted Microscopy.

Carl Zeiss, Inc., Microscopy & Imaging Systems
One Zeiss Drive, Thornwood, NY 10594 micro@zeiss.com, www.zeiss.com/micro

Being a scientist, you're more than familiar with the rigorous demands of your research. Discover the Axiovert 200, a new standard in inverted microscopy from Zeiss. Superior performance, brilliant fluorescence, greater stability, flexibility and reliability set it apart from the pack. Uncompromising quality guarantees you the edge you need for success. A powerful tool with impact, you'll see more and achieve more with the new Axiovert 200. **For further details call 800.233.2343.**

ZEISS

MBL/WHOI LIBRARY
WH 1B37 S